Republic of Iraq
Ministry of Higher Education and Scientific Research
University of Al-Qadisiyah
College of Sciences
Department of Chemistry

Synthesis and Characterization of New Heterocyclic Polymers and Study of the Potential Biological Activity

A Thesis Submitted to

The Council of the College of Sciences - University of Al- Qadisiyah

As a Partial Fulfillment of the Requirements for the Degree of PhD of Sciences in Organic Chemistry

Submitted by

Nidal Hassoun Thamer

M.Sc. in Chemistry - University of Al- Qadisiyah 2025- 2026

Supervised by

Prof. Mohammed Ali Mutar (PhD)

2026 A.D. **1448 A.H.**

بِسْمِ اللَّهِ الرَّحْمَٰنِ الرَّحِيمِ

﴿ وَيَسْأَلُونَكَ عَنِ الرُّوحِ قُلِ الرُّوحُ مِنْ أَمْرِ رَبِّي

وَمَا أُوتِيتُمْ مِنَ الْعِلْمِ إِلَّا قَلِيلًا ﴾

صَدَقَ اللهُ العَلِيُّ العَظيم

(الاسراء 85)

Language Proofreader's Declaration

I hereby certify that the PhD thesis entitled (**Synthesis and Characterization of New Heterocyclic Polymers and Study of the Potential Biological Activity**) has been reviewed linguistically, and all linguistic errors have been corrected. The thesis is now qualified for discussion.

Signature:

Name: Sahar Abdulameer Haraj
Academic Rank : Professor

Date: ____ / ____ / 2026

Declaration of Scientific Evaluation

I hereby certify that the PhD thesis entitled (**Synthesis and Characterization of New Heterocyclic Polymers and Study of the Potential Biological Activity**) has been scientifically evaluated by me and is part of the requirements for obtaining a PhD degree in Chemistry.

Signature:

Name: Sadiq Abdul Hussein Kareem

Academic Rank : Professor

Date: ____ / ____ / 2026

Declaration of Scientific Evaluation

I hereby certify that the PhD thesis entitled (**Synthesis and Characterization of New Heterocyclic Polymers and Study of the Potential Biological Activity**) has been scientifically evaluated by me and is part of the requirements for obtaining a PhD degree in Chemistry.

Signature:

Name: Maha Abdul Wahab Younis Mohammed

Academic Rank: Professor

Date: ____ / ____ / 2026

Supervisor's Declaration

I hereby certify that the preparation of this thesis entitled (**Synthesis and Characterization of New Heterocyclic Polymers and Study of the Potential Biological Activity**) was conducted under my supervision in the Department of Chemistry, College of Sciences, Al-Qadisiyah University, and is part of the requirements for obtaining a PhD degree in organic Chemistry.

Signature:

Name: Prof. Dr. Mohamed Ali Mutar

Academic Rank: Professor

Address: Al-Qadisiyah University / College of Sciences / Department of Chemistry

Date: 2026/ /

Recommendation of the Head of the Department of Chemistry

Based on the available recommendations, I nominate this thesis for defense.

Signature:

Name: Prof. Dr. Bassam Faron Abed

Address: Al-Qadisiyah University / College of Science / Department of Chemistry

Date: 2026/ /

EXAMINATION COMMITTEE CERTIFICATION

We certify that we have read this Dissertation entitled (Synthesis and Characterization of New Heterocyclic Polymers and Study of the Potential Biological Activity) and as an examining committee examined the student (Nidal Hassoun Thamer), in its content and what is related to it, and that in our opinion it meets the standards of a dissertation for the degree of master of science in chemical with the grade of distinction.

Signature
Name: Professor.Dr. Ibtisam Khalifa Jassim
Date: / / 2026
(Chairman)

Signature:
Name: Professor.Dr. Mohammed Ali Mutar
Date: / / 2026
(Supervisor)

Signature:
Name:Professor.Dr.Moayad Nahma Mohammed
Date: / / 2026
(Member)

Signature
Name:Professor.Dr.Muqdad Irhaeem Kadhim
Date: / / 2026
(Member)

Signature:
Name:Asst.Prof.Dr. Tiba Ibrahim Mohammed
Date: / / 2026
(Member)

Signature:
Name: Asst. Prof. Dr. Loay Ali Khalil
Date: / / 2026
(Member)

Signature:
Name: Professor.Dr. Bassam Faron Abed
Date: / / 2026

Approved by the Head of the Chemical Department

Approved by the Dean of the College Science
Signature:
Name: Professor.Dr. Salwan Ali Obaid
Date: / / 2026

Dedication

I humbly dedicate this dissertation to Almighty Allah, praying that he may accept it with his gracious acceptance and make it beneficial and sincerely devoted to him.

I dedicate this humble research to God Almighty, hoping that he will accept it from me in the best possible way.

To the teacher of humanity and the source of wisdom, our prophet Muhammad (peace and blessings be upon him and his family), whose guidance continues to illuminate the path of knowledge and virtue.

To my beloved father, my wisdom and inspiration, my guiding light on the straight path, my support, my strength, and my refuge after Allah. Your unwavering love, sacrifices, and encouragement have been the foundation of every step in my journey. This achievement is dedicated to You with all my love and gratitude.

To my beloved mother, the fountain of patience, optimism, and hope; the symbol of unconditional love and the balm of healing. To the one whose sincere prayes for me absence, have always been my greatest source of strength and blessing. With profound love , gratitude, and appreciation, I dedicate this work to you.

To my beloved brothers and my brothers nephews, whos Presence in my life has blessed me with strength, love, and boundless confidence. Your constant support, and faith in me have been an invaluable source of inspiration throughout my journey. With heartfelt gratitude and affection, I dedicate this work you.

To all my esteemed teachers, who have carried the noblest mission in life the mission of education and who have paved the way for knowledge and enlightenment. Your guidance, dedication, and generosity in sharing your knowledge have left a lasting impact on my academic journey. With sincere respect and gratitude, I dedicate this work to you.

Acknowledgements

All praise is due to Allah, as befits the majesty of his countenance and the greatest of his sovereignty. May the finest blessing and peace be upon the master of the messenger and the seal of the prophets, prophet Muhammad (peace and blessings be upon him), and upon his family and all his companions.

First and foremost, I thank Almighty Allah, how granted me the strength, patience and perseverance to complete this work.

I would like to express my sincere gratitude, deepest appreciation, and highest respect to my esteemed supervisor, prof. Dr. Mohammed Ali Mutar, for kindly accepting to supervise my dissertation. His invaluable guidance, constructive advice, and continues support throughout every stage of this work were instrumental in the successful completion of this research. He never hesitated to provide his advice and assistance whenever needed and served as a constant source of encouragement, inspiration, and support. I am profoundly that for his generous help, careful follow-up, and unwavering dedication throughout the entire research period.

I would also like to extend my sincere thanks and profound appreciation to Prof.Dr.Salwan Ali Ubaid, Dean of college of Sciences.

My heartfelt thanks and deepest appreciation are also extended to Prof. Bassam Faroun Abdul , Head of the department of Chemistry.

I would also like to express my sincere gratitude to all my respected professors, the staff members of the department of chemistry , and to everyone who has supported, guided , taught, and encouraged me throughout this academic journey.

May Allah grand success to all

List of Contents

Dedication VI
Acknowledgements VIII
List of Tables XXIII
List of Figures XXVII
List of Schemes XLVII
List of Abbreviations LII
Summary LIV
Chapter One Introduction 1
1.1 Introduction 2
1.2 Aim of the work 4
Chapter Two Theoretical Part 7
2.1 Polyheteroatomic Heterocycles 8
2.1.1 Overview on the Heterocyclic 8
2.1.2 Natural Occurrence 12
2.1.3 Strategies for the Synthesis of Heterocyclic 15
2.2 Heterocycles With More Heteroatoms 17
2.2.1 Importance in Nature and Applications 18
2.2.2 Five-Membered Heterocycles 22
2.3 Synthesis of Heterocyclic Polymers 27
2.3.1 Heterocyclic Formation Polymerization 28
2.3.2 Heterocyclic Polymers from Preforme Heterocyclie Monomers(64). 30
2.3.3 Heterocyclic Polymers by a Reaction on the Polymer 31
2.3.4 Functional Heterocyclic Polymers 32
2.3.5 Oxadiazoles and Thiadiazole Containing Polymers 33
2.4 Nucleophilic A Romatic Displacement PoIymerization(118, 119). 40
2.4.1 Mechanism(120). 40
2.4.2 Reaction Conditions Nucleophile 40
2.4.3 Side Reactions 41
2.4.4 Masked Bisphenol. 43
2.5 Applications. 43
2.5.1 Drug Design 47
2.5.2 Molecular Docking 48

Contents

2.6 CANCER....50
Chapter Three Experimental work....51
3.1 Materials and instrument....52
3.1.1 Materials:- 52
3.1.2 Instrument....54
3.2 Synthesis of the Thiosemicarbazones compounds (1-9). 55
3.2.1 Synthesis of Thiosemicarbazones of 2-(pyridin-2-ylmethylene) hydrazine-1-carbothioamide compound(1). 55
3.2.2 Synthesis of Thiosemicarbazones of 2-(1-(4-aminophenyl) ethylidene) hydrazine-1-carbothioamide compound(2). 56
3.2.3 Synthesis of Thiosemicarbazones of 2-(1-(4-nitrophenyl)ethylidene)hydrazine-1-carbothioamide compound(3). 56
3.2.4 Synthesis of Thiosemicarbazones of 2-(diphenylmethylene)hydrazine-1-carbothioamide compound(4). 57
3.2.5 Synthesis of Thiosemicarbazones of 2-(6-hydroxybenzylidene) hydrazine-1-carbothioamide compound(5). 57
3.2.6 Synthesis of 2-(thiophen-2-ylmethylene)hydrazine-1-carbothioamide thiosemicarbazon compound(6). 58
3.2.7 Synthesis of 2-(furan-2-ylmethylene)hydrazine-1-carbothioamide thiosemicarbazon compound(7). 58
3.2.8 Synthesis of (Z)-2-(1-(thiophen-2-yl)ethylidene)hydrazine-1-carbothioamide thiosemicarbazone compound(8). 59
3.2.9 Synthesis of N, N-dimethyl amino benzaldeyde thiosemicarbazone compound(9). 59
3.3 Synthesis of 2-(4-Substituted-benzylidene hydrazono)-1, 3-Thiazolidine-4-one compounds (10-17). 60
3.3.1 Synthesis of N-(Carboxymethyl) 2-(pyridin-2-ylmethylene)hydrazine-1-carbothioamide compound (10). 60
3.3.2 Synthesis of N-(Carboxymethyl) -4-Aminoacetophenone thiosemicarbazone compound(11). 60
3.3.3 Synthesis of N-(Carboxymethyl) 4-Nitroacetophenone thiosemicarbazone compound(12). 61
3.3.4 Synthesis of N-(Carboxymethyl) benzophenone thiosemicarbazone compound(13). 61
3.3.5 Synthesis of N-(Carboxymethyl) salicylaldehyde thiosemicarbazone compound(14). 62

3.3.6 Synthesis of 3-((thiophen-2-ylmethylene)amino)-2-thioxoimidazolidin-4-one compound(15).....62

3.3.7 Synthesis of 3-((furan-2-ylmethylene)amino)-2-thioxoimidazolidin-4-one compound(16).....63

3.3.8 Synthesis of (E)-3-((1-(thiophen-2-yl)ethylidene)amino)-2-thioxoimidazolidin-4-one compound(17).....63

3.4 Synthesis of 5-styryl-2-amino -1, 3, 4-thiadiazole (18-20).....64

3.4.1 Synthesis of N-(5-aminophthaloyl) thiosemicarbazide Compound(18). 64

3.4.2 Synthesis of 5-amino-2-(2-aminophenyl)-2, 5-dihydro-1, 3, 4-thiadiazol-2-ol compound(19).....64

3.4.3 Synthesis of 5-amino-2-(5-amino-2-hydroxyphenyl)-2, 5-dihydro-1, 3, 4-thiadiazol-2 compound(20).....65

3.5 Synthesis of Imide compounds(21-23) 65

3.5.1 Synthesis of 3-amino-5-(5-(5-(1, 3-dioxo-1, 3-dihydroisobenzofuran-5-carbonyl)-3-methylene-1-oxoisoindolin-2-yl)-4, 5-dihydro-1, 3, 4-thiadiazol-2-yl)benzoic acid compound(21). 66

3.5.2 Synthesis of 2-(5-(2-aminophenyl)-1, 3, 4-thiadiazol-2-yl)-1, 3-dioxoisoindoline-5-carboxylic acid compound(22).....66

3.5.3 Synthesis of 2-(5-(5-amino-2-hydroxyphenyl)-1, 3, 4-thiadiazol-2-yl)-5-(1, 3-dioxo-1, 3-dihydroisobenzofuran-5-yl)isoindoline-1, 3-dione compound(23). 67

3.6 Synthesis 1-(3-(derivative)-1, 5-dioxo-1, 5-dihydrobenzo[e] [1, 3] oxazepin -4(3H)-yl) thiourea compounds. (24-26).....67

3.6.1 Synthesis of 1-(8-(1, 3-dioxo-1, 3-dihydroisobenzofuran-5-carbonyl)-1, 5-dioxo-3-(pyridin-2-yl)-1, 5-dihydrobenzo[e][1, 3]oxazepin-4(3H)-yl)urea. (Compound24) 68

3.6.2 Synthesis of 3-(4-aminophenyl)-3-methyl-1, 5-dioxo-4-thioureido-1, 3, 4, 5-tetrahydrobenzo[e][1, 3]oxazepine-8-carboxylic acid compound(25). 68

3.6.3 Synthesis of 1-(3-(3-(dimethylamino)phenyl)-1, 5-dioxo-9-(4-(3-oxobutanoyl)phenyl)-1, 5-dihydrobenzo[e][1, 3]oxazepin-4(3H)-yl)urea compound(26).69

3.7 Synthesis of 2-chloro-N-(5-mercapto-1, 3, 4- thiadiazole-2-yl) acetamide compound(27). 69

3.7.1 Synthesis of (5-mercapto-1, 3, 4-thiadiazol-2-yl)glycinoyl chloridecompound(27).....70

3.8 Synthesis of N-(5-mercapto-1, 3, 4-thiadiazole-2-yl)-2-ureidoacetamide compound(28). 70

3.8.1 *Synthesis* of N-carbamoyl-2-((5-mercapto-1, 3, 4-thiadiazol-2 yl)amino)acetamide compound(28).....70

3.9 *Synthesis* of some 2, 3-dihydroquinosulin4-one derivatives.(29 -31) 70

3.9.1 *Synthesis* of 1-(4-oxo-2-(thiophen-2-yl)-1, 4-dihydroquinazolin-3(2H)-yl)thiourea compound(29). 71

3.9.2 *Synthesis* of 1-(2-(furan-2-yl)-4-oxo-1, 4-dihydroquinazolin-3(2H)-yl)thiourea compound(30). 71

3.9.3 *Synthesis* of 1-(4-oxo-2-(thiophen-2-yl)-1, 4-dihydroquinazolin-3(2H)-yl)thiourea compound(31). 72

3.10 *Synthesis* of Thiosemicarbazones compound(32). 72

3.10.1 *Synthesis* of 1, 1'-(1, 4-phenylenebis(methaneylylidene))bis(thiourea) compound(32). 72

3.11 *Synthesis* of (tetrazole)compounds compound(33). 73

3.11.1 *Synthesis* of 1, 1'-(1, 4-phenylenebis(4, 5-dihydro-1H-tetrazole-5, 1-diyl))bis(thiourea) compound(33). 73

3.12 *Synthesis* (tetrazole) compounds. (34) 73

3.12.1 *Synthesis* of 2, 2'-((Z)-indoline-2, 3-diylidene)bis(hydrazine-1-carbothioamide) compound(34). 73

3.13 *Synthesis* of tetrazole compound.(35) 74

3.13.1 *Synthesis* of 1, 1'-(dispiro[tetrazole-5, 2'-indoline-3', 5"-tetrazol]-1, 1"(4H, 4"H)-diyl)bis(thiourea) compound(35). 74

3.14 *Synthesis* of 2-iminothiazolidin-4-one compound. (Compound36) 74

3.14.1 *Synthesis* of 2-iminothiazolidin-4-one compound(36). 75

3.15 *Synthesis* of Mannich reaction compounds(37-40) 75

3.15.1 *Synthesis* of 3-((3-(4-aminophenoxy)phenyl)amino)-3, 4-dihydro-2H-thiazolo[3, 2-a][1, 3, 5]triazin-6(7H)-one compound(37). 75

3.15.2 *Synthesis* of 3-((4-aminophenyl)amino)-3, 4-dihydro-2H-thiazolo[3, 2-a][1, 3, 5]triazin-6(7H)-one compound (38). 76

3.15.3 *Synthesis* of 3-((2-((2-((2-minoethyl)amino)ethyl)amino) ethyl)amino)-3, 4-dihydro-2H-thiazolo[3, 2-a][1, 3, 5]triazin-6(7H)-one compound(39). 76

3.15.4 *Synthesis* of 3-((6-aminopyridin-2-yl)amino)-3, 4-dihydro-2H-thiazolo[3, 2-a][1, 3, 5]triazin-6(7H)-one compound(40). 77

3.16 Synthesis of copolymer (methyl acrylic acid-co- Itaconic anhydride) (MAA-CO-IAN). 77

3.16.1 *Synthesis* of copolymer (MAA-CO-IAN) 78

3.17 Synthesis of copolymer (dimethyl acrylic amide-co- Citraconic anhydride) (DMA-CO-CAN). 78

3.17.1 *Synthesis* of copolymer (DMA-CO-CAN). 78

3.18 Synthesis of copolymer (MAA-CO-IAN) with Thiosemicarbazones compounds (1-9). 78

3.18.1 Synthesis of copolymer(1) (MAA-Co-IAN) with compound(1). 79

3.18.2 Synthesis of copolymer(2) (MAA-Co-IAN) with compound(2). 79

3.18.3 Synthesis of copolymer(3) (MAA-Co-IAN) with compound(3). 79

3.18.4 Synthesis of copolymer(4) (MAA-Co-IAN) with compound(4). 80

3.18.5 Synthesis of copolymer(5) (MAA-Co-IAN) with compound(5). 80

3.18.6 Synthesis of copolymer(6) (MAA-Co-IAN) with compound(6). 80

3.18.7 Synthesis of copolymer(7) (MAA-Co-IAN) with compound(7). 81

3.18.8 Synthesis of copolymer(8) (MAA-Co-IAN) with compound(8). 81

3.18.9 Synthesis of copolymer(9) (MAA-Co-IAN) with compound(9). 81

3.19 Synthesis of copolymer (MAA-CO-IAN) with thiosemicarbazide derivatives compounds. (10-17) 82

3.19.1 Synthesis of copolymer(10) (MAA-CO-IAN) with compound(10). 82

3.19.2 Synthesis of copolymer(11) (MAA-CO-IAN) with compound(11). 82

3.19.3 Synthesis of copolymer(12) (MAA-CO-IAN) with compound(12). 83

3.19.4 Synthesis of copolymer(13) (MAA-CO-IAN) with compound(13). 83

3.19.5 Synthesis of copolymer(14) (MAA-CO-IAN) with compound(14). 83

3.19.6 Synthesis of copolymer(15) (MAA-CO-IAN) with compound(15). 84

3.19.7 Synthesis of copolymer(16) (MAA-CO-IAN) with compound(16). 84

3.19.8 Synthesis of copolymer(17) (MAA-CO-IAN) with compound(17). 84

3.20 Synthesis of copolymer (MAA-CO-IAN) with compounds (18-20). 85

3.20.1 Synthesis of copolymer(18) (MAA-CO-IAN) with compound(18). 85

3.20.2 Synthesis of copolymer(19) (MAA-CO-IAN) with compound(19). 85

3.20.3 Synthesis of copolymer(20) (MAA-CO-IAN) with compound(20). 86

3.21 Synthesis of copolymer(1) (MAA-CO-IAN) with Imide compounds (21-23). 86

3.21.1 Synthesis of copolymer(21) (MAA-CO-IAN) with compound(21) 86

3.21.2 Synthesis of copolymer(32) (MAA-CO-IAN) with compound(22) 86

3.21.3 Synthesis of copolymer(23) (MAA-CO-IAN) with compound(23) 87

3.22 Synthesis of copolymer (MAA-CO-IAN) with compounds (24-26). 87

3.22.1 Synthesis of copolymer(24) (MAA-CO-IAN) with compound (24). 87

3.22.2 Synthesis of copolymer(25) (MAA-CO-IAN) with compound (25). 88

3.22.3 Synthesis of copolymer(26) (MAA-CO-IAN) with compound (26). 88

3.23 Synthesis of copolymer (MAA-CO-IAN) with compound(27) 88
3.23.1 Synthesis of copolymer(27) (MAA-CO-IAN) with compound (27). 89
3.24 Synthesis of copolymer (MAA-CO-IAN) with compound(28). 89
3.24.1 Synthesis of copolymer(28) (MAA-CO-IAN) with compound (28). 89
3.25 Synthesis of copolymer (MAA-CO-IAN) with compounds (29-31) 89
3.25.1 Synthesis of copolymer(29) (MAA-CO-IAN) with compound (29). 90
3.25.2 Synthesis of copolymer(30) (MAA-CO-IAN) with compound (30). 90
3.25.3 Synthesis of copolymer(31) (MAA-CO-IAN) with compound (31). 90
3.26 Synthesis of copolymer (MAA-CO-IAN) with compound(32) 91
3.26.1 Synthesis of copolymer(32) (MAA-CO-IAN) with compound (32). 91
3.27 *Synthesis* of copolymer (MAA-CO-IAN) with compound(33)..... 91
3.27.1 Synthesis of copolymer(33) (MAA-CO-IAN) with compound (33). 91
3.28 *Synthesis* of copolymer (MAA-CO-IAN) with compound (34)..... 91
3.28.1 Synthesis of copolymer(34) (MAA-CO-IAN) with compound (34). 92
3.29 *Synthesis* of copolymer (MAA-CO-IAN) with compound (35)..... 92
3.29.1 Synthesis of copolymer(35) (MAA-CO-IAN) with compound (35). 92
3.30 Synthesis of copolymer (MAA-CO-IAN) with compound (36). 92
3.30.1 Synthesis of copolymer(36) (MAA-CO-IAN) with compound (36). 93
3.31 *Synthesis* of copolymer (MAA-CO-IAN) with Compounds (37-40)..... 93
3.31.1 Synthesis of copolymer(37) (MAA-CO-IAN) with compound(37). 93
3.31.2 Synthesis of copolymer(38) (MAA-CO-IAN) with compound(38). 94
3.31.3 Synthesis of copolymer(39) (MAA-CO-IAN) with compound(39). 94
3.31.4 Synthesis of copolymer(40) (MAA-CO-IAN) with compound(40). 94
3.32 Synthesis of copolymer (DMA-CO-CAN) with Thiosemicarbazones compounds(3). 95
3.32.1 Synthesis of copolymer(41) (DMA-CO-CAN) with compound(3). 95
3.33 Synthesis of copolymer (DMA-CO-CAN) with compounds (13), (14), (16), (17). . 95
3.33.1 Synthesis of copolymer(42) (DMA-CO-CAN) with compound(13). 95
3.33.2 Synthesis of copolymer(43) (DMA-CO-CAN) with compound(14). 96
3.33.3 Synthesis of copolymer(44) (DMA-CO-CAN) with compound(16). 96
3.33.4 Synthesis of copolymer(45) (DMA-CO-CAN) with compound(17). 96
3.34 Synthesis of copolymer (DMA-CAN) with compounds(18-20)..... 97
3.34.1 Synthesis of copolymer(46) (DMA-CO-CAN) with compound(18). 97

3.34.2 Synthesis of copolymer(47) (DMA-CO-CAN) with compound(19). 97
3.34.3 Synthesis of copolymer(48) (DMA-CO-CAN) with compound(20). 97
3.35 Synthesis of copolymer (DMA-CO-CAN) with compounds with (24-25). 98
3.35.1 Synthesis of copolymer(49) (DMA-CO-CAN) with compound(24). 98
3.35.2 Synthesis of copolymer(50) (DMA-CO-CAN) with compound(25). 98
3.36 Synthesis of copolymer (DMA-CO-CAN) with compound (28). 98
3.36.1 Synthesis of copolymer(51) (DMA-CO-CAN) with compound(28). 99
3.37 Synthesis of copolymer (DMA-CO-CAN) with compounds (31). 99
3.37.1 Synthesis of copolymer(52) (DMA-CO-CAN) with compound(31). 99
3.38 Synthesis of copolymer (DMA-CO-CAN) with compound(34). 99
3.38.1 Synthesis of copolymer(53) (DMA-CO-CAN) with compound (34). 100
3.39 Synthesis of copolymer (DMA-CO-CAN) with compound(35). 100
3.39.1 Synthesis of copolymer(54) (DMA-CO-CAN) with compound(35). 100
3.40 *Synthesis* of copolymer (DMA-CO-CAN) with compounds (37-40). 100
3.40.1 Synthesis of copolymer(55) (DMA-CO-CAN) with compound(37). 101
3.40.2 Synthesis of copolymer(56) (DMA-CO-CAN) with compound(38). 101
3.40.3 Synthesis of copolymer(57) (DMA-CO-CAN) with compound(39). 101
3.40.4 Synthesis of copolymer(58) (DMA-CO-CAN) with compound(40). 102
3.41 Study of thermogravimetric analysis (*TGA*) 102
3.42 Differential Scanning calorimeter analysis (DSC) study 102
3.43 Study of molecules docking 103
3.43.1 Molecules Library Preparation 103
3.44 Study of Biological Activity: 105
3.44.1 Preparation of the Culture Medium: 105
3.44.2 Processing Method : 105
3.45 Cytotoxicity Assays Cell Lines 106
3.45.1 Cancer Cell Lines: 106
3.45.2 Cytotoxicity MTT Assays: 106
3.46 DPPH Radical Scavenging activity: 109
3.47 Statistical analysis 109
Chapter Four Results and Discussion 113
4.1 Synthesis of the Thiosemicarbazones compounds (1-9). 114
4.1.1 Synthesis of Thiosemicarbazones of 2-(pyridin-2-ylmethylene)hydrazine-1-

carbothioamide compound(1). 114

4.1.2 Synthesis of Thiosemicarbazones of 2-(1-(4-aminophenyl)ethylidene)hydrazine-1-carbothioamide compound(2). 116

4.1.3 Synthesis of the Thiosemicarbazones for 2-(1-(4-nitrophenyl)ethylidene)hydrazine-1carbothioamide compound(3). 118

4.1.4 Synthesis of the Thiosemicarbazones for 2-(diphenylmethylene)hydrazine-1-carbothioamide compound(4). 120

4.1.5 Synthesis of the Thiosemicarbazones for 2-(2-hydroxybenzylidene) hydrazine-1-carbothioamide compound(5). 122

4.1.6 Synthesis of 2-(thiophen-2-ylmethylene)hydrazine-1-carbothioamide thiosemicarbazon compound(6). 124

4.1.7 Synthesis of 2-(furan-2-ylmethylene)hydrazine-1-carbothioamide thiosemicarbazon compound(7). 126

4.1.8 Synthesis of (Z)-2-(1-(thiophen-2-yl)ethylidene)hydrazine-1-carbothioamide thiosemicarbazone compound(8). 128

4.1.9 Synthesis of the Thiosemicarbazones for N, N-dimethyaminebenzaldehyde compound(9). 130

4.2 Synthesis of 2-(4-Substituted-benzylidene hydrazono)-1, 3-Thiazolidine-4-one compounds.(10 -17) 132

4.2.1 Synthesis of (Z)-3-((pyridin-2-ylmethylene)amino)-2-thioxoimidazolidin-4-one compound(10). 132

4.2.2 Synthesis of (E)-3-((1-(2-aminophenyl)ethylidene)amino)-2-thioxoimidazolidin-4-one compound(11). 135

4.2.3 Synthesis of (E)-3-((1-(4-nitrophenyl)ethylidene)amino)-2-thioxoimidazolidin-4-one compound(12). 137

4.2.4 Synthesis of (Z)-3-((cyclohexa-2, 4-dien-1-yl(phenyl)methylene)amino)-2-thioxoimidazolidin-4-one compound(13). 139

4.2.5 Synthesis of (E)-3-((1-(2-hydroxyphenyl)ethylidene)amino)-2-thioxoimidazolidin-4-one compound(14). 141

4.2.6 Synthesis of 3-((thiophen-2-ylmethylene)amino)-2-thioxoimidazolidin-4-one compound(15). 143

4.2.7 Synthesis of 3-((furan-2-ylmethylene)amino)-2-thioxoimidazolidin-4-one compound(16). 145

4.2.8 Synthesis of of (E)-3-((1-(thiophen-2-yl)ethylidene)amino)-2-thioxoimidazolidin-4-one compound(17). 147

4.3 Synthesis of 5-styryl-2-amino -1, 3, 4-thiadiazole (18-20) 149

4.3.1 Synthesis of N-(5-aminophthaloyl) thiosemicarbazide compound(1). 149

4.3.2 Synthesis of 5-amino-2-(2-aminophenyl)-2, 5-dihydro-1, 3, 4-thiadiazol-2-ol compound(19).....151

4.3.3 Synthesis of 5-amino-2-(5-amino-2-hydroxyphenyl)-2, 5-dihydro-1, 3, 4-thiadiazol-2 compound(20).....153

4.4 Synthesis of Imide compounds(21-23) 155

4.4.1 Synthesis of 3-amino-5-(5-(5-(1, 3-dioxo-1, 3-dihydroisobenzofuran-5-carbonyl)-3-methylene-1-oxoisoindolin-2-yl)-4, 5-dihydro-1, 3, 4-thiadiazol-2-yl)benzoic acid compound(21). 155

4.4.2 Synthesis of 5-(2-(5-(2-aminophenyl)-5-hydroxy-2, 5-dihydro-1, 3, 4-thiadiazol-2-yl)-3-methylene-1-oxoisoindoline-5-carbonyl) isobenzofuran-1, 3-dione compound(22). 158

4.4.3 Synthesis of 2-(5-(5-amino-2-hydroxyphenyl)-5-hydroxy-2, 5-dihydro-1, 3, 4-thiadiazol-2-yl)-5-(1, 3-dioxo-1, 3-dihydroisobenzofuran-5-carbonyl)isoindoline-1, 3-dione compound(23). 160

4.5 Synthesis 1-(3-(derivative)-1, 5-dioxo-1, 5-dihydrobenzo[e] [1, 3] oxazepin -4(3H)-yl) thiourea compounds. (24-26).....162

4.5.1 Synthesis of 1-(8-(1, 3-dioxo-1, 3-dihydroisobenzofuran-5-carbonyl)-1, 5-dioxo-3-(pyridin-2-yl)-1, 5-dihydrobenzo[e][1, 3]oxazepin-4(3H)-yl)urea compound(24). 162

4.5.2 Synthesis of 3-(2-aminophenyl)-1, 5-dioxo-4-ureido-1, 3, 4, 5-tetrahydrobenzo[e][1, 3]oxazepine-8-carboxylic acid compound(25). 165

4.5.3 Synthesis of 1-(3-(3-(dimethylamino)phenyl)-1, 5-dioxo-9-(4-(3-oxobutanoyl)phenyl)-1, 5-dihydrobenzo[e][1, 3]oxazepin-4(3H)-yl)urea compound(26). 167

4.6 Synthesis of (5-mercapto-1, 3, 4-thiadiazol-2-yl)glycinoyl chloride compound(27). 169

4.7 Synthesis of N-(5-mercapto-1, 3, 4-thiadiazole-2-yl)-2-ureidoacetamide compound(28). 172

4.8 Synthesis of some 2, 3-dihydroquinosulin4-one derivatives.(29 -31) 174

4.8.1 Synthesis of 1-(4-oxo-2-(thiophen-2-yl)-1, 4-dihydroquinazolin-3(2H)-yl)thiourea compound(29). 174

4.8.2 *Synthesis* of 1-(2-(furan-2-yl)-4-oxo-1, 4-dihydroquinazolin-3(2H)-yl)thiourea compound(30).....177

4.8.3 *Synthesis* of 1-(4-oxo-2-(thiophen-2-yl)-1, 4-dihydroquinazolin-3(2H)-yl)thiourea compound(31). 179

4.9 Synthesis of 1, 1'-(1, 4- phenylenebis(methaneylylidene))bis(thiourea) compound(32). 181

4.10 *Synthesis* of 1, 1'-(1, 4-phenylenebis(4, 5-dihydro-1H-tetrazole-5, 1-

diyl))bis(thiourea) compound(33). 184

4.11 Synthesis of 2, 2'-((Z)-indoline-2, 3-diylidene)bis(hydrazine-1-carbothioamide) compound(34). 186

4.12 Synthesis of 1, 1'-(dispiro[tetrazole-5, 2'-indoline-3', 5''-tetrazol]-1, 1''(4H, 4''H)-diyl)bis(thiourea) compound(35). 188

4.13 *Synthesis* of 2-iminothiazolidin-4-one compound(36). 190

4.14 Synthesis of Mannich reaction compounds(37-40) 192

4.14.1 Synthesis of 3-((3-(4-aminophenoxy)phenyl)amino)-3, 4-dihydro-2H-thiazolo[3, 2-a][1, 3, 5]triazin-6(7H)-one compound(37). 192

4.14.2 Synthesis of 3-((4-aminophenyl)amino)-3, 4-dihydro-2H-thiazolo[3, 2-a][1, 3, 5]triazin-6(7H)-one compound(38). 194

4.14.3 Synthesis of 3-((2-((2-((2-minoethyl)amino)ethyl)amino) ethyl)amino)-3, 4-dihydro-2H-thiazolo[3, 2-a][1, 3, 5]triazin-6(7H)-one compound(39). 196

4.14.4 Synthesis of 3-((6-aminopyridin-2-yl)amino)-3, 4-dihydro-2H-thiazolo[3, 2-a][1, 3, 5]triazin-6(7H)-one compound(40). 198

4.15 Synthesis of copolymer (methyl acrylic acid-co - Itaconic anhydride) (MAA-CO-IAN) . 201

4.16 Synthesis of copolymer (N, N-dimethylacrylamide-CO -Citraconic anhydride) (DMA-CO-CAN). 202

4.17 Synthesis of copolymer (MAA-CO-IAN) with Thiosemicarbazones compounds (1-9). 205

4.17.1 Synthesis of copolymer(1) (MAA-Co-IAN) with compound(1). 205

4.17.2 Synthesis of copolymer(2) (MAA-Co-IAN) with compound(2). 207

4.17.3 Synthesis of copolymer (3) (MAA-Co-IAN) with compound(3). 209

4.17.4 Synthesis of copolymer(4) (MAA-Co-IAN) with compound(4). 211

4.17.5 Synthesis of copolymer(5) (MAA-Co-IAN) with compound(5). 213

4.17.6 Synthesis of copolymer(6) (MAA-Co-IAN) with compound(6). 215

4.17.7 Synthesis of copolymer(7) (MAA-Co-IAN) with compound(7). 217

4.17.8 Synthesis of copolymer(8) (MAA-Co-IAN) with compound(8). 219

4.17.9 Synthesis of copolymer(9) (MAA-Co-IAN) with compound(9). 222

4.18 Synthesis of copolymer (MAA-CO-IAN) with thiosemicarbazide derivatives compounds. (10-17) 224

4.18.1 Synthesis of copolymer(10) (MAA-Co-IAN) with compound(10). 224

4.18.2 Synthesis of copolymer(11) (MAA-CO-IAN) with compound(11). 226

4.18.3 Synthesis of copolymer(12) (MAA-CO-IAN) with compound(12). 228

4.18.4 Synthesis of copolymer(13) (MAA-CO-IAN) with compound(13). 230
4.18.5 Synthesis of copolymer(14) (MAA-CO-IAN) with compound(14). 231
4.18.6 Synthesis of copolymer(15) (MAA-CO-IAN) with compound(15). 233
4.18.7 Synthesis of copolymer(16) (MAA-CO-IAN) with compound(16). 235
4.18.8 Synthesis of copolymer(17) (MAA-CO-IAN) with compound(17). 237
4.19 Synthesis of copolymer (MAA-CO-IAN) with compounds (18-20). 239
4.19.1 Synthesis of copolymer(18) (MAA-CO-IAN) with compound(18). 239
4.19.2 Synthesis of copolymer(19) (MAA-CO-IAN) with compound(19). 241
4.20 Synthesis of copolymer(1) (MAA-CO-IAN) with Imide compounds (21-23). 245
4.20.1 Synthesis of copolymer(21) (MAA-CO-IAN) with compound(21) 245
4.20.2 Synthesis of copolymer(32) (MAA-CO-IAN) with compound(22) 247
4.20.3 Synthesis of copolymer(23) (MAA-CO-IAN) with compound(23) 249
4.21 Synthesis of copolymer (MAA-CO-IAN) with compounds (24-26). 251
4.21.1 Synthesis of copolymer(24) (MAA-CO-IAN) with compound (24). 251
4.21.2 Synthesis of copolymer(25) (MAA-CO-IAN) with compound (25). 253
4.21.3 Synthesis of copolymer(26) (MAA-CO-IAN) with compound (26). 255
4.22 Synthesis of copolymer(27) (MAA-CO-IAN) with compound(27) 257
4.23 Synthesis of copolymer (MAA-CO-IAN) with compounds (29-31) 261
4.23.1 Synthesis of copolymer(29) (MAA-CO-IAN) with compound (29). 261
4.23.2 Synthesis of copolymer(30) (MAA-CO-IAN) with compound (30). 263
4.23.3 Synthesis of copolymer(31) (MAA-CO-IAN) with compound (31). 265
4.24 Synthesis of copolymer(32) (MAA-CO-IAN) with compound (32). 267
4.25 *Synthesis* of copolymer(33) (MAA-CO-IAN) with compound(33). 269
4.26 *Synthesis* of copolymer(34)(MAA-CO-IAN) with compound (34). 271
4.27 *Synthesis* of copolymer(35)(MAA-CO-IAN) with compound (35). 273
4.28 Synthesis of copolymer(36) (MAA-CO-IAN) with compound (36). 275
4.29 Synthesis of copolymer (MAA-CO-IAN) with Compounds (37-40). 277
4.29.1 Synthesis of copolymer(37) (MAA-CO-IAN) with compound(37). 277
4.29.2 Synthesis of copolymer(38) (MAA-CO-IAN) with compound(38). 279
4.29.3 Synthesis of copolymer(39) (MAA-CO-IAN) with compound(39). 281
4.29.4 Synthesis of copolymer(40) (MAA-CO-IAN) with compound(40). 283
4.30 Synthesis of copolymer(41) (DMA-CO-CAN) with compound(3). 285
4.31 Synthesis of copolymer (DMA-CO-CAN) with compounds (13), (14), (16), (17).287

4.31.1 Synthesis of copolymer(42) (DMA-CO-CAN) with compound(13). 287
4.31.2 Synthesis of copolymer(43) (DMA-CO-CAN) with compound(14). 289
4.31.3 Synthesis of copolymer(44) (DMA-CO-CAN) with compound(16). 291
4.31.4 Synthesis of copolymer(45) (DMA-CO-CAN) with compound(17). 293
4.32 Synthesis of copolymer (DMA-CAN) with compounds(18-20). 295
4.32.1 Synthesis of copolymer(46) (DMA-CO-CAN) with compound(18). 295
4.32.2 Synthesis of copolymer(47) (DMA-CO-CAN) with compound(19). 297
4.32.3 Synthesis of copolymer(48) (DMA-CO-CAN) with compound(20). 299
4.33 Synthesis of copolymer (DMA-CO-CAN) with compounds with (24-25). 301
4.33.1 Synthesis of copolymer(49) (DMA-CO-CAN) with compound(24). 301
4.33.2 Synthesis of copolymer(50) (DMA-CO-CAN) with compound(25). 303
4.34 Synthesis of copolymer (51) (DMA-CO-CAN) with compound (28). 305
4.35 Synthesis of copolymer(52) (DMA-CO-CAN) with compound(31). 307
4.36 Synthesis of copolymer(53) (DMA-CO-CAN) with compound (34). 309
4.37 Synthesis of copolymer(54) (DMA-CO-CAN) with compound(35). 311
4.38 *Synthesis* of copolymer (DMA-CO-CAN) with compounds (37-40). 313
4.38.1 Synthesis of copolymer(55) (DMA-CO-CAN) with compound(37). 313
4.38.2 Synthesis of copolymer(56) (DMA-CO-CAN) with compound(38). 315
4.38.3 Synthesis of copolymer(57) (DMA-CO-CAN) with compound(39). 317
4.38.4 Synthesis of copolymer(58) (DMA-CO-CAN) with compound(40). 319
4.39 Thermo gravimetric analysis (TGA) 321
4.40 Differential Scanning calorimeter analysis (DSC) study 324
4.41 Molecules Library Preparation 331
4.42 Receptors preparation 333
4.43 Ligand–Protein molecular docking 334
4.44 Results 335
4.45 Interpretation of molecular docking results 340
4.46 Molecules Library Preparation 343
4.47 Receptors preparation 345
4.48 Ligand–Protein molecular docking 346
4.49 Results 346
4.50 Interpretation of molecular docking results 352
4.51 Molecules Library Preparation 355

4.52 Receptors preparation.....357
4.53 Ligand–Protein molecular docking 357
4.54 Results 358
4.55 Interpretation of molecular docking results 362
4.56 Molecules Library Preparation.....367
4.57 Receptors preparation.....368
4.58 Ligand–Protein molecular docking 369
4.59 Results 369
4.60 Interpretation of molecular docking results 375
4.61 Biological activity: 379
4.61.1 Cytotoxic potential of copolymer (1) on colon Cell Line(HCT-116).....379
4.61.2 Antioxidant Activity of copolymer(1) Extract via DPPH Assay. 385
4.61.3 Cytotoxic potential of copolymer (2) on colon Cell Line(HCT-116).....386
4.61.4 Antioxidant Activity of copolymer(2) Extract via DPPH Assay.....391
4.61.5 Cytotoxic potential of copolymer (3) on colon Cell Line (HCT-116).....392
4.61.6 Antioxidant Activity of copolymer(3) Extract via DPPH Assay.....397
4.61.7 Cytotoxic potential of copolymer (4) on colon Cell Line (HCT-116).....398
4.61.8 Antioxidant Activity of Extract copolymer(4) via DPPH Assay. 403
4.61.9 Cytotoxic potential of copolymer (5) on colon Cell Line (HCT-116).....404
4.61.10 Antioxidant Activity of copolymer(5)and copolymer(6) Extract via DPPH Assay. 411
4.61.11 Cytotoxic against of copolymer(6) on skin cancer Cell Lines(A431) in comparison with normal cell line (Hdfn). 412
4.61.12 Cytotoxic against of copolymer(7) on skin cancer Cell Lines(A431) in comparison with normal cell line (Hdfn). 417
4.61.13 Antioxidant Activity of copolymer(7)and copolymer(8) Extract via DPPH Assay. 422
4.61.14 Cytotoxic against of copolymer(8) on skin cancer Cell Lines(A431) in comparison with normal cell line (Hdfn). 422
4.61.15 Cytotoxic against of copolymer(9) on skin cancer Cell Lines(A431) in comparison with normal cell line (Hdfn). 427
4.61.16 Antioxidant Activity of copolymer(9) Extract via DPPH Assay. 431
4.61.17 Antioxidant Activity of copolymer(10)and Extract via DPPH Assay. 440
4.62 Antimicrobial and Antifungal Activity of Tested Copolymers. 445

4.62.1 Antibacterial Activity 445
4.62.2 Effect of polymers on E. coli and P. aeruginosa: 446
4.63 Antifungal Activity 455
Chapter Five Conclusions and Recommendations and future work 465
5.1 Conclusions 466
5.2 Recommendations and future work 469
References 470
References 471
الخلاصة: ..... أ

List of Tables

Table (2- 1): Common name endings for heterocyclic compounds. 10
Table (2- 2): Main five-membered polyheteroatomic heterocycles. 22

Table (3- 1): Elemental analysis data of compound (1) (calculated vs. found values). 56
Table (3- 2): Elemental analysis data of compound (2) (calculated vs. found values). 56
Table (3- 3): Elemental analysis data of compound (3) (calculated vs. found values). 56
Table (3- 4): Elemental analysis data of compound (4) (calculated vs. found values). 57
Table (3- 5): Elemental analysis data of compound (5) (calculated vs. found values). 57
Table (3- 6): Elemental analysis data of compound (6) (calculated vs. found values). 58
Table (3- 7): Elemental analysis data of compound (7) (calculated vs. found values). 58
Table (3- 8): Elemental analysis data of compound (8) (calculated vs. found values). 59
Table (3- 9): Elemental analysis data of compound (9) (calculated vs. found values. 59
Table (3- 10): Elemental analysis data of compound (10) (calculated vs. found values). 60
Table (3- 11): Elemental analysis data of compound (11) (calculated vs. found values) 60
Table (3- 12): Elemental analysis data of compound (12) (calculated vs. found values) 61
Table (3- 13): Elemental analysis data of compound (13) (calculated vs. found values). 61
Table (3- 14): Elemental analysis data of compound (14) (calculated vs. found values). 62
Table (3- 15): Elemental analysis data of compound (15) (calculated vs. found values). 62
Table (3- 16): Elemental analysis data of compound (16) (calculated vs. found values). 63
Table (3- 17): Elemental analysis data of compound (17) (calculated vs. found values). 63
Table (3- 18): Elemental analysis data of compound (18) (calculated vs. found values). 64
Table (3- 19): Elemental analysis data of compound (19) (calculated vs. found values). 65
Table (3- 20): Elemental analysis data of compound (20) (calculated vs. found values). 65
Table (3- 21): Elemental analysis data of compound (21) (calculated vs. found values). 66
Table (3- 22): Elemental analysis data of compound (22) (calculated vs. found values). 66
Table (3- 23): Elemental analysis data of compound (23) (calculated vs. found values) 67
Table (3- 24): Elemental analysis data of compound (24) (calculated vs. found values). 68
Table (3- 25): Elemental analysis data of compound (25) (calculated vs. found values) 68
Table (3- 26): Elemental analysis data of compound (26) (calculated vs. found values). 69
Table (3- 27): Elemental analysis data of compound (27) (calculated vs. found values). 70
Table (3- 28): Elemental analysis data of compound (28) (calculated vs. found values). 70
Table (3- 29): Elemental analysis data of compound (29) (calculated vs. found values). 71
Table (3- 30): Elemental analysis data of compound (30) (calculated vs. found values). 71
Table (3- 31): Elemental analysis data of compound (31) (calculated vs. found values). 72
Table (3- 32): Elemental analysis data of compound (32) (calculated vs. found values). 72
Table (3- 33): Elemental analysis data of compound (33) (calculated vs. found values). 73
Table (3- 34): Elemental analysis data of compound (34) (calculated vs. found values). 74
Table (3- 35): Elemental analysis data of compound (35) (calculated vs. found values). 74
Table (3- 36): Elemental analysis data of compound (36) (calculated vs. found values). 75
Table (3- 37): Elemental analysis data of compound (37) (calculated vs. found values). 76
Table (3- 38): Elemental analysis data of compound (38) (calculated vs. found values). 76

Table (3- 39): Elemental analysis data of compound (39) (calculated vs. found values). 77
Table (3- 40): Elemental analysis data of compound (40) (calculated vs. found values). 77
Table (3- 41): Kits used in this study 106
Table (3- 42): The color, yield and melting point of synthesis of compounds.....110
Table (4- 1): Some Thermal Stability Characteristics Curves Thermal Gravimetric Analysis (TGA) of polymers represents the temperature of decomposition.....323
Table (4- 2): Shows the Thermal parameter obtained from DSc. 327
Table (4- 3): The binding affinity and rmsd result of copolymers with 5IKQ 335
Table (4- 4): Name of copolymers and smiles 336
Table (4- 5): Details of the best pose of protein 5IKQ. 337
Table (4- 6): The binding affinity and rmsd result of compounds with 5IKQ 347
Table (4- 7): Details of the best pose of protein 5IKQ 348
Table (4- 8): Name of compounds and smiles.....349
Table (4- 9): The binding affinity and rmsd result of compounds with 8C7Y 358
Table (4- 10): Name of copolymers and smiles 359
Table (4- 11): Details of the best pose of protein 8C7Y.....360
Table (4- 12): The binding affinity and rmsd result of copolymers with 5IKQ 370
Table (4- 13): Details of the best pose of protein 5IKQ.....371
Table (4- 14): Name of copolymers and smiles 372
Table (4- 15): Cytotoxic potentials of copolymer(1) on colon cancer cell line vs normal cell line after 24 hrs.; 37 Cº.....380
Table (4- 16): Cytotoxic potentials of copolymer(1) on colon cancer cell line vs normal cell line after 48 hrs.; 37 Cº.....382
Table (4- 17): Cytotoxic potentials of copolymer(1) on colon cancer cell line vs normal cell line after 72 hrs.; 37 Cº.....384
Table (4- 18): DPPH radical scavenging activity of copolymer(1) and Vit-C. 385
Table (4- 19): Cytotoxic potentials of copolymer(2) on colon cancer cell line vs normal cell line after 24 hrs.; 37 Cº.....387
Table (4- 20): Cytotoxic potentials of copolymer(2) on colon cancer cell line vs normal cell line after 48 hrs.; 37 Cº.....388
Table (4- 21): Cytotoxic potentials of o copolymer(2) on colon cancer cell line vs normal cell line after 72 hrs.; 37 Cº.....390
Table (4- 22): DPPH radical scavenging activity of copolymer(2) and Vit-C. 391
Table (4- 23): Cytotoxic potentials of copolymer(3) on colon cancer cell line vs normal cell line after 24 hrs.; 37 Cº.....393
Table (4- 24): Cytotoxic potentials of copolymer(3) on colon cancer cell line vs normal cell line after 48 hrs.; 37 Cº.....395
Table (4- 25): Cytotoxic potentials of copolymer(3) on colon cancer cell line vs normal cell line after 72 hrs.; 37 Cº.....396
Table (4- 26): DPPH radical scavenging activity of copolymer(3) and Vit-C. 397
Table (4- 27): Cytotoxic potentials of copolymer(4) on colon cancer cell line vs normal cell line after 24 hrs.; 37 Cº.....398
Table (4- 28): Cytotoxic potentials of copolymer(4) on colon cancer cell line vs normal cell line

after 48 hrs.; 37 Cº.....400
Table (4- 29): Cytotoxic potentials of copolymer(4) on colon cancer cell line vs normal cell line after 72 hrs.; 37 Cº.....402
Table (4- 30): DPPH radical scavenging activity of copolymer(4) and Vit-C. 404
Table (4- 31): Cytotoxic potentials of copolymer(5) on colon cancer cell line vs normal cell line after 24 hrs.; 37 Cº.....405
Table (4- 32): Cytotoxic potentials of copolymer(5) on colon cancer cell line vs normal cell line after 48 hrs.; 37 Cº.....406
Table (4- 33): Cytotoxic potentials of copolymer(5) on colon cancer cell line vs normal cell line after 72 hrs.; 37 Cº.....408
Table (4- 34): DPPH radical scavenging activity of copolymer(5) and copolymer(6), Vit-C. ...412
Table (4- 35): Cytotoxic potentials of copolymer(6) on skin cancer cell line vs normal cell line after 24 hrs.; 37 C°. 413
Table (4- 36): Cytotoxic potentials of copolymer(6) on skin cancer cell line vs normal cell line after 48 hrs.; 37 C°. 414
Table (4- 37): Cytotoxic potentials of copolymer(6) on skin cancer cell line vs normal cell line after 72 hrs.; 37 C°. 416
Table (4- 38): Cytotoxic potentials of copolymer(7) compound on skin cancer cell line vs normal cell line after 24 hrs.; 37 C° 417
Table (4- 39): Cytotoxic potentials of copolymer(7) on skin cancer cell line vs normal cell line after 48 hrs.; 37 C°. 419
Table (4- 40): Cytotoxic potentials of copolymer(7) on skin cancer cell line vs normal cell line after 72 hrs.; 37 C°. 420
Table (4- 41): DPPH radical scavenging activity of copolymer(7) and copolymer(8), Vit-C. ...422
Table (4- 42): Cytotoxic potentials of copolymer(8) on skin cancer cell line vs normal cell line after 24 hrs.; 37 C°. 423
Table (4- 43): Cytotoxic potentials of copolymer(8) on skin cancer cell line vs normal cell line after 48 hrs.; 37 C°. 424
Table (4- 44): Cytotoxic potentials of copolymer(8) on skin cancer cell line vs normal cell line after 72 hrs.; 37 C°. 426
Table (4- 45): Cytotoxic potentials of copolymer(9) on skin cancer cell line vs normal cell line after 24 hrs.; 37 C°. 427
Table (4- 46): Cytotoxic potentials of copolymer(9) on skin cancer cell line vs normal cell line after 48 hrs.; 37 C° 429
Table (4- 47): Cytotoxic potentials of copolymer(9) on skin cancer cell line vs normal cell line after 72 hrs.; 37 C°. 430
Table (4- 48): DPPH radical scavenging activity of copolymer(9) and Vit-C. 432
Table (4- 49): Cytotoxic potentials of copolymer(10) on skin cancer cell line vs normal cell line after 24 hrs.; 37 C°. 433
Table (4- 50): Cytotoxic potentials of copolymer(10) on skin cancer cell line vs normal cell line after 48 hrs.; 37 C°. 434
Table (4- 51): Cytotoxic potentials of copolymer(10) on skin cancer cell line vs normal cell line after 72 hrs.; 37 C° 436

Table (4- 52): DPPH radical scavenging activity of copolymer(10) and Vit-C. 440
Table (4- 53): DPPH radical scavenging activity of vitamin-C. 440
Table (4- 54): Antibactrial activities of (copolymer1 and copolymer2) on both *Escherichia coli* and *Pseudomonas aeruginosa* 446
Table (4- 55): Antibacterial activities of (copolymer(3) and copolymer(4)) on both *Escherichia coli* and *Pseudomonas aeruginosa* 447
Table (4- 56): Antibacterial activities of (copolymer(5) and copolymer(6)) on both *Escherichia coli* and *Pseudomonas aeruginosa* 448
Table (4- 57): Antibacterial activities of (copolymer(7) and copolymer(8)) on both *Escherichia coli* and *Pseudomonas aeruginosa* 449
Table (4- 58): Antibacterial activities of (copolymer(9) and copolymer(10)) on both *Escherichia coli* and *Pseudomonas aeruginosa* 450
Table (4- 59): Antibacterial activities of (copolymer(1) and copolymer(2)) on both *Staphylococcus aureus* and *Enterococcus faecalis* 451
Table (4- 60): Antibacterial activities of (copolymer(3) and copolymer(4)) on both *Staphylococcus aureus* and *Enterococcus faecalis* 451
Table (4- 61): Antibacterial activities of (copolymer(5) and copolymer(6)) on both *Staphylococcus aureus* and *Enterococcus faecalis* 452
Table (4- 62): Antibacterial activities of (copolymer(7) and copolymer(7)) on both *Staphylococcus aureus* and *Enterococcus faecalis* 453
Table (4- 63): Antibacterial activities of (copolymer(9) and copolymer(10)) on both *Staphylococcus aureus* and *Enterococcus faecalis* 454
Table (4- 64): Antifungal activities of (copolymer(1) and copolymer(2)) on *Candida albicans* and *Aspergillus niger* 455
Table (4- 65): Antifungal activities of (copolymer(3) and copolymer(4)) on *Candida albicans* and *Aspergillus niger* 456
Table (4- 66): Anti Antifungal activities of (copolymer(5) and copolymer(6)) on *Candida albicans* 457
Table (4- 67): Anti Antifungal activities of (copolymer(7) and copolymer(8)) on *Candida albicans* and *Aspergillus niger* 458
Table (4- 68): Anti Antifungal activities of (copolymer(9) and copolymer(10)) on *Candida albicans* and *Aspergillus niger* 459

List of Figures

Figure (2- 1): Differences between heterocyclic and isocyclic compounds: (a) (4-dimethylaminophenyl) pentazole, an isocyclic compound; (b) Cyclopenta-1, 3-diene, isocyclic and carbocyclic compound; (c) Borazine, an inorganic heterocyclic compound; (d) Pyridine, an or organic heterocyclic aromatic compound. 8
Figure (2- 2): Common monocyclic compounds with trivial and systematic name. 11
Figure (2- 3): Common benzofused aromatic heterocycles. 12
Figure (2- 4): Representation of the pigments of life: Heme and Chlorophyll a. 13
Figure (2- 5): Vitamin C or ascorbic acid structure. 13
Figure (2- 6): Tryptophan structure. 14
Figure (2- 7): Some selected organometallic C-H functionalization of heterocycles. (a) Pd(II) catalyzed sequential C-H functionalization of oxazole. (b) Nickel catalyzed THF functionalization. (c) Organ magnesium metallation/functionalization of pyrimidine. 16
Figure (2- 8): Selected example of cyclization of acyclic reactant. (a) Prins Cyclization. (b) 1, 3-dipolar Cycloaddition (c) Cycloisomerization of functionalized allenes (d) Annulation of strained cyclopropanes.(e)Hantzsch cyclocondensation. 17
Figure (2- 9): DNA structure and its nitrogenous bases. 18
Figure (2- 10): Some important B vitamins. 20
Figure (2- 11): Structures of histidine and histamine. 20
Figure (2- 12): Examples of benzodiazepines. 21
Figure (2- 13): The abundance of five-membered heterocycles within top 200 drugs. 23
Figure (2- 14): Main benzofused aromatic heterocycles with more heteroatoms. 23
Figure (2- 15): Timolol chemical structure. 24
Figure (2- 16): X-ray co-crystal structures of timolol in the β-adrenergic receptor. 25
Figure (2- 17): Comparison between furazabol (a) and stanozolol (b) structures. 27
Figure (2- 18): 38
Figure (2- 19): 39
Figure (2- 20): Examples of natural pharmacologically active heterocyclic compounds. 43
Figure (2- 21): Some of the top brand name small molecules drugs. 44
Figure (2- 22): Some pyridine agrochemicals. 45
Figure (2- 34): Derivatives of pyrroles, furans, and thiophenes as agrochemicals. 45
Figure (2- 24): Examples of dyestuff containing heterocyclic structures. 46
Figure (2- 25): Examples of highly efficient organic light-emitting diodes (OLEDs) and novel electroluminescence mechanism using thermally activated delayed fluorescence (TADF). 46
Figure (2- 26): Flowchart of a usual clustering analysis for structure-based drug design 47
Figure (3- 1): structure of thiosemicarbazones of 2-(pyridin-2-ylmethylene)hydrazine-1-carbothioamide compound(1). 55
Figure (3- 2): structure of thiosemicarbazones of 2-(1-(4-aminophenyl) ethylidene) hydrazine-1-carbothioamide compound (2). 56
Figure (3- 3): structure of thiosemicarbazones of 2-(1-(4-nitrophenyl)ethylidene)hydrazine-1-carbothioamide compound(3). 56
Figure (3- 4): structure thiosemicarbazones of 2-(diphenylmethylene)hydrazine-1-carbothioamide

compound(4). 57
Figure (3- 5): structure of thiosemicarbazones of 2-(6-hydroxybenzylidene)hydrazine-1-carbothioamide compound(5). 57
Figure (3- 6): structure of 2-(thiophen-2-ylmethylene)hydrazine-1-carbothioamide compound(6) 58
Figure (3- 7): structure of 2-(furan-2-ylmethylene)hydrazine-1-carbothioamide thiosemicarbazon compound(7). 58
Figure (3- 8): structure of (Z)-2-(1-(thiophen-2-yl)ethylidene)hydrazine-1-carbothioamide thiosemicarbazone compound(8). 59
Figure (3- 9): structure of N, N-dimethyl amino benzaldeyde thiosemicarbazone compound(9).59
Figure (3- 10): structure of N-(Carboxymethyl) 2-(pyridin-2-ylmethylene)hydrazine-1-carbothioamide compound(10). 60
Figure (3- 11): structure of N-(Carboxymethyl) -4-Aminoacetophenone thiosemicarbazone compound(11) 60
Figure (3- 12): structure of N-(Carboxymethyl) 4-Nitroacetophenone thiosemicarbazone compound(12). 61
Figure (3- 13): structure of N-(Carboxymethyl) benzophenone thiosemicarbazone compound(13). 61
Figure (3- 14): structure of N-(Carboxymethyl) salicylaldehyde thiosemicarbazone compound(14). 62
Figure (3- 15): structure of 3-((thiophen-2-ylmethylene)amino)-2-thioxoimidazolidin-4-one compound(15). 62
Figure (3- 16): structure of 3-((furan-2-ylmethylene)amino) -2-thioxoimidazolidin-4-one compound(16). 63
Figure (3- 17): structure of (E)-3-((1-(thiophen-2-yl)ethylidene)amino)-2-thioxoimidazolidin-4-one compound(17)..... 63
Figure (3- 18): structure of N-(5-aminophthaloyl) thiosemicarbazide compound(18). 64
Figure (3- 19): structure of 5-amino-2-(2-aminophenyl)-2, 5-dihydro-1, 3, 4-thiadiazol-2-ol compound(19). 64
Figure (3- 20): structure of 5-amino-2-(5-amino-2-hydroxyphenyl)-2, 5-dihydro-1, 3, 4-thiadiazol-2 compound(20). 65
Figure (3- 21): structure of 3-amino-5-(5-(5-(1, 3-dioxo-1, 3-dihydroisobenzofuran-5-carbonyl)-3-methylene-1-oxoisoindolin-2-yl)-4, 5-dihydro-1, 3, 4-thiadiazol-2-yl)benzoic acid compound(21). 66
Figure (3- 22): structure of 2-(5-(2-aminophenyl)-1, 3, 4-thiadiazol-2-yl)-1, 3-dioxoisoindoline-5-carboxylic acid compound(22). 66
Figure (3- 23): structure of 2-(5-(5-amino-2-hydroxyphenyl)-1, 3, 4-thiadiazol-2-yl)-5-(1, 3-dioxo-1, 3-dihydroisobenzofuran-5-yl)isoindoline-1, 3-dione compound(23). 67
Figure (3- 24): structure of 1-(8-(1, 3-dioxo-1, 3-dihydroisobenzofuran-5-carbonyl)-1, 5-dioxo-3-(pyridin-2-yl)-1, 5-dihydrobenzo[e][1, 3]oxazepin-4(3H)-yl)urea compound(24)..... 68
Figure (3- 25): structure of 3-(4-aminophenyl)-3-methyl-1, 5-dioxo-4-thioureido-1, 3, 4, 5-tetrahydrobenzo[e][1, 3]oxazepine-8-carboxylic acid compound(25). 68
Figure (3- 26): structure of 1-(3-(3-(dimethylamino)phenyl)-1, 5-dioxo-9-(4-(3-

oxobutanoyl)phenyl)-1, 5-dihydrobenzo[e][1, 3]oxazepin-4(3H)-yl)urea compound(26). 69
Figure (3- 27): structure of (5-mercapto-1, 3, 4-thiadiazol-2-yl) glycinoyl chloridecompound(27). 70
Figure (3- 28): structure of N-carbamoyl-2-((5-mercapto-1, 3, 4-thiadiazol-2 yl)amino)acetamide compound(28). 70
Figure (3- 29): structure of 1-(4-oxo-2-(thiophen-2-yl)-1, 4-dihydroquinazolin-3(2H)-yl)thiourea compound(29). 71
Figure (3- 30): structure 1-(2-(furan-2-yl)-4-oxo-1, 4-dihydroquinazolin-3(2H)-yl)thiourea compound(30). 71
Figure (3- 31): structure of (Z)-N-(3-amino-2-formylphenyl)-2-(1-(thiophen-2-yl)ethylidene)hydrazine-1-carbothioamide compound(31).....72
Figure (3- 32): structure of 1, 1'-(1, 4-phenylenebis(methaneylylidene))bis(thiourea) compound(32). 72
Figure (3- 33): structure of 1, 1'-(1, 4-phenylenebis(4, 5-dihydro-1H-tetrazole-5, 1-diyl))bis(thiourea) compound(33). 73
Figure (3- 34): structure of 2, 2'-((Z)-indoline-2, 3-diylidene)bis(hydrazine-1-carbothioamide) compound(34). 73
Figure (3- 35): structure of 1, 1'-(dispiro[tetrazole-5, 2'-indoline-3', 5''-tetrazol]-1, 1''(4H, 4''H)-diyl)bis(thiourea) compound(35). 74
Figure (3- 36): structure of 2-iminothiazolidin-4-one compound(36). 75
Figure (3- 37): structure of 3-((3-(4-aminophenoxy)phenyl)amino)-3, 4-dihydro-2H-thiazolo[3, 2-a][1, 3, 5]triazin-6(7H)-one compound(37). 75
Figure (3- 38): structure of 3-((4-aminophenyl)amino)-3, 4-dihydro-2H-thiazolo[3, 2-a][1, 3, 5]triazin-6(7H)-one compound(38).....76
Figure (3- 39): structure of 3-((2-((2-((2-minoethyl)amino)ethyl)amino) ethyl)amino)-3, 4-dihydro-2H-thiazolo[3, 2-a][1, 3, 5]triazin-6(7H)-one compound(39).....76
Figure (3- 40): structure of 3-((6-aminopyridin-2-yl)amino)-3, 4-dihydro-2H-thiazolo[3, 2-a][1, 3, 5]triazin-6(7H)-onecompound(40).....77
Figure (3- 41): structure of copolymer (MAA-CO-IAN) 78
Figure (3- 42): structure of copolymer (DMA-CO-CAN). 78
Figure (3- 43): structure copolymer(1) (MAA-Co-IAN) with compound(1). 79
Figure (3- 44): structure of copolymer(2) (MAA-Co-IAN) with compound(2). 79
Figure (3- 45): structure of copolymer(3) (MAA-Co-IAN) with compound(3). 79
Figure (3- 46): structure of copolymer(4) (MAA-Co-IAN) with compound(4). 80
Figure (3- 47): structure of copolymer(5) (MAA-Co-IAN) with compound(5). 80
Figure (3- 48): structure of copolymer(6) (MAA-Co-IAN) with compound(6). 80
Figure (3- 49): structure of copolymer (7) (MAA-Co-IAN) with compound (7). 81
Figure (3- 50): structure of copolymer(8) (MAA-Co-IAN) with compound(8). 81
Figure (3- 51): structure of copolymer(9) (MAA-Co-IAN) with compound(9). 81
Figure (3- 52): structure of copolymer(10) (MAA-CO-IAN) with compound(10). 82
Figure (3- 53): structure of copolymer(11) (MAA-CO-IAN) with compound(11). 82
Figure (3- 54): structure of copolymer(12) (MAA-CO-IAN) with compound(12). 83
Figure (3- 55): structure of copolymer(13) (MAA-CO-IAN) with compound(13). 83

Figure (3- 56): structure of copolymer(14) (MAA-CO-IAN) with compound(14). 83
Figure (3- 57): structure of copolymer(15) (MAA-CO-IAN) with compound(15). 84
Figure (3- 58): structure of copolymer(16) (MAA-CO-IAN) with compound(16). 84
Figure (3- 59): *structure* of copolymer(17) (MAA-CO-IAN) with compound(17). 84
Figure (3- 60): structure of copolymer(18) (MAA-CO-IAN) with compound(18). 85
Figure (3- 61): structure of copolymer(19) (MAA-CO-IAN) with compound(9). 85
Figure (3- 62): structure of copolymer(20) (MAA-CO-IAN) with compound(20). 86
Figure (3- 63): structure of copolymer(21) (MAA-CO-IAN) with compound(21) 86
Figure (3- 64): structure of copolymer(22) (MAA-CO-IAN) with compound(22) 86
Figure (3- 65): structure of copolymer(23) (MAA-CO-IAN) with compound(23) 87
Figure (3- 66): structure of copolymer(24) (MAA-CO-IAN) with compound (24). (Compound28) 87
Figure (3- 67): structure of copolymer(25) (MAA-CO-IAN) with compound (25). 88
Figure (3- 68): structure of copolymer(1) (MAA-CO-IAN) with compound (26). 88
Figure (3- 69): structure of copolymer(27) (MAA-CO-IAN) with compound (27). 89
Figure (3- 70): structure of copolymer(1) (MAA-CO-IAN) with compound (28). 89
Figure (3- 71): structure of copolymer(29) (MAA-CO-IAN) with compound (29). 90
Figure (3- 72): structure of copolymer(30) (MAA-CO-IAN) with compound (30). 90
Figure (3- 73): structure of copolymer(31) (MAA-CO-IAN) with compound (31). 90
Figure (3- 74): structure of copolymer(32) (MAA-CO-IAN) with compound (32). 91
Figure (3- 75): structure of copolymer(33) (MAA-CO-IAN) with compound (33). 91
Figure (3- 76): structure of copolymer(34) (MAA-CO-IAN) with compound (34). 92
Figure (3- 77): structure of copolymer(35) (MAA-CO-IAN) with compound (35). 92
Figure (3- 78): structure of copolymer(36) (MAA-CO-IAN) with compound (36). 93
Figure (3- 79): structure of copolymer(37) (MAA-CO-IAN) with compound(37). 93
Figure (3- 80): structure of copolymer(38) (MAA-CO-IAN) with compound(38). 94
Figure (3- 81): structure of copolymer(39) (MAA-CO-IAN) with compound(39). 94
Figure (3- 82): structure of copolymer(40) (MAA-CO-IAN) with compound(40). 94
Figure (3- 83): structure of copolymer(41) (MAA-CO-IAN) with compound(3). 95
Figure (3- 84): structure of copolymer(42) (DMA-CO-CAN) with compound(13). 95
Figure (3- 85): structure of copolymer(43) (DMA-CO-CAN) with compound(14). 96
Figure (3- 86): structure of copolymer(44) (DMA-CO-CAN) with compound(16). 96
Figure (3- 87): structure of copolymer(45) (DMA-CO-CAN) with compound(17). 96
Figure (3- 88): structure of copolymer(46) (DMA-CO-CAN) with compound(18). 97
Figure (3- 89): structure of copolymer(47) (DMA-CO-CAN) with compound(19). 97
Figure (3- 90): structure of copolymer(48) (DMA-CO-CAN) with compound(20). (Compound53) 97
Figure (3- 91): structure of copolymer(49) (DMA-CO-CAN) with compound(24). 98
Figure (3- 92): structure of copolymer(50) (DMA-CO-CAN) with compound(25). 98
Figure (3- 93): structure of copolymer(51) (DMA-CO-CAN) with compound(28). 99
Figure (3- 94): structure of copolymer(52) (DMA-CO-CAN) with compound(31). 99
Figure (3- 95): structure of copolymer(53) (DMA-CO-CAN) with compound (34). 100
Figure (3- 96): structure of copolymer(54) (DMA-CO-CAN) with compound(35). 100

Figure (3- 97): structure of copolymer(55) (DMA-CO-CAN) with compound(37). 101
Figure (3- 98): structure of copolymer(56) (DMA-CO-CAN) with compound(38). 101
Figure (3- 99): structure of copolymer(57) (DMA-CO-CAN) with compound(39). 101
Figure (3- 100): structure of copolymer(58) (DMA-CO-CAN) with compound(40). 102
Figure (3- 101): Schematic representation of the docking procedure, analysis of ligands and reactivity 104
Figure (4- 1): FTIR Spectrum of 2-(pyridin-2-ylmethylene)hydrazine-1- carbothioamide compound(1). 115
Figure (4- 2): ^{1}HNMR Spectrum of 2-(pyridin-2-ylmethylene)hydrazine-1- carbothioamide compound(1). 115
Figure (4- 3): ^{13}C-NMR Spectrum of 2-(pyridin-2-ylmethylene)hydrazine-1- carbothioamide. (Compound1) 116
Figure (4- 4): FTIR Spectrum of 2-(1-aminophenyl)ethylidene)hydrazine-1-carbothioamide compound(2). 117
Figure (4- 5): ^{1}HNMR Spectrum of 2-(pyridin-2-ylmethylene)hydrazine-1- carbothioamide compound(2). 117
Figure (4- 6): ^{13}C-NMR Spectrum of 2-(pyridin-2-ylmethylene)hydrazine-1- carbothioamide compound(2). 118
Figure (4- 7): FTIR Spectrum of(4-nitrophenyl)ethylidene)hydrazine-1-carbothioamide compound(3). 119
Figure (4- 8): ^{1}HNMR Spectrum of(4-nitrophenyl)ethylidene)hydrazine-1-carbothioamide compound(3). 119
Figure (4- 9): ^{13} CNMR Spectrum of(4-nitrophenyl)ethylidene)hydrazine-1-carbothioamide compound(3). 120
Figure (4- 10): FTIR Spectrum of 2-(diphenylmethylene)hydrazine-1-carbothioamide compound(4). 121
Figure (4- 11): ^{1}HNMR Spectrum of 2-(diphenylmethylene)hydrazine-1-carbothioamide compound(4). 121
Figure (4- 12): ^{13} CNMR Spectrum of 2-(diphenylmethylene)hydrazine-1-carbothioamide compound(4). 122
Figure (4- 13): FTIR Spectrum of 2-(2-hydroxybenzylidene)hydrazine-1-carbothioamide compound(5). 123
Figure (4- 14): ^{1}HNMR Spectrum of 2-(2-hydroxybenzylidene)hydrazine-1-carbothioamide compound(5). 123
Figure (4- 15): ^{13} CNMR Spectrum of 2-(2-hydroxybenzylidene)hydrazine-1-carbothioamide compound(5). 124
Figure (4- 16): FTIR Spectrum 2-(thiophen-2-ylmethylene)hydrazine-1-carbothioamide thiosemicarbazon compound(6). 125
Figure (4- 17):) ^{1}HNMR Spectrum 2-(thiophen-2-ylmethylene)hydrazine-1-carbothioamide thiosemicarbazon compound(6). 125
Figure (4- 18): ^{13} CNMR Spectrum 2-(thiophen-2-ylmethylene)hydrazine-1-carbothioamide thiosemicarbazon compound(6). 126
Figure (4- 19): FTIR spectrum of 2-(furan-2-ylmethylene)hydrazine-1-carbothioamide

thiosemicarbazon compound(7). 126
Figure (4- 20): ^{1}HNMR Spectrum of 2-(furan-2-ylmethylene)hydrazine-1-carbothioamide thiosemicarbazon compound(7). 127
Figure (4- 21): ^{13} CNMR Spectrum of 2-(furan-2-ylmethylene)hydrazine-1-carbothioamide thiosemicarbazon compound(7). 127
Figure (4- 22): FTIR spectrum of (Z)-2-(1-(thiophen-2-yl)ethylidene)hydrazine-1-carbothioamide thiosemicarbazone compound(8). 128
Figure (4- 23): ^{1}HNMR spectrum of (Z)-2-(1-(thiophen-2-yl)ethylidene)hydrazine-1-carbothioamide thiosemicarbazone compound(8). 129
Figure (4- 24): ^{13}C-NMR spectrum of (Z)-2-(1-(thiophen-2-yl)ethylidene)hydrazine-1-carbothioamide thiosemicarbazone compound(8). 130
Figure (4- 25): FTIR spectrum of Thiosemicarbazones for N, N-dimethyaminebenzaldehyde compound(9). 131
Figure (4- 26): ^{1}HNMR spectrum of Thiosemicarbazones for N, N-dimethyaminebenzaldehyde compound(9). 131
Figure (4- 27): ^{13}C-NMR spectrum of Thiosemicarbazones for N, N-dimethyaminebenzaldehyde compound(9). 132
Figure (4- 28): mechanism2-thioxoimidazolidin-4-one compounds 132
Figure (4- 29): FTIR spectrum of (Z)-3-((pyridin-2-ylmethylene)amino)-2-thioxoimidazolidin-4-one compound(10). 133
Figure (4- 30): ^{1}HNMR spectrum of (Z)-3-((pyridin-2-ylmethylene)amino)-2-thioxoimidazolidin-4-one compound(10). 134
Figure (4- 31): ^{13}C-NMR spectrum of (Z)-3-((pyridin-2-ylmethylene)amino)-2-thioxoimidazolidin-4-one compound(10). 134
Figure (4- 32): FTIR spectrum of (E)-3-((1-(2-aminophenyl)ethylidene)amino)-2-thioxoimidazolidin-4-one compound(11). 135
Figure (4- 33): ^{1}HNMR spectrum of (E)-3-((1-(2-aminophenyl)ethylidene)amino)-2-thioxoimidazolidin-4-one compound(11). 136
Figure (4- 34): ^{13}C-NMR spectrum of (E)-3-((1-(2-aminophenyl)ethylidene)amino)-2-thioxoimidazolidin-4-one compound(11). 137
Figure (4- 35): FTIR spectrum of (E)-3-((1-(4-nitrophenyl)ethylidene)amino)-2-thioxoimidazolidin-4-one compound(12). 138
Figure (4- 36): ^{1}HNMR spectrum of (E)-3-((1-(4-nitrophenyl)ethylidene)amino)-2-thioxoimidazolidin-4-one compound(12). 138
Figure (4- 37): ^{13}C-NMR spectrum of (E)-3-((1-(4-nitrophenyl)ethylidene)amino)-2-thioxoimidazolidin-4-one compound(12). 139
Figure (4- 38): FTIR spectrum of (Z)-3-((cyclohexa-2, 4-dien-1-yl(phenyl)methylene)amino)-2-thioxoimidazolidin-4-one compound(13). 140
Figure (4- 39): ^{1}HNMR spectrum of (Z)-3-((cyclohexa-2, 4-dien-1-yl(phenyl) methylene) amino)-2-thioxoimidazolidin-4-one compound(13). 140
Figure (4- 40): ^{13}C-NMR spectrum of (Z)-3-((cyclohexa-2, 4-dien-1-yl(phenyl)methylene)amino)-2-thioxoimidazolidin-4-one compound(13). 141
Figure (4- 41): FTIR spectrum of (E)-3-((1-(2-hydroxyphenyl)ethylidene)amino)-2-

thioxoimidazolidin-4-one compound(14). 142
Figure (4- 42): ^{1}HNMR spectrum of (E)-3-((1-(2-hydroxyphenyl)ethylidene)amino)-2-thioxoimidazolidin-4-one compound(14). 142
Figure (4- 43): ^{13}C-NMR spectrum of (E)-3-((1-(2-hydroxyphenyl)ethylidene)amino)-2-thioxoimidazolidin-4-one compound(14). 143
Figure (4- 44): FTIR spectrum of of 3-((thiophen-2-ylmethylene)amino)-2-thioxoimidazolidin-4-one compound(15). 144
Figure (4- 45): ^{1}HNMR spectrum of 3-((thiophen-2-ylmethylene)amino)-2-thioxoimidazolidin-4-one compound(15). 144
Figure (4- 46): ^{13}C-NMR spectrum of 3-((thiophen-2-ylmethylene)amino)-2-thioxoimidazolidin-4-one compound(15). 145
Figure (4- 47): FTIR spectrum of 3-((furan-2-ylmethylene)amino)-2-thioxoimidazolidin-4-one compound(16). 146
Figure (4- 48): ^{1}HNMR spectrum of 3-((furan-2-ylmethylene)amino)-2-thioxoimidazolidin-4-one compound(16). 146
Figure (4- 49): ^{13}C-NMR spectrum of3-((furan-2-ylmethylene)amino)-2-thioxoimidazolidin-4-one compound(16). 147
Figure (4- 50): FTIR spectrum of (E)-3-((1-(thiophen-2-yl)ethylidene)amino)-2-thioxoimidazolidin-4-one compound(17). 148
Figure (4- 51): ^{1}HNMR spectrum of (E)-3-((1-(thiophen-2-yl)ethylidene)amino)-2-thioxoimidazolidin-4-one compound(17). 148
Figure (4- 52): ^{13}C-NMR spectrum of (E)-3-((1-(thiophen-2-yl)ethylidene)amino)-2-thioxoimidazolidin-4-one compound(17). 149
Figure (4- 53): FTIR structure of synthesis of N-(5-aminophthaloyl) thiosemicarbazide compound(18). 150
Figure (4- 54): ^{1}HNMR structure of synthesis of N-(5-aminophthaloyl) thiosemicarbazide compound(18). 150
Figure (4-55): ^{13}C-NMR structure of synthesis of N-(5-aminophthaloyl) thiosemicarbazide compound(18). 151
Figure (4- 56): FTIR structure of 5-styryl-2-amino -1, 3, 4-thiadiazole compound for anthranilic acid compound(19). 152
Figure (4- 57): ^{1}HNMR structure of 5-styryl-2-amino -1, 3, 4-thiadiazole compound for anthranilic acid compound(19). 152
Figure (4- 58): ^{13}C-NMR structure of 5-styryl-2-amino -1, 3, 4-thiadiazole compound for anthranilic acid compound(19). 153
Figure (4- 59): FTIR structure of 5-styryl-2-amino -1, 3, 4-thiadiazole compound for 5-amino -2-hydroxybenzoic acid compound(20). 154
Figure (4- 60): ^{1}HNMR structure of 5-styryl-2-amino -1, 3, 4-thiadiazole compound for 5-amino -2-hydroxybenzoic acid compound(20). 154
Figure (4- 61): ^{13}C-NMR structure of 5-styryl-2-amino -1, 3, 4-thiadiazole compound for 5-amino -2-hydroxybenzoic acid compound(20). 155
Figure (4- 62): FTIR structure of 3-amino-5-(5-(5-(1, 3-dioxo-1, 3-dihydroisobenzofuran-5-carbonyl)-3-methylene-1-oxoisoindolin-2-yl)-4, 5-dihydro-1, 3, 4-thiadiazol-2-yl)benzoic acid

compound(21). 156
Figure (4- 63): ^{1}HNMR spectrum of 3-amino-5-(5-(5-(1, 3-dioxo-1, 3-dihydroisobenzofuran-5-carbonyl)-3-methylene-1-oxoisoindolin-2-yl)-4, 5-dihydro-1, 3, 4-thiadiazol-2-yl)benzoic acid compound(21). 157
Figure (4- 64): ^{13}C-NMR spectrum of 3-amino-5-(5-(5-(1, 3-dioxo-1, 3-dihydroisobenzofuran-5-carbonyl)-3-methylene-1-oxoisoindolin-2-yl)-4, 5-dihydro-1, 3, 4-thiadiazol-2-yl)benzoic acid compound(21). 157
Figure (4- 65): FTIR spectrum of 5-(2-(5-(2-aminophenyl)-5-hydroxy-2, 5-dihydro-1, 3, 4-thiadiazol-2-yl)-3-methylene-1-oxoisoindoline-5-carbonyl)isobenzofuran-1, 3-dione compound(22). 158
Figure (4- 66): ^{1}HNMR spectrum of 5-(2-(5-(2-aminophenyl)-5-hydroxy-2, 5-dihydro-1, 3, 4-thiadiazol-2-yl)-3-methylene-1-oxoisoindoline-5-carbonyl)isobenzofuran-1, 3-dione compound(22). 159
Figure (4- 67): ^{13}C-NMR spectrum of 5-(2-(5-(2-aminophenyl)-5-hydroxy-2, 5-dihydro-1, 3, 4-thiadiazol-2-yl)-3-methylene-1-oxoisoindoline-5-carbonyl)isobenzofuran-1, 3-dione compound(22). 159
Figure (4- 68): FTIR spectrum of 2-(5-(5-amino-2-hydroxyphenyl)-5-hydroxy-2, 5-dihydro-1, 3, 4-thiadiazol-2-yl)-5-(1, 3-dioxo-1, 3-dihydroisobenzofuran-5-carbonyl)isoindoline-1, 3-dione compound(23). 160
Figure (4- 69): ^{1}HNMR spectrum of 2-(5-(5-amino-2-hydroxyphenyl)-5-hydroxy-2, 5-dihydro-1, 3, 4-thiadiazol-2-yl)-5-(1, 3-dioxo-1, 3-dihydroisobenzofuran-5-carbonyl)isoindoline-1, 3-dione compound(23). 161
Figure (4- 70): ^{13}C-NMR spectrum of 2-(5-(5-amino-2-hydroxyphenyl)-5-hydroxy-2, 5-dihydro-1, 3, 4-thiadiazol-2-yl)-5-(1, 3-dioxo-1, 3-dihydroisobenzofuran-5-carbonyl)isoindoline-1, 3-dione compound(23). 162
Figure (4- 71): FTIR spectrum of 2-(5-(5-amino-2-hydroxyphenyl)-5-hydroxy-2, 5-dihydro-1, 3, 4-thiadiazol-2-yl)-5-(1, 3-dioxo-1, 3-dihydroisobenzofuran-5-carbonyl)isoindoline-1, 3-dione compound(24). 163
Figure (4- 72): ^{1}HNMR spectrum of 2-(5-(5-amino-2-hydroxyphenyl)-5-hydroxy-2, 5-dihydro-1, 3, 4-thiadiazol-2-yl)-5-(1, 3-dioxo-1, 3-dihydroisobenzofuran-5-carbonyl)isoindoline-1, 3-dione compound(24). 164
Figure (4- 73): ^{13}C-NMR spectrum of 2-(5-(5-amino-2-hydroxyphenyl)-5-hydroxy-2, 5-dihydro-1, 3, 4-thiadiazol-2-yl)-5-(1, 3-dioxo-1, 3-dihydroisobenzofuran-5-carbonyl)isoindoline-1, 3-dione compound(24). 164
Figure (4- 74): FTIR spectrum of 2-(5-(5-amino-2-hydroxyphenyl)-5-hydroxy-2, 5-dihydro-1, 3, 4-thiadiazol-2-yl)-5-(1, 3-dioxo-1, 3-dihydroisobenzofuran-5-carbonyl)isoindoline-1, 3-dione compound(25). 165
Figure (4- 75): ^{1}HNMR spectrum of 2-(5-(5-amino-2-hydroxyphenyl)-5-hydroxy-2, 5-dihydro-1, 3, 4-thiadiazol-2-yl)-5-(1, 3-dioxo-1, 3-dihydroisobenzofuran-5-carbonyl)isoindoline-1, 3-dione compound(25). 166
Figure (4- 76): ^{13}C-NMR spectrum of 2-(5-(5-amino-2-hydroxyphenyl)-5-hydroxy-2, 5-dihydro-1, 3, 4-thiadiazol-2-yl)-5-(1, 3-dioxo-1, 3-dihydroisobenzofuran-5-carbonyl)isoindoline-1, 3-dione compound(25). 167

Figure (4- 77): FTIR spectrum of 1-(3-(3-(dimethylamino)phenyl)-1, 5-dioxo-9-(4-(3-oxobutanoyl)phenyl)-1, 5-dihydrobenzo[e][1, 3]oxazepin-4(3H)-yl)urea compound(26). 168
Figure (4- 78): ^{1}HNMR spectrum of 1-(3-(3-(dimethylamino)phenyl)-1, 5-dioxo-9-(4-(3-oxobutanoyl)phenyl)-1, 5-dihydrobenzo[e][1, 3]oxazepin-4(3H)-yl)urea compound(26). 168
Figure (4- 79): ^{13}C-NMR spectrum of 1-(3-(3-(dimethylamino)phenyl)-1, 5-dioxo-9-(4-(3-oxobutanoyl)phenyl)-1, 5-dihydrobenzo[e][1, 3]oxazepin-4(3H)-yl)urea compound(26). 169
Figure (4- 80): FTIR spectrum of (5-mercapto-1, 3, 4-thiadiazol-2-yl)glycinoyl chloride compound(27). 170
Figure (4- 81): ^{13}C-NMR spectrum of (5-mercapto-1, 3, 4-thiadiazol-2-yl)glycinoyl chloride compound(27). 171
Figure (4- 82): ^{13}C-NMR spectrum of (5-mercapto-1, 3, 4-thiadiazol-2-yl)glycinoyl chloride compound(27). 171
Figure (4- 83): FTIR spectrum of N-(5-mercapto-1, 3, 4-thiadiazole-2-yl)-2-ureidoacetamide compound(28). 172
Figure (4- 84): ^{1}HNMR spectrum of N-(5-mercapto-1, 3, 4-thiadiazole-2-yl)-2-ureidoacetamide compound(28). 173
Figure (4- 85): ^{13}C-NMR spectrum of N-(5-mercapto-1, 3, 4-thiadiazole-2-yl)-2-ureidoacetamide compound(28). 174
Figure (4- 86): FTIR spectrum of 1-(4-oxo-2-(thiophen-2-yl)-1, 4-dihydroquinazolin-3(2H)-yl)thiourea compound(29). 175
Figure (4- 87): ^{1}HNMR spectrum of 1-(4-oxo-2-(thiophen-2-yl)-1, 4-dihydroquinazolin-3(2H)-yl)thiourea compound(29). 176
Figure (4- 88): ^{13}C-NMR spectrum of 1-(4-oxo-2-(thiophen-2-yl)-1, 4-dihydroquinazolin-3(2H)-yl)thiourea compound(29). 176
Figure (4- 89): FTIR spectrum of 1-(2-(furan-2-yl)-4-oxo-1, 4-dihydroquinazolin-3(2H)-yl)thiourea compound(30). 177
Figure (4- 90): ^{1}HNMR spectrum of 1-(2-(furan-2-yl)-4-oxo-1, 4-dihydroquinazolin-3(2H)-yl) thiourea compound(30). 178
Figure (4- 91): ^{13}C-NMR spectrum of 1-(2-(furan-2-yl)-4-oxo-1, 4-dihydroquinazolin-3(2H)-yl)thiourea compound(30). 179
Figure (4- 92): ^{13}C-NMR spectrum of 1-(4-oxo-2-(thiophen-2-yl)-1, 4-dihydroquinazolin-3(2H)-yl)thiourea compound(31). 180
Figure (4- 93): ^{13}C-NMR spectrum of 1-(4-oxo-2-(thiophen-2-yl)-1, 4-dihydroquinazolin-3(2H)-yl)thiourea compound(31). 180
Figure (4- 94): ^{13}C-NMR spectrum of (Z)-N-(3-amino-2-formylphenyl)-2-(1-(thiophen-2-yl)ethylidene)hydrazine-1-carbothioamide compound(31). 181
Figure (4- 95): FTIR spectrum of 1, 1'-(1, 4-phenylenebis(methaneylylidene))bis(thiourea) compound(32). 182
Figure (4- 96): ^{1}HNMR spectrum of 1, 1'-(1, 4-phenylenebis(methaneylylidene))bis(thiourea) compound(32). 183
Figure (4- 97): ^{13}C-NMR spectrum of 1, 1'-(1, 4-phenylenebis(methaneylylidene)) bis(thiourea) compound(32). 183
Figure (4- 98): FTIR spectrum of 1, 1'-(1, 4-phenylenebis(4, 5-dihydro-1H-tetrazole-5, 1-

diyl))bis(thiourea) compound(33). 184
Figure (4- 99): ^{1}HNMR spectrum of 1, 1'-(1, 4-phenylenebis(4, 5-dihydro-1H-tetrazole-5, 1-diyl))bis(thiourea) compound(33). 185
Figure (4- 100): ^{13}C-NMR spectrum of 1, 1'-(1, 4-phenylenebis(4, 5-dihydro-1H-tetrazole-5, 1-diyl))bis(thiourea) compound(33). 186
Figure (4- 101): FTIR spectrum of 2, 2'-((Z)-indoline-2, 3-diylidene)bis(hydrazine-1-carbothioamide) compound(34). 187
Figure (4- 102): ^{1}HNMR spectrum of 2, 2'-((Z)-indoline-2, 3-diylidene)bis(hydrazine-1-carbothioamide) compound(34). 187
Figure (4- 103): ^{13}C-NMR spectrum of 2, 2'-((Z)-indoline-2, 3-diylidene)bis(hydrazine-1-carbothioamide) compound(34). 188
Figure (4- 104): FTIR spectrum of synthesis of 1, 1'-(dispiro[tetrazole-5, 2'-indoline-3', 5''-tetrazol]-1, 1''(4H, 4''H)-diyl)bis(thiourea) compound(35). 189
Figure (4- 105): ^{1}HNMR spectrum of synthesis of 1, 1'-(dispiro[tetrazole-5, 2'-indoline-3', 5''-tetrazol]-1, 1''(4H, 4''H)-diyl)bis(thiourea) compound(35). 189
Figure (4- 106): ^{1}HNMR spectrum of synthesis of 1, 1'-(dispiro[tetrazole-5, 2'-indoline-3', 5''-tetrazol]-1, 1''(4H, 4''H)-diyl)bis(thiourea) compound(35). 190
Figure (4- 107): ^{13}C-NMR spectrum of 2-iminothiazolidin-4-one compound(36). 191
Figure (4- 108): ^{13}C-NMR spectrum of 2-iminothiazolidin-4-one compound(36). 191
Figure (4- 109): ^{13}C-NMR spectrum of 2-iminothiazolidin-4-one compound(36). 192
Figure (4- 110): FTIR spectrum of 3-((3-(4-aminophenoxy)phenyl)amino)-3, 4-dihydro-2H-thiazolo[3, 2-a][1, 3, 5]triazin-6(7H)-one compound(37). 193
Figure (4- 111): ^{1}HNMR spectrum of 3-((3-(4-aminophenoxy)phenyl)amino)-3, 4-dihydro-2H-thiazolo[3, 2-a][1, 3, 5]triazin-6(7H)-one compound(37). 193
Figure (4- 112): ^{13}C-NMR spectrum of 3-((3-(4-aminophenoxy)phenyl)amino)-3, 4-dihydro-2H-thiazolo[3, 2-a][1, 3, 5]triazin-6(7H)-one compound(37). 194
Figure (4- 113): FTIR spectrum of 3-((4-aminophenyl)amino)-3, 4-dihydro-2H-thiazolo[3, 2-a][1, 3, 5]triazin-6(7H)-one compound(38). 195
Figure (4- 114):^{1}HNMR spectrum of 3-((4-aminophenyl)amino)-3, 4-dihydro-2H-thiazolo[3, 2-a][1, 3, 5]triazin-6(7H)-one compound(38). 195
Figure (4- 115):^{13}C-NMR spectrum of 3-((4-aminophenyl)amino)-3, 4-dihydr-2H-thiazolo[3, 2-a][1, 3, 5]triazin-6(7H)-one compound(38). 196
Figure (4- 116):FTIR spectrum of 3-((2-((2-((2-minoethyl)amino)ethyl)amino) ethyl)amino)-3, 4-dihydro-2H-thiazolo[3, 2-a][1, 3, 5]triazin-6(7H)-one compound(39). 197
Figure (4- 117): ^{1}HNMR spectrum of 3-((2-((2-((2-minoethyl)amino)ethyl)amino) ethyl)amino)-3, 4-dihydro-2H-thiazolo[3, 2-a][1, 3, 5]triazin-6(7H)-one compound(39). 198
Figure (4- 118):^{13}C-NMR spectrum of 3-((2-((2-((2-minoethyl)amino)ethyl)amino) ethyl)amino)-3, 4-dihydro-2H-thiazolo[3, 2-a][1, 3, 5]triazin-6(7H)-one compound(39). 198
Figure (4- 119):FTIR spectrum of 3-((6-aminopyridin-2-yl)amino)-3, 4-dihydro-2H-thiazolo[3, 2-a][1, 3, 5]triazin-6(7H)-one compound(40). 199
Figure (4- 120):^{1}HNMR spectrum of 3-((6-aminopyridin-2-yl)amino)-3, 4-dihydro-2H-thiazolo[3, 2-a][1, 3, 5]triazin-6(7H)-one compound(40). 200
Figure (4- 121):^{13}C-NMR spectrum of 3-((6-aminopyridin-2-yl)amino)-3, 4-dihydro-2H-

thiazolo[3, 2-a][1, 3, 5]triazin-6(7H)-one compound(40). 200
Figure (4- 122): FTIR spectrum of synthesis of copolymer (methyl acrylic acid-co - Itaconic anhydride) (MAA-CO-IAN). 201
Figure (4- 123):1HNMR spectrum of synthesis of copolymer (methyl acrylic acid-co - Itaconic anhydride) (MAA-CO-IAN). 202
Figure (4- 124): ^{13}C-NMR spectrum of synthesis of copolymer (methyl acrylic acid-co - Itaconic anhydride) (MAA-CO-IAN). 202
Figure (4- 125):FTIR spectrum of copolymer (N, N-dimethylacrylamide-Citraconic anhydride) 203
Figure (4- 126):^{1}HNMR spectrum of copolymer (N, N-dimethylacrylamide-Citraconic anhydride). 204
Figure (4- 127):^{13}C-NMR spectrum of copolymer (N, N-dimethylacrylamide-Citraconic anhydride)..... 204
Figure (4- 128): structure copolymer(1) (MAA-Co-IAN) with compound(1). 206
Figure (4- 129):structure copolymer(1) (MAA-Co-IAN) with compound(1). 206
Figure (4- 130):structure copolymer(1) (MAA-Co-IAN) with compound(1). 207
Figure (4- 131):FTIR spectrum of syntheses of copolymer(2) (MAA-Co-IAN) with compound(2). 208
Figure (4- 132):^{1}HNMR spectrum of syntheses of copolymer(2) (MAA-Co-IAN) with compound(2). 208
Figure (4- 133):^{13}C-NMR spectrum of syntheses of copolymer(2) (MAA-Co-IAN) with compound(2). 209
Figure (4- 134): FTIR spectrum of copolymer(3) (MAA-Co-IAN) with compound(3). 210
Figure (4- 135): ^{1}HNMR spectrum of copolymer(3) (MAA-Co-IAN) with compound(3). 210
Figure (4- 136): ^{13}C-NMR spectrum of copolymer(3) (MAA-Co-IAN) with compound(3). 211
Figure (4- 137): FTIR spectrum of copolymer(4) (MAA-Co-IAN) with compound(4). 212
Figure (4- 138): ^{1}HNMR spectrum of copolymer(4) (MAA-Co-IAN) with compound(4). 212
Figure (4- 139): ^{13}C-NMR spectrum of copolymer(4) (MAA-Co-IAN) with compound(4). 213
Figure (4- 140): FTIR spectrum of copolymer (5) (MAA-Co-IAN) with compound(5). 214
Figure (4- 141): ^{1}HNMR spectrum of copolymer (5) (MAA-Co-IAN) with compound(5). 214
Figure (4- 142): ^{13}C-NMR spectrum of copolymer (5) (MAA-Co-IAN) with compound(5). 215
Figure (4- 143): FTIR spectrum of copolymer (6) (MAA-Co-IAN) with compound(6). 216
Figure (4- 144): 1HNMR spectrum of copolymer (6) (MAA-Co-IAN) with compound(6). 216
Figure (4- 145): ^{13}C-NMR spectrum of copolymer (6) (MAA-Co-IAN) with compound(6). 217
Figure (4- 146): FTIR spectrum of copolymer (7) (MAA-Co-IAN) with compound(7). 218
Figure (4- 147): ^{1}HNMR spectrum of copolymer (7) (MAA-Co-IAN) with compound(7). 218
Figure (4- 148): ^{13}C-NMR spectrum of copolymer (7) (MAA-Co-IAN) with compound(7). 219
Figure (4- 149): FTIR spectrum of copolymer (8) (MAA-Co-IAN) with compound(8). 220
Figure (4- 150): ^{1}HNMR spectrum of copolymer (8) (MAA-Co-IAN) with compound(8). 221
Figure (4- 151): ^{13}C-NMR spectrum of copolymer (8) (MAA-Co-IAN) with compound(8). 221
Figure (4- 152): FTIR spectrum of copolymer (9) (MAA-Co-IAN) with compound(9). 222
Figure (4- 153): ^{1}HNMR spectrum of copolymer (9) (MAA-Co-IAN) with compound(9). 223
Figure (4- 154): ^{13}C-NMR spectrum of copolymer (9) (MAA-Co-IAN) with compound(9). 223

Figure (4- 155): FTIR spectrum of copolymer(10) (MAA-Co-IAN) with compound(10). 224
Figure (4- 156): ^{1}HNMR spectrum of copolymer(10) (MAA-Co-IAN) with compound(10). ...225
Figure (4- 157): ^{13}C-NMR spectrum of copolymer(10) (MAA-Co-IAN) with compound(10). .225
Figure (4- 158): FTIR spectrum of copolymer(11) (MAA-CO-IAN) with compound(11).....226
Figure (4- 159): ^{1}HNMR spectrum of copolymer(11) (MAA-CO-IAN) with compound(11)....227
Figure (4- 160): ^{13}C-NMR spectrum of copolymer(11) (MAA-CO-IAN) with compound(11). 227
Figure (4- 161): FTIR spectrum of copolymer(12) (MAA-CO-IAN) with compound(12). 228
Figure (4- 162): ^{1}HNMR spectrum of copolymer(12) (MAA-CO-IAN) with compound(12)....229
Figure (4- 163): ^{13}C-NMR spectrum of copolymer(12) (MAA-CO-IAN) with compound(12). 229
Figure (4- 164): ^{1}HNMR spectrum of copolymer(13) (MAA-CO-IAN) with compound(13)....230
Figure (4- 165): ^{13}C-NMR spectrum of copolymer(13) (MAA-CO-IAN) with compound(13). 231
Figure (4- 166): FTIR spectrum of copolymer(14) (MAA-CO-IAN) with compound(14). 232
Figure (4- 167): ^{1}HNMR spectrum of copolymer(14) (MAA-CO-IAN) with compound(14)....233
Figure (4- 168): ^{13}C-NMR spectrum of copolymer(14) (MAA-CO-IAN) with compound(14). 233
Figure (4- 169): FTIR spectrum of copolymer(15) (MAA-CO-IAN) with compound(15). 234
Figure (4- 170): ^{1}HNMR spectrum of copolymer(15) (MAA-CO-IAN) with compound(15)....234
Figure (4- 171): ^{13}C-NMR spectrum of copolymer(15) (MAA-CO-IAN) with compound(15). 235
Figure (4- 172): FTIR spectrum of copolymer(16) (MAA-CO-IAN) with compound(16). 236
Figure (4- 173): ^{1}HNMR spectrum of copolymer(16) (MAA-CO-IAN) with compound(16)....236
Figure (4- 174): ^{13}C-NMR spectrum of copolymer(16) (MAA-CO-IAN) with compound(16). 237
Figure (4- 175): FTIR spectrum of copolymer(17) (MAA-CO-IAN) with compound(17). 238
Figure (4- 176): ^{1}HNMR spectrum of copolymer(17) (MAA-CO-IAN) with compound(17)....238
Figure (4- 177): ^{13}C-NMR spectrum of copolymer(17) (MAA-CO-IAN) with compound(17). 239
Figure (4- 178): FTIR spectrum of copolymer(18) (MAA-CO-IAN) with compound(18). 240
Figure (4- 179): ^{1}HNMR spectrum of copolymer(18) (MAA-CO-IAN) with compound(18)....240
Figure (4- 180): ^{13}C-NMR spectrum of copolymer(18) (MAA-CO-IAN) with compound(18). 241
Figure (4- 181): FTIR spectrum of copolymer(19) (MAA-CO-IAN) with compound(19). 242
Figure (4- 182): ^{1}HNMR spectrum of copolymer(19) (MAA-CO-IAN) with compound(19)....242
Figure (4- 183): ^{13}C-NMR spectrum of copolymer(19) (MAA-CO-IAN) with compound(19). 243
Figure (4- 184): FTIR spectrum of copolymer(20) (MAA-CO-IAN) with compound(20). 244
Figure (4- 185): ^{1}HNMR spectrum of copolymer(20) (MAA-CO-IAN) with compound(20)....244
Figure (4- 186): ^{13}C-NMR spectrum of copolymer(20) (MAA-CO-IAN) with compound(20). 245
Figure (4- 187): FTIR spectrum of copolymer(21) (MAA-CO-IAN) with compound(21) 246
Figure (4- 188): ^{1}HNMR spectrum of copolymer(21) (MAA-CO-IAN) with compound(21) ...246
Figure (4- 189): ^{13}C-NMR spectrum of copolymer(21) (MAA-CO-IAN) with compound(21). 247
Figure (4- 190): FTIR spectrum of copolymer(32) (MAA-CO-IAN) with compound(22) 248
Figure (4- 191): ^{1}HNMR spectrum of copolymer(32) (MAA-CO-IAN) with compound(22) ...248
Figure (4- 192): ^{13}C-NMR spectrum of copolymer(32) (MAA-CO-IAN) with compound(22). 249
Figure (4- 193): FTIR spectrum of copolymer(23) (MAA-CO-IAN) with compound(23). 250
Figure (4- 194): ^{1}HNMR spectrum of copolymer(23) (MAA-CO-IAN) with compound(23) ...250
Figure (4- 195): ^{13}C-NMR spectrum of copolymer(23) (MAA-CO-IAN) with compound(23) .251
Figure (4- 196): FTIR spectrum of copolymer(24) (MAA-CO-IAN) with compound (24). 252
Figure (4- 197): ^{1}HNMR spectrum of copolymer(24) (MAA-CO-IAN) with compound (24)...252

Figure (4- 198): ^{13}C-NMR spectrum of copolymer(24) (MAA-CO-IAN) with compound (24).253
Figure (4- 199): FTIR spectrum of copolymer(25) (MAA-CO-IAN) with compound (25). 254
Figure (4- 200): ^{1}HNMR spectrum of copolymer(25) (MAA-CO-IAN) with compound (25)...254
Figure (4- 201): ^{13}C-NMR spectrum of copolymer(25) (MAA-CO-IAN) with compound (25).255
Figure (4- 202): FTIR spectrum of copolymer(26) (MAA-CO-IAN) with compound (26). 256
Figure (4- 203): ^{1}HNMR spectrum of copolymer(26) (MAA-CO-IAN) with compound (26)...256
Figure (4- 204): ^{13}C-NMR spectrum of copolymer(26) (MAA-CO-IAN) with compound (26).257
Figure (4- 205): FTIR spectrum of copolymer (27) (MAA-CO-IAN) with compound(27). 258
Figure (4- 206): ^{1}HNMR spectrum of copolymer (27) (MAA-CO-IAN) with compound(27) ..258
Figure (4- 207): ^{13}C-NMR spectrum of copolymer(27) (MAA-CO-IAN) with compound(27). 259
Figure (4- 208): FTIR spectrum of copolymer (28) (MAA-CO-IAN) with compound(28). 260
Figure (4- 209): ^{1}HNMR spectrum of copolymer (28) (MAA-CO-IAN) with compound(28)...260
Figure (4- 210): ^{13}C-NMR spectrum of copolymer(28) (MAA-CO-IAN) with compound(28). 261
Figure (4- 211): FTIR spectrum of copolymer(29) (MAA-CO-IAN) with compound (29). 262
Figure (4- 212): ^{1}HNMR spectrum of copolymer(29) (MAA-CO-IAN) with compound (29)...262
Figure (4- 213): ^{13}C-NMR spectrum of copolymer(29) (MAA-CO-IAN) with compound (29).263
Figure (4- 214): FTIR spectrum of copolymer(30) (MAA-CO-IAN) with compound (30). 264
Figure (4- 215): ^{1}HNMR spectrum of copolymer(30) (MAA-CO-IAN) with compound (30)...264
Figure (4- 216): ^{13}C-NMR spectrum of copolymer(30) (MAA-CO-IAN) with compound (30).265
Figure (4- 217): FTIR spectrum of copolymer(31) (MAA-CO-IAN) with compound (31). 266
Figure (4- 218): ^{1}HNMR spectrum of copolymer(31) (MAA-CO-IAN) with compound (31)...266
Figure (4- 219): ^{13}C-NMR spectrum of copolymer(31) (MAA-CO-IAN) with compound (31).267
Figure (4- 220): FTIR spectrum of copolymer(32) (MAA-CO-IAN) with compound (32). 268
Figure (4- 221): ^{1}HNMR spectrum of copolymer(32) (MAA-CO-IAN) with compound (32)...268
Figure (4- 222): ^{13}C-NMR spectrum of copolymer(32) (MAA-CO-IAN) with compound (32).269
Figure (4- 223): FTIR spectrum of copolymer (33) (MAA-CO-IAN) with compound(33). 270
Figure (4- 224): ^{1}HNMR spectrum of copolymer(33) (MAA-CO-IAN) with compound(33)....270
Figure (4- 225): ^{13}C-NMR spectrum of copolymer(33) (MAA-CO-IAN) with compound(33). 271
Figure (4- 226): FTIR spectrum of copolymer(34) (MAA-CO-IAN) with compound (34). 272
Figure (4- 227): ^{1}HNMR spectrum of copolymer (34) (MAA-CO-IAN) with compound (34)..272
Figure (4- 228): ^{13}C-NMR spectrum of copolymer(34) (MAA-CO-IAN) with compound (34).273
Figure (4- 229): FTIR spectrum of copolymer(35) (MAA-CO-IAN) with compound (35). 274
Figure (4- 230): ^{1}HNMR spectrum of copolymer(35) (MAA-CO-IAN) with compound (35)...274
Figure (4- 231): ^{13}C-NMR spectrum of copolymer (35) (MAA-CO-IAN) with compound (35). 275
Figure (4- 232): FTIR spectrum of copolymer(36) (MAA-CO-IAN) with compound (36). 276
Figure (4- 233): ^{1}HNMR spectrum of copolymer(36) (MAA-CO-IAN) with compound (36)..276
Figure (4- 234):^{13}C-NMR spectrum of copolymer(36)(MAA-CO-IAN) with compound (36). 277
Figure (4- 235): FTIR spectrum of copolymer(37) (MAA-CO-IAN) with compound(37). 278
Figure (4- 236): ^{1}HNMR spectrum of copolymer(37) (MAA-CO-IAN) with compound(37)....278
Figure (4- 237): ^{13}C-NMR spectrum of copolymer(37) (MAA-CO-IAN) with compound(37). 279
Figure (4- 238): FTIR spectrum of copolymer(38) (MAA-CO-IAN) with compound(38). 280
Figure (4- 239): ^{1}HNMR spectrum of copolymer(38) (MAA-CO-IAN) with compound(38)....280

Figure (4- 240): ^{13}C-NMR spectrum of copolymer(38) (MAA-CO-IAN) with compound(38). 281
Figure (4- 241): FTIR spectrum of copolymer(39) (MAA-CO-IAN) with compound(39). 282
Figure (4- 242): ^{1}HNMR spectrum of copolymer(39) (MAA-CO-IAN) with compound(39)....282
Figure (4- 243): ^{13}C-NMR spectrum of copolymer(39) (MAA-CO-IAN) with compound(39). 283
Figure (4- 244): FTIR spectrum of copolymer(40) (MAA-CO-IAN) with compound(40). 284
Figure (4- 245): ^{1}HNMR spectrum of copolymer(40) (MAA-CO-IAN) with compound(40)....284
Figure (4- 246): ^{13}C-NMR spectrum of copolymer(40) (MAA-CO-IAN) with compound(40). 285
Figure (4- 247): FTIR spectrum of copolymer(41) (DMA-CO-CAN) with compound(3).....286
Figure (4- 248): ^{1}HNMR spectrum of copolymer(41) (DMA-CO-CAN) with compound(3). ...286
Figure (4- 249): ^{13}C-NMR spectrum of copolymer(41) (DMA-CO-CAN) with compound(3)..287
Figure (4- 250): FTIR spectrum of copolymer(42) (DMA-CO-CAN) with compound(13).....288
Figure (4- 251): ^{1}HNMR spectrum of copolymer(42) (DMA-CO-CAN) with compound(13). .288
Figure (4- 252): ^{13}C-NMR spectrum of copolymer(42) (DMA-CO-CAN) with compound(13). 289
Figure (4- 253): FTIR spectrum of copolymer(43) (DMA-CO-CAN) with compound(14).....290
Figure (4- 254): ^{1}HNMR spectrum of copolymer(43) (DMA-CO-CAN) with compound(14). .290
Figure (4- 255): ^{13}C-NMR spectrum of copolymer(43) (DMA-CO-CAN) with compound(14). 291
Figure (4- 256): FTIR spectrum of copolymer(44) (DMA-CO-CAN) with compound(16).....292
Figure (4- 257): ^{1}HNMR spectrum of copolymer(44) (DMA-CO-CAN) with compound(16). .292
Figure (4- 258): ^{13}C-NMR spectrum of copolymer(44) (DMA-CO-CAN) with compound(16). 293
Figure (4- 259): FTIR spectrum of copolymer(45) (DMA-CO-CAN) with compound(17).....294
Figure (4- 260): ^{1}HNMR spectrum of copolymer(45) (DMA-CO-CAN) with compound(17). .294
Figure (4- 261): ^{13}C-NMR spectrum of copolymer(45) (DMA-CO-CAN) with compound(17). 295
Figure (4- 262): FTIR spectrum of copolymer(46) (DMA-CO-CAN) with compound(18).....296
Figure (4- 263): ^{1}HNMR spectrum of copolymer(46) (DMA-CO-CAN) with compound(18). .296
Figure (4- 264): ^{13}C-NMR spectrum of copolymer(46) (DMA-CO-CAN) with compound(18). 297
Figure (4- 265): FTIR spectrum of copolymer(47) (DMA-CO-CAN) with compound(19).....298
Figure (4- 266): ^{1}HNMR spectrum of copolymer(47) (DMA-CO-CAN) with compound(19). .298
Figure (4- 267): ^{13}C-NMR spectrum of copolymer(47) (DMA-CO-CAN) with compound(19). 299
Figure (4- 268): FTIR spectrum of copolymer(48) (DMA-CO-CAN) with compound(20).....300
Figure (4- 269): ^{1}HNMR spectrum of copolymer(48) (DMA-CO-CAN) with compound(20). .300
Figure (4- 270): ^{13}C-NMR spectrum of copolymer(48) (DMA-CO-CAN) with compound(20). 301
Figure (4- 271): FTIR spectrum of copolymer(49) (DMA-CO-CAN) with compound(24).....302
Figure (4- 272): ^{1}HNMR spectrum of copolymer(49) (DMA-CO-CAN) with compound(24). .302
Figure (4- 273): ^{13}C-NMR spectrum of copolymer(49) (DMA-CO-CAN) with compound(24). 303
Figure (4- 274): FTIR spectrum of copolymer(50) (DMA-CO-CAN) with compound(25).....304

Figure (4- 275): ^{1}HNMR spectrum of copolymer(50) (DMA-CO-CAN) with compound(25). .304
Figure (4- 276): ^{13}C-NMR spectrum of copolymer(50) (DMA-CO-CAN) with compound(25). 305
Figure (4- 277): FTIR spectrum of copolymer (51) (DMA-CO-CAN) with compound (28). 306
Figure (4- 278): ^{1}HNMR spectrum of copolymer (51) (DMA-CO-CAN) with compound (28).306
Figure (4- 279): ^{13}C-NMR spectrum of copolymer (51) (DMA-CO-CAN) with compound (28). 307
Figure (4- 280): FTIR spectrum of copolymer(52) (DMA-CO-CAN) with compound(31). 308
Figure (4- 281): ^{1}HNMR spectrum of copolymer(52) (DMA-CO-CAN) with compound(31). .308
Figure (4- 282): ^{13}C-NMR spectrum of copolymer(52) (DMA-CO-CAN) with compound(31). 309
Figure (4- 283): FTIR spectrum of copolymer(53) (DMA-CO-CAN) with compound (34). 310
Figure (4- 284): ^{1}HNMR spectrum of copolymer(53) (DMA-CO-CAN) with compound (34). 310
Figure (4- 285): ^{13}C-NMR spectrum of copolymer(53) (DMA-CO-CAN) with compound (34). 311
Figure (4- 286): FTIR spectrum of copolymer(54) (DMA-CO-CAN) with compound(35). 312
Figure (4- 287): ^{1}HNMR spectrum of copolymer(54) (DMA-CO-CAN) with compound(35). .312
Figure (4- 288): ^{13}C-NMR spectrum of copolymer(54) (DMA-CO-CAN) with compound(35). 313
Figure (4- 289): FTIR spectrum of copolymer(55) (DMA-CO-CAN) with compound(37). 314
Figure (4- 290): ^{1}HNMR spectrum of copolymer(55) (DMA-CO-CAN) with compound(37). .314
Figure (4- 291): ^{13}C-NMR spectrum of copolymer(55) (DMA-CO-CAN) with compound(37). 315
Figure (4- 292): FTIR spectrum of copolymer(56) (DMA-CO-CAN) with compound(38). 316
Figure (4- 293): ^{1}HNMR spectrum of copolymer(56) (DMA-CO-CAN) with compound(38). .316
Figure (4- 294): ^{13}C-NMR spectrum of copolymer(56) (DMA-CO-CAN) with compound(38). 317
Figure (4- 295): FTIR spectrum of copolymer(57) (DMA-CO-CAN) with compound(39). 318
Figure (4- 296): ^{1}HNMR spectrum of copolymer(57) (DMA-CO-CAN) with compound(39). .318
Figure (4- 297): ^{13}C-NMR spectrum of copolymer(57) (DMA-CO-CAN) with compound(39). 319
Figure (4- 298): FTIR spectrum of copolymer(58) (DMA-CO-CAN) with compound(40). 320
Figure (4- 299): ^{1}HNMR spectrum of copolymer(58) (DMA-CO-CAN) with compound(40). .320
Figure (4- 300): ^{13}C-NMR spectrum of copolymer(58) (DMA-CO-CAN) with compound(40). 321
Figure (4- 301): TGA and DSC curve for copolymer (1).....327
Figure (4- 302): TGA and DSC curve for copolymer (2).....327
Figure (4- 303): TGA and DSC curve for copolymer (3).....328
Figure (4- 304): TGA and DSC curve for copolymer (4).....328
Figure (4- 305): TGA and DSC curve for copolymer (5).....328
Figure (4- 306): TGA and DSC curve for copolymer (6).....329
Figure (4- 307): TGA and DSC curve for copolymer (7).....329
Figure (4- 308): TGA and DSC curve for copolymer (8).....330

Figure (4- 309): TGA and DSC curve for copolymer (9).....330
Figure (4- 310): TGA and DSC curve for copolymer (10).....331
Figure (4- 311): Schematic representation of the docking procedure, analysis of ligands and reactivity.....332
Figure (4- 312): 2D structures of selected copolymers (ligands).....333
Figure (4- 313): Crystal structures of the 5IKQ proteins.....334
Figure (4- 314): 2D and 3D of the best pose.....340
Figure (4- 315): Schematic representation of the docking procedure, analysis of ligands and reactivity.....344
Figure (4- 316): 2D structures of selected copolymers (ligands).....345
Figure (4- 317): Crystal structures of the 5IKQ proteins.....346
Figure (4- 318): 2D and 3D of the best pose.....351
Figure (4- 319): Schematic representation of the docking procedure, analysis of ligands and reactivity.....356
Figure (4- 320): 2D structures of selected copolymers (ligands).....356
Figure (4- 321): Crystal structures of the 8C7Y proteins.....357
Figure (4- 322): 2D and 3D of the best pose.....362
Figure (4- 323): Schematic representation of the docking procedure, analysis of ligands and reactivity.....367
Figure (4- 324): 2D structures of selected copolymers (ligands).....368
Figure (4- 325): Crystal structures of the 5IKQ proteins.....369
Figure (4- 326): 2D and 3D of the best pose.....375
Figure (4- 327): Cytotoxic potentials o copolymer(1) on colon cancer cell line vs normal cell line after 24 hrs.; 37 Cº.....380
Figure (4- 328): Cytotoxic potentials of copolymer(1) on colon cancer cell line vs normal cell line after 24 hrs.; 37 Cº.....381
Figure (4- 329): Cytotoxic potentials of copolymer(1) on colon cancer cell line vs normal cell line after 48 hrs.; 37 Cº.....382
Figure (4- 330): Cytotoxic potentials of copolymer(1) on colon cancer cell line vs normal cell line after 48 hrs.; 37 Cº.....383
Figure (4- 331): Cytotoxic potentials of copolymer(1) on colon cancer cell line vs normal cell line after 72 hrs.; 37 Cº.....384
Figure (4- 332): Cytotoxic potentials of copolymer(1) on colon cancer cell line vs normal cell line after 72 hrs.; 37 Cº.....385
Figure (4- 333): DPPH radical scavenging activity of copolymer(1) and vitamin C 386
Figure (4- 334): Cytotoxic potentials of copolymer(2) on colon cancer cell line vs normal cell line after 24 hrs.; 37 Cº.....387
Figure (4- 335): Cytotoxic potentials of copolymer(2) on colon cancer cell line vs normal cell line after 24 hrs.; 37 Cº.....387
Figure (4- 336): Cytotoxic potentials of copolymer(2) on colon cancer cell line vs normal cell line after 48 hrs.; 37 Cº.....389
Figure (4- 337): Cytotoxic potentials of copolymer(2) on colon cancer cell line vs normal cell line after 72 hrs.; 37 Cº.....390

Figure (4- 338): Cytotoxic potentials of o copolymer(2) n colon cancer cell line vs normal cell line after 72 hrs.; 37 Cº.....391
Figure (4- 339): DPPH radical scavenging activity of copolymer(2) and vitamin-C 392
Figure (4- 340): Cytotoxic potentials of copolymer(3) on colon cancer cell line vs normal cell line after 24 hrs.; 37 Cº.....393
Figure (4- 341): Cytotoxic potentials of copolymer(3) on colon cancer cell line vs normal cell line after 24 hrs.; 37 Cº.....394
Figure (4- 342): Cytotoxic potentials of copolymer(3) on colon cancer cell line vs normal cell line after 48 hrs.; 37 Cº.....395
Figure (4- 343): Cytotoxic potentials of copolymer(3) on colon cancer cell line vs normal cell line after 48 hrs.; 37 Cº.....395
Figure (4- 344): Cytotoxic potentials of copolymer(3) on colon cancer cell line vs normal cell line after 72 hrs.; 37 Cº.....396
Figure (4- 345): Cytotoxic potentials of copolymer(3) on colon cancer cell line vs normal cell line after 72 hrs.; 37 Cº.....397
Figure (4- 346): DPPH radical scavenging activity of copolymer(3) and vitamin-C 398
Figure (4- 347): Cytotoxic potentials of copolymer(4) on colon cancer cell line vs normal cell line after 24 hrs.; 37 Cº.....399
Figure (4- 348): Cytotoxic potentials of copolymer(4) on colon cancer cell line vs normal cell line after 24 hrs.; 37 Cº.....399
Figure (4- 349): Cytotoxic potentials of copolymer(4) on colon cancer cell line vs normal cell line after 48 hrs.; 37 Cº.....400
Figure (4- 350): Cytotoxic potentials of copolymer(4) on colon cancer cell line vs normal cell line after 48 hrs.; 37 Cº.....401
Figure (4- 351): Cytotoxic potentials of copolymer(4) on colon cancer cell line vs normal cell line after 72 hrs.; 37 Cº.....402
Figure (4- 352): Cytotoxic potentials of copolymer(4) on colon cancer cell line vs normal cell line after 72 hrs.; 37 Cº.....403
Figure (4- 353): DPPH radical scavenging activity of copolymer(4) and vitamin-C 404
Figure (4- 354): Cytotoxic potentials of copolymer(5) on colon cancer cell line vs normal cell line after 24 hrs.; 37 Cº.....405
Figure (4- 355): Cytotoxic potentials of copolymer(5) on colon cancer cell line vs normal cell line after 24 hrs.; 37 Cº.....406
Figure (4- 356): Cytotoxic potentials of copolymer(5) on colon cancer cell line vs normal cell line after 48 hrs.; 37 Cº.....407
Figure (4- 357): Cytotoxic potentials of copolymer(5) on colon cancer cell line vs normal cell line after 48 hrs.; 37 Cº.....407
Figure (4- 358): Cytotoxic potentials of copolymer(5) on colon cancer cell line vs normal cell line after 72 hrs.; 37 Cº.....409
Figure (4- 359): Cytotoxic potentials of copolymer(5) on colon cancer cell line vs normal cell line after 72 hrs.; 37 Cº.....409
Figure (4- 360): DPPH radical scavenging activity of copolymer(5) and copolymer(6) with vitamin-C.....412

Figure (4- 361): Cytotoxic potentials of copolymer(6) on skin cancer cell line vs normal cell line after 24 hrs.; 37 C.....413
Figure (4- 362): Cytotoxic potentials of copolymer(6) on skin cancer cell line vs normal cell line after 24 hrs.; 37 C.....414
Figure (4- 363): Cytotoxic potentials of copolymer(6) on skin cancer cell line vs normal cell line after 48 hrs.; 37 C°.....415
Figure (4- 364): Cytotoxic potentials of copolymer(6) on skin cancer cell line vs normal cell line after 48 hrs.; 37 C°.....415
Figure (4- 365): Cytotoxic potentials of copolymer(6) on skin cancer cell line vs normal cell line after 72 hrs.; 37 C°.....416
Figure (4- 366): Cytotoxic potentials of copolymer(6) on skin cancer cell line vs normal cell line after 72 hrs.; 37 C°.....417
Figure (4- 367): Cytotoxic potentials of copolymer(7) on skin cancer cell line vs normal cell line after 24 hrs.; 37 C°.....418
Figure (4- 368): Cytotoxic potentials of copolymer(7) on skin cancer cell line vs normal cell line after 24 hrs.; 37 C°.....418
Figure (4- 369): Cytotoxic potentials of copolymer(7) on skin cancer cell line vs normal cell line after 48 hrs.; 37 C°.....419
Figure (4- 370): Cytotoxic potentials of copolymer(7) on skin cancer cell line vs normal cell line after 48 hrs.; 37 C°.....420
Figure (4- 371): Cytotoxic potentials of copolymer(7) on skin cancer cell line vs normal cell line after 72 hrs.; 37 C°.....421
Figure (4- 372): Cytotoxic potentials of copolymer(7) on skin cancer cell line vs normal cell line after 72 hrs.; 37 C°.....421
Figure (4- 373): DPPH radical scavenging activity of copolymer(7) and copolymer(8) with vitamin-C.....422
Figure (4- 374): Cytotoxic potentials of copolymer(8) on skin cancer cell line vs normal cell line after 24 hrs.; 37 C°.....423
Figure (4- 375): Cytotoxic potentials of copolymer(8) on skin cancer cell line vs normal cell line after 24 hrs.; 37 C°.....424
Figure (4- 376): Cytotoxic potentials of copolymer(8) on skin cancer cell line vs normal cell line after 48 hrs.; 37 C°.....425
Figure (4- 377): Cytotoxic potentials of copolymer(8) on skin cancer cell line vs normal cell line after 48 hrs.; 37 C° 425
Figure (4- 378): Cytotoxic potentials of copolymer(8) on skin cancer cell line vs normal cell line after 72 hrs.; 37 C°.....426
Figure (4- 379): Cytotoxic potentials of copolymer(8) on skin cancer cell line vs normal cell line after 72 hrs.; 37 C°.....427
Figure (4- 380): Cytotoxic potentials of copolymer(9) on skin cancer cell line vs normal cell line after 24 hrs.; 37 C°.....428
Figure (4- 381): Cytotoxic potentials of copolymer(9) on skin cancer cell line vs normal cell line after 24 hrs.; 37 C°.....428
Figure (4- 382): Cytotoxic potentials of copolymer(9) on skin cancer cell line vs normal cell line

after 48 hrs.; 37 C° 429
Figure (4- 383): Cytotoxic potentials of copolymer(9) on skin cancer cell line vs normal cell line after 48 hrs.; 37 C° 430
Figure (4- 384): Cytotoxic potentials of copolymer(9) on skin cancer cell line vs normal cell line after 72 hrs.; 37 C°. 431
Figure (4- 385): Cytotoxic potentials of copolymer(9) on skin cancer cell line vs normal cell line after 72 hrs.; 37 C° 431
Figure (4- 386): DPPH radical scavenging activity of copolymer(9) and vitamin -C 432
Figure (4- 387): Cytotoxic potentials of copolymer(10) on skin cancer cell line vs normal cell line after 24 hrs.; 37 C°. 433
Figure (4- 388): Cytotoxic potentials of copolymer(10) on skin cancer cell line vs normal cell line after 24 hrs.; 37 C°. 434
Figure (4- 389): Cytotoxic potentials of copolymer(10) on skin cancer cell line vs normal cell line after 48 hrs.; 37 C°. 435
Figure (4- 390): Cytotoxic potentials of copolymer(10) on skin cancer cell line vs normal cell line after 72 hrs.; 37 C°. 436
Figure (4- 391): Cytotoxic potentials of copolymer(10) on skin cancer cell line vs normal cell line after 72 hrs.; 37 C° 437
Figure (4- 392): DPPH radical scavenging activity of copolymer(10) with vitamin -C 440
Figure (4- 393): Antibacterial activities of (copolymer(1) and copolymer(2)) on both *Escherichia coli* and *Pseudomonas aeruginosa* 446
Figure (4- 394): Antibacterial activities of (copolymer(3) and copolymer(4)) on both *Escherichia coli* ad *Pseudomonas aeruginosa* 447
Figure (4- 395): Antibacterial activities of (copolymer(5) and copolymer(6)) on both *Escherichia coli* and *Pseudomonas aeruginosa* 448
Figure (4- 396): Antibacterial activities of (copolymer(7) and copolymer(8)) on both *Escherichia coli* and *Pseudomonas aeruginosa* 449
Figure (4- 397): Antibacterial activities of (copolymer(9) and copolymer(10)) on both *Escherichia coli* and *Pseudomonas aeruginosa* 450
Figure (4- 398): Antibacterial activities of (copolymer(1) and copolymer(2)) on both *Staphylococcus aureus* and *Enterococcus faecalis* 451
Figure (4- 399): Antibacterial activities of (copolymer(3) and copolyme4)) on both *Staphylococcus aureus* and *Enterococcus faecalis* 452
Figure (4- 400): Antibacterial activities of (copolymer(5) and copolymer(6)) on both Staphylococcus aureus and Enterococcus faecalis 453
Figure (4- 401): Antibacterial activities of (copolymer(7) and copolymer(8)) on both *Staphylococcus aureus* and *Enterococcus faecalis* 454
Figure (4- 402): Antibacterial activities of (copolymer(8) and copolymer(10)) on both Staphylococcus aureus and Enterococcus faecalis 455
Figure (4- 403): Antifungal activities of (copolymer(1) and copolymer(2)) on *Candida albicans* and *AspergDillus niger* 456
Figure (4- 404): Anti Antifungal activities of (copolymer(3) and copolymer(4)) on *Candida albicans* and *Aspergillus niger* 457

Figure (4- 405): Antibacterial activities of (copolymer(5) and copolymer(6)) on both Staphylococcus aureus and Enterococcus faecalis.....458
Figure (4- 406): Anti Antifungal activities of (copolymer(7) and copolymer(8)) on *Candida albicans* and *Aspergillus niger*.....459
Figure (4- 407): Antifungal activities of (copolymer(9) and copolymer(10)) on *Candida albicans* and *Aspergillus niger*.....460

List of Schemes

Scheme (1) Synthesis of new Schiff bases to obtain the intermediate of thiosemcarbazone compounds (1-9) LVI
Scheme (2): Synthesis of a series of 2-(4-substituted-benzylidene hydrazono)-1, 3- thiazolidine-4-one compounds (10-17) LVII
Scheme (3) Synthesis of 5-Styryli-2-amino-1, 3, 4-thiadiazole (18-20) ……LVIII
Scheme (4) Synthesis of the imide compounds (21-23) LVIII
Scheme (5) Cyclization step to obtain 1, 3-oxazepine-4, 7-dione derivatives compounds (24-26) LIX
Scheme (6) Reaction of 2-amino 1, 3, 4-thiadiazole-5-thiol compound with chloroacetylchloride and urea to obtain compound (28)..... LIX
Scheme (7) Synthesis of 2, 3-dihydroquinosulin-4-one derivatives (29-31) …… LX
Scheme (8) Synthesis of Tetrazole derivatives (32-33) LX
Scheme (9) Synthesis of 2-iminothiazolidine – 4- one (36) LXI
Scheme (10) Synthesis of Mannich compound derivatives (37-40)..... LXI
Scheme (11) Radical photopolymerization of vinyl monomers / Polymerization of copolymers …… LXII
Scheme (12) Synthesis of copolymers containing five and six cyclic member's heterocyclic compounds …… LXXVII
Scheme (2- 1): Possible strategies for the synthesis of polysubstituted heterocycles.....15
Scheme (2- 2): Cyosine tautomeric equilibrium. 19
Scheme (2- 3): Knorr's synthesis of antipyrine.....25
Scheme (2- 4): Synthesis of Polybenzimidazole, Polybenzoxazole and Polybenzthiazole by Condensation Polymerization. 28
Scheme (2- 5): Synthesis of polyimides from aromatic diisocyanates. 29
Scheme (2- 6): Synthesis of Polybenzimidazole and Polyquinoxaline.....29
Scheme (2- 7): Synthesis and structures of poly(arylene ether)s. 31
Scheme (2- 8): synthesis scheme of poly(aryl ether) polymers using various aryl (Ar) units. 31
Scheme (2- 9): Synthesis of post-polymerization modification of poly(arylene ether ketone)s via cyclization 32
Scheme (2- 10): Synthesis of 1,2,4-triazole-functionalized poly(arylene ether ketone. 32
Scheme (2- 11): Synthesis of Poly(1,3,4-oxadiazole) by Polycondensation of Bis(tetrazole) with Terephthaloyl Chloride.....33
Scheme (2- 12): Synthesis of 1,3,4-Oxadiazole derivative via thermal cyclization of diacylhydrazine. 34
Scheme (2- 13): Synthesis of 1,3,4-Oxadiazole 35
Scheme (2- 14): Synthesis of 1,3,4-oxadiazole derivative via thermal cyclodehydration. 35
Scheme (2- 15): Synthesis of bis(1,2,4-oxadiazole) derivative. 36
Scheme (2- 16): Synthesis of polymerization of nitrile oxide yields poly-1,2,5-oxadiazoles. 36
Scheme (2- 17): Synthesis of terephthalonitrile di-N-oxide. 36
Scheme (2- 18): Synthesis of poly (1,2,4-oxadiazole N-oxide> 37
Scheme (2- 19): Mechanism of cycloreversion of 3,4-diphenyl-1,2,5-oxadiazoleThermal cleavage

of 1,2,5-oxadiazole. 37
Scheme (2- 20): Mechanism for the thermal decomposition to form phenyl. 38
Scheme (2- 21): Mechanism of thermal degradation of 1,3,4-oxadiazole ring. 39
Scheme (2- 22): Meisenheimer Complex 40
Scheme (2- 23): mechanism of the polymerization reaction. 42
Scheme (2- 24): Schematic illustration of docking a small molecule ligand (green) to a protein target (black) producing a stable complex. 48
Scheme (4-1): Synthesis Thiosemicarbazones of 2-(pyridin-2-ylmethylene)hydrazine-1-carbothioamide compound(1). 114
Scheme (4-2): Mechanism of Schiff base. 114
Scheme (4- 3): Synthesis of 2-(1-(4-aminophenyl)ethylidene)hydrazine-1-carbothioamide compound(2). 116
Scheme (4-4): Synthesis of (4-nitrophenyl)ethylidene)hydrazine-1-carbothioamide compound(3). 118
Scheme (4-5): Synthesis of 2-(diphenylmethylene)hydrazine-1-carbothioamide compound(4). 120
Scheme (4-6): Synthesis of 2-(2-hydroxybenzylidene)hydrazine-1-carbothioamide compound(5). 122
Scheme (4-7): Synthesis2-(thiophen-2-ylmethylene)hydrazine-1-carbothioamide thiosemicarbazon compound(6). 124
Scheme (4-8): Synthesis of 2-(furan-2-ylmethylene)hydrazine-1-carbothioamide thiosemicarbazon compound(7). 126
Scheme (4-9): synthesis of (Z)-2-(1-(thiophen-2-yl)ethylidene)hydrazine-1-carbothioamide thiosemicarbazone compound(8). 128
Scheme (4-10): synthesis of the Thiosemicarbazones for N, N-dimethyaminebenzaldehyde compound(9). 130
Scheme (4-11): synthesis of (Z)-3-((pyridin-2-ylmethylene)amino)-2-thioxoimidazolidin-4-one compound(10). 132
Scheme (4-12): synthesis of (E)-3-((1-(2-aminophenyl)ethylidene)amino)-2-thioxoimidazolidin-4-one compound(11). 135
Scheme (4-13): synthesis of (E)-3-((1-(4-nitrophenyl)ethylidene)amino)-2-thioxoimidazolidin-4-one compound(12). 137
Scheme (4-14): Synthesis of (Z)-3-((cyclohexa-2, 4-dien-1-yl(phenyl) methylene) amino)-2-thioxoimidazolidin-4-one compound(13). 139
Scheme (4-15): synthesis of (E)-3-((1-(2-hydroxyphenyl)ethylidene)amino)-2-thioxoimidazolidin-4-one compound(14). 141
Scheme (4-16): synthesis of 3-((thiophen-2-ylmethylene)amino)-2-thioxoimidazolidin-4-one compound(15). 143
Scheme (4-17): synthesis of 3-((furan-2-ylmethylene)amino)-2-thioxoimidazolidin-4-one compound(16). 145
Scheme (4-18): synthesis of (E)-3-((1-(thiophen-2-yl)ethylidene)amino)-2-thioxoimidazolidin-4-one compound(17). 147
Scheme (4-19): synthesis of N-(5-aminophthaloyl) thiosemicarbazide compound(18). 149

Scheme (4-20): synthesis of 5-amino-2-(2-aminophenyl)-2, 5-dihydro-1, 3, 4-thiadiazol-2-ol compound(19). 151
Scheme (4-21): synthesis of 5-amino-2-(5-amino-2-hydroxyphenyl)-2, 5-dihydro-1, 3, 4-thiadiazol-2 compound(20). 153
Scheme (4-22): synthesis of 3-amino-5-(5-(5-(1, 3-dioxo-1, 3-dihydroisobenzofuran-5-carbonyl)-3-methylene-1-oxoisoindolin-2-yl)-4, 5-dihydro-1, 3, 4-thiadiazol-2-yl)benzoic acid compound(21). 155
Scheme (4-23): synthesis of 5-(2-(5-(2-aminophenyl)-5-hydroxy-2, 5-dihydro-1, 3, 4-thiadiazol-2-yl)-3-methylene-1-oxoisoindoline-5-carbonyl)isobenzofuran-1, 3-dione compound(22)..... 158
Scheme (4-24): synthesis of 2-(5-(5-amino-2-hydroxyphenyl)-5-hydroxy-2, 5-dihydro-1, 3, 4-thiadiazol-2-yl)-5-(1, 3-dioxo-1, 3-dihydroisobenzofuran-5-carbonyl)isoindoline-1, 3-dione compound(23). 160
Scheme (4-25): synthesis of 1-(8-(1, 3-dioxo-1, 3-dihydroisobenzofuran-5-carbonyl)-1, 5-dioxo-3-(pyridin-2-yl)-1, 5-dihydrobenzo[e][1, 3]oxazepin-4(3H)-yl)urea compound(24). 162
Scheme (4-26): Mechanism of synthesis 1, 3 oxazepine 162
Scheme (4-27): synthesis of 3-(2-aminophenyl)-1, 5-dioxo-4-ureido-1, 3, 4, 5-tetrahydrobenzo[e][1, 3]oxazepine-8-carboxylic acid compound(25). 165
Scheme (4-28): synthesis of 1-(3-(3-(dimethylamino)phenyl)-1, 5-dioxo-9-(4-(3-oxobutanoyl)phenyl)-1, 5-dihydrobenzo[e][1, 3]oxazepin-4(3H)-yl)urea compound(26). 167
Scheme (4-29): synthesis of (5-mercapto-1, 3, 4-thiadiazol-2-yl)glycinoyl chloride compound(27). 169
Scheme (4-30): synthesis of N-(5-mercapto-1, 3, 4-thiadiazole-2-yl)-2-ureidoacetamide compound(28). 172
Scheme (4-31): synthesis of 1-(4-oxo-2-(thiophen-2-yl)-1, 4-dihydroquinazolin-3(2H)-yl)thiourea compound(29). 174
Scheme (4-32): Mechanism synthesis of some 2, 3-dihydroquinosulin4-one derivatives..... 174
Scheme (4-33): synthesis of 1-(2-(furan-2-yl)-4-oxo-1, 4-dihydroquinazolin-3(2H)-yl)thiourea compound(30). 177
Scheme (4-34): synthesis of 1-(4-oxo-2-(thiophen-2-yl)-1, 4-dihydroquinazolin-3(2H)-yl)thiourea compound(31). 179
Scheme (4-35): synthesis of 1, 1'-(1, 4-phenylenebis(methaneylylidene))bis(thiourea) compound(32). 181
Scheme (4-36): of Mechanism of synthesis tetrazole 181
Scheme (4-37): synthesis of 1, 1'-(1, 4-phenylenebis(4, 5-dihydro-1H-tetrazole-5, 1-diyl))bis(thiourea) compound(33). 184
Scheme (4-38): structure of synthesis of 2, 2'-((Z)-indoline-2, 3-diylidene)bis(hydrazine-1-carbothioamide) compound(34). 186
Scheme (4-39): Synthesis of 1, 1'-(dispiro[tetrazole-5, 2'-indoline-3', 5''-tetrazol]-1, 1''(4H, 4''H)-diyl)bis(thiourea) compound(35). 188
Scheme (4-40): synthesis of 2-iminothiazolidin-4-one compound(36). 190
Scheme (4-41): synthesis of 3-((3-(4-aminophenoxy)phenyl)amino)-3, 4-dihydro-2H-thiazolo[3, 2-a][1, 3, 5]triazin-6(7H)-one compound(37). 192
Scheme (4-42): synthesis of 3-((4-aminophenyl)amino)-3, 4-dihydro-2H-thiazolo[3, 2-a][1, 3,

5]triazin-6(7H)-one compound(38).....194
Scheme (4-43): synthesis of 3-((2-((2-((2-minoethyl)amino)ethyl)amino) ethyl)amino)-3, 4-dihydro-2H-thiazolo[3, 2-a][1, 3, 5]triazin-6(7H)-one compound(39).....196
Scheme (4-44): synthesis of 3-((6-aminopyridin-2-yl)amino)-3, 4-dihydro-2H-thiazolo[3, 2-a][1, 3, 5]triazin-6(7H)-one compound(40).....198
Scheme (4-45): synthesis of copolymer (methyl acrylic acid-co - Itaconic anhydride) (MAA-CO-IAN). 201
Scheme (4-46): synthesis of copolymer (N, N-dimethylacrylamide-Citraconic anhydride) (DMA-CO-CAN) 203
Scheme (4-47): synthesis of copolymer (1) (MAA-Co-IAN) with compound(1). 205
Scheme (4-48): Mechanism of synthesis copolymer with compounds.....205
Scheme (4-49): Syntheses of copolymer(2) (MAA-Co-IAN) with compound(2).....207
Scheme (4-50): synthesis of copolymer(3) (MAA-Co-IAN) with compound(3). 209
Scheme (4-51): synthesis of copolymer(4) (MAA-Co-IAN) with compound(4). 211
Scheme (4-52): synthesis of copolymer(5) (MAA-Co-IAN) with compound(5). 213
Scheme (4-53): synthesis of copolymer(6) (MAA-Co-IAN) with compound(6). 215
Scheme (4-54): synthesis of copolymer(7) (MAA-Co-IAN) with compound(7). 217
Scheme (4-55): synthesis of copolymer(8) (MAA-Co-IAN) with compound(8). 219
Scheme (4-56): synthesis of copolymer(9) (MAA-Co-IAN) with compound(9). 222
Scheme (4-57): synthesis of copolymer(10) (MAA-Co-IAN) with compound(10). 224
Scheme (4-58): synthesis of copolymer(11) (MAA-CO-IAN) with compound(11).....226
Scheme (4-59): synthesis of copolymer(12) (MAA-CO-IAN) with compound(12). 228
Scheme (4-60): synthesis of copolymer(13) (MAA-CO-IAN) with compound(13). 230
Scheme (4-61): synthesis of copolymer(14) (MAA-CO-IAN) with compound(14). 231
Scheme (4-62): synthesis of copolymer(15) (MAA-CO-IAN) with compound(15). 233
Scheme (4-63): synthesis of copolymer(16) (MAA-CO-IAN) with compound(16). 235
Scheme (4-64): synthesis of copolymer(17) (MAA-CO-IAN) with compound(17). 237
Scheme (4-65): synthesis of copolymer(18) (MAA-CO-IAN) with compound(18). 239
Scheme (4-66): synthesis of copolymer(19) (MAA-CO-IAN) with compound(19). 241
Scheme (4-67): synthesis of copolymer(20) (MAA-CO-IAN) with compound(20). 243
Scheme (4-68): synthesis of copolymer(21) (MAA-CO-IAN) with compound(21) 245
Scheme (4-69): synthesis of copolymer(32) (MAA-CO-IAN) with compound(22) 247
Scheme (4-70): synthesis of copolymer(23) (MAA-CO-IAN) with compound(23) 249
Scheme (4-71): synthesis of copolymer(24) (MAA-CO-IAN) with compound (24). 251
Scheme (4-72): synthesis of copolymer(25) (MAA-CO-IAN) with compound (25). 253
Scheme (4-73): synthesis of copolymer(26) (MAA-CO-IAN) with compound (26). 255
Scheme (4-74): synthesis of copolymer (27) (MAA-CO-IAN) with compound(27) 257
Scheme (4-75): synthesis of copolymer(28) (MAA-CO-IAN) with compound(28). 259
Scheme (4-76): synthesis of copolymer(29) (MAA-CO-IAN) with compound (29). 261
Scheme (4-77): synthesis of copolymer(30) (MAA-CO-IAN) with compound (30). 263
Scheme (4-78): synthesis of copolymer(31) (MAA-CO-IAN) with compound (31). 265
Scheme (4-79): synthesis of copolymer(32) (MAA-CO-IAN) with compound (32). 267
Scheme (4-80): synthesis of copolymer(33) (MAA-CO-IAN) with compound(33). 269

Scheme (4-81): synthesis of copolymer(34) (MAA-CO-IAN) with compound (34). 271
Scheme (4-82): synthesis of copolymer(35) (MAA-CO-IAN) with compound (35). 273
Scheme (4-83): synthesis of copolymer(36) (MAA-CO-IAN) with compound (36). 275
Scheme (4-84): synthesis of copolymer(37) (MAA-CO-IAN) with compound(37). 277
Scheme (4-85): synthesis of copolymer(38) (MAA-CO-IAN) with compound(38). 279
Scheme (4-86): synthesis of copolymer(39) (MAA-CO-IAN) with compound(39). 281
Scheme (4-87): synthesis of copolymer(40) (MAA-CO-IAN) with compound(40). 283
Scheme (4-88): synthesis of copolymer(41) (DMA-CO-CAN) with compound(3). 285
Scheme (4-89): synthesis3of copolymer(42) (DMA-CO-CAN) with compound(13). 287
Scheme (4-90): synthesis of copolymer(43) (DMA-CO-CAN) with compound(14). 289
Scheme (4-91): synthesis of copolymer(44) (DMA-CO-CAN) with compound(16). FTIR spectrum of copolymer(44) (DMA-CO-CAN) with compound(16). 291
Scheme (4-92): synthesis of copolymer(45) (DMA-CO-CAN) with compound(17). 293
Scheme (4-93): synthesis of copolymer(46) (DMA-CO-CAN) with compound(18) 295
Scheme (4-94): synthesis of copolymer(47) (DMA-CO-CAN) with compound(19). 297
Scheme (4-95): synthesis of copolymer(48) (DMA-CO-CAN) with compound(20). 299
Scheme (4-96): synthesis of copolymer(49) (DMA-CO-CAN) with compound(24). 301
Scheme (4-97): synthesis of copolymer(50) (DMA-CO-CAN) with compound(25). 303
Scheme (4-98): synthesis of copolymer (51) (DMA-CO-CAN) with compound (28). 305
Scheme (4-99): synthesis of copolymer(52) (DMA-CO-CAN) with compound(31). 307
Scheme (4-100): synthesis of copolymer(53) (DMA-CO-CAN) with compound (34). 309
Scheme (4-101): synthesis of copolymer(54) (DMA-CO-CAN) with compound(35). 311
Scheme (4-102): synthesis of copolymer(55) (DMA-CO-CAN) with compound(37). 313
Scheme (4-103): synthesis of copolymer(56) (DMA-CO-CAN) with compound(38). FTIR spectrum of copolymer(56) (DMA-CO-CAN) with compound(38). 315
Scheme (4-104): synthesis of copolymer(57) (DMA-CO-CAN) with compound(39). 317
Scheme (4-105): synthesis of copolymer(58) (DMA-CO-CAN) with compound(40). 319

List of Abbreviations

Abbreviations	Name
FTIR	Fourier Transform Infrared Spectroscopy
1HNMR	Proton Nuclear Magnetic Resonance
13C-NMR	Carbon-13 Nuclear Magnetic Resonance
m.p	Melting Point
Å	Angstrom
ºC	Degree Celsius
MAA-CO-IAN	methyl acrylic acid-co - Itaconic anhydride
DMA-CO-CAN	dimethylacrylamide-CO -Citraconic anhydride
TGA	Thermo gravimetric analysis.
DT	disintegration temperature.
Ti	Initial disintegration temperature.
Top	Optimum disintegration temperature.
Tf	Final disintegration temperature. The final degree of dissociation temperature
T50%	Temperature of 50% weight loss, acquired by TGA.
T Residual	Residual weight ratio at 800 °C in Argon from TGA.
T Char	Char% at 600 °C.
DSC	Differential Scanning calorimeter analysis
Tg	Temperature Glass Transition
Tc	Degree of Crystallization
DFT	density functional theory
RMS	root-mean-square
MOE	Molecular Operating Environment
PDB	Protein Data Bank.
RMSD	Root Mean Square Deviation
EDTA	Ethylene Diamine Tetraacetic acid

List of Abbreviations

RPMI	Roswell Park Memorial Institue
ARG, VAL.ALA.TYR	Amino Acids
DPPH	2, 2-Diphenyl -1-1- picrylhydrazyl
HdFn	Human Dermal Fibroblast nnormal
Ppm	Parts Per Million
IC_{50}	Half Maximal Inhibitory Concentration
MTT	3-(4, 5-dimethylthiazole-2-yl)-2, 5-diphenyl tetrazolium bromide

Summary

All living organisms have the ability to defense themselves from exogenous pathogens and repair tissue damage that results from infection. Discovering inflammatory response has led to significant advantages in the treatment of inflammatory diseases which are related to various physiological and pathological processes. Physiology of disease is not yet completely understood. However, inflammation is known to be adaptive response and promoted by detrimental stimuli. Primarily, an acute inflammatory stimulus is evaluated by infection or tissue injuries that triggers distribution of blood ingredients (plasma and leukocytes) through infected or injured area. Additionally, this local event may lead to chronic inflammation and autoimmune diseases in further cases which is originated from malfunction of tissue due to homeostatic imbalance of one or several biological mechanisms.

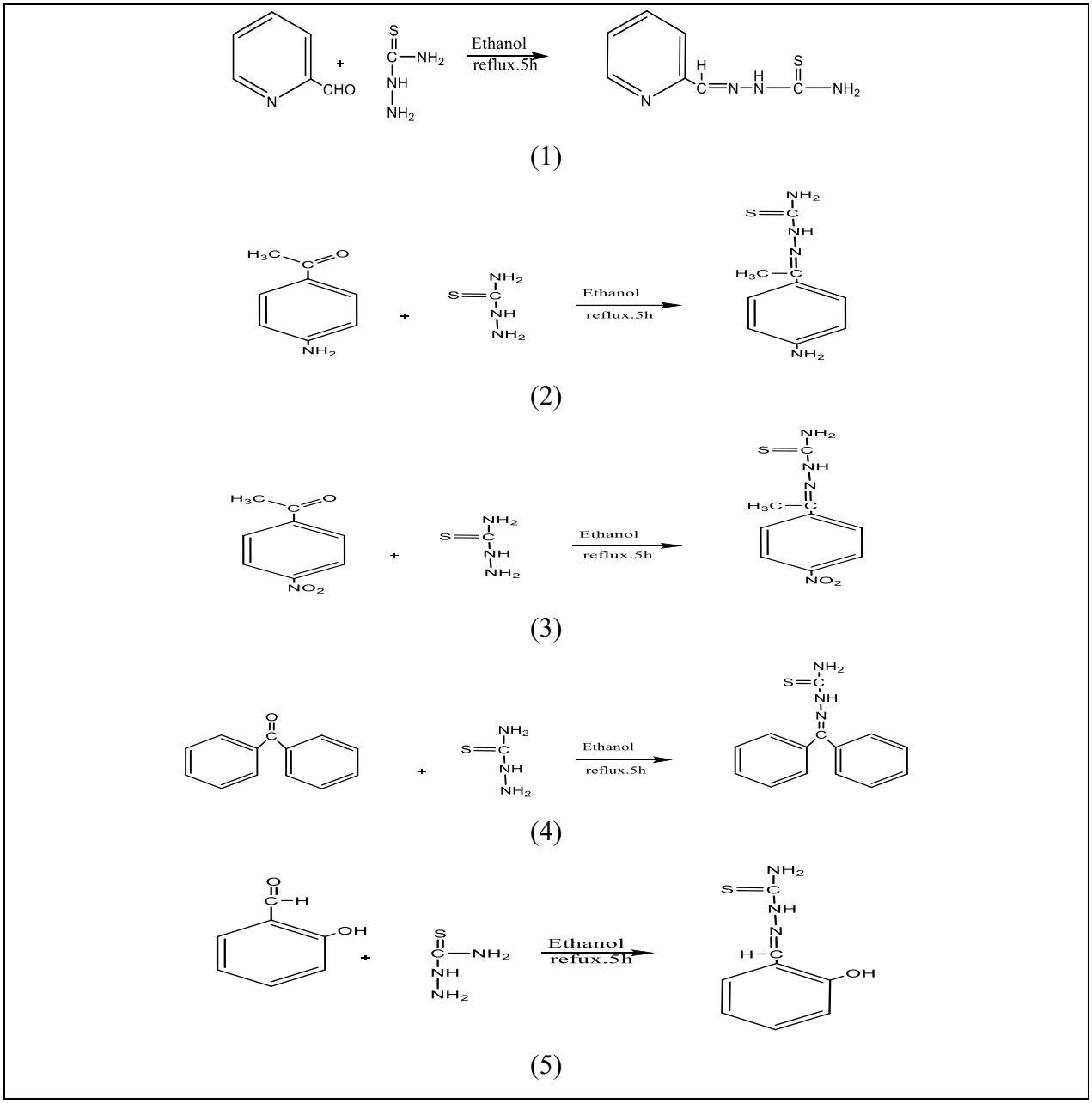
The utility of thiosemicarbazides in organic synthesis demonstrates their importance in the synthesis of several heterocycles. Their reactions with systems containing C=O and C=N groups is one of the methods for the preparation of biologically active compounds viz. pyrazole, thiazole, triazole, thiadiazole, oxadiazole, triazine and thiadiazine. The formation of C−N and C=N bonds as opposed to the N−N bond formation is reflected in their extensive use for the preparation of these heterocycles in excellent yields.

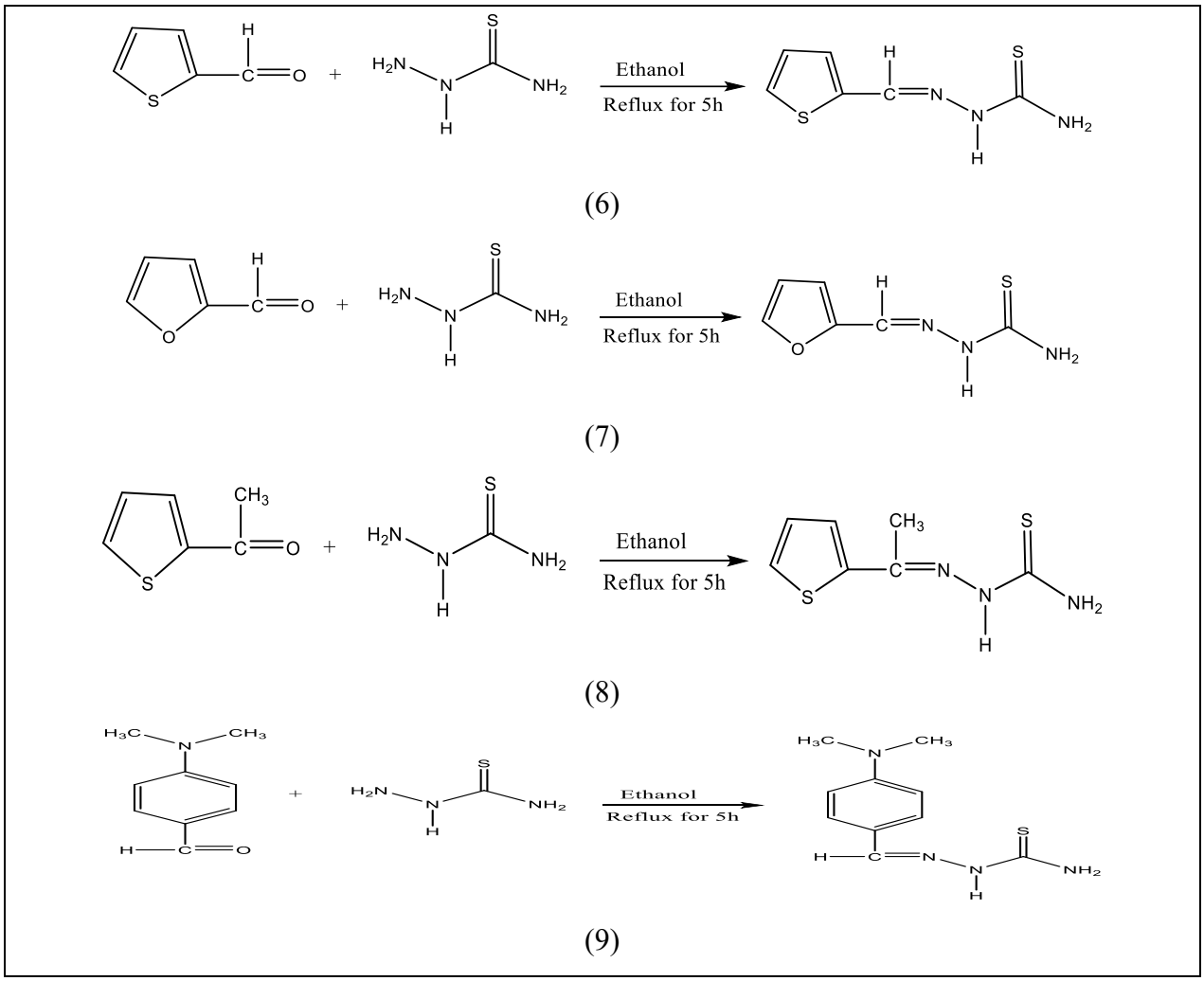
New classes of copolymers derived from copolymers containing five and six cyclic member's heterocyclic compounds have been of great interest on account of their variety of applications particularly in the field of chemotherapeutic, antimicrobial and fungicide concerning the immobilization through chemical bonds of some biologically active compounds on the (methyl acrylic acid- Itaconic anhydride) and (N, N-dimethylacrylamide-Citraconic anhydride) copolymers. The high reactivity of the anhydride cycle of the polymer has allowed us to obtain conjugates in which the biologically active compounds of some heterocyclic compounds are immobilized on the polymeric support through amide bonds. The

chemical structures of the synthesized compounds and copolymers were determined by some spectroscopy techniques such as [FTIR , ^{1}HNMR, ^{13}CNMR and Elemental Analysis (CHNS)]. Some physical properties of synthesized compounds were determined such as melting points and colors**.**

This work includes Twelfth different parts as shown below

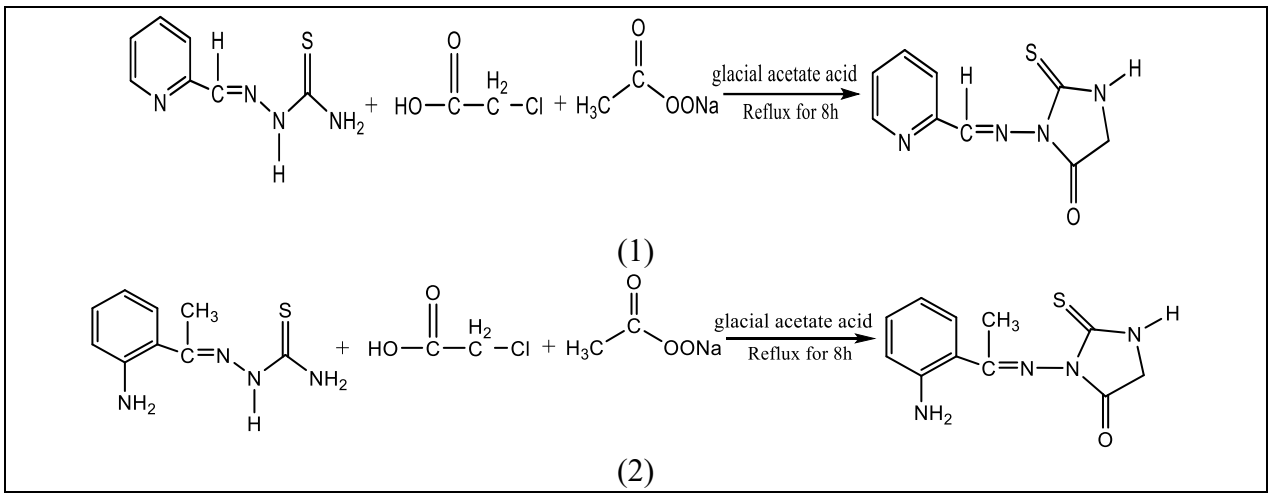
1- **First part:** This part involved the synthesis of new Schiff bases to obtain the intermediate of thiosemcarbazone compounds (**1-9**) by reaction thiosemicarbazide with several aromatic ketones and aldehydes as shown in Scheme (1).

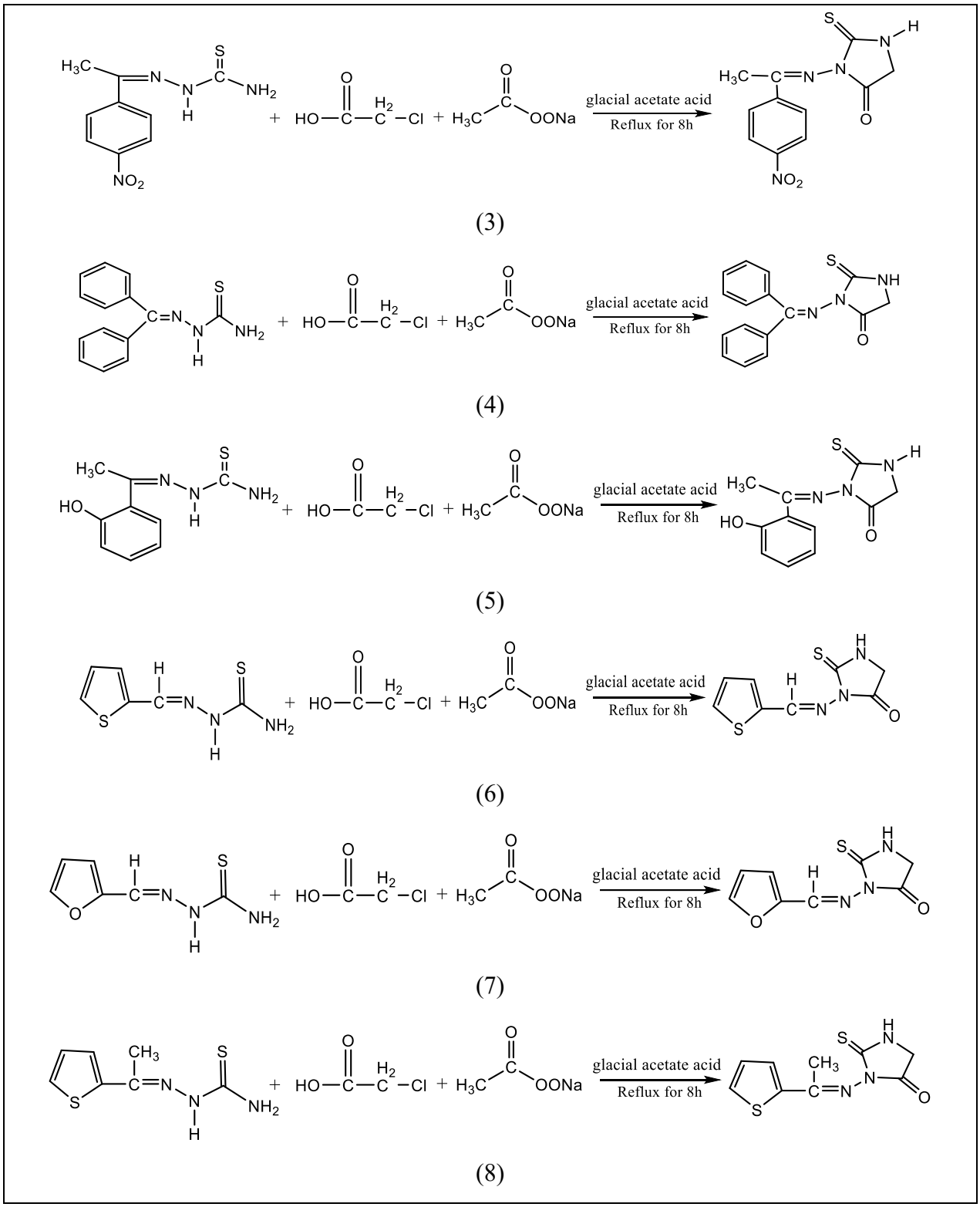




Scheme (1)

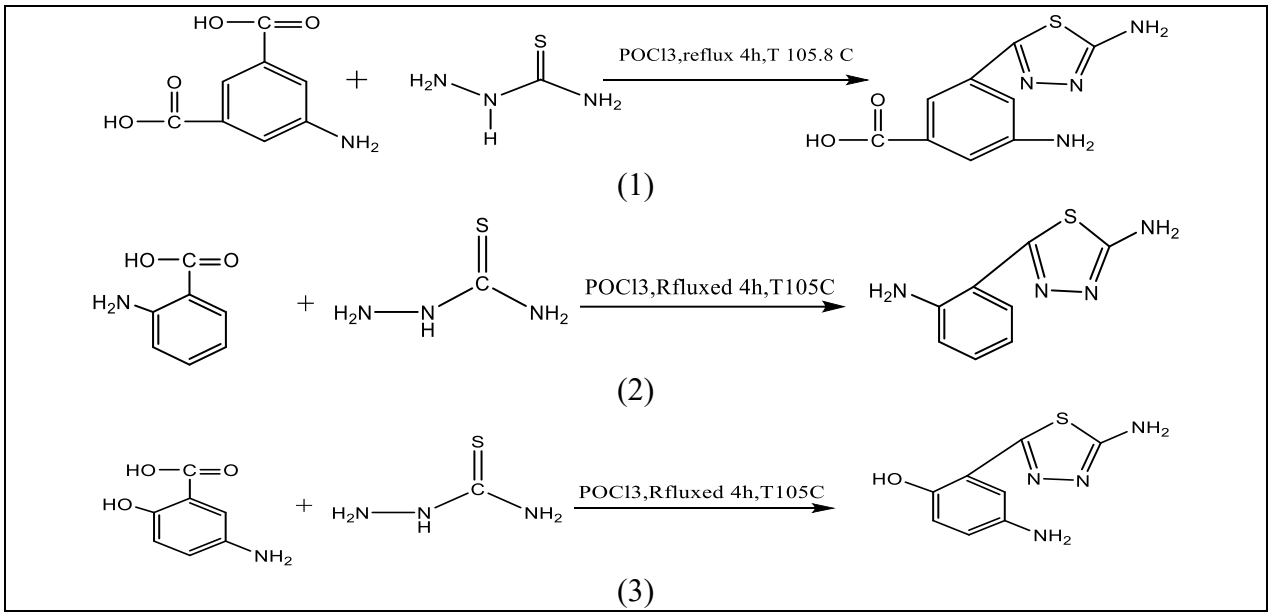
2- **Second part:** Treatment of compounds (**1, 2, 3, 4, 6, 7, 8)** with Chloroacetic acid and anhydrous sodium acetate, a series of 2-(4-substituted-benzylidene hydrazono)-1, 3- thiazolidine-4-one compounds (**10-17**) were synthesized as shown in Scheme (2).





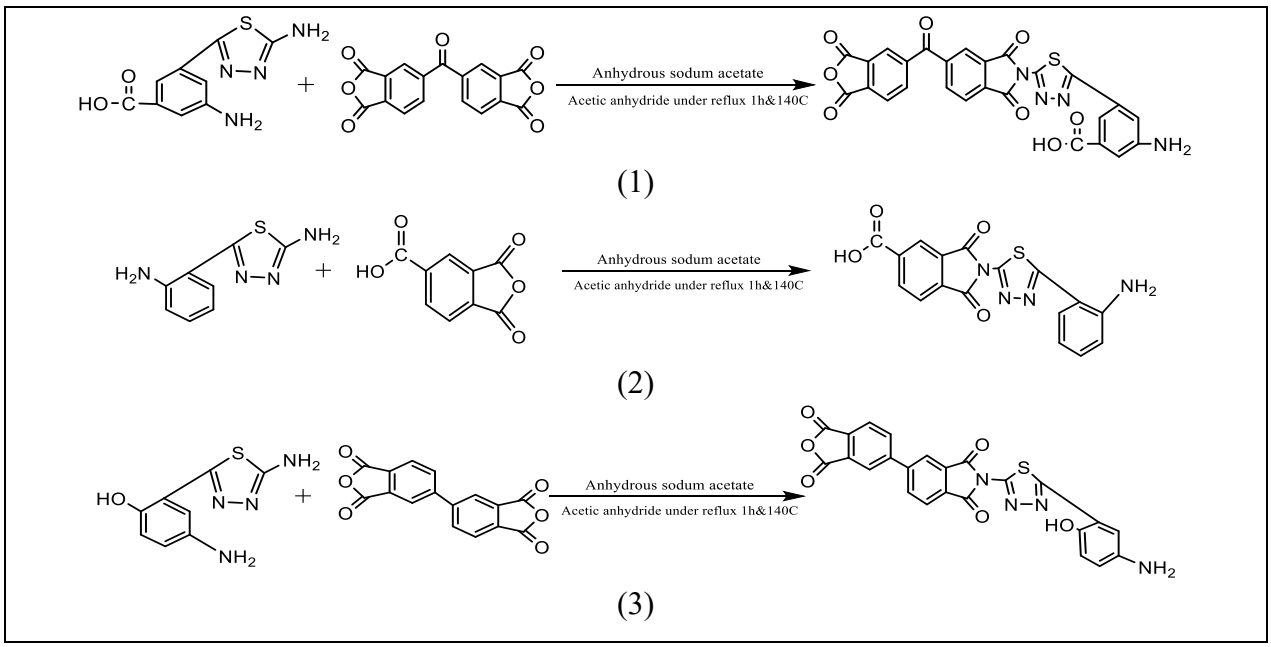
Scheme (2):

3- Third part: 5-Styryli-2-amino-1, 3, 4-thiadiazole (**18-20**) was synthesized from the reaction of 5-amino phthalic acid, Anthranilic acid and 5-amino-2-hydroxybenzoic acid with thiosemicarbazide in presence of $POCl_3$ as shown in Scheme (3)



Scheme (3)

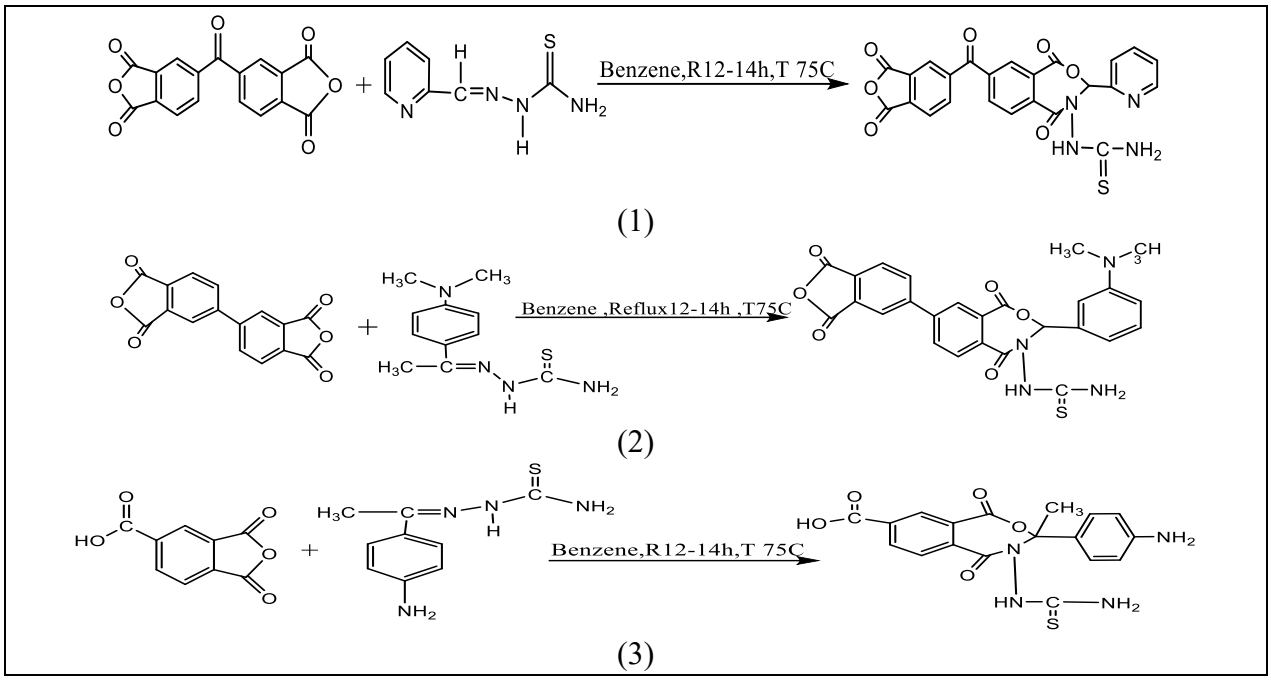
4- Fourth part: The imide compounds (21-**23**) were synthesized from the reaction of 5-Styryli-2-amino-1, 3, 4-thiadiazole (**18-20**) with 3, 3', 4, 4'-Benzophenne tetracarboxylic acid anhydride, trimellitic anhydride and 3, 3;4, 4'- Biphenyl tetracarboxylic acid anhydride in 3:2 solutions of acetic acid and pyridine as shown in Scheme (4).



Scheme (4)

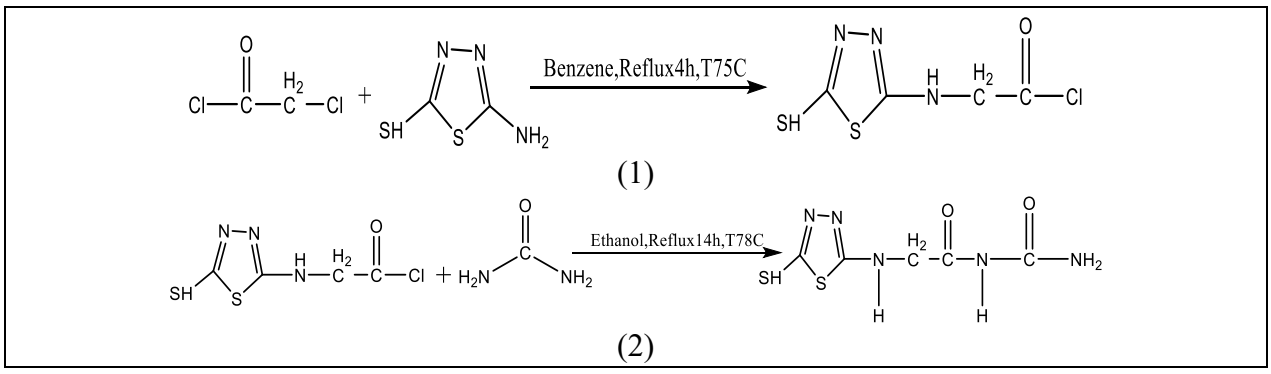
5- Fifth part: Cyclization step was achieved by treatment thiosemcarbazone compounds (**1, 2, 9**) with trimellitic anhydride and, 3', 4, 4'-Benzophenne tetracarboxylic acid anhydride to obtain1, 3-oxazepine-4, 7-dione derivatives

compounds (**24-26**) as shown in Scheme (5).



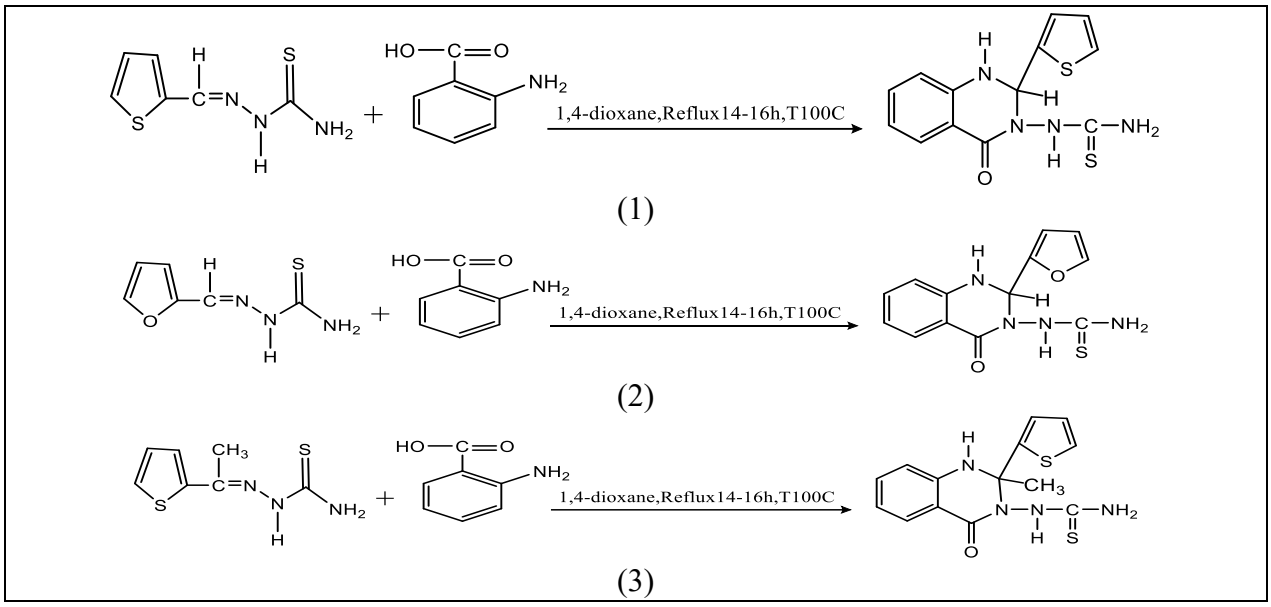
Scheme (5)

6- **Sixth part**: The reaction of 2-amino 1, 3, 4-thiadiazole-5-thiol compound with chloroacetylchloride produced compound (**27**) then treated with urea to obtained compound (**28**) as shown in Scheme (6)



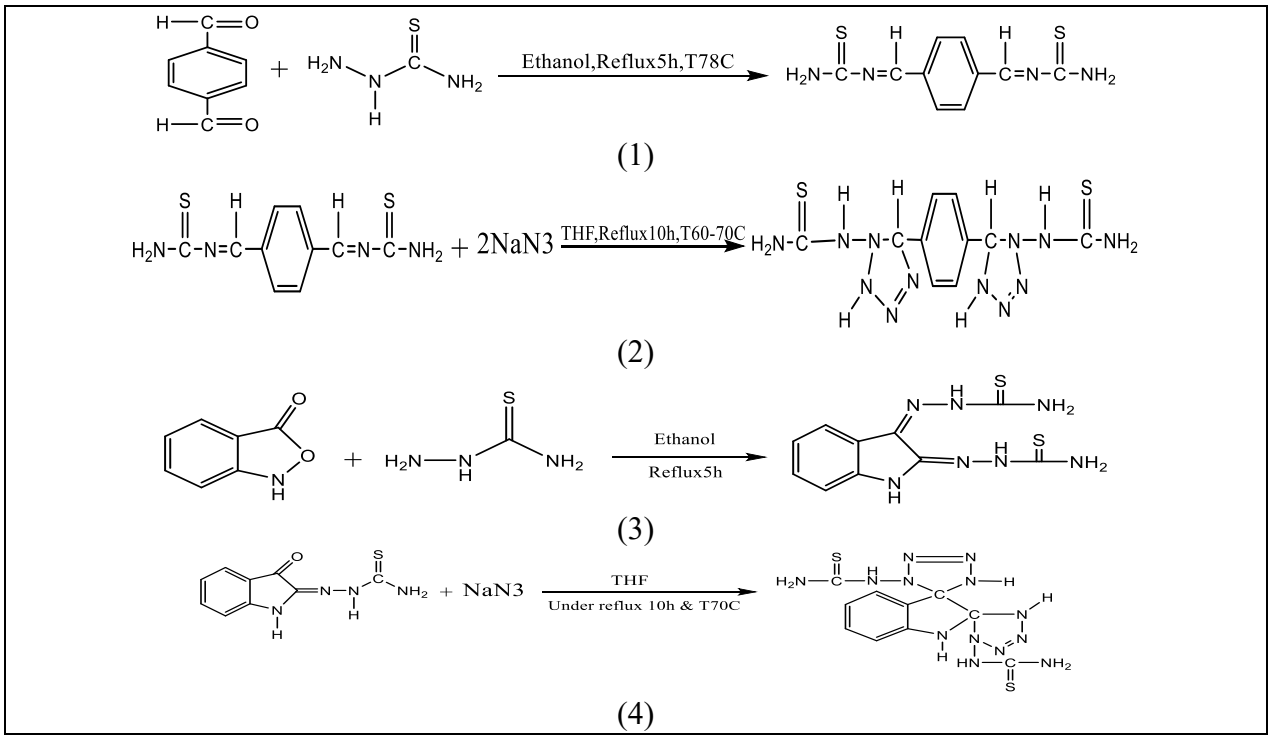
Scheme (6)

7- **Seventh part:** 2, 3-dihydroquinosulin-4-one derivatives **(29-31)** were synthesized from the reaction of Schiff bases derivatives (8, 9, 10) with of anthranilic acid as shown in Scheme (7)



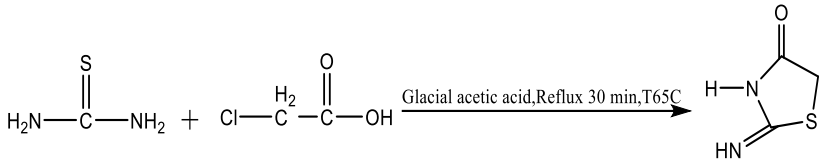
Scheme (7)

8- Eighth part: Tetrazole derivatives **(32-33)** were synthesized from the reaction of sodium azide with Schiff bases derivatives that obtained from reaction of terphthaldehyde and Isatin with thiosemicarbazide **(34-35)** as shown in Scheme (8)



Scheme (8)

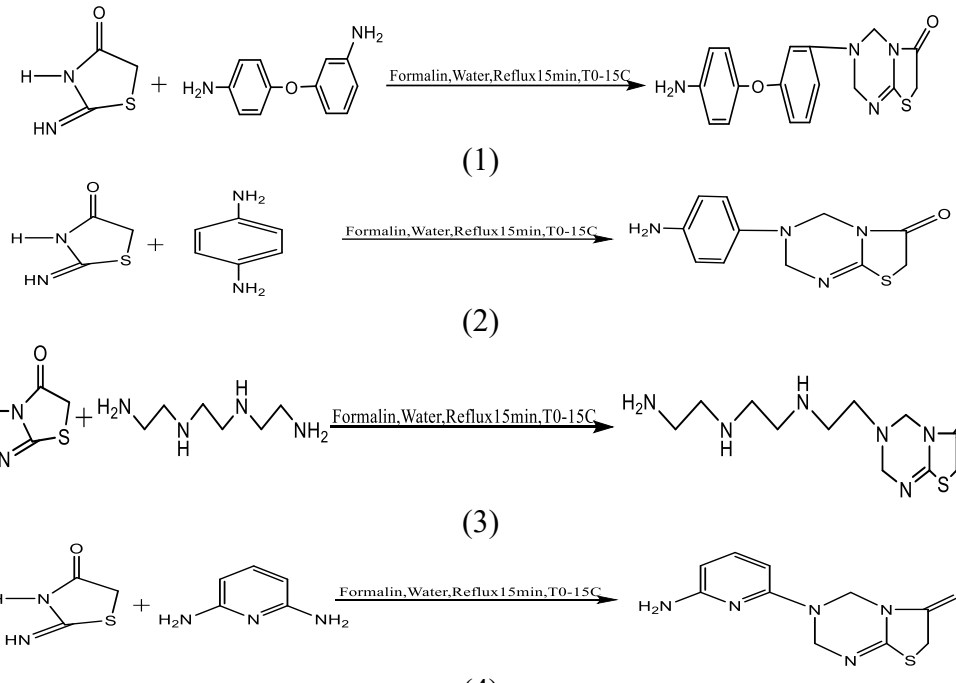
9- Ninth part :2- iminothiazolidine – 4- one **(36)** was synthesized from the reaction of thiourea with of monochloroacetic acid as shown in Scheme (9)



(1)

Scheme (9)

10- Tenth part: Mannich compound derivatives **(37-40)** were synthesized from the reaction of **compound (36)** with 1, 4-phenylenediamine a, 3, 4'-Diamino diphenyl ether, triethylenetetramine, 2, 6-diamino pyridine **in** presence of **formalin** as shown in Scheme (10)



(1)

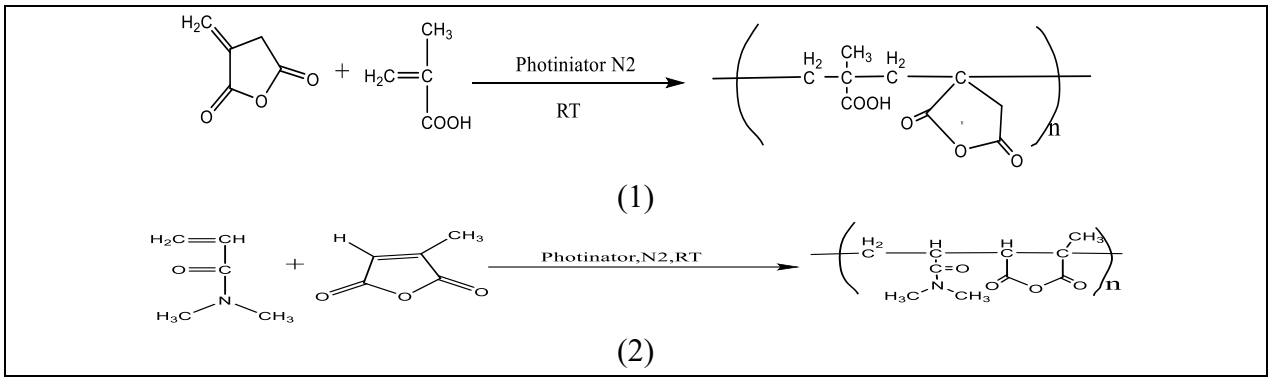
(2)

(3)

(4)

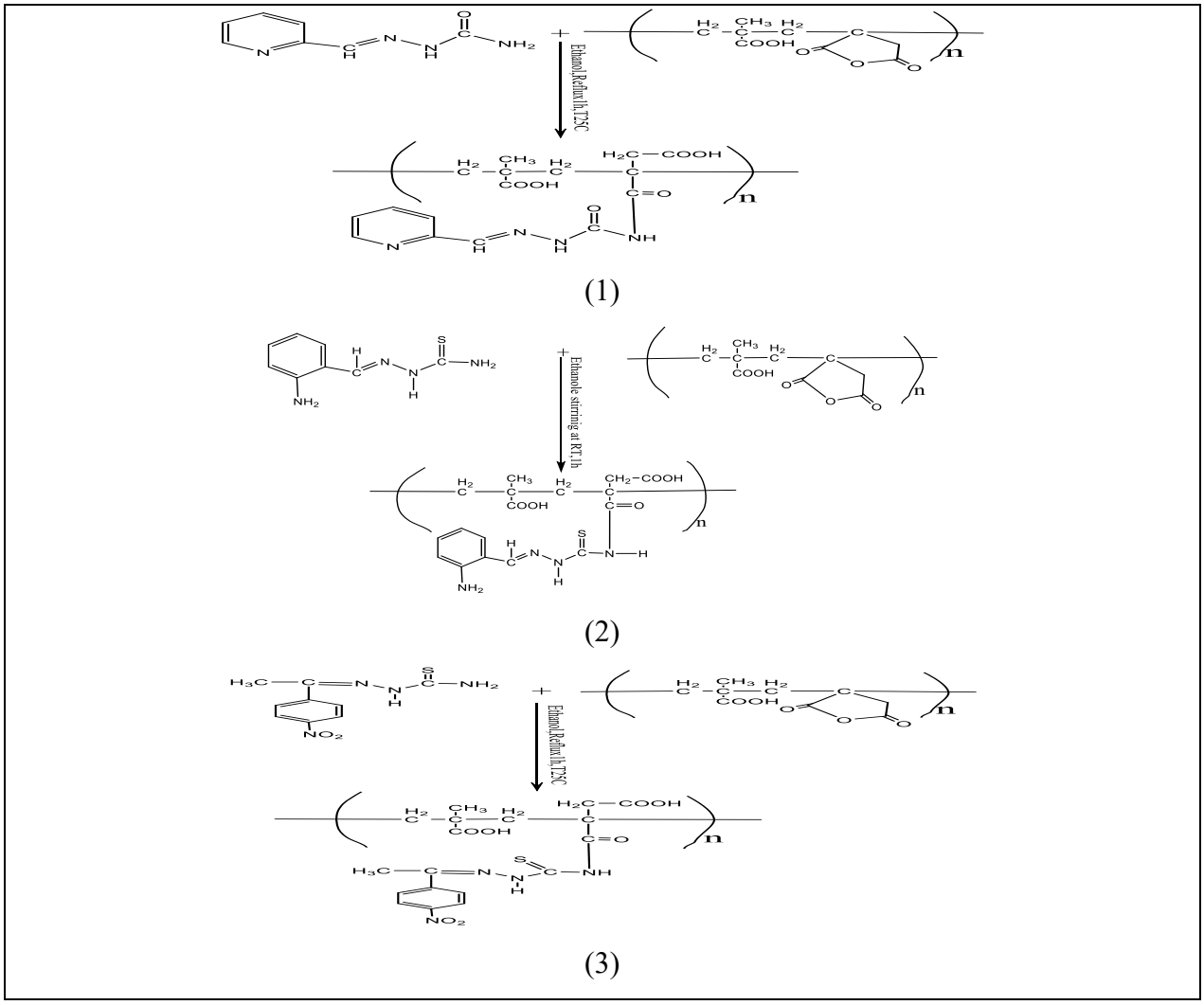
Scheme (10)

11- Eleventh part: Radical photopolymerization of vinyl monomers (methyl acrylic acid, Itaconicanhydride, N, N-dimethylacrylamide and Citraconic anhydride) carried out using 1-hydroxy cyclohexyl phenol ketone as the initiator affording copolymers (methyl methacrylate- Itaconic anhydride) and (N, N-dimethyl acrylamide-Citraconic anhydride). Polymerization of copolymers as shown in scheme (11).

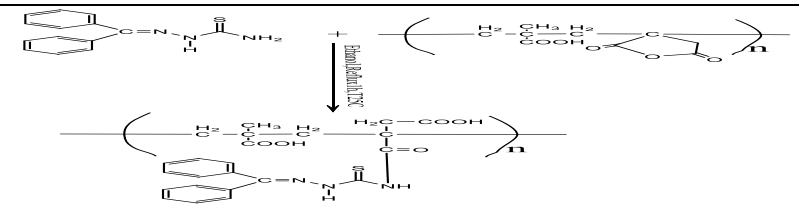


Scheme (11)

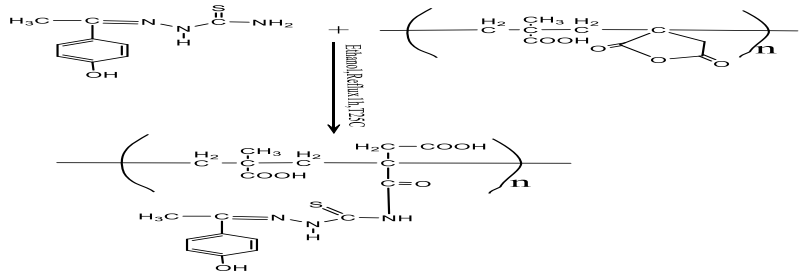
12- Twelfth part: copolymers were synthesized containing five and six cyclic member's heterocyclic compounds concerning the immobilization through chemical bonds of some biologically active compounds on the (methyl acrylic acid- Itaconic anhydride) **(1-40)** and (N, N-dimethyl acrylamide-Citraconic anhydride) **(41-58)** copolymers as shown in Scheme (12)



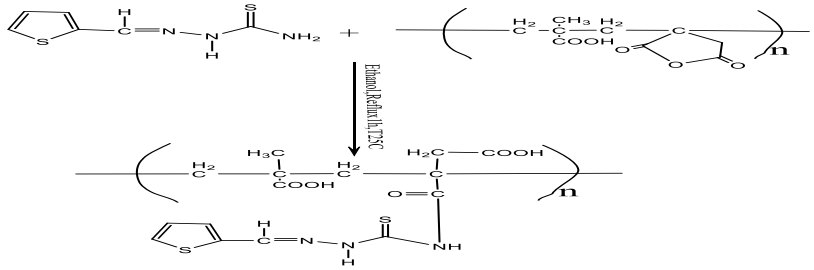
Summary


Ethanol,Reflux,6h,TFSC

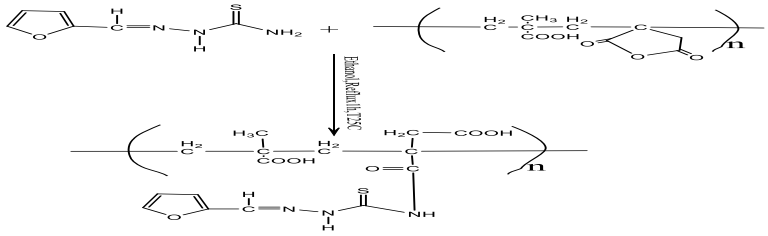
(4)


Ethanol,Reflux,6h,TFSC

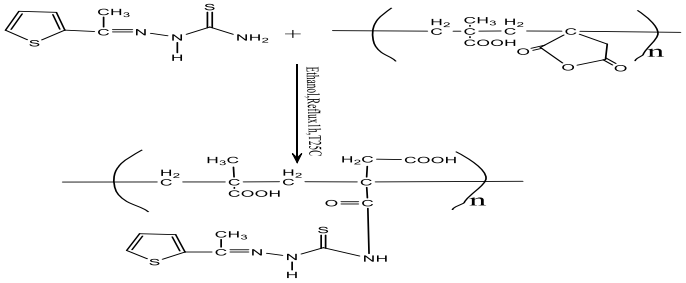
(5)


Ethanol,Reflux,6h,TFSC

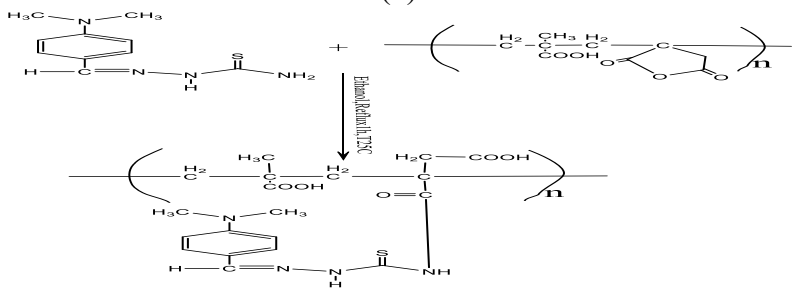
(6)


Ethanol,Reflux,6h,TFSC

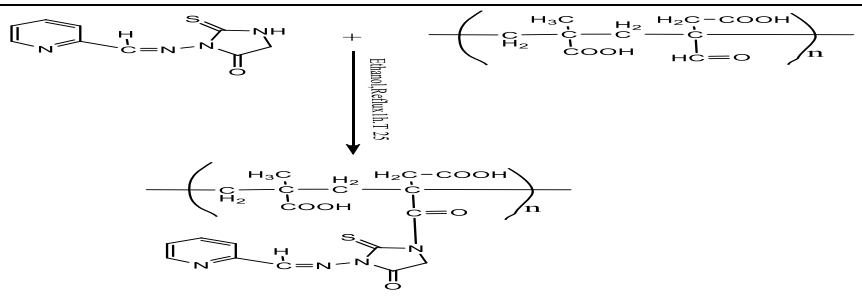
(7)


Ethanol,Reflux,6h,TFSC

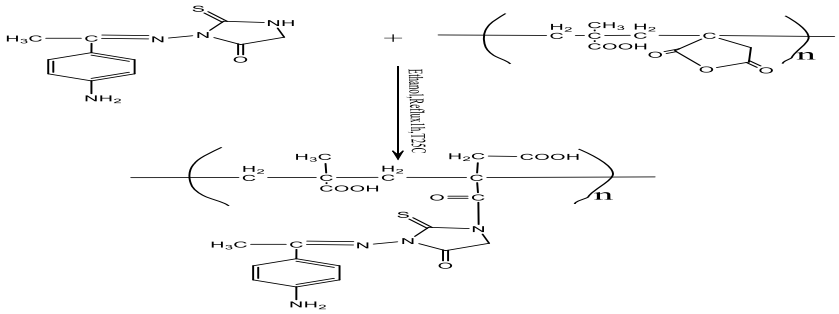
(8)


Ethanol,Reflux,6h,TFSC

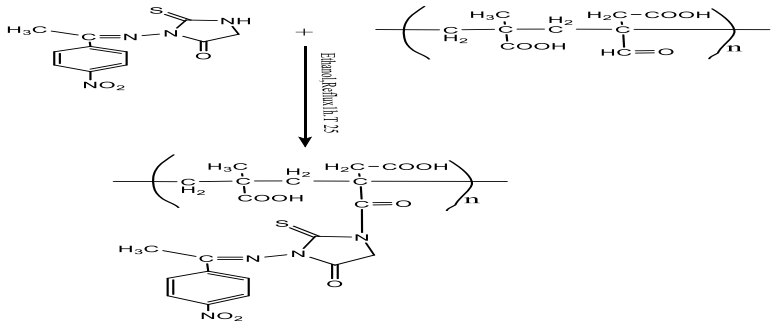
(9)


Ethanol,Reflux,6h,T 25

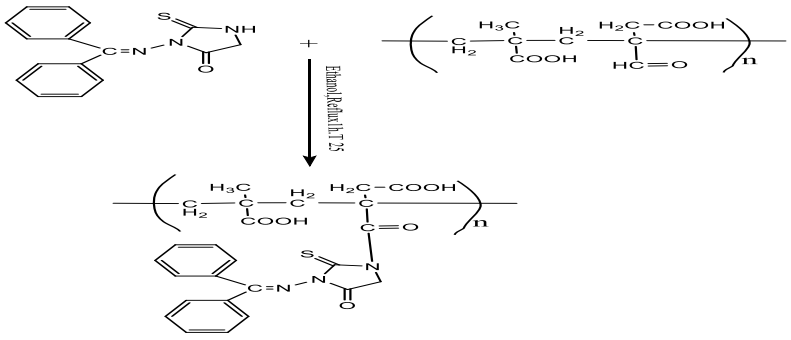
(10)


Ethanol,Reflux,6h,T25C

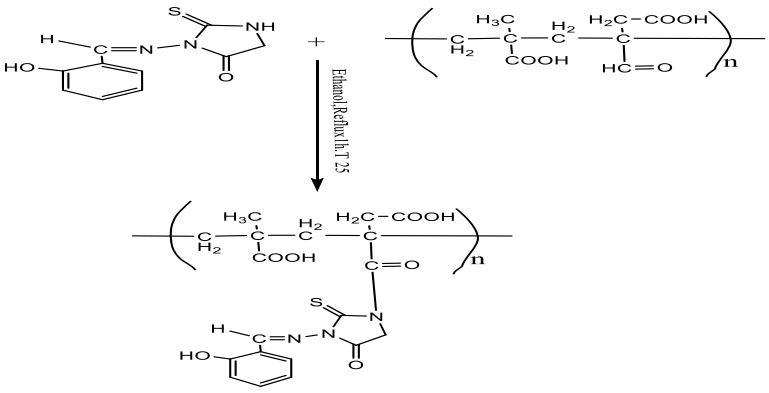
(11)


Ethanol,Reflux,6h,T 25

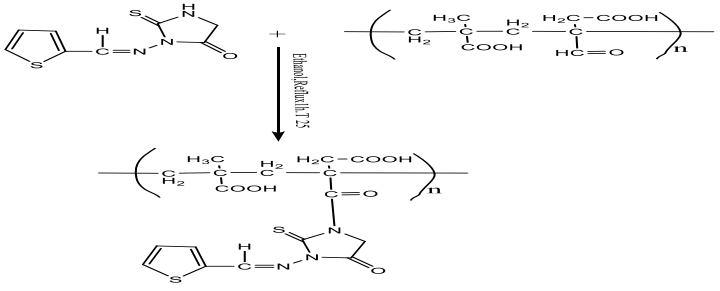
(12)


Ethanol,Reflux,6h,T 25

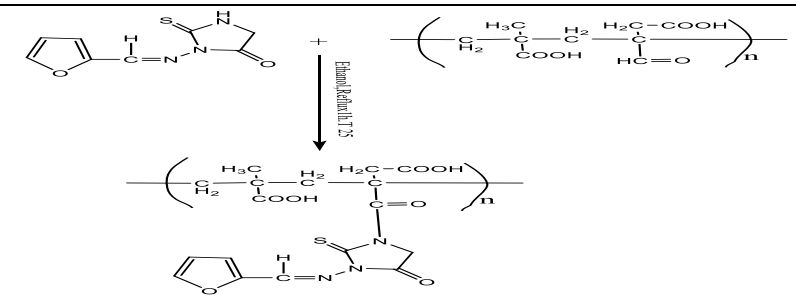
(13)



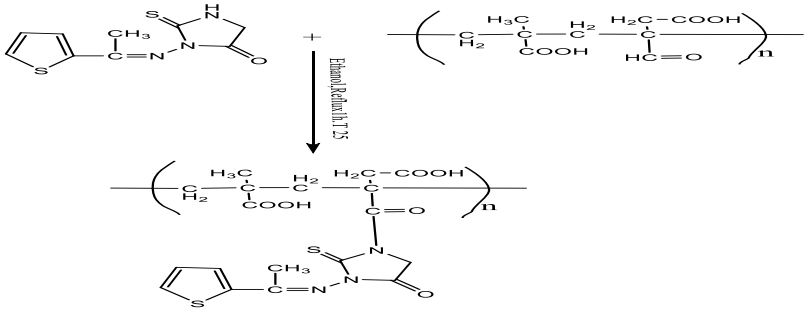
(14)



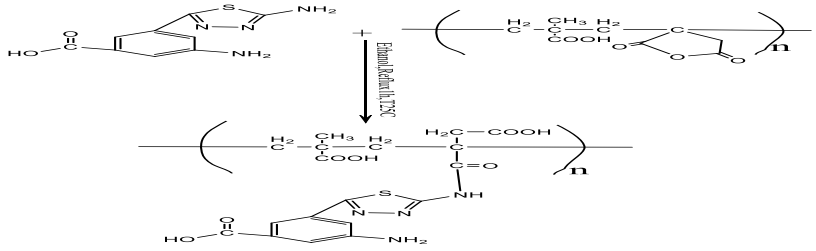
(15)



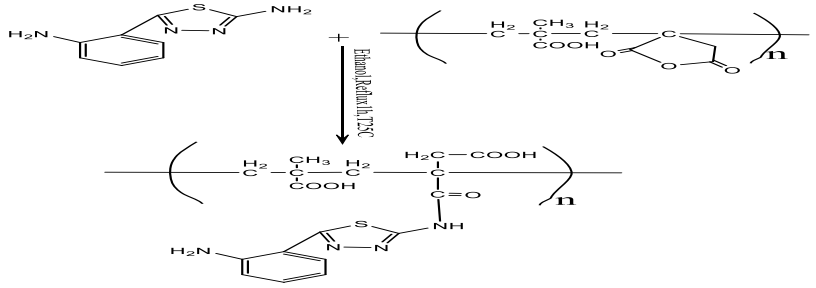
(16)



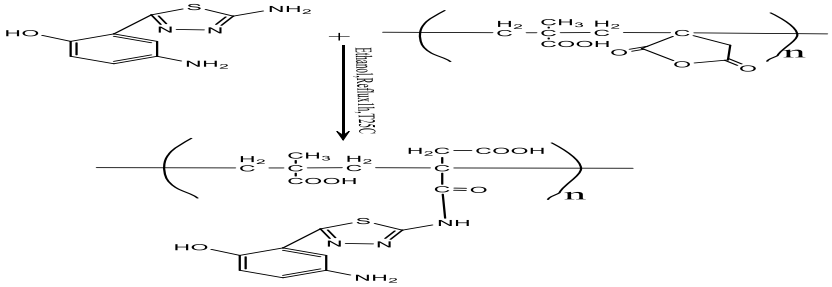
(17)



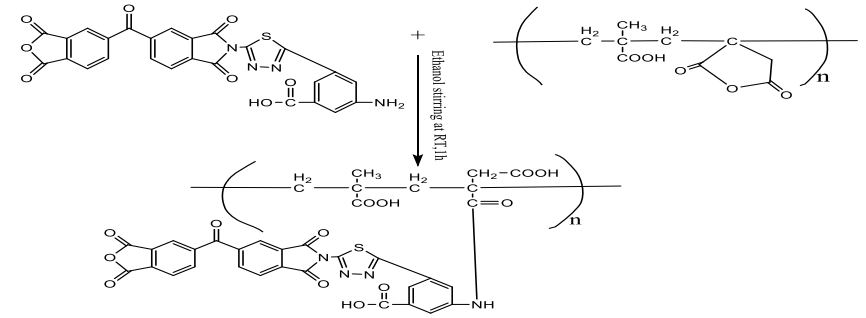
(18)



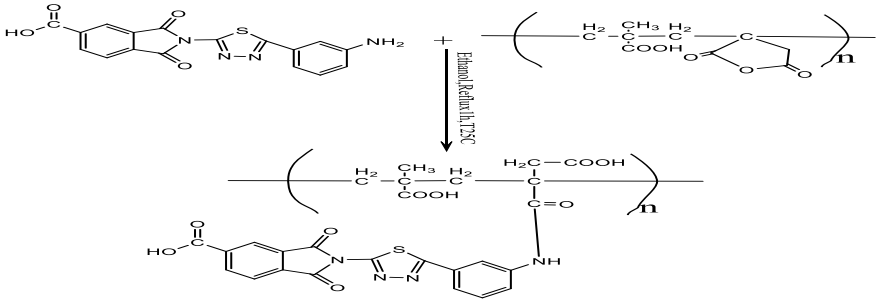
(19)



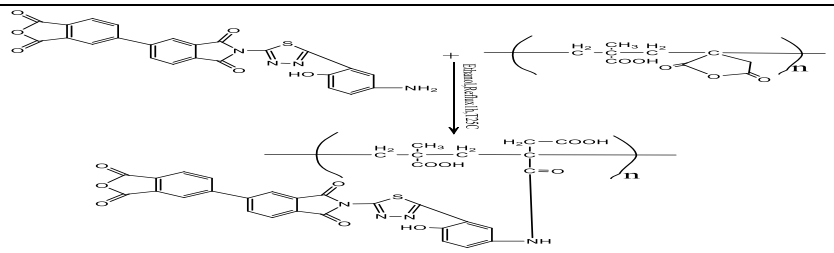
(20)



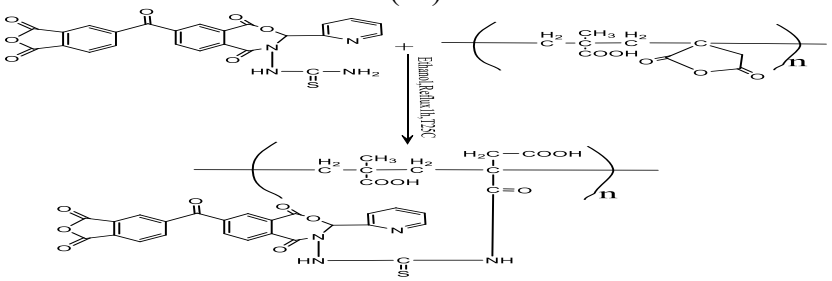
(21)



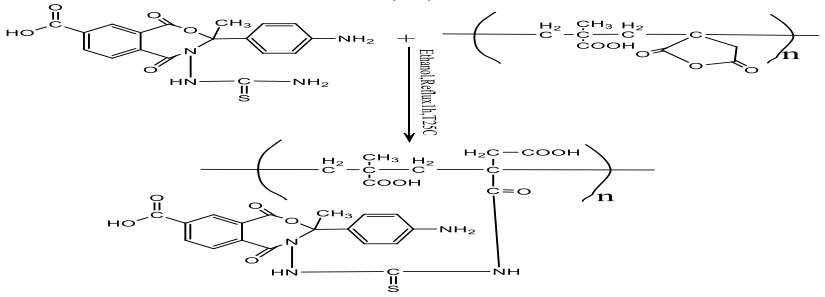
(22)



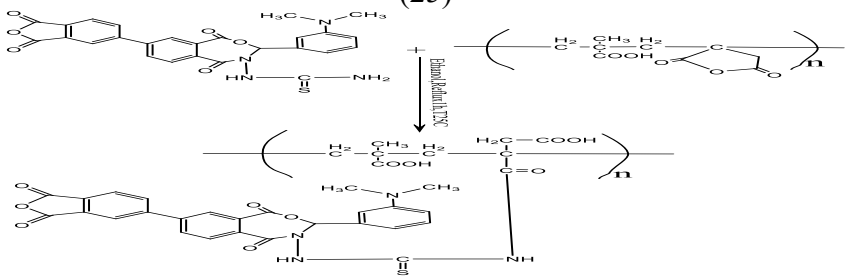
(23)



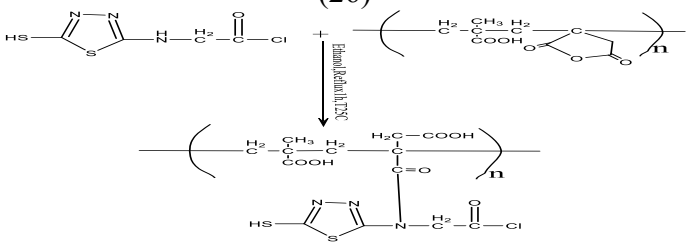
(24)



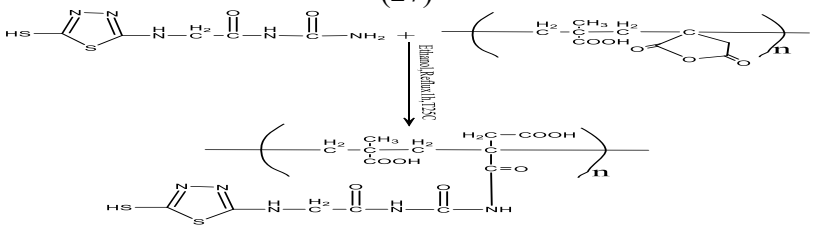
(25)



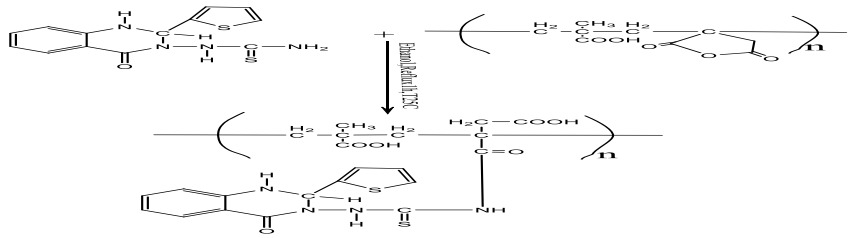
(26)



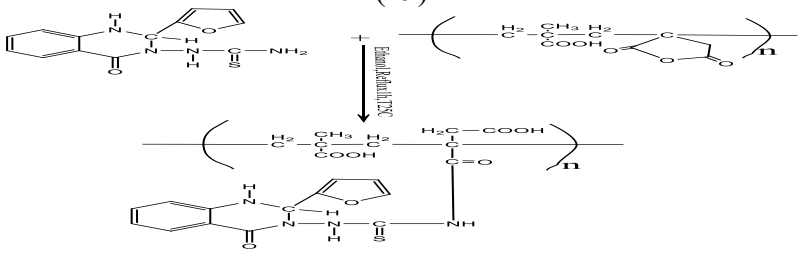
(27)



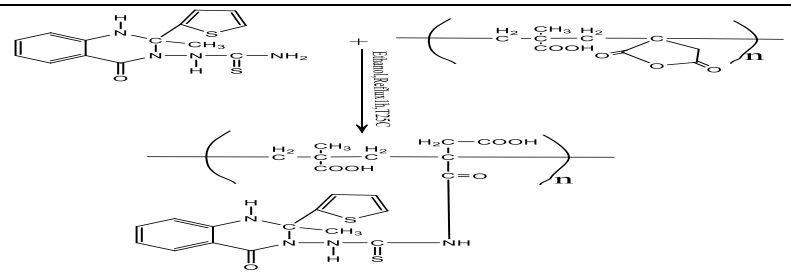
(28)



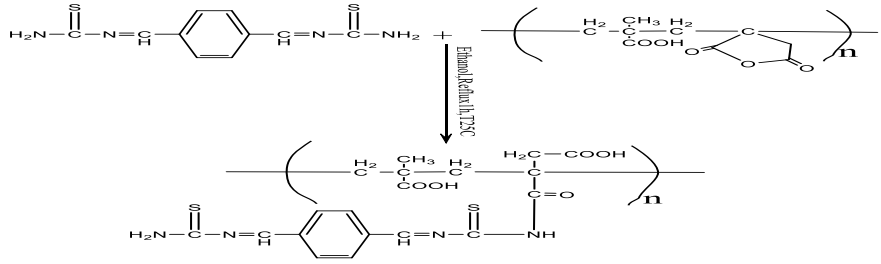
(29)



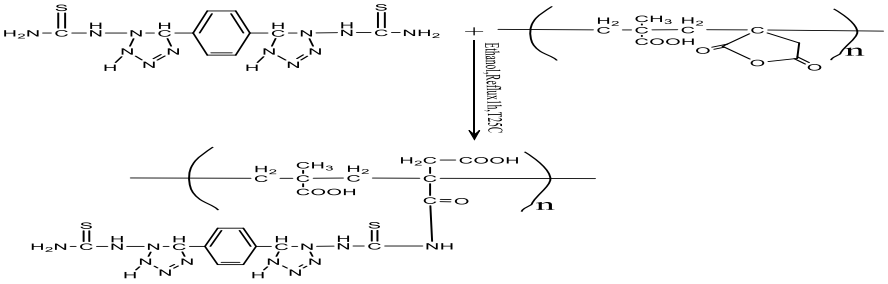
(30)



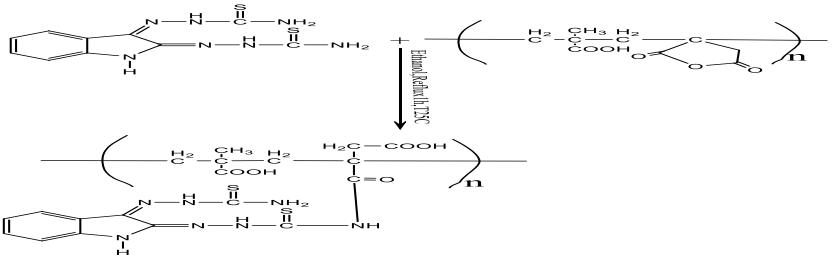
(31)



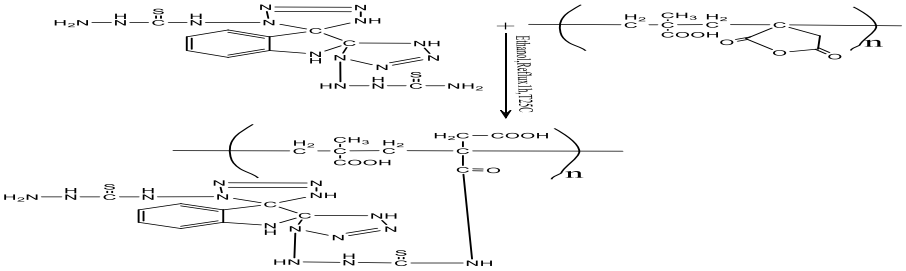
(32)



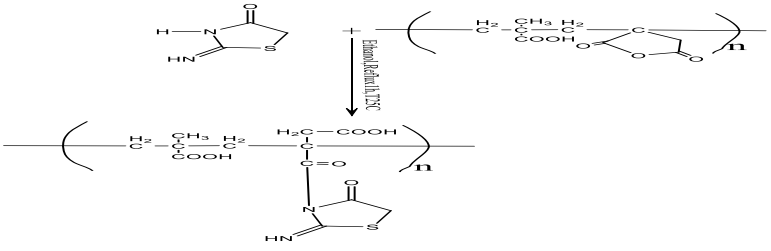
(33)



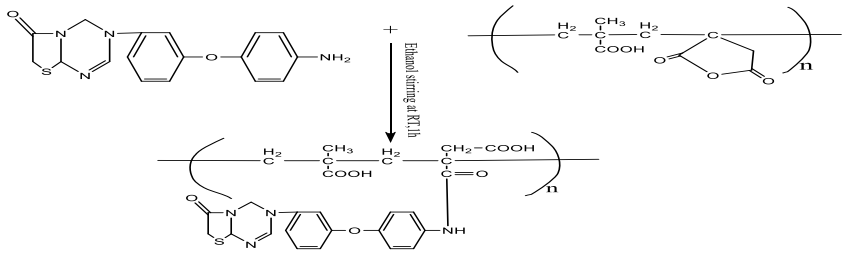
(34)



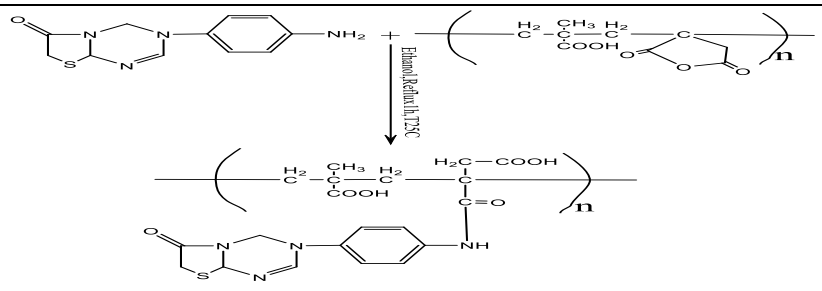
(35)



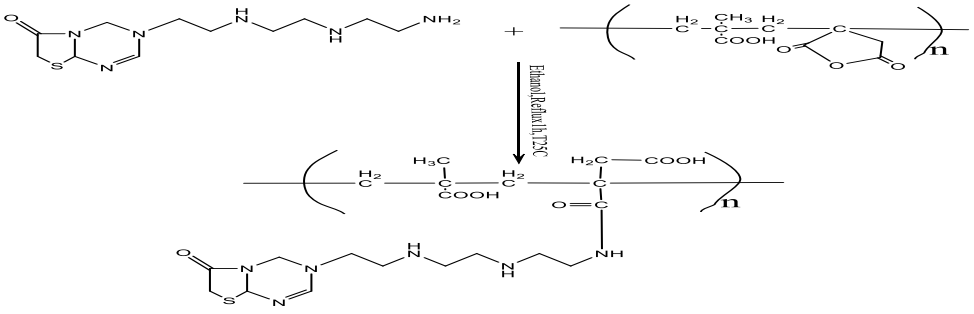
(36)



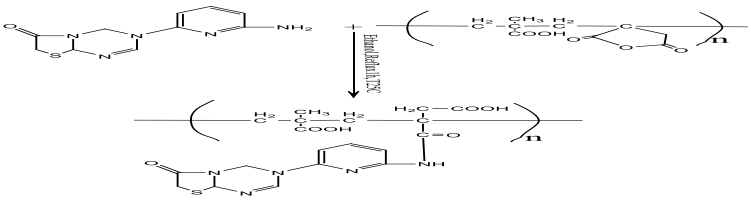
(37)



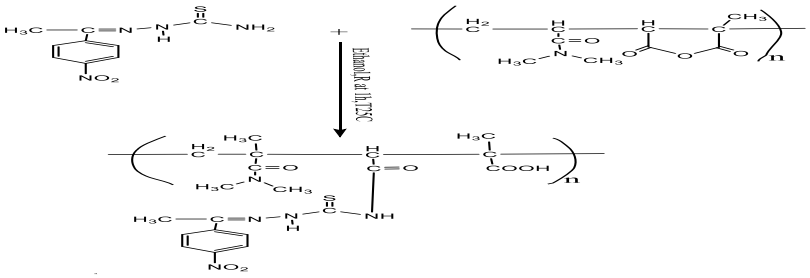
(38)



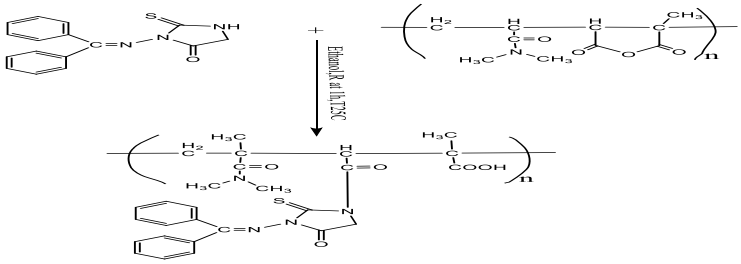
(39)



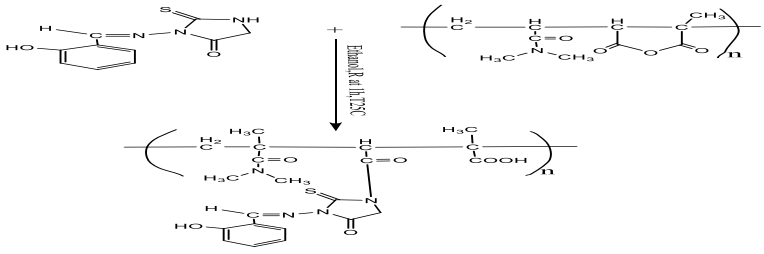
(40)



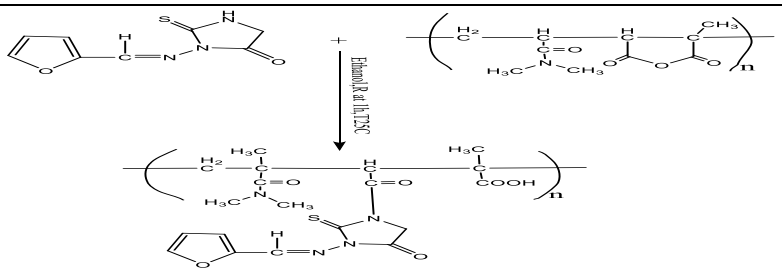
(41)



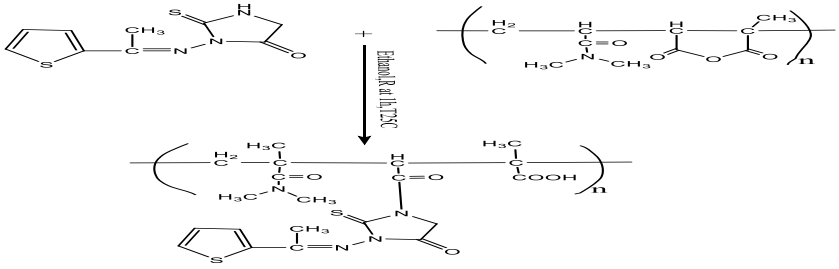
(42)



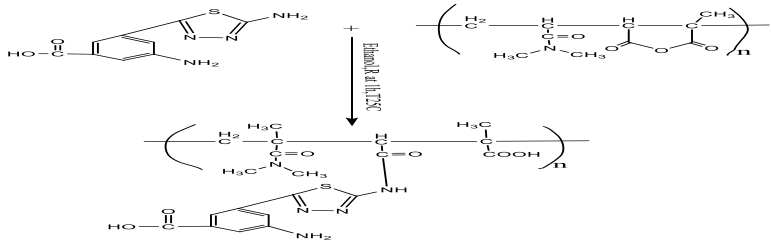
(43)



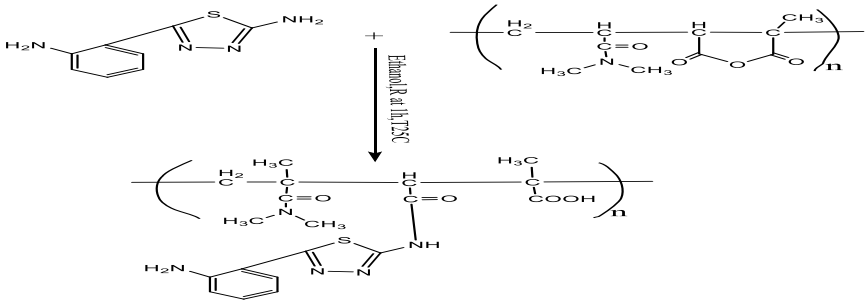
(44)



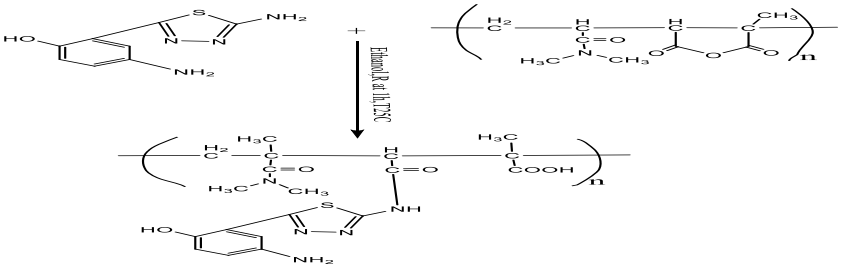
(45)



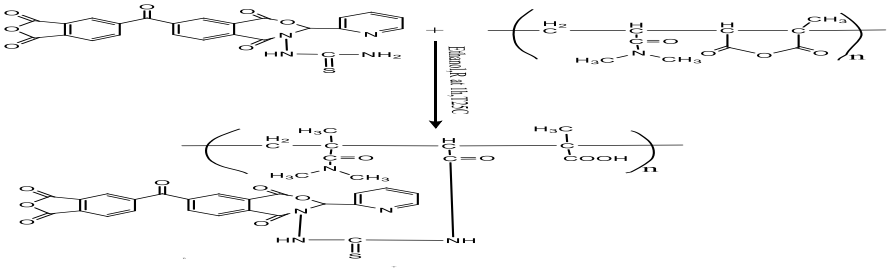
(46)



(47)

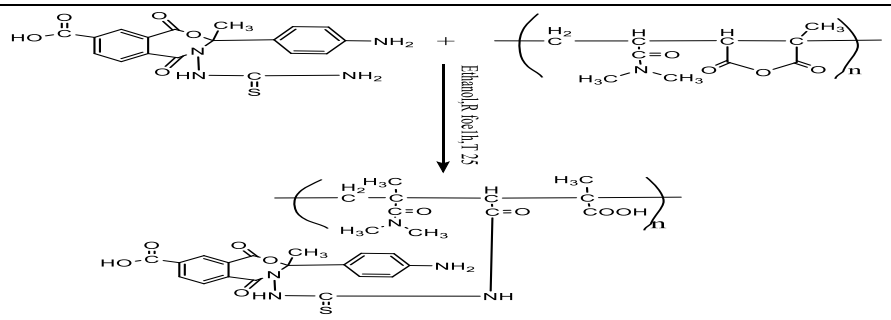


(48)

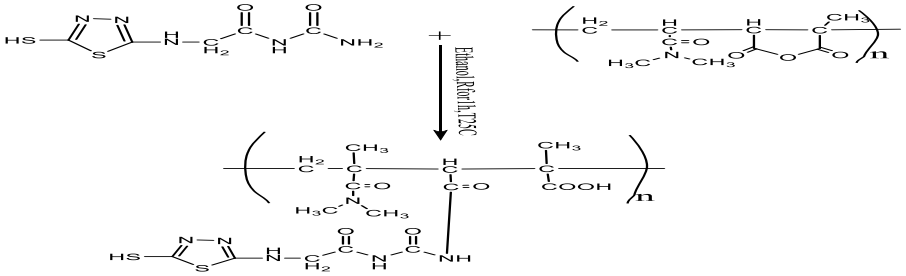


(49)

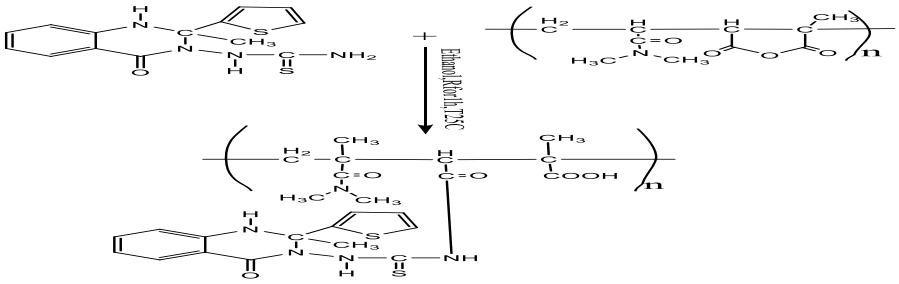
Summary


Ethanol,R.foe.1h,T.25

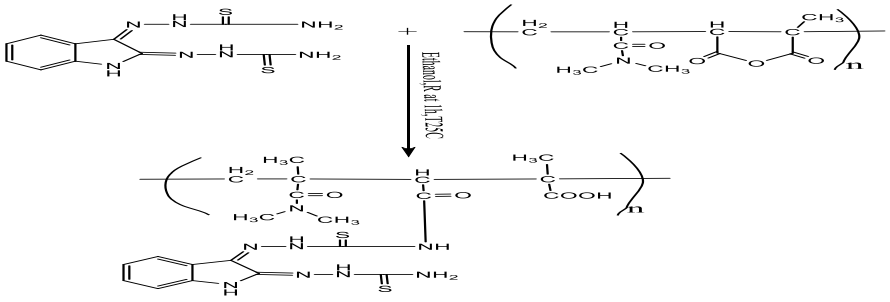
(50)


Ethanol,Rfor1h.T25C

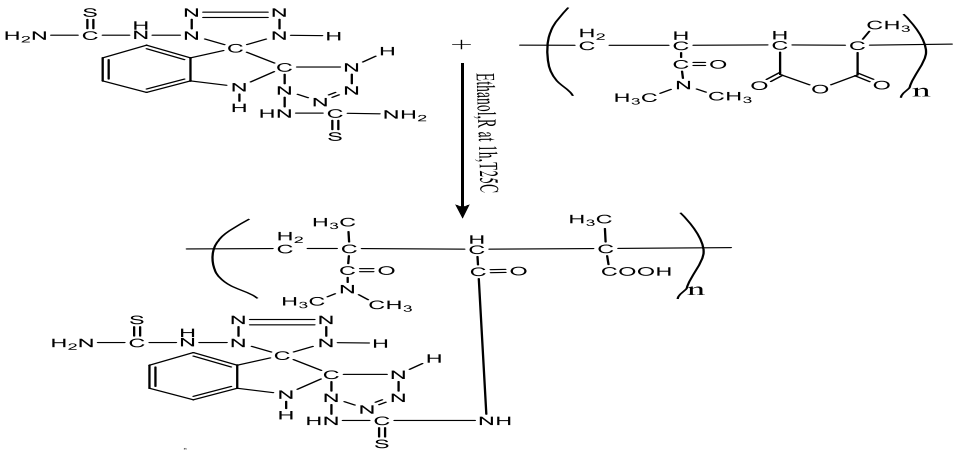
(51)


Ethanol,Rfor1h.T25C

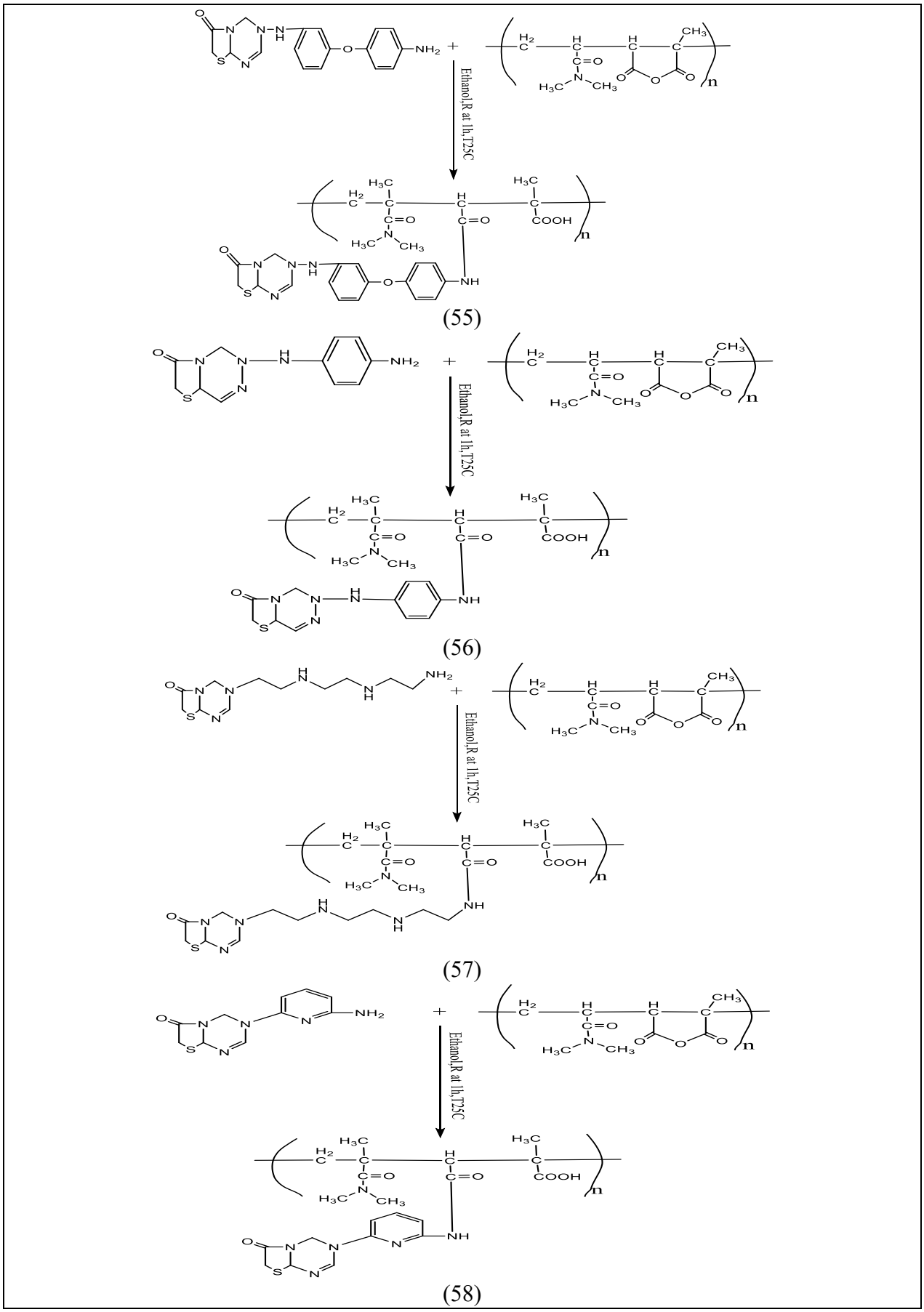
(52)


Ethanol,R at 1h.T25C

(53)


Ethanol,R at 1h.T25C

(54)


Ethanol,R at 1h,T25C
(55)
Ethanol,R at 1h,T25C
(56)
Ethanol,R at 1h,T25C
(57)
Ethanol,R at 1h,T25C
(58)

Scheme (12)

Thermogravimetric analysis (TGA) indicated that the copolymers (1-10) containing phenyl group as substituent in the pyridine ring and heterocyclic compounds had maximum thermal stability. It seems that using a bulkier substituent in the 4-position of the pyridine ring of diamine monomers causes improvement of solubility and thermal stability of resulting copolymers.

Glass transition temperature for copolymers are studied using differential scanning calorimeter (DSC). Exothermic peak of dendrimers appeared in the DSC measurement. The glass transition temperature of the copolymers increased with molecular weight, and the variation was consistent with theoretical calculations.

The molecular docking of ten synthetic copolymers (1-10) was calculated. Molecular docking facilitates the analysis of interactions between two compounds, thereby enabling the creation of a stable complex that can be utilized in various experiments. The results from the docking study can then be used for energy profiling, strength, and stability of the complexes. The ligand utilized can be any small molecule; the target protein may be a protein, carbohydrate, or nucleic acid. The data collected from the docking studies can be stored as raw data in databases for future experiments and uses.

Molecular docking is a computational approach used to predict the binding of molecules, referred to as ligands, to appropriate receptor proteins.

It is a tool utilized for various computational purposes, including drug discovery. It has become an essential tool in in drug development. It is used to study ligand-receptor binding interactions using measures such as docking scores, g-scores, binding free energies, etc. Such a method allows researchers to study small molecules and ensure that they can yield beneficial results before taking them for wet lab experiments.

The antimicrobial activity of the modified copolymer was tested against various microorganisms these four types of bacteria are Gram-positive (Staphylococcus aureus) and Gram-negative (Klebsiella pneumoniae, Pseudomonas aeruginosa, Escherichia coli), and two fungal (*Candida albicans***,** Aspergillus niger). In general,

the copolymers showed good antimicrobial activity against the previously mentioned microorganism. The Evaluation of biological activity of some newly synthesized of copolymers containing heterocycles compounds and to develop new drug candidates for cancer treatment against cancer cell line and cancer cell line incorporating different pharmacophore as hybrid molecules possessing antioxidant and antimicrobial activities.

The synthesis of some copolymers should advance our understanding of derivatives' biological activities investigate these compounds' prospective applications as antibiotics and identify the structure-activity correlations associated with such applications. Thus, we describe herein the synthesis, identification, and studied the biological activities to develop new therapeutics for this drug.

Ten of new copolymers synthesized **(10)** was evaluated for their cytotoxicity activity against the cancer cell lines used were the colon cancer cell line caco2 and skin cancer cell line revealed increased inhibition compare to the normal cell line. This interpretation is supported by the consistent decrease in IC_{50} values from 24 to 72 hours across all compounds, as well as the maintained difference between colon cancer (HCT-116) and normal (HdFn) cell lines.

Chapter One

Introduction

1.1 Introduction

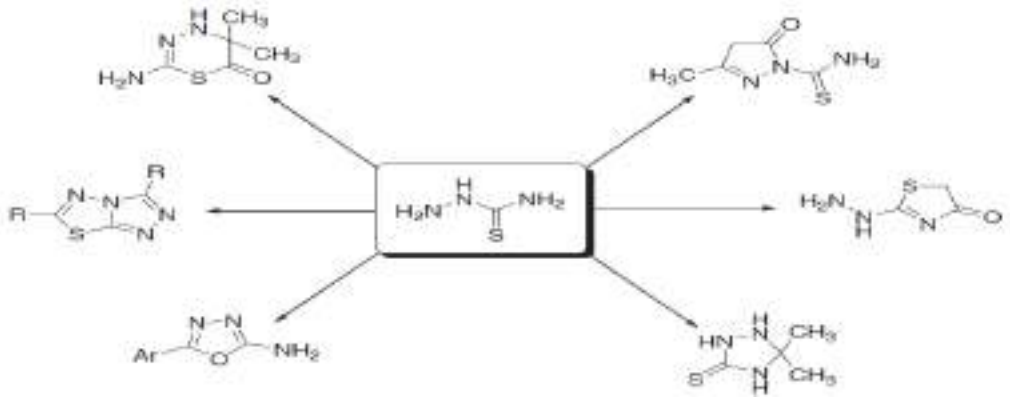
Heterocyclic compounds are one of the largest categories related to organic-anchored substances, and they have a profound effect on human evolution. Some examples of heterocyclic compounds that are essential for human life include glucose, DNA, and vitamins B1, B2, C, and D (1) .heterocyclic polymers ideal for applications where high thermal stability is required, such as the aerospace industry. The advancement in the fields related to science and technology has resulted in designing and synthesis of various heterocyclic polymers with tailored properties. Heterocyclic polymers display specific thermal, mechanical, and photophysical properties as a result of the electronic effect and ring tension related to heterocyclic structures, this resulted in producing various applications in manufacturing, biological-based materials, organic photovoltaics, and light-emitting diodes, (2) . Functional polymer science is an interdisciplinary field that encompasses polymer chemistry, materials science, biology, and the environment. It is a relatively new field, having developed in the 1960s (3) .

Heterocyclic polymers have various potential applications, but their synthesis can be challenging. Direct attachment of all the modified heterocycles to the polymer backbones that utilizes reactive heterocyclic monomers that have been synthesized is considered as a typical synthetic technique. However, the lengthy procedure related to reaction, challenging conditions in term of polymerization, challenges with numerous substituent inclusion, and affordable heterocyclic monomers usually hamper this kind of synthesis technique (4). However, acetylenic polymers, which are synthesized from triple-bond building blocks, possess electronically unsaturated double bonds, fused aromatic rings, or fused heterocyclic units in their main chain.

Many polymers with reactive functional groups are now synthesized, tested and used not only for their macromolecular properties, but also for the properties of their functional groups. These functional groups provide an approach to a subsequent modification of the polymer for specific end applications (5).

Nowadays a strong demand prevails for functional polymers with very specific properties. Functional groups give the polymer structure of special characters substantially different from the inherent properties of the basic polymer chain (6) . In recent years some comprehensive work has been published on functional monomer and their polymers (7-10) . The antimicrobial property of the polymers plays an important role for many of its applications. Contamination by microorganisms is of great concern in several areas such as medical devices, health care products, water purification systems, hospital and dental equipments, etc. One possible way to avoid the microbial contamination is to develop materials possessing antimicrobial activities. Consequently, biocidal polymers have received much attention in recent years (11).

Thiosemicarbazones and the corresponding metal complexes are widely known as having a large range of biological applications, such as antiviral, antimalarial, antifungal, (12, 13).The compound pacetamidobenzaldehyde thiosemicarbazone, commercially available as thiacetazone, has long been employed in the treatment of tuberculosis (14) .The activity of these compounds is strongly dependent upon the nature of the heteroaromatic ring and the position of attachment to the ring, as well as the form of the thiosemicarbazone moiety. Some thiazole, thiosemicarbazole, imidazole, benzothiazole derivatives (15-19) and isatin (20-22) are mentioned in literature to show antimicrobial (23-26) antifungal (27), antihelmitic (28) pesticide and herbicidal properties.



The high reactivity of anhydride ring in the copolymers based on anhydride acid toward the nucleophilic reagents (29-32) would suggest the possibility of its

opening by various nucleophilic compounds in order to obtain new products with potential biological activity. There are many systems mentioned in the literature (33), obtained through the opening of the anhydride ring of anhydride copolymer with some vinyl monomers, especially with the methacrylate, under the action of heterocyclic compounds. It must be mentioned that these copolymers are biocompatible, and some of them present an important intrinsic biological activity (34, 35).

1.2 Aim of the work

1. To synthesize of new series of new copolymers derived from poly (**MAA-IAN**) and poly (**DMA-CON)** containing five and six cyclic member's heterocyclic compounds have been of great interest on account of their variety of applications particularly in the field of chemotherapeutic, antimicrobial and fungicide.
2. To synthesize a series of new Schiff Bases derivatives by reaction with several aromatic of aldehydes and ketones.
3. To synthesize of 5-Styryli-2-amino-1, 3, 4-thiadiazole derivatives from the reaction of 5-amino phthalic acid, Anthranilic acid and 5-amino-2-hydroxybenzoic acid with thiosemicarbazide.
4. To synthesize of 2-(4-substituted-benzylidene hydrazono)-1, 3-thiazolidine-4-one compounds from Treatment of Schiff Bases with Chloroacetic acid and anhydrous sodium acetate
5. To synthesize of new Oxazepines derivatives and cyclization by the treatment of Schiff bases with anhydride acid.
6. To synthesize of new imides derivatives from the reaction of 3, 3', 4, 4'benzophenone tetracarboxylic dianhydride, Trimellitic anhydride and 3, 3, 4, 4-Biphenyl tetra carboxylic dianhydride with 5-Styryli-2-amino-1, 3, 4-thiadiazole.
7. To synthesize of new acetamide derivatives from the reaction of 2-amino 1, 3, 4-thiadiazole-5-thiol with chloro acetyl chloride.

8. To synthesize of new ureidoacetamide derivatives from the reaction of urea acetamide compound.
9. To synthesize f 2, 3-dihydroquinosulin-4-one derivatives from the reaction of Schiff bases derivatives with of anthranilic acid.
10. To synthesis of tetrazole derivatives from the reaction of Schiff bases derivatives that obtained from terphthaldehyde and Isatin with of sodium azide.
11. To synthesize of 2- iminothiazolidine – 4- one from the reaction of thiourea with of mono chloro acetic acid
12. To synthesize of Mannich compound derivatives from the reaction of formalin with 1, 4-phenylenediamine and Triethylenetetramine compounds.
13. To synthesize new copolymers (methyl acrylic acid- Itaconic anhydride) and (N, N-dimethyl acrylamide-Citraconic anhydride) by radical photopolymerization of vinyl monomers (methyl methacrylate, Itaconicanhydride, N, N-dimethylacrylamide and Citraconic anhydride) carried out using 1-hydroxy cyclohexyl phenol ketone as the initiator
14. To synthesize new heterocyclic compounds that allowed to react with (methyl acrylic acid- Itaconic anhydride) and (N, N-dimethyl acrylamide-Citraconic anhydride) copolymers to obtain higher biological active products. Several studies have demonstrated the antimicrobial and antifungal action of these compounds using four bacterial strains klebsiella pneumonia, Staphylococcus aureus, Escherichia coli, Pseudomonas Aeruginosa, and two fungi Aspergillus Niger, and Candida Albicans respectively.
15. To synthesize novel heterocyclic copolymers, which possess great thermal stability and processability. In addition, synthesis of novel functional heterocyclic copolymers based on previous structure-property relationships, the target polymer structure is designed. An effective

synthetic method **is** then developed for the monomers. and then polymerization conditions are optimized.

Finally, the new polymers synthesized are characterized and the properties are evaluated:

1. To Identify the chemical structures of the synthesized compounds by various spectroscopic techniques such as Nuclear Magnetic Resonance Spectroscopy ^{1}HNMR, ^{13}CNMR, Fourier Transform Infrared Spectroscopy (FTIR) and CHNOS analysis.
2. To Evaluate the biological activity of some newly synthesized copolymers and to develop new drug candidates for cancer treatment against the colon cancer cell line_caco2 and skin cancer cell line incorporating different pharmacophore as hybrid molecules possessing antioxidant and antimicrobial activities.
3. To study findings for the first time the synthesis of some should advance our understanding of derivatives' biological activities investigate these compounds' prospective applications as antibiotics and identify the structure-activity correlations associated with such applications. Thus, we describe herein the synthesis, identification, and studied the biological activities to develop new therapeutics for this drug.

Chapter Two
Theoretical Part

2. Theoretical Part

2.1 Polyheteroatomic Heterocycles

2.1.1 Overview on the Heterocyclic

Two hundred years ago, the chemical science was an undivided field; around 1900 a division into inorganic, organic and physical chemistry became necessary. Over the years, a progressive segmentation into subdisciplines, very often interconnected, has become necessary. Heterocyclic included inside compounds have been studied since half of 1800s due to their wide occurrence in nature; however the heterocyclic chemistry was born as a branch of organic chemistry only after the Second World War. Two main types of molecular structures could be recognized in organic chemistry: the aliphatic acyclic compounds, in which the atoms form a chain, and the cyclic (aliphatic or aromatic) compounds, in which the atoms form a ring. If only one element take part to the formation of a cyclic compound, then we refer to an isocyclic compound (e.g. if the ring consists of C-atoms only, then we speak of carbocyclic compound). Cyclic compounds with at least two different atoms in the ring are known as heterocyclic compounds. The ring itself is called a heterocyclic. If the ring contains no C-atom, then we speak of an inorganic heterocyclic. If at least one ring atom is a C-atom, then the molecule is an organic heterocyclic compound. In this case, all the ring atoms which are not carbon are called heteroatom (Fig.2-1).

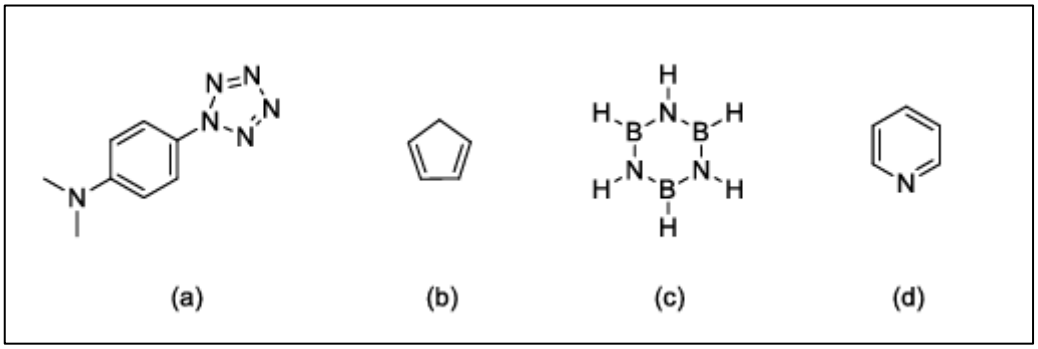


Figure (2- 1): Differences between heterocyclic and isocyclic compounds: (a) (4-dimethylaminophenyl) pentazole, an isocyclic compound; (b) Cyclopenta-1, 3-diene, isocyclic and carbocyclic compound; (c) Borazine, an inorganic heterocyclic compound; (d) Pyridine, an or organic heterocyclic aromatic compound.

Nitrogen, oxygen and sulfur are the most common heteroatoms, but heterocyclic rings containing other heteroatoms are also widely known. In a 1983 report, the International Union of Pure and Applied Chemistry (IUPAC) recognized 15 elements coming from groups II to IV of theperiodic system capable of forming cyclic structures with carbon atoms (36).

To determine the stability and reactivity of heterocyclic compounds, it is useful to compare them with their carbocyclic analogues. In principle, it is possible to derive every heterocycle from a carbocyclic compound by replacing appropriate CH2 or CH groups by heteroatoms. If one limits oneself to monocyclic systems, one can distinguish four types of heterocyclic as follows (37).

1- Saturated heterocyclic (heterocycloalkanes): in this category, there are no multiple bonds between the ring atoms. The compounds react largely like their aliphatic analogues.

2- Partially unsaturated systems (heterocycloalkenes): if the multiple bonds are between two C-atoms of the ring compounds react essentially like alkenes or alkynes. The heteroatom can also be involved in a double bond, with reactivity close to the corresponding acyclic double bonds.

3- Systems with the greatest possible number of noncumulated double bonds (heteroannulenes): each heteroatom can donate one electron pair to the conjugated system and its nonbonding electron pair does not contribute (as in pyridine), or else, one electron pair of the heteroatom is incorporated into the conjugated system (delocalization of the electrons, such as in furane or pyrrole). 4-Heteroaromatic systems (heteroarenes): this includes heteroannulenes, which comply with the HÜCKEL rule, i.e. which possess $(4n + 2)$ π-electrons delocalized over the ring.

In 1887 and 1888, Hantzsch (38) and Widman (39) independently introduced methods for naming fiveand six-membered nitrogen monocycles. The system was extended to include rings of other sizes, additional heteroatoms, and the expression of various levels of hydrogenation. In 1957, the IUPAC Commission on Nomenclature of Organic Chemistry codified this extension of the Hantzsch-

Widman system as part of its rules for the nomenclature of organic chemistry (40).

Nowadays the extended Hantzsch-Widman system accomplishes several tasks. First, the identity of the different atoms is established by placing different prefixes for each type of non-carbon atom. The three mainly used prefixes are oxa-, thia-, and aza- for oxygen, sulfur, and nitrogen, respectively (the final 'a' is elided before a vowel). Second, the position of the heteroatoms is denoted by ring atom numbers. Numbering starts at an oxygen, sulfur or nitrogen (in decreasing order of preference) and continues in such a way that the heteroatoms are assigned the lowest possible numbers. Third, the size and degree of unsaturation of the ring is determined by the suffix at the end (Table2-1); partially saturated rings are indicated by the prefixes 'dihydro', 'tetrahydro', etc.

Table (2- 1): Common name endings for heterocyclic compounds.

	Ring with Nitrogen			Ring without Nitrogen		
Ring size	**Maximum unsaturation**	**One double Bond**	**Saturated**	**Maximum Unsaturation**	**One double bond**	**Saturated**
3	**-irine**	**-**	**-iridine**	**-irene**	**-**	**-irane**
4	**-ete**	**-etine**	**-etidine**	**-ete**	**-etene**	**-etane**
5	**-ole**	**-oline**	**-olidine**	**-ole**	**-olene**	**-olane**
6	**-ine**	**-**	**-inane**	**-in**	**-**	**-ane**
7	**-epine**	**-**	**-**	**-epin**	**-**	**-epane**
8	**-ocine**	**-**	**-ocin**	**-ocin**	**-**	**-ocane**
9	**-onine**	**-**	**-**	**-onin**	**-**	**-onane**
10	**-ecine**	**-**	**-**	**-ecin**	**-**	**-ecane**

In compounds with maximum instauration, if the double bonds can be arranged in more than one way, their positions are defined by indicating the nitrogen or carbon atoms which are not multiply bonded, and consequently carry an 'extra' hydrogen atom, by 1H-, 2H- etc. In partially saturated compounds, the positions of the hydrogen atoms can be indicated by 1, 2- dihydro', etc. (together with the 1H-type notation if necessary); alternatively, the position of the double bonds can be specified; for example 'Δ^3- indicates that a double bond is between atoms 3 and 4. A positively charged ring is denoted by the suffix '-ium'. Many heterocyclics, as well as many other organic compounds, were identified early on, and received trivial names which are still preferred.

Fig. (2-2) shows some of the most known monocyclic compounds, with the common (trivial) name in red and a systematic name based on the Hantzsch-Widman system given in black.

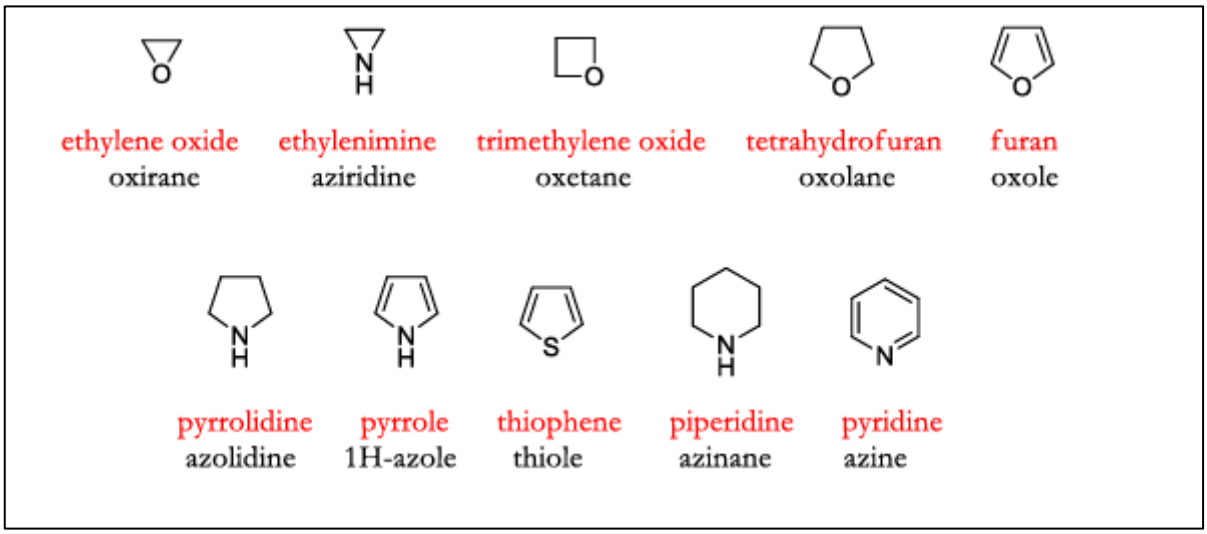


Figure (2- 2): Common monocyclic compounds with trivial and systematic name.

Among these common monocyclic compounds, there are some which belong to a well-defined type of heterocycles of the four cited before: the aromatic heterocycles. In particular, the most used in organic synthesis, and not just, are the five-membered rings, like furan, pyrrole and thiophene, and the six- membered rings, like pyridine.

When is an heterocycle aromatic? To establish the aromaticity of a heterocyclic compound, it needs to respect some criteria which must be applied to each compound that we want to call aromatic. They are the following:

1-The molecule must be cyclic;

2-Every atom in the ring must have an occupied p orbital, which overlaps with p orbitals on either side. In this way, the molecule is fully conjugated;

3-The molecule must be planar;

4-The molecule must contain an even number of pairs of π electrons and it must satisfy Huckel's rule: (4n+2)π electrons, where n is an integer starting from zero.

In the case of heterocycles, this latter rule is fulfilled thanks to the lone pair on the heteroatom that is delocalized inside the π electrons system of the ring. For example, furan has got the oxygen atom which is sp^2 hybridized. One lone pair is in

the π system and the other in the plane of the ring (analogous to C-H bond on the other positions). The sum of π electrons is 6, so furan is aromatic. If these aromatic rings, both five- and six-membered, are fused with benzene ring, it can be possible to obtain new aromatic heterocycles with different structures, as showed in (Fig 2-3) below

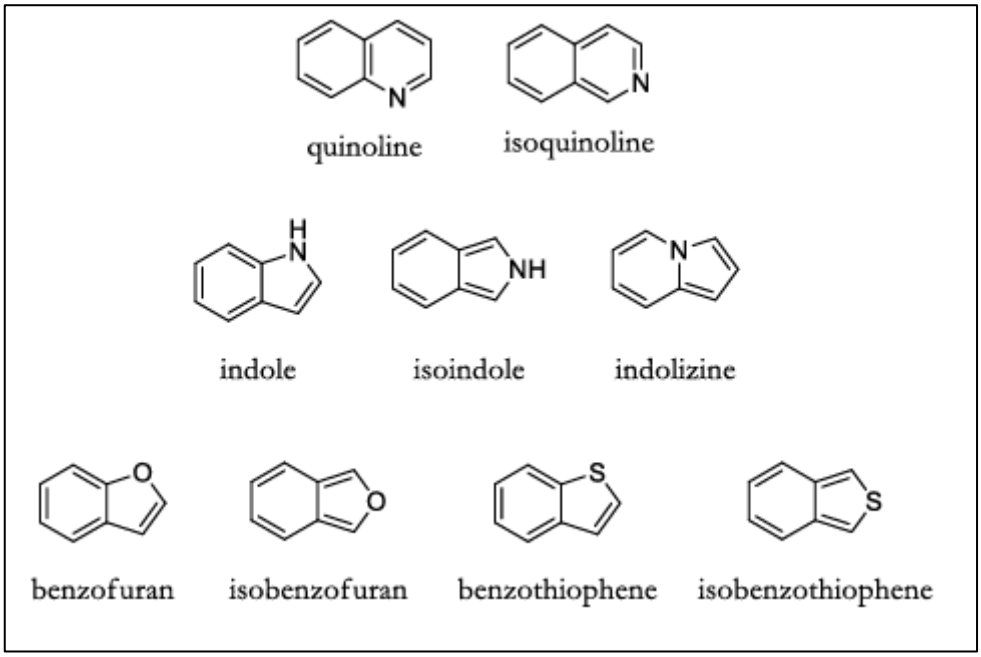


Figure (2- 3): Common benzofused aromatic heterocycles.

All these structures are planar containing 10 π-electrons including the non-bonding electron pair of heteroatom as in monocyclic heterocycles. These 10 π-electrons are delocalized over the ring. Because of the involvement of non-bonding lone pair of heteroatom in aromatization, it makes the five- and six-membered rings more prone to attack by electrophilic reagents.

2.1.2 Natural Occurrence

Heterocycles are by far one of the largest and most significant classes of organic compounds, mainly because they are the basis of life. This is not an overstatement if we think that the majority of macromolecules constituting living organisms are built around heterocyclic motifs.

The first natural molecules that may come to mind are, for sure, Heme and Chlorophyll, which are the oxygen carriers in animals and plants, respectively (Fig. 2-4). Both of them are derivatives of porphyrin, aromatic heterocyclic macrocycles

composed of four modified pyrrole subunits (in the case of Heme) or three modified pyrrole subunits and one of pyrroline (in the case of Chlorophyll), interconnected at their α carbon atoms via methine bridges (=CH−).

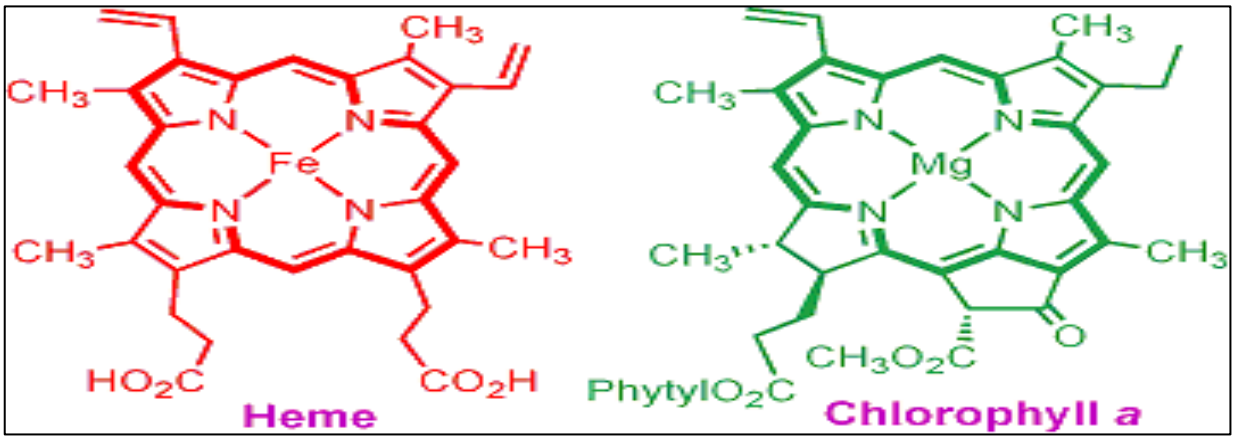


Figure (2- 4): Representation of the pigments of life: Heme and Chlorophyll a.

Heterocycles are also present in most vitamins, an organic compound required by an organism as a vital nutrient in limited amounts (41), it cannot be synthesized in sufficient quantities by the organism and must be obtained from the diet. One of the most remarkable vitamins is Vitamin C or ascorbic acid, very important for our life because it is involved in several collagen synthesis reactions for wound- healing and for preventing bleeding from capillaries, but also it acts as an antioxidant against free radicals and the oxidative stress (Fig. 2-5). (42) It has to take it by eating many fruits, vegetables and beef liver in order to prevent diseases derived by its deficiency, like the scurvy.

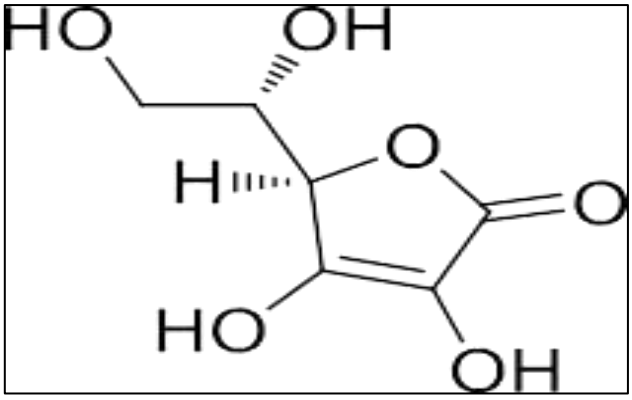


Figure (2- 5): Vitamin C or ascorbic acid structure.

Moreover, heterocycles are found in another class of organic molecules, fundamental for organisms: the amino acids, essential for the construction of several

proteins. These biologically important organic compounds are composed of amine ($-NH_2$) and carboxylic acid (-COOH) functional groups, along with a side-chain specific to each amino acid. Precisely, this latter differentiates properties and characteristics of a single amino acid and it is also maintained after that the new protein is formed.

Recent estimates tell that about 500 amino acids are known, 22 of these ones are present in the eukaryote organisms, available to synthetize proteins, and only 9 are essential amino acids, that means they are not produced *de novo* by the organism and they have to be assimilated from the diet. One of these essential amino acids contain an heterocycle and it is tryptophan (Fig. 2-6), which have an indole functional group and is the biochemical precursor of important compounds, like serotonin and the Vitamin B3 or nicotinic acid.

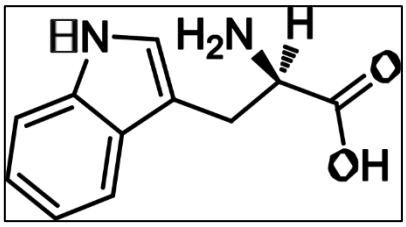


Figure (2- 6): Tryptophan structure.

It is possible to continue with an almost infinite series of examples that demonstrate the spread occurrence of heterocyclic compounds in nature, which certainly is the best teacher and source of inspiration for synthetic chemists.

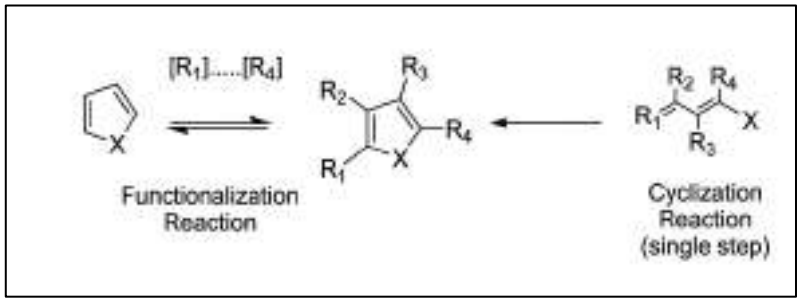
Why does nature utilize heterocycles? The answer to this question is provided by the fact that heterocycles are able to get involved in an extraordinarily wide range of reaction types. Depending on the pH of the medium, they may behave as acids or bases, forming anions or cations. Some interact readily with electrophilic reagents, others with nucleophiles, yet others with both. Some are easily oxidized, but resist reduction, while others can be readily hydrogenated but are stable toward the action of oxidizing agents. Certain amphoteric heterocyclic systems simultaneously demonstrate all of the above-mentioned properties. The ability of many heterocycles to produce stable complexes with metal ions has great biochemical significance.

2.1.3 Strategies for the Synthesis of Heterocyclic

Chemistry of heterocyclic compounds is so vast that it is almost impossible to summarize in a single chapter their several ways of synthesis. However, from a conceptual point of view, it is possible to divide the preparation of polyfunctionalized heterocycles using two major strategies (Scheme 2-1), or combination of both of these:

1- Incorporation of functional group in a pre-existing heterocycle.

2-Ring construction through cyclization of acyclic precursors.



Scheme (2- 1): Possible strategies for the synthesis of polysubstituted heterocycles.

Nowadays, formation of cyclic core followed by incorporation of further functionalization is a frequent approach to access heterocycles. Electrophilic or nucleophilic substitution are often used, and recently organometallic C-H functionalization has been developed (Fig. 2-7). (43)

Even these type of functionalization are extremely important, however, increasing the complexity of the system, regioselectivity remains a big problem to overcome. Presence of different heteroatoms, for example, could influence greatly the electronic feature of the ring, leading to low yield of desired products. (44)

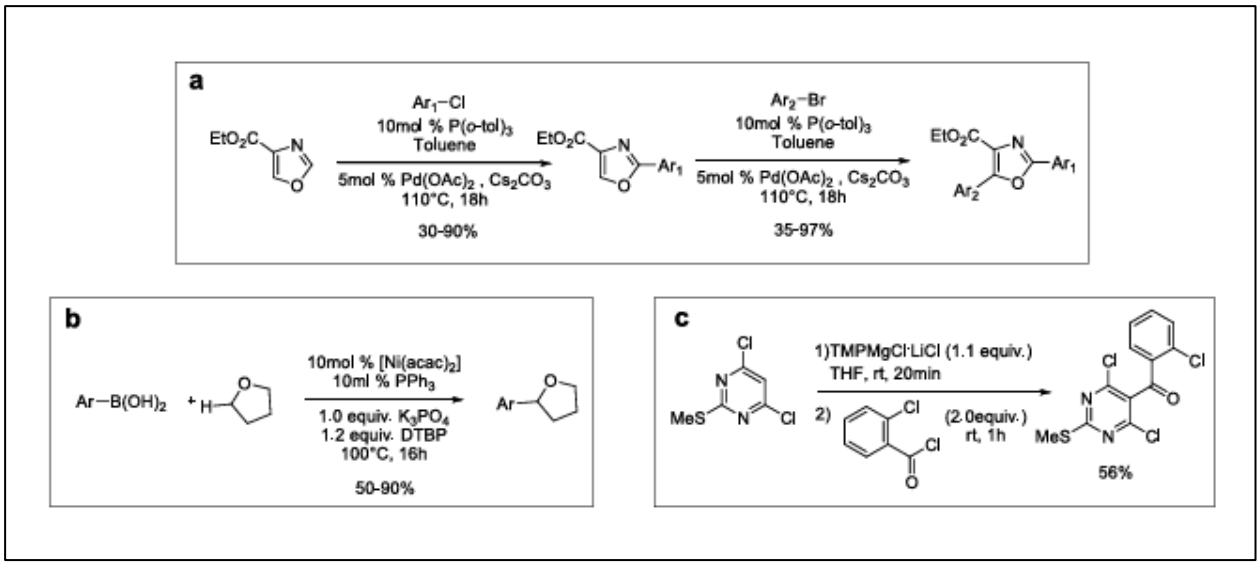


Figure (2- 7): Some selected organometallic C-H functionalization of heterocycles. (a) Pd(II) catalyzed sequential C-H functionalization of oxazole. (b) Nickel catalyzed THF functionalization. (c) Organ magnesium metallation/functionalization of pyrimidine.

Differently, cyclization reactions give well defined polysubstitution, generally with high regio- and stereochemical control. For this reason, the cyclization of acyclic precursors that contain linearly encoded functional group, is still largely used for the synthesis of heterocycles. In literature, we can come across several typology of ex-novo synthesis of polysubstituted heterocycles: unimolecular reaction that involved intramolecular cyclization of bifunctional molecules; but also multicomponent process such as cycloaddition, annulation reactions, cyclocondensation and several other types (Fig.2-8). (45) In these reactions, key steps are frequently the instauration of a carbon heteroatom linkage. Most common, σ bond forming reactions such as nucleophilic displacements at satured or unsatured carbon, and condensation reaction have been reported. Additionally ring closure reactions involving conjugated π-systems are extremely useful in preparation of five or six membered ring heterocycles.

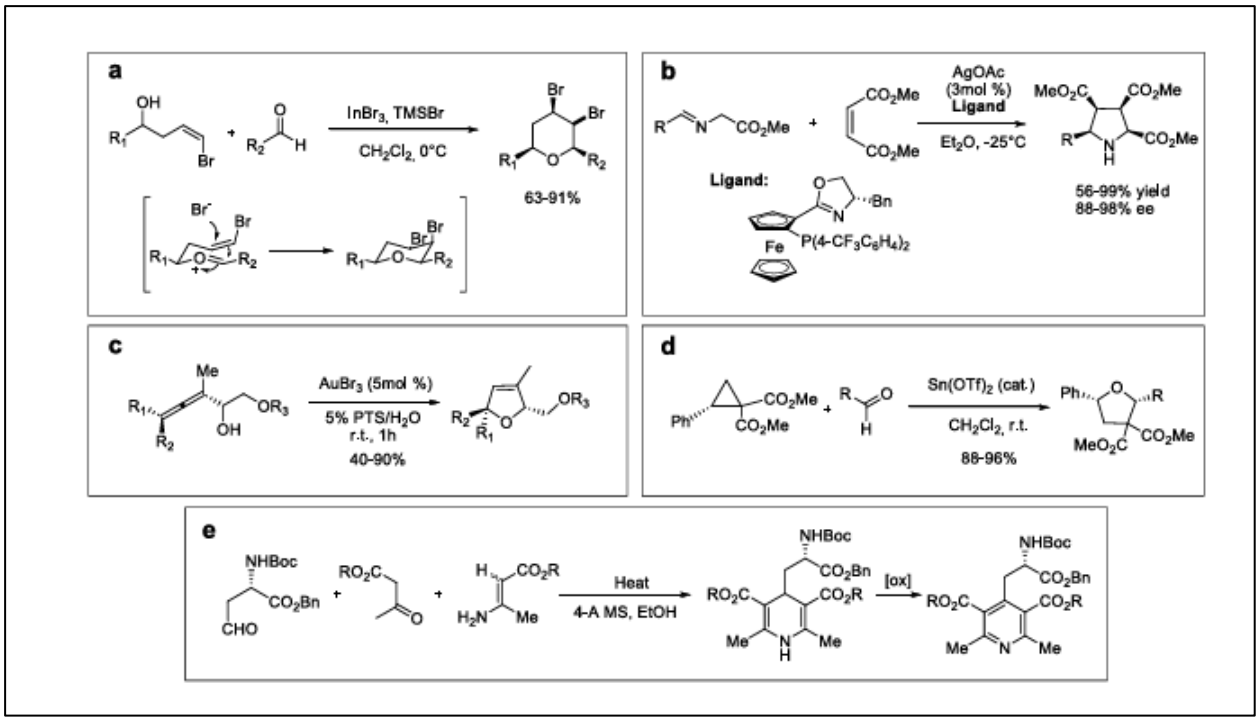


Figure (2- 8): Selected example of cyclization of acyclic reactant. (a) Prins Cyclization. (b) 1, 3-dipolar Cycloaddition (c) Cycloisomerization of functionalized allenes (d) Annulation of strained cyclopropanes.(e)Hantzsch cyclocondensation.

Naturally, it is not possible to define which approach is the best or the worst, but it all depends on the type of application it is intended. Nevertheless, it is possible to state that a functionalization approach could be favorable for diversity oriented synthesis application, where starting from the same core it is possible to create several congeners. Instead, the cyclization approach could be extremely useful in target oriented synthesis, since several step of protection/deprotection, reduction/oxidation and so on, could be avoided creating the heterocyclic core de novo.

2.2 Heterocycles With More Heteroatoms

In the previous section of this thesis, it was developed the general theme of the heterocycles, their main features and their importance for the formation of natural and synthetic compounds. However, this is only the beginning because the heterocyclic chemistry is open to a more complex world that looks over the simple heterocycles and their derivatives. So, now we have to consider the common case where more than one heteroatom is present in the ring.

The usual rules for stems to indicate ring size and suffixes for degree of saturation are used, as are the prefixes for the various heteroatoms. They are listed in the following order of priorities, derived from the main groups of the Periodic System, and then within each group by increasing atomic number:

Group VI (O>S>Se>Te)> Group V (N>P>As)> Group IV (Si>Ge)> Group III (B).

This listing can be simplified greatly by taking out the most commonly found heteroatoms in their order, which gives O>S>N>P. Each heteroatom is then given a number as found in the ring, with that of highest priority given position

2.2.1 Importance in Nature and Applications

When we think about polyheteroatomic heterocycles, we obviously deal with heterocyclic compounds with similar, if not identical, characteristics, and the same will be also the pool where they can be caught: nature.

The most immediate example that we can bring is undoubtedly DNA, the molecule that encodes the genetic instructions used in the development and the functioning of all known living organisms.

Nucleotides, the building blocks of our nucleic acid, are composed of a five-carbon sugar (ribose or deoxyribose), at least one phosphate group and a nitrogenous base. The latter exists in 4 different types and all four are derivatives of pyrimidine and purine ring structures. In fact, there are adenine and guanine for the purine bases and then, thymine and cytosine for the pyrimidine bases (Fig. 2-9).

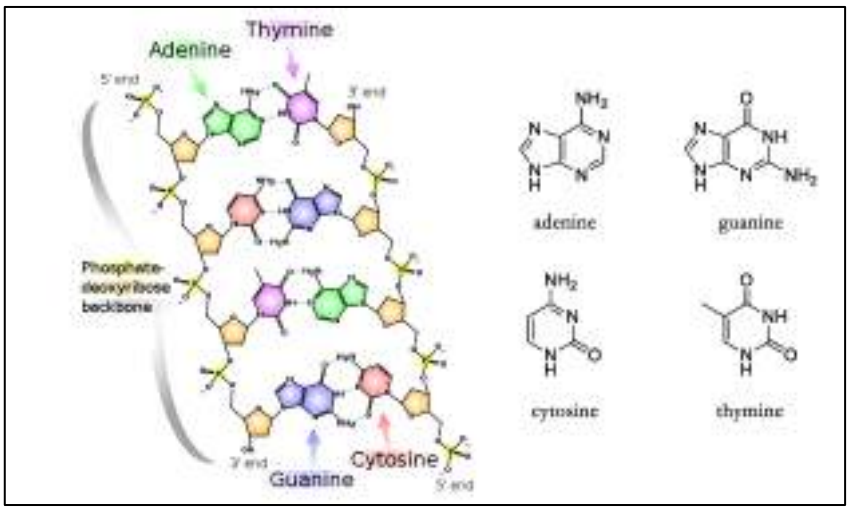
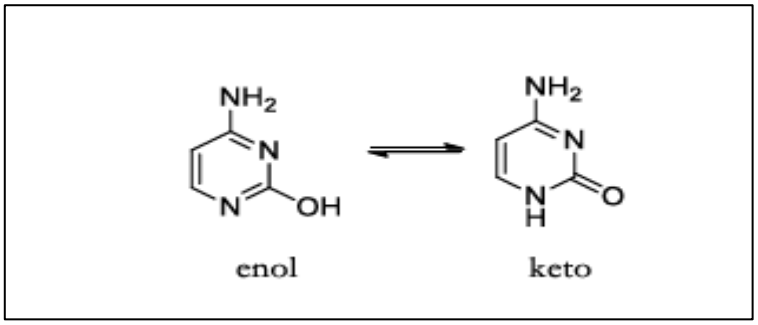


Figure (2- 9): DNA structure and its nitrogenous bases.

Four of the nitrogenous bases (also uracil in RNA instead of thymine) possess carbonyl groups. In early studies, the oxygen was written in the tautomeric hydroxyl form, and this confused the structural assignment of their bonding to the pentose. The tautomerism is expressed in (Sch.2-2) for cytosine as an example, where the enol form can be viewed as a hydroxypyrimidine.



Scheme (2- 2): Cyosine tautomeric equilibrium.

In the solid state, only the keto form is observed, but in an aqueous solution, a small amount of the enol form is present in the tautomeric equilibrium. Recognition of the keto form as dominant played a significant role in the unraveling of the structure of the nucleic acids and led J. D. Watson and F. Crick (46) to propose the famous double helix held together by H-bonds to the carbonyl oxygens.

Another class of natural organic compounds that it must be taking into account are vitamins. We have already mentioned some examples of these important molecules because they are vital for our organism and are specific co-factors behaving as the "helper molecules" that assist enzyme's biological activity in biochemical transformations. A particular attention goes to vitamins belonging to the B family, which are all water-soluble and contain an heterocyclic motif with more than one heteroatom (Fig. 2-10).

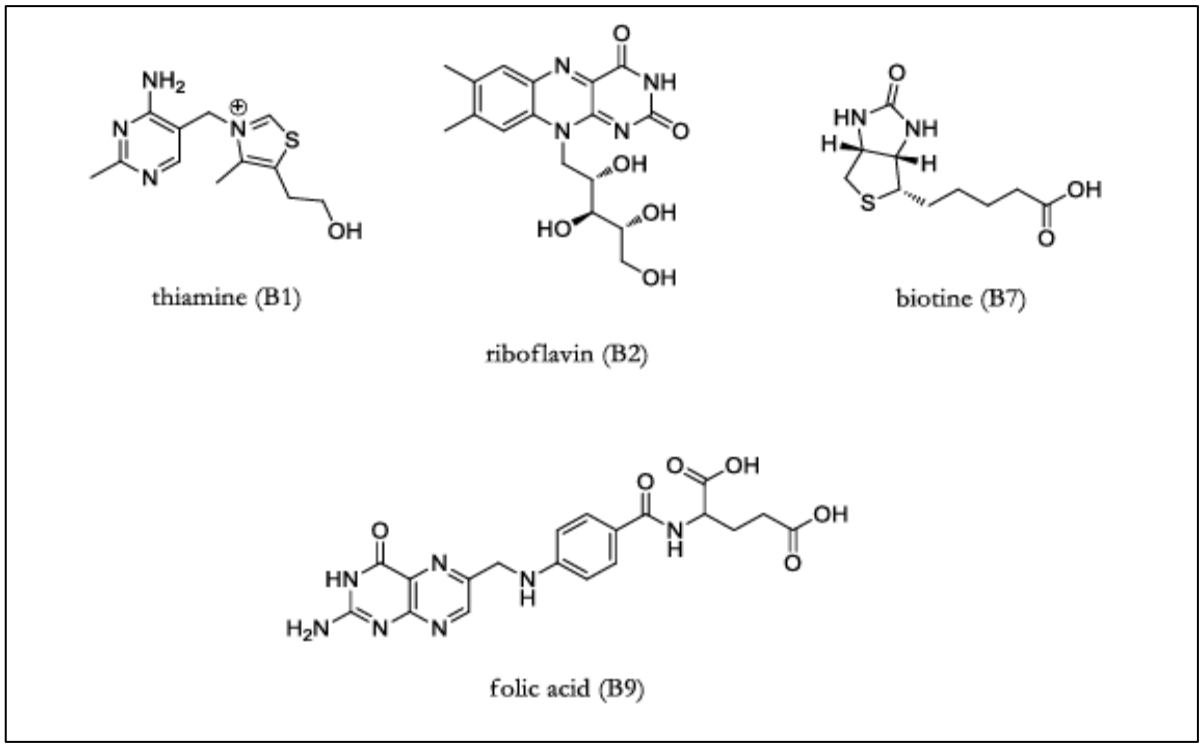


Figure (2- 10): Some important B vitamins.

The final group to consider is the amino acid family from which all proteins are constructed we have already discussed previously.

One of the essential amino acids with an heterocyclic side chain is histidine, containing an imidazole functional group. Histidine on biological decarboxylation is the precursor of the notorious histamine, which in the human body plays a crucial role in the immune response, including allergic reactions and it is useful in the creation of a vast family of pharmaceuticals called antihistamines (Fig.2-11).

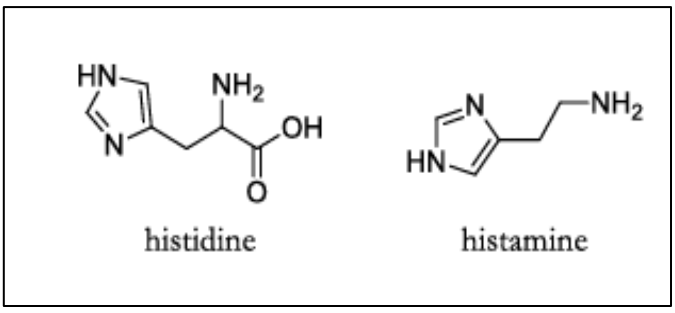


Figure (2- 11): Structures of histidine and histamine.

Aromatic and non-aromatic polyheteroatomic heterocyclic rings are a predominant architectural constant of pharmaceuticals and allow for variable interactions with the biological target which are not possible using simpler

carbocyclic motifs.

Perhaps some the most common drugs used nowadays and, probably everyday, are based on 7- membered rings and they are the benzodiazepines. Benzodiazepines are a psychoactive drug, whose core chemical structure is the fusion of a benzene ring and a diazepine ring. Different ones are used for the treatment of seizures, insomnia, depression, or anxiety. Examples of benzodiazepines include alprazolam and diazepam ((Fig. 2-12).

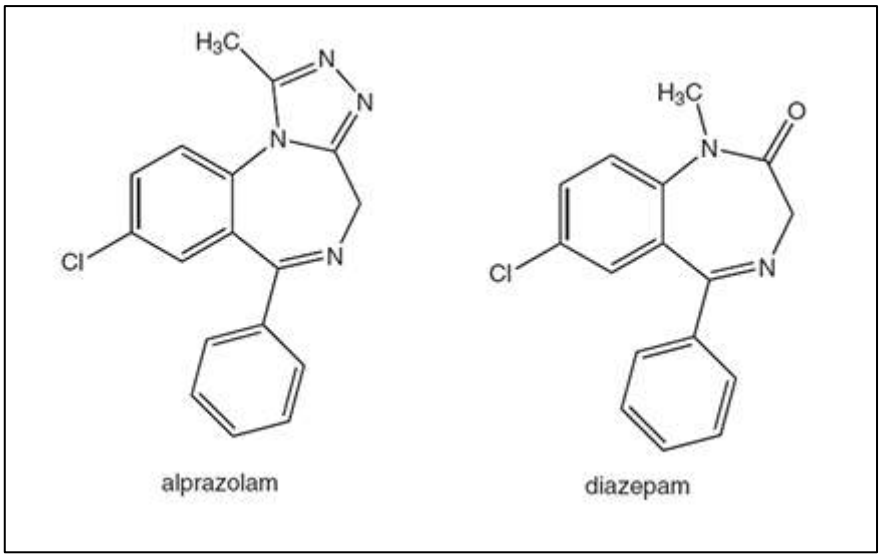


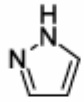
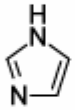
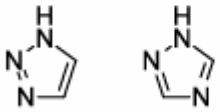
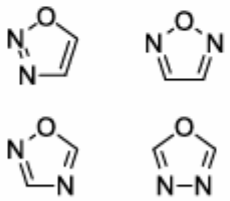
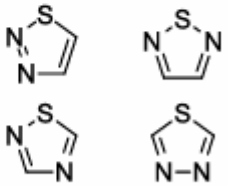
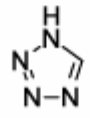
Figure (2- 12): Examples of benzodiazepines.

Benzodiazepines work by increasing the efficiency of a natural brain chemical, neurotransmitter gamma-aminobutyric acid (GABA), to decrease the excitability of neurons. This reduces the communication between neurons and, therefore, has a calming effect on many of the functions of the brain. The fastest compound, related to the speed of onset, is precisely diazepam that is rapidly absorbed by the organism, but it has a long half-life of around 40-250 hours. For this reason, diazepam and benzodiazepines with analogous features are called long-acting compounds, which have the advantage of a reduced severity of rebound effects and withdrawal, but at the same time they have a risk of accumulation in the elderly and in individuals with severely impaired liver function.

2.2.2 Five-Membered Heterocycles

Now, it is time to focused the attention on five-membered heterocyclic compounds (Table 2-2), because they are particularly important due to their remarkable variety of applications. Their chemistry, synthesis and transformations have, therefore, received considerable attention and importance.

Table (2- 2): Main five-membered polyheteroatomic heterocycles.

HETEROATOM		
N	**O**	**S**
 pyrazole	 isoxazole	 isothiazole
 imidazole	 oxazole	 thiazole
 triazoles	 oxadiazoles	 thiadiazoles
 tetrazole		

Five-membered heterocycles with more than one heteroatom are ubiquitous in nature and their significance is hinted, as seen above, by their presence in an enormous number of natural products, such as adenine, histidine, caffeine, uric acid and so on. Due to this common presence, they are known to interact with the receptor sites on enzymes, and hence their synthesis opens new horizons in enzyme receptor interactions for curing physiological disorders (47) . To confirm this, in (Fig. 2-13) is shown the abundance of five-membered heterocycles in general within top 200

drugs: the relevance of these rings in biologically active compounds is highlighted by the fact that in 59 drugs is present a five-membered heterocycle.

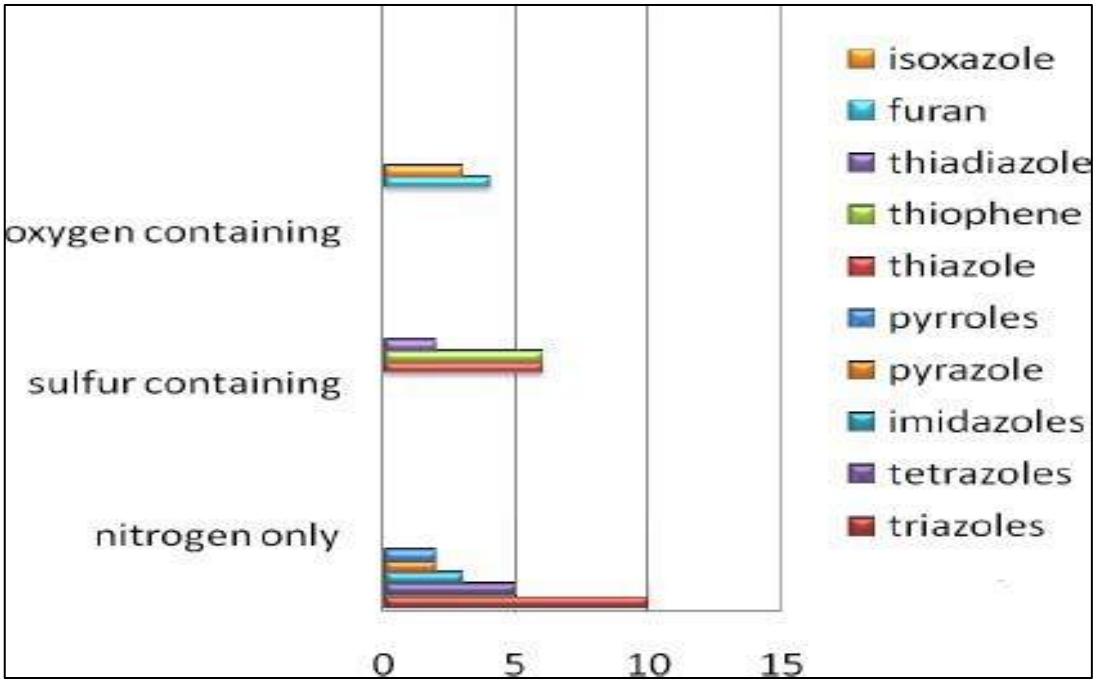


Figure (2- 13): The abundance of five-membered heterocycles within top 200 drugs.

As presented in the initial overview on the heterocycles, the aromatic cycles can be fused with benzene ring to give rise to various possible structures. This is also valid to the aromatic polyheteroatomic heterocycles, as showed in (Fig. 2-14). In fact, it may be useful to synthetize them because they are compounds better to employ in some organic synthetic ways compared to the monocyclic ones, taking advantage of their major stability.

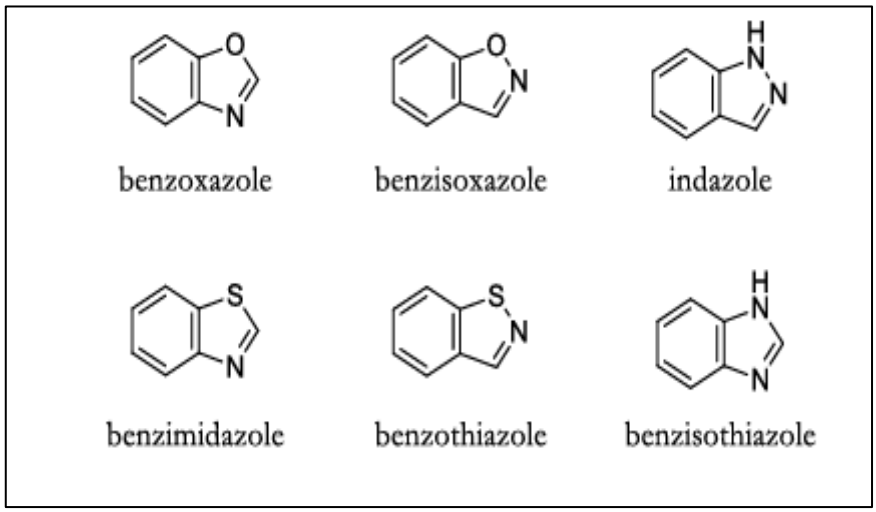


Figure (2- 14): Main benzofused aromatic heterocycles with more heteroatoms.

The number of substituents, their chemical structures and their positions on the heterocyclic ring are of crucial importance in determining the characteristic of a whole molecule. Versatile methodologies exist for attaching a wide variety of functional groups and a large numbers of analogs of a certain scaffold type could be synthesized using multiparallel synthesis. This approach is especially used in pharmaceutical industry during the high-throughput screening (HTS), wherein large libraries of chemicals are tested for their ability to interact with a specific target. A direct route to broad coverage aims at the development of a novel heterocyclic scaffold, which in turns is derivatized with standard reactions in order to create a thematic library. The novel scaffold material may be prepared in bulk and then appropriately portioned for multiple derivatizations in parallel. The latter may involve common reactions, but the resulting products are novel (48). One of the best examples on importance of substituents in aromatic heterocycles containing drugs is observed in

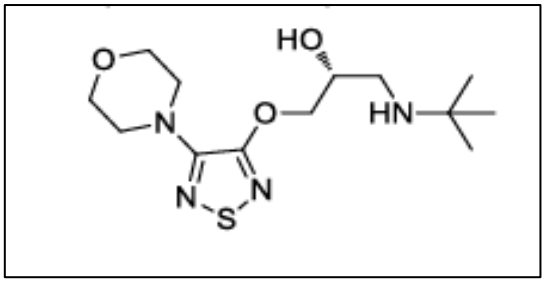


Figure (2- 15): Timolol chemical structure.

timolol (Fig. 2-15), a β-adrenergic receptor blocker indicated for treating glaucoma, heart attacks and hypertension. In its ophthalmic form (brand name: Timoptol in Italy) is used to lower intraocular pressure by reduction of aqueous humour production. (49) In a recent report, (50) an X-ray co-crystal structure of timolol within the β_2-adrenergic receptor (Fig. 2-16) disclosed its better biological activity compared with the analogous β-blockers which have a carbazole system as core.

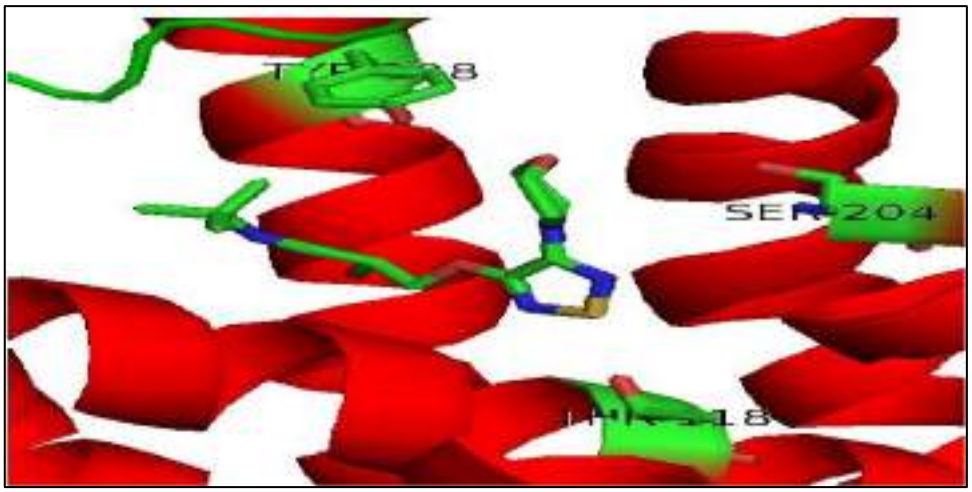
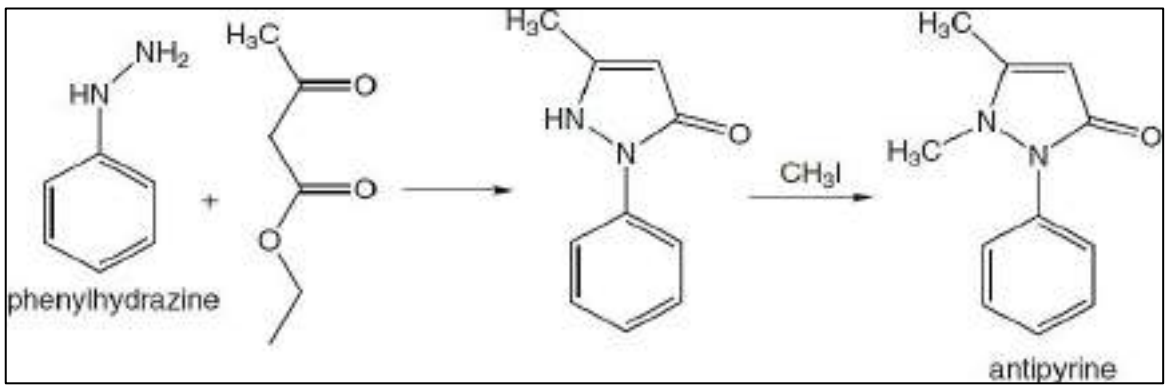


Figure (2- 16): X-ray co-crystal structures of timolol in the β-adrenergic receptor.

In fact, this data nicely exemplifies the stronger binding of timolol, as its morpholine group is involved in an extra hydrogen-bonding network with nearby amino acids (Asn, Tyr, Ser) and the thiadiazole motif itself protrudes deeper into the actual binding pocket which results in stronger interactions.

As every type of heterocycles, also five-membered ring was soon transfer from nature to medicinal and clinical fields with the development of new drugs. The first synthetic heterocyclic pharmaceutical seems to be antipyrine (Sch.2-3). Antipyrine is a pyrazole analgesic and an antipyretic, like aspirin. Ludwig Knorr used Emil Fischer's discovery of phenylhydrazine to synthesize antipyrine, and in 1883, Knorr was granted a patent on the synthesis. (51) In 1899, four years after market introduction, sales had grown to almost 800 metric tons. (52) More recently, antipyrine has been used in a solution with benzocaine to relieve ear pain and swelling caused by middle ear infections.



Scheme (2- 3): Knorr's synthesis of antipyrine.

Furthermore, the progress of more and more synthetic drugs brought to the involvement of this family of heterocycles also in pharmaceutical products of particular relevance, as the synthesis of anabolic steroids, the derivatives of natural steroids, like testosterone or cholesterol.

Anabolic steroids are drugs that are structurally related to the natural cyclic steroid ring system and have similar effects to testosterone in the body. They increase protein within cells, especially in skeletal muscles. They also have androgenic and virilizing properties, including the development and maintenance of masculine characteristics such as the growth of the vocal cords, testicles and body hair. Anabolic steroids were first made in the 1930s and are now used therapeutically in medicine to stimulate bone growth and appetite, induce male puberty and treat chronic wasting conditions, such as cancer and AIDS. However, equally to all the medicines, health risks can be produced by long-term use or excessive doses; exactly some sportive athletes can get into these risks when they assume this substances to improve their performances. For these reasons, anabolic steroids are classified as doping agents.

One signifiable example of these cited compounds, where a polyheteroatomic heterocycle is present, is furazabol (17β-hydroxy-17α-methyl-5α-androstano[2, 3-c] furazan) that is an anabolic steroid doping agent and its chemical structure is the same as that of stanozolol except for a furazan ring fused to the steroidal skeleton in place of the pyrazole (Fig. 2-17). It is used clinically as an hypolipidaemic and anabolic agent. This latter because it was demonstrates that it possess a very good myotrophic/androgenic ratio, that is the relationship between the increasing of muscle weight and the androgenic activity, which emphasis or develop male characteristics in a person. In general, steroids containing more heteroatoms inside the five-membered ring are of great interest since they have been found to be highly potent anabolic steroids with low androgenic activity (53) .

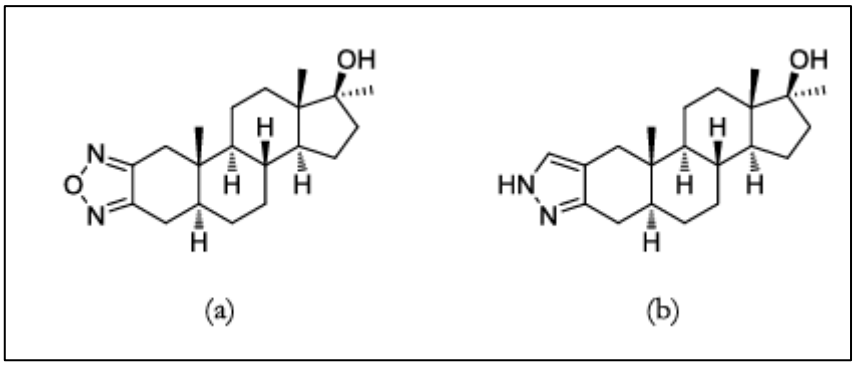


Figure (2- 17): Comparison between furazabol (a) and stanozolol (b) structures.

This last example of pharmaceutical compound introduces the real aim of this thesis, that deals with polyheteroatomic heterocycles, but more in particular with 1, 2, 5-oxadiazole, or even called furazans, and their related synthesis because it is possible get an improvement or an innovation on the synthetic pathways of these molecules, of which we already know surprising features and advantages towards clinical and medicinal uses. But it is still not enough.

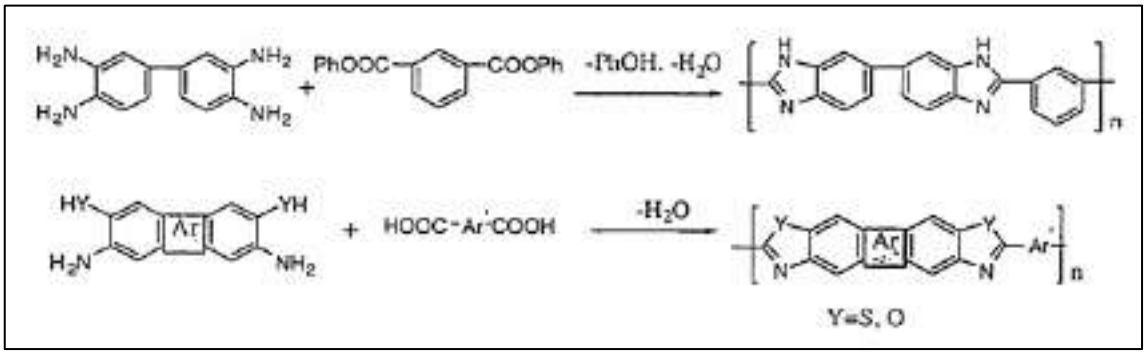
2.3 Synthesis of Heterocyclic Polymers

During the past decade, significant efforts have been carried out to synthesize new heterocyclic polymers. This incorporation of heterocyclic group into a polyrmer chain generally enhances properties such as strength, modulus and Tg. Functional heterocyclic polymers containing functional groups are of interest. In this section we survey the synthesis of heterocyclic polymers and functional heterocyclic polymers with special functionality such as fluorescent properties. There are three synthetic strategies currently employed to introduce a heterocyclic group into polymers. One method involves the use of a heterocyclic formation reaction for a polymenzation reaction. Another method involves incorporation of a heterocyclic moiety into a monomer. One of these approaches uses a heterocyclic activated nucleophilic aromatic substitution reaction, which is described in the next section. The last method involves a polymer precursor which is convened to a heterocyclic polymer by a reaction on the polymer.

2.3.1 Heterocyclic Formation Polymerization

Polyimides and polybenzazoles are major heterocyclic polymers. Besides polybenzazoles, polyhydantoins. polyparabanic acids, polyquinolines, and polyquinoxalines are commercial or widely studied heterocyclic polymers. Each of these polymers is synthesized from different monomers by a distinct chemical reaction.

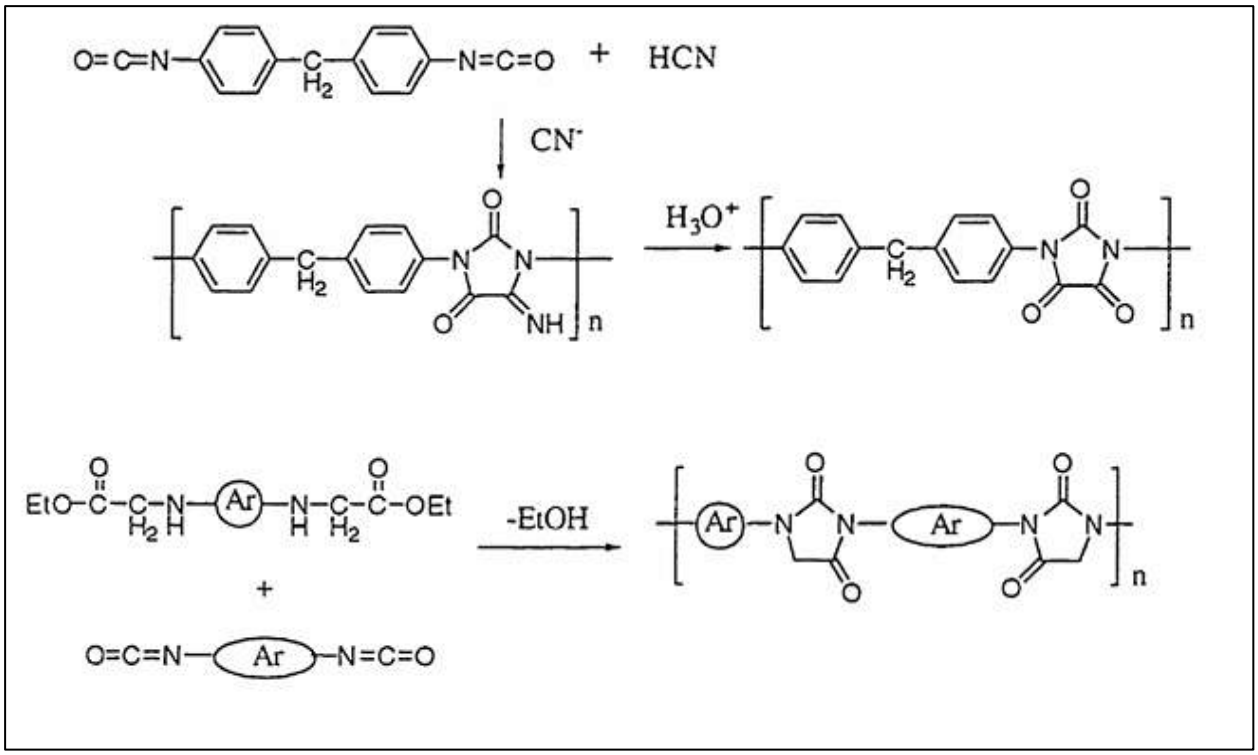
Polybenzimidazoles are synthesized by melt condensation of aromatic tetraamines and phenyl esters of aromatic dicarboxylic acids (54) . This process consists of two steps. The mixture of tetraamine and phenyl esters of aromatic dicarboxylic acids was first heated to 200-300°C to give an oligomer, which solidified. The solid was then heated to 350-400°C in vacuo affording high molecular weight polybenzimidazole powder (Scheme 2-4). Polybenzimidazoles have also been synthesized by polyphosphoric acid solution condensation (55) .



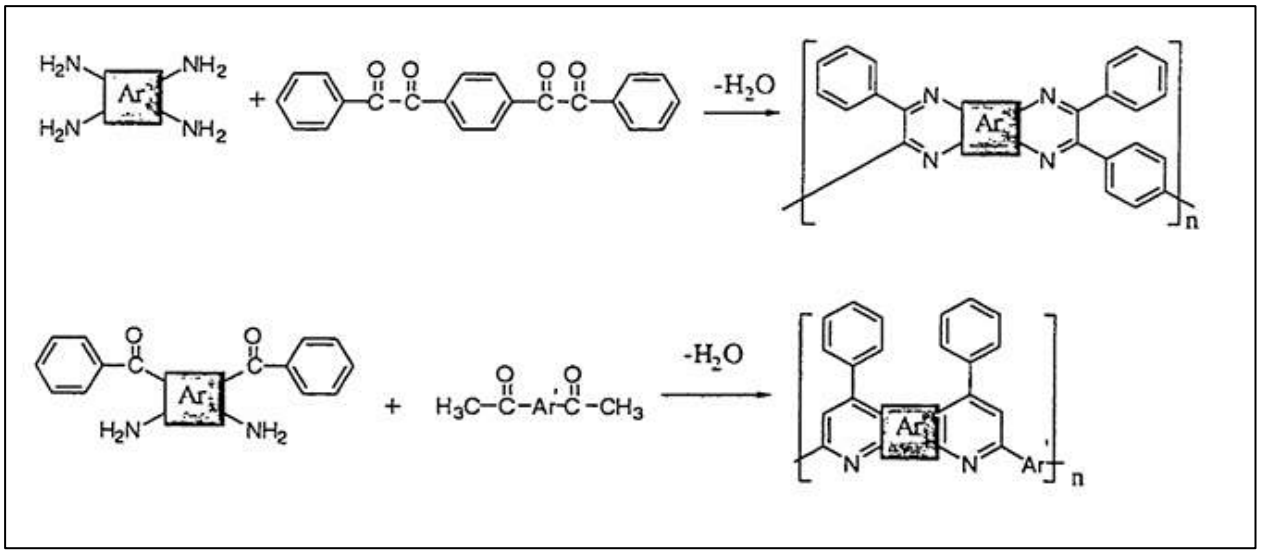
Scheme (2- 4): Synthesis of Polybenzimidazole, Polybenzoxazole and Polybenzthiazole by Condensation Polymerization.

Polybenzoxzoles and poIybenzthiazoles are synthesized by a similar method in polyphosphoric acid (56) (Sch.2-5). Polybenzoxazoles can be obtained from bis(o-aminophenol) and aromatic dicarhoxylic acid, and polybenzthiazoles can be obtained from bis O-aminobenzenethiol and aromatic dicarboxylic acid. Polyoxydiazoles are synthesized from aromatic hydrazides and aromatic dicarhoxylic acid chlorides by a 2-step method (57) .

Polyhydantoins, and poly (parabanic acid)s are used for vanishes, and coatings. Polyhydantoins are synthesized from aromatic bisamic acid esters and aromatic diisocyanates (58) .



Scheme (2- 5): Synthesis of polyimides from aromatic diisocyanates.



Scheme (2- 6): Synthesis of Polybenzimidazole and Polyquinoxaline.

Poly(parabanic acid)s are synthesized by a reaction of aromatic diisocyanates and hydrogen cyanide. Diisocyanates and HCN are reacted in the presence of sodium cyanide in NMP at room temperature and the polyiminohydantoin obtained is hydrolyzed to poly(parabanic acid) in the presence of sulfuric acid catalyst by heating (59) .(Sch.2-6).

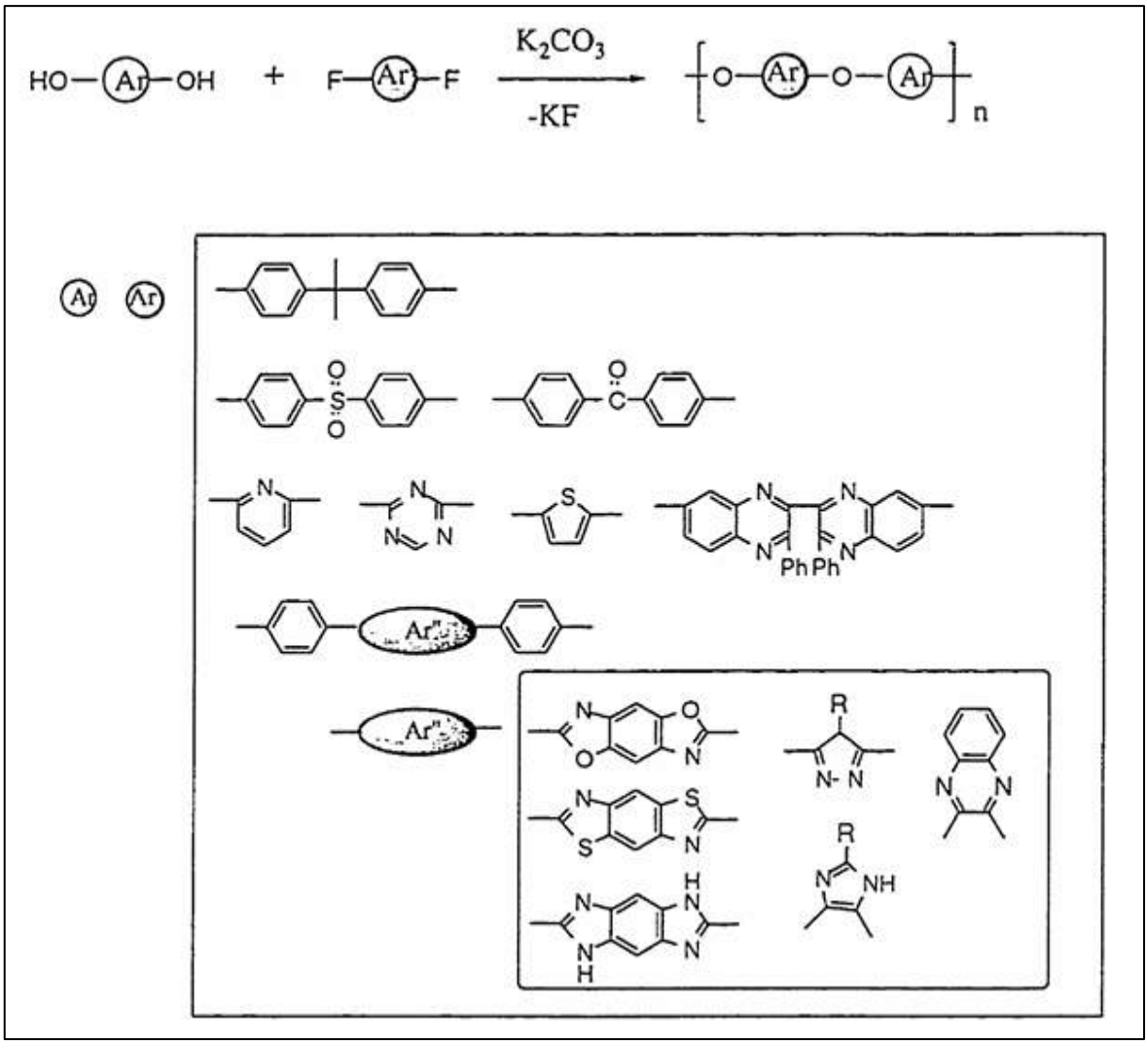
Polyquinoxalines are obtained by the reaction between aromatic tetraamines

and aromatic bis(l.2-diketone)s in m-creso1/xylene at low temperature(60-62) . Polyquinolines are obtained by the reaction of aromatic bis(o-aminoketone) and aromatic diacetyl compound in m- cresol/ phosphorus pentoxide at 135°C (63) .

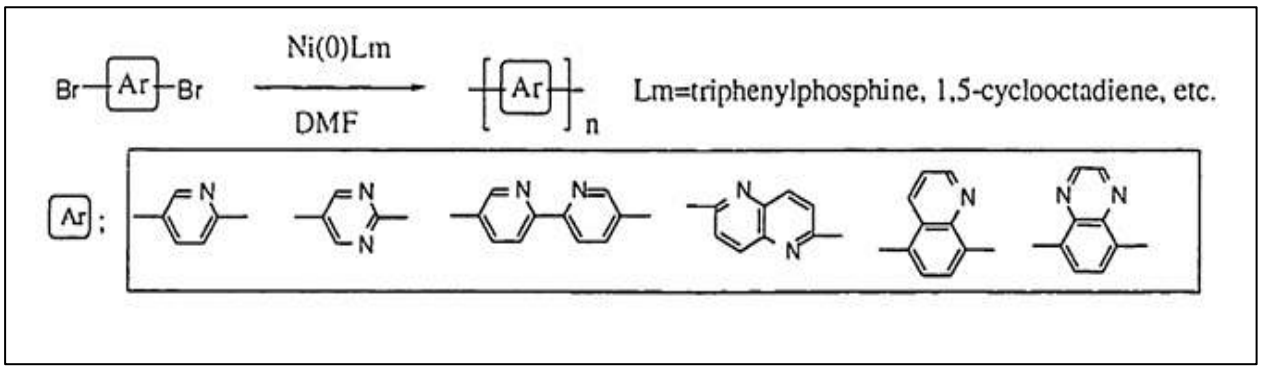
Heterocyclic Polymers from Preforme Heterocyclie Monomers (64) .

A number of heterocyclic polymers have been synthesized by polymerization of monomers which have performed heterocyclic groups. This method does not rely on a high yield for the heterocyclic formation reaction and therefore broadens the types of structures or the monomers. Many new heterocyclic polymers have been synthesized by a nucleophilic aromatic substitution reaction (Sch.2-7). In this polymerization reaction, a heterocyclic group is incorporated into a bisphenol or an aromatic activated dihalide. In many cases, heterocyc1ic group words as an activating group. 1, 3, 4-Oxadiazole (65) , 1, 3.4-thiadiazole (66) quinoxaline and benzoxazole (67) ahave been used successfully. Halogen atoms bound directly to the heteroaromatic ring are also strongly activated toward the nucleophilic attack. This approach has been used for a number of six-membered heteroaromatic systams such as 2, 6-difluoropyridine (68) . 2, 6-difluoropyrazine (69) , and halogenated triazinesn (70) .It has also been used with five-membered heteroaromatic systems based on benzthiazole (71), thiophene (72), and oxazole (73).

Yamamoto has synthesized a series of p-conjugated polymers containing nitrogen containing heterocyclic polymers such as pyridine (74), pyrimidine (75), quinolone (76), and quinoxaline (77) by dehaloganation polycondensation using a nickel complex as a catalyst (Sch.2-8).



Scheme (2- 7): Synthesis and structures of poly(arylene ether)s.

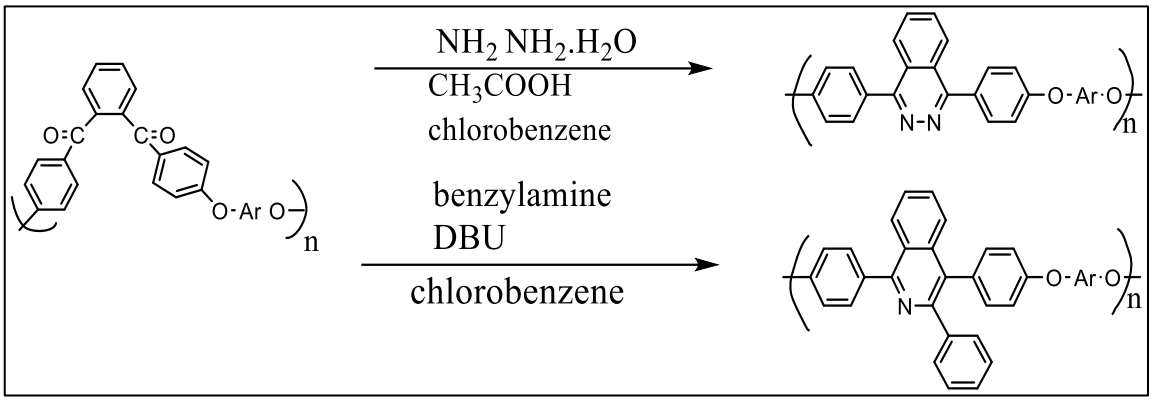


Scheme (2- 8): synthesis scheme of poly(aryl ether) polymers using various aryl (Ar) units.

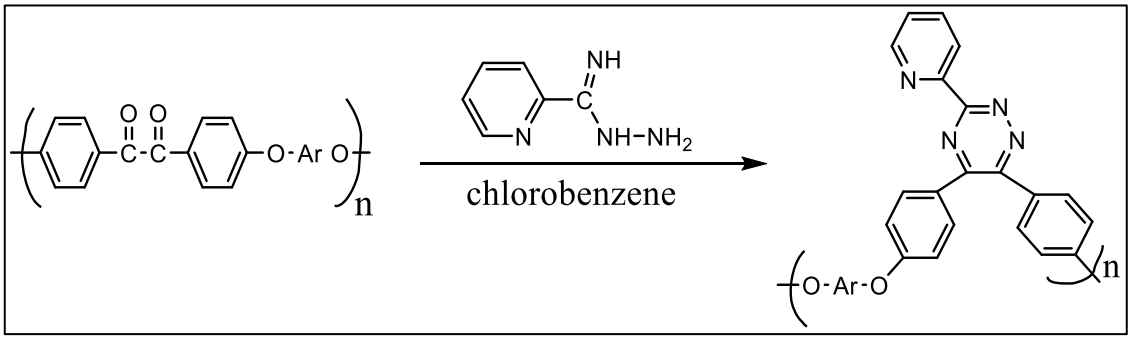
2.3.2 Heterocyclic Polymers by a Reaction on the Polymer

Another approach to incorporate a heterocyclic ring into a polymer is the use of a polymer precursor. Such a precursor polymer is particularly useful for the introduction of heterocyclic functionality which cannot tolerate the polymerization

conditions. Singh reported the synthesis of poly (aryl ether isoquinoline)s and poly(arylether phthalazine)s from high molecular weight poly(aryl ether)s containing a 1, 2 dibenzoylbenzene group (78).



Scheme (2- 9): Synthesis of post-polymerization modification of poly(arylene ether ketone)s via cyclization



Scheme (2- 10): Synthesis of 1,2,4-triazole-functionalized poly(arylene ether ketone.

The 1.2 - dibenzoylbenzene moiety is converted by treatment with hydrazine to phthalazine (79) , and by treatment with benzylamine the presence of 1, 8-diazabicyclo[5.4.O]undecene (DBU) to isoquinoline (80) .Strukelj reported the synthesis of poly(aryl ether pyridyltriazine)s from poly(aryl ether benzil)s by the reaction with (2-pyridyl)hydrazine (81) .

2.3.3 Functional Heterocyclic Polymers

Besides high thermal stability or good mechanical properties, heterocyclic polymers with special functionality have received great attention. Functionalities that have been incorporated are conductivity, nonlinear optical activity, fluorescent properties, etc..

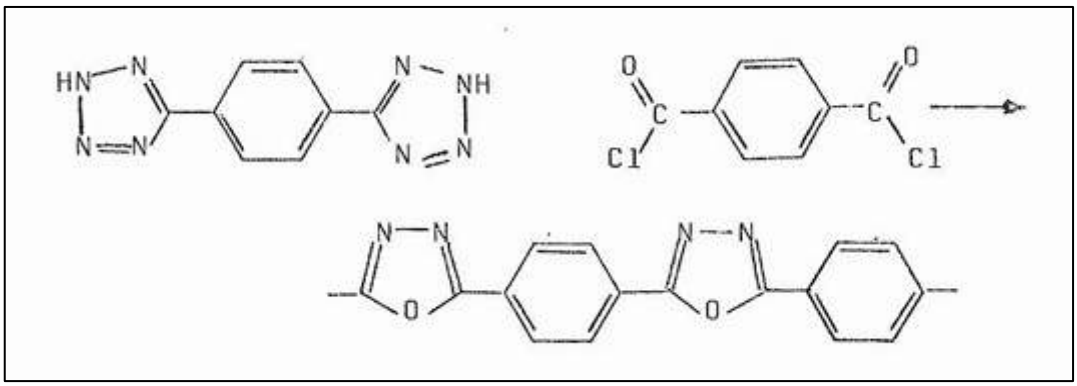
Some con|ugatnd heterocyclic polymers, such as polypyrrole. polythiophene,

exhibit conductivity when they are doped (82). They arc synthesized by chemical or electrochemical oxidative polymerization. Recently many organometallic catalyzed reactions such the Still reaction (83), have been applind to synthesize conjugated heterocyclic polymers.

Oxazoles, or quinoxaline derivatives display nonlinear optical behavior. Brittain synthesized polycarbonates, polyformals, and polyethers containing these NLO chromophores (84). Bcnzoxazole and benzthiazolc groups have a chromophoric effect on the fluorescence of conjugated systems (85). Electro and photoactive polybenzthiazole rod-coil copolymers were synthesized and thus supramolecular stricture for enhanced functional and solid state photophysized properties were studied (86, 87). Oxadiazoles, oxazoles, and triazole containing electroactive polymers were synthesized and films of these polymers Frere used for electron transport layers in a light emitting diode (88).

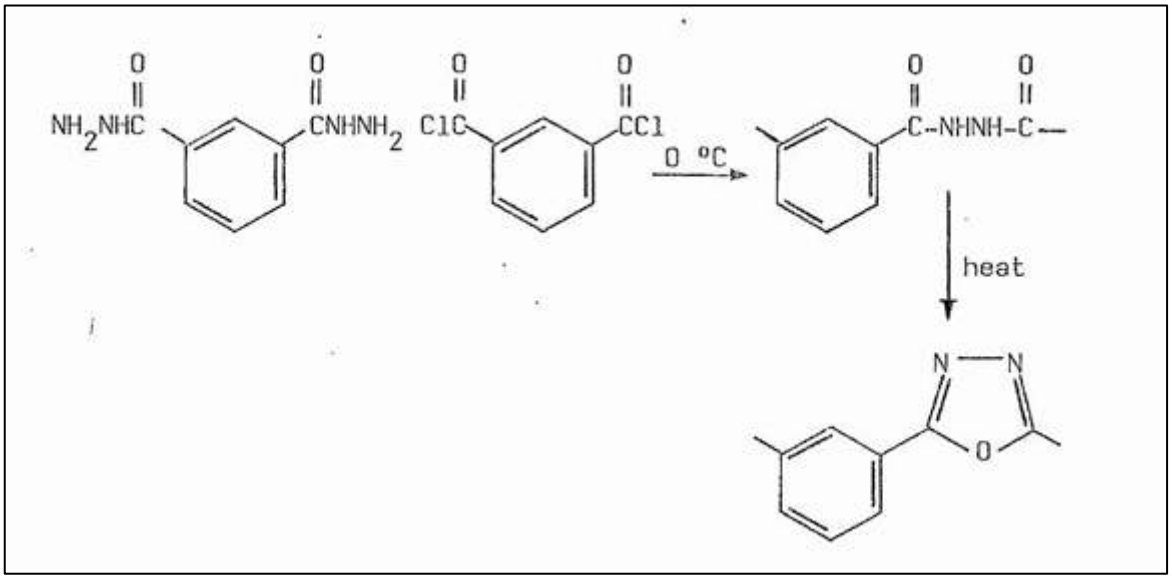
2.3.4 Oxadiazoles and Thiadiazole Containing Polymers

The oxadiazole and thiediazole ring systems have been known for almost a century and have found uses in several important fields, such as the dye (89-91) industries. (92-96) and pharmaceutical It was however not until 1958 that Huisgen (97, 98) and coworkers began to study fifieZr uses in polymers. (99) Abshire and Marvel prepared, in 1961, a series of 12 polymers from bis-tetrazoles and diacid chlorides, (Sch.2-11), based on the original reaction of Huisgen. These polymers were however of too low molecular weight for fibre production.



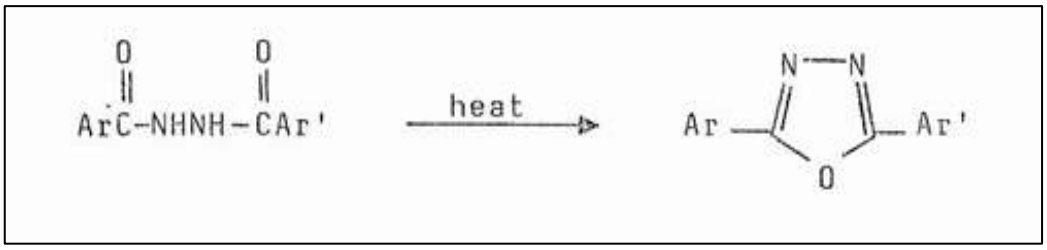
Scheme (2- 11): Synthesis of Poly(1,3,4-oxadiazole) by Polycondensation of Bis(tetrazole) with Terephthaloyl Chloride.

In 1964, Frazer (100) and co-workers developed one of the most popular synthetic routes to polyoxadiazoles, through the cyclodehydration of polyhydrazides. The polyhydrazides were prepared by the low temperature solution polymerisation technique as developed by Frazer and Wallenberger, and were of high molecular weight. They also had the advantage of solubility in dipolar aprotic solvents such as dimethyl. sulphoxide and N, N-dimethylacetamide, and could thus be processed into fibres and films. These could then be con verted by heat treatment to the more thermally stable oxa diazoles. (Sch.2-12)



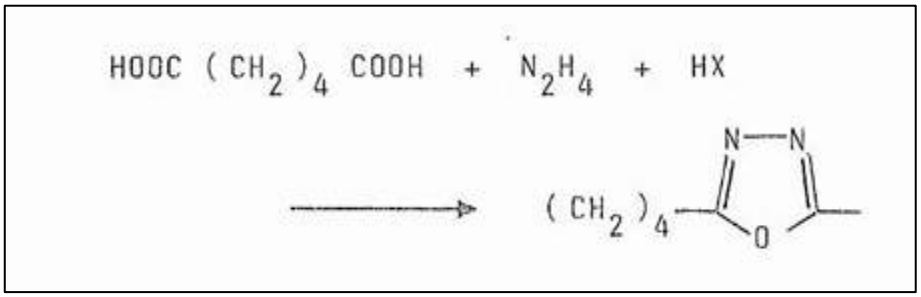
Scheme (2- 12): Synthesis of 1,3,4-Oxadiazole derivative via thermal cyclization of diacylhydrazine.

he properties and uses of polymers based on 1, 3, 4--oxadiazoles have been investigated by the Furukawa Electric Company (Japan). The polymers are hydrolytically stable, partially crystalline and can be oriented to a higher degree of crystallinity by drawing. They are found to be more stable than polymers based on triazoles, but less stable than those based on thiadiazoles. Poly-1, 3, 4-oxadiazoles can be prepared by a wide range of reactions, only two of which, (the most commonly used), will be discussed. The first method, already mentioned, is that used by Frazer and coworkers (99), and is based on Stolie's (101) early observations on the cycJodehydration of diaroylhydrazines. (Sch.2-13).



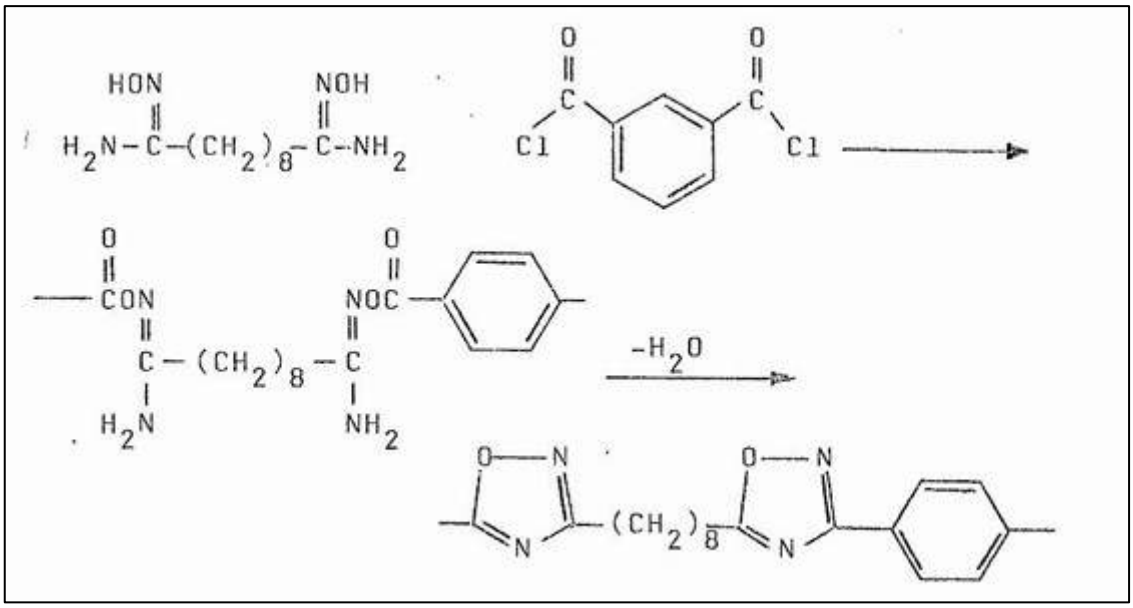
Scheme (2- 13): Synthesis of 1,3,4-Oxadiazole .

Chemical dehydrating agents, such as phosphorus pentoxide, phosphorus pentachloride, oxalyl chloride, thionyl chloride, polyphosphoric acid and fuming sulphuric acid can also be used. However, thermal dehydration is chosen preferentially to these. The second method, first used by Iwakura et al (102) is a one-step solution polymerisation by reaction of dicarboxylic acid, or the corresponding nitrile, amide or ester, with hydrazine or its salts in polyphosphoric acid or fuming sulphuric acid. Reaction temperatures of 85 - 200 °C are usually employed and a 20 - 30% excess of hydrazine is often used, since this favours the formation of polymer of high molecular weight. (Sch. 2-14).



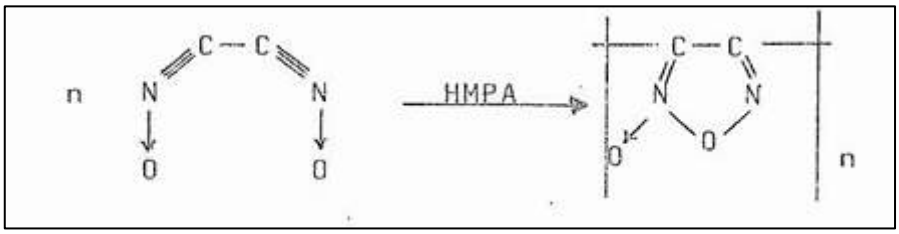
Scheme (2- 14): Synthesis of 1,3,4-oxadiazole derivative via thermal cyclodehydration.

A larger number of poly-1, 3, 4-oxadiazoles have been made. They are most frequently used as films or fibres, produced from solutions of fuming sulphuric acid. They are flame-resistant and liave favourable tensile properties. However, the other isomeric forms of the oxadiazole ring, namely the 1, 2, 4- and 1, 2, 5- systems have received very little attention since the mid-sixties. The most widely used synthesis of poly-1, 2, 4-oxadiazoles is the polymerisation of diamidoximes with diacid chlorides. (103) In many instances, the intermediate polyacylamidoxime can be isolated, and this on subsequent dehydration yields the polyoxadiazole. (Sch.2-15).



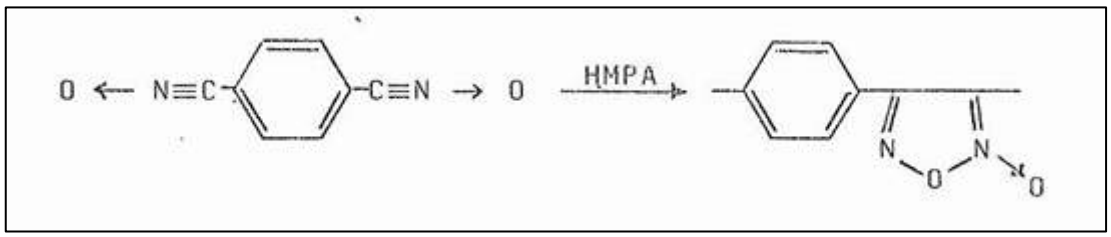
Scheme (2- 15): Synthesis of bis(1,2,4-oxadiazole) derivative.

The polymerisation of nitrile oxides (104-106) yields poly- -1 , 2, 5-oxadiazoles. (Sch.2-16). Two paths are possible however for the polymerisation of terephthalonitrile di-N-oxide.



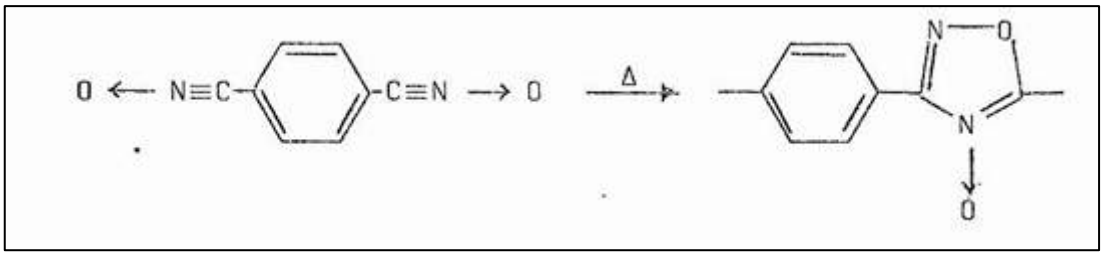
Scheme (2- 16): Synthesis of polymerization of nitrile oxide yields poly-1,2,5-oxadiazoles.

In solution poly(1, 2, 5-oxadiazole N-oxides) are formed using such solvents as dimethylacetamide, dioxan, hexamethyl- phosphoramide (HMPA) and dimethylforniamide. Reactions can occur at ambient or low temperature. (Sch2-17).



Scheme (2- 17): Synthesis of terephthalonitrile di-N-oxide.

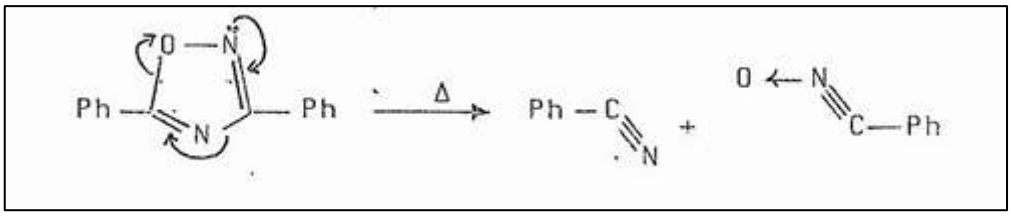
The solid state polymerisation of terephthalonitrile di-N -oxide, however, gives the poly(1, 2, 4-oxadiazole N-oxide) (Sch.2- 18).



Scheme (2- 18): Synthesis of poly (1,2,4-oxadiazole N-oxide>

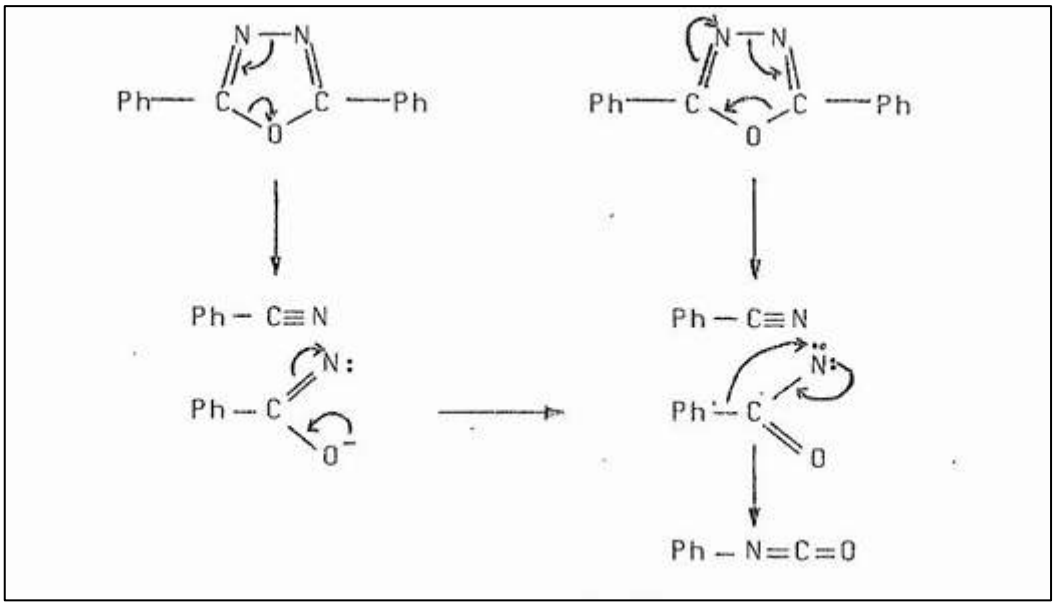
In terms of tractability and solubility, these polymers are quite similar to poly-1, 3, 4-oxadiazoles. However they possess considerably less thermal stability and have lower glass transition temperatures (Tg), than analogous 1, 3, 4-oxadiazole-based polymers .(107)

The reason for the difference in stability between the 1.3.4- and the 1, 2, 4-oxadiazole system has been sliown to relate to the proportion of delocalisation energy, i.e. the 1.3.4-system is more stable as it has the higher délocalisa tion energy, as found from molecular orbital calculations. In addition, the 1, 2, 4-system can decompose by a retro-cycloaddition, to a nitrile and a nitrile oxide. (Sch.2-19). More complex pathways are also possible. In the 1, 3, 4-system



Scheme (2- 19): Mechanism of cycloreversion of 3,4-diphenyl-1,2,5-oxadiazoleThermal cleavage of 1,2,5-oxadiazole.

the ring also cleaves, but not until temperatures (108) 400 °C. (Sch.2-20). This lack of thermal, stability is, no doubt, one of the reasons why the 1, 2, 4- and the 1, 2, 5- systems have been much less studied.



Scheme (2- 20): Mechanism for the thermal decomposition to form phenyl.

In the mid-sixties, Preston (109-111) prepared a range of polyamides based on the oxadiazole-containing diamines shown in (Fig.2-18).

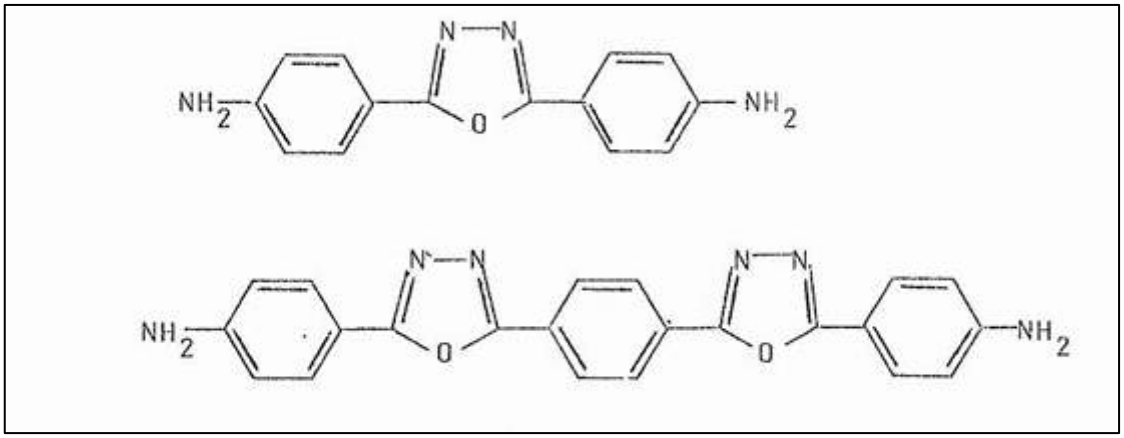


Figure (2- 18):Synthesis of polyamides based on the oxadiazole-containing diamines

At the same time, (112) published a paper detailing the preparation of two bisphenols containing a 1, 3, 4- -oxadiazole ring. Polycarbonates were prepared by the transestérification of the bisphenols with diphenyl carbonate Polyesters were prepared by reaction with diphenyl esters. The structures of the two bisphenols are shown in (Fig.2- 19) .

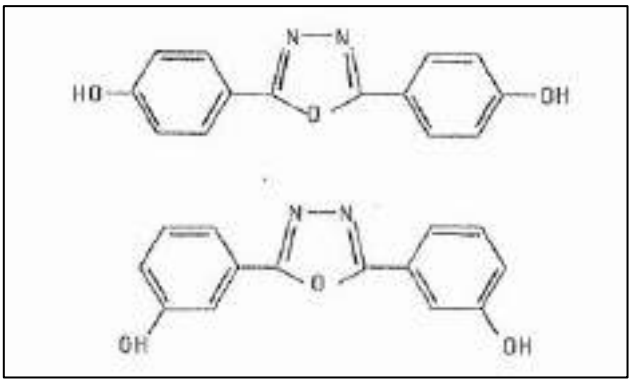
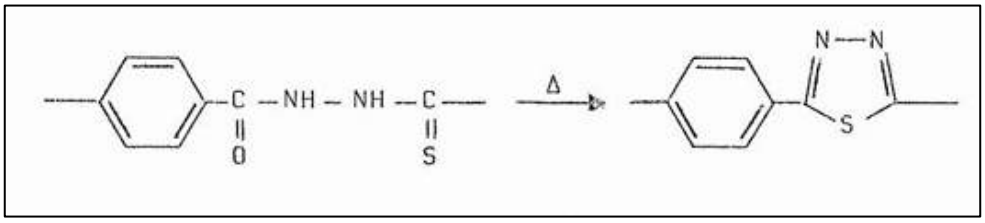


Figure (2- 19): Synthesis of oxadiazole ring

Oxadiazole-containing polymers with other functional groups have been prepared; amide and imide functional (113) groups by Bruma et a.I and ether functional groups by CL - Steinmann.(114)

or the three isomeric forms of thiadiazole, only two, the 1, 3, 4- and the 1, 2, 5-forms have been used in polymers. Thiadiazole-containing polymers have received less attention than the oxadiazole-containing polymers, not because their properties are inferior, (for they are indeed not), but for the reason that thiadiazole precursors are less accessible. Poly-1, 3, 4-thiadiazole fibres have been prepared in a manner analogous to that of poly-1, 3, 4-oxadiazoles - the cyclodehydration of a polyoxythiahydrazide fibre. (Sch.2-21). This cyclisation occurs at lower temperatures and at a faster rate than the corresponding cyclisation to oxa diazoles. Fabrication of the polyoxythiahydrazide is easy, due to its high solubility in pyridine and dimethylacetamide Thiadiazole-containing polymers exhibit the same desired chemical and thermal stability as oxadiazoles, but they are somewhat more tractable. Various patents and papers have been published, which describe thiadiazole-containing polymers and the fibres obtained from these polymers. (115, 116) The main uses of these polymers are as packing materials, high strength fibres and electrical insulators. (117)



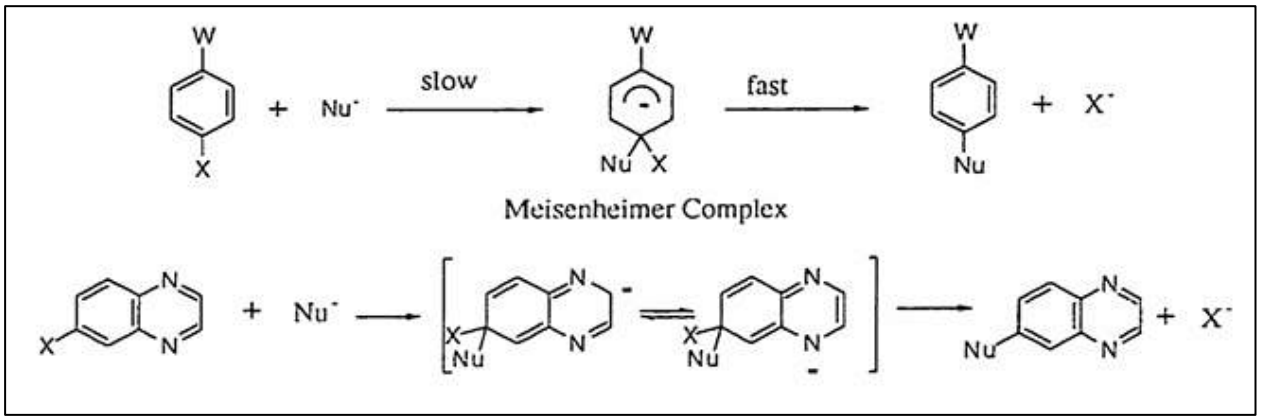
Scheme (2- 21): Mechanism of thermal degradation of 1,3,4-oxadiazole ring.

2.4 Nucleophilic Aromatic Displacement PoIymerization.(118, 119)

Poly (aryl ether)s are an important class of commercial polymers and functional derivatives of these polymers have been of interest recently. The most commonly used synthetic route to poly (aryl ether)s involves generation of an ether linkage by a nucleophilic aromatic substitution reaction (S_NAr) as the polymer forming reaction. Many of the new polymers described in this thesis were synthesized by this S_NAr reaction. In this section, a survey of".S_NAr reactions is presented. Emphasis was put on the choice of reaction conditions.

2.4.1 Mechanism.(120)

Nucleophilic displacement takes place via a two-step addition-elimination mchanism (Sch.2-22). The first step, the formation of the Meisenheimer complex, is usually the rnie determining step.



Scheme (2- 22): Meisenheimer Complex

2.4.2 Reaction Conditions Nucleophile.

Genially speaking the reactivity of the nuclrophile, such as phenolate, is not as crucial as the activated halides to obtain high molecular weight polymers. The more basic the phenolate is, the more reactive it is. Bis(4-hydroxy pheny1)sulfone cannot form a high molecular weight polymer with bis(4-chloropheny1)sulfone in DMAc; however, it forms a high molecular weight polymer in NMP at higher temperatures (121). In some cases, bisphenol a gave lower molecular weight than other bisphenols presumably because of reductive dehalogenation reactions or ether cleavages (122).

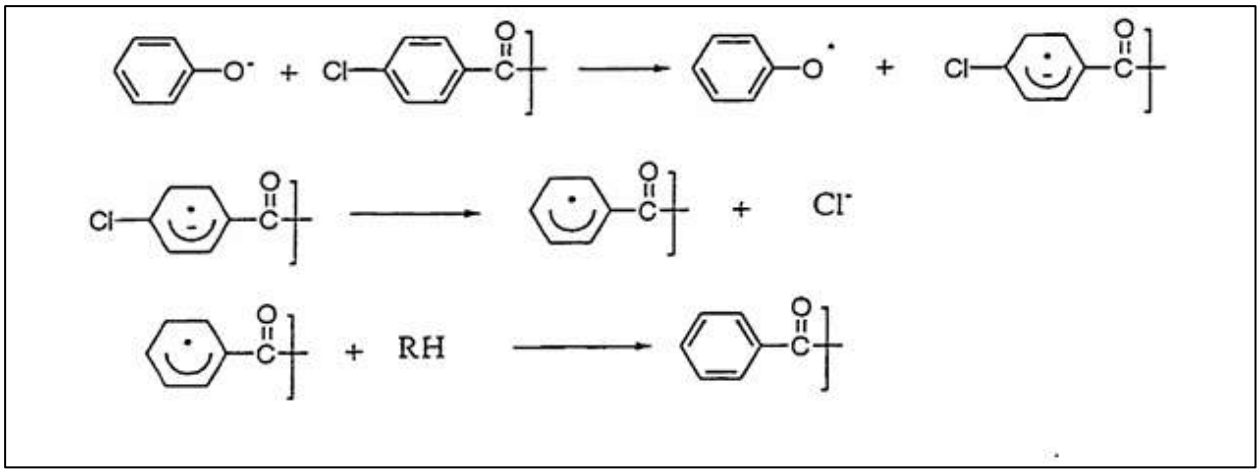
A- Base

In general, the order of the reactivity of the phenolate salt is CS>K>>Na (123).

Higher polarizable cations intenact more effectively with the solvent. The lithium, calcium or magnesium salts of phenols are not useful due to their insolubility in a polar solvent. The use of most reactive cesium phenolate can lower the reaction temperature and can shorten the reaction time . In high temperature reactions, potassium salts sometimes cause side reactions so sodium carbonate was used instead (124). Mixed metal carbonates have been used to prepare dendrimers (125).The addition of $MgCO_3$, or $CaCO_3$, removes the fluoride ion, which cause side reactions, form the reaction system because MgF_2 or CaF_2 is insoluble in the dipolar aprotic solvent used. A combination of alkaline earth metal carbonate, such as calcium carbonate, and sodium or potassium or cesium carbonate were used to prepare poly(arylene ether)s (126). Bisphenols were reacted with activated aryl halides in the presence of a catalytic amount of potassium carbonate and equimolar amounts of calcium carbonate in diphenyl sulfone at 300°C. The viscosities of the formed polymer were much higher than those of polymers prepared with equimolar amounts of potassium carbonate.

2.4.3 Side Reactions

The displacement of chlorine from his(chloroary1 ketone)s with bisphenoxides to form high molecule wright PAKs is more difficult. A competitive reductive dehalogenation reaction via a $S_{RN}1$ (substitution, radical-nucleophilic, unimolecular) reaction mechanism has been shown to account for the formation of low molecular weight PAKs (127) (Sch.2-23). Factors contributing to the occurrence of the $S_{RN}1$ reaction during the synthesis of poly(arylene ether ketone)s were studied (128). With a strong nucleophile, obtained from bisphenol A, high molecular weight polymers were formed exclusively via a nucleophilic aromatic substitution in the polymerization with 1.3-bis (4-chlorohenzoyl) benzene.



Scheme (2- 23): mechanism of the polymerization reaction.

On the other hand, oligomeric products were obtained from the weaker nucleophile from hydroquinone. In this case, both mechanisms were operative. The S_{RN} 1 pathway, which was responsible for the formation of oligometric products, could be eliminated by the addition of a suitable radical scavenger (129) such as trtraphenylhydnzine. The order of the radical stability in four amide solvents, 1.3-dimethyl-3, 4, 5.6- tetrahydro-2(1 H)-pyrimidinone (DMPU), 1 -meihyl-2-pyrrolidinone (NMP). 1.1.3.3- tetramcthylurea (TMU) and N, N-dimethylacetamide (MAC) agreed with the order of the molecular weight of the poly(ary1ene ether ketone)s formed in these solvents. This result supported the termination reaction by S_{RN} mechanism (130) .

In the polymerization of 1-chloro-4-(4-fluorobenzoyl) naphthalene in NMP, BPA gave a lower molecular weight polymer than hydroquinone. The authors suggested that the isopropylidene group in BPA worked as a hydrogen source for the termination by a S_{RN1} mechanism (131).

Aryl ether cleavages of poly(aryl ether ketone)s (PEKs) and poly(aryl ether sulfone)s (PESs) have been studied (132). Aryl ethers in PESs were significantly cleaved above 280°C. While aryl ethers in PEKs were not cleaved up to 300°C in the presence of potassium fluoride in diphenyl sulfone. High molecular weight poly(ether ketone)s were found to react with 4, 4'- difluorobenzophenone in the presence of potassium carbonate in diphenylsulfone at 330°C, yielding low molecular weight poly(ether ketone) with fluorophenyl end groups. The aryl ether

bonds were cleaved by the phenoxide under the reaction condition, which led to ether interchange (133).

2.4.4 Masked Bisphenol.

Silylated bisphenols (134), bisphenol carbonates (Scheme 1 - 11) (135), and polycarbonate have been used as masked bisphenols for the polymerization. The use of masked bisphenols eliminates the dehydration step and thus can shorten the reaction time. In addition, it alleviates the difficulty in handling unstable monomers. Masked thiophenols are also successfully polymerized to form high molecular weight poly(arylrne sulfide)s (136).

2.5 Applications.

Heterocycles are therefore inextricably interlaced into the life processes and the vital interest of the pharmaceutical and agrochemical industries in heterocycles is often connected with their natural occurrence.In fact, among the vast number of pharmacologically active heterocyclic compounds, many of which are in regular clinical use, some of these are natural products, for example antibiotics such as penicillin and cephalosporin, alkaloids such as vinblastine, ellipticine, morphine, and reserpine, and cardiac glycosides such as those of the Digitalis plant (Fig.2-20).

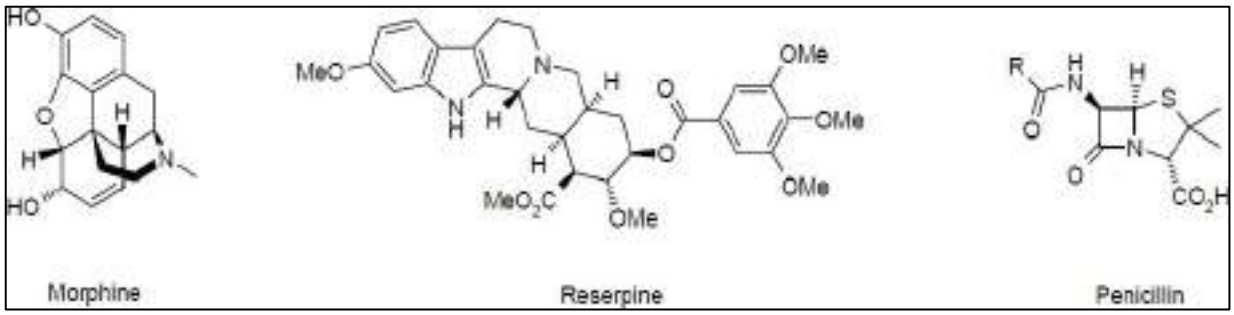


Figure (2- 20): Examples of natural pharmacologically active heterocyclic compounds.

The large majority of drugs (137) (Fig.2-21) and biologically active compounds, like antitumor, antibiotic, anti- inflammatory, antidepressant, antimalarial, anti-HIV, antimicrobial, antibacterial, antifungal, antiviral, antidiabetic, hypnotics, and vasopressor modifiers agents, include synthetic heterocycles as central structural moiety.

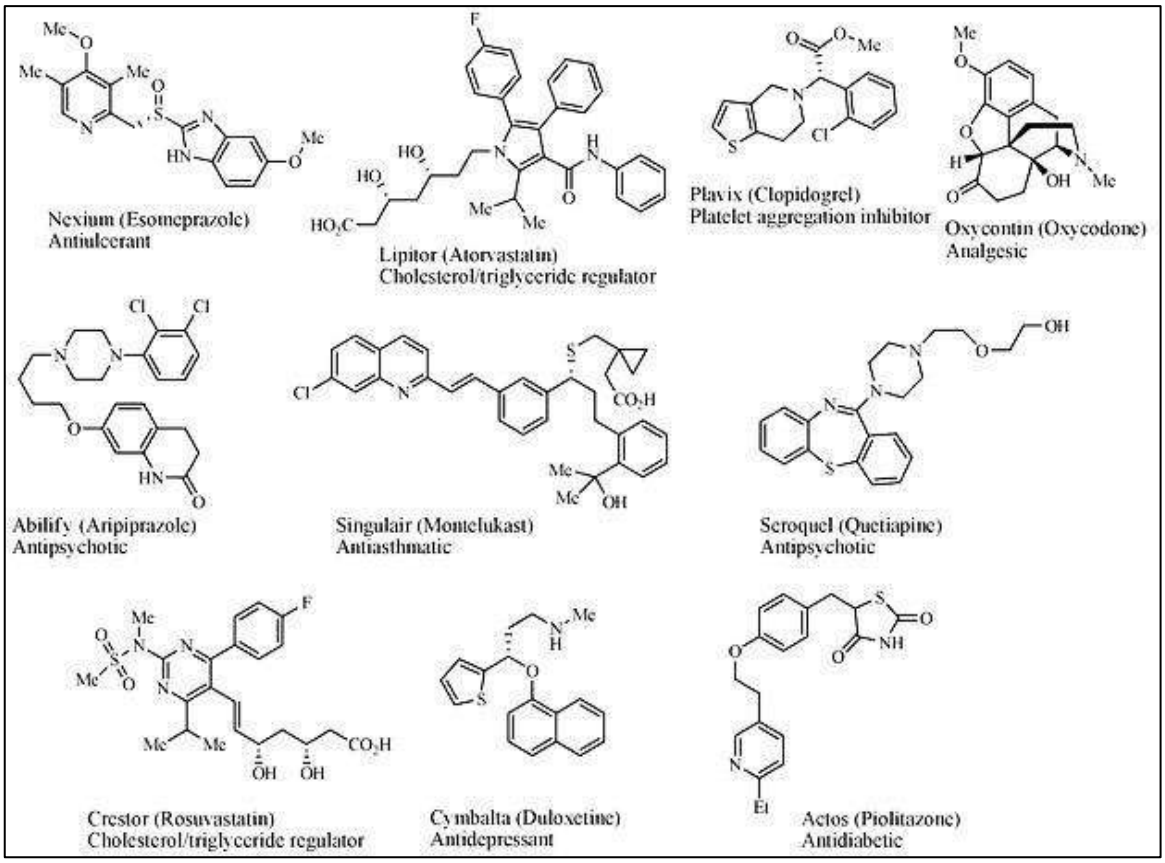


Figure (2- 21): Some of the top brand name small molecules drugs.

It is also possible to find a great variety of heterocycles in agrochemical compounds because they serve as pesticides, insecticides, herbicides, fungicides and rodenticides. Since the discovery in the 1940s of the powerful insecticides, like 1, 1-bis(*p*-chlorophenyl)-2, 2, 2-trichloroethane (DDT), research on pesticides and plant growth regulators (PGRs) became a major activity of many industrial firms and heterocycles being prominent among them. Some of these chemical compounds were synthetized early in the 1850s, but they were commercialized just after the 1950s to contrast the negative effects of DDT in humans and animals. The most sold are all derivatives of pyridine because they exhibit a variety of types of biochemical activity; For example, there are herbicides like picloram, diquat, paraquat and fluridone or insecticides like chlorpyrifos (Fig.2-22).

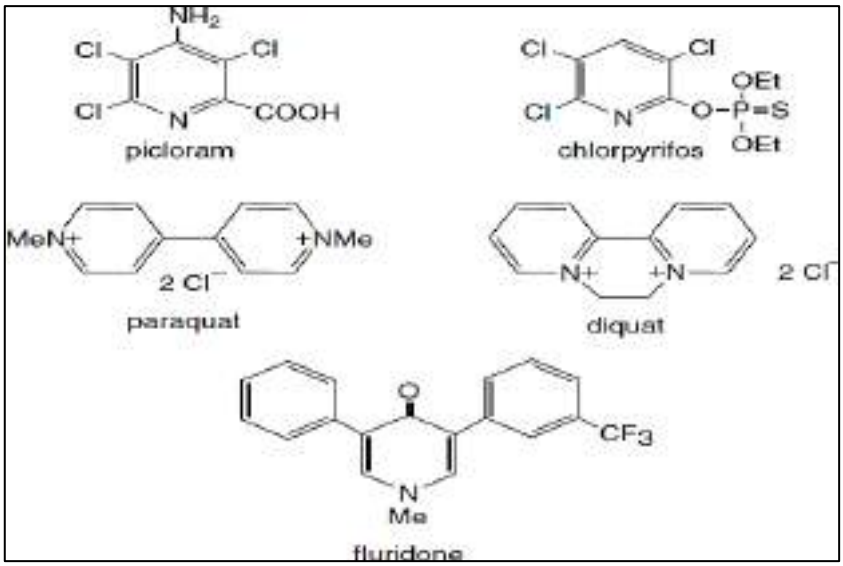


Figure (2- 22): Some pyridine agrochemicals.

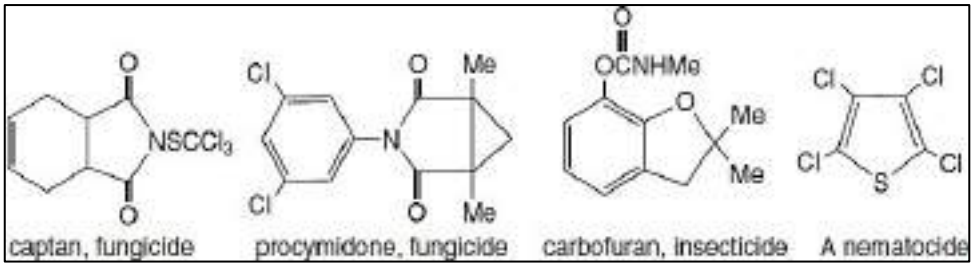


Figure (2-23): Derivatives of pyrroles, furans, and thiophenes as agrochemicals.

However, in research of the 2000s, many derivatives of various five-membered rings have been introduced successfully as agrochemicals (Fig.2-23).

Besides the great importance in medicinal and agrochemistry, heterocyclic chemistry is an inexhaustible resource of novel compounds. Since rings can be of any size, from three-membered upward, and since the heteroatoms can be drawn in almost any combination from a large number of elements (though nitrogen, oxygen, and sulfur are still by far the most commons), the number of possible heterocyclic systems is almost limitless, making available compounds with the most diverse physical, chemical, and biological properties.(138) Practical applications include dyestuffs (Fig.2-24), copolymers, solvents, photographic sensitizers and developers, and antioxidants and vulcanization accelerators in the rubber industry(139).

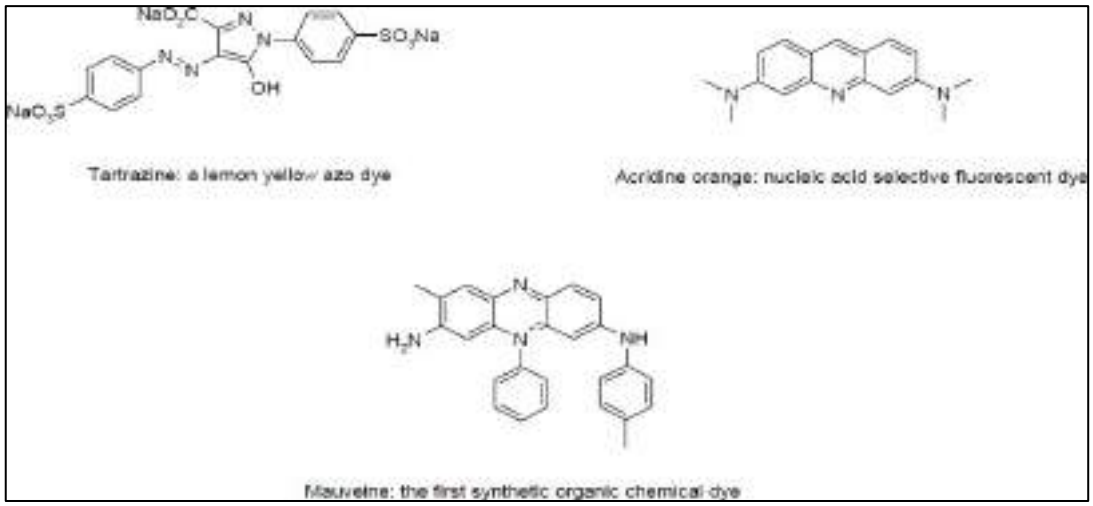


Figure (2- 23): Examples of dyestuff containing heterocyclic structures.

Furthermore, heterocycles found a large application as organic conductors, semiconductors, molecular wires, and organic light-emitting diodes (OLEDs) (Fig.2-25) (140).

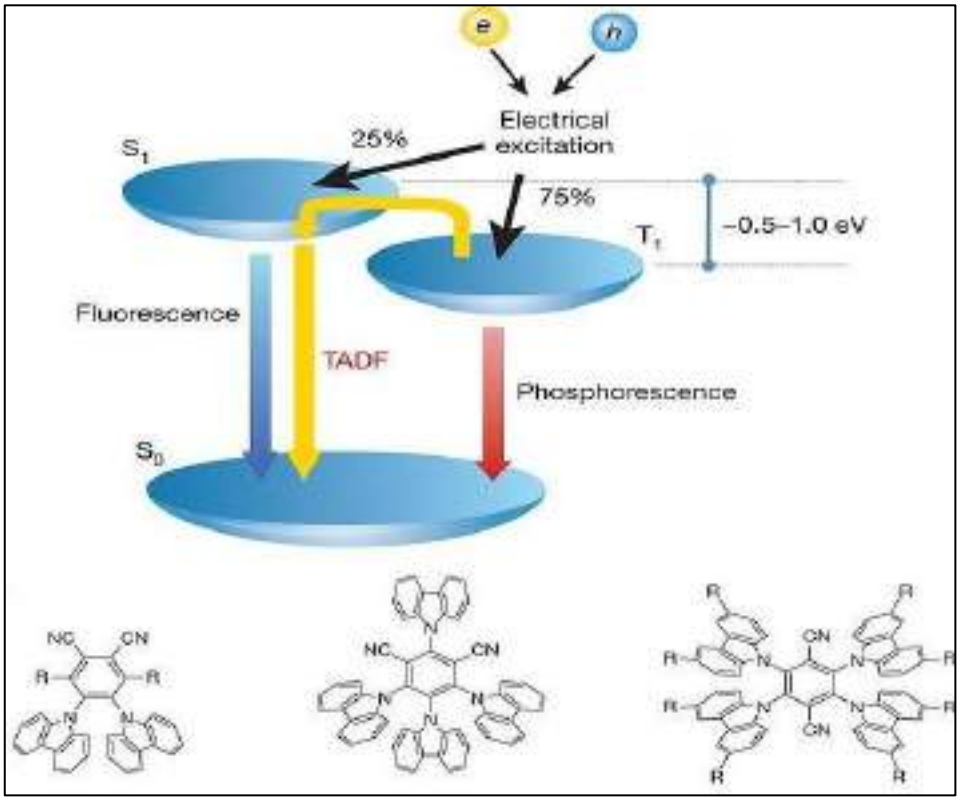


Figure (2- 24): Examples of highly efficient organic light-emitting diodes (OLEDs) and novel electroluminescence mechanism using thermally activated delayed fluorescence (TADF).

At last, but not the least, they are valuable synthetic intermediates. Therefore, substantial attention has been paid to develop efficient and straightforward methods

to synthesize heterocycles (141). Therefore, an enormous number of heterocyclic compounds is known and this number continues to increase very rapidly. Over 31 million compounds are now recorded in Chemical Abstracts and a very large proportion of these are heterocyclic.

2.5.1 Drug Design

Drug design, often referred to as rational drug design or simply rational design, is the inventive process of finding new medications based on the knowledge of a biological target. The drug is most commonly an organic small molecule that activates or inhibits the function of a bio molecule such as a protein, which in turn results in a therapeutic benefit to the patient. In the most basic sense, drug design involves the design of molecules that are complementary in shape and charge to the bio molecular target with which they interact and therefore will bind to it. Drug design frequently but not necessarily relies on computer modeling techniques. This type of modeling is sometimes referred to as computer-aided drug design. Finally, drug design that relies on the knowledge of the three-dimensional structure of the bio molecular target is known as structure-based drug design. In addition to small molecules, biopharmaceuticals and especially therapeutic antibodies are an increasingly important class of drugs and computational methods for improving the affinity, selectivity, and stability of this protein-based therapeutics have also been developed.

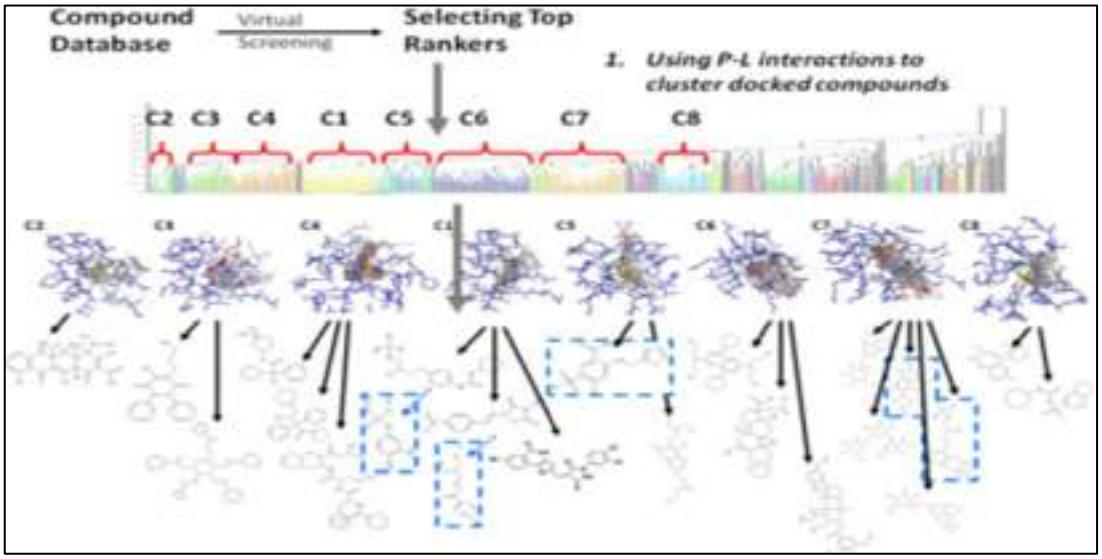
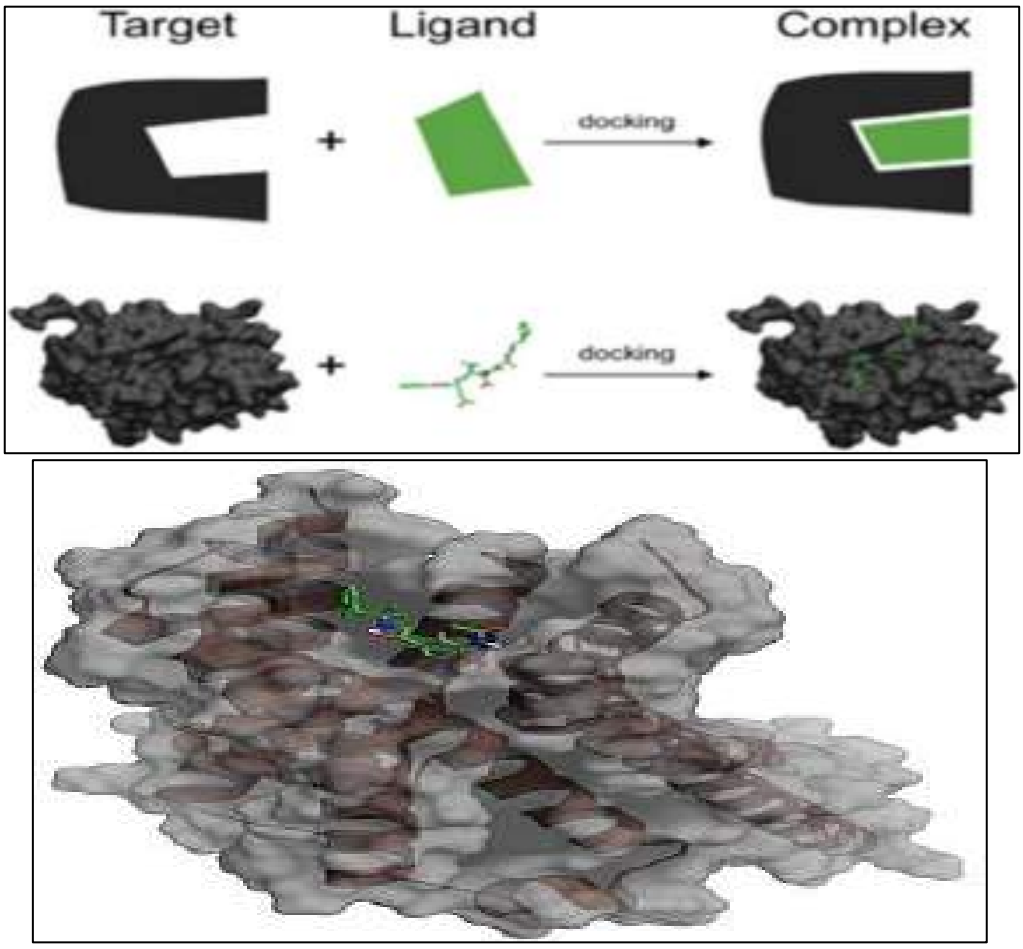


Figure (2- 25): Flowchart of a usual clustering analysis for structure-based drug design

2.5.2 Molecular Docking

In the field of molecular modeling, docking is a method which predicts the preferred orientation of one molecule to a second when bound to each other to form a stable complex. Knowledge of the preferred orientation in turn may be used to predict the strength of association or binding affinity between two molecules using, for example, scoring functions.



Scheme (2- 24): Schematic illustration of docking a small molecule ligand (green) to a protein target (black) producing a stable complex.

The associations between biologically relevant molecules such as proteins, nucleic acids, carbohydrates, and lipids play a central role in signal transduction. Furthermore, the relative orientation of the two interacting partners may affect the type of signal produced (e.g., agonism vs antagonism). Therefore, docking is useful for predicting both the strength and type of signal produced.

Molecular docking is one of the most frequently used methods in structure-based drug design, due to its ability to predict the binding conformation of small

molecule ligands to the appropriate target binding site. Characterization of the binding behavior plays an important role in rational design of drugs as well as to elucidate fundamental biochemical processes.

A- Docking Approaches (142).

Two approaches are particularly popular within the molecular docking community. One approach uses a matching technique that describes the protein and the ligand as complementary surfaces. The second approach simulates the actual docking process in which the ligand-protein pair wise interaction energies are calculated. Both approaches have significant advantages as well as some limitations.

B- Mechanics of Docking

To perform a docking screen, the first requirement is a structure of the protein of interest. Usually the structure has been determined using a biophysical technique such as x-ray crystallography or NMR spectroscopy, but can also derive from homology modeling construction. This protein structure and a database of potential ligands serve as inputs to a docking program. The success of a docking program depends on two components: the search algorithm and the scoring function.

C- Application(143) .

A binding interaction between a small molecule ligand and an enzyme protein may result in activation or inhibition of the enzyme. If the protein is a receptor, ligand binding may result in agonism or antagonism. Docking is most commonly used in the field of drug design — most drugs are small organic molecules, and docking may be applied to:

1-Hit identification – docking combined with a scoring function can be used to quickly screen large databases of potential drugs in silico to identify molecules that are likely to bind to protein target of interest (see virtual screening).

2-Lead optimization – docking can be used to predict in where and in which relative orientation a ligand binds to a protein (also referred to as the binding mode or pose). This information may in turn be used to design more potent and selective analogs.

3-Bioremediation – Protein ligand docking can also be used to predict pollutants

that can be degraded by enzymes.

2.6 CANCER

Cancer is a group of diseases involving abnormal cell growth with the potential to invade or spread to other parts of the body. Not all tumors are cancerous; benign tumors do not spread to other parts of the body. Possible signs and symptoms include a lump, abnormal bleeding, prolonged cough, unexplained weight loss and a change in bowel movements. While these symptoms may indicate cancer, they may have other causes. Over 100 types of cancers affect humans. Tobacco use is the cause of about 22% of cancer deaths. Another 10% is due to obesity, poor diet, lack of physical activity, and excessive drinking of alcohol. Other factors include certain infections, exposure to ionizing radiation and environmental pollutants. In the developing world nearly 20% of cancers are due to infections such as hepatitis B, hepatitis C and human papilloma virus infection. These factors act, at least partly, by changing the genes of a cell. Typically many genetic changes are required before cancer develops.

Chapter Three

Experimental Work

3. Experimental Work

3.1 Materials and Instrument

3.1.1 Materials:

No.	Substances	Formula	Company	Purity %	Mw
1	Thiosemicrbazid	CH_5N_3S	Sigma-Aldrich	99	91.13
2	Pyridine carboxaldehyde	C_6H_5NO	Sigma-Aldrich	99	107.11
3	4-Amino acetophenone	C_8H_9NO	Merck KGaA	98	135.16
4	4-Bromo acetophenone	C_7H_5BrO	Sigma-Aldrich	99	185.03
5	4-Nitro acetophenone	$C_8H_7NO_3$	Sigma-Aldrich	99	165.14
6	4-hyroxy acetophenone	$C_8H_8O_2$	Sigma-Aldrich	99	136.15
7	Benzophenone	$C_{13}H_{10}O$	Merck KGaA	98	182.22
8	Salicylaledhyde	$C_7H_6O_2$	Sigma-Aldrich	99	122.12
9	Glacial acid	CH_3COOH	B.D.H	99	60.052
10	Chloroacetic acid	C_2H_3ClO	Sigma-Aldrich	99	94.5
11	Anhydrouse sodium acetate	CH_3COONa	Sigma-Aldrich	99	82.03
12	Thiophene-2-Carboxxaldehyde	C_5H_4OS	Sigma-Aldrich	99	112.15
13	Furfural	$C_5H_4O_2$	Sigma-Aldrich	99	99.10
14	2-Acetyl thiophene	C_6H_6OS	Sigma-Aldrich	99	126.18
15	N, N-dimethyl amino benzaldehyde	$C_9H_{11}NO$	Sigma-Aldrich	98	149.19
16	Ethanol	C_2H_6O	Scharlau	99.9	46.06
17	Ethyl chloroacetatte	$C_3H_5O_2cl_2$	Sigma-Aldrich	99	122.55
18	Sodium acetate	$C_2H_3NaO_2$	Sigma-Aldrich	99	82.03
19	5-Amino phthalic acid	$C_8H_7NO_4$	Sigma-	99	181.15

No.	Substances	Formula	Company	Purity %	Mw
			Aldrich		
20	Athranilic acid	$C_7H_7NO_2$	Sigma-Aldrich	99	137.14
21	5-Amino-2-hydroxybenzoic acid	$C_{14}H_{14}N_2O_5$	Sigma-Aldrich	99	290.27
22	Phosphoryl trichloride	$POCl_3$	Riedel-Dehaen	98	153.33
23	Potassium hydroxide	KOH	B.D.H	98	56.106
24	Acid anhydride	$C_4H_6O_3$	B.D.H	99	102.09
25	3, 3, 4, 4-Benzophenone tetracarboxylic dianhydride	$C_{17}H_6O_7$	Sigma-Aldrich	98	322.23
26	Tirphthelitic anhydride	$C_8H_4O_3$	Sigma-Aldrich	98.5	148.11
27	Pyridine	C_5H_5N	Sigma-Aldrich	99	79.10
28	3, 3.4, 4-Biphenyl tetra carboxylic dianhydride	$C_{16}H_6O_6$	Sigma-Aldrich	99	294.22
29	Dry benzene	C_6H_6	Merck KGaA	99.9	78.11
30	Chloro acetyl chloride	$C_2H_2Cl_2O$	Merck KGaA	98	112.94
31	2-Amino -1, 3, 4-thiadia zol-5-thiol	$C_2H_3N_3S_2$	Sigma-Aldrich	98	133.20
32	Urea	CH_4N_2O	Merck KGaA	98	60.06
33	1, 4-dioxane	$C_4H_8O_2$	Merck KGaA	99	88.11
34	Terephthalic acid	$C_8H_6O_4$	Sigma-Aldrich	99	166.13
35	Tetrahydrofuran	C_4H_8O	Merck KGaA	99	72.11
36	Sodium Azide	N_3Na	Sigma-Aldrich	99	65.010
37	Isatin	$C_8H_5NO_2$	Sigma-Aldrich	98	147.13
38	Mercapto acetic acid (Thioglycolic acid)	$C_2H_4O_2S$	Sigma-Aldrich	99	92.12
39	Thiourea	CH_4N_2S	Merck KGaA	98	76.12
40	Mono chloro acetic acid	$ClCH_2COOH$	Sigma-Aldrich	99.5	94.50

No.	Substances	Formula	Company	Purity %	Mw
41	Methanol	CH_3OH	Sigma-Aldrich	99	32.042
42	Sodium bicarbonate	$C_2H_2Na_2O_6$	Merck KGaA	99	168.01
43	Formalin	$C_2H_4O_2$	B.D.H		60.05
44	Magnesium sulfate	MgO_4S	B.D.H	99	120.37
45	3, 4 -Diamino diphenyl ether	$C_{12}H_{12}N_2O$	Sigma-Aldrich	99	200.24
46	2-aminothiazol	$C_3H_4N_2S$	Sigma-Aldrich	99	100.14
47	1, 4-phenylenediamine	$C_6H_8N_2$	Sigma-Aldrich	99	108.14
48	Triethylenetetramine	$C_6H_{18}N_4$	Sigma-Aldrich	99	146.23
49	2, 6-Diamino pyridine	$C_5H_7N_3$	Thomas Baker	99	109.13
50	Itaconic anhydride	$C_5H_4O_3$	Sigma-Aldrich	99	112.08
51	Methacrylic acid	$C_4H_6O_2$	Normapur	98	86.09
52	1-Hydroxycyclohexyl phenyl ketone	$C_{13}H_{16}O_2$	Sigma-Aldrich	99	204.26
53	Citraconic anhydride	$C_5H_4O_3$	Sigma-Aldrich	99	112.08
54	N, N dimethyl acrylic amide	C_5H_9NO	Sigma-Aldrich	99	99.13
55	Aniline	C_6H_7N	Merck KGaA	99	93.13
56	Anhydrous DMF	C_3H_7NO	B.D.H	98	73.09
57	Acetone	C_3H_6O	B.D.H	99.8	58.08
58	Sulfuric acid	H_2SO_4	Sigma-Aldrich	99	98.08
59	Sodium hydroxide	NaOH	Sigma-Aldrich	99	40.00

3.1.2 Instrument

1. **^{1}H-NMR Spectra:** were registered using a Bruker , ultra-shield 500Mhz , spectrometer (Switzerland) using DMSO d6 a solvent , at the university of Tehran in Iran .

2. **Fourier Transform Infrared (FTIR) Spectroscopy:** it was used the Fourier transport infrared spectrophotometer of type FT-IR -8400 s supplied by the Bruker company , Germany in the characterization of the recorder preparation compound by the detection the active group, and detect the type of bounds that bind the particles of the mineral , Department University of Baghdad.
3. **Vacuum drying oven k-vo27 , K&K scientific suppler , Korea .**
4. **Degree of Fusion (Melting points) :** were measured the penile and lattice Stuart smp30 melting point apparatus Hotplate stirrer : model - 81 , albinos , the Netherlands . Vacuum drying oven k-vo27 , K&K scientific suppler , Korea .
5. **Thermo gravimetric "analysis" (TGA)** as well as a differential scanning calorimetry (DSC), Measurement utilizing a heating rate of 10° C/min in Argon atmosphere in the temperature range of (30-800°C) measurement using apparatus Perkin Elmer in the laboratory of Tehran University Iran.

3.2 Synthesis of the Thiosemicarbazones compounds (1-9).

A mixture of aromatic aldehyde and ketone pyridine carboxaldehyde, 4-amino acetophenone, 4- nitro acetophenone, , benzophenone, salicylaldehyde thiophene-2-carboxaldehyde, Furfural, 2-Acetyl thiophene, N, N-dimethyl amino benzaldeyde, compounds (1-9) (0.01 mole), thiosemicarbazide (0.01 mole) in 20 mL of ethanol, and four drops of glacial acetic acid were heated under reflux for 5 hours at 78°C. The product was cooled to room temperature, and the solid was filtered, dried, and purified to *via* recrystallization with ethanol.

3.2.1 Synthesis of Thiosemicarbazones of 2-(pyridin-2-ylmethylene) hydrazine-1-carbothioamide compound(1).

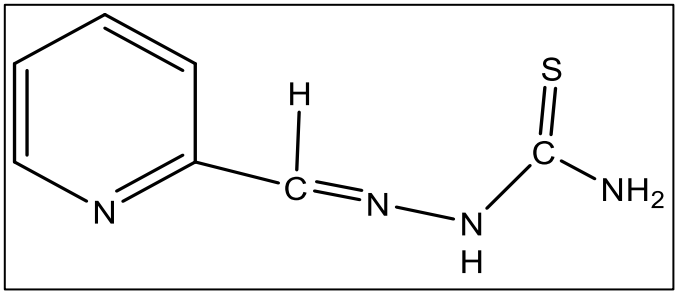


Figure (3-): structure of thiosemicarbazones of 2-(pyridin-2-ylmethylene)hydrazine-1-carbothioamide compound(1).

Table (3- 1): Elemental analysis data of compound (1) (calculated vs. found values).

CHNS	%C	%H	%N	%S
Calculated	46.60	4.99	31.07	17.75
Found	46.90	5.29	31.37	18.05

3.2.2 Synthesis of Thiosemicarbazones of 2-(1-(4-aminophenyl) ethylidene) hydrazine-1-carbothioamide compound(2).

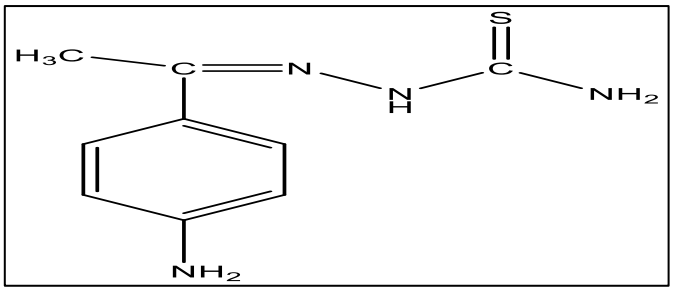


Figure (3- 1): structure of thiosemicarbazones of 2-(1-(4-aminophenyl) ethylidene) hydrazine-1-carbothioamide compound (2).

Table (3- 2): Elemental analysis data of compound (2) (calculated vs. found values).

CHNS	%C	%H	%N	%S
Calculated	48.62	5.47	26.92	15.38
Found	48.92	5.77	27.22	15.68

3.2.3 Synthesis of Thiosemicarbazones of 2-(1-(4-nitrophenyl)ethylidene)hydrazine-1-carbothioamide compound(3).

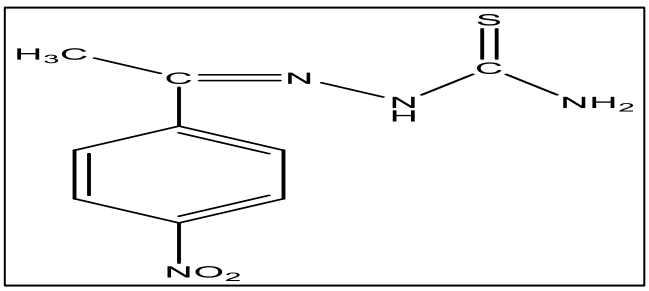


Figure (3- 2): structure of thiosemicarbazones of 2-(1-(4-nitrophenyl)ethylidene)hydrazine-1-carbothioamide compound(3).

Table (3- 3): Elemental analysis data of compound (3) (calculated vs. found values).

CHNOS	%C	%H	%N	%O	%S
Calculated	45.37	4.20	3.522	13.44	13.44
Found	45.67	4.50	23.82	13.74	13.74

3.2.4 Synthesis of Thiosemicarbazones of 2-(diphenylmethylene)hydrazine-1-carbothioamide compound(4).

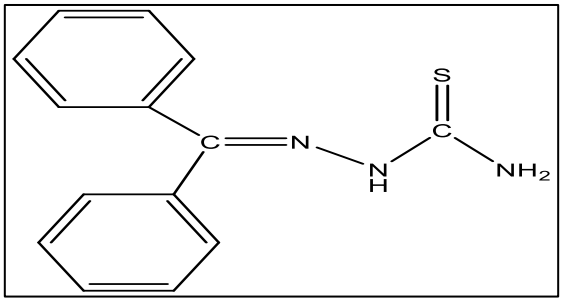


Figure (3- 3): structure thiosemicarbazones of 2-(diphenylmethylene)hydrazine-1-carbothioamide compound(4).

Table (3- 4): Elemental analysis data of compound (4) (calculated vs. found values).

CHNS	%C	%H	%N	%S
Calculated	64.36	5.09	6.47	12.54
Found	65.88	5.39	16.77	12.84

3.2.5 Synthesis of Thiosemicarbazones of 2-(6-hydroxybenzylidene) hydrazine-1-carbothioamide compound(5).

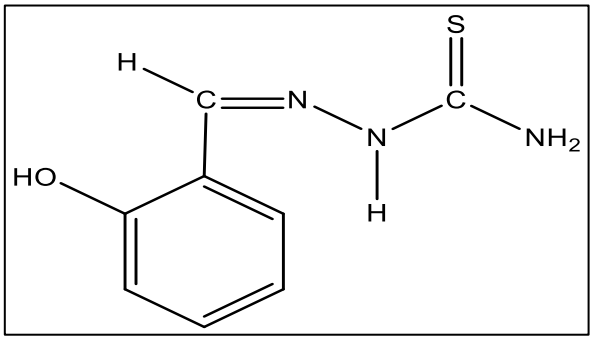


Figure (3- 4): structure of thiosemicarbazones of 2-(6-hydroxybenzylidene)hydrazine-1-carbothioamide compound(5).

Table (3- 5): Elemental analysis data of compound (5) (calculated vs. found values).

CHNOS	%C	%H	%N	%O	%S
Calculated	49.17	4.60	21.15	3.86	20.09
Found	49.47	4.90	21.18	4.06	20.39

3.2.6 Synthesis of 2-(thiophen-2-ylmethylene)hydrazine-1-carbothioamide thiosemicarbazon compound(6).

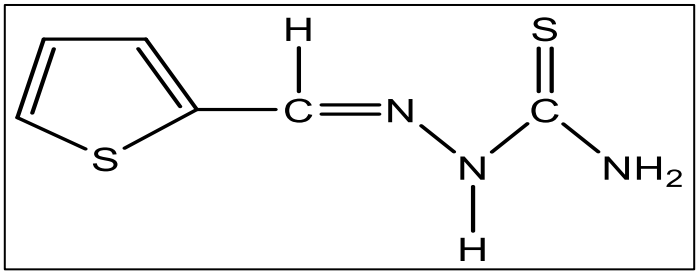


Figure (3- 5): structure of 2-(thiophen-2-ylmethylene)hydrazine-1-carbothioamide compound(6)

Table (3- 6): Elemental analysis data of compound (6) (calculated vs. found values).

CHNS	%C	%H	%N	%S
Calculated	38.79	4.30	22.58	34.40
Found	39.09	4.60	23.88	34.70

3.2.7 Synthesis of 2-(furan-2-ylmethylene)hydrazine-1-carbothioamide thiosemicarbazon compound(7).

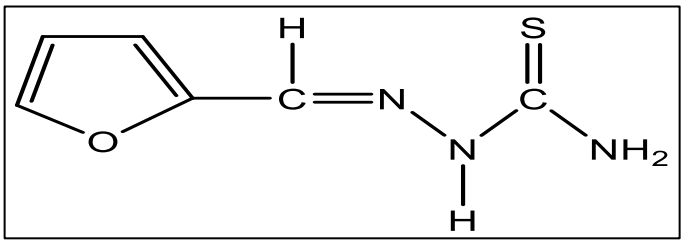


Figure (3- 6): structure of 2-(furan-2-ylmethylene)hydrazine-1-carbothioamide thiosemicarbazon compound(7).

Table (3- 7): Elemental analysis data of compound (7) (calculated vs. found values).

CHNOS	%C	%H	%N	%O	%S
Calculated	46.15	4.12	17.94	9.87	20.51
Found	46.45	4.42	18.24	10.17	20.18

3.2.8 Synthesis of (Z)-2-(1-(thiophen-2-yl)ethylidene)hydrazine-1-carbothioamide thiosemicarbazone compound(8).

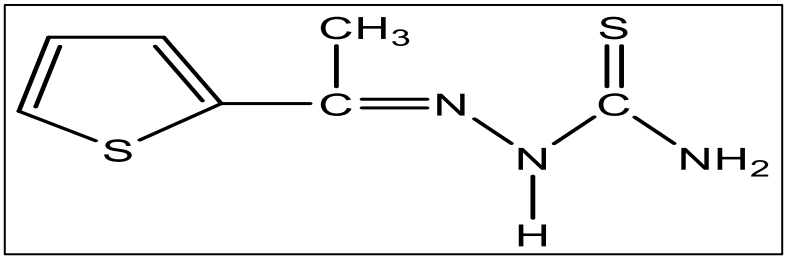


Figure (3- 7): structure of (Z)-2-(1-(thiophen-2-yl)ethylidene)hydrazine-1-carbothioamide thiosemicarbazone compound(8).

Table (3- 8): Elemental analysis data of compound (8) (calculated vs. found values).

CHNS	%C	%H	%N	%S
Calculated	42	5	21	32
Found	42. 3	5.3	21.3	32.3

3.2.9 Synthesis of N, N-dimethyl amino benzaldeyde thiosemicarbazone compound(9).

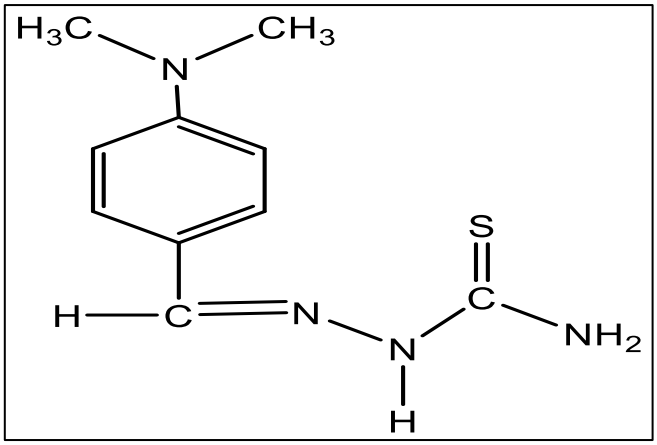


Figure (3- 8): structure of N, N-dimethyl amino benzaldeyde thiosemicarbazone compound(9).

Table (3- 9): Elemental analysis data of compound (9) (calculated vs. found values.

CHNOS	%C	%H	%N	%S
Calculated	49.0.5	5.30	25.22	14.14
Found	49.35	5.60	25.52	14.71

3.3 Synthesis of 2-(4-Substituted-benzylidene hydrazono)-1, 3-Thiazolidine-4-one compounds (10-17).

A mixture of Thiosemicarbazide derivatives compounds (1-8) was prepared by heating and continuous stirring for 0.01 mole chloroacetic acid and 0.01 mole anhydrous sodium acetate 0.01 mole in 20 ml glacial acetate acid under reflux for 8 h . The produced were left to cool via poured into ice cold water, and separated solid was filtered off, washed with water, dried, and recrystallized by absolute ethanol.

3.3.1 Synthesis of N-(Carboxymethyl) 2-(pyridin-2-ylmethylene)hydrazine-1-carbothioamide compound (10).

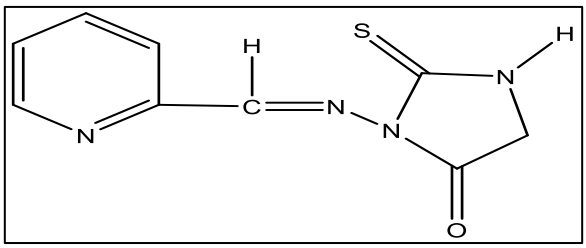


Figure (3- 9): structure of N-(Carboxymethyl) 2-(pyridin-2-ylmethylene)hydrazine-1-carbothioamide compound(10).

Table (3- 10): Elemental analysis data of compound (10) (calculated vs. found values).

CHNOS	%C	%H	%N	%O	%S
Calculated	49.03	3.63	27.96	2	15.98
Found	49.33	3.93	28.26	2.2	16.28

3.3.2 Synthesis of N-(Carboxymethyl) -4-Aminoacetophenone thiosemicarbazone compound(11).

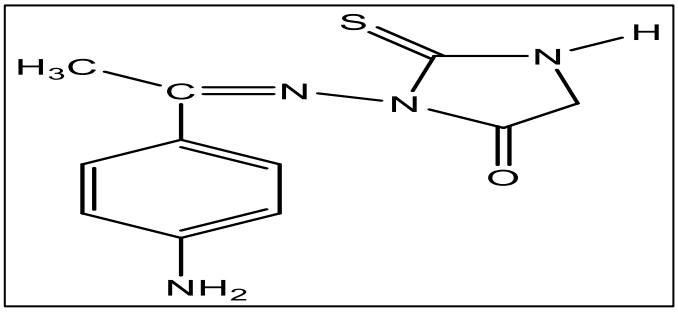


Figure (3- 10): structure of N-(Carboxymethyl) -4-Aminoacetophenone thiosemicarbazone compound(11).

Table (3- 11): Elemental analysis data of compound (11) (calculated vs. found values)

CHNOS	%C	%H	%N	%O	%S
Calculated	44.51	3.03	24.96	11.7	14.24
Found	44.81	3.39	25.26	12	14.54

3.3.3 Synthesis of N-(Carboxymethyl) 4-Nitroacetophenone thiosemicarbazone compound(12).

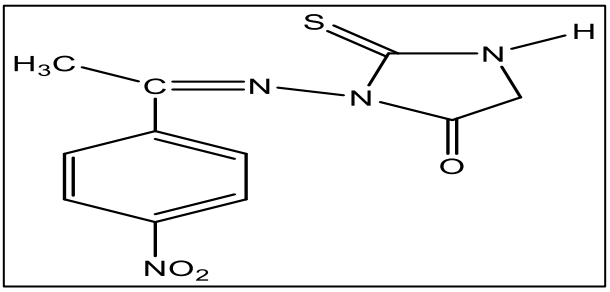


Figure (3- 11): structure of N-(Carboxymethyl) 4-Nitroacetophenone thiosemicarbazone compound(12).

Table (3- 12): Elemental analysis data of compound (12) (calculated vs. found values)

CHNOS	%C	%H	%N	%O	%S
Calculated	49.22	3.03	24.21	9.14	12.90
Found	49.52	3.33	24.51	9.44	13.20

3.3.4 Synthesis of N-(Carboxymethyl) benzophenone thiosemicarbazone compound(13).

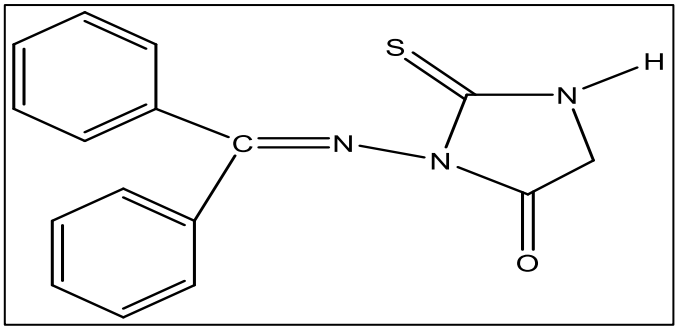


Figure (3- 12): structure of N-(Carboxymethyl) benzophenone thiosemicarbazone compound(13).

Table (3- 13): Elemental analysis data of compound (13) (calculated vs. found values).

CHNOS	%C	%H	%N	%O	%S
Calculated	65.08	4.40	14.23	4.05	10.84
Found	65.38	4.70	14.53	4.25	11.14

3.3.5 Synthesis of N-(Carboxymethyl) salicylaldehyde thiosemicarbazone compound(14).

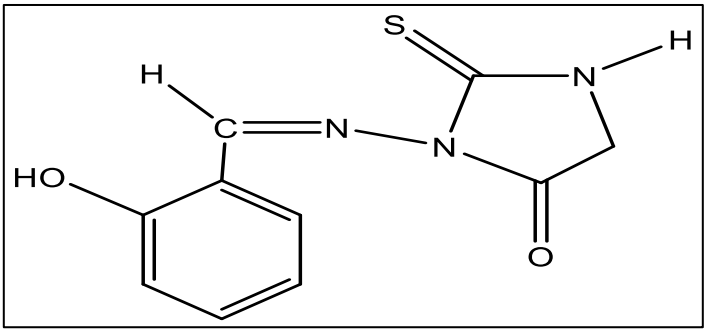


Figure (3- 13): structure of N-(Carboxymethyl) salicylaldehyde thiosemicarbazone compound(14).

Table (3- 14): Elemental analysis data of compound (14) (calculated vs. found values).

CHNOS	%C	%H	%N	%O	%S
Calculated	49.16	3.82	20.97	11.14	13.61
Found	49.36	4.12	21.17	11.44	13.91

3.3.6 Synthesis of 3-((thiophen-2-ylmethylene)amino)-2-thioxoimidazolidin-4-one compound(15).

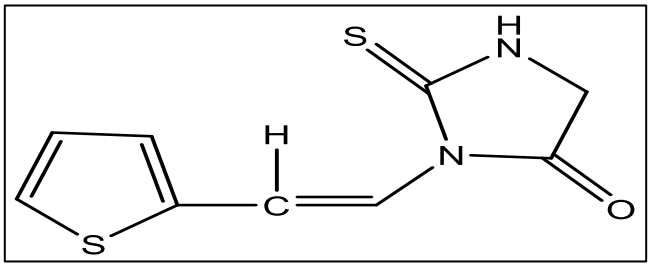


Figure (3- 14): structure of 3-((thiophen-2-ylmethylene)amino)-2-thioxoimidazolidin-4-one compound(15).

Table (3- 15): Elemental analysis data of compound (15) (calculated vs. found values).

CHNOS	%C	%H	%N	%O	%S
Calculated	42.66	3.11	18.66	7.13	28.44
Found	42.96	3.41	18.96	7.43	28.74

3.3.7 Synthesis of 3-((furan-2-ylmethylene)amino)-2-thioxoimidazolidin-4-one compound(16).

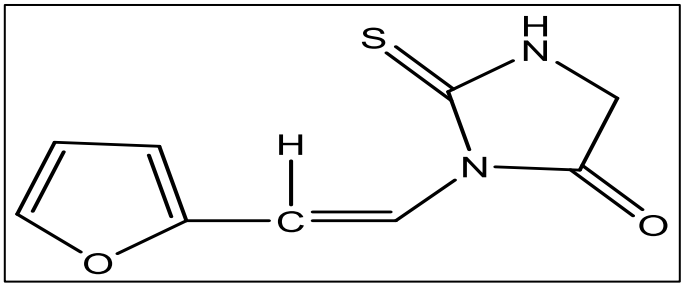


Figure (3- 15): structure of 3-((furan-2-ylmethylene)amino) -2-thioxoimidazolidin-4-one compound(16).

Table (3- 16): Elemental analysis data of compound (16) (calculated vs. found values).

CHNOS	%C	%H	%N	%O	%S
Calculated	45.94	2.34	20.09	15.33	15.31
Found	46.24	3.64	20.39	15.63	15.61

3.3.8 Synthesis of (E)-3-((1-(thiophen-2-yl)ethylidene)amino)-2-thioxoimidazolidin-4-one compound(17).

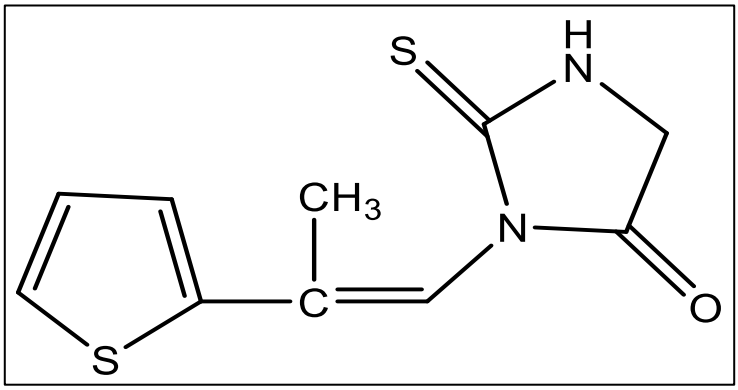


Figure (3- 16): structure of (E)-3-((1-(thiophen-2-yl)ethylidene)amino)-2-thioxoimidazolidin-4-one compound(17).

Table (3- 17): Elemental analysis data of compound (17) (calculated vs. found values).

CHNOS	%C	%H	%N	%O	%S
Calculated	45.18	3.76	20.4	12.59	16.47
Found	45.48	4.06	20.80	12.89	16.77

3.4 Synthesis of 5-styryl-2-amino -1, 3, 4-thiadiazole (18-20)

The mixture (0.01 mol) from acids 5-amino phthalic acid , Anthranilic acid, 5-amino-2-hydroxybenzoic acid with (0.01 mol) thiosemicarbazide in (10 ml) of $POCl_3$ was refluxed 4 hours, the excess of $POCl_3$ was removed and the residue was dissolved in distilled water (50 ml) then heated for 1 h. After that, the resulting product was cooled, filtered, and neutralized with KOH. The precipitate was filtered, dried, and recrystallized in ethanol.

3.4.1 Synthesis of N-(5-aminophthaloyl) thiosemicarbazide Compound(18).

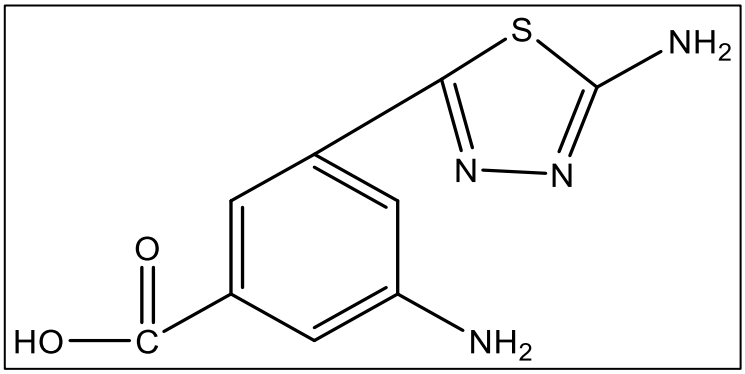


Figure (3- 17): structure of N-(5-aminophthaloyl) thiosemicarbazide compound(18).

Table (3- 18): Elemental analysis data of compound (18) (calculated vs. found values).

CHNOS	%C	%H	%N	%O	%S
Calculated	47.57	3.52	24.66	14.09	14.09
Found	47.77	3.72	24.86	14.29	14.29

3.4.2 Synthesis of 5-amino-2-(2-aminophenyl)-2, 5-dihydro-1, 3, 4-thiadiazol-2-ol compound(19).

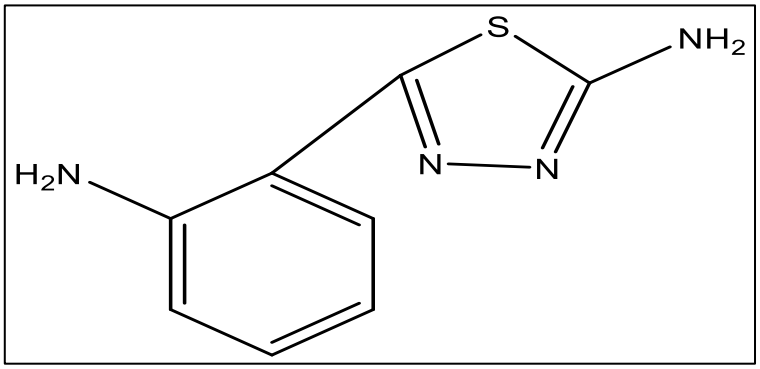


Figure (3- 18): structure of 5-amino-2-(2-aminophenyl)-2, 5-dihydro-1, 3, 4-thiadiazol-2-ol compound(19).

Table (3- 19): Elemental analysis data of compound (19) (calculated vs. found values).

CHNS	%C	%H	%N	%S
Calculated	45.71	3.66	26.66	15.23
Found	45.91	3.96	26.86	15.43

3.4.3 Synthesis of 5-amino-2-(5-amino-2-hydroxyphenyl)-2, 5-dihydro-1, 3, 4-thiadiazol-2 compound(20).

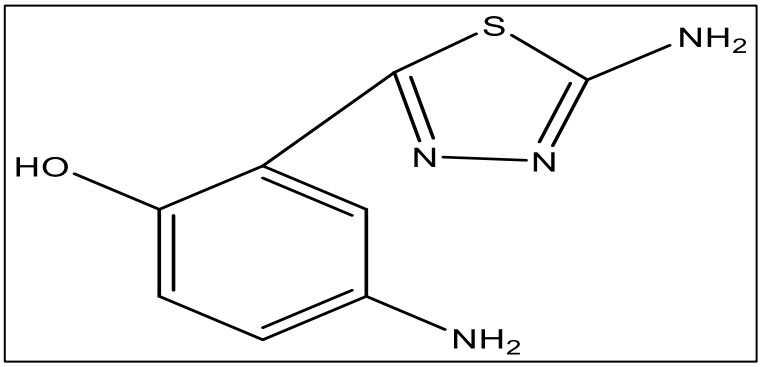


Figure (3- 19): structure of 5-amino-2-(5-amino-2-hydroxyphenyl)-2, 5-dihydro-1, 3, 4-thiadiazol-2 compound(20).

Table (3- 20): Elemental analysis data of compound (20) (calculated vs. found values).

CHNOS	%C	%H	%N	%O	%S
Calculated	45.47	3.7	24.77	9.81	15.15
Found	45.67	4	24.97	10.01	15.35

3.5 Synthesis of Imide compounds(21-23)

For a 250 mL round-bottomed flask, additions were made of dianhydride acids 3, 3', 4, 4'-Benzophenone tetracarboxylic dianhydride, Trimellitic anhydride, 3, 3, 4, 4-Biphenyl tetra carboxylic dianhydride (6.8mole), (21.2mole) compound from (21-23), and 80 ml of a 3:2 solution of acetic acid and pyridine. The mixture was stirred for two hours at room temperature before being refluxed for one hour at 60 °C. Filtered, and dried solid.

3.5.1 Synthesis of 3-amino-5-(5-(5-(1, 3-dioxo-1, 3-dihydroisobenzofuran-5-carbonyl)-3-methylene-1-oxoisoindolin-2-yl)-4, 5-dihydro-1, 3, 4-thiadiazol-2-yl)benzoic acid compound(21).

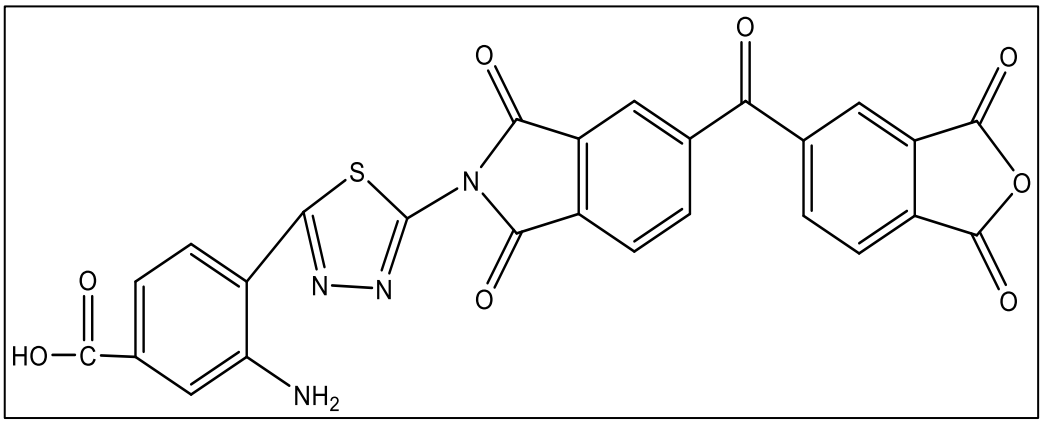


Figure (3- 20): structure of 3-amino-5-(5-(5-(1, 3-dioxo-1, 3-dihydroisobenzofuran-5-carbonyl)-3-methylene-1-oxoisoindolin-2-yl)-4, 5-dihydro-1, 3, 4-thiadiazol-2-yl)benzoic acid compound(21).

Table (3- 21): Elemental analysis data of compound (21) (calculated vs. found values).

CHNOS	%C	%H	%N	%O	%S
Calculated	57.56	2.58	10.33	23.63	5.90
Found	57.86	3.88	10.63	23.93	6.20

3.5.2 Synthesis of 2-(5-(2-aminophenyl)-1, 3, 4-thiadiazol-2-yl)-1, 3-dioxoisoindoline-5-carboxylic acid compound(22).

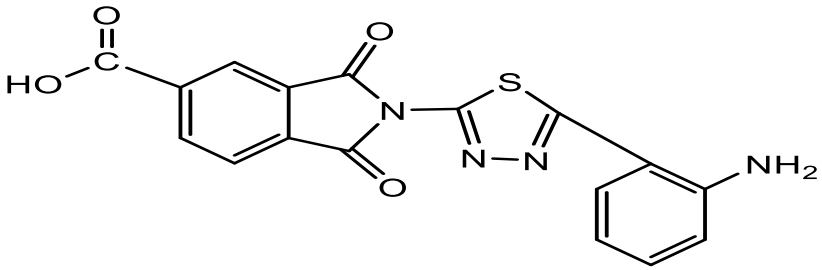


Figure (3- 21): structure of 2-(5-(2-aminophenyl)-1, 3, 4-thiadiazol-2-yl)-1, 3-dioxoisoindoline-5-carboxylic acid compound(22).

Table (3- 22): Elemental analysis data of compound (22) (calculated vs. found values).

CHNOS	%C	%H	%N	%O	%S
Calculated	58.36	2.72	10.89	21.81	6.22
Found	58.56	2.92	11.09	22.01	6.42

3.5.3 Synthesis of 2-(5-(5-amino-2-hydroxyphenyl)-1, 3, 4-thiadiazol-2-yl)-5-(1, 3-dioxo-1, 3-dihydroisobenzofuran-5-yl)isoindoline-1, 3-dione compound(23).

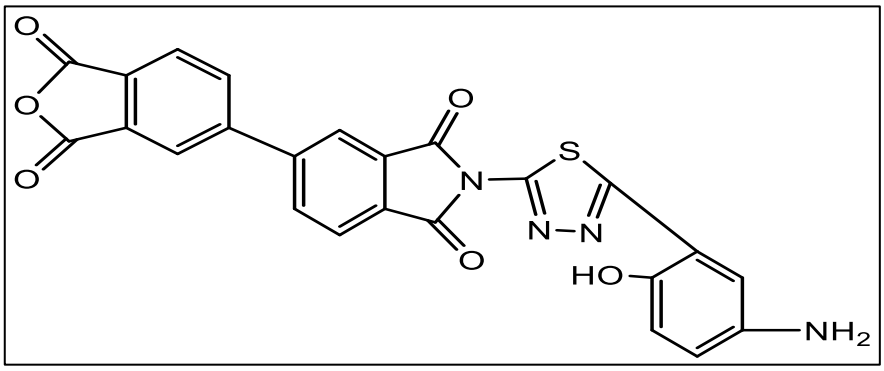


Figure (3- 22): structure of 2-(5-(5-amino-2-hydroxyphenyl)-1, 3, 4-thiadiazol-2-yl)-5-(1, 3-dioxo-1, 3-dihydroisobenzofuran-5-yl)isoindoline-1, 3-dione compound(23).

Table (3- 23): Elemental analysis data of compound (23) (calculated vs. found values)

CHNOS	%C	%H	%N	%O	%S
Calculated	56.60	2.64	10.56	24.12	6.03
Found	56.80	2.84	10.76	24.35	6.05

3.6 Synthesis 1-(3-(derivative)-1, 5-dioxo-1, 5-dihydrobenzo[e] [1, 3] oxazepin -4(3H)-yl) thiourea compounds. (24-26)

A 0.0 25 mole from thiosemcarbazone derivatives (1), (2), (9) compounds and 0.025 mole from anhydride acids 3, 3', 4, 4'-Benzophenone tetracarboxylic dianhydride, Trimellitic anhydride, 3, 3, 4, 4-Biphenyl tetra carboxylic dianhydride in 20 mL from dry benzene was mixed, refluxed, and stirring on a water bath at 75 °C for 12-14 h.

3.6.1 Synthesis of 1-(8-(1, 3-dioxo-1, 3-dihydroisobenzofuran-5-carbonyl)-1, 5-dioxo-3-(pyridin-2-yl)-1, 5-dihydrobenzo[e][1, 3]oxazepin-4(3H)-yl)urea. (Compound24)

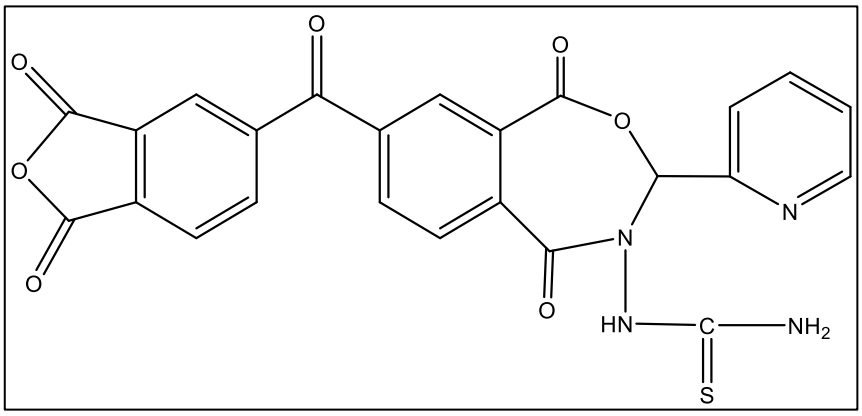


Figure (3- 23): structure of 1-(8-(1, 3-dioxo-1, 3-dihydroisobenzofuran-5-carbonyl)-1, 5-dioxo-3-(pyridin-2-yl)-1, 5-dihydrobenzo[e][1, 3]oxazepin-4(3H)-yl)urea compound(24).

Table (3- 24): Elemental analysis data of compound (24) (calculated vs. found values).

CHNOS	%C	%H	%N	%O	%S
Calculated	55.59	2.70	10.81	25.36	6.17
Found	55.79	2.90	11.01	25.56	6.37

3.6.2 Synthesis of 3-(4-aminophenyl)-3-methyl-1, 5-dioxo-4-thioureido-1, 3, 4, 5-tetrahydrobenzo[e][1, 3]oxazepine-8-carboxylic acid compound(25).

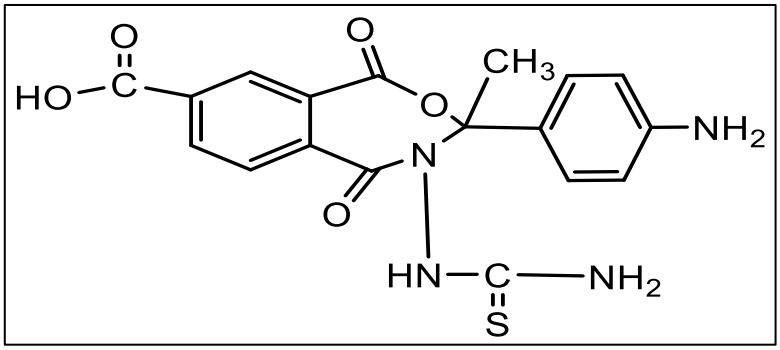


Figure (3- 24): structure of 3-(4-aminophenyl)-3-methyl-1, 5-dioxo-4-thioureido-1, 3, 4, 5-tetrahydrobenzo[e][1, 3]oxazepine-8-carboxylic acid compound(25).

Table (3- 25): Elemental analysis data of compound (25) (calculated vs. found values)

CHNOS	%C	%H	%N	%O	%S
Calculated	50.74	3.48	13.93	23.89	7.96
Found	50.94	3.68	14.13	24.09	8.16

3.6.3 Synthesis of 1-(3-(3-(dimethylamino)phenyl)-1, 5-dioxo-9-(4-(3-oxobutanoyl)phenyl)-1, 5-dihydrobenzo[e][1, 3]oxazepin-4(3H)-yl)urea compound(26).

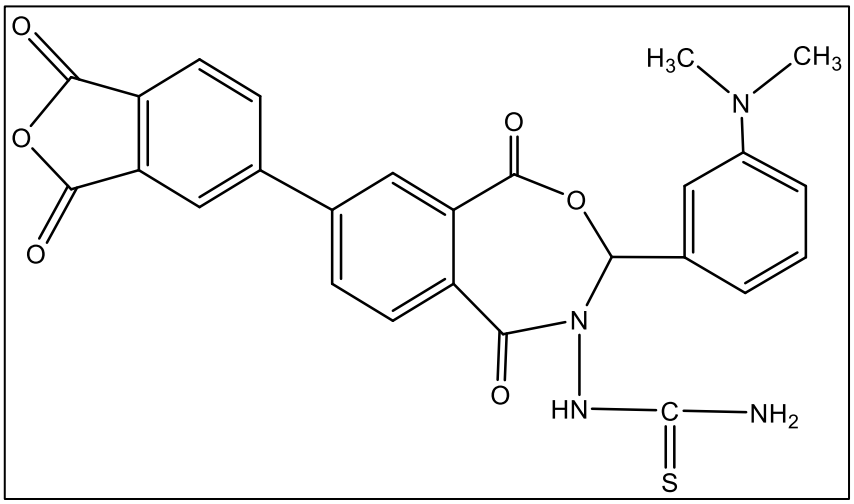


Figure (3- 25): structure of 1-(3-(3-(dimethylamino)phenyl)-1, 5-dioxo-9-(4-(3-oxobutanoyl)phenyl)-1, 5-dihydrobenzo[e][1, 3]oxazepin-4(3H)-yl)urea compound(26).

Table (3- 26): Elemental analysis data of compound (26) (calculated vs. found values).

CHNOS	%C	%H	%N	%O	%S
Calculated	58.13	4.15	10.56	18.13	6.03
Found	58.33	4.35	10.76	18.33	6.23

3.7 Synthesis of 2-chloro-N-(5-mercapto-1, 3, 4- thiadiazole-2-yl) acetamide compound(27).

Freshly 2.5 mL of distilled chloro acetyl chloride was dissolved in 100 mL dry benzene, and gradually added to a mixture of 0.033 mole (4.3 g) from 2-amino 1, 3, 4-thiadiazole-5-thiol in 30 mL dry benzene. The mixture was refluxed via a water bath for 4 h. and benzene solvent was distilled off. The product was washed with distilled water, dried, and recrystallized using absolute ethanol.

3.7.1 Synthesis of (5-mercapto-1, 3, 4-thiadiazol-2-yl)glycinoyl chloridecompound(27).

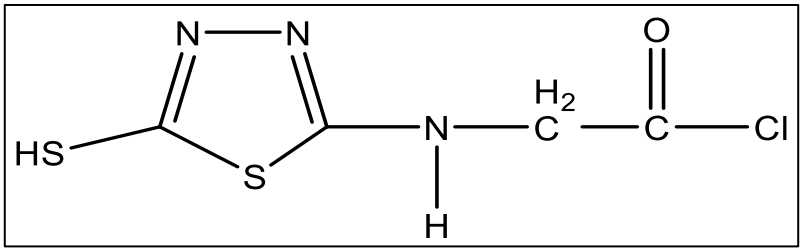


Figure (3- 26): structure of (5-mercapto-1, 3, 4-thiadiazol-2-yl) glycinoyl chloridecompound(27).

Table (3- 27): Elemental analysis data of compound (27) (calculated vs. found values).

CHNOS	%C	%H	%N	%O	%S
Calculated	22.96	1.91	20.09	24.42	30.62
Found	23.26	2.21	20.39	24.62	30.92

3.8 Synthesis of N-(5-mercapto-1, 3, 4-thiadiazole-2-yl)-2-ureidoacetamide compound(28).

Exact 0.01mole (4.18 g) from compound (27) was refluxed with 0.02 mole, (1.2 g) from urea for 14h. In 20 mL from absolute ethanol. Then the reaction mixture was filtered, recrystallized the product by ethanol, and dried to give the final product.

3.8.1 *Synthesis* of N-carbamoyl-2-((5-mercapto-1, 3, 4-thiadiazol-2 yl)amino)acetamide compound(28).

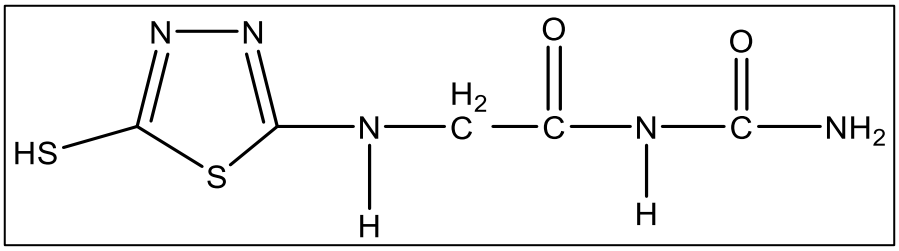


Figure (3- 27): structure of N-carbamoyl-2-((5-mercapto-1, 3, 4-thiadiazol-2 yl)amino)acetamide compound(28).

Table (3- 28): Elemental analysis data of compound (28) (calculated vs. found values).

CHNOS	%C	%H	%N	%O	%S
Calculated	25.75	3	30.04	13.75	27.46
Found	26.05	3.3	30.34	13.95	27.76

3.9 *Synthesis* of some 2, 3-dihydroquinosulin4-one derivatives.(29 -31)

(0.06mole) of some Schiff bases derivatives (6), (7), (8) was dissolved in (10ml) of (1, 4-dioxane) and added to (0.06mole, 0.095gm) of anthranilic acid dissolved in (5ml) of (1, 4 - dioxane), then the mixture was refluxed for (14-16) hours, The mixture was cooled, and then filtered, washed with cold water, recrystallized with absolute ethanol, and dried at a temperature of 100C.

3.9.1 *Synthesis* of 1-(4-oxo-2-(thiophen-2-yl)-1, 4-dihydroquinazolin-3(2H)-yl)thiourea compound(29).

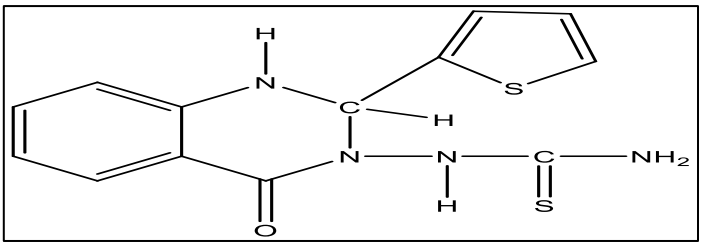


Figure (3- 28): structure of 1-(4-oxo-2-(thiophen-2-yl)-1, 4-dihydroquinazolin-3(2H)-yl)thiourea compound(29).

Table (3- 29): Elemental analysis data of compound (29) (calculated vs. found values).

CHNOS	%C	%H	%N	%O	%S
Calculated	41.71	3.20	33.68	4.17	7.111
Found	42.01	3.50	32.98	4.37	17.41

3.9.2 *Synthesis* of 1-(2-(furan-2-yl)-4-oxo-1, 4-dihydroquinazolin-3(2H)-yl)thiourea compound(30).

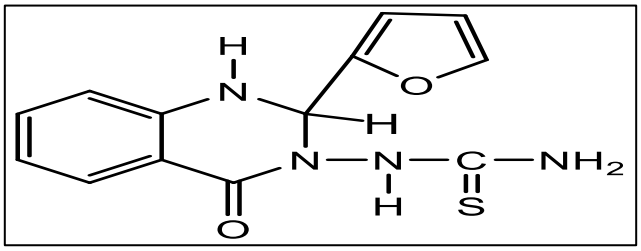


Figure (3- 29): structure 1-(2-(furan-2-yl)-4-oxo-1, 4-dihydroquinazolin-3(2H)-yl)thiourea compound(30).

Table (3- 30): Elemental analysis data of compound (30) (calculated vs. found values).

CHNOS	%C	%H	%N	%O	%S
Calculated	44.06	4.16	31.44	7.93	11.11
Found	44.36	4.36	31.74	8.13	11.41

3.9.3 *Synthesis* of 1-(4-oxo-2-(thiophen-2-yl)-1, 4-dihydroquinazolin-3(2H)-yl)thiourea compound(31).

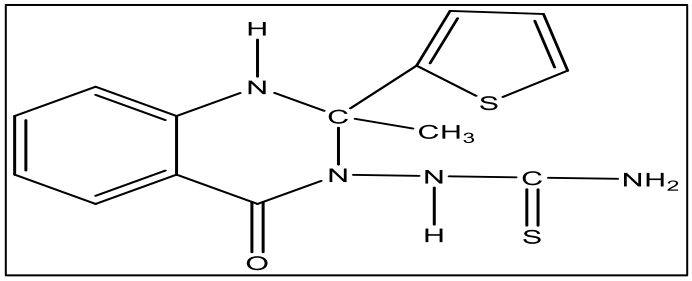


Figure (3- 30): structure of (Z)-N-(3-amino-2-formylphenyl)-2-(1-(thiophen-2-yl)ethylidene)hydrazine-1-carbothioamide compound(31).

Table (3- 31): Elemental analysis data of compound (31) (calculated vs. found values).

CHNOS	%C	%H	%N	%O	%S
Calculated	45.73	4.40	17.61	10.84	20.22
Found	46.03	4.60	17.91	11.04	20.42

3.10 *Synthesis* of Thiosemicarbazones compound(32).

A mixture of Terpathaldehyde (0.01 mole), thiosemicarbazide (0.01 mole) in 20 mL of ethanol, and four drops of glacial acetic acid were heated under reflux for 5 hours at 78 °C. The product was cooled to room temperature, and the solid was filtered, dried, and purified *via* recrystallization with ethanol.

3.10.1*Synthesis* of 1, 1'-(1, 4-phenylenebis(methaneylylidene))bis(thiourea) compound(32).

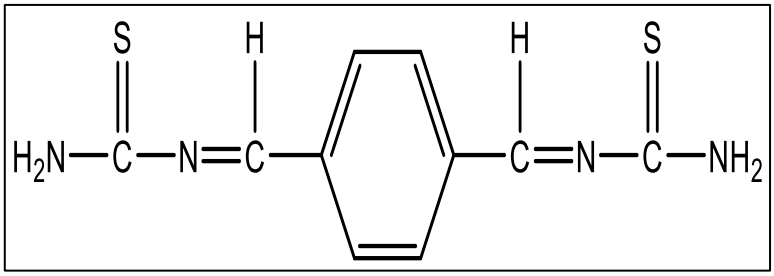


Figure (3- 31): structure of 1, 1'-(1, 4-phenylenebis(methaneylylidene))bis(thiourea) compound(32).

Table (3- 32): Elemental analysis data of compound (32) (calculated vs. found values).

CHNOS	%C	%H	%N	%S
Calculated	47.45	2.82	31.63	17.07
Found	47.64	3.12	31.83	18.27

3.11 *Synthesis* of (tetrazole)compounds compound(33).

Schiff base (0.001mol) from (32) compound was dissolved in (10 ml) of THF followed by adding (0.002mol) sodium azide. The mixture was heated in water bath at (60-70)ºC for (10hrs). then, the mixture of reaction was filtered, the resulted was purified by absolute ethanol.

3.11.1*Synthesis* of 1, 1'-(1, 4-phenylenebis(4, 5-dihydro-1H-tetrazole-5, 1-diyl))bis(thiourea) compound(33).

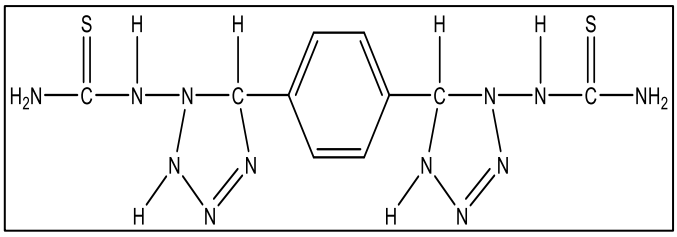


Figure (3- 32): structure of 1, 1'-(1, 4-phenylenebis(4, 5-dihydro-1H-tetrazole-5, 1-diyl))bis(thiourea) compound(33).

Table (3- 33): Elemental analysis data of compound (33) (calculated vs. found values).

CHNOS	%C	%H	%N	%S
Calculated	42.72	3.3	35.8	17.48
Found	43.08	3.50	36.10	17.68

3.12 *Synthesis* (tetrazole) compounds. (34)

A mixture of Isatin (0.01 mole), thiosemicarbazide (0.01 mole) in 20 mL of ethanol, and four drops of glacial acetic acid were heated under reflux for 5 hours at 78 °C. The product was cooled to room temperature, and the solid was filtered, dried, and purified *via* recrystallization with ethanol.

3.12.1*Synthesis* of 2, 2'-((Z)-indoline-2, 3-diylidene)bis(hydrazine-1-carbothioamide) compound(34).

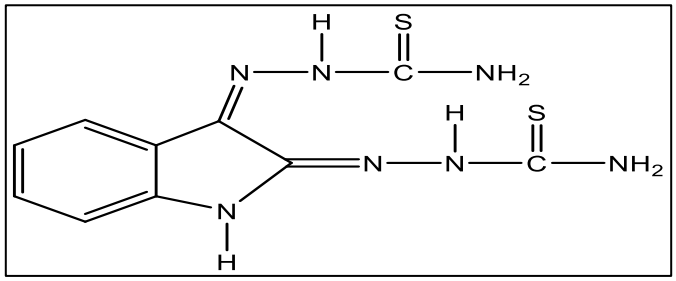


Figure (3- 33): structure of 2, 2'-((Z)-indoline-2, 3-diylidene)bis(hydrazine-1-carbothioamide) compound(34).

Table (3- 34): Elemental analysis data of compound (34) (calculated vs. found values).

CHNOS	%C	%H	%N	%S
Calculated	**45.97**	**4.21**	**37.54**	**2.261**
Found	**46.17**	**4.41**	**37.74**	**12.46**

3.13 *Synthesis* of tetrazole compound.(35)

Schiff base of Isatin (0.001mol) from compound (34) was dissolved in (10 ml) of THF followed by adding (0.002mol) sodium azide. The mixture was heated in water bath at (60-70)ºC for (10hrs). then, the mixture of reaction was filtered, the resulted was purified by absolute ethanol.

3.13.1*Synthesis* of 1, 1'-(dispiro[tetrazole-5, 2'-indoline-3', 5''-tetrazol]-1, 1''(4H, 4''H)-diyl)bis(thiourea) compound(35).

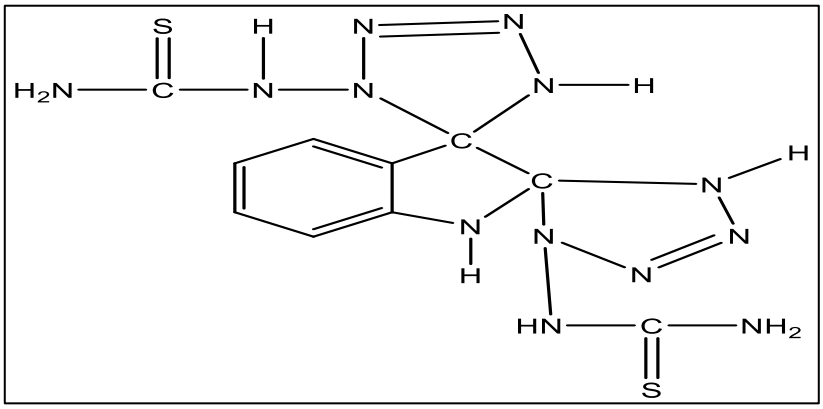


Figure (3- 34): structure of 1, 1'-(dispiro[tetrazole-5, 2'-indoline-3', 5''-tetrazol]-1, 1''(4H, 4''H)-diyl)bis(thiourea) compound(35).

Table (3- 35): Elemental analysis data of compound (35) (calculated vs. found values).

CHNOS	%C	%H	%N	%S
Calculated	**45.66**	**3.43**	**38.02**	**16.88**
Found	**45.96**	**3.73**	**38.32**	**17.08**

3.14 *Synthesis* of 2-iminothiazolidin-4-one compound. (Compound36)

6 gram of thiourea with 7.2 gm of mono chloro acetic acid in glacial acetic acid, are refluxed for half an hours at 118, to give a solid, filter, and wash with methyl alcohol. Then dissolve in lest amount of water, then basified with sodium bicarbonate (3%) solution to give a white crystal. Dried and crystallized.

3.14.1*Synthesis* of 2-iminothiazolidin-4-one compound(36).

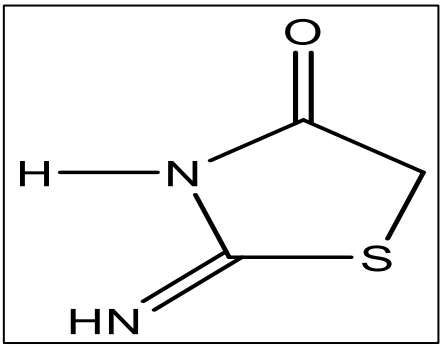


Figure (3- 35): structure of 2-iminothiazolidin-4-one compound(36).

Table (3- 36): Elemental analysis data of compound (36) (calculated vs. found values).

CHNOS	%C	%H	%N	%O	%S
Calculated	31.03	2.44	24.13	13.82	27.58
Found	31.33	3.74	24.43	14.12	27.88

3.15 *Synthesis* of Mannich reaction compounds(37-40)

0.92 gm (8 mole) from compound (36) in 1.92 ml (0.024 mole) of formalin add dropwise with stirring 1gm (8 mole) of 25 % aqueous solution of aliphatic amine at 0-5 °C . After the addition is complete .The reaction mixture is stirred without cooling for another 15 min. after which it is treated with worm (30 -40°C) benzene (four portions 20 ml each) .The benzene layer is dried with magnesium sulphate, the benzene is removed by distillation to one fifth of its original volume.

3.15.1*Synthesis* of 3-((3-(4-aminophenoxy)phenyl)amino)-3, 4-dihydro-2H-thiazolo[3, 2-a][1, 3, 5]triazin-6(7H)-one compound(37).

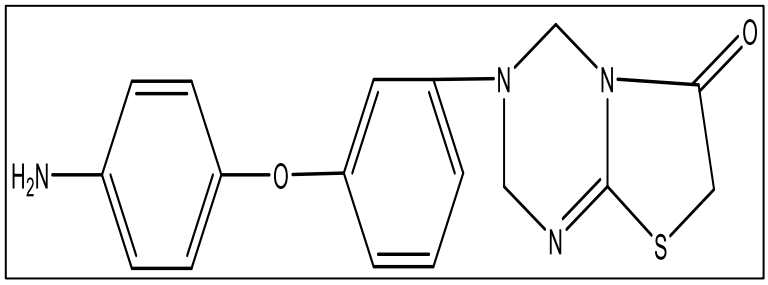


Figure (3- 36): structure of 3-((3-(4-aminophenoxy)phenyl)amino)-3, 4-dihydro-2H-thiazolo[3, 2-a][1, 3, 5]triazin-6(7H)-one compound(37).

Table (3- 37): Elemental analysis data of compound (37) (calculated vs. found values).

CHNOS	%C	%H	%N	%O	%S
Calculated	57.46	4.78	19.71	9.04	9.01
Found	57.76	5.08	20.01	9.34	9.31

3.15.2 *Synthesis* of 3-((4-aminophenyl)amino)-3, 4-dihydro-2H-thiazolo[3, 2-a][1, 3, 5]triazin-6(7H)-one compound (38).

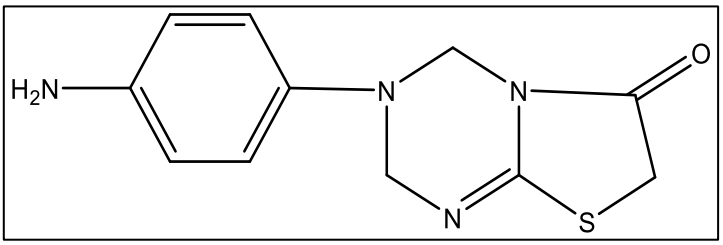


Figure (3- 37): structure of 3-((4-aminophenyl)amino)-3, 4-dihydro-2H-thiazolo[3, 2-a][1, 3, 5]triazin-6(7H)-one compound(38).

Table (3- 38): Elemental analysis data of compound (38) (calculated vs. found values).

CHNOS	%C	%H	%N	%O	%S
Calculated	48.19	4.94	26.61	4.91	12.10
Found	48.49	5.24	26.91	5.21	12.46

3.15.3 *Synthesis* of 3-((2-((2-((2-minoethyl)amino)ethyl)amino) ethyl)amino)-3, 4-dihydro-2H-thiazolo[3, 2-a][1, 3, 5]triazin-6(7H)-one compound(39).

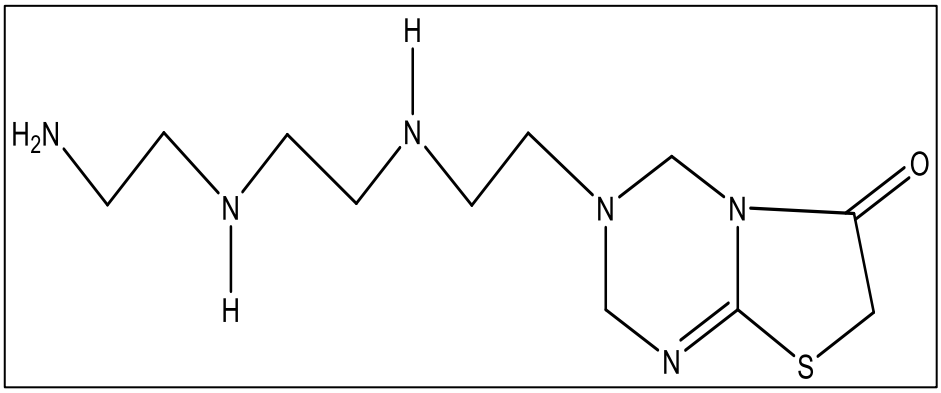


Figure (3- 38): structure of 3-((2-((2-((2-minoethyl)amino)ethyl)amino) ethyl)amino)-3, 4-dihydro-2H-thiazolo[3, 2-a][1, 3, 5]triazin-6(7H)-one compound(39).

Table (3- 39): Elemental analysis data of compound (39) (calculated vs. found values).

CHNOS	%C	%H	%N	%O	%S
Calculated	43.85	7.64	29.56	8.32	10.63
Found	44.15	7.94	29.86	8.62	10.93

3.15.4*Synthesis* of 3-((6-aminopyridin-2-yl)amino)-3, 4-dihydro-2H-thiazolo[3, 2-a][1, 3, 5]triazin-6(7H)-one compound(40).

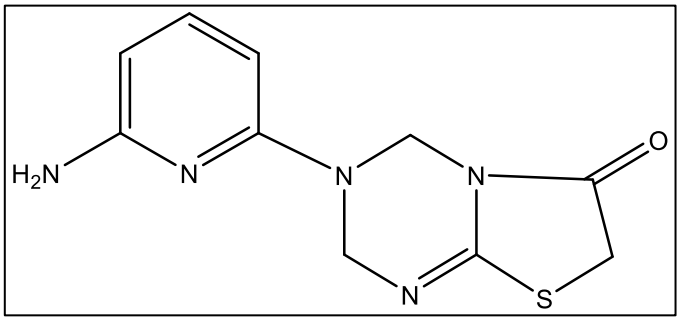


Figure (3- 39): structure of 3-((6-aminopyridin-2-yl)amino)-3, 4-dihydro-2H-thiazolo[3, 2-a][1, 3, 5]triazin-6(7H)-onecompound(40).

Table (3- 40): Elemental analysis data of compound (40) (calculated vs. found values).

CHNOS	%C	%H	%N	%O	%S
Calculated	45.45	4.54	31.81	4.58	12.12
Found	45.75	4.84	32.11	4.88	12.42

3.16 Synthesis of copolymer (methyl acrylic acid-co- Itaconic anhydride) (MAA-CO-IAN).

The MAA-CO-IAN used in this study was synthesized by a modified solution polymerization of the monomers methyl acrylic acid (MAA)(5gm) , Itaconic anhydride (IAN) (5 gm) . The polymerization reaction was carried out in a reactor (Flask 250 ml) under intensive mixing and nitrogen atmosphere at room temperature for 30 minute under stirring. The copolymers were synthesized in presence of 1-hydroxycyclohexyl phenyl ketone (0.1gm) as initiator.

3.16.1*Synthesis* of copolymer (MAA-CO-IAN) .

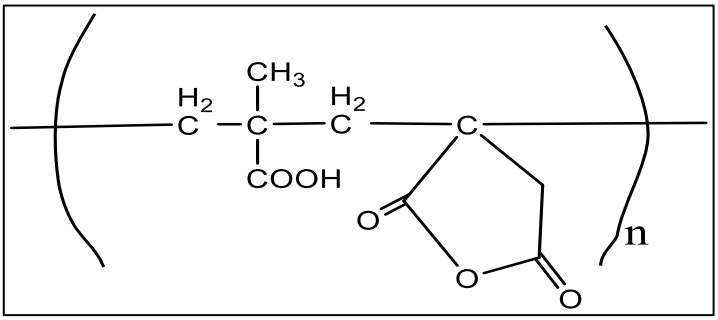


Figure (3- 40): structure of copolymer (MAA-CO-IAN).

3.17 Synthesis of copolymer (dimethyl acrylic amide-co- Citraconic anhydride) (DMA-CO-CAN).

The DMA -C0-CAN used in this study was synthesized by a modified solution polymerization of the monomers N, N dimethyl acrylic amide (DMA) (5 gm), Citraconic anhydride (CAN) (5 gm). The polymerization reaction was carried out in a reactor (Flask 250 ml) under intensive mixing and nitrogen atmosphere at room temperature for 30 minute under stirring. The copolymers were synthesized in presence of 1-hydroxycyclohexyl phenyl ketone (0.1gm) as initiator.

3.17.1*Synthesis* of copolymer (DMA-CO-CAN).

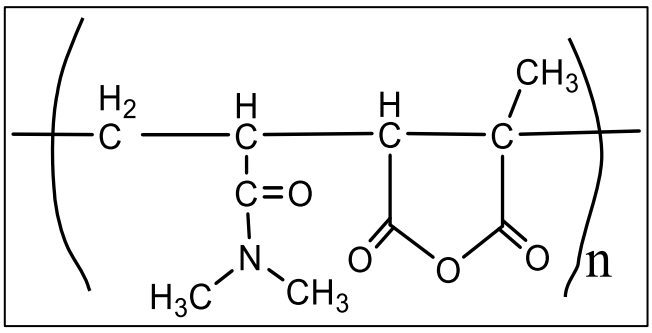


Figure (3- 41): structure of copolymer (DMA-CO-CAN).

3.18 Synthesis of copolymer (MAA-CO-IAN) with Thiosemicarbazones compounds (1-9).

By mixing of 0.5 mol of amine compounds (1), (2), (3), (4), (5), (6), (7), (8), (9), with 0.5 mol from copolymer (MAA-CO-IAN) in 20 ml of absolute ethanol with stirring at room temperature. The precipitate was filtered off and washed in ether and recrystallized from ethanol.

3.18.1 Synthesis of copolymer(1) (MAA-Co-IAN) with compound(1).

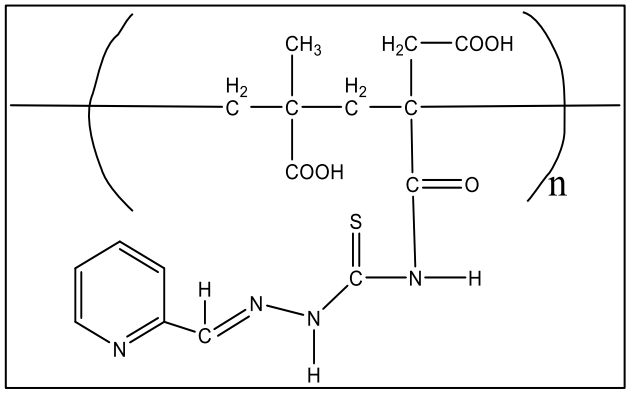


Figure (3- 42): structure copolymer(1) (MAA-Co-IAN) with compound(1).

3.18.2 Synthesis of copolymer(2) (MAA-Co-IAN) with compound(2).

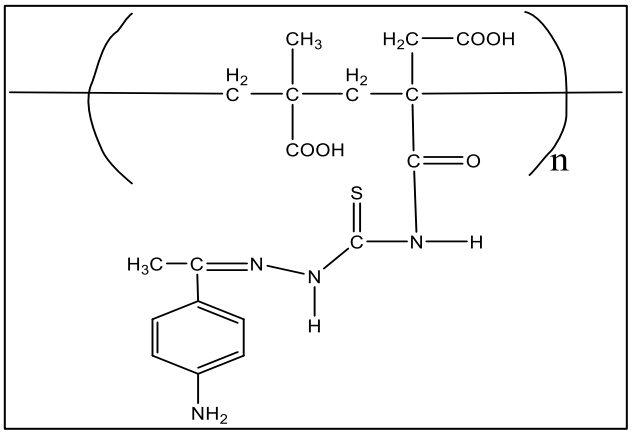


Figure (3- 43): structure of copolymer(2) (MAA-Co-IAN) with compound(2).

3.18.3 Synthesis of copolymer(3) (MAA-Co-IAN) with compound(3).

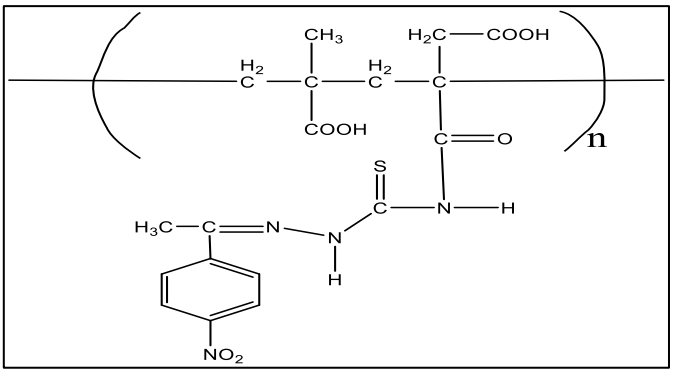


Figure (3- 44): structure of copolymer(3) (MAA-Co-IAN) with compound(3).

3.18.4 Synthesis of copolymer(4) (MAA-Co-IAN) with compound(4).

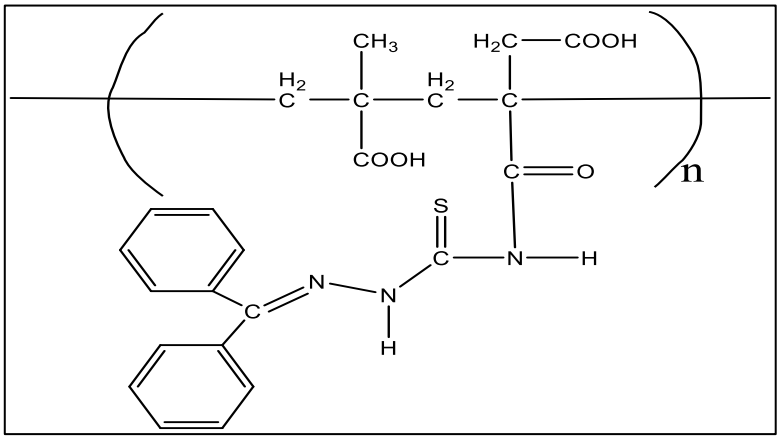


Figure (3- 45): structure of copolymer(4) (MAA-Co-IAN) with compound(4).

3.18.5 Synthesis of copolymer(5) (MAA-Co-IAN) with compound(5).

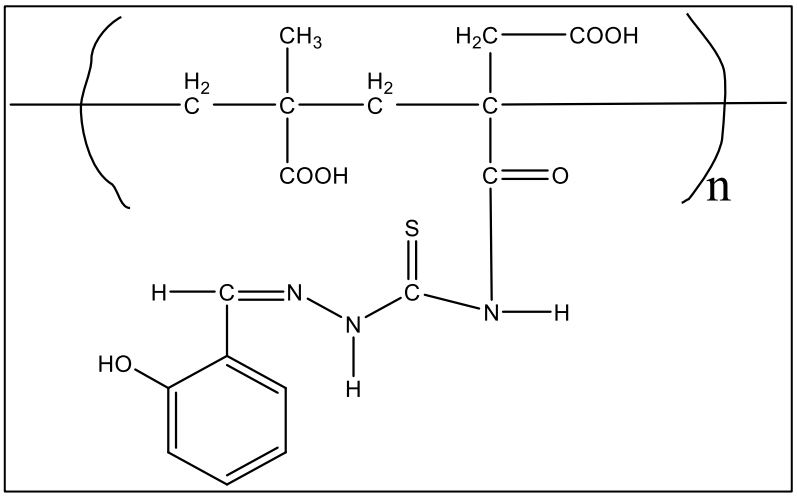


Figure (3- 46): structure of copolymer(5) (MAA-Co-IAN) with compound(5).

3.18.6 Synthesis of copolymer(6) (MAA-Co-IAN) with compound(6).

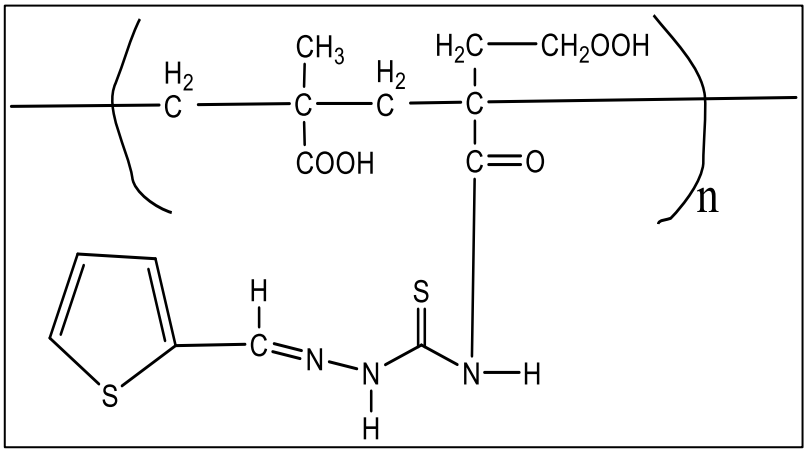


Figure (3- 47): structure of copolymer(6) (MAA-Co-IAN) with compound(6).

3.18.7 Synthesis of copolymer(7) (MAA-Co-IAN) with compound(7).

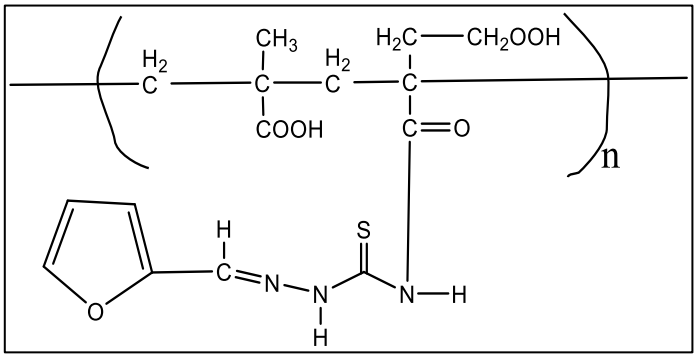


Figure (3- 48): structure of copolymer (7) (MAA-Co-IAN) with compound (7).

3.18.8 Synthesis of copolymer(8) (MAA-Co-IAN) with compound(8).

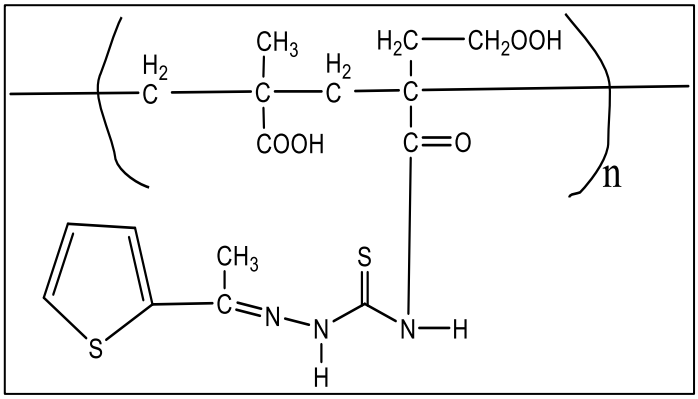


Figure (3- 49): structure of copolymer(8) (MAA-Co-IAN) with compound(8).

3.18.9 Synthesis of copolymer(9) (MAA-Co-IAN) with compound(9).

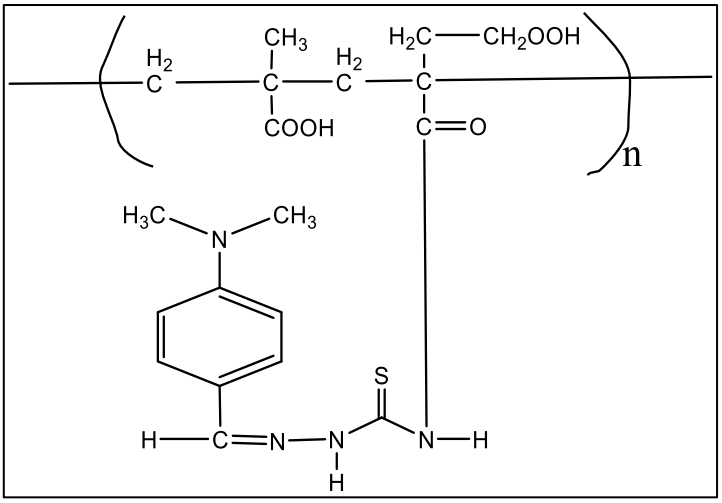


Figure (3- 50): structure of copolymer(9) (MAA-Co-IAN) with compound(9).

3.19 Synthesis of copolymer (MAA-CO-IAN) with thiosemicarbazide derivatives compounds. (10-17)

A mixture of 0.5 mol of thiosemicarbazide derivatives compounds (10), (11), (12), (13), (14), (15), (16), (17), with 0.5 mol from copolymer (MAA-CO-IAN) in 20 ml of absolute ethanol with stirring at room temperature. The precipitate was filtered off and washed in ether and recrystallized from ethanol.

3.19.1 Synthesis of copolymer(10) (MAA-CO-IAN) with compound(10).

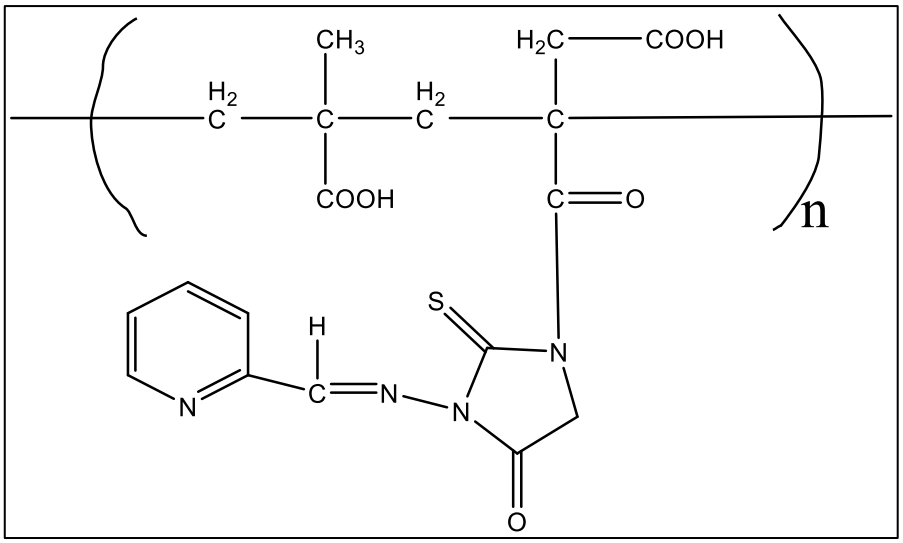


Figure (3- 51): structure of copolymer(10) (MAA-CO-IAN) with compound(10).

3.19.2 Synthesis of copolymer(11) (MAA-CO-IAN) with compound(11).

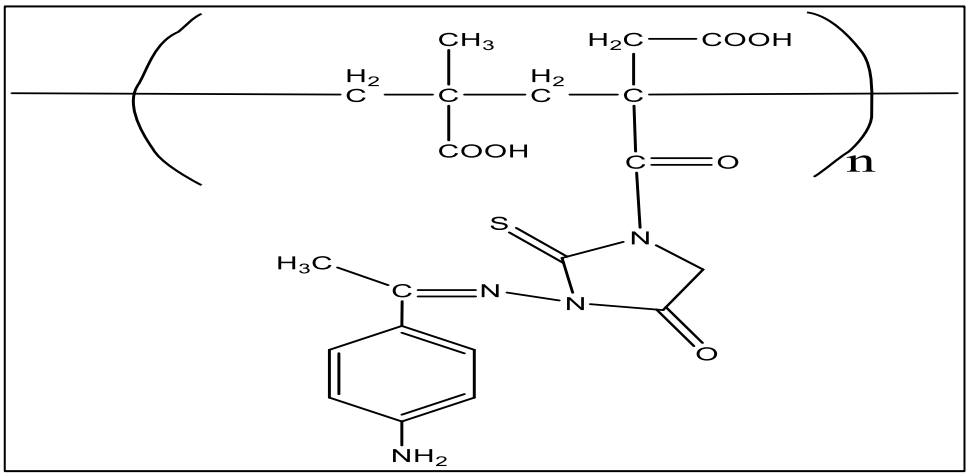


Figure (3- 52): structure of copolymer(11) (MAA-CO-IAN) with compound(11).

3.19.3 Synthesis of copolymer(12) (MAA-CO-IAN) with compound(12).

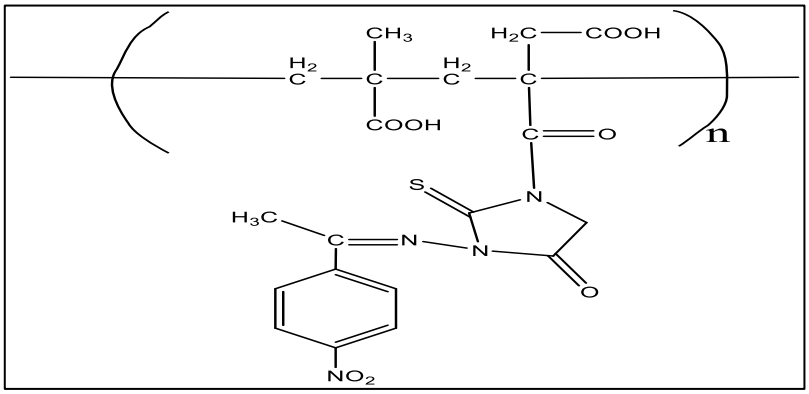


Figure (3- 53): structure of copolymer(12) (MAA-CO-IAN) with compound(12).

3.19.4 Synthesis of copolymer(13) (MAA-CO-IAN) with compound(13).

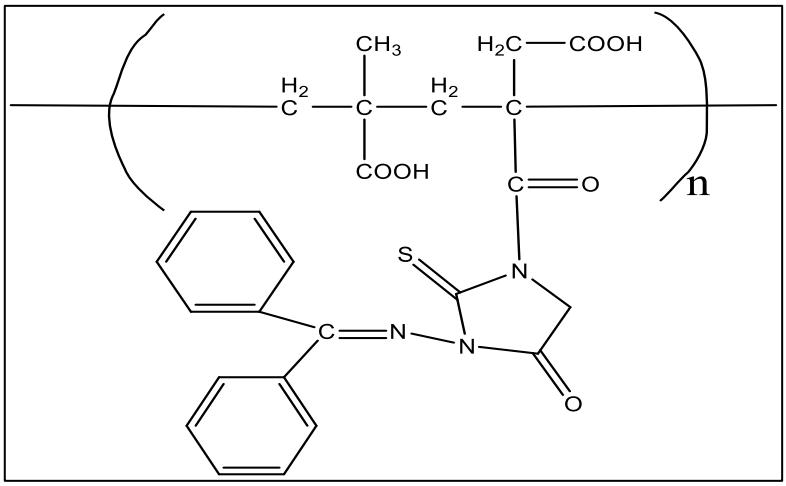


Figure (3- 54): structure of copolymer(13) (MAA-CO-IAN) with compound(13).

3.19.5 Synthesis of copolymer(14) (MAA-CO-IAN) with compound(14).

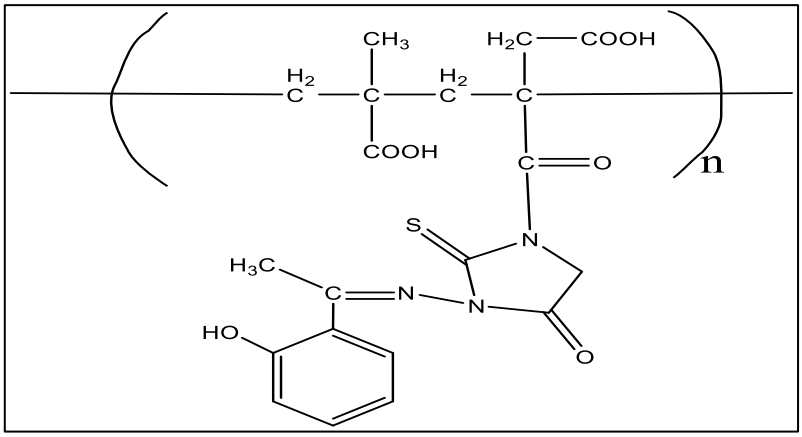


Figure (3- 55): structure of copolymer(14) (MAA-CO-IAN) with compound(14).

3.19.6 Synthesis of copolymer(15) (MAA-CO-IAN) with compound(15).

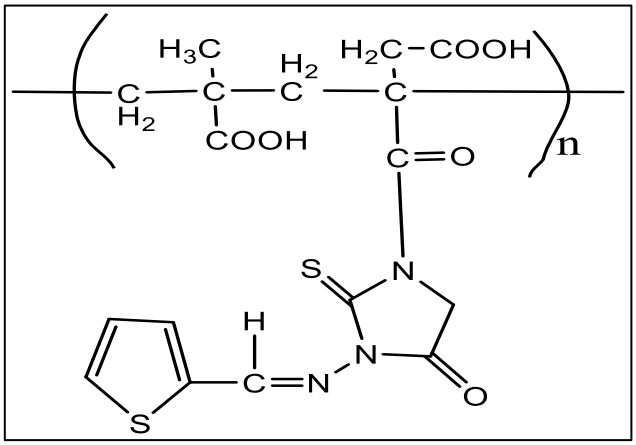


Figure (3- 56): structure of copolymer(15) (MAA-CO-IAN) with compound(15).

3.19.7 Synthesis of copolymer(16) (MAA-CO-IAN) with compound(16).

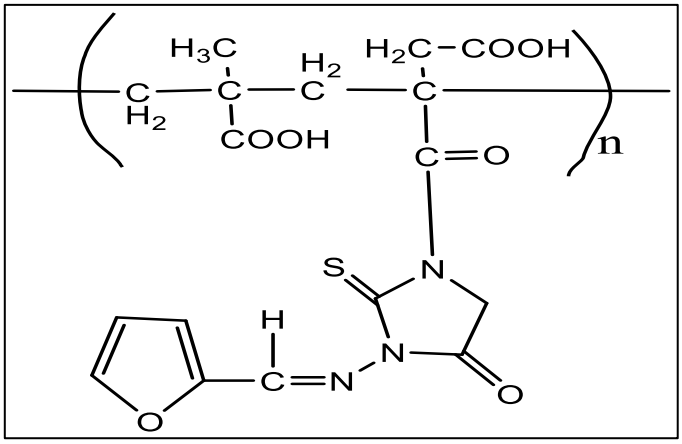


Figure (3- 57): structure of copolymer(16) (MAA-CO-IAN) with compound(16).

3.19.8Synthesis of copolymer(17) (MAA-CO-IAN) with compound(17).

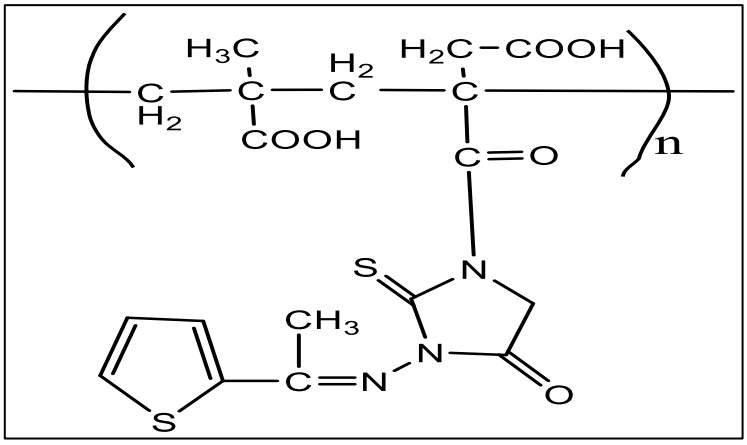


Figure (3- 58): *structure* of copolymer(17) (MAA-CO-IAN) with compound(17).

3.20 Synthesis of copolymer (MAA-CO-IAN) with compounds (18-20).

The mixture (0.01 mol) from (18) (19) (20) compounds with 0.5 mol from copolymer (MAA-CO-IAN) in 20 ml of absolute ethanol with stirring at room temperature. The precipitate was filtered off and washed in ether and recrystallized from ethanol.

3.20.1 Synthesis of copolymer(18) (MAA-CO-IAN) with compound(18).

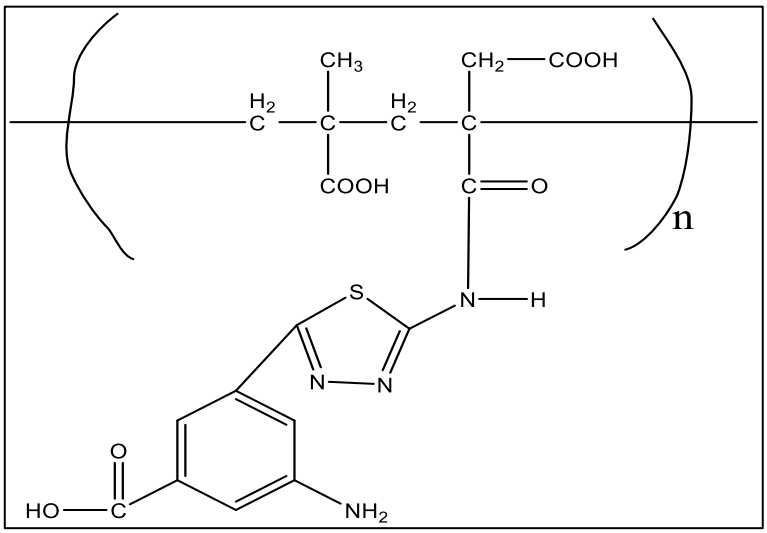


Figure (3- 59): structure of copolymer(18) (MAA-CO-IAN) with compound(18).

3.20.2 Synthesis of copolymer(19) (MAA-CO-IAN) with compound(19).

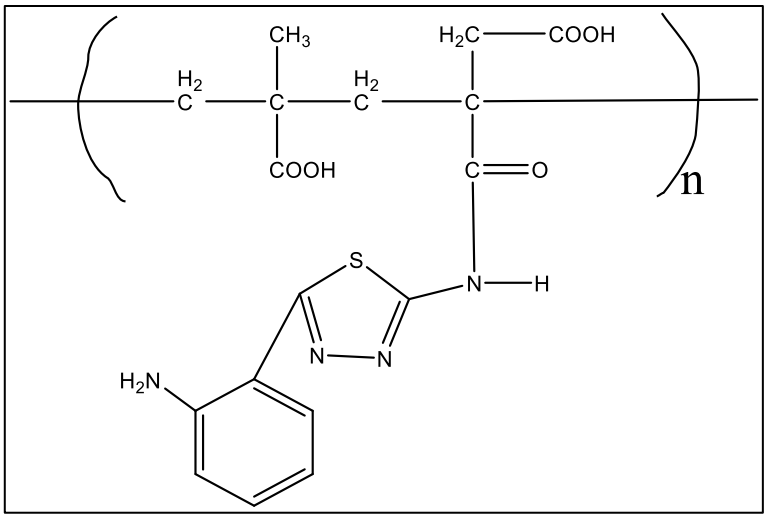


Figure (3- 60): structure of copolymer(19) (MAA-CO-IAN) with compound(9).

3.20.3 Synthesis of copolymer(20) (MAA-CO-IAN) with compound(20).

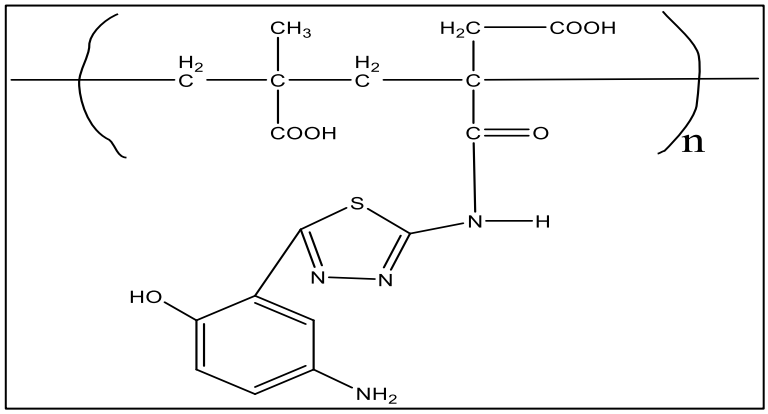


Figure (3- 61): structure of copolymer(20) (MAA-CO-IAN) with compound(20)

3.21 Synthesis of copolymer(1) (MAA-CO-IAN) with Imide compounds (21-23).

The mixture **(**0.5) from (21), (22), (23) compounds with 0.5 mol from copolymer (MAA-CO-IAN) in 20 ml of absolute ethanol with stirring at room temperature. The precipitate was filtered off and washed in ether and recrystallized from ethanol.

3.21.1 Synthesis of copolymer(21) (MAA-CO-IAN) with compound(21) .

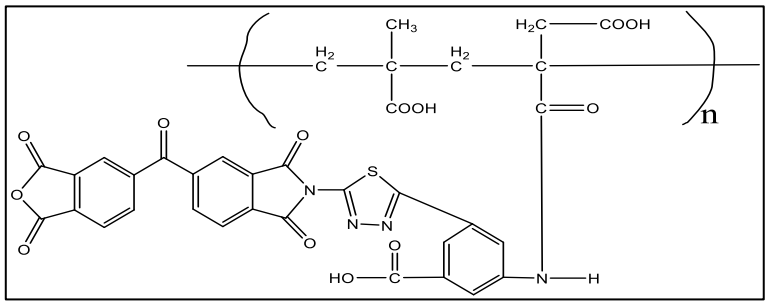


Figure (3- 62): structure of copolymer(21) (MAA-CO-IAN) with compound(21) .

3.21.2 Synthesis of copolymer(32) (MAA-CO-IAN) with compound(22) .

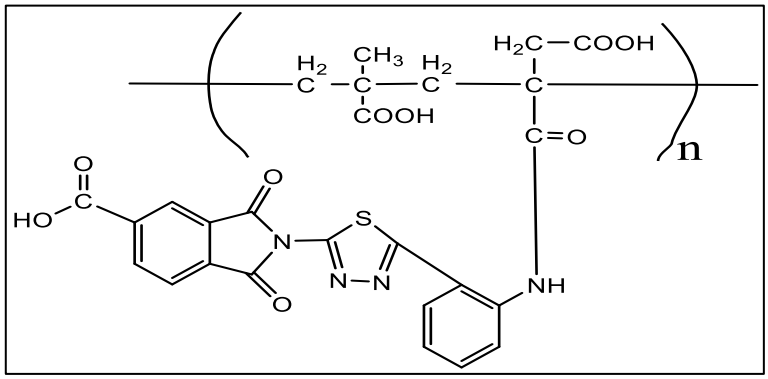


Figure (3- 63): structure of copolymer(22) (MAA-CO-IAN) with compound(22) .

3.21.3 Synthesis of copolymer(23) (MAA-CO-IAN) with compound(23) .

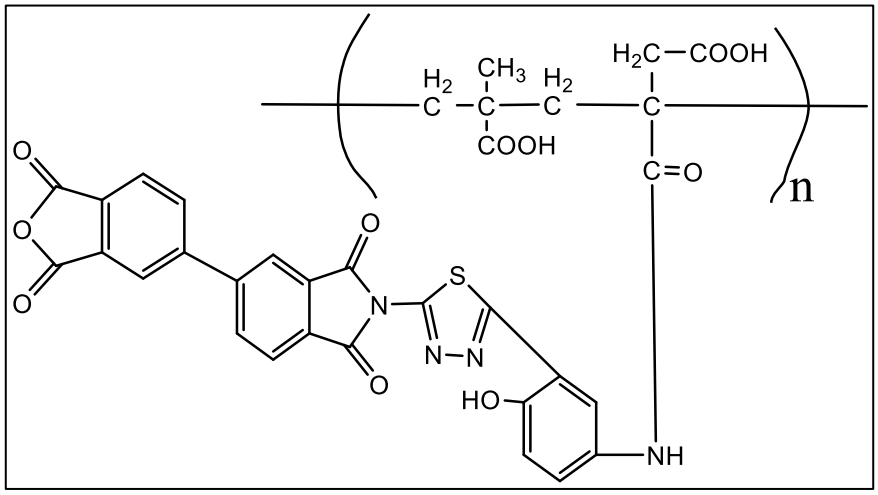


Figure (3- 64): structure of copolymer(23) (MAA-CO-IAN) with compound(23) .

3.22 Synthesis of copolymer (MAA-CO-IAN) with compounds (24-26).

A 0. 5 mole from thiosemcarbazone derivatives (24), (25), (26) compounds with 0.5 mol from copolymer (MAA-CO-IAN) in 20 ml of absolute ethanol with stirring at room temperature. The precipitate was filtered off and washed in ether and recrystallized from ethanol.

3.22.1 Synthesis of copolymer(24) (MAA-CO-IAN) with compound (24).

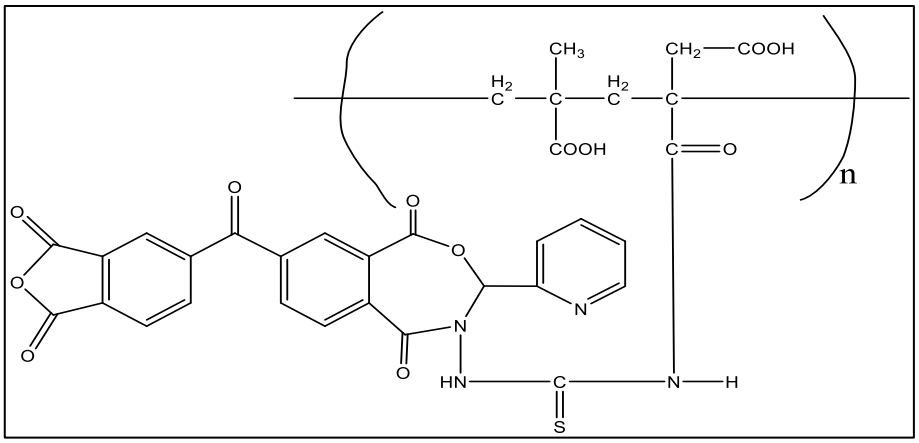


Figure (3- 65): structure of copolymer(24) (MAA-CO-IAN) with compound (24). (Compound28).

3.22.2 Synthesis of copolymer(25) (MAA-CO-IAN) with compound (25).

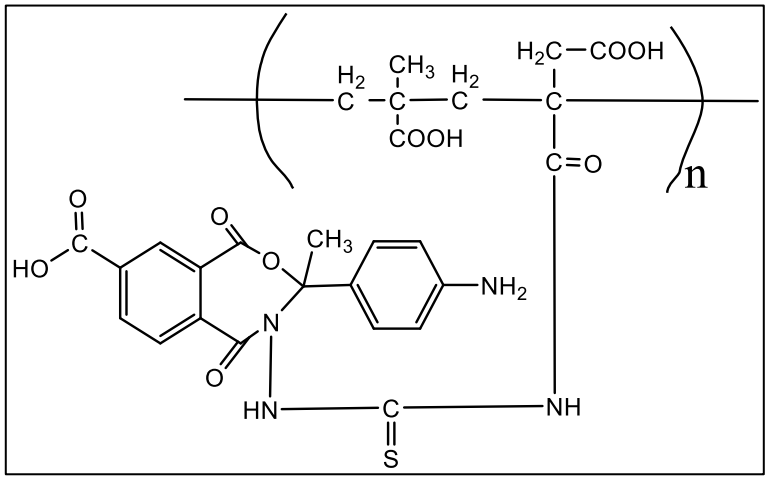


Figure (3- 66): structure of copolymer(25) (MAA-CO-IAN) with compound (25).

3.22.3 Synthesis of copolymer(26) (MAA-CO-IAN) with compound (26).

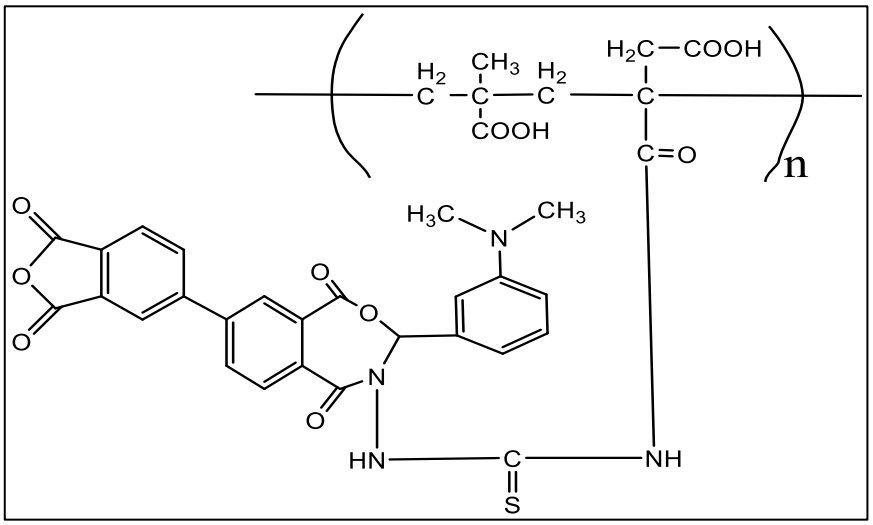


Figure (3- 67): structure of copolymer(1) (MAA-CO-IAN) with compound (26).

3.23 Synthesis of copolymer (MAA-CO-IAN) with compound(27) .

A 0. 5 mole from compound (27) with 0.5 mol from copolymer (MAA-CO-IAN) in 20 ml of absolute ethanol with stirring at room temperature. The precipitate was filtered off and washed in ether and recrystallized from ethanol.

3.23.1 Synthesis of copolymer(27) (MAA-CO-IAN) with compound (27).

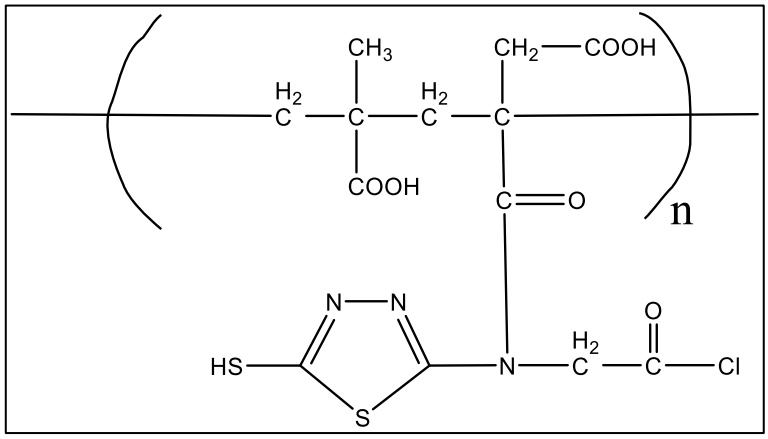


Figure (3- 68): structure of copolymer(27) (MAA-CO-IAN) with compound (27).

3.24 Synthesis of copolymer (MAA-CO-IAN) with compound(28).

A 0.5 mole from (28) compound with 0.5 mol from copolymer (MAA-CO-IAN) in 20 ml of absolute ethanol with stirring at room temperature. The precipitate was filtered off and washed in ether and recrystallized from ethanol.

3.24.1 Synthesis of copolymer(28) (MAA-CO-IAN) with compound (28).

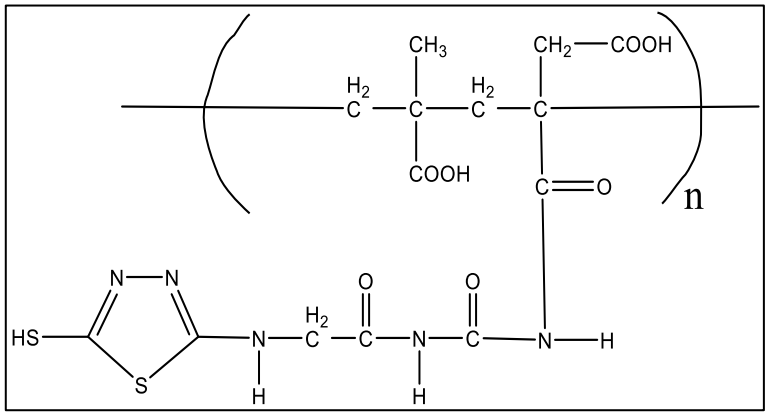


Figure (3- 69): structure of copolymer(1) (MAA-CO-IAN) with compound (28).

3.25 Synthesis of copolymer (MAA-CO-IAN) with compounds (29-31) .

A 0. 5 mole from (29) (30) (31) compounds with 0.5 mol from copolymer (MAA-CO-IAN) in 20 ml of absolute ethanol with stirring at room temperature. The precipitate was filtered off and washed in ether and recrystallized from ethanol.

3.25.1 Synthesis of copolymer(29) (MAA-CO-IAN) with compound (29).

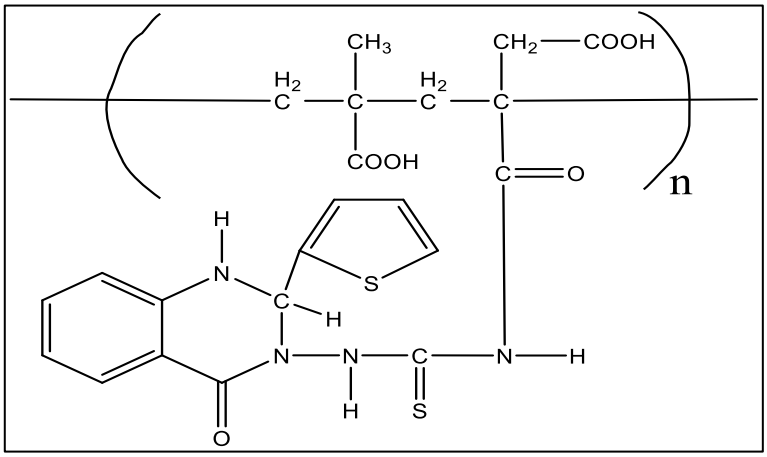


Figure (3- 70): structure of copolymer(29) (MAA-CO-IAN) with compound (29).

3.25.2 Synthesis of copolymer(30) (MAA-CO-IAN) with compound (30).

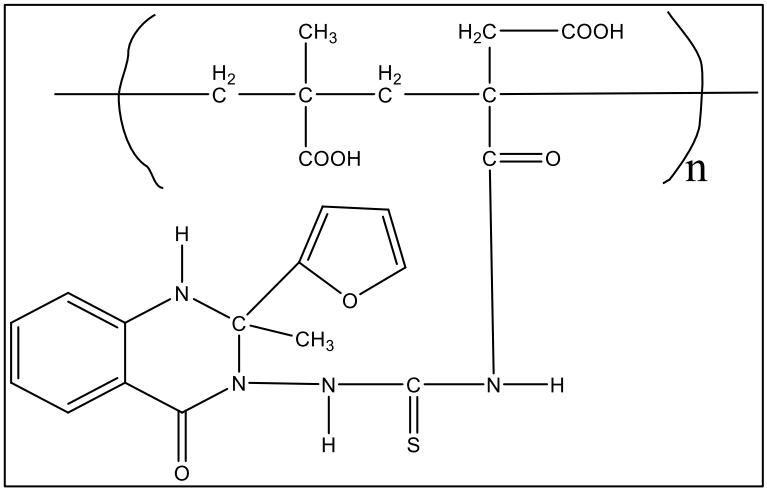


Figure (3- 71): structure of copolymer(30) (MAA-CO-IAN) with compound (30).

3.25.3 Synthesis of copolymer(31) (MAA-CO-IAN) with compound (31).

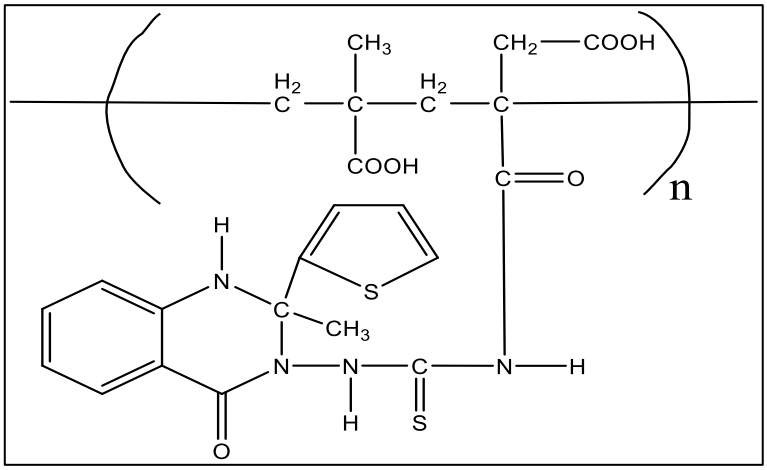


Figure (3- 72): structure of copolymer(31) (MAA-CO-IAN) with compound (31).

3.26 Synthesis of copolymer (MAA-CO-IAN) with compound(32) .

By mixing 0.5 from (32) compound with 0.5 mol from copolymer (MAA-CO-IAN) in 20 ml of absolute ethanol with stirring at room temperature. The precipitate was filtered off and washed in ether and recrystallized from ethanol.

3.26.1 Synthesis of copolymer(32) (MAA-CO-IAN) with compound (32).

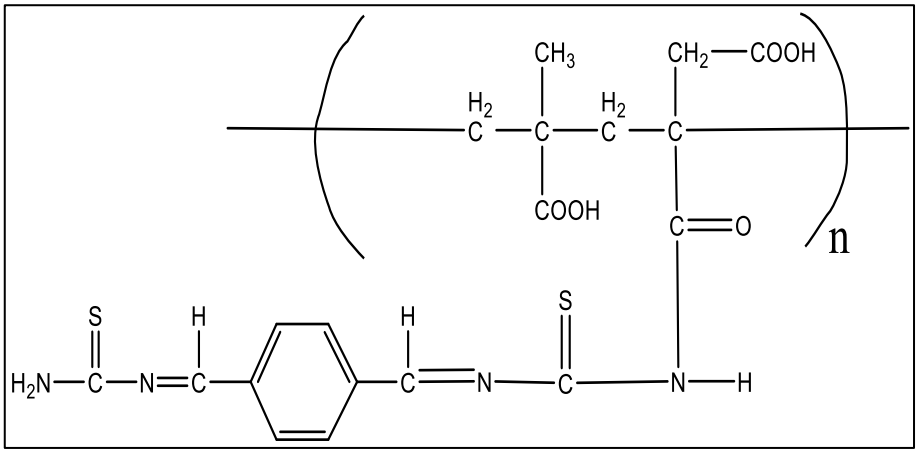


Figure (3- 73): structure of copolymer(32) (MAA-CO-IAN) with compound (32).

3.27 *Synthesis* of copolymer (MAA-CO-IAN) with compound(33).

By mixing 0.5 from (33) compound with 0.5 mol from copolymer (MAA-CO-IAN) in 20 ml of absolute ethanol with stirring at room temperature. The precipitate was filtered off and washed in ether and recrystallized from ethanol.

3.27.1 Synthesis of copolymer(33) (MAA-CO-IAN) with compound (33).

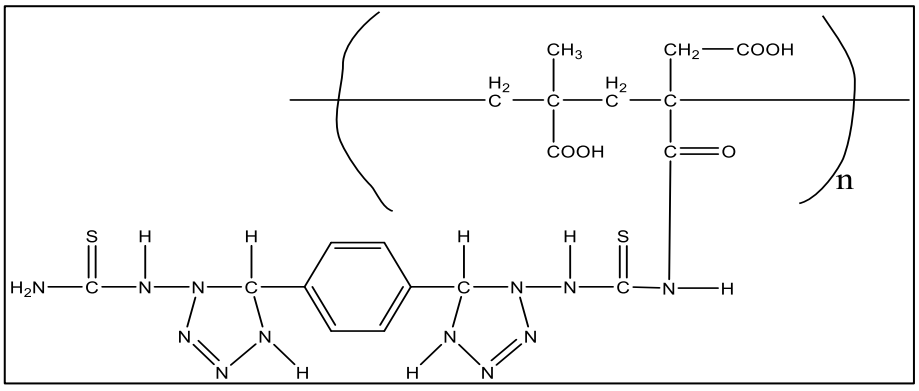


Figure (3- 74): structure of copolymer(33) (MAA-CO-IAN) with compound (33).

3.28 *Synthesis* of copolymer (MAA-CO-IAN) with compound (34).

A mixture of 0.5 from (34) compound with 0.5 mol from copolymer (MAA-CO-IAN) in 20 ml of absolute ethanol with stirring at room temperature. The precipitate was filtered off and washed in ether and recrystallized from ethanol.

3.28.1 Synthesis of copolymer(34) (MAA-CO-IAN) with compound (34).

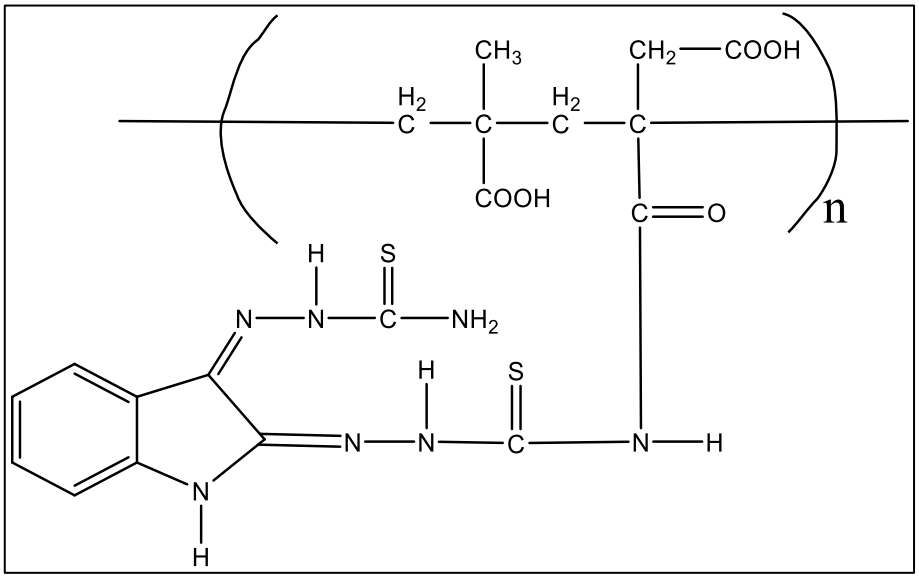


Figure (3- 75): structure of copolymer(34) (MAA-CO-IAN) with compound (34).

3.29 *Synthesis* of copolymer (MAA-CO-IAN) with compound (35).

A mixture of 0.5 from (35) compound with (0.5) mol from copolymer (MAA-CO-IAN) in 20 ml of absolute ethanol with stirring at room temperature. The precipitate was filtered off and washed in ether and recrystallized from ethanol.

3.29.1 Synthesis of copolymer(35) (MAA-CO-IAN) with compound (35).

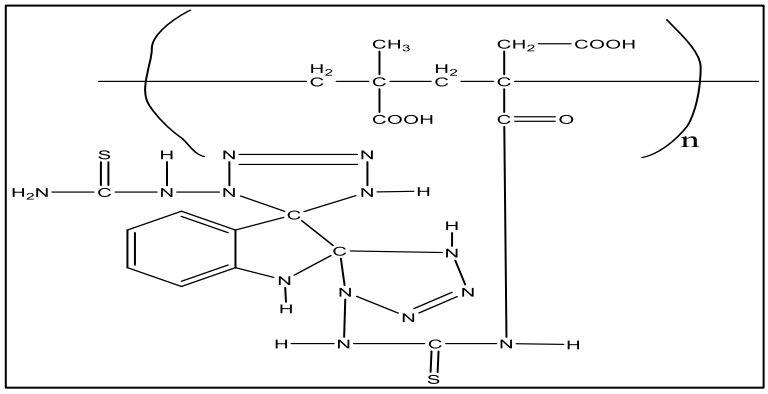


Figure (3- 76): structure of copolymer(35) (MAA-CO-IAN) with compound (35)

3.30 Synthesis of copolymer (MAA-CO-IAN) with compound (36).

By mixing of 0.5 mol of (36) compound with 0.5 mol from copolymer (MAA-CO-IAN) in 20 ml of absolute ethanol with stirring at room temperature. The precipitate was filtered off and washed in ether and recrystallized from ethanol.

3.30.1 Synthesis of copolymer(36) (MAA-CO-IAN) with compound (36).

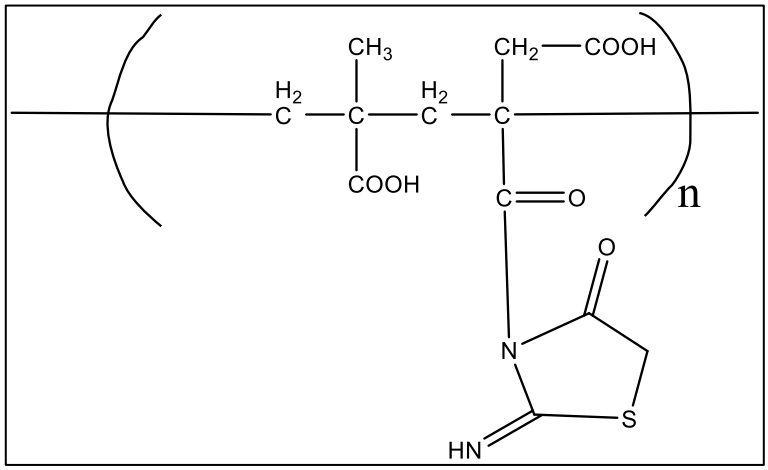


Figure (3- 77): structure of copolymer(36) (MAA-CO-IAN) with compound (36).

3.31 *Synthesis* of copolymer (MAA-CO-IAN) with Compounds (37-40).

Mixing of 0.5 mol from (37), (38), (39), (40) compounds with 0.5 mol from copolymer (MAA-CO-IAN) in 20 ml of absolute ethanol with stirring at room temperature. The precipitate was filtered off and washed in ether and recrystallized from ethanol.

3.31.1 Synthesis of copolymer(37) (MAA-CO-IAN) with compound(37).

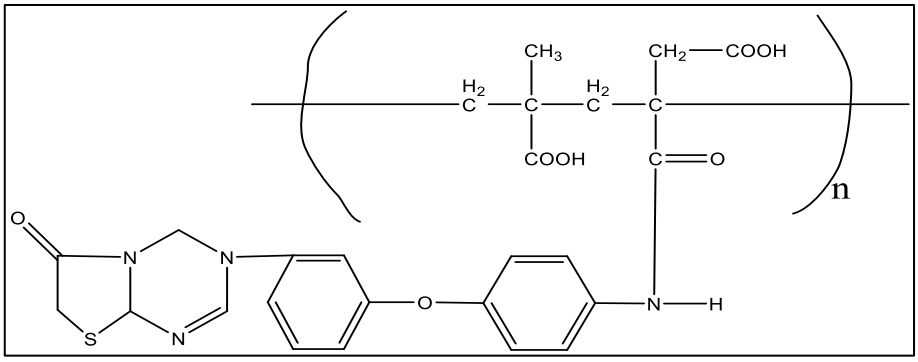


Figure (3- 78): structure of copolymer(37) (MAA-CO-IAN) with compound(37).

3.31.2 Synthesis of copolymer(38) (MAA-CO-IAN) with compound(38).

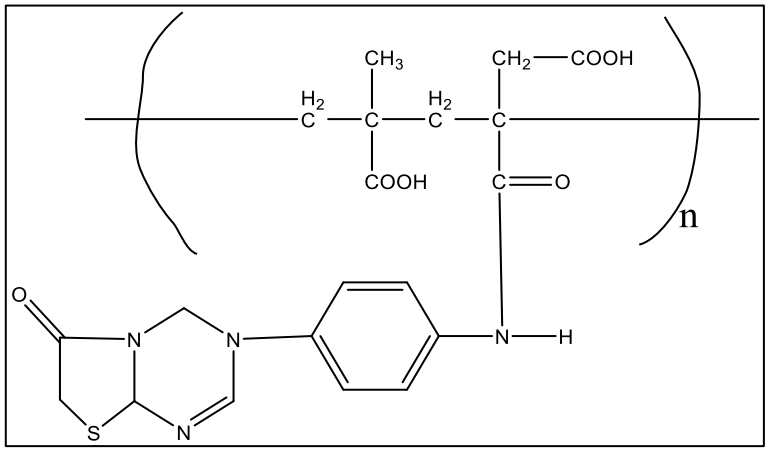


Figure (3- 79): structure of copolymer(38) (MAA-CO-IAN) with compound(38).

3.31.3 Synthesis of copolymer(39) (MAA-CO-IAN) with compound(39).

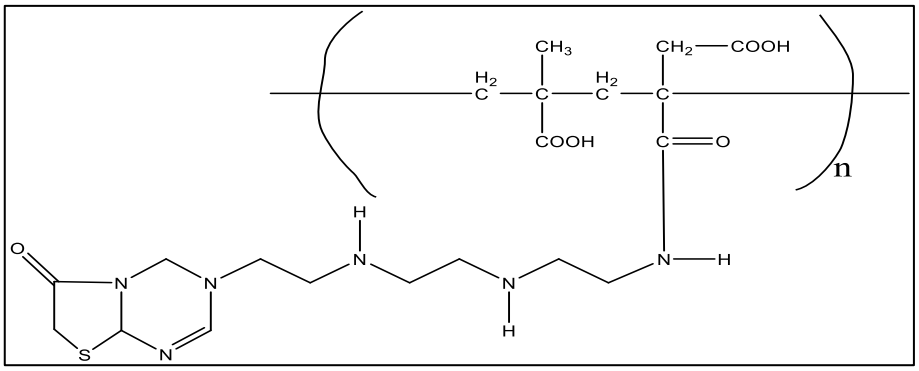


Figure (3- 80): structure of copolymer(39) (MAA-CO-IAN) with compound(39).

3.31.4 Synthesis of copolymer(40) (MAA-CO-IAN) with compound(40).

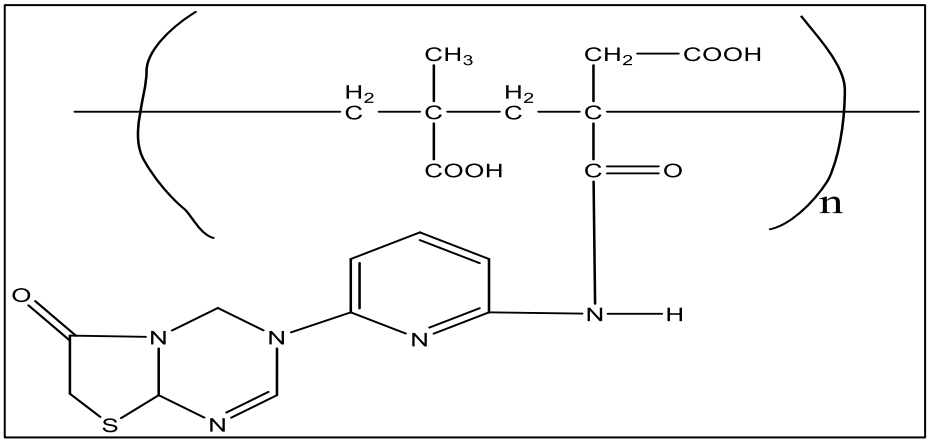


Figure (3- 81): structure of copolymer(40) (MAA-CO-IAN) with compound(40).

3.32 Synthesis of copolymer (DMA-CO-CAN) with Thiosemicarbazones compounds(3).

By mixing of 0.5 mol of (3) compounds with 0.5 mol from copolymer (DMA-CO-CAN) in 20 ml of absolute ethanol with stirring at room temperature. The precipitate was filtered off and washed in ether and recrystallized from ethanol.

3.32.1 Synthesis of copolymer(41) (DMA-CO-CAN) with compound(3).

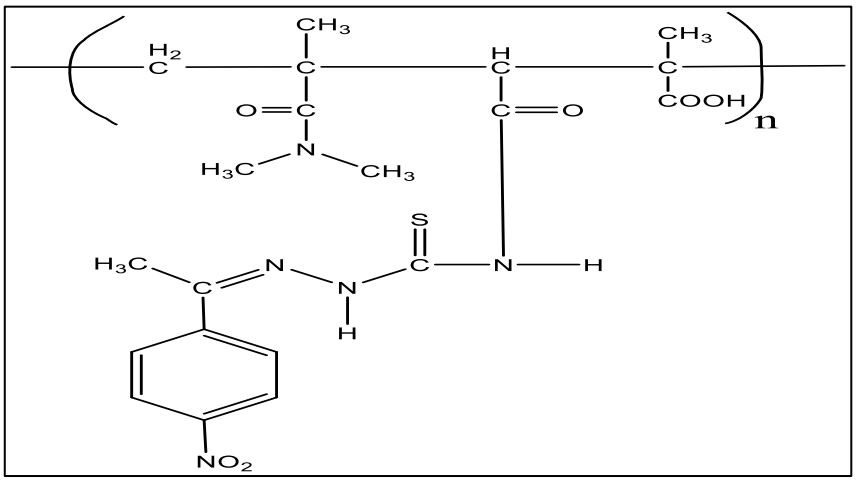


Figure (3- 82): structure of copolymer(41) (MAA-CO-IAN) with compound(3).

3.33 Synthesis of copolymer (DMA-CO-CAN) with compounds (13), (14), (16), (17).

A mixture of 0.5 mol of thiosemicarbazide derivatives (13), (14), (16), (17), compounds with 0.5 mol from copolymer (DMA-CO-CAN) in 20 ml of absolute ethanol with stirring at room temperature. The precipitate was filtered off and washed in ether and recrystallized from ethanol.

3.33.1 Synthesis of copolymer(42) (DMA-CO-CAN) with compound(13).

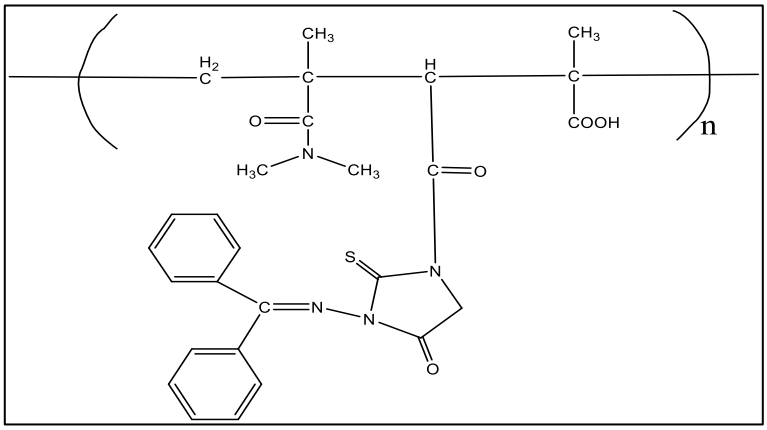


Figure (3- 83): structure of copolymer(42) (DMA-CO-CAN) with compound(13).

3.33.2 Synthesis of copolymer(43) (DMA-CO-CAN) with compound(14).

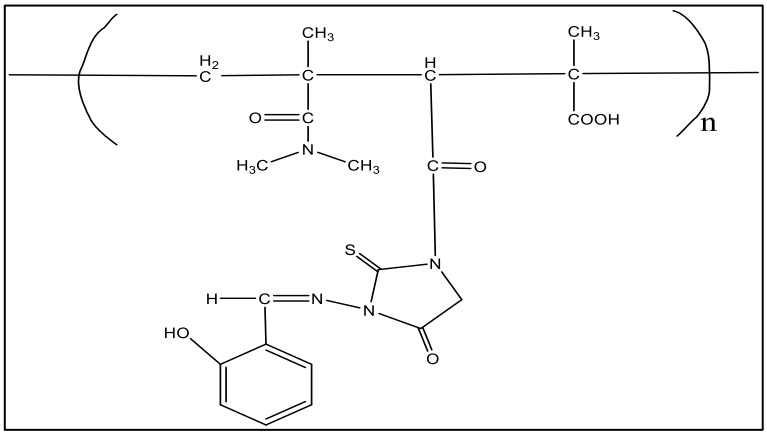


Figure (3- 84): structure of copolymer(43) (DMA-CO-CAN) with compound(14).

3.33.3. Synthesis of copolymer(44) (DMA-CO-CAN) with compound(16).

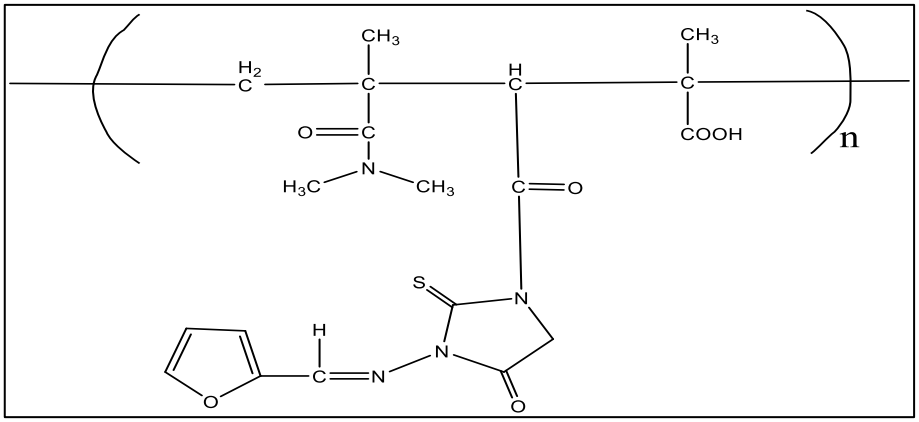


Figure (3- 85): structure of copolymer(44) (DMA-CO-CAN) with compound(16).

3.33.4 Synthesis of copolymer(45) (DMA-CO-CAN) with compound(17).

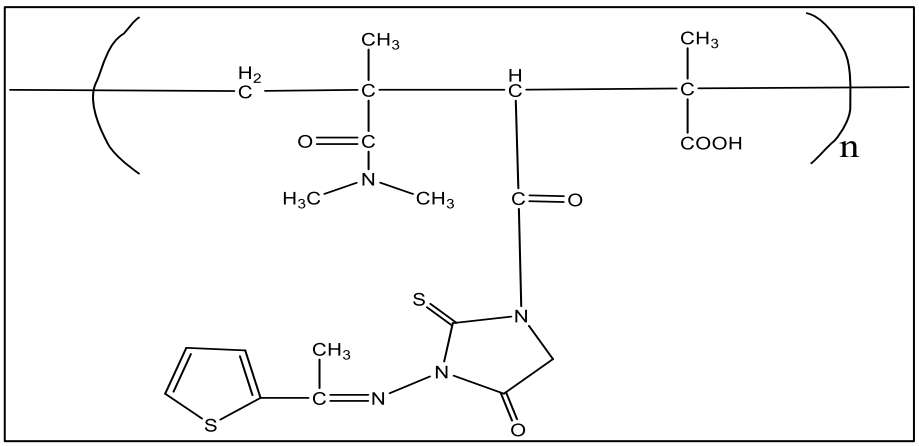


Figure (3- 86): structure of copolymer(45) (DMA-CO-CAN) with compound(17).

3.34 Synthesis of copolymer (DMA-CAN) with compounds(18-20).

The mixture (0.01 mol) from (18), (19), (20) compounds with 0.5 mol from copolymer (DMA-CAN) in 20 ml of absolute ethanol with stirring at room temperature. The precipitate was filtered off and washed in ether and recrystallized from ethanol.

3.34.1 Synthesis of copolymer(46) (DMA-CO-CAN) with compound(18).

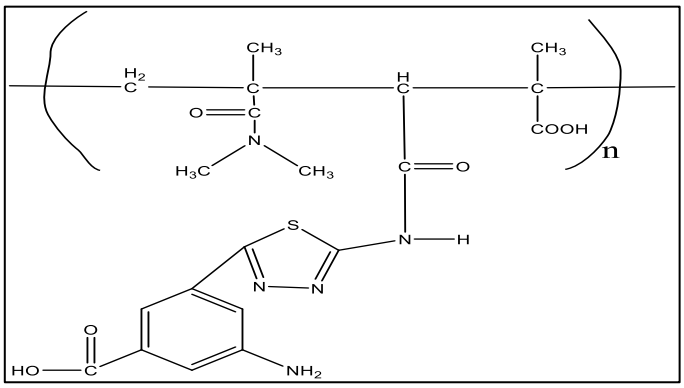


Figure (3- 87): structure of copolymer(46) (DMA-CO-CAN) with compound(18).

3.34.2 Synthesis of copolymer(47) (DMA-CO-CAN) with compound(19).

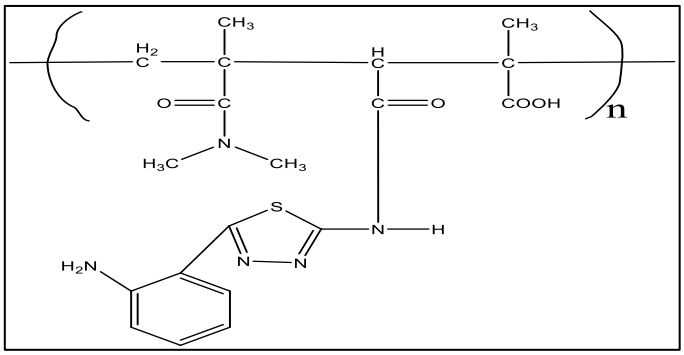


Figure (3- 88): structure of copolymer(47) (DMA-CO-CAN) with compound(19).

3.34.3 Synthesis of copolymer(48) (DMA-CO-CAN) with compound(20).

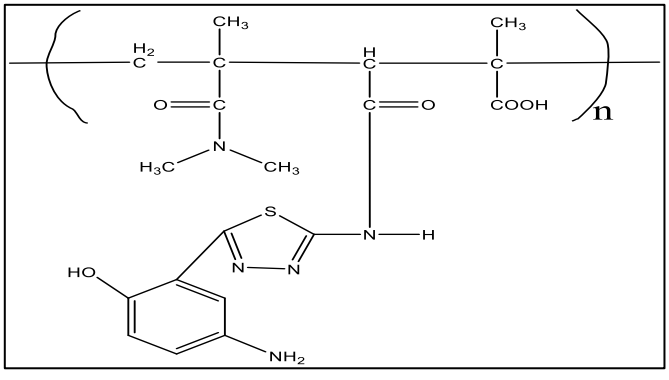


Figure (3- 89): structure of copolymer(48) (DMA-CO-CAN) with compound(20).

(Compound53)

3.35 Synthesis of copolymer (DMA-CO-CAN) with compounds with (24-25).

The mixture **(**0.5) from (24), (25), compounds with 0.5 mol from copolymer (DMA-CO-CAN) in 20 ml of absolute ethanol with stirring at room temperature. The precipitate was filtered off and washed in ether and recrystallized from ethanol.

3.35.1 Synthesis of copolymer(49) (DMA-CO-CAN) with compound(24).

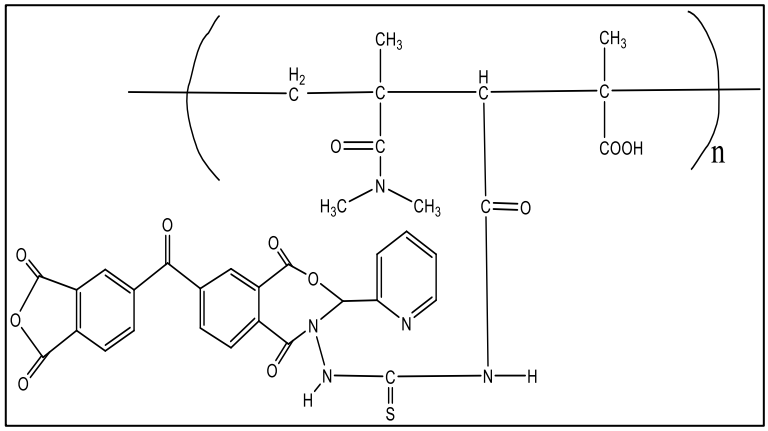


Figure (3- 90): structure of copolymer(49) (DMA-CO-CAN) with compound(24).

3.35.2 Synthesis of copolymer(50) (DMA-CO-CAN) with compound(25).

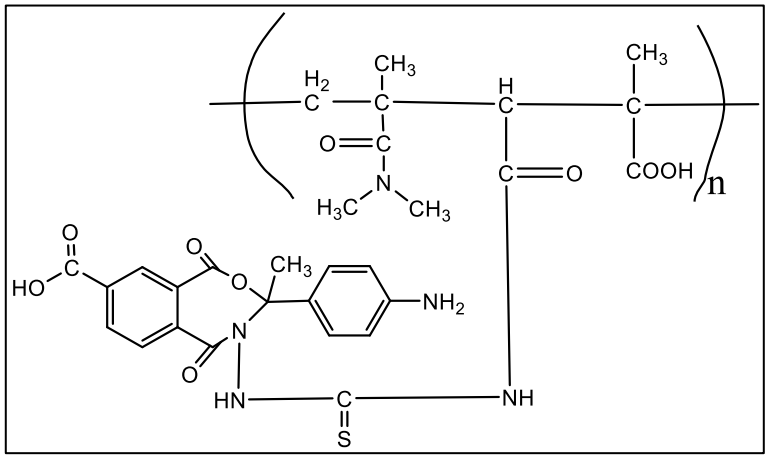


Figure (3- 91): structure of copolymer(50) (DMA-CO-CAN) with compound(25).

3.36 Synthesis of copolymer (DMA-CO-CAN) with compound (28).

A 0. 5 mole from (28) compound with 0.5 mol from copolymer (DMA-CO-CAN) in 20 ml of absolute ethanol with stirring at room temperature. The precipitate was filtered off and washed in ether and recrystallized from ethanol.

3.36.1 Synthesis of copolymer(51) (DMA-CO-CAN) with compound(28).

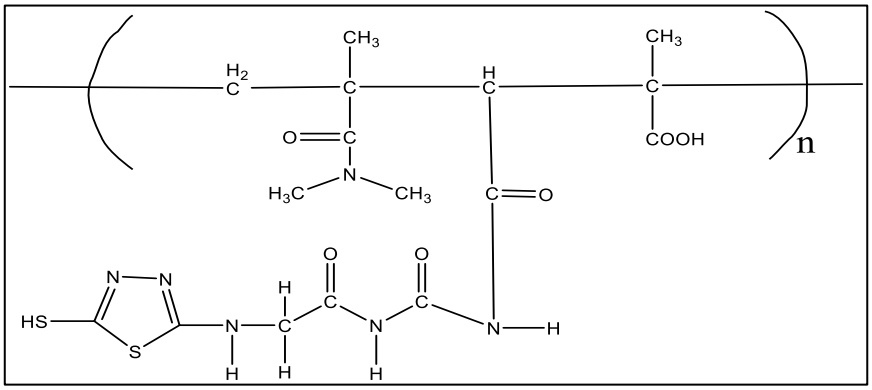


Figure (3- 92): structure of copolymer(51) (DMA-CO-CAN) with compound(28).

3.37 Synthesis of copolymer (DMA-CO-CAN) with compounds (31).

A 0. 5 mole from (31) compound with 0.5 mol copolymer(DMA-CO-CAN) in 20 ml of absolute ethanol with stirring at room temperature. The precipitate was filtered off and washed in ether and recrystallized from ethanol.

3.37.1 Synthesis of copolymer(52) (DMA-CO-CAN) with compound(31).

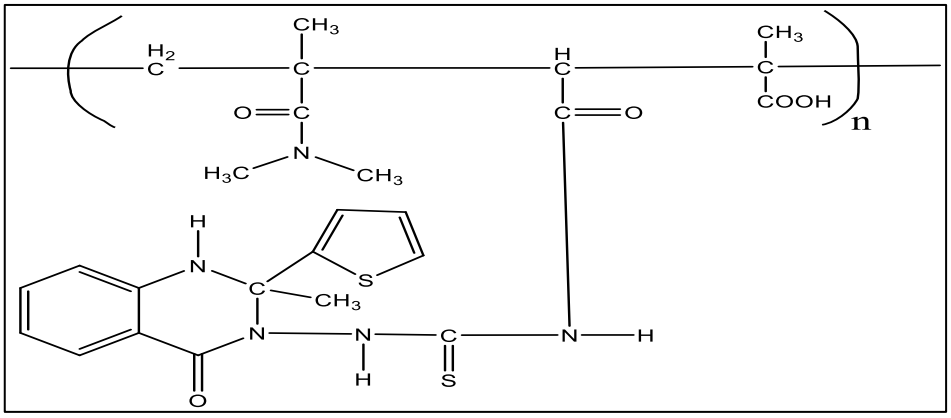


Figure (3- 93): structure of copolymer(52) (DMA-CO-CAN) with compound(31).

3.38 Synthesis of copolymer (DMA-CO-CAN) with compound(34).

A mixture of 0.5 from (34) compound with 0.5 mol from copolymer(DMA-CO-CAN) in 20 ml of absolute ethanol with stirring at room temperature. The precipitate was filtered off and washed in ether and recrystallized from ethanol.

3.38.1 Synthesis of copolymer(53) (DMA-CO-CAN) with compound (34).

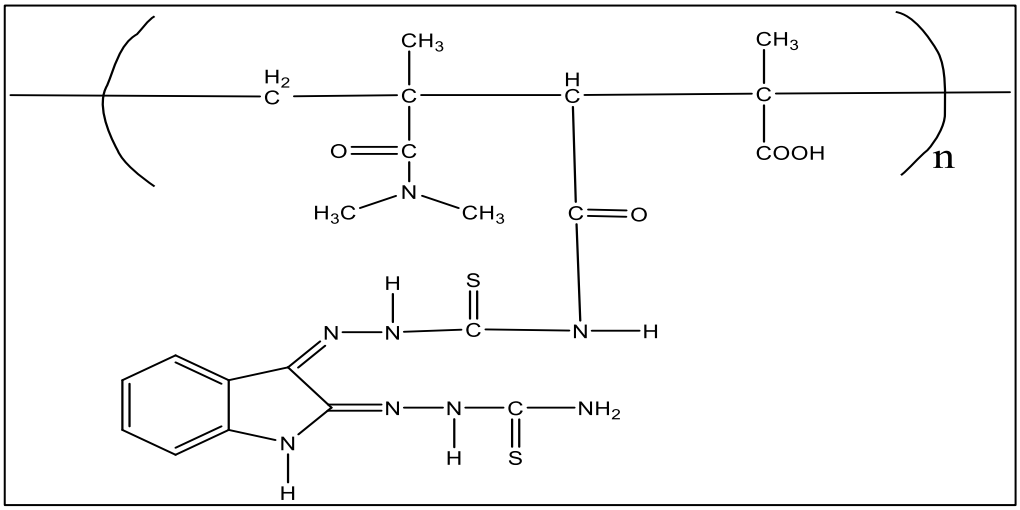


Figure (3- 94): structure of copolymer(53) (DMA-CO-CAN) with compound (34).

3.39 Synthesis of copolymer (DMA-CO-CAN) with compound(35).

A mixture of (0.5) from (35) compound with (0.5) mol from copolymer (DMA-CO-CAN) in 20 ml of absolute ethanol with stirring at room temperature. The precipitate was filtered off and washed in ether and recrystallized from ethanol.

3.39.1 Synthesis of copolymer(54) (DMA-CO-CAN) with compound(35).

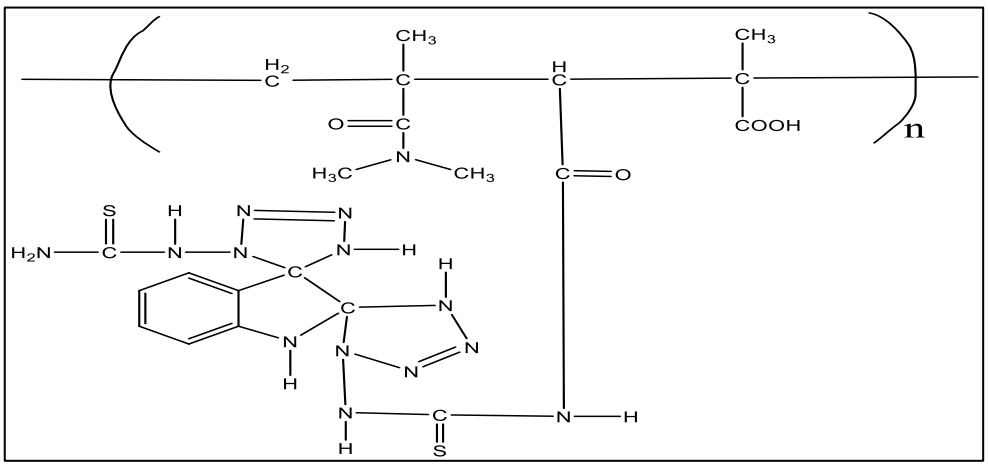


Figure (3- 95): structure of copolymer(54) (DMA-CO-CAN) with compound(35).

3.40 *Synthesis* of copolymer (DMA-CO-CAN) with compounds (37-40).

Mixing of 0.5 mol from (37), (38), (39), (40) compounds with 0.5 mol from copolymer (DMA-CO-CAN) in 20 ml of absolute ethanol with stirring at room temperature. The precipitate was filtered off and washed in ether and recrystallized from ethanol.

3.40.1 Synthesis of copolymer(55) (DMA-CO-CAN) with compound(37).

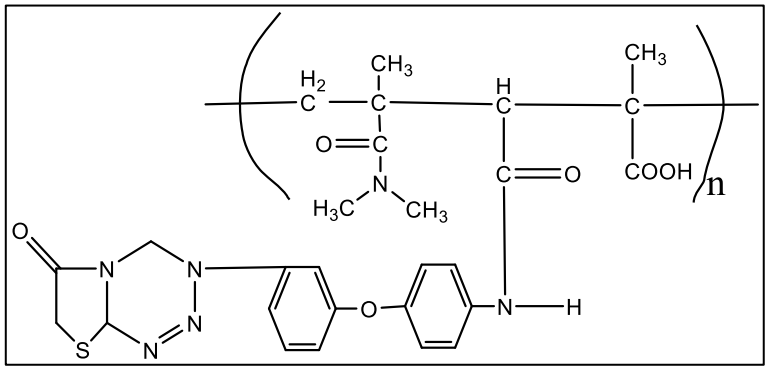


Figure (3- 96): structure of copolymer(55) (DMA-CO-CAN) with compound(37).

3.40.2 Synthesis of copolymer(56) (DMA-CO-CAN) with compound(38).

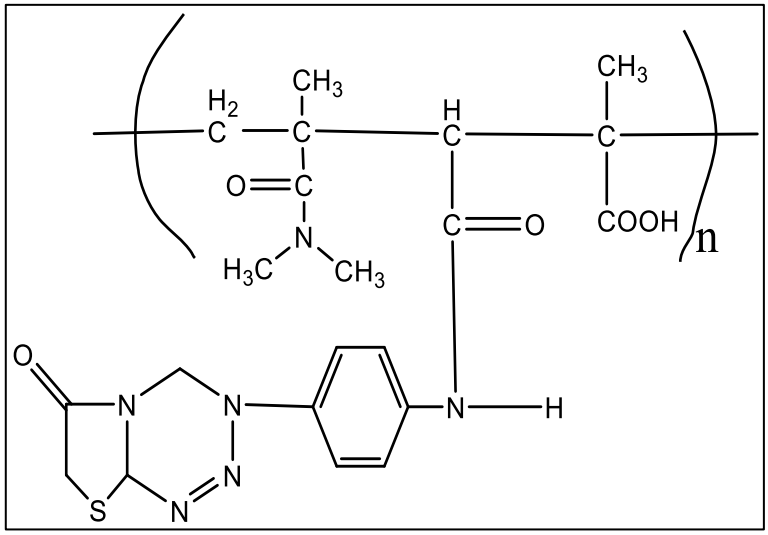


Figure (3- 97): structure of copolymer(56) (DMA-CO-CAN) with compound(38).

3.40.3 Synthesis of copolymer(57) (DMA-CO-CAN) with compound(39).

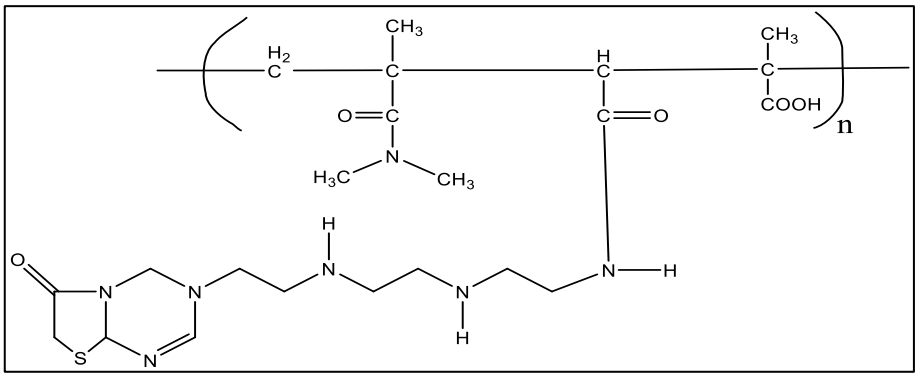


Figure (3- 98): structure of copolymer(57) (DMA-CO-CAN) with compound(39).

3.40.4 Synthesis of copolymer(58) (DMA-CO-CAN) with compound(40).

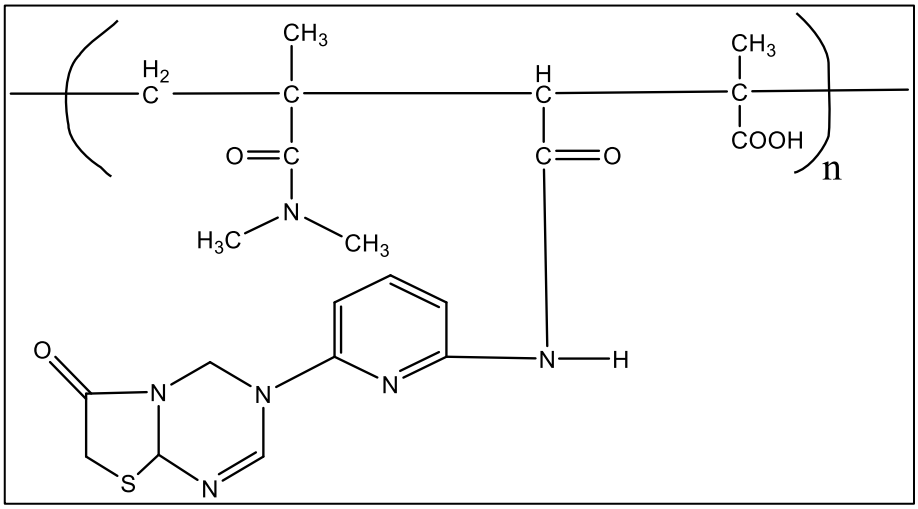


Figure (3- 99): structure of copolymer(58) (DMA-CO-CAN) with compound(40).

3.41 Study of thermogravimetric analysis (*TGA*)

Thermogravimetric analysis (*TGA*) involves determining changes in mass as a function of temperature. It is commonly used to research degradation temperatures, absorbed content of materials, levels of inorganic and organic parts contained in a material and analyze solvent residues. It employs a sensitive electronic balance from which the sample is suspended in a furnace controlled by a temperature programmer (144).

The furnace environment is controlled by continuously purging the system with air or nitrogen as required. A characteristic curve will be obtained displaying mass against temperature that provides information regarding the composition of the sample. For example, organic polymers heated in air will burn and release combustion products. Consequently, sample mass will decrease continuously until all the sample has burned giving a balance reading of close to zero depending on any inorganic impurities that may be present (145).

3.42 Differential Scanning calorimeter analysis (DSC) study

DSC measures the amount of energy absorbed or released by a sample as it is heated, cooled or held at a constant temperature. It is achieved by placing two temperature probes in the furnace and simultaneously measuring the temperature of the sample and furnace temperature while heating the sample at a constant rate. This

technique is used for polymer and pharmaceutical applications. The DSC will be resulted in a heat input against temperature curve. Differential Scanning Calorimetry, is a technique of thermal analysis that investigates how material's heat capacity (Cp) is transformed by temperature. A known mass sample is heated or cooled and the variations in its heat capacity are observed as alterations in the heat flow. This allows to reveal transitions such as melts glass transitions (Tg), and the melting point (Tm) the degree of crystallization (Tc) (146).

DSC analysis revealed glass transition temperatures around (66-110^{o}C) that are typical for structures of this type. Differences between the numbers obtained during first and second heating and cooling could be referred to the changes happening in materials. The observation of "Tm" can be explained by the same reasons, as it does not appear during the second cycle. Crystallization of heterocyclic polymer synthesized is explained by its higher molecular weight and crosslinking.

3.43 Study of molecules docking

3.43.1 Molecules Library Preparation

The newly copolymers **(1, 2, 3, 4, 5)** were synthesized and characterization to using in molecular docking process, Chemdraw Ultra 12.0 (https://chemdraw pro.software.informer.com/12.0/) software was utilized to generate the 3D structures of the compounds **(1, 2, 3, 4, 5)** and followed by energy minimization. The structures were pre-optimized with semi-empirical AM1 method using Hyperchem 8.08 software. The structures were optimized using density functional theory DFT method by employing the B3LYP/6-31G basis set to obtain the most stable conformation. The convergent value of maximum force, root-mean-square (RMS) force, maximum displacement and RMS displacement are set by default and achieved "YES". All values are positive after calculating vibrational frequencies for ligands; those results indicate that the ligands are stable. The optimized structures were combined in one database on MOE software (Molecular Operating Environment (MOE), 2019) in order to study the affinity of ligands (figure 2). Also, figure 1 illustrates the schematic representation of the docking procedure, analysis

of ligands, and reactivity.

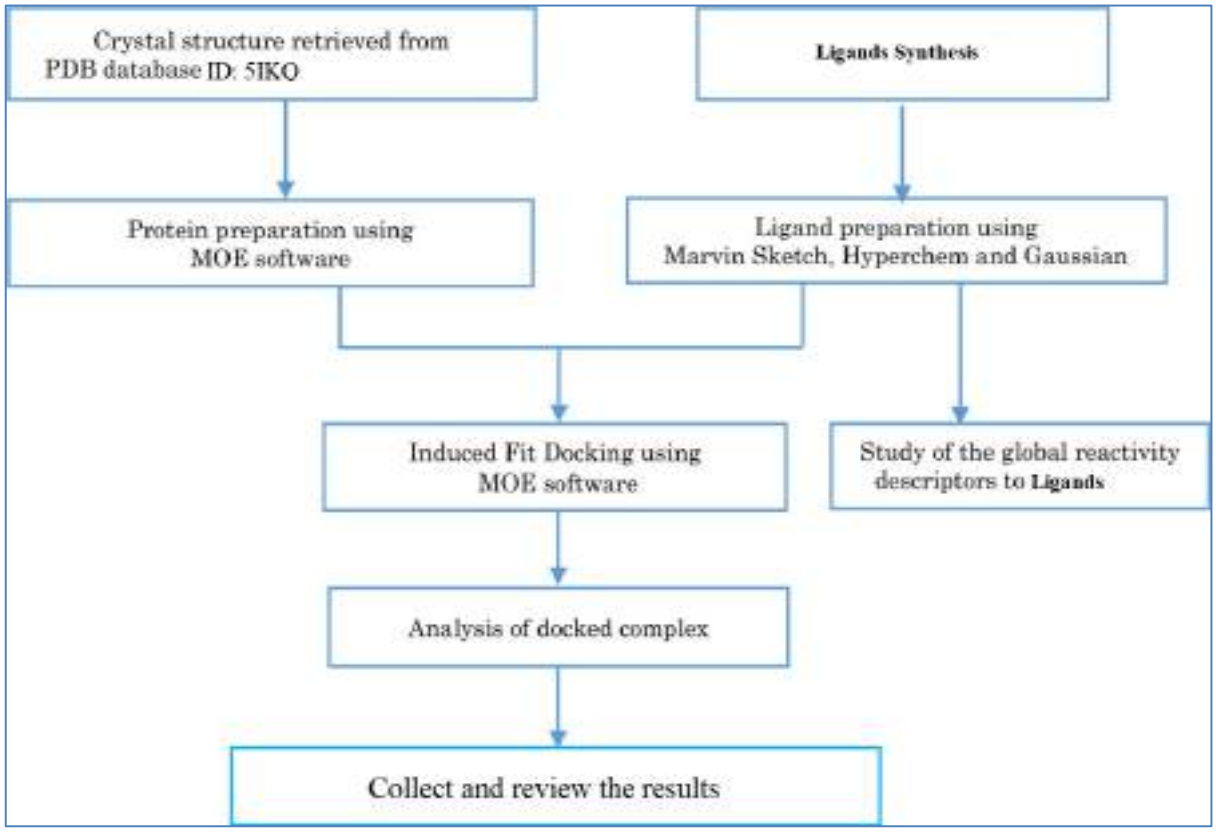


Figure (3- 100): Schematic representation of the docking procedure, analysis of ligands and reactivity

3.44 Study of Biological Activity:

The biological activity of some prepared copolymers **(**1, 2 , 3 , 4 , 5 , 6 , 7 , 8 , 9 , 10) was studied . This thesis included the use of four types of pathogenic bacteria that were identified and isolated using chemical and microscopic tests. These four types of bacteria are Gram-positive (Staphylococcus aureus) and Gram-negative (Klebsiella pneumonia, Pseudomonas aeruginosa, Escherichia coli), and two fungal (*Candida albicans***,** Aspergillus niger) which were obtained from the Biotechnology research center , University of Nahrin, Iraq . The inhibitory effect of these copolymers on bacterial growth and fungi was examined, and the diameters of the inhibition zones were measured after 24 hours of incubation at a temperature of 37°C.

3.44.1 Preparation of the Culture Medium:

Muller–Hinton agar was prepared by dissolving 38 g of the dehydrated medium in 1000 mL of distilled water. The solution was heated until complete dissolution. The pH was adjusted to 6.8 using a calibrated pH meter. The medium was sterilized by autoclaving at 121°C under 15 psi pressure for 15 minutes. After sterilization, the medium was poured into sterile Petri dishes to a uniform depth 3–4 mm and allowed to solidify. The plates were stored at 37°C until use.

3.44.2 Processing Method :

The prepared bacteria were spread on the culture medium in Petri dishes using a loopful method. were created in these plates using a sterile cork borer, sterilized with alcohol. Afterward, Single colonies from each bacterial isolate were cultured on nutrient agar and incubated at 37°C for 18–24 hours. Colonies were then transferred into 5 mL of sterile normal saline and mixed thoroughly using a vortex mixer. The turbidity of the suspension was adjusted to match 0.5 McFarland standard, corresponding to approximately 1.5×10^8 CFU/mL.

3.45 Cytotoxicity Assays Cell Lines

3.45.1 Cancer Cell Lines:

Study of, the cancer cell lines used were cytotoxic effect of copolymers on human colorectal carcinoma cell line (HCT116) and human malignant melanoma cell line (A375) with human dermal fibroblasts (HdFn) as normal cell line using MTT assay that can be used in cancer and toxicology research This step was done at the department of pharmacology, Faculty of Medicine, Center for Natural Product Research and Drug Discovery, University of Nahrain, Baghdad, Iraq IC 50 was also measured.

3.45.2 Cytotoxicity MTT Assays:

The Principle It is one of the colorimetric assays used to estimate cytotoxicity by measuring the metabolic activity of cells, and is commonly applied to estimate the inhibitory or lethal ability of extracts and compounds against cancer cells.The test depends on the ability of oxidation and reduction enzymes (Oxidoreductase enzymes) and the cellular ability based on the ability of the NADPH enzyme Dehydrogenase to reduce Phosphate buffer saline solution (1M, pH 7.2) MTT Phosphate buffer saline (PBS) was prepared by dissolving NaCl 8 g, potassium chloride (KCl) 0.2 g, KH2PO4 0.4 g and Na2HPO4.7H2O 1.4 g in 800 mL of D.W, as the higher the percentage of Phosphate buffer compound formed, The more effectiveness, which means an increase in the percentage of viable cells (147).

A-Kit Contente

Table (3- 41): Kits used in this study

Kits	Company – origin
3 – (4, 5 – dimethylthiazol – 2 – yl) – 2, 5 diphenyltetrazolium bromide (MTT kit)	Intron Biotech – Korea

B- Procedure Assay

The steps of the Procedure were followed were prepared according to Manish and Thankamani (148).

1- **Phosphate buffer saline solution (1M, pH 7.2):** Phosphate buffer saline (PBS) was prepared by dissolving NaCl 8 g, potassium chloride (KCl) 0.2 g, KH_2PO_4 0.4 g and $Na_2HPO_4.7H_2O$ 1.4 g in 800 mL of D.W. After that, pH was adjusted to 7.2. Then, the volume was completed to

2- 1000 mL with D.W.

3- Trypsin solution (1%): To prepare this solution, 1 g of trypsin was dissolved in 100 mL of PBS, then, the mixture was sterilized by Millipore filter 0.22 µ.

4- EDTA solution (1%): To prepare this solution, 1 g of ethylene–diamine–tetra acetic acid (EDTA) was dissolved in 100 mL of PBS. Then, the mixture was sterilized by autoclaving.

5- Trypsin-EDTA solution: A 20 mL of trypsin solution, 10 mL of EDTA solution and 370 mL of PBS were mixed together and stored at 4°C.

6- **Roswell Park Memorial Institute (RPMI)-1640 medium:** Package RPMI 100 mL that is ready prepare and use in this study.

7- 4–(2–hydroxyethyl) –1 piperazine–ethane sulfonic acid (HEPES) and

8- L–glutamine were already present in the medium, as illustrated by manufacturer. Also, these following ingredients were added directly to the medium and mixed thoroughly:

A-Penicillin: (10^3 IU),

B-Streptomycin: (0.001 g),

C-Sodium bicarbonate: (1%),

D-Fetal bovine serum: (15%).

9- **Serum free medium:** Is RPMI-1640 medium that is free of fetal bovine serum.

10- **MTT kit contents:** MTT solution (1 mL × 10 vials) 10 mL and Solubilization solution (50 mL × 2 bottles) 100 mL, both solutions were ready to use.

11- Cell line culture and maintenance: Culture and maintenance of cell line was done as follow:

A- All cell lines A375, HCT116 and HdFn were suspended in RPMI-1640 medium and allow propagating in culture (96–well plate) in a humidified atmosphere with 5% CO_2 at 37°C until a monolayer is formed.

B- When the cells grown formed a confluent (70–80%) monolayer, the growth medium was discarded from the plate and adherent cells were washed with PBS solution, twice times.

C- From trypsin EDTA solution 2 or 3 mL was added to the plate and the plate was turned over to cover the monolayer completely along with gentle shaking.

D- The plate was incubated at 37°C for 2 min. until the cells detached from the surface of the plate.

E- The activity of trypsin was stopped by the addition of complete RPMI 1640 media and cells were distributed into other plate containing fresh RPMI medium and the plate were incubated at 37°C in 5% CO_2 incubator.

F- The cell concentration required was achieved by counting the cell using hemocytometer and applying the following formula:

$$\boldsymbol{Total\ cell\frac{count}{mL} = Cell\ count \times Dilution\ factor\ (sample\ volume) \times 10^4}$$

12- Protocol: 3 – (4, 5 – dimethylthiazol – 2 – yl) – 2, 5 – diphenyltetrazolium bromide assay or MTT assay was assayed as following:

A- Cancer cells were re-cultured in (96-well plates) by volume of 200 µL culture medium per well.

B- The plates were incubated at 37°C for 24hrs.

C- After incubation for 24hrs., the medium was discarded and two–fold of serial dilution of compounds name (25, 50, 100, 200 and 400 µg/mL) 200 µL from each concentration were added to the wells.

D- Triplicates were performed at each concentration and control and the plates were incubated in a CO_2 incubator 37°C; 5% CO_2 for 24hrs.

E- Following incubation, 10µL of MTT solution was added to each well and the plates were incubated in CO_2 incubator for 4hrs. in dark.

F- The medium was carefully removed and 100 µL of solubilization solution was added into each well and incubated for 5min.

G- The absorbance was measured by utilizing a microplate reader (ELISA) at 575 nm.

The data was subjected to statistical analysis in order to calculate the concentration of compounds required to cause 50% reduction in cell viability for each cell line (IC_{50}).

3.46 DPPH Radical Scavenging activity:

The DPPH radical scavenging activity was evaluated according to Rajesh and Natavar (149), by preparing a DPPH solution (0.0043 g in 3.3 mL methanol:DMSO, 9:1 v/v) protected from light. Different concentrations of (1 to 10) at (0.500–0.0625 mg/mL) were prepared, while ascorbic acid was used as a standard at the same concentrations. Then, 0.1 mL of compounds (1 to 10) concentration was added to 3.9 mL of DPPH solution and incubated at 37°C for 30 mins. After cooling, the absorbance was measured at 517 nm for 4 times. The percentage of radical scavenging activity was calculated using the following formula:

$$\boldsymbol{DPPH\ radical\ scavenging\ activity}\ (\%) = \left(\mathbf{1} - \frac{\boldsymbol{Absorbance\ of\ sample}}{\boldsymbol{Absorbance\ of\ standard}}\right) \times \mathbf{100}$$

3.47 Statistical analysis

IBM SPSS Statistics version 31.0.0.0 was used to calculated the mean and stander division (SD). Also, used Graph Pad Prism version 10 (GraphPad Software Incorpo rated, La Jolla, California), for determine the IC_{50}.(150)

Table (3- 42): The color, yield and melting point of synthesis of compounds

Compounds	Formula	Color	m.p / ^{0}C	Weight (gm)	Yield (%)
1	$C_7H_9N_4S$	Pink	215-220 dec.	3.5	92
2	$C_9H_{12}N_4S$	Orange	193-195dec	3	93
3	$C_8H_4Cl_4O_6P_2$	Yellow	300 dec	2.3	92
4	$C_8H_4Cl_4O_6P_2$	White	191-194 dec	2.3	93
5	$C_8H_9N_3OS$	White	230-233 dec.	1.9	90
6	$C_8H_7N_3OS_2$	White	234-237	5.3	94
7	$C_6H_8N_3OS$	Brown	248-251 dec	3.5	94
8	$C_7H_{10}N_3S_2$	White	168-171 dec	3.9	92
9	$C_{10}H_{14}N_4S$	White	167-170 dec	3.4	94
10	$C_9H_8N_3OS$	Olive	258-261 dec	3.5	92
11	$C_{11}H_{12}N_4OS$	Brown	168-172 dec	3.8	95
12	$C_{11}H_{10}N_4O_3S$	Yellow	245-248 dec	4.1	95
13	$C_{16}H_{13}N_3OS$	White	261-264 dec	4.3	94
14	$C_{10}H_9N_3O_2S$	White	241-244 dec	3.5	94
15	$C_8H_7N_3OS_2$	White	234-237 dec	5.3	94
16	$C_8H_7N_3O_2S$	Brown	240-244 dec	4.2	92
17	$C_9H_9N_3OS_2$	White	263-266 dec	5.2	94
18	$C_9H_8N_4O_2S$	Brown	-	5.2	96
19	$C_8H_8N_4S$	Brown	212-215 dec	4.2	95
20	$C_8H_8N_4OS$	Brown	-	4.5	93
21	$C_{26}H_{12}N_4O_8S$	Brown	-	4.2	93
22	$C_{25}H_{14}N_4O_7S$	White	203-207 dec	3	90
23	$C_{25}H_{12}N_4O_7S$	Yellow	209-212 dec	3.9	9.2
24	$C_{24}H_{14}N_4O_8$	Yellow	195-199 dec	1	83
25	$C_{17}H_{14}N_4O_6$	White	230-233 dec	0.73	76
26	$C_{27}H_{22}N_4O_6$	Orange	197-200 dec	1.02	82
27	$C_4H_4ClN_3OS_2$	Pink	187-189 dec	7.5	96
28	$C_5H_7N_5O_2S_2$	Pink	190-193 dec	5.08	94
29	$C_{13}H_{12}N_4OS_2$	Brown	-	2.7	90
30	$C_{14}H_{14}N_4O_2S$	Black	-	2.7	90
31	$C_{14}H_{14}N_4OS_2$	Brown	186-188 dec	2.9	90
32	$C_{10}H_{10}N_4S_2$	White	194-197 dec	2	91
33	$C_{10}H_{14}N_{12}O_2$	Orange	205-208 dec	3	92
34	$C_{10}H_{11}N_7S_2$	White	199-203 dec	2.1	91
35	$C_{10}H_{13}N_{13}S_2$	Orange	201-204 dec	3.9	92
36	$C_3H_4N_2OS$	White	217-220 dec	12	97
37	$C_{17}H_{17}N_5O_2S$	Brown	240-243 dec	1.8	94
38	$C_{11}H_{13}N_5OS$	Black	-	1.7	90
39	$C_{11}H_{23}N_7OS$	White	-	1.7	90

40	$C_{10}H_{12}N_6OS$	White	-	1.7	90
41	$C_{15}H_{24}O_2$	White	-	10	99
42	$C_{14}H_{23}NO_4$	White	-	10	99
43	$C_{18}H_{24}N_4O_5S$	Light pink	-	0.9	90
44	$C_{20}H_{28}N_4O_5S$	Light orange	-	0.9	90
45	$C_{20}H_{26}N_4O_7S$	Light yellow	-	0.9	90
46	$C_{25}H_{29}N_3O_5S$	White	-	0.9	90
47	$C_{19}H_{25}N_3O_6S$	White	-	0.9	90
48	$C_{17}H_{23}N_3O_5S_2$	Light yellow	-	0.9	90
49	$C_{17}H_{23}N_3O_6S$	Light brown	-	0.9	90
50	$C_{18}H_{30}N_4O_5S$	White	-	0.9	90
51	$C_{25}H_{29}N_3O_5S$	White	-	0.9	90
52	$C_{21}H_{30}N_4O_5S$	White	-	0.9	90
53	$C_{20}H_{24}N_4O_6S$	Light green	-	0.9	90
54	$C_{22}H_{28}N_4O_6S$	Light brawn	-	0.9	90
55	$C_{22}H_{26}N_4O_8S$	Light yellow	-	0.9	90
56	$C_{27}H_{29}N_3O_6S$	White	-	0.9	90
57	$C_{22}H_{27}N_3O_7S$	White	-	0.9	90
58	$C_{19}H_{23}N_3O_6S_2$	White	-	0.9	90
59	$C_{21}H_{28}N_4O_6S$	Light brown	-	0.9	90
60	$C_{22}H_{29}N_5O_6S$	Light brown	-	0.9	90
61	$C_{21}H_{29}N_5O_4S$	Light brown	-	0.9	90
62	$C_{21}H_{29}N_5O_5S$	Light brown	-	0.9	90
63	$C_{37}H_{28}N_4O_{13}S$	Light brown	-	0.9	90
64	$C_{36}H_{28}N_4O_{11}S$	White	-	0.9	90
65	$C_{36}H_{28}N_4O_{11}S$	Light yellow	-	0.9	90
66	$C_{35}H_{32}N_4O_{11}S$	Light yellow	-	0.9	90
67	$C_{29}H_{34}N_4O_9S$	White	-	0.9	90
68	$C_{37}H_{36}N_4O_{11}S$	Light orange	-	0.9	90
69	$C_{15}H_{20}ClN_3O_6S_2$	Light pink	-	0.9	90
70	$C_{16}H_{23}N_5O_7S_2$	Light pink	-	0.9	90
71	$C_{24}H_{28}N_4O_6S_2$	Light brown	-	0.9	90
72	$C_{25}H_{30}N_4O_7S$	Lead	-	0.9	90
73	$C_{25}H_{30}N_4O_6S_2$	Light brown	-	0.9	90
74	$C_{21}H_{26}N_4O_5S_2$	White	-	0.9	90
75	$C_{21}H_{30}N_{12}O_5S_2$	Light orange	-	0.9	90
76	$C_{21}H_{27}N_7O_5S_2$	White	-	0.9	90
77	$C_{21}H_{29}N_{13}O_5S_2$	Light orange	-	0.9	90
78	$C_{14}H_{20}N_2O_6S$	White	-	0.9	90
79	$C_{28}H_{33}N_5O_7S$	Light brown	-	0.9	90
80	$C_{22}H_{29}N_5O_6S$	Lead	-	0.9	90
81	$C_{22}H_{39}N_7O_6S$	White	-	0.9	90

82	**$C_{21}H_{28}N_6O_6S$**	**White**	**-**	**0.9**	**90**
83	**$C_{22}H_{32}N_4O_5S$**	**White**	**-**	**0.9**	**90**
84	**$C_{29}H_{34}N_4O_5S$**	**White**	**-**	**0.9**	**90**
85	**$C_{23}H_{30}N_4O_6S$**	**White**	**-**	**0.9**	**90**
86	**$C_{22}H_{30}N_4O_5S_2$**	**White**	**-**	**0.9**	**90**
87	**$C_{21}H_{28}N_4O_6S$**	**Light brown**	**-**	**0.9**	**90**
88	**$C_{22}H_{29}N_5O_6S$**	**Light brown**	**-**	**0.9**	**90**
89	**$C_{21}H_{29}N_5O_4S$**	**Light brown**	**-**	**0.9**	**90**
90	**$C_{21}H_{29}N_5O_5S$**	**Light brown**	**-**	**0.9**	**90**
91	**$C_{37}H_{35}N_5O_{11}S$**	**Light yellow**	**-**	**0.9**	**90**
92	**$C_{31}H_{37}N_5O_9S$**	**White**	**-**	**0.9**	**90**
93	**$C_{18}H_{28}N_6O_6S_2$**	**Light pink**	**-**	**0.9**	**90**
94	**$C_{27}H_{35}N_5O_5S_2$**	**Light brown**	**-**	**0.9**	**90**
95	**$C_{23}H_{32}N_8O_4S_2$**	**White**	**-**	**0.9**	**90**
96	**$C_{23}H_{34}N_{14}O_4S_2$**	**Light orange**	**-**	**0.9**	**90**
97	**$C_{30}H_{38}N_6O_6S$**	**Lead**	**-**	**0.9**	**90**
98	**$C_{24}H_{34}N_6O_5S$**	**White**	**-**	**0.9**	**90**
99	**$C_{24}H_{43}N_7O_5S$**	**White**	**-**	**0.9**	**90**
100	**$C_{23}H_{33}N_7O_5S$**	**White**	**-**	**0.9**	**90**

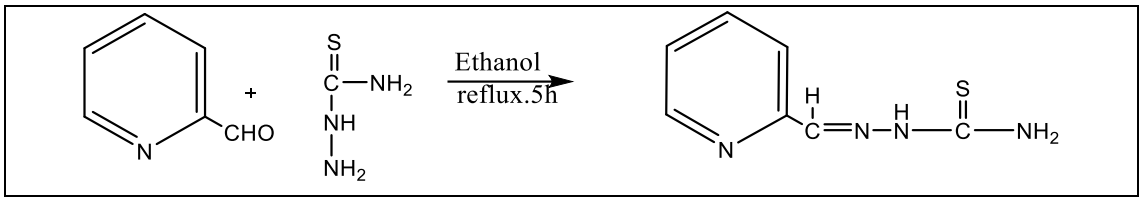
Chapter Four

Results and Discussion

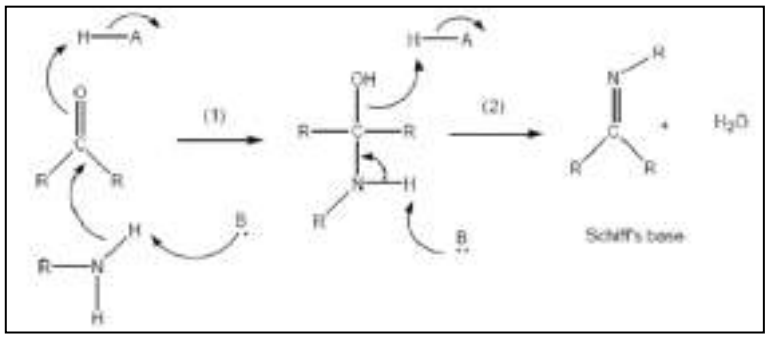
4. Results and discussion

4.1 Synthesis of the Thiosemicarbazones compounds (1-9).

4.1.1 Synthesis of Thiosemicarbazones of 2-(pyridin-2-ylmethylene)hydrazine-1-carbothioamide compound(1).



Scheme (4-1): Synthesis Thiosemicarbazones of 2-(pyridin-2-ylmethylene)hydrazine-1-carbothioamide compound(1).



Scheme (4-2): Mechanism of Schiff base.

FTIR Spectrum of 2-(pyridin-2-ylmethylene)hydrazine-1-carbothioamide compound(1).

The FTIR spectrum of Thiosemicarbazones for 2-(pyridin-2-ylmethylene)hydrazine-1- carbothioamide as shown in (fig.4-1) which indicates absorption bands at 3432 and 3260 cm^{-1} to $–NH_2$ stretching , absorption band at 3157 cm^{-1} to C-H (aromatic), absorption band at 1608 cm^{-1} to C=N, absorption band at 1147 Cm^{-1} to C=S, absorption band at 1526 Cm^{-1} to C=C (aromatic).

(151-153)

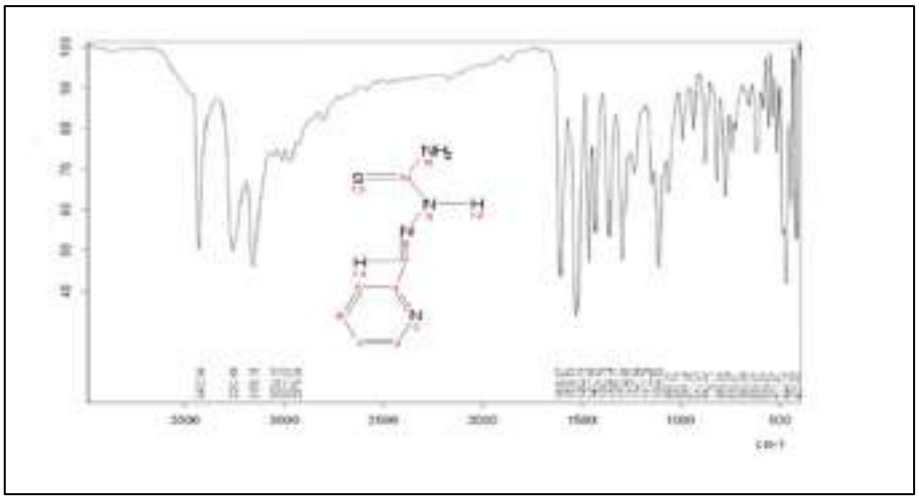


Figure (4- 1): FTIR Spectrum of 2-(pyridin-2-ylmethylene)hydrazine-1- carbothioamide compound(1).

^{1}HNMR spectrum of Thiosemicarbazones for Pyridine carboxaldehyde compound(1).

^{1}HNMR spectrum of Thiosemicarbazones for Pyridine carboxaldehyde in (Fig.4-2) the major signals at δ 1.3 ppm is characteristic of DMSO-d6 as solvent , singlate at (7.3-8.8 δ ppm) to (3H, Hetro phenyl ring), single at (3.5 ppm) to $–NH_2$, singles at (2.5 ppm) to =CH. (151-153)

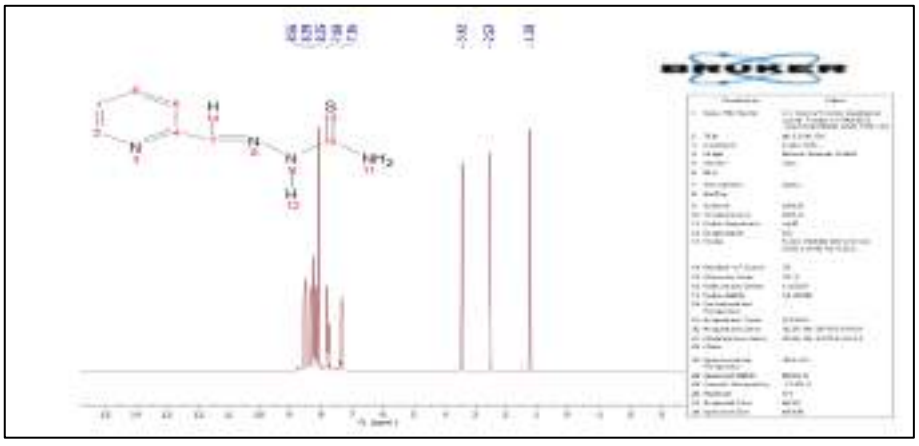


Figure (4- 2): ^{1}HNMR Spectrum of 2-(pyridin-2-ylmethylene)hydrazine-1- carbothioamide compound(1).

^{13}C-NMR spectrum of Thiosemicarbazones for Pyridine carboxaldehyde compound(1).

The signals of olefinic and aromatic carbons appear in the third region between 122 and 136 ppm, single related to C=N at 142 ppm , single related to C-N at 64 ppm, single related to C=S at 180 ppm. **(151, 152)**

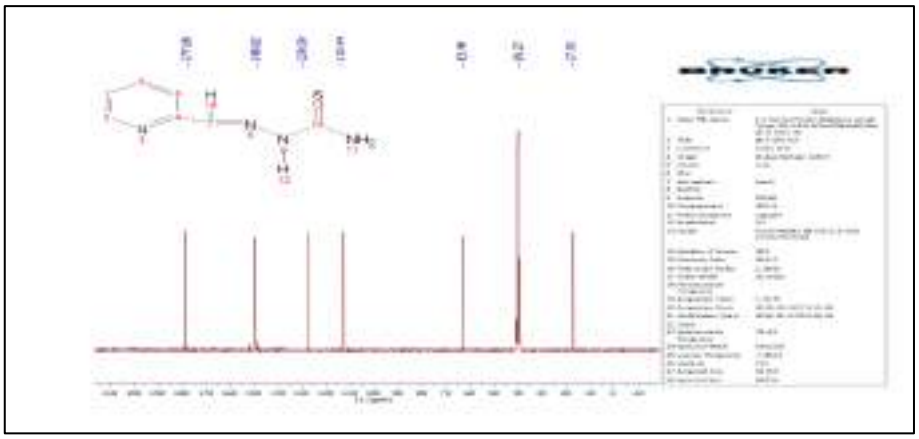
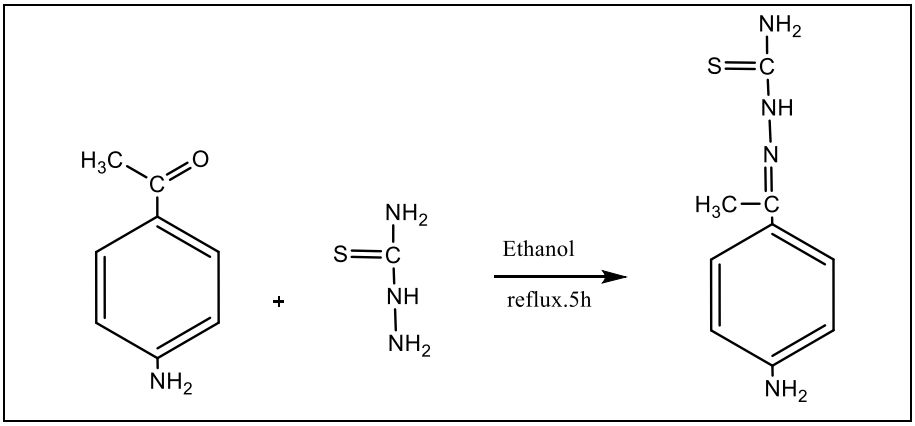


Figure (4- 3): ^{13}C-NMR Spectrum of 2-(pyridin-2-ylmethylene)hydrazine-1-carbothioamide. (Compound1)

4.1.2 Synthesis of Thiosemicarbazones of 2-(1-(4-aminophenyl)ethylidene)hydrazine-1-carbothioamide compound(2).



Scheme (4- 3): Synthesis of 2-(1-(4-aminophenyl)ethylidene)hydrazine-1-carbothioamide compound(2).

FTIR spectrum of 2-(1-(4-aminophenyl)ethylidene)hydrazine-1-carbothioamide compound(2).

The FTIR spectrum of 2-(1-(4-aminophenyl)ethylidene)hydrazine-1-carbothioamide as shown in (fig.4-4) which indicates absorption bands at 3445 and 3388 cm^{-1} to $–NH_2$ stretching , absorption band at 3309 cm^{-1} to C-H (aromatic), absorption band at 1589 cm^{-1} to C=N, absorption band at 1183 Cm^{-1} to C=S, absorption band at 1486 Cm^{-1} to C=C (aromatic), and absorption band at 1278 Cm^{-1} to CH_3. (151-153)

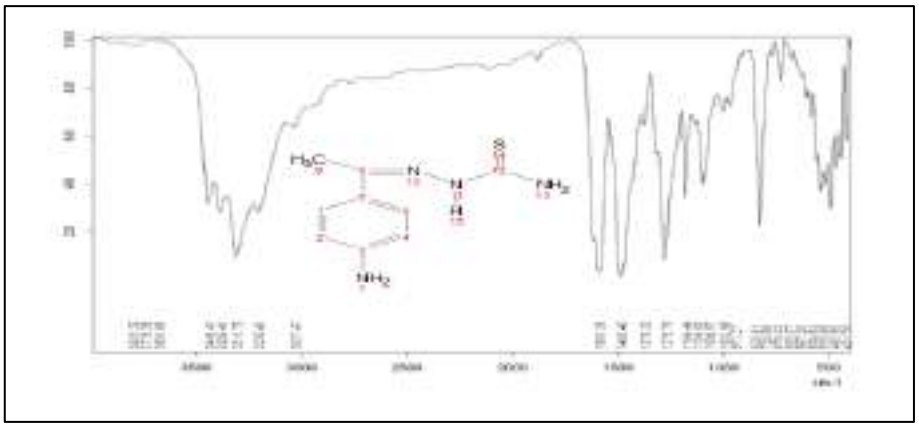


Figure (4- 4): FTIR Spectrum of 2-(1-aminophenyl)ethylidene)hydrazine-1-carbothioamide compound(2).

^{1}HNMR spectrum of 2-(1-(4-aminophenyl)ethylidene)hydrazine-1-carbothioamide compound(2).

^{1}HNMR spectrum of Thiosemicarbazones for amino acetophenone in (Fig.4-5) the major signal at δ 2.3 ppm is characteristic of DMSO-d6 as solvent , singles at (6.5-8.2 δ ppm) to (4H, phenyl ring), single at (3.5 ppm) to $–NH_2$. single at (1.3 ppm) to $–CH_3$. (151-153)

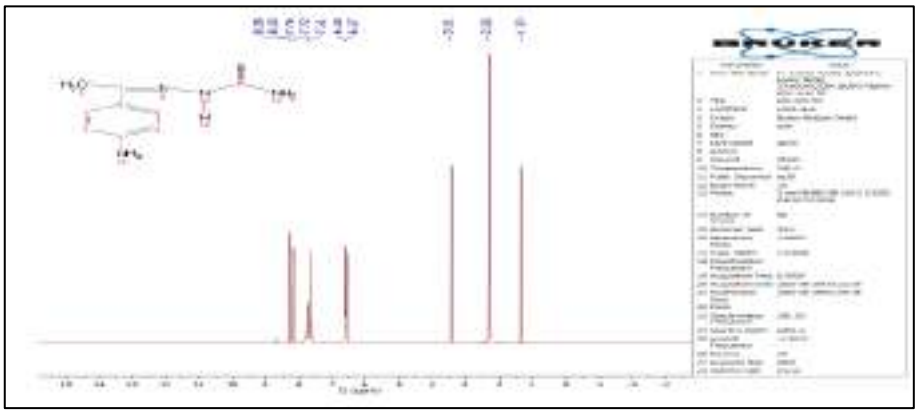


Figure (4- 5): ^{1}HNMR Spectrum of 2-(pyridin-2-ylmethylene)hydrazine-1- carbothioamide compound(2).

^{13}C-NMR spectrum of 2-(1-(4-aminophenyl)ethylidene)hydrazine-1-carbothioamide compound(2).

The signals of olefinic and aromatic carbons appear in the third region between 114 and 129 ppm, singles related to C=N at 150 ppm , single related to C-N at 64 ppm, singles related to C=S at 179 ppm, single related to CH_3-C (Secondary) at 18 ppm. (151-153)

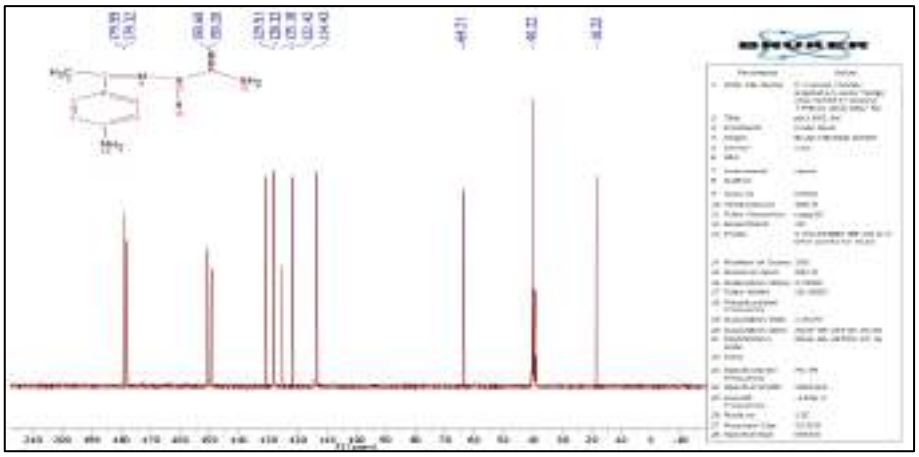
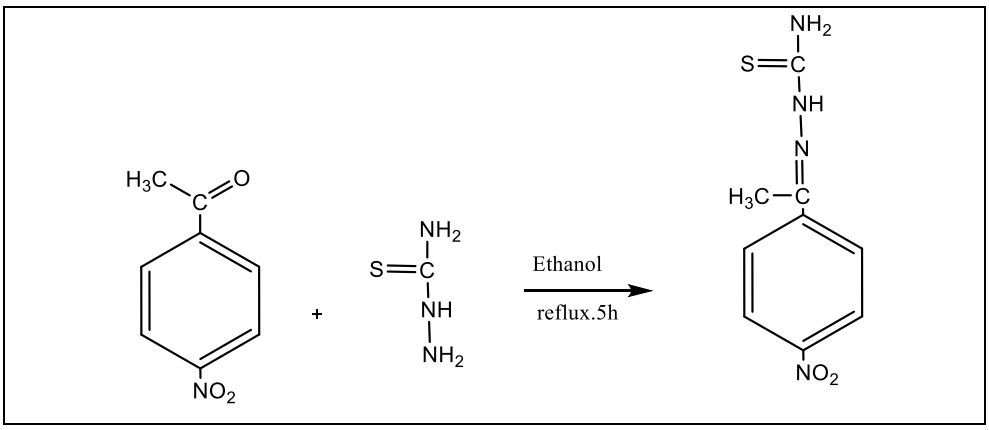


Figure (4- 6): ^{13}C-NMR Spectrum of 2-(pyridin-2-ylmethylene)hydrazine-1-carbothioamide compound(2).

4.1.3 Synthesis of the Thiosemicarbazones for 2-(1-(4-nitrophenyl)ethylidene)hydrazine-1carbothioamide compound(3).



Scheme (4-4): Synthesis of (4-nitrophenyl)ethylidene)hydrazine-1-carbothioamide compound(3).

FTIR Spectrum of 2-(1-(4-nitrophenyl)ethylidene)hydrazine-1-carbothioamide compound(3).

The FTIR spectrum of Thiosemicarbazones for 4-nitro acetophenone as shown in (fig.4-7) which indicates absorption bands at 3477 and 3355 cm^{-1} to $–NH_2$ stretching , absorption band at 3195 cm^{-1} to C-H (aromatic), absorption band at 1582 cm^{-1} to C=N, absorption band at 1078 Cm^{-1} to C=S, absorption band at 1445 Cm^{-1} to C=C (aromatic), absorption band at 1504 Cm^{-1} to NO_2, and absorption band at 1393 Cm^{-1} to CH_3. (151-153)

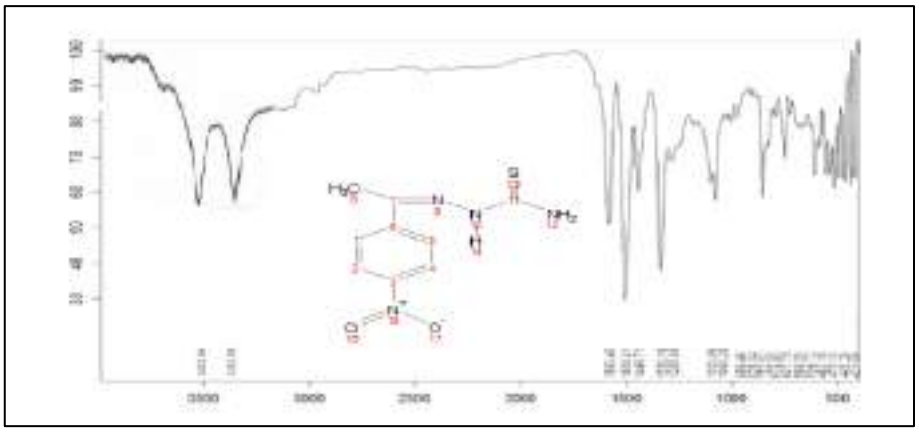


Figure (4- 7): FTIR Spectrum of(4-nitrophenyl)ethylidene)hydrazine-1-carbothioamide compound(3).

^{1}HNMR Spectrum of (4-nitrophenyl)ethylidene)hydrazine-1-carbothioamide compound(3).

^{1}HNMR Spectrum of (4-nitrophenyl)ethylidene)hydrazine-1-carbothioamide in (fig.4-8) the major signal at δ 2.3 ppm is characteristic of DMSO-d6 as solvent , singlate at (8.2-8.5 δ ppm) to (4H, phenyl ring), single at (3.4 ppm) to $–NH_2$. singles at (1.3 ppm) to $–CH_3$. **(151-153)**

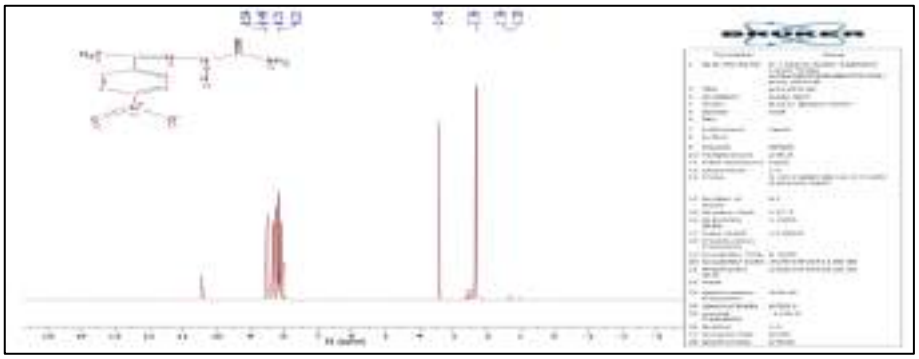


Figure (4- 8): ^{1}HNMR Spectrum of(4-nitrophenyl)ethylidene)hydrazine-1-carbothioamide compound(3).

^{13} CNMR Spectrum of (4-nitrophenyl)ethylidene) hydrazine-1-carbothioamide compound(3).

^{13} CNMR Spectrum of (4-nitrophenyl)ethylidene)hydrazine-1-carbothioamide the signals of olefinic and aromatic carbons appear in the third region between 124 and 128 ppm, singles related to C=N at 144 ppm , single related to C-N at 64 ppm, singles related to C=S at 179 ppm, single related to CH_3-C(Secondary) at 18 ppm. (151-153)

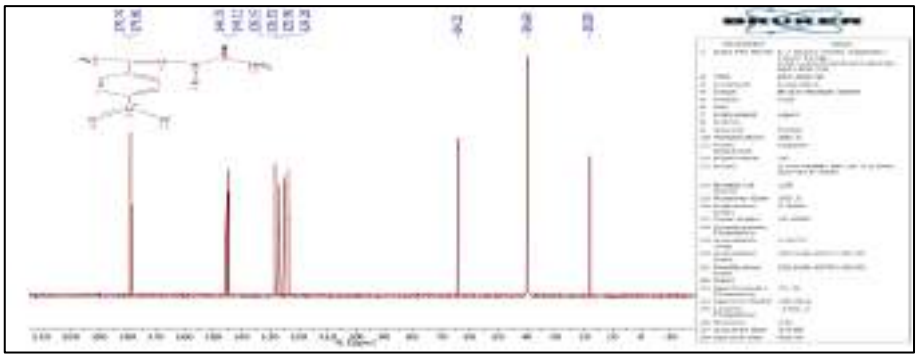
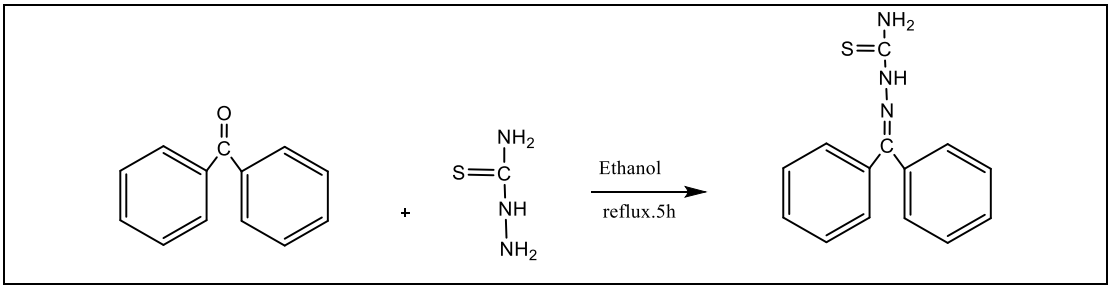


Figure (4- 9): ^{13} CNMR Spectrum of(4-nitrophenyl)ethylidene)hydrazine-1-carbothioamide compound(3).

4.1.4 Synthesis of the Thiosemicarbazones for 2-(diphenylmethylene)hydrazine-1-carbothioamide compound(4).



Scheme (4-5): Synthesis of 2-(diphenylmethylene)hydrazine-1-carbothioamide compound(4).

FTIR Spectrum of 2-(diphenylmethylene)hydrazine-1-carbothioamide compound(4).

The FTIR Spectrum of 2-(diphenylmethylene)hydrazine-1-carbothioamide FTIR spectrum of Thiosemicarbazones for benzophenone as shown in (fig4-10) which indicates absorption bands at 3367 and 3263 cm^{-1} to $–NH_2$ stretching , absorption band at 3179 cm^{-1} to C-H (aromatic), absorption band at 2998 cm^{-1} to C-H(alphatic), absorption band at 1644 cm^{-1} to C=N, absorption band at 1163 Cm^{-1} to C=S, absorption band at 1530 Cm^{-1} to C=C (aromatic). (151-153)

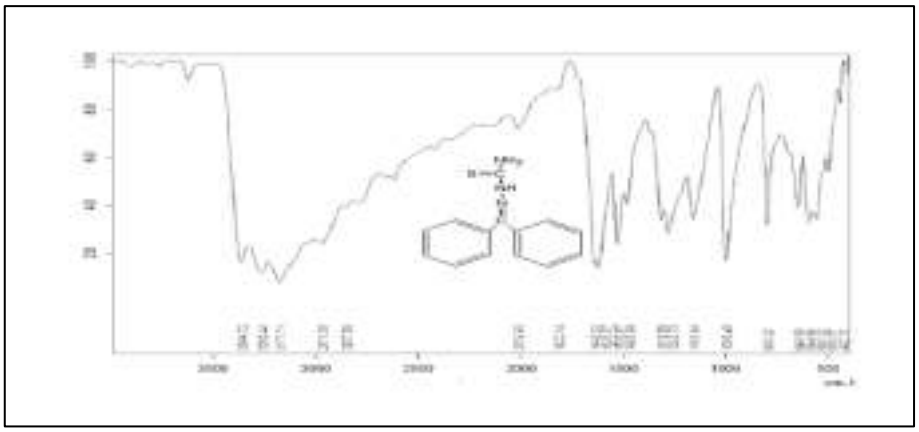


Figure (4- 10): FTIR Spectrum of 2-(diphenylmethylene)hydrazine-1-carbothioamide compound(4).

^{1}HNMR Spectrum of 2-(diphenylmethylene)hydrazine-1-carbothioamide compound(4).

^{1}HNMR Spectrum of 2-(diphenylmethylene)hydrazine-1-carbothioamide in (fig.4-11) the major signal at δ 2.5 ppm is characteristic of DMSO-d6 as solvent , singlate at (7.1-8.8 δ ppm) to (10H, phenyl ring), single at (4.5 ppm) to $–NH_2$. (151-153)

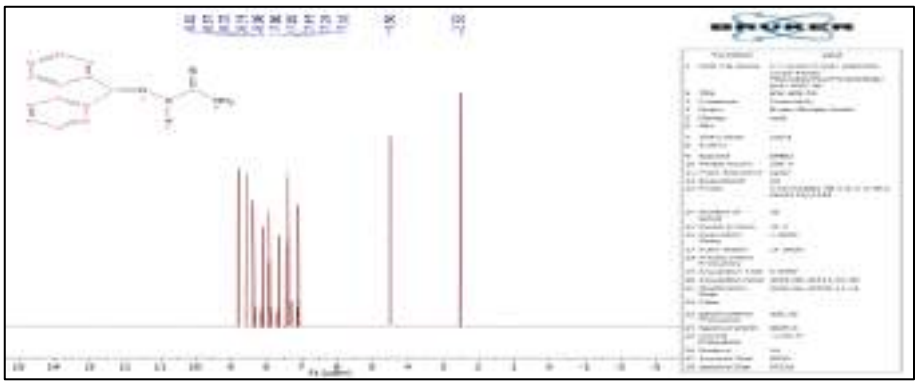


Figure (4- 11): ^{1}HNMR Spectrum of 2-(diphenylmethylene)hydrazine-1-carbothioamide compound(4).

^{13} CNMR Spectrum of 2-(diphenylmethylene)hydrazine-1-carbothioamide compound(4).

^{13} CNMR Spectrum of 2-(diphenylmethylene)hydrazine-1-carbothioamide the signals of olefinic and aromatic carbons appear in the third region between 122 and 136 ppm, single related to C=N at 140 ppm , single related to C-N at 64 ppm, single related to C=S at 182 ppm. (151-153)

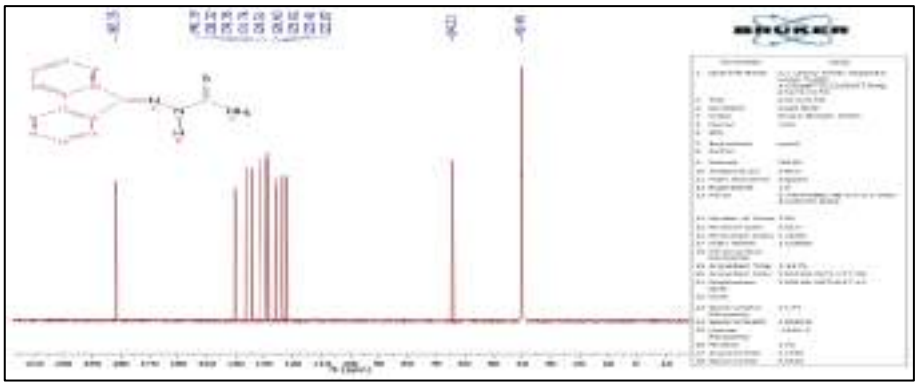
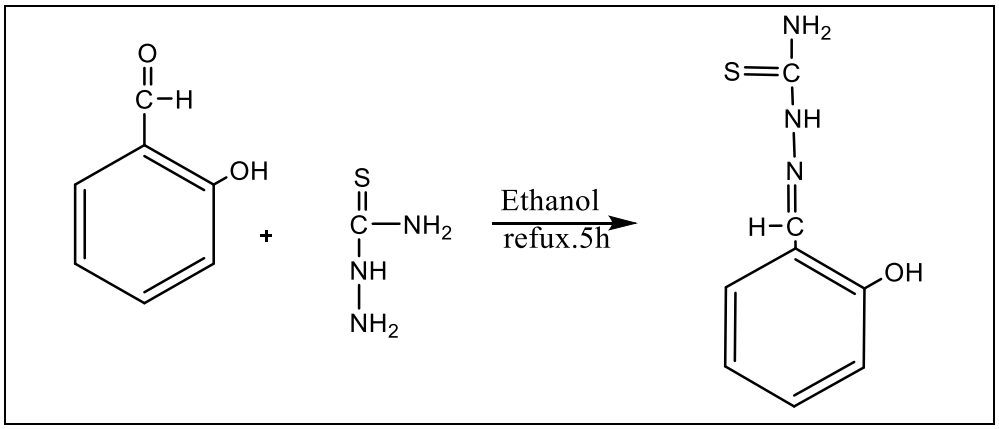


Figure (4- 12): ^{13} CNMR Spectrum of 2-(diphenylmethylene)hydrazine-1-carbothioamide compound(4).

4.1.5 Synthesis of the Thiosemicarbazones for 2-(2-hydroxybenzylidene) hydrazine-1-carbothioamide compound(5).



Scheme (4-6): Synthesis of 2-(2-hydroxybenzylidene)hydrazine-1-carbothioamide compound(5).

FTIR Spectrum of 2-(2-hydroxybenzylidene)hydrazine-1-carbothioamide compound(5).

FTIR Spectrum of 2-(2-hydroxybenzylidene)hydrazine-1-carbothioamide the as shown in (fig.4-13) which indicates absorption bands at 3442 Cm^{-1} to OH and 3318cm^{-1} to $–NH_2$ stretching , absorption band at 3172 cm^{-1} to C-H(aromatic) , absorption band at 2988 cm^{-1} to C-H(alphatic), absorption band at 1611 cm^{-1} to C=N, absorption band at 1150 Cm^{-1} to C=S, absorption band at 1537 Cm^{-1} to C=C (aromatic). (151-153)

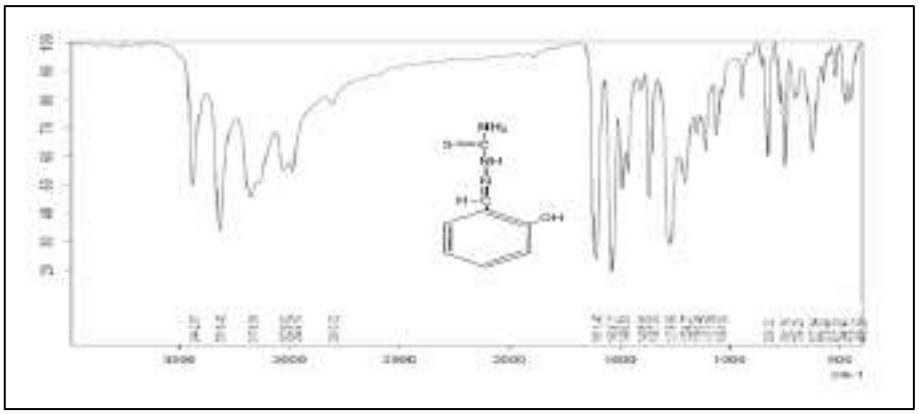


Figure (4- 13): FTIR Spectrum of 2-(2-hydroxybenzylidene)hydrazine-1-carbothioamide compound(5).

^{1}HNMR Spectrum of 2-(2-hydroxybenzylidene) hydrazine-1-carbothioamide compound(5).

^{1}HNMR Spectrum of 2-(2-hydroxybenzylidene)hydrazine-1-carbothioamide in (fig.4-14) the major signal at δ 2.5 ppm is characteristic of DMSO-d6 as solvent , singlate at (6.8-8.4 δ ppm) to (4H, phenyl ring), single at (3.4 ppm) to $–NH_2$, single at (9.9 ppm) to (H, OH). (151-153)

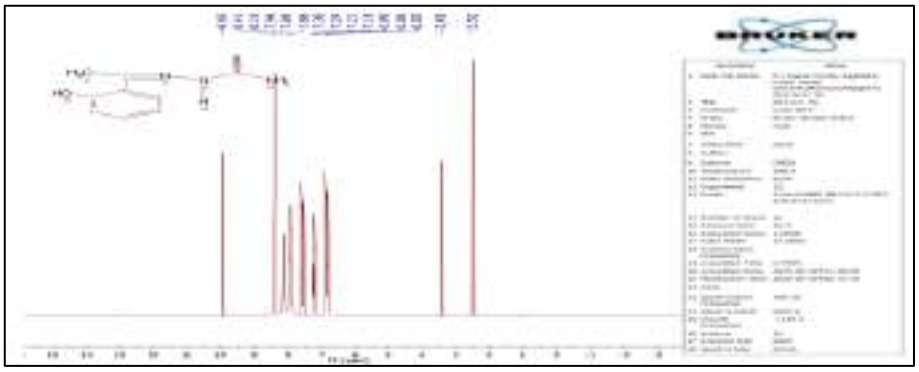


Figure (4- 14): ^{1}HNMR Spectrum of 2-(2-hydroxybenzylidene)hydrazine-1-carbothioamide compound(5).

^{13} CNMR Spectrum of 2-(2-hydroxybenzylidene)hydrazine-1-carbothioamide compound(5).

^{13} CNMR Spectrum of 2-(2-hydroxybenzylidene)hydrazine-1-carbothioamide the signals of olefinic and aromatic carbons appear in the third region between 118 and 133 ppm, single related to C=N at 158 ppm , single related to C-N at 64 ppm, single related to C=S at 178 ppm. (151-153)

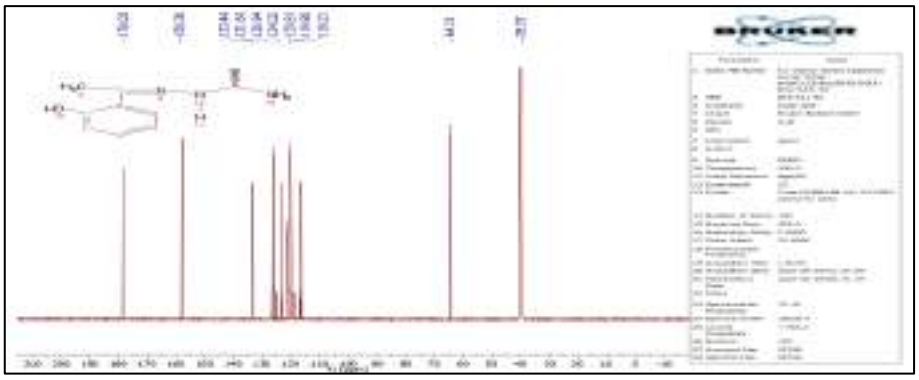
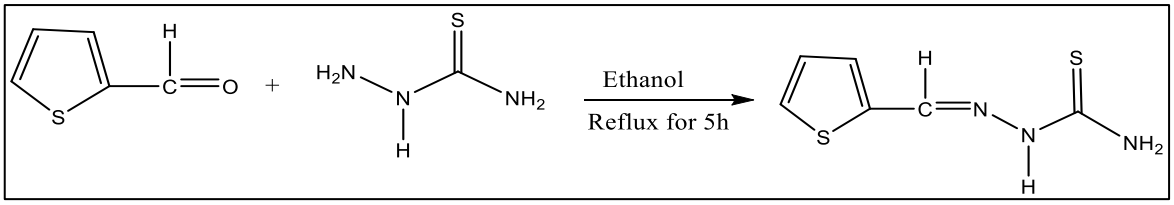


Figure (4- 15): ^{13} CNMR Spectrum of 2-(2-hydroxybenzylidene)hydrazine-1-carbothioamide compound(5).

4.1.6 Synthesis of 2-(thiophen-2-ylmethylene)hydrazine-1-carbothioamide thiosemicarbazon compound(6).



Scheme (4-7): Synthesis2-(thiophen-2-ylmethylene)hydrazine-1-carbothioamide thiosemicarbazon compound(6).

FTIR spectrum2-(thiophen-2-ylmethylene)hydrazine-1-carbothioamide thiosemicarbazon compound(6).

The FTIR spectrum2-(thiophen-2-ylmethylene)hydrazine-1-carbothioamide thiosemicarbazon as shown in Figure (4- 16) which indicates absorption bands at 3365 and 3261 cm^{-1} to $–NH_2$ stretching , absorption band at 3176 cm^{-1} to C-H (Hetero phenyl ring), absorption band at 2966 cm^{-1} to C-H(alphatic),absorption band at 1618 cm^{-1} to C=N, absorption band at 1284 Cm^{-1} to C=S, absorption band at 1531 Cm^{-1} to C=C (Hetero phenyl ring) .(151-153)

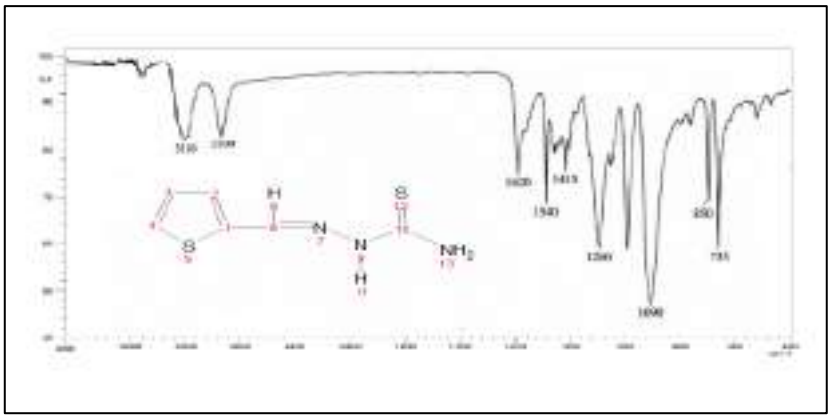


Figure (4- 16): FTIR Spectrum 2-(thiophen-2-ylmethylene)hydrazine-1-carbothioamide thiosemicarbazon compound(6).

^{1}HNMR spectrum2-(thiophen-2-ylmethylene)hydrazine-1-carbothioamide thiosemicarbazon compound(6).

^{1}HNMR spectrum2-(thiophen-2-ylmethylene)hydrazine-1-carbothioamide thiosemicarbazon in (fig.4-17) the major signal at δ 2.5 ppm is characteristic of DMSO-d6 as solvent , singles at (7.0-8.3 δ ppm) to (3H, Hetro phenyl ring), single at (3.3 ppm) to $–NH_2$, single at (4.5 ppm) to =CH (151-153).

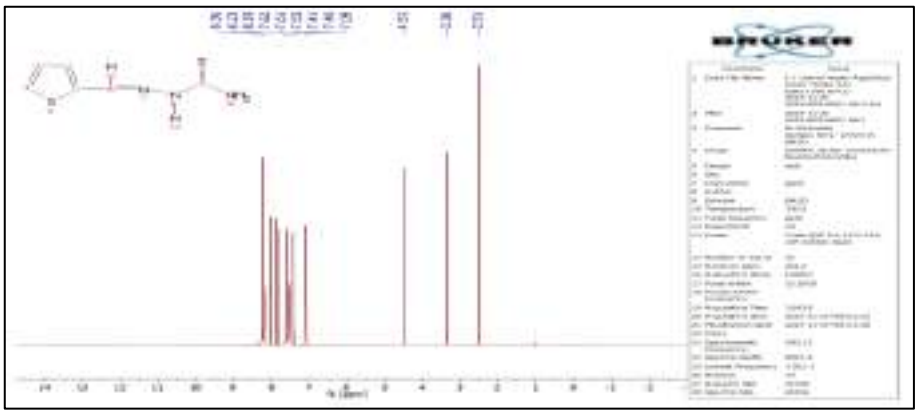


Figure (4- 17):) ^{1}HNMR Spectrum 2-(thiophen-2-ylmethylene)hydrazine-1-carbothioamide thiosemicarbazon compound(6).

^{13}C-NMR spectrum 2-(thiophen-2-ylmethylene)hydrazine-1-carbothioamide thiosemicarbazon compound(6).

^{13} CNMR Spectrum 2-(thiophen-2-ylmethylene)hydrazine-1-carbothioamide thiosemicarbazon the signals of olefinic and aromatic carbons appear in the third region between 126 and 131 ppm, single related to C=N at 139 ppm , single related to C-N at 64 ppm, single related to C=S at 178 ppm (151, 152).

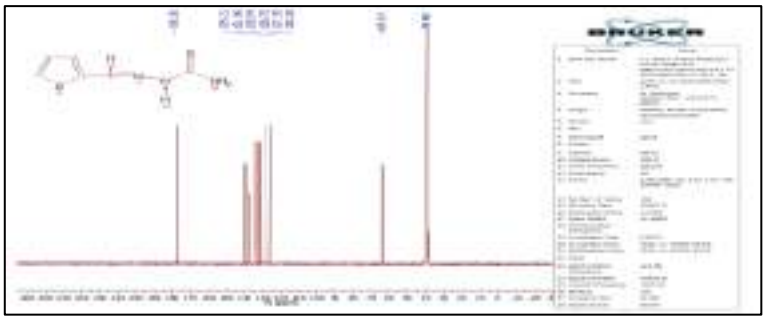
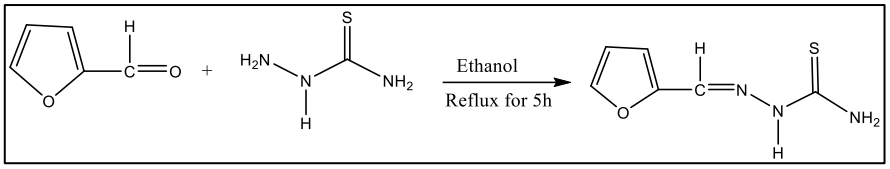


Figure (4- 18): ^{13} CNMR Spectrum 2-(thiophen-2-ylmethylene)hydrazine-1-carbothioamide thiosemicarbazon compound(6).

4.1.7 Synthesis of 2-(furan-2-ylmethylene)hydrazine-1-carbothioamide thiosemicarbazon compound(7).



Scheme (4-8): Synthesis of 2-(furan-2-ylmethylene)hydrazine-1-carbothioamide thiosemicarbazon compound(7).

FTIR spectrum of 2-(furan-2-ylmethylene)hydrazine-1-carbothioamide thiosemicarbazon compound(7).

The FTIR spectrum of 2-(furan-2-ylmethylene)hydrazine-1-carbothioamide thiosemicarbazon as shown in (fig.4-19) which indicates absorption bands at 3415 and 3278 cm^{-1} to $–NH_2$ stretching , absorption band at 3176 cm^{-1} to C-H (Hetero phenyl ring), absorption band at 2985 cm^{-1} to C-H(alphatic),absorption band at 1618 cm^{-1} to C=N, absorption band at 1269 Cm^{-1} to C=S, absorption band at 1606 Cm^{-1} to C=C (Hetero phenyl ring), absorption band at 1056 Cm^{-1} to C-O(151-153).

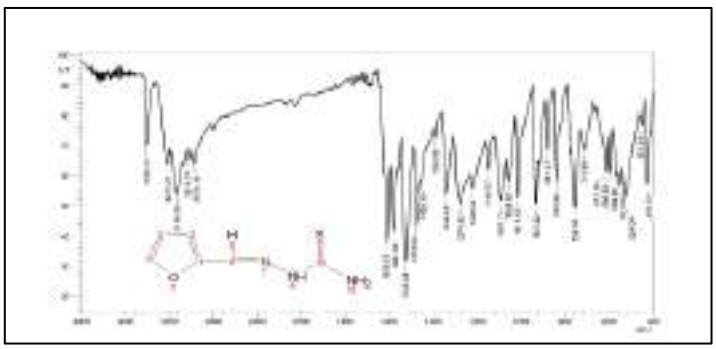


Figure (4- 19): FTIR spectrum of 2-(furan-2-ylmethylene)hydrazine-1-carbothioamide thiosemicarbazon compound(7).

^{1}HNMR spectrum of 2-(furan-2-ylmethylene)hydrazine-1-carbothioamide thiosemicarbazon compound(7).

^{1}HNMR spectrum of 2-(furan-2-ylmethylene)hydrazine-1-carbothioamide thiosemicarbazon in (fig.4-20) the major signal at δ 2.5 ppm is characteristic of DMSO-d6 as solvent , singles at (6.5-8.3 δ ppm) to (3H, Hetro phenyl ring), single at (3.3 ppm) to $-NH_2$, single at (4.5 ppm) to =CH. (151-153)

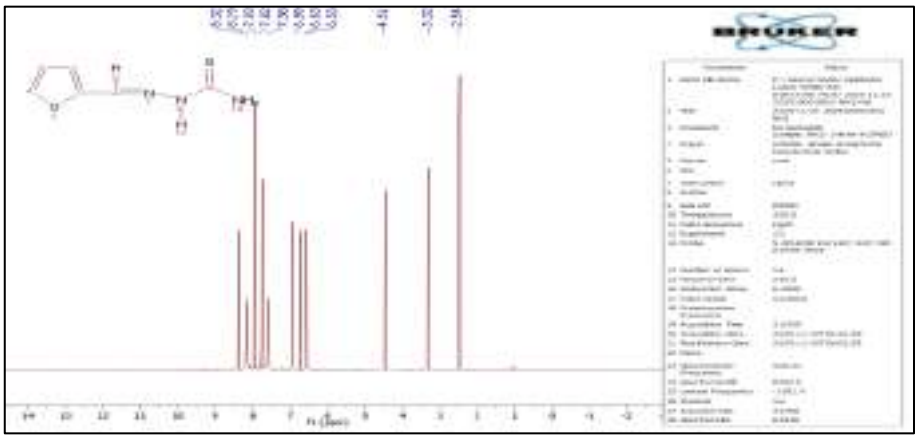


Figure (4- 20): ^{1}HNMR Spectrum of 2-(furan-2-ylmethylene)hydrazine-1-carbothioamide thiosemicarbazon compound(7).

^{13}C-NMR spectrum of 2-(furan-2-ylmethylene)hydrazine-1-carbothioamide thiosemicarbazon compound(7).

The signals of olefinic and aromatic carbons appear in the third region between 111 and 132 ppm, single related to C=N at 150 ppm , single related to C-N at 64 ppm, single related to C=S at 178 ppm (151-153).

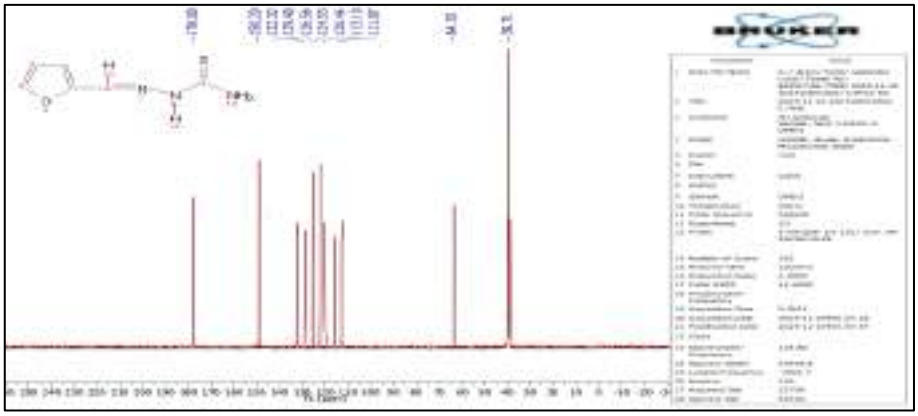
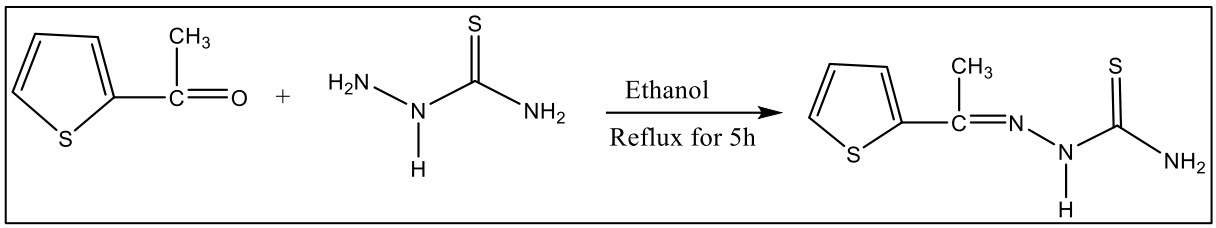


Figure (4- 21): ^{13} CNMR Spectrum of 2-(furan-2-ylmethylene)hydrazine-1-carbothioamide thiosemicarbazon compound(7).

4.1.8 Synthesis of (Z)-2-(1-(thiophen-2-yl)ethylidene)hydrazine-1-carbothioamide thiosemicarbazone compound(8).



Scheme (4-9): synthesis of (Z)-2-(1-(thiophen-2-yl)ethylidene)hydrazine-1-carbothioamide thiosemicarbazone compound(8).

FTIR spectrum of (Z)-2-(1-(thiophen-2-yl)ethylidene)hydrazine-1-carbothioamide thiosemicarbazone compound(8).

The FTIR spectrum of (Z)-2-(1-(thiophen-2-yl)ethylidene)hydrazine-1-carbothioamide thiosemicarbazone as shown in (fig.4-22) which indicates absorption bands at 3307 cm^{-1} to $–NH_2$ stretching , absorption band at 3188 cm^{-1} to C-H (Hetero phenyl ring), absorption band at 2986 cm^{-1} to C-H(alphatic), absorption band at 1562 cm^{-1} to C=N, absorption band at 1290 Cm^{-1} to C=S, absorption band at 1471 Cm^{-1} to C=C (Hetero phenyl ring), absorption band at 1373 Cm^{-1} to CH_3 .(151-153)

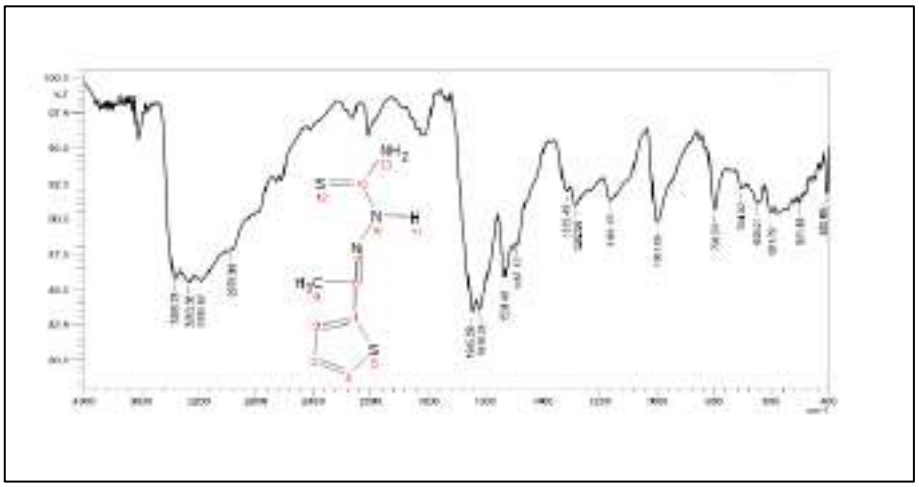


Figure (4- 22): FTIR spectrum of (Z)-2-(1-(thiophen-2-yl)ethylidene)hydrazine-1-carbothioamide thiosemicarbazone compound(8).

^{1}HNMR spectrum of (Z)-2-(1-(thiophen-2-yl)ethylidene)hydrazine-1-carbothioamide thiosemicarbazone compound(8).

^{1}HNMR spectrum of (Z)-2-(1-(thiophen-2-yl)ethylidene)hydrazine-1-carbothioamide thiosemicarbazone in (fig.4-23) the major signal at δ 2.3 ppm is characteristic of DMSO-d6 as solvent , singles at (7.1-8.3 δ ppm) to (3H, Hetro phenyl ring), single at (3.3 ppm) to $–NH_2$, single at (4.5 ppm) to =CH, single at (1.3 ppm) to CH_3. (151-153)

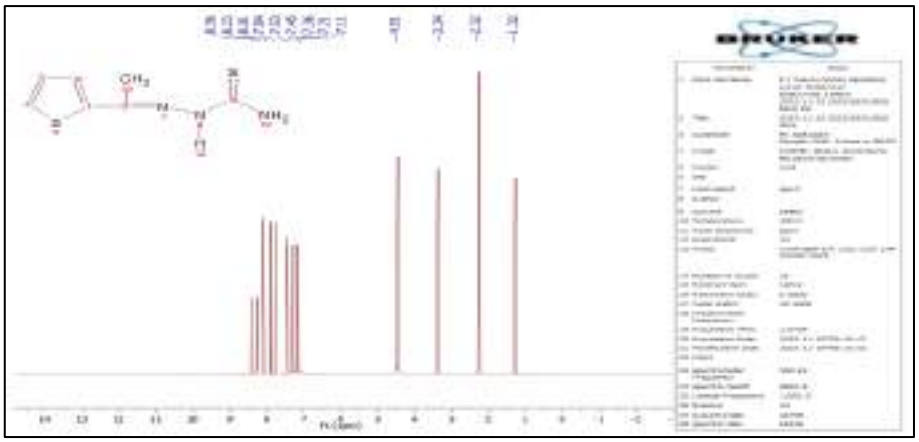


Figure (4- 23): ^{1}HNMR spectrum of (Z)-2-(1-(thiophen-2-yl)ethylidene)hydrazine-1-carbothioamide thiosemicarbazone compound(8).

^{13}C-NMR spectrum of (Z)-2-(1-(thiophen-2-yl)ethylidene)hydrazine-1-carbothioamide thiosemicarbazone compound(8).

^{13}C-NMR spectrum of (Z)-2-(1-(thiophen-2-yl)ethylidene)hydrazine-1-carbothioamide thiosemicarbazone the signals of olefinic and aromatic carbons appear in the third region between 126 and 127 ppm, singles related to C=N at 143-144 ppm , single related to C-N at 64 ppm, single related to C=S at 181 ppm, single related to CH_3 at 15 ppm. (151-153)

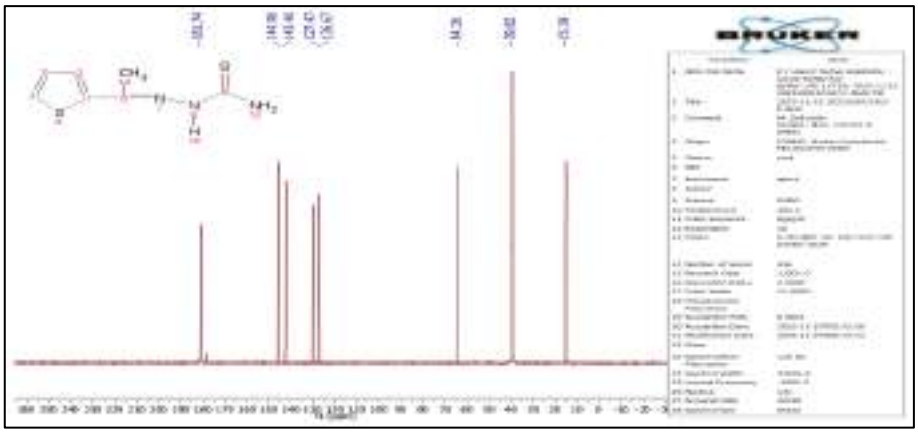
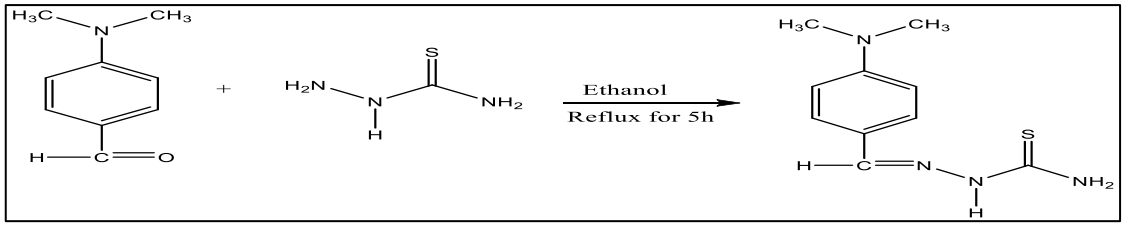


Figure (4- 24): ^{13}C-NMR spectrum of (Z)-2-(1-(thiophen-2-yl)ethylidene)hydrazine-1-carbothioamide thiosemicarbazone compound(8).

4.1.9 Synthesis of the Thiosemicarbazones for N, N-dimethyaminebenzaldehyde compound(9).



Scheme (4-10): synthesis of the Thiosemicarbazones for N, N-dimethyaminebenzaldehyde compound(9).

FTIR spectrum of Thiosemicarbazones for N, N-dimethyaminebenzaldehyde compound(9).

The FTIR spectrum of Thiosemicarbazones for N, N-dimethyaminebenzaldehyde as shown in (fig.4-25) which indicates absorption bands at 3334 and 3264 cm^{-1} to $–NH_2$ stretching , absorption band at 3176 cm^{-1} to C-H(aromatic) , absorption band at 2985 and 2924 cm^{-1} to C-H(alphatic),absorption band at 2985 cm^{-1} to C-H (CH_3), , absorption band at 1606 cm^{-1} to C=N, absorption band at 1257 Cm^{-1} to C=S, absorption band at 1562 Cm^{-1} to C=C (aromatic). (151-153)

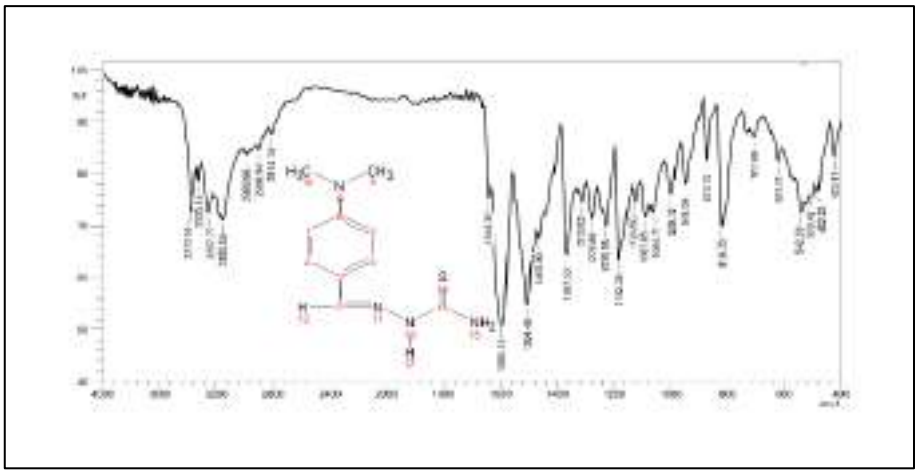


Figure (4- 25): FTIR spectrum of Thiosemicarbazones for N, N-dimethyaminebenzaldehyde compound(9).

^{1}HNMR spectrum of Thiosemicarbazones for N, N-dimethyaminebenzaldehyde compound(9).

^{1}HNMR spectrum of Thiosemicarbazones for N, N-dimethyaminebenzaldehyde in (fig.4-26) the major signal at δ 2.9 ppm is characteristic of DMSO-d6 as solvent , singlate at (6.6-8.0 δ ppm) to (4H, phenyl ring), single at (4.5 ppm) to $–NH_2$, singles at 2.5 ppm to =CH, singles at 3.3 ppm to CH_3-N. (151-153)

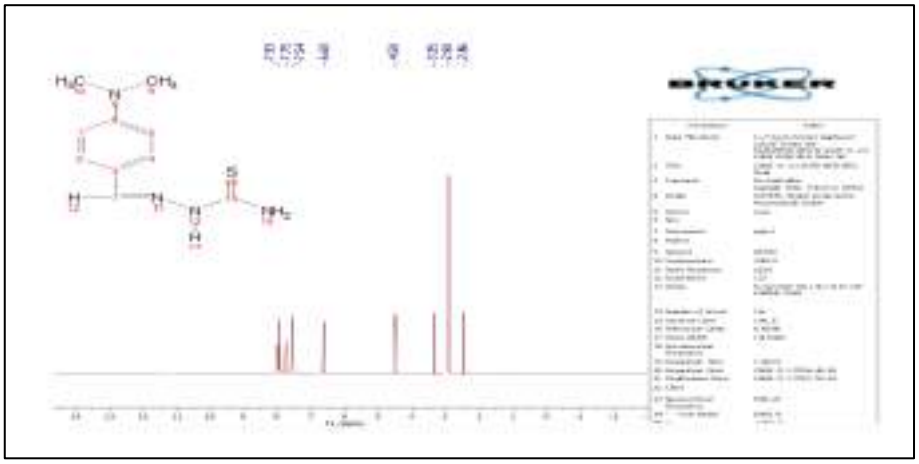


Figure (4- 26): ^{1}HNMR spectrum of Thiosemicarbazones for N, N-dimethyaminebenzaldehyde compound(9).

^{13}C-NMR spectrum of Thiosemicarbazones for N, N-dimethyaminebenzaldehyde compound(9).

^{13}C-NMR spectrum of Thiosemicarbazones for N, N-

dimethyaminebenzaldehyde the signals of olefinic and aromatic carbons appear in the third region between 110 and 129 ppm , singles related to C=N at 152 ppm , single related to C-N at 64 ppm. singles related to C=S at 178-181 ppm. (151-153)

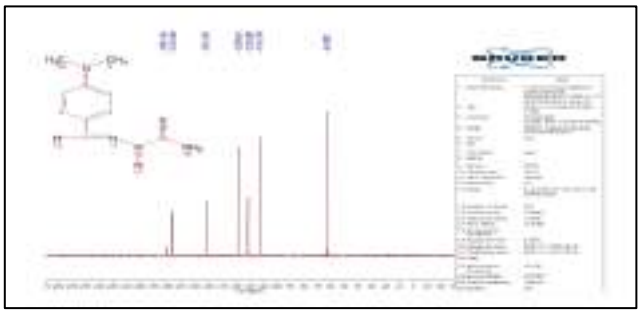
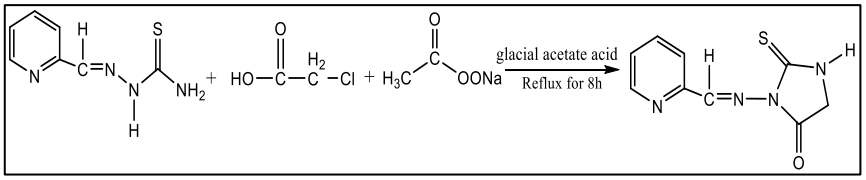


Figure (4- 27): ^{13}C-NMR spectrum of Thiosemicarbazones for N, N-dimethyaminebenzaldehyde compound(9).

4.2 Synthesis of 2-(4-Substituted-benzylidene hydrazono)-1, 3-Thiazolidine-4-one compounds.(10 -17)

4.2.1 Synthesis of (Z)-3-((pyridin-2-ylmethylene)amino)-2-thioxoimidazolidin-4-one compound(10).



Scheme (4-11): synthesis of (Z)-3-((pyridin-2-ylmethylene)amino)-2-thioxoimidazolidin-4-one compound(10).

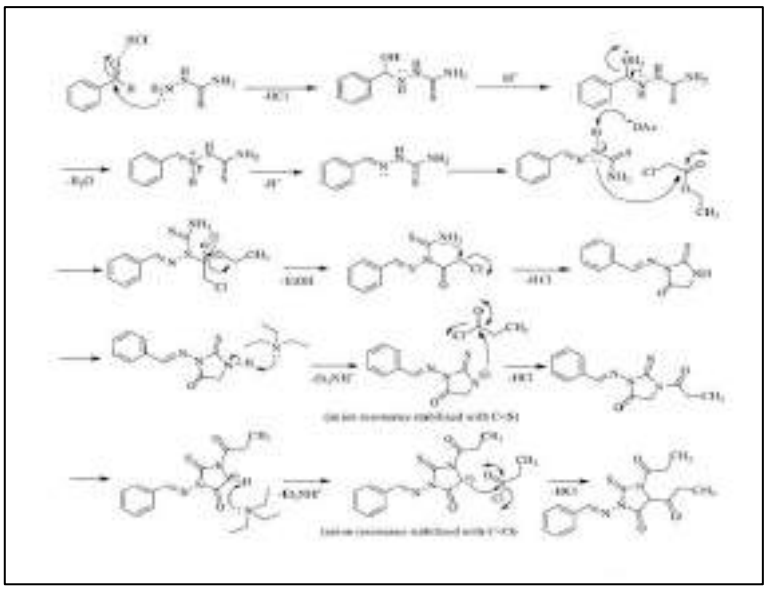


Figure (4- 28): mechanism2-thioxoimidazolidin-4-one compounds

FTIR spectrum of (Z)-3-((pyridin-2-ylmethylene)amino)-2-thioxoimidazolidin-4-one compound(10).

The FTIR spectrum of the preparation of of (Z)-3-((pyridin-2-ylmethylene)amino)-2-thioxoimidazolidin-4-one as shown in (fig.4-29) which indicates absorption band at 3263 to –NH , absorption band at 3045 Cm^{-1} to C-H (aromatic) , absorption band at 2960 and 2924 cm^{-1} to C-H(alphatic), absorption band at 1635 Cm^{-1} to C=N, absorption band at 1192 Cm^{-1} to C=S, absorption band at 1573 Cm^{-1} to C=C (aromatic), absorption band at 1134 Cm^{-1} to C-O, absorption band at 1035 Cm^{-1} to C-N, absorption band at 1708 Cm^{-1} to C=O. (151-153)

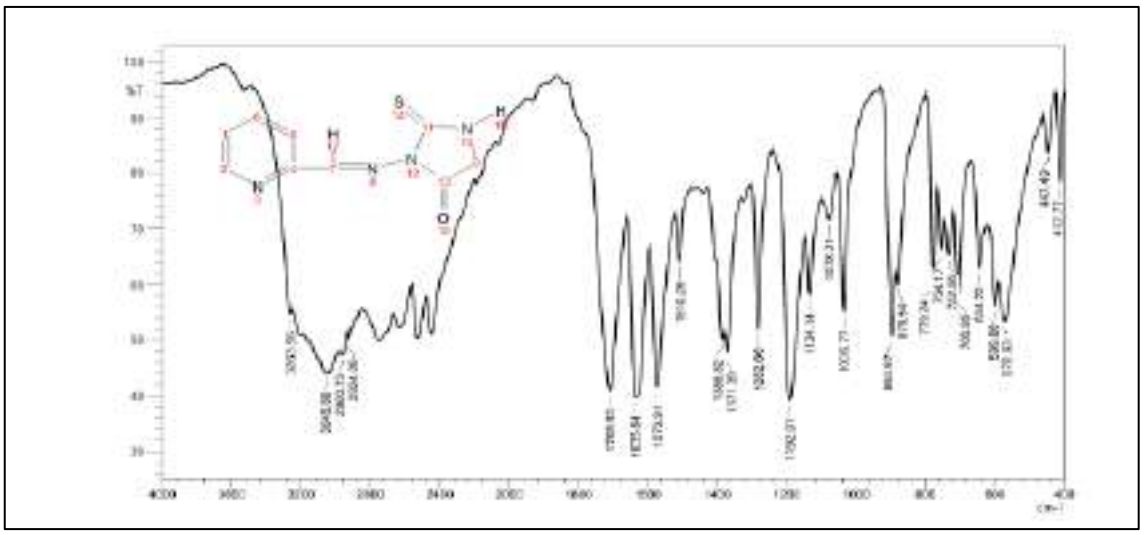


Figure (4- 29): FTIR spectrum of (Z)-3-((pyridin-2-ylmethylene)amino)-2-thioxoimidazolidin-4-one compound(10).

^{1}HNMR spectrum of (Z)-3-((pyridin-2-ylmethylene)amino)-2-thioxoimidazolidin-4-one compound(10).

^{1}HNMR spectrum of (Z)-3-((pyridin-2-ylmethylene)amino)-2-thioxoimidazolidin-4-one in (fig.4-30) the major signal at δ 1.8 ppm is characteristic of DMSO-d6 as solvent , singlate at (7.4-8.8 δ ppm) to (4H, phenyl ring), multiplet singlate at (3.4 to 4.1 ppm) to –NH. (151-153)



Figure (4- 30): ^{1}HNMR spectrum of (Z)-3-((pyridin-2-ylmethylene)amino)-2-thioxoimidazolidin-4-one compound(10).

^{13}C-NMR spectrum of (Z)-3-((pyridin-2-ylmethylene)amino)-2-thioxoimidazolidin-4-one compound(10).

The signals of olefinic and aromatic carbons appear in the third region between 122 and 136 ppm , singles related to C=N at 151-166 ppm , single related to C-N at 64 ppm, singles related to C=O (amide) at 174 ppm, single related to C=S at 176 ppm. (151-153)

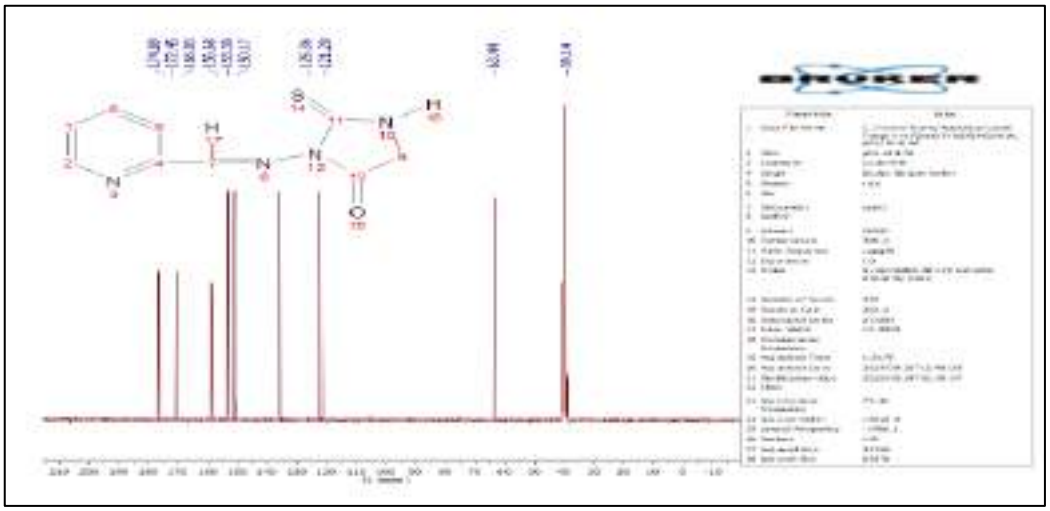
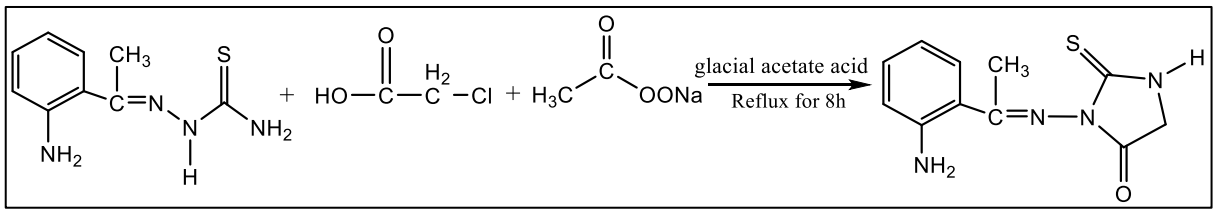


Figure (4- 31): ^{13}C-NMR spectrum of (Z)-3-((pyridin-2-ylmethylene)amino)-2-thioxoimidazolidin-4-one compound(10).

4.2.2 Synthesis of (E)-3-((1-(2-aminophenyl)ethylidene)amino)-2-thioxoimidazolidin-4-one compound(11).



Scheme (4-12): synthesis of (E)-3-((1-(2-aminophenyl)ethylidene)amino)-2-thioxoimidazolidin-4-one compound(11).

FTIR spectrum of (E)-3-((1-(2-aminophenyl)ethylidene)amino)-2-thioxoimidazolidin-4-one compound(11).

The FTIR spectrum of (E)-3-((1-(2-aminophenyl)ethylidene)amino)-2-thioxoimidazolidin-4-one as shown in (fig.4-32) which indicates absorption band at 3273 to –NH , absorption band at 3165 Cm^{-1} to C-H (aromatic) , absorption band at 2931 cm^{-1} to C-H(alphatic),absorption band at 1616 Cm^{-1} to C=N, absorption band at 1190 Cm^{-1} to C=S, absorption band at 1558 Cm^{-1} to C=C (aromatic), absorption band at 1056 Cm^{-1} to C-O, absorption band at 1153 Cm^{-1} to C-N, absorption band at 1724 Cm^{-1} to C=O, absorption band at 1328 Cm^{-1} to CH_3. (151-153)

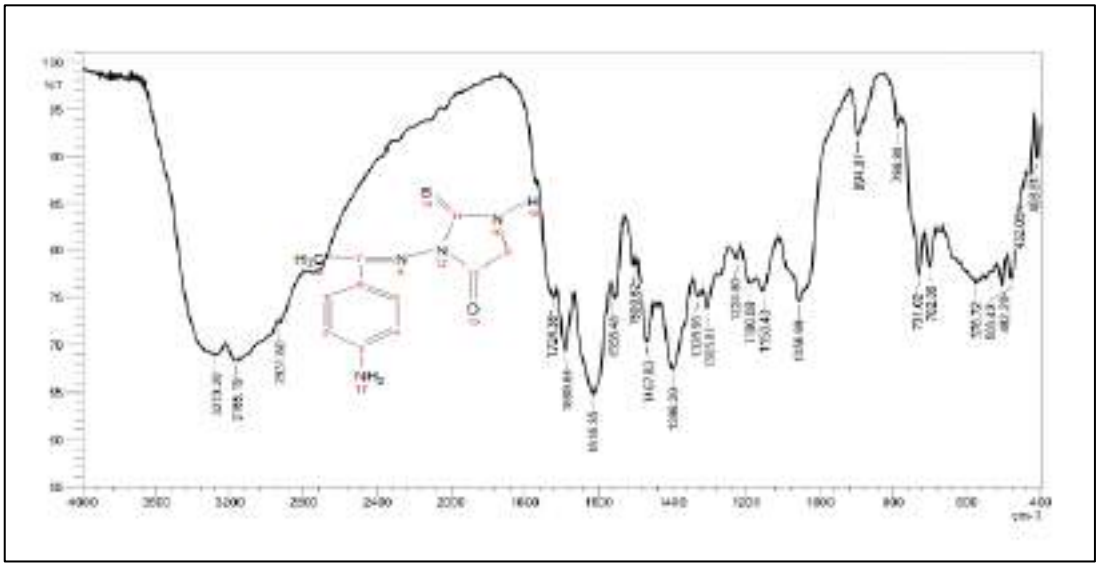


Figure (4- 32): FTIR spectrum of (E)-3-((1-(2-aminophenyl)ethylidene)amino)-2-thioxoimidazolidin-4-one compound(11).

^{1}HNMR spectrum of (E)-3-((1-(2-aminophenyl)ethylidene)amino)-2-

thioxoimidazolidin-4-one compound(11).

[1]HNMR spectrum of (E)-3-((1-(2-aminophenyl)ethylidene)amino)-2-thioxoimidazolidin-4-one in (fig.4-33) the major signal at δ 1.8 ppm is characteristic of DMSO-d6 as solvent , singlate at (7.6-8.1 δ ppm) to (4H, phenyl ring), multiplet singlate at (3.8 to 4.1 ppm) to –NH, singlate at (1.3 ppm) to –CH_3. (151-153)

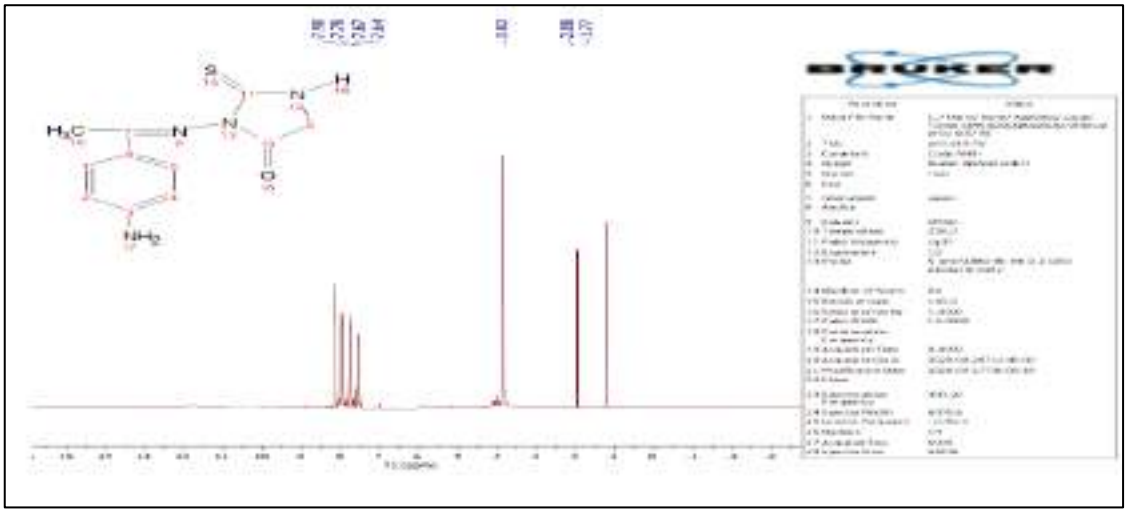


Figure (4- 33): [1]HNMR spectrum of (E)-3-((1-(2-aminophenyl)ethylidene)amino)-2-thioxoimidazolidin-4-one compound(11).

[13]C-NMR spectrum of (E)-3-((1-(2-aminophenyl)ethylidene)amino)-2-thioxoimidazolidin-4-one compound(11).

The signals of olefinic and aromatic carbons appear in the third region between 118 to 136 ppm , singles related to C=N at 158 ppm , single related to C-N at 64 ppm, singles related to C=O (amide) at 174 ppm, single related to C=S at 175 ppm, single related to CH_3-C (Secondary) at 45 ppm. (151-153)

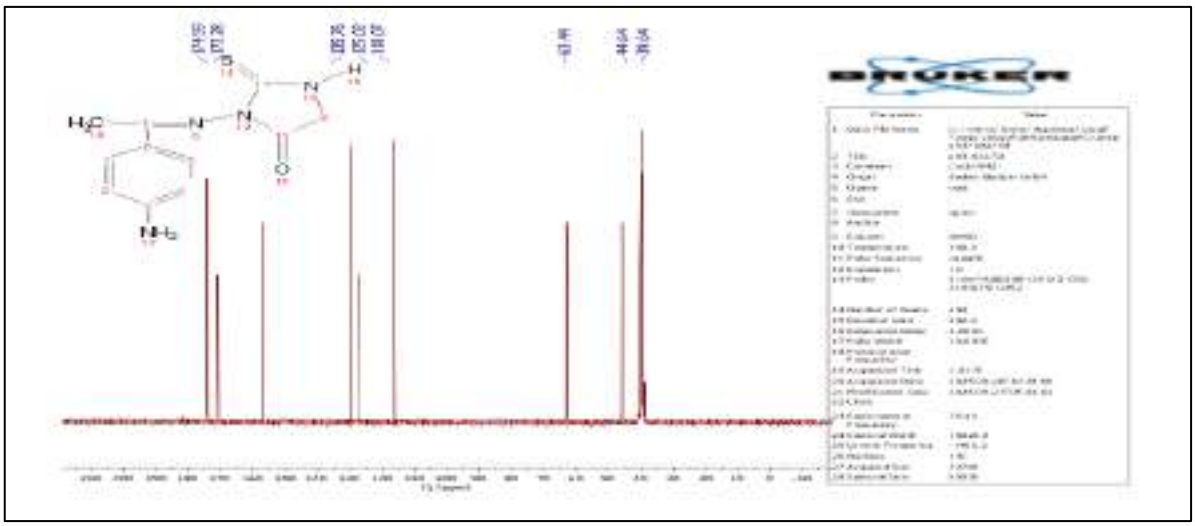
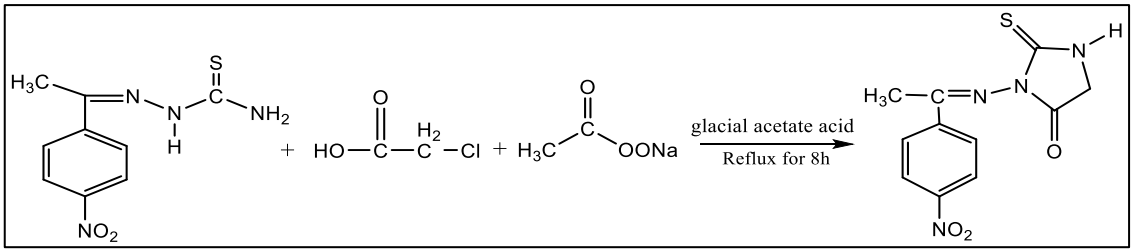


Figure (4- 34): ^{13}C-NMR spectrum of (E)-3-((1-(2-aminophenyl)ethylidene)amino)-2-thioxoimidazolidin-4-one compound(11).

4.2.3 Synthesis of (E)-3-((1-(4-nitrophenyl)ethylidene)amino)-2-thioxoimidazolidin-4-one compound(12).



Scheme (4-13): synthesis of (E)-3-((1-(4-nitrophenyl)ethylidene)amino)-2-thioxoimidazolidin-4-one compound(12).

FTIR spectrum of (E)-3-((1-(4-nitrophenyl)ethylidene)amino)-2-thioxoimidazolidin-4-one compound(12).

The FTIR spectrum of the preparation(E)-3-((1-(4-nitrophenyl) ethylidene) amino)-2-thioxoimidazolidin-4-one as shown in (fig.4-35) which indicates absorption band at 3367 to –NH , absorption band at 3261 Cm^{-1} to C-H (aromatic) , absorption band at 3176 and 2966 cm^{-1} to C-H(alphatic), absorption band at 1618 Cm^{-1} to C=N, absorption band at 1483 Cm^{-1} to C=C (aromatic), absorption band at 1082 Cm^{-1} to C-O, absorption band at 1161 Cm^{-1} to C-N, absorption band at 1641 Cm^{-1} to C=O, absorption band at 1315 Cm^{-1} to CH_3, absorption band at 1529 Cm^{-1} to NO_2. (151-153)

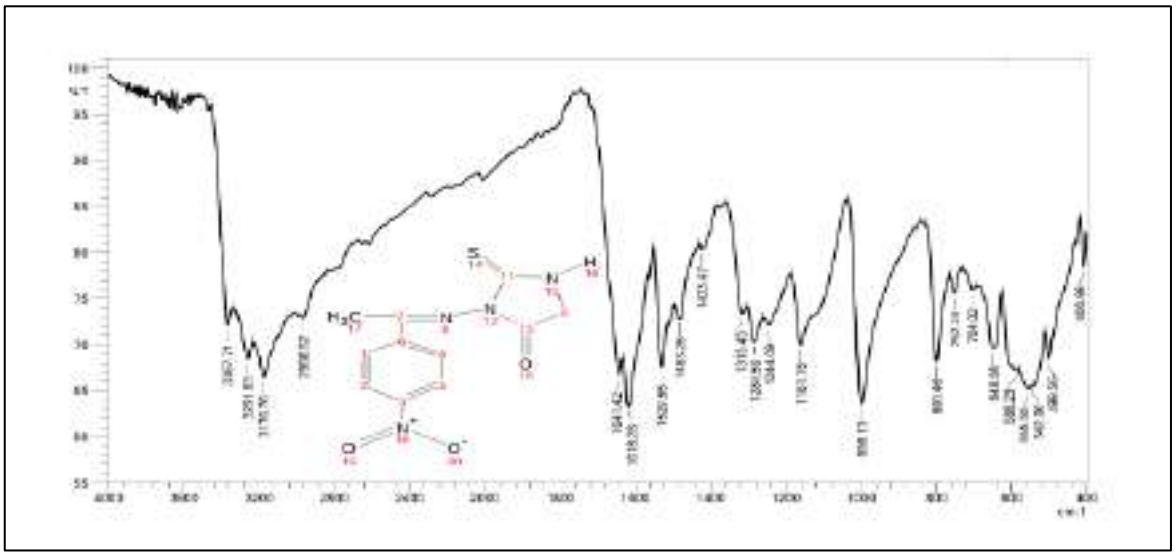


Figure (4- 35): FTIR spectrum of (E)-3-((1-(4-nitrophenyl)ethylidene)amino)-2-thioxoimidazolidin-4-one compound(12).

^{1}HNMR spectrum of 3-((4-hydroxybenzylidene) amino)-2-thioxoimidazolidin -4-one compound for nitro acetophenone compound(12).

^{1}HNMR spectrum of (E)-3-((1-(4-nitrophenyl)ethylidene)amino)-2-thioxoimidazolidin-4-one in (fig.4-36) the major signal at δ 2.3 ppm is characteristic of DMSO-d6 as solvent , singlate at (8.1-8.5 δ ppm) to (4H, phenyl ring), multiplet singles at (3.4 to 3.9 ppm) to –NH, singlate at (1.8 ppm) to –CH_3. (151-153)

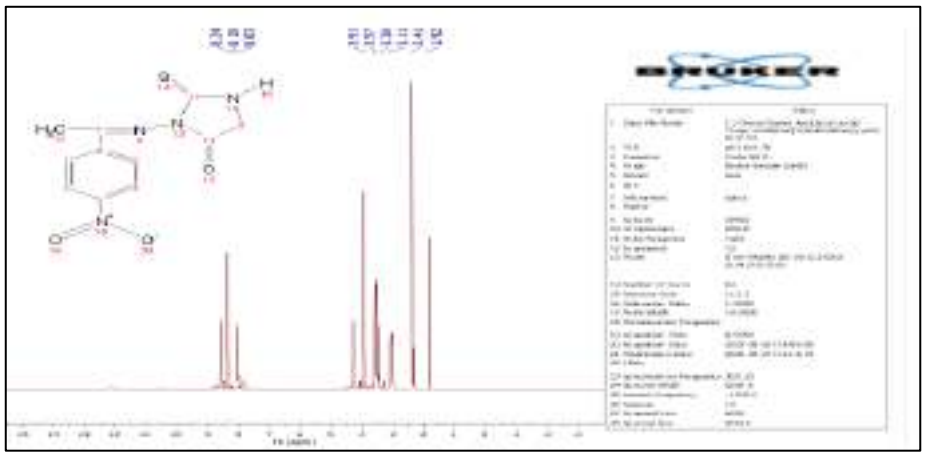


Figure (4- 36): ^{1}HNMR spectrum of (E)-3-((1-(4-nitrophenyl)ethylidene)amino)-2-thioxoimidazolidin-4-one compound(12).

^{13}C-NMR spectrum of (E)-3-((1-(4-nitrophenyl)ethylidene)amino)-2-thioxoimidazolidin-4-one compound(12).

The signals of olefinic and aromatic carbons appear in the third region between 123 to 136 ppm , single related to C=N at 158 ppm , single related to C-N at 64 ppm, single related to C=O (amide) at 168 ppm, single related to C=S at 177 ppm, single related to CH_3-C (Secondary) at 33 ppm. (151-153)

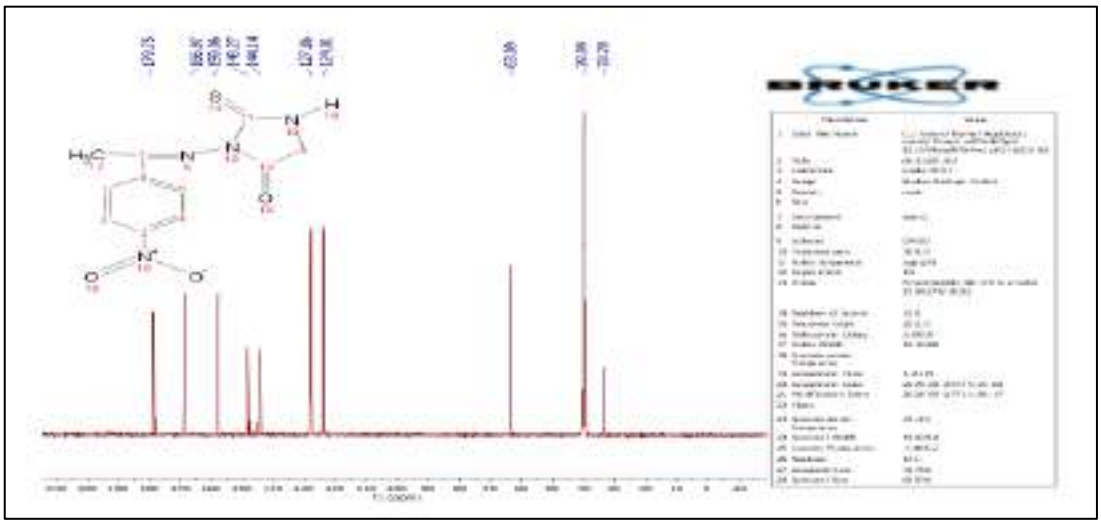
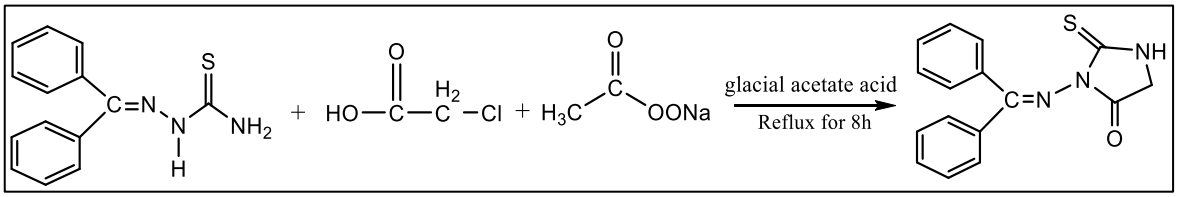


Figure (4- 37): ^{13}C-NMR spectrum of (E)-3-((1-(4-nitrophenyl)ethylidene)amino)-2-thioxoimidazolidin-4-one compound(12).

4.2.4 Synthesis of (Z)-3-((cyclohexa-2, 4-dien-1-yl(phenyl)methylene)amino)-2-thioxoimidazolidin-4-one compound(13).



Scheme (4-14): Synthesis of (Z)-3-((cyclohexa-2, 4-dien-1-yl(phenyl) methylene) amino)-2-thioxoimidazolidin-4-one compound(13).

FTIR spectrum of (Z)-3-((cyclohexa-2, 4-dien-1-yl(phenyl) methylene) amino)-2-thioxoimidazolidin-4-one compound(13).

The FTIR spectrum of the preparation of (Z)-3-((cyclohexa-2, 4-dien-1-yl(phenyl)methylene)amino)-2-thioxoimidazolidin-4-one as shown in (fig.4-38) which indicates absorption band at 3415 and 3378 to –NH , absorption band at 3315 Cm^{-1} to C-H (aromatic) , absorption band at 3089 and 2987 cm^{-1} to C-H(alphatic),

absorption band at 1695 Cm^{-1} to C=N, absorption band at 1462 Cm^{-1} to C=C (aromatic), absorption band at 1056 Cm^{-1} to C-O, absorption band at 1186 Cm^{-1} to C-N, absorption band at 1728 Cm^{-1} to C=O. (151-153)

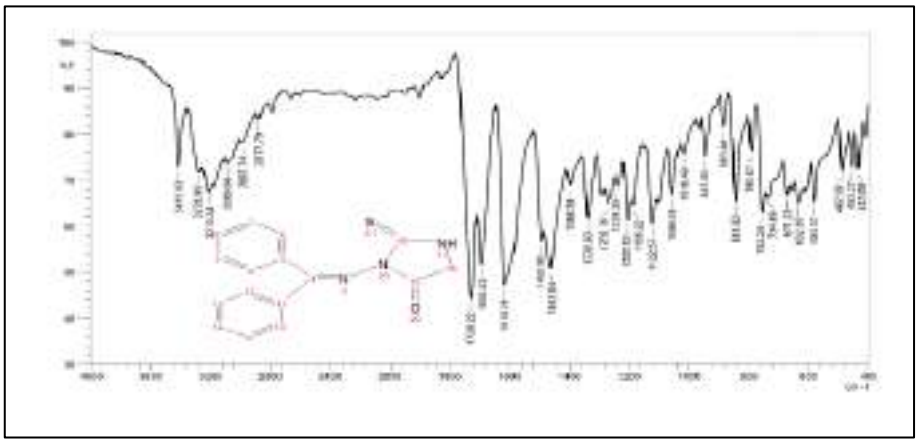


Figure (4- 38): FTIR spectrum of (Z)-3-((cyclohexa-2, 4-dien-1-yl(phenyl)methylene)amino)-2-thioxoimidazolidin-4-one compound(13).

^{1}HNMR spectrum of (Z)-3-((cyclohexa-2, 4-dien-1-yl(phenyl)methylene)amino)-2-thioxoimidazolidin-4-one compound(13).

^{1}HNMR spectrum of (Z)-3-((cyclohexa-2, 4-dien-1-yl(phenyl)methylene)amino)-2-thioxoimidazolidin-4-one in (fig.4-39) the major signal at δ 2.5 ppm is characteristic of DMSO-d6 as solvent , singlate at (7.3-8.6 δ ppm) to (10H, phenyl ring), multiplet singles at (3.4 to 4.0 ppm) to –NH. (151-153)

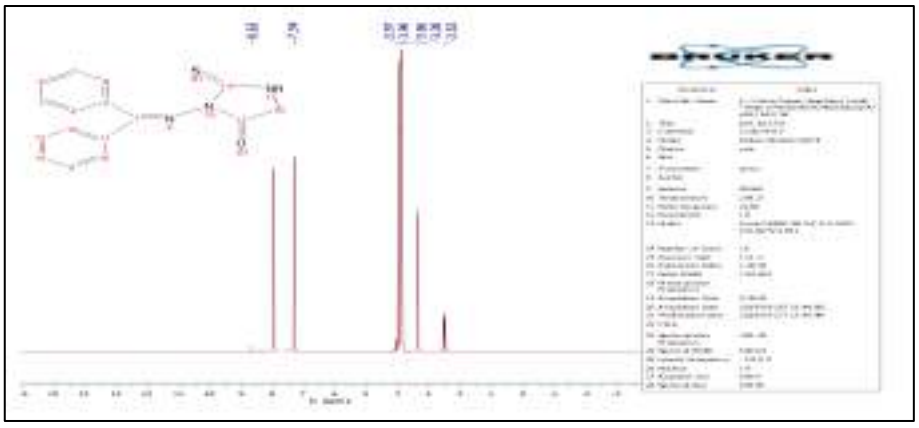


Figure (4- 39): ^{1}HNMR spectrum of (Z)-3-((cyclohexa-2, 4-dien-1-yl(phenyl) methylene) amino)-2-thioxoimidazolidin-4-one compound(13).

^{13}C-NMR spectrum of (Z)-3-((cyclohexa-2, 4-dien-1-yl(phenyl)methylene)amino)-2-thioxoimidazolidin-4-one compound(13).

The signals of olefinic and aromatic carbons appear in the third region between 118 to 126 ppm , singles related to C=N at 158 ppm , single related to C-N at 66 ppm, single related to C=O (amide) at 168 ppm, single related to C=S at 174 ppm. (151-153)

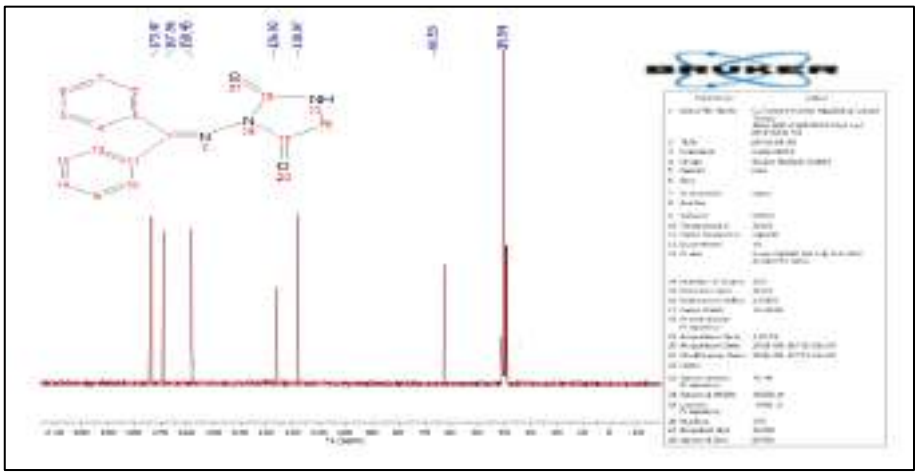
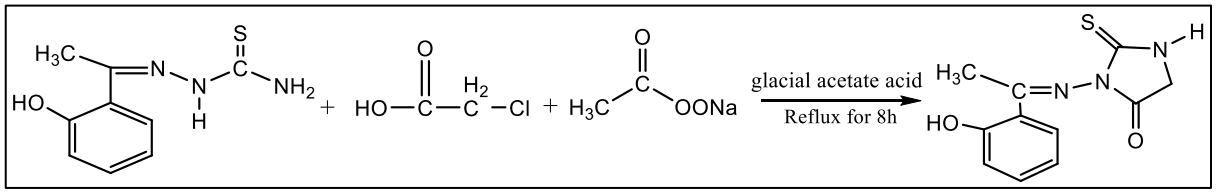


Figure (4- 40): ^{13}C-NMR spectrum of (Z)-3-((cyclohexa-2, 4-dien-1-yl(phenyl)methylene)amino)-2-thioxoimidazolidin-4-one compound(13).

4.2.5 Synthesis of (E)-3-((1-(2-hydroxyphenyl)ethylidene)amino)-2-thioxoimidazolidin-4-one compound(14).



Scheme (4-15): synthesis of (E)-3-((1-(2-hydroxyphenyl)ethylidene)amino)-2-thioxoimidazolidin-4-one compound(14).

FTIR spectrum of (E)-3-((1-(2-hydroxyphenyl)ethylidene)amino)-2-thioxoimidazolidin-4-one compound(14).

The FTIR spectrum of the preparation of (E)-3-((1-(2-hydroxyphenyl)ethylidene)amino)-2-thioxoimidazolidin-4-one as shown in (fig.4-41) which indicates absorption band at 3365 and 3261 to –NH , absorption band at 3176 Cm^{-1} to C-H (aromatic) , absorption band at 2966 cm^{-1} to C-H(alphatic),absorption band at 1618 Cm^{-1} to C=N, absorption band at 1483 Cm^{-1} to

C=C (aromatic), absorption band at 1016 Cm^{-1} to C-O, absorption band at 1161 Cm^{-1} to C-N, absorption band at 1643 Cm^{-1} to C=O. (151-153)

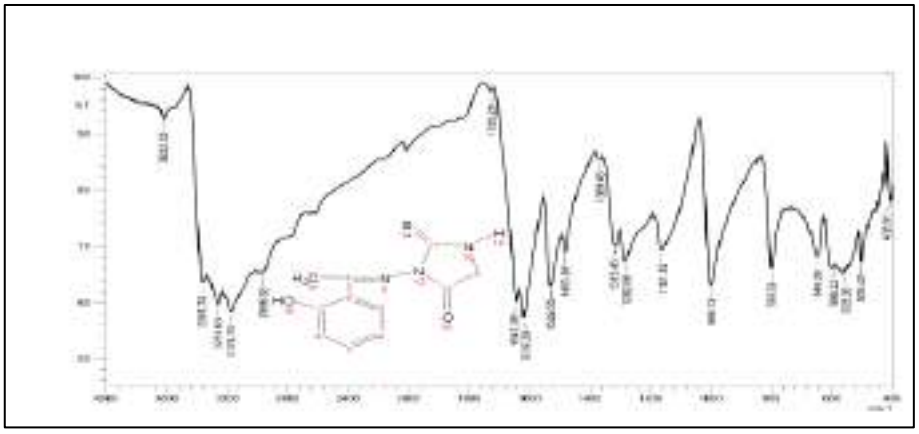


Figure (4- 41): FTIR spectrum of (E)-3-((1-(2-hydroxyphenyl)ethylidene)amino)-2-thioxoimidazolidin-4-one compound(14).

^{1}HNMR spectrum of (E)-3-((1-(2-hydroxyphenyl)ethylidene)amino)-2-thioxoimidazolidin-4-one compound(14).

^{1}HNMR spectrum of (E)-3-((1-(2-hydroxyphenyl)ethylidene)amino)-2-thioxoimidazolidin-4-one in (fig.4-42) the major signal at δ 2.5 ppm is characteristic of DMSO-d6 as solvent , singlate at (6.8-7.7 δ ppm) to (4H, phenyl ring), multiplet singles at (3.5 to 4.0 ppm) to –NH, singlate at (9.9 ppm) to –OH. (151-153)

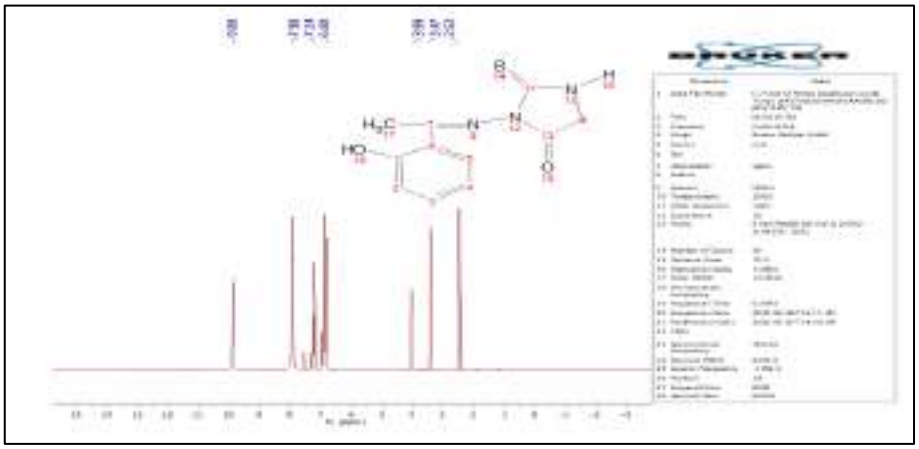


Figure (4- 42): ^{1}HNMR spectrum of (E)-3-((1-(2-hydroxyphenyl)ethylidene)amino)-2-thioxoimidazolidin-4-one compound(14).

^{13}C-NMR spectrum of (E)-3-((1-(2-hydroxyphenyl)ethylidene)amino)-2-thioxoimidazolidin-4-one compound(14).

The signals of olefinic and aromatic carbons appear in the third region between 116 to 133 ppm , singles related to C=N at 141 ppm , single related to C-N at 66 ppm, singles related to C=O (amide) at 168 ppm, single related to C=S at 178 ppm. (151-153)

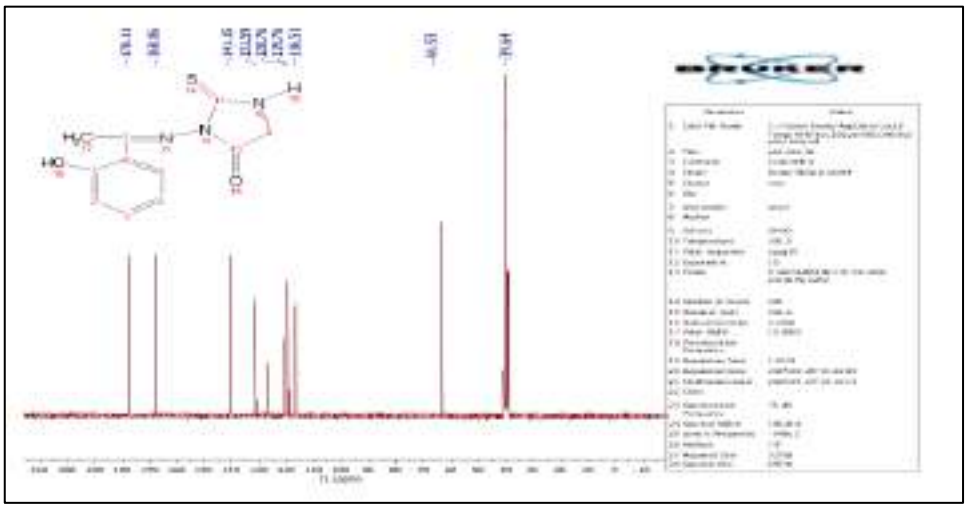
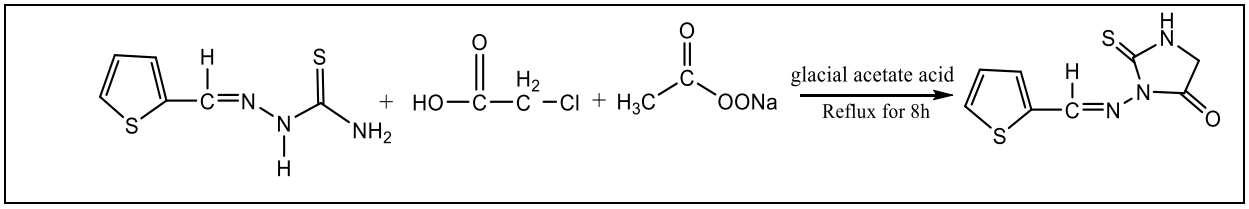


Figure (4- 43): ^{13}C-NMR spectrum of (E)-3-((1-(2-hydroxyphenyl)ethylidene)amino)-2-thioxoimidazolidin-4-one compound(14).

4.2.6 Synthesis of 3-((thiophen-2-ylmethylene)amino)-2-thioxoimidazolidin-4-one compound(15).



Scheme (4-16): synthesis of 3-((thiophen-2-ylmethylene)amino)-2-thioxoimidazolidin-4-one compound(15).

FTIR spectrum of 3-((thiophen-2-ylmethylene)amino)-2-thioxoimidazolidin-4-one compound(15).

The FTIR spectrum of the preparation of 3-((thiophen-2-ylmethylene)amino)-2-thioxoimidazolidin-4-one as shown in (fig.4-44) which indicates absorption band at 3309 to –NH , absorption band at 3182 Cm^{-1} to C-H (aromatic) , absorption band at 2970 and 2895 cm^{-1} to C-H(alphatic), absorption band at 1560 Cm^{-1} to C=N,

absorption band at 1192 Cm^{-1} to C=S, absorption band at 1573 Cm^{-1} to C=C (Hetro phenyl ring), absorption band at 1120 Cm^{-1} to C-O, absorption band at 1006 Cm^{-1} to C-N, absorption band at 1707 Cm^{-1} to C=O, absorption band at 1053 Cm^{-1} to C-S. (151-153)

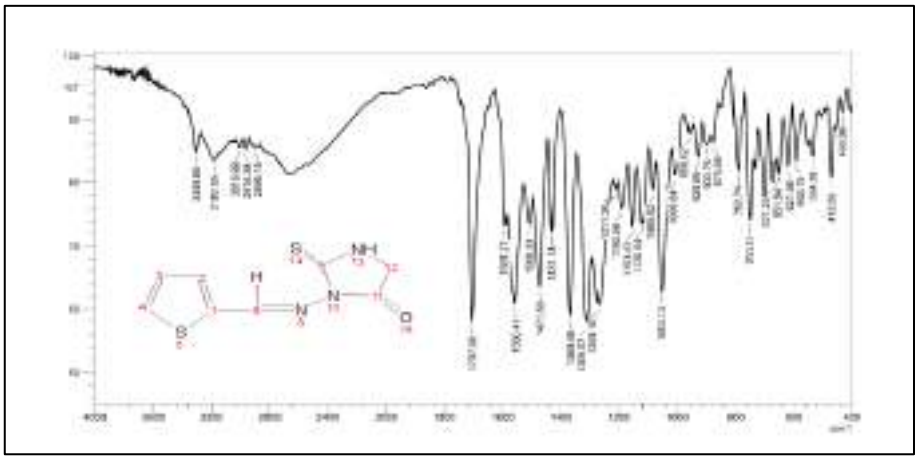


Figure (4- 44): FTIR spectrum of of 3-((thiophen-2-ylmethylene)amino)-2-thioxoimidazolidin-4-one compound(15).

^{1}HNMR spectrum of of 3-((thiophen-2-ylmethylene)amino)-2-thioxoimidazolidin-4-one compound(15).

^{1}HNMR spectrum of of 3-((thiophen-2-ylmethylene)amino)-2-thioxoimidazolidin-4-one in (fig.4-45) the major signal at δ 1.8 ppm is characteristic of DMSO-d6 as solvent , singlate at (7.0-8.4 δ ppm) to (3H, Hetro phenyl ring), multiplet singlate at (3.4 to 4.1 ppm) to –NH, single at 2.5 ppm to =CH**.** (151-153)

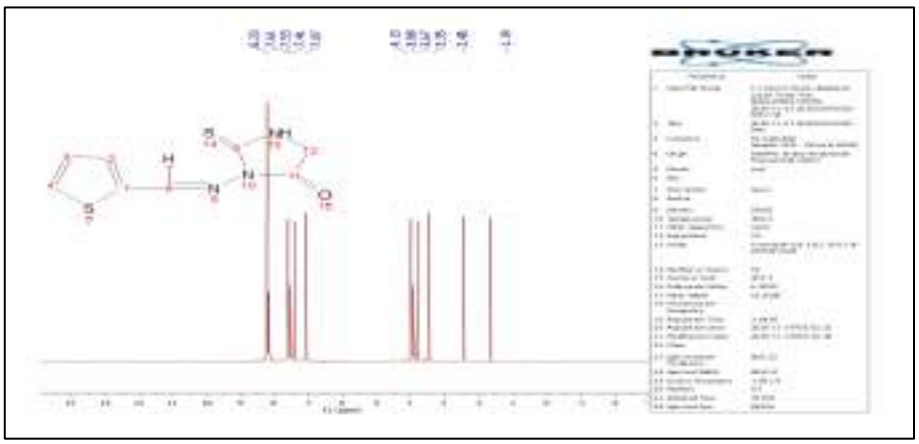


Figure (4- 45): ^{1}HNMR spectrum of 3-((thiophen-2-ylmethylene)amino)-2-thioxoimidazolidin-4-one compound(15).

^{13}C-NMR spectrum of of 3-((thiophen-2-ylmethylene)amino)-2-

thioxoimidazolidin-4-one compound(15).

The signals of olefinic and aromatic carbons appear in the third region between 126 and 128 ppm , singles related to C=N at 145 ppm , single related to C-N at 64 ppm, singles related to C=O (amide) at 174 ppm, single related to C=S at 182 ppm. (151-153)

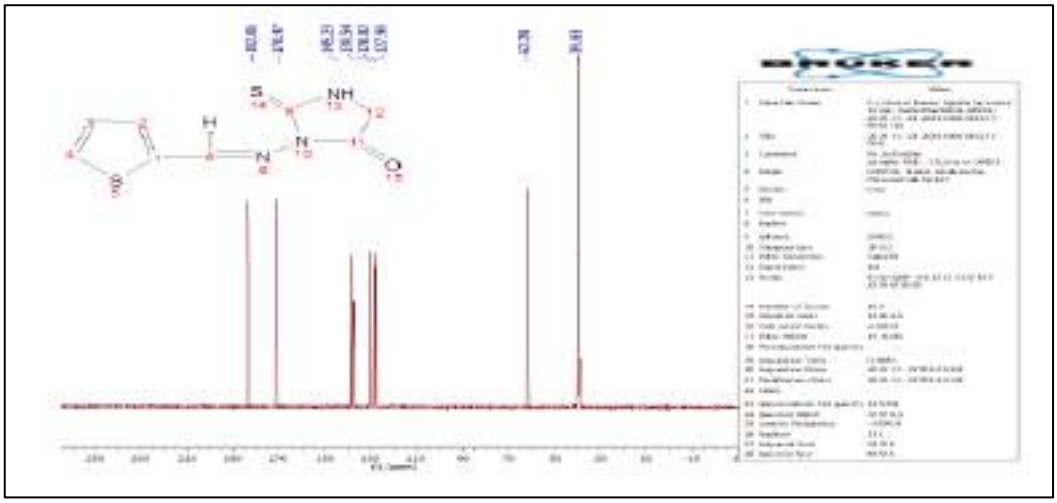
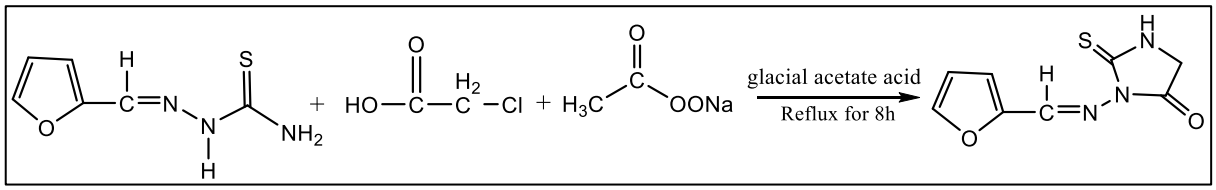


Figure (4- 46): ^{13}C-NMR spectrum of 3-((thiophen-2-ylmethylene)amino)-2-thioxoimidazolidin-4-one compound(15).

4.2.7 Synthesis of 3-((furan-2-ylmethylene)amino)-2-thioxoimidazolidin-4-one compound(16).



Scheme (4-17): synthesis of 3-((furan-2-ylmethylene)amino)-2-thioxoimidazolidin-4-one compound(16).

FTIR spectrum of 3-((4-hydroxybenzylidene) amino)-2-thioxoimidazolidin -4-one compound for furfural.

The FTIR spectrum of the preparation of 3-((furan-2-ylmethylene)amino)-2-thioxoimidazolidin-4-one as shown in (fig.4-47) which indicates absorption band at 3332 and 3248 to –NH , absorption band at 3178 Cm^{-1} to C-H (Hetro phenyl ring) , absorption band at 2989 and 2924 cm^{-1} to C-H(alphatic), absorption band at 1566 Cm^{-1} to C=N, absorption band at 1193 Cm^{-1} to C=S, absorption band at 1510 Cm^{-1}

to C=C (Hetro phenyl ring), absorption band at 1143 Cm^{-1} to C-O, absorption band at 1105 Cm^{-1} to C-N, absorption band at 1703 Cm^{-1} to C=O. (151-153)

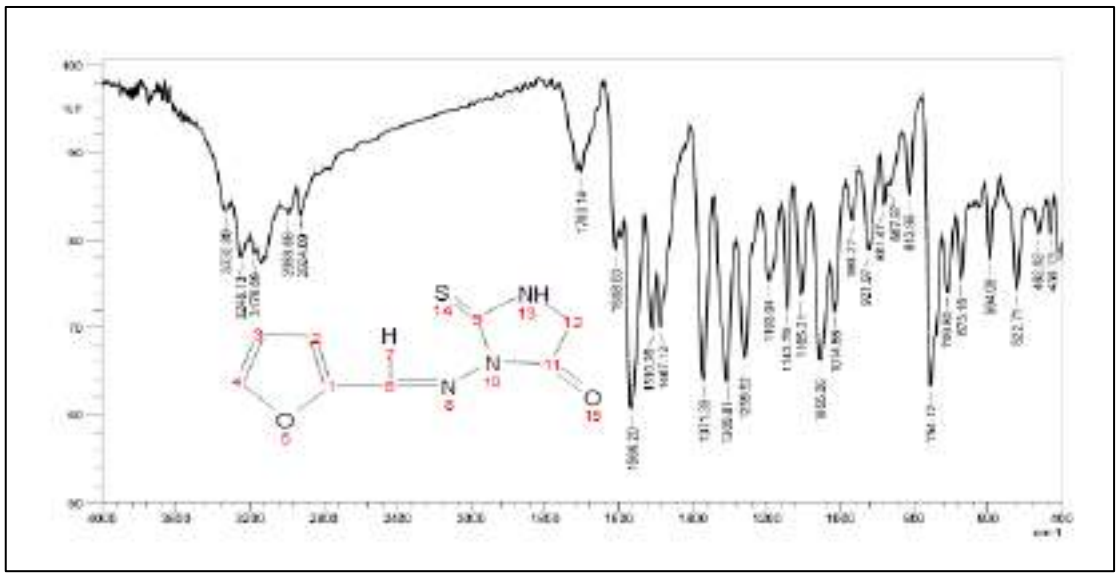


Figure (4- 47): FTIR spectrum of 3-((furan-2-ylmethylene)amino)-2-thioxoimidazolidin-4-one compound(16).

^{1}HNMR spectrum of 3-((furan-2-ylmethylene)amino)-2-thioxoimidazolidin-4-one compound(16).

^{1}HNMR spectrum of 3-((furan-2-ylmethylene)amino)-2-thioxoimidazolidin-4-one in (fig.4-48) the major signal at δ 1.8 ppm is characteristic of DMSO-d6 as solvent , singlate at (6.0-8.2 δ ppm) to (3H, Hetro phenyl ring), multiplet singlate at (3.4 to 4.1 ppm) to –NH, single at 2.5 ppm to =CH**.** Silverstien, R.M., Webster, F.X and Kiemle, D.J.(2005). (151-153)

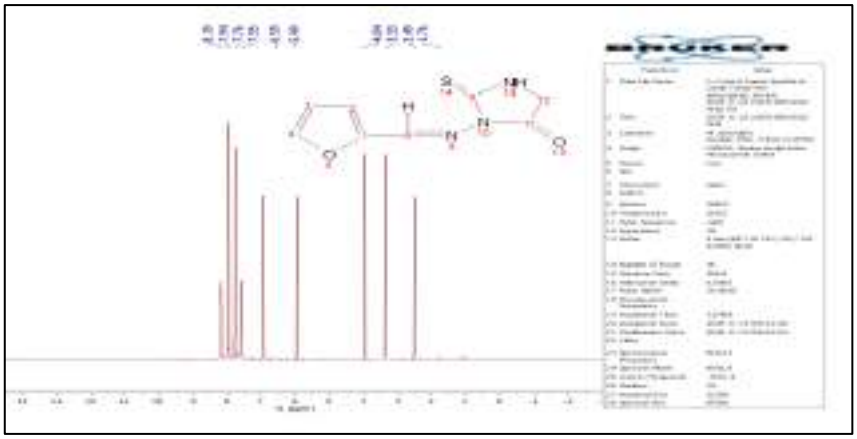


Figure (4- 48): ^{1}HNMR spectrum of 3-((furan-2-ylmethylene)amino)-2-thioxoimidazolidin-4-one compound(16).

^{13}C-NMR spectrum of 3-((furan-2-ylmethylene)amino)-2-thioxoimidazolidin-4-one compound(16).

The signals of olefinic and aromatic carbons appear in the third region between 112 and 113 ppm , singles related to C=N at 143-150 ppm , single related to C-N at 64 ppm, singles related to C=O (amide) at 174-176 ppm, single related to C=S at 183 ppm. (151-153)

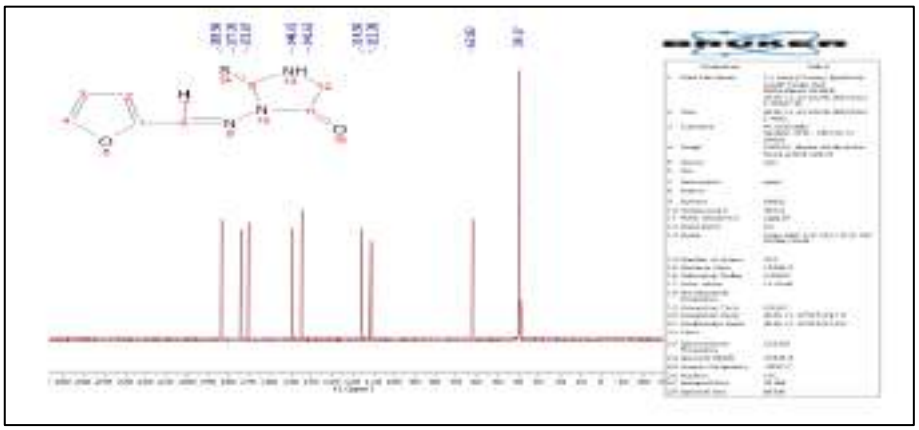
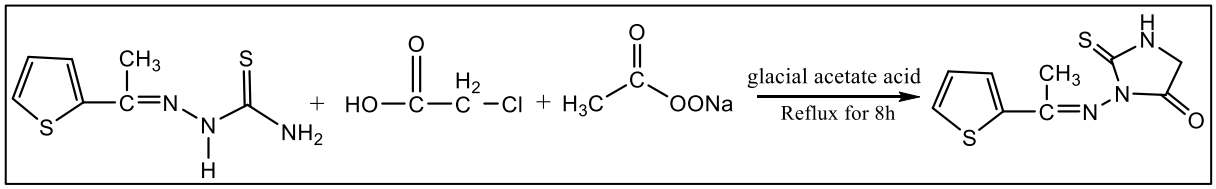


Figure (4- 49): ^{13}C-NMR spectrum of3-((furan-2-ylmethylene)amino)-2-thioxoimidazolidin-4-one compound(16).

4.2.8 Synthesis of (E)-3-((1-(thiophen-2-yl)ethylidene)amino)-2-thioxoimidazolidin-4-one compound(17).



Scheme (4-18): synthesis of (E)-3-((1-(thiophen-2-yl)ethylidene)amino)-2-thioxoimidazolidin-4-one compound(17).

FTIR spectrum of (E)-3-((1-(thiophen-2-yl)ethylidene)amino)-2-thioxoimidazolidin-4-one compound(17).

The FTIR spectrum of the preparation of (E)-3-((1-(thiophen-2-yl)ethylidene)amino)-2-thioxoimidazolidin-4-one as shown in (fig.4-50) which indicates absorption band at 3431and 3304 to –NH , absorption band at 3182 Cm^{-1} to C-H (aromatic) , absorption band at 3072 and 2987 cm^{-1} to C-H(alphatic), absorption band at 1598 Cm^{-1} to C=N, absorption band at 1199 Cm^{-1} to C=S,

absorption band at 1409 Cm^{-1} to C=C. (Hetro phenyl ring), absorption band at 1114 Cm^{-1} to C-N, absorption band at 1712 Cm^{-1} to C=O, absorption band at 1334 Cm^{-1} to CH_3. (151-153)

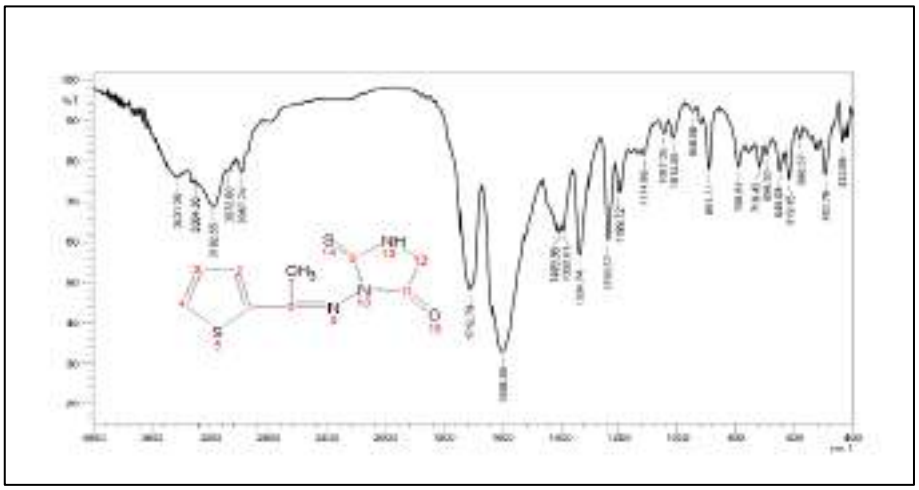


Figure (4- 50): FTIR spectrum of (E)-3-((1-(thiophen-2-yl)ethylidene)amino)-2-thioxoimidazolidin-4-one compound(17).

^{1}HNMR spectrum of (E)-3-((1-(thiophen-2-yl)ethylidene)amino)-2-thioxoimidazolidin-4-one compound(17).

^{1}HNMR spectrum of (E)-3-((1-(thiophen-2-yl)ethylidene)amino)-2-thioxoimidazolidin-4-one in (fig.4-51) the major signal at δ 1.8 ppm is characteristic of DMSO-d6 as solvent , singlate at (7.2-8.6 δ ppm) to (3H, Hetro phenyl ring), multiplet singlate at (3.4 to 4.1 ppm) to –NH, single at 2.5 ppm to =CH**.** (151-153)

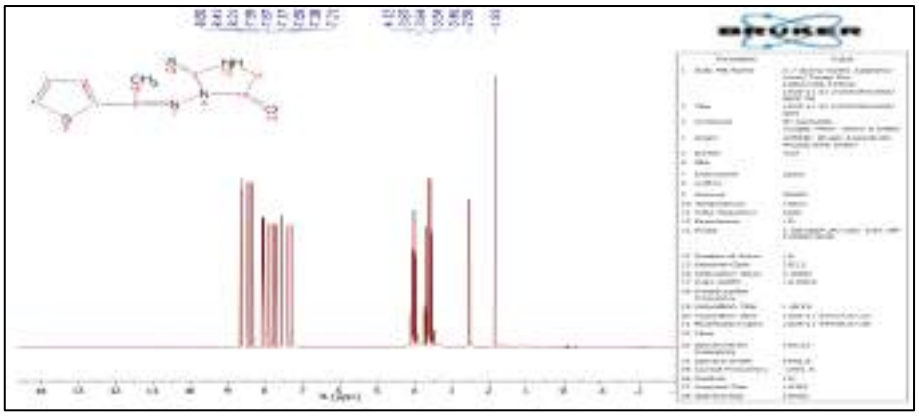


Figure (4- 51): ^{1}HNMR spectrum of (E)-3-((1-(thiophen-2-yl)ethylidene)amino)-2-thioxoimidazolidin-4-one compound(17).

^{13}C-NMR spectrum of (E)-3-((1-(thiophen-2-yl)ethylidene)amino)-2-thioxoimidazolidin-4-one compound(17).

The signals of olefinic and aromatic carbons appear in the third region between 126 and 128 ppm , singles related to C=N at 154 ppm , single related to C-N at 64 ppm, singles related to C=O (amide) at 175 ppm, singles related to C=S at 178-182 ppm, single related to CH_3 at 15 ppm. (151-153)

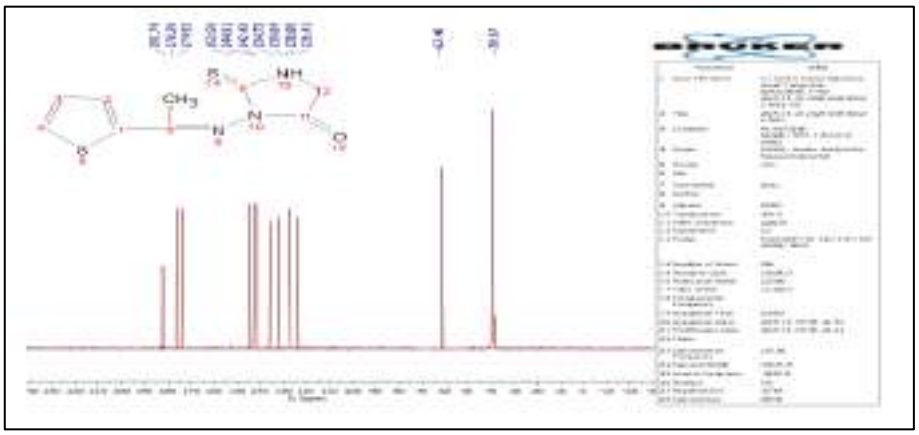
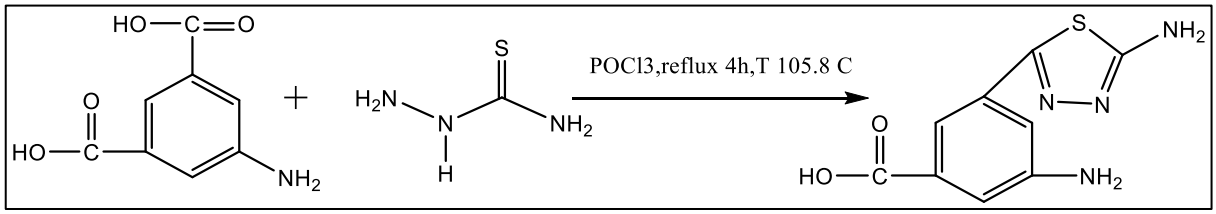


Figure (4- 52): ^{13}C-NMR spectrum of (E)-3-((1-(thiophen-2-yl)ethylidene)amino)-2-thioxoimidazolidin-4-one compound(17).

4.3 Synthesis of 5-styryl-2-amino -1, 3, 4-thiadiazole (18-20)

4.3.1 Synthesis of N-(5-aminophthaloyl) thiosemicarbazide compound(1).



Scheme (4-19): synthesis of N-(5-aminophthaloyl) thiosemicarbazide compound(18).

FTIR spectrum of N-(5-aminophthaloyl) thiosemicarbazide compound(18).

The FTIR spectrum of synthesis OF N-(5-aminophthaloyl) thiosemicarbazide as shown in (fig.4-53) which indicates absorption band at 3562 to $–NH_2$, overlapping with a –OH group , absorption band at 3000 Cm^{-1} to C-H (aromatic) , absorption band at 2812 cm^{-1} to C-H(alphatic), absorption band at 1539 Cm^{-1} to C=C (aromatic), absorption band at 1633 Cm^{-1} to C=O (carboxylic), absorption band at 1161 Cm^{-1} to C-N. (151-153)

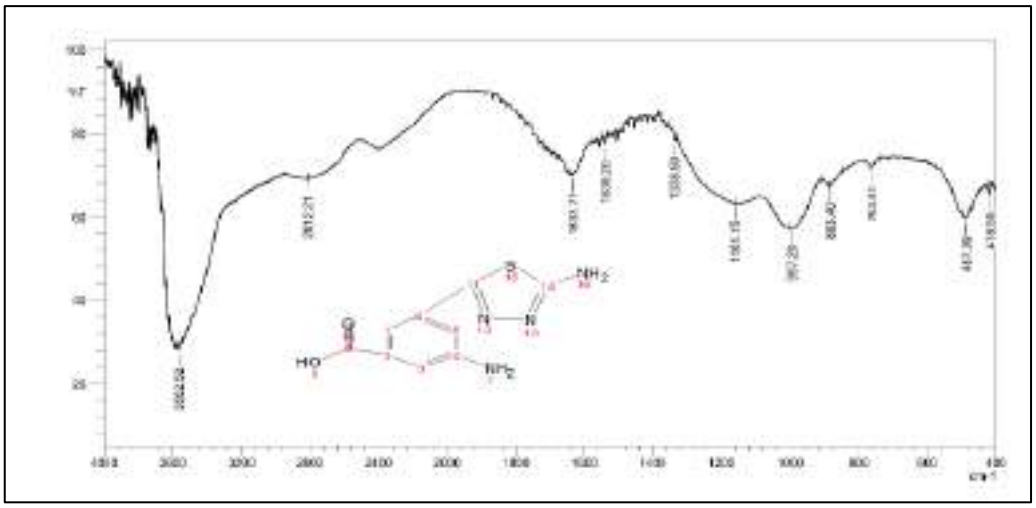


Figure (4- 53): FTIR structure of synthesis of N-(5-aminophthaloyl) thiosemicarbazide compound(18).

[1]HNMR spectrum of 5-styryl-2-amino -1, 3, 4-thiadiazole compound for 5-amino Phthalic acid compound(18).

[1]HNMR spectrum of 5-styryl-2-amino -1, 3, 4-thiadiazole compound for 5-amino Phthalic acid in (fig.4-54) the major signal at δ 2.5 ppm is characteristic of DMSO-d6 as solvent , singles at (6.6-7.7 δ ppm) to (4H, phenyl ring), multiplet singlate at (3.4 ppm) to $–NH_2$, singles at (8.3 ppm) to (H, OH). (151-153)

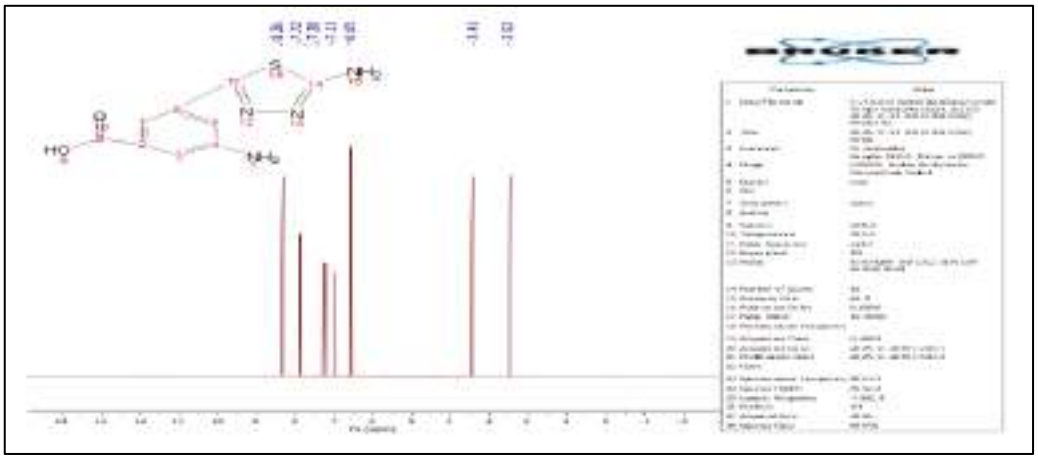


Figure (4- 54): [1]HNMR structure of synthesis of N-(5-aminophthaloyl) thiosemicarbazide compound(18).

^{13}C-NMR spectrum of 5-styryl-2-amino -1, 3, 4-thiadiazole compound for 5-amino Phthalic acid compound(18).

The signals of olefinic and aromatic carbons appear in the third region between 111 and 135 ppm , single related to C-S at 56 ppm , singles related to C=N at 155-161 ppm , single related to C-N at 64 ppm, single related to C=O (acid) at 169ppm. (151-153)

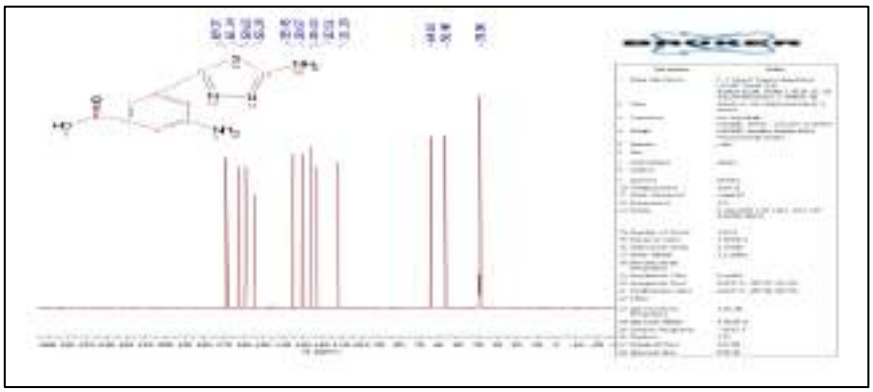
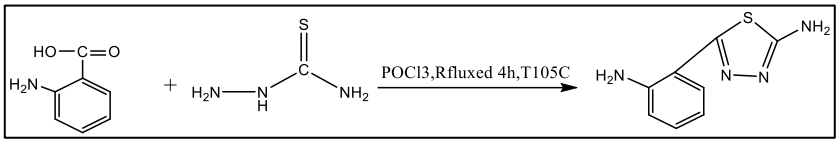


Figure (4-55): ^{13}C-NMR structure of synthesis of N-(5-aminophthaloyl) thiosemicarbazide compound(18).

4.3.2 Synthesis of 5-amino-2-(2-aminophenyl)-2, 5-dihydro-1, 3, 4-thiadiazol-2-ol compound(19).



Scheme (4-20): synthesis of 5-amino-2-(2-aminophenyl)-2, 5-dihydro-1, 3, 4-thiadiazol-2-ol compound(19).

FTIR spectrum of 5-styryl-2-amino -1, 3, 4-thiadiazole compound for anthranilic acid compound(19).

The FTIR spectrum of the preparation of 5-styryl-2-amino -1, 3, 4-thiadiazole compound for anthranilic acid as shown in (fig.4-56) which indicates absorption band at 3481 and 3415 to $-NH_2$ group , absorption band at 3236 Cm^{-1} to C-H (aromatic) , absorption band at 2998 cm^{-1} to C-H(alphatic), absorption band at 1456 Cm^{-1} to C=C (aromatic), absorption band at 1637 Cm^{-1} to C=O (carboxylic), absorption band at 1141 Cm^{-1} to C-N, absorption band at 1554 Cm^{-1} to C=N .(151-153)

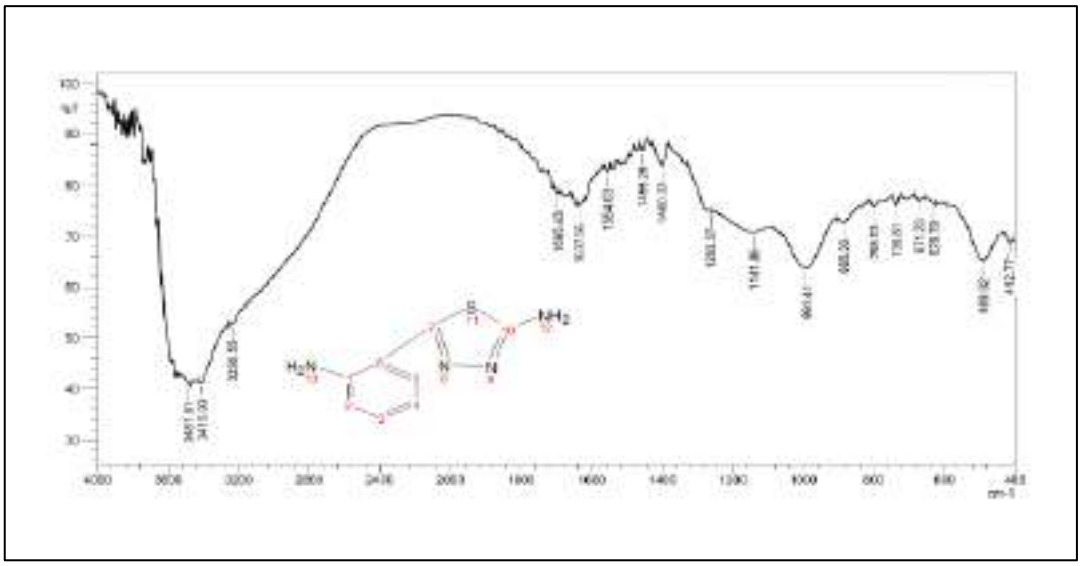


Figure (4- 56): FTIR structure of 5-styryl-2-amino -1, 3, 4-thiadiazole compound for anthranilic acid compound(19).

^{1}HNMR spectrum of 5-styryl-2-amino -1, 3, 4-thiadiazole compound for anthranilic acid compound(19).

^{1}HNMR spectrum of 5-styryl-2-amino -1, 3, 4-thiadiazole compound for anthranilic acid in (fig.4-57) the major signal at δ 2.5 ppm is characteristic of DMSO-d6 as solvent , singles at (7.4-8.2 δ ppm) to (4H, phenyl ring), multiplet singlate at (3.4 ppm) to $–NH_2$. (151-153)

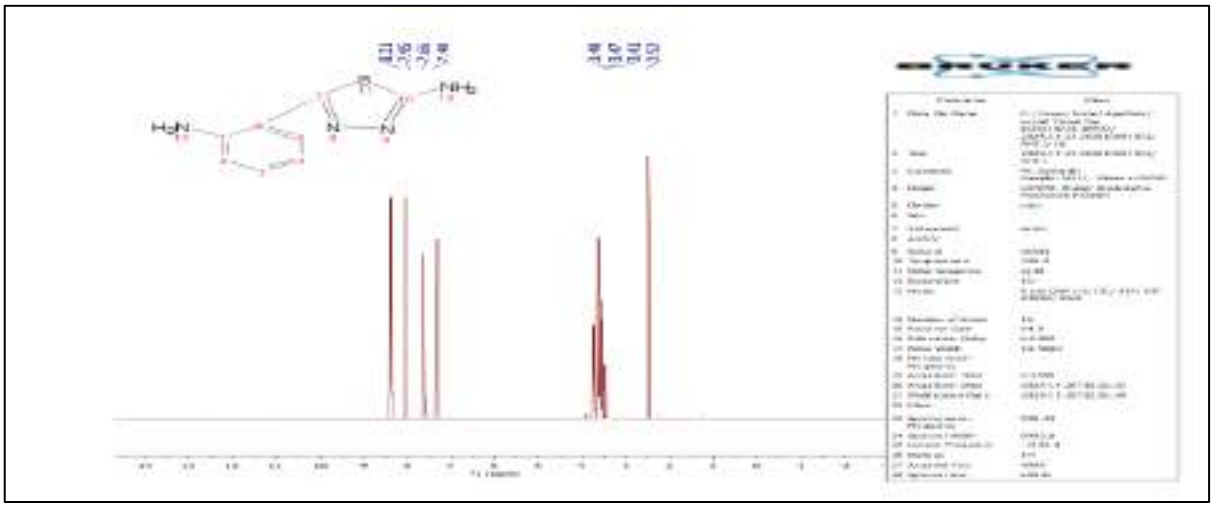


Figure (4- 57): ^{1}HNMR structure of 5-styryl-2-amino -1, 3, 4-thiadiazole compound for anthranilic acid compound(19).

^{13}C-NMR spectrum of 5-styryl-2-amino -1, 3, 4-thiadiazole compound for anthranilic acid compound(19).

The signals of olefinic and aromatic carbons appear in the third region between 125 and 136 ppm , single related to C-S at 56 ppm , singles related to C=N at 154-162 ppm , single related to C-N at 64 ppm, singles related to C=O (acid) at 169-172 ppm. (151-153)

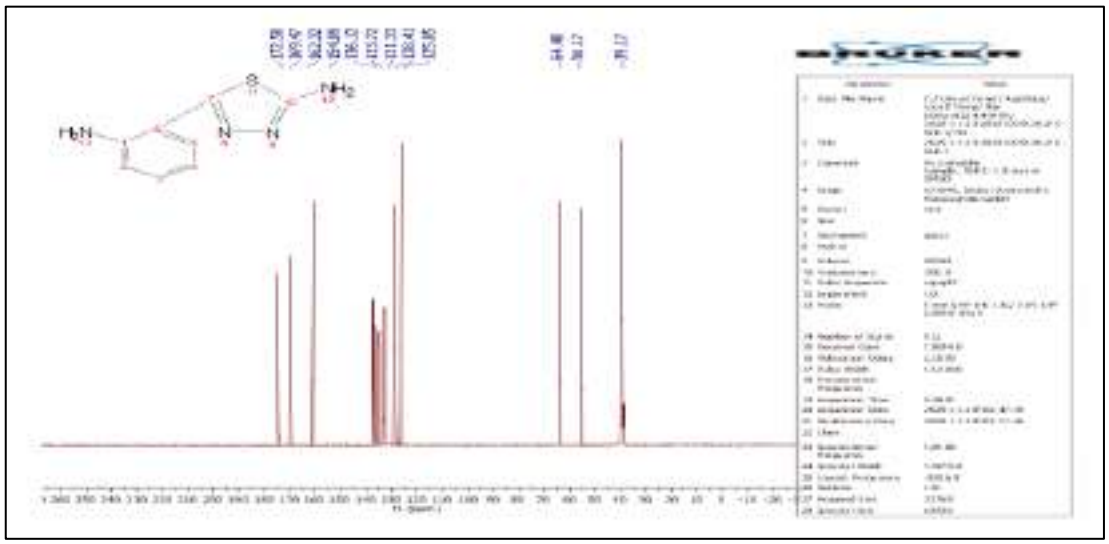
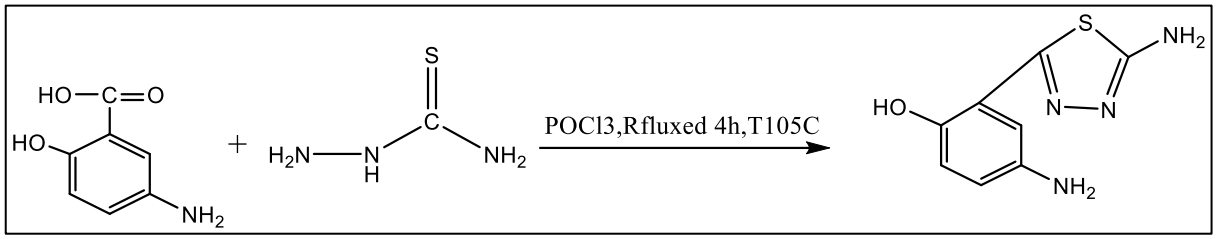


Figure (4- 58): ^{13}C-NMR structure of 5-styryl-2-amino -1, 3, 4-thiadiazole compound for anthranilic acid compound(19).

4.3.3 Synthesis of 5-amino-2-(5-amino-2-hydroxyphenyl)-2, 5-dihydro-1, 3, 4-thiadiazol-2 compound(20).



Scheme (4-21): synthesis of 5-amino-2-(5-amino-2-hydroxyphenyl)-2, 5-dihydro-1, 3, 4-thiadiazol-2 compound(20).

FTIR spectrum of 5-styryl-2-amino -1, 3, 4-thiadiazole compound for 5-amino -2-hydroxybenzoic acid compound(20).

The FTIR spectrum of the preparation of 5-styryl-2-amino -1, 3, 4-thiadiazole compound for 5-amino -2-hydroxybenzoic acid as shown in (fig.4-59) which indicates absorption band at 3560 to $–NH_2$, overlapping with a –OH group ,

absorption band at 3000 Cm^{-1} to C-H (aromatic) , absorption band at 1452 Cm^{-1} to C=C (aromatic), absorption band at 1631 Cm^{-1} to C=O (carboxylic), absorption band at 1182 Cm^{-1} to C-N. (151-153)

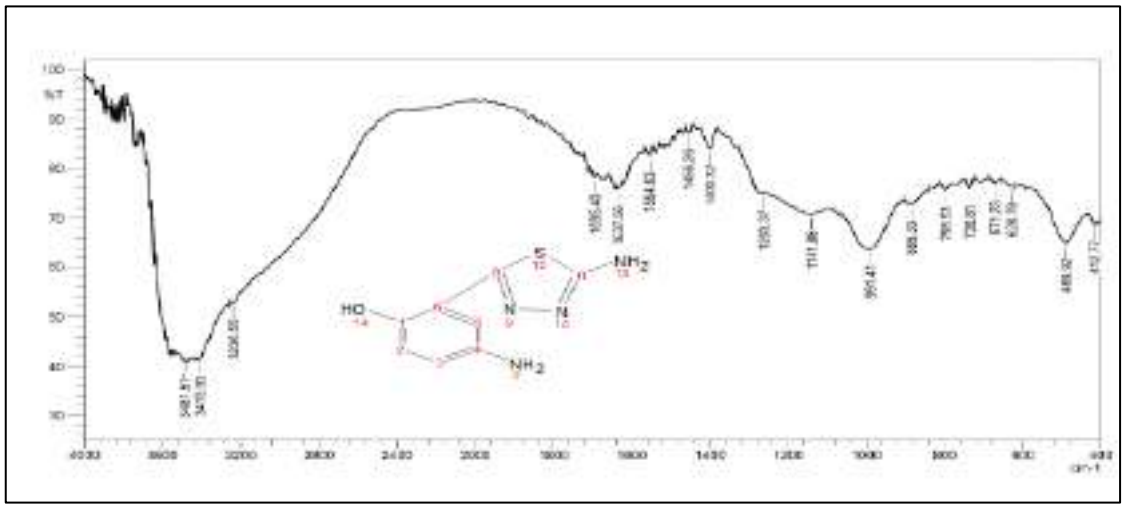


Figure (4- 59): FTIR structure of 5-styryl-2-amino -1, 3, 4-thiadiazole compound for 5-amino -2-hydroxybenzoic acid compound(20).

^{1}HNMR spectrum of 5-styryl-2-amino -1, 3, 4-thiadiazole compound for 5-amino -2-hydroxybenzoic acid compound(20).

^{1}HNMR spectrum of 5-styryl-2-amino -1, 3, 4-thiadiazole compound for 5-amino -2-hydroxybenzoic acid in (fig.4-60) the major signal at δ 2.5 ppm is characteristic of DMSO-d6 as solvent , singles at (6.6-8.0 δ ppm) to (4H, phenyl ring), multiplet singlate at (3.4 ppm) to $–NH_2$, singles at (8.7 ppm) to (H, OH). (151-153)

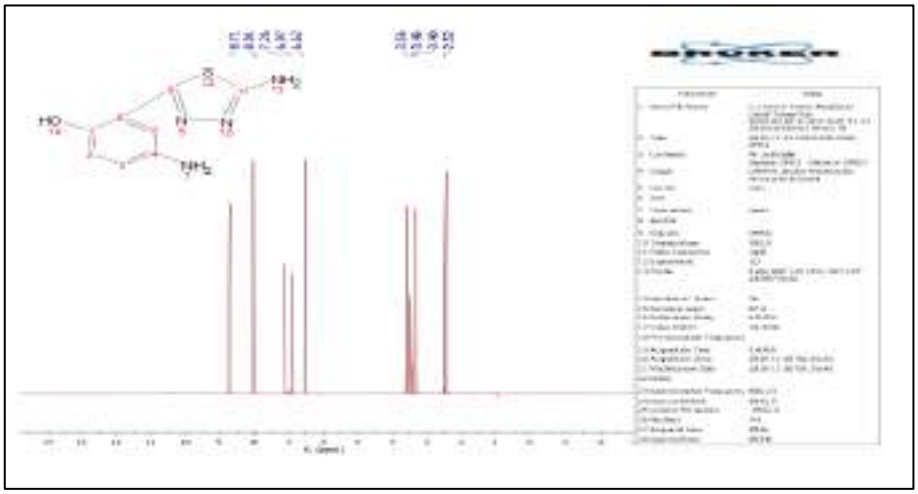


Figure (4- 60): ^{1}HNMR structure of 5-styryl-2-amino -1, 3, 4-thiadiazole compound for 5-amino -2-hydroxybenzoic acid compound(20).

^{13}C-NMR spectrum of 5-styryl-2-amino -1, 3, 4-thiadiazole compound for 5-amino -2-hydroxybenzoic acid compound(20).

The signals of olefinic and aromatic carbons appear in the third region between 115 and 134 ppm , single related to C-S at 56 ppm , singles related to C=N at 152-162 ppm , single related to C-N at 64 ppm, single related to C=O (acid) at 172ppm. (151-153)

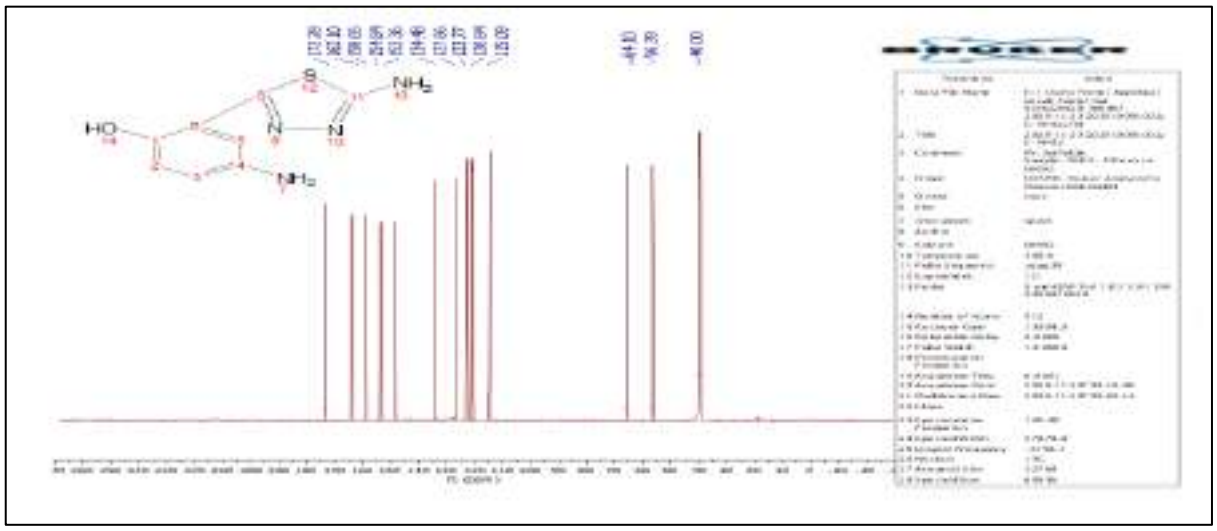
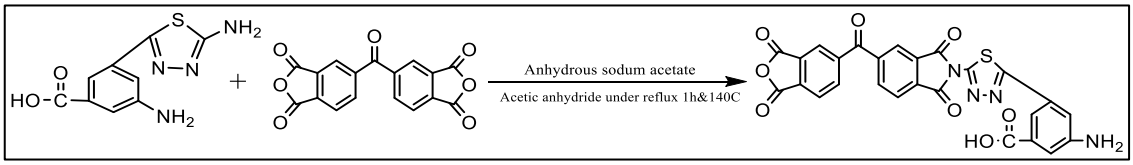


Figure (4- 61): ^{13}C-NMR structure of 5-styryl-2-amino -1, 3, 4-thiadiazole compound for 5-amino -2-hydroxybenzoic acid compound(20).

4.4 Synthesis of Imide compounds(21-23)

4.4.1 Synthesis of 3-amino-5-(5-(5-(1, 3-dioxo-1, 3-dihydroisobenzofuran-5-carbonyl)-3-methylene-1-oxoisoindolin-2-yl)-4, 5-dihydro-1, 3, 4-thiadiazol-2-yl)benzoic acid compound(21).



Scheme (4-22): synthesis of 3-amino-5-(5-(5-(1, 3-dioxo-1, 3-dihydroisobenzofuran-5-carbonyl)-3-methylene-1-oxoisoindolin-2-yl)-4, 5-dihydro-1, 3, 4-thiadiazol-2-yl)benzoic acid compound(21).

FTIR spectrum of imide for 3, 3', 4, 4'-benzophenone tetracarboxylic acid anhydride with 5-amino phthalic acid compound(21).

The FTIR spectrum of the preparation of imide compound for 3, 3', 4, 4'-benzophenone tetracarboxylic acid anhydride with 5-amino phthalic acid as shown in (fig.4-62) which indicates absorption band at 3456 to NH_2 overlapping with a –OH group, absorption band at 3074 Cm^{-1} to C-H (aromatic) , absorption band at 2966 and 2889 cm^{-1} to C-OH (alphatic), absorption band at 1539 Cm^{-1} to C=C (aromatic), absorption band at 1635 Cm^{-1} to C=O (amide), absorption band at 1714 Cm^{-1} to C=O (carboxylic acid), absorption band at 1163 Cm^{-1} to C-N. (151-153)

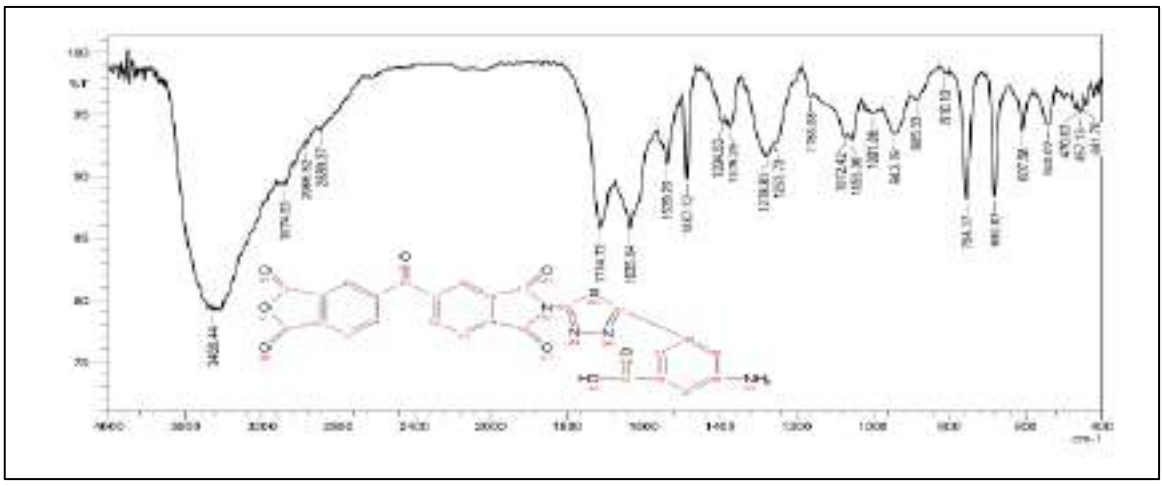


Figure (4- 62): FTIR structure of 3-amino-5-(5-(5-(1, 3-dioxo-1, 3-dihydroisobenzofuran-5-carbonyl)-3-methylene-1-oxoisoindolin-2-yl)-4, 5-dihydro-1, 3, 4-thiadiazol-2-yl)benzoic acid compound(21).

^{1}HNMR spectrum of imide for 3, 3', 4, 4'-benzophenone tetracarboxylic acid anhydride with 5-amino phthalic acid compound(21).

^{1}HNMR spectrum of imide for 3, 3', 4, 4'-benzophenone tetracarboxylic acid anhydride with 5-amino phthalic acid in (fig.63) the major signal at δ 1.8 ppm is characteristic of DMSO-d6 as solvent , multiplet singlate at (7.3-8.1 ppm) to (9H, phenyl ring), singles at (8.9 ppm) to (1H, OH), singlate at (3.4 ppm) to $–NH_2$. (151-153)

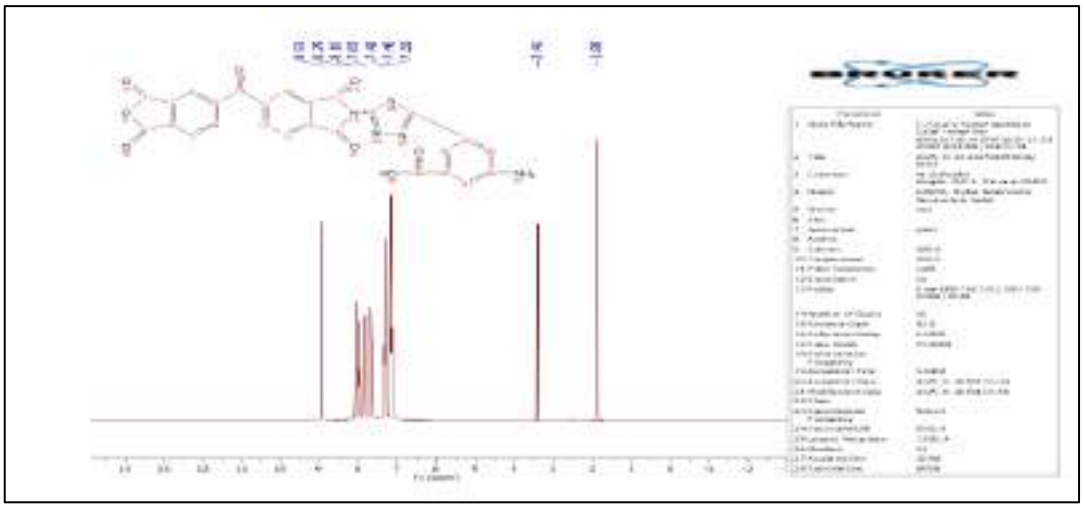


Figure (4- 63): ^{1}HNMR spectrum of 3-amino-5-(5-(5-(1, 3-dioxo-1, 3-dihydroisobenzofuran-5-carbonyl)-3-methylene-1-oxoisoindolin-2-yl)-4, 5-dihydro-1, 3, 4-thiadiazol-2-yl)benzoic acid compound(21).

^{13}C-NMR spectrum of 3-amino-5-(5-(5-(1, 3-dioxo-1, 3-dihydroisobenzofuran-5-carbonyl)-3-methylene-1-oxoisoindolin-2-yl)-4, 5-dihydro-1, 3, 4-thiadiazol-2-yl)benzoic acid compound(21).

The signals of olefinic and aromatic carbons appear in the third region between 123 and 134 ppm , singles related to C-S at 56 ppm , singles related to C=N at 166ppm , single related to C-N at 64 ppm, single related to C=O at 173 ppm. (151-153)

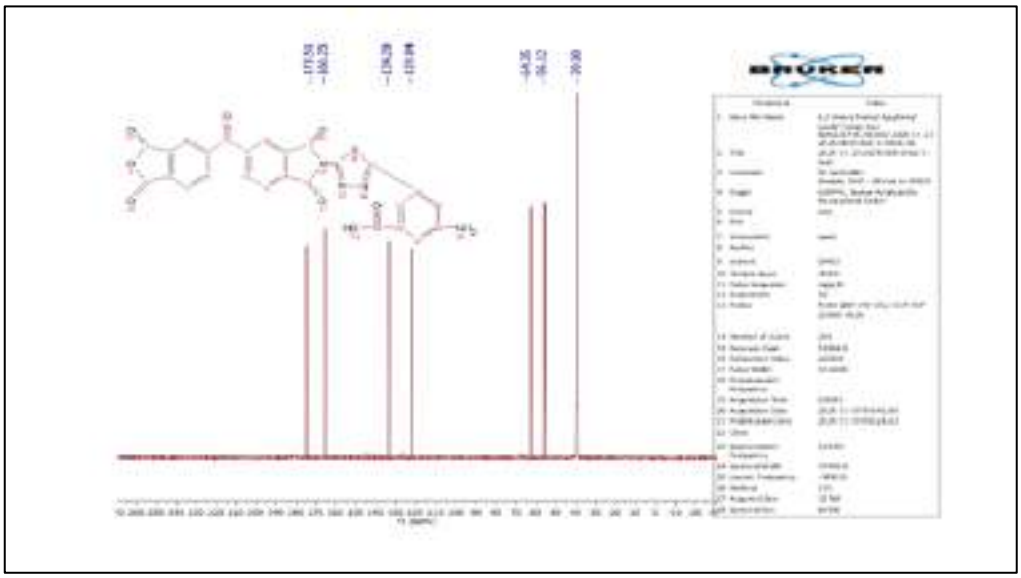
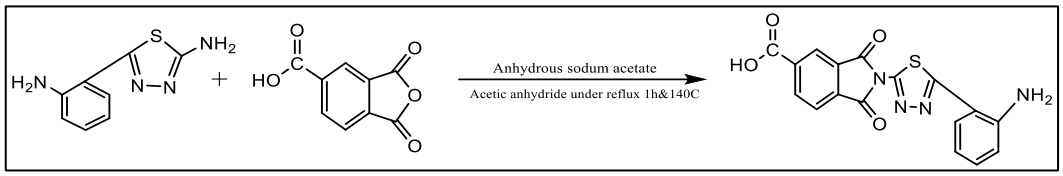


Figure (4- 64): ^{13}C-NMR spectrum of 3-amino-5-(5-(5-(1, 3-dioxo-1, 3-dihydroisobenzofuran-5-carbonyl)-3-methylene-1-oxoisoindolin-2-yl)-4, 5-dihydro-1, 3, 4-thiadiazol-2-yl)benzoic acid compound(21).

4.4.2 Synthesis of 5-(2-(5-(2-aminophenyl)-5-hydroxy-2, 5-dihydro-1, 3, 4-thiadiazol-2-yl)-3-methylene-1-oxoisoindoline-5-carbonyl) isobenzofuran-1, 3-dione compound(22).



Scheme (4-23): synthesis of 5-(2-(5-(2-aminophenyl)-5-hydroxy-2, 5-dihydro-1, 3, 4-thiadiazol-2-yl)-3-methylene-1-oxoisoindoline-5-carbonyl)isobenzofuran-1, 3-dione compound(22).

FTIR spectrum of imide for trimellitic anhydride compound(22).

The FTIR spectrum of the preparation of imide for trimellitic anhydride as shown in (fig.4-65) which indicates absorption band at 3477 and 3412 to $–NH_2$ group , absorption band at 3034 Cm^{-1} to C-H (aromatic) , absorption band at 1492 Cm^{-1} to C=C (aromatic), absorption band at 1635 Cm^{-1} to C=O (anhydride acid), absorption band at 1714 Cm^{-1} to C=O (ketone) , absorption band at 1149 Cm^{-1} to C-N, absorption band at 1620 Cm^{-1} to C=N. (151-153)

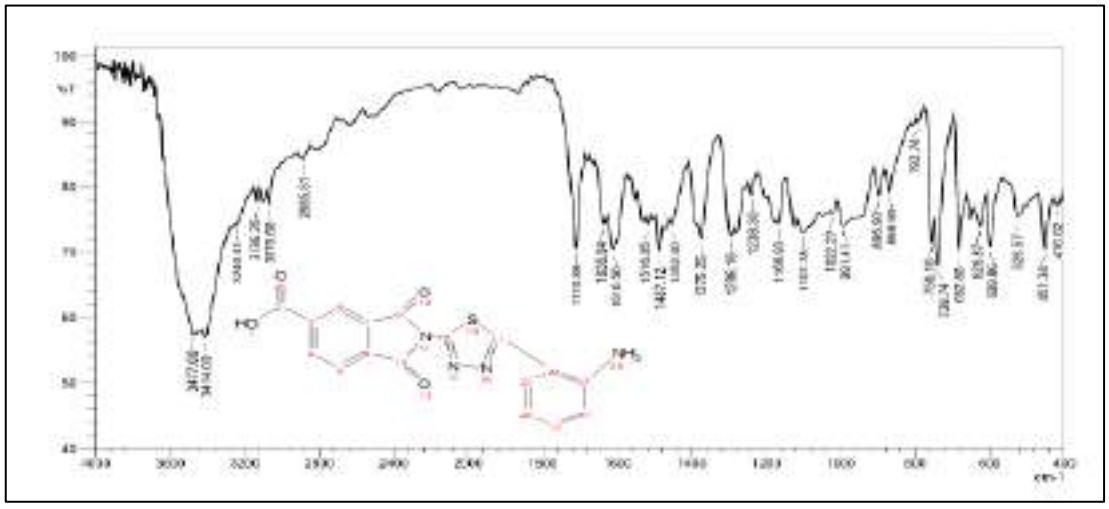


Figure (4- 65): FTIR spectrum of 5-(2-(5-(2-aminophenyl)-5-hydroxy-2, 5-dihydro-1, 3, 4-thiadiazol-2-yl)-3-methylene-1-oxoisoindoline-5-carbonyl)isobenzofuran-1, 3-dione compound(22).

^{1}HNMR spectrum of imide for trimellitic anhydride compound(22).

^{1}HNMR spectrum of imide for trimellitic anhydride in (fig.4-66) the major signal at δ 2.5 ppm is characteristic of DMSO-d6 as solvent , singles at (7.4-8.6 δ ppm) to (10H, phenyl ring), multiplet singlate at (3.4 ppm) to $–NH_2$. (151-153)

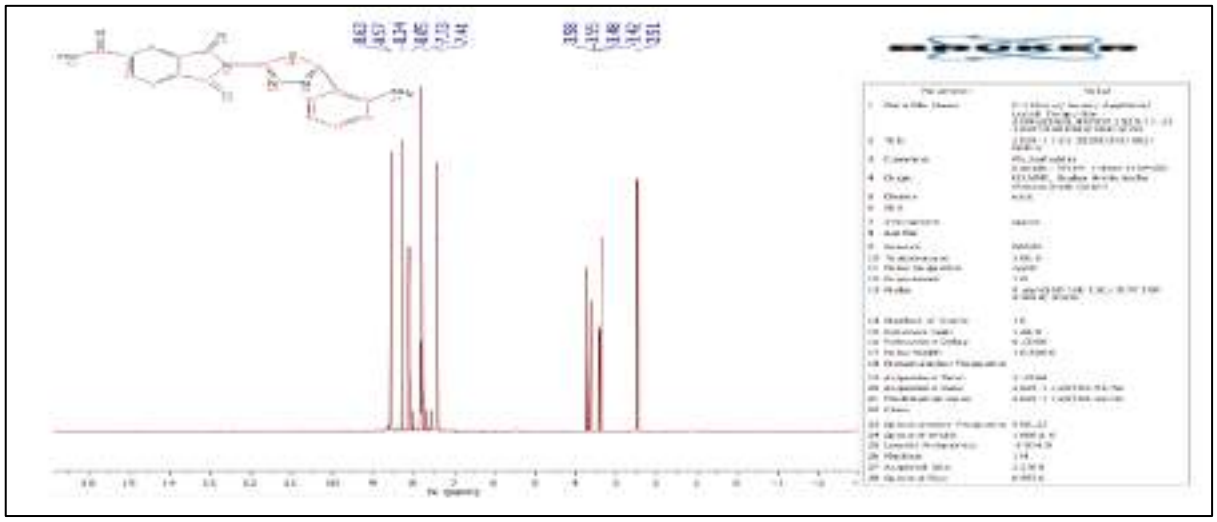


Figure (4- 66): ^{1}HNMR spectrum of 5-(2-(5-(2-aminophenyl)-5-hydroxy-2, 5-dihydro-1, 3, 4-thiadiazol-2-yl)-3-methylene-1-oxoisoindoline-5-carbonyl)isobenzofuran-1, 3-dione compound(22).

^{13}C-NMR spectrum of imide for trimellitic anhydride compound(22).

The signals of olefinic and aromatic carbons appear in the third region between 124 and 133 ppm , single related to C-S at 56 ppm , singles related to C=N at 148 ppm , single related to C-N at 64 ppm, singles related to C=O (acid) at 164-169 ppm. (151-153)

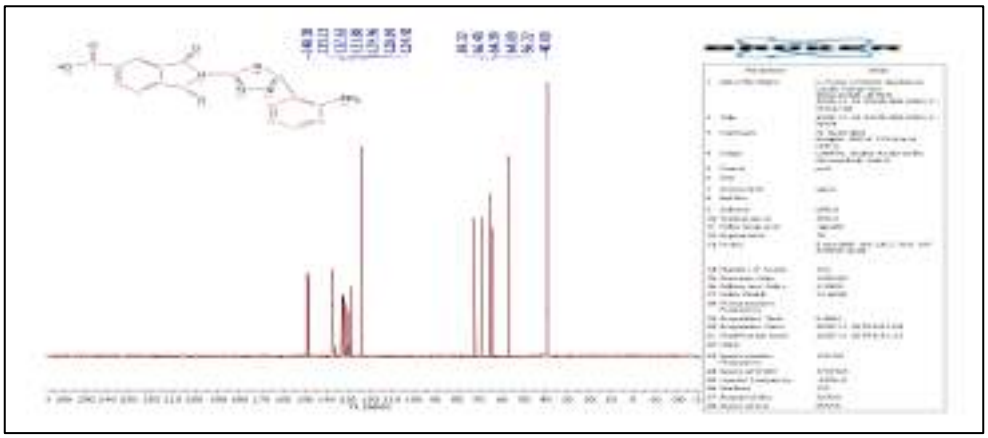
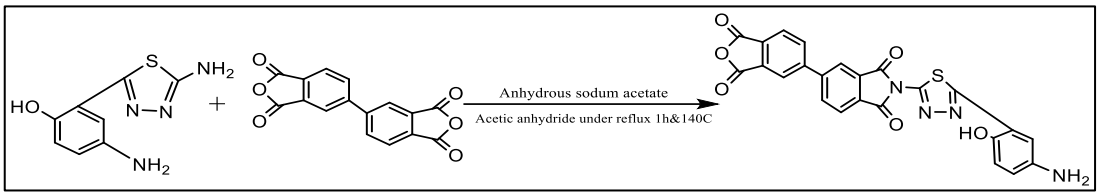


Figure (4- 67): ^{13}C-NMR spectrum of 5-(2-(5-(2-aminophenyl)-5-hydroxy-2, 5-dihydro-1, 3, 4-thiadiazol-2-yl)-3-methylene-1-oxoisoindoline-5-carbonyl)isobenzofuran-1, 3-dione compound(22).

4.4.3 Synthesis of 2-(5-(5-amino-2-hydroxyphenyl)-5-hydroxy-2, 5-dihydro-1, 3, 4-thiadiazol-2-yl)-5-(1, 3-dioxo-1, 3-dihydroisobenzofuran-5-carbonyl)isoindoline-1, 3-dione compound(23).



Scheme (4-24): synthesis of 2-(5-(5-amino-2-hydroxyphenyl)-5-hydroxy-2, 5-dihydro-1, 3, 4-thiadiazol-2-yl)-5-(1, 3-dioxo-1, 3-dihydroisobenzofuran-5-carbonyl)isoindoline-1, 3-dione compound(23).

FTIR spectrum of 2-(5-(5-amino-2-hydroxyphenyl)-5-hydroxy-2, 5-dihydro-1, 3, 4-thiadiazol-2-yl)-5-(1, 3-dioxo-1, 3-dihydroisobenzofuran-5-carbonyl)isoindoline-1, 3-dione compound(23).

The FTIR spectrum of the preparation of 2-(5-(5-amino-2-hydroxyphenyl)-5-hydroxy-2, 5-dihydro-1, 3, 4-thiadiazol-2-yl)-5-(1, 3-dioxo-1, 3-dihydroisobenzofuran-5-carbonyl)isoindoline-1, 3-dione as shown in (fig.4-68) which indicates absorption band at 3477 to $–NH_2$, and 3414 to –OH group , absorption band at 3136 Cm^{-1} to C-H (aromatic) , absorption band at 1516 Cm^{-1} to C=C (aromatic), absorption band at 1635 Cm^{-1} to C=O (anhydride acid), absorption band at 1710 Cm^{-1} to C=O (Ketone), absorption band at 1166 Cm^{-1} to C-N. (151-153)

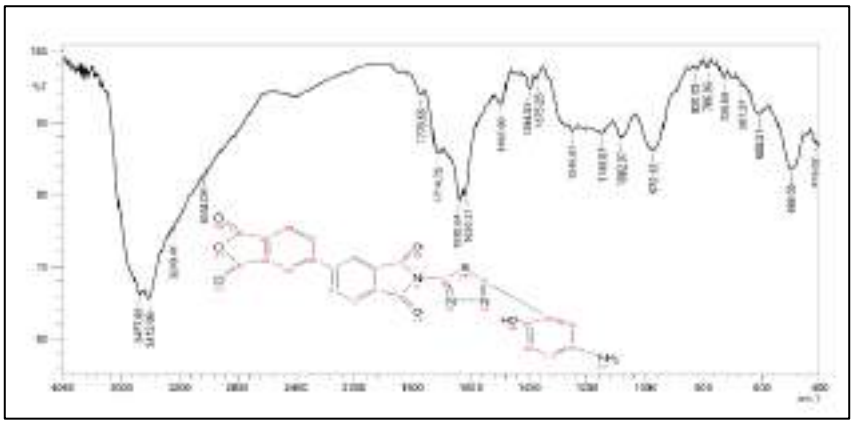


Figure (4- 68): FTIR spectrum of 2-(5-(5-amino-2-hydroxyphenyl)-5-hydroxy-2, 5-dihydro-1, 3, 4-thiadiazol-2-yl)-5-(1, 3-dioxo-1, 3-dihydroisobenzofuran-5-carbonyl)isoindoline-1, 3-dione compound(23).

^{1}HNMR spectrum of 2-(5-(5-amino-2-hydroxyphenyl)-5-hydroxy-2, 5-dihydro-1, 3, 4-thiadiazol-2-yl)-5-(1, 3-dioxo-1, 3-dihydroisobenzofuran-5-carbonyl)isoindoline-1, 3-dione compound(23).

^{1}HNMR spectrum of 2-(5-(5-amino-2-hydroxyphenyl)-5-hydroxy-2, 5-dihydro-1, 3, 4-thiadiazol-2-yl)-5-(1, 3-dioxo-1, 3-dihydroisobenzofuran-5-carbonyl)isoindoline-1, 3-dione in (fig.4-69) the major signal at δ 2.5 ppm is characteristic of DMSO-d6 as solvent , singles at (7.3-8.6 δ ppm) to (9H, phenyl ring), singlate at (3.5 ppm) to $–NH_2$, singles at (12.1 ppm) to (H, OH). (151-153)

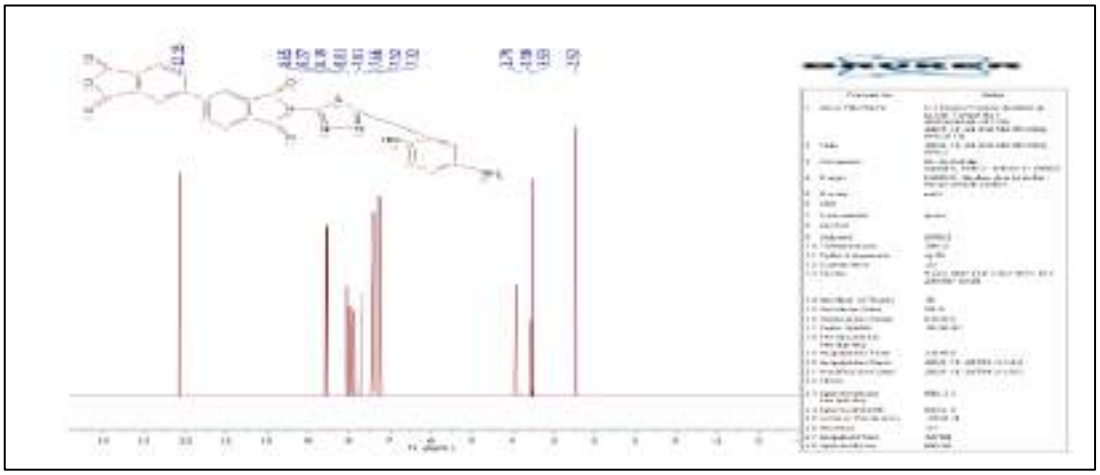


Figure (4- 69): ^{1}HNMR spectrum of 2-(5-(5-amino-2-hydroxyphenyl)-5-hydroxy-2, 5-dihydro-1, 3, 4-thiadiazol-2-yl)-5-(1, 3-dioxo-1, 3-dihydroisobenzofuran-5-carbonyl)isoindoline-1, 3-dione compound(23).

^{13}C-NMR spectrum of 2-(5-(5-amino-2-hydroxyphenyl)-5-hydroxy-2, 5-dihydro-1, 3, 4-thiadiazol-2-yl)-5-(1, 3-dioxo-1, 3-dihydroisobenzofuran-5-carbonyl)isoindoline-1, 3-dione compound(23).

The signals of olefinic and aromatic carbons appear in the third region between 114 and 133 ppm , single related to C-S at 56 ppm , single related to C=N at 148 ppm , single related to C-N at 64 ppm, singles related to C=O (acid) at 168ppm. (151-153)

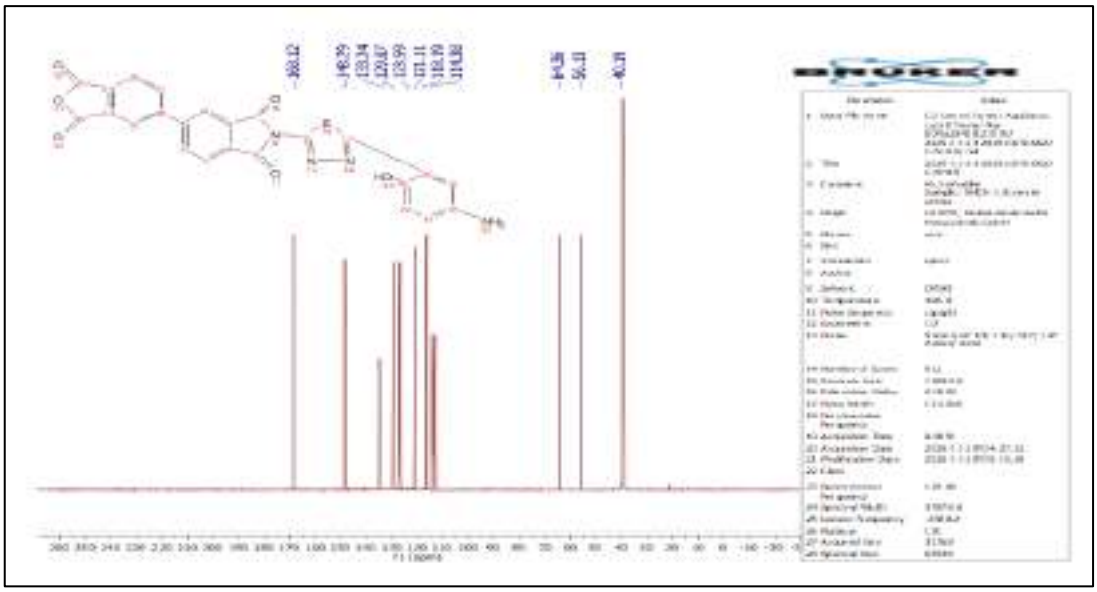
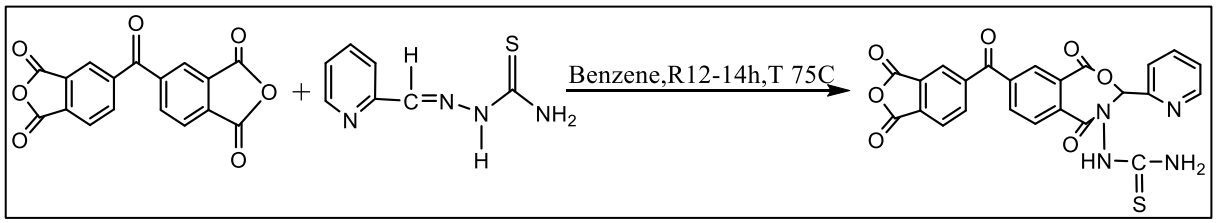


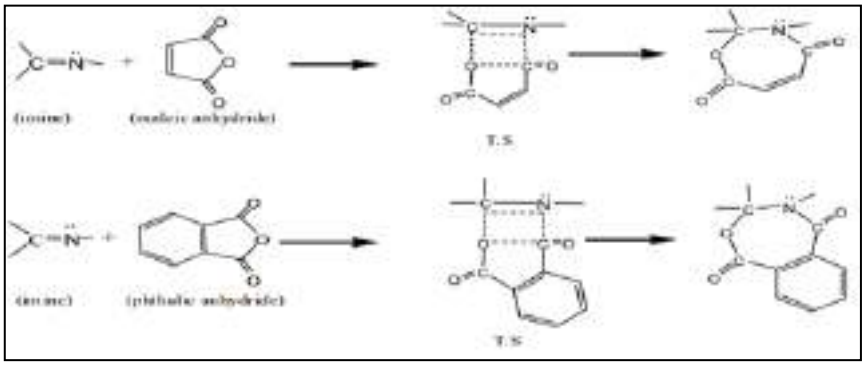
Figure (4- 70): ^{13}C-NMR spectrum of 2-(5-(5-amino-2-hydroxyphenyl)-5-hydroxy-2, 5-dihydro-1, 3, 4-thiadiazol-2-yl)-5-(1, 3-dioxo-1, 3-dihydroisobenzofuran-5-carbonyl)isoindoline-1, 3-dione compound(23).

4.5 Synthesis 1-(3-(derivative)-1, 5-dioxo-1, 5-dihydrobenzo[e] [1, 3] oxazepin -4(3H)-yl) thiourea compounds. (24-26)

4.5.1 Synthesis of 1-(8-(1, 3-dioxo-1, 3-dihydroisobenzofuran-5-carbonyl)-1, 5-dioxo-3-(pyridin-2-yl)-1, 5-dihydrobenzo[e][1, 3]oxazepin-4(3H)-yl)urea compound(24).



Scheme (4-25): synthesis of 1-(8-(1, 3-dioxo-1, 3-dihydroisobenzofuran-5-carbonyl)-1, 5-dioxo-3-(pyridin-2-yl)-1, 5-dihydrobenzo[e][1, 3]oxazepin-4(3H)-yl)urea compound(24).



Scheme (4-26): Mechanism of synthesis 1, 3 oxazepine

FTIR spectrum of 1-(3-(derivative)-1, 5-dioxo-1, 5-dihydrobenzo[e] [1, 3] oxazepin -4(3H)-yl) thiourea compound for pyridine carboxaldehyde compound(24).

The FTIR spectrum of 1-(3-(derivative)-1, 5-dioxo-1, 5-dihydrobenzo[e] [1, 3] oxazepin -4(3H)-yl) thiourea compound for pyridine carboxaldehyde as shown in (fig.4-71) which indicates absorption bands at 3442 cm^{-1} to $–NH_2$ stretching and absorption bands at 3288 cm^{-1} to –NH , absorption band at 3174 cm^{-1} to C-H(aromatic) , absorption band at 2995and 2900 cm^{-1} to C-H(alphatic), absorption band at 1591 cm^{-1} to C=N, absorption band at 1232 Cm^{-1} to C=S, absorption band at 1517 Cm^{-1} to C=C (aromatic), absorption bands at 1134 Cm^{-1} to C-N, absorption bands at 1715 Cm^{-1} to C=O (ester), absorption bands at 1643 Cm^{-1} to C=O (Ketone). (151-153)

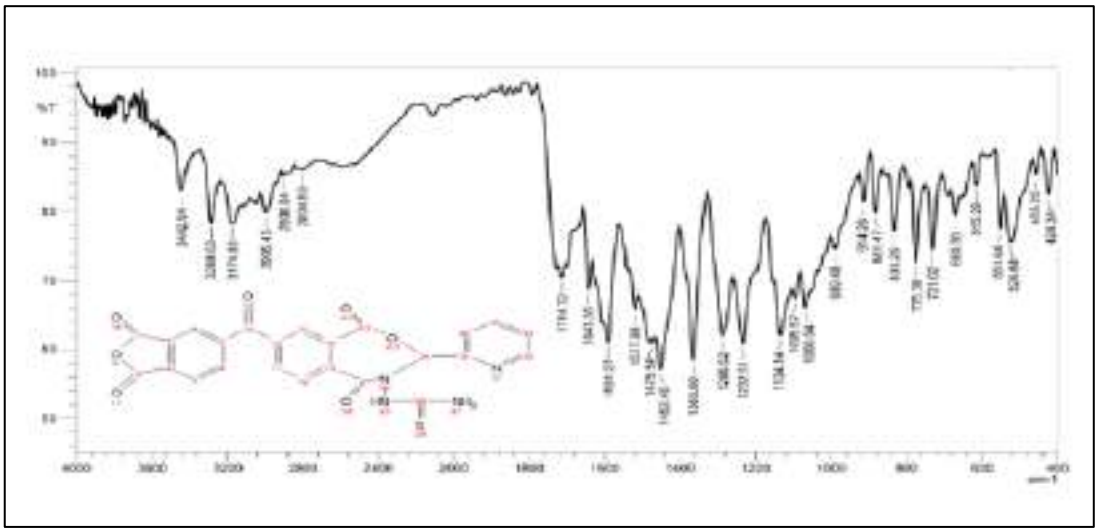


Figure (4- 71): FTIR spectrum of 2-(5-(5-amino-2-hydroxyphenyl)-5-hydroxy-2, 5-dihydro-1, 3, 4-thiadiazol-2-yl)-5-(1, 3-dioxo-1, 3-dihydroisobenzofuran-5-carbonyl)isoindoline-1, 3-dione compound(24).

^{1}HNMR spectrum of 1-(3-(derivative)-1, 5-dioxo-1, 5-dihydrobenzo[e] [1, 3] oxazepin -4(3H)-yl) thiourea compound for pyridine carboxaldehyde compound(24).

^{1}HNMR spectrum of 1-(3-(derivative)-1, 5-dioxo-1, 5-dihydrobenzo[e] [1, 3] oxazepin -4(3H)-yl) thiourea compound for pyridine carboxaldehyde in (fig.4-72) the major signal at δ 1.4 ppm is characteristic of DMSO-d6 as solvent , singles at

(7.3-8.7 δ ppm) to (10H, phenyl ring), singles at (3.4-4.3 ppm) to $–NH_2$, singlate at (2.5 ppm) to =CH. Silverstien, R.M., Webster, F.X and Kiemle, D.J.(2005). (151, 152)

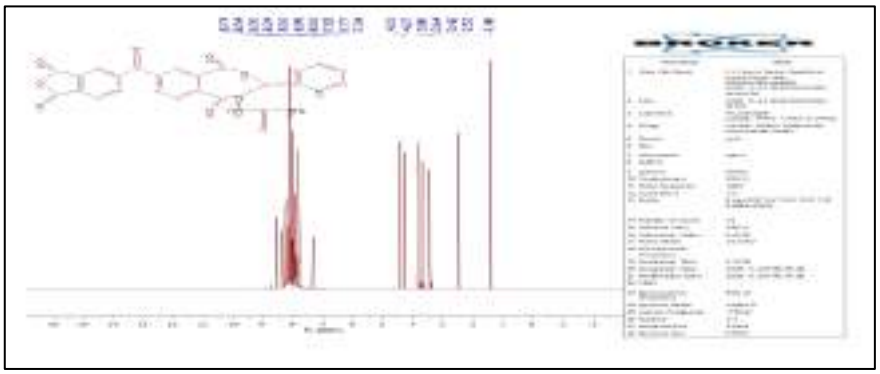


Figure (4- 72): ^{1}HNMR spectrum of 2-(5-(5-amino-2-hydroxyphenyl)-5-hydroxy-2, 5-dihydro-1, 3, 4-thiadiazol-2-yl)-5-(1, 3-dioxo-1, 3-dihydroisobenzofuran-5-carbonyl)isoindoline-1, 3-dione compound(24).

^{13}C-NMR spectrum of1-(3-(derivative)-1, 5-dioxo-1, 5-dihydrobenzo[e] [1, 3] oxazepin -4(3H)-yl) thiourea compound for pyridine carboxaldehyde compound(24).

The signals of olefinic and aromatic carbons appear in the third region between 120 and 136 ppm , singles related to C=S at 194 ppm , singles related to C=N at 154 ppm , single related to C-N at 63 ppm, single related to C=O (Acid)at 178 ppm. , singles related to C=O (Ester)at 168 ppm, single related to C=O (Ketone) at 193 ppm. (151-153)

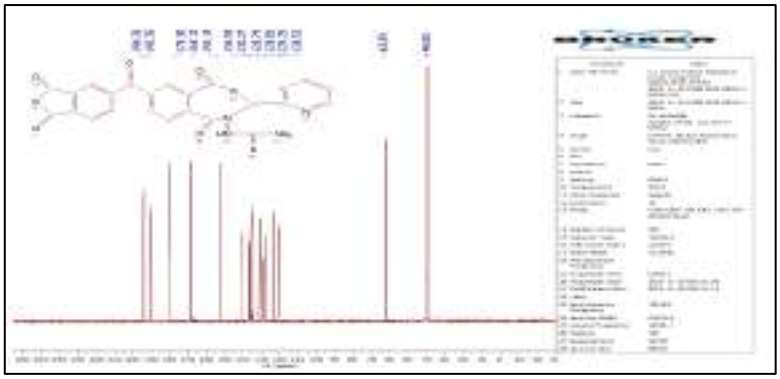
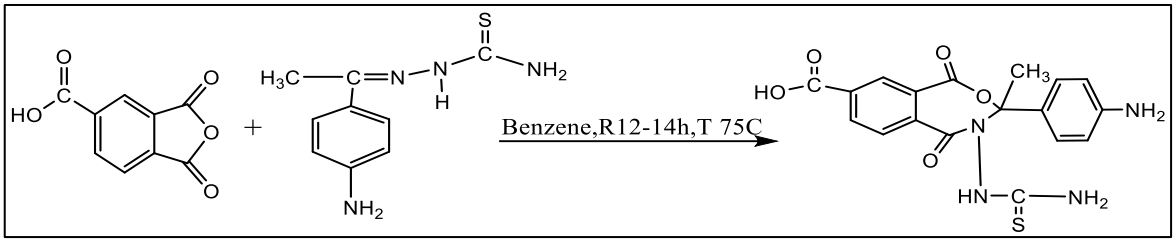


Figure (4- 73): ^{13}C-NMR spectrum of 2-(5-(5-amino-2-hydroxyphenyl)-5-hydroxy-2, 5-dihydro-1, 3, 4-thiadiazol-2-yl)-5-(1, 3-dioxo-1, 3-dihydroisobenzofuran-5-carbonyl)isoindoline-1, 3-dione compound(24).

4.5.2 Synthesis of 3-(2-aminophenyl)-1, 5-dioxo-4-ureido-1, 3, 4, 5-tetrahydrobenzo[e][1, 3]oxazepine-8-carboxylic acid compound(25).



Scheme (4-27): synthesis of 3-(2-aminophenyl)-1, 5-dioxo-4-ureido-1, 3, 4, 5-tetrahydrobenzo[e][1, 3]oxazepine-8-carboxylic acid compound(25).

FTIR spectrum of 3-(2-aminophenyl)-1, 5-dioxo-4-ureido-1, 3, 4, 5-tetrahydrobenzo[e][1, 3]oxazepine-8-carboxylic acid compound(25).

The FTIR spectrum of 3-(2-aminophenyl)-1, 5-dioxo-4-ureido-1, 3, 4, 5-tetrahydrobenzo[e][1, 3]oxazepine-8-carboxylic acid as shown in (fig.4-74) which indicates absorption bands at 3441 cm^{-1} to $–NH_2$ stretching and absorption bands at 3311 cm^{-1} to -OH , absorption band at 3178 cm^{-1} to C-H(aromatic) , absorption band at 3062 cm^{-1} to N-H (alphatic), absorption band at 1591 cm^{-1} to C=N, absorption band at 1232 Cm^{-1} to C=S, absorption band at 1606 Cm^{-1} to C=C (aromatic), absorption bands at 1116 Cm^{-1} to C-N, absorption bands at 1716 Cm^{-1} to C=O (ester), absorption bands at 1653 Cm^{-1} to C=O (Acid), absorption bands at 1388 Cm^{-1} to CH_3. (151-153)

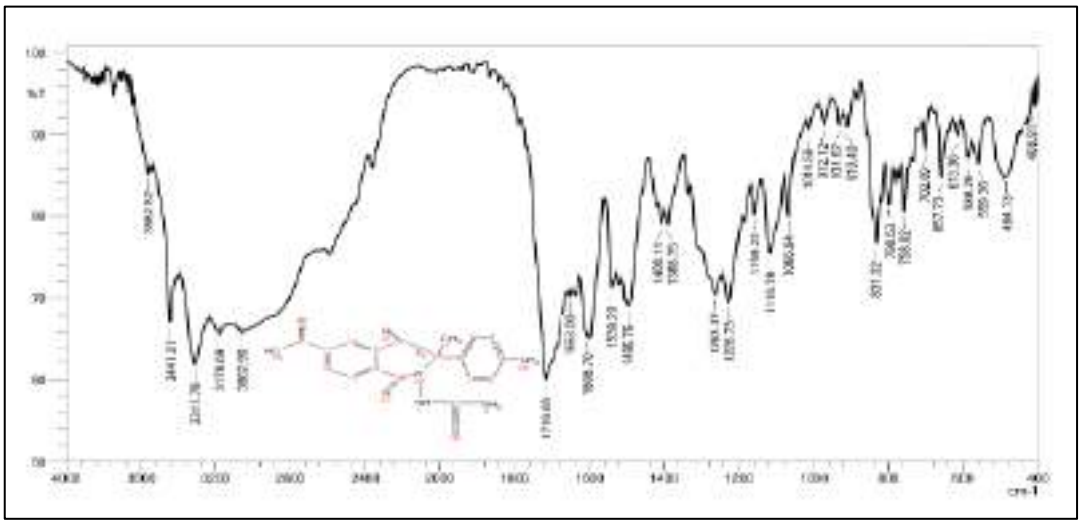


Figure (4- 74): FTIR spectrum of 2-(5-(5-amino-2-hydroxyphenyl)-5-hydroxy-2, 5-dihydro-1, 3, 4-thiadiazol-2-yl)-5-(1, 3-dioxo-1, 3-dihydroisobenzofuran-5-carbonyl)isoindoline-1, 3-dione compound(25).

^{1}HNMR spectrum of 3-(2-aminophenyl)-1, 5-dioxo-4-ureido-1, 3, 4, 5-tetrahydrobenzo[e][1, 3]oxazepine-8-carboxylic acid compound(25).

^{1}HNMR spectrum of 3-(2-aminophenyl)-1, 5-dioxo-4-ureido-1, 3, 4, 5-tetrahydrobenzo[e][1, 3]oxazepine-8-carboxylic acid in (fig4-75) the major signal at δ 2.4 ppm is characteristic of DMSO-d6 as solvent , singles at (7.0-8.5 δ ppm) to (7 H, phenyl ring), single at (3.4 ppm) to $–NH_2$, singlate at (2.5 ppm) to =CH, single at (6.5 ppm) to –OH, singlate at (1.3 ppm) to CH_3**.** (151-153)

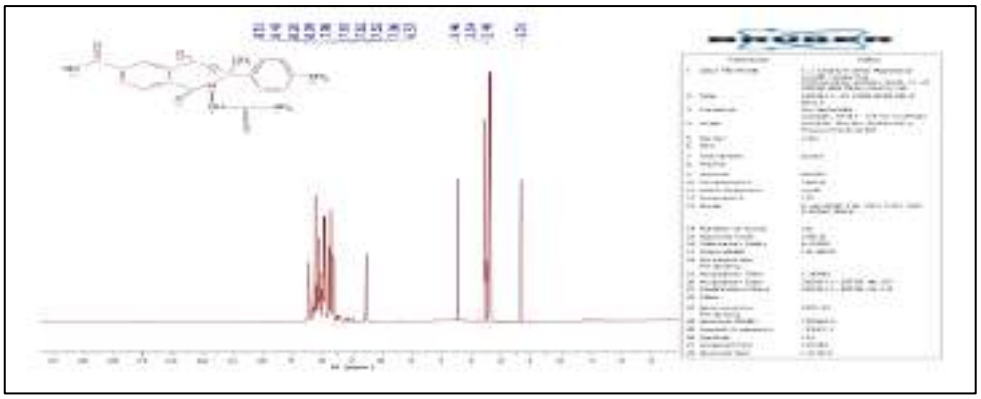


Figure (4- 75): ^{1}HNMR spectrum of 2-(5-(5-amino-2-hydroxyphenyl)-5-hydroxy-2, 5-dihydro-1, 3, 4-thiadiazol-2-yl)-5-(1, 3-dioxo-1, 3-dihydroisobenzofuran-5-carbonyl)isoindoline-1, 3-dione compound(25).

^{13}C-NMR spectrum of 3-(2-aminophenyl)-1, 5-dioxo-4-ureido-1, 3, 4, 5-tetrahydrobenzo[e][1, 3]oxazepine-8-carboxylic acid compound(25).

The signals of olefinic and aromatic carbons appear in the third region between 113 and 136 ppm , singles related to C=S at 194 ppm , singles related to C=N at 148 ppm , single related to C-N at 63 ppm, singles related to C=O (Acid)at 178 ppm, single related to C=O (Ketone) at 193 ppm, single related to CH_3 at 13 ppm. (151-153)

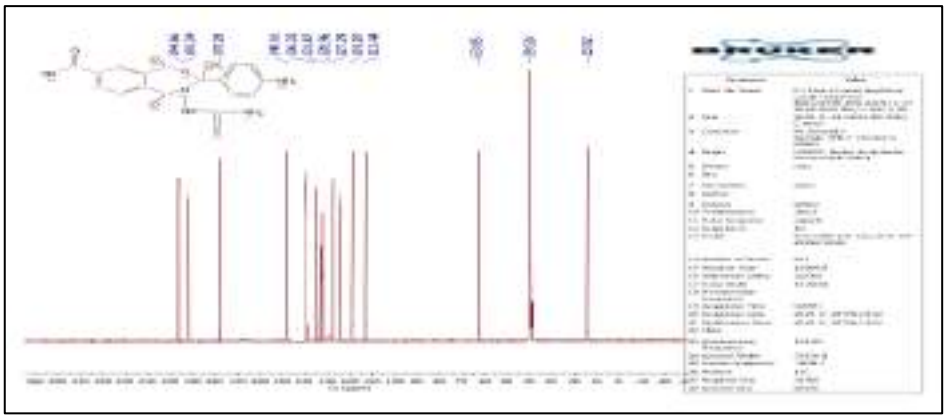
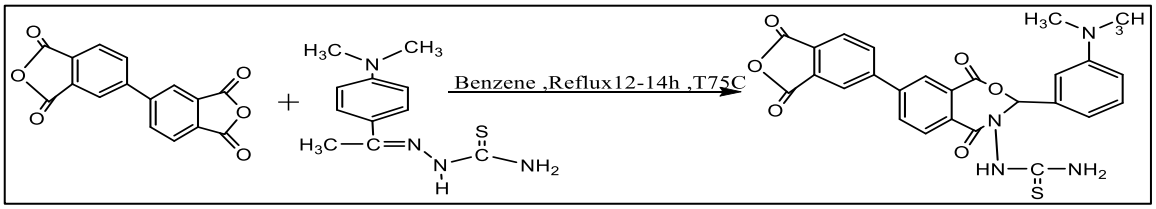


Figure (4- 76): ^{13}C-NMR spectrum of 2-(5-(5-amino-2-hydroxyphenyl)-5-hydroxy-2, 5-dihydro-1, 3, 4-thiadiazol-2-yl)-5-(1, 3-dioxo-1, 3-dihydroisobenzofuran-5-carbonyl)isoindoline-1, 3-dione compound(25).

4.5.3 Synthesis of 1-(3-(3-(dimethylamino)phenyl)-1, 5-dioxo-9-(4-(3-oxobutanoyl)phenyl)-1, 5-dihydrobenzo[e][1, 3]oxazepin-4(3H)-yl)urea compound(26).



Scheme (4-28): synthesis of 1-(3-(3-(dimethylamino)phenyl)-1, 5-dioxo-9-(4-(3-oxobutanoyl)phenyl)-1, 5-dihydrobenzo[e][1, 3]oxazepin-4(3H)-yl)urea compound(26).

FTIR spectrum of 1-(3-(3-(dimethylamino)phenyl)-1, 5-dioxo-9-(4-(3-oxobutanoyl)phenyl)-1, 5-dihydrobenzo[e][1, 3]oxazepin-4(3H)-yl)urea compound(26).

The FTIR spectrum of 1-(3-(3-(dimethylamino)phenyl)-1, 5-dioxo-9-(4-(3-oxobutanoyl)phenyl)-1, 5-dihydrobenzo[e][1, 3]oxazepin-4(3H)-yl)urea as shown in (fig.4-77) which indicates absorption bands at 3411 cm^{-1} to $–NH_2$ and 3377 cm^{-1} to –NH stretching , absorption band at 3269 and 3132 cm^{-1} to C-H (aromatic), absorption band at 2987 cm^{-1} to C-H (CH_3), absorption band at 1514 cm^{-1} to C=N, absorption band at 1278 Cm^{-1} to C=S, absorption band at 1458 Cm^{-1} to C=C (aromatic), absorption bands at 1178 Cm^{-1} to C-N, absorption bands at 1712 Cm^{-1} to C=O (Ketone), absorption bands at 1651 Cm^{-1} to C=O (Acid). (151-153)

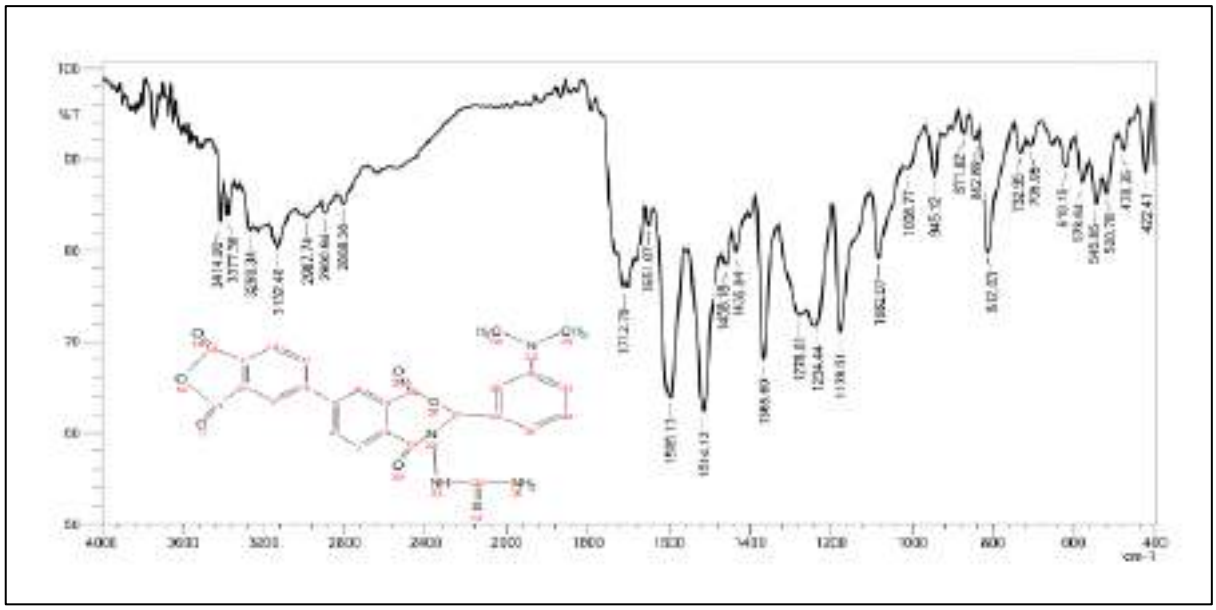


Figure (4- 77): FTIR spectrum of 1-(3-(3-(dimethylamino)phenyl)-1, 5-dioxo-9-(4-(3-oxobutanoyl)phenyl)-1, 5-dihydrobenzo[e][1, 3]oxazepin-4(3H)-yl)urea compound(26).

^{1}HNMR spectrum of 1-(3-(3-(dimethylamino)phenyl)-1, 5-dioxo-9-(4-(3-oxobutanoyl)phenyl)-1, 5-dihydrobenzo[e][1, 3]oxazepin-4(3H)-yl)urea compound(26).

^{1}HNMR spectrum of 1-(3-(3-(dimethylamino)phenyl)-1, 5-dioxo-9-(4-(3-oxobutanoyl)phenyl)-1, 5-dihydrobenzo[e][1, 3]oxazepin-4(3H)-yl)urea in (fig.4-78) singlate at (6.7-8.3 δ ppm) to (10 H, phenyl ring), singlate at (4.3 ppm) to -NH, singlate at (2.4 ppm) to =CH, singlate at (1.3 ppm) to (CH_3)**,** singlate at (2.8 ppm) to N-CH_3. (151-153)

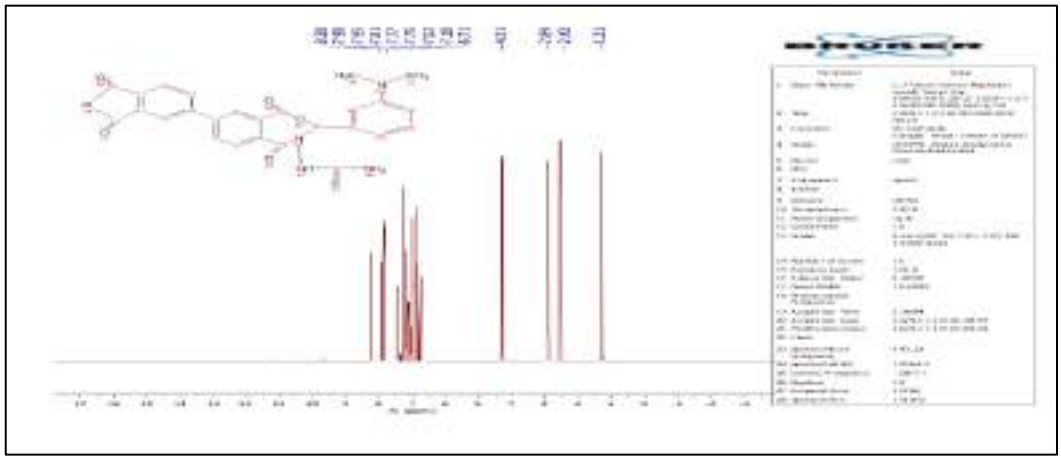


Figure (4- 78): ^{1}HNMR spectrum of 1-(3-(3-(dimethylamino)phenyl)-1, 5-dioxo-9-(4-(3-oxobutanoyl)phenyl)-1, 5-dihydrobenzo[e][1, 3]oxazepin-4(3H)-yl)urea compound(26).

^{13}C-NMR spectrum of 1-(3-(3-(dimethylamino)phenyl)-1, 5-dioxo-9-(4-(3-oxobutanoyl)phenyl)-1, 5-dihydrobenzo[e][1, 3]oxazepin-4(3H)-yl)urea compound(26).

The signals of olefinic and aromatic carbons appear in the third region between 111 and 134 ppm , singles related to C=S at 195 ppm , singles related to C=N at 151 ppm , , singles related to C-N at 63 ppm, singles related to C=O (acid) at 178 ppm, single related to CH3 (acid) at 13 ppm. (151-153)

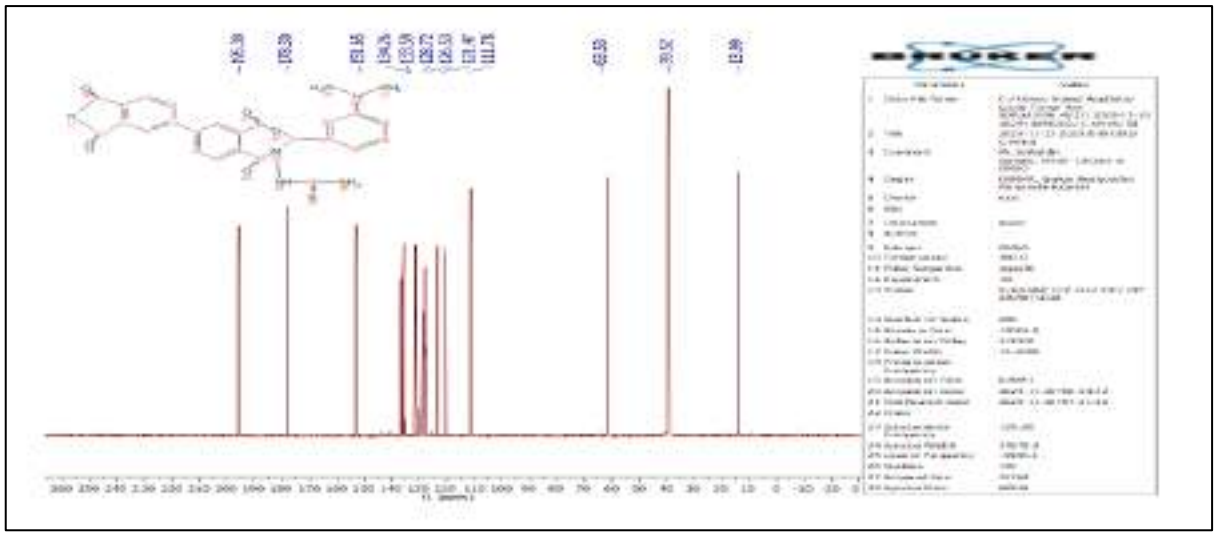
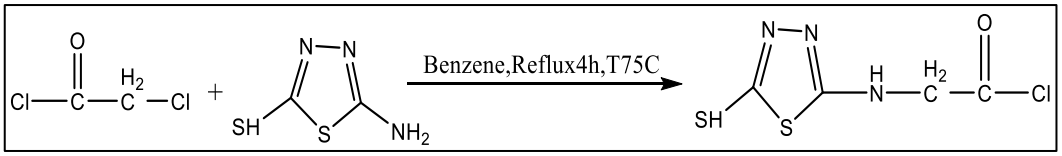


Figure (4- 79): ^{13}C-NMR spectrum of 1-(3-(3-(dimethylamino)phenyl)-1, 5-dioxo-9-(4-(3-oxobutanoyl)phenyl)-1, 5-dihydrobenzo[e][1, 3]oxazepin-4(3H)-yl)urea compound(26).

4.6 Synthesis of (5-mercapto-1, 3, 4-thiadiazol-2-yl)glycinoyl chloride compound(27).



Scheme (4-29): synthesis of (5-mercapto-1, 3, 4-thiadiazol-2-yl)glycinoyl chloride compound(27).

FTIR spectrum of (5-mercapto-1, 3, 4-thiadiazol-2-yl)glycinoyl chloride compound(27).

The FTIR spectrum of (5-mercapto-1, 3, 4-thiadiazol-2-yl)glycinoyl chloride. compound as shown in (fig.4-80) which indicates absorption bands at 3336 to $–NH_2$ and 3469 and 3255 Cm^{-1} to –NH , absorption band at 3061 Cm^{-1} to C-H (aromatic) ,

absorption band at 1599 cm^{-1} to C=N, absorption band at 2755 Cm^{-1} to SH, absorption band at 1573 Cm^{-1} to C=C (aromatic), absorption band at 1134 Cm^{-1} to C-N , absorption band at 1705 Cm^{-1} to C=O Acid chloride), absorption band at 1635 Cm^{-1} to C=N**,** absorption band at 779 Cm^{-1} to C-Cl. (151-153)

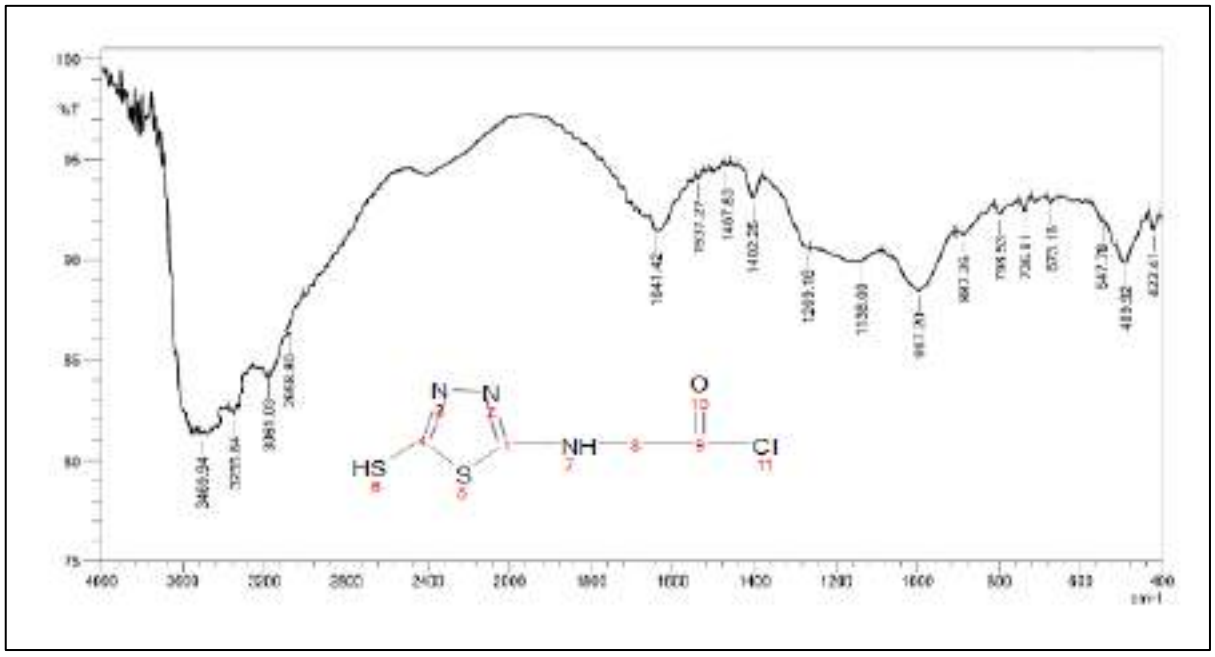


Figure (4- 80): FTIR spectrum of (5-mercapto-1, 3, 4-thiadiazol-2-yl)glycinoyl chloride compound(27).

^{1}HNMR spectrum of (5-mercapto-1, 3, 4-thiadiazol-2-yl)glycinoyl chloride compound(27).

^{1}HNMR spectrum of (5-mercapto-1, 3, 4-thiadiazol-2-yl)glycinoyl chloride. compound in (fig.4-81) the major signal at δ 1.5-2.1 ppm is characteristic of DMSO-d6 as solvent , multiplet singlate at (4.1-4.3 ppm) to SH. multiplet singlate at (3.3ppm) to NH**.** Silverstien, R.M., Webster, F.X and Kiemle, D.J.(2005). (151-153)

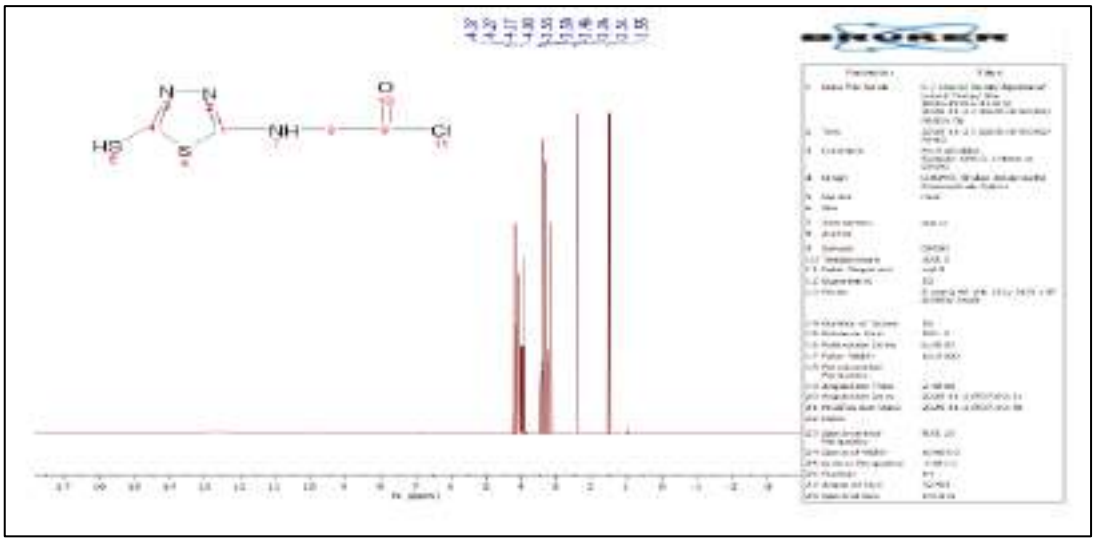


Figure (4- 81): ^{13}C-NMR spectrum of (5-mercapto-1, 3, 4-thiadiazol-2-yl)glycinoyl chloride compound(27).

^{13}C-NMR spectrum compound of (5-mercapto-1, 3, 4-thiadiazol-2-yl)glycinoyl chloride compound(27).

Single related to C-S at 68 ppm , singles related to C=N at 153 ppm , single related to C-N at 62 ppm, singles related to C=O at 169-172 ppm, single related to C-Cl at 78 ppm.. (151-153)

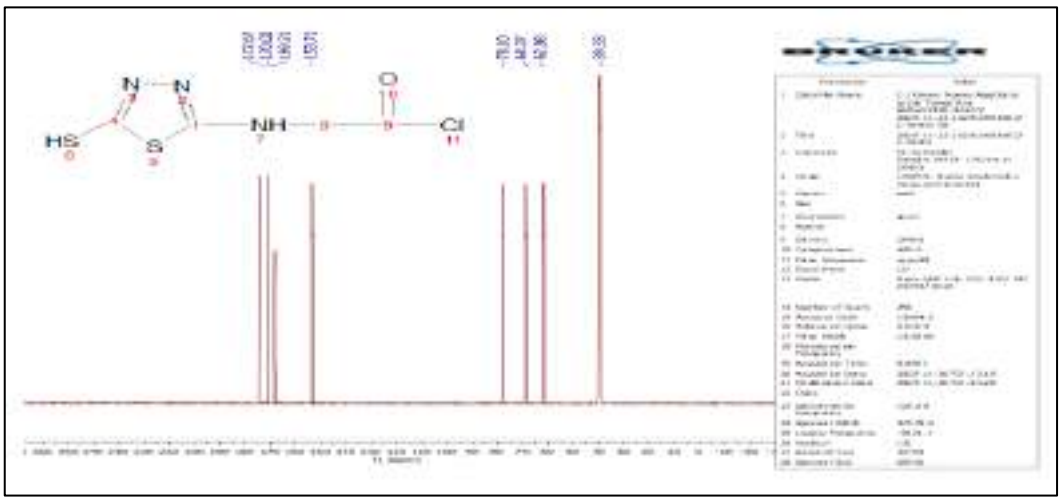
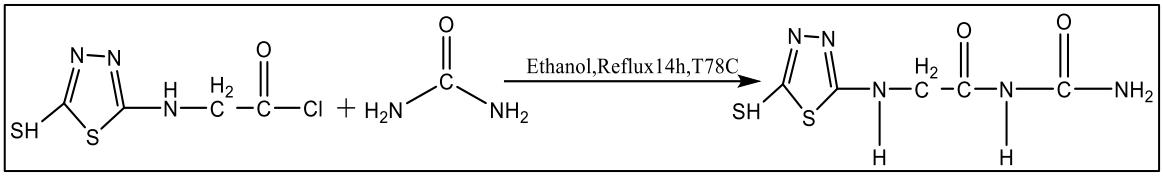


Figure (4- 82): ^{13}C-NMR spectrum of (5-mercapto-1, 3, 4-thiadiazol-2-yl)glycinoyl chloride compound(27).

4.7 Synthesis of N-(5-mercapto-1, 3, 4-thiadiazole-2-yl)-2-ureidoacetamide compound(28).



Scheme (4-30): synthesis of N-(5-mercapto-1, 3, 4-thiadiazole-2-yl)-2-ureidoacetamide compound(28).

FTIR spectrum of *N-(5-mercapto-1, 3, 4-thiadiazole-2-yl)-2-ureidoacetamide* compound(28).

The FTIR spectrum of N-(5-mercapto-1, 3, 4-thiadiazole-2-yl)-2-ureidoacetamide compound as shown in (fig.4-83) which indicates absorption bands at 3550 to $–NH_2$ and 3408 Cm^{-1} to –NH , absorption band at 3194 Cm^{-1} to C-H (aromatic) , absorption band at 2981 cm^{-1} to C-H(alphatic), absorption band at 1599 cm^{-1} to C=N, absorption band at 2755 Cm^{-1} to SH, absorption band at 1510 Cm^{-1} to C=C (aromatic), absorption bands at 1155 Cm^{-1} to C-N , absorption band at 1618 Cm^{-1} to C=O (Amide), absorption band at 1689 Cm^{-1} to C=O (Amide), absorption bands at 1560 Cm^{-1} to C=N. (151-153)

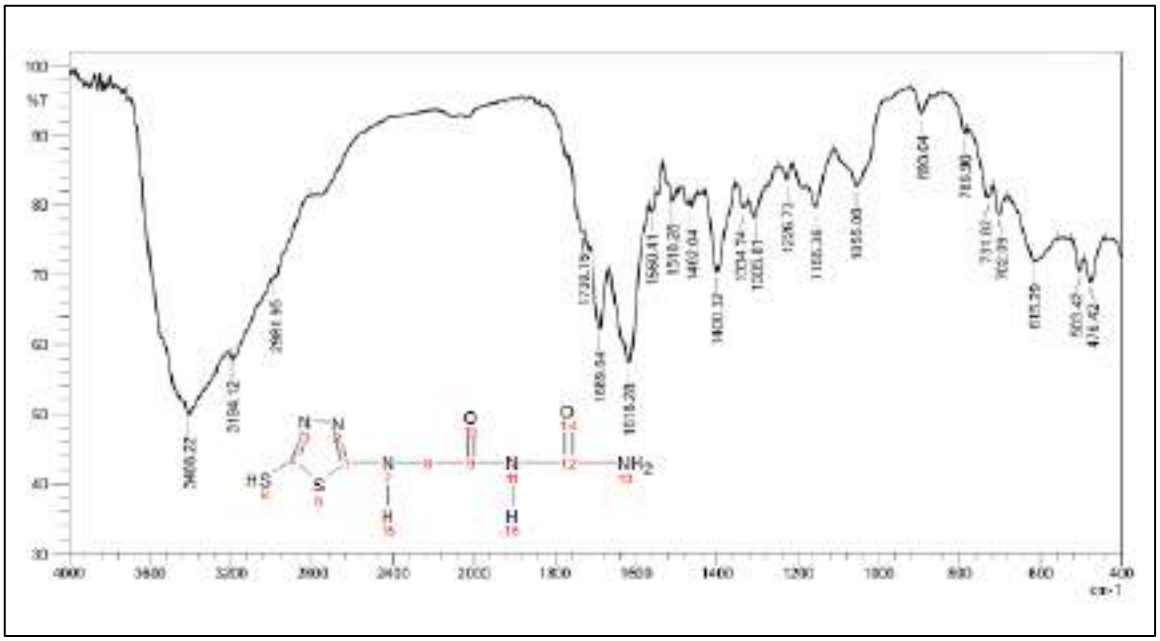


Figure (4- 83): FTIR spectrum of N-(5-mercapto-1, 3, 4-thiadiazole-2-yl)-2-ureidoacetamide compound(28).

^{1}HNMR spectrum of N-(5-mercapto-1, 3, 4- thiadiazole-2-yl) ureidoacetamide compound compound(28).

^{1}HNMR spectrum of N-(5-mercapto-1, 3, 4-thiadiazole-2-yl)-2-ureidoacetamide compound in (fig.4-84) multiplet singlate at (3.7-4.2 ppm) to SH. multiplet singlate at (3.1-3.6 ppm) to NH_2**,** singlate at (2, 3 ppm) to CH_2. Silverstien, R.M., Webster, F.X and Kiemle, D.J.(2005). (151-153)

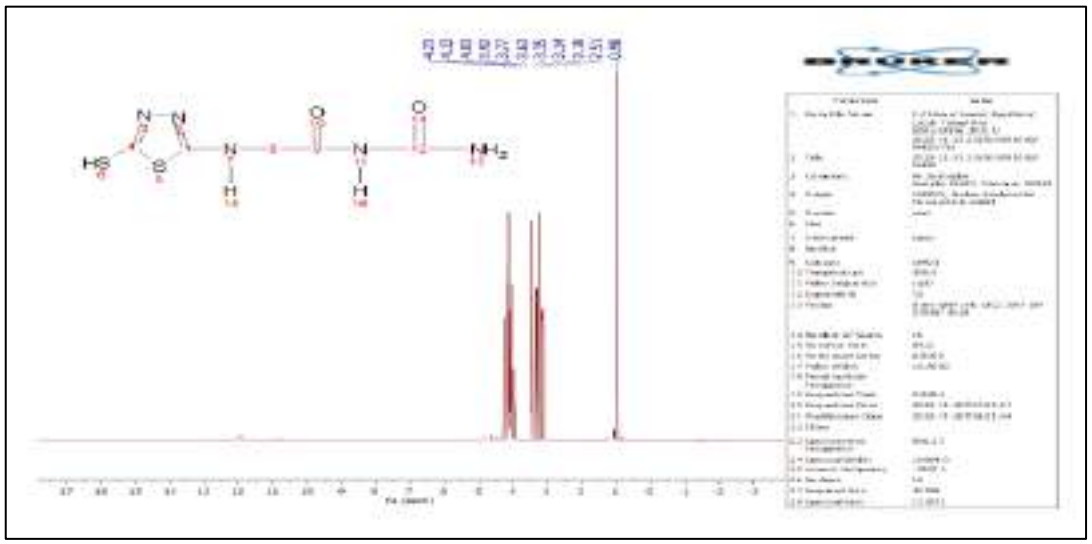


Figure (4- 84): ^{1}HNMR spectrum of N-(5-mercapto-1, 3, 4-thiadiazole-2-yl)-2-ureidoacetamide compound(28).

^{13}C-NMR spectrum compound of N-(5-mercapto-1, 3, 4- thiadiazole-2-yl) ureidoacetamide compound compound(28).

Single related to C-S at 56 ppm , singles related to C=N at 156-160 ppm , singles related to C-N at 62 ppm, singles related to C=O (amide) at 162-174 ppm. (151-153)

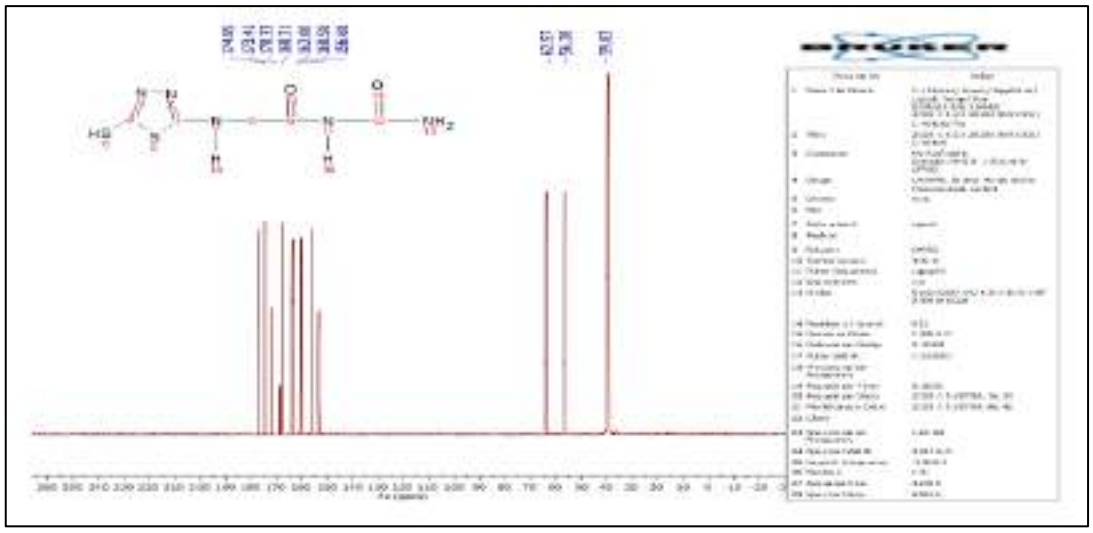
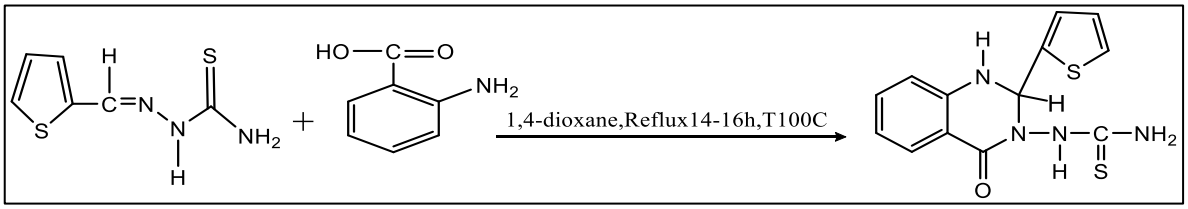


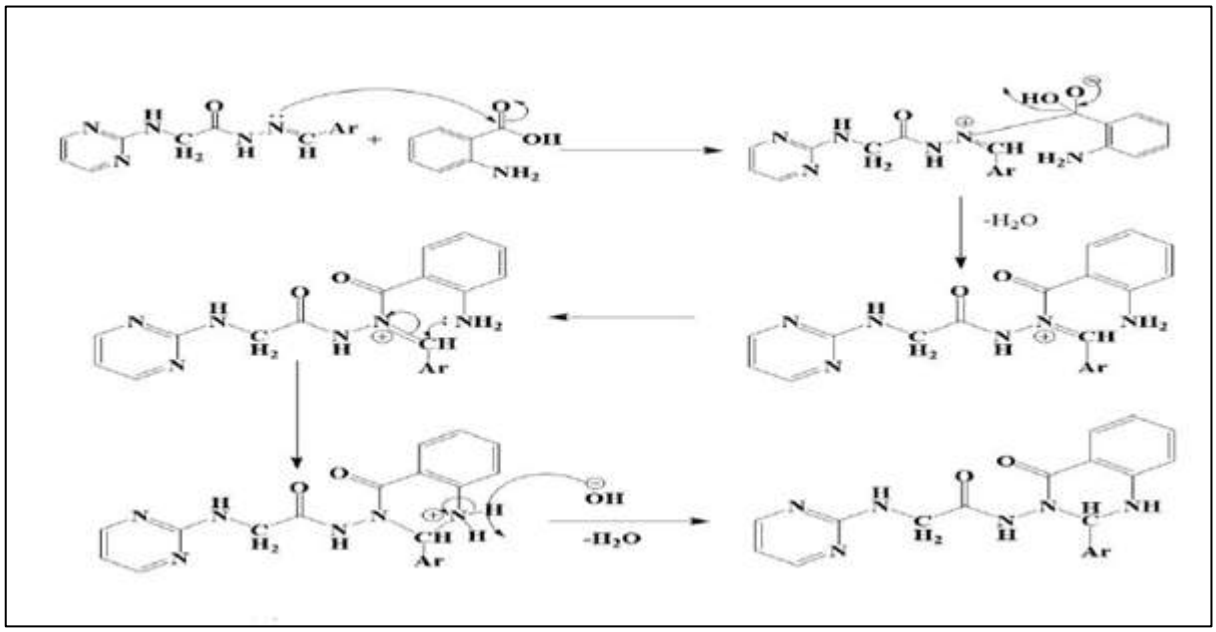
Figure (4- 85): ^{13}C-NMR spectrum of N-(5-mercapto-1, 3, 4-thiadiazole-2-yl)-2-ureidoacetamide compound(28).

4.8 Synthesis of some 2, 3-dihydroquinosulin4-one derivatives.(29 -31)

4.8.1 Synthesis of 1-(4-oxo-2-(thiophen-2-yl)-1, 4-dihydroquinazolin-3(2H)-yl)thiourea compound(29).



Scheme (4-31): synthesis of 1-(4-oxo-2-(thiophen-2-yl)-1, 4-dihydroquinazolin-3(2H)-yl)thiourea compound(29).



Scheme (4-32): Mechanism synthesis of some 2, 3-dihydroquinosulin4-one derivatives

FTIR spectrum of 1-(4-oxo-2-(thiophen-2-yl)-1, 4-dihydroquinazolin-3(2H)-yl)thiourea compound(29).

The FTIR spectrum of the preparation of 1-(4-oxo-2-(thiophen-2-yl)-1, 4-dihydroquinazolin-3(2H)-yl)thiourea as shown in (fig.4-86) which indicates absorption band at 3448 to $–NH_2$, absorption band at 3182 Cm^{-1} to C-H (aromatic) , absorption band at 2964 Cm^{-1} to C-H (Aliphatic), absorption band at 1192 Cm^{-1} to C=S, absorption band at 1589 Cm^{-1} to C=C (phenyl ring), absorption band at 1080 Cm^{-1} to C-N, absorption band at 1691 Cm^{-1} to C=O, absorption band at 1045 Cm^{-1} to C-S. (151-153)

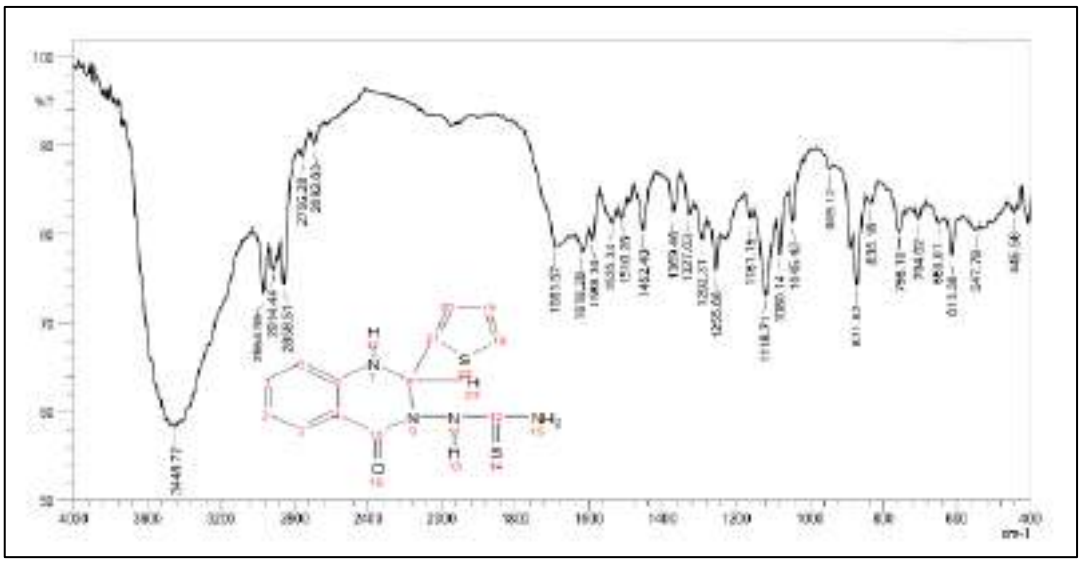


Figure (4- 86): FTIR spectrum of 1-(4-oxo-2-(thiophen-2-yl)-1, 4-dihydroquinazolin-3(2H)-yl)thiourea compound(29).

^{1}HNMR spectrum of 1-(4-oxo-2-(thiophen-2-yl)-1, 4-dihydroquinazolin-3(2H)-yl)thiourea compound(29).

^{1}HNMR spectrum of 1-(4-oxo-2-(thiophen-2-yl)-1, 4-dihydroquinazolin-3(2H)-yl)thiourea in (fig.4-87) singles at (6.5-8.3 δ ppm) to (4H, phenyl ring), multiplet singlate at (3.3 to 4.1 ppm) to $–NH_2$, single at 2.5 ppm to =CH**.** (151-153)

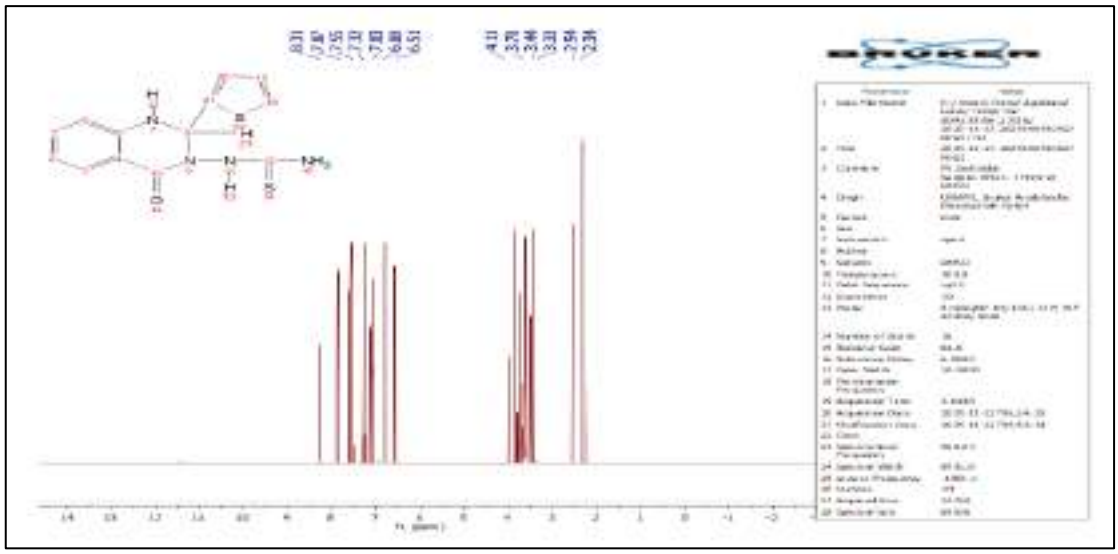


Figure (4- 87): ^{1}HNMR spectrum of 1-(4-oxo-2-(thiophen-2-yl)-1, 4-dihydroquinazolin-3(2H)-yl)thiourea compound(29).

^{13}C-NMR spectrum of 1-(4-oxo-2-(thiophen-2-yl)-1, 4-dihydroquinazolin-3(2H)-yl)thiourea compound(29).

The signals of olefinic and aromatic carbons appear in the third region between 114 and 136ppm , singles related to C=N at 152ppm , single related to C-N at 66 ppm, singles related to C=O (amide) at 170 ppm, single related to C=S at 178 ppm. (151-153)

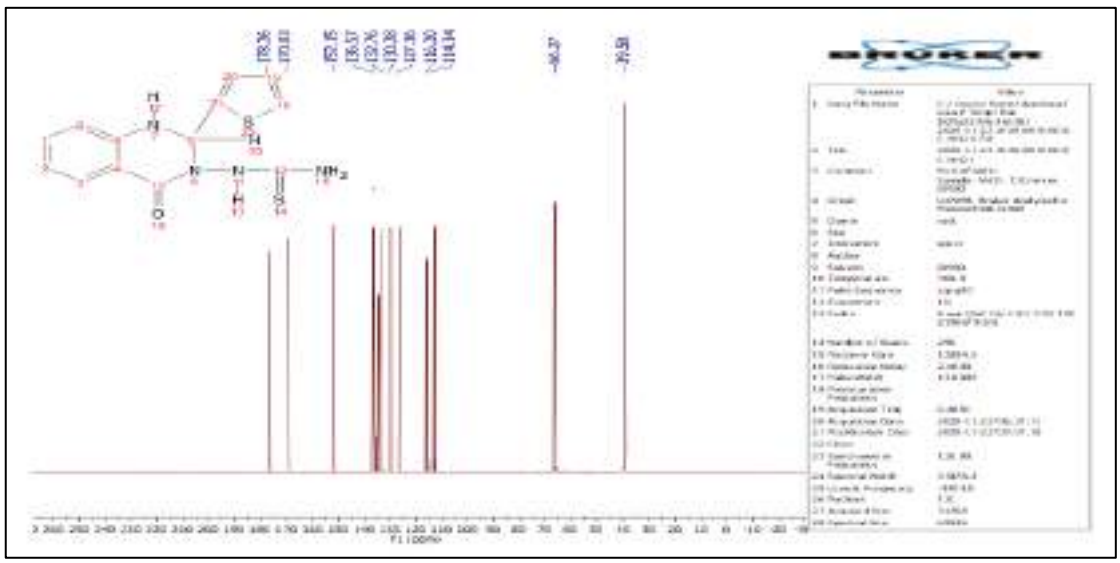
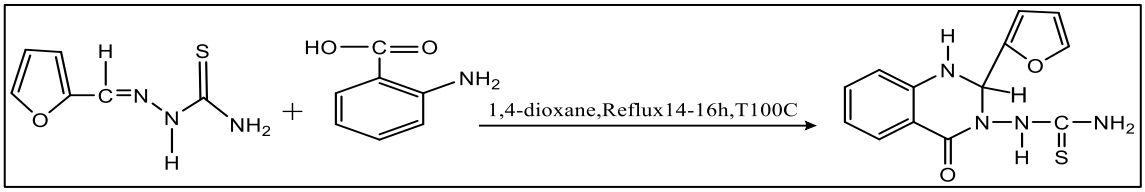


Figure (4- 88): ^{13}C-NMR spectrum of 1-(4-oxo-2-(thiophen-2-yl)-1, 4-dihydroquinazolin-3(2H)-yl)thiourea compound(29).

4.8.2 *Synthesis* of 1-(2-(furan-2-yl)-4-oxo-1, 4-dihydroquinazolin-3(2H)-yl)thiourea compound(30).



Scheme (4-33): synthesis of 1-(2-(furan-2-yl)-4-oxo-1, 4-dihydroquinazolin-3(2H)-yl)thiourea compound(30).

FTIR spectrum of 1-(2-(furan-2-yl)-4-oxo-1, 4-dihydroquinazolin-3(2H)-yl)thiourea compound(30).

The FTIR spectrum of the preparation of 1-(2-(furan-2-yl)-4-oxo-1, 4-dihydroquinazolin-3(2H)-yl)thiourea as shown in (fig.4-89) which indicates absorption band at 3475 to $–NH_2$ and 3427 to -NH , absorption band at 3182 Cm^{-1} to C-H (aromatic) , absorption band at 2964 and 2856 Cm^{-1} to C-H (Aliphatic), absorption band at 1116 Cm^{-1} to C=S, absorption band at 1514 Cm^{-1} to C=C (phenyl ring), absorption band at 1080 Cm^{-1} to C-N, absorption band at 1668 Cm^{-1} to C=O, absorption band at 1047 Cm^{-1} to C-O. (151-153)

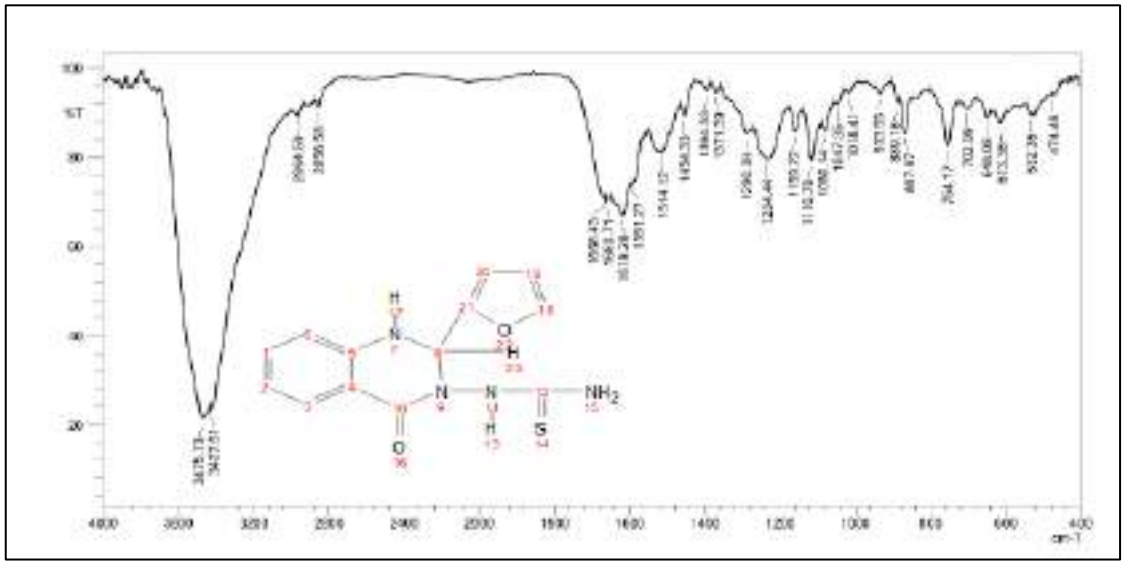


Figure (4- 89): FTIR spectrum of 1-(2-(furan-2-yl)-4-oxo-1, 4-dihydroquinazolin-3(2H)-yl)thiourea compound(30).

^{1}HNMR spectrum of 1-(2-(furan-2-yl)-4-oxo-1, 4-dihydroquinazolin-3(2H)-yl)thiourea compound(30).

^{1}HNMR spectrum of 1-(2-(furan-2-yl)-4-oxo-1, 4-dihydroquinazolin-3(2H)-yl)thiourea in (fig.4-90) the major signal at δ 1.8 ppm is characteristic of DMSO-d6 as solvent , singles at (6.4-8.0 δ ppm) to (4H, phenyl ring), multiplet singlate at (3.4 to 4.1 ppm) to $–NH_2$, single at 2.5 ppm to =CH**.** (151-153)

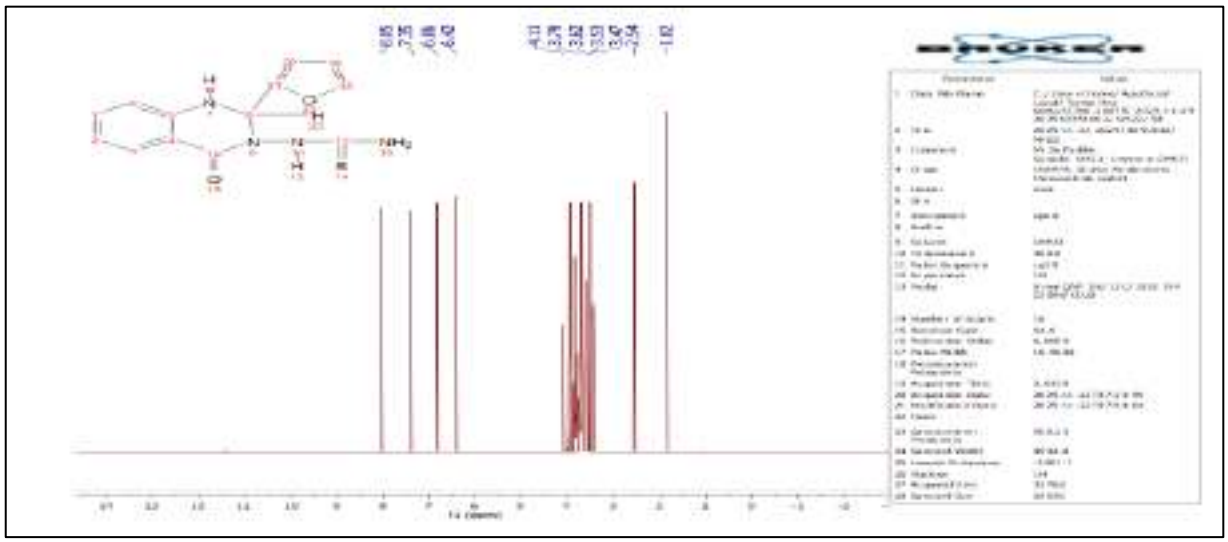


Figure (4- 90): ^{1}HNMR spectrum of 1-(2-(furan-2-yl)-4-oxo-1, 4-dihydroquinazolin-3(2H)-yl) thiourea compound(30).

^{13}C-NMR spectrum of 1-(2-(furan-2-yl)-4-oxo-1, 4-dihydroquinazolin-3(2H)-yl)thiourea compound(30).

The signals of olefinic and aromatic carbons appear in the third region between 110 and 134 ppm , singles related to C=N at 152ppm , single related to C-N at 66 ppm, singles related to C=O (amide) at 170 ppm, single related to C=S at 178 ppm. (151-153)

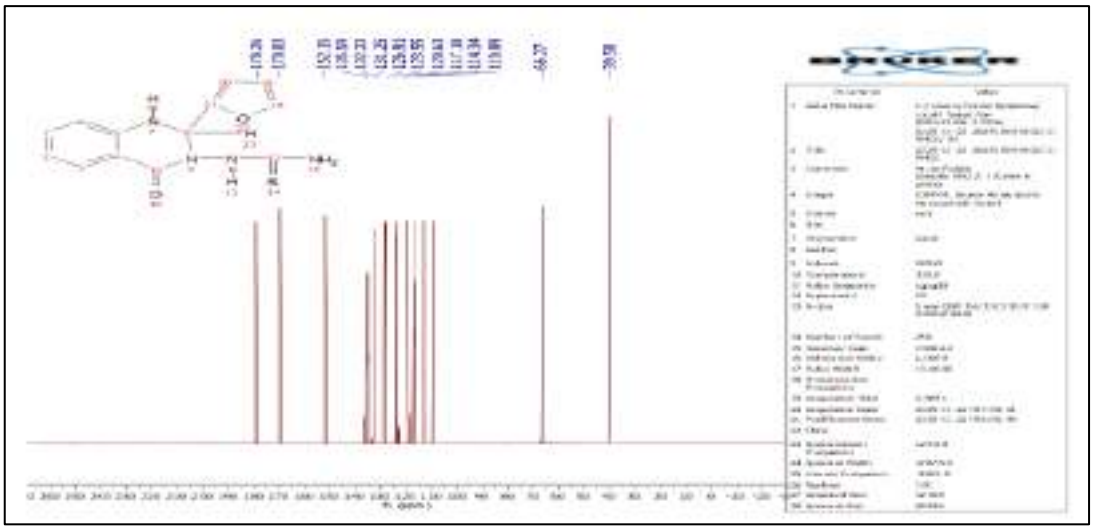
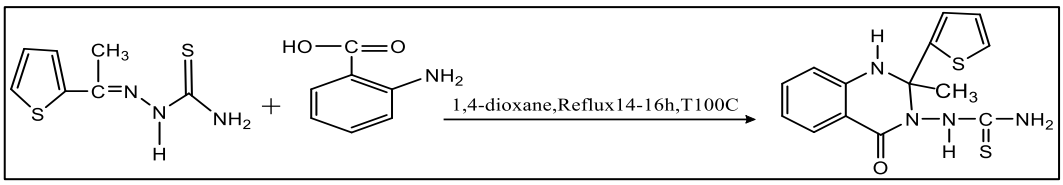


Figure (4- 91): ^{13}C-NMR spectrum of 1-(2-(furan-2-yl)-4-oxo-1, 4-dihydroquinazolin-3(2H)-yl)thiourea compound(30).

4.8.3 *Synthesis* of 1-(4-oxo-2-(thiophen-2-yl)-1, 4-dihydroquinazolin-3(2H)-yl)thiourea compound(31).



Scheme (4-34): synthesis of 1-(4-oxo-2-(thiophen-2-yl)-1, 4-dihydroquinazolin-3(2H)-yl)thiourea compound(31).

FTIR spectrum of 1-(4-oxo-2-(thiophen-2-yl)-1, 4-dihydroquinazolin-3(2H)-yl)thiourea compound(31).

The FTIR spectrum of the preparation of 1-(4-oxo-2-(thiophen-2-yl)-1, 4-dihydroquinazolin-3(2H)-yl)thiourea as shown in (fig.4-92) which indicates absorption band at 3471 to $–NH_2$ and 3263 to -NH, absorption band at 3170 Cm^{-1} to C-H (aromatic) , absorption band at 2964 Cm^{-1} to C-H (Aliphatic), absorption band at 1161Cm^{-1} to C=S, absorption band at 1531 Cm^{-1} to C=C (phenyl ring), absorption band at 1246 Cm^{-1} to C-N, absorption band at 1643 Cm^{-1} to C=O, absorption band at 1002 Cm^{-1} to C-S, absorption band at 1317 Cm^{-1} to CH_3**.** (151-153)

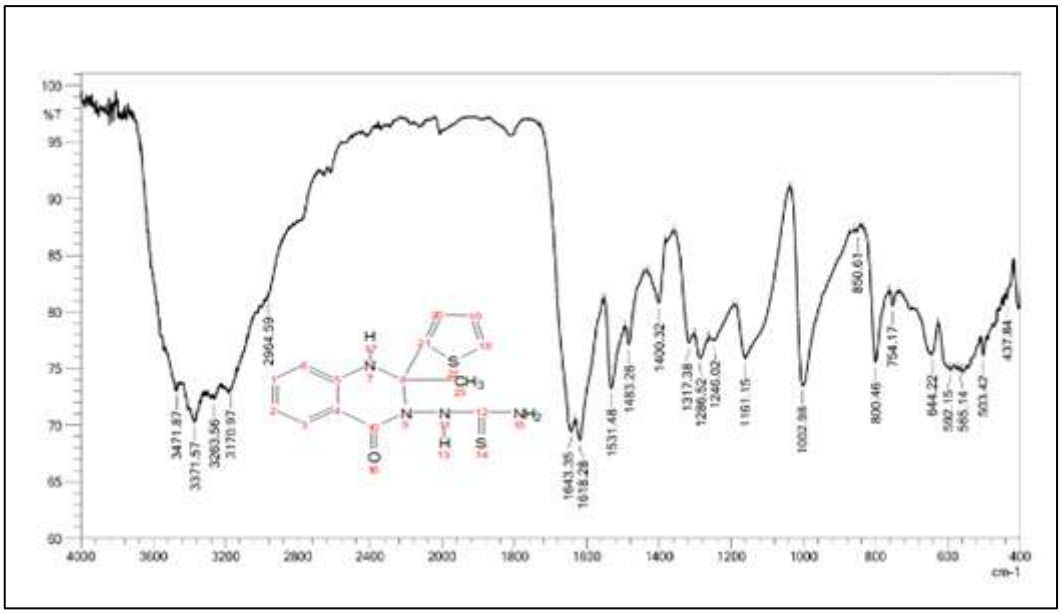


Figure (4- 92): ^{13}C-NMR spectrum of 1-(4-oxo-2-(thiophen-2-yl)-1, 4-dihydroquinazolin-3(2H)-yl)thiourea compound(31).

^{1}HNMR spectrum of 1-(4-oxo-2-(thiophen-2-yl)-1, 4-dihydroquinazolin-3(2H)-yl)thiourea compound(31).

^{1}HNMR spectrum of 1-(4-oxo-2-(thiophen-2-yl)-1, 4-dihydroquinazolin-3(2H)-yl)thiourea in (fig.4-93) singles at (6.4-8.6 δ ppm) to (4H, phenyl ring), multiplet singlate at (3.3 to 4.1 ppm) to $-NH_2$, singles at 2.3-2.5 ppm to =CH**,** singles at 1.3 ppm to CH_3. Silverstien, R.M., Webster, F.X and Kiemle, D.J.(2005). (151-153)

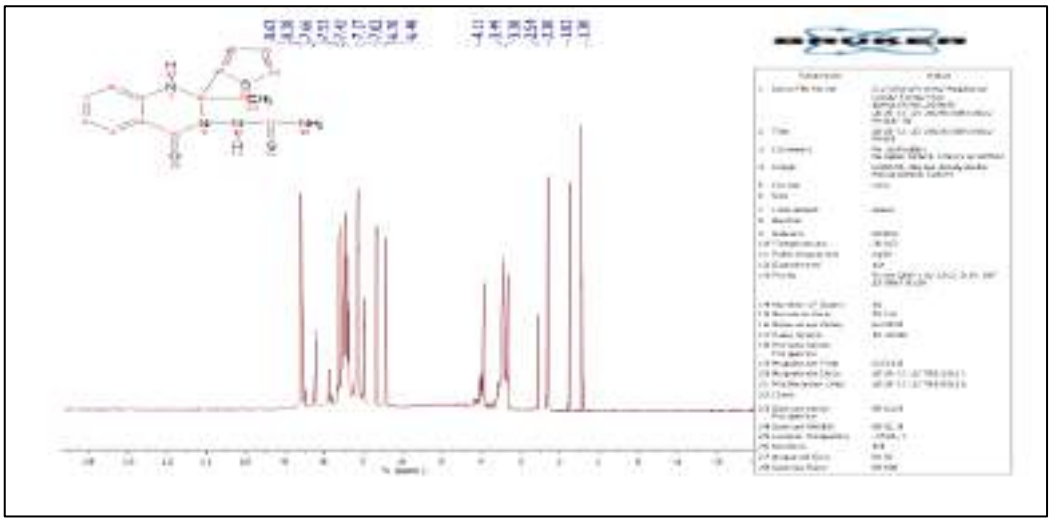


Figure (4- 93): ^{13}C-NMR spectrum of 1-(4-oxo-2-(thiophen-2-yl)-1, 4-dihydroquinazolin-3(2H)-yl)thiourea compound(31).

^{13}C-NMR spectrum of 1-(4-oxo-2-(thiophen-2-yl)-1, 4-dihydroquinazolin-3(2H)-yl)thiourea compound(31).

The signals of olefinic and aromatic carbons appear in the third region between 110 and 133ppm , single related to C=N at 152ppm , single related to C-N at 67 ppm, singles related to C=O (amide) at 170 ppm, singles related to C=S at 178-182 ppm. (151-153)

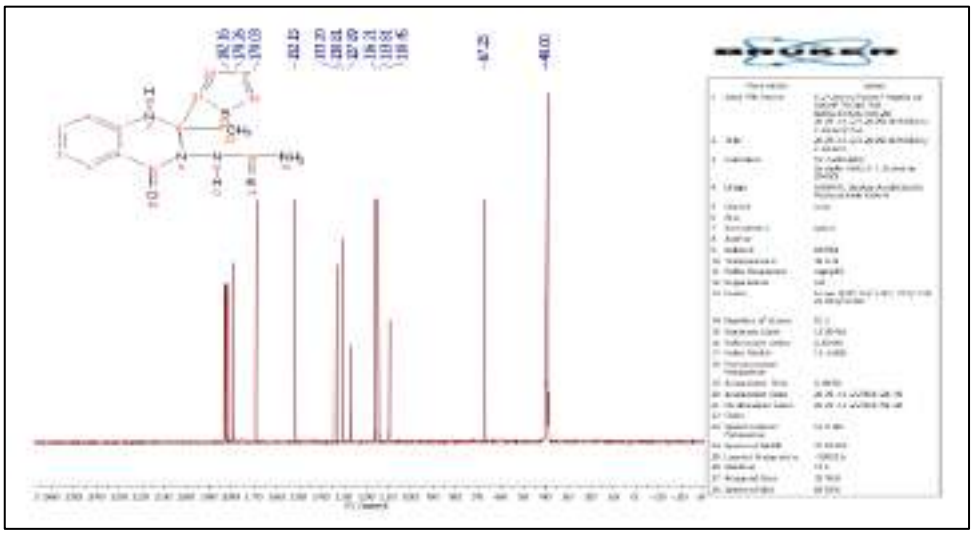
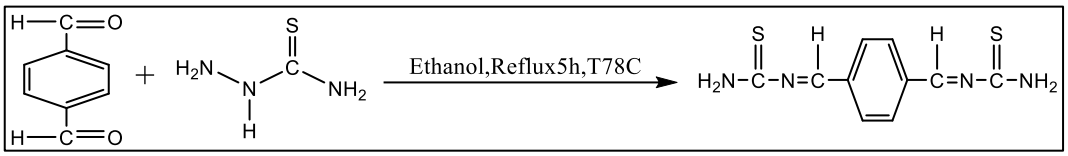
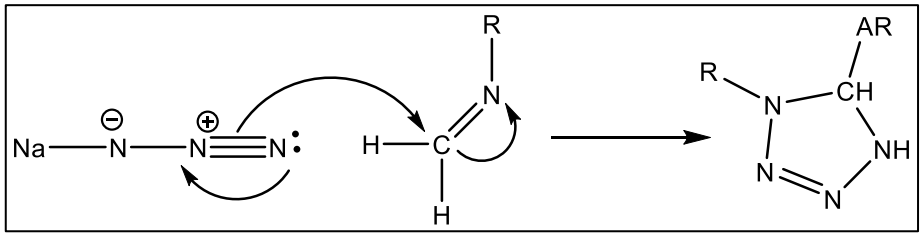


Figure (4- 94): ^{13}C-NMR spectrum of (Z)-N-(3-amino-2-formylphenyl)-2-(1-(thiophen-2-yl)ethylidene)hydrazine-1-carbothioamide compound(31).

4.9 Synthesis of 1, 1'-(1, 4- phenylenebis(methaneylylidene))bis(thiourea) compound(32).



Scheme (4-35): synthesis of 1, 1'-(1, 4-phenylenebis(methaneylylidene))bis(thiourea) compound(32).



Scheme (4-36): of Mechanism of synthesis tetrazole

FTIR spectrum of 1, 1'-(1, 4-phenylenebis(methaneylylidene))bis(thiourea) compound(32).

The FTIR spectrum of 1, 1'-(1, 4-phenylenebis(methaneylylidene))bis(thiourea) as shown in (fig.4-95) which indicates absorption bands at 3369 and 3261 cm^{-1} to $–NH_2$ stretching , absorption band at 3178 cm^{-1} to C-H (aromatic), absorption band at 2995 and 2970 cm^{-1} to C-H(alphatic), absorption band at 1645cm^{-1} to C=N, absorption band at 1284 Cm^{-1} to C=S, absorption band at 1531Cm^{-1} to C=C (aromatic). (151-153)

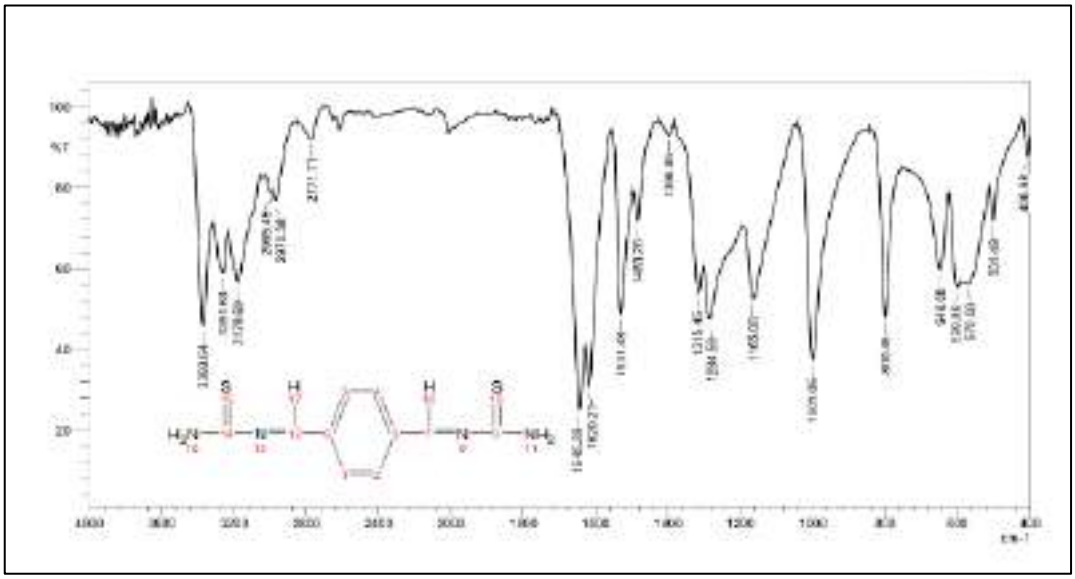


Figure (4- 95): FTIR spectrum of 1, 1'-(1, 4-phenylenebis(methaneylylidene))bis(thiourea) compound(32).

^{1}HNMR spectrum of 1, 1'-(1, 4- phenylenebis(methaneylylidene)) bis(thiourea) compound(32).

^{1}HNMR spectrum of 1, 1'-(1, 4- phenylenebis(methaneylylidene))bis(thiourea) in (fig.4-96) the major signal at δ 2.5 ppm is characteristic of DMSO-d6 as solvent , singlate at (7.3-8.6 δ ppm) to (4H, phenyl ring), single at (3.2-4.5 ppm) to $–NH_2$. (151-153)

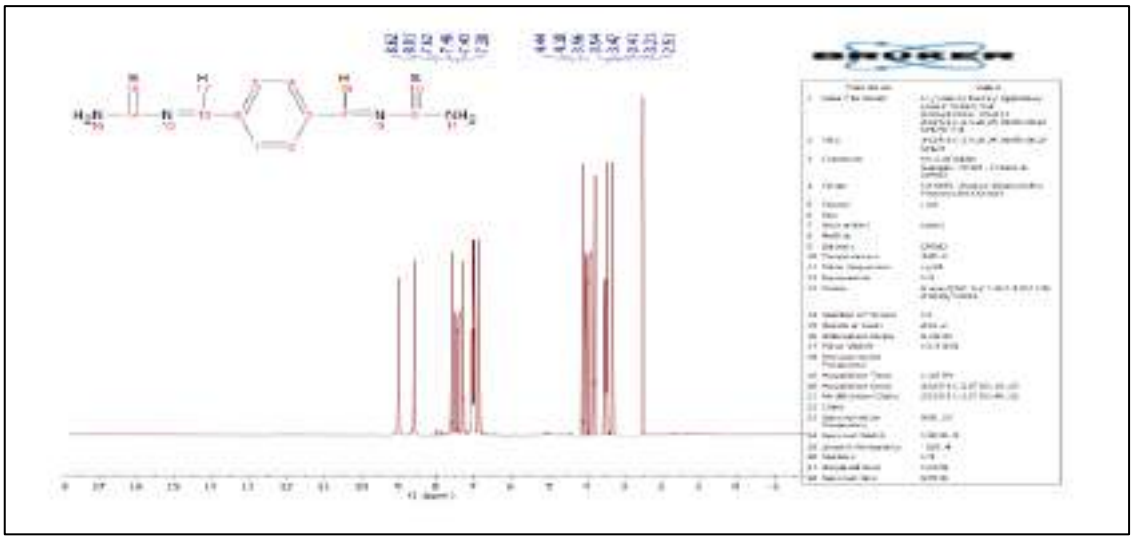


Figure (4- 96): ^{1}HNMR spectrum of 1, 1'-(1, 4-phenylenebis(methaneylylidene))bis(thiourea) compound(32).

^{13}C-NMR spectrum of 1, 1'-(1, 4- phenylenebis(methaneylylidene)) bis(thiourea) compound(32).

The signals of olefinic and aromatic carbons appear in the third region between 110 and 132 ppm, single related to C=N at 140 ppm , single related to C-N at 64 ppm, single related to C=S at 182 ppm. (151-153)

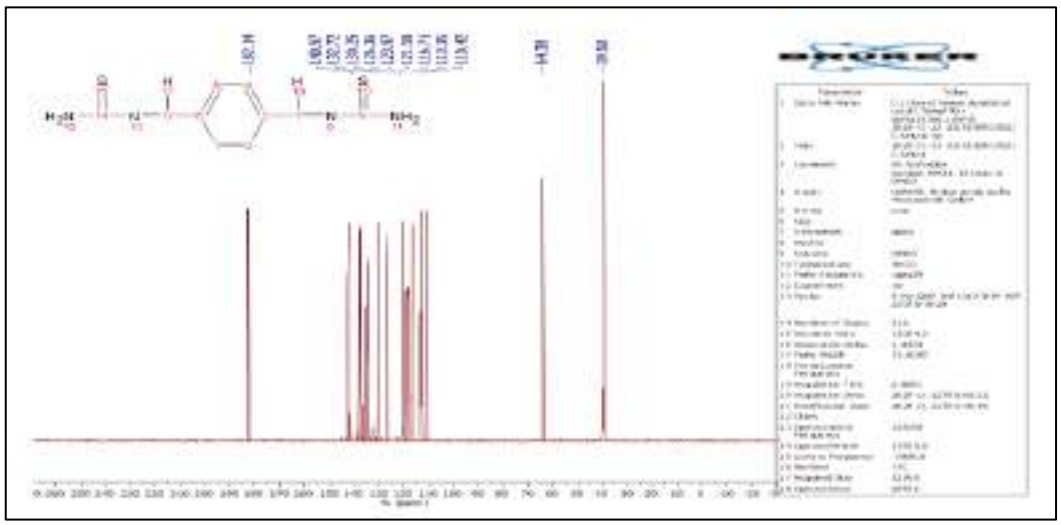
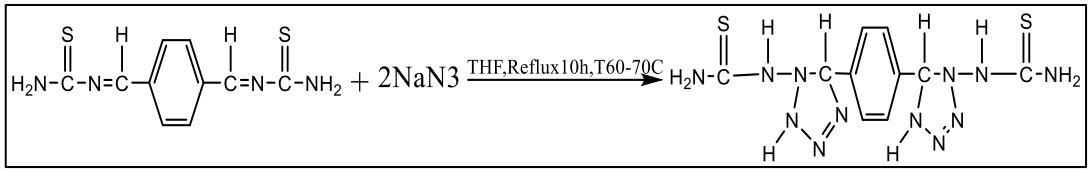


Figure (4- 97): ^{13}C-NMR spectrum of 1, 1'-(1, 4-phenylenebis(methaneylylidene)) bis(thiourea) compound(32).

4.10 *Synthesis* of 1, 1'-(1, 4-phenylenebis(4, 5-dihydro-1H-tetrazole-5, 1-diyl))bis(thiourea) compound(33).



Scheme (4-37): synthesis of 1, 1'-(1, 4-phenylenebis(4, 5-dihydro-1H-tetrazole-5, 1-diyl))bis(thiourea) compound(33).

FTIR spectrum of 1, 1'-(1, 4-phenylenebis(4, 5-dihydro-1H-tetrazole-5, 1-diyl))bis(thiourea) compound(33).

The FTIR spectrum of 1, 1'-(1, 4-phenylenebis(4, 5-dihydro-1H-tetrazole-5, 1-diyl))bis(thiourea) as shown in (fig.4-98) which indicates absorption bands at 3464 and 3415 cm^{-1} to $–NH_2$ stretching and 3232 Cm^{-1} to -NH, absorption band at 3176 cm^{-1} to C-H (aromatic), absorption band at 2879 and 2791 cm^{-1} to C-H(alphatic),absorption band at 1680cm^{-1} to C=N, absorption band at 1271 Cm^{-1} to C=S, absorption band at 1543Cm^{-1} to C=C (aromatic), absorption band at 1398-1462 Cm^{-1} to N=N, absorption band at 1238 Cm^{-1} to C-N. (151-153)

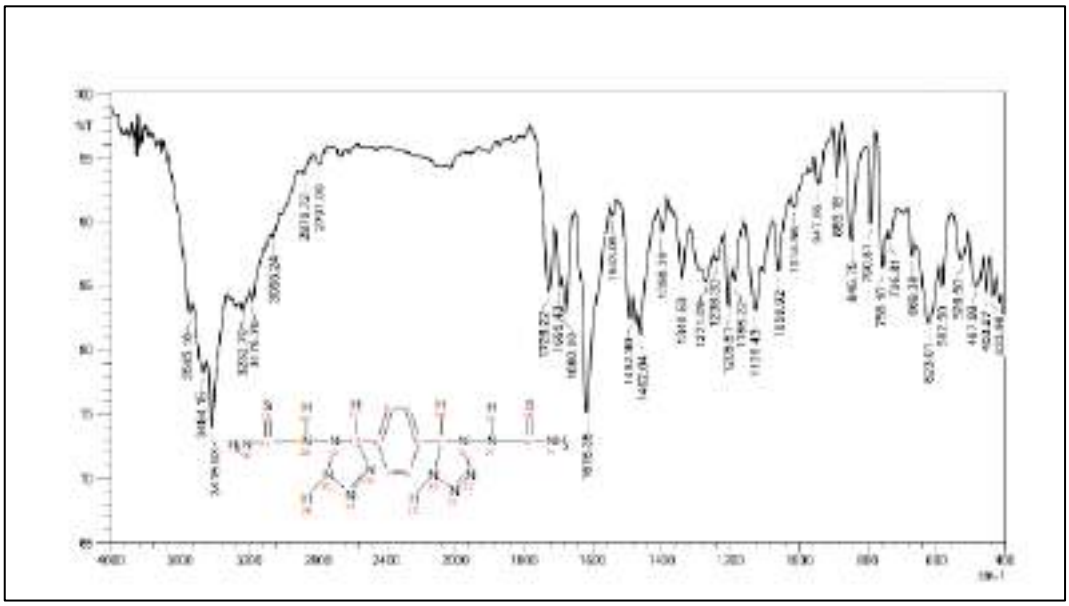


Figure (4- 98): FTIR spectrum of 1, 1'-(1, 4-phenylenebis(4, 5-dihydro-1H-tetrazole-5, 1-diyl))bis(thiourea) compound(33).

^{1}HNMR spectrum of 1, 1'-(1, 4-phenylenebis(4, 5-dihydro-1H-tetrazole-5, 1-diyl))bis(thiourea) compound(32).

^{1}HNMR spectrum of 1, 1'-(1, 4-phenylenebis(4, 5-dihydro-1H-tetrazole-5, 1-diyl))bis(thiourea) in (fig.4-99) the major signal at δ 2.5 ppm is characteristic of DMSO-d6 as solvent , singlate at (6.7-7.8 δ ppm) to (4H, phenyl ring), singles at (3.5 ppm) to $–NH_2$. (151-153)

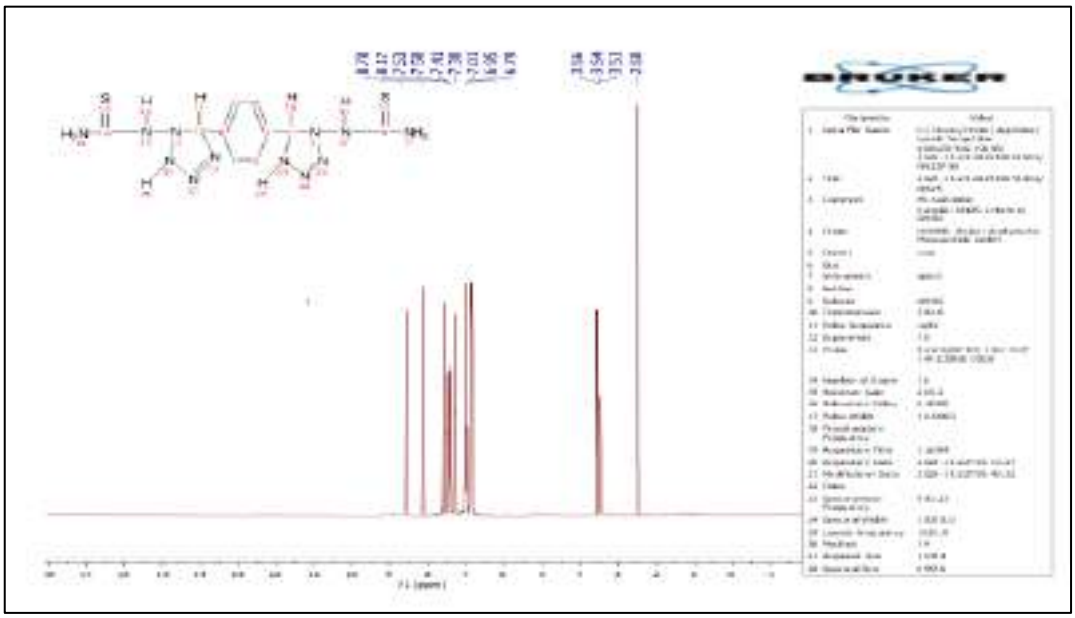


Figure (4- 99): ^{1}HNMR spectrum of 1, 1'-(1, 4-phenylenebis(4, 5-dihydro-1H-tetrazole-5, 1-diyl))bis(thiourea) compound(33).

^{13}C-NMR spectrum of 1, 1'-(1, 4-phenylenebis(4, 5-dihydro-1H-tetrazole-5, 1-diyl))bis(thiourea) compound(33).

The signals of olefinic and aromatic carbons appear in the third region between 111 and 130 ppm, single related to C=N at 150 ppm , single related to C-N at 64 ppm, single related to C=S at 182 ppm. (151-153)

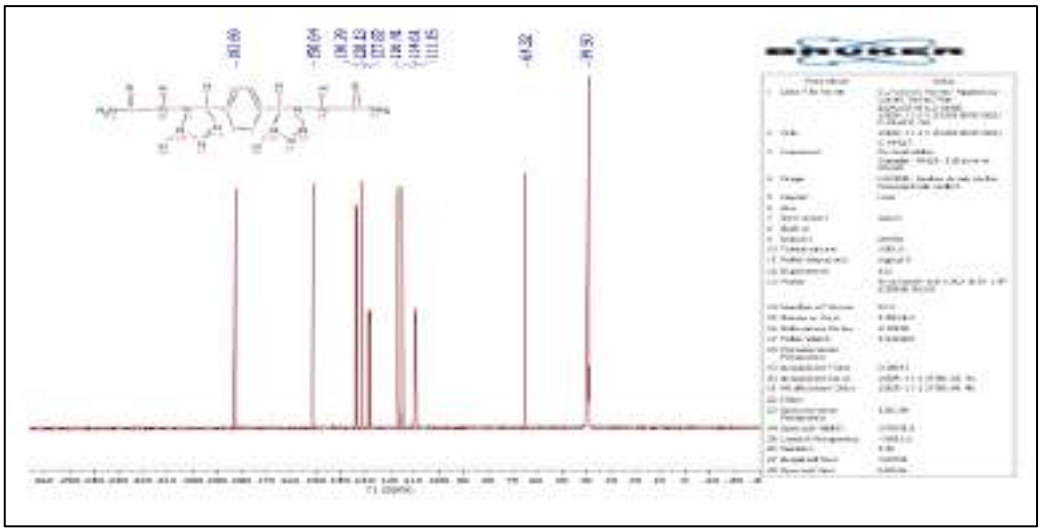
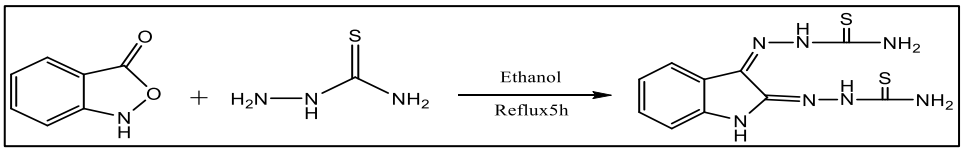


Figure (4- 100): ^{13}C-NMR spectrum of 1, 1'-(1, 4-phenylenebis(4, 5-dihydro-1H-tetrazole-5, 1-diyl))bis(thiourea) compound(33).

4.11 Synthesis of 2, 2'-((Z)-indoline-2, 3-diylidene)bis(hydrazine-1-carbothioamide) compound(34).



Scheme (4-38): structure of synthesis of 2, 2'-((Z)-indoline-2, 3-diylidene)bis(hydrazine-1-carbothioamide) compound(34).

FTIR spectrum of 2, 2'-((Z)-indoline-2, 3-diylidene)bis(hydrazine-1-carbothioamide) compound(34).

The FTIR spectrum of 2, 2'-((Z)-indoline-2, 3-diylidene)bis(hydrazine-1-carbothioamide) as shown in (fig.4-101) which indicates absorption bands at 3468 and 3385 cm^{-1} to $–NH_2$ stretching, and 3261 Cm^{-1} to -NH , absorption band at 3180 cm^{-1} to C-H (aromatic), absorption band at 2970 cm^{-1} to C-H(alphatic), absorption band at 1641cm^{-1} to C=N, absorption band at 1284 Cm^{-1} to C=S, absorption band at 15 29Cm^{-1} to C=C (aromatic). (151-153)

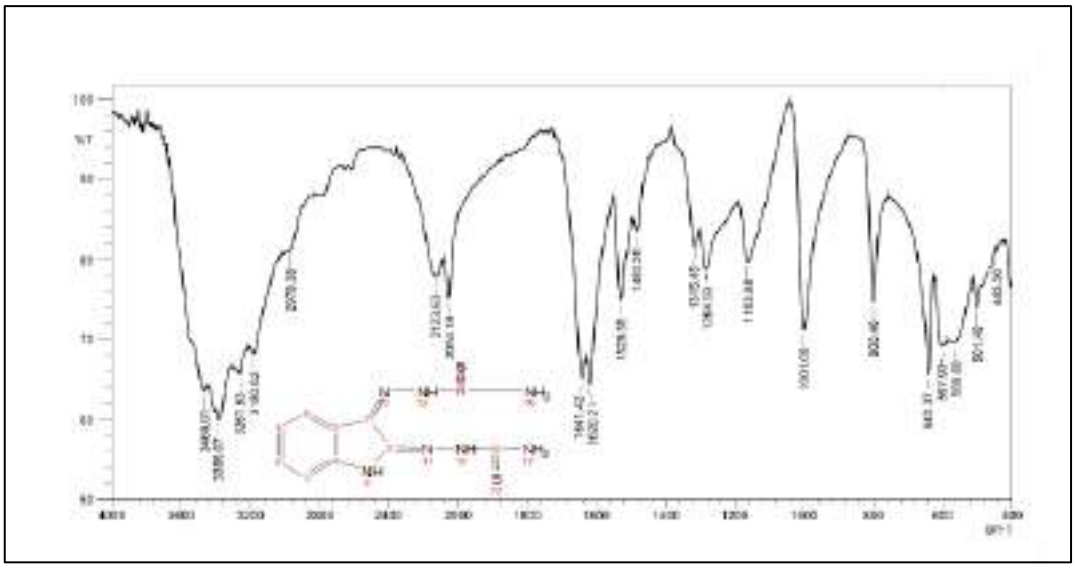


Figure (4- 101): FTIR spectrum of 2, 2'-((Z)-indoline-2, 3-diylidene)bis(hydrazine-1-carbothioamide) compound(34).

^{1}HNMR spectrum of 2, 2'-((Z)-indoline-2, 3-diylidene)bis(hydrazine-1-carbothioamide) compound(34).

^{1}HNMR spectrum of 2, 2'-((Z)-indoline-2, 3-diylidene)bis(hydrazine-1-carbothioamide) in (fig.4-102) the major signal at δ 2.5 ppm is characteristic of DMSO-d6 as solvent , singlate at (6.8-8.5δ ppm) to (4H, phenyl ring), single at (3.5-4.5 ppm) to $–NH_2$. **(151-153)**

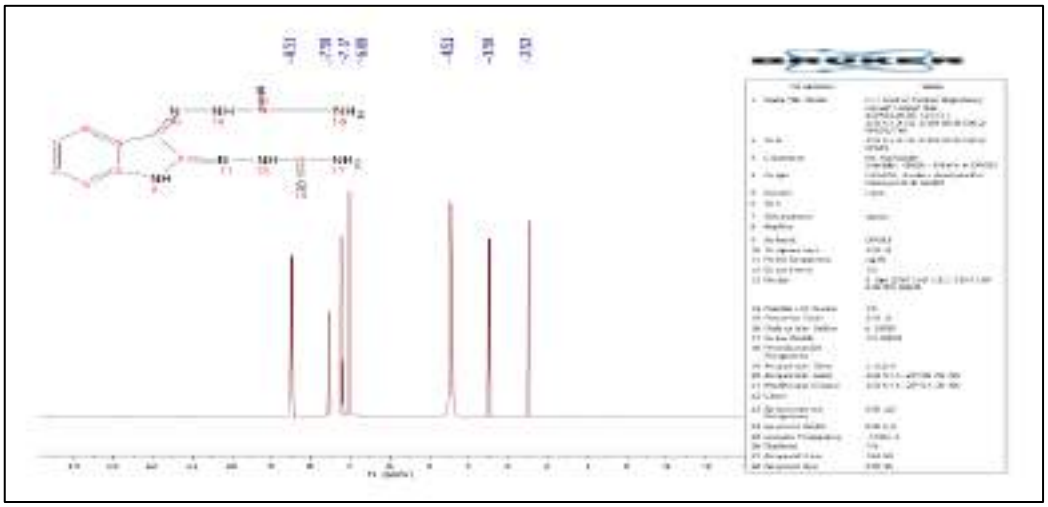


Figure (4- 102): ^{1}HNMR spectrum of 2, 2'-((Z)-indoline-2, 3-diylidene)bis(hydrazine-1-carbothioamide) compound(34).

^{13}C-NMR spectrum of 2, 2'-((Z)-indoline-2, 3-diylidene)bis(hydrazine-1-carbothioamide) compound(34).

The signals of olefinic and aromatic carbons appear in the third region between 120 and 130 ppm, single related to C=N at 151 ppm , single related to C-N at 64 ppm, single related to C=S at 180 ppm. (151-153)

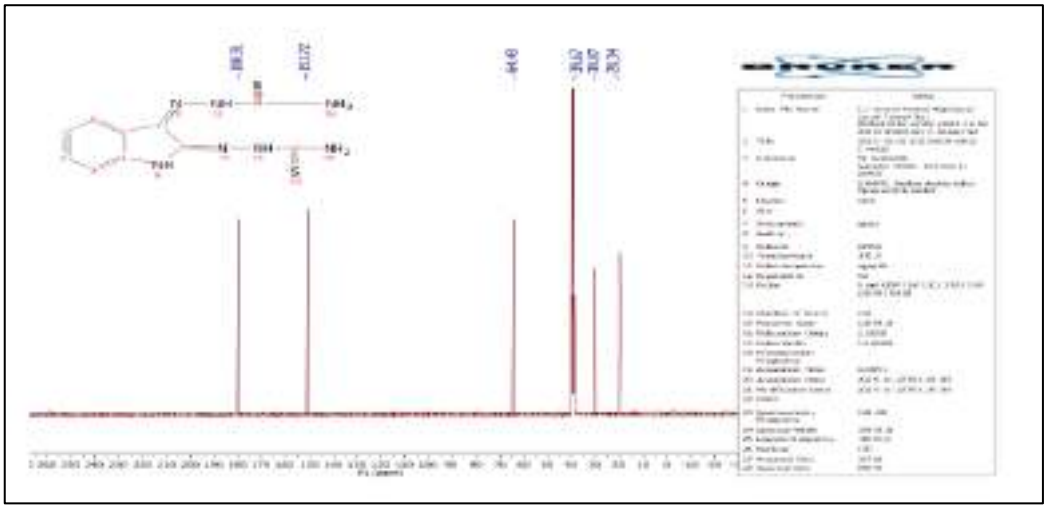
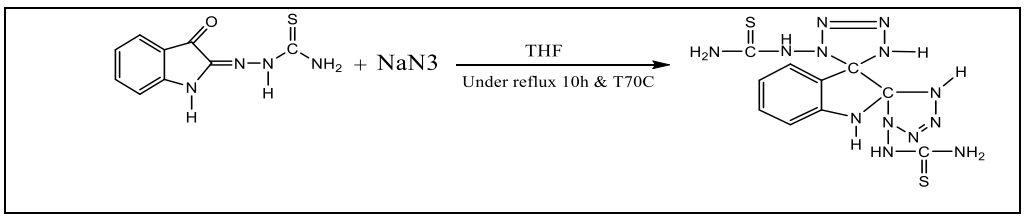


Figure (4- 103): ^{13}C-NMR spectrum of 2, 2'-((Z)-indoline-2, 3-diylidene)bis(hydrazine-1-carbothioamide) compound(34).

4.12 Synthesis of 1, 1'-(dispiro[tetrazole-5, 2'-indoline-3', 5''-tetrazol]-1, 1''(4H, 4''H)-diyl)bis(thiourea) compound(35).



Scheme (4-39): Synthesis of 1, 1'-(dispiro[tetrazole-5, 2'-indoline-3', 5''-tetrazol]-1, 1''(4H, 4''H)-diyl)bis(thiourea) compound(35).

FTIR spectrum of synthesis of 1, 1'-(dispiro[tetrazole-5, 2'-indoline-3', 5''-tetrazol]-1, 1''(4H, 4''H)-diyl)bis(thiourea) compound(35).

The FTIR spectrum of 1, 1'-(dispiro[tetrazole-5, 2'-indoline-3', 5''-tetrazol]-1, 1''(4H, 4''H)-diyl)bis(thiourea) as shown in (fig.4-104) which indicates absorption bands at 3475 and 3414 cm^{-1} to $–NH_2$ stretching and 3286 and 3219 Cm^{-1} to -NH, absorption band at 3093 cm^{-1} to C-H (aromatic), absorption band at 2989 and 2879 cm^{-1} to C-H(alphatic),absorption band at 1618cm^{-1} to C=N, absorption band at 1269

Cm^{-1} to C=S, absorption band at 1592 Cm^{-1} to C=C (aromatic), absorption band at 1396-1463 Cm^{-1} to N=N, absorption band at 1238 Cm^{-1} to C-N. (151-153)

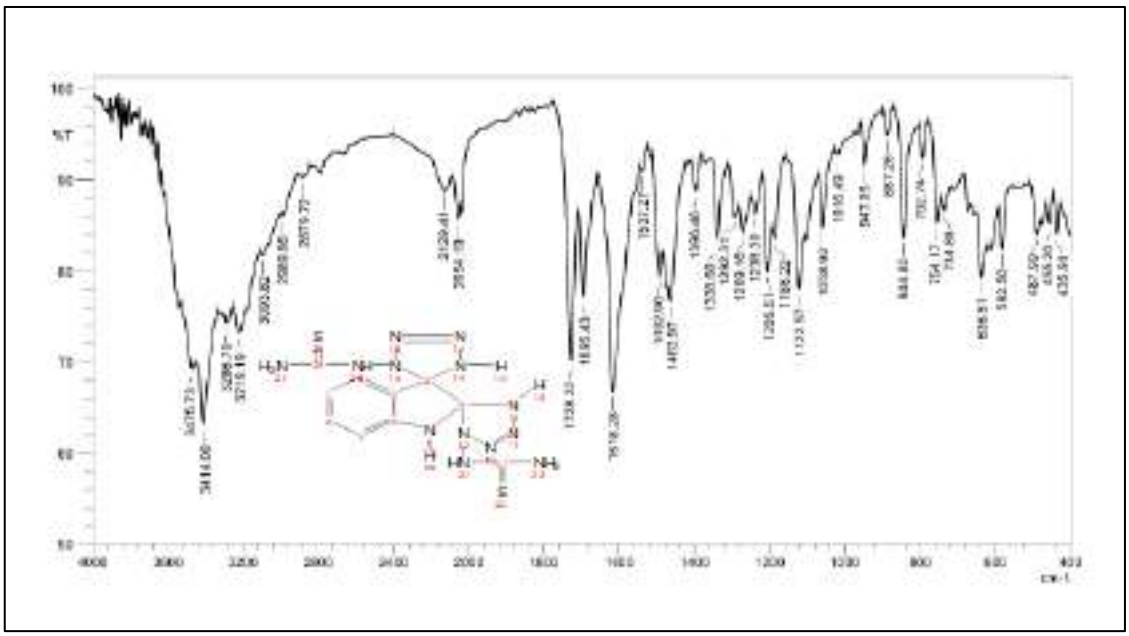


Figure (4- 104): FTIR spectrum of synthesis of 1, 1'-(dispiro[tetrazole-5, 2'-indoline-3', 5''-tetrazol]-1, 1''(4H, 4''H)-diyl)bis(thiourea) compound(35).

^{1}HNMR spectrum of synthesis of 1, 1'-(dispiro[tetrazole-5, 2'-indoline-3', 5''-tetrazol]-1, 1''(4H, 4''H)-diyl)bis(thiourea) compound(35).

^{1}HNMR spectrum of 1, 1'-(dispiro[tetrazole-5, 2'-indoline-3', 5''-tetrazol]-1, 1''(4H, 4''H)-diyl)bis(thiourea) in (fig.4-105) the major signal at δ 2.5 ppm is characteristic of DMSO-d6 as solvent , singlate at (6.7-8.3 δ ppm) to (4H, phenyl ring), single at (3.5 ppm) to $–NH_2$. (151-153)

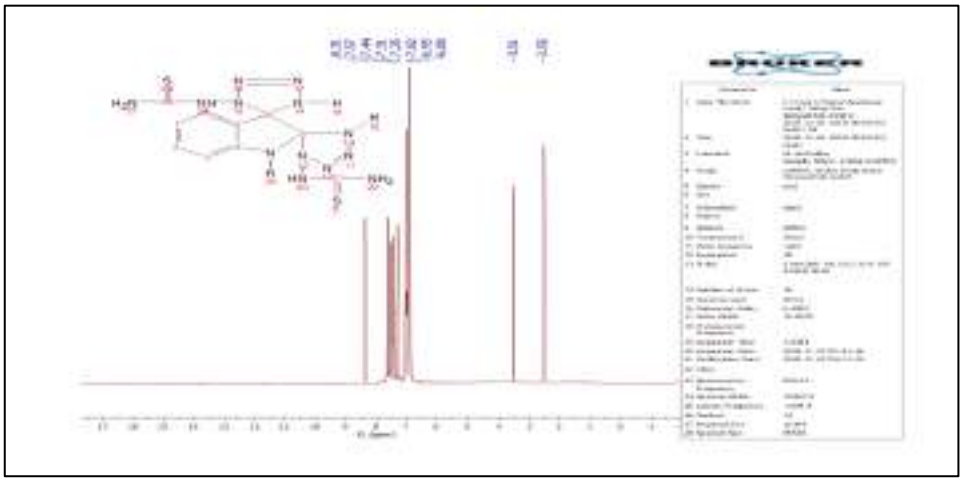


Figure (4- 105): ^{1}HNMR spectrum of synthesis of 1, 1'-(dispiro[tetrazole-5, 2'-indoline-3', 5''-tetrazol]-1, 1''(4H, 4''H)-diyl)bis(thiourea) compound(35).

^{13}C-NMR spectrum of synthesis of 1, 1'-(dispiro[tetrazole-5, 2'-indoline-3', 5''-tetrazol]-1, 1''(4H, 4''H)-diyl)bis(thiourea) compound(35).

The signals of olefinic and aromatic carbons appear in the third region between 111 and 132 ppm, single related to C=N at 150-162 ppm , single related to C-N at 66 ppm, single related to C=S at 178-182 ppm. (151-153)

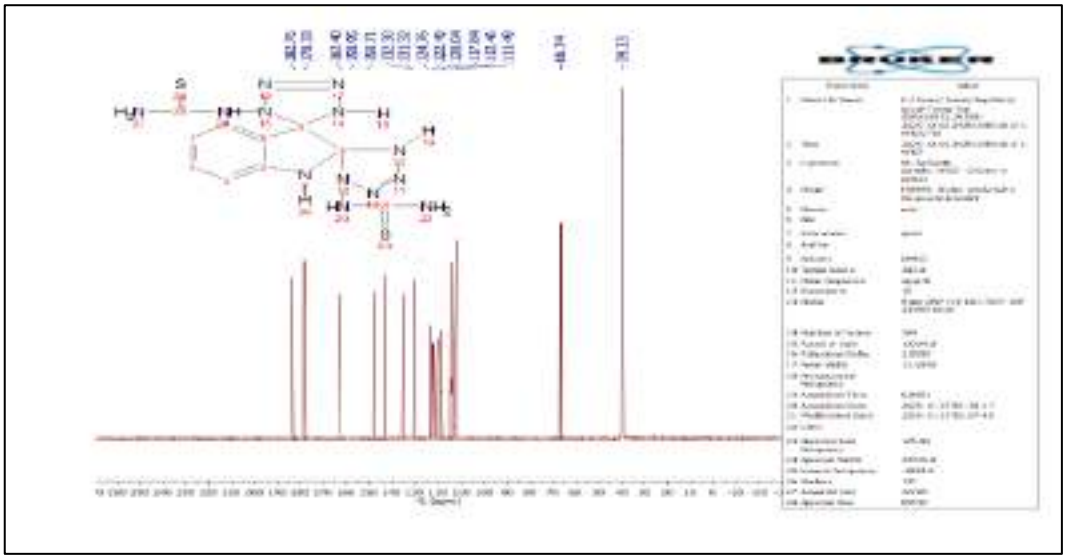
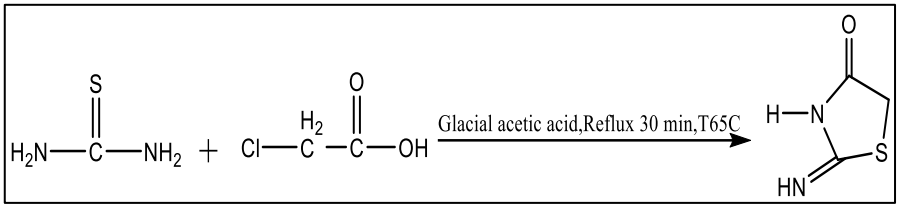


Figure (4- 106): ^{1}HNMR spectrum of synthesis of 1, 1'-(dispiro[tetrazole-5, 2'-indoline-3', 5''-tetrazol]-1, 1''(4H, 4''H)-diyl)bis(thiourea) compound(35).

4.13 *Synthesis* of 2-iminothiazolidin-4-one compound(36).



Scheme (4-40): synthesis of 2-iminothiazolidin-4-one compound(36).

FTIR spectrum of 2-iminothiazolidine 4-one compound(36).

The FTIR spectrum of 2-iminothiazolidine 4-one as shown in (fig.4-107) which indicates absorption bands at 3475 and 3417 cm^{-1} to –NH stretching, absorption band at 3174 cm^{-1} to C-H (aromatic), absorption band at 1589cm^{-1} to C=N, absorption band at 1089 Cm^{-1} to C-S, absorption band at 1494 Cm^{-1} to C=C (aromatic), absorption band at 1236 Cm^{-1} to C-N, absorption band at 1668 Cm^{-1} to C=O. (151-153)

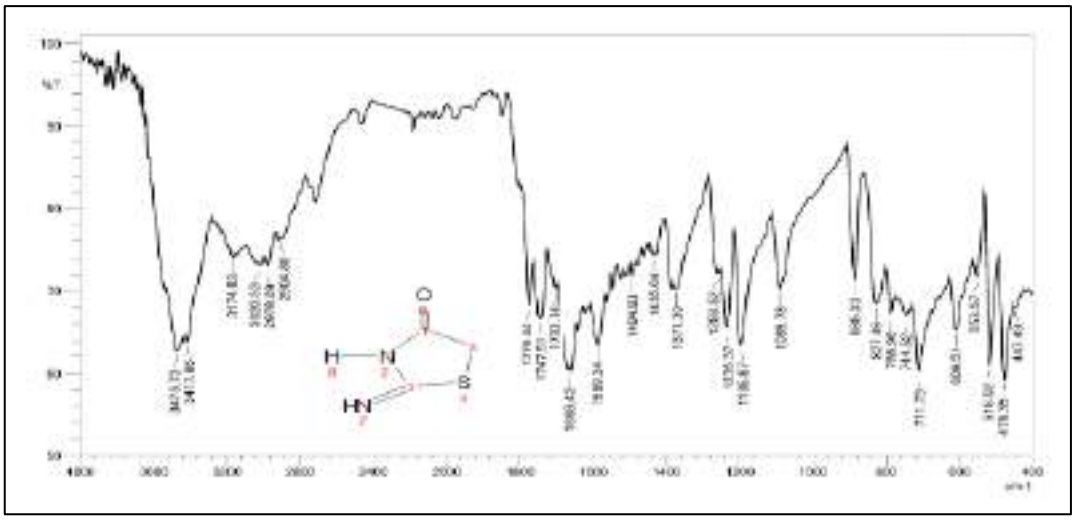


Figure (4- 107): ^{13}C-NMR spectrum of 2-iminothiazolidin-4-one compound(36).

^{1}HNMR spectrum of Thiosemicarbazones for 2-iminothiazolidine 4-one compound(36).

^{1}HNMR spectrum of 2-iminothiazolidine 4-one in (fig.4-108) the major signal at δ 2.5 ppm is characteristic of DMSO-d6 as solvent , singles at (4.3 ppm) to –NH, single at (2.5 ppm) to –CH_2. (151-153)

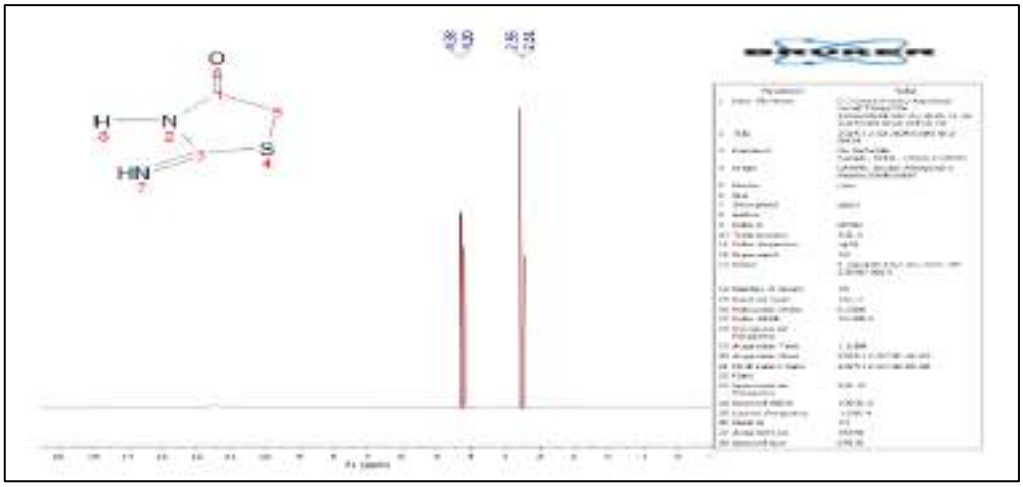


Figure (4- 108): ^{13}C-NMR spectrum of 2-iminothiazolidin-4-one compound(36).

^{13}C-NMR spectrum of Tetrazole derivatives for 2-iminothiazolidine 4-one compound(36).

The signals of olefinic and aromatic carbons appear in the third region between 110 and 119 ppm, single related to C=N at 150-162 ppm , single related to C-N at 66 ppm, single related to C=S at 178 ppm, single related to C=O at 175 ppm. (151-153)

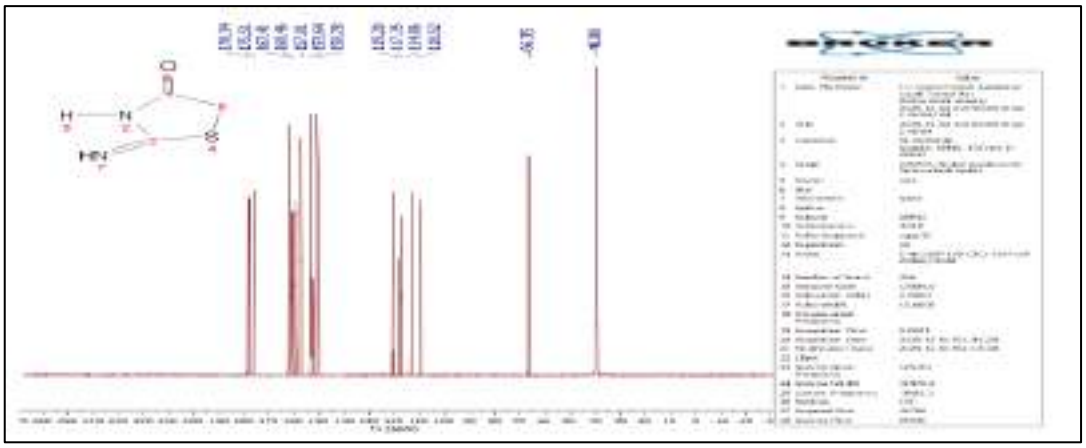
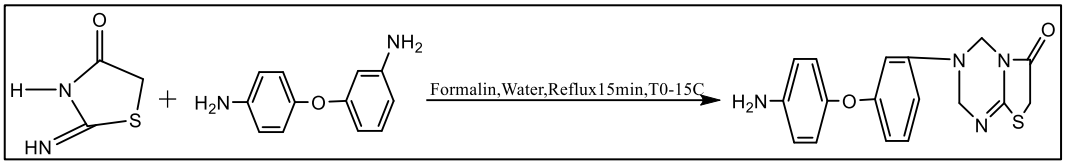


Figure (4- 109): ^{13}C-NMR spectrum of 2-iminothiazolidin-4-one compound(36).

4.14 Synthesis of Mannich reaction compounds(37-40)

4.14.1 Synthesis of 3-((3-(4-aminophenoxy)phenyl)amino)-3, 4-dihydro-2H-thiazolo[3, 2-a][1, 3, 5]triazin-6(7H)-one compound(37).



Scheme (4-41): synthesis of 3-((3-(4-aminophenoxy)phenyl)amino)-3, 4-dihydro-2H-thiazolo[3, 2-a][1, 3, 5]triazin-6(7H)-one compound(37).

FTIR spectrum of 3-((3-(4-aminophenoxy)phenyl)amino)-3, 4-dihydro-2H-thiazolo[3, 2-a][1, 3, 5]triazin-6(7H)-one compound(37).

The FTIR spectrum of 3-((3-(4-aminophenoxy)phenyl)amino)-3, 4-dihydro-2H-thiazolo[3, 2-a][1, 3, 5]triazin-6(7H)-one as shown in (fig.4-110) which indicates absorption bands at 3452 and 3250 cm^{-1} to $–NH_2$ stretching , absorption band at 3034 cm^{-1} to C-H (aromatic), absorption band at 1633cm^{-1} to C=N, absorption band at 1535 Cm^{-1} to C=C (aromatic), absorption band at 1238 Cm^{-1} to C-N, absorption band at 1114 Cm^{-1} to C-S**,** absorption band at 1166 Cm^{-1} to C-O, absorption band at 1664 Cm^{-1} to C=O. (151-153)

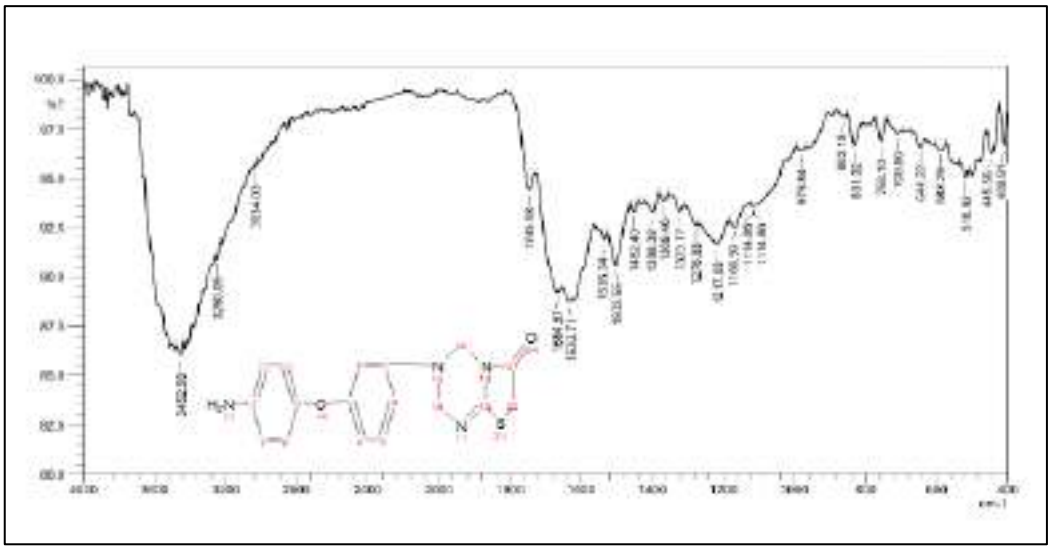


Figure (4- 110): FTIR spectrum of 3-((3-(4-aminophenoxy)phenyl)amino)-3, 4-dihydro-2H-thiazolo[3, 2-a][1, 3, 5]triazin-6(7H)-one compound(37).

^{1}HNMR spectrum of3-((3-(4-aminophenoxy)phenyl)amino)-3, 4-dihydro-2H-thiazolo[3, 2-a][1, 3, 5]triazin-6(7H)-one compound(37).

^{1}HNMR spectrum of 3-((3-(4-aminophenoxy)phenyl)amino)-3, 4-dihydro-2H-thiazolo[3, 2-a][1, 3, 5]triazin-6(7H)-one in (fig.4-111) singles at (7.1-7.4 δ ppm) to (8 H, phenyl ring), single at (3.4 ppm) to $–NH_2$, singlate at (2.5 δ ppm) to CH_2**.** (151-153)

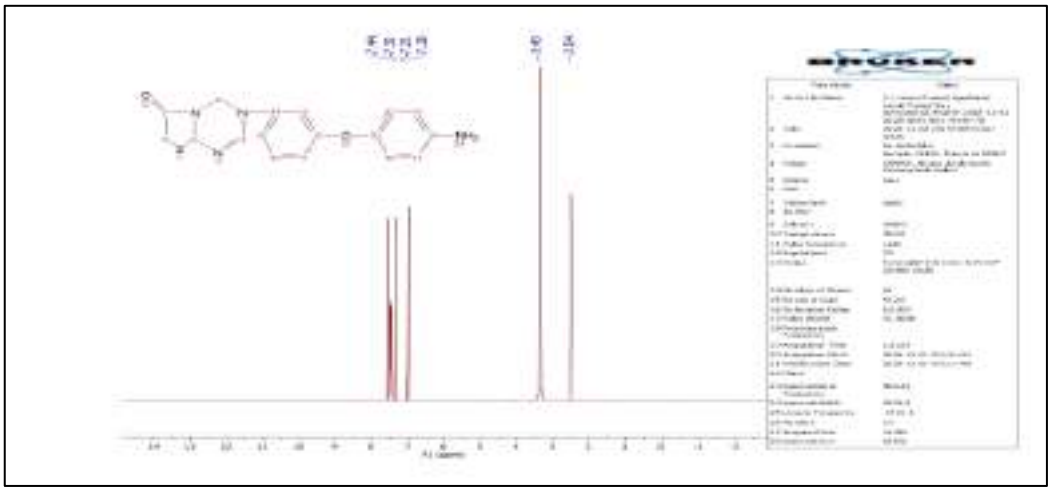


Figure (4- 111): ^{1}HNMR spectrum of 3-((3-(4-aminophenoxy)phenyl)amino)-3, 4-dihydro-2H-thiazolo[3, 2-a][1, 3, 5]triazin-6(7H)-one compound(37).

^{13}C-NMR spectrum of 3-((3-(4-aminophenoxy)phenyl)amino)-3, 4-dihydro-2H-thiazolo[3, 2-a][1, 3, 5]triazin-6(7H)-one compound(37).

The signals of olefinic and aromatic carbons appear in the third region between 111 and 128 ppm, single related to C=N at 150-162 ppm , single related to C-N at 66 ppm, single related to C-S at 56 ppm, single related to C=O at 168 ppm. (151-153)

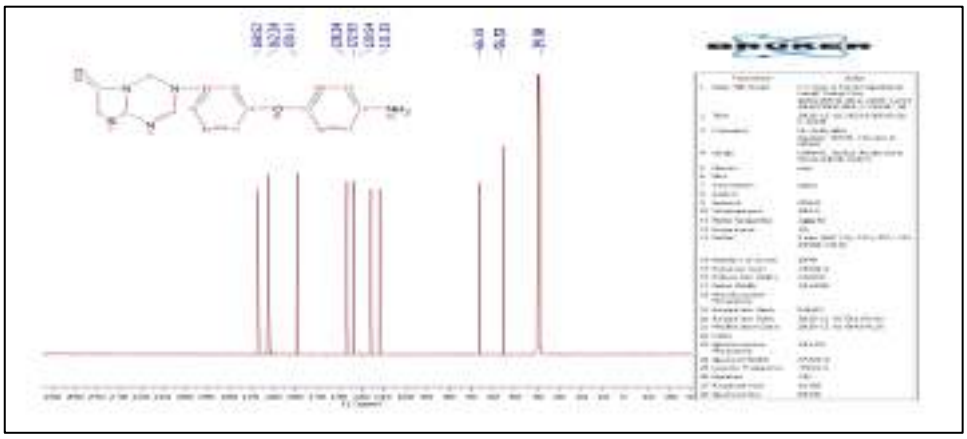
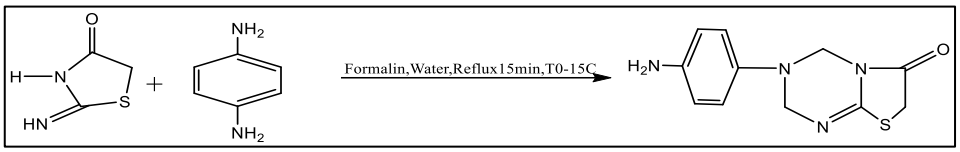


Figure (4- 112): ^{13}C-NMR spectrum of 3-((3-(4-aminophenoxy)phenyl)amino)-3, 4-dihydro-2H-thiazolo[3, 2-a][1, 3, 5]triazin-6(7H)-one compound(37).

4.14.2 Synthesis of 3-((4-aminophenyl)amino)-3, 4-dihydro-2H-thiazolo[3, 2-a][1, 3, 5]triazin-6(7H)-one compound(38).



Scheme (4-42): synthesis of 3-((4-aminophenyl)amino)-3, 4-dihydro-2H-thiazolo[3, 2-a][1, 3, 5]triazin-6(7H)-one compound(38).

FTIR spectrum of 3-((4-aminophenyl)amino)-3, 4-dihydro-2H-thiazolo[3, 2-a][1, 3, 5]triazin-6(7H)-one compound(38).

The FTIR spectrum of 3-((4-aminophenyl)amino)-3, 4-dihydro-2H-thiazolo[3, 2-a][1, 3, 5]triazin-6(7H)-one as shown in (fig.4-113) which indicates absorption bands at 3508 cm^{-1} to $–NH_2$ stretching , absorption band at 3174 cm^{-1} to C-H (aromatic), absorption band at 1633 cm^{-1} to C=N, absorption band at 1454 Cm^{-1} to C=C (aromatic), absorption band at 1247 Cm^{-1} to C-N, absorption band at 1026 Cm^{-1} to C-S**,** absorption band at 1193 Cm^{-1} to C-O, absorption band at 1681 Cm^{-1} to

C=O. (151-153)

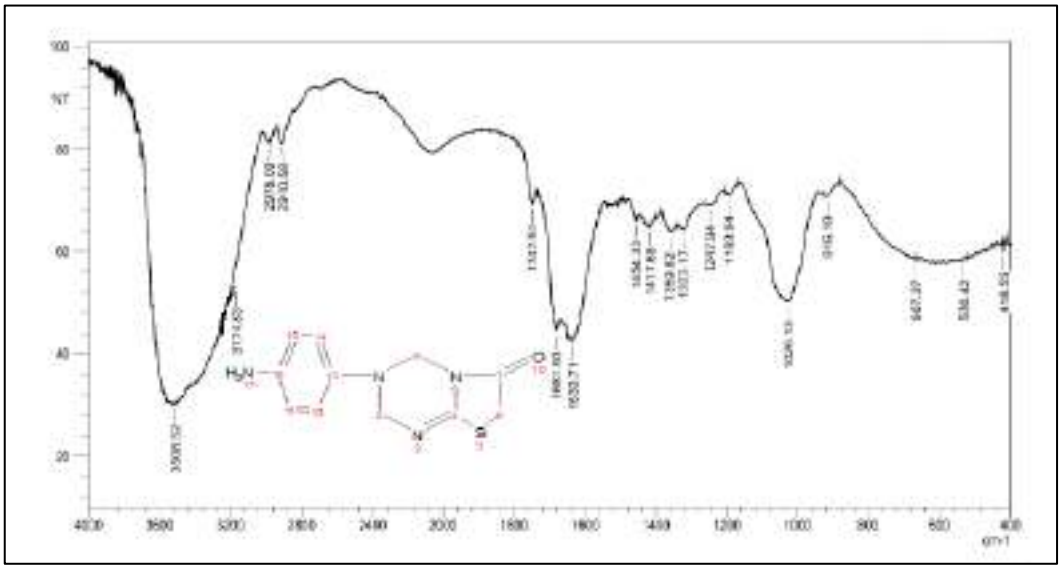


Figure (4- 113): FTIR spectrum of 3-((4-aminophenyl)amino)-3, 4-dihydro-2H-thiazolo[3, 2-a][1, 3, 5]triazin-6(7H)-one compound(38).

^{1}HNMR spectrum of 3-((4-aminophenyl)amino)-3, 4-dihydro-2H-thiazolo[3, 2-a][1, 3, 5]triazin-6(7H)-one compound(38).

^{1}HNMR spectrum of 3-((4-aminophenyl)amino)-3, 4-dihydro-2H-thiazolo[3, 2-a][1, 3, 5]triazin-6(7H)-one in (fig.4-114) singles 00at (6.6-8.4 δ ppm) to (4H, phenyl ring), single at (3.2-4.8 ppm) to $–NH_2$, singlate at (2.5 δ ppm) to CH_2**.** (151-153)

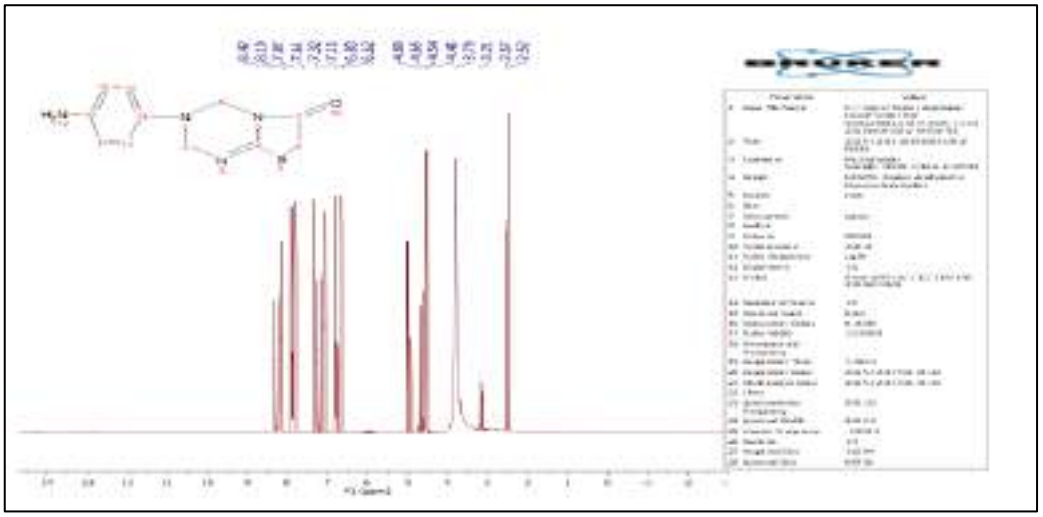


Figure (4- 114):^{1}HNMR spectrum of 3-((4-aminophenyl)amino)-3, 4-dihydro-2H-thiazolo[3, 2-a][1, 3, 5]triazin-6(7H)-one compound(38).

^{13}C-NMR spectrum of 3-((4-aminophenyl)amino)-3, 4-dihydro-2H-thiazolo[3, 2-a][1, 3, 5]triazin-6(7H)-one compound(38).

The signals of olefinic and aromatic carbons appear in the third region between 111 and 128 ppm, single related to C=N at 148 ppm , single related to C-N at 82-84 ppm, single related to C-S at 55 ppm, single related to C=O at 175 ppm. (151-153)

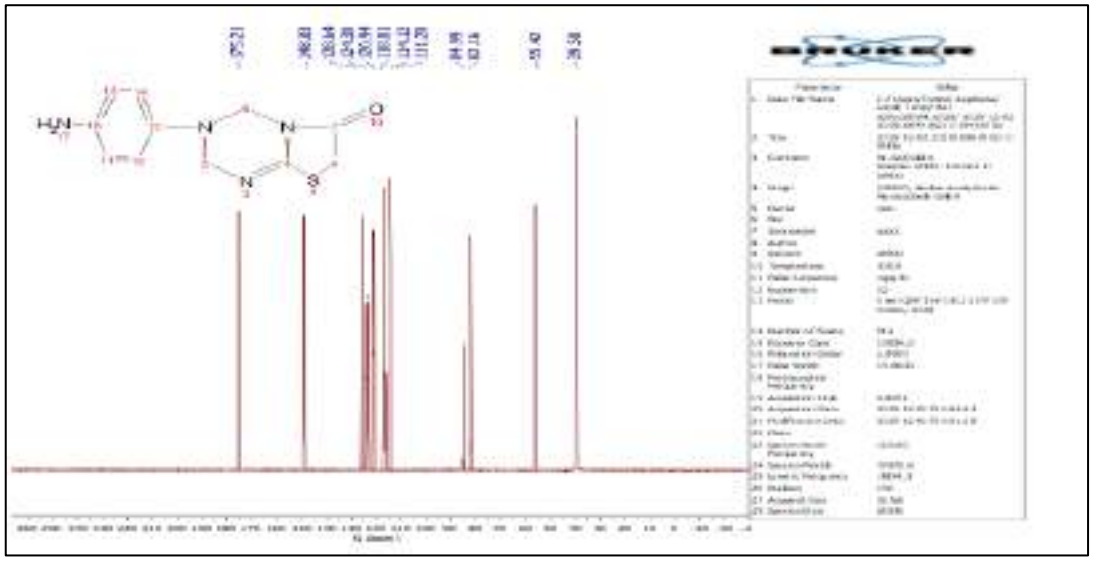
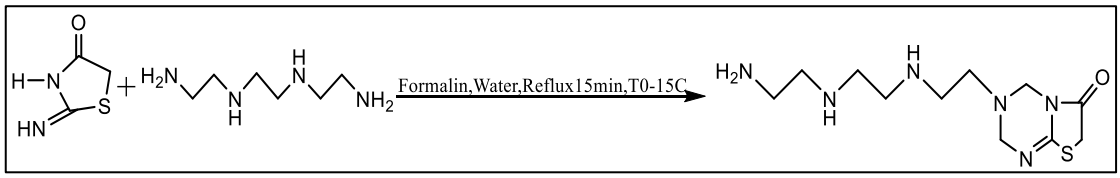


Figure (4- 115):^{13}C-NMR spectrum of 3-((4-aminophenyl)amino)-3, 4-dihydr-2H-thiazolo[3, 2-a][1, 3, 5]triazin-6(7H)-one compound(38).

4.14.3 Synthesis of 3-((2-((2-((2-minoethyl)amino)ethyl)amino) ethyl)amino)-3, 4-dihydro-2H-thiazolo[3, 2-a][1, 3, 5]triazin-6(7H)-one compound(39).



Scheme (4-43): synthesis of 3-((2-((2-((2-minoethyl)amino)ethyl)amino) ethyl)amino)-3, 4-dihydro-2H-thiazolo[3, 2-a][1, 3, 5]triazin-6(7H)-one compound(39).

FTIR spectrum of 3-((2-((2-((2-minoethyl)amino)ethyl)amino) ethyl)amino)-3, 4-dihydro-2H-thiazolo[3, 2-a][1, 3, 5]triazin-6(7H)-one compound(39).

The FTIR spectrum of 3-((2-((2-((2-minoethyl)amino)ethyl)amino) ethyl)amino)-3, 4-dihydro-2H-thiazolo[3, 2-a][1, 3, 5]triazin-6(7H)-one as shown in (fig.4-116) which indicates absorption bands at 3441 cm^{-1} to $–NH_2$ stretching , absorption band at 3134 cm^{-1} to C-H (aromatic), absorption band at 2955cm^{-1} to C-

H (Aliphatic), absorption band at 1651 cm^{-1} to C=N, absorption band at 1620 Cm^{-1} to C=C (aromatic), absorption band at 1224 Cm^{-1} to C-N, absorption band at 1058 Cm^{-1} to C-S**,** absorption band at 1109 Cm^{-1} to C-O, absorption band at 1681 Cm^{-1} to C=O. (151-153)

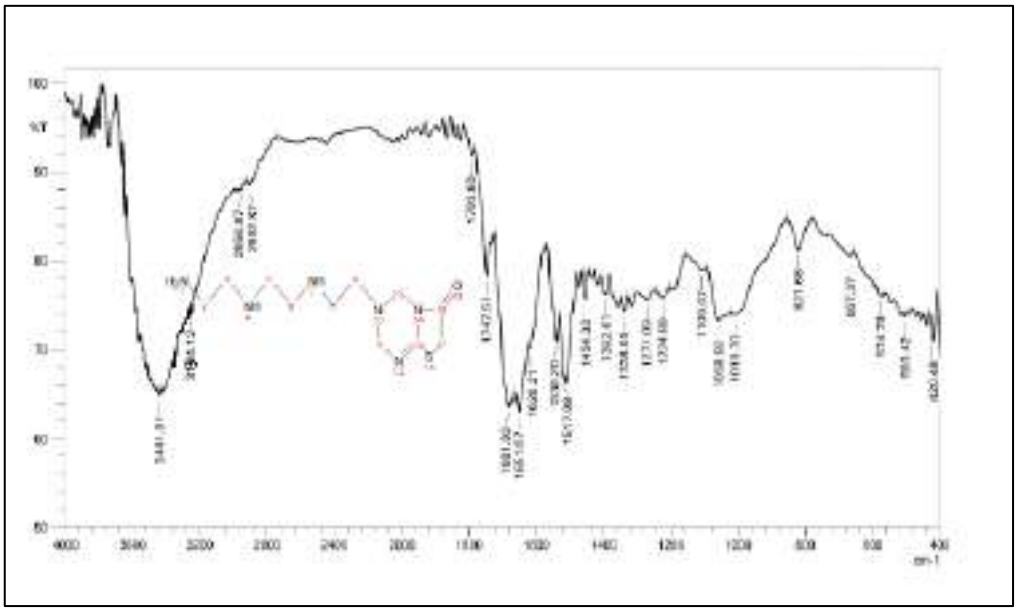


Figure (4- 116):FTIR spectrum of 3-((2-((2-((2-minoethyl)amino)ethyl)amino) ethyl)amino)-3, 4-dihydro-2H-thiazolo[3, 2-a][1, 3, 5]triazin-6(7H)-one compound(39).

^{1}HNMR spectrum of 3-((2-((2-((2-minoethyl)amino)ethyl)amino) ethyl)amino)-3, 4-dihydro-2H-thiazolo[3, 2-a][1, 3, 5]triazin-6(7H)-one compound(39).

^{1}HNMR spectrum of 3-((2-((2-((2-minoethyl)amino)ethyl)amino) ethyl)amino)-3, 4-dihydro-2H-thiazolo[3, 2-a][1, 3, 5]triazin-6(7H)-one in (fig.4-117) singles at (3.2-4.8 ppm) to $–NH_2$, singles at (2.5-3.0 δ ppm) to CH_2**.** (150-152)

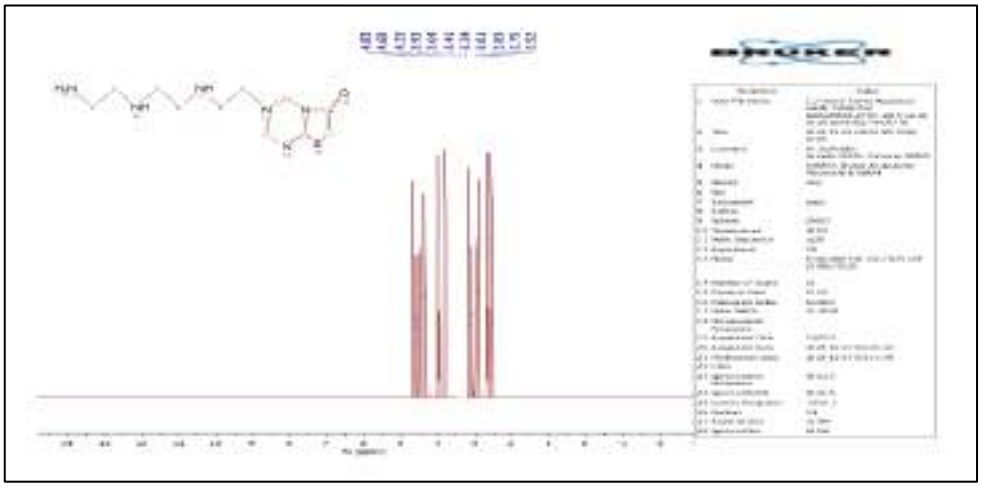


Figure (4- 117): ^{1}HNMR spectrum of 3-((2-((2-((2-minoethyl)amino)ethyl)amino) ethyl)amino)-3, 4-dihydro-2H-thiazolo[3, 2-a][1, 3, 5]triazin-6(7H)-one compound(39).

^{13}C-NMR spectrum of3-((2-((2-((2-minoethyl)amino)ethyl)amino) ethyl)amino)-3, 4-dihydro-2H-thiazolo[3, 2-a][1, 3, 5]triazin-6(7H)-one compound(39).

Single related to C=N at 148 ppm , single related to C-N at 82-84 ppm, single related to C-S at 55 ppm, single related to C=O at 168 ppm. (151-153)

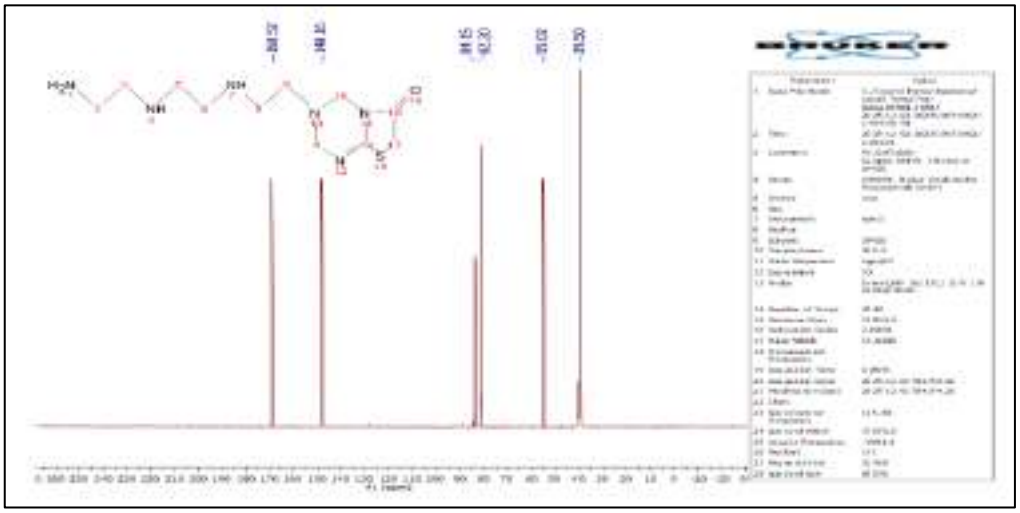
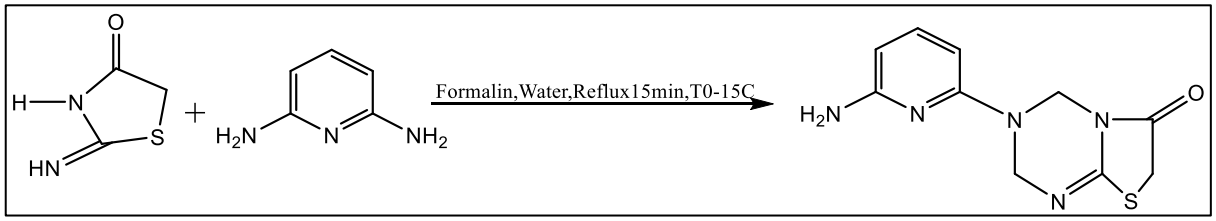


Figure (4- 118):^{13}C-NMR spectrum of 3-((2-((2-((2-minoethyl)amino)ethyl)amino) ethyl)amino)-3, 4-dihydro-2H-thiazolo[3, 2-a][1, 3, 5]triazin-6(7H)-one compound(39).

4.14.4Synthesis of 3-((6-aminopyridin-2-yl)amino)-3, 4-dihydro-2H-thiazolo[3, 2-a][1, 3, 5]triazin-6(7H)-one compound(40).



Scheme (4-44): synthesis of 3-((6-aminopyridin-2-yl)amino)-3, 4-dihydro-2H-thiazolo[3, 2-a][1, 3, 5]triazin-6(7H)-one compound(40).

FTIR spectrum of 3-((6-aminopyridin-2-yl)amino)-3, 4-dihydro-2H-thiazolo[3, 2-a][1, 3, 5]triazin-6(7H)-one compound(40).

The FTIR spectrum of 3-((6-aminopyridin-2-yl)amino)-3, 4-dihydro-2H-thiazolo[3, 2-a][1, 3, 5]triazin-6(7H)-one as shown in (fig.4-119) which indicates

absorption bands at 3410 cm^{-1} to $–NH_2$ stretching , absorption band at 3134 cm^{-1} to C-H (aromatic), absorption band at 2972 Cm^{-1} to C-H (Aliphatic), absorption band at 1643 cm^{-1} to C=N, absorption band at 1579 Cm^{-1} to C=C (Hetro phenyl ring), absorption band at 1228 Cm^{-1} to C-N, absorption band at 1039 Cm^{-1} to C-S**,** absorption band at 1103 Cm^{-1} to C-O, absorption band at 1681 Cm^{-1} to C=O. (151-153)

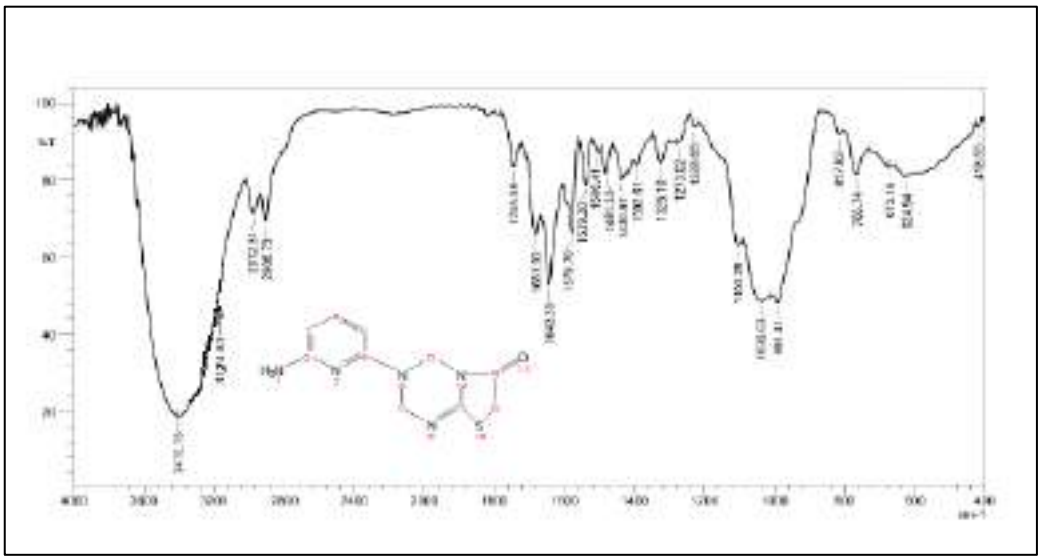


Figure (4- 119):FTIR spectrum of 3-((6-aminopyridin-2-yl)amino)-3, 4-dihydro-2H-thiazolo[3, 2-a][1, 3, 5]triazin-6(7H)-one compound(40).

^{1}HNMR spectrum of 3-((6-aminopyridin-2-yl)amino)-3, 4-dihydro-2H-thiazolo[3, 2-a][1, 3, 5]triazin-6(7H)-one compound(40).

^{1}HNMR spectrum of 3-((6-aminopyridin-2-yl)amino)-3, 4-dihydro-2H-thiazolo[3, 2-a][1, 3, 5]triazin-6(7H)-one in (fig.4-120) singles at (3.2-3.4 ppm) to –NH_2, singles at (2.5 δ ppm) to CH_2, singles at (6.2-7.5 ppm) to (3H heteropheny ring). (151-153)

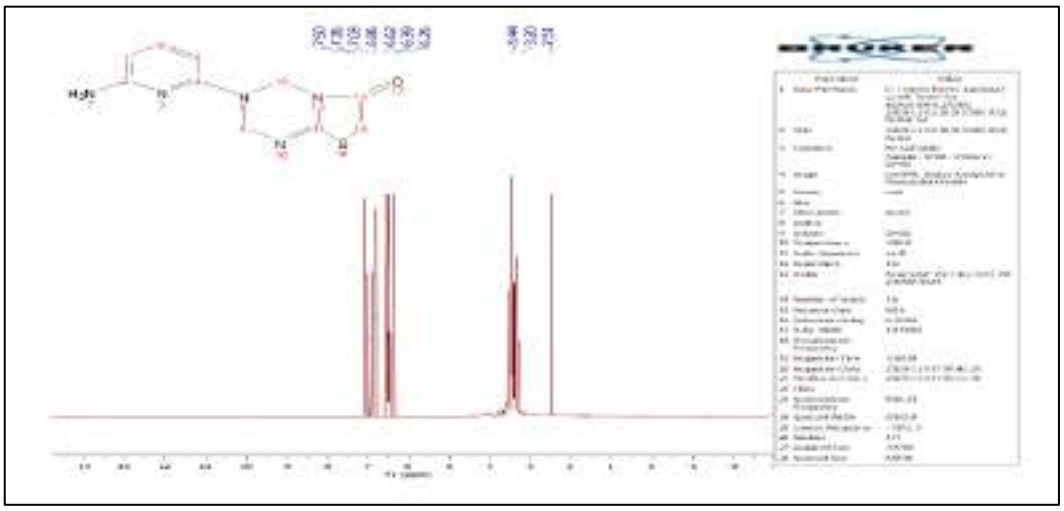


Figure (4- 120):^{1}HNMR spectrum of 3-((6-aminopyridin-2-yl)amino)-3, 4-dihydro-2H-thiazolo[3, 2-a][1, 3, 5]triazin-6(7H)-one compound(40).

^{13}C-NMR spectrum of 3-((6-aminopyridin-2-yl)amino)-3, 4-dihydro-2H-thiazolo[3, 2-a][1, 3, 5]triazin-6(7H)-one compound(40).

Single related to C=N at 148 ppm , single related to C-N at 82-84 ppm, single related to C-S at 55 ppm, single related to C=O at 168 ppm. (151-153)

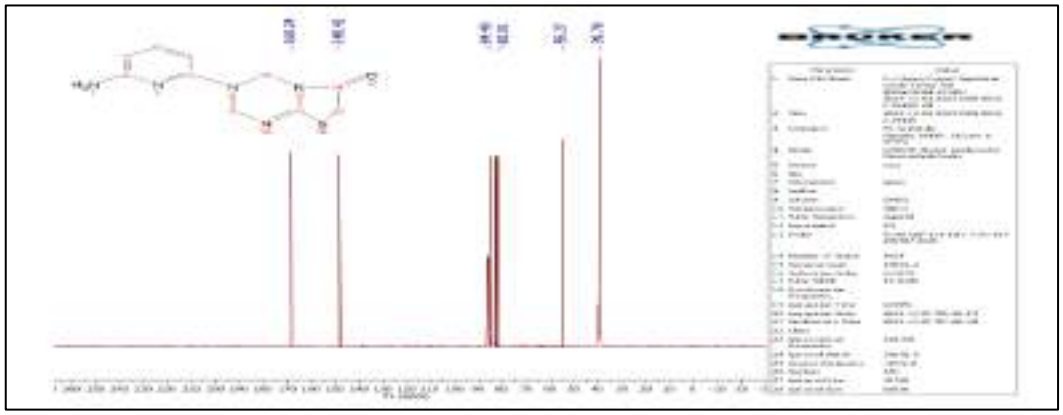
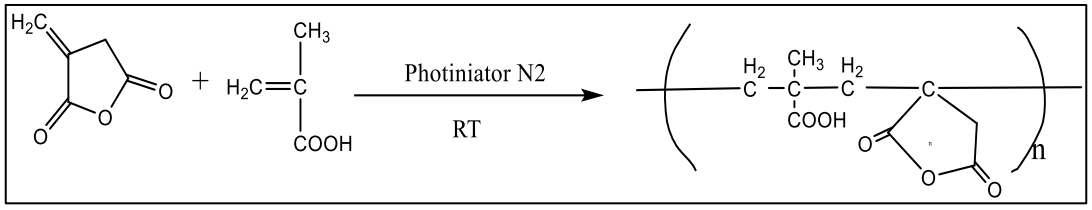


Figure (4- 121):^{13}C-NMR spectrum of 3-((6-aminopyridin-2-yl)amino)-3, 4-dihydro-2H-thiazolo[3, 2-a][1, 3, 5]triazin-6(7H)-one compound(40).

4.15 Synthesis of copolymer (methyl acrylic acid-co - Itaconic anhydride) (MAA-CO-IAN) .



Scheme (4-45): synthesis of copolymer (methyl acrylic acid-co - Itaconic anhydride) (MAA-CO-IAN).

FTIR spectrum of Copolymer (methyl acrylic acid-co- Itaconic anhydride).

The FTIR spectrum of copolymer (methyl acrylic acid- Itaconic anhydride) as shown in (fig.4-122*)* which indicates absorption bands at 3411 to OH, absorption band at 3107 cm^{-1} to C-H (heterocyclic ring), absorption band at 2929 cm^{-1} to CH_2(aliphatic), absorption band at 1708 Cm^{-1} to C=O for ester, absorption band at 1699 Cm^{-1} to C=O (carboxylic acid), absorption band at 1309 Cm^{-1} to CH_3, absorption band at 1166 Cm^{-1} to C-O. (151-153)

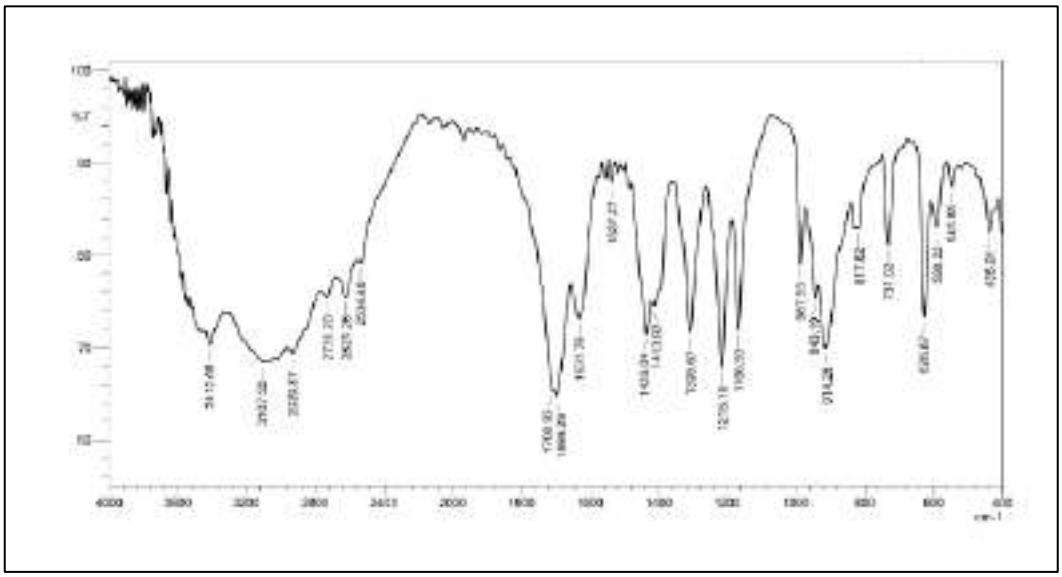


Figure (4- 122): FTIR spectrum of synthesis of copolymer (methyl acrylic acid-co - Itaconic anhydride) (MAA-CO-IAN).

^{1}HNMR spectrum of Copolymer (methyl acrylic acid- Itaconic anhydride)

^{1}HNMR spectrum of polymer for Copolymer (methyl acrylic acid- Itaconic anhydride) in (fig.4-123) singles at (5.7-6.2 δ ppm) to (4H, Heterocyclic ring), single at (12.5 ppm) to –OH, single at (2.5 ppm) to $–CH_3$, singles at (3.3 ppm) to $–CH_2$. (151-153)

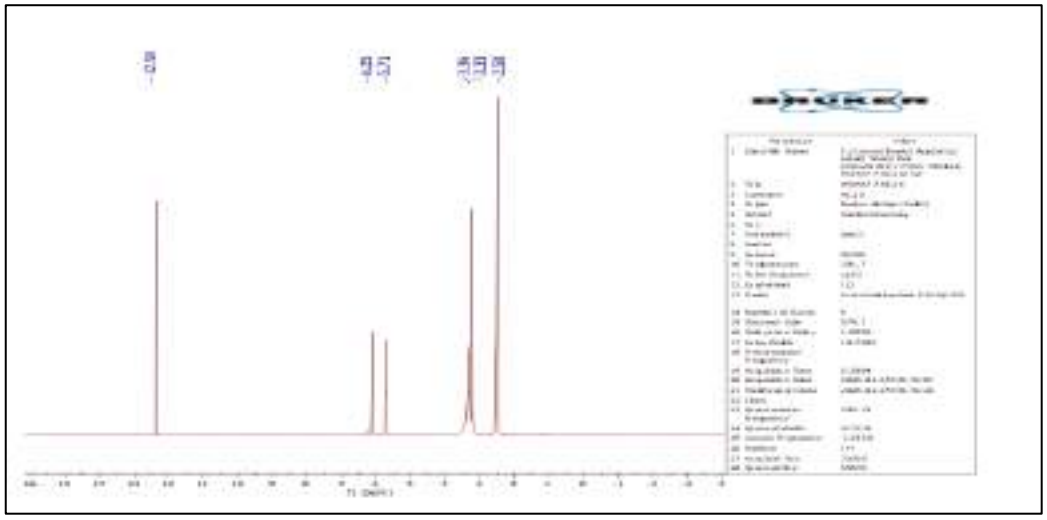


Figure (4- 123):1HNMR spectrum of synthesis of copolymer (methyl acrylic acid-co - Itaconic anhydride) (MAA-CO-IAN).

^{13}C-NMR spectrum of Copolymer (methyl acrylic acid- Itaconic anhydride)

Single related to C=O at 198 ppm (ester), single related to C=O (acid) at 178 ppm, single related to CH_3 at 18 ppm, single related to C-O at 76 ppm. (151-153)

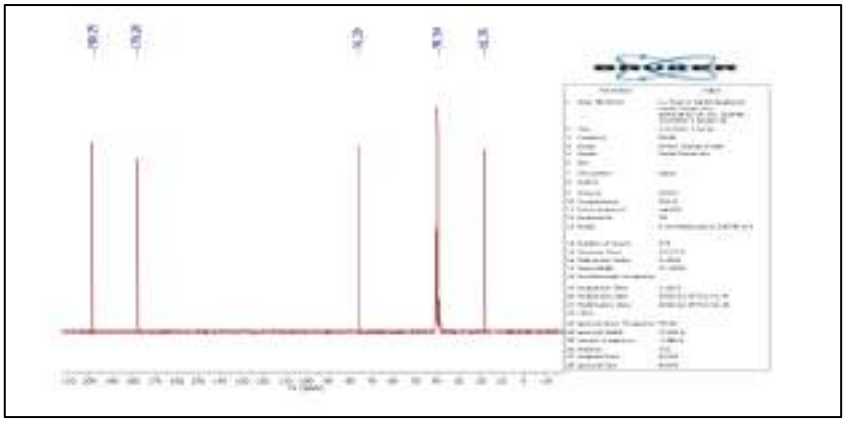
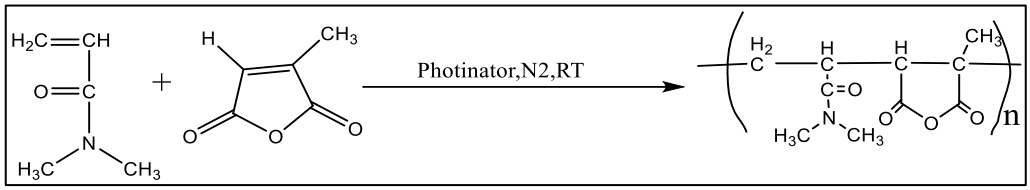


Figure (4- 124): ^{13}C-NMR spectrum of synthesis of copolymer (methyl acrylic acid-co - Itaconic anhydride) (MAA-CO-IAN).

4.16 Synthesis of copolymer (N, N-dimethylacrylamide-CO -Citraconic

anhydride) (DMA-CO-CAN).



Scheme (4-46): synthesis of copolymer (N, N-dimethylacrylamide-Citraconic anhydride) (DMA-CO-CAN) .

FTIR spectrum of Copolymer (N, N-dimethylacrylamide-Citraconic anhydride)

The FTIR spectrum of copolymer (N, N-dimethylacrylamide-Citraconic anhydride) as shown in (fig.4-125) which indicates absorption bands at 3074 to OH, absorption band at 3107 cm^{-1} to C-H (heterocyclic ring), absorption band at 2995 cm^{-1} to CH_2(aliphatic), absorption band at 1768 Cm^{-1} to C=O for ester, absorption band at 1697 Cm^{-1} to C=O (carboxylic acid), absorption band at 1315 Cm^{-1} to CH_3, absorption band at 1190 Cm^{-1} to C-O. (151-153)

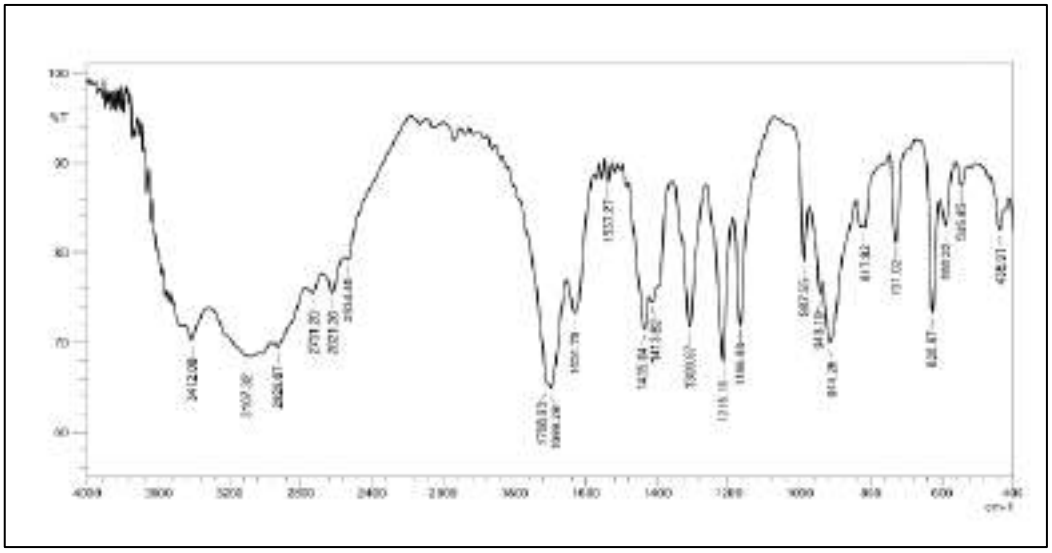


Figure (4- 125):FTIR spectrum of copolymer (N, N-dimethylacrylamide-Citraconic anhydride) .

^{1}HNMR spectrum of Copolymer (N, N-dimethylacrylamide-Citraconic anhydride)

^{1}HNMR spectrum of of copolymer (N, N-dimethylacrylamide-Citraconic anhydride) in (fig.4-126) singles at (5.7-6.1 δ ppm) to (1H, Heterocyclic ring), single at (1.2 ppm) to $–CH_3$, singles at (2.0-2.5 ppm) to $–CH_2$. (151-153)

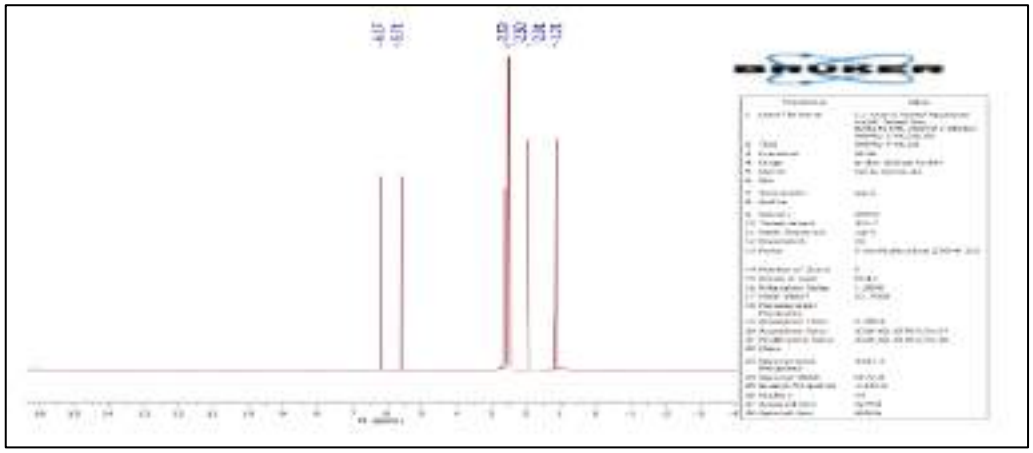


Figure (4- 126):^{1}HNMR spectrum of copolymer (N, N-dimethylacrylamide-Citraconic anhydride).

^{13}C-NMR spectrum of Copolymer (N, N-dimethylacrylamide-Citraconic anhydride)

Single related to C=O at 198 ppm (ester), single related to C=O (acid) at 178 ppm, single related to CH_3 at 20 ppm, single related to C-O at 76 ppm. (151-153)

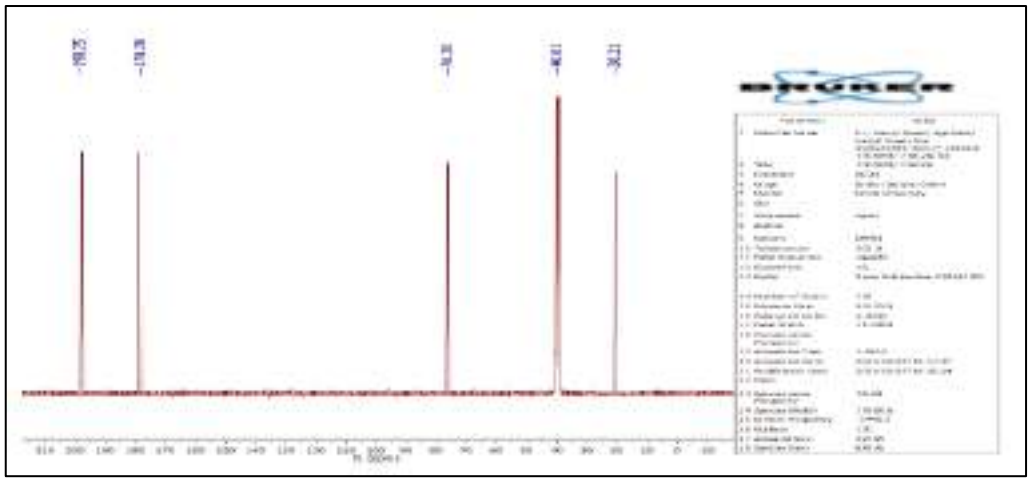
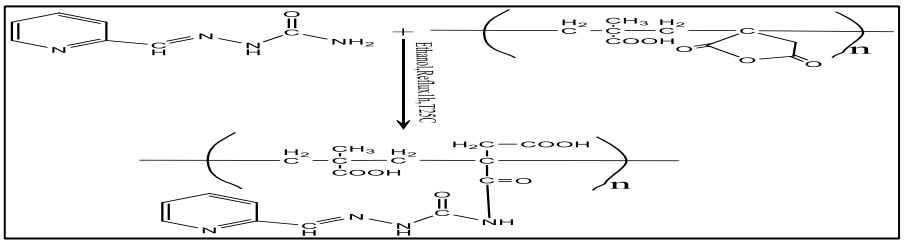


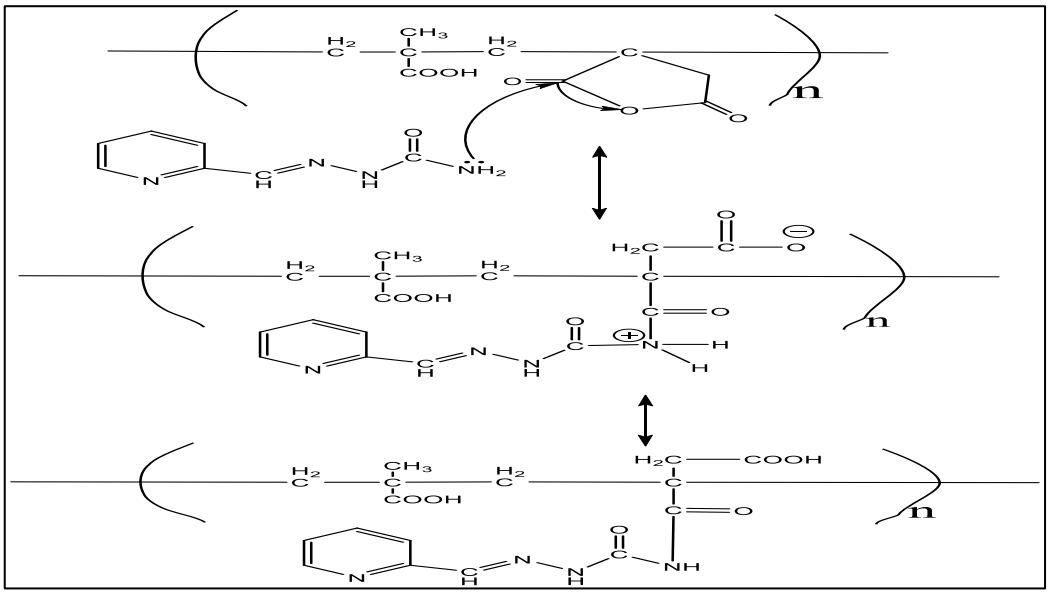
Figure (4- 127):^{13}C-NMR spectrum of copolymer (N, N-dimethylacrylamide-Citraconic anhydride).

4.17 Synthesis of copolymer (MAA-CO-IAN) with Thiosemicarbazones compounds (1-9).

4.17.1 Synthesis of copolymer(1) (MAA-Co-IAN) with compound(1).



Scheme (4-47): synthesis of copolymer (1) (MAA-Co-IAN) with compound(1).



Scheme (4-48): Mechanism of synthesis copolymer with compounds

FTIR spectrum of copolymer(1) (MAA-Co-IAN) with compound(1).

The FTIR spectrum of copolymer(1) (MAA-Co-IAN) with compound(1) as shown in (fig.4-128) which indicates absorption bands at 3414 to OH and 3292 cm^{-1} to $–NH_2$ stretching, absorption band at 3157 cm^{-1} to C-H (hetro phenyl ring), absorption band at 2974 cm^{-1} to CH_2(aliphatic) , absorption band at 1633 cm^{-1} to C=N, absorption band at 1178 Cm^{-1} to C=S, absorption band at 1537 Cm^{-1} to C=C (Hetro phenyl ring), absorption band at 1710 Cm^{-1} to C=O for carboxylic acid, absorption band at 1699 Cm^{-1} to C=O (amide), absorption band at 1390 Cm^{-1} to CH_3, absorption band at 1085 Cm^{-1} to C-O. (151-153)

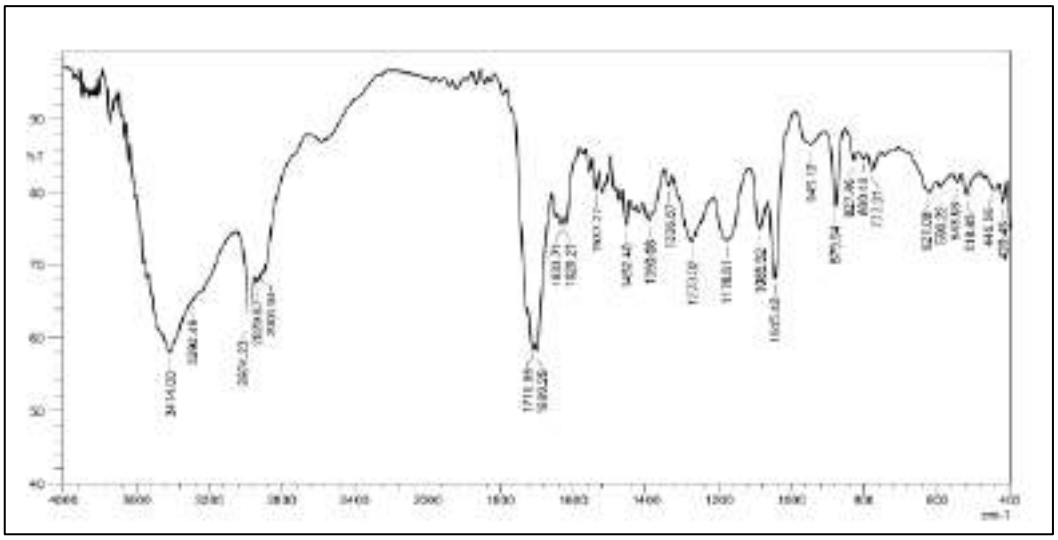


Figure (4- 128): structure copolymer(1) (MAA-Co-IAN) with compound(1).

^{1}HNMR spectrum of copolymer(1) (MAA-Co-IAN) with compound(1).

^{1}HNMR spectrum of copolymer(1) (MAA-Co-IAN) with compound(1) in (fig.4-129) singles at (7.3-7.7 δ ppm) to (3H, Hetro phenyl ring), single at (3.3 ppm) to –NH, single at (9.5 ppm) to –OH, single at (4.5 ppm) to –NH (amide), single at (0.9 ppm) to $–CH_3$, singles at (1.8 ppm) to $–CH_2$. (151-153)

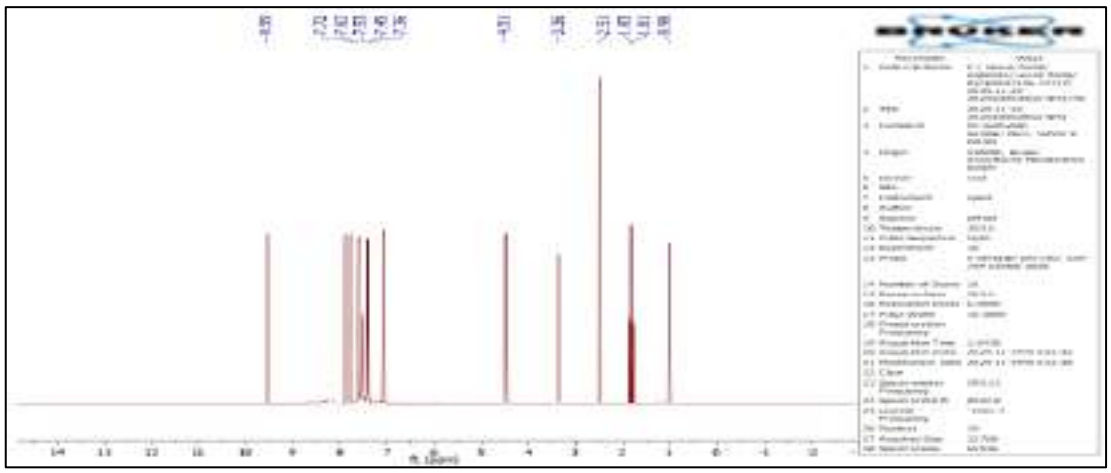


Figure (4- 129):structure copolymer(1) (MAA-Co-IAN) with compound(1).

^{13}C-NMR spectrum of copolymer(1) (MAA-Co-IAN) with compound(1).

The signals of olefinic and aromatic carbons appear in the third region between 124 and 127 ppm, single related to C=N at 142 ppm, single related to C-N at 64 ppm, single related to C=S at 210 ppm, single related to CH_3 at 18 ppm, single related to C=O (amide) at 166 ppm, single related to C=O (COOH) at 173 ppm. (151-153)

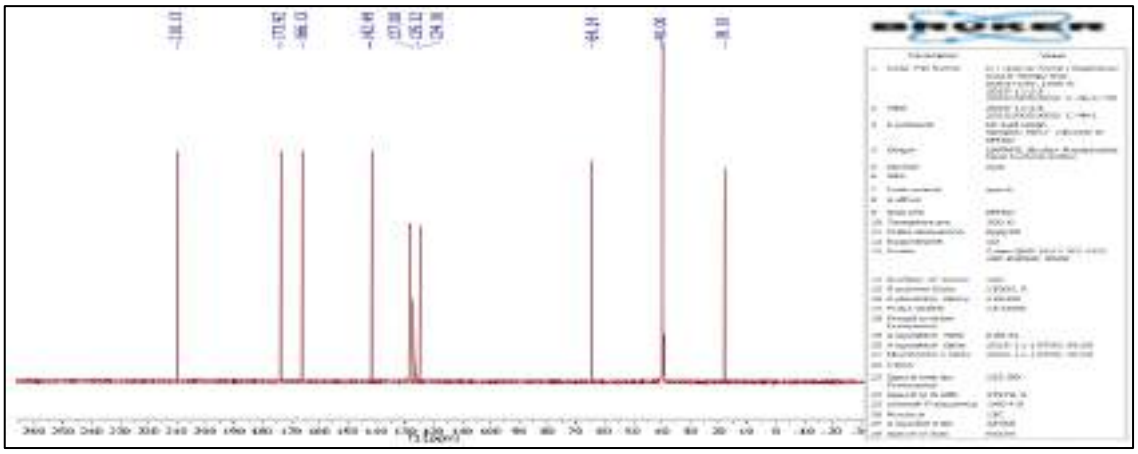
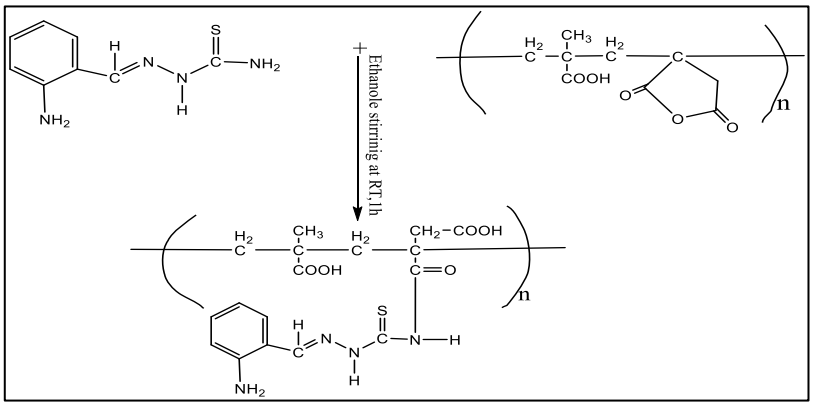


Figure (4- 130):structure copolymer(1) (MAA-Co-IAN) with compound(1).

4.17.2 Synthesis of copolymer(2) (MAA-Co-IAN) with compound(2).



Scheme (4-49): Syntheses of copolymer(2) (MAA-Co-IAN) with compound(2).

FTIR spectrum of copolymer(2) (MAA-Co-IAN) with compound(2).

The FTIR spectrum of copolymer(2) (MAA-Co-IAN) with compound(2) as shown in (fig.4-131) which indicates absorption bands at 3417 to -OH and 3219 cm^{-1} to $–NH_2$ stretching, absorption band at 3207 cm^{-1} to C-H (aromatic), absorption band at 2974 cm-1 to CH_2(aliphatic), absorption band at 1633 cm^{-1} to C=N, absorption band at 1182 Cm^{-1} to C=S, absorption band at 1492 Cm^{-1} to C=C (aromatic), and absorption band at 1392 Cm^{-1} to CH_3, absorption band at 1703 Cm-1 to C=O for carboxylic acid, absorption band at 1633 Cm^{-1} to C=O (amide), absorption band at 1082 Cm^{-1} to C-O. (151-153)

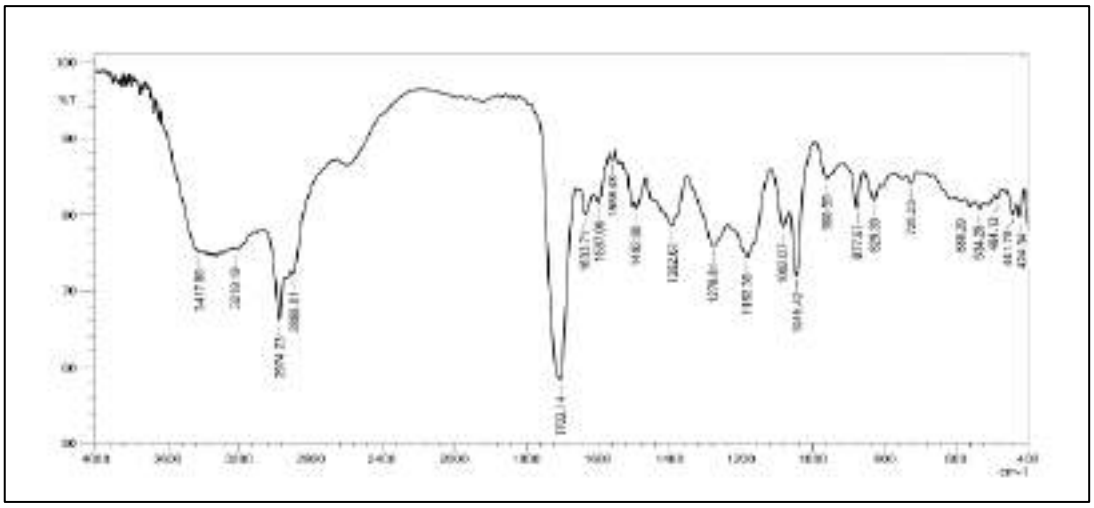


Figure (4- 131):FTIR spectrum of syntheses of copolymer(2) (MAA-Co-IAN) with compound(2).

^{1}HNMR spectrum of copolymer(2) (MAA-Co-IAN) with compound(2).

^{1}HNMR spectrum of copolymer(2) (MAA-Co-IAN) with compound(2) as shown in **(**fig.4-132) singles at (7.5-8.2 δ ppm) to (4H, phenyl ring), singles at 3.2-3.4 ppm) to $–NH_2$. single at (1.2 ppm) to $–CH_3$, single at (10.3 ppm) to –OH, single at (4.5 ppm) to –NH (amide), singles at (2.3 ppm) to $–CH_2$. (151-153)

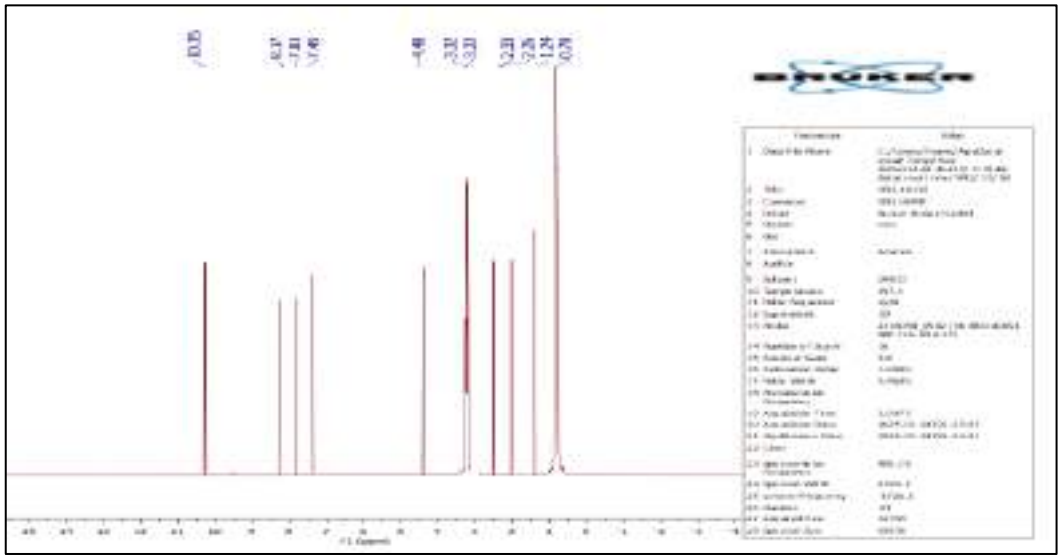


Figure (4- 132):^{1}HNMR spectrum of syntheses of copolymer(2) (MAA-Co-IAN) with compound(2).

^{13}C-NMR spectrum of copolymer(2) (MAA-Co-IAN) with compound(2).

The signals of olefinic and aromatic carbons appear in the third region between 124 and 135 ppm, singles related to C=N at 147- 150 ppm, single related to C-N at

64 ppm, singles related to C=S at 179 ppm, single related to CH_3-C (Secondary) at 18 ppm, single related to CH_3 at 18 ppm, single related to C=O (amide) at 166 ppm, single related to C=O (COOH) at 173 ppm. (151-153)

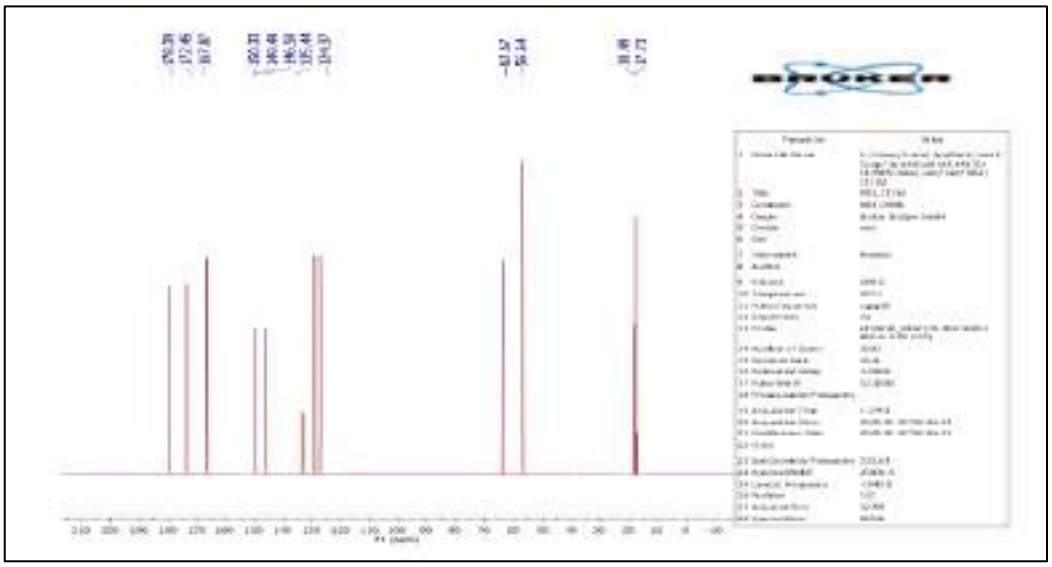
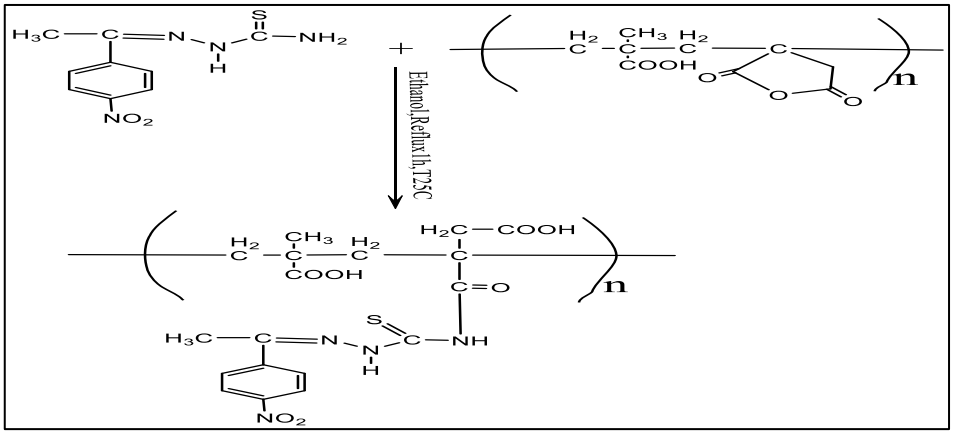


Figure (4- 133):^{13}C-NMR spectrum of syntheses of copolymer(2) (MAA-Co-IAN) with compound(2).

4.17.3 Synthesis of copolymer (3) (MAA-Co-IAN) with compound(3).



Scheme (4-50): synthesis of copolymer(3) (MAA-Co-IAN) with compound(3).

FTIR spectrum of copolymer (3) (MAA-Co-IAN) with compound(3).

The FTIR spectrum of copolymer (3) (MAA-Co-IAN) with compound(3) as shown in (fig.4-134) which indicates absorption bands at 3473 to -OH and 3414 cm^{-1} to –NH stretching, absorption band at 3197 cm^{-1} to C-H (aromatic), absorption band at 2999 cm-1 to C-H (aliphatic), absorption band at 1577 cm^{-1} to C=N, absorption band at 1076 Cm^{-1} to C=S, absorption band at 1481 Cm^{-1} to C=C (aromatic),

absorption band at 1506 Cm^{-1} to NO_2, and absorption band at 1334 Cm^{-1} to CH_3**,** absorption band at 1703 Cm-1 to C=O for carboxylic acid, absorption band at 1654 Cm-1 to C=O (amide), absorption band at 1103 Cm-1 to C-O. (151-153)

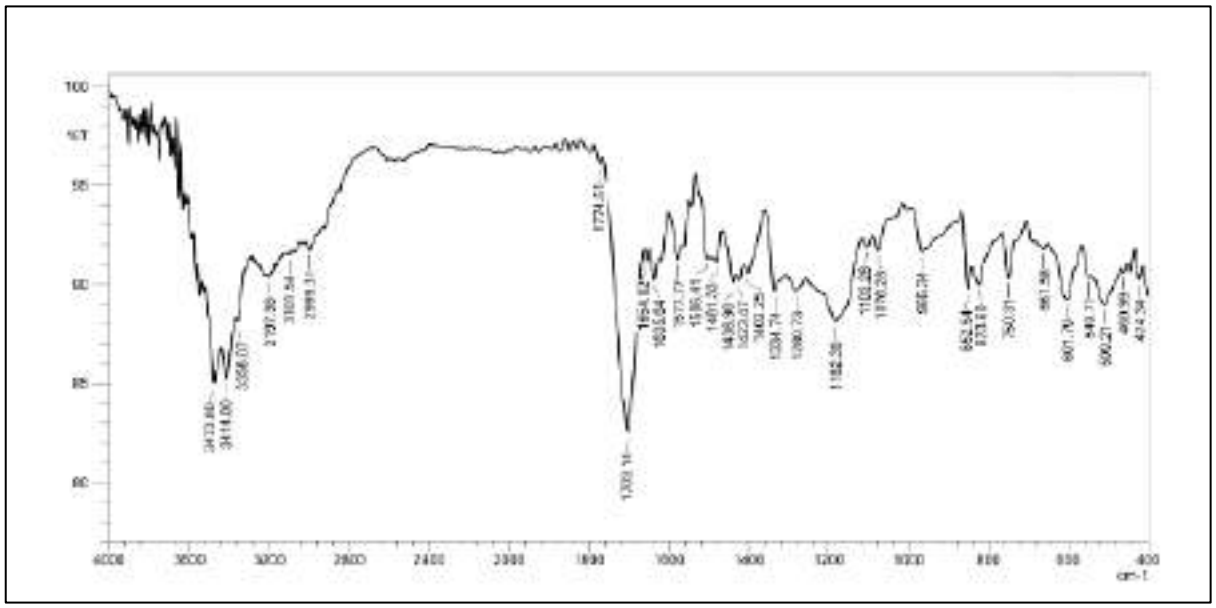


Figure (4- 134): FTIR spectrum of copolymer(3) (MAA-Co-IAN) with compound(3).

^{1}HNMR spectrum of copolymer (3) (MAA-Co-IAN) with compound(3).

^{1}HNMR spectrum of copolymer (3) (MAA-Co-IAN) with compound(3) in (fig.4-135) singles at (7.3-8.1 δ ppm) to (4H, phenyl ring), single at (3.3 ppm) to –NH, single at (4.4 ppm) to –NH (amide), singles at (0.9 ppm) to $–CH_3$, single at (11.7 ppm) to –OH, singles at (2.0-2.4 ppm) to $–CH_2$. (151-153)

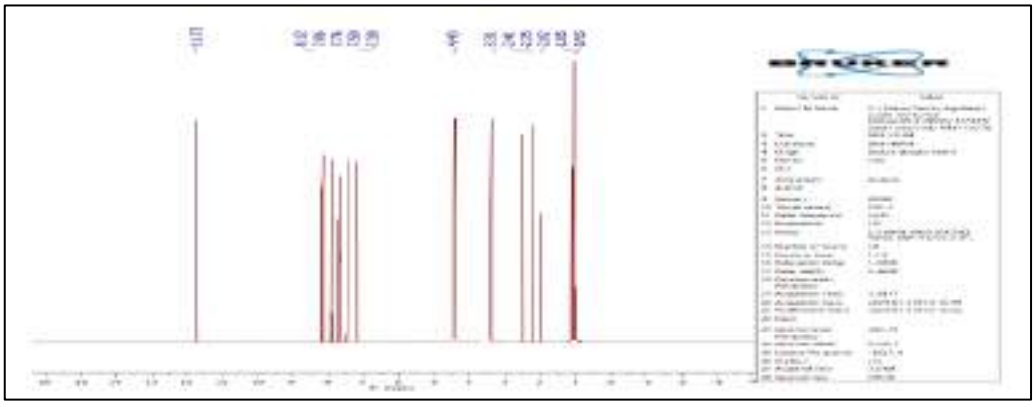


Figure (4- 135): ^{1}HNMR spectrum of copolymer(3) (MAA-Co-IAN) with compound(3).

^{13}C-NMR spectrum of copolymer (3) (MAA-Co-IAN) with compound(3).

The signals of olefinic and aromatic carbons appear in the third region between 124 and 133 ppm, singles related to C=N at 143-146 ppm, single related to C-N at 75 ppm, singles related to C=S at 192 ppm, single related to CH_3-C(Secondary) at 18 ppm, single related to CH_3 at 18 ppm, single related to C=O (amide) at 166 ppm, single related to C=O (COOH) at 177ppm. (151-153)

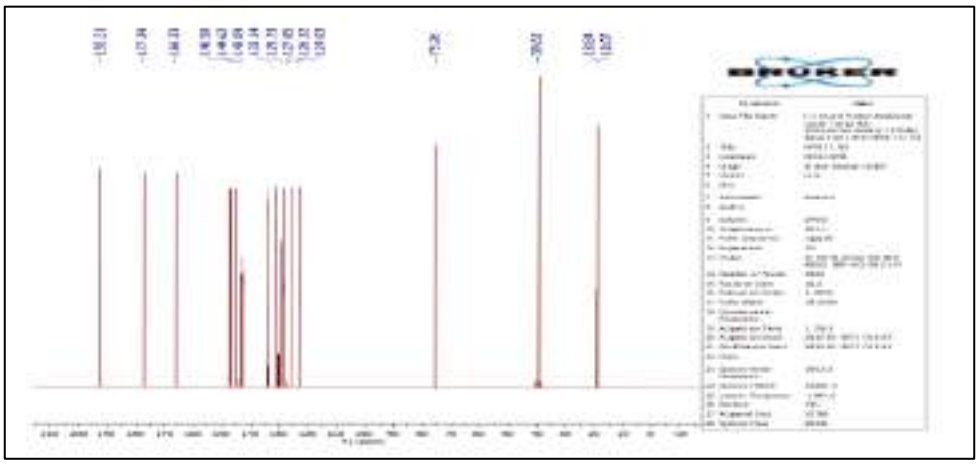
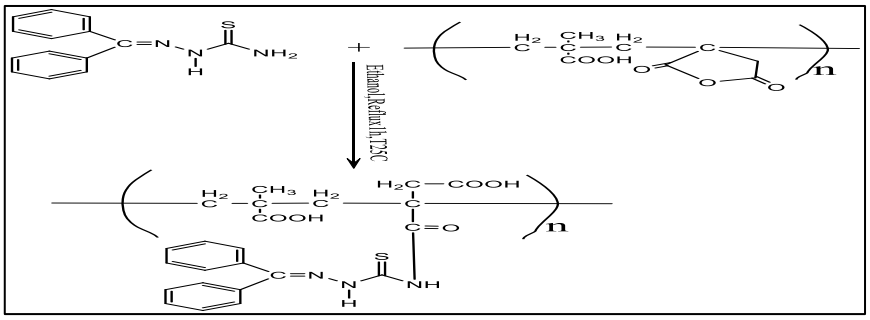


Figure (4- 136): ^{13}C-NMR spectrum of copolymer(3) (MAA-Co-IAN) with compound(3).

4.17.4 Synthesis of copolymer(4) (MAA-Co-IAN) with compound(4).



Scheme (4-51): synthesis of copolymer(4) (MAA-Co-IAN) with compound(4).

FTIR spectrum of copolymer(4) (MAA-Co-IAN) with compound(4).

The FTIR spectrum of copolymer (4) (MAA-Co-IAN) with compound(4) as shown in (fig.4-137) which indicates absorption bands at 3415 cm^{-1} to –OH overlapping with –NH stretching, absorption band at 2976 cm^{-1} to C-H (aromatic), absorption band at 2897 cm-1 to C-H (aliphatic), absorption band at 1537 cm^{-1} to C=N, absorption band at 1176 Cm^{-1} to C=S, absorption band at 1452 Cm^{-1} to C=C (aromatic), and absorption band at 1386 Cm-1 to CH_3, absorption band at 1703 Cm-1 to C=O for carboxylic acid, absorption band at 1643 Cm-1 to C=O (amide),

absorption band at 1047 Cm-1 to C-O. (151-153)

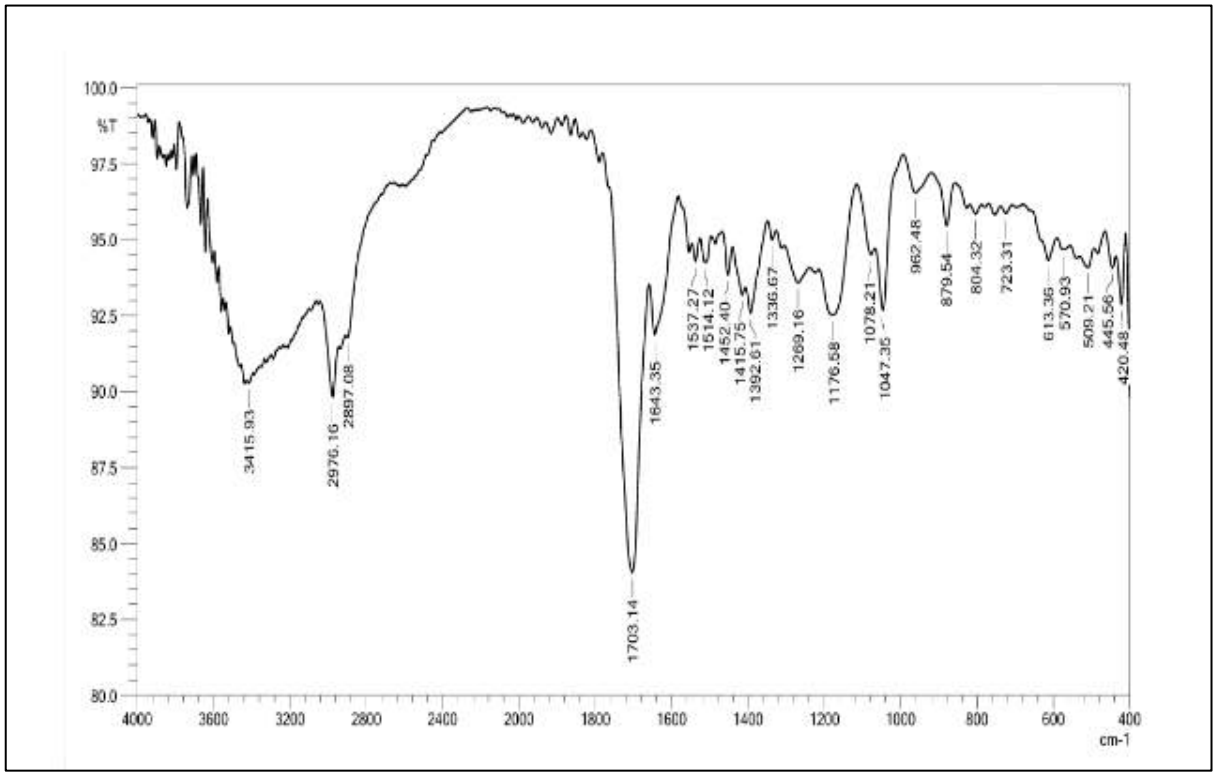


Figure (4- 137): FTIR spectrum of copolymer(4) (MAA-Co-IAN) with compound(4).

[1]HNMR spectrum of copolymer(4) (MAA-Co-IAN) with compound(4).

[1]HNMR spectrum of copolymer (4) (MAA-Co-IAN) with compound(4) in (fig.4-138) singles at (7.1-8.8 δ ppm) to (10H, phenyl ring), single at (3.5 ppm) to –NH. singles at (1.0 ppm) to $–CH_3$, single at (4.5 ppm) to –NH (amide), singles at (1.0 ppm) to –CH3, single at (11.3 ppm) to –OH (COOH), singles at (2.5 ppm) to $–CH_2$. (151-153)

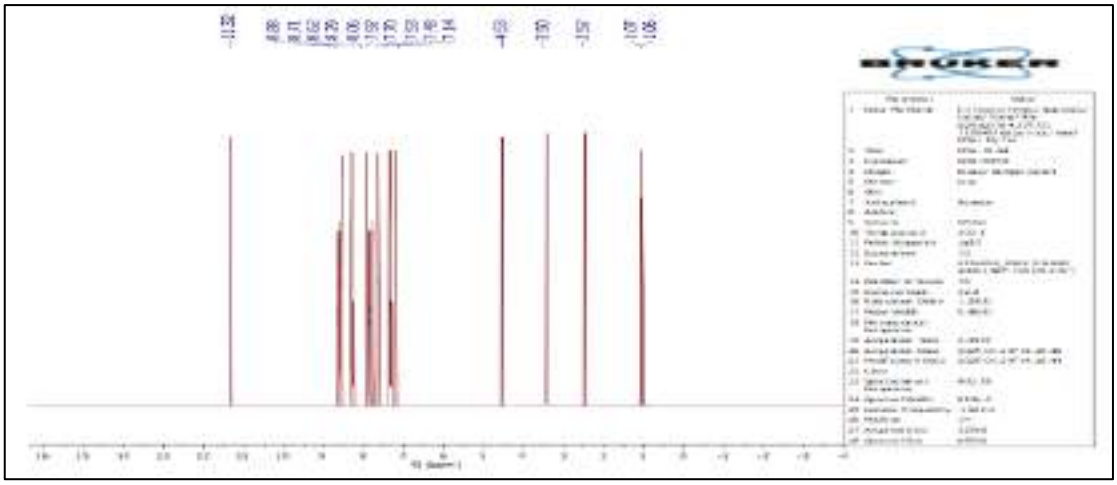


Figure (4- 138): [1]HNMR spectrum of copolymer(4) (MAA-Co-IAN) with compound(4).

^{13}C-NMR spectrum of copolymer(4) (MAA-Co-IAN) with compound(4).

The signals of olefinic and aromatic carbons appear in the third region between 117 and 133 ppm, single related to C=N at 150 ppm, single related to C-N at 72 ppm, single related to C=S at 182 ppm, single related to CH_3-C(Secondary) at 18 ppm, single related to CH_3 at 18 ppm, single related to C=O (amide) at 166 ppm, single related to C=O (COOH) at 173 ppm. (151-153)

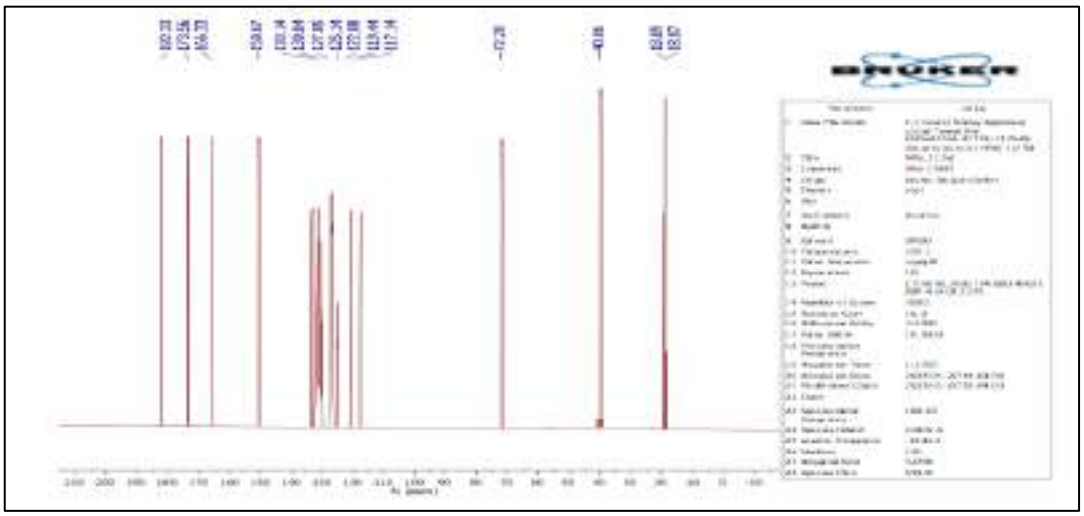
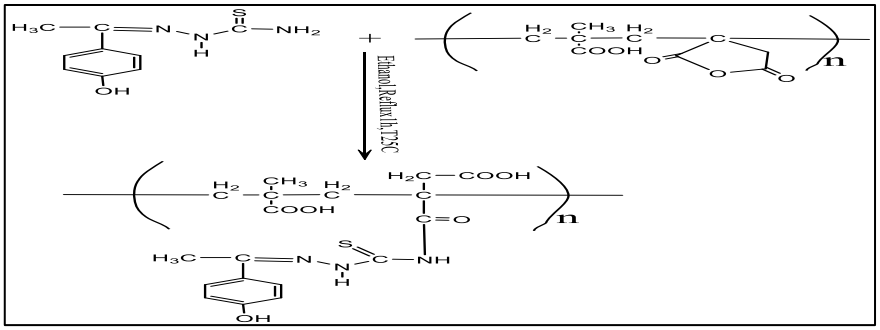


Figure (4- 139): ^{13}C-NMR spectrum of copolymer(4) (MAA-Co-IAN) with compound(4).

4.17.5Synthesis of copolymer(5) (MAA-Co-IAN) with compound(5).



Scheme (4-52): synthesis of copolymer(5) (MAA-Co-IAN) with compound(5).

FTIR spectrum of copolymer(5) (MAA-Co-IAN) with compound(5).

The FTIR spectrum of copolymer(5) (MAA-Co-IAN) with compound(5) as shown in (fig.4-140) which indicates absorption bands at 3441 Cm^{-1} to OH and 3317cm^{-1} to –NH stretching, absorption band at 3188cm^{-1} to C-H (aromatic), absorption band at 2991 cm^{-1} to C-H (aliphatic), absorption band at 1537 cm-1 to C=N, absorption band at 1188 Cm-1 to C=S, absorption band at 1487 Cm^{-1} to C=C (aromatic), and absorption band at 1392Cm^{-1} to CH_3, , absorption band at 1701 Cm-

[1] to C=O for carboxylic acid, absorption band at 1631 Cm^{-1} to C=O (amide), absorption band at 1037 Cm-1 to C-O. (151-153)

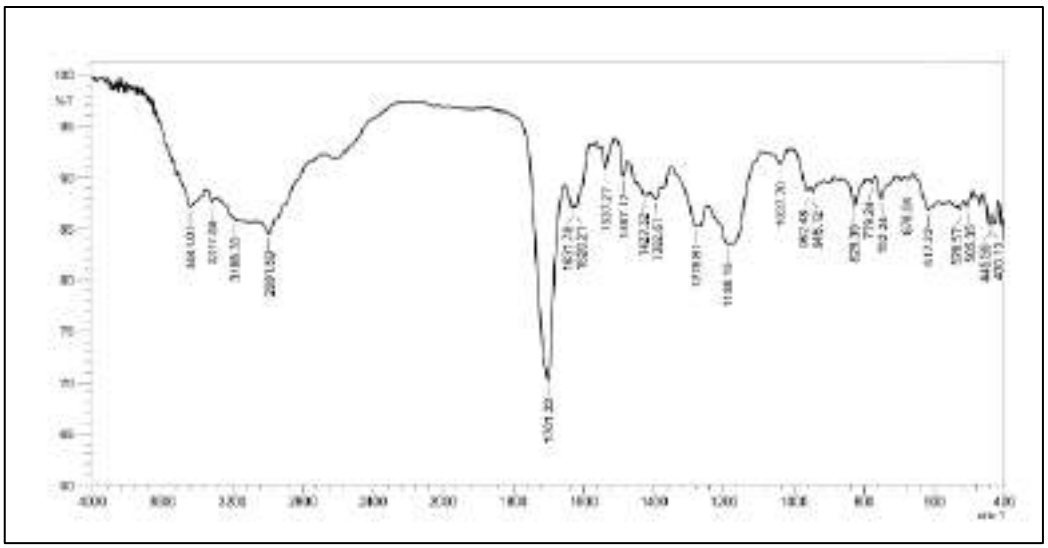


Figure (4- 140): FTIR spectrum of copolymer (5) (MAA-Co-IAN) with compound(5).

[1]HNMR spectrum of copolymer(5) (MAA-Co-IAN) with compound(5).

[1]HNMR spectrum of copolymer(5) (MAA-Co-IAN) with compound(5) in (fig.4-141) singles at (6.0-7.3 δ ppm) to (4H, phenyl ring), single at (3.5 ppm) to –NH, single at (5.7 ppm) to (H, OH). single at (4.5 ppm) to –NH (amide), singles at (1.0 ppm) to –CH3, single at (11.3 ppm) to –OH (COOH), singles at (2.5 ppm) to –CH_2. (151-153)

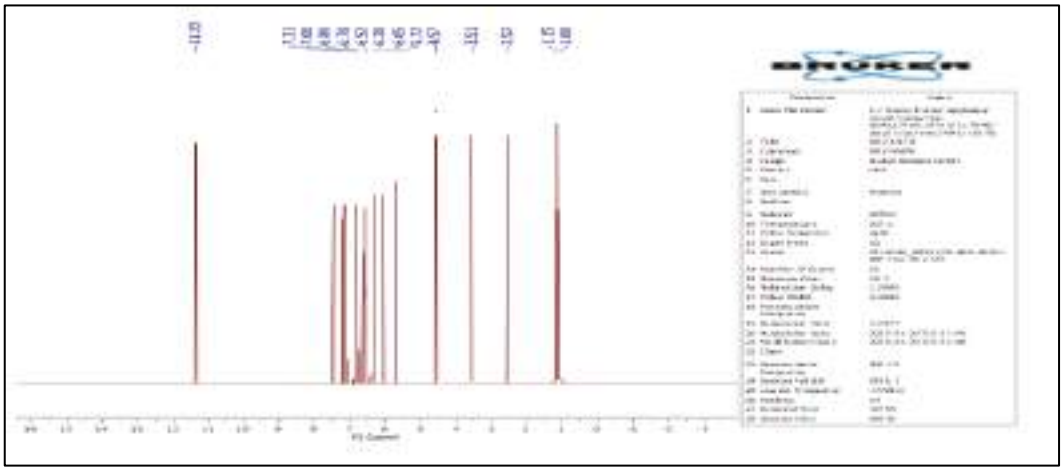


Figure (4- 141): [1]HNMR spectrum of copolymer (5) (MAA-Co-IAN) with compound(5).

^{13}C-NMR spectrum of copolymer(5) (MAA-Co-IAN) with compound(5).

The signals of olefinic and aromatic carbons appear in the third region between 118 and 133 ppm, single related to C=N at 152-157 ppm, single related to C-N at 72 ppm, single related to C=S at 183 ppm, single related to CH_3-C(Secondary) at 18 ppm, single related to CH_3 at 18 ppm, single related to C=O (amide) at 166 ppm, single related to C=O (COOH) at 173 ppm. (151-153)

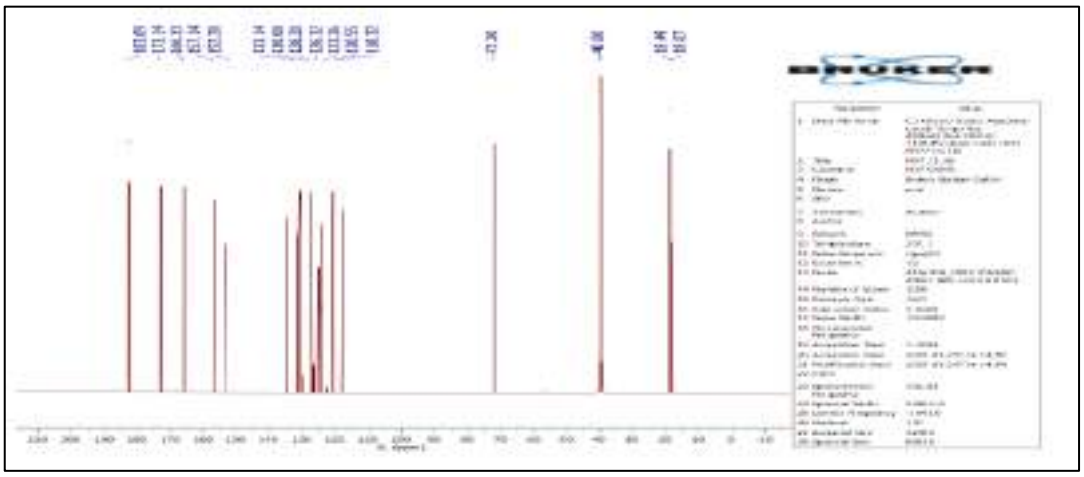
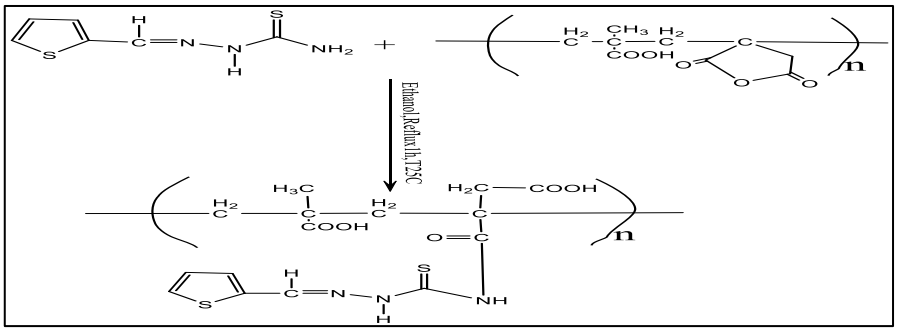


Figure (4- 142): ^{13}C-NMR spectrum of copolymer (5) (MAA-Co-IAN) with compound(5).

4.17.6Synthesis of copolymer(6) (MAA-Co-IAN) with compound(6).



Scheme (4-53): synthesis of copolymer(6) (MAA-Co-IAN) with compound(6).

FTIR spectrum of copolymer(6) (MAA-Co-IAN) with compound(6).

The FTIR spectrum of copolymer(6) (MAA-Co-IAN) with compound(6) as shown in (fig.4-143) which indicates absorption bands at 3545 to –OH Cm^{-1} and 3448 and 3412 cm^{-1} to –NH stretching, absorption band at 3232 cm^{-1} to C-H (Hetero phenyl ring), absorption band at 2978 cm^{-1} to C-H (aliphatic), absorption band at 1616 cm^{-1} to C=N, absorption band at 1271 Cm^{-1} to C=S, absorption band at 1537 Cm^{-1} to C=C (Hetero phenyl ring),), absorption band at 1043 Cm^{-1} to C-O,

absorption band at 1182 Cm^{-1} to C-N, absorption band at 1701 Cm^{-1} to C=O (COOH), absorption band at 1635 Cm^{-1} to C=O (amide), absorption band at 1388 Cm^{-1} to CH_3. (151-153)

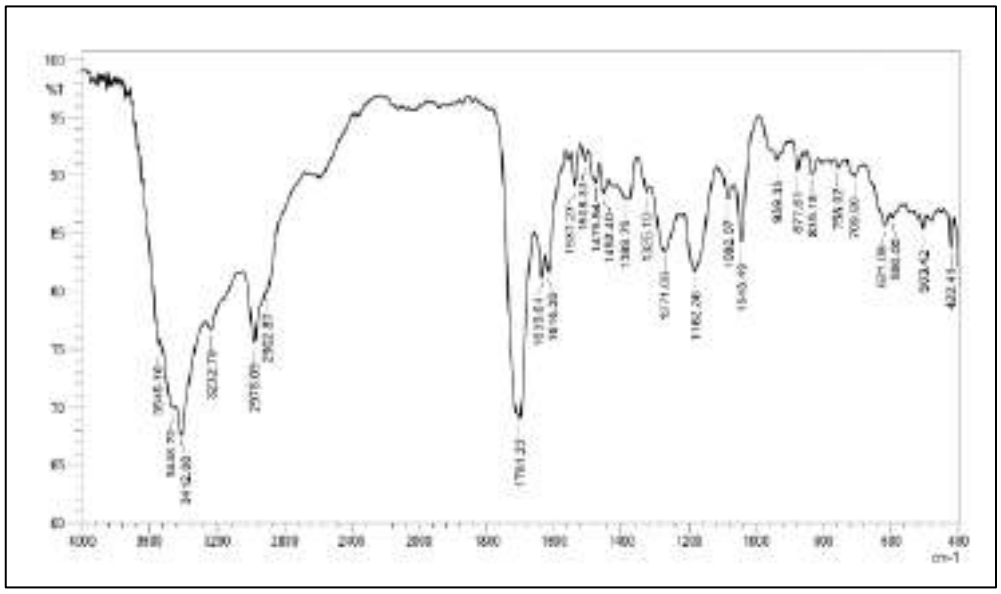


Figure (4- 143): FTIR spectrum of copolymer (6) (MAA-Co-IAN) with compound(6).

^{1}HNMR spectrum of copolymer(6) (MAA-Co-IAN) with compound(6).

^{1}HNMR spectrum of copolymer(6) (MAA-Co-IAN) with compound(6) in (fig.4-144) singles at (6.7-8.0 δ ppm) to (3H, Hetro phenyl ring), single at (3.3 ppm) to –NH, single at (3.5 ppm) to –NH, single at (4.4ppm) to –NH (amide), singles at (0.9 ppm) to $–CH_3$, single at (11.0 ppm) to –OH (COOH), singles at (2.3 ppm) to $–CH_2$. (151-153)

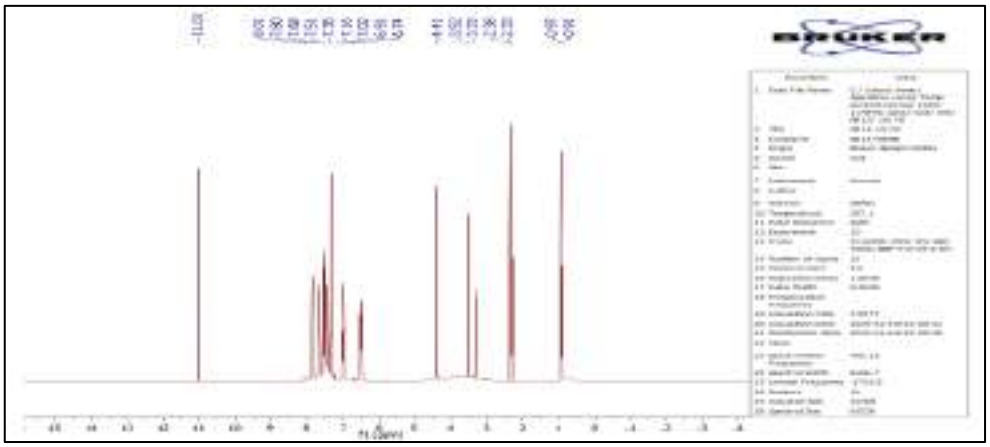


Figure (4- 144): 1HNMR spectrum of copolymer (6) (MAA-Co-IAN) with compound(6).

^{13}C-NMR spectrum of polymer 1 for thiophene-2- carboxaldehyde

The signals of olefinic and aromatic carbons appear in the third region between 126 and 131 ppm, singles related to C=N at 139 ppm, singles related to C-N at 64 ppm, single related to C=S at 195 ppm, single related to CH_3-C(Secondary) at 18 ppm, single related to CH_3 at 18 ppm, singles related to C=O (amide) at 166 ppm, single related to C=O (COOH) at 178 ppm. (151-153)

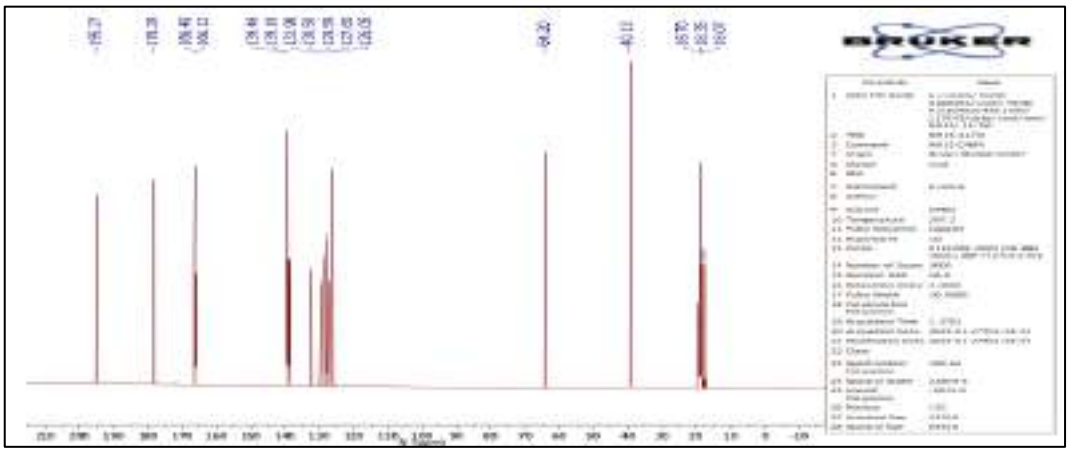
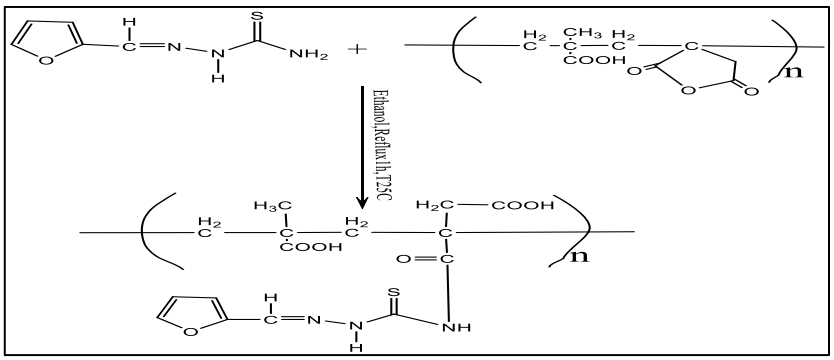


Figure (4- 145): ^{13}C-NMR spectrum of copolymer (6) (MAA-Co-IAN) with compound(6).

4.17.7Synthesis of copolymer(7) (MAA-Co-IAN) with compound(7).



Scheme (4-54): synthesis of copolymer(7) (MAA-Co-IAN) with compound(7).

FTIR spectrum of copolymer(7) (MAA-Co-IAN) with compound(7).

The FTIR spectrum of copolymer(7) (MAA-Co-IAN) with compound(7) as shown in (fig.4-146) which indicates absorption bands at 3417Cm^{-1} to –OH overlapping with –NH. stretching, absorption band at 2974 cm^{-1} to C-H (Hetero phenyl ring), absorption band at 2889 cm^{-1} to C-H (aliphatic), absorption band at 1523 Cm^{-1} to C=N, absorption band at 1269 Cm^{-1} to C=S, absorption band at 1477 Cm^{-1} to C=C (Hetero phenyl ring), absorption band at 1045 Cm^{-1} to C-O, absorption

band at 1187 Cm^{-1} to C-N, absorption band at 1701 Cm^{-1} to C=O (COOH), absorption band at 1627 Cm^{-1} to C=O (amide), absorption band at 1392 Cm^{-1} to CH_3. (151-153)

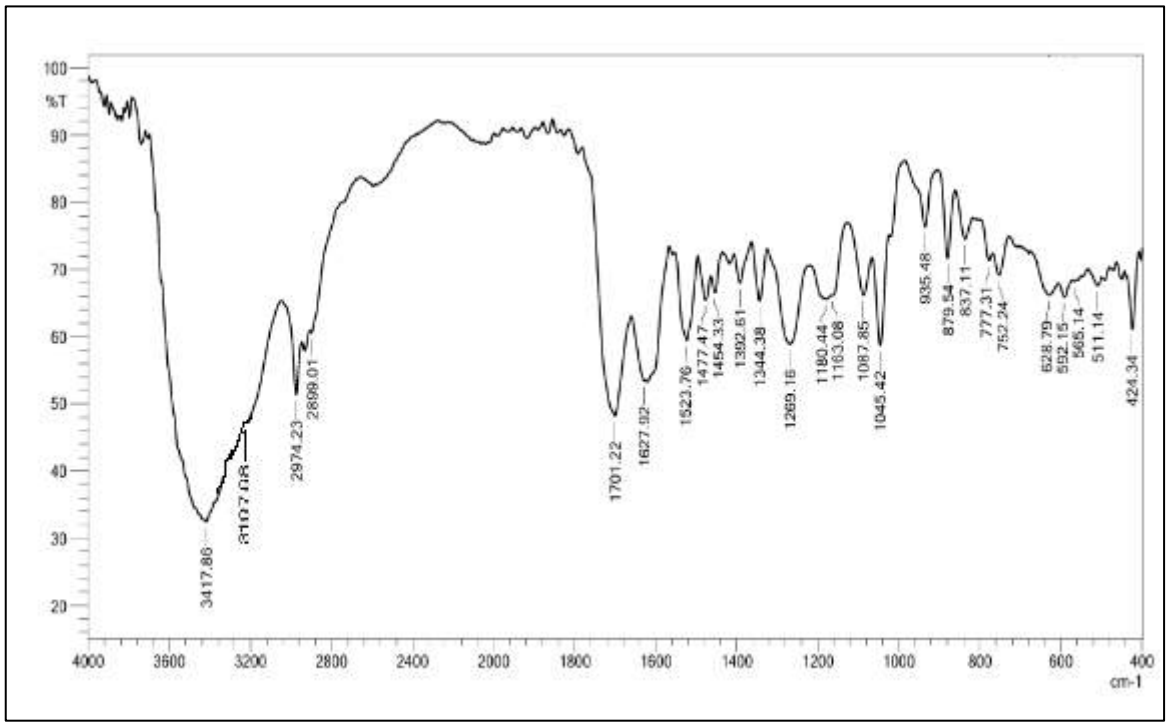


Figure (4- 146): FTIR spectrum of copolymer (7) (MAA-Co-IAN) with compound(7).

[1]HNMR spectrum of copolymer(7) (MAA-Co-IAN) with compound(7).

[1]HNMR spectrum of copolymer(7) (MAA-Co-IAN) with compound(7) in (fig.4-147) singles at (6.5-8.1 δ ppm) to (3H, Hetro phenyl ring), single at (3.4 ppm) to –NH, single at (4.4ppm) to –NH (amide), singlate at (1.0 ppm) to $–CH_3$, single at (11.4 ppm) to –OH (COOH), singles at (2.5 ppm) to $–CH_2$. (151-153)

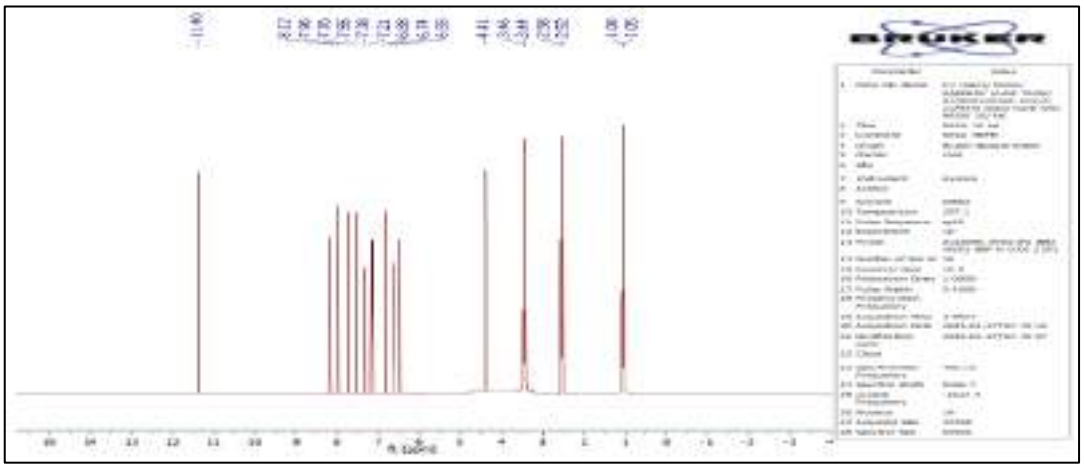


Figure (4- 147): [1]HNMR spectrum of copolymer (7) (MAA-Co-IAN) with compound(7).

^{13}C-NMR spectrum of copolymer(7) (MAA-Co-IAN) with compound(7).

The signals of olefinic and aromatic carbons appear in the third region between 114 and 133 ppm, single related to C=N at 145-150 ppm, single related to C-N at 64 ppm, single related to C=S at 1194 ppm, single related to CH_3-C(Secondary) at 18 ppm, single related to C=O (amide) at 166 ppm, single related to C=O (COOH) at 178 ppm. (151-153)

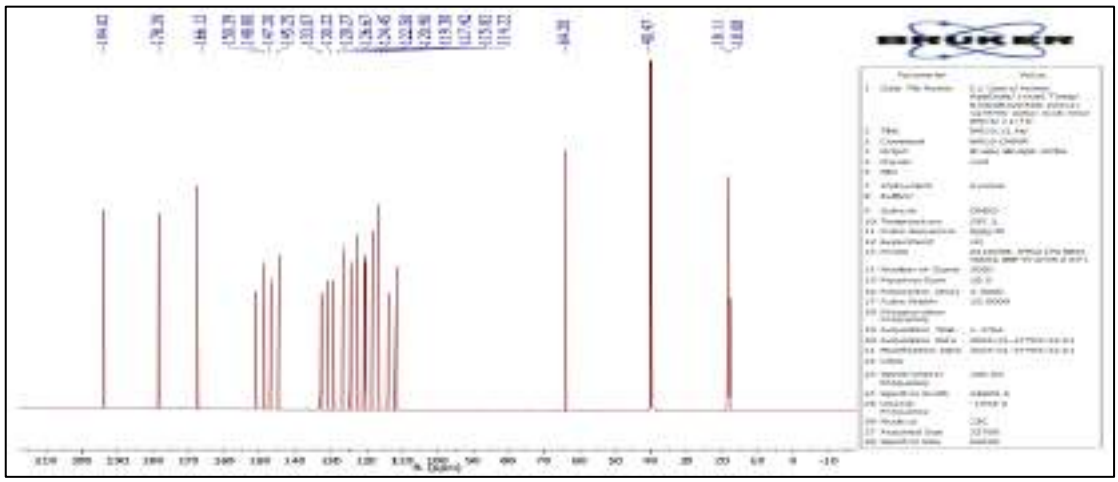
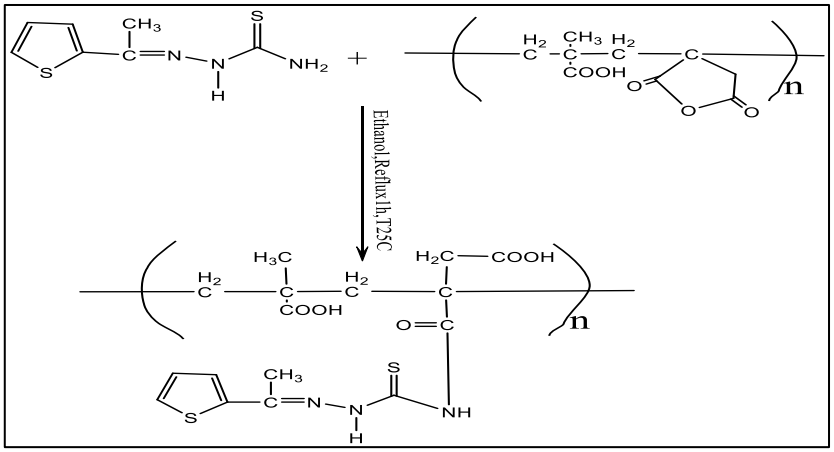


Figure (4- 148): ^{13}C-NMR spectrum of copolymer (7) (MAA-Co-IAN) with compound(7).

4.17.8 Synthesis of copolymer(8) (MAA-Co-IAN) with compound(8).



Scheme (4-55): synthesis of copolymer(8) (MAA-Co-IAN) with compound(8).

FTIR spectrum of copolymer(8) (MAA-Co-IAN) with compound(8).

The FTIR spectrum of copolymer(8) (MAA-Co-IAN) with compound(8) as shown in (fig.4-149) which indicates absorption bands at 3457 cm^{-1} to –OH overlapping with –NH stretching, absorption band at 3070 cm^{-1} to C-H (Hetero phenyl ring), absorption band at 2949 cm^{-1} to C-H(aliphatic), absorption band at

1612 cm^{-1} to C=N, absorption band at 1290 Cm^{-1} to C=S, absorption band at 1487 Cm^{-1} to C=C (Hetero phenyl ring), absorption band at 1031 Cm^{-1} to C-O, absorption band at 1199 Cm^{-1} to C-N, absorption band at 1708 Cm^{-1} to C=O (COOH), absorption band at 1699 Cm^{-1} to C=O (amide), absorption band at 1336 Cm^{-1} to CH_3.(151-153)

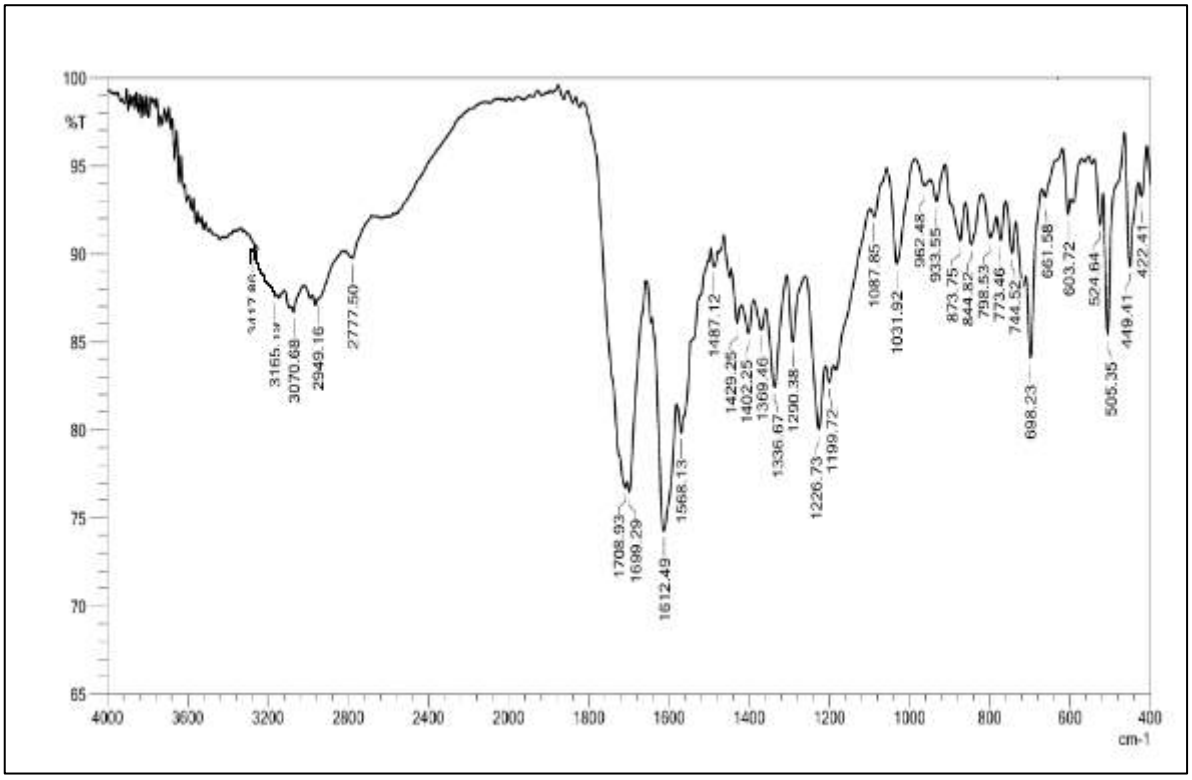


Figure (4- 149): FTIR spectrum of copolymer (8) (MAA-Co-IAN) with compound(8).

^{1}HNMR spectrum of copolymer(8) (MAA-Co-IAN) with compound(8). ^{1}HNMR spectrum of copolymer(8) (MAA-Co-IAN) with compound(8) in (fig.4-150) singles at (7.3-8.3 δ ppm) to (3H, Hetro phenyl ring), singles at (3.5 ppm) to –NH, singles at (4.3ppm) to –NH (amide), singles at (1.3 ppm) to $–CH_3$, single at (12.3 ppm) to –OH (COOH), singles at (2.5 ppm) to $–CH_2$. (151-153)

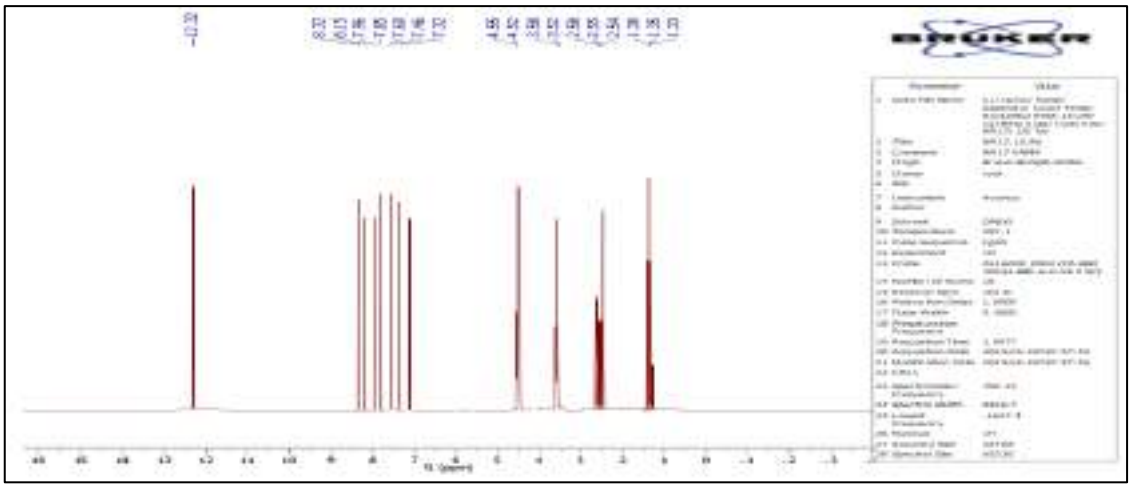


Figure (4- 150): ^{1}HNMR spectrum of copolymer (8) (MAA-Co-IAN) with compound(8).

^{13}C-NMR spectrum of copolymer(8) (MAA-Co-IAN) with compound(8).

The signals of olefinic and aromatic carbons appear in the third region between 128 and 131 ppm, single related to C=N at 150 ppm, single related to C-N at 64 ppm, single related to C=S at 195 ppm, singles related to CH_3 at 15 ppm, single related to CH_3 at 18 ppm, singles related to C=O (amide) at 164 ppm, singles related to C=O (COOH) at 175 ppm. (151-153)

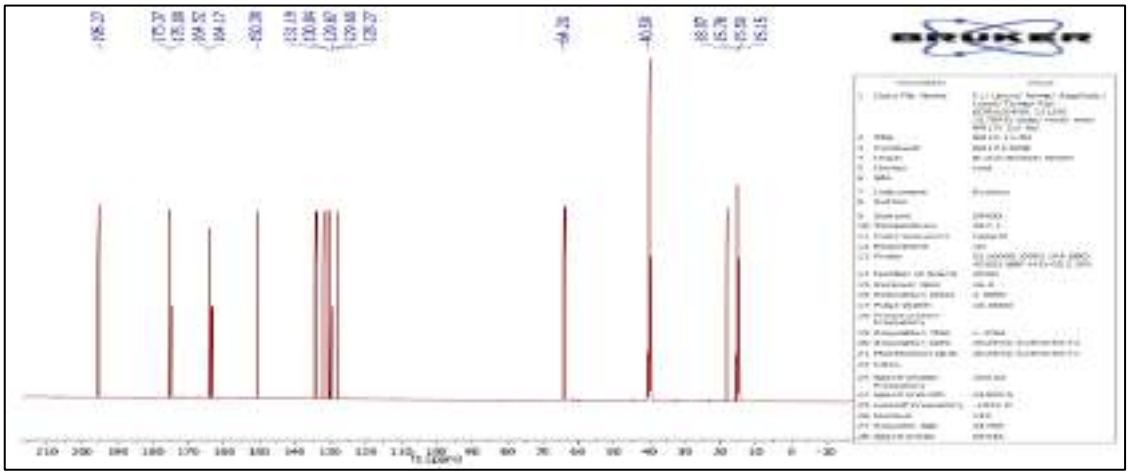
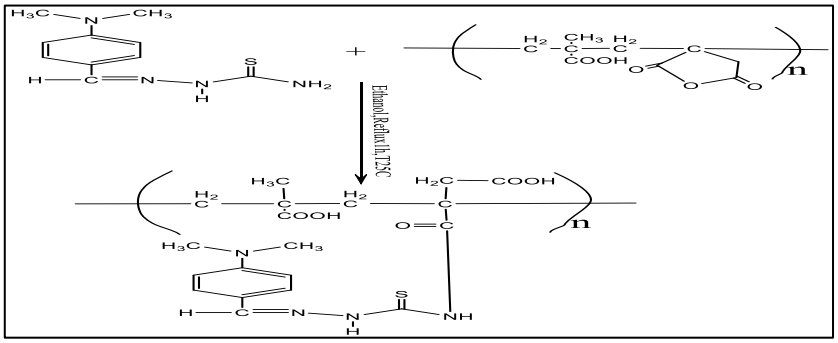


Figure (4- 151): ^{13}C-NMR spectrum of copolymer (8) (MAA-Co-IAN) with compound(8).

4.17.9 Synthesis of copolymer(9) (MAA-Co-IAN) with compound(9).



Scheme (4-56): synthesis of copolymer(9) (MAA-Co-IAN) with compound(9).

FTIR spectrum of copolymer(9) (MAA-Co-IAN) with compound(9).

The FTIR spectrum of copolymer (9) (MAA-Co-IAN) with compound(9) as shown in (fig.4-152) which indicates absorption bands at 3396 Cm^{-1} to -OH and 3253 cm^{-1} to –NH stretching , absorption band at 2974 cm^{-1} to C-H(aromatic), absorption band at 2897 cm^{-1} to C-H (aliphatic), , absorption band at 1637 cm^{-1} to C=N, absorption band at 1271 Cm^{-1} to C=S, absorption band at 1539 Cm^{-1} to C=C (aromatic), absorption band at 1045 Cm^{-1} to C-O, absorption band at 1182 Cm^{-1} to C-N, absorption band at 1710 Cm^{-1} to C=O (COOH), absorption band at 1699 Cm^{-1} to C=O (amide), absorption band at 1392 Cm^{-1} to CH_3. (151-153)

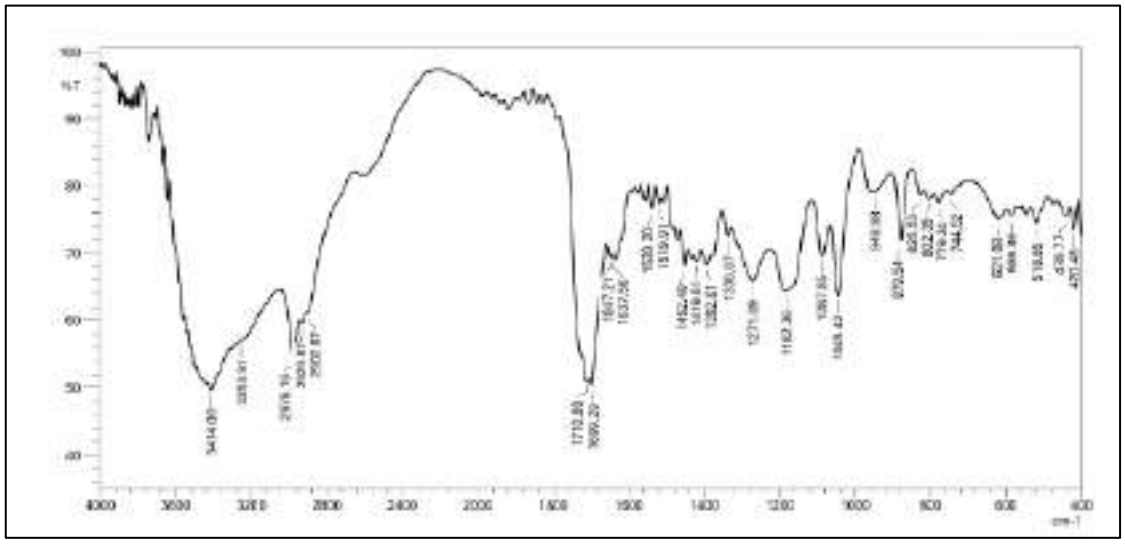


Figure (4- 152): FTIR spectrum of copolymer (9) (MAA-Co-IAN) with compound(9).

^{1}HNMR spectrum of copolymer(9) (MAA-Co-IAN) with compound(9).

^{1}HNMR spectrum of copolymer(9) (MAA-Co-IAN) with compound(9) in (fig.4-153) the major signal at δ 2.9 ppm is characteristic of DMSO-d6 as solvent, singlate at (7.1-8.2 δ ppm) to (4H, phenyl ring), single at (3.3 ppm) to –NH, singles at 3.3 ppm to CH_3-N, singles at (4.0-4.5 ppm) to –NH (amide), singles at (1.3 ppm) to –CH_3, single at (12.3 ppm) to –OH (COOH), singles at (2.5 ppm) to –CH_2. (151-153)

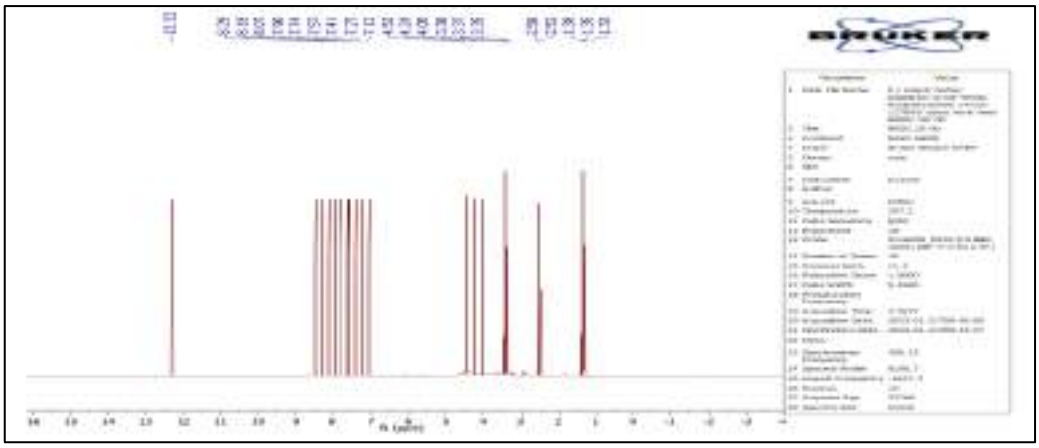


Figure (4- 153): ^{1}HNMR spectrum of copolymer (9) (MAA-Co-IAN) with compound(9).

^{13}C-NMR of copolymer(9) (MAA-Co-IAN) with compound(9).

The signals of olefinic and aromatic carbons appear in the third region between 110 and 129 ppm, singles related to C=N at 154 ppm, single related to C-N at 64 ppm. singles related to C=S at 193 ppm, single related to CH_3 at 18 ppm, single related to CH_3 at 18 ppm, single related to C=O (amide) at 166 ppm, single related to C=O (COOH) at 178 ppm. (151-153)

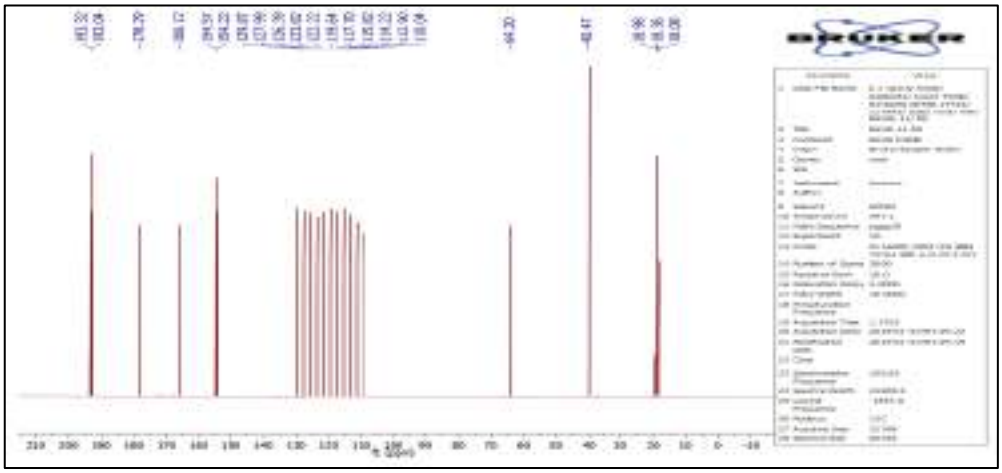
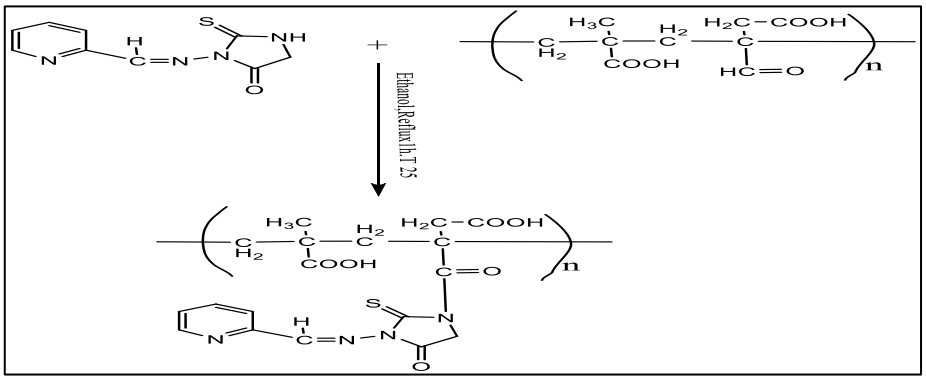


Figure (4- 154): ^{13}C-NMR spectrum of copolymer (9) (MAA-Co-IAN) with compound(9).

4.18 Synthesis of copolymer (MAA-CO-IAN) with thiosemicarbazide derivatives compounds. (10-17)

4.18.1 Synthesis of copolymer(10) (MAA-Co-IAN) with compound(10).



Scheme (4-57): synthesis of copolymer(10) (MAA-Co-IAN) with compound(10).

FTIR spectrum of copolymer(10) (MAA-Co-IAN) with compound(10).

The FTIR spectrum of the preparation of copolymer(10) (MAA-Co-IAN) with compound(10) as shown in (fig.4-155) which indicates absorption band at 3479 cm^{-1} to –OH, absorption band at 3415 Cm^{-1} to C-H (aromatic), absorption band at 2958 Cm^{-1} to C-H (aliphatic) , absorption band at 1643 Cm^{-1} to C=N, absorption band at 1170 Cm^{-1} to C=S, absorption band at 1539 Cm^{-1} to C=C (aromatic), absorption band at 1082 Cm^{-1} to C-O, absorption band at 1045 Cm^{-1} to C-N, absorption band at 1695 Cm^{-1} to C=O(COOH), absorption band at 1681 Cm^{-1} to C=O(amide), absorption band at 1342 Cm^{-1} to CH_3. (151-153)

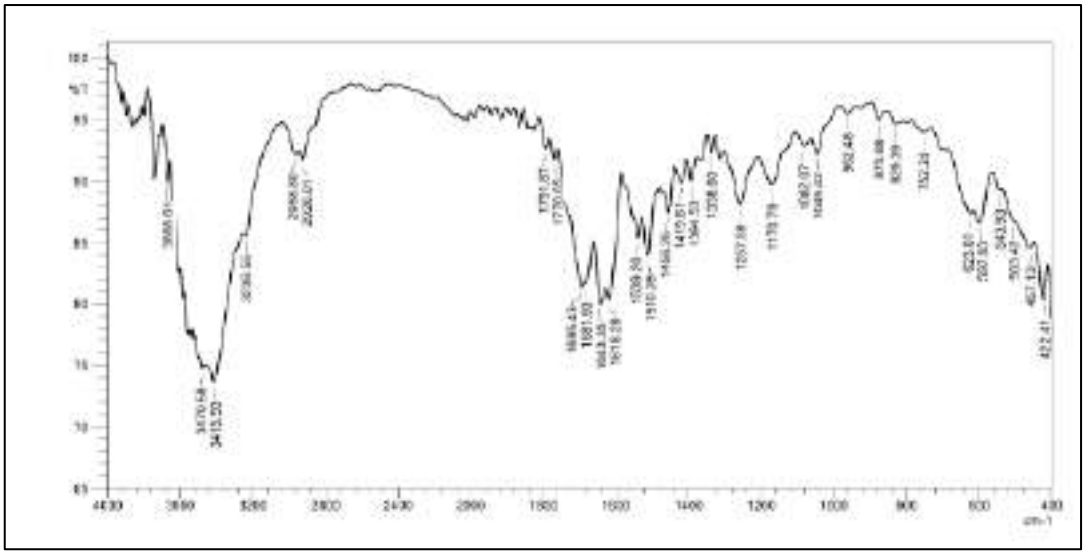


Figure (4- 155): FTIR spectrum of copolymer(10) (MAA-Co-IAN) with compound(10).

^{1}HNMR spectrum of copolymer(10) (MAA-Co-IAN) with compound(10).

^{1}HNMR spectrum of copolymer(10) (MAA-Co-IAN) with compound(10) in (fig.4-156) Singles at (7.4-8.8 δ ppm) to (4H, phenyl ring), multiplet singlate at (3.4 to 4.1 ppm) to –NH, singlate at (12.3 ppm) to –OH, single at (1.2 ppm) to $–CH_3$, singles at (2.0-2.5 ppm) to $–CH_2$. (151-153)

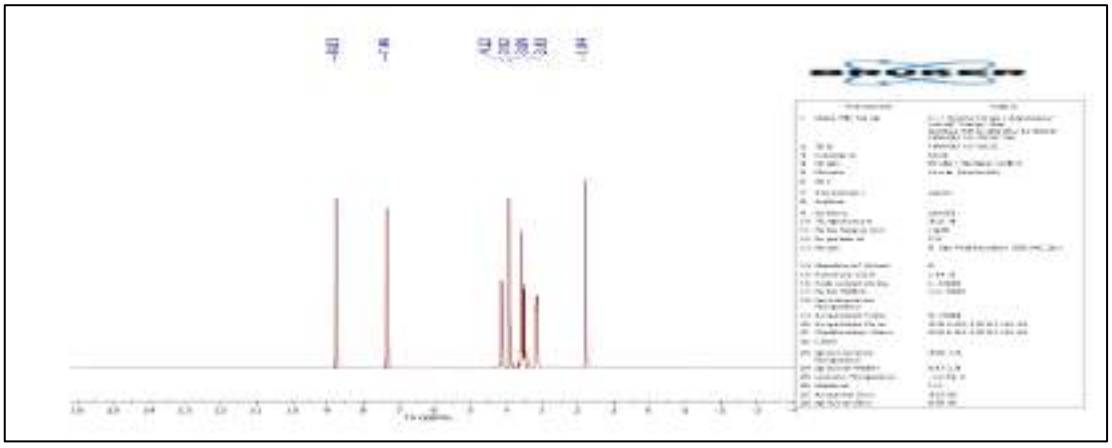


Figure (4- 156): ^{1}HNMR spectrum of copolymer(10) (MAA-Co-IAN) with compound(10).

^{13}C-NMR spectrum of copolymer(10) (MAA-Co-IAN) with compound(10).

The signals of olefinic and aromatic carbons appear in the third region between 122 and 136 ppm, singles related to C=N at 151-166 ppm, single related to C-N at 64 ppm, singles related to C=O (amide) at 174 ppm, single related to C=S at 176 ppm. (151-153)

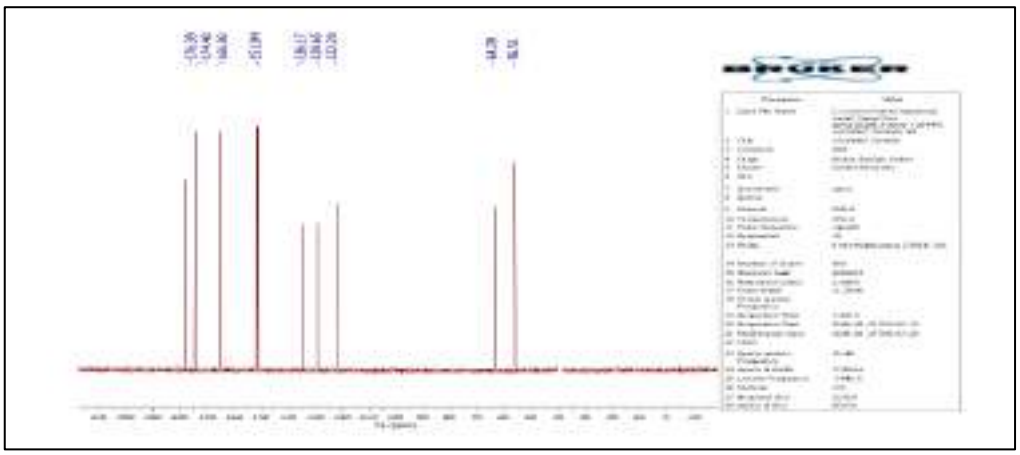
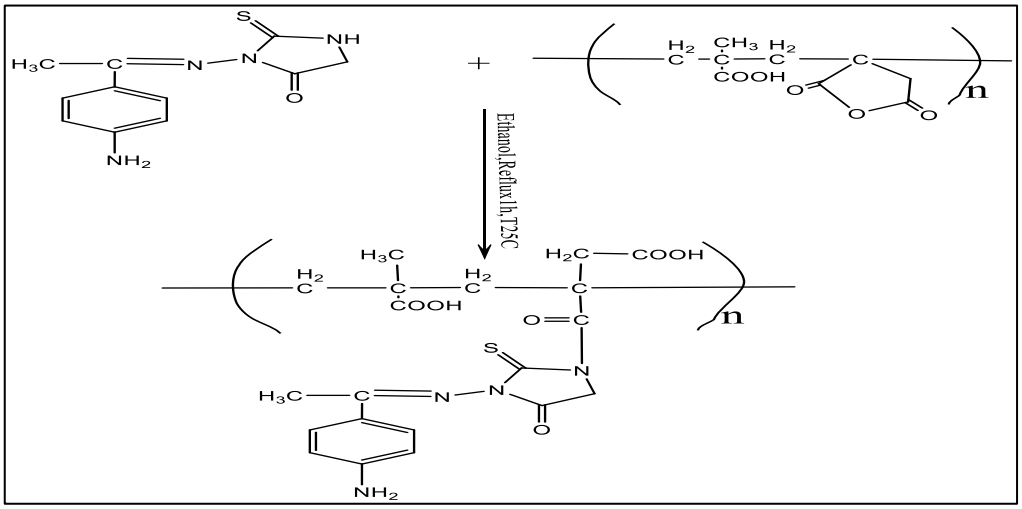


Figure (4- 157): ^{13}C-NMR spectrum of copolymer(10) (MAA-Co-IAN) with compound(10).

4.18.2 Synthesis of copolymer(11) (MAA-CO-IAN) with compound(11).



Scheme (4-58): synthesis of copolymer(11) (MAA-CO-IAN) with compound(11).

FTIR spectrum of copolymer(11) (MAA-CO-IAN) with compound(11).

The FTIR spectrum of copolymer(11) (MAA-CO-IAN) with compound(11) as shown in (fig.4-158) which indicates absorption bands at 3466 to -OH and 3134 cm^{-1} to $–NH_2$ stretching, absorption band at 3005 cm^{-1} to C-H (aromatic), absorption band at 2935 cm-1 to CH_2(aliphatic), absorption band at 1633 cm^{-1} to C=N, absorption band at 1182 Cm^{-1} to C=S, absorption band at 1492 Cm^{-1} to C=C (aromatic), and absorption band at 1392 Cm^{-1} to CH_3, absorption band at 1703 Cm-1 to C=O for carboxylic acid, absorption band at 1633 Cm^{-1} to C=O (amide), absorption band at 1082 Cm^{-1} to C-O. (151-153)

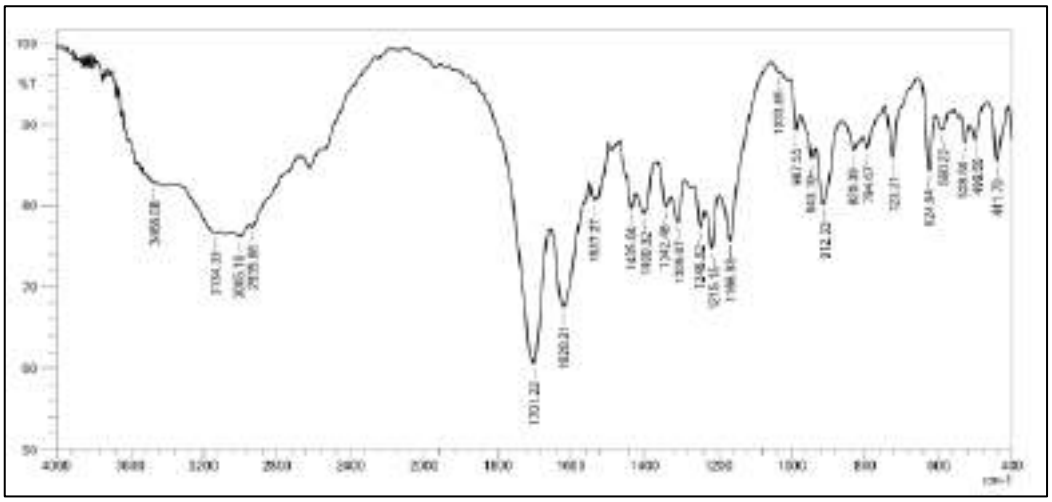


Figure (4- 158): FTIR spectrum of copolymer(11) (MAA-CO-IAN) with compound(11).

^{1}HNMR spectrum of copolymer(11) (MAA-CO-IAN) with compound(11).

^{1}HNMR spectrum of copolymer(11) (MAA-CO-IAN) with compound(11) in (fig.4-159) singles at (7.5-8.2 δ ppm) to (4H, phenyl ring), singles at 3.2-3.4 ppm) to $–NH_2$. single at (1.2 ppm) to $–CH_3$, single at (10.3 ppm) to –OH, single at (4.5 ppm) to –NH (amide), singles at (2.3 ppm) to $–CH_2$. (151-153)

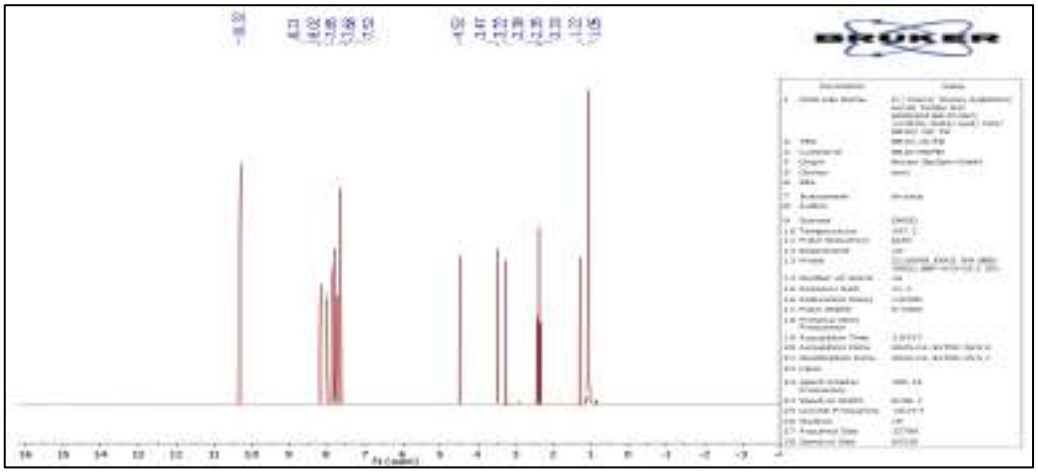


Figure (4- 159): ^{1}HNMR spectrum of copolymer(11) (MAA-CO-IAN) with compound(11).

^{13}C-NMR spectrum of copolymer(11) (MAA-CO-IAN) with compound(11).

The signals of olefinic and aromatic carbons appear in the third region between 124 and 135 ppm, singles related to C=N at 147- 150 ppm, single related to C-N at 64 ppm, singles related to C=S at 179 ppm, single related to CH_3-C (Secondary) at 18 ppm, single related to CH_3 at 18 ppm, single related to C=O (amide) at 166 ppm, single related to C=O (COOH) at 173 ppm. (151-153)

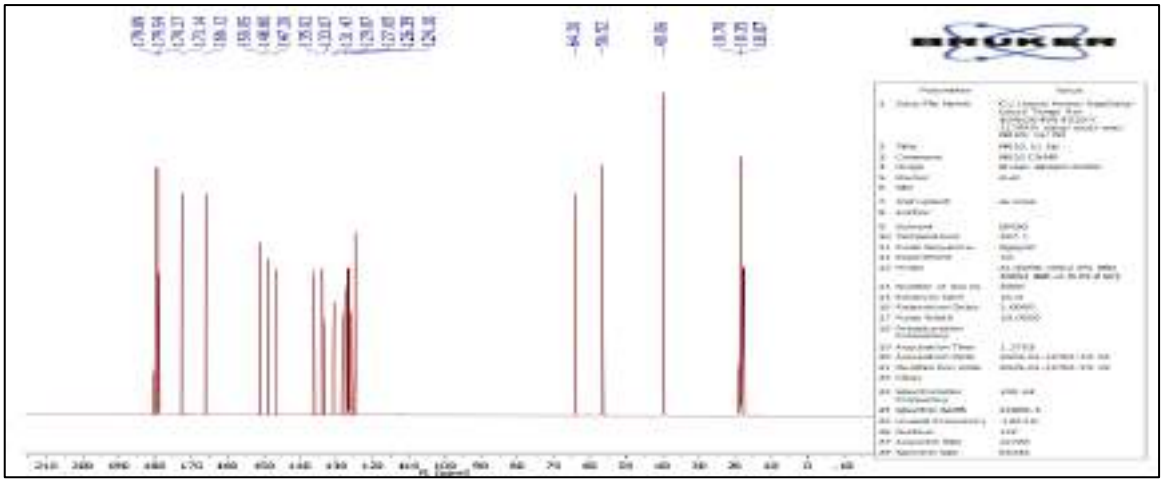
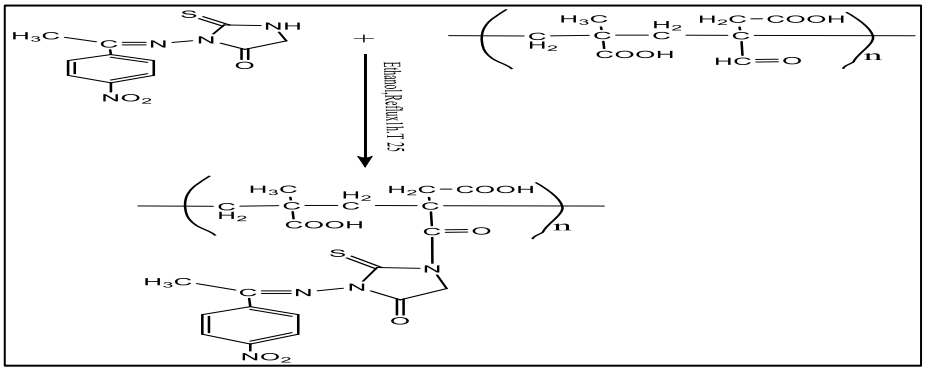


Figure (4- 160): ^{13}C-NMR spectrum of copolymer(11) (MAA-CO-IAN) with compound(11).

4.18.3 Synthesis of copolymer(12) (MAA-CO-IAN) with compound(12).



Scheme (4-59): synthesis of copolymer(12) (MAA-CO-IAN) with compound(12).

FTIR spectrum of copolymer(12) (MAA-CO-IAN) with compound(12).

The FTIR spectrum of copolymer(12) (MAA-CO-IAN) with compound(12) as shown in (fig.4-161) which indicates absorption band at 3134 to –OH, absorption band at 3059 Cm^{-1} to C-H (aromatic), absorption band at 2981 Cm^{-1} to C-H (aliphatic), absorption band at 1598 Cm^{-1} to C=N, absorption band at 1514 Cm^{-1} to C=C (aromatic), absorption band at 1031 Cm^{-1} to C-O, absorption band at 1105 Cm^{-1} to C-N, absorption band at 1641 Cm^{-1} to C=O, absorption band at 1338 Cm^{-1} to CH_3, absorption band at 1564 Cm^{-1} to NO_2, absorption band at 1697 Cm^{-1} to C=O(COOH), absorption band at 1620 Cm^{-1} to C=O (amide). (151-153)

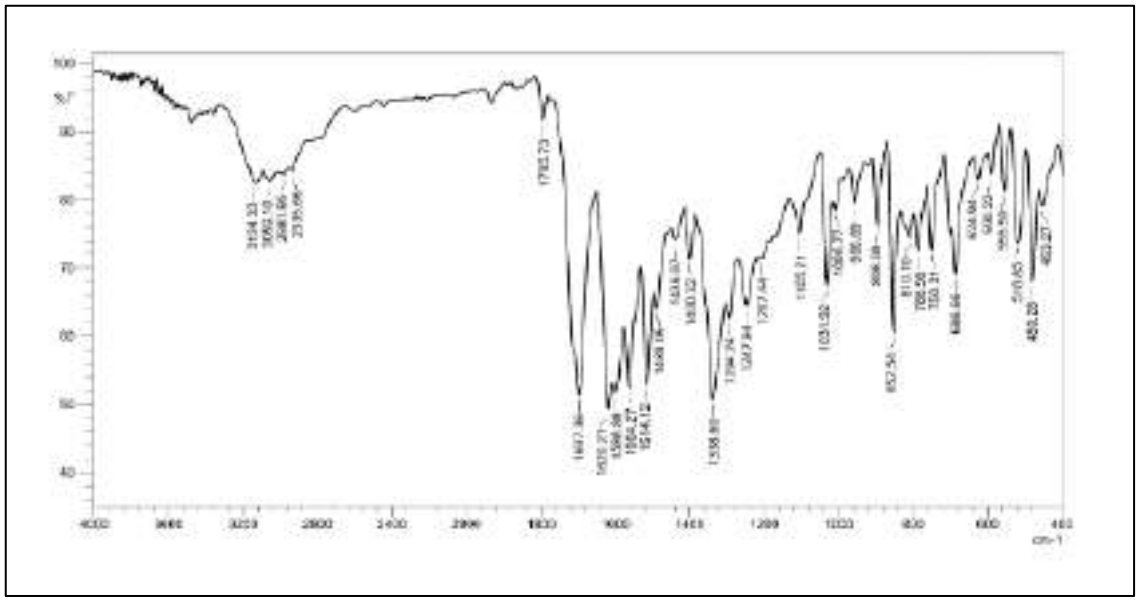


Figure (4- 161): FTIR spectrum of copolymer(12) (MAA-CO-IAN) with compound(12).

^{1}HNMR spectrum of copolymer(12) (MAA-CO-IAN) with compound(12).

^{1}HNMR spectrum of copolymer(12) (MAA-CO-IAN) with compound(12) in (fig.4-162) Singles at (8.1-8.5 δ ppm) to (4H, phenyl ring), multiplet singles at (3.4 to 3.9 ppm) to –NH, singlate at (1.8 ppm) to $–CH_3$. singlate at (1.3 ppm) to $–CH_3$, singles at (2.5 ppm) to $–CH_2$. single at (12 ppm) to –OH. (151-153)

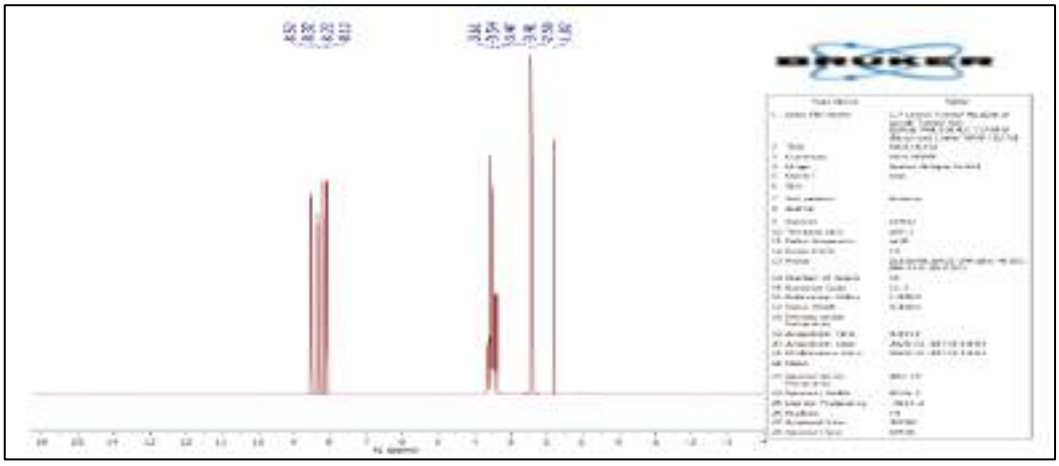


Figure (4- 162): ^{1}HNMR spectrum of copolymer(12) (MAA-CO-IAN) with compound(12).

^{13}C-NMR spectrum of copolymer(12) (MAA-CO-IAN) with compound(12).

The signals of olefinic and aromatic carbons appear in the third region between 115 to 129 ppm, single related to C=N at 158 ppm, single related to C-N at 64 ppm, single related to C=O (amide) at 174 ppm, single related to C=S at 197 ppm, single related to CH_3-C (Secondary) at 33 ppm. (151-153)

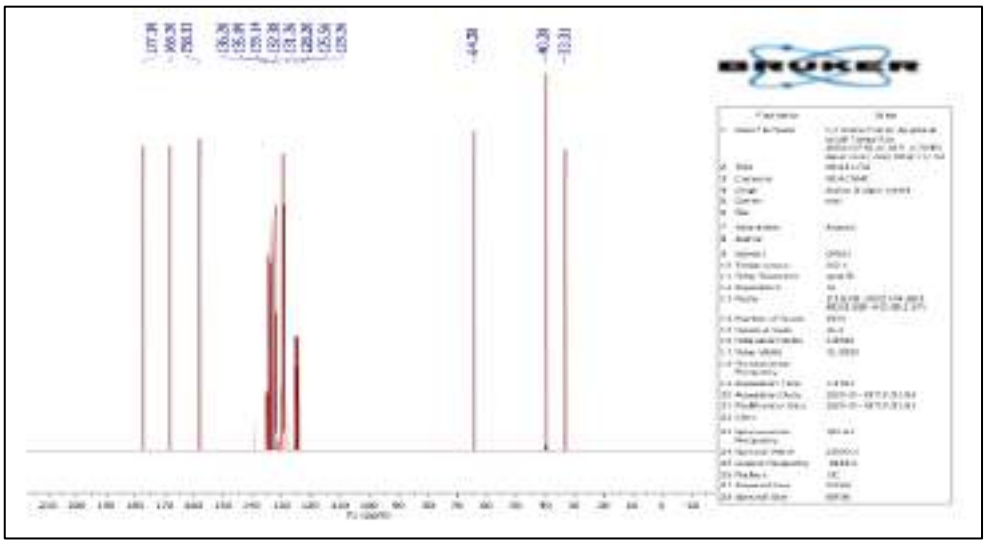
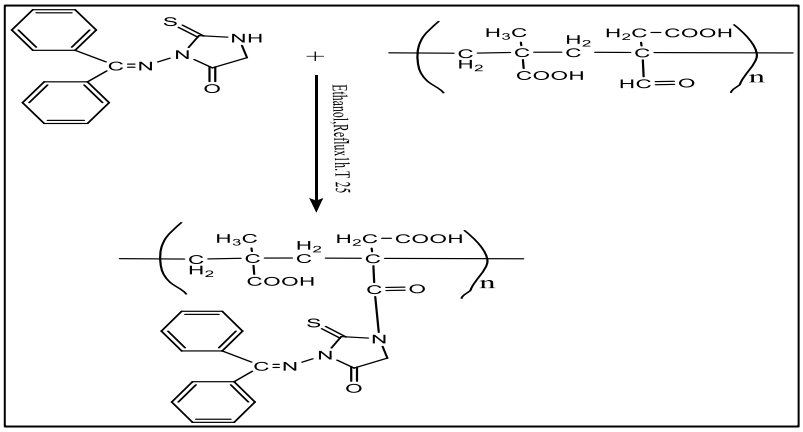


Figure (4- 163): ^{13}C-NMR spectrum of copolymer(12) (MAA-CO-IAN) with compound(12).

4.18.4Synthesis of copolymer(13) (MAA-CO-IAN) with compound(13).



Scheme (4-60): **synthesis of copolymer(13) (MAA-CO-IAN) with compound(13).**

FTIR spectrum of copolymer(13) (MAA-CO-IAN) with compound(13).

The FTIR spectrum of copolymer(13) (MAA-CO-IAN) with compound(13) as shown in (fig.4-164)which indicates absorption band at 3414 to –OH, absorption band at 3226 Cm^{-1} to C-H (aromatic), absorption band at 2937 Cm^{-1} to C-H (alphatic), absorption band at 1622 Cm^{-1} to C=N, absorption band at 1539 Cm^{-1} to C=C (aromatic), absorption band at 1093 Cm^{-1} to C-O, absorption band at 1134 Cm^{-1} to C-N, absorption band at 1701 Cm^{-1} to C=O (COOH), absorption band at 1649 Cm^{-1} to C=O (amide), absorption band at 1390 Cm^{-1} to CH_3. (151-153)

^{1}HNMR spectrum of copolymer(13) (MAA-CO-IAN) with compound(13).

^{1}HNMR spectrum of copolymer(13) (MAA-CO-IAN) with compound(13) in (fig.4-165). Singles at (7.3-8.6 δ ppm) to (10H, phenyl ring), multiplet singles at (3.4 to 4.0 ppm) to –NH. singlate at (1.3 ppm) to $–CH_3$, singlate at (10.3 ppm) to –OH, singles at (2.3 ppm) to $–CH_2$. (151-153)

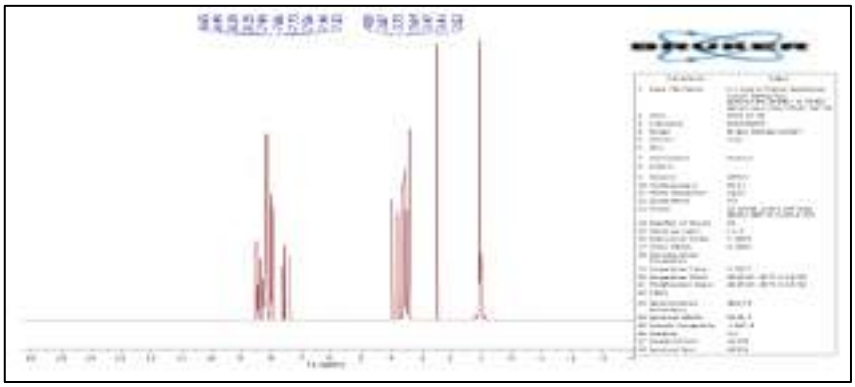


Figure (4- 164): ^{1}HNMR spectrum of copolymer(13) (MAA-CO-IAN) with compound(13).

^{13}C-NMR spectrum of copolymer(13) (MAA-CO-IAN) with compound(13).

The signals of olefinic and aromatic carbons appear in the third region between 118 to 126 ppm, singles related to C=N at 158 ppm, single related to C-N at 66 ppm, single related to C=O (amide) at 174 ppm, single related to C=S at 194 ppm. (151-153)

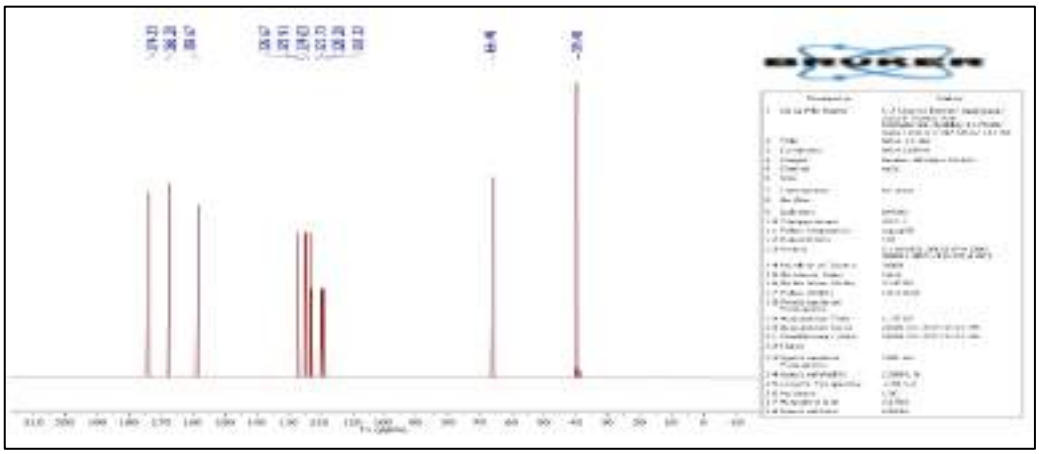
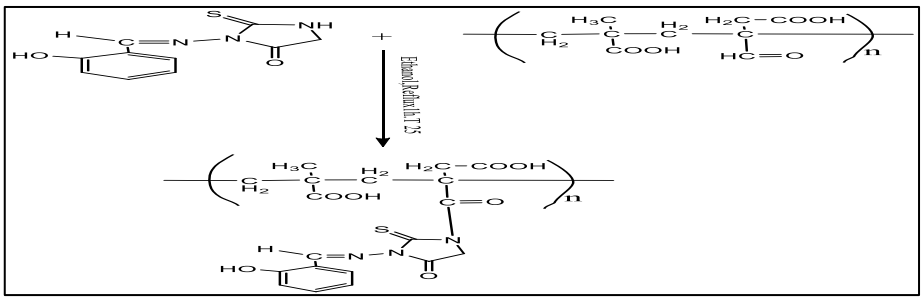


Figure (4- 165): ^{13}C-NMR spectrum of copolymer(13) (MAA-CO-IAN) with compound(13).

4.18.5Synthesis of copolymer(14) (MAA-CO-IAN) with compound(14).



Scheme (4-61): synthesis of copolymer(14) (MAA-CO-IAN) with compound(14).

FTIR spectrum of copolymer(14) (MAA-CO-IAN) with compound(14).

The FTIR spectrum of copolymer(14) (MAA-CO-IAN) with compound(14 as shown in (fig.4-166) which indicates absorption band at 3441 Cm^{-1} to –OH, absorption band at 3317 Cm^{-1} to N-H, absorption band at 3172 Cm^{-1} to C-H (aromatic), absorption band at 2987 Cm^{-1} to C-H (aliphatic) , absorption band at 1616 Cm^{-1} to C=N, absorption band at 1537 Cm^{-1} to C=C (aromatic), absorption band at 1035 Cm^{-1} to C-O, absorption band at 1197 Cm^{-1} to C-N, absorption band at 1710 Cm^{-1} to C=O (COOH), absorption band at 1697 Cm^{-1} to C=O (amide), absorption band at 1390 Cm^{-1} to CH_3.(151-153)

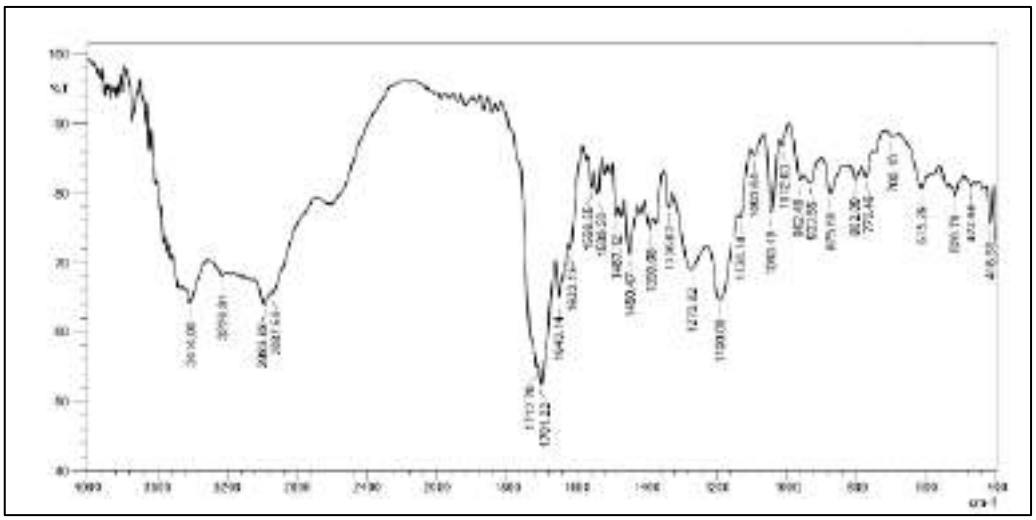


Figure (4- 166): FTIR spectrum of copolymer(14) (MAA-CO-IAN) with compound(14).

^{1}HNMR spectrum of copolymer(14) (MAA-CO-IAN) with compound(14).

^{1}HNMR spectrum of copolymer(14) (MAA-CO-IAN) with compound(14) in (fig.4-167) , singles at (6.8-8.7 δ ppm) to (4H, phenyl ring), multiplet singles at (3.5 to 4.0 ppm) to –NH, singlate at (9.9 ppm) to –OH. singlate at (1.3 ppm) to $–CH_3$, singlate at (11.5 ppm) to –OH(phenol), singles at (2.3 ppm) to $–CH_2$. (151-153)

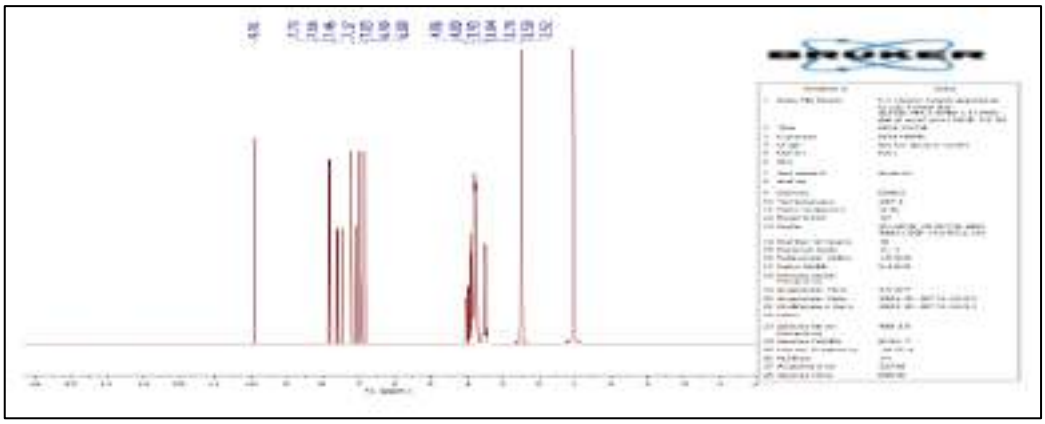


Figure (4- 167): ^{1}HNMR spectrum of copolymer(14) (MAA-CO-IAN) with compound(14).

^{3}C-NMR spectrum of copolymer(14) (MAA-CO-IAN) with compound(14).

The signals of olefinic and aromatic carbons appear in the third region between 116 to 133 ppm, singles related to C=N at 141 ppm, single related to C-N at 66 ppm, singles related to C=O (amide) at 178 ppm, single related to C=S at 198 ppm. (151-153)

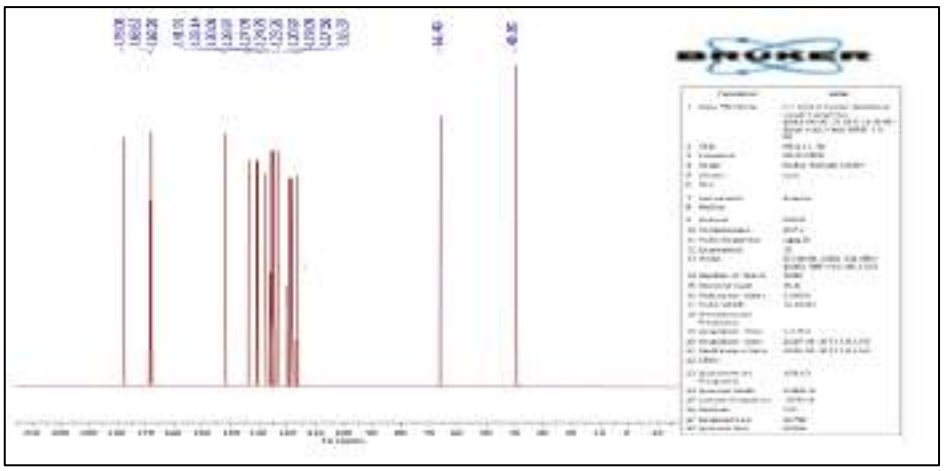
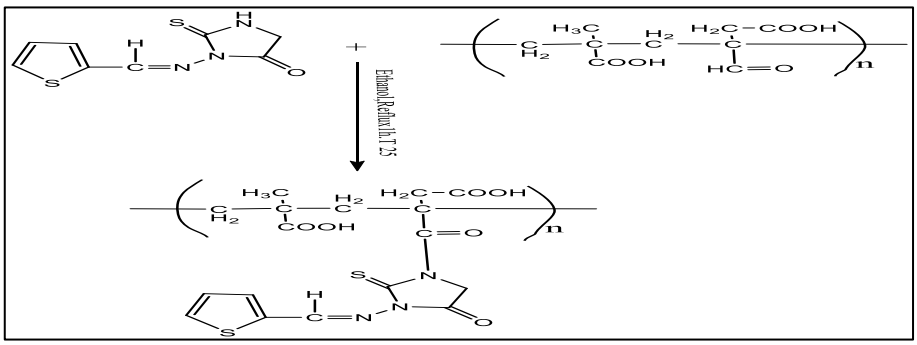


Figure (4- 168): ^{13}C-NMR spectrum of copolymer(14) (MAA-CO-IAN) with compound(14).

4.18.6 Synthesis of copolymer(15) (MAA-CO-IAN) with compound(15).



Scheme (4-62): synthesis of copolymer(15) (MAA-CO-IAN) with compound(15).

FTIR spectrum of copolymer(15) (MAA-CO-IAN) with compound(15).

The FTIR spectrum spectrum of copolymer(15) (MAA-CO-IAN) with compound(15) as shown in (fig.4-169) which indicates absorption band at 3410 Cm^{-1} to –OH, absorption band at 3095 Cm^{-1} to C-H (aromatic), absorption band at 2972 Cm^{-1} to C-H (aliphatic), absorption band at 1577 Cm^{-1} to C=N, absorption band at 1217 Cm^{-1} to C=S, absorption band at 1577 Cm^{-1} to C=C (Heterocyclic ring), absorption band at 1039 Cm^{-1} to C-O, absorption band at 1097 Cm^{-1} to C-N, absorption band at 1708 Cm^{-1} to C=O, absorption band at 1342 Cm^{-1} to CH_3. (151-153)

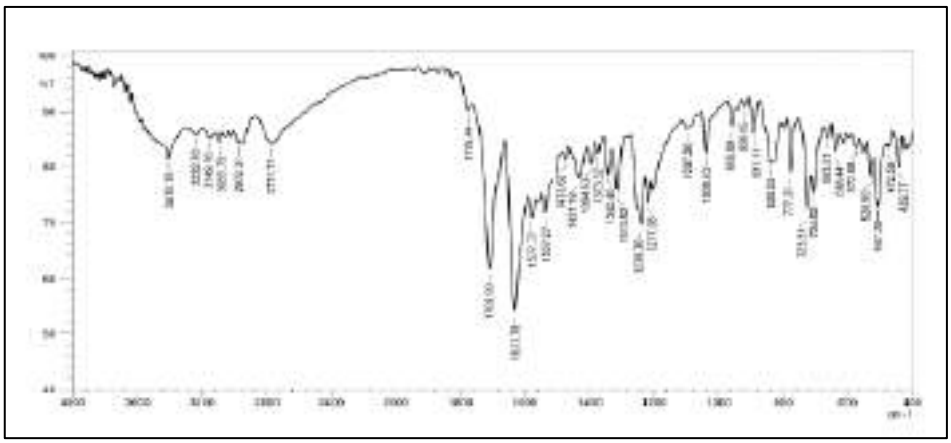


Figure (4- 169): FTIR spectrum of copolymer(15) (MAA-CO-IAN) with compound(15).

^{1}HNMR spectrum of copolymer(15) (MAA-CO-IAN) with compound(15).

^{1}HNMR spectrum of copolymer(15) (MAA-CO-IAN) with compound(15) in (fig.4-170) singles at (7.7-8.2 δ ppm) to (3H, Heterocyclic ring), single at 2.5 ppm to CH_2**,** single at 0.9 ppm to CH_3, single at (11.4ppm) to –OH (COOH), singles at (2.3 ppm) to –CH_2, single at 3.2-4.3 ppm to =CH (Thiophene**).** (151-153)

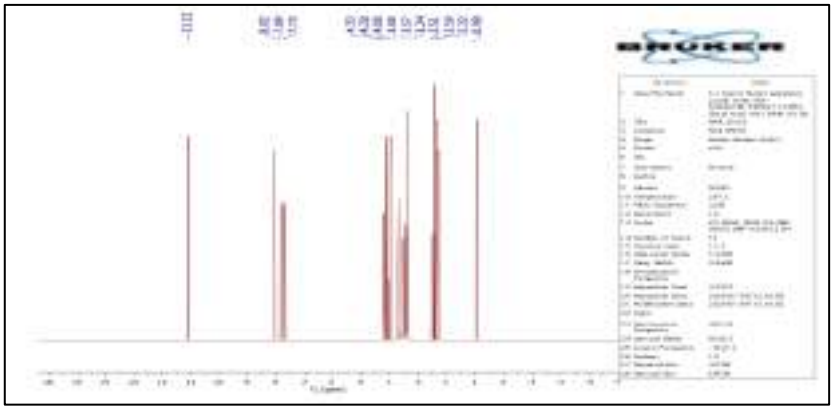


Figure (4- 170): ^{1}HNMR spectrum of copolymer(15) (MAA-CO-IAN) with compound(15).

^{13}C-NMR spectrum of copolymer(15) (MAA-CO-IAN) with compound(15).

The signals of olefinic and aromatic carbons appear in the third region between 126 and 132 ppm, singles related to C=N at 141 ppm, single related to C-N at 65 ppm, singles related to C=O (amide) at 174 ppm, single related to C=S at 196 ppm, singles related to C=O (COOH) at 178 ppm. (151-153)

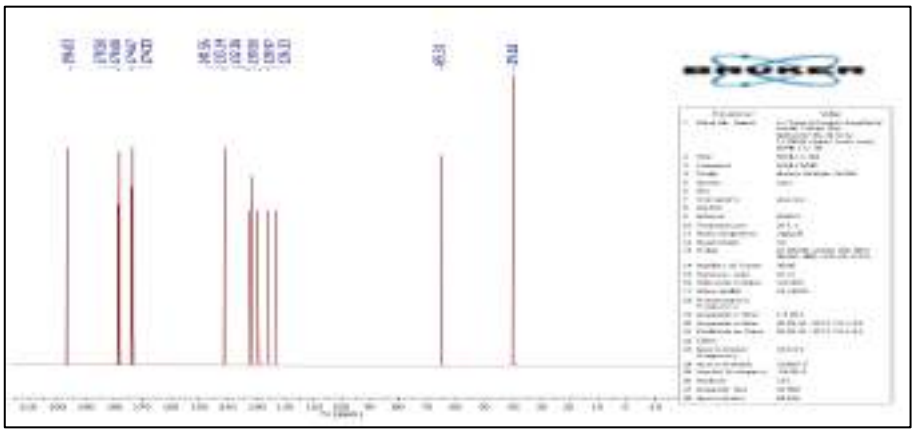
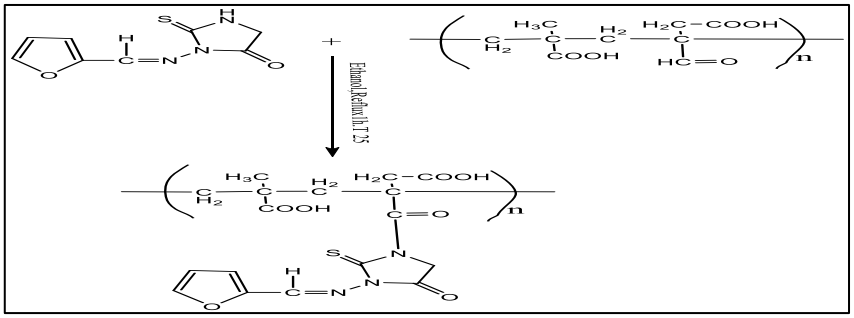


Figure (4- 171): ^{13}C-NMR spectrum of copolymer(15) (MAA-CO-IAN) with compound(15).

4.18.7Synthesis of copolymer(16) (MAA-CO-IAN) with compound(16).



Scheme (4-63): synthesis of copolymer(16) (MAA-CO-IAN) with compound(16).

FTIR spectrum of copolymer(16) (MAA-CO-IAN) with compound(16).

The FTIR spectrum of the preparation of copolymer(16) (MAA-CO-IAN) with compound(16) as shown in (fig.4-172) which indicates absorption band at 3560 Cm^{-1} to –OH, absorption band at 3178 Cm^{-1} to C-H (Hetro phenyl ring), absorption band at 2916 Cm^{-1} to C-H (aliphatic) absorption band at 1554 Cm^{-1} to C=N, absorption band at 1205 Cm^{-1} to C=S, absorption band at 1415 Cm^{-1} to C=C (Hetro phenyl ring), absorption band at 1338 Cm^{-1} to CH_3, absorption band at 1730 Cm^{-1} to C=O(COOH), absorption band at 1647 Cm^{-1} to C=O(amide). (151-153)

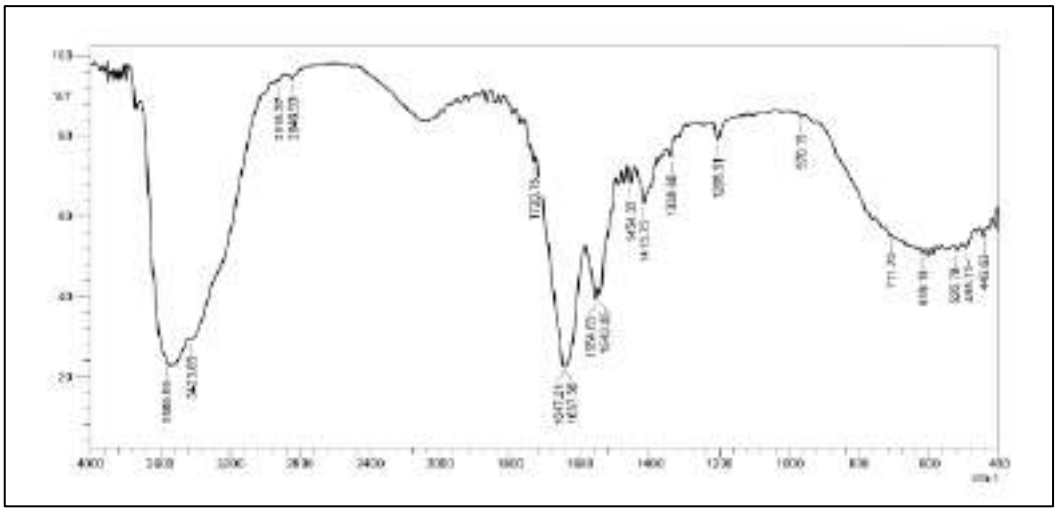


Figure (4- 172): FTIR spectrum of copolymer(16) (MAA-CO-IAN) with compound(16).

^{1}HNMR spectrum of copolymer(16) (MAA-CO-IAN) with compound(16).

^{1}HNMR spectrum of copolymer(16) (MAA-CO-IAN) with compound(16) in (fig.4-173), singles at (6.5-8.2 δ ppm) to (3H, Heterocyclic ring), multiple singlate at (3.4 to 4.1 ppm) to –NH, single at 2.5 ppm to =CH**,** single at 2.5 ppm to –CH_3**,** single at 2.3 ppm to –CH_2**,** single at 11.2 ppm to –OH**.** (151-153)

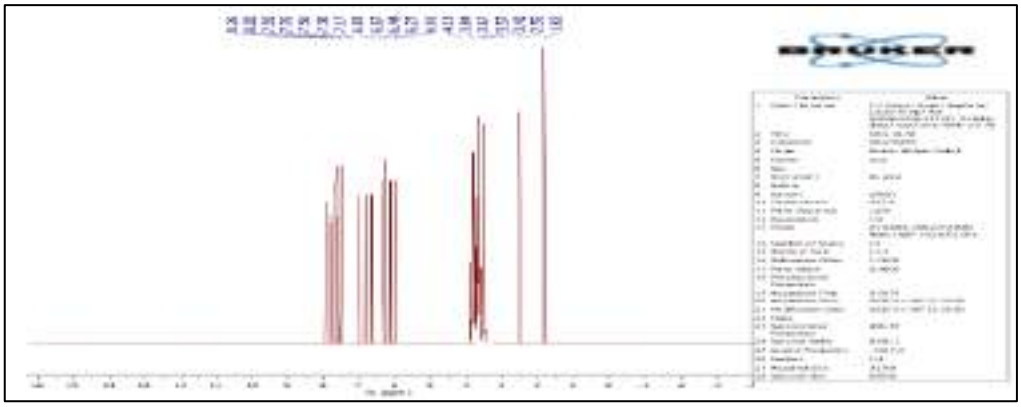


Figure (4- 173): ^{1}HNMR spectrum of copolymer(16) (MAA-CO-IAN) with compound(16).

^{13}C-NMR spectrum of copolymer(16) (MAA-CO-IAN) with compound(16).

The signals of olefinic and aromatic carbons appear in the third region between 124 and 126ppm, singles related to C=N at 143-150 ppm, single related to C-N at 64 ppm, singles related to C=O (amide) at 174-178 ppm, single related to C=S at 193 ppm. (151-153)

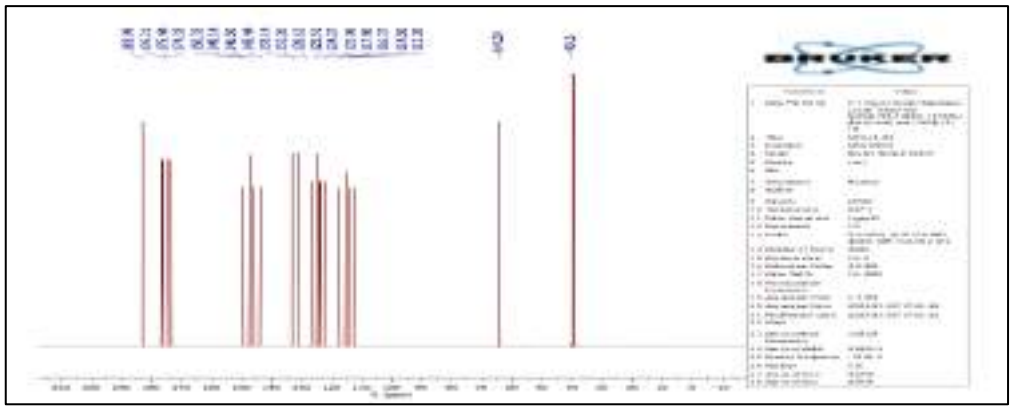
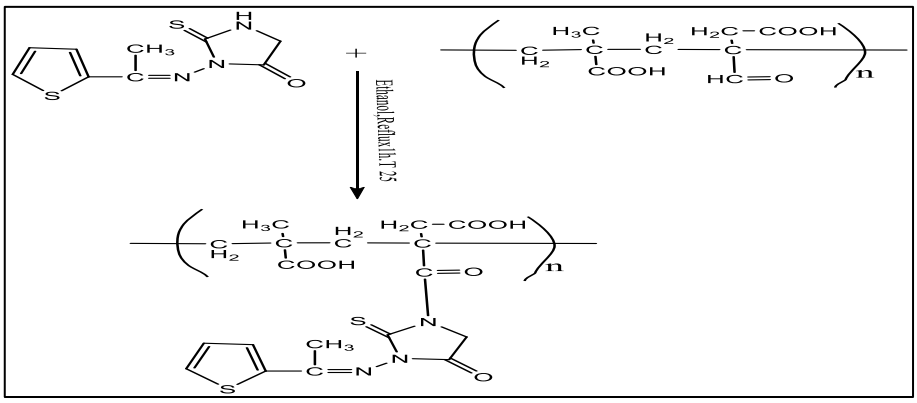


Figure (4- 174): ^{13}C-NMR spectrum of copolymer(16) (MAA-CO-IAN) with compound(16).

4.18.8 Synthesis of copolymer(17) (MAA-CO-IAN) with compound(17).



Scheme (4-64): synthesis of copolymer(17) (MAA-CO-IAN) with compound(17).

FTIR spectrum of copolymer(17) (MAA-CO-IAN) with compound(17).

The FTIR spectrum of the preparation of copolymer(17) (MAA-CO-IAN) with compound(17) as shown in (fig.4-175) which indicates absorption band at 3417Cm^{-1} to –OH, absorption band at 3182 Cm^{-1} to C-H (aromatic), absorption band at 1554 Cm^{-1} to C=N, absorption band at 1199 Cm^{-1} to C=S, absorption band at 1473 Cm^{-1} to C=C (Hetro phenyl ring), absorption band at 1120 Cm^{-1} to C-N, absorption band at 1728 Cm^{-1} to C=O (COOH), absorption band at 1645 Cm^{-1} to C=O (amide)absorption band at 1338 Cm^{-1} to CH_3. (151-153)

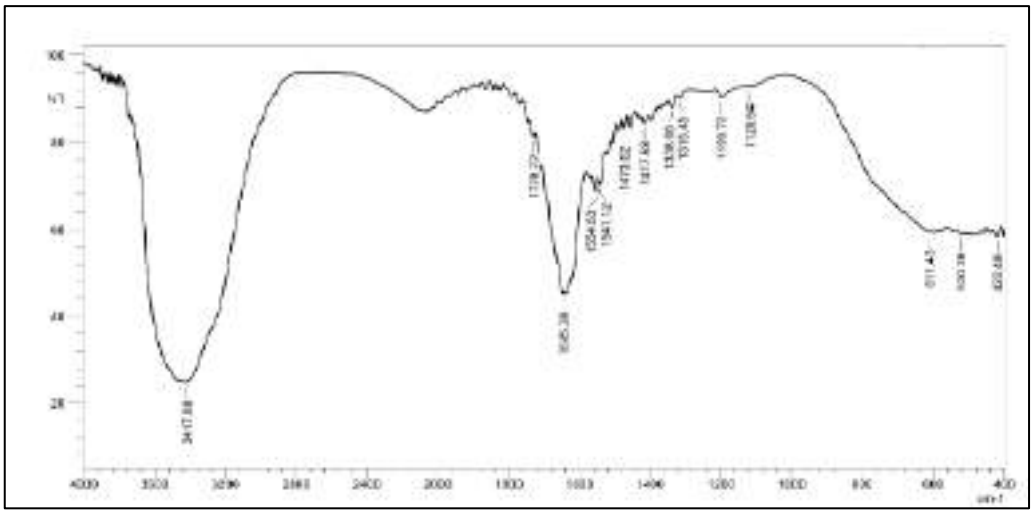


Figure (4- 175): FTIR spectrum of copolymer(17) (MAA-CO-IAN) with compound(17).

^{1}HNMR spectrum of copolymer(17) (MAA-CO-IAN) with compound(17).

^{1}HNMR spectrum of copolymer(17) (MAA-CO-IAN) with compound(17) in (fig.4-176) t, singles at (7.2-8.6 δ ppm) to (3H, Hetro phenyl ring), multiple singlate at (4.4 ppm) to –NH, single at 2.5 ppm to =CH**,** single at 11.2 ppm to –OH single at 2.2 ppm to $–CH_2$**,** single at 1.2 ppm to $–CH_3$**.** (151-153)

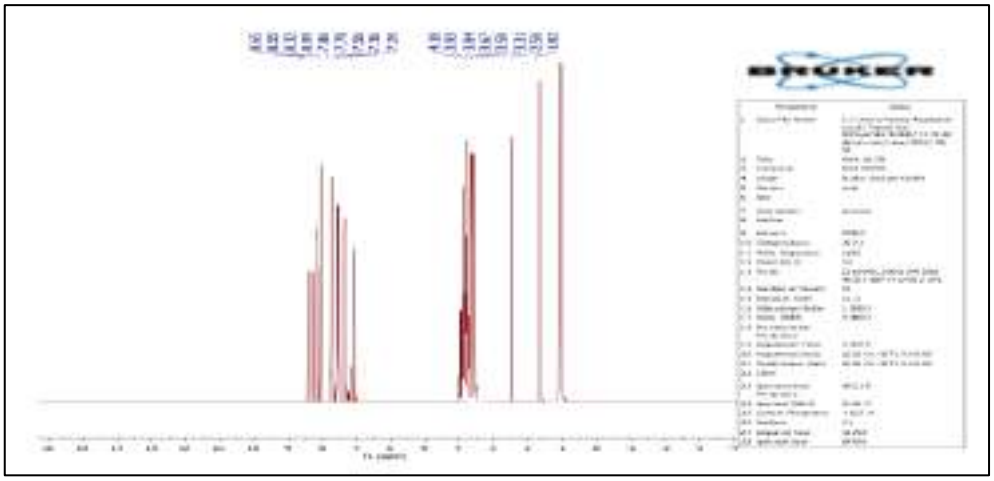


Figure (4- 176): ^{1}HNMR spectrum of copolymer(17) (MAA-CO-IAN) with compound(17).

^{13}C-NMR spectrum of copolymer(17) (MAA-CO-IAN) with compound(17).

The signals of olefinic and aromatic carbons appear in the third region between 126 and 128 ppm, singles related to C=N at 154 ppm, single related to C-N at 64 ppm, singles related to C=O (amide) at 175 ppm, singles related to C=S at 178-182 ppm, single related to CH_3 at 15 ppm. (151-153)

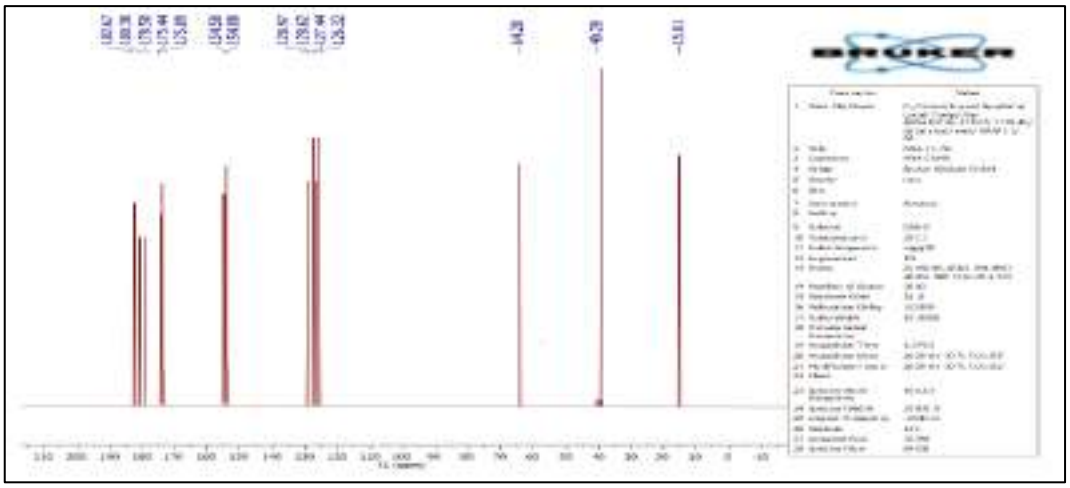
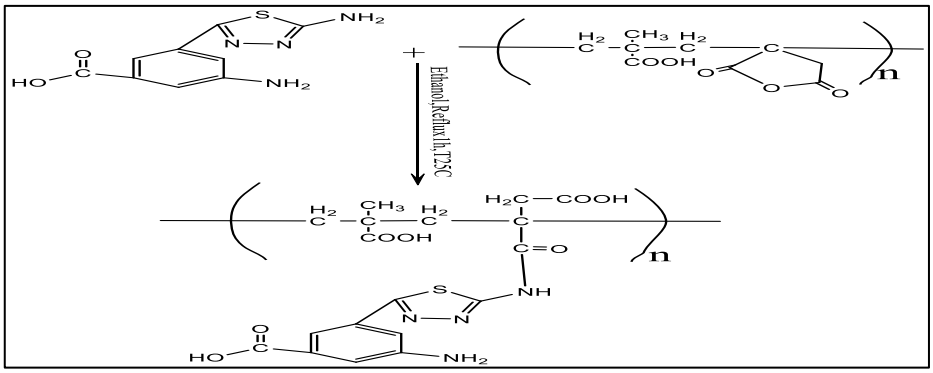


Figure (4- 177): ^{13}C-NMR spectrum of copolymer(17) (MAA-CO-IAN) with compound(17).

4.19 Synthesis of copolymer (MAA-CO-IAN) with compounds (18-20).

4.19.1 Synthesis of copolymer(18) (MAA-CO-IAN) with compound(18).



Scheme (4-65): synthesis of copolymer(18) (MAA-CO-IAN) with compound(18).

FTIR spectrum of copolymer(18) (MAA-CO-IAN) with compound(18).

The FTIR spectrum of copolymer(18) (MAA-CO-IAN) with compound(18) as shown in (fig.4-178) which indicates absorption band at 3469 Cm^{-1} to –OH and 3415 $Cm^{-1}$to $–NH_2$, absorption band at 3000 Cm^{-1} to C-H (aromatic), absorption band at 2978 Cm^{-1} to C-H (alphatic), absorption band at 1533 Cm^{-1} to C=N, absorption band at 1479 Cm^{-1} to C=C (aromatic), absorption band at 1697 Cm^{-1} to C=O (carboxylic), absorption band at 1641Cm^{-1} to C=O (amide), absorption band at 1166 Cm^{-1} to C-N, absorption band at 1386 Cm^{-1} to CH_3.(151-153)

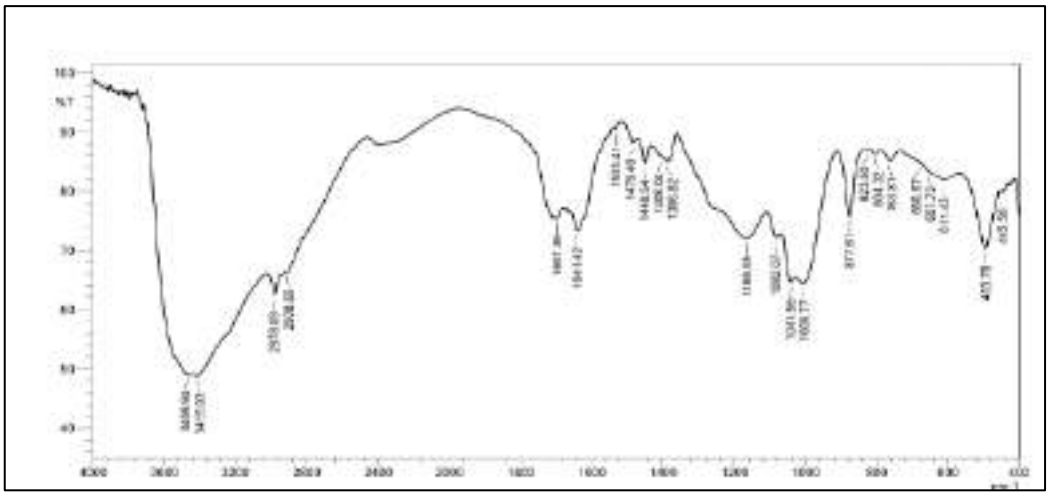


Figure (4- 178): FTIR spectrum of copolymer(18) (MAA-CO-IAN) with compound(18).

^{1}HNMR spectrum of copolymer(18) (MAA-CO-IAN) with compound(18).

^{1}HNMR spectrum of copolymer(18) (MAA-CO-IAN) with compound(18) in (fig.4-179) singles at (7.3-7.5 δ ppm) to (4H, phenyl ring), singlate at (3.4 ppm) to –NH_2, singlate at (5.3 ppm) to –NH(amide), single at (11.3 ppm) to (COOH), singlate at (2.4 ppm) to –CH_2**,** singlate at (1.2 ppm) to –CH_3. (151-153)

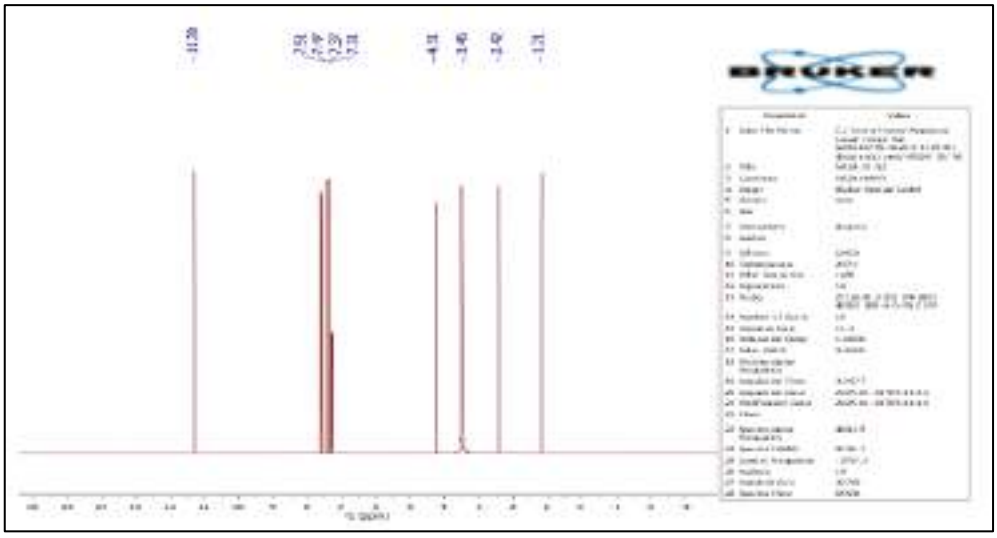


Figure (4- 179): ^{1}HNMR spectrum of copolymer(18) (MAA-CO-IAN) with compound(18).

^{13}C-NMR spectrum of copolymer(18) (MAA-CO-IAN) with compound(18). The signals of olefinic and aromatic carbons appear in the third region between 126 and 135 ppm, single related to C-S at 56 ppm, single related to C=N at 157ppm, single related to C-N at 64 ppm, single related to C=O (acid) at 183ppm, single related to C=O (amide) at 173ppm, singles related to CH_3 at 18 ppm. (151-153)

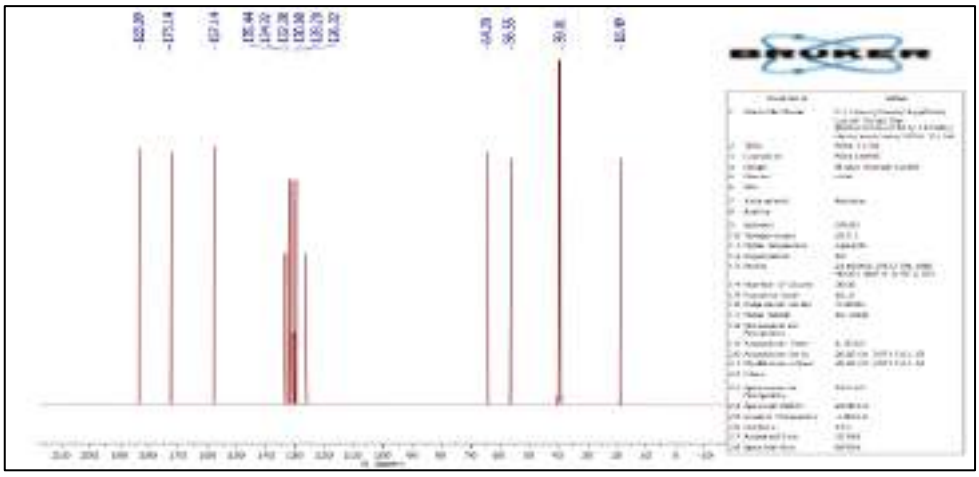
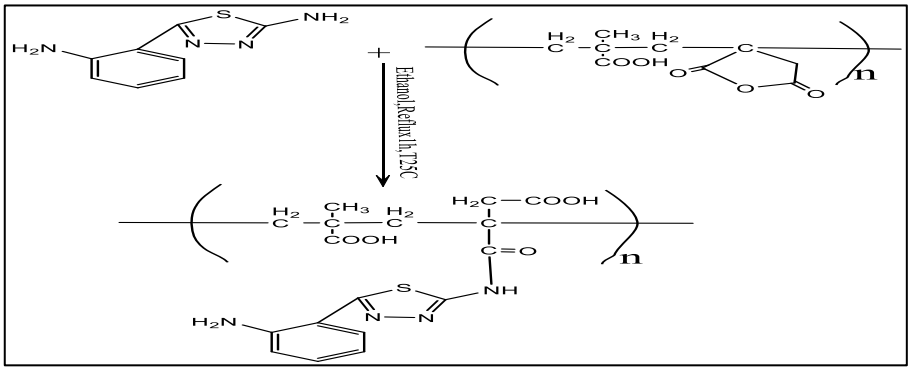


Figure (4- 180): ^{13}C-NMR spectrum of copolymer(18) (MAA-CO-IAN) with compound(18).

4.19.2 Synthesis of copolymer(19) (MAA-CO-IAN) with compound(19).



Scheme (4-66): synthesis of copolymer(19) (MAA-CO-IAN) with compound(19).

FTIR spectrum of copolymer(19) (MAA-CO-IAN) with compound(19).

The FTIR spectrum of copolymer(19) (MAA-CO-IAN) with compound(19) as shown in (fig.4-181) which indicates absorption band at 3400 Cm^{-1} to –OH and 3412 $Cm^{-1}$to $–NH_2$, absorption band at 3232 Cm^{-1} to C-H (aromatic), absorption band at 2985 Cm^{-1} to C-H (alphatic), absorption band at 1552 Cm^{-1} to C=N, absorption band at 1487 Cm^{-1} to C=C (aromatic), absorption band at 1708 Cm^{-1} to C=O (carboxylic), absorption band at 1697Cm^{-1} to C=O (amide), absorption band at 1178 Cm^{-1} to C-N, absorption band at 1373 Cm^{-1} to CH_3. (151-153)

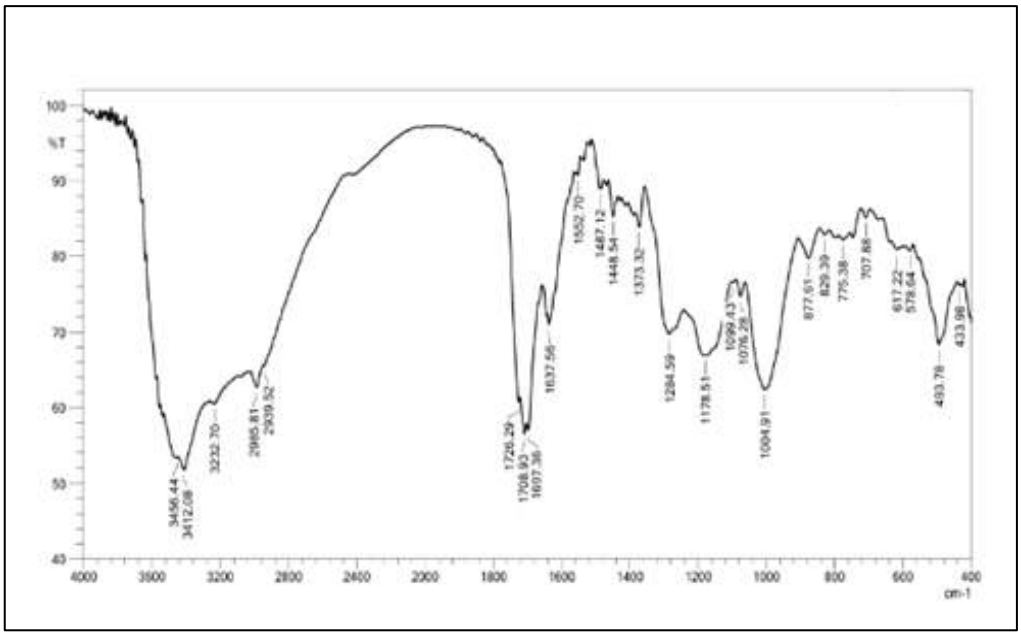


Figure (4- 181): FTIR spectrum of copolymer(19) (MAA-CO-IAN) with compound(19).

^{1}HNMR spectrum of copolymer(19) (MAA-CO-IAN) with compound(19).

^{1}HNMR spectrum of copolymer(19) (MAA-CO-IAN) with compound(19) in (fig.4-182) singles at (6.3-7.5 δ ppm) to (4H, phenyl ring), singlate at (3.4 ppm) to $–NH_2$, singlate at (4.4 ppm) to –NH (amide), single at (10.5 ppm) to (COOH), singlate at (2.4 ppm) to $–CH_2$**,** singles at (1.2 ppm) to $–CH_3$. (151-153)

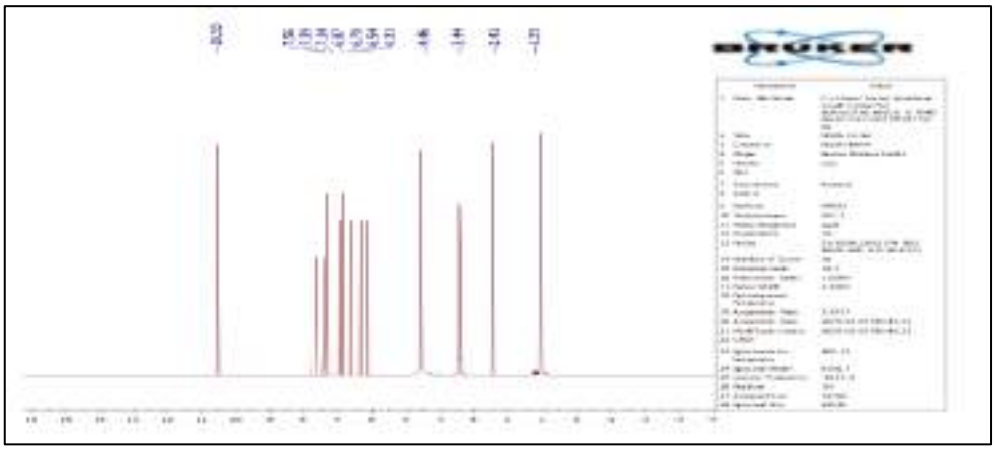


Figure (4- 182): ^{1}HNMR spectrum of copolymer(19) (MAA-CO-IAN) with compound(19).

^{13}C-NMR spectrum of copolymer(19) (MAA-CO-IAN) with compound(19).

The signals of olefinic and aromatic carbons appear in the third region between 126 and 135 ppm, single related to C-S at 56 ppm, single related to C=N at 157ppm, singles related to C-N at 63 ppm, single related to C=O (acid) at 183ppm, single

related to C=O (amide) at 173ppm, singles related to CH_3 at 18 ppm. (151-153)

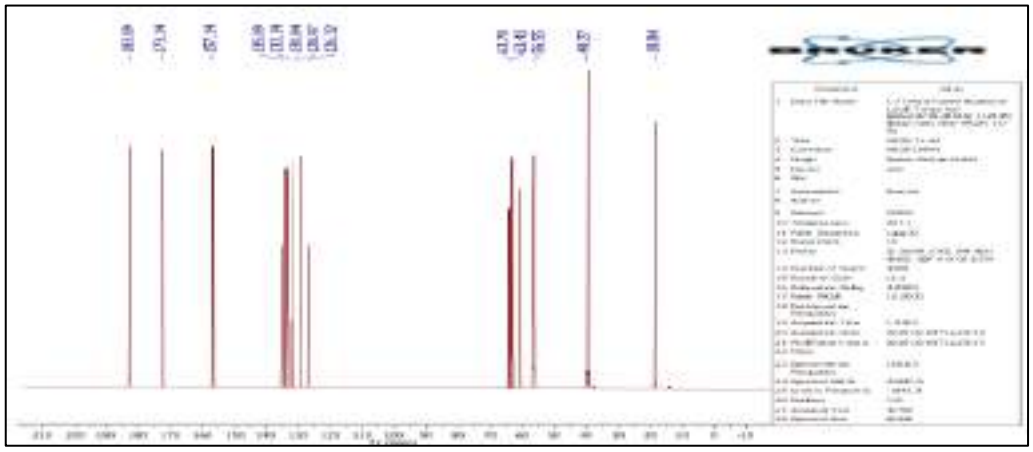
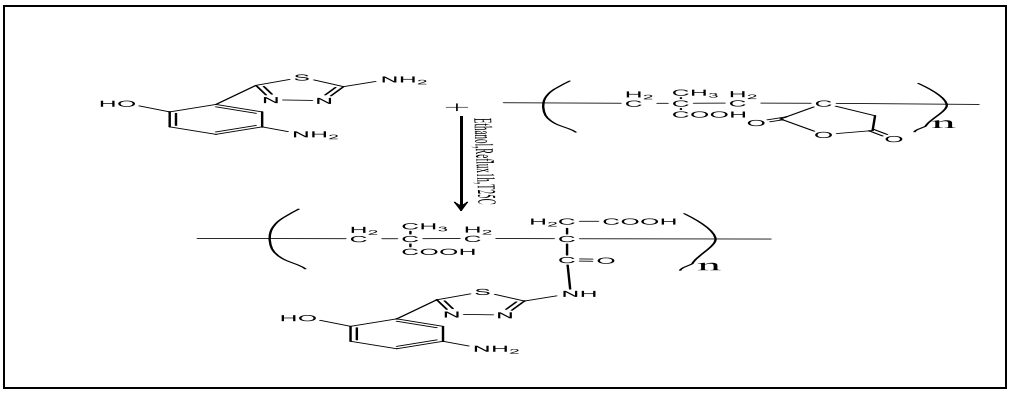


Figure (4- 183): ^{13}C-NMR spectrum of copolymer(19) (MAA-CO-IAN) with compound(19).

4-19-3:- Synthesis of copolymer(20) (MAA-CO-IAN) with compound(20).



Scheme (4-67): synthesis of copolymer(20) (MAA-CO-IAN) with compound(20).

FTIR spectrum of copolymer(20) (MAA-CO-IAN) with compound(20).

The FTIR spectrum of copolymer(20) (MAA-CO-IAN) with compound(20) as shown in (fig.4-184) which indicates absorption band at 3400 to $–NH_2$, overlapping with a –OH group, absorption band at 3000 Cm^{-1} to C-H (aromatic), absorption band at 2985 Cm^{-1} to C-H (aliphatic), absorption band at 1568 Cm^{-1} to C=N, absorption band at 1504 Cm^{-1} to C=C (aromatic), absorption band at 1708 Cm^{-1} to C=O (carboxylic), absorption band at 1633Cm^{-1} to C=O (amide), absorption band at 1145 Cm^{-1} to C-N, absorption band at 1371 Cm^{-1} to CH_3. (151-153)

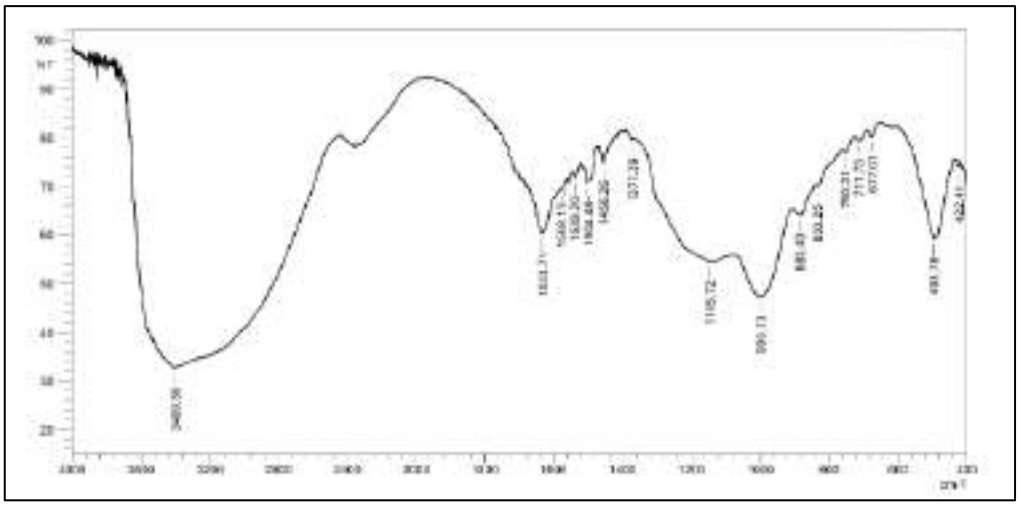


Figure (4- 184): FTIR spectrum of copolymer(20) (MAA-CO-IAN) with compound(20).

^{1}HNMR spectrum of copolymer(20) (MAA-CO-IAN) with compound(20).

^{1}HNMR spectrum of copolymer(20) (MAA-CO-IAN) with compound(20) in (fig.4-185) singles at (6.0-7.6 δ ppm) to (4H, phenyl ring), singlate at (3.3 ppm) to $–NH_2$, singlate at (4.4 ppm) to –NH (amide), single at (10.3 ppm) to (COOH), singlate at (2.4 ppm) to $–CH_2$**,** singles at (0.9 ppm) to $–CH_3$. (151-153)

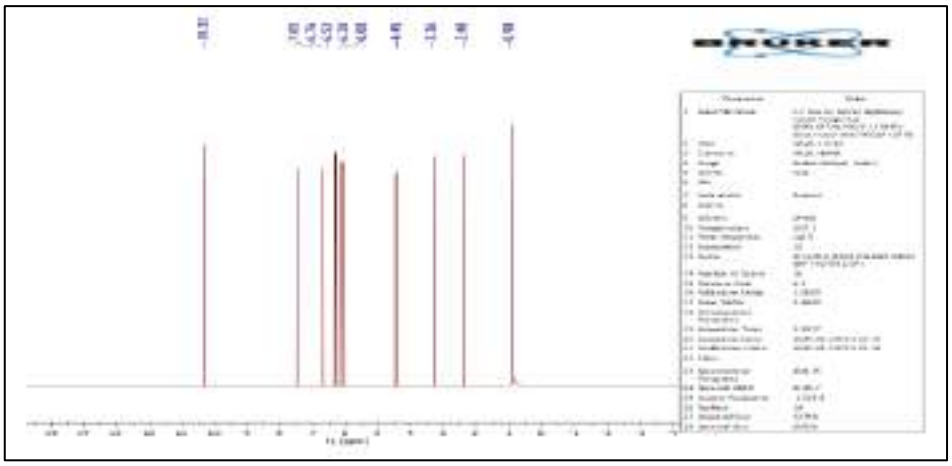


Figure (4- 185): ^{1}HNMR spectrum of copolymer(20) (MAA-CO-IAN) with compound(20).

^{13}C-NMR spectrum of copolymer(20) (MAA-CO-IAN) with compound(20). The signals of olefinic and aromatic carbons appear in the third region between 118 and 132ppm, single related to C-S at 56 ppm, single related to C=N at 153ppm, singles related to C-N at 63 ppm, single related to C=O (acid) at 183ppm, single related to C=O (amide) at 173ppm, singles related to CH_3 at 18 ppm. (151-153)

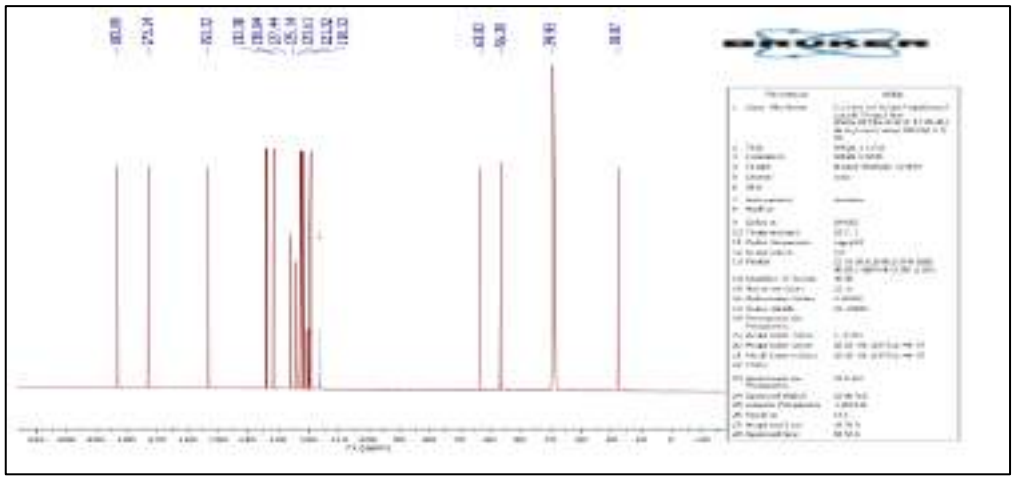
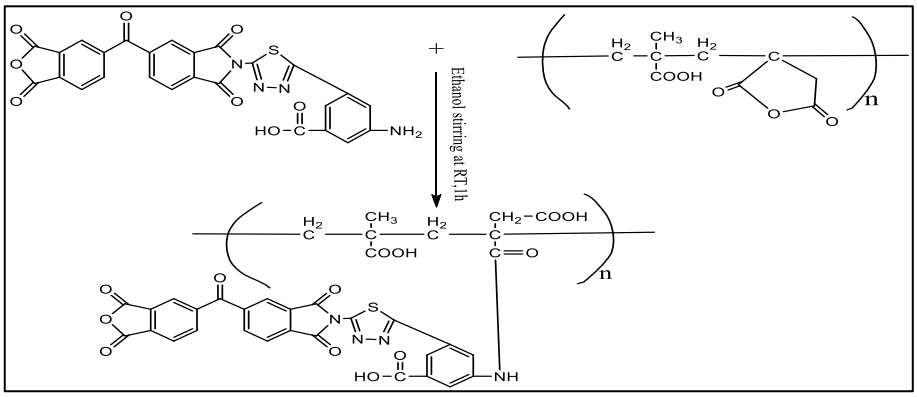


Figure (4- 186): ^{13}C-NMR spectrum of copolymer(20) (MAA-CO-IAN) with compound(20).

4.20 Synthesis of copolymer(1) (MAA-CO-IAN) with Imide compounds (21-23).

4.20.1 Synthesis of copolymer(21) (MAA-CO-IAN) with compound(21) .



Scheme (4-68): synthesis of copolymer(21) (MAA-CO-IAN) with compound(21) .

FTIR spectrum of copolymer(21) (MAA-CO-IAN) with compound(21) .

The FTIR spectrum of copolymer(21) (MAA-CO-IAN) with compound(21) as shown in (fig.4-187) which indicates absorption band at 3419 Cm^{-1} to -OH overlapping with NH, absorption band at 3070 to C-H (aromatic), absorption band at 2981 to C-H (aliphatic), absorption band at 1541 Cm^{-1} to C-H to C=N, absorption band at 1489 Cm^{-1} to C=C (aromatic), absorption band at 1637 Cm^{-1} to C=O (amide), absorption band at 1712 Cm^{-1} to C=O (carboxylic acid), absorption band at 1178 Cm^{-1} to C-N, absorption band at 1390 Cm^{-1} to CH_3.(151-153)

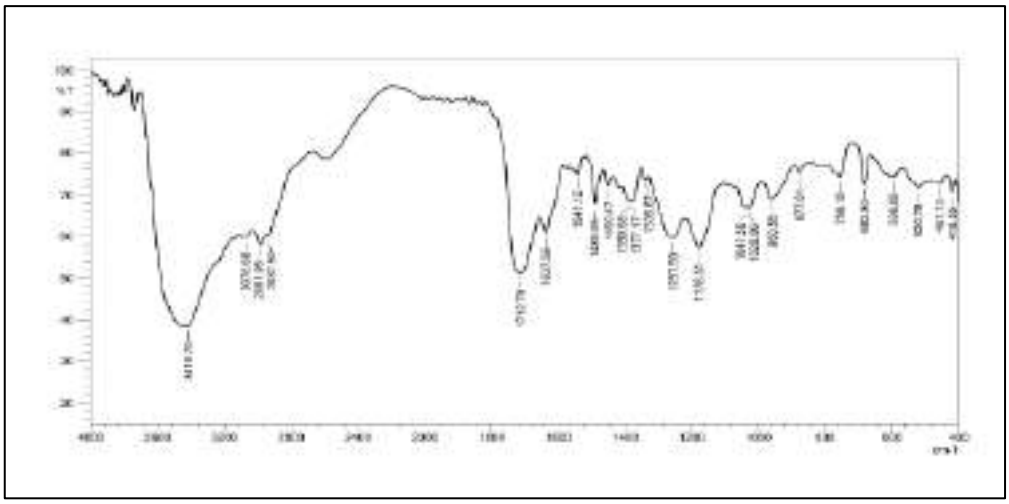


Figure (4- 187): FTIR spectrum of copolymer(21) (MAA-CO-IAN) with compound(21) .

^{1}HNMR spectrum of copolymer(21) (MAA-CO-IAN) with compound(21).

^{1}HNMR spectrum of copolymer(21) (MAA-CO-IAN) with compound(21) in (fig.4-188) singles at (6.3-9.0 δ ppm) to (9H, phenyl ring), singles at (3.4 ppm) to –NH, singlate at (4.2-5.1 ppm) to –NH (amide), single at (11.5 ppm) to (COOH), singles at (2.5 ppm) to $–CH_2$**,** singles at (1.0 ppm) to $–CH_3$. (151-153)

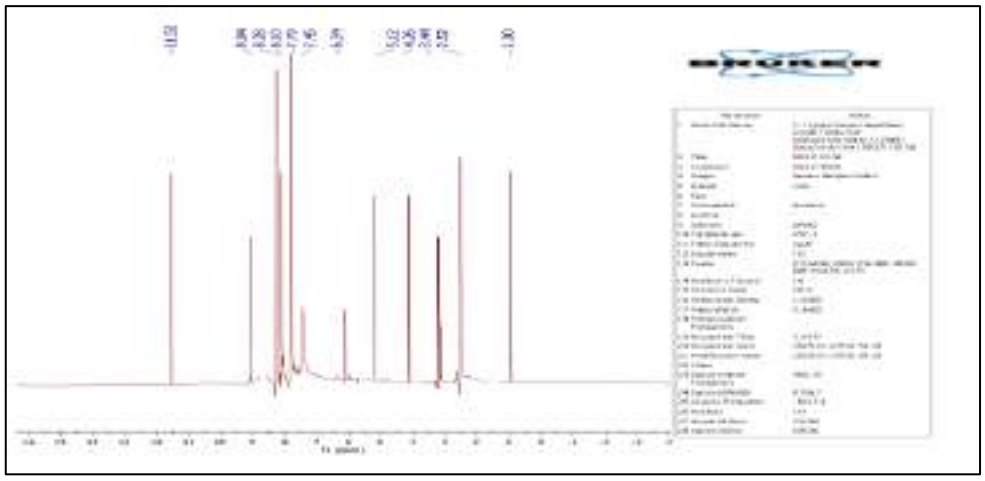


Figure (4- 188): ^{1}HNMR spectrum of copolymer(21) (MAA-CO-IAN) with compound(21) .

^{13}C-NMR spectrum of copolymer(21) (MAA-CO-IAN) with compound(21)

. The signals of olefinic and aromatic carbons appear in the third region between 125 and 135 ppm, singles related to C-S at 56 ppm, singles related to C=N at 166 ppm, single related to C-N at 64 ppm, single related to C=O (amide) at 173 ppm, single related to C=O (acid) at 182 ppm. (151-153)

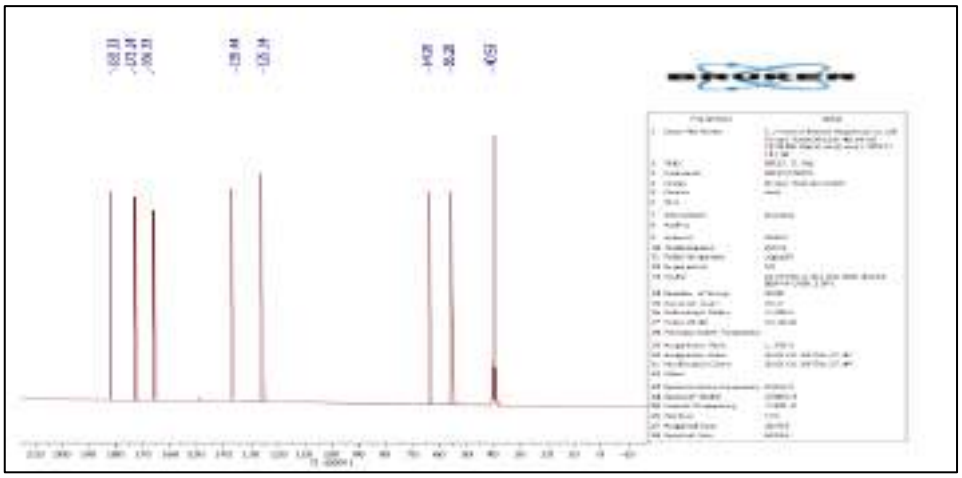
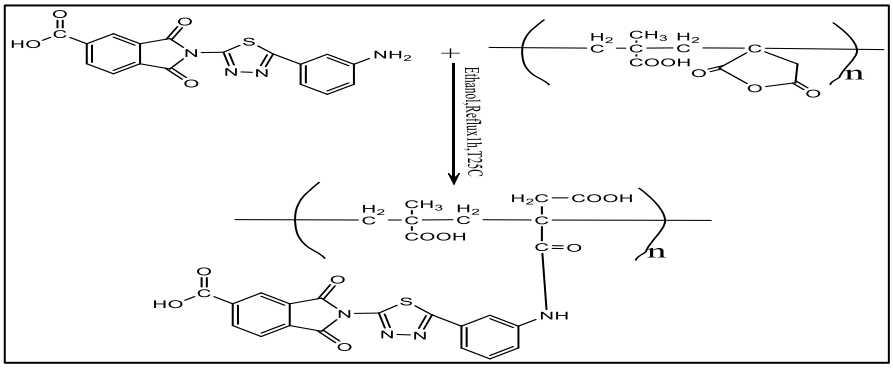


Figure (4- 189): ^{13}C-NMR spectrum of copolymer(21) (MAA-CO-IAN) with compound(21).

4.20.2 Synthesis of copolymer(32) (MAA-CO-IAN) with compound(22) .



Scheme (4-69): synthesis of copolymer(32) (MAA-CO-IAN) with compound(22)

FTIR spectrum of copolymer(32) (MAA-CO-IAN) with compound(22) .

The FTIR spectrum of copolymer(32) (MAA-CO-IAN) with compound(22) as shown in (fig.4-190) which indicates absorption band at 3136 Cm^{-1} to -OH overlapping with NH, absorption band at 3072 to C-H (aromatic), absorption band at 2882 to C-H (aliphatic), absorption band at 1604 Cm^{-1} to C-H to C=N, absorption band at 1487 Cm^{-1} to C=C (aromatic), absorption band at 1635 Cm^{-1} to C=O (amide), absorption band at 1712 Cm^{-1} to C=O (carboxylic acid), absorption band at 1166 Cm^{-1} to C-N, absorption band at 1377 Cm^{-1} to CH_3. (151-153)

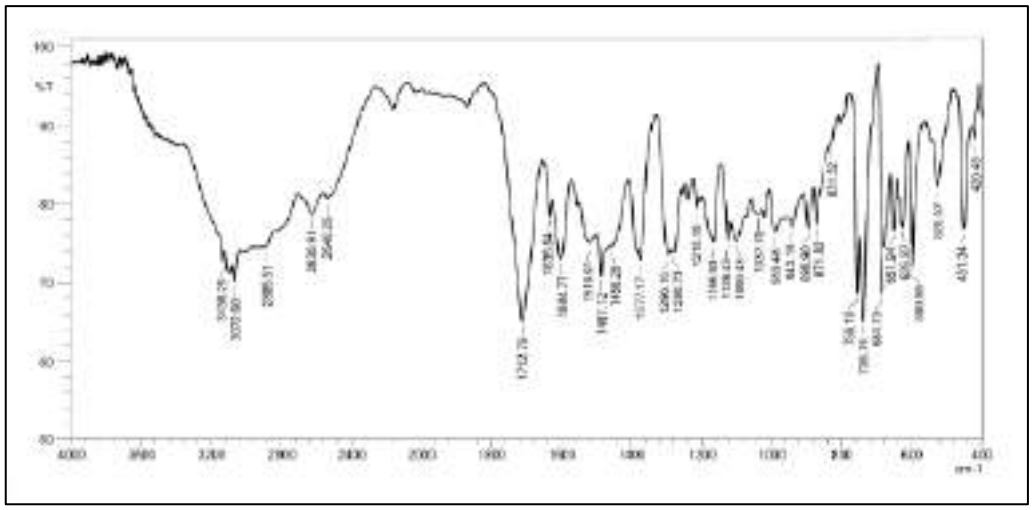


Figure (4- 190): FTIR spectrum of copolymer(32) (MAA-CO-IAN) with compound(22) .

^{1}HNMR spectrum of copolymer(32) (MAA-CO-IAN) with compound(22).

^{1}HNMR spectrum of copolymer(32) (MAA-CO-IAN) with compound(22) in (fig.4-191) singles at (6.2-9.0 δ ppm) to (10H, phenyl ring), singles at (3.4 ppm) to –NH, singlate at (4.2-5.1 ppm) to –NH (amide), single at (11.5 ppm) to (COOH), singles at (2.5 ppm) to $–CH_2$**,** singles at (1.0 ppm) to $–CH_3$. (151-153)

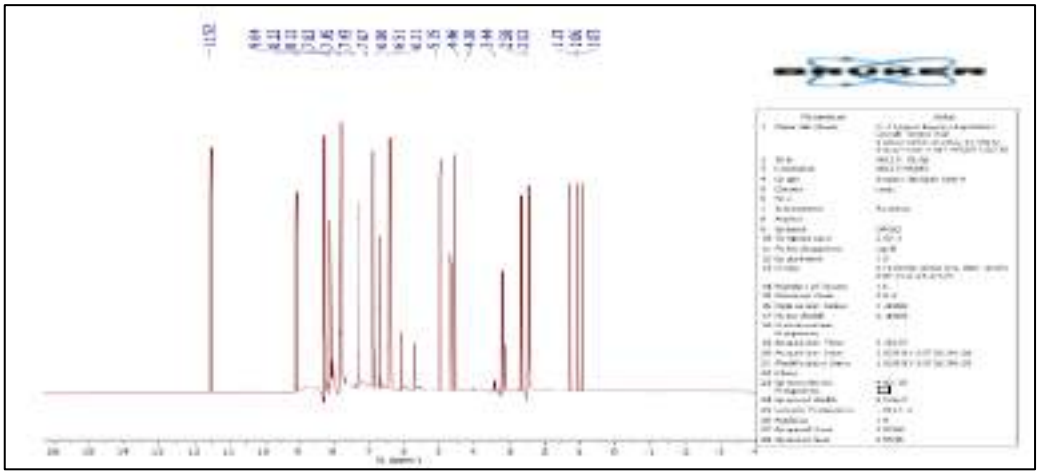


Figure (4- 191): ^{1}HNMR spectrum of copolymer(32) (MAA-CO-IAN) with compound(22) .

^{13}C-NMR spectrum of copolymer(32) (MAA-CO-IAN) with compound(22) . The signals of olefinic and aromatic carbons appear in the third region between 125 and 135 ppm, singles related to C-S at 56 ppm, singles related to C=N at 166 ppm, single related to C-N at 64 ppm, single related to C=O (amide) at 172 ppm, single related to C=O (acid) at 182 ppm. (151-153)

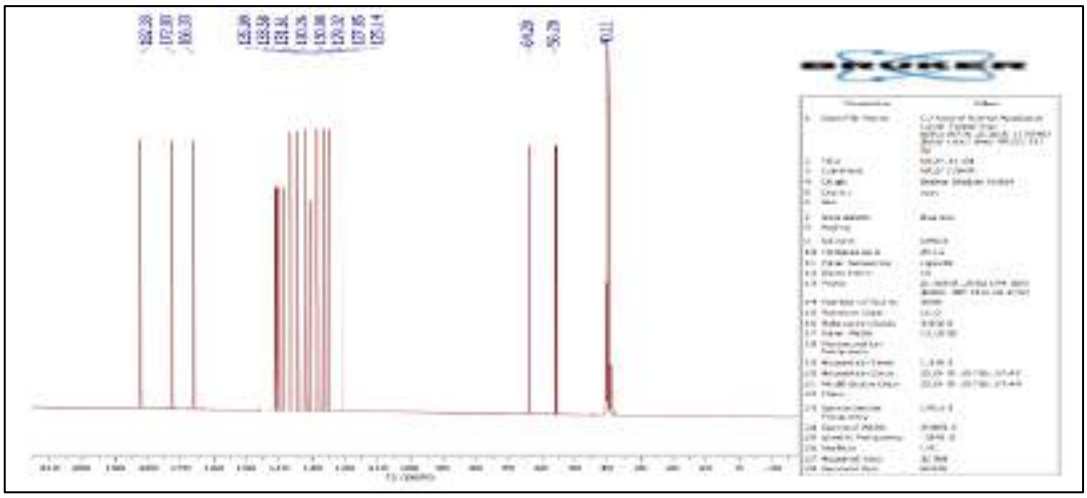
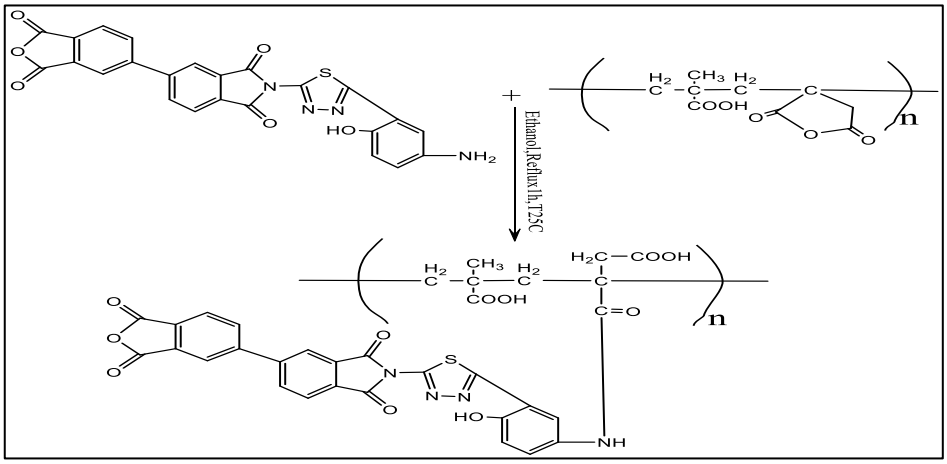


Figure (4- 192): ^{13}C-NMR spectrum of copolymer(32) (MAA-CO-IAN) with compound(22).

4.20.3 Synthesis of copolymer(23) (MAA-CO-IAN) with compound(23) .



Scheme (4-70): synthesis of copolymer(23) (MAA-CO-IAN) with compound(23) .

FTIR spectrum of copolymer(23) (MAA-CO-IAN) with compound(23) .

The FTIR spectrum of copolymer(23) (MAA-CO-IAN) with compound(23) as shown in (fig.4-193) which indicates absorption band at 3116 Cm^{-1} to -OH overlapping with NH, absorption band at 3001 to C-H (aromatic), absorption band at 2872 to C-H (aliphatic), absorption band at 1562 Cm^{-1} to C-H to C=N, absorption band at 1492 Cm^{-1} to C=C (aromatic), absorption band at 1633 Cm^{-1} to C=O (amide), absorption band at 1712 Cm^{-1} to C=O (carboxylic acid), absorption band at 1168 Cm^{-1} to C-N, absorption band at 1390 Cm^{-1} to CH_3. (151-153)

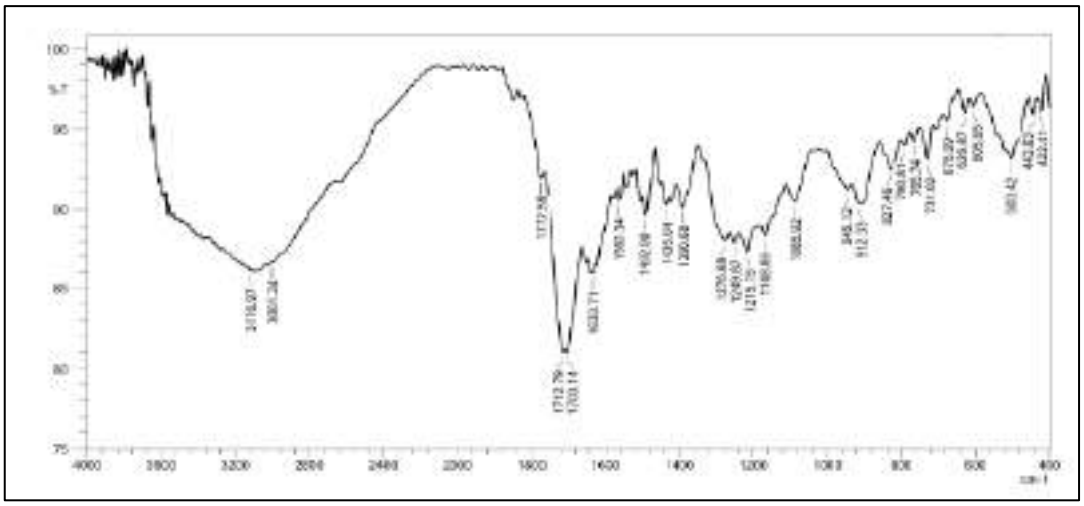


Figure (4- 193): FTIR spectrum of copolymer(23) (MAA-CO-IAN) with compound(23).

^{1}HNMR spectrum of copolymer(23) (MAA-CO-IAN) with compound(23) . ^{1}HNMR spectrum of copolymer(23) (MAA-CO-IAN) with compound(23) in (fig. 4-194) singles at (6.1-8.5 δ ppm) to (9H, phenyl ring), singles at (3.4 ppm) to –NH, singlate at (4.2-5.1 ppm) to –NH (amide), single at (10.5 ppm) to (COOH), singles at (2.5 ppm) to $–CH_2$**,** singles at (1.0 ppm) to $–CH_3$. (151-153)

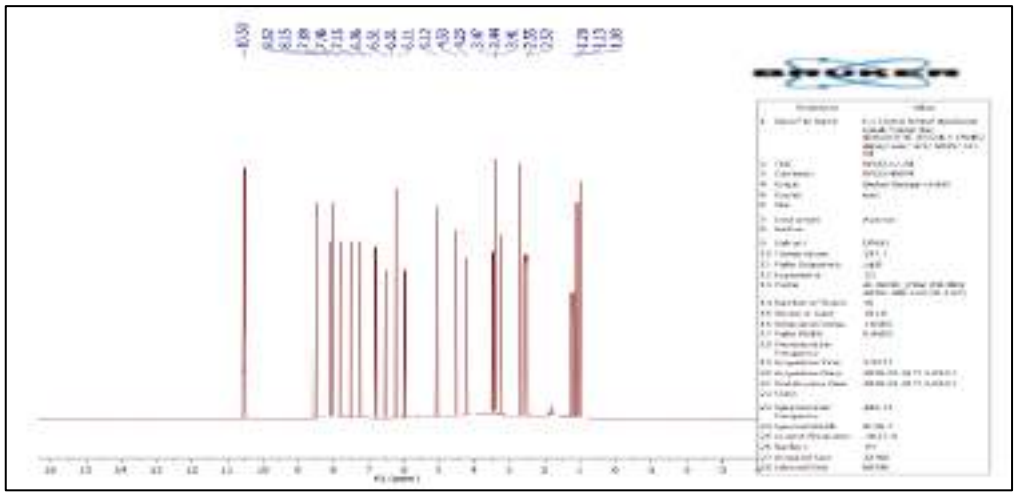


Figure (4- 194): ^{1}HNMR spectrum of copolymer(23) (MAA-CO-IAN) with compound(23) .

^{13}C-NMR spectrum of copolymer(23) (MAA-CO-IAN) with compound(23) . The signals of olefinic and aromatic carbons appear in the third region between 126 and 135 ppm, singles related to C-S at 56 ppm, singles related to C=N at 166 ppm, single related to C-N at 64 ppm, single related to C=O (amide) at 173 ppm, single related to C=O (acid) at 182 ppm. (151-153)

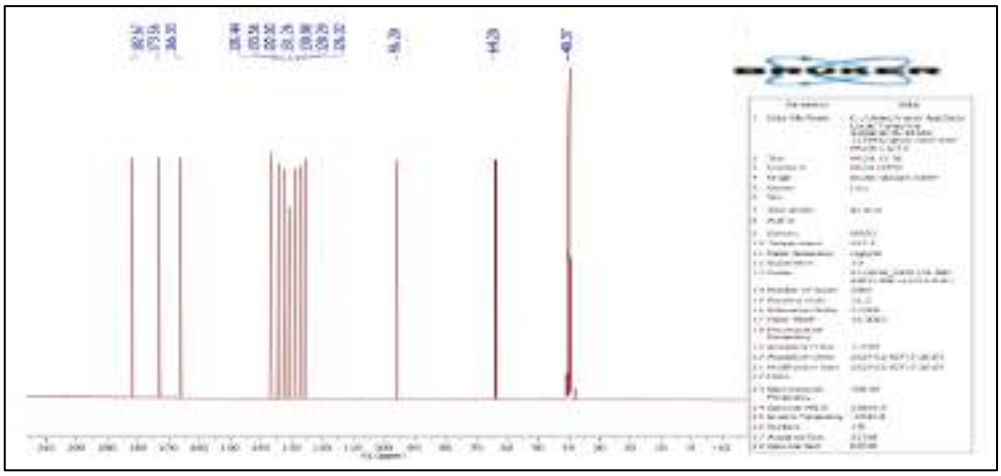
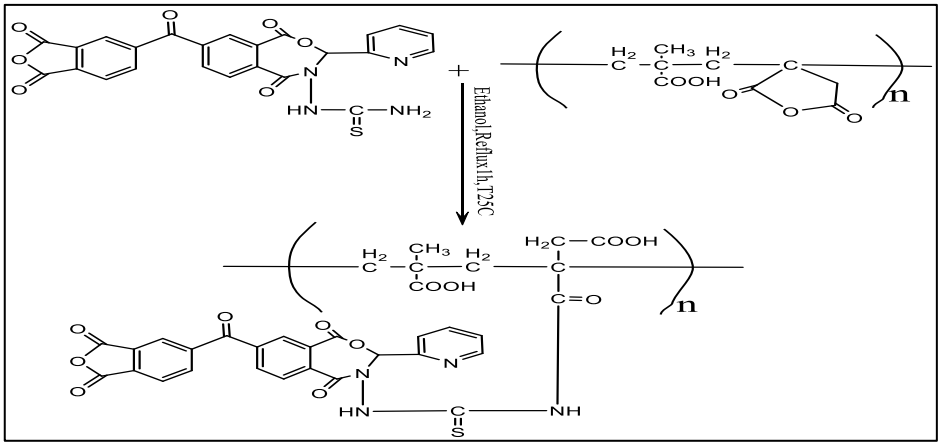


Figure (4- 195): ^{13}C-NMR spectrum of copolymer(23) (MAA-CO-IAN) with compound(23)

4.21 Synthesis of copolymer (MAA-CO-IAN) with compounds (24-26).

4.21.1 Synthesis of copolymer(24) (MAA-CO-IAN) with compound (24).



Scheme (4-71): synthesis of copolymer(24) (MAA-CO-IAN) with compound (24).

FTIR spectrum of copolymer(24) (MAA-CO-IAN) with compound (24).

The FTIR spectrum of copolymer(24) (MAA-CO-IAN) with compound (24) as shown in (fig.4-196) which indicates absorption bands at 3475 cm^{-1} to –OH and 3414 Cm^{-1} to –NH, absorption band at 3174 cm^{-1} to C-H(aromatic) , absorption band at 2981 cm^{-1} to C-H(aliphatic), absorption band at 1284 Cm^{-1} to C=S, absorption band at 1556 Cm^{-1} to C=C (aromatic), absorption bands at 1180 Cm^{-1} to C-N, absorption bands at 1714 Cm^{-1} to C=O (ester), absorption bands at 1639 Cm^{-1} to C=O (acid), absorption bands at 1392 Cm^{-1} to CH_3, absorption bands at 1701 Cm^{-1} to C=O Ketone), absorption bands at 1070 Cm^{-1} to C-O. (151-153)

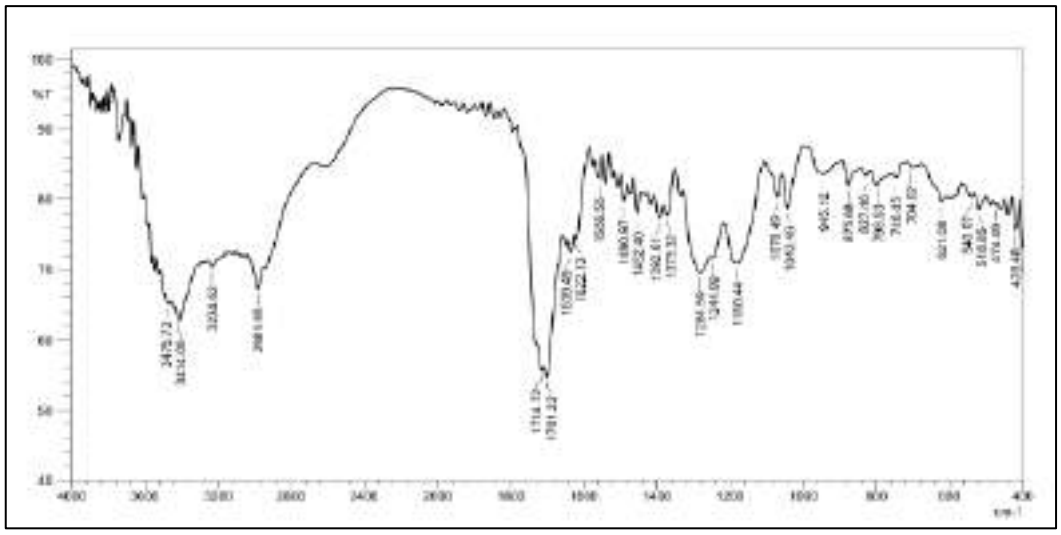


Figure (4- 196): FTIR spectrum of copolymer(24) (MAA-CO-IAN) with compound (24).

^{1}HNMR spectrum of copolymer(24) (MAA-CO-IAN) with compound (24). ^{1}HNMR spectrum of copolymer(24) (MAA-CO-IAN) with compound (24) in (fig.4-197) singles at (7.3-7.8 δ ppm) to (10H, phenyl ring), singles at (3. 3 ppm) to –NH, singles at (4. 3 ppm) to –NH (amide), singlate at (2.4 ppm) to CH_2, singlate at (0.9 ppm) to CH_3, singlate at (11.4 ppm) to OH (COOH). (151-153)

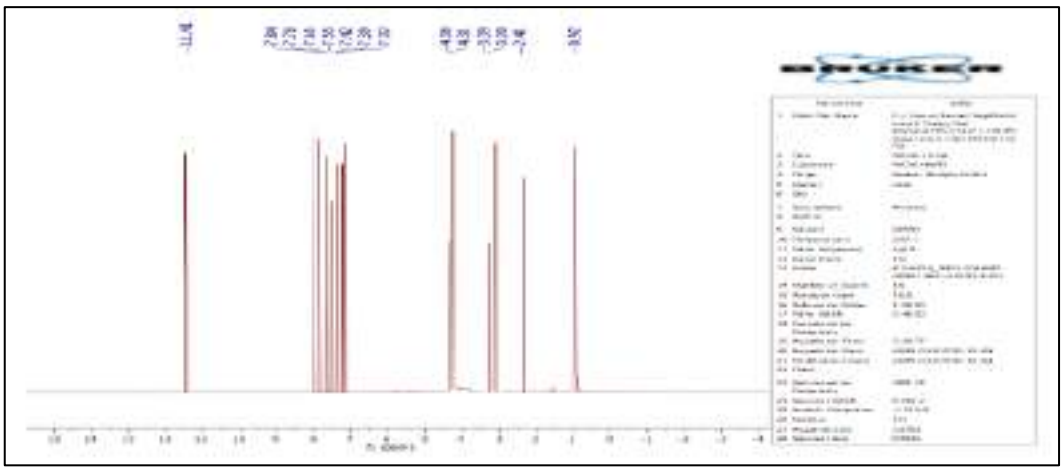


Figure (4- 197): ^{1}HNMR spectrum of copolymer(24) (MAA-CO-IAN) with compound (24).

^{13}C-NMR spectrum of copolymer(24) (MAA-CO-IAN) with compound (24). The signals of olefinic and aromatic carbons appear in the third region between 121 and 134 ppm, singles related to C=S at 194 ppm, single related to C-N at 63 ppm, single related to C=O (Acid) at 166 ppm, singles related to C=O (Ester) at 174 ppm, singles related to C=O (Ketone) at 210 ppm, singles related to CH_3 at 19 ppm. (151-153)

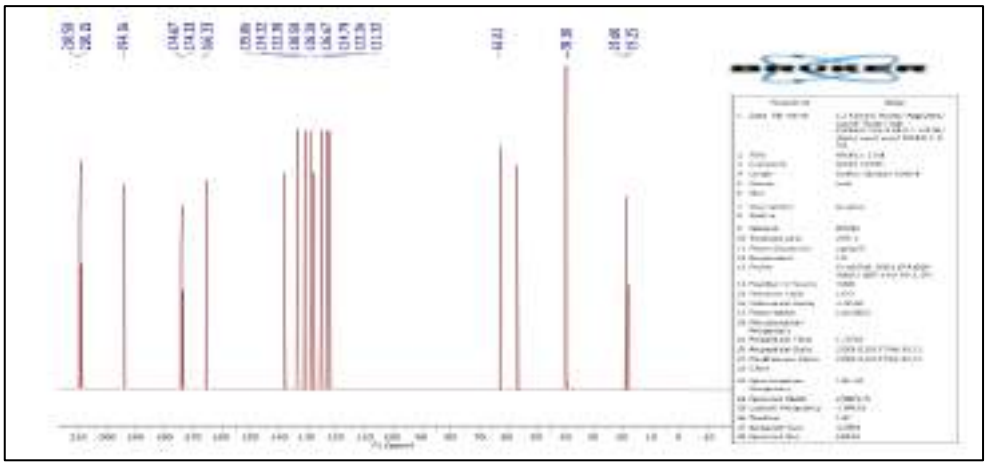
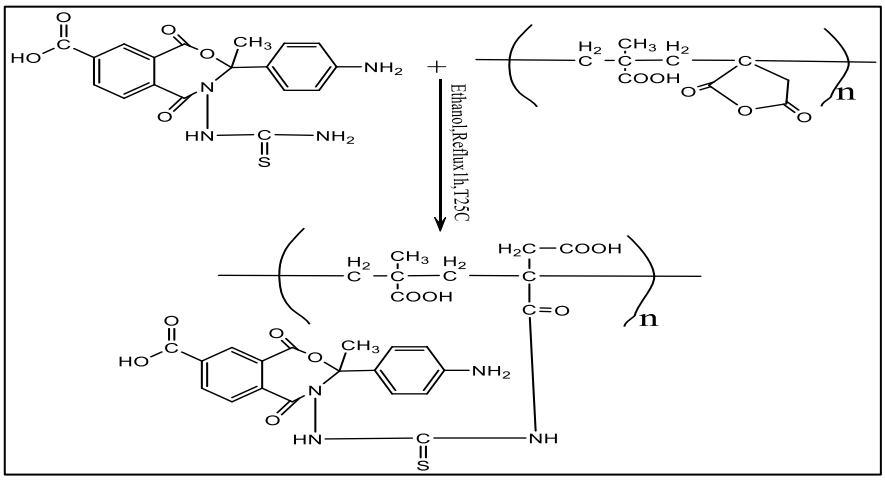


Figure (4- 198): ^{13}C-NMR spectrum of copolymer(24) (MAA-CO-IAN) with compound (24).

4.21.2. Synthesis of copolymer(25) (MAA-CO-IAN) with compound (25).



Scheme (4-72): synthesis of copolymer(25) (MAA-CO-IAN) with compound (25).

FTIR spectrum of copolymer(25) (MAA-CO-IAN) with compound (25).

The FTIR spectrum of copolymer(25) (MAA-CO-IAN) with compound (25) as shown in (fig.4-199) which indicates absorption bands at 3441 cm^{-1} to –OH and 3319 Cm^{-1} to –NH, absorption band at 3076 cm^{-1} to C-H (aromatic) , absorption band at 2987 cm^{-1} to C-H (aliphatic), absorption band at 1263 Cm^{-1} to C=S, absorption band at 1598 Cm^{-1} to C=C (aromatic), absorption bands at 1182 Cm^{-1} to C-N, absorption bands at 1714 Cm^{-1} to C=O (ester), absorption bands at 1649 Cm^{-1} to C=O (acid), absorption bands at 1336 Cm^{-1} to CH_3, absorption bands at 1070 Cm^{-1} to C-O. (151-153)

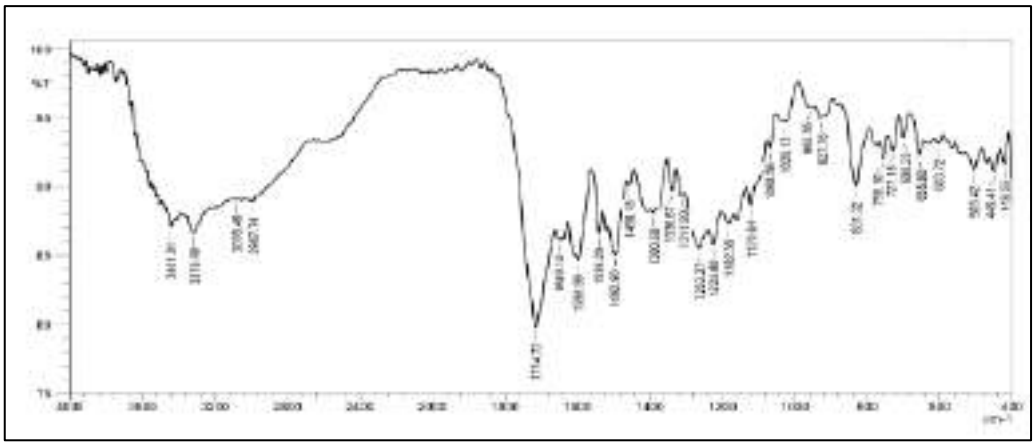


Figure (4- 199): FTIR spectrum of copolymer(25) (MAA-CO-IAN) with compound (25).

^{1}HNMR spectrum of copolymer(25) (MAA-CO-IAN) with compound (25).

^{1}HNMR spectrum of copolymer(25) (MAA-CO-IAN) with compound (25) in (fig.4-200) singles at (7.5-7.8 δ ppm) to (7H, phenyl ring), single at (3. 3 ppm) to –NH, single at (4. 3 ppm) to –NH (amide), singlate at (2.3 ppm) to CH_2, singlate at (0.9 ppm) to CH_3, singlate at (11.4 ppm) to OH (COOH). (151-153)

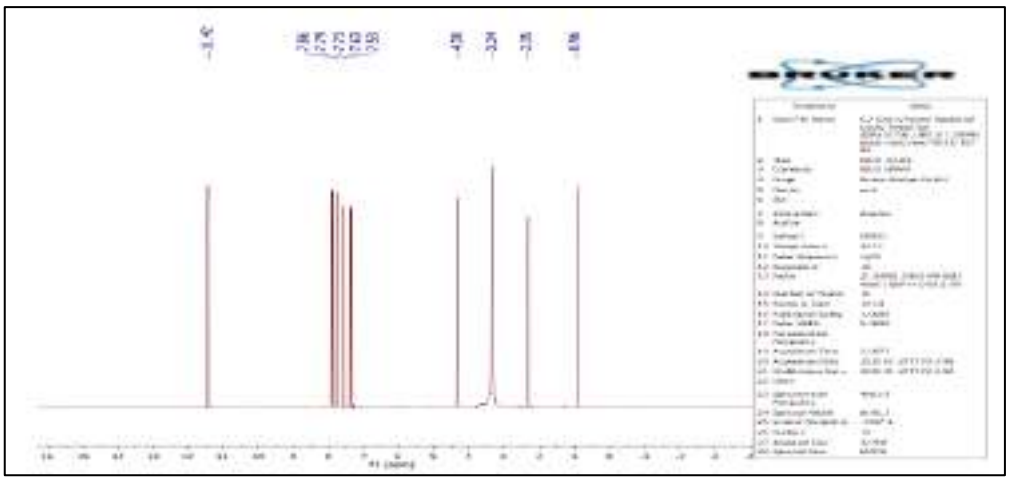


Figure (4- 200): ^{1}HNMR spectrum of copolymer(25) (MAA-CO-IAN) with compound (25).

^{13}C-NMR spectrum of copolymer(25) (MAA-CO-IAN) with compound (25). The signals of olefinic and aromatic carbons appear in the third region between 112 and 136 ppm, singles related to C=S at 194 ppm, single related to C-N at 63 ppm, singles related to C=O (Acid) at 166 ppm, singles related to C=O (Ester) at 174 ppm, singles related to C=O (Ketone) at 210 ppm, singles related to CH_3 at 19 ppm. (151-153)

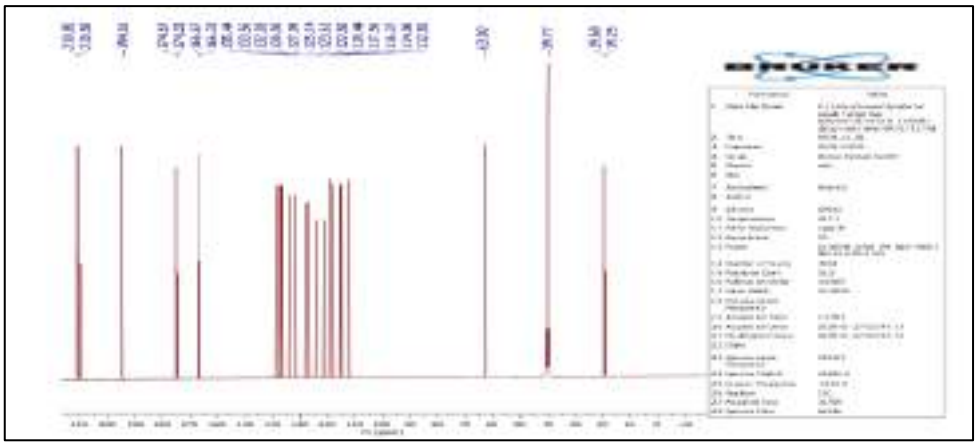
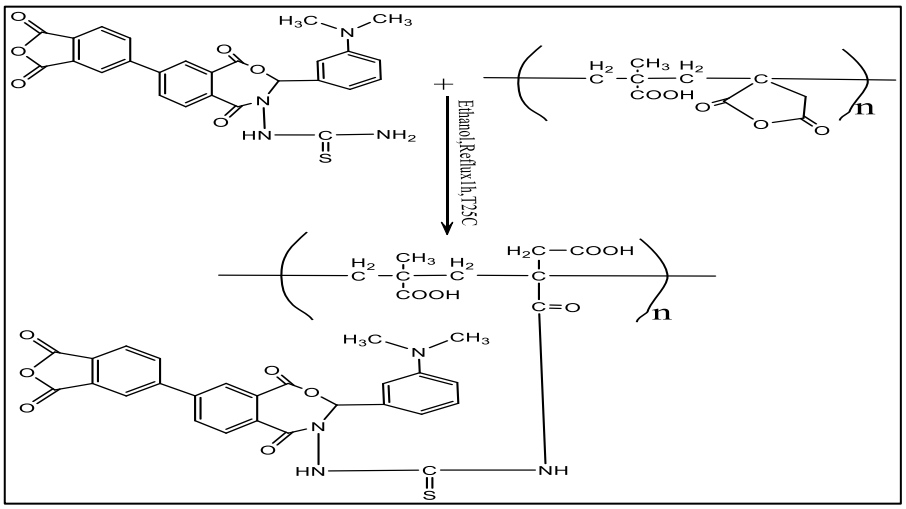


Figure (4- 201): ^{13}C-NMR spectrum of copolymer(25) (MAA-CO-IAN) with compound (25).

4.21.3 Synthesis of copolymer(26) (MAA-CO-IAN) with compound (26).



Scheme (4-73): synthesis of copolymer(26) (MAA-CO-IAN) with compound (26).

FTIR spectrum of copolymer(26) (MAA-CO-IAN) with compound (26).of

The FTIR spectrum of copolymer(26) (MAA-CO-IAN) with compound (26) as shown in (fig.4-202) which indicates absorption bands at 3504 cm^{-1} to –OH and 3414, 3377 Cm^{-1} to –NH, absorption band at 3076 cm^{-1} to C-H (aromatic) , absorption band at 2989 cm^{-1} to C-H (aliphatic), absorption band at 1247 Cm^{-1} to C=S, absorption band at 1515 Cm^{-1} to C=C (aromatic), absorption bands at 1178 Cm^{-1} to C-N, absorption bands at 1712 Cm^{-1} to C=O (ester), absorption bands at 1701 Cm^{-1} to C=O (acid), absorption bands at 1336 Cm^{-1} to CH_3, absorption bands at 1083Cm^{-1} to C-O. (151-153)

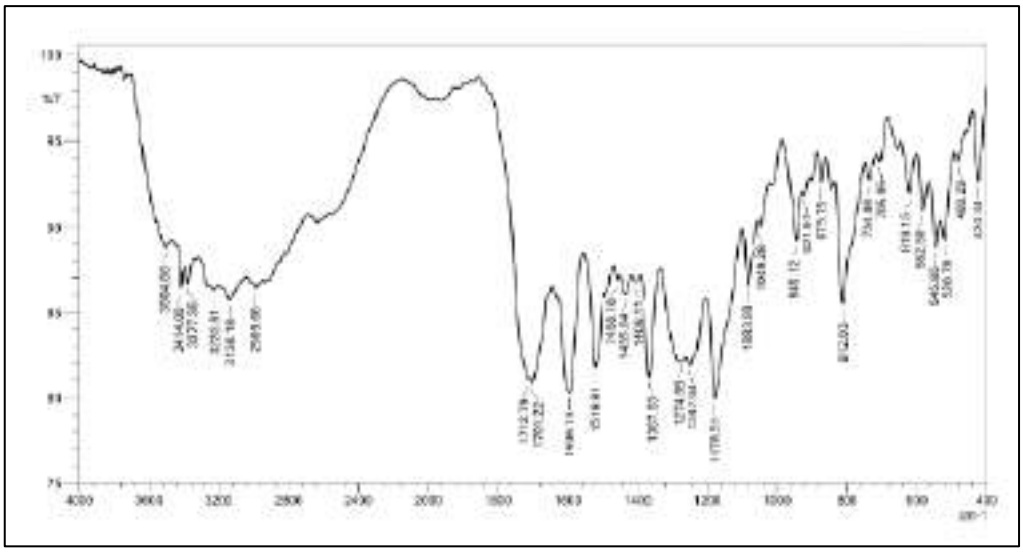


Figure (4- 202): FTIR spectrum of copolymer(26) (MAA-CO-IAN) with compound (26).

^{1}HNMR spectrum of copolymer(26) (MAA-CO-IAN) with compound (26).

^{1}HNMR spectrum of copolymer(26) (MAA-CO-IAN) with compound (26) in (fig.4-203) singles at (6.0-8.3 δ ppm) to (10H, phenyl ring), single at (3.0-3.4ppm) to –NH, single at (4.3 ppm) to –NH (amide), singlate at (2.3 ppm) to CH_2, singles at (1.0-1.3 ppm) to CH_3, singlate at (11.3 ppm) to OH (COOH). (151-153)

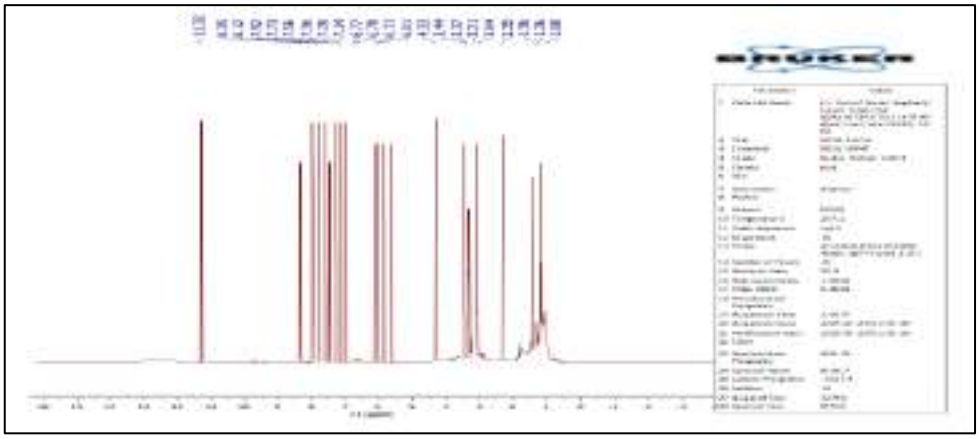


Figure (4- 203): ^{1}HNMR spectrum of copolymer(26) (MAA-CO-IAN) with compound (26).

^{13}C-NMR spectrum of copolymer(26) (MAA-CO-IAN) with compound (26). The signals of olefinic and aromatic carbons appear in the third region between 112 and 135 ppm, singles related to C=S at 194-205 ppm, single related to C-N at 64 ppm, singles related to C=O (Acid) at 168 ppm, singles related to C=O (Ester) at 174 ppm, singles related to CH_3 at 18 ppm. (151-153)

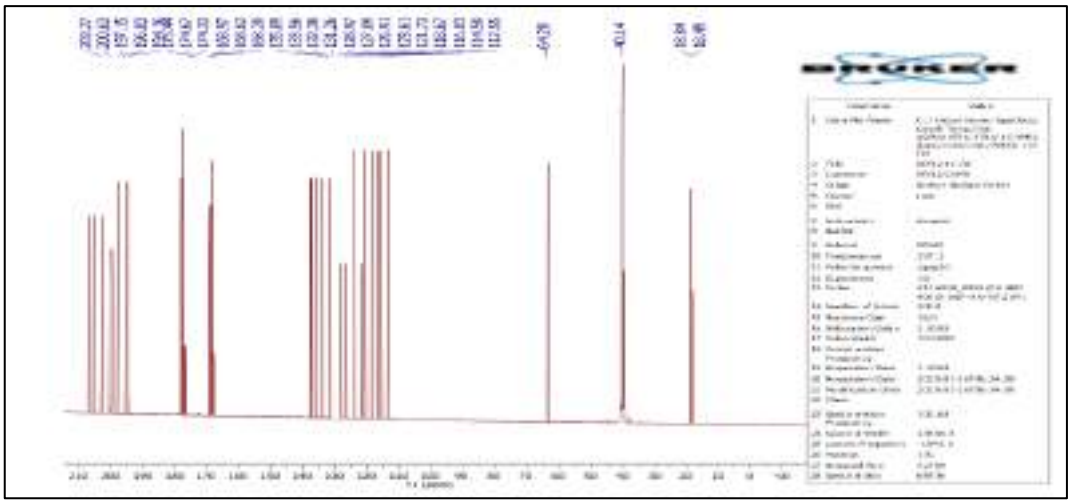
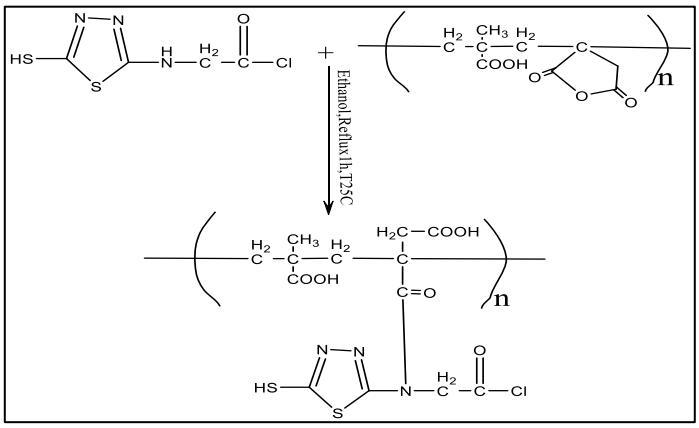


Figure (4- 204): ^{13}C-NMR spectrum of copolymer(26) (MAA-CO-IAN) with compound (26).

4.22 Synthesis of copolymer(27) (MAA-CO-IAN) with compound(27) .



Scheme (4-74): synthesis of copolymer (27) (MAA-CO-IAN) with compound(27) .

FTIR spectrum of copolymer (27) (MAA-CO-IAN) with compound(27) .

The FTIR spectrum of copolymer(27) (MAA-CO-IAN) with compound(27) as shown in (fig.4-205) which indicates absorption bands at 3412 to -OH overlapping with –NH , absorption band at 3061 Cm^{-1} to C-H (aromatic) , absorption band at 2980 Cm^{-1} to C-H (aliphatic), absorption band at 1573Cm^{-1} to C=N, absorption band at 2755 Cm^{-1} to SH, absorption band at 1504 Cm^{-1} to C=C (aromatic), absorption band at 1728 Cm^{-1} to C=O (Acid chloride), absorption band at 744 Cm^{-1} to C-Cl. absorption band at 1631 Cm^{-1} to C=O (amide), absorption band at 1371 Cm^{-1} to CH_3. (151-153)

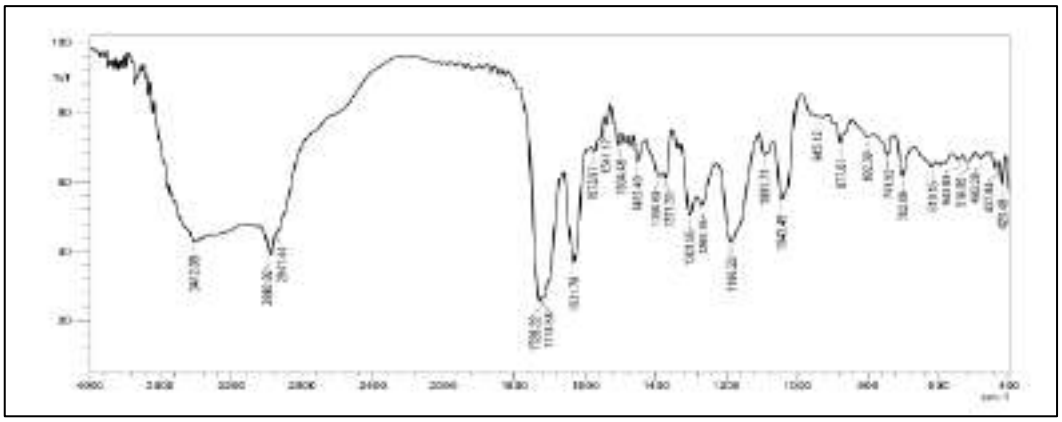


Figure (4- 205): FTIR spectrum of copolymer (27) (MAA-CO-IAN) with compound(27).

^{1}HNMR spectrum of copolymer (27) (MAA-CO-IAN) with compound(27).

^{1}HNMR spectrum of copolymer(27) (MAA-CO-IAN) with compound(27) in (fig.4-206) multiple singlate at (3.1-4.3 ppm) to SH. multiple singlate at (10.3ppm) to OH (COOH)**,** singlate at (2.3 ppm) to CH_2, singles at (0.9-1.0 ppm) to CH_3**.** (151-153)

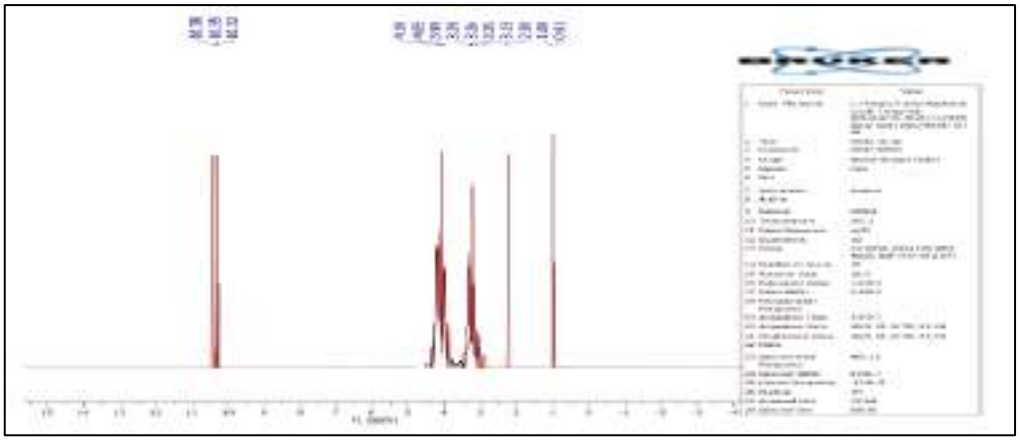


Figure (4- 206): ^{1}HNMR spectrum of copolymer (27) (MAA-CO-IAN) with compound(27) .

^{13}C-NMR spectrum of copolymer(27) (MAA-CO-IAN) with compound(27) . Single related to C-S at 68 ppm, singles related to C=N at 153 ppm, single related to C-N at 62 ppm, singles related to C=O (amid) at 187 ppm, single related to C-Cl at 78 ppm, singles related to C=O (acid) at 173 ppm, single related to CH_3 (acid) at 18 ppm. (151-153)

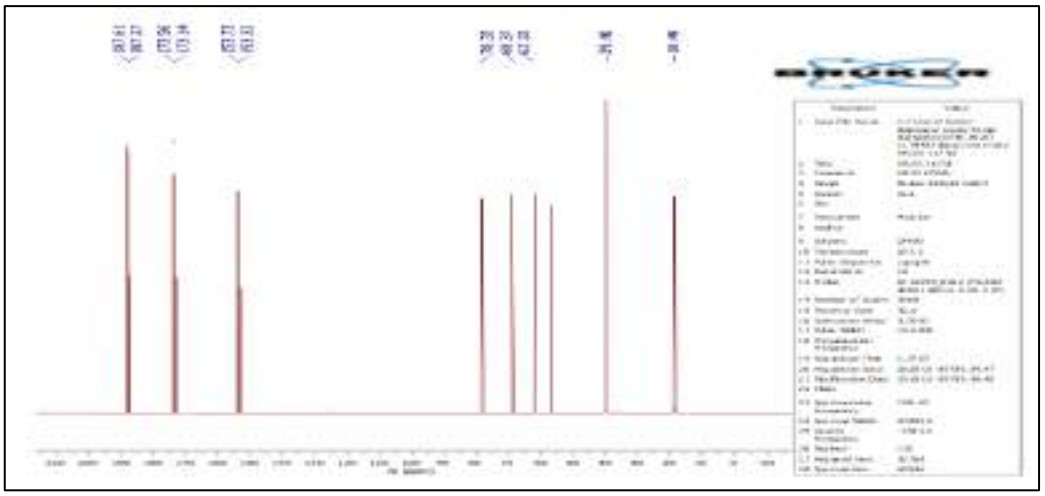
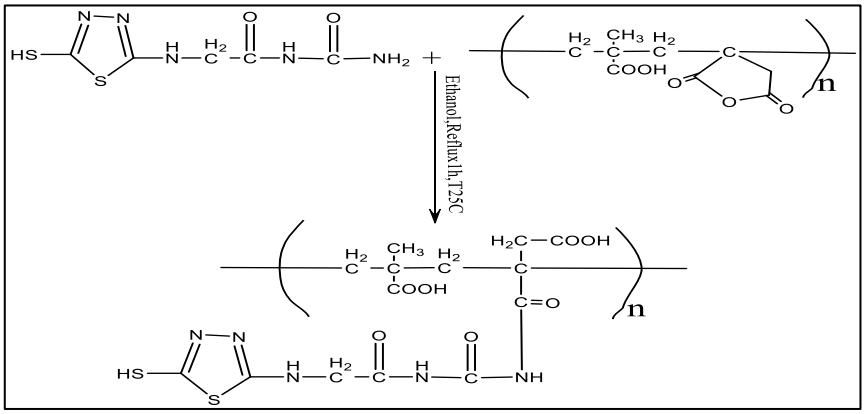


Figure (4- 207): ^{13}C-NMR spectrum of copolymer(27) (MAA-CO-IAN) with compound(27).

4-23:- Synthesis of copolymer(28) (MAA-CO-IAN) with compound(28).



Scheme (4-75): synthesis of copolymer(28) (MAA-CO-IAN) with compound(28).

The FTIR spectrum of copolymer(28) (MAA-CO-IAN) with compound(28 as shown in (fig.4-208) which indicates absorption bands at 3410 to -OH overlapping with –NH , absorption band at 3194 Cm^{-1} to C-H (aromatic) , absorption band at 2976 Cm^{-1} to C-H (aliphatic), absorption band at 1556 Cm^{-1} to C=N, absorption band at 2755 Cm^{-1} to SH, absorption band at 1510 Cm^{-1} to C=C (aromatic), absorption band at 1697 Cm^{-1} to C=O (Acid), absorption band at 1618 Cm^{-1} to C=O (amide), absorption band at 1336 Cm^{-1} to CH_3. (151-153)

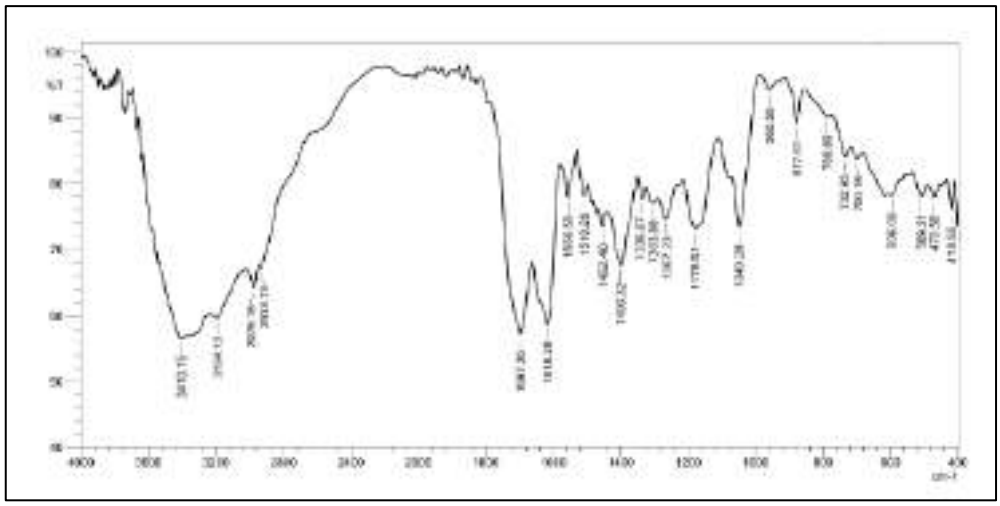


Figure (4- 208): FTIR spectrum of copolymer (28) (MAA-CO-IAN) with compound(28).

^{1}HNMR spectrum of copolymer(28) (MAA-CO-IAN) with compound(28).

^{1}HNMR spectrum of copolymer(28) (MAA-CO-IAN) with compound(28) in (fig.4-209) multiple singlate at (3.1-4.3 ppm) to SH. multiple singlate at (10.8ppm) to OH (COOH)**,** singlate at (2.3 ppm) to CH_2, singles at (0.9ppm) to CH_3**.** (151-153)

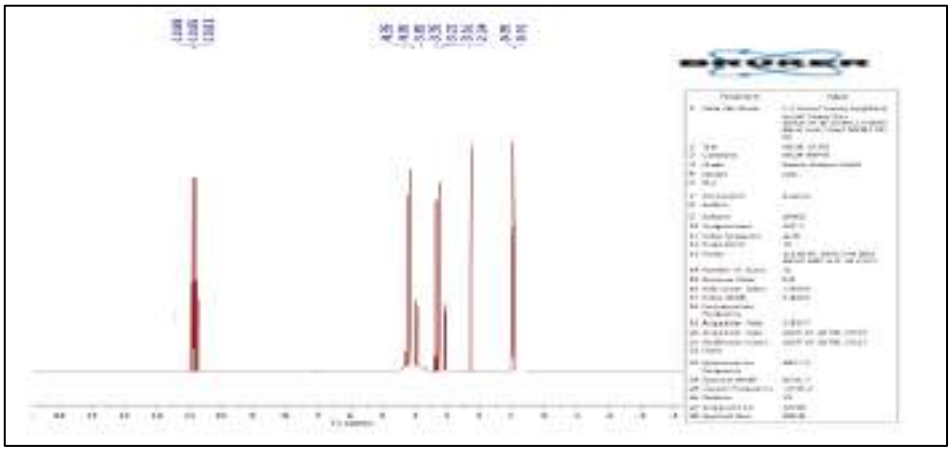


Figure (4- 209): ^{1}HNMR spectrum of copolymer (28) (MAA-CO-IAN) with compound(28).

^{13}C-NMR spectrum of copolymer(28) (MAA-CO-IAN) with compound(28).

Single related to C-S at 68 ppm, singles related to C=N at 154 ppm, single related to C-N at 62 ppm, singles related to C=O (amid) at 186 ppm, single related to C-Cl at 78 ppm, singles related to C=O (acid) at 174 ppm, single related to CH_3 (acid) at 18 ppm. (151-153)

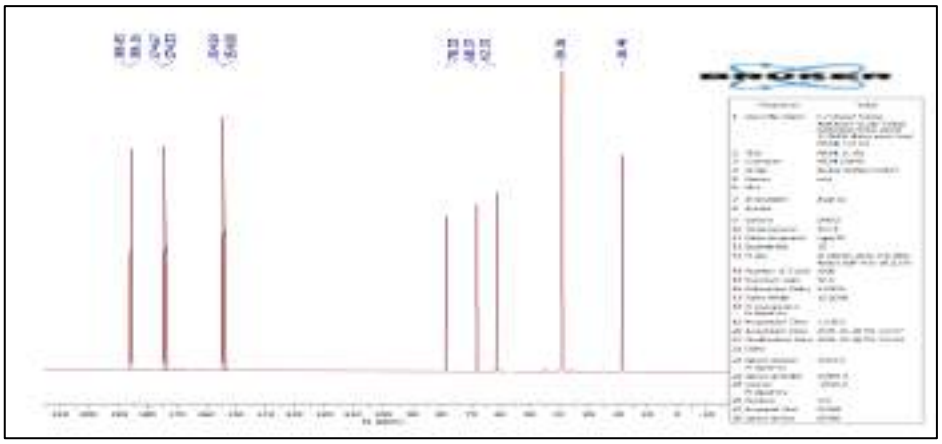
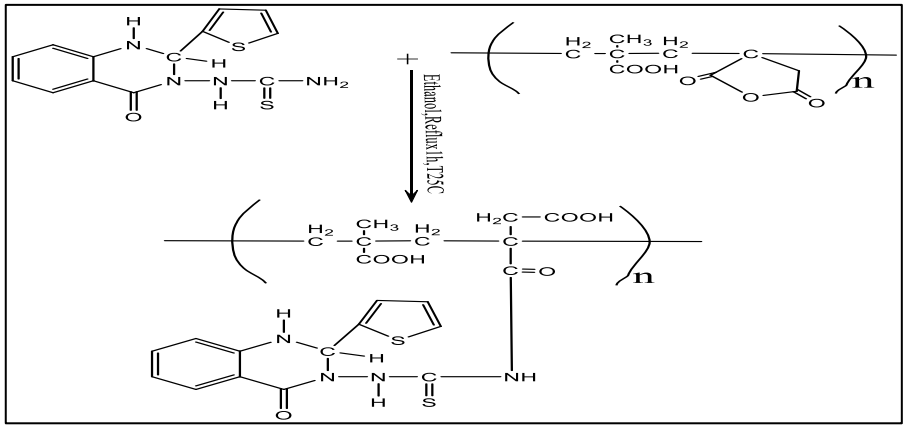


Figure (4- 210): ^{13}C-NMR spectrum of copolymer(28) (MAA-CO-IAN) with compound(28).

4.23 Synthesis of copolymer (MAA-CO-IAN) with compounds (29-31) .

4.23.1 Synthesis of copolymer(29) (MAA-CO-IAN) with compound (29).



Scheme (4-76): synthesis of copolymer(29) (MAA-CO-IAN) with compound (29).

FTIR spectrum of copolymer(29) (MAA-CO-IAN) with compound (29).

The FTIR spectrum of copolymer(29) (MAA-CO-IAN) with compound (29) as shown in (fig.4-211) which indicates absorption band at 3466 Cm^{-1} to –OH and 3408 Cm^{-1} to–NH, absorption band at 3226 Cm^{-1} to C-H (aromatic), absorption band at 2981 Cm^{-1} to C-H (aliphatic), absorption band at 1273 Cm^{-1} to C=S, absorption band at 1537 Cm^{-1} to C=C (phenyl ring), absorption band at 1043 Cm^{-1} to C-N, absorption band at 1083 Cm^{-1} to C-O , absorption band at 1710 Cm^{-1} to C=O(acid), absorption band at 1697 Cm^{-1} to C=O(amide), absorption band at 612 Cm^{-1} to C-S, absorption band at 1390 Cm^{-1} to CH_3. (151-153)

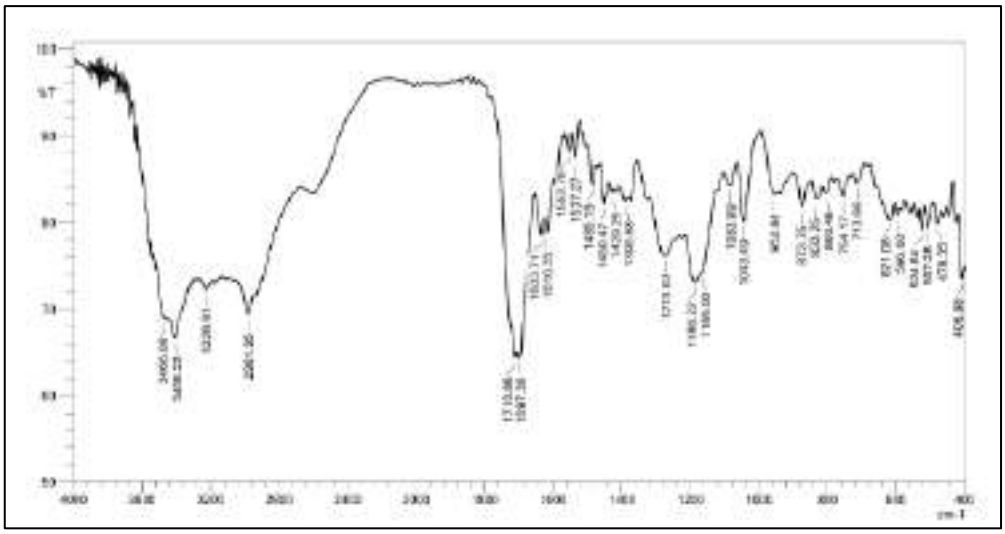


Figure (4- 211): FTIR spectrum of copolymer(29) (MAA-CO-IAN) with compound (29).

^{1}HNMR spectrum of copolymer(29) (MAA-CO-IAN) with compound (29).

^{1}HNMR spectrum of copolymer(29) (MAA-CO-IAN) with compound (29) in (fig.4-212) singles at (6.5-8.3 δ ppm) to (4H, phenyl ring), multiple singlate at (3.3 to 4.0 ppm) to –NH, single at 2.5 ppm to CH_2**,** single at 1.0 ppm to CH_3**,** singles at 12.0-12.5 ppm to OH (COOH). (151-153)

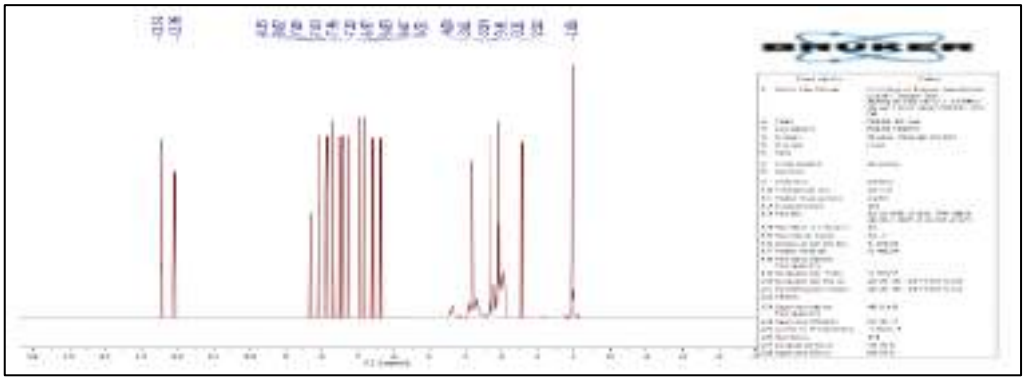


Figure (4- 212): ^{1}HNMR spectrum of copolymer(29) (MAA-CO-IAN) with compound (29).

^{13}C-NMR spectrum of copolymer(29) (MAA-CO-IAN) with compound (29). The signals of olefinic and aromatic carbons appear in the third region between 115 and 136ppm, single related to C-N at 66 ppm, singles related to C=O (amide) at 166 ppm, singles related to C=S at 193-210 ppm, singles related to C=O (acid) at 173 ppm, singles related to CH_3 at 18 ppm. (151-153)

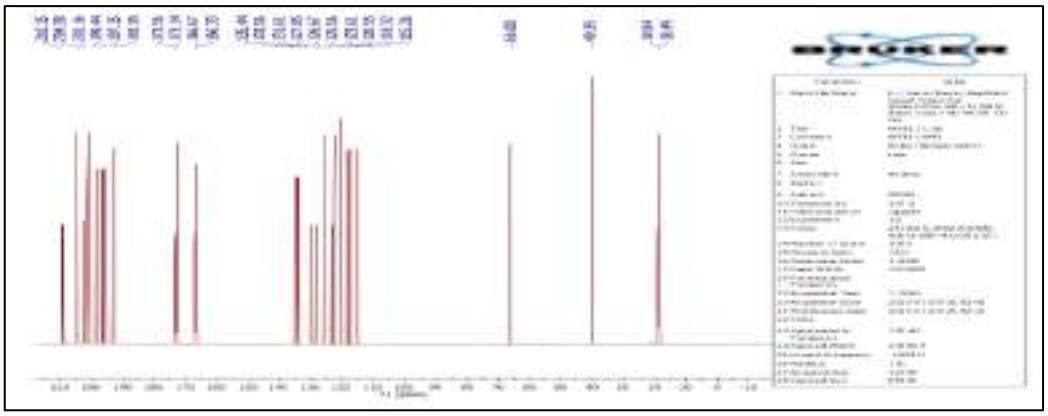
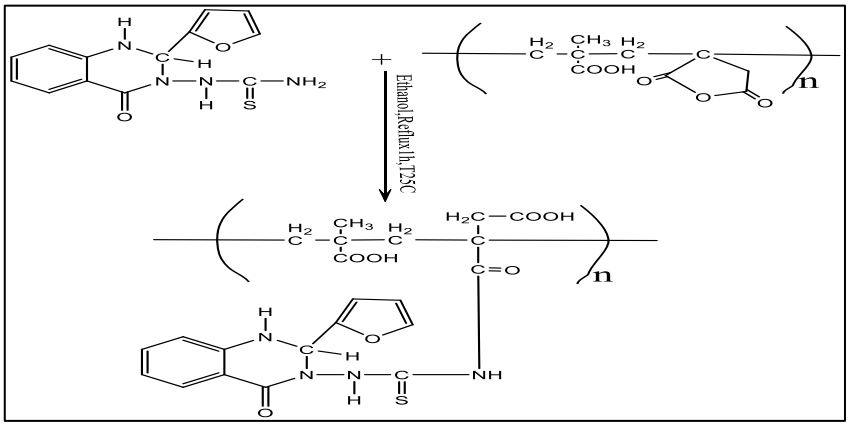


Figure (4- 213): ^{13}C-NMR spectrum of copolymer(29) (MAA-CO-IAN) with compound (29).

4.23.2 Synthesis of copolymer(30) (MAA-CO-IAN) with compound (30).



Scheme (4-77): synthesis of copolymer(30) (MAA-CO-IAN) with compound (30).

FTIR spectrum of copolymer(30) (MAA-CO-IAN) with compound (30).

The FTIR spectrum of copolymer(30) (MAA-CO-IAN) with compound (30) as shown in (fig.4-214) which indicates absorption band at 3460Cm^{-1} to –OH and 3412 Cm^{-1} to–NH, absorption band at 3234 Cm^{-1} to C-H (aromatic), absorption band at 2974 Cm^{-1} to C-H (aliphatic), absorption band at 1257 Cm^{-1} to C=S, absorption band at 1485 Cm^{-1} to C=C (phenyl ring), absorption band at 1047 Cm^{-1} to C-N, absorption band at 1087 Cm^{-1} to C-O , absorption band at 1699 Cm^{-1} to C=O(acid), absorption band at 1635 Cm^{-1} to C=O(amide), absorption band at 622 Cm^{-1} to C-S, absorption band at 1386 Cm^{-1} to CH_3. (151-153)

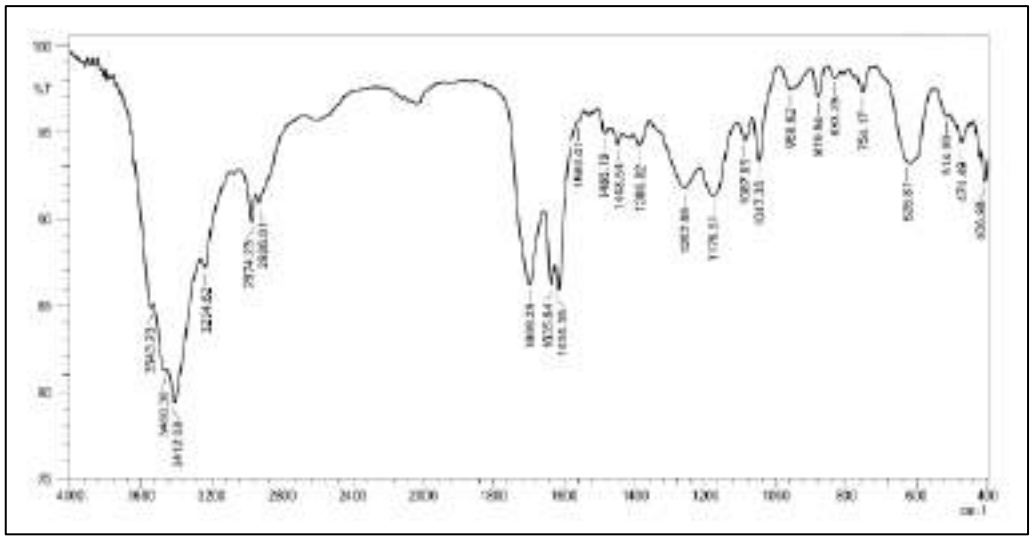


Figure (4- 214): FTIR spectrum of copolymer(30) (MAA-CO-IAN) with compound (30).

^{1}HNMR spectrum of copolymer(30) (MAA-CO-IAN) with compound (30).

^{1}HNMR spectrum of copolymer(30) (MAA-CO-IAN) with compound (30) in (fig.4-215) singles at (6.0-7.7 δ ppm) to (4H, phenyl ring), multiple singles at (3.3 to 4.0 ppm) to –NH, single at 2.5 ppm to CH_2**,** single at 1.0 ppm to CH_3**,** singles at 11.2 ppm to OH (COOH). (151-153)

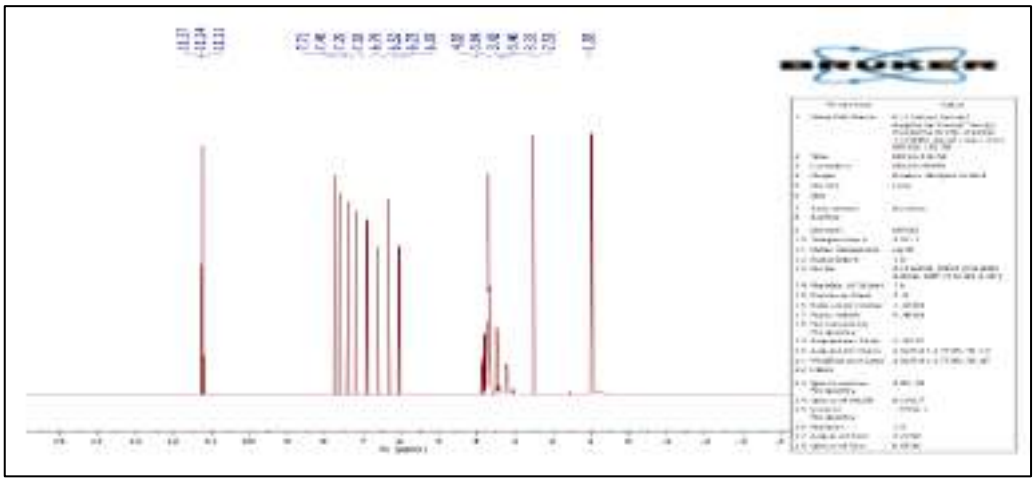


Figure (4- 215): ^{1}HNMR spectrum of copolymer(30) (MAA-CO-IAN) with compound (30).

^{13}C-NMR spectrum of copolymer(30) (MAA-CO-IAN) with compound (30). The signals of olefinic and aromatic carbons appear in the third region between 115 and 133ppm, single related to C-N at 66 ppm, singles related to C=O (amide) at 166 ppm, singles related to C=S at 190-210 ppm, singles related to C=O (acid) at 172 ppm, singles related to CH_3 at 18 ppm. (151-153)

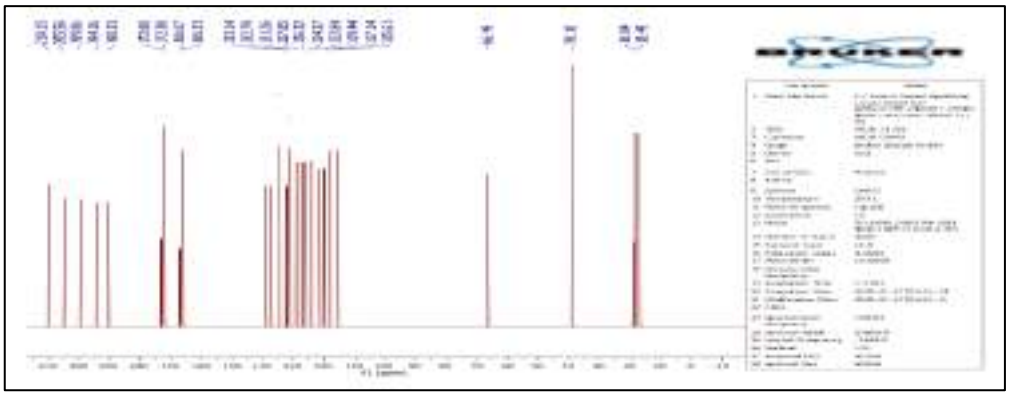
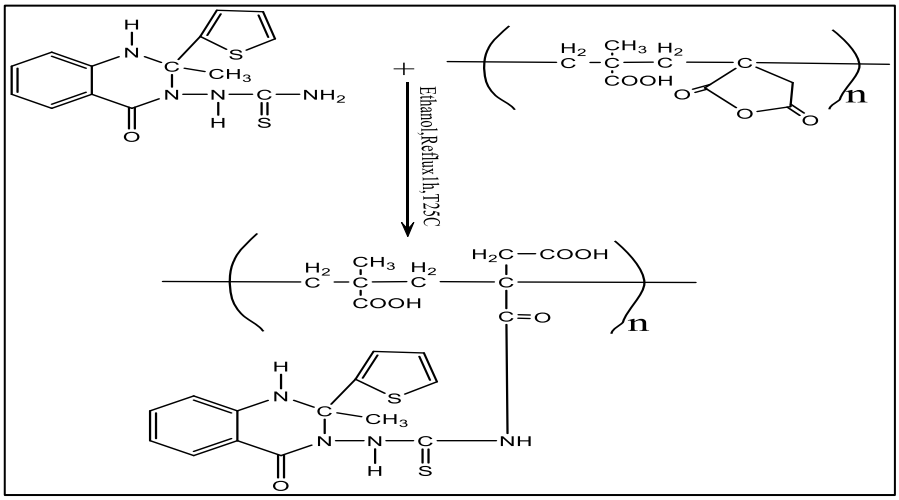


Figure (4- 216): ^{13}C-NMR spectrum of copolymer(30) (MAA-CO-IAN) with compound (30).

4.23.3 Synthesis of copolymer(31) (MAA-CO-IAN) with compound (31).



Scheme (4-78): synthesis of copolymer(31) (MAA-CO-IAN) with compound (31).

FTIR spectrum of copolymer(31) (MAA-CO-IAN) with compound (31).

The FTIR spectrum of copolymer(31) (MAA-CO-IAN) with compound (31) as shown in (fig.4-217) which indicates absorption band at 3414 Cm^{-1} to –OH and 3236 Cm^{-1} to–NH, absorption band at 3182 Cm^{-1} to C-H (aromatic), absorption band at 2974 Cm^{-1} to C-H (aliphatic), absorption band at 1238 Cm^{-1} to C=S, absorption band at 1537 Cm^{-1} to C=C (phenyl ring), absorption band at 1045 Cm^{-1} to C-N, absorption band at 1087 Cm^{-1} to C-O , absorption band at 1707 Cm^{-1} to C=O(acid), absorption band at 1616 Cm^{-1} to C=O(amide), absorption band at 632 Cm^{-1} to C-S, absorption band at 1390 Cm^{-1} to CH_3. (151-153)

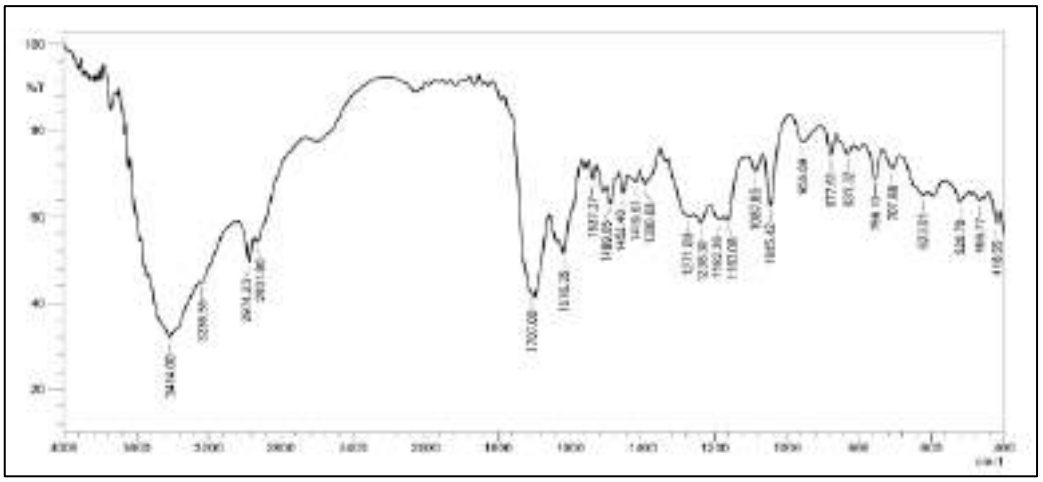


Figure (4- 217): FTIR spectrum of copolymer(31) (MAA-CO-IAN) with compound (31).

^{1}HNMR spectrum of copolymer(31) (MAA-CO-IAN) with compound (31).

^{1}HNMR spectrum of copolymer(31) (MAA-CO-IAN) with compound (31) in (fig.4-218) singles at (6.5-8.3 δ ppm) to (4H, phenyl ring), multiple singlate at (3.3 to 4.0 ppm) to –NH, singles at 2.3 ppm to CH_2**,** single at 1.0 ppm to CH_3**,** singles at 12.0 ppm to OH (COOH). (151-153)

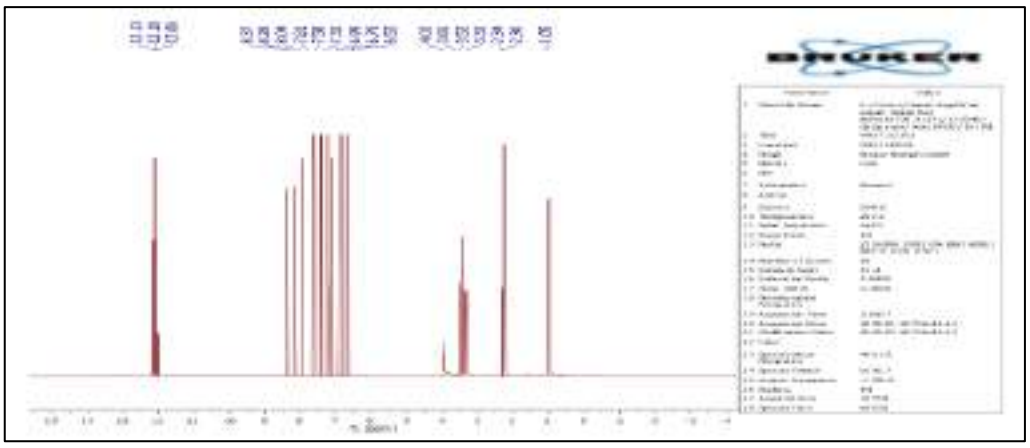


Figure (4- 218): ^{1}HNMR spectrum of copolymer(31) (MAA-CO-IAN) with compound (31).

^{13}C-NMR spectrum of copolymer(31) (MAA-CO-IAN) with compound (31).

The signals of olefinic and aromatic carbons appear in the third region between 110 and 135ppm, single related to C-N at 56 ppm, singles related to C=O (amide) at 166 ppm, singles related to C=S at 190-210 ppm, singles related to C=O (acid) at 172 ppm, singles related to CH_3 at 18 ppm. (151-153)

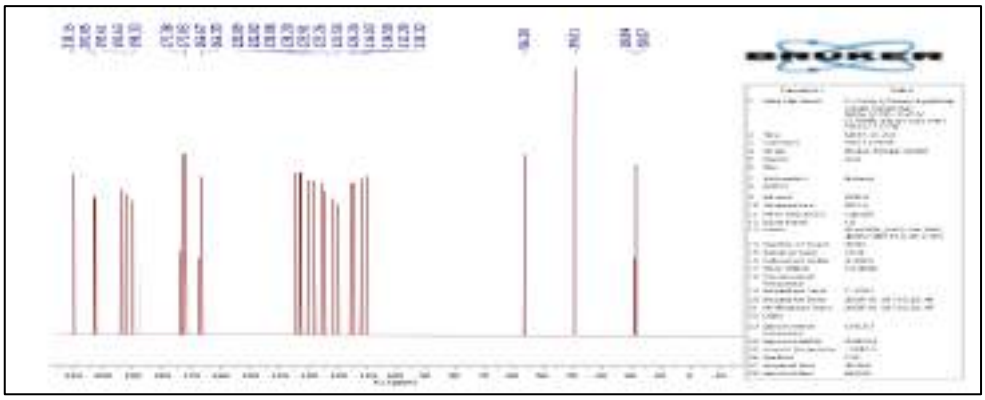
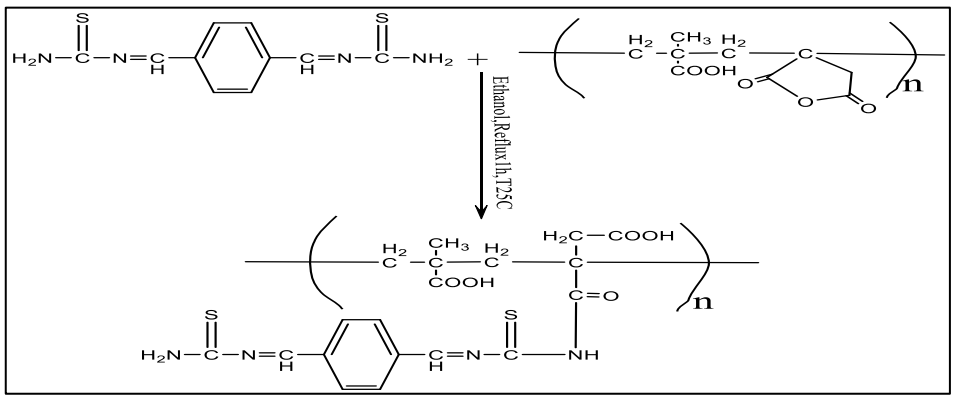


Figure (4- 219): ^{13}C-NMR spectrum of copolymer(31) (MAA-CO-IAN) with compound (31).

4.24 Synthesis of copolymer(32) (MAA-CO-IAN) with compound (32).



Scheme (4-79): synthesis of copolymer(32) (MAA-CO-IAN) with compound (32).

FTIR spectrum of copolymer(32) (MAA-CO-IAN) with compound (32).

The FTIR spectrum of copolymer(32) (MAA-CO-IAN) with compound (32) as shown in (fig.4-220) which indicates absorption band at 3390 Cm^{-1} to –OH and 3236 Cm^{-1} to–NH, absorption band at 3172 Cm^{-1} to C-H (aromatic), absorption band at 2978 Cm^{-1} to C-H (aliphatic), absorption band at 1274 Cm^{-1} to C=S, absorption band at 1552 Cm^{-1} to C=C (phenyl ring), absorption band at 1043 Cm^{-1} to C-N, absorption band at 1083 Cm^{-1} to C-O , absorption band at 1710 Cm^{-1} to C=O(acid), absorption band at 1697 Cm^{-1} to C=O(amide), absorption band at 1633 Cm^{-1} to C=N, absorption band at 1390 Cm^{-1} to CH_3. (151-153)

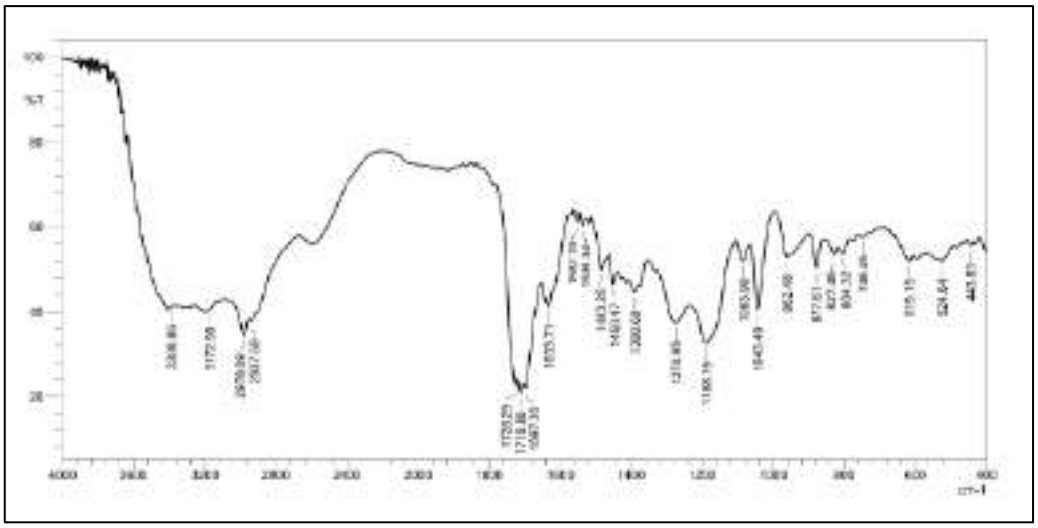


Figure (4- 220): FTIR spectrum of copolymer(32) (MAA-CO-IAN) with compound (32).

^{1}HNMR spectrum of copolymer(32) (MAA-CO-IAN) with compound (32).

^{1}HNMR spectrum of copolymer(32) (MAA-CO-IAN) with compound (32) in (fig.4-221) singles at (6.5-8.3 δ ppm) to (4H, phenyl ring), multiple singlate at (3.3) to –NH, multiple singlate at (4.3) to –NH(amide), singles at 2.3 ppm to CH_2**,** single at 1.0 ppm to CH_3**,** singles at 12.5 ppm to OH (COOH). (151-153)

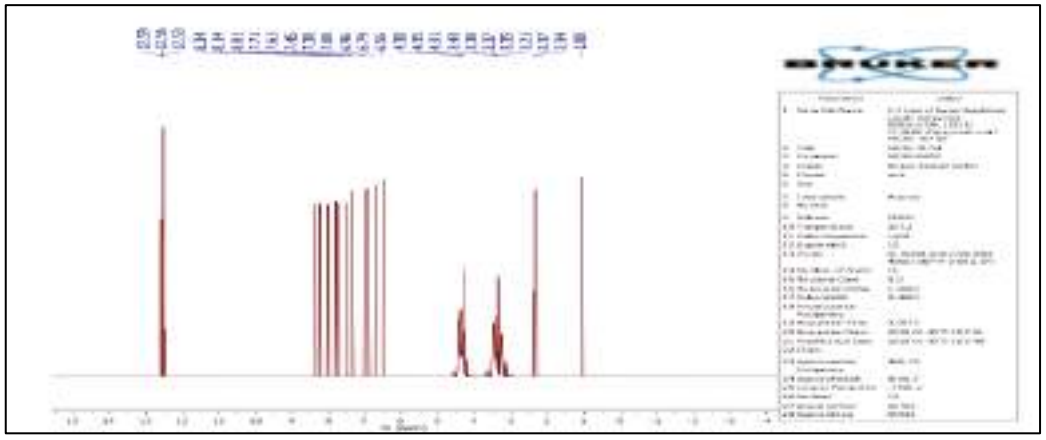


Figure (4- 221): ^{1}HNMR spectrum of copolymer(32) (MAA-CO-IAN) with compound (32).

^{13}C-NMR spectrum of copolymer(32) (MAA-CO-IAN) with compound (32).

The signals of olefinic and aromatic carbons appear in the third region between 112 and 130 ppm, single related to C-N at 56 ppm, singles related to C=O (amide) at 166 ppm, singles related to C=S at 192-210 ppm, singles related to C=O (acid) at 173 ppm, singles related to CH_3 at 18 ppm, single related to C=N at 141 ppm. (151-153)

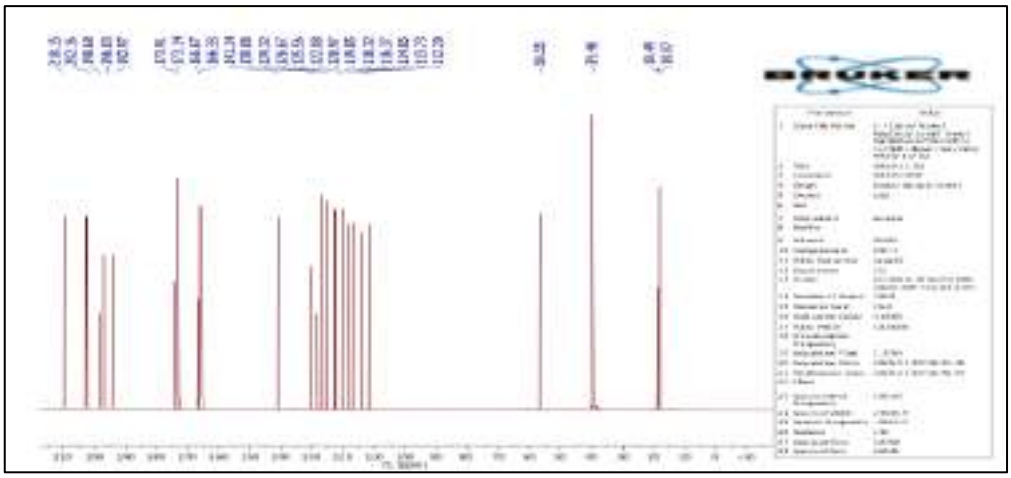
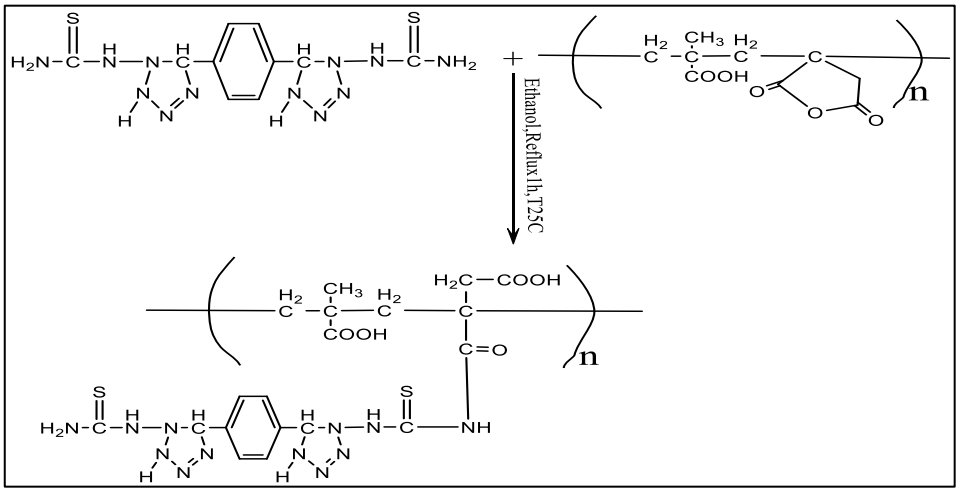


Figure (4- 222): ^{13}C-NMR spectrum of copolymer(32) (MAA-CO-IAN) with compound (32).

4.25 *Synthesis* of copolymer(33) (MAA-CO-IAN) with compound(33).



Scheme (4-80): synthesis of copolymer(33) (MAA-CO-IAN) with compound(33).

FTIR spectrum of copolymer (33) (MAA-CO-IAN) with compound(33).

The FTIR spectrum of copolymer (MAA-CO-IAN) with compound(33) in (fig.4-223) which indicates absorption band at 3415 Cm^{-1} to –OH and 3211and 3172 Cm^{-1} to–NH, absorption band at 3055 Cm^{-1} to C-H (aromatic), absorption band at 2991 Cm^{-1} to C-H (aliphatic), absorption band at 1271 Cm^{-1} to C=S, absorption band at 1462 Cm^{-1} to C=C (phenyl ring), absorption band at 1058 Cm^{-1} to C-N, absorption band at 1086 Cm^{-1} to C-O , absorption band at 1726 Cm^{-1} to C=O(acid), absorption band at 1699 Cm^{-1} to C=O (amide), absorption band at 1618 Cm^{-1} to C=N, absorption band at 1338 Cm^{-1} to CH_3, absorption band at 1490 Cm^{-1} to N=N. (151-153)

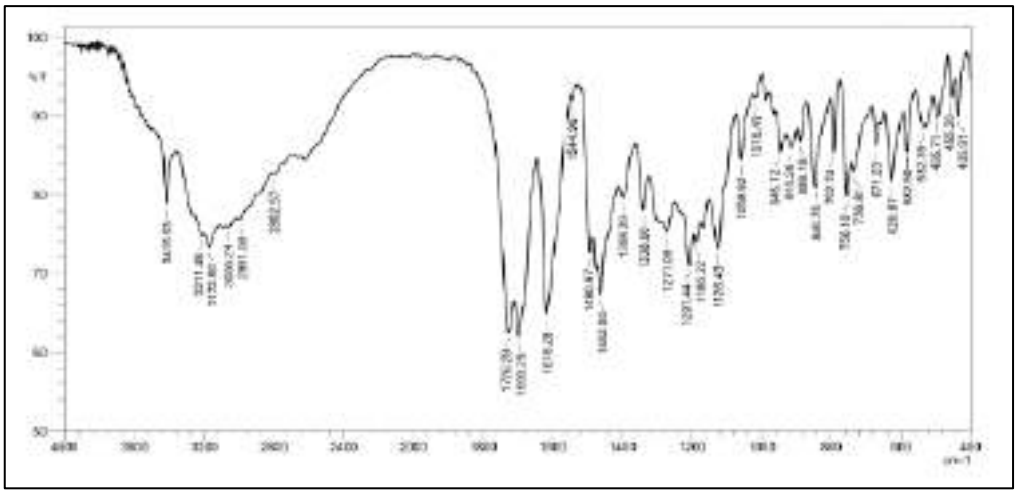


Figure (4- 223): FTIR spectrum of copolymer (33) (MAA-CO-IAN) with compound(33).

^{1}HNMR spectrum of copolymer (33) (MAA-CO-IAN) with compound(33).

^{1}HNMR spectrum of copolymer (33) (MAA-CO-IAN) with compound(33) in (fig.4-224) singles at (6.5-8.3 δ ppm) to (4H, phenyl ring), multiple singlate at (3.3) to –NH, multiple singlate at (4.3) to –NH(amide), singles at 2.5 ppm to CH_2**,** single at 1.0-1.3 ppm to CH_3**,** singles at 11.3 ppm to OH (COOH). (151-153)

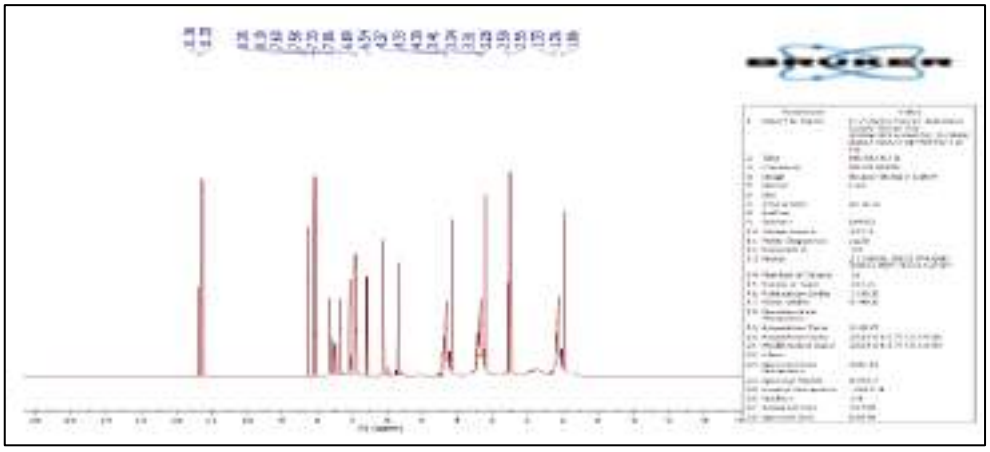


Figure (4- 224): ^{1}HNMR spectrum of copolymer(33) (MAA-CO-IAN) with compound(33).

^{13}C-NMR spectrum of copolymer(33) (MAA-CO-IAN) with compound(33). The signals of olefinic and aromatic carbons appear in the third region between 112 and 130 ppm, single related to C-N at 56 ppm, singles related to C=O (amide) at 166 ppm, singles related to C=S at 195-205 ppm, singles related to C=O (acid) at 173 ppm, singles related to CH_3 at 18 ppm, single related to C=N at 150 ppm. (151-153)

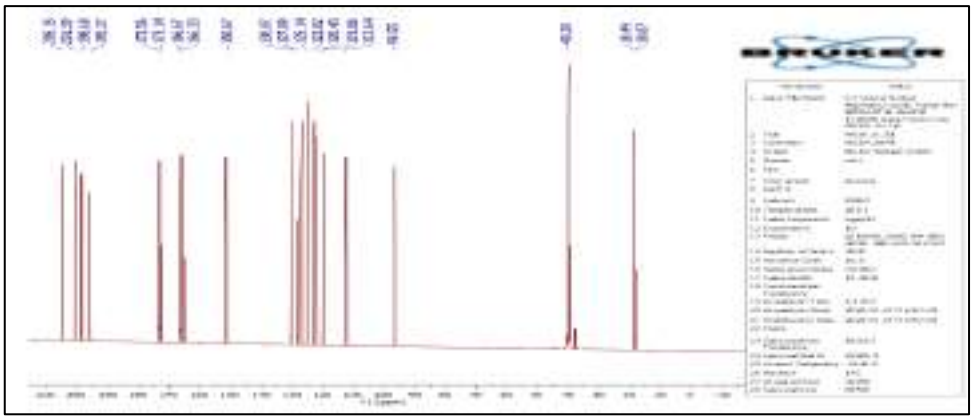
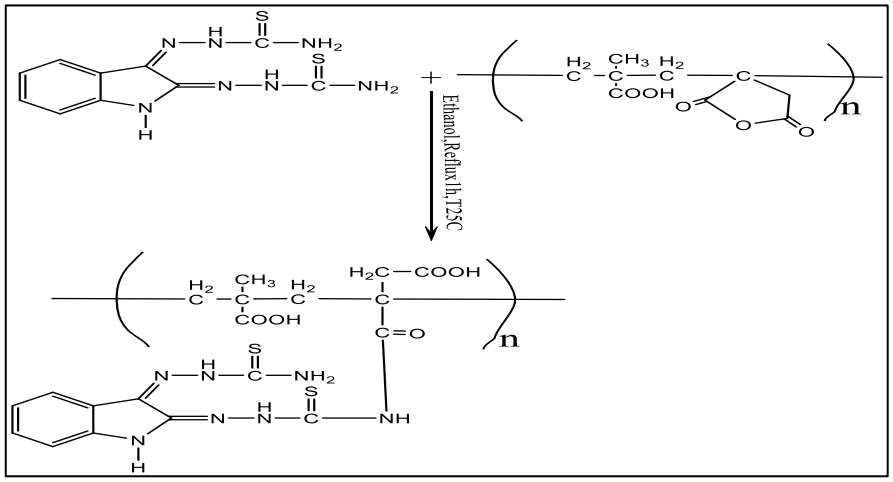


Figure (4- 225): ^{13}C-NMR spectrum of copolymer(33) (MAA-CO-IAN) with compound(33).

4.26 *Synthesis* of copolymer(34)(MAA-CO-IAN) with compound (34).



Scheme (4-81): synthesis of copolymer(34) (MAA-CO-IAN) with compound (34).

FTIR spectrum of copolymer(34) (MAA-CO-IAN) with compound (34).

The FTIR spectrum of copolymer (34) (MAA-CO-IAN) with compound (34) as shown in (fig.4-226) which indicates absorption band at 3367 Cm^{-1} to –OH and 3261 Cm^{-1} to–NH, absorption band at 3176 Cm^{-1} to C-H (aromatic), absorption band at 2997 Cm^{-1} to C-H (aliphatic), absorption band at 1284 Cm^{-1} to C=S, absorption band at 1531 Cm^{-1} to C=C (phenyl ring), absorption band at 1001 Cm^{-1} to C-N, absorption band at 1165 Cm^{-1} to C-O , absorption band at 1699 Cm^{-1} to C=O(acid), absorption band at 1645 Cm^{-1} to C=O(amide), absorption band at 1618 Cm^{-1} to C=N, absorption band at 1396 Cm^{-1} to CH_3. (151-153)

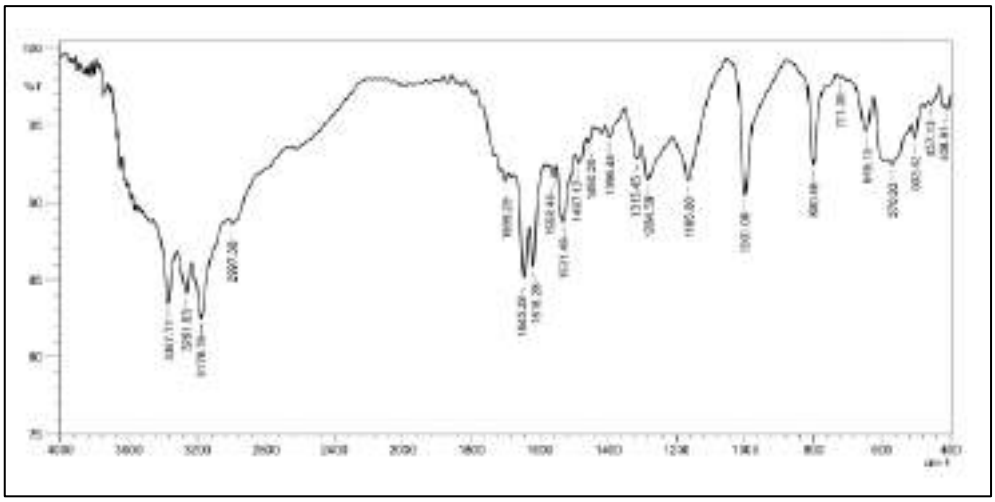


Figure (4- 226): FTIR spectrum of copolymer(34) (MAA-CO-IAN) with compound (34).

^{1}HNMR spectrum of copolymer (34) (MAA-CO-IAN) with compound (34).

^{1}HNMR spectrum of copolymer(34) (MAA-CO-IAN) with compound (34) in (fig.4-227) singles at (7.2-8.7 δ ppm) to (4H, phenyl ring), multiple singlate at (3.3) to –NH, multiple singlate at (4.5) to –NH(amide), singles at 2.3 ppm to CH_2**,** single at 1.0 ppm to CH_3**,** singles at 8.7 ppm to OH (COOH.(151-153)

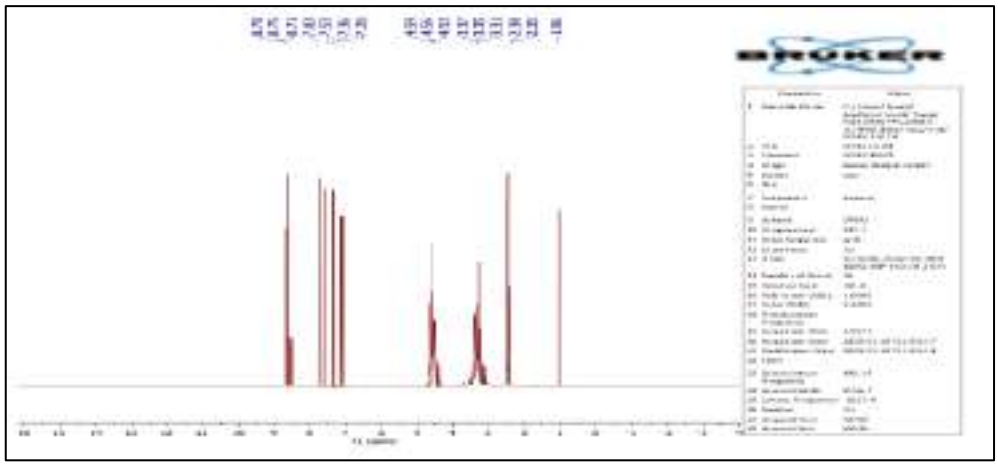


Figure (4- 227): ^{1}HNMR spectrum of copolymer (34) (MAA-CO-IAN) with compound (34).

^{13}C-NMR spectrum of copolymer(34) (MAA-CO-IAN) with compound (34).

The signals of olefinic and aromatic carbons appear in the third region between 117 and 127ppm, single related to C-N at 56 ppm, singles related to C=O (amide) at 164 ppm, singles related to C=S at 195-210 ppm, singles related to C=O (acid) at 173 ppm, singles related to CH_3 at 18 ppm, single related to C=N at 141 ppm. (151-153)

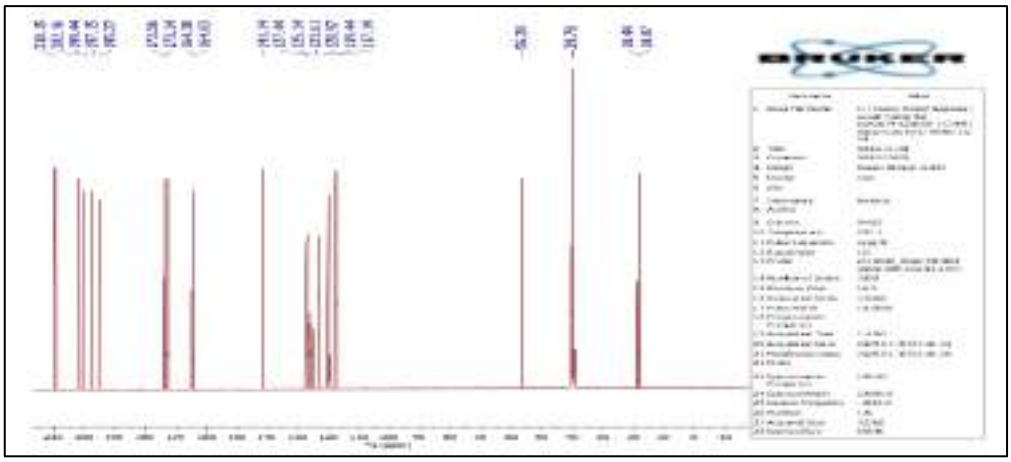
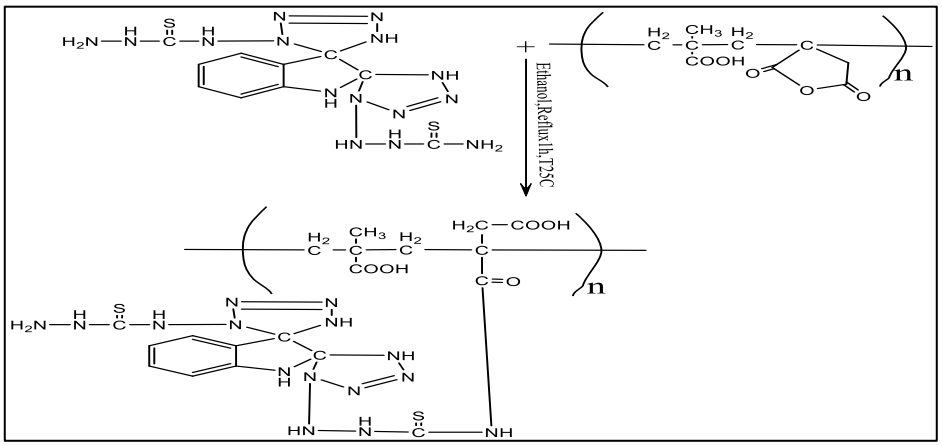


Figure (4- 228): ^{13}C-NMR spectrum of copolymer(34) (MAA-CO-IAN) with compound (34).

4.27 *Synthesis* of copolymer(35)(MAA-CO-IAN) with compound (35).



Scheme (4-82): synthesis of copolymer(35) (MAA-CO-IAN) with compound (35).

FTIR spectrum of copolymer (35) (MAA-CO-IAN) with compound (35).

The FTIR spectrum of copolymer (35) (MAA-CO-IAN) with compound (35) as shown in (fig.4-229) which indicates absorption band at 3415 Cm^{-1} to –OH and 3213 Cm^{-1} to–NH, absorption band at 3174 Cm^{-1} to C-H (aromatic), absorption band at 2987 Cm^{-1} to C-H (aliphatic), absorption band at 1290 Cm^{-1} to C=S, absorption band at 1462 Cm^{-1} to C=C (phenyl ring), absorption band at 1056 Cm^{-1} to C-N, absorption band at 1056 Cm^{-1} to C-O , absorption band at 1728 Cm^{-1} to C=O(acid), absorption band at 1695 Cm^{-1} to C=O (amide), absorption band at 1618 Cm^{-1} to C=N, absorption band at 1396 Cm^{-1} to CH_3, absorption band at 1492 Cm^{-1} to N=N. (151-153)

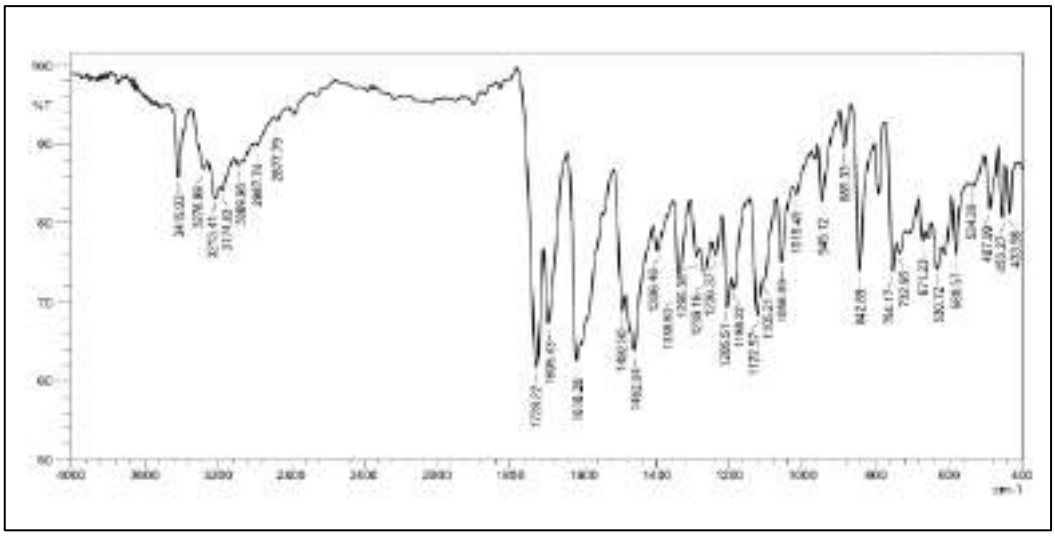


Figure (4- 229): FTIR spectrum of copolymer(35) (MAA-CO-IAN) with compound (35).

^{1}HNMR spectrum of copolymer(35) (MAA-CO-IAN) with compound (35). ^{1}HNMR spectrum of copolymer(35) (MAA-CO-IAN) with compound (35) in (fig.4-230) singles at (6.5-8.3 δ ppm) to (4H, phenyl ring), multiple singlate at (3.3) to –NH, multiple singlate at (5.2-5.6) to –NH(amide), singlate at 2.5 ppm to CH_2**,** single at 1.0-1.1 ppm to CH_3**,** singles at 11.3 ppm to OH (COOH). (151-153)

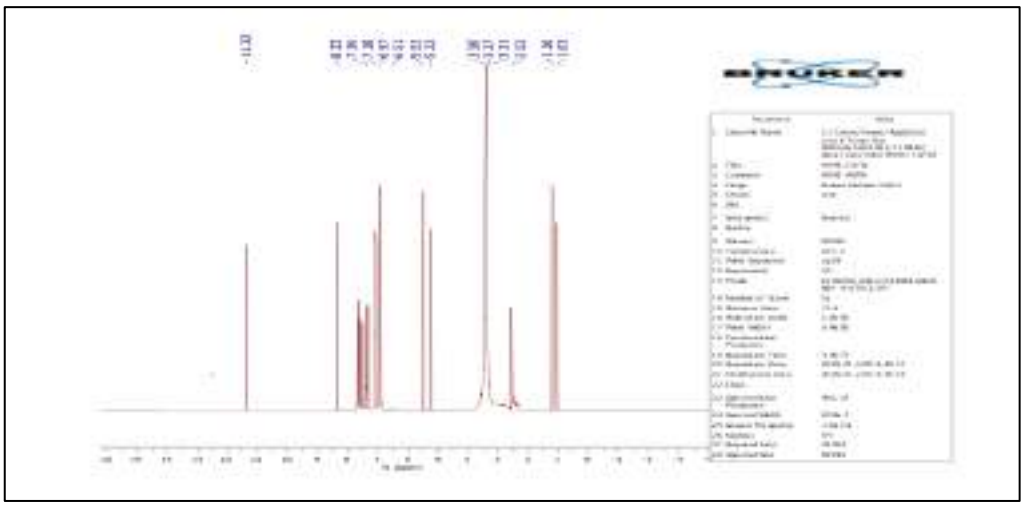


Figure (4- 230): ^{1}HNMR spectrum of copolymer(35) (MAA-CO-IAN) with compound (35).

^{13}C-NMR spectrum of copolymer(35) (MAA-CO-IAN) with compound (35). The signals of olefinic and aromatic carbons appear in the third region between 111 and 134 ppm, single related to C-N at 56 ppm, singles related to C=O (amide) at 164 ppm, singles related to C=S at 200-205 ppm, singles related to C=O (acid) at 180 ppm, singles related to CH_3 at 18 ppm, single related to C=N at 143 ppm. (151-153)

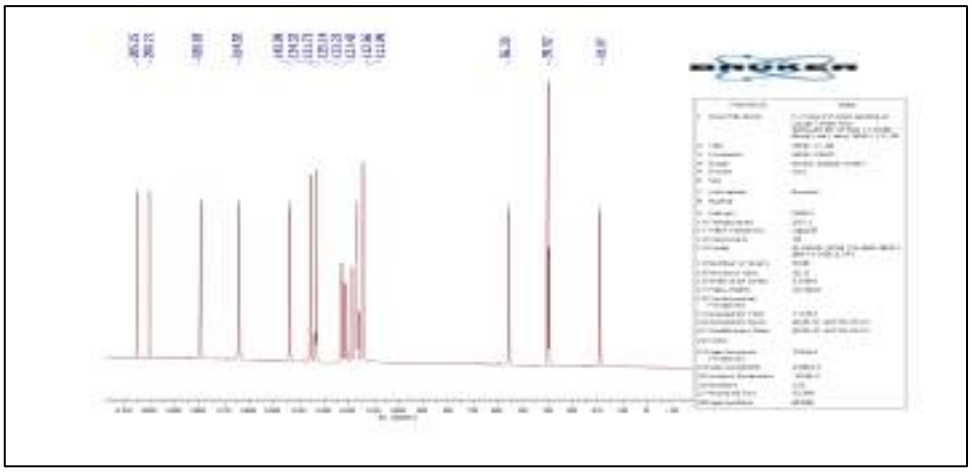
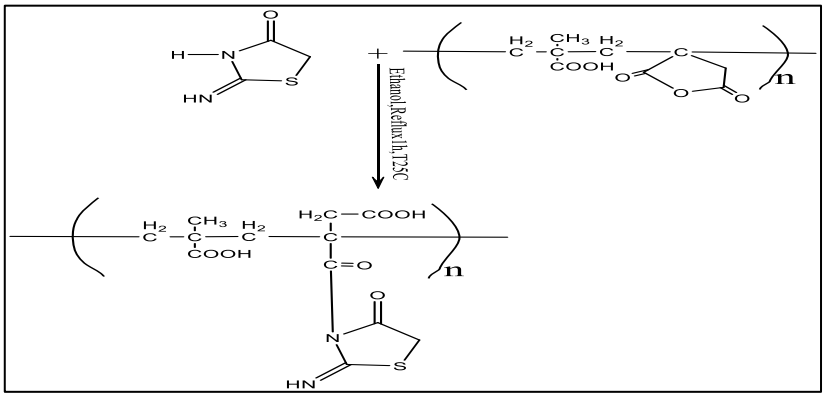


Figure (4- 231): ^{13}C-NMR spectrum of copolymer (35) (MAA-CO-IAN) with compound (35).

4.28 Synthesis of copolymer(36) (MAA-CO-IAN) with compound (36).



Scheme (4-83): synthesis of copolymer(36) (MAA-CO-IAN) with compound (36).

FTIR spectrum of copolymer (MAA-CO-IAN) with compound (36).

The FTIR spectrum of copolymer(36) (MAA-CO-IAN) with compound (36) in (fig.4-232) which indicates absorption bands at 3410 Cm^{-1} to OH and 3236 cm^{-1} to –NH stretching, absorption band at 3174 Cm^{-1} to C-H (aromatic), absorption band at 2978 cm^{-1} to C-H (aliphatic), absorption band at 1570 cm^{-1} to C=N, absorption band at 613 Cm^{-1} to C-S, absorption band at 1481 Cm^{-1} to C=C (aromatic), absorption band at 1271 Cm^{-1} to C-N, absorption band at 1708 Cm^{-1} to C=O (acid), absorption band at 1637 Cm^{-1} to C=O(amide), absorption band at 1334 Cm^{-1} to CH_3**,** absorption band at 1186 Cm^{-1} to C-O. (151-153)

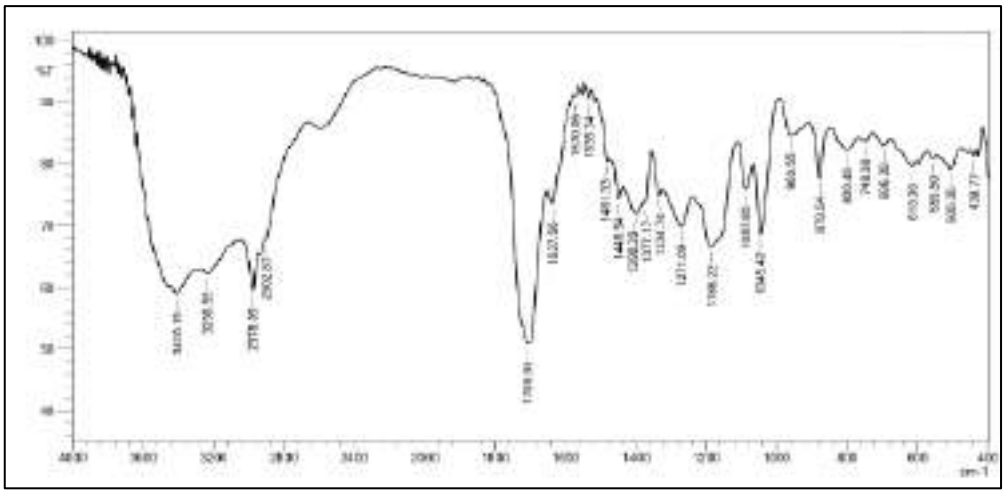


Figure (4- 232): FTIR spectrum of copolymer(36) (MAA-CO-IAN) with compound (36).

^{1}HNMR spectrum of copolymer(36) (MAA-CO-IAN) with compound (36).

^{1}HNMR spectrum of copolymer(36) (MAA-CO-IAN) with compound (36) in (fig.4-233) singles at (3.3) to –NH, singles at (4.1-5.6) to –NH(amide), singlate at 2.5 ppm to CH_2**,** singlate at 1.0 ppm to CH_3**,** singles at 11.3 ppm to OH (COOH). (151-153)

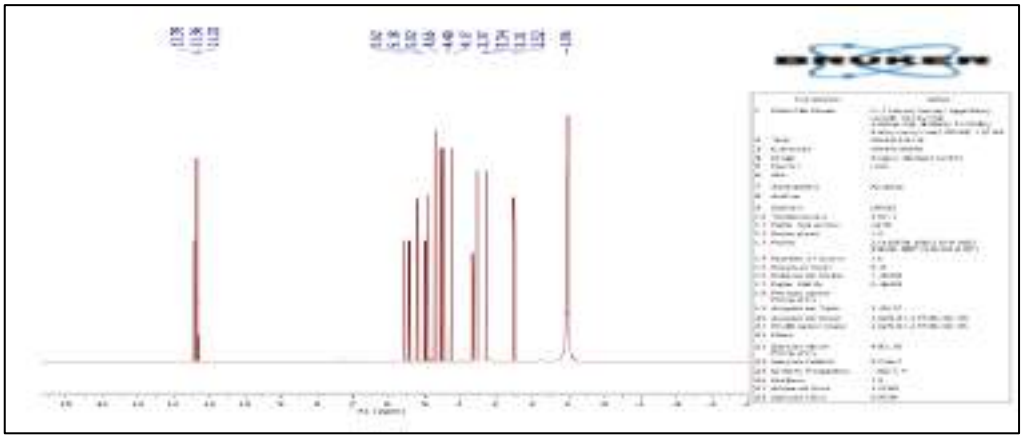


Figure (4- 233): ^{1}HNMR spectrum of copolymer(36) (MAA-CO-IAN) with compound (36).

^{13}C-NMR spectrum of copolymer(36) (MAA-CO-IAN) with compound (36).

Single related to C=N at 156 ppm, single related to C-N at 63 ppm, single related to C-S at 56 ppm, single relates to C=O (amide) at 174 ppm, single relates to C=O (acid) at 183 ppm, single related to CH_3 18 ppm. (151-153)

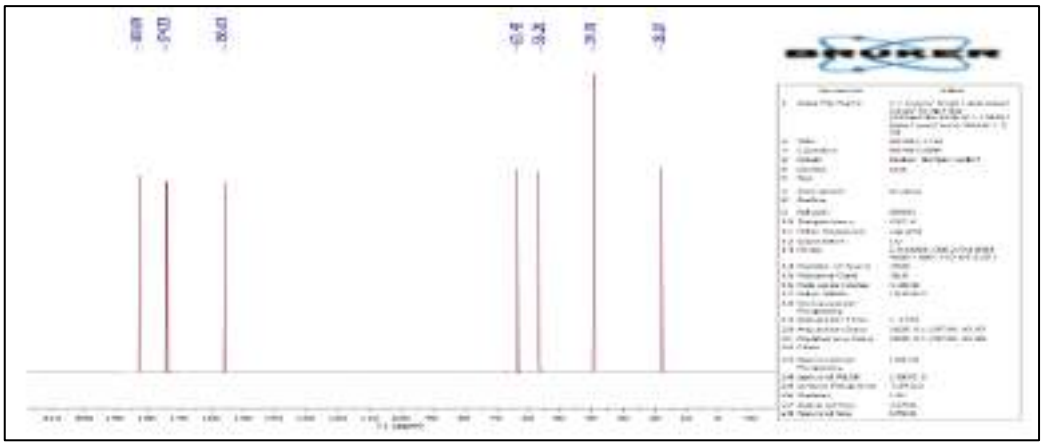
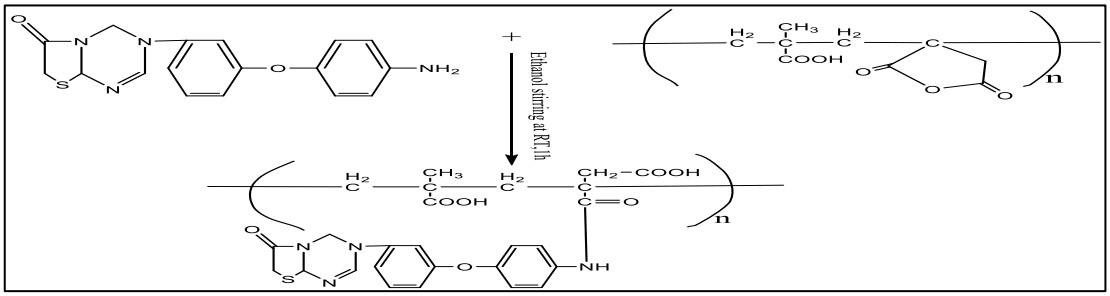


Figure (4- 234):^{13}C-NMR spectrum of copolymer(36)(MAA-CO-IAN) with compound (36).

4.29 Synthesis of copolymer (MAA-CO-IAN) with Compounds (37-40).



4.29.1Synthesis of copolymer(37) (MAA-CO-IAN) with compound(37).

Scheme (4-84): synthesis of copolymer(37) (MAA-CO-IAN) with compound(37).

FTIR spectrum of copolymer(37) (MAA-CO-IAN) with compound(37).

The FTIR spectrum of copolymer(37) (MAA-CO-IAN) with compound(37) as shown in (fig.4-235) which indicates absorption bands at 3415Cm^{-1} to OH overlapping with –NH stretching, absorption band at 3174 Cm^{-1} to C-H (aromatic), absorption band at 2954 cm^{-1} to C-H (aliphatic), absorption band at 1539 Cm^{-1} to C=N, absorption band at 613 Cm^{-1} to C-S, absorption band at 1510 Cm^{-1} to C=C (aromatic), absorption band at 1255 Cm^{-1} to C-N, absorption band at 1676 Cm^{-1} to C=O (acid), absorption band at 1643 Cm^{-1} to C=O(amide), absorption band at 1361Cm^{-1} to CH_3**,** absorption band at 1172 Cm^{-1} to C-O. (151-153)

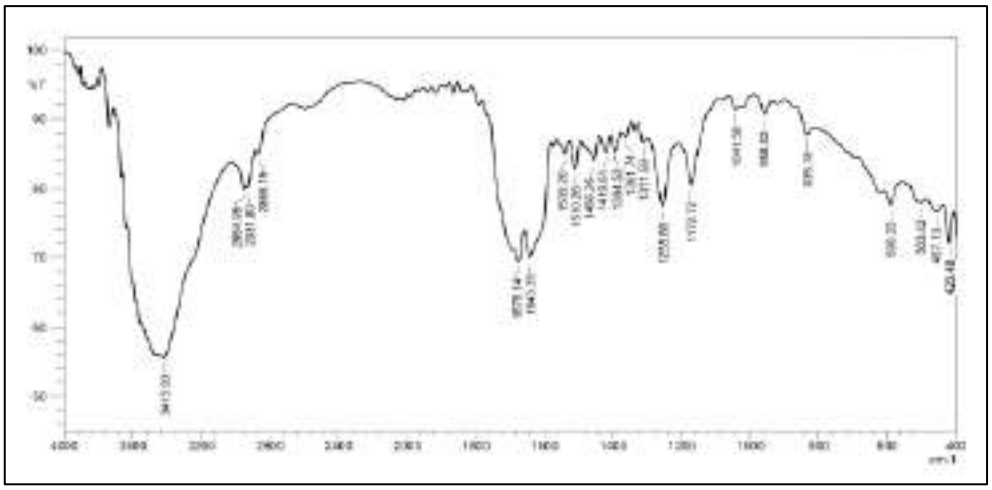


Figure (4- 235): FTIR spectrum of copolymer(37) (MAA-CO-IAN) with compound(37).

^{1}HNMR spectrum of copolymer(37) (MAA-CO-IAN) with compound(37).

^{1}HNMR spectrum of copolymer(37) (MAA-CO-IAN) with compound(37) in (fig.4-236) singles at (6.5-8.3 δ ppm) to (4H, phenyl ring), multiple singlate at (3.2) to –NH, singlate at (4.5) to –NH(amide), singlate at 2.5 ppm to CH_2**,** single at 0.9 ppm to CH_3**,** singles at 11.3 ppm to OH (COOH). (151-153)

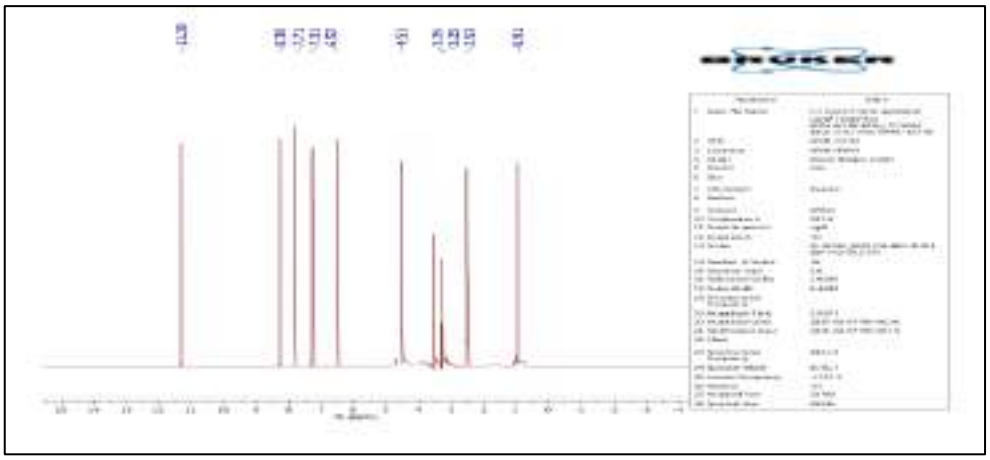


Figure (4- 236): ^{1}HNMR spectrum of copolymer(37) (MAA-CO-IAN) with compound(37).

Figure (9)

^{13}C-NMR spectrum of copolymer(37) (MAA-CO-IAN) with compound(37). The signals of olefinic and aromatic carbons appear in the third region between 128 and 135 ppm, single related to C=N at 156 ppm, single related to C-N at 63 ppm, single related to C-S at 56 ppm, single relates to C=O (amide) at166- 174 ppm, single relates to C=O (acid) at 182 ppm, single related to CH_3 18 ppm. (151-153)

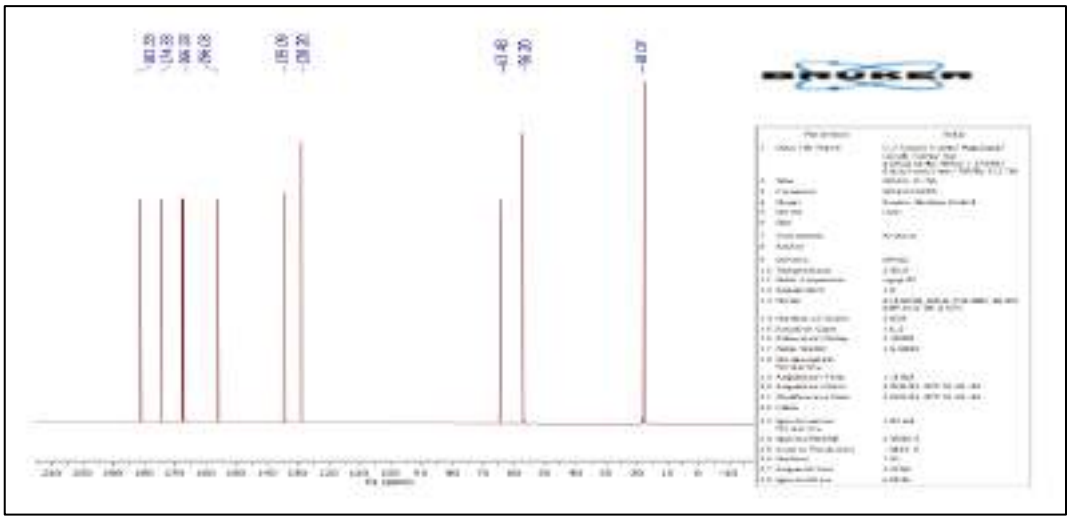
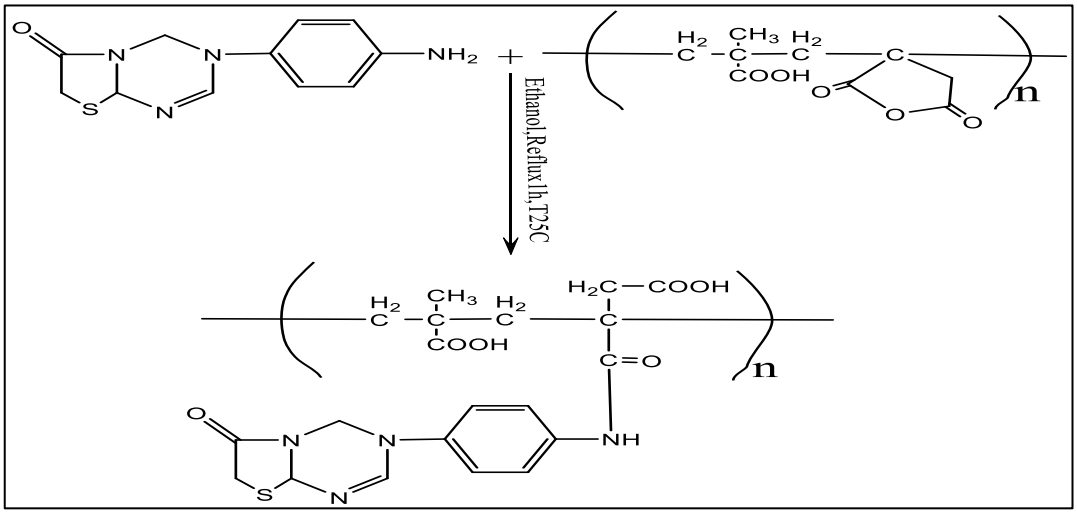


Figure (4- 237): ^{13}C-NMR spectrum of copolymer(37) (MAA-CO-IAN) with compound(37).

4.29.2 Synthesis of copolymer(38) (MAA-CO-IAN) with compound(38).



Scheme (4-85): synthesis of copolymer(38) (MAA-CO-IAN) with compound(38).

FTIR spectrum of copolymer(38) (MAA-CO-IAN) with compound(38).]

The FTIR spectrum of copolymer(38) (MAA-CO-IAN) with compound(38) as shown in (fig.4-238) which indicates absorption bands at 3414Cm^{-1} to OH and 3238 Cm^{-1} to –NH stretching, absorption band at 3114 Cm^{-1} to C-H (aromatic), absorption band at 2976 cm^{-1} to C-H (aliphatic), absorption band at 1539 Cm^{-1} to C=N, absorption band at 617 Cm^{-1} to C-S, absorption band at 1510 Cm^{-1} to C=C (aromatic), absorption band at 1269 Cm^{-1} to C-N, absorption band at 1712 Cm^{-1} to C=O (acid), absorption band at 1639 Cm^{-1} to C=O(amide), absorption band at 1392Cm^{-1} to CH_3**,** absorption band at 1186 Cm^{-1} to C-O. (151-153)

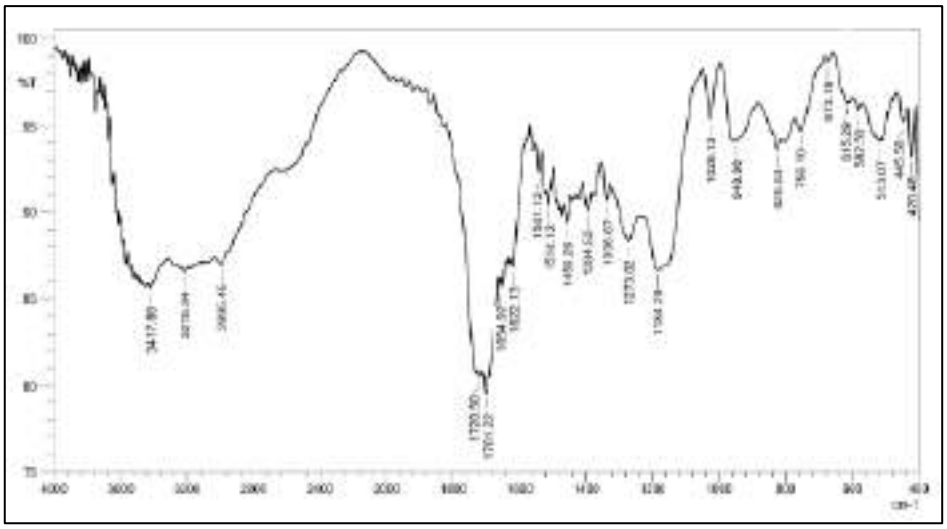


Figure (4- 238): FTIR spectrum of copolymer(38) (MAA-CO-IAN) with compound(38).

^{1}HNMR spectrum of copolymer(38) (MAA-CO-IAN) with compound(38).

^{1}HNMR spectrum of copolymer(38) (MAA-CO-IAN) with compound(38) in (fig.4-239) singles at (6.5-8.3 δ ppm) to (4H, phenyl ring), multiple singlate at (3.2) to –NH, singlate at (4.5) to –NH(amide), singlate at 2.5 ppm to CH_2**,** single at 0.9 ppm to CH_3**,** singles at 11.3 ppm to OH (COOH). (151-153)

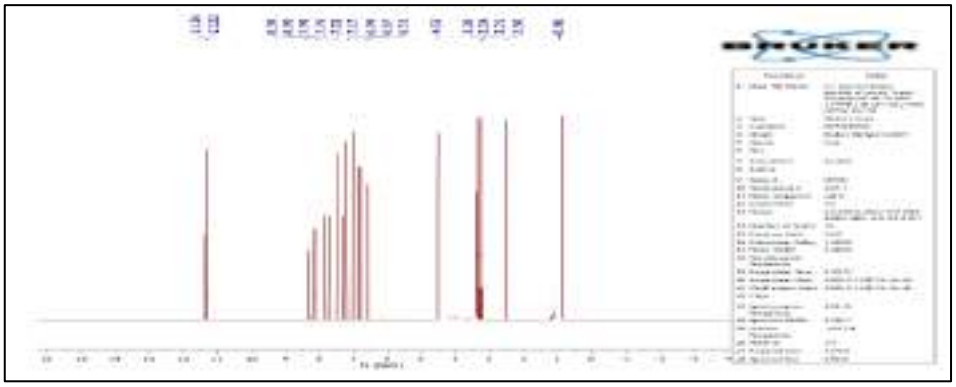


Figure (4- 239): ^{1}HNMR spectrum of copolymer(38) (MAA-CO-IAN) with compound(38).

^{13}C-NMR spectrum of copolymer(38) (MAA-CO-IAN) with compound(38).

The signals of olefinic and aromatic carbons appear in the third region between 126 and 135 ppm, single related to C=N at 156 ppm, single related to C-N at 63 ppm, single related to C-S at 56 ppm, single relates to C=O (amide) at166- 174 ppm, single relates to C=O (acid) at 182 ppm, single related to CH_3 18 ppm. (151-153)

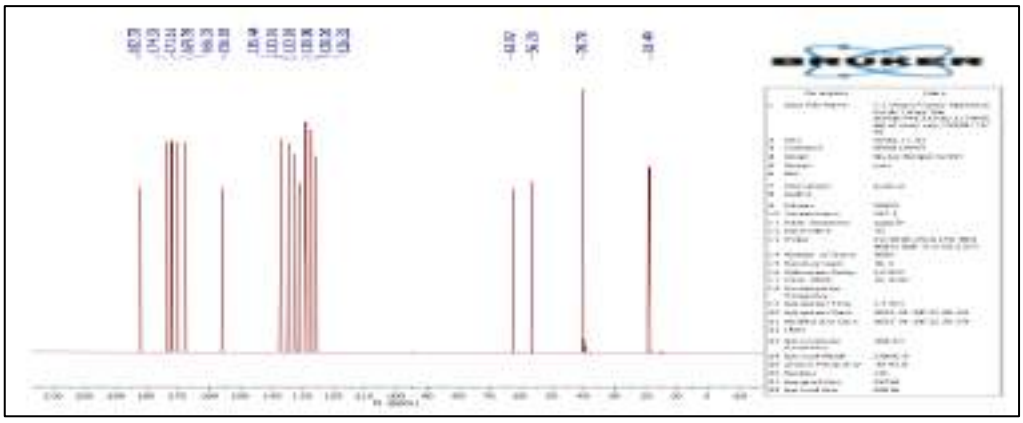
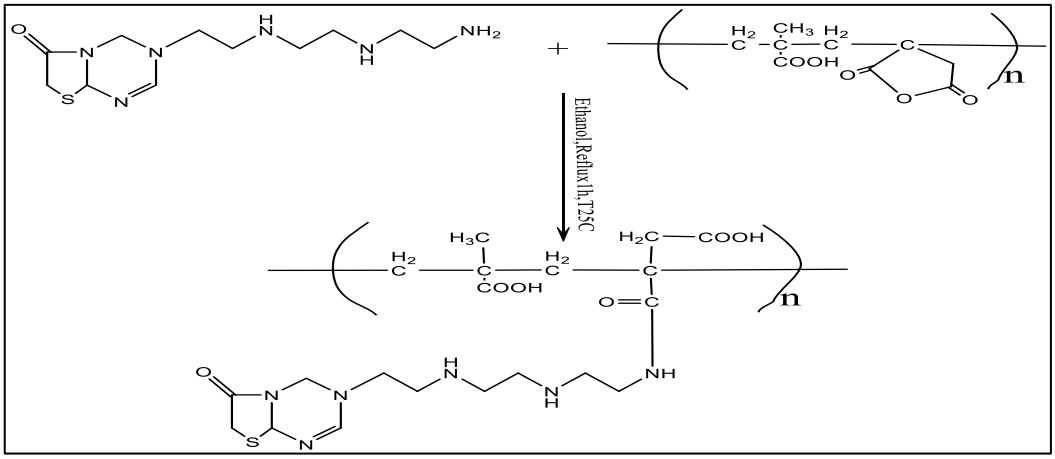


Figure (4- 240): ^{13}C-NMR spectrum of copolymer(38) (MAA-CO-IAN) with compound(38).

4.29.3 Synthesis of copolymer(39) (MAA-CO-IAN) with compound(39).



Scheme (4-86): synthesis of copolymer(39) (MAA-CO-IAN) with compound(39).

FTIR spectrum of copolymer(39) (MAA-CO-IAN) with compound(39).

The FTIR spectrum of copolymer(39) (MAA-CO-IAN) with compound(39) as shown in (fig.4-241) which indicates absorption bands at 3412 Cm^{-1} to OH overlapping with –NH stretching, absorption band at 3117 Cm^{-1} to C-H (aromatic), absorption band at 2974 cm^{-1} to C-H (aliphatic), absorption band at 1660 Cm^{-1} to C=N, absorption band at 624 Cm^{-1} to C-S, absorption band at 1539 Cm^{-1} to C=C (aromatic), absorption band at 1259 Cm^{-1} to C-N, absorption band at 1712 Cm^{-1} to C=O (acid), absorption band at 1643 Cm^{-1} to C=O(amide), absorption band at 1390 Cm^{-1} to CH_3, absorption band at 1087 Cm^{-1} to C-O. (151-153)

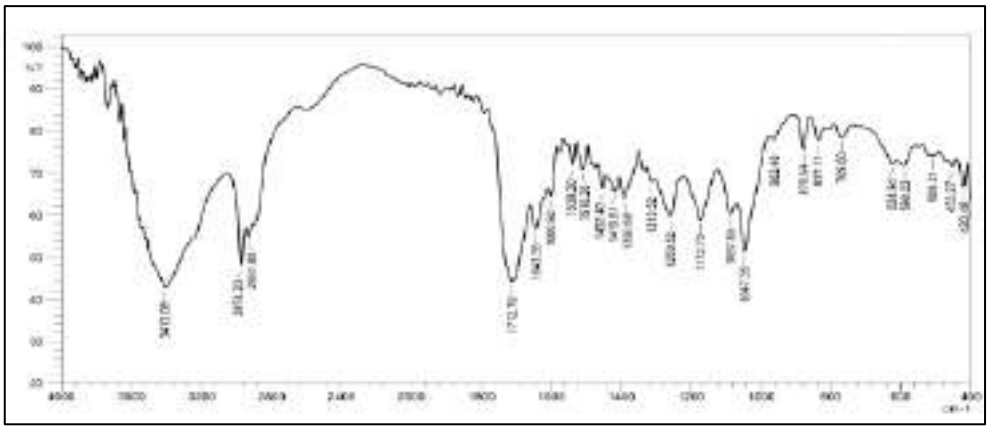


Figure (4- 241): FTIR spectrum of copolymer(39) (MAA-CO-IAN) with compound(39).

^{1}HNMR spectrumof copolymer(39) (MAA-CO-IAN) with compound(39).

^{1}HNMR spectrum of copolymer(39) (MAA-CO-IAN) with compound(39) in (fig.4-242) singles at (6.5-8.3 δ ppm) to (4H, phenyl ring), multiple singlate at (3.2) to –NH, singlate at (4.5) to –NH(amide), singlate at 2.5 ppm to CH_2**,** single at 0.9 ppm to CH_3**,** singles at 11.3 ppm to OH (COOH). (151-153)

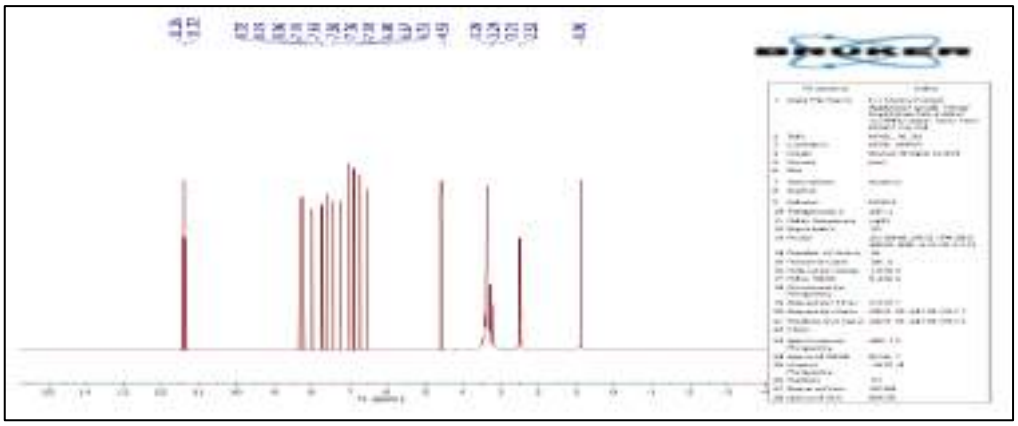


Figure (4- 242): ^{1}HNMR spectrum of copolymer(39) (MAA-CO-IAN) with compound(39).

^{13}C-NMR spectrum of copolymer(39) (MAA-CO-IAN) with compound(39).

The signals of olefinic and aromatic carbons appear in the third region between 126 and 135 ppm, single related to C=N at 156 ppm, single related to C-N at 63 ppm, single related to C-S at 56 ppm, single relates to C=O (amide) at166- 174 ppm, single relates to C=O (acid) at 182 ppm, single related to CH_3 18 ppm. (151-153)

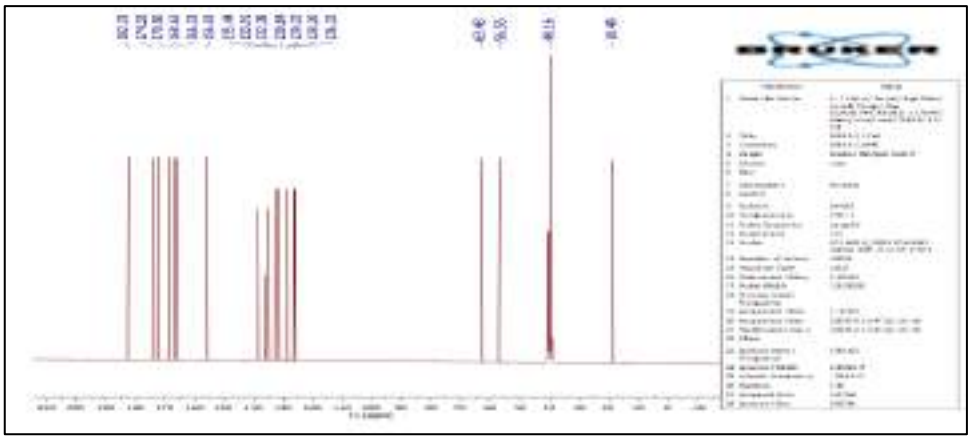
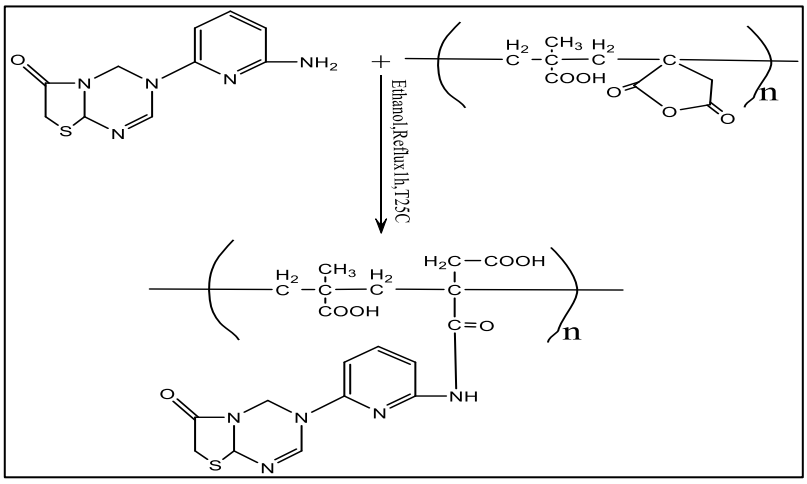


Figure (4- 243): ^{13}C-NMR spectrum of copolymer(39) (MAA-CO-IAN) with compound(39).

4.29.4 Synthesis of copolymer(40) (MAA-CO-IAN) with compound(40).



Scheme (4-87): synthesis of copolymer(40) (MAA-CO-IAN) with compound(40).

FTIR spectrum of copolymer(40) (MAA-CO-IAN) with compound(40).

The FTIR spectrum of copolymer(40) (MAA-CO-IAN) with compound(40) as shown in (fig.4-244) which indicates absorption bands at 3437 Cm^{-1} to OH overlapping with –NH stretching, absorption band at 3117 Cm^{-1} to C-H (aromatic), absorption band at 2974 cm^{-1} to C-H (aliphatic), absorption band at 1660 Cm^{-1} to C=N, absorption band at 624 Cm^{-1} to C-S, absorption band at 1539 Cm^{-1} to C=C (aromatic), absorption band at 1259 Cm^{-1} to C-N, absorption band at 1712 Cm^{-1} to C=O (acid), absorption band at 1643 Cm^{-1} to C=O(amide), absorption band at 1390 Cm^{-1} to CH_3, absorption band at 1087 Cm^{-1} to C-O. (151-153)

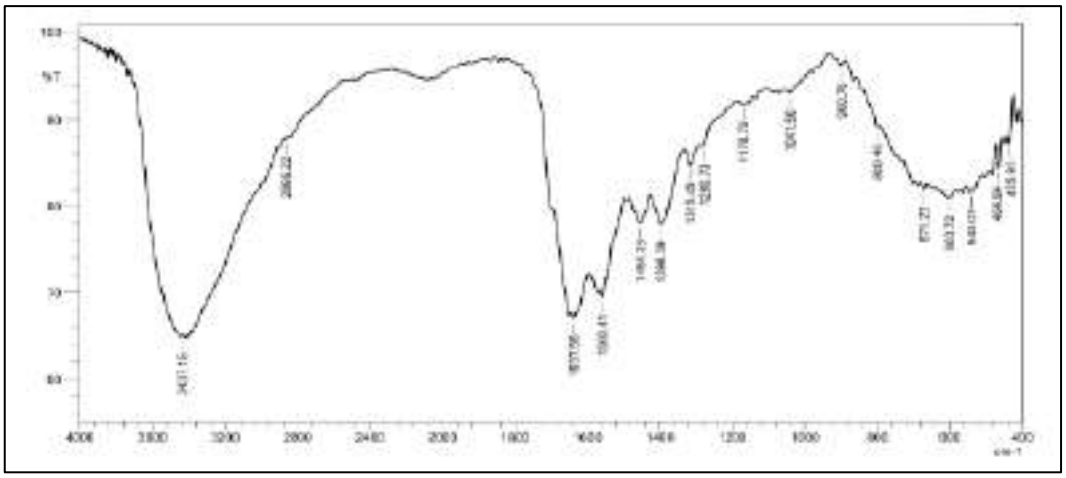


Figure (4- 244): FTIR spectrum of copolymer(40) (MAA-CO-IAN) with compound(40).

^{1}HNMR spectrum of copolymer(40) (MAA-CO-IAN) with compound(40).

^{1}HNMR spectrum of copolymer(40) (MAA-CO-IAN) with compound(40) in (fig.4-245) singles at (3.2-3.4 ppm) to $–NH_2$, singles at (2.5 δ ppm) to CH_2**,** singles at (6.2-7.5 ppm) to (3H heterophony ring). (151-153)

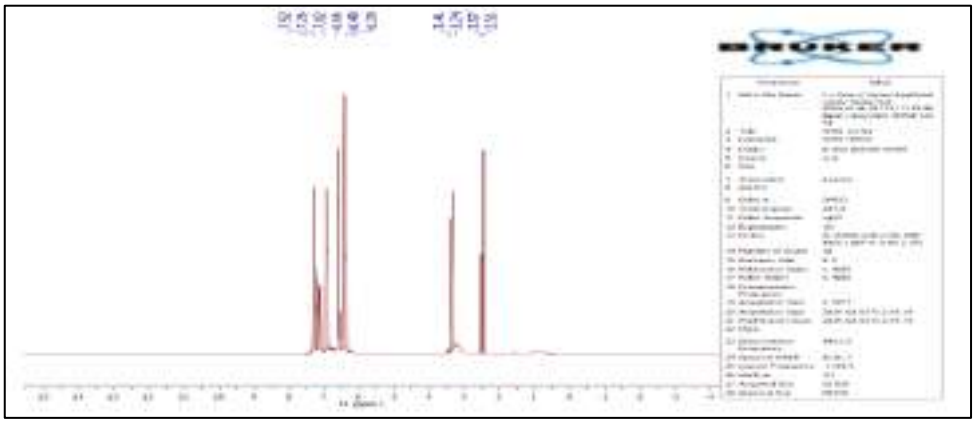


Figure (4- 245): ^{1}HNMR spectrum of copolymer(40) (MAA-CO-IAN) with compound(40).

^{13}C-NMR spectrum of copolymer(40) (MAA-CO-IAN) with compound(40).

Single related to C=N at 148 ppm, single related to C-N at 82-84 ppm, single related to C-S at 55 ppm, single related to C=O at 168 ppm. Pavia, L.D., Lampman, L.G., Kris, S.G., Vyvyan, R.J.(2009). Introduction to Spectrophotometer. 4 th.book cole general learning.(151-153)

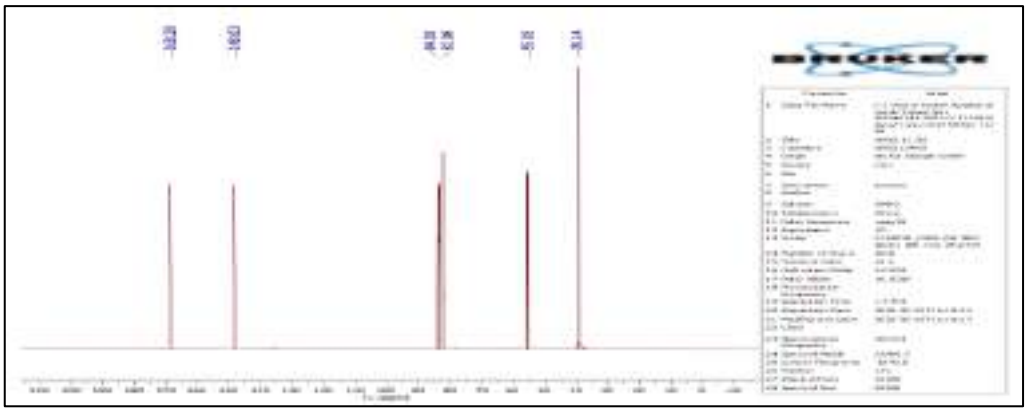
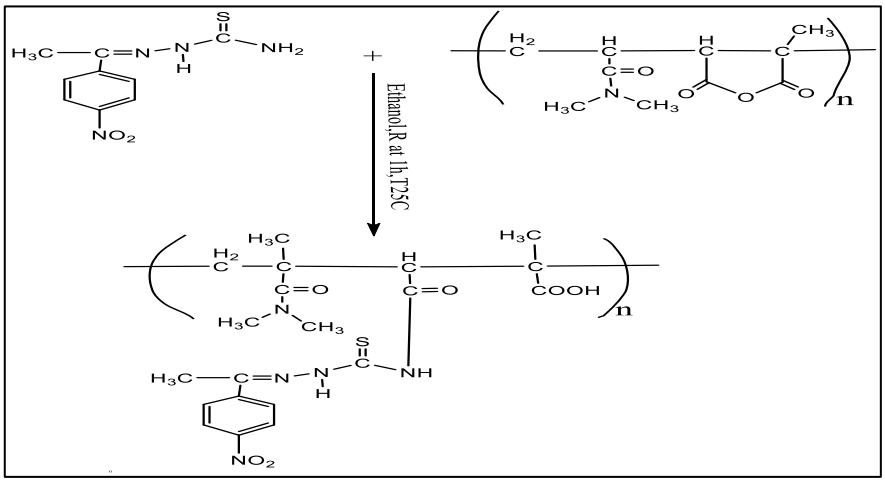


Figure (4- 246): ^{13}C-NMR spectrum of copolymer(40) (MAA-CO-IAN) with compound(40).

4.30 Synthesis of copolymer(41) (DMA-CO-CAN) with compound(3).



Scheme (4-88): synthesis of copolymer(41) (DMA-CO-CAN) with compound(3).

FTIR spectrum of copolymer(41) (DMA-CO-CAN) with compound(3).

The FTIR spectrum of copolymer(41) (DMA-CO-CAN) with compound(3) as shown in (fig.4-247) which indicates absorption bands at 3566 to -OH over lapping with –NH stretching, absorption band at 3197 cm^{-1} to C-H (aromatic), absorption band at 2976 cm-1 to C-H (aliphatic), absorption band at 1539 cm^{-1} to C=N, absorption band at 1045 Cm^{-1} to C=S, absorption band at 1452 Cm^{-1} to C=C (aromatic), absorption band at 1388 Cm^{-1} to NO_2, and absorption band at 1315 Cm^{-1} to CH_3**,** absorption band at 1703 Cm-1 to C=O for carboxylic acid, absorption band at 1641 Cm^{-1} to C=O (amide), absorption band at 1083 Cm^{-1} to C-O. (151-153)

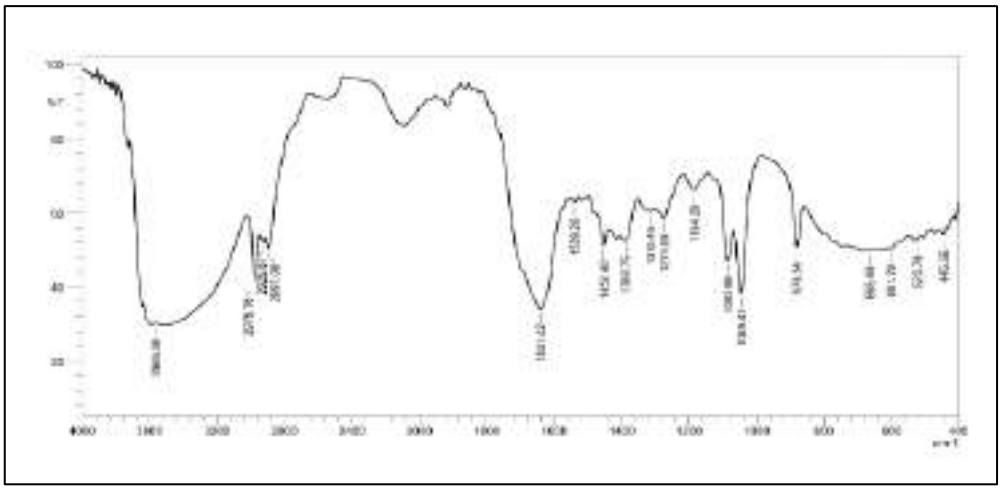


Figure (4- 247): FTIR spectrum of copolymer(41) (DMA-CO-CAN) with compound(3).

^{1}HNMR spectrum of copolymer(41) (DMA-CO-CAN) with compound(3).

^{1}HNMR spectrum of copolymer(41) (DMA-CO-CAN) with compound(3) in (fig. 4-248) singles at (7.3-8.1 δ ppm) to (4H, phenyl ring), singles at (3.3-4.0 ppm) to –NH, singlate at (0.9 ppm) to $–CH_3$, single at (11.7 ppm) to –OH, singles at (2.5 ppm) to $–CH_2$. (151-153)

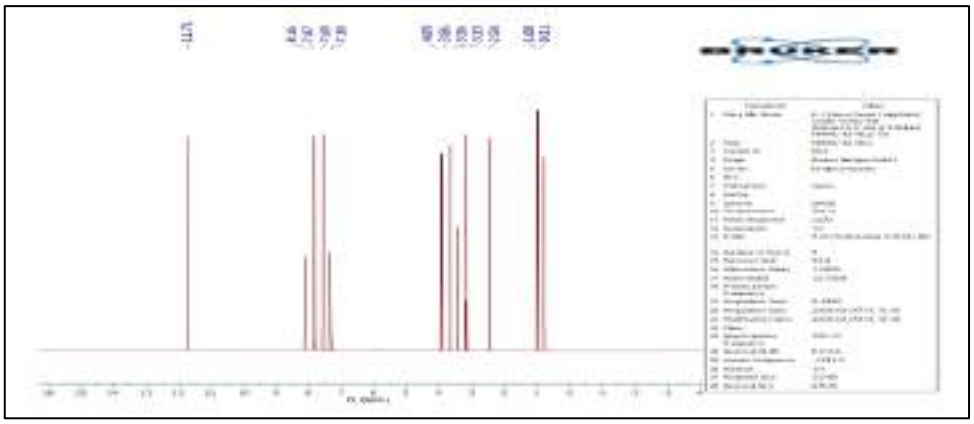


Figure (4- 248): ^{1}HNMR spectrum of copolymer(41) (DMA-CO-CAN) with compound(3).

^{13}C-NMR spectrum of copolymer(41) (DMA-CO-CAN) with compound(3). The signals of olefinic and aromatic carbons appear in the third region between 124 and 133 ppm, singles related to C=N at 143-146 ppm, single related to C-N at 55 ppm, singles related to C=S at 192 ppm, single related to CH_3-C(Secondary) at 18 ppm, single related to CH_3 at 18 ppm, single related to C=O (amide) at 166 ppm, single related to C=O (COOH) at 177ppm. (151-153)

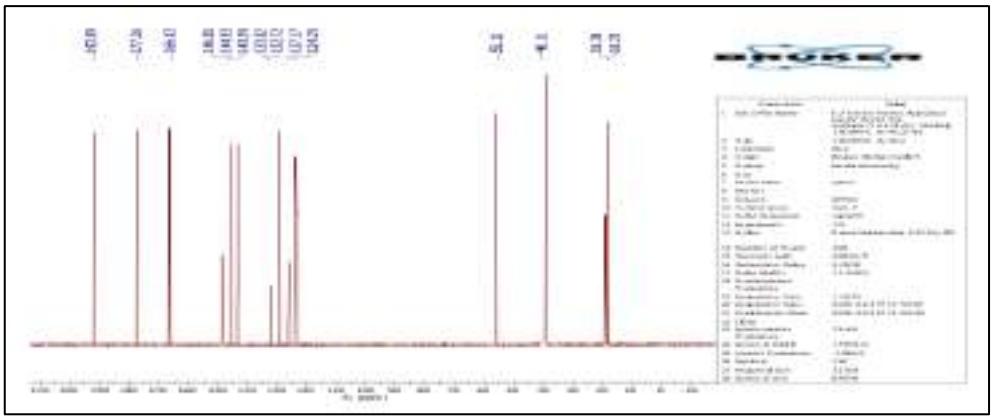
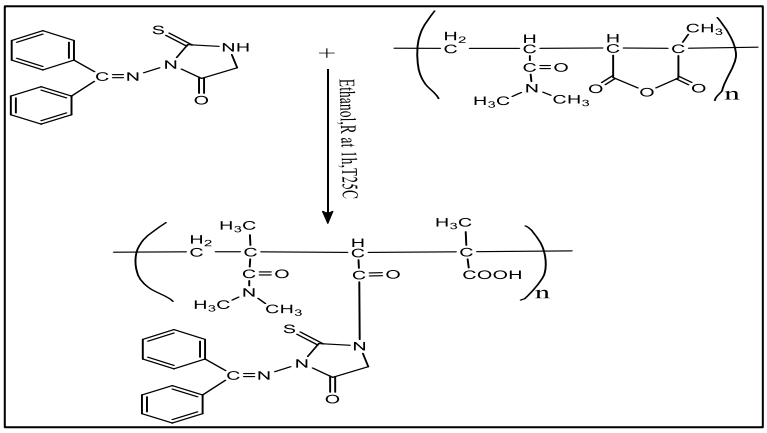


Figure (4- 249): ^{13}C-NMR spectrum of copolymer(41) (DMA-CO-CAN) with compound(3).

4.31 Synthesis of copolymer (DMA-CO-CAN) with compounds (13), (14), (16), (17).

4.31.1 Synthesis of copolymer(42) (DMA-CO-CAN) with compound(13).



Scheme (4-89): synthesis3of copolymer(42) (DMA-CO-CAN) with compound(13).

FTIR spectrum of copolymer(42) (DMA-CO-CAN) with compound(13).

The FTIR spectrum of copolymer(42) (DMA-CO-CAN) with compound(13) as shown in (fig.4-250) which indicates absorption bands at 3437 cm^{-1} to –OH overlapping with –NH stretching, absorption band at 3179 cm^{-1} to C-H (aromatic), absorption band at 2976 cm-1 to C-H (aliphatic), absorption band at 1552 cm^{-1} to C=N, absorption band at 1170 Cm^{-1} to C=S, absorption band at 1450 Cm^{-1} to C=C (aromatic), absorption band at 1710 Cm-1 to C=O for carboxylic acid, absorption band at 1390 Cm-1 to CH_3 , absorption band at 1645 Cm^{-1} to C=O (amide), absorption band at 1085 Cm^{-1} to C-O. (151-153)

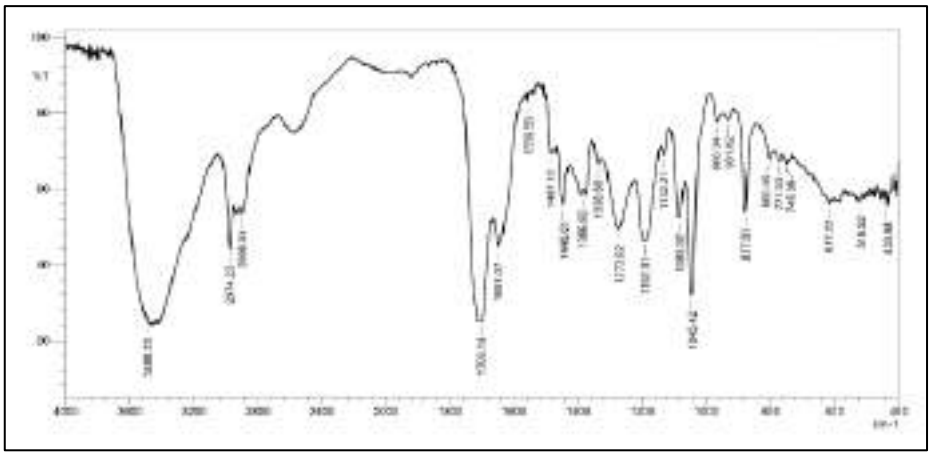


Figure (4- 250): FTIR spectrum of copolymer(42) (DMA-CO-CAN) with compound(13).

^{1}HNMR spectrum of copolymer(42) (DMA-CO-CAN) with compound(13

^{1}HNMR spectrum of copolymer(42) (DMA-CO-CAN) with compound(13) in (fig.4-251) singles at (7.7-8.1 δ ppm) to (10H, phenyl ring), single at (4.0 ppm) to –NH. singles at (1.0 ppm) to $–CH_3$, single at (4.5 ppm) to –NH (amide), single at (1.0 ppm) to $–CH_3$, single at (10 ppm) to –OH (COOH), singles at (2.0-2.5 ppm) to $–CH_2$. (151-153)

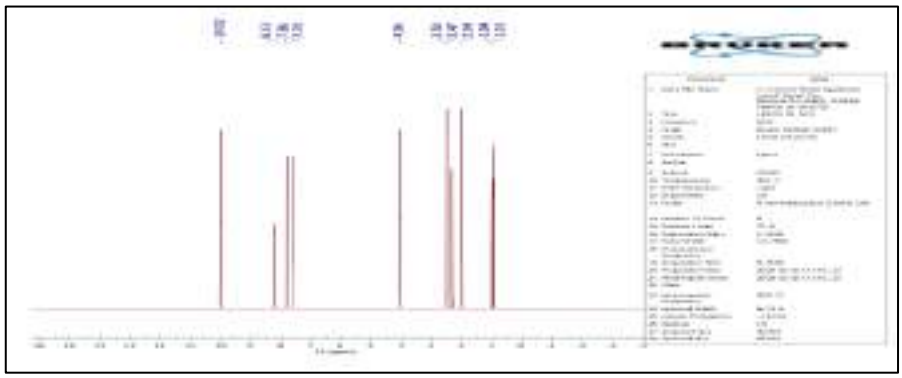


Figure (4- 251): ^{1}HNMR spectrum of copolymer(42) (DMA-CO-CAN) with compound(13).

^{13}C-NMR spectrum of copolymer(42) (DMA-CO-CAN) with compound(13)

The signals of olefinic and aromatic carbons appear in the third region between 115 and 133 ppm, single related to C=N at 150 ppm, single related to C-N at 56 ppm, single related to C=S at 192 ppm, single related to CH_3-C(Secondary) at 18 ppm, single related to C=O (amide) at 166 ppm, single related to C=O (COOH) at 183 ppm. (151-153)

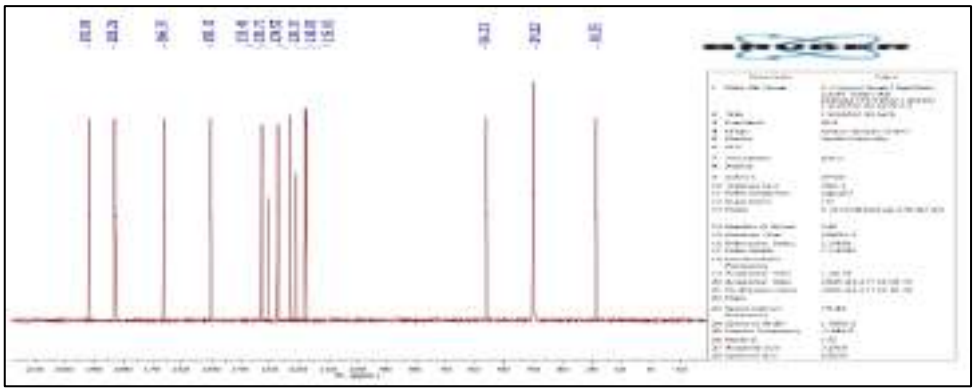
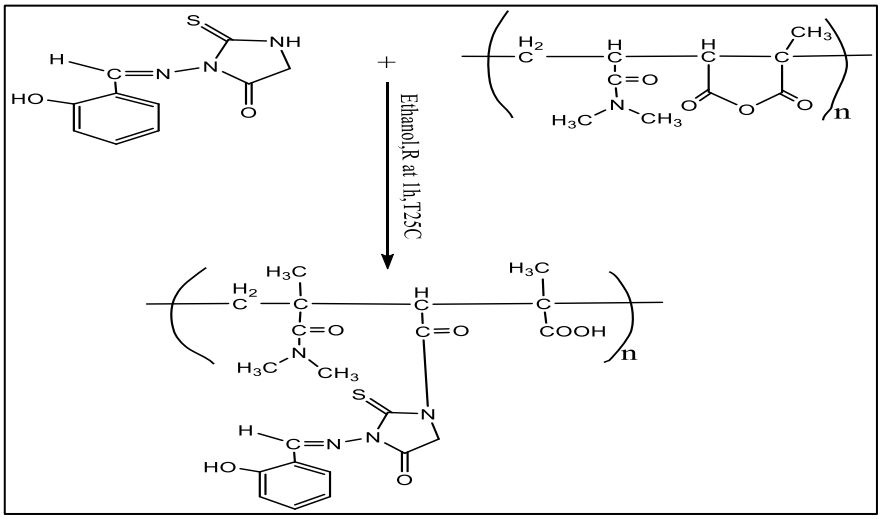


Figure (4- 252): ^{13}C-NMR spectrum of copolymer(42) (DMA-CO-CAN) with compound(13).

4.31.2 Synthesis of copolymer(43) (DMA-CO-CAN) with compound(14).



Scheme (4-90): synthesis of copolymer(43) (DMA-CO-CAN) with compound(14).

FTIR spectrum of copolymer(43) (DMA-CO-CAN) with compound(14).

The FTIR spectrum of copolymer(43) (DMA-CO-CAN) with compound(14) as shown in (fig.4-253*)* which indicates absorption bands at 3431 Cm^{-1} to OH over lapping with –NH stretching, absorption band at 3118 cm^{-1} to C-H (aromatic), absorption band at 2991 cm^{-1} to C-H (aliphatic), absorption band at 1539 cm-1 to C=N, absorption band at 1219 Cm-1 to C=S, absorption band at 1452 Cm^{-1} to C=C (aromatic), absorption band at 1699 Cm^{-1} to C=O for carboxylic acid, absorption band at 1643 Cm^{-1} to C=O (amide), absorption band at 1033 Cm-1 to C-O, absorption band at 1338 Cm-1 to CH_3. (151-153)

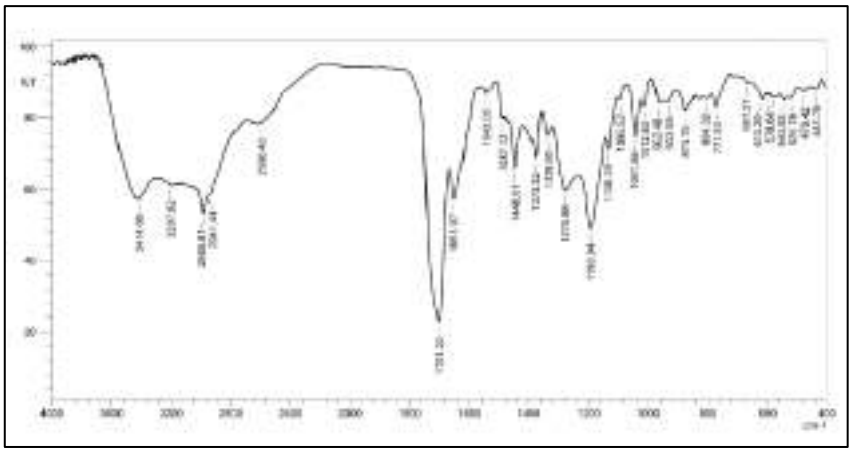


Figure (4- 253): FTIR spectrum of copolymer(43) (DMA-CO-CAN) with compound(14).

^{1}HNMR spectrum of copolymer(43) (DMA-CO-CAN) with compound(14).

^{1}HNMR spectrum of copolymer(43) (DMA-CO-CAN) with compound(14) in (fig.4-254) singles at (6.9-8.3 δ ppm) to (4H, phenyl ring), single at (3.5 ppm) to –NH, single at (5.7 ppm) to (H, OH). single at (4.5 ppm) to –NH (amide), singles at (1.0 ppm) to –CH3, single at (11.3 ppm) to –OH (COOH), singles at (2.5 ppm) to –CH_2, single at (11.3 ppm) to –OH (phenolic). (151-153)

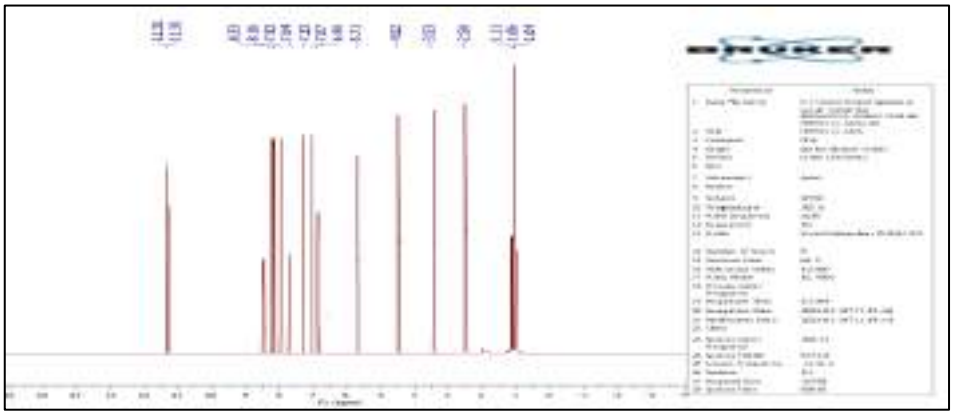


Figure (4- 254): ^{1}HNMR spectrum of copolymer(43) (DMA-CO-CAN) with compound(14).

^{13}C-NMR spectrum of copolymer(43) (DMA-CO-CAN) with compound(14). The signals of olefinic and aromatic carbons appear in the third region between 117 and 133 ppm, single related to C=N at 152-157 ppm, single related to C-N at 72 ppm, single related to C=S at 193 ppm, single related to CH_3-C(Secondary) at 18 ppm, single related to C=O (amide) at 166 ppm, single related to C=O (COOH) at 173 ppm. (151-153)

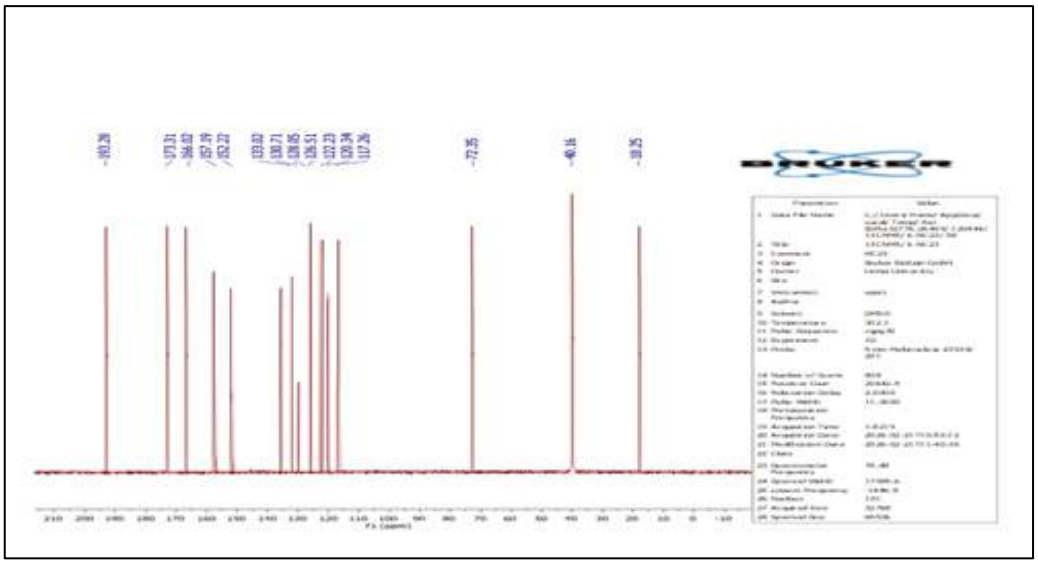
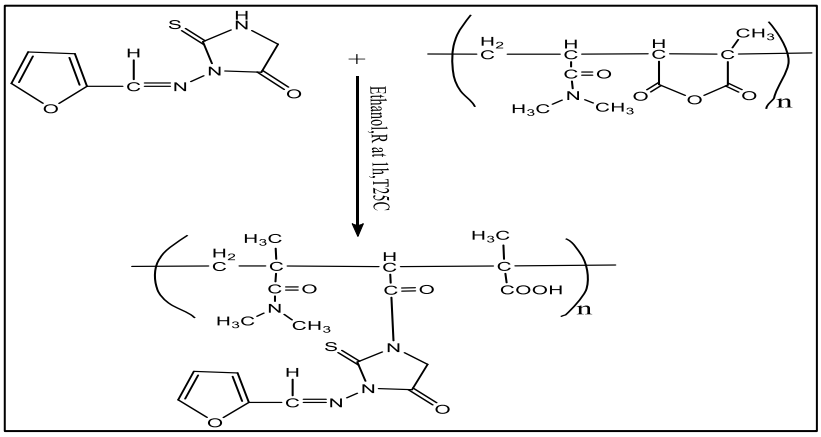


Figure (4- 255): ^{13}C-NMR spectrum of copolymer(43) (DMA-CO-CAN) with compound(14).

4.31.3 Synthesis of copolymer(44) (DMA-CO-CAN) with compound(16).



Scheme (4-91): synthesis of copolymer(44) (DMA-CO-CAN) with compound(16). FTIR spectrum of copolymer(44) (DMA-CO-CAN) with compound(16).

The FTIR spectrum of copolymer(44) (DMA-CO-CAN) with compound(16) as shown in (fig.4-256) which indicates absorption bands at 3458 Cm^{-1} to –OH and 3417 Cm^{-1} to –NH. stretching, absorption band at 3176 cm^{-1} to C-H (Hetero phenyl ring), absorption band at 2985 cm^{-1} to C-H (aliphatic), absorption band at 1543 Cm^{-1} to C=N, absorption band at 1276 Cm^{-1} to C=S, absorption band at 1487 Cm^{-1} to C=C (Heterocyclic ring), absorption band at 1041 Cm^{-1} to C-O, absorption band at 1187 Cm^{-1} to C-N, absorption band at 1701 Cm^{-1} to C=O (COOH), absorption band at 1651 Cm^{-1} to C=O (amide), absorption band at 1373 Cm^{-1} to CH_3. (151-153)

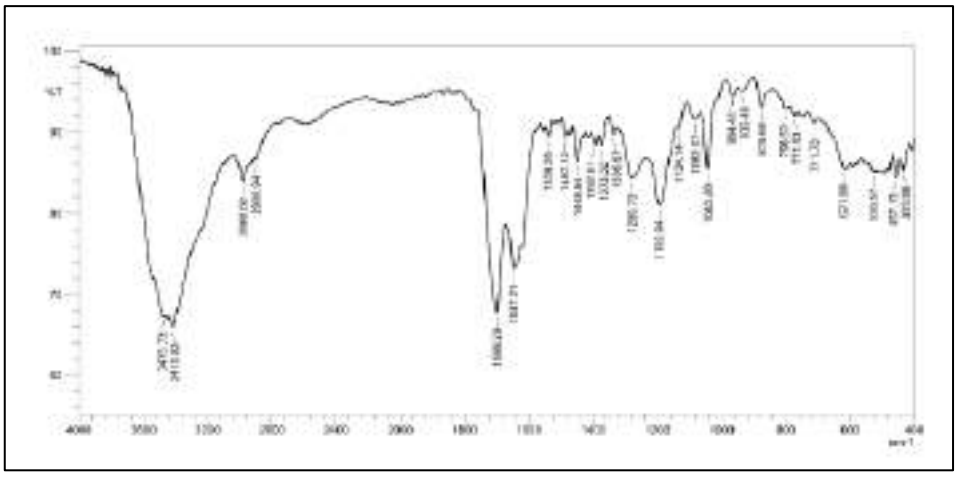


Figure (4- 256): FTIR spectrum of copolymer(44) (DMA-CO-CAN) with compound(16).

^{1}HNMR spectrum of copolymer(44) (DMA-CO-CAN) with compound(16).

^{1}HNMR spectrum of copolymer(44) (DMA-CO-CAN) with compound(16) in (fig.4-257) singles at (6.5-8.1 δ ppm) to (3H, Hetro phenyl ring), single at (3.4 ppm) to –NH, single at (4.4ppm) to –NH (amide), singlate at (1.0 ppm) to $–CH_3$, single at (11.4 ppm) to –OH (COOH), singles at (2.5 ppm) to $–CH_2$. (151-153)

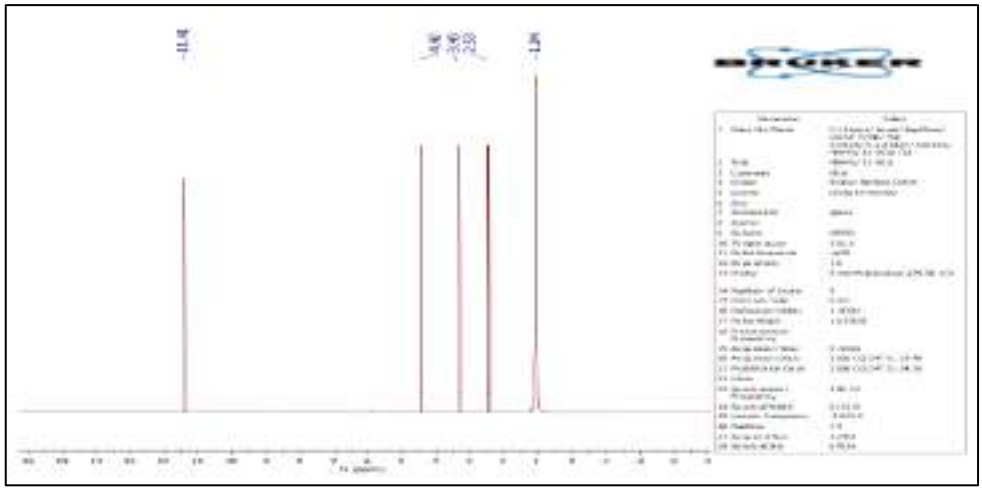


Figure (4- 257): ^{1}HNMR spectrum of copolymer(44) (DMA-CO-CAN) with compound(16).

^{13}C-NMR spectrum of copolymer(44) (DMA-CO-CAN) with compound(16).

The signals of olefinic and aromatic carbons appear in the third region between 114 and 133 ppm, single related to C=N at 145-150 ppm, single related to C-N at 56 ppm, single related to C=S at 194 ppm, single related to CH_3-C(Secondary) at 18 ppm, single related to C=O (amide) at 166 ppm, single related to C=O (COOH) at 178 ppm. (151-153)

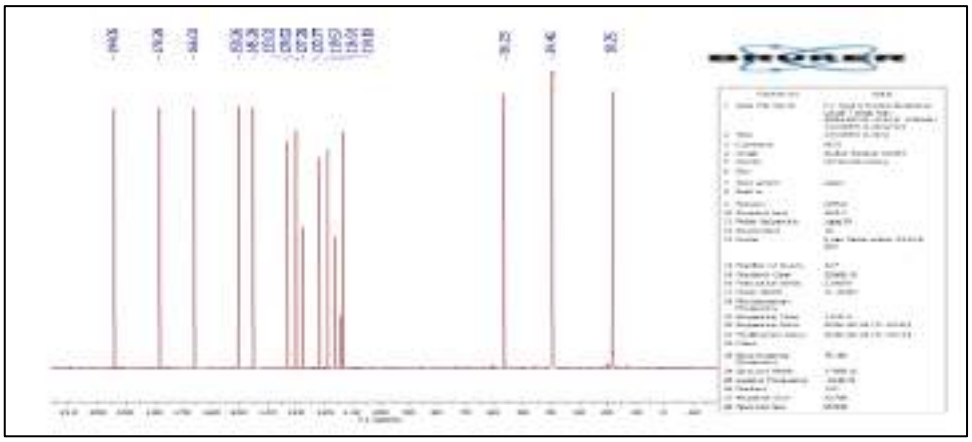
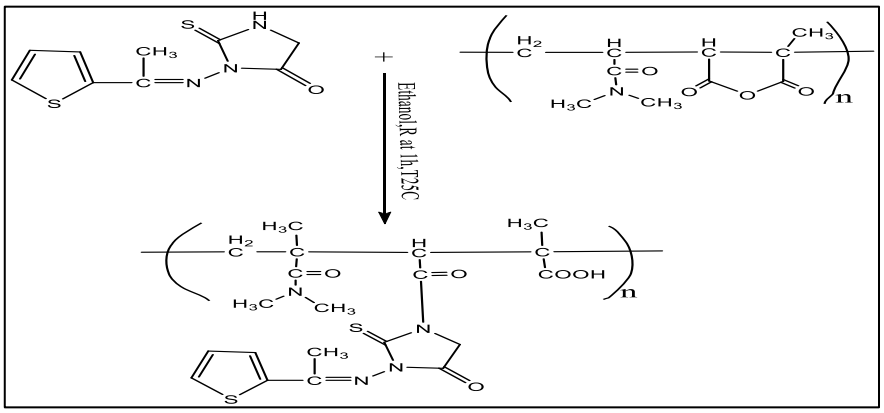


Figure (4- 258): ^{13}C-NMR spectrum of copolymer(44) (DMA-CO-CAN) with compound(16).

4.31.4 Synthesis of copolymer(45) (DMA-CO-CAN) with compound(17).



Scheme (4-92): synthesis of copolymer(45) (DMA-CO-CAN) with compound(17).

FTIR spectrum of copolymer(45) (DMA-CO-CAN) with compound(17).

The FTIR spectrum of copolymer(45) (DMA-CO-CAN) with compound(17) as shown in (fig.4-259) which indicates absorption bands at 3475 cm^{-1} to –OH overlapping with –NH stretching, absorption band at 3070 cm^{-1} to C-H (Heterocyclic ring), absorption band at 2974 cm^{-1} to C-H (aliphatic), absorption band at 1556cm^{-1} to C=N, absorption band at 1273 Cm^{-1} to C=S, absorption band at 1487 Cm^{-1} to C=C (Heterocyclic ring), absorption band at 1085 Cm^{-1} to C-O, absorption band at 1192 Cm^{-1} to C-N, absorption band at 1703 Cm^{-1} to C=O (COOH), absorption band at 1651 Cm^{-1} to C=O (amide), absorption band at 1338 Cm^{-1} to CH_3. (151-153)

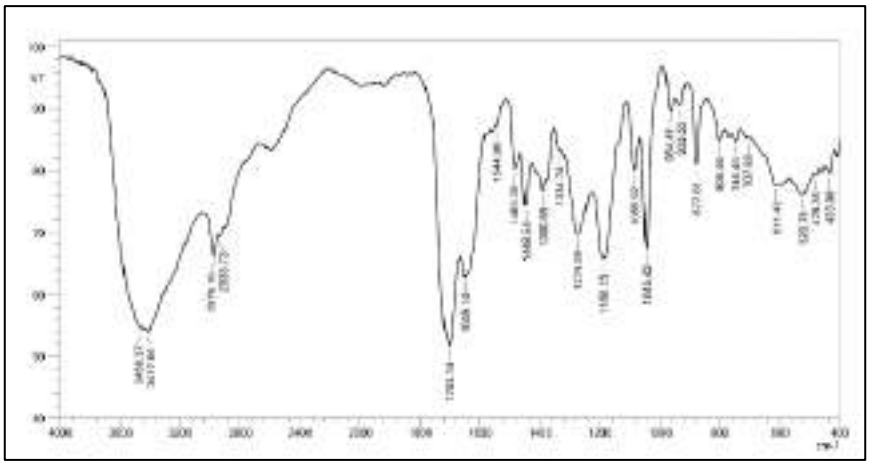


Figure (4- 259): FTIR spectrum of copolymer(45) (DMA-CO-CAN) with compound(17).

^{1}HNMR spectrum of copolymer(45) (DMA-CO-CAN) with compound(17).

^{1}HNMR spectrum of copolymer(45) (DMA-CO-CAN) with compound(17) in (fig.4-260) singles at (7.3-8.3 δ ppm) to (3H, Heterocyclic ring), singles at (3.5 ppm) to –NH, singles at (4.3ppm) to –NH (amide), singles at (1.0 ppm) to $–CH_3$, single at (12.3 ppm) to –OH (COOH), singles at (2.5 ppm) to $–CH_2$. (151-153)

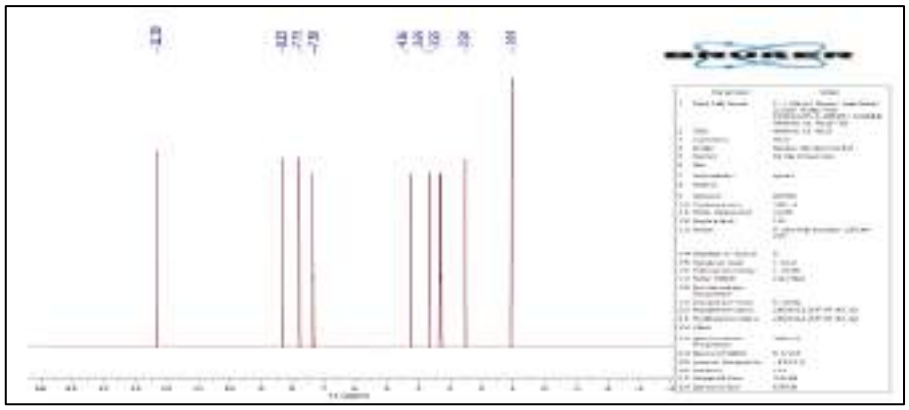


Figure (4- 260): ^{1}HNMR spectrum of copolymer(45) (DMA-CO-CAN) with compound(17).

^{13}C-NMR spectrum of copolymer(45) (DMA-CO-CAN) with compound(17).

The signals of olefinic and aromatic carbons appear in the third region between 128 and 131 ppm, single related to C=N at 150 ppm, single related to C-N at 64 ppm, single related to C=S at 195 ppm, single related to CH_3 at 18 ppm, single related to C=O (amide) at 164 ppm, singles related to C=O (COOH) at 175 ppm. (151-153)

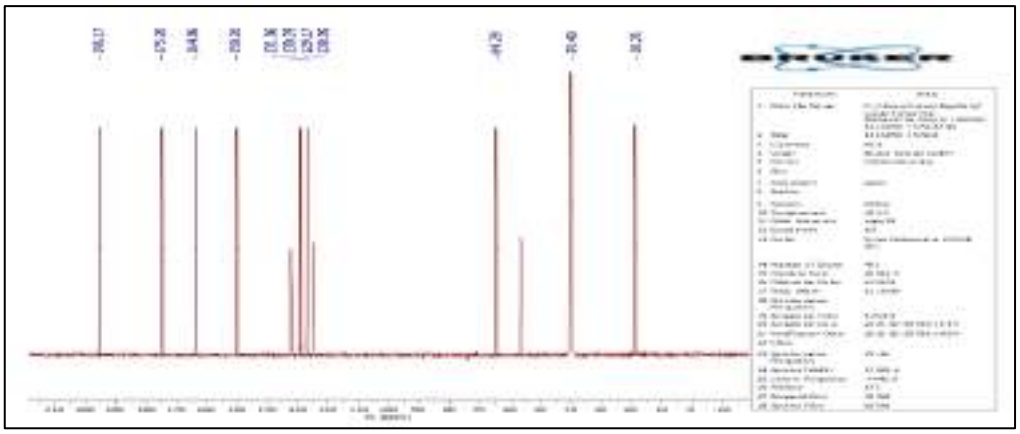
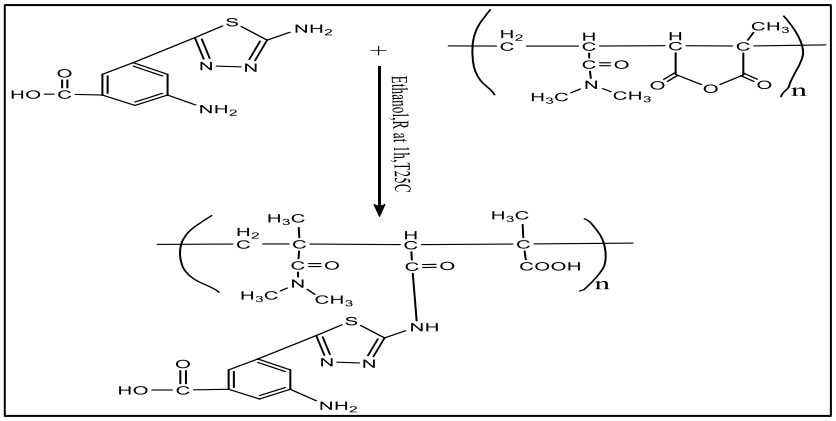


Figure (4- 261): ^{13}C-NMR spectrum of copolymer(45) (DMA-CO-CAN) with compound(17).

4.32 Synthesis of copolymer (DMA-CAN) with compounds(18-20).

4.32.1 Synthesis of copolymer(46) (DMA-CO-CAN) with compound(18).



Scheme (4-93): synthesis of copolymer(46) (DMA-CO-CAN) with compound(18)

FTIR spectrum of copolymer(46) (DMA-CO-CAN) with compound(18).

The FTIR spectrum of copolymer(46) (DMA-CO-CAN) with compound(18) as shown in (fig.4-262) which indicates absorption band at 3545 Cm^{-1} to –OH, absorption band at 35469 and 3412 Cm^{-1} to $–NH_2$, absorption band at 3234 Cm^{-1} to C-H (aromatic), absorption band at 2976 Cm^{-1} to C-H (aliphatic), absorption band at 1539 Cm^{-1} to C=N, absorption band at 1485 Cm^{-1} to C=C (aromatic), absorption band at 1703 Cm^{-1} to C=O (carboxylic), absorption band at 1651Cm^{-1} to C=O (amide), absorption band at 1190 Cm^{-1} to C-N, absorption band at 1377 Cm^{-1} to CH_3. (151-153)

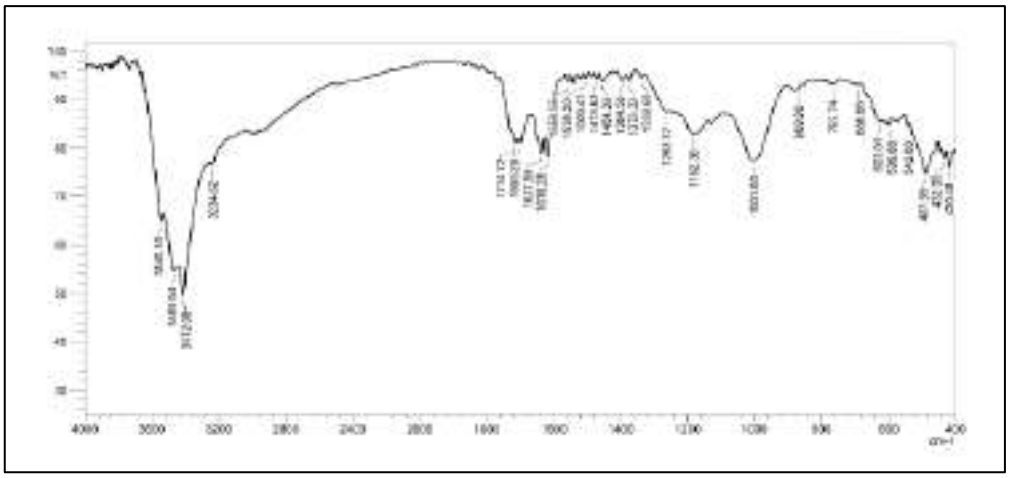


Figure (4- 262): FTIR spectrum of copolymer(46) (DMA-CO-CAN) with compound(18).

^{1}HNMR spectrum of copolymer(46) (DMA-CO-CAN) with compound(18).

^{1}HNMR spectrum of copolymer(46) (DMA-CO-CAN) with compound(18) in (fig.4-263) singles at (7.3-7.5 δ ppm) to (4H, phenyl ring), singlate at (3.4 ppm) to –NH_2, singlate at (4.5 ppm) to –NH(amide), single at (11.3 ppm) to (COOH), singlate at (2.4 ppm) to –CH_2**,** singlate at (1.2 ppm) to –CH_3. (151-153)

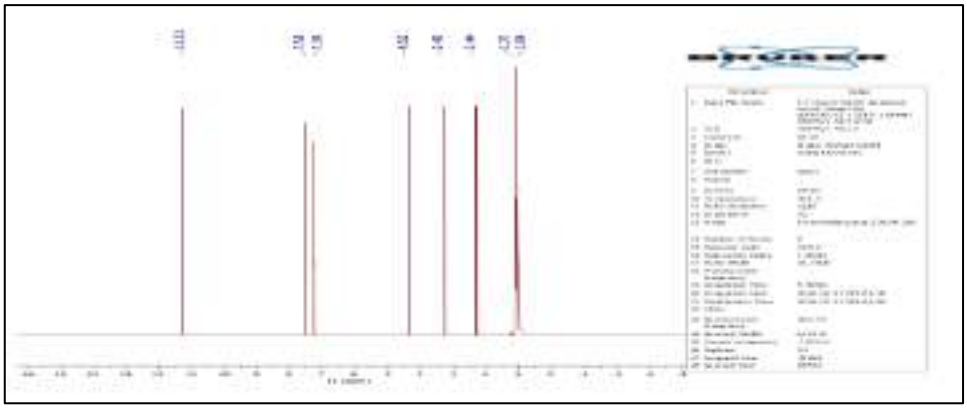


Figure (4- 263): ^{1}HNMR spectrum of copolymer(46) (DMA-CO-CAN) with compound(18).

^{13}C-NMR spectrum of copolymer(46) (DMA-CO-CAN) with compound(18).

The signals of olefinic and aromatic carbons appear in the third region between 126 and 135 ppm, single related to C-S at 56 ppm, single related to C=N at 157ppm, single related to C-N at 64 ppm, single related to C=O (acid) at 183ppm, single related to C=O (amide) at 173ppm, singles related to CH_3 at 18 ppm. (151-153)

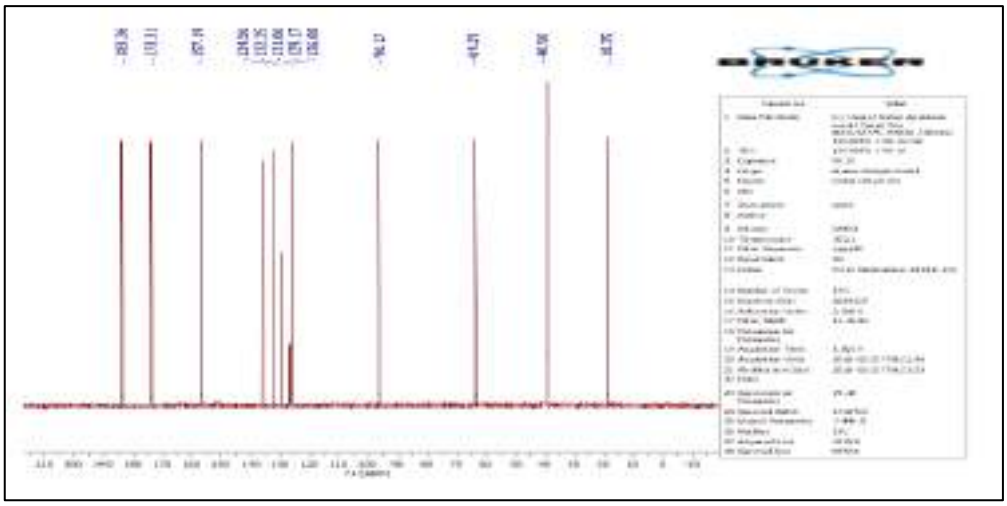
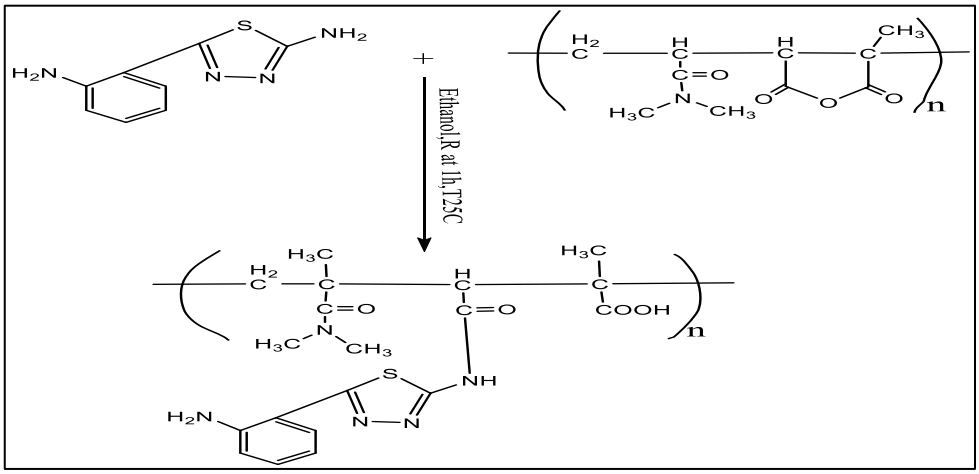


Figure (4- 264): ^{13}C-NMR spectrum of copolymer(46) (DMA-CO-CAN) with compound(18).

4.32.2 Synthesis of copolymer(47) (DMA-CO-CAN) with compound(19).



Scheme (4-94): synthesis of copolymer(47) (DMA-CO-CAN) with compound(19).

FTIR spectrum of copolymer(47) (DMA-CO-CAN) with compound(19).

The FTIR spectrum of copolymer(47) (DMA-CO-CAN) with compound(19) as shown in (fig.4-265) which indicates absorption band at 3547 Cm^{-1} to –OH and 3471 and 3414 $Cm^{-1}$to $–NH_2$, absorption band at 3238 Cm^{-1} to C-H (aromatic), absorption band at 2976 Cm^{-1} to C-H (aliphatic), absorption band at 1544 Cm^{-1} to C=N, absorption band at 1448 Cm^{-1} to C=C (aromatic), absorption band at 1703 Cm^{-1} to C=O (carboxylic), absorption band at 1649Cm^{-1} to C=O (amide), absorption band at 1188 Cm^{-1} to C-N, absorption band at 1390 Cm^{-1} to CH_3. (151-153)

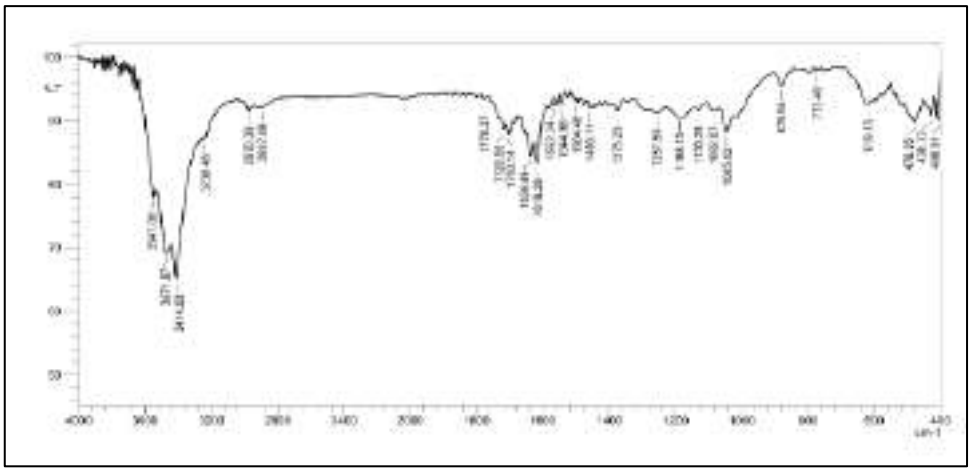


Figure (4- 265): FTIR spectrum of copolymer(47) (DMA-CO-CAN) with compound(19).

^{1}HNMR spectrum of copolymer(47) (DMA-CO-CAN) with compound(19).

^{1}HNMR spectrum of copolymer(47) (DMA-CO-CAN) with compound(19) in (fig.4-266) singles at (6.3-7.5 δ ppm) to (4H, phenyl ring), singles at (3.4 ppm) to –NH_2, single at (10.5 ppm) to (COOH), singlate at (2.4 ppm) to –CH_2**,** singles at (1.2 ppm) to –CH_3. (151-153)

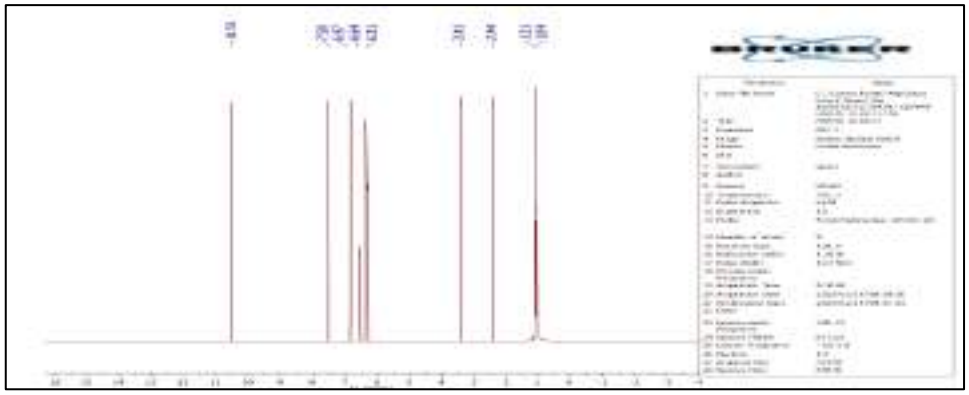


Figure (4- 266): ^{1}HNMR spectrum of copolymer(47) (DMA-CO-CAN) with compound(19).

^{13}C-NMR spectrum of copolymer(47) (DMA-CO-CAN) with compound(19).

The signals of olefinic and aromatic carbons appear in the third region between 126 and 135 ppm, single related to C-S at 56 ppm, single related to C=N at 157ppm, singles related to C-N at 63 ppm, single related to C=O (acid) at 183ppm, single related to C=O (amide) at 173ppm, singles related to CH_3 at 18 ppm. (151-153)

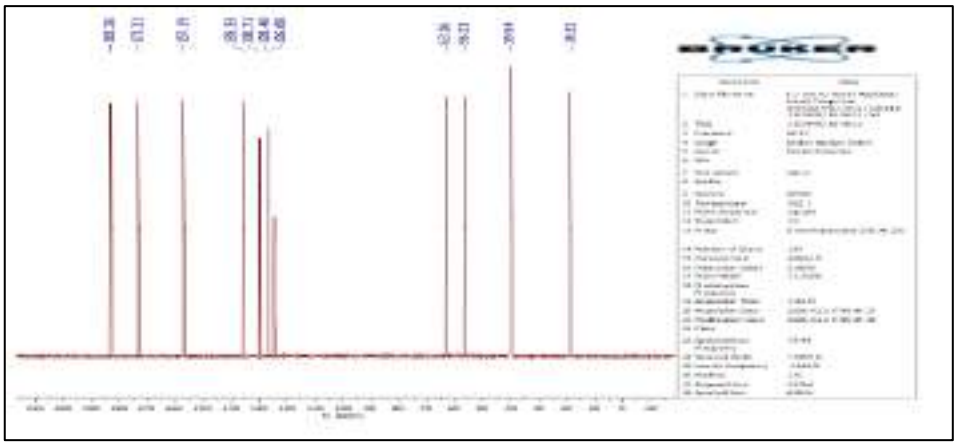
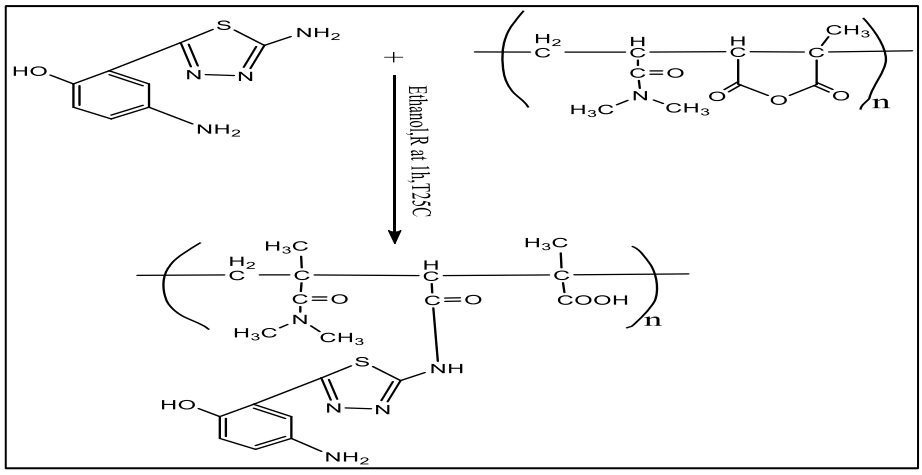


Figure (4- 267): ^{13}C-NMR spectrum of copolymer(47) (DMA-CO-CAN) with compound(19).

4.32.3 Synthesis of copolymer(48) (DMA-CO-CAN) with compound(20).



Scheme (4-95): synthesis of copolymer(48) (DMA-CO-CAN) with compound(20).

FTIR spectrum of copolymer(48) (DMA-CO-CAN) with compound(20).

The FTIR spectrum of copolymer(48) (DMA-CO-CAN) with compound(2) as shown in (fig.4-268*)* which indicates absorption band at 3408 Cm^{-1} to –OH and 3343 Cm^{-1} to $–NH_2$, absorption band at 3000 Cm^{-1} to C-H (aromatic), absorption band at 2980 Cm^{-1} to C-H (aliphatic), absorption band at 1539 Cm^{-1} to C=N, absorption band at 1487 Cm^{-1} to C=C (aromatic), absorption band at 1699 Cm^{-1} to C=O (carboxylic), absorption band at 1647 Cm^{-1} to C=O (amide), absorption band at 1193 Cm^{-1} to C-N, absorption band at 1373 Cm^{-1} to CH_3. (151-153)

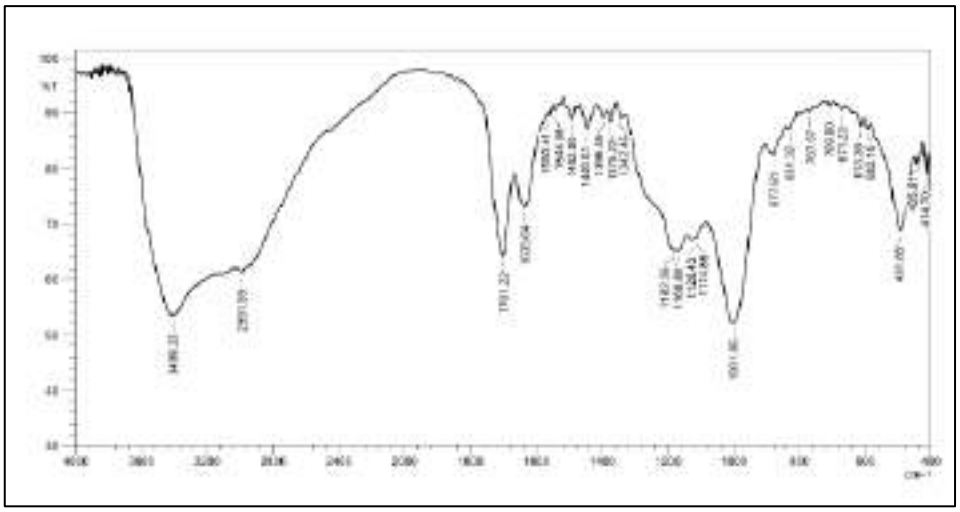


Figure (4- 268): FTIR spectrum of copolymer(48) (DMA-CO-CAN) with compound(20).

^{1}HNMR spectrum of copolymer(48) (DMA-CO-CAN) with compound(20).

^{1}HNMR spectrum of copolymer(48) (DMA-CO-CAN) with compound(20) in (fig.4-269) singles at (5.7-6.3 δ ppm) to (4H, phenyl ring), singlate at (3.3 ppm) to –NH_2, singlate at (3.9 ppm) to –NH (amide), single at (10.3 ppm) to (COOH), singlate at (2.4 ppm) to –CH_2**,** singles at (1.0 ppm) to –CH_3. (151-153)

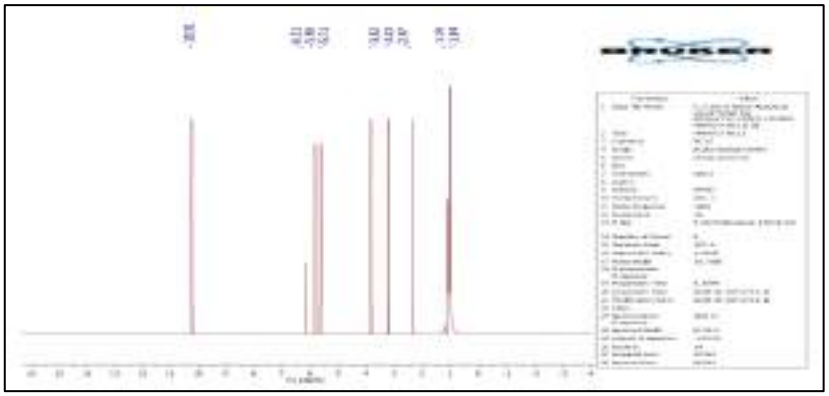


Figure (4- 269): ^{1}HNMR spectrum of copolymer(48) (DMA-CO-CAN) with compound(20).

^{13}C-NMR spectrum of copolymer(48) (DMA-CO-CAN) with compound(20).

The signals of olefinic and aromatic carbons appear in the third region between 118 and 132ppm, single related to C-S at 56 ppm, single related to C=N at 153ppm, singles related to C-N at 63 ppm, single related to C=O (acid) at 183ppm, single related to C=O (amide) at 173ppm, singles related to CH_3 at 18 ppm. (151-153)

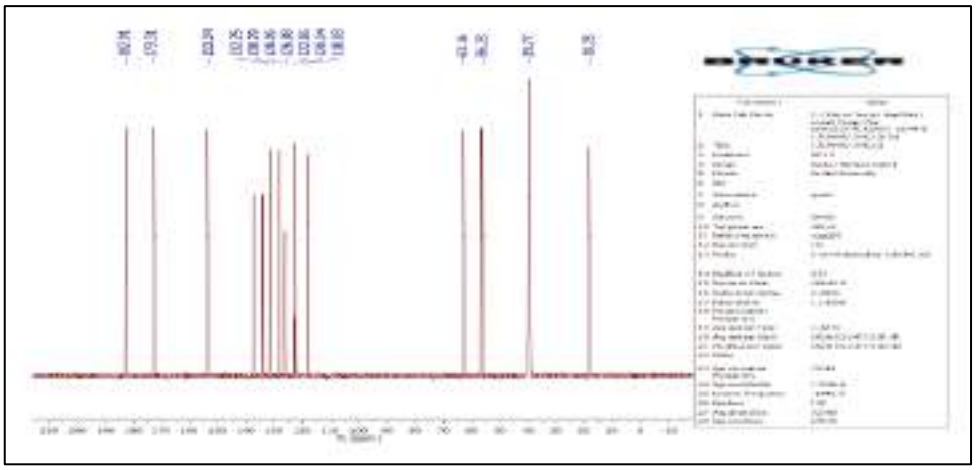
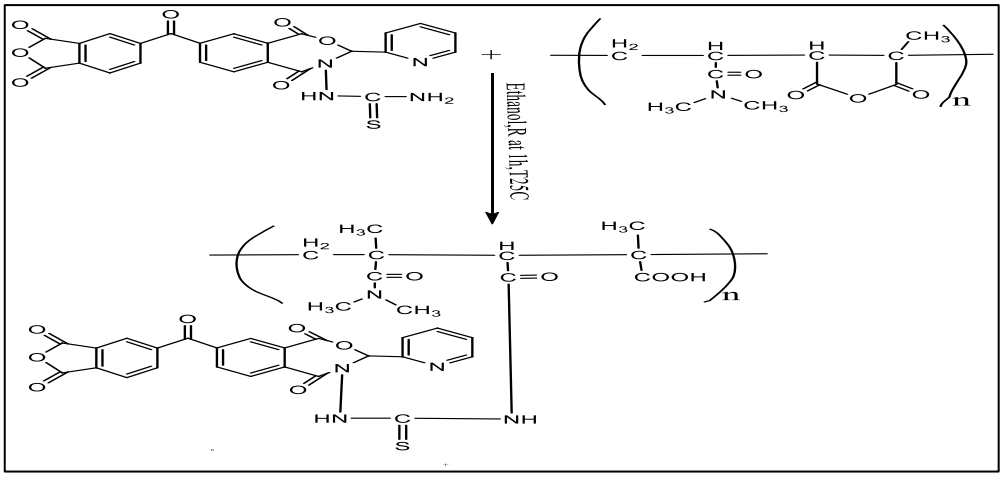


Figure (4- 270): ^{13}C-NMR spectrum of copolymer(48) (DMA-CO-CAN) with compound(20).

4.33 Synthesis of copolymer (DMA-CO-CAN) with compounds with (24-25).

4.33.1 Synthesis of copolymer(49) (DMA-CO-CAN) with compound(24).



Scheme (4-96): synthesis of copolymer(49) (DMA-CO-CAN) with compound(24).

FTIR spectrum of copolymer(49) (DMA-CO-CAN) with compound(24).

The FTIR spectrum of copolymer(49) (DMA-CO-CAN) with compound(24) as shown in (fig.4-271) which indicates absorption bands at 3543 cm^{-1} to –OH and 3471and 3412 Cm^{-1} to –NH, absorption band at 3234 cm^{-1} to C-H(aromatic) , absorption band at 2980 cm^{-1} to C-H(aliphatic), absorption band at 1284 Cm^{-1} to C=S, absorption band at 1539 Cm^{-1} to C=C (aromatic), absorption bands at 1193 Cm^{-1} to C-N, absorption bands at 1714 Cm^{-1} to C=O (ester), absorption bands at 1641 Cm^{-1} to C=O (acid), absorption bands at 1392 Cm^{-1} to CH_3, absorption bands at 1699 Cm^{-1} to C=O Ketone), absorption bands at 1043 Cm^{-1} to C-O. (151-153)

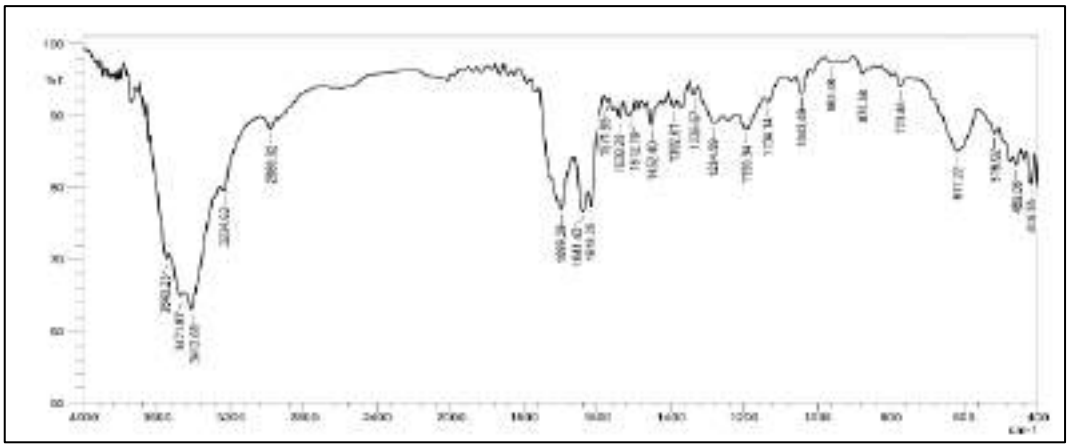


Figure (4- 271): FTIR spectrum of copolymer(49) (DMA-CO-CAN) with compound(24).

^{1}HNMR spectrum of copolymer(49) (DMA-CO-CAN) with compound(24).

^{1}HNMR spectrum of copolymer(49) (DMA-CO-CAN) with compound(24) in (fig.4-272) singles at (7.3-7.8 δ ppm) to (10H, phenyl ring), singles at (3. 4 ppm) to –NH, singles at (4. 3 ppm) to –NH (amide), singles at (2.0-2.4 ppm) to CH_2, singlate at (1.0 ppm) to CH_3, singlate at (11.4 ppm) to OH (COOH). (151-153)

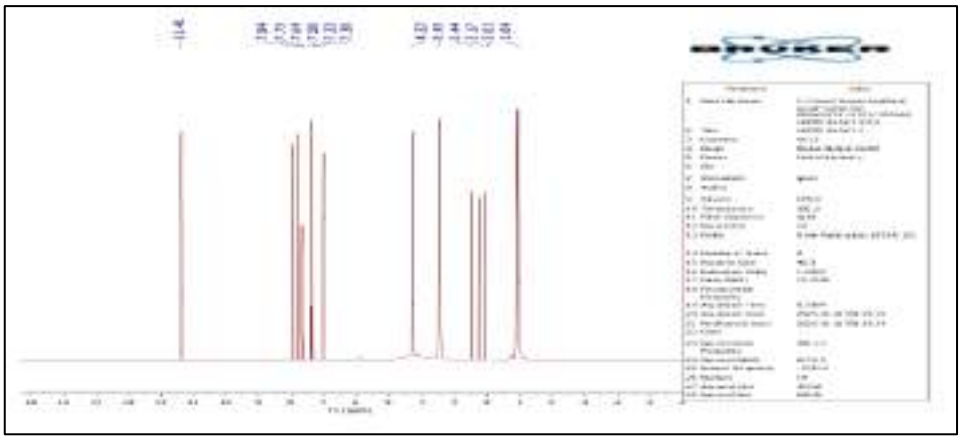


Figure (4- 272): ^{1}HNMR spectrum of copolymer(49) (DMA-CO-CAN) with compound(24).

^{13}C-NMR spectrum of copolymer(49) (DMA-CO-CAN) with compound(24).

The signals of olefinic and aromatic carbons appear in the third region between 121 and 134 ppm, singles related to C=S at 194 ppm, single related to C-N at 56 ppm, single related to C=O (Acid) at 166 ppm, singles related to C=O (Ester) at 174 ppm, singles related to C=O (Ketone) at 210 ppm, singles related to CH_3 at 19 ppm. (151-153)

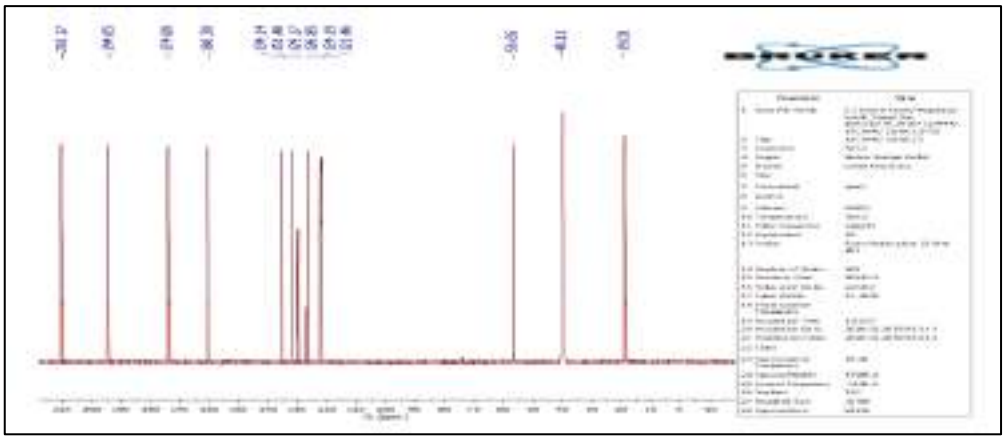
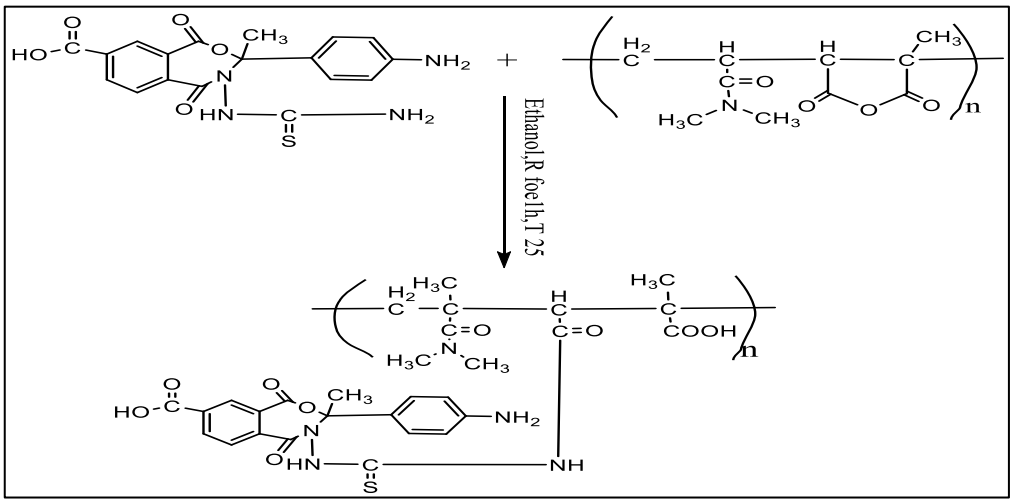


Figure (4- 273): ^{13}C-NMR spectrum of copolymer(49) (DMA-CO-CAN) with compound(24).

4.33.2 Synthesis of copolymer(50) (DMA-CO-CAN) with compound(25).



Scheme (4-97): synthesis of copolymer(50) (DMA-CO-CAN) with compound(25).

FTIR spectrum of copolymer(50) (DMA-CO-CAN) with compound(25).

The FTIR spectrum of copolymer(50) (DMA-CO-CAN) with compound(25) as shown in (fig.4-274) which indicates absorption bands at 3421 cm^{-1} to –OH over lapping with –NH2, absorption band at 3076 cm^{-1} to C-H (aromatic) , absorption band at 2974 cm^{-1} to C-H (aliphatic), absorption band at 1274 Cm^{-1} to C=S, absorption band at 1450 Cm^{-1} to C=C (aromatic), absorption bands at 1195 Cm^{-1} to C-N, absorption bands at 1703 Cm^{-1} to C=O (ester), absorption bands at 1651 Cm^{-1} to C=O (acid), absorption bands at 1336 Cm^{-1} to CH_3, absorption bands at 1087 Cm^{-1} to C-O.(151-153)

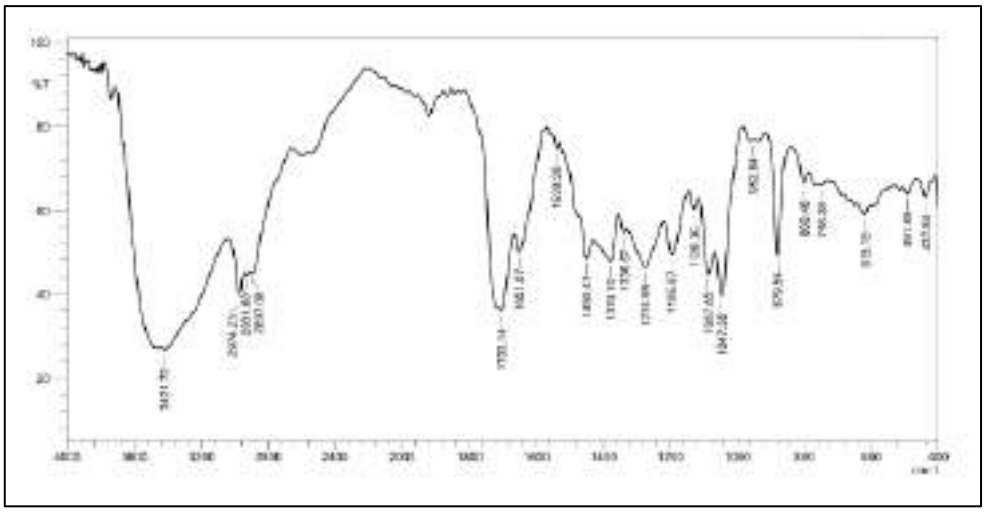


Figure (4- 274): FTIR spectrum of copolymer(50) (DMA-CO-CAN) with compound(25).

^{1}HNMR spectrum of copolymer(50) (DMA-CO-CAN) with compound(25).

^{1}HNMR spectrum of copolymer(50) (DMA-CO-CAN) with compound(25) in (fig.4-275) singles at (7.5-7.8 δ ppm) to (7H, phenyl ring), single at (3. 3 ppm) to –NH, single at (4. 3 ppm) to –NH (amide), singlate at (2.0-2.5 ppm) to CH_2, singlate at (0.9 ppm) to CH_3, singlate at (11.4 ppm) to OH (COOH). (151-153)

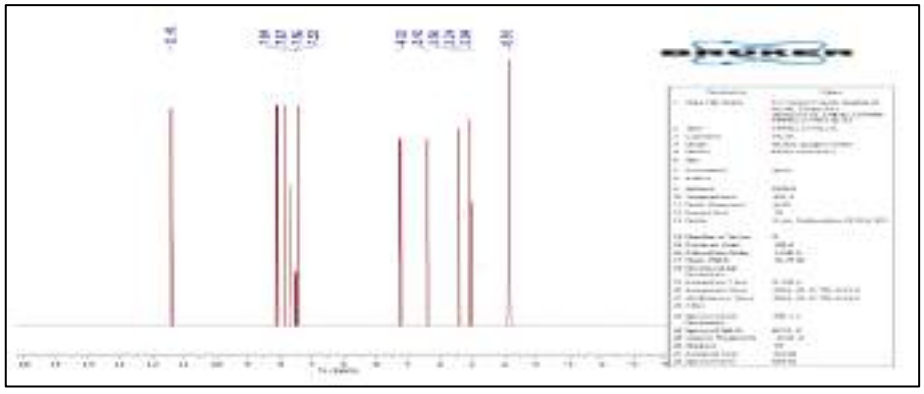


Figure (4- 275): ^{1}HNMR spectrum of copolymer(50) (DMA-CO-CAN) with compound(25).

^{13}C-NMR spectrum of copolymer(50) (DMA-CO-CAN) with compound(25).

The signals of olefinic and aromatic carbons appear in the third region between 112 and 136 ppm, singles related to C=S at 194 ppm, single related to C-N at 56 ppm, singles related to C=O (Acid) at 166 ppm, singles related to C=O (Ester) at 174 ppm, singles related to C=O (Ketone) at 210 ppm, singles related to CH_3 at 19 ppm. (151-153)

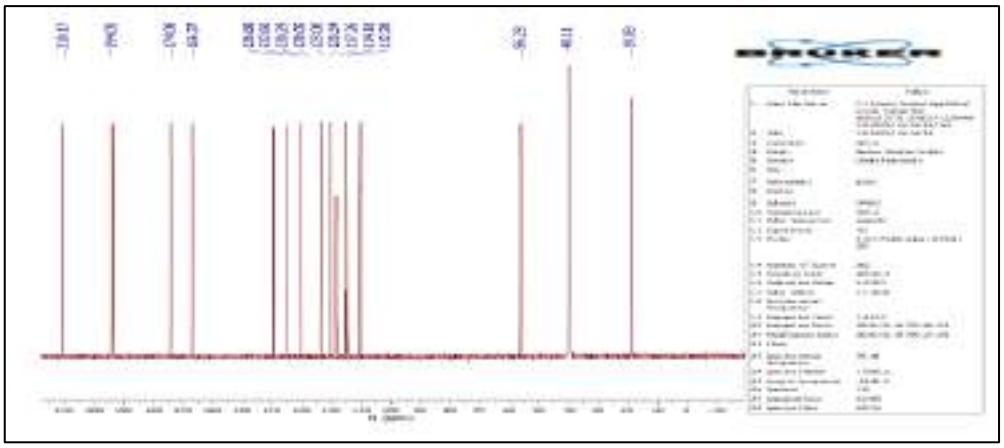
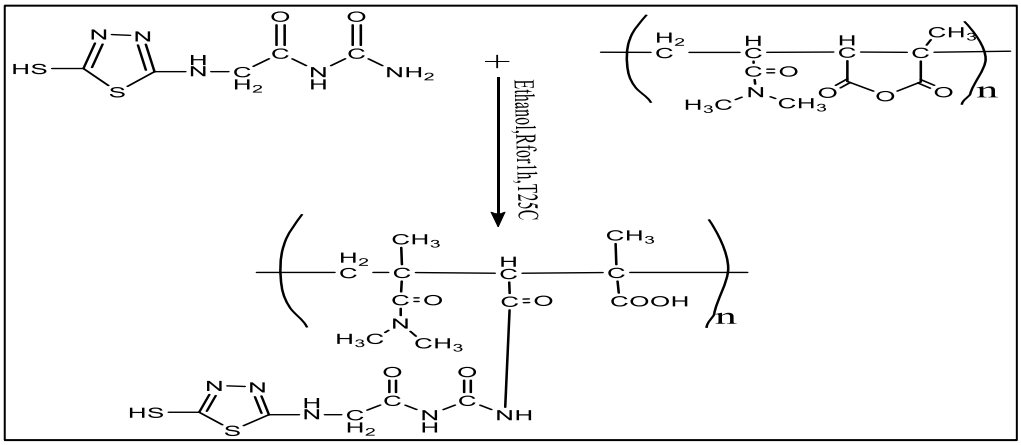


Figure (4- 276): ^{13}C-NMR spectrum of copolymer(50) (DMA-CO-CAN) with compound(25).

4.34 Synthesis of copolymer (51) (DMA-CO-CAN) with compound (28).



Scheme (4-98): synthesis of copolymer (51) (DMA-CO-CAN) with compound (28).

FTIR spectrum of copolymer (51) (DMA-CO-CAN) with compound (28).

The FTIR spectrum of copolymer (51) (DMA-CO-CAN) with compound (28) as shown in (fig.4-277) which indicates absorption bands at 3448 to -OH overlapping with –NH , absorption band at 3174 Cm^{-1} to C-H (aromatic) , absorption band at 2926 Cm^{-1} to C-H (aliphatic), absorption band at 1552 Cm^{-1} to C=N, absorption band at 2755 Cm^{-1} to SH, absorption band at 1467 Cm^{-1} to C=C (aromatic), absorption band at 1695 Cm^{-1} to C=O (Acid), absorption band at 1614 Cm^{-1} to C=O (amide), absorption band at 1330 Cm^{-1} to CH_3.(151-153)

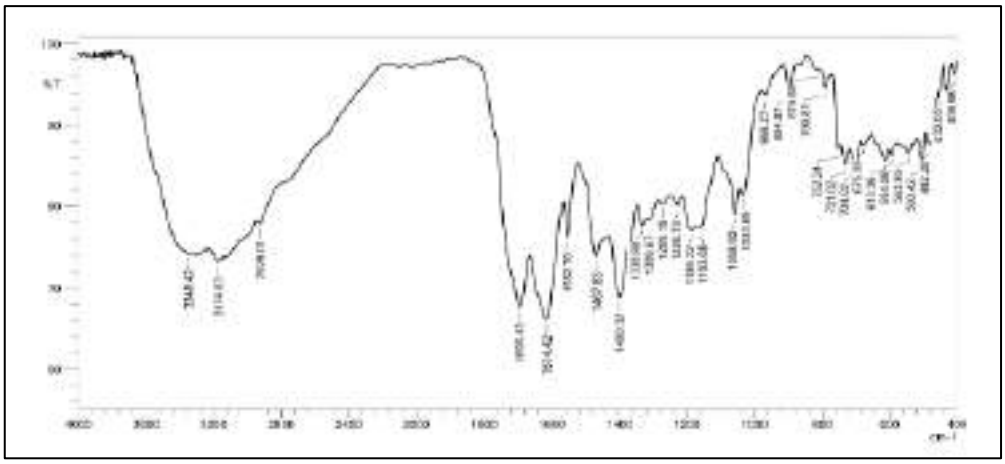


Figure (4- 277): FTIR spectrum of copolymer (51) (DMA-CO-CAN) with compound (28).

^{1}HNMR spectrum of copolymer (51) (DMA-CO-CAN) with compound (28).

^{1}HNMR spectrum of copolymer (51) (DMA-CO-CAN) with compound (28) in (fig.4-278) multiple singlate at (4.3 ppm) to SH, singlate at (3.4 ppm) to -NH, multiple singlate at (10.8ppm) to OH (COOH)**,** singlate at (2.4 ppm) to CH_2, singles at (0.9ppm) to CH_3**.** (151-153)

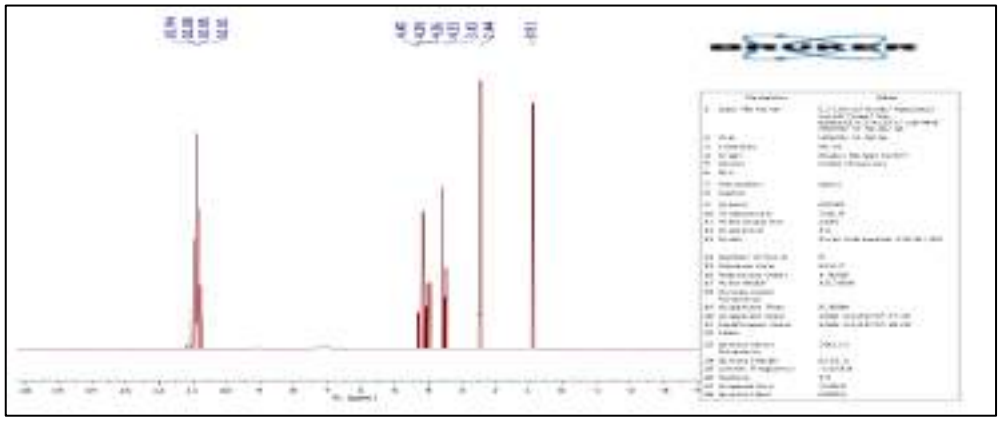


Figure (4- 278): ^{1}HNMR spectrum of copolymer (51) (DMA-CO-CAN) with compound (28).

^{13}C-NMR spectrum of copolymer (51) (DMA-CO-CAN) with compound (28).

The single related to C-S at 68 ppm, singles related to C=N at 154 ppm, single related to C-N at 62 ppm, singles related to C=O (amid) at 186 ppm, single related to C-Cl at 78 ppm, singles related to C=O (acid) at 174 ppm, single related to CH_3 (acid) at 18 ppm. (151-153)

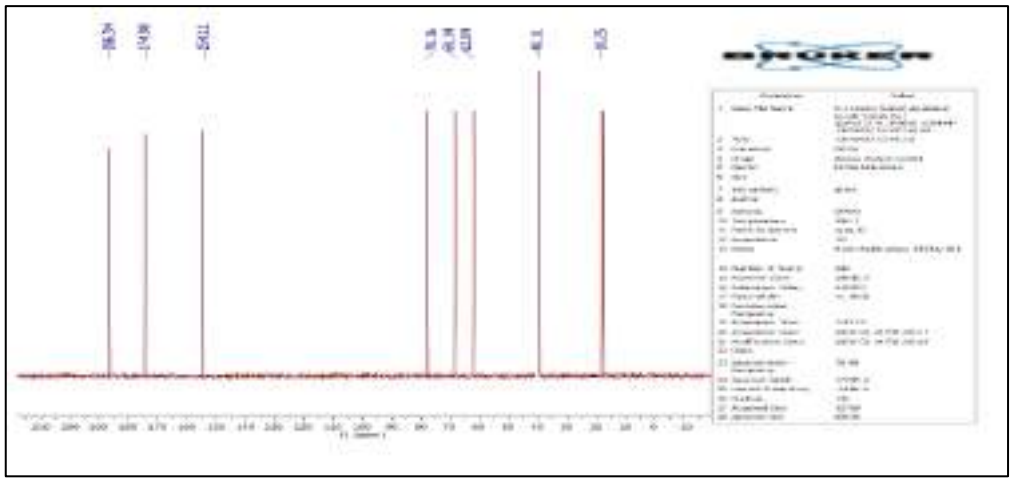
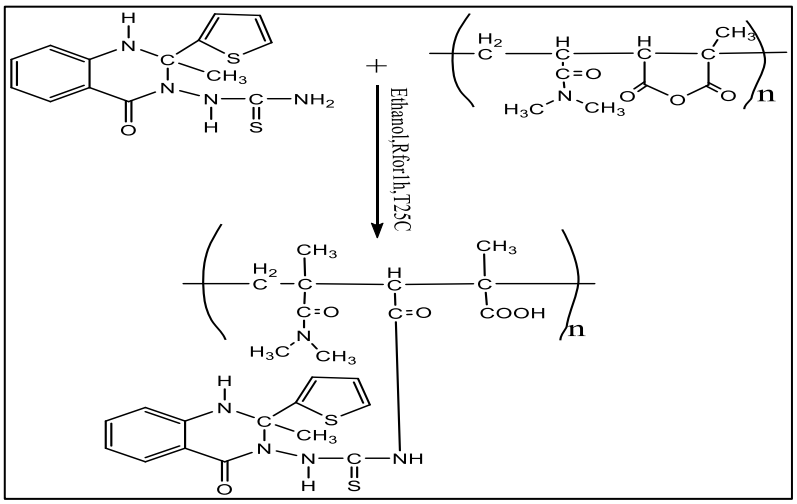


Figure (4- 279): ^{13}C-NMR spectrum of copolymer (51) (DMA-CO-CAN) with compound (28).

4.35 Synthesis of copolymer(52) (DMA-CO-CAN) with compound(31).



Scheme (4-99): synthesis of copolymer(52) (DMA-CO-CAN) with compound(31).

FTIR spectrum of copolymer(52) (DMA-CO-CAN) with compound(31).

The FTIR spectrum of the preparation of copolymer(52) (DMA-CO-CAN) with compound(31) as shown in(fig.4-280) which indicates absorption band at 3547 Cm^{-1} to –OH and 3471 and 3414 Cm^{-1} to–NH, absorption band at 3236 Cm^{-1} to C-H (aromatic), absorption band at 2926 Cm^{-1} to C-H (aliphatic), absorption band at 1271 Cm^{-1} to C=S, absorption band at 1525 Cm^{-1} to C=C (phenyl ring), absorption band at 1039 Cm^{-1} to C-N, absorption band at 1166 Cm^{-1} to C-O , absorption band at 1703 Cm^{-1} to C=O(acid), absorption band at 1635 Cm^{-1} to C=O(amide), absorption band at 615 Cm^{-1} to C-S, absorption band at 1402 Cm^{-1} to CH_3. (151-153)

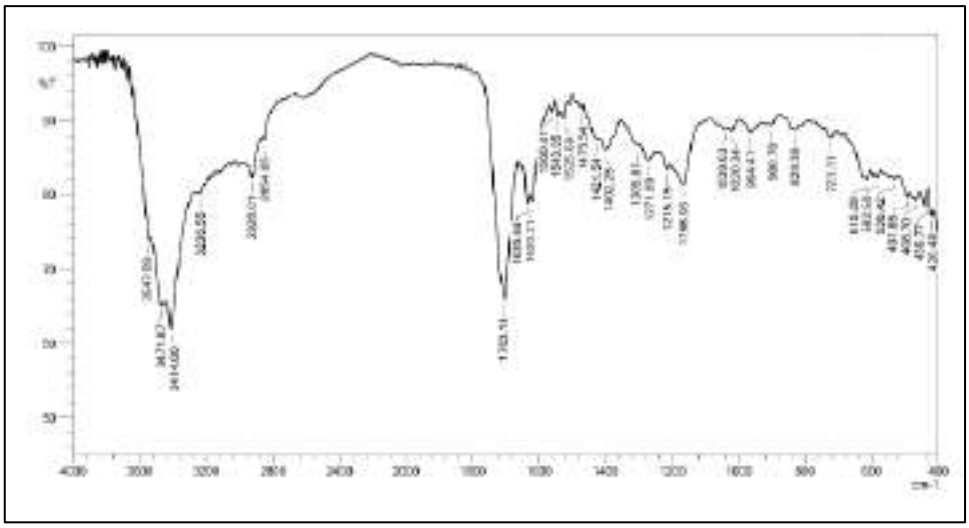


Figure (4- 280): FTIR spectrum of copolymer(52) (DMA-CO-CAN) with compound(31).

^{1}HNMR spectrum of copolymer(52) (DMA-CO-CAN) with compound(31).

^{1}HNMR spectrum of copolymer(52) (DMA-CO-CAN) with compound(31) in (fig.4-281) singles at (6.5-8.3 δ ppm) to (4H, phenyl ring), singles at (3.3 to 4.5 ppm) to –NH, singles at 2.3 ppm to CH_2**,** single at 1.0 ppm to CH_3**,** singles at 12.0 ppm to OH (COOH). (151-153)

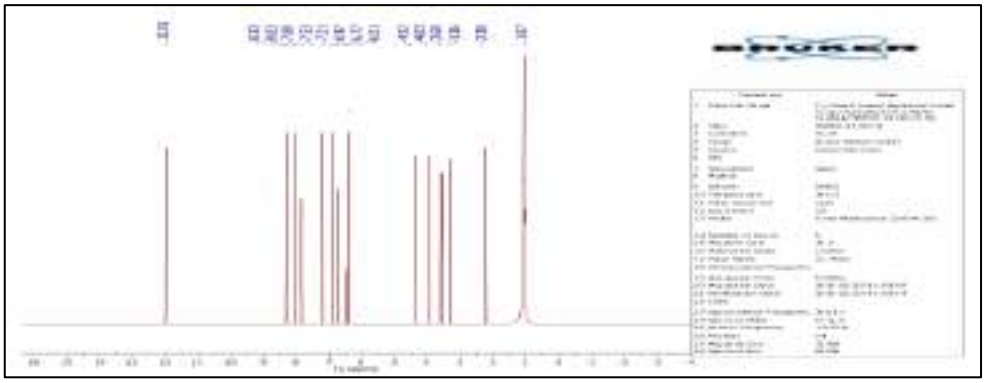


Figure (4- 281): ^{1}HNMR spectrum of copolymer(52) (DMA-CO-CAN) with compound(31).

^{13}C-NMR spectrum of copolymer(52) (DMA-CO-CAN) with compound(31). The signals of olefinic and aromatic carbons appear in the third region between 110 and 135ppm, single related to C-N at 56 ppm, singles related to C=O (amide) at 166 ppm, singles related to C=S at 190-210 ppm, singles related to C=O (acid) at 172 ppm, singles related to CH_3 at 18 ppm. (151-153)

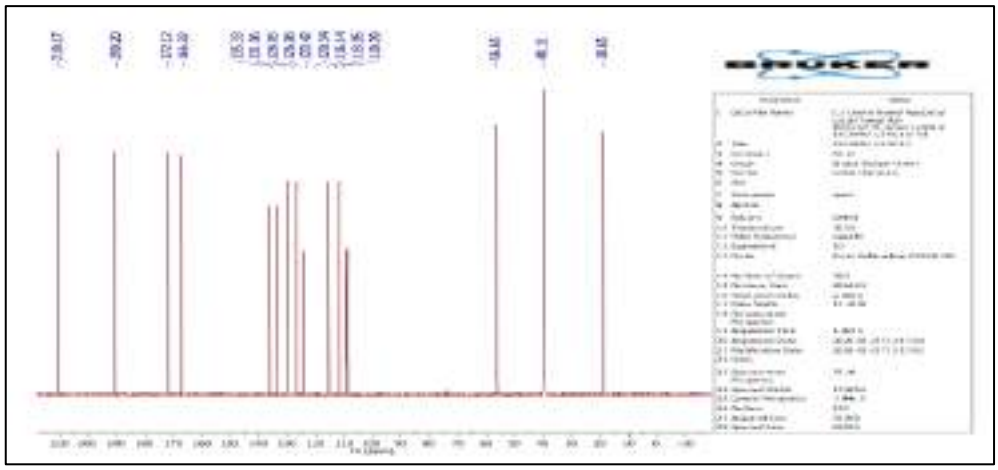
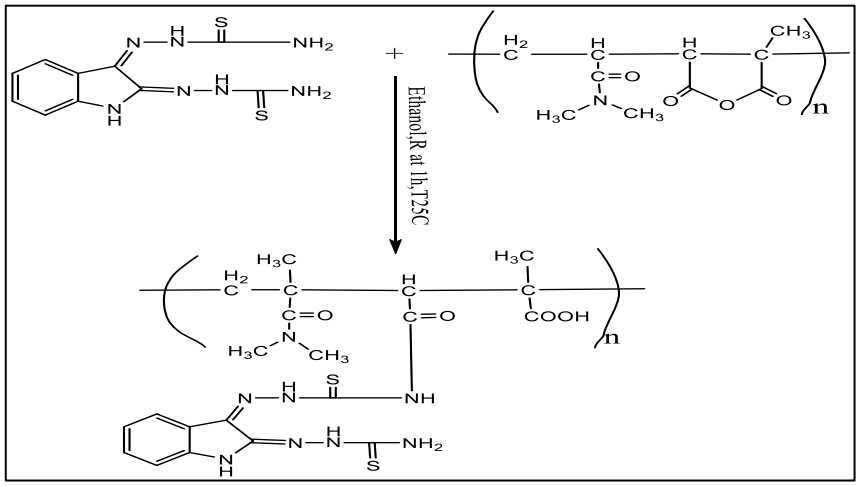


Figure (4- 282): ^{13}C-NMR spectrum of copolymer(52) (DMA-CO-CAN) with compound(31).

4.36 Synthesis of copolymer(53) (DMA-CO-CAN) with compound (34).



Scheme (4-100): synthesis of copolymer(53) (DMA-CO-CAN) with compound (34).

FTIR spectrum of copolymer(53) (DMA-CO-CAN) with compound (34).

The FTIR spectrum of copolymer(53) (DMA-CO-CAN) with compound (34) as shown in (fig.4-283) which indicates absorption band at 3421 Cm^{-1} to –OH over lapping with –NH, absorption band at 3176 Cm^{-1} to C-H (aromatic), absorption band at 2995 Cm^{-1} to C-H (aliphatic), absorption band at 1273 Cm^{-1} to C=S, absorption band at 1504 Cm^{-1} to C=C (phenyl ring), absorption band at 1060 Cm^{-1} to C-N, absorption band at 1128Cm^{-1} to C-O , absorption band at 1728 Cm^{-1} to C=O(acid), absorption band at 1697 Cm^{-1} to C=O(amide), absorption band at 1622 Cm^{-1} to C=N, absorption band at 1336 Cm^{-1} to CH_3. (151-153)

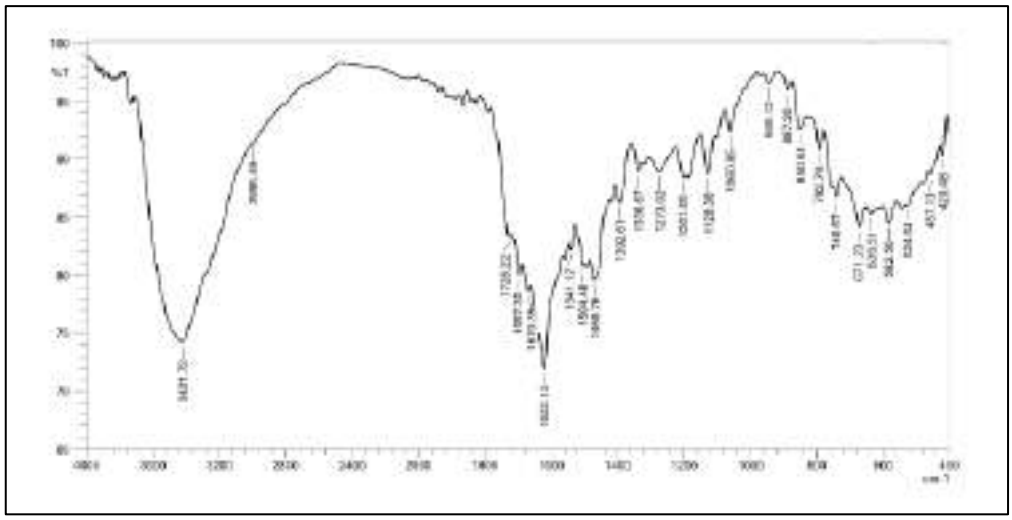


Figure (4- 283): FTIR spectrum of copolymer(53) (DMA-CO-CAN) with compound (34).

^{1}HNMR spectrum of copolymer(53) (DMA-CO-CAN) with compound (34). ^{1}HNMR spectrum of copolymer(53) (DMA-CO-CAN) with compound (34) in (fig.4-284) singles at (6.2-7.8 δ ppm) to (4H, phenyl ring), multiple singlate at (3.2-4.1) to –NH, singles at 2.3 ppm to CH_2**,** single at 1.0 ppm to CH_3**,** singles at 8.7 ppm to OH (COOH). (151-153)

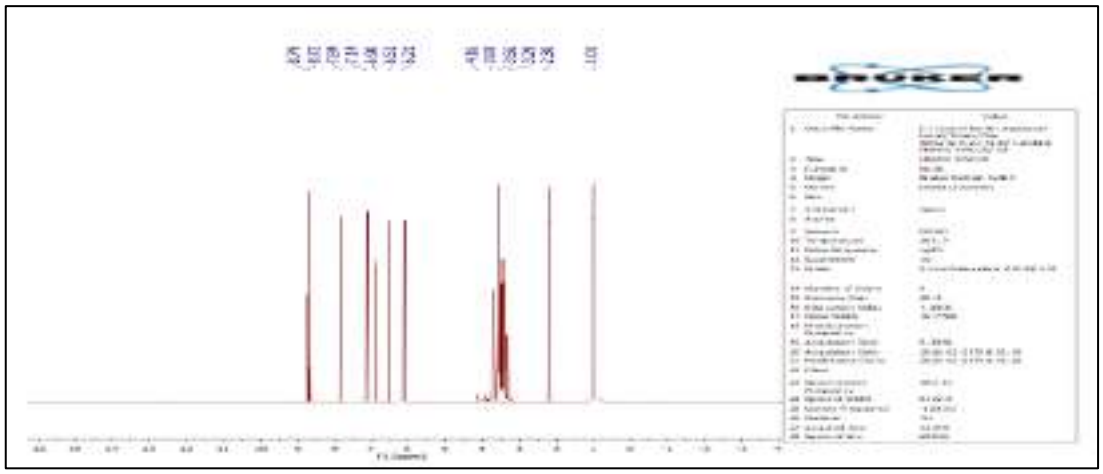


Figure (4- 284): ^{1}HNMR spectrum of copolymer(53) (DMA-CO-CAN) with compound (34).

^{13}C-NMR spectrum of copolymer(53) (DMA-CO-CAN) with compound (34).

The signals of olefinic and aromatic carbons appear in the third region between 117 and 127ppm, single related to C-N at 56 ppm, singles related to C=O (amide) at 164 ppm, singles related to C=S at 195-210 ppm, singles related to C=O (acid) at 173 ppm, singles related to CH_3 at 18 ppm, single related to C=N at 141 ppm. (151-

153)

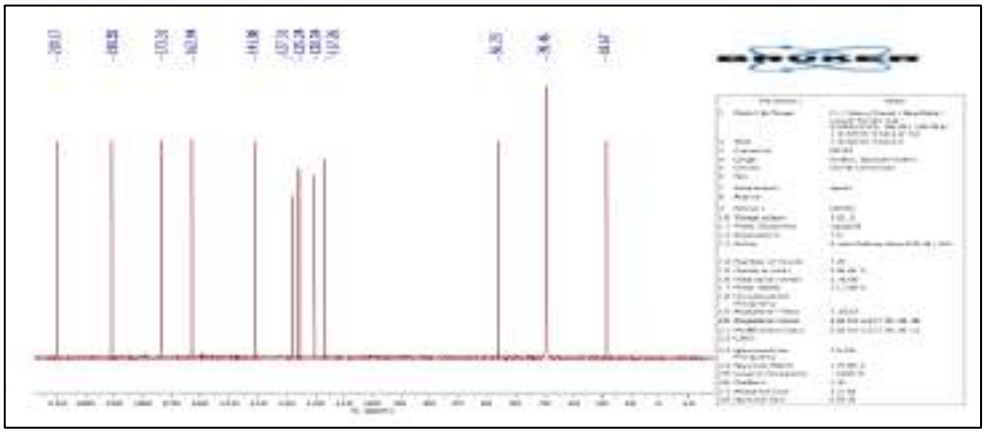
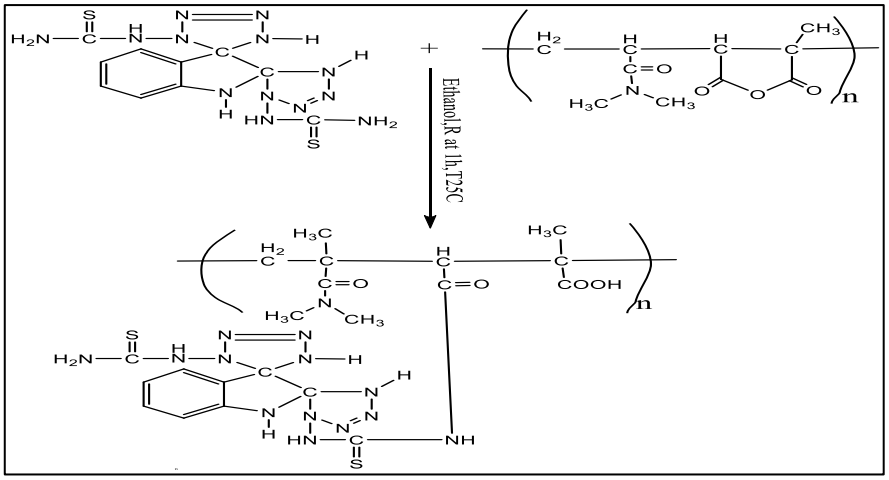


Figure (4- 285): ^{13}C-NMR spectrum of copolymer(53) (DMA-CO-CAN) with compound (34).

4.37 Synthesis of copolymer(54) (DMA-CO-CAN) with compound(35).



Scheme (4-101): synthesis of copolymer(54) (DMA-CO-CAN) with compound(35).

FTIR spectrum of copolymer(54) (DMA-CO-CAN) with compound(35).

The FTIR spectrum of copolymer(54) (DMA-CO-CAN) with compound(35) as shown in (fig.4-286) which indicates absorption band at 3441 Cm^{-1} to –OH over lapping with –NH, absorption band at 3174 Cm^{-1} to C-H (aromatic), absorption band at 2974 Cm^{-1} to C-H (aliphatic), absorption band at 1251 Cm^{-1} to C=S, absorption band at 1452 Cm^{-1} to C=C (phenyl ring), absorption band at 1041 Cm^{-1} to C-N, absorption band at 1114 Cm^{-1} to C-O , absorption band at 1703Cm^{-1} to C=O(acid), absorption band at 1631 Cm^{-1} to C=O (amide), absorption band at 1556 Cm^{-1} to C=N, absorption band at 1319 Cm^{-1} to CH_3, absorption band at 1396 Cm^{-1} to N=N. (151-153)

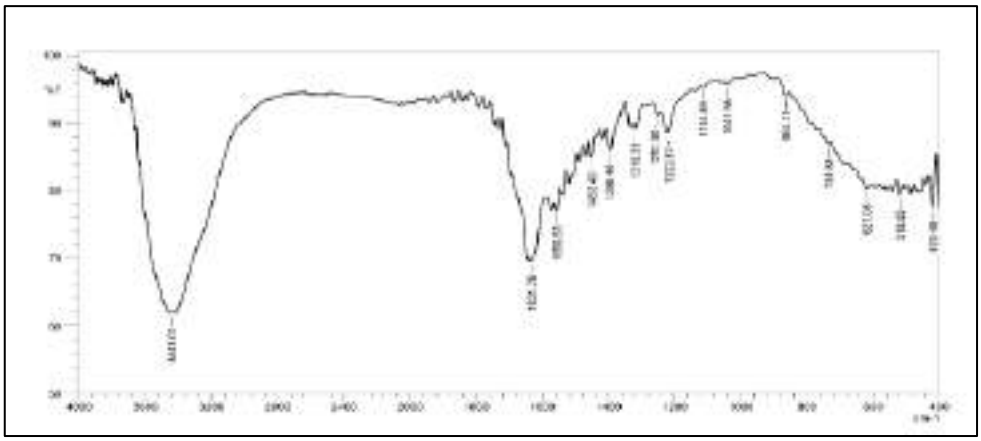


Figure (4- 286): FTIR spectrum of copolymer(54) (DMA-CO-CAN) with compound(35).

^{1}HNMR spectrum of copolymer(54) (DMA-CO-CAN) with compound(35).

^{1}HNMR spectrum of copolymer(54) (DMA-CO-CAN) with compound(35) in (fig.4-287) singles at (6.3-8.3 δ ppm) to (4H, phenyl ring), multiple singlate at (3.4) to –NH, multiple singlate at (4.5) to –NH(amide), singlate at 2.5 ppm to CH_2**,** single at 1.0ppm to CH_3**,** singles at 11.3 ppm to OH (COOH). (151-153)

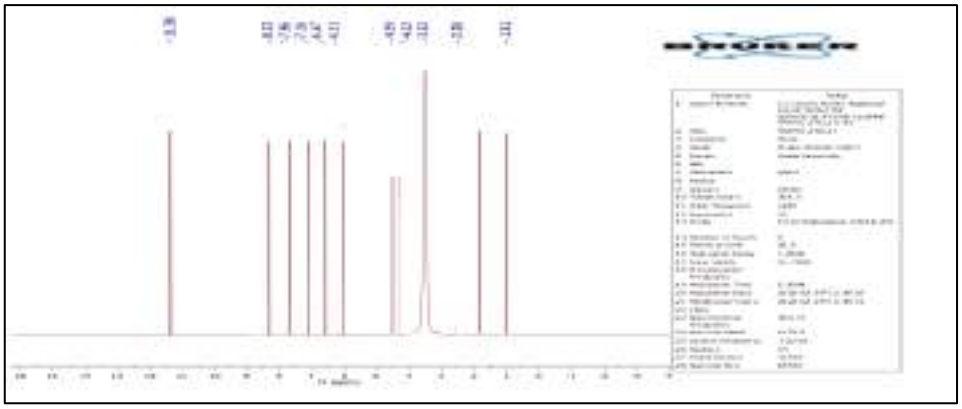


Figure (4- 287): ^{1}HNMR spectrum of copolymer(54) (DMA-CO-CAN) with compound(35).

^{13}C-NMR spectrum of copolymer(54) (DMA-CO-CAN) with compound(35).

The signals of olefinic and aromatic carbons appear in the third region between 111 and 134 ppm, single related to C-N at 56 ppm, singles related to C=O (amide) at 164 ppm, singles related to C=S at 200-205 ppm, singles related to C=O (acid) at 180 ppm, singles related to CH_3 at 18 ppm, single related to C=N at 143 ppm. (151-153)

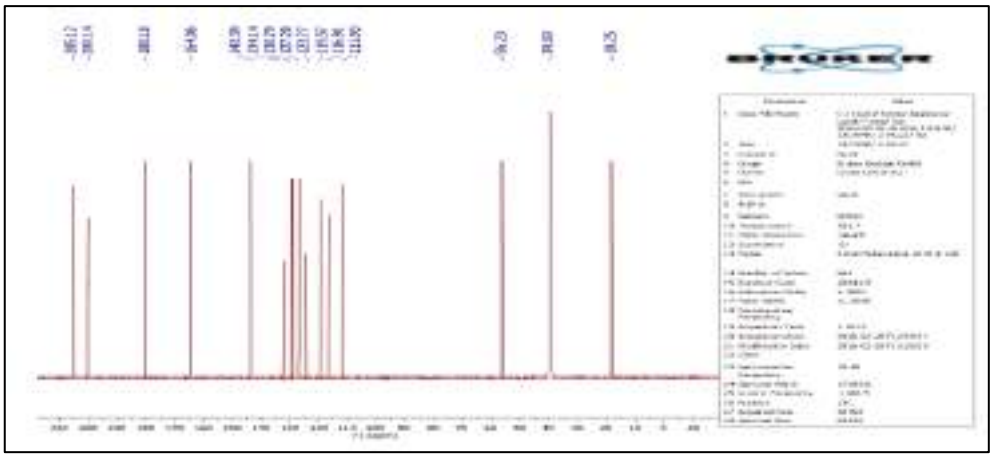
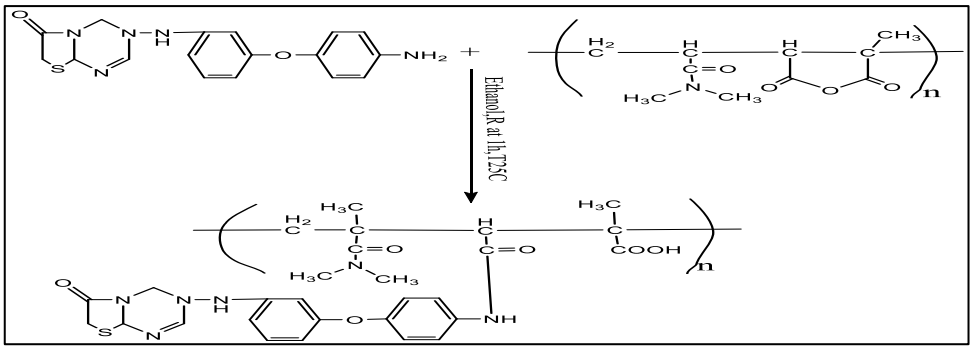


Figure (4- 288): ^{13}C-NMR spectrum of copolymer(54) (DMA-CO-CAN) with compound(35).

4.38 *Synthesis* of copolymer (DMA-CO-CAN) with compounds (37-40).

4.38.1 Synthesis of copolymer(55) (DMA-CO-CAN) with compound(37).



Scheme (4-102): synthesis of copolymer(55) (DMA-CO-CAN) with compound(37).

FTIR spectrum of copolymer(55) (DMA-CO-CAN) with compound(37).

The FTIR spectrum of copolymer(55) (DMA-CO-CAN) with compound(37) as shown in (fig.4-289) which indicates absorption bands at 3435 Cm^{-1} to OH overlapping with –NH stretching, absorption band at 3174 Cm^{-1} to C-H (aromatic), absorption band at 2954 cm^{-1} to C-H (aliphatic), absorption band at 1539 Cm^{-1} to C=N, absorption band at 678 Cm^{-1} to C-S, absorption band at 1539 Cm^{-1} to C=C (aromatic), absorption band at 1274 Cm^{-1} to C-N, absorption band at 1695 Cm^{-1} to C=O (acid), absorption band at 1633 Cm^{-1} to C=O(amide), absorption band at 1336Cm^{-1} to CH_3**,** absorption band at 1180 Cm^{-1} to C-O.(151-153)

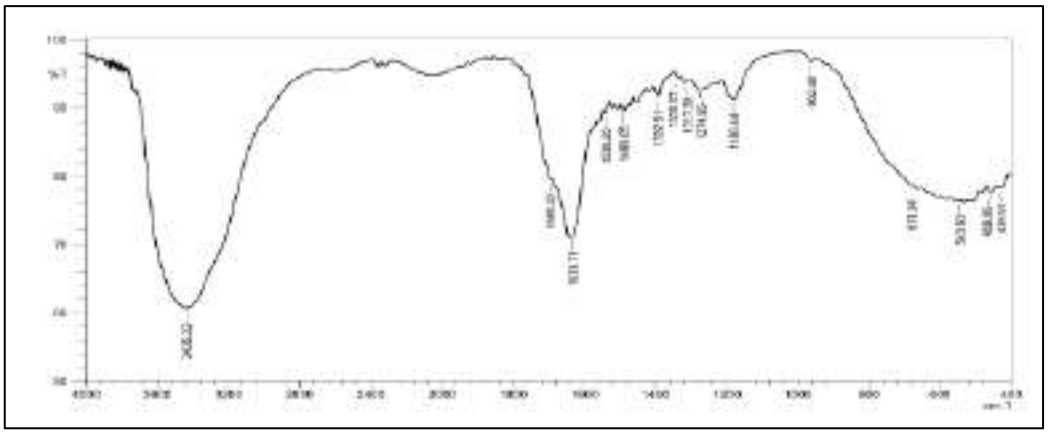


Figure (4- 289): FTIR spectrum of copolymer(55) (DMA-CO-CAN) with compound(37).

^{1}HNMR spectrum of copolymer(55) (DMA-CO-CAN) with compound(37).

^{1}HNMR spectrum of copolymer(55) (DMA-CO-CAN) with compound(37) in (fig.4-290) singles at (6.5-8.3 δ ppm) to (6H, phenyl ring), multiple singlate at (3.2) to –NH, singlate at (4.5) to –NH(amide), singlate at 2.5 ppm to CH_2**,** single at 1.0 ppm to CH_3**,** singles at 5.7 ppm to OH (COOH). (151-153)

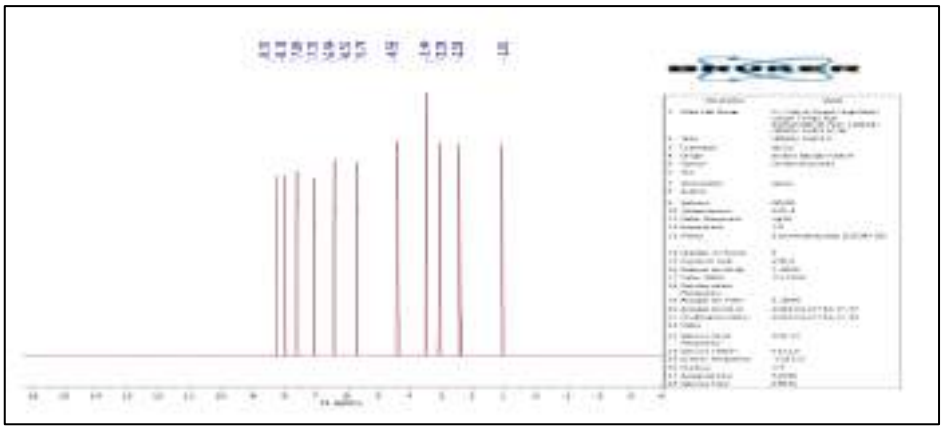


Figure (4- 290): ^{1}HNMR spectrum of copolymer(55) (DMA-CO-CAN) with compound(37).

^{13}C-NMR spectrum of copolymer(55) (DMA-CO-CAN) with compound(37).

The signals of olefinic and aromatic carbons appear in the third region between 128 and 135 ppm, single related to C=N at 156 ppm, single related to C-N at 63 ppm, single related to C-S at 56 ppm, single relates to C=O (amide) at166- 174 ppm, single relates to C=O (acid) at 182 ppm, single related to CH_3 18 ppm. (151-153)

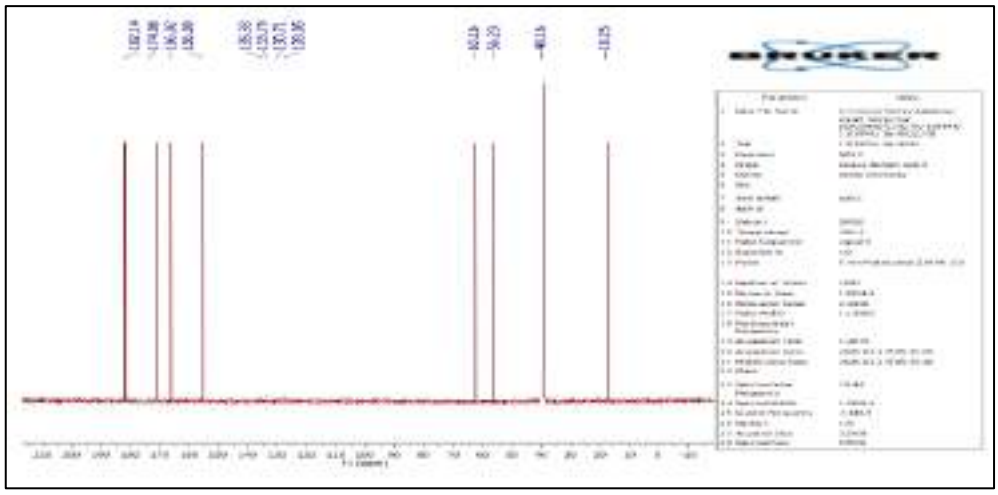
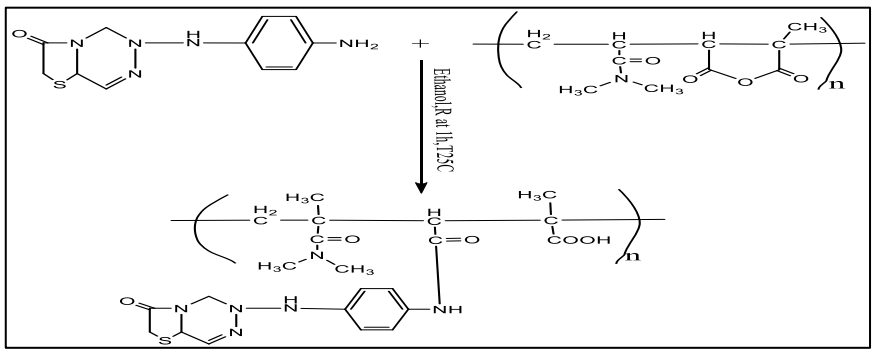


Figure (4- 291): ^{13}C-NMR spectrum of copolymer(55) (DMA-CO-CAN) with compound(37).

4.38.2 Synthesis of copolymer(56) (DMA-CO-CAN) with compound(38).



Scheme (4-103): synthesis of copolymer(56) (DMA-CO-CAN) with compound(38). FTIR spectrum of copolymer(56) (DMA-CO-CAN) with compound(38).

The FTIR spectrum of copolymer(56) (DMA-CO-CAN) with compound(38) as shown in (fig.4-292) which indicates absorption bands at 3421Cm^{-1} to over lapping with –NH stretching, absorption band at 3114 Cm^{-1} to C-H (aromatic), absorption band at 2976 cm^{-1} to C-H (aliphatic), absorption band at 1517 Cm^{-1} to C=N, absorption band at 680 Cm^{-1} to C-S, absorption band at 1452Cm^{-1} to C=C (aromatic), absorption band at 1222 Cm^{-1} to C-N, absorption band at 1712 Cm^{-1} to C=O (acid), absorption band at 1645 Cm^{-1} to C=O(amide), absorption band at 1390 Cm^{-1} to CH_3**,** absorption band at 1134 Cm^{-1} to C**-**O. (151-153)

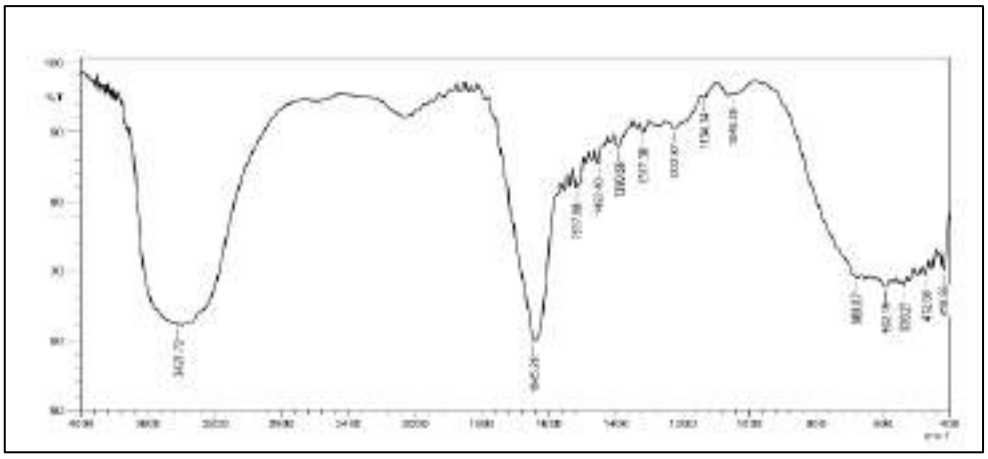


Figure (4- 292): FTIR spectrum of copolymer(56) (DMA-CO-CAN) with compound(38).

^{1}HNMR spectrum of copolymer(56) (DMA-CO-CAN) with compound(38).

^{1}HNMR spectrum of copolymer(56) (DMA-CO-CAN) with compound(38) in (fig.4-293) singles at (6.5-8.3 δ ppm) to (4H, phenyl ring), multiple singlate at (3.5) to –NH, singlate at (4.5) to –NH(amide), singlate at 2.5 ppm to CH_2**,** single at 1.0 ppm to CH_3**,** singles at 5.8 ppm to OH (COOH). (151-153)

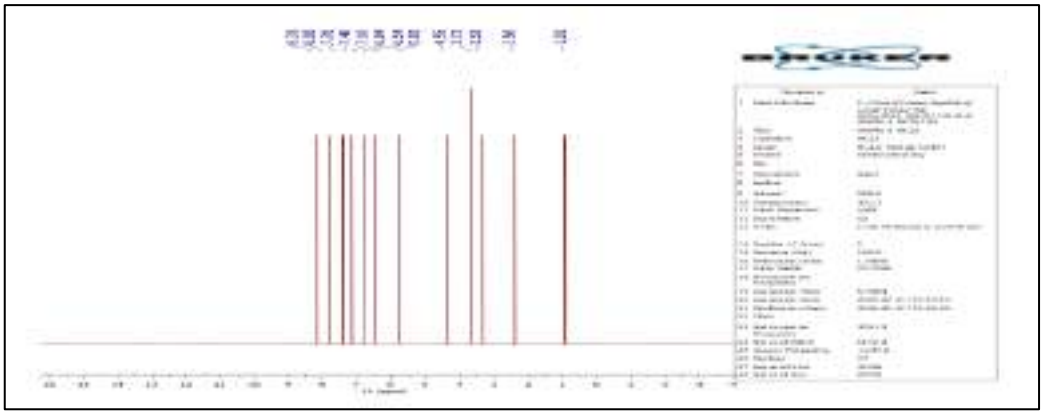


Figure (4- 293): ^{1}HNMR spectrum of copolymer(56) (DMA-CO-CAN) with compound(38).

^{13}C-NMR spectrum of copolymer(56) (DMA-CO-CAN) with compound(38).

The signals of olefinic and aromatic carbons appear in the third region between 126 and 135 ppm, single related to C=N at 156 ppm, single related to C-N at 63 ppm, single related to C-S at 56 ppm, single relates to C=O (amide) at166- 174 ppm, single relates to C=O (acid) at 182 ppm, single related to CH_3 18 ppm. (151-153)

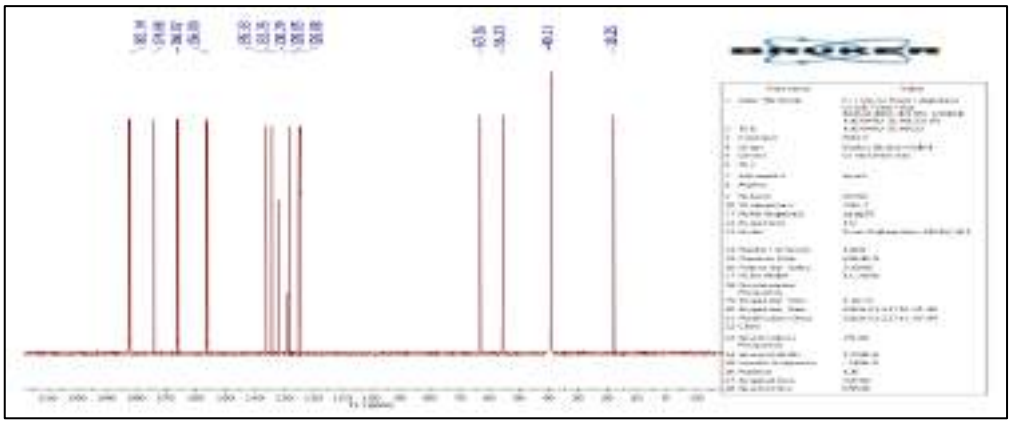
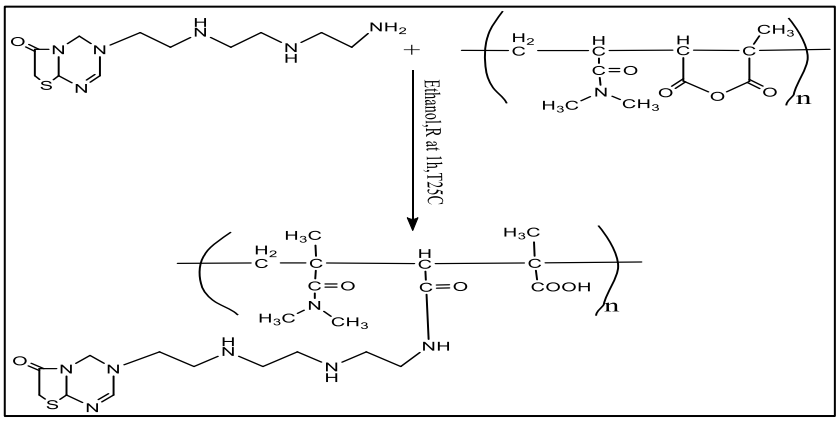


Figure (4- 294): ^{13}C-NMR spectrum of copolymer(56) (DMA-CO-CAN) with compound(38).

4.38.3 Synthesis of copolymer(57) (DMA-CO-CAN) with compound(39).



Scheme (4-104): synthesis of copolymer(57) (DMA-CO-CAN) with compound(39).

FTIR spectrum of copolymer(57) (DMA-CO-CAN) with compound(39).

The FTIR spectrum of copolymer(57) (DMA-CO-CAN) with compound(39) as shown in (fig.4-295) which indicates absorption bands at 3419Cm^{-1} to OH over lapping with –NH stretching, absorption band at 3117 Cm^{-1} to C-H (aromatic), absorption band at 2972 cm^{-1} to C-H (aliphatic), absorption band at 1564Cm^{-1} to C=N, absorption band at 623 Cm^{-1} to C-S, absorption band at 1446 Cm^{-1} to C=C (heterocyclic ring), absorption band at 1249 Cm^{-1} to C-N, absorption band at 1641 Cm^{-1} to C=O (acid), absorption band at 1625 Cm^{-1} to C=O(amide), absorption band at 1327 Cm^{-1} to CH_3**,** absorption band at 1138 Cm^{-1} to C-O. (151-153)

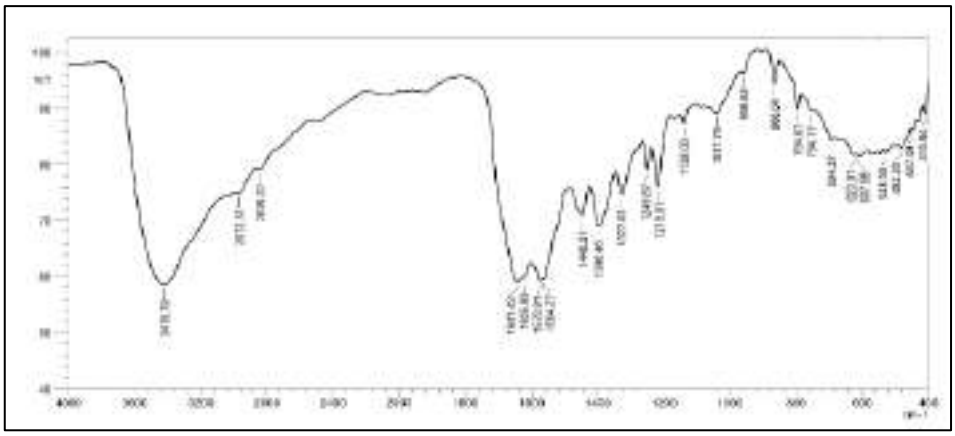


Figure (4- 295): FTIR spectrum of copolymer(57) (DMA-CO-CAN) with compound(39).

^{1}HNMR spectrum of copolymer(57) (DMA-CO-CAN) with compound(39).

^{1}HNMR spectrum of copolymer(57) (DMA-CO-CAN) with compound(39) in (fig.4-296) singles at (6.5-8.3 δ ppm) to (4H, heterocyclic ring)), multiple singlate at (3.2) to –NH, singlate at (4.5) to –NH(amide), singlate at 2.0-2.5 ppm to CH_2**,** single at 1.0 ppm to CH_3**,** singles at 5.6 ppm to OH (COOH). (151-153)

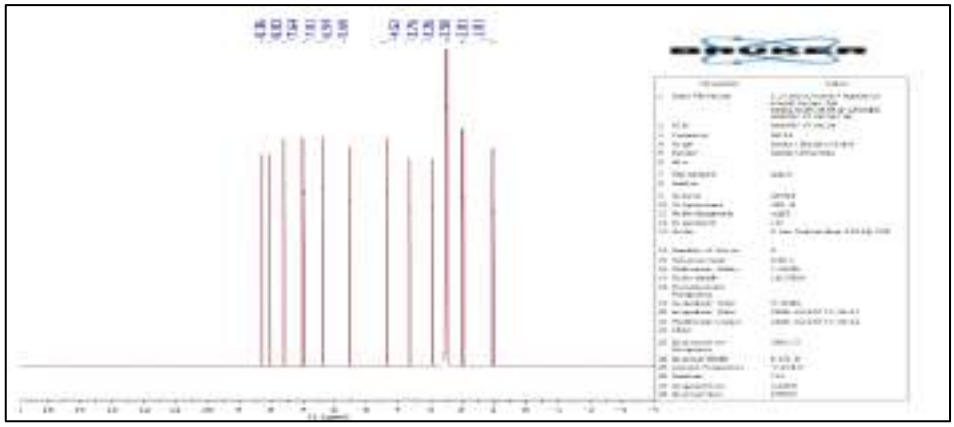


Figure (4- 296): ^{1}HNMR spectrum of copolymer(57) (DMA-CO-CAN) with compound(39).

^{13}C-NMR spectrum of copolymer(57) (DMA-CO-CAN) with compound(39).

The signals of olefinic and aromatic carbons appear in the third region between 126 and 135 ppm, single related to C=N at 156 ppm, single related to C-N at 63 ppm, single related to C-S at 56 ppm, single relates to C=O (amide) at166- 174 ppm, single relates to C=O (acid) at 182 ppm, single related to CH_3 18 ppm. (151-153)

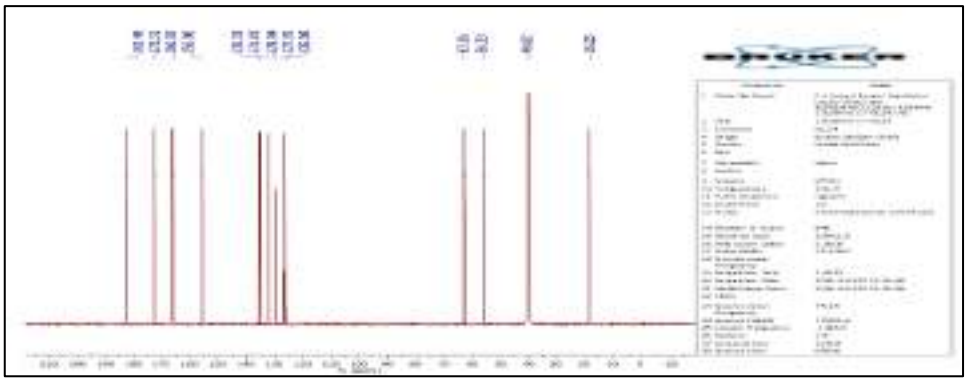
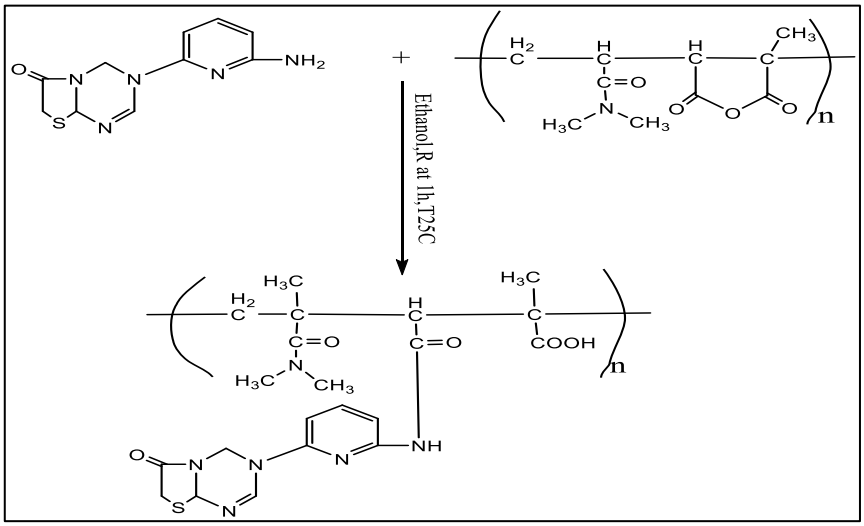


Figure (4- 297): ^{13}C-NMR spectrum of copolymer(57) (DMA-CO-CAN) with compound(39).

4.38.4 Synthesis of copolymer(58) (DMA-CO-CAN) with compound(40).



Scheme (4-105): synthesis of copolymer(58) (DMA-CO-CAN) with compound(40).

FTIR spectrum of copolymer(58) (DMA-CO-CAN) with compound(40).

The FTIR spectrum of copolymer(58) (DMA-CO-CAN) with compound(40) as shown in (fig.4-298) which indicates absorption bands at 3462 Cm^{-1} to OH and 3414 Cm^{-1} with –NH stretching, absorption band at 3117 Cm^{-1} to C-H (aromatic), absorption band at 2974 cm^{-1} to C-H (aliphatic), absorption band at 1579 Cm^{-1} to C=N, absorption band at 615 Cm^{-1} to C-S, absorption band at 1541 Cm^{-1} to C=C (aromatic), absorption band at 1320 Cm^{-1} to C-N, absorption band at 1701 Cm^{-1} to C=O (acid), absorption band at 1637 Cm^{-1} to C=O(amide), absorption band at 1377 Cm^{-1} to CH_3, absorption band at 1128 Cm^{-1} to C-O. (151-153)

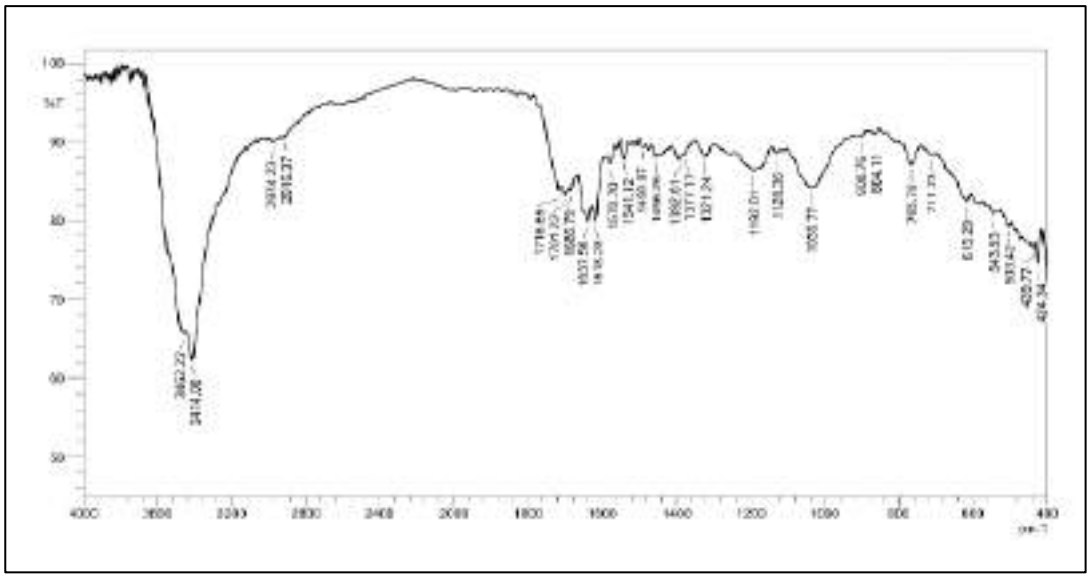


Figure (4- 298): FTIR spectrum of copolymer(58) (DMA-CO-CAN) with compound(40).

^{1}HNMR spectrum of copolymer(58) (DMA-CO-CAN) with compound(40).

^{1}HNMR spectrum of copolymer(58) (DMA-CO-CAN) with compound(40) in (fig.4-299) singles at (3.2-3.4 ppm) to $–NH_2$, singles at (2.5 δ ppm) to CH_2**,** single at (6.1 δ ppm) to CH(COOH), singles at (1.2 δ ppm) to CH_3. (151-153)

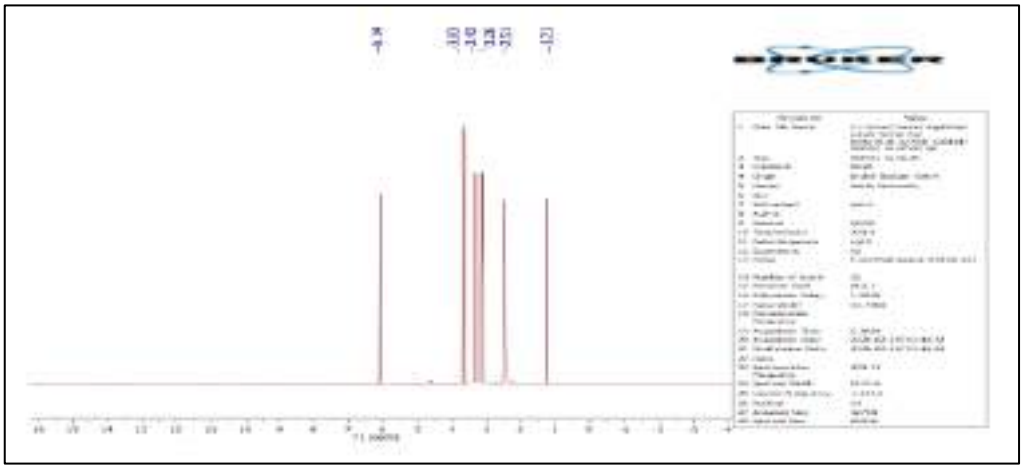


Figure (4- 299): ^{1}HNMR spectrum of copolymer(58) (DMA-CO-CAN) with compound(40).

^{13}C-NMR spectrum of copolymer(58) (DMA-CO-CAN) with compound(40).

The single related to C=N at 148 ppm, single related to C-N at 82-84 ppm, single related to C-S at 55 ppm, single related to C=O at 168 ppm. (151-153)

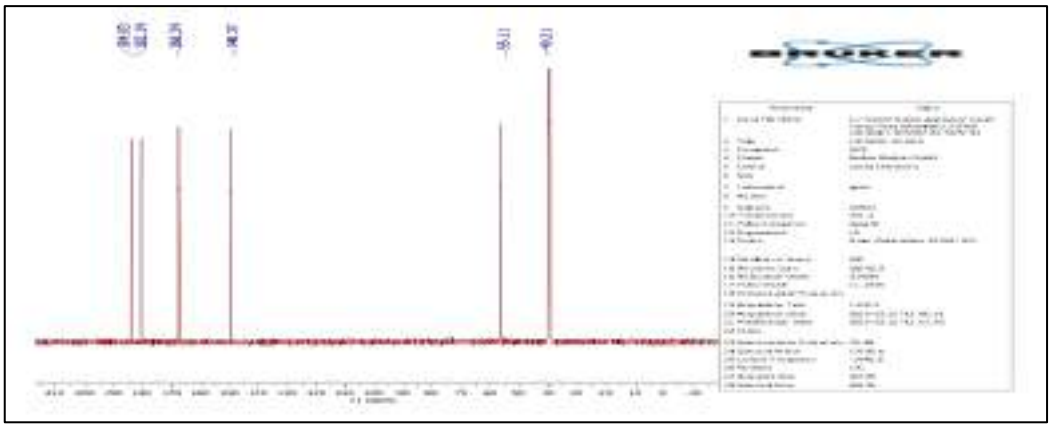


Figure (4- 300): ^{13}C-NMR spectrum of copolymer(58) (DMA-CO-CAN) with compound(40).

4.39 Thermo gravimetric analysis (TGA)

Research Thermogravimetric Analysis (TGA) involves evaluating changes in mass only as function to temperature. This is widely utilized check for temperatures of degradation, chemical content consumed, amounts of inorganic as well as organic sections found in a sample, as well as solvent remains evaluation. It employs a sensitive electronic balance from which the sample is suspended in a furnace controlled by a temperature programmer. The thermal properties of the copolymers were investigated by means of Thermogravimetric analysis (TGA) in nitrogen atmosphere at heating rate of 10ºC/ min.

Tiny volatile molecules that lead first peak at T = (80 °C), then unreacted monomers. The second peak causes quick degradation of a copolymers at T =400 °C. It has been shown which heterocyclic polymers having at least one β-hydrogen decompose to an olefin as well as acid end groups through a cyclic intermolecular transition state.

After preheating weight loss can be caused by contamination of samples with traces of solvents. All phenomena observed in the temperature range from 15 to 350ºC could be referred to water evaporation, melting of residual monomer in the range 383-424ºC, breaking of H-bonds and starting of the polycondensation or cross-linking. The form of TGA curves allows the assumption, that the weight loss happening at 70ºC due to breaking of the H-bond in backbone of heterocyclic polymers. This TGA plot shows the decomposition of heterocyclic polymers in

nitrogen at a heating rate of 10ºC /min. The decomposition occurs in three mass-loss steps with the release of water carbon monoxide and carbon dioxide. The TGA curve provides the decomposition rate and is helpful for evaluating the mass-loss steps accurately. The results such as Ti, Top, Tf, T50%, T Residue at 800 ºC as well as the production of char at 600ºC is epitomized in Table (4-1). This temperature of 50 percent loss of weight (heterocyclic polymers) for a typical index for heterocyclic polymers thermal stabilization for all around 800ºC.

The temperatures of 50% weight loss of heterocyclic polymers as a standard indication for thermal stability of copolymers were all above 800°C, which indicates excellent thermal stability of copolymers. The stability of the copolymers increased with the increase in content of aromatic rings.

The char yields of these copolymers at 600°C between 9 % and 20 % in nitrogen, which was good for copolymers. All the copolymers left more than 20 % char yields at 800°C in nitrogen atmosphere, which indicate they could meet high temperature resistant requirements as some special materials in fiber reinforcements, fire retardants and curing agents However, the weight residue of copolymer(2) (17) and copolymer(4) (18) at 800°C were the highest for any copolymers of this series, (17% and18 %) respectively.

Through TGA experiments, it was found that both rates of the first weight monomer. Then an exothermic behavior observed at high temperature region. The results are summarized in Table (4-2). These results indicated that the heterocyclic polymers containing phenyl group as substituent in the heterocyclic ring had maximum thermal stability. It seems that using a bulkier substituent in the 4-position of the heterocyclic ring of diamine monomers causes improvement of solubility and thermal stability of resulting copolymers.

The study of copolymers decomposition allows us to understand the thermal stability of the material, as well as direct us to the creation of new and better structures with greater thermal resistance. It was proposed that the thermal decomposition of heterocyclic polymers occurs stepwise. At the first stage of the

destruction, aromatic compounds are formed (benzene, derivatives of phenol, aniline). On the second step - low-molecular compounds (hydrocarbons, carbon dioxide, aliphatic amines, etc.), followed by carbonization. At higher temperatures, lower molecular weight compounds are identified. This may be because the main chain scission is less targeted to solely the low energy bonds. This leads to other volatile products such as CO, CO_2 or diphenyl ether, which are identified at 650 °C. At 750 °C and higher, dibenzofuran, biphenyl and naphthalene are identified. Phenol has been identified as the main decomposition product at temperatures above 650 °C [3]. Another major decomposition product is reported to be furan. This can be associated to a ring closure reaction occurring between diradicals at the ether groups

Further its spontaneous splitting with chain end split there in thermal degeneration for copolymers as well as clarified that its immediate at one-step radical transition raised by temperature suggests that β splitting happens on a chain end before radical transition since the β split rate is quicker as temperature increases. for this situation of a copolymers, there is an aliphatic chain, in which at least two carbon atoms are closest, suggesting that the likelihood of spontaneous scission is so small. The disintegration started with the disintegration of hydroxyl as well as carboxylic end groups of heterocyclic polymers, as well as a sharp decrease at molecular weight through water, was also observed in the comparable aliphatic polymer as heterocyclic polymers at these temperatures.

Table (4- 1): Some Thermal Stability Characteristics Curves Thermal Gravimetric Analysis (TGA) of polymers represents the temperature of decomposition.

Dendrimers	T_i C°	T_{op1} C°	T_f C°	$T_{50\%}$ C°	Residue at °C800	Char %At 600°C
copolymer 1	**300**	**400**	**700**	**390**	**6**	**9**
copolymer 2	**150**	**325**	**700**	**380**	**17**	**19**
copolymer 3	**350**	**150**	**700**	**400**	**10**	**15**
copolymer 4	**145**	**340**	**700**	**325**	**18**	**23**
Copolymer 5	**300**	**420**	**700**	**360**	**10**	**15**
Copolymer 6	**300**	**430**	**705**	**400**	**10**	**15**
Copolymer 7	**154**	**350**	**700**	**360**	**18**	**20**
Copolymer 8	**310**	**410**	**700**	**405**	**10**	**15**
Copolymer 9	**300**	**400**	**710**	**390**	**12**	**15**
Copolymer 10	**305**	**400**	**700**	**395**	**15**	**20**

This is the major disintegration.

DT: disintegration temperature.

Ti: Initial disintegration temperature.

Top: Optimum disintegration temperature.

Tf: Final disintegration temperature. The final degree of dissociation temperature.

T50%: Temperature of 50% weight loss, acquired by TGA.

Char% at 600 °C.

T Residual weight ratio at 800 °C in Argon from TGA.

4.40 Differential Scanning calorimeter analysis (DSC) study

DSC measures the amount of energy absorbed or released by a sample as it is heated, cooled or held at a constant temperature. It is achieved by placing two temperature probes in the furnace and simultaneously measuring the temperature of the sample and furnace temperature while heating the sample at a constant rate. This technique is used for polymer and pharmaceutical applications. The DSC will be resulted in a heat input against temperature curve. Differential Scanning Calorimetry, is a technique of thermal analysis that investigates how material's heat capacity (Cp) is transformed by temperature. A known mass sample is heated or cooled and the variations in its heat capacity are observed as alterations in the heat flow. This allows to reveal transitions such as melts glass transitions (Tg), and the melting point (Tm) the degree of crystallization (Tc).

DSC analysis revealed glass transition temperatures around (66-110^{o}C) that are typical for structures of this type. Differences between the numbers obtained during first and second heating and cooling could be referred to the changes happening in materials. The observation of "Tm" can be explained by the same reasons, as it does not appear during the second cycle. Crystallization of heterocyclic polymer synthesized is explained by its higher molecular weight and crosslinking.

The results of (copolymer 1) showed the curve of a sharp exothermic peak in (fig.4-301) the value of the glass transition (Tg) of the mixture (66°C) indicating that the flow of temperature and then increase the rate of absorption of the sample to reach the melting point (Tm) at (583°C), is completely dissolved and then the rate

of absorption of the sample to the heat and through the curve was set the degree of crystallization (Tc) of the mixture (335°C).

The results of (copolymer 2) showed the curve of a sharp exothermic peak in (fig.4-302) the value of the glass transition (Tg) of the mixture (65°C), indicating an increase in the flow of temperature and then increase the rate of absorption of the sample to the temperature until it reaches the melting point (Tm) at (450°C). In the curve, the crystallization rate (Tc) was determined for the mixture (310°C).

The results of (copolymer 3) showed The curve of a sharp exothermic peak in (fig.4303) the value of the glass transition (Tg) of the mixture (45°C), indicating an increase in the flow of temperature and then increase the rate of absorption of the sample to the temperature until the melting point (Tm) at (483°C) if completely melted and then the rate of absorption of the sample to heat and by the curve was set the crystallization rate (Tc) of the mixture (340°C).

The results of (co polymer 4) showed The curve of a sharp exothermic peak in (fig.4-304) the value of the glass transition (Tg) of the mixture (106°C), indicating an increase in the flow of temperature and after that the rate of absorption of the sample to the temperature until it reaches the melting point (Tm) at (445°C) and then the rate of absorption of the sample to heat and by the curve of the formation of (Tc) of the mixture (305°C).

The results of (copolymer 5) showed The curve of a sharp exothermic peak in (fig.4-305) the value of the glass transition (Tg) of the mixture (110°C), indicating an increase in the flow of temperature and after that the rate of absorption of the sample to the temperature until it reaches the melting point (Tm) at (487°C) and then the rate of absorption of the sample to heat and by the curve of the formation of (Tc) of the mixture (340°C).

The results of (copolymer 6) showed The curve of a sharp exothermic peak in (fig.4-306) the value of the glass transition (Tg) of the mixture (107°C), indicating an increase in the flow of temperature and after that the rate of absorption of the sample to the temperature until it reaches the melting point (Tm) at 474(°C) and then

the rate of absorption of the sample to heat and by the curve of the formation of (Tc) of the mixture (345°C).

The results of (copolymer 7) showed The curve of a sharp exothermic peak in (fig.4-307) the value of the glass transition (Tg) of the mixture (109°C), indicating an increase in the flow of temperature and after that the rate of absorption of the sample to the temperature until it reaches the melting point (Tm) at (450°C) and then the rate of absorption of the sample to heat and by the curve of the formation of (Tc) of the mixture (306°C).

The results of (copolymer 8) showed The curve of a sharp exothermic peak in (fig.4-308) the value of the glass transition (Tg) of the mixture (102°C), indicating an increase in the flow of temperature and after that the rate of absorption of the sample to the temperature until it reaches the melting point (Tm) at (473°C) and then the rate of absorption of the sample to heat and by the curve of the formation of (Tc) of the mixture (351°C).

The results of (copolymer 9) showed The curve of a sharp exothermic peak in (fig.4-309) the value of the glass transition (Tg) of the mixture (102°C), indicating an increase in the flow of temperature and after that the rate of absorption of the sample to the temperature until it reaches the melting point (Tm) at (473°C) and then the rate of absorption of the sample to heat and by the curve of the formation of (Tc) of the mixture (361°C).

The results of (copolymer 10) showed The curve of a sharp exothermic peak in (fig.4-310) the value of the glass transition (Tg) of the mixture (104°C), indicating an increase in the flow of temperature and after that the rate of absorption of the sample to the temperature until it reaches the melting point (Tm) at (480°C) and then the rate of absorption of the sample to heat and by the curve of the formation of (Tc) of the mixture (304°C)(154).

Table (4- 2): Shows the Thermal parameter obtained from DSc.

Dendrimers	Tg (c^o)	Tm (c^o)	TC (c^o)
copolymer 1	66	583	335
copolymer 2	65	450	310
copolymer 3	45	483	340
copolymer 4	106	445	305
copolymer 5	110	487	340
copolymer 6	107	474	345
copolymer 7	109	450	306
copolymer 8	102	473	351
copolymer 9	102	473	361
copolymer 10	104	480	304

Tg: Temperature Glass Transition

Tm: Melting Point

Tc: Degree of Crystallization

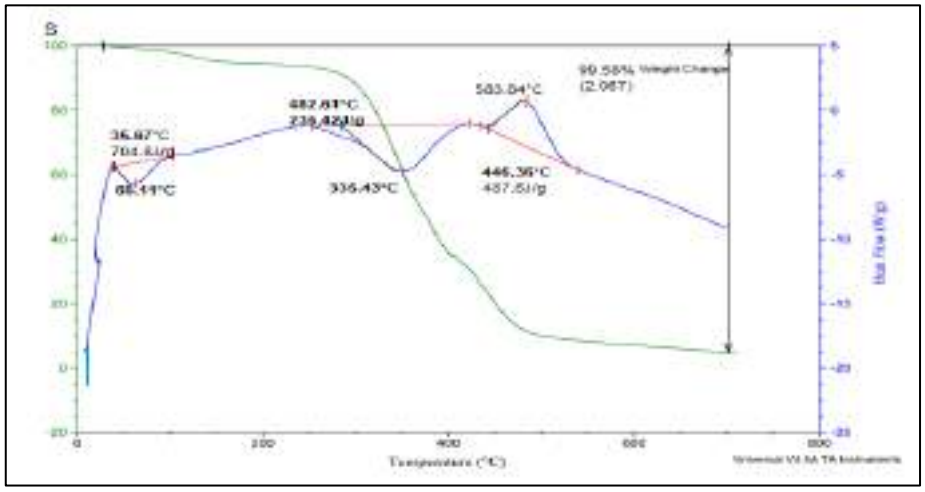


Figure (4- 301): TGA and DSC curve for copolymer (1)

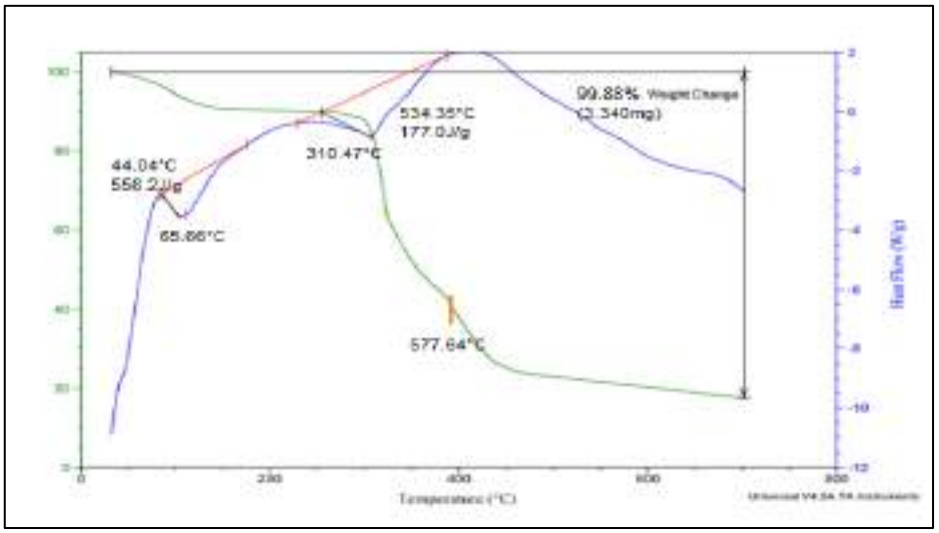


Figure (4- 302): TGA and DSC curve for copolymer (2).

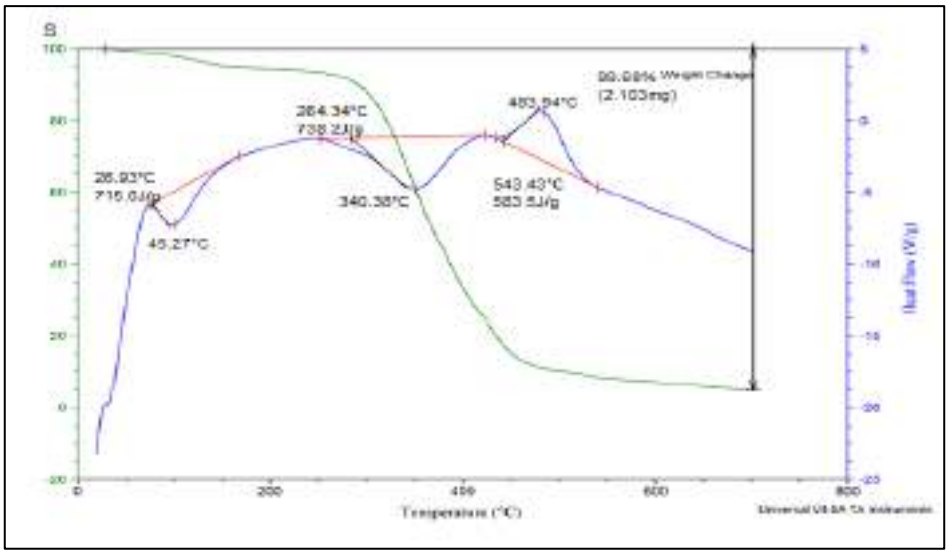


Figure (4- 303): TGA and DSC curve for copolymer (3).

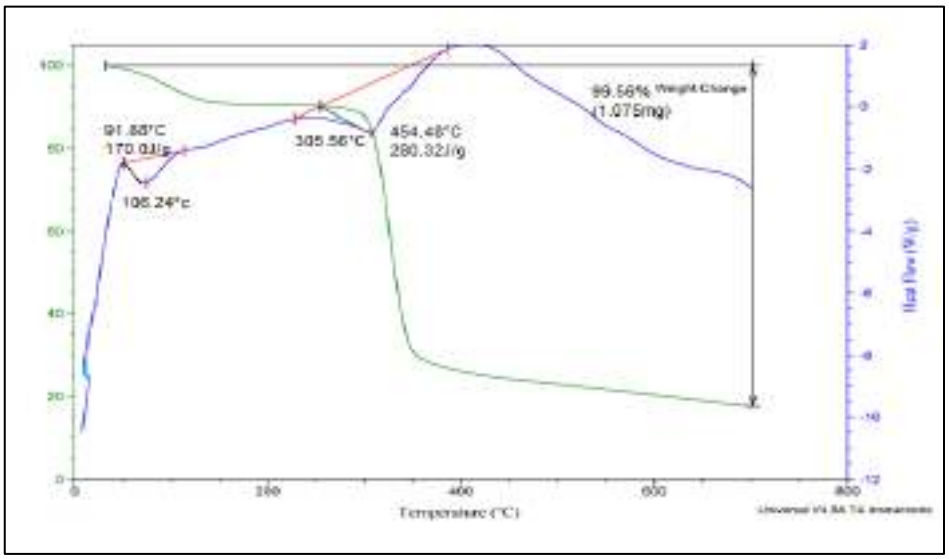


Figure (4- 304): TGA and DSC curve for copolymer (4).

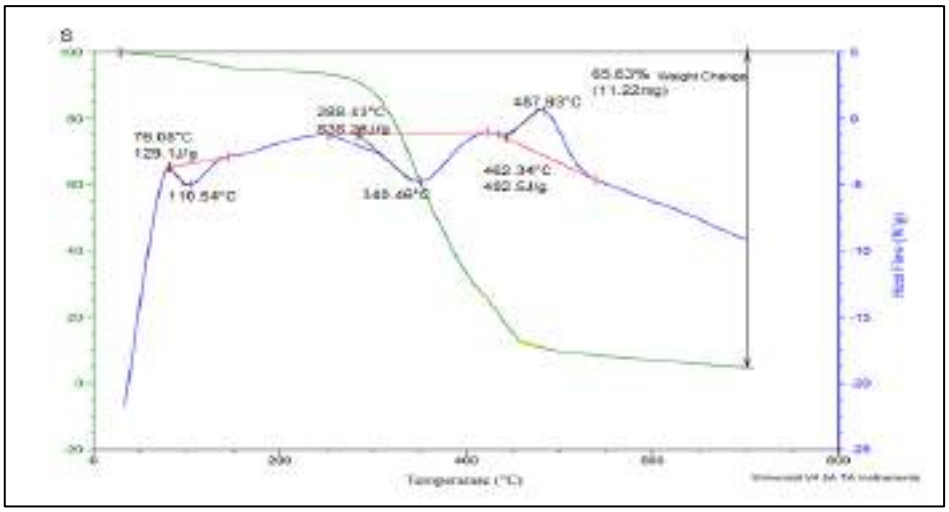


Figure (4- 305): TGA and DSC curve for copolymer (5)

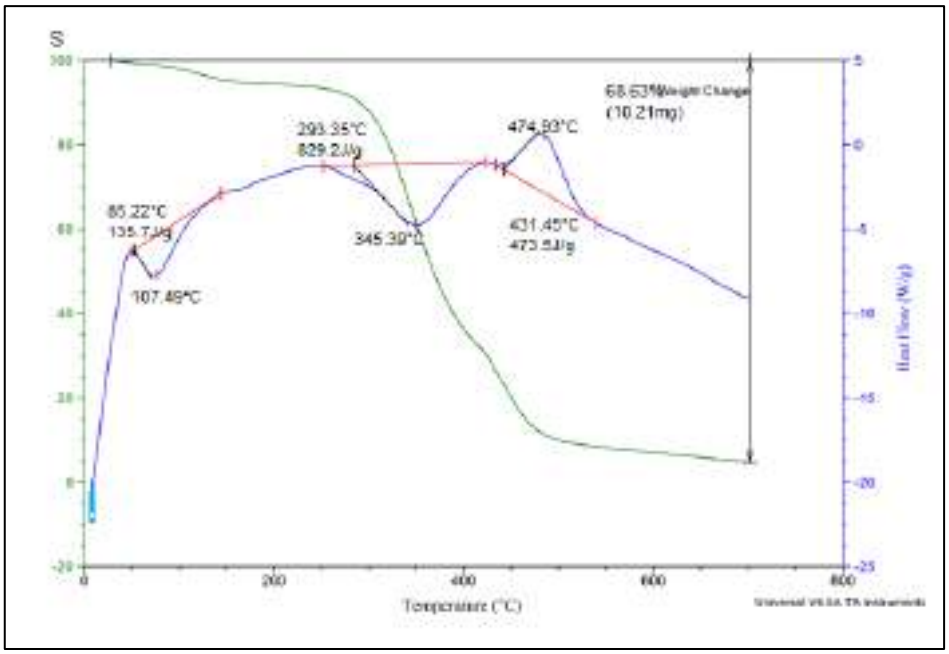


Figure (4- 306): TGA and DSC curve for copolymer (6)

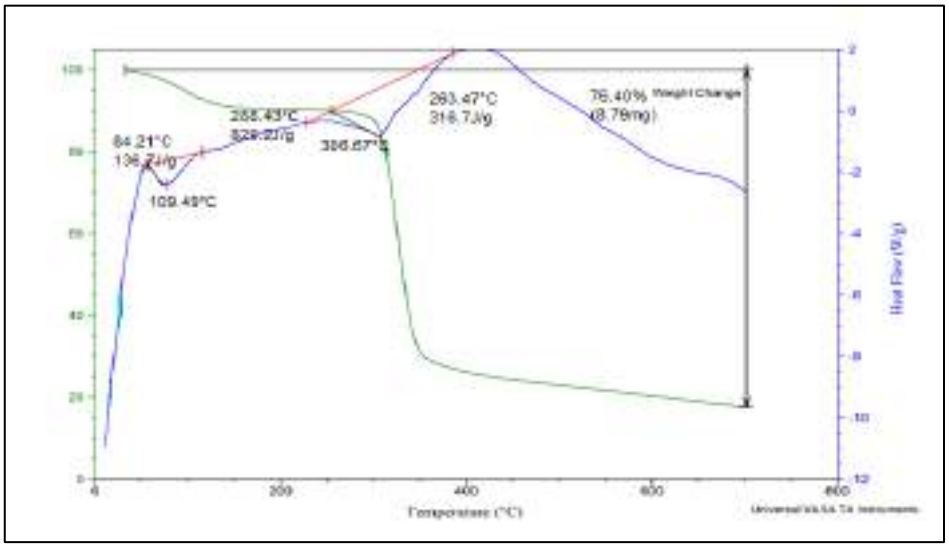


Figure (4- 307): TGA and DSC curve for copolymer (7)

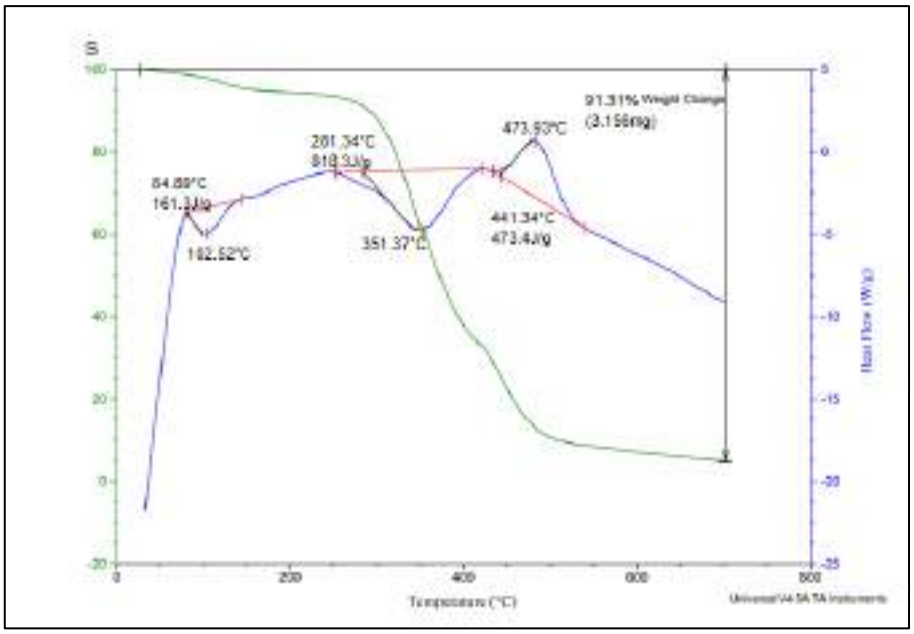


Figure (4- 308): TGA and DSC curve for copolymer (8)

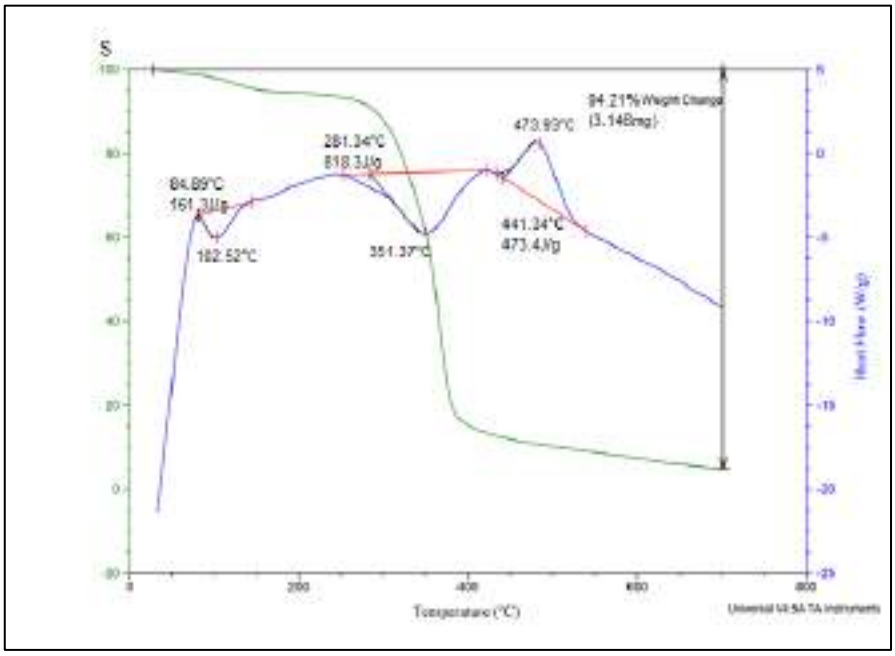


Figure (4- 309): TGA and DSC curve for copolymer (9).

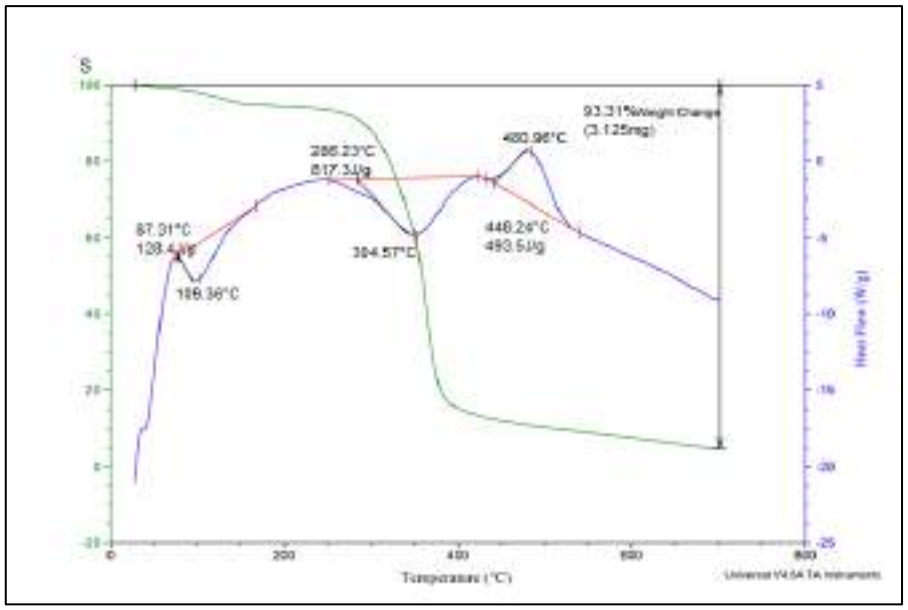


Figure (4- 310): TGA and DSC curve for copolymer (10)

4.41 Molecules Library Preparation

The newly copolymers **(1, 2, 3, 4, 5)** were synthesized and characterization to using in molecular docking process, Chemdraw Ultra 12.0 (https://chemdraw pro.software.informer.com/12.0/) software was utilized to generate the 3D structures of the copolymers **(1, 2, 3, 4, 5)** and followed by energy minimization. The structures were pre-optimized with semi-empirical AM1 method using Hyperchem 8.08 software. The structures were optimized using density functional theory DFT method by employing the B3LYP/6-31G basis set to obtain the most stable conformation. The convergent value of maximum force, root-mean-square (RMS) force, maximum displacement and RMS displacement are set by default and achieved "YES". All values are positive after calculating vibrational frequencies for ligands; those results indicate that the ligands are stable. The optimized structures were combined in one database on MOE software (Molecular Operating Environment (MOE), 2019) in order to study the affinity of ligands (fig.4-311). Also, (fig.4-312) illustrates the schematic representation of the docking procedure, analysis of ligands, and reactivity.

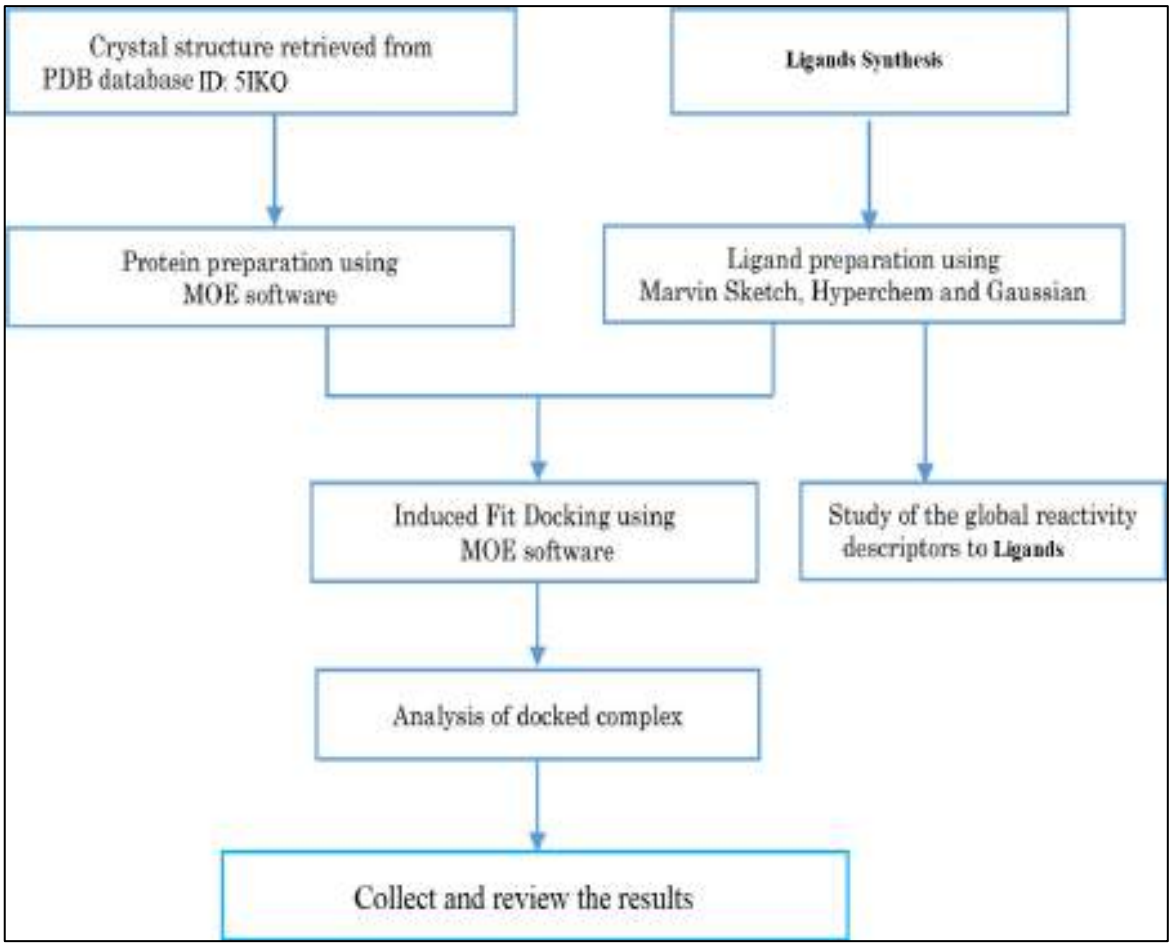


Figure (4- 311): Schematic representation of the docking procedure, analysis of ligands and reactivity.

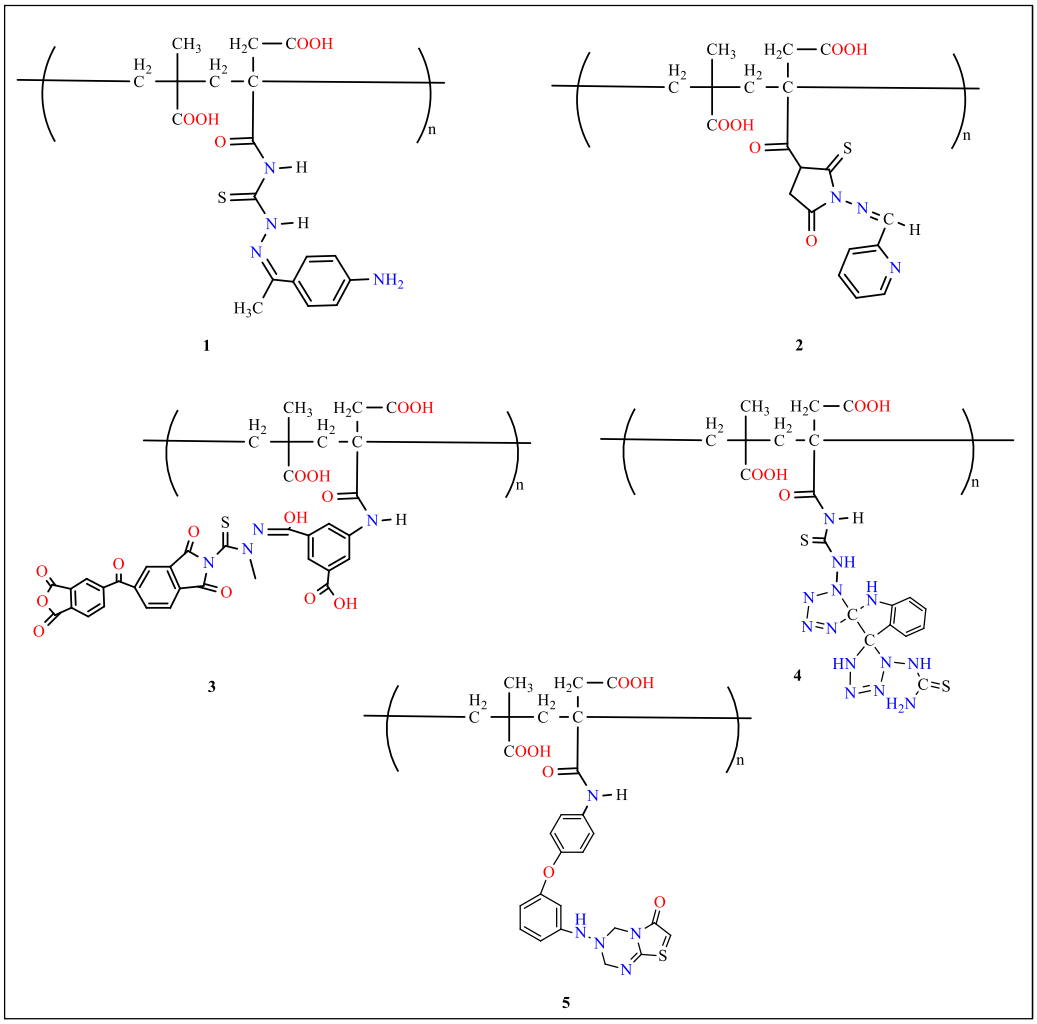


Figure (4- 312): 2D structures of selected copolymers (ligands).

4.42 Receptors preparation

The crystal structures of the proteins (5IKQ) (fig.4-313) was selected from the Protein Data Bank. Because the water molecule in the active site of the target proteins plays an important role, it was inserted in the active sites to ensure making a hydrogen bond between the ligand and the target. After that, the proteins structure was prepared by correcting the missing bonds, which were broken in X-ray diffraction, and then the hydrogen atoms were added also Importantly, PDB is a trusted source for the crystal structure of biological macromolecules worldwide.



Figure (4- 313): Crystal structures of the 5IKQ proteins.

4.43 Ligand–Protein molecular docking

All the docking and scoring calculations were performed using the molecular operation environment software (MOE) (Molecular Operating Environment (MOE), 2015). The crystal structure of the protein (5IKQ) (fig.4-314) at a resolution of 2.41 Å was obtained from the Protein Data Bank. A resolution between 1.4 and 2.5 Å is considered a good quality for docking studies. It is known that the best score of RMSD values should be less than 2 Å with an energy score less than or equal to -7 kcal/mol. These two values are often used as criteria to validate the result of the molecular docking.

4.44 Results

Molecular docking is used as a fundamental tool in the drug discovery pipeline. In the present study, MOE software was applied to perform all molecular docking calculations and predict the binding modes of the prepared copolymers (1, 2, 3, 4, 5) with the protein (5IKQ) (fig.4-315). The predicted binding affinities and features of the investigated copolymers (1, 2, 3, 4, 5) toward 5IKQ are listed in the next tables. These tables show the best binding poses of copolymers (1, 2, 3, 4, 5) against target proteins. The 2D and 3D representations of interactions of the inspected compounds with the key amino acid residues of the (5IKQ) proteins are illustrated in the next figures and tables. Copolymers **(**1, 2, 3, 4, 5) showed good binding affinity values (Table 4-3 and Table 4-4) with proteins (5IKQ). The binding and mode of interactions of the copolymers (1, 2, 3, 4, 5) with the (5IKQ) protein are shown in 2D and 3D figures. From the interactions, it has been shown that primarily there are different types of interactions (hydrogen bonding and hydrophobic interactions). Interactions were further examined for bond lengths and hydrogen bonds in the active site and were illustrated in the last figures. The results from these figures showed that copolymers (1, 2, 3, 4, 5) interact with different amino acid residues in three different interactions: H-donor, H-acceptor, and H-pi, as well as two H-acceptor and pi-H interactions with the water and different amino acids. The distance and energy binding of interaction are listed in the next tables.

Table (4- 3): The binding affinity and rmsd result of copolymers with 5IKQ

copolymers	Mseq	Binding Affinity Kcal/mol	Rmsd (Å)	E_conf	E_place	E_score1	E_refine	E_score2
1- pose1	1	-8.86025	2.08114	-78.6068	-14.873	-7.83803	-30.8679	-8.86025
1- pose2	1	-8.75955	1.82947	-68.4186	-17.193	-9.55507	-23.8441	-8.75955
1- pose 3	1	-8.73728	1.90884	-72.1545	-14.4796	-7.87096	-26.1557	-8.73728
1- pose4	1	-8.5055	1.57438	-67.6256	-13.9314	-9.03801	-27.6035	-8.5055
1- pose5	1	-8.42658	2.675783	-81.9659	-13.3956	-9.62877	-29.5028	-8.42658
2- pose1	2	-9.44451	1.671818	40.4138	-19.8614	-10.7862	-36.2559	-9.44451
2- pose2	2	-9.35767	1.810745	26.57492	-14.5323	-6.92877	-34.4458	-9.35767
2- pose3	2	-9.07746	2.036561	35.98328	-15.0122	-8.45539	-33.2926	-9.07746
2- pose4	2	-8.74918	2.519033	32.3657	-19.0868	-9.29892	-27.2741	-8.74918
2- pose5	2	-8.71826	2.986262	19.85469	-17.799	-9.29369	-28.429	-8.71826
3- pose1	3	-10.9057	2.737868	-65.1087	-10.6965	-1.03132	-44.9006	-10.9057
3- pose2	3	-10.1356	2.149911	-28.6178	-8.44451	-0.97669	-31.2845	-10.1356
3- pose3	3	-9.52989	2.269534	-44.6756	-7.73784	-4.65685	-27.5974	-9.52989
3- pose4	3	-9.35724	2.505816	-38.55	-9.11851	-6.31719	-37.378	-9.35724
3- pose5	3	-9.10584	1.834705	-59.3458	-6.44576	-5.42663	-23.6841	-9.10584
4- pose1	4	-9.3609	1.404223	57.64496	-9.86849	-8.39081	-18.3877	-9.3609
4- pose2	4	-8.99693	1.417554	42.31095	-12.6907	-5.98669	-30.1937	-8.99693

copolymers	Mseq	Binding Affinity Kcal/mol	Rmsd (Å)	E_conf	E_place	E_score1	E_refine	E_score2
4- pose3	4	-7.99033	3.163848	34.99519	-14.7753	-3.31437	-15.3159	-7.99033
4- pose4	4	-7.85363	2.40338	40.73356	-11.1429	-4.77025	-11.822	-7.85363
4- pose5	4	-7.44025	2.331456	34.51871	-10.0238	-4.11574	-11.9307	-7.44025
5- pose1	5	-10.3596	3.109696	53.72296	-14.6647	-3.98222	-43.9637	-10.3596
5- pose2	5	-9.78001	2.697975	-100.47	-16.0096	-4.83203	-50.2214	-9.78001
5- pose3	5	-9.54237	2.076265	-124.989	-23.5164	-10.0736	-34.2528	-9.54237
5- pose4	5	-9.48936	2.509375	-126.512	-16.7475	-1.87792	-44.918	-9.48936
5- pose5	5	-9.46836	2.05639	-112.857	-17.5376	-7.46597	-42.8605	-9.46836
Standard	Std	-7.17611	2.096395	-46.0659	-14.1648	-10.165	-37.0982	-7.17611

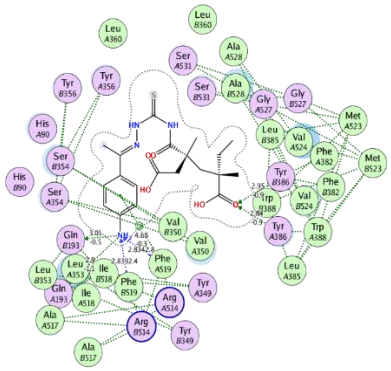
Table (4- 4): Name of copolymers and smiles

Copolymers	Binding Affinity Kcal/mol	Rmsd (Å)	Smile
1- pose1	-8.86025	2.08114	S=C(N/N=C(\C)/c1ccc(N)cc1)NC(=O)[C@@](CC(=O)O)(C[C@@](C(=O)O)(CC)C)C
1- pose2	-8.75955	1.82947	S=C(N/N=C(\C)/c1ccc(N)cc1)NC(=O)[C@@](CC(=O)O)(C[C@@](C(=O)O)(CC)C)C
1- pose 3	-8.73728	1.90884	S=C(N/N=C(\C)/c1ccc(N)cc1)NC(=O)[C@@](CC(=O)O)(C[C@@](C(=O)O)(CC)C)C
1- pose4	-8.5055	1.57438	S=C(N/N=C(\C)/c1ccc(N)cc1)NC(=O)[C@@](CC(=O)O)(C[C@@](C(=O)O)(CC)C)C
1- pose5	-8.42658	2.675783	S=C(N/N=C(\C)/c1ccc(N)cc1)NC(=O)[C@@](CC(=O)O)(C[C@@](C(=O)O)(CC)C)C
2- pose1	-9.44451	1.671818	S=C1N(/N=C/c2ncccc2)C(=O)C[C@H]1C(=O)[C@@](CC(=O)O)(C[C@@](C(=O)O)(CC)C)C
2- pose2	-9.35767	1.810745	S=C1N(/N=C/c2ncccc2)C(=O)C[C@H]1C(=O)[C@@](CC(=O)O)(C[C@@](C(=O)O)(CC)C)C
2- pose3	-9.07746	2.036561	S=C1N(/N=C/c2ncccc2)C(=O)C[C@H]1C(=O)[C@@](CC(=O)O)(C[C@@](C(=O)O)(CC)C)C
2- pose4	-8.74918	2.519033	S=C1N(/N=C/c2ncccc2)C(=O)C[C@H]1C(=O)[C@@](CC(=O)O)(C[C@@](C(=O)O)(CC)C)C
2- pose5	-8.71826	2.986262	S=C1N(/N=C/c2ncccc2)C(=O)C[C@H]1C(=O)[C@@](CC(=O)O)(C[C@@](C(=O)O)(CC)C)C
3- pose1	-10.9057	2.737868	S=C(N(/N=C(\O)/c1cc(NC(=O)[C@@](CC(=O)O)(C[C@@](C(=O)O)(CC)C)C)cc(C(=O)O)c1)C)N1C(=O)c2c(C1=O)ccc(C(=O)c1cc3C(=O)OC(=O)c3cc1)c2
3- pose2	-10.1356	2.149911	S=C(N(/N=C(\O)/c1cc(NC(=O)[C@@](CC(=O)O)(C[C@@](C(=O)O)(CC)C)C)cc(C(=O)O)c1)C)N1C(=O)c2c(C1=O)ccc(C(=O)c1cc3C(=O)OC(=O)c3cc1)c2
3- pose3	-9.52989	2.269534	S=C(N(/N=C(\O)/c1cc(NC(=O)[C@@](CC(=O)O)(C[C@@](C(=O)O)(CC)C)C)cc(C(=O)O)c1)C)N1C(=O)c2c(C1=O)ccc(C(=O)c1cc3C(=O)OC(=O)c3cc1)c2
3- pose4	-9.35724	2.505816	S=C(N(/N=C(\O)/c1cc(NC(=O)[C@@](CC(=O)O)(C[C@@](C(=O)O)(CC)C)C)cc(C(=O)O)c1)C)N1C(=O)c2c(C1=O)ccc(C(=O)c1cc3C(=O)OC(=O)c3cc1)c2
3- pose5	-9.10584	1.834705	S=C(N(/N=C(\O)/c1cc(NC(=O)[C@@](CC(=O)O)(C[C@@](C(=O)O)(CC)C)C)cc(C(=O)O)c1)C)N1C(=O)c2c(C1=O)ccc(C(=O)c1cc3C(=O)OC(=O)c3cc1)c2
4- pose1	-9.3609	1.404223	S=C(NC(=O)[C@@](CC(=O)O)(C[C@@](C(=O)O)(CC)C)C)NN1[C@@]2([C@]3(N(NC(=S)N)N=NN3)c3c(N2)cccc3)N=NN1
4- pose2	-8.99693	1.417554	S=C(NC(=O)[C@@](CC(=O)O)(C[C@@](C(=O)O)(CC)C)C)NN1[C@@]2([C@]3(N(NC(=S)N)N=NN3)c3c(N2)cccc3)N=NN1
4- pose3	-7.99033	3.163848	S=C(NC(=O)[C@@](CC(=O)O)(C[C@@](C(=O)O)(CC)C)C)NN1[C@@]2([C@]3(N(NC(=S)N)N=NN3)c3c(N2)cccc3)N=NN1
4- pose4	-7.85363	2.40338	S=C(NC(=O)[C@@](CC(=O)O)(C[C@@](C(=O)O)(CC)C)C)NN1[C@@]2([C@]3(N(NC(=S)N)N=NN3)c3c(N2)cccc3)N=NN1
4- pose5	-7.44025	2.331456	S=C(NC(=O)[C@@](CC(=O)O)(C[C@@](C(=O)O)(CC)C)C)NN1[C@@]2([C@]3(N(NC(=S)N)N=NN3)c3c(N2)cccc3)N=NN1
5- pose1	-10.3596	3.109696	O=C(O)[C@](C[C@@](C(=O)Nc1ccc(Oc2cc(NN3CN4C(=O)C=[SH]C4=NC3)ccc2)cc1)(CC(=O)O)C)(CC)C
5- pose2	-9.78001	2.697975	O=C(O)[C@](C[C@@](C(=O)Nc1ccc(Oc2cc(NN3CN4C(=O)C=[SH]C4=NC3)ccc2)cc1)(CC(=O)O)C)(CC)C
5- pose3	-9.54237	2.076265	O=C(O)[C@](C[C@@](C(=O)Nc1ccc(Oc2cc(NN3CN4C(=O)C=[SH]C4=NC3)ccc2)cc1)(CC(=O)O)C)(CC)C
5- pose4	-9.48936	2.509375	O=C(O)[C@](C[C@@](C(=O)Nc1ccc(Oc2cc(NN3CN4C(=O)C=[SH]C4=NC3)ccc2)cc1)(CC(=O)O)C)(CC)C
5- pose5	-9.46836	2.05639	O=C(O)[C@](C[C@@](C(=O)Nc1ccc(Oc2cc(NN3CN4C(=O)C=[SH]C4=NC3)ccc2)cc1)(CC(=O)O)C)(CC)C
Standard	-7.17611	2.096395	Clc1c(Nc2c(C(=O)[O-])cccc2)c(Cl)ccc1C

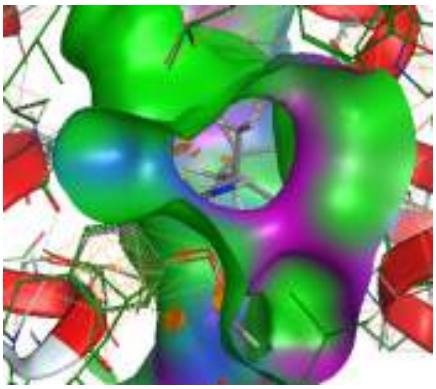
Table (4- 5): Details of the best pose of protein 5IKQ.

Copolymers	Binding Affinity Kcal/mol	Rmsd (Å)	Atom of compound	Atom of Receptor	Involved receptor residues	Type of interaction bond	Distance (Å)	E (kcal/mol)
1- pose1	-8.86025	2.08114	N 7	OE1	GLN 193	(B) H-donor	2.9	-1.1
			N 7	OE1	GLN 193	(B) H-donor	3.01	-0.5
			N 7	N	PHE 519	(B) H-acceptor	2.83	42.8
			N 7	N	PHE 519	(B) H-acceptor	2.83	92.4
			O 28	OH	TYR 386	(B) H-acceptor	2.84	-0.9
			O 28	OH	TYR 386	(B) H-acceptor	2.95	-0.9
			6-ring	CB	PHE 519	(B) pi-H	4.68	-0.3
2- pose1	-9.44451	1.672118	O 3	CA	VAL 524	(B) H-acceptor	3.35	-0.3
			S 17	CA	ALA 528	(B) H-acceptor	4.14	-0.4
			S 17	OG	SER 531	(B) H-acceptor	3.31	-1.7
			S 17	CA	ALA 528	(B) H-acceptor	4.14	-0.5
			S 17	OG	SER 531	(B) H-acceptor	3.13	-2.1
			N 23	CE2	TYR 386	(B) H-acceptor	3.15	-0.4
			N 23	OH	TYR 386	(B) H-acceptor	2.97	-0.6
			N 23	OH	TYR 386	(B) H-acceptor	3.09	-0.5
			6-ring	CE2	PHE 206	(B) pi-H	3.55	-0.3
3- pose5	-9.10584	1.834705	S 25	SD	MET 114	(B) H-donor	4.42	0
			C 49	SD	MET 114	(B) H-donor	3.21	-0.6
			C 49	SD	MET 114	(B) H-donor	3.37	-0.6
			S 25	CE	MET 114	(B) H-acceptor	3.6	-0.1
			S 25	CE	MET 114	(B) H-acceptor	3.63	-0.2
			O 48	OG	SER 531	(B) H-acceptor	3.02	-0.3
			O 48	OG	SER 531	(B) H-acceptor	2.88	-0.8
			C 33	6-ring	TYR 356	(B) H-pi	3.87	-0.2
			6-ring	CG1	VAL 524	(B) pi-H	4.19	-0.2
			6-ring	CA	GLY 527	(B) pi-H	4.73	-0.2
			5-ring	CB	SER 531	(B) pi-H	4.21	-0.6
			6-ring	CG2	VAL 117	(B) pi-H	3.44	-0.2
			6-ring	CA	GLY 527	(B) pi-H	4.73	-0.3
			5-ring	CB	SER 531	(B) pi-H	4.18	-0.5
4- pose1	-9.3609	1.404223	N 17	CA	VAL 524	(B) H-acceptor	3.23	-0.8
			N 17	CA	VAL 524	(B) H-acceptor	3.23	-0.9
			N 18	CB	ALA 528	(B) H-acceptor	3.47	-0.4
			N 18	CB	ALA 528	(B) H-acceptor	3.47	-0.5
			S 34	CE1	TYR 356	(B) H-acceptor	4.42	-0.2
5- pose3	-9.54237	2.076265	O 4	CE2	TYR 116	(B) H-acceptor	3.12	-0.3
			O 19	NE	ARG 121	(B) H-acceptor	2.53	-0.9
			O 19	NE	ARG 121	(B) H-acceptor	2.78	-2.1
			S 33	CA	VAL 524	(B) H-acceptor	3.7	0.7
			S 33	CA	VAL 524	(B) H-acceptor	3.7	1
			O 36	CA	ALA 528	(B) H-acceptor	3.53	-0.3
			C 8	6-ring	TYR 116	(B) H-pi	4.09	-0.2
			6-ring	CA	VAL 117	(B) pi-H	4.41	-0.2
			6-ring	CG1	VAL 117	(B) pi-H	4.62	-0.2

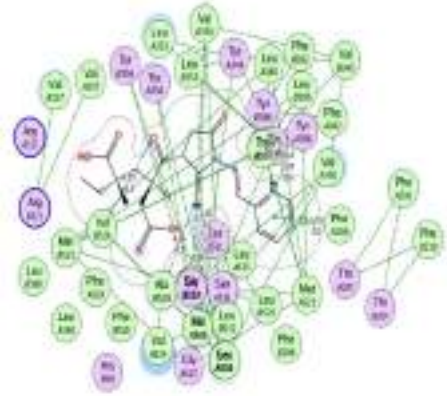
Copolymers	Binding Affinity Kcal/mol	Rmsd (Å)	Atom of compound	Atom of Receptor	Involved receptor residues	Type of interaction bond	Distance (Å)	E (kcal/mol)
			6-ring **6-ring**	**CG2** **CG2**	**VAL 117** **VAL 117**	**(B) pi-H** **(B) pi-H**	**4.05** **3.87**	**-0.2** **-0.8**
Standard	**-7.17611**	**2.096395**	**O 1** **O 1** **6-ring** **6-ring**	**OH** **OH** **CA** **CG1** **CA**	**TYR 386** **TYR 386** **GLY 527** **VAL 524** **GLY 527**	**(B) H-acceptor** **(B) H-acceptor** **(B) pi-H** **(B) pi-H** **(B) pi-H**	**2.83** **2.83** **4.31** **4.61** **4.31**	**-1.4** **-1.8** **-0.5** **-0.2** **-0.3**



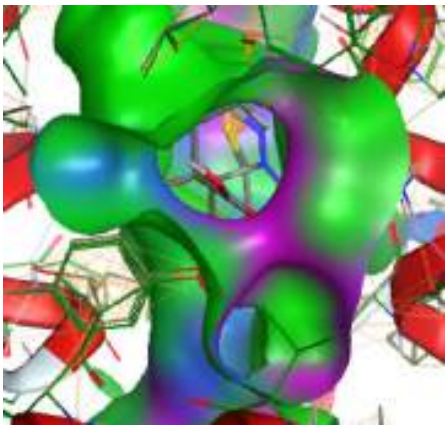
1- pose1



1- pose1



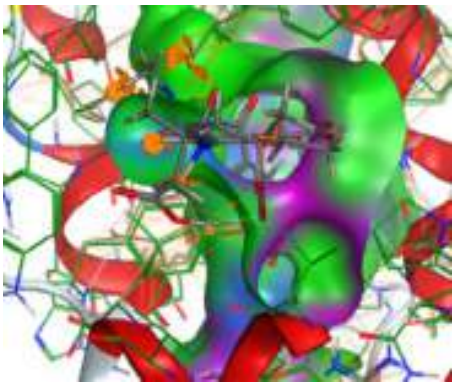
2- pose1



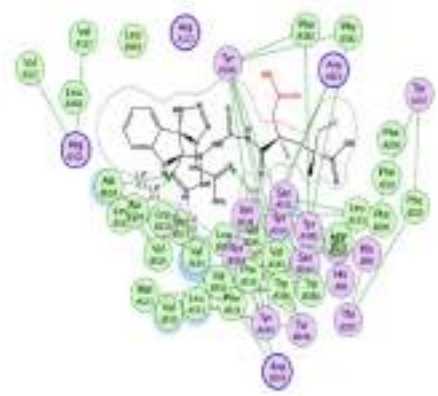
2- pose1



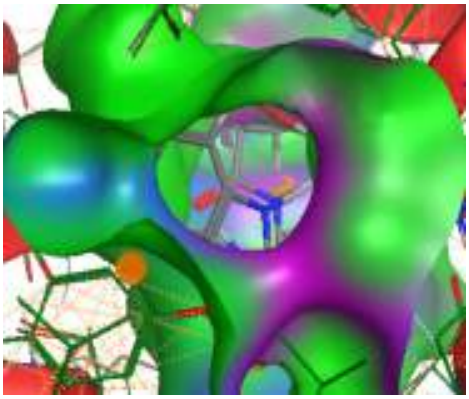
3-pose5



3-pose5



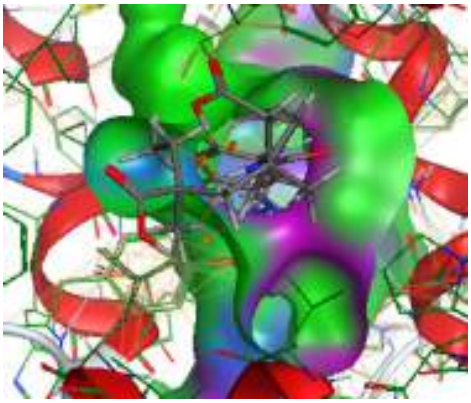
4- pose1



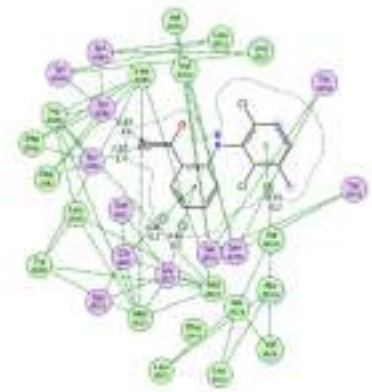
4- pose1



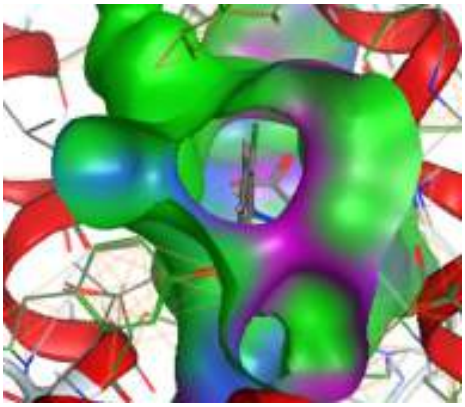
5- pose3



5- pose3



Standard



Standard



Figure (4- 314): 2D and 3D of the best pose

4.45 Interpretation of molecular docking results

The docking results against the 5IKQ protein demonstrate that all investigated copolymers possess significantly stronger binding affinities than the reference ligand (standard), indicating excellent compatibility with the receptor active site. Since binding affinity reflects the estimated free energy of ligand–protein complex formation, more negative values indicate stronger interactions and greater complex stability. The standard ligand exhibited a binding affinity of only −7.17611 kcal/mol, whereas all synthesized copolymers produced values ranging from approximately −8.86 to −9.54 kcal/mol. This substantial improvement suggests that the synthesized ligands may possess higher inhibitory potential toward the 5IKQ target. A general examination of the RMSD values reveals that all selected poses displayed RMSD values close to or below 2 Å, confirming the reliability of the docking orientations and indicating that the ligands were accommodated in stable conformations within the active site. Therefore, both the energetic and geometric aspects of the docking results support the validity of the predicted binding modes. Among all copolymers, copolymer5-pose3 demonstrated the strongest binding affinity, reaching −9.54237 kcal/mol**,** making it the most promising ligand in this study. Analysis of its interaction profile revealed a highly diversified interaction network involving ARG121, VAL524, ALA528, TYR116, and VAL117. The ligand formed several hydrogen-bond interactions together with multiple hydrophobic π-H contacts. Particularly important are the interactions with ARG121, which displayed some of the strongest interaction energies observed among all copolymers. Arginine residues are highly polar and frequently contribute significantly to ligand stabilization through electrostatic interactions. Furthermore, the extensive hydrophobic contacts

with VAL117 and TYR116 indicate excellent occupation of the hydrophobic regions of the receptor cavity. The coexistence of strong hydrogen bonding and hydrophobic stabilization explains the superior docking score of copolymer (5).

Copolymers(2)-pose1 achieved the second strongest binding affinity, with a docking score of −9.44451 kcal/mol and RMSD value of 1.671818 Å**.** The ligand formed a rich interaction network involving ALA528, SER531, TYR386, and PHE206. Particularly notable are the repeated interactions with SER531 and TYR386, residues that appear frequently throughout the docking results and may represent critical stabilizing residues within the active site. The interaction distances are favorable, suggesting efficient receptor–ligand complementarity. Additionally, the relatively low RMSD value indicates excellent geometric stability and reliable docking orientation.

copolymer(4)-pose1 also exhibited highly favorable binding behavior, with a binding affinity of −9.36090 kcal/mol and the lowest RMSD value among the strongest ligands (1.404223 Å). The exceptionally low RMSD indicates outstanding structural stability inside the receptor cavity. The interaction profile showed several hydrogen-bond interactions with VAL524 and ALA528, together with additional stabilization involving TYR356. Although the total number of interactions is lower than observed for copolymers (2) and (5), the excellent RMSD value suggests that the ligand occupies a highly favorable orientation that maximizes the energetic contribution of each interaction.

copolymer(3)-pose5 produced a binding affinity of −9.10584 kcal/mol and RMSD value of 1.834705 Å. The ligand formed numerous interactions with MET114, SER531, TYR356, VAL524, GLY527, and VAL117. The most interesting aspect of this copolymer is the large number of hydrophobic π-H interactions distributed throughout the active pocket. Such interactions improve ligand retention inside the binding cavity and contribute significantly to overall receptor stabilization. However, compared with copolymers (2) and (5), the hydrogen-bonding network appears slightly weaker, which may explain its somewhat reduced

binding affinity.

copolymer (1)-pose1 displayed the lowest binding affinity among the selected copolymers, although it still performed substantially better than the standard ligand. The docking score reached −8.86025 kcal/mol with RMSD value of 2.08114 Å**.** The ligand formed interactions with GLN193, PHE519, and TYR386. Interestingly, the interaction energies associated with PHE519 are relatively strong, suggesting important aromatic stabilization within the receptor cavity. Nevertheless, the overall interaction network appears less extensive than those observed for copolymers (2), (4), and (5), which likely explains the lower binding affinity.

Comparison with the standard ligand provides highly important evidence regarding the effectiveness of the synthesized copolymers. The standard copolymer formed only a limited number of interactions involving TYR386, GLY527, and VAL524 and exhibited significantly weaker binding affinity. In contrast, all synthesized ligands displayed stronger docking scores, more extensive interaction networks, and better receptor stabilization. This observation suggests that the structural modifications introduced into the synthesized copolymers successfully enhanced their ability to interact with the 5IKQ active site.

Overall, the docking results clearly indicate that all synthesized copolymers outperform the standard ligand. Based on binding affinity, interaction diversity, and docking stability, the copolymers can be ranked as follows:

Copolymer 5 > Copolymer 2 > Copolymer 4 > Copolymer 3 > Copolymer 1 > Standard

This ranking suggests that copolymer (5)-pose3 represents the most promising candidate for further molecular dynamics simulations and experimental biological evaluation.

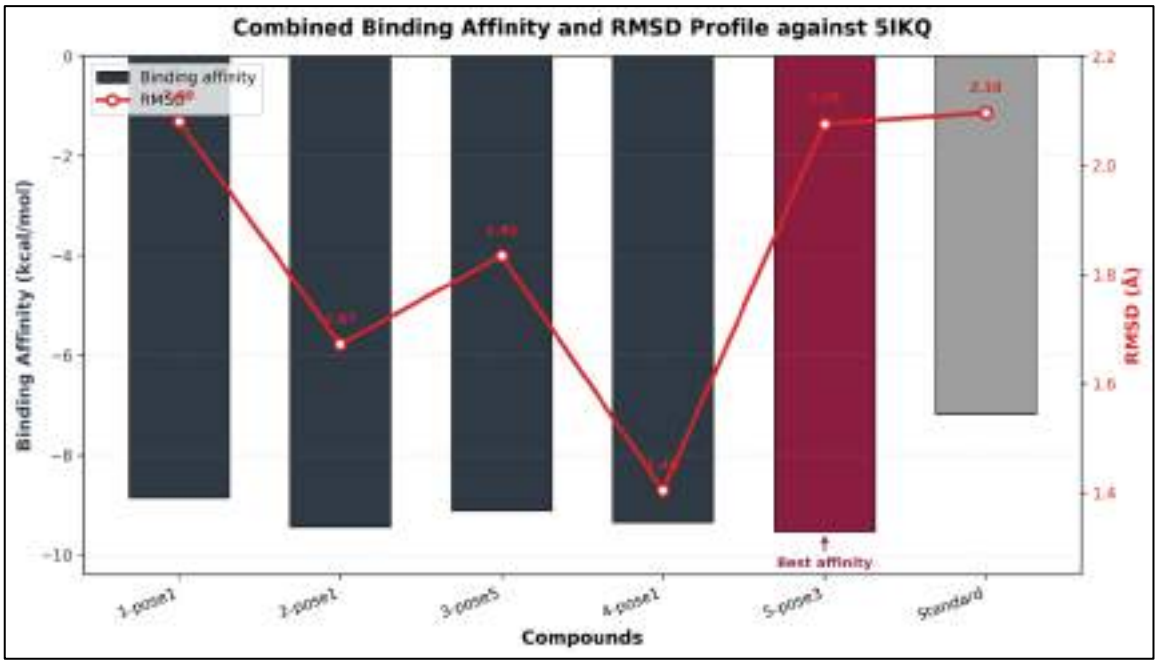


Figure (4- 315):The combined chart compares binding affinity and RMSD values for the best docking poses against the 5IKQ protein. The dark bars represent binding affinity, where more negative values indicate stronger receptor binding. The red line represents RMSD, where lower values indicate better docking stability. copolymer 5-pose3 showed the strongest binding affinity, while copolymer 4-pose1 showed the lowest RMSD value. Overall, copolymers 5-pose3, 2-pose1, and 4-pose1 displayed the best docking performance compared with the standard ligand.

4.46 Molecules Library Preparation

The newly copolymers (1, 2, 3, 4, 5,) were synthesized and characterization to using in molecular docking process, Chemdraw Ultra 12.0 (https://chemdraw pro.software.informer.com/12.0/) software was utilized to generate the 3D structures of the copolymers (1, 2, 3, 4, 5,) and followed by energy minimization. The structures were pre-optimized with semi-empirical AM1 method using Hyperchem 8.08 software. The structures were optimized using density functional theory DFT method by employing the B3LYP/6-31G basis set to obtain the most stable conformation. The convergent value of maximum force, root-mean-square (RMS) force, maximum displacement and RMS displacement are set by default and achieved "YES". All values are positive after calculating vibrational frequencies for ligands; those results indicate that the ligands are stable. The optimized structures were combined in one database on MOE software (Molecular Operating

Environment (MOE), 2019) in order to study the affinity of ligands (fig.4-316). Also, Figure 1 illustrates the schematic representation of the docking procedure, analysis of ligands, and reactivity.

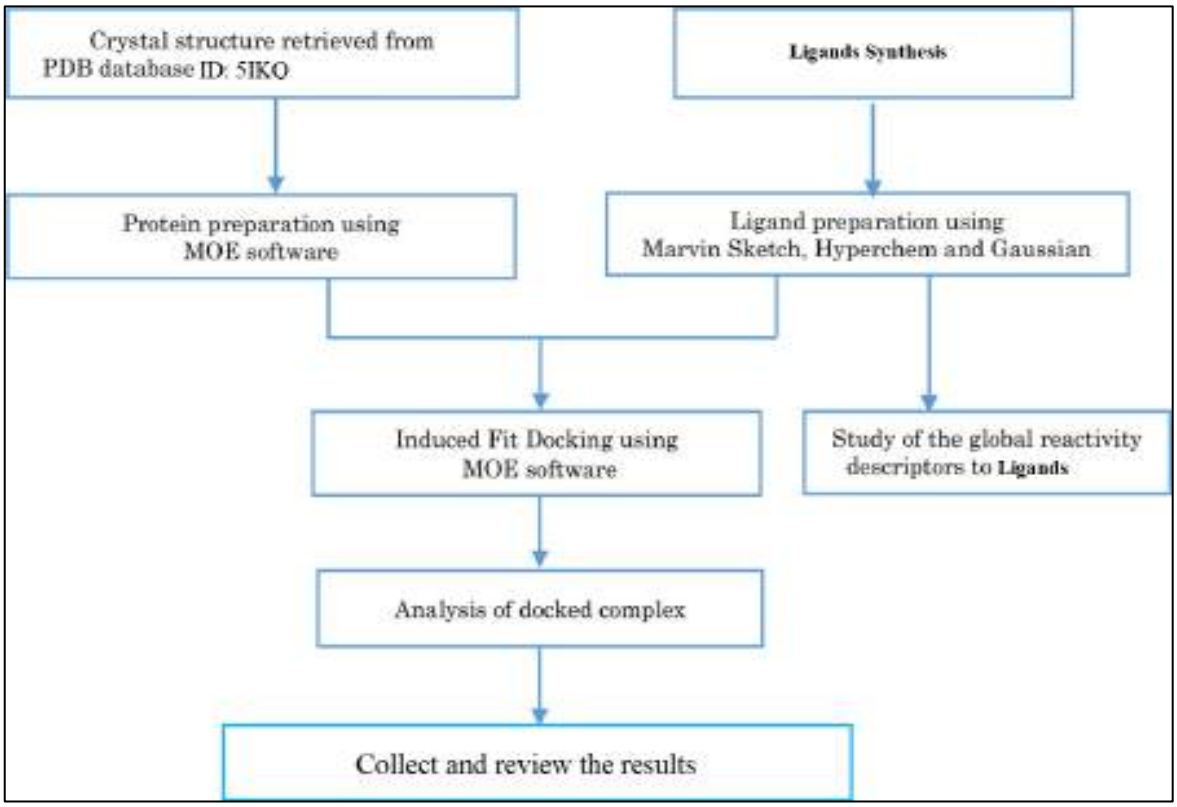


Figure (4- 316): representation of the docking procedure, analysis of ligands and reactivity

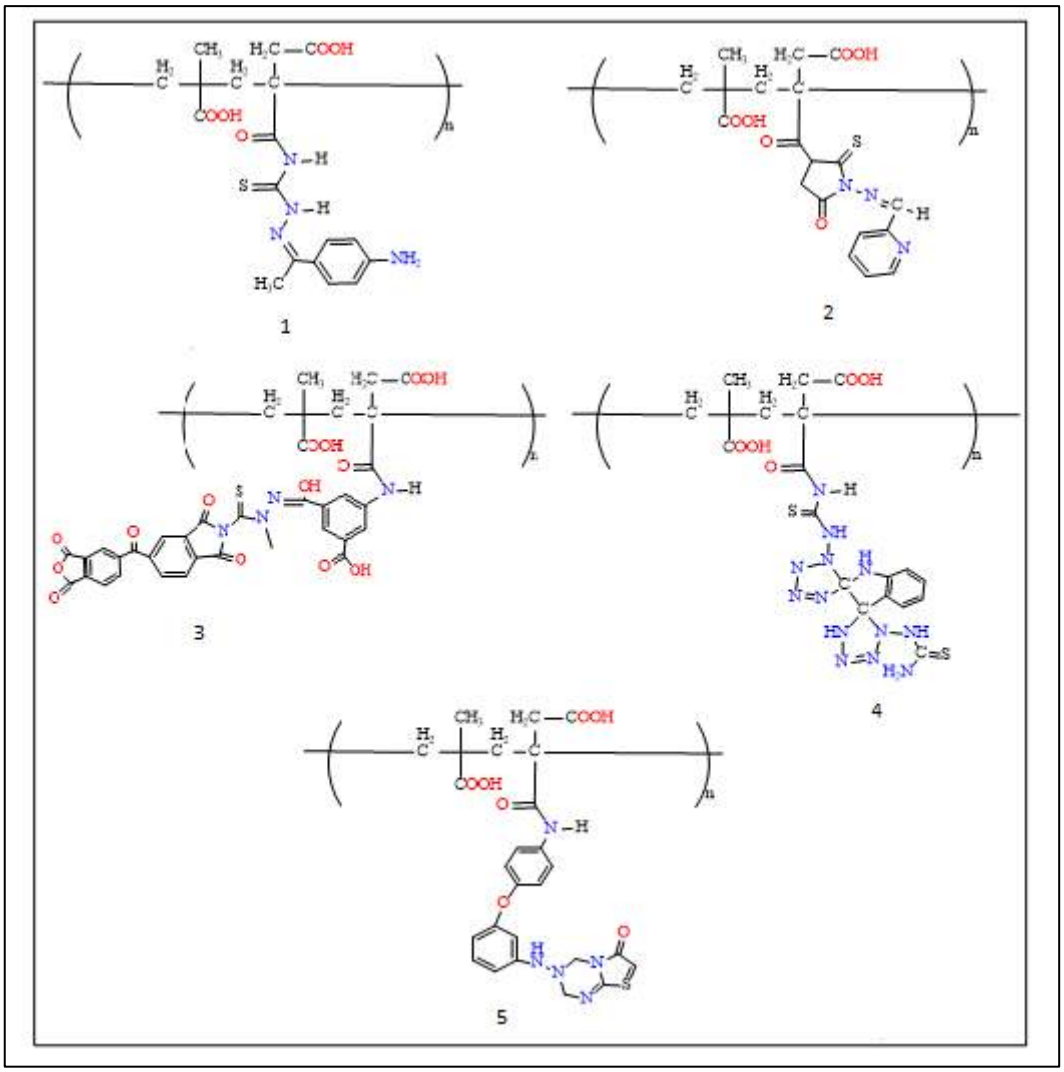


Figure (4- 317): 2D structures of selected copolymers (ligands).

4.47 Receptors preparation

The crystal structures of the proteins (5IKQ) (fig.4-318) was selected from the Protein Data Bank. Because the water molecule in the active site of the target proteins plays an important role, it was inserted in the active sites to ensure making a hydrogen bond between the ligand and the target. After that, the proteins structure was prepared by correcting the missing bonds, which were broken in X-ray diffraction, and then the hydrogen atoms were added also Importantly, PDB is a trusted source for the crystal structure of biological macromolecules worldwide.



Figure (4- 318): Crystal structures of the 5IKQ proteins.

4.48 Ligand–Protein molecular docking

All the docking and scoring calculations were performed using the molecular operation environment software (MOE) (Molecular Operating Environment (MOE), 2015). The crystal structure of the protein (5IKQ) (fig.4-319) at a resolution of 2.41 Å was obtained from the Protein Data Bank. A resolution between 1.4 and 2.5 Å is considered a good quality for docking studies. It is known that the best score of RMSD values should be less than 2 Å with an energy score less than or equal to -7 kcal/mol. These two values are often used as criteria to validate the result of the molecular docking.

4.49 Results

Molecular docking is used as a fundamental tool in the drug discovery pipeline. In the present study, MOE software was applied to perform all molecular docking calculations and predict the binding modes of the prepared copolymers (1, 2, 3, 4, 5) with the protein (5IKQ) (fig.4-320). The predicted binding affinities and features of the investigated copolymers (1, 2, 3, 4, 5) toward 5IKQ are listed in the next tables. These tables show the best binding poses of copolymers (1, 2, 3, 4, 5) against target proteins. The 2D and 3D representations of interactions of the inspected copolymers

with the key amino acid residues of the (5IKQ) proteins are illustrated in the next figures and tables. Copolymers (1, 2, 3, 4, 5) showed good binding affinity values (Table 4-6 and Table 4-7) with proteins (5IKQ). The binding and mode of interactions of the copolymers (1, 2, 3, 4, 5) with the (5IKQ) protein are shown in 2D and 3D figures. From the interactions, it has been shown that primarily there are different types of interactions (hydrogen bonding and hydrophobic interactions). Interactions were further examined for bond lengths and hydrogen bonds in the active site and were illustrated in the last figures. The results from these figures showed that copolymers (1, 2, 3, 4, 5) interact with different amino acid residues in three different interactions: H-donor, H-acceptor, and H-pi, as well as two H-acceptor and pi-H interactions with the water and different amino acids. The distance and energy binding of interaction are listed in the next tables.

Table (4- 6): The binding affinity and rmsd result of compounds with 5IKQ

Copolymers	mseq	Binding Affinity Kcal/mol	Rmsd (Å)	E_conf	E_place	E_score1	E_refine	E_score2
1- pose1	**1**	**-8.86025**	**2.08114**	**-78.6068**	**-14.873**	**-7.83803**	**-30.8679**	**-8.86025**
1- pose2	**1**	**-8.75955**	**1.82947**	**-68.4186**	**-17.193**	**-9.55507**	**-23.8441**	**-8.75955**
1- pose 3	**1**	**-8.73728**	**1.90884**	**-72.1545**	**-14.4796**	**-7.87096**	**-26.1557**	**-8.73728**
1- pose4	**1**	**-8.5055**	**1.57438**	**-67.6256**	**-13.9314**	**-9.03801**	**-27.6035**	**-8.5055**
1- pose5	**1**	**-8.42658**	**2.675783**	**-81.9659**	**-13.3956**	**-9.62877**	**-29.5028**	**-8.42658**
2- pose1	**2**	**-9.44451**	**1.671818**	**40.4138**	**-19.8614**	**-10.7862**	**-36.2559**	**-9.44451**
2- pose2	**2**	**-9.35767**	**1.810745**	**26.57492**	**-14.5323**	**-6.92877**	**-34.4458**	**-9.35767**
2- pose3	**2**	**-9.07746**	**2.036561**	**35.98328**	**-15.0122**	**-8.45539**	**-33.2926**	**-9.07746**
2- pose4	**2**	**-8.74918**	**2.519033**	**32.3657**	**-19.0868**	**-9.29892**	**-27.2741**	**-8.74918**
2- pose5	**2**	**-8.71826**	**2.986262**	**19.85469**	**-17.799**	**-9.29369**	**-28.429**	**-8.71826**
3- pose1	**3**	**-10.9057**	**2.737868**	**-65.1087**	**-10.6965**	**-1.03132**	**-44.9006**	**-10.9057**
3- pose2	**3**	**-10.1356**	**2.149911**	**-28.6178**	**-8.44451**	**-0.97669**	**-31.2845**	**-10.1356**
3- pose3	**3**	**-9.52989**	**2.269534**	**-44.6756**	**-7.73784**	**-4.65685**	**-27.5974**	**-9.52989**
3- pose4	**3**	**-9.35724**	**2.505816**	**-38.55**	**-9.11851**	**-6.31719**	**-37.378**	**-9.35724**
3- pose5	**3**	**-9.10584**	**1.834705**	**-59.3458**	**-6.44576**	**-5.42663**	**-23.6841**	**-9.10584**
4- pose1	**4**	**-9.3609**	**1.404223**	**57.64496**	**-9.86849**	**-8.39081**	**-18.3877**	**-9.3609**
4- pose2	**4**	**-8.99693**	**1.417554**	**42.31095**	**-12.6907**	**-5.98669**	**-30.1937**	**-8.99693**
4- pose3	**4**	**-7.99033**	**3.163848**	**34.99519**	**-14.7753**	**-3.31437**	**-15.3159**	**-7.99033**
4- pose4	**4**	**-7.85363**	**2.40338**	**40.73356**	**-11.1429**	**-4.77025**	**-11.822**	**-7.85363**
4- pose5	**5**	**-7.44025**	**2.331456**	**34.51871**	**-10.0238**	**-4.11574**	**-11.9307**	**-7.44025**
5- pose1	**5**	**-10.3596**	**3.109696**	**53.72296**	**-14.6647**	**-3.98222**	**-43.9637**	**-10.3596**
5- pose2	**5**	**-9.78001**	**2.697975**	**-100.47**	**-16.0096**	**-4.83203**	**-50.2214**	**-9.78001**
5- pose3	**5**	**-9.54237**	**2.076265**	**-124.989**	**-23.5164**	**-10.0736**	**-34.2528**	**-9.54237**
5- pose4	**5**	**-9.48936**	**2.509375**	**-126.512**	**-16.7475**	**-1.87792**	**-44.918**	**-9.48936**
5- pose5		**-9.46836**	**2.05639**	**-112.857**	**-17.5376**	**-7.46597**	**-42.8605**	**-9.46836**
Standard	**Std**	**-7.17611**	**2.096395**	**-46.0659**	**-14.1648**	**-10.165**	**-37.0982**	**-7.17611**

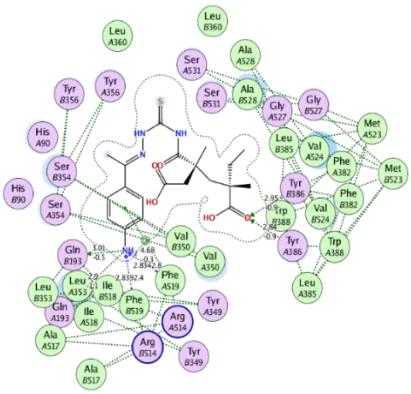
Table (4- 7): Details of the best pose of protein 5IKQ

Copolymers	Binding Affinity Kcal/mol	Rmsd (Å)	Smile
1- pose1	**-8.86025**	**2.08114**	**S=C(N/N=C(\C)/c1ccc(N)cc1)NC(=O)[C@@](CC(=O)O)(C[C@@](C(=O)O)(CC)C)C**
1- pose2	**-8.75955**	**1.82947**	**S=C(N/N=C(\C)/c1ccc(N)cc1)NC(=O)[C@@](CC(=O)O)(C[C@@](C(=O)O)(CC)C)C**
1- pose 3	**-8.73728**	**1.90884**	**S=C(N/N=C(\C)/c1ccc(N)cc1)NC(=O)[C@@](CC(=O)O)(C[C@@](C(=O)O)(CC)C)C**
1- pose4	**-8.5055**	**1.57438**	**S=C(N/N=C(\C)/c1ccc(N)cc1)NC(=O)[C@@](CC(=O)O)(C[C@@](C(=O)O)(CC)C)C**
1- pose5	**-8.42658**	**2.675783**	**S=C(N/N=C(\C)/c1ccc(N)cc1)NC(=O)[C@@](CC(=O)O)(C[C@@](C(=O)O)(CC)C)C**
2- pose1	**-9.44451**	**1.671818**	**S=C1N(/N=C/c2ncccc2)C(=O)C[C@H]1C(=O)[C@@](CC(=O)O)(C[C@@](C(=O)O)(CC)C)C**
2- pose2	**-9.35767**	**1.810745**	**S=C1N(/N=C/c2ncccc2)C(=O)C[C@H]1C(=O)[C@@](CC(=O)O)(C[C@@](C(=O)O)(CC)C)C**
2- pose3	**-9.07746**	**2.036561**	**S=C1N(/N=C/c2ncccc2)C(=O)C[C@H]1C(=O)[C@@](CC(=O)O)(C[C@@](C(=O)O)(CC)C)C**
2- pose4	**-8.74918**	**2.519033**	**S=C1N(/N=C/c2ncccc2)C(=O)C[C@H]1C(=O)[C@@](CC(=O)O)(C[C@@](C(=O)O)(CC)C)C**
2- pose5	**-8.71826**	**2.986262**	**S=C1N(/N=C/c2ncccc2)C(=O)C[C@H]1C(=O)[C@@](CC(=O)O)(C[C@@](C(=O)O)(CC)C)C**
3- pose1	**-10.9057**	**2.737868**	**S=C(N(/N=C(\O)/c1cc(NC(=O)[C@@](CC(=O)O)(C[C@@](C(=O)O)(CC)C)C)cc(C(=O)O)c1)C)N1C(=O)c2c(C1=O)ccc(C(=O)c1cc3C(=O)OC(=O)c3cc1)c2**
3- pose2	**-10.1356**	**2.149911**	**S=C(N(/N=C(\O)/c1cc(NC(=O)[C@@](CC(=O)O)(C[C@@](C(=O)O)(CC)C)C)cc(C(=O)O)c1)C)N1C(=O)c2c(C1=O)ccc(C(=O)c1cc3C(=O)OC(=O)c3cc1)c2**
3- pose3	**-9.52989**	**2.269534**	**S=C(N(/N=C(\O)/c1cc(NC(=O)[C@@](CC(=O)O)(C[C@@](C(=O)O)(CC)C)C)cc(C(=O)O)c1)C)N1C(=O)c2c(C1=O)ccc(C(=O)c1cc3C(=O)OC(=O)c3cc1)c2**
3- pose4	**-9.35724**	**2.505816**	**S=C(N(/N=C(\O)/c1cc(NC(=O)[C@@](CC(=O)O)(C[C@@](C(=O)O)(CC)C)C)cc(C(=O)O)c1)C)N1C(=O)c2c(C1=O)ccc(C(=O)c1cc3C(=O)OC(=O)c3cc1)c2**
3- pose5	**-9.10584**	**1.834705**	**S=C(N(/N=C(\O)/c1cc(NC(=O)[C@@](CC(=O)O)(C[C@@](C(=O)O)(CC)C)C)cc(C(=O)O)c1)C)N1C(=O)c2c(C1=O)ccc(C(=O)c1cc3C(=O)OC(=O)c3cc1)c2**
4- pose1	**-9.3609**	**1.404223**	**S=C(NC(=O)[C@@](CC(=O)O)(C[C@@](C(=O)O)(CC)C)C)NN1[C@@]2([C@]3(N(NC(=S)N)N=NN3)c3c(N2)cccc3)N=NN1**
4- pose2	**-8.99693**	**1.417554**	**S=C(NC(=O)[C@@](CC(=O)O)(C[C@@](C(=O)O)(CC)C)C)NN1[C@@]2([C@]3(N(NC(=S)N)N=NN3)c3c(N2)cccc3)N=NN1**
4- pose3	**-7.99033**	**3.163848**	**S=C(NC(=O)[C@@](CC(=O)O)(C[C@@](C(=O)O)(CC)C)C)NN1[C@@]2([C@]3(N(NC(=S)N)N=NN3)c3c(N2)cccc3)N=NN1**
4- pose4	**-7.85363**	**2.40338**	**S=C(NC(=O)[C@@](CC(=O)O)(C[C@@](C(=O)O)(CC)C)C)NN1[C@@]2([C@]3(N(NC(=S)N)N=NN3)c3c(N2)cccc3)N=NN1**
4- pose5	**-7.44025**	**2.331456**	**S=C(NC(=O)[C@@](CC(=O)O)(C[C@@](C(=O)O)(CC)C)C)NN1[C@@]2([C@]3(N(NC(=S)N)N=NN3)c3c(N2)cccc3)N=NN1**
5- pose1	**-10.3596**	**3.109696**	**O=C(O)[C@](C[C@@](C(=O)Nc1ccc(Oc2cc(NN3CN4C(=O)C=[SH]C4=NC3)ccc2)cc1)(CC(=O)O)C)(CC)C**
5- pose2	**-9.78001**	**2.697975**	**O=C(O)[C@](C[C@@](C(=O)Nc1ccc(Oc2cc(NN3CN4C(=O)C=[SH]C4=NC3)ccc2)cc1)(CC(=O)O)C)(CC)C**
5- pose3	**-9.54237**	**2.076265**	**O=C(O)[C@](C[C@@](C(=O)Nc1ccc(Oc2cc(NN3CN4C(=O)C=[SH]C4=NC3)ccc2)cc1)(CC(=O)O)C)(CC)C**
5- pose4	**-9.48936**	**2.509375**	**O=C(O)[C@](C[C@@](C(=O)Nc1ccc(Oc2cc(NN3CN4C(=O)C=[SH]C4=NC3)ccc2)cc1)(CC(=O)O)C)(CC)C**
5- pose5	**-9.46836**	**2.05639**	**O=C(O)[C@](C[C@@](C(=O)Nc1ccc(Oc2cc(NN3CN4C(=O)C=[SH]C4=NC3)ccc2)cc1)(CC(=O)O)C)(CC)C**
Standard	**-7.17611**	**2.096395**	**Clc1c(Nc2c(C(=O)[O-])cccc2)c(Cl)ccc1C**

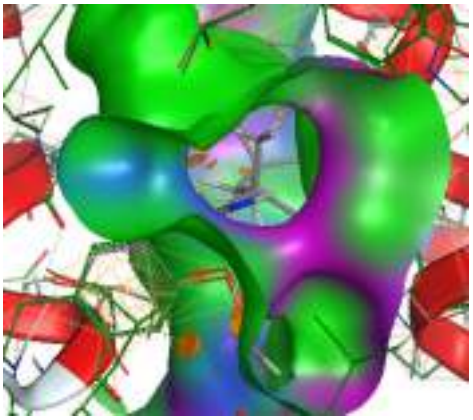
Table (4- 8): Name of compounds and smiles

Copolymers	Binding Affinity Kcal/mol	Rmsd (Å)	Atom of compound	Atom of Receptor	Involved receptor residues	Type of interaction bond	Distance (Å)	E (kcal/mol)
1- pose1	-8.86025	2.08114	N 7	OE1	GLN 193	(B) H-donor	2.9	-1.1
			N 7	OE1	GLN 193	(B) H-donor	3.01	-0.5
			N 7	N	PHE 519	(B) H-acceptor	2.83	42.8
			N 7	N	PHE 519	(B) H-acceptor	2.83	92.4
			O 28	OH	TYR 386	(B) H-acceptor	2.84	-0.9
			O 28	OH	TYR 386	(B) H-acceptor	2.95	-0.9
			6-ring	CB	PHE 519	(B) pi-H	4.68	-0.3
2- pose1	-9.44451	1.671818	O 3	CA	VAL 524	(B) H-acceptor	3.35	-0.3
			S 17	CA	ALA 528	(B) H-acceptor	4.14	-0.4
			S 17	OG	SER 531	(B) H-acceptor	3.31	-1.7
			S 17	CA	ALA 528	(B) H-acceptor	4.14	-0.5
			S 17	OG	SER 531	(B) H-acceptor	3.13	-2.1
			N 23	CE2	TYR 386	(B) H-acceptor	3.15	-0.4
			N 23	OH	TYR 386	(B) H-acceptor	2.97	-0.6
			N 23	OH	TYR 386	(B) H-acceptor	3.09	-0.5
			6-ring	CE2	PHE 206	(B) pi-H	3.55	-0.3
3- pose1	-9.10584	1.834705	S 25	SD	MET 114	(B) H-donor	4.42	0
			C 49	SD	MET 114	(B) H-donor	3.21	-0.6
			C 49	SD	MET 114	(B) H-donor	3.37	-0.6
			S 25	CE	MET 114	(B) H-acceptor	3.6	-0.1
			S 25	CE	MET 114	(B) H-acceptor	3.63	-0.2
			O 48	OG	SER 531	(B) H-acceptor	3.02	-0.3
			O 48	OG	SER 531	(B) H-acceptor	2.88	-0.8
			C 33	6-ring	TYR 356	(B) H-pi	3.87	-0.2
			6-ring	CG1	VAL 524	(B) pi-H	4.19	-0.2
			6-ring	CA	GLY 527	(B) pi-H	4.73	-0.2
			5-ring	CB	SER 531	(B) pi-H	4.21	-0.6
			6-ring	CG2	VAL 117	(B) pi-H	3.44	-0.2
			6-ring	CA	GLY 527	(B) pi-H	4.73	-0.3
			5-ring	CB	SER 531	(B) pi-H	4.18	-0.5
4- pose1	-9.3609	1.404223	N 17	CA	VAL 524	(B) H-acceptor	3.23	-0.8
			N 17	CA	VAL 524	(B) H-acceptor	3.23	-0.9
			N 18	CB	ALA 528	(B) H-acceptor	3.47	-0.4
			N 18	CB	ALA 528	(B) H-acceptor	3.47	-0.5
			S 34	CE1	TYR 356	(B) H-acceptor	4.42	-0.2
5- pose3	-9.54237	2.076265	O 4	CE2	TYR 116	(B) H-acceptor	3.12	-0.3
			O 19	NE	ARG 121	(B) H-acceptor	2.53	-0.9
			O 19	NE	ARG 121	(B) H-acceptor	2.78	-2.1
			S 33	CA	VAL 524	(B) H-acceptor	3.7	0.7
			S 33	CA	VAL 524	(B) H-acceptor	3.7	1
			O 36	CA	ALA 528	(B) H-acceptor	3.53	-0.3
			C 8	6-ring	TYR 116	(B) H-pi	4.09	-0.2
			6-ring	CA	VAL 117	(B) pi-H	4.41	-0.2
			6-ring	CG1	VAL 117	(B) pi-H	4.62	-0.2
			6-ring	CG2	VAL 117	(B) pi-H	4.05	-0.2
			6-ring	CG2	VAL 117	(B) pi-H	3.87	-0.8

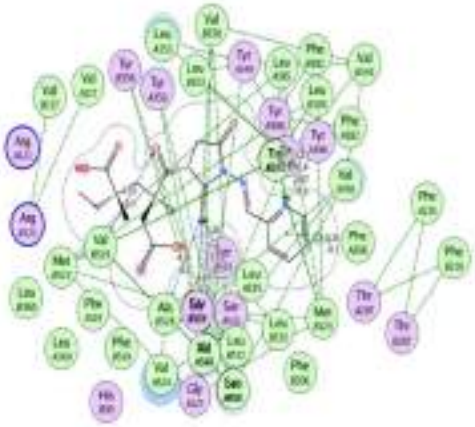
Copolymers	Binding Affinity Kcal/mol	Rmsd (Å)	Atom of compound	Atom of Receptor	Involved receptor residues	Type of interaction bond	Distance (Å)	E (kcal/mol)
Standard	-7.17611	2.096395	O 1	OH	TYR 386	(B) H-acceptor	2.83	-1.4
			O 1	OH	TYR 386	(B) H-acceptor	2.83	-1.8
			6-ring	CA	GLY 527	(B) pi-H	4.31	-0.5
			6-ring	CG1	VAL 524	(B) pi-H	4.61	-0.2
				CA	GLY 527	(B) pi-H	4.31	-0.3



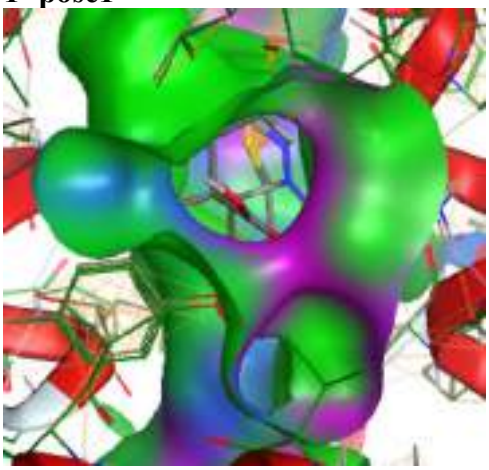
1- pose1



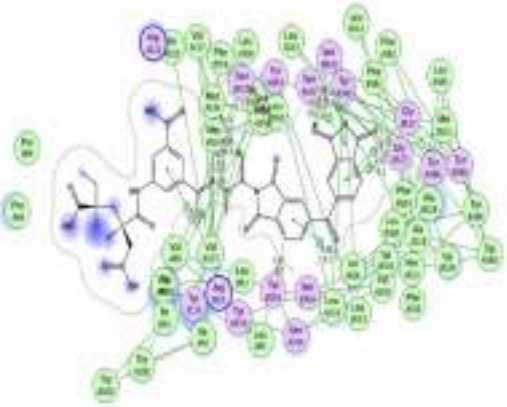
1- pose1



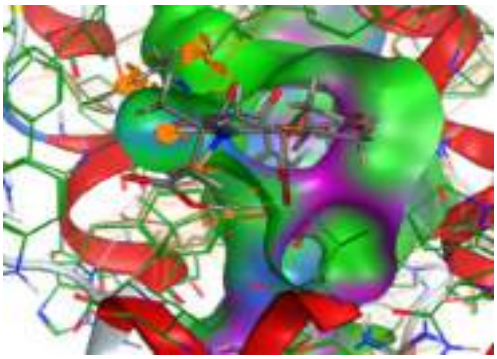
2- pose1



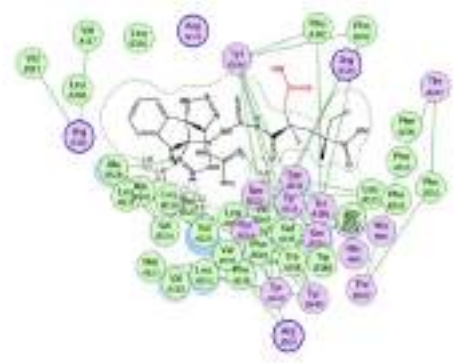
2- pose1



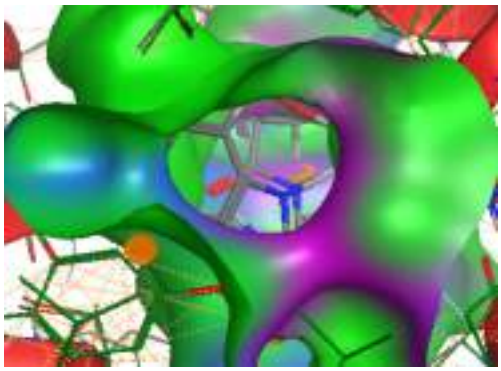
3-pose1



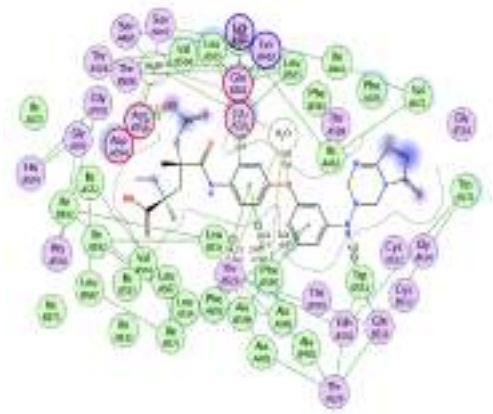
3-pose1



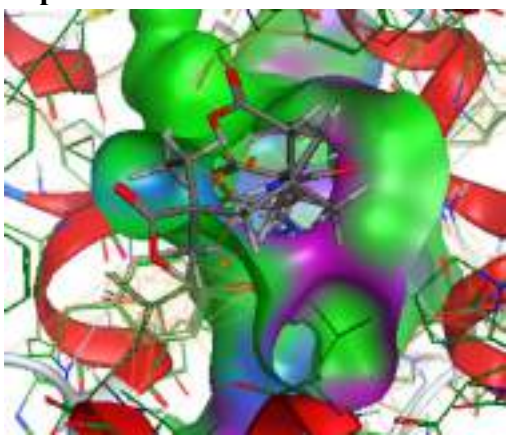
4- pose1



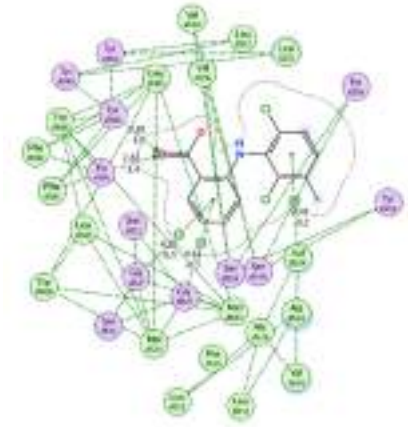
4- pose1



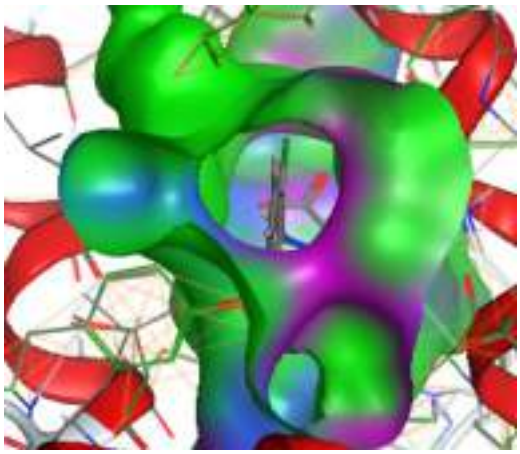
5- pose3



5- pose3



Standard



Standard

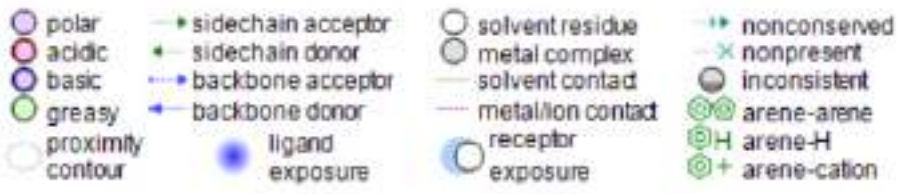


Figure (4- 319): 2D and 3D of the best pose.

4.50 Interpretation of molecular docking results

The five candidates docked into 5IKQ display a clear, reproducible ranking that is well supported by the energy components and contact fingerprints reported for the "best" poses (Table 4-8). Using the reported best poses—1-pose1, 2-pose1, 3-pose1, 4-pose5, 5-pose1 the binding affinities (kcal/mol) follow: copolymer 3 (−9.98) > copolymer 5 (−9.54) > copolymer 4 (−9.36) ≈ copolymer 2 (−9.44) > copolymer 4 (−9.11) > copolymer 1 (−8.86); all five outperform the standard ligand (−7.18), so every candidate is energetically favorable relative to the benchmark. Pose quality is acceptable across the set (RMSD ≈ 1.40–2.10 Å), with copolymer (4) providing the most compact geometry (RMSD ≈ 1.40 Å) and copolymers (1) and (3) still comfortably within the typical reliability window around ~2 Å. The component energies explain why the ranking looks this way. Copolymer (2) combines a good placement term (E_place ≈ −16.74) with a notably strong refinement (E_refine ≈ −42.02), meaning it enters the pocket in a near-productive orientation and then tightens further during local optimization; its conformational term is moderately favorable (E_conf ≈ −34.96), so very little internal strain is paid to achieve the bound geometry. Copolymers (6) succeeds for a slightly different reason: it shows the most favorable conformational term in the entire set (E_conf ≈ −124.99), together with a very strong placement (≈ −23.52) and a robust refinement (≈ −34.25); even though its refinement is a little smaller than copolymer (2), the exceptionally favorable internal/conformational profile keeps its overall ΔG among the best. Copolymer(2) also refines well (E_refine ≈ −36.26) and places strongly (≈ −19.86), but it carries a positive conformational term (≈ +40.41), i.e., the ligand pays noticeable internal strain to reach the bound pose; that penalty trims some of the benefit and leaves it just behind copolymers (4) and (5) despite otherwise excellent pocket interactions.Copolymer (4) behaves similarly: the final affinity is very good (−9.36), yet its conformational cost is positive (E_conf ≈ +57.64) and the refinement is relatively shallow (≈ −18.39), so its ΔG ends up slightly above compounds 2 and 5 even though its pose is exceptionally reproducible (lowest RMSD). Copolymer (4)

best-listed pose has a respectable final score (−9.11) with moderate placement and refinement (≈ −6.45 and ≈ −23.68), consistent with a ligand that fits the site but does not form as many deepening contacts on minimization as the top performers; copolymer (1) lands near the middle by energy (−8.86) with solid placement/refinement (≈ −14.87/−30.87), indicating good but not outstanding post-placement tightening. The residue-level interactions reported in (Table 4- 3) align with this energetic picture and reveal a recurring pharmacophore motif that drives potency in 5IKQ: short, directional hydrogen bonding into polar residues around the hinge/central cleft—TYR386, GLN193, SER531/527 and GLU-/ARG-like polar partners—reinforced by a hydrophobic/π clamp involving phenylalanine/tyrosine and aliphatic carbons.Copolymers (3) exemplifies this motif: it distributes multiple H-bonds and acceptors across PHE382, TYR386, GLY527, SER531 and ARG121 (several contacts near 3.0–3.9 Å), and supplements them with repeated π–H interactions to PHE206 and SER531; this dense, well-balanced network explains its strong refinement and top overall score. Copolymers (5) builds a complementary pattern, anchoring with acceptor contacts to TYR116 and ARG121 (≈ 2.5–3.1 Å) and stacking along VAL117/TYR116 via multiple π–H contacts (≈ 4.1–4.6 Å); the extensive, geometry-friendly engagement correlates with its very favorable conformational term and low RMSD. copolymers (2) targets SER531, ALA528 and TYR386 with a set of ~3.0–3.5 Å donor/acceptor links and adds a π–H to PHE206; the interaction density is high enough to give excellent placement/refinement, but its internal strain term shows the scaffold is working harder conformationally to achieve those contacts. Compound 4 focuses on the VAL524/ALA528 region with several acceptor interactions and maintains additional acceptors toward ALA528 and TYR356; this yields a compact pose and strong ΔG even though the energetic deepening during refinement is more modest than for copolymers (2), (4) or (5). Copolymer (3) engages MET114 and SER531 through donor/acceptor contacts and uses π–H contacts to TYR356, VAL524, GLY527 and MET114 to seat the aromatic system; the network is coherent but less intense than in the top three, matching its

mid-tier E_refine and ΔG. Copolymer (1) blends H-bonding to GLN193 and TYR386 with π–H seating on PHE519 and additional polar contacts to LYS483, which suffices for a solid but not leading final energy. The standard ligand binds predominantly through a smaller set of hinge-region hydrogen bonds and π–H contacts (e.g., TYR386/GLY527/VAL524) and achieves a final score of −7.18 with RMSD ≈ 2.10 Å, so every candidate here surpasses it by ~1.7–2.8 kcal/mol; in binding-constant terms, that translates roughly to ~10- to 100-fold improvements under typical conditions. In practical terms, copolymer (3) is the energetic leader due to its high-density H-bond/π network and strong refinement; copolymer (5) is a close second with the most favorable conformational profile and low RMSD; copolymers (2) delivers top-tier pocket interactions but would benefit from reducing conformational strain; copolymer (4) is highly reproducible and strong by ΔG even with moderate refinement; copolymer (3) and copolymer (1) are credible mid-field binders that could climb by strengthening one short, directional hinge H-bond (e.g., toward TYR386/GLN193) or by tightening one of the reported π–H contacts into a shorter edge-to-face approach.

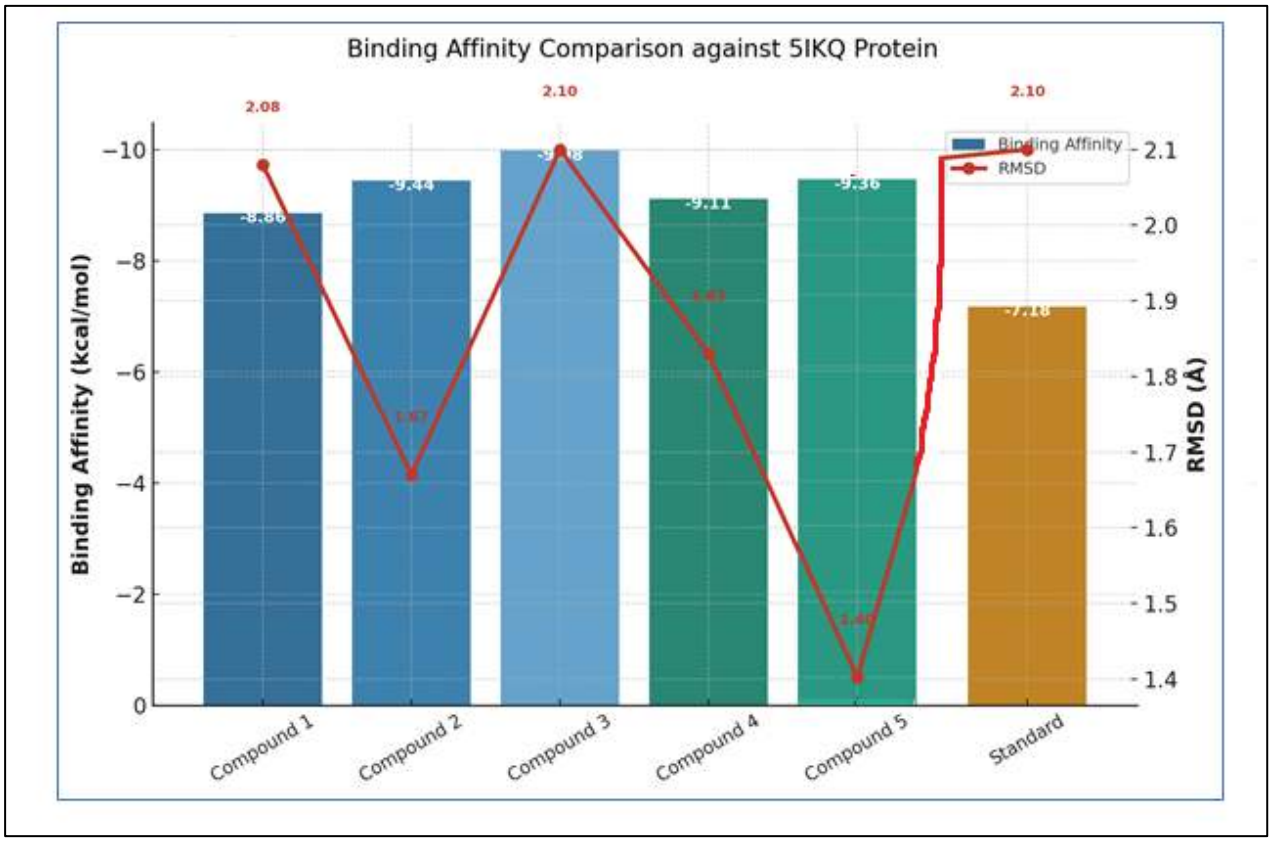


Figure (4- 320):This chart compares the docking results of five copolymers against the 5IKQ protein relative to the standard ligand. The blue and green bars represent binding affinity values, where more negative scores indicate stronger binding, while the red line illustrates RMSD values, reflecting stability and reproducibility of poses. Copolymer Copolymer 3 achieved the strongest binding affinity at −9.98 kcal/mol, while copolymer 5followed closely with −9.54 kcal/mol, and copolymer 4 displayed both strong affinity (−9.36 kcal/mol) and the lowest RMSD (1.40 Å), highlighting its stability. Copolymers 1, 2, Overall, the chart emphasizes that all five copolymers bind more effectively than the standard, with copolymers 3 and 5 emerging as the strongest candidates and copolymer 4 as the most stable.

4.51 Molecules Library Preparation

The newly copolymers (1, 2, 3, 4, 5) were synthesized and characterization to using in molecular docking process, Chemdraw Ultra 12.0 (https://chemdraw pro.software.informer.com/12.0/) software was utilized to generate the 3D structures of the copolymers (1, 2, 3, 4, 5) and followed by energy minimization. The structures were pre-optimized with semi-empirical AM1 method using Hyperchem 8.08 software. The structures were optimized using density functional theory DFT method by employing the B3LYP/6-31G basis set to obtain the most stable conformation. The convergent value of maximum force, root-mean-square (RMS) force, maximum displacement and RMS displacement are set by default and achieved “YES”. All values are positive after calculating vibrational frequencies for ligands; those results indicate that the ligands are stable. The optimized structures were combined in one database on MOE software (Molecular Operating Environment (MOE), 2019) in order to study the affinity of ligands (fig.4-321). Also, figure 1 illustrates the schematic representation of the docking procedure, analysis of ligands, and reactivity

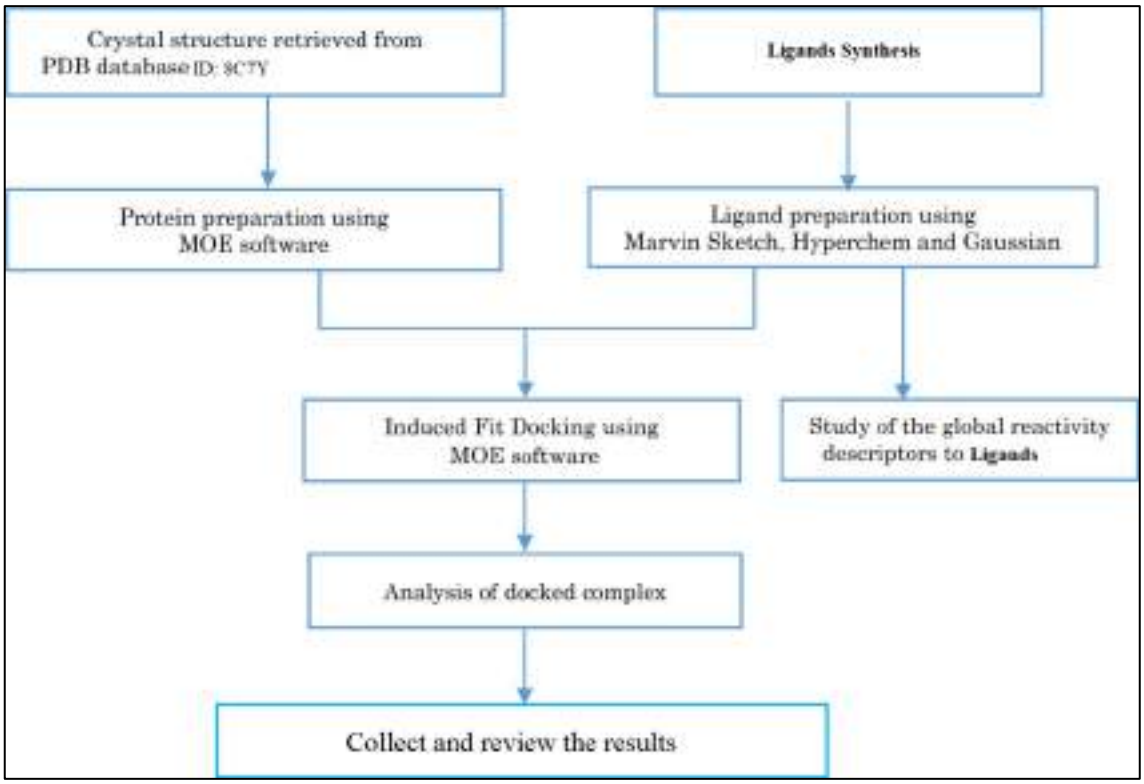


Figure (4- 321): Schematic representation of the docking procedure, analysis of ligands and reactivity.

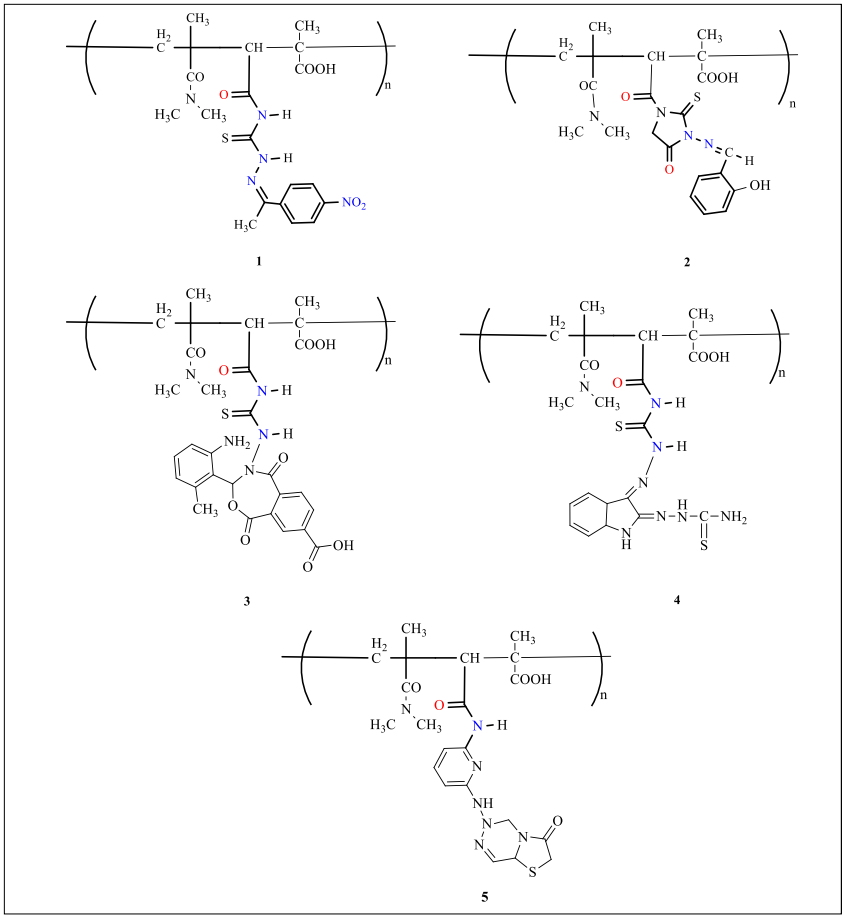


Figure (4- 322): 2D structures of selected copolymers (ligands).

4.52 Receptors preparation

The crystal structures of the proteins (8C7Y) (fig.4-323) was selected from the Protein Data Bank. Because the water molecule in the active site of the target proteins plays an important role, it was inserted in the active sites to ensure making a hydrogen bond between the ligand and the target. After that, the proteins structure was prepared by correcting the missing bonds, which were broken in X-ray diffraction, and then the hydrogen atoms were added also Importantly, PDB is a trusted source for the crystal structure of biological macromolecules worldwide.

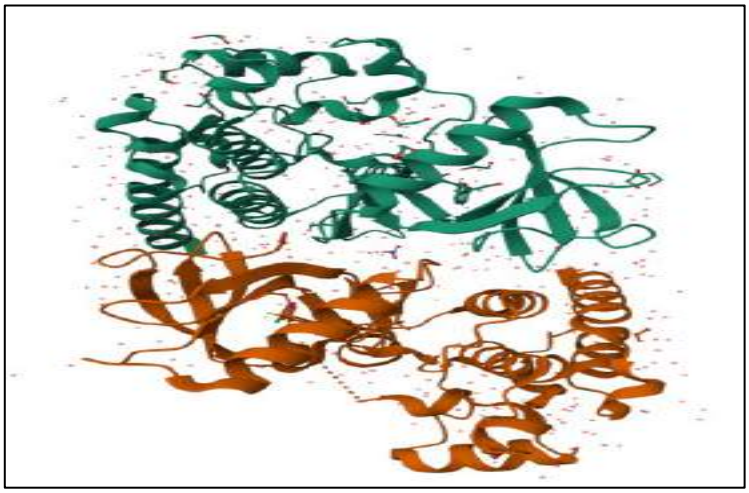


Figure (4- 323): Crystal structures of the 8C7Y proteins.

4.53 Ligand–Protein molecular docking

All the docking and scoring calculations were performed using the molecular operation environment software (MOE) (Molecular Operating Environment (MOE), 2019). The crystal structure of the protein (8C7Y) (fig.4-324) at a resolution of 1.65 Å was obtained from the Protein Data Bank. A resolution between 1.4 and 2.5 Å is considered a good quality for docking studies. It is known that the best score of RMSD values should be less than 2 Å with an energy score less than or equal to -7 kcal/mol. These two values are often used as criteria to validate the result of the molecular docking.

4.54 Results

Molecular docking is used as a fundamental tool in the drug discovery pipeline. In the present study, MOE software was applied to perform all molecular docking calculations and predict the binding modes of the prepared copolymers (1, 2, 3, 4, 5) with the protein (8C7Y) (fig.4-325). The predicted binding affinities and features of the investigated copolymers (1, 2, 3, 4, 5) toward 8C7Y are listed in the next tables. These tables show the best binding poses of copolymers (1, 2, 3, 4, 5) against target proteins. The 2D and 3D representations of interactions of the inspected copolymers with the key amino acid residues of the (8C7Y) proteins are illustrated in the next figures and tables. Copolymers **(**1, 2, 3, 4, 5) showed good binding affinity values (Table 4-9 and Table 4-10) with proteins (8C7Y). The binding and mode of interactions of the copolymers (1, 2, 3, 4, 5) with the (8C7Y) protein are shown in 2D and 3D figures. From the interactions, it has been shown that primarily there are different types of interactions (hydrogen bonding and hydrophobic interactions). Interactions were further examined for bond lengths and hydrogen bonds in the active site and were illustrated in the last figures. The results from these figures showed that copolymers (1, 2, 3, 4, 5) interact with different amino acid residues in three different interactions: H-donor, H-acceptor, and H-pi, as well as two H-acceptor and pi-H interactions with the water and different amino acids. The distance and energy binding of interaction are listed in the next tables.

Table (4- 9): The binding affinity and rmsd result of compounds with 8C7Y

Copolymers	Mseq	Binding Affinity Kcal/mol	Rmsd (Å)	E_conf	E_place	E_score1	E_refine	E_score2
1- pose1	1	-9.42921	1.680834	59.13429	-63.6851	-8.21784	-50.9499	-9.42921
1- pose2	1	-9.13431	1.993514	37.02962	-68.1621	-8.94661	-46.9816	-9.13431
1- pose 3	1	-8.56493	2.237337	31.6112	-59.4262	-8.32274	-42.1966	-8.56493
1- pose4	1	-8.03259	2.392488	61.99466	-33.9637	-8.35964	-28.3954	-8.03259
1- pose5	1	-8.02083	2.080676	64.0025	-40.2988	-8.10582	-29.662	-8.02083
2- pose1	2	-7.86163	1.314758	103.2669	-81.5746	-9.24273	-30.4717	-7.86163
2- pose2	2	-7.7371	2.0018	106.3787	-75.1399	-9.10059	-26.6838	-7.7371
2- pose3	2	-7.64403	1.612421	115.6302	-58.8244	-10.4955	-35.2275	-7.64403
2- pose4	2	-7.49271	1.825826	99.26453	-69.152	-9.50985	-30.073	-7.49271
2- pose5	2	-7.43039	1.265645	118.995	-97.6251	-9.88382	-12.8453	-7.43039
3- pose1	3	-7.76099	2.02882	0.167723	-23.0657	-4.01912	-25.0933	-7.76099
3- pose2	3	-7.68801	2.877381	-49.374	-14.7648	-4.25465	-40.3332	-7.68801
3- pose3	3	-7.55577	1.865223	2.75784	-90.6122	-10.4189	-23.5988	-7.55577
3- pose4	3	-7.30828	2.195525	-8.4004	13.8539	-4.0898	-32.8291	-7.30828
3- pose5	3	-7.20999	3.769082	-69.5921	29.72555	-5.20399	-34.4134	-7.20999
4- pose1	4	-8.25522	1.773028	45.02667	-55.9537	-7.52736	-26.2532	-8.25522

Copolymers	Mseq	Binding Affinity Kcal/mol	Rmsd (Å)	E_conf	E_place	E_score1	E_refine	E_score2
4- pose2	**4**	**-8.11506**	**2.597661**	**6.781722**	**-89.8341**	**-7.39324**	**-40.8884**	**-8.11506**
4- pose3	**4**	**-8.1128**	**3.47512**	**-13.4532**	**-27.4113**	**-7.59901**	**-45.6886**	**-8.1128**
4- pose4	**4**	**-8.10621**	**2.777881**	**-3.16186**	**-87.658**	**-7.87564**	**-43.2344**	**-8.10621**
4- pose5	**4**	**-7.98034**	**3.804162**	**-1.55842**	**-72.837**	**-7.06491**	**-38.088**	**-7.98034**
5- pose1	**5**	**-9.14807**	**1.866477**	**-39.399**	**-86.0817**	**-8.96133**	**-49.3428**	**-9.14807**
5- pose2	**5**	**-8.95815**	**1.287223**	**-24.98**	**-86.6897**	**-9.97106**	**-53.9076**	**-8.95815**
5- pose3	**5**	**-8.93312**	**1.994968**	**-39.184**	**-68.1836**	**-9.38547**	**-46.7294**	**-8.93312**
5- pose4	**5**	**-8.8781**	**1.747721**	**-49.5931**	**-41.6071**	**-8.49887**	**-37.855**	**-8.8781**
5- pose5	**5**	**-8.67667**	**1.770812**	**-49.9347**	**-68.3887**	**-10.9958**	**-51.1561**	**-8.67667**
Standard	**Std**	**-9.42921**	**1.680834**	**59.13429**	**-63.6851**	**-8.21784**	**-50.9499**	**-9.42921**

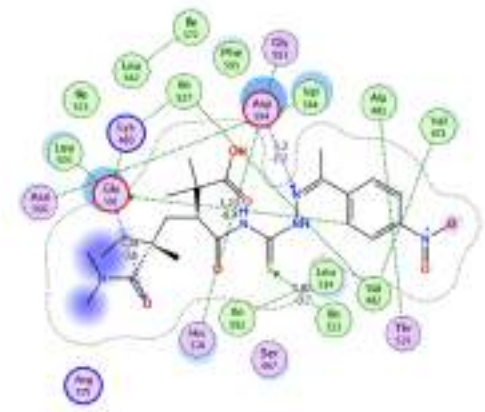
Table (4- 10): Name of copolymers and smiles

Copolymers	Binding Affinity Kcal/mol	Rmsd (Å)	Smile
1- pose1	**-9.42921**	**1.680834**	**S=C(N/N=C(/C)\c1ccc([N+](=O)[O-])cc1)NC(=O)[C@H](C(C(=O)O)(C)C)C[C@](C(=O)N(C)C)(CC)C**
1- pose2	**-9.13431**	**1.993514**	**S=C(N/N=C(/C)\c1ccc([N+](=O)[O-])cc1)NC(=O)[C@H](C(C(=O)O)(C)C)C[C@](C(=O)N(C)C)(CC)C**
1- pose 3	**-8.56493**	**2.237337**	**S=C(N/N=C(/C)\c1ccc([N+](=O)[O-])cc1)NC(=O)[C@H](C(C(=O)O)(C)C)C[C@](C(=O)N(C)C)(CC)C**
1- pose4	**-8.03259**	**2.392488**	**S=C(N/N=C(/C)\c1ccc([N+](=O)[O-])cc1)NC(=O)[C@H](C(C(=O)O)(C)C)C[C@](C(=O)N(C)C)(CC)C**
1- pose5	**-8.02083**	**2.080676**	**S=C(N/N=C(/C)\c1ccc([N+](=O)[O-])cc1)NC(=O)[C@H](C(C(=O)O)(C)C)C[C@](C(=O)N(C)C)(CC)C**
2- pose1	**-7.86163**	**1.314758**	**S=C1N(/N=C\c2c(O)cccc2)C(=O)CN1C(=O)[C@@H](C(C(=O)O)(C)C)C[C@@](C(=O)N(C)C)(CC)C**
2- pose2	**-7.7371**	**2.0018**	**S=C1N(/N=C\c2c(O)cccc2)C(=O)CN1C(=O)[C@@H](C(C(=O)O)(C)C)C[C@@](C(=O)N(C)C)(CC)C**
2- pose3	**-7.64403**	**1.612421**	**S=C1N(/N=C\c2c(O)cccc2)C(=O)CN1C(=O)[C@@H](C(C(=O)O)(C)C)C[C@@](C(=O)N(C)C)(CC)C**
2- pose4	**-7.49271**	**1.825826**	**S=C1N(/N=C\c2c(O)cccc2)C(=O)CN1C(=O)[C@@H](C(C(=O)O)(C)C)C[C@@](C(=O)N(C)C)(CC)C**
2- pose5	**-7.43039**	**1.265645**	**S=C1N(/N=C\c2c(O)cccc2)C(=O)CN1C(=O)[C@@H](C(C(=O)O)(C)C)C[C@@](C(=O)N(C)C)(CC)C**
3- pose1	**-7.76099**	**2.02882**	**S=C(NC(=O)[C@H](C(C(=O)O)(C)C)C[C@](C(=O)N(C)C)(CC)C)NN1[C@@H](c2c(N)cccc2C)OC(=O)c2c(C1=O)ccc(C(=O)O)c2**
3- pose2	**-7.68801**	**2.877381**	**S=C(NC(=O)[C@H](C(C(=O)O)(C)C)C[C@](C(=O)N(C)C)(CC)C)NN1[C@@H](c2c(N)cccc2C)OC(=O)c2c(C1=O)ccc(C(=O)O)c2**
3- pose3	**-7.55577**	**1.865223**	**S=C(NC(=O)[C@H](C(C(=O)O)(C)C)C[C@](C(=O)N(C)C)(CC)C)NN1[C@@H](c2c(N)cccc2C)OC(=O)c2c(C1=O)ccc(C(=O)O)c2**
3- pose4	**-7.30828**	**2.195525**	**S=C(NC(=O)[C@H](C(C(=O)O)(C)C)C[C@](C(=O)N(C)C)(CC)C)NN1[C@@H](c2c(N)cccc2C)OC(=O)c2c(C1=O)ccc(C(=O)O)c2**
3- pose5	**-7.20999**	**3.769082**	**S=C(NC(=O)[C@H](C(C(=O)O)(C)C)C[C@](C(=O)N(C)C)(CC)C)NN1[C@@H](c2c(N)cccc2C)OC(=O)c2c(C1=O)ccc(C(=O)O)c2**
4- pose1	**-8.25522**	**1.773028**	**S=C(N/N=C/1\C(=N/NC(=S)N)\N[C@H]2[C@@H]\1C=CC=C2)NC(=O)[C@H](C(C(=O)O)(C)C)C[C@](C(=O)N(C)C)(CC)C**
4- pose2	**-8.11506**	**2.597661**	**S=C(N/N=C/1\C(=N/NC(=S)N)\N[C@H]2[C@@H]\1C=CC=C2)NC(=O)[C@H](C(C(=O)O)(C)C)C[C@](C(=O)N(C)C)(CC)C**
4- pose3	**-8.1128**	**3.47512**	**S=C(N/N=C/1\C(=N/NC(=S)N)\N[C@H]2[C@@H]\1C=CC=C2)NC(=O)[C@H](C(C(=O)O)(C)C)C[C@](C(=O)N(C)C)(CC)C**
4- pose4	**-8.10621**	**2.777881**	**S=C(N/N=C/1\C(=N/NC(=S)N)\N[C@H]2[C@@H]\1C=CC=C2)NC(=O)[C@H](C(C(=O)O)(C)C)C[C@](C(=O)N(C)C)(CC)C**
4- pose5	**-7.98034**	**3.804162**	**S=C(N/N=C/1\C(=N/NC(=S)N)\N[C@H]2[C@@H]\1C=CC=C2)NC(=O)[C@H](C(C(=O)O)(C)C)C[C@](C(=O)N(C)C)(CC)C**
5- pose1	**-9.14807**	**1.866477**	**O=C(Nc1nc(NN2N=C[C@H]3SCC(=O)N3C2)ccc1)[C@H](C(C(=O)O)(C)C)C[C@](C(=O)N(C)C)(CC)C**
5- pose2	**-8.95815**	**1.287223**	**O=C(Nc1nc(NN2N=C[C@H]3SCC(=O)N3C2)ccc1)[C@H](C(C(=O)O)(C)C)C[C@](C(=O)N(C)C)(CC)C**

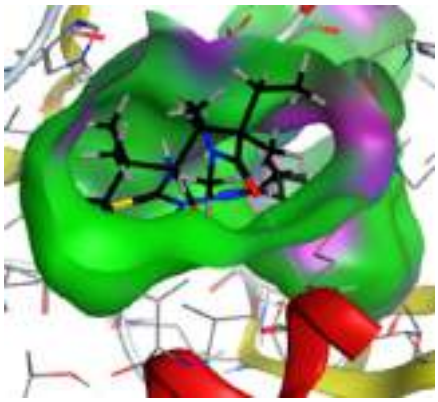
Copolymers	Binding Affinity Kcal/mol	Rmsd (Å)	Smile
5- pose3	**-8.93312**	**1.994968**	**O=C(Nc1nc(NN2N=C[C@H]3SCC(=O)N3C2)ccc1)[C@H](C(C(=O)O)(C)C)C[C@](C(=O)N(C)C)(CC)C**
5- pose4	**-8.8781**	**1.747721**	**O=C(Nc1nc(NN2N=C[C@H]3SCC(=O)N3C2)ccc1)[C@H](C(C(=O)O)(C)C)C[C@](C(=O)N(C)C)(CC)C**
5- pose5	**-8.67667**	**1.770812**	**O=C(Nc1nc(NN2N=C[C@H]3SCC(=O)N3C2)ccc1)[C@H](C(C(=O)O)(C)C)C[C@](C(=O)N(C)C)(CC)C**
Standard	**-9.42921**	**1.680834**	**S=C(N/N=C(/C)\c1ccc([N+](=O)[O-])cc1)NC(=O)[C@H](C(C(=O)O)(C)C)C[C@](C(=O)N(C)C)(CC)C**

Table (4- 11): Details of the best pose of protein 8C7Y

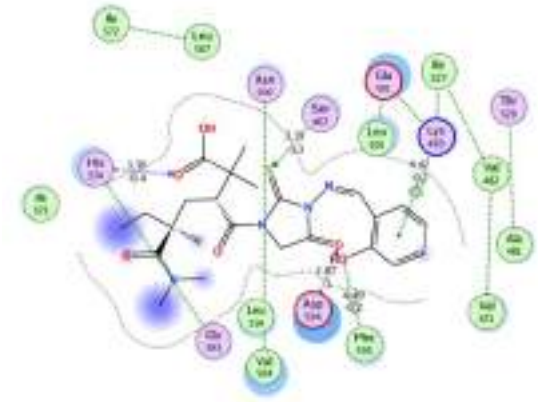
Copolymers	Binding Affinity Kcal/mol	Rmsd (Å)	Atom of compound	Atom of Receptor	Involved receptor residues	Type of interaction bond	Distance (Å)	E (kcal/mol)
1- pose1	**-9.42921**	**1.680834**	**C 1** **N 8** **S 12** **O 31**	**OE2** **N** **CG2** **CA**	**GLU 501 (B)** **ASP 594 (B)** **ILE 513 (B)** **GLU 501 (B)**	**H-donor** **H-acceptor** **H-acceptor** **H-acceptor**	**3.23** **3.3** **3.82** **3.38**	**-0.4** **-2.2** **-0.7** **-0.6**
2- pose1	**-7.86163**	**1.314758**	**O 8** **S 9** **O 33** **O 31** **6-ring**	**N** **OG** **CA** **6-ring** **CB**	**ASP 594 (B)** **SER 467 (B)** **HIS 574 (B)** **PHE 595 (B)** **LYS 483 (B)**	**H-acceptor** **H-acceptor** **H-acceptor** **H-pi** **pi-H**	**2.87** **3.19** **3.36** **4.49** **4.42**	**-1** **-1.3** **-0.4** **-0.2** **-0.2**
3- pose1	**-7.76099**	**2.02882**	**S 3** **S 3** **O 38** **O 39** **O 49** **C 26** **6-ring** **6-ring**	**OG** **NZ** **CA** **NZ** **ND2** **6-ring** **CE** **CA**	**SER 467 (B)** **LYS 483 (B)** **GLY 593 (B)** **LYS 483 (B)** **ASN 500 (B)** **PHE 595 (B)** **LYS 483 (B)** **GLY 593 (B)**	**H-acceptor** **H-acceptor** **H-acceptor** **H-acceptor** **H-acceptor** **H-pi** **pi-H** **pi-H**	**3.13** **4.32** **3.15** **3.07** **2.99** **4.84** **4.72** **4.32**	**-2.1** **-0.5** **-0.6** **-0.5** **-3.7** **-0.4** **-0.4** **-0.4**
4- pose1	**-8.25522**	**1.773028**	**C 23** **N 32** **N 34** **S 3** **S 3** **O 37**	**OE2** **OG1** **O** **CB** **CA** **CA**	**GLU 501 (B)** **THR 529 (B)** **GLN 530 (B)** **LEU 514 (B)** **GLY 593 (B)** **GLU 501 (B)**	**H-donor** **H-donor** **H-donor** **H-acceptor** **H-acceptor** **H-acceptor**	**3.39** **3.37** **2.88** **3.95** **3.44** **3.26**	**-0.7** **-0.5** **-1.4** **-0.6** **-0.8** **-0.7**
5- pose1	**-9.14807**	**1.866477**	**C 16** **C 29** **S 30** **S 30** **O 36** **S 30** **S 30** **O 38** **6-ring**	**O** **O** **O** **O** **O** **CB** **CG2** **CD** **CB**	**HIS 574 (B)** **ASP 594 (B)** **ALA 481 (B)** **ILE 527 (B)** **HIS 574 (B)** **LYS 483 (B)** **THR 529 (B)** **ARG 575 (B)** **ASP 594 (B)**	**H-donor** **H-donor** **H-donor** **H-donor** **H-donor** **H-acceptor** **H-acceptor** **H-acceptor** **pi-H**	**3.33** **3.3** **4.29** **3.51** **2.88** **3.7** **3.63** **3.58** **4.06**	**-0.3** **-0.4** **0** **0.1** **-3.9** **-0.3** **-0.5** **-0.3** **-0.3**
Standard	**-8.62212**	**1.924656**	**N1 1** **N2 6** **O1 10** **N3 16**	**OE2** **O** **O** **N**	**GLU 501** **GLN 530** **HOH 913** **CYS 532**	**(B) H-donor** **(B) H-donor** **(B) H-acceptor** **(B) H-acceptor**	**2.84** **2.87** **2.68** **2.91**	**-5.5** **-5.0** **-2.4** **-5.3**



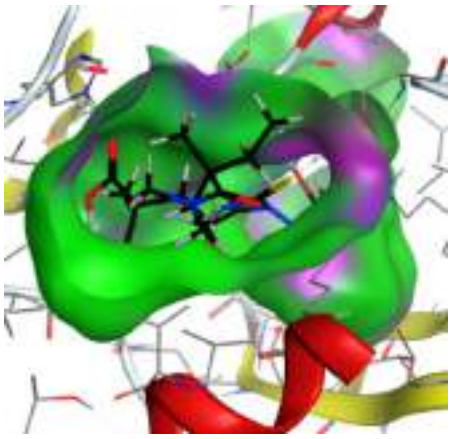
1- pose1



1- pose1



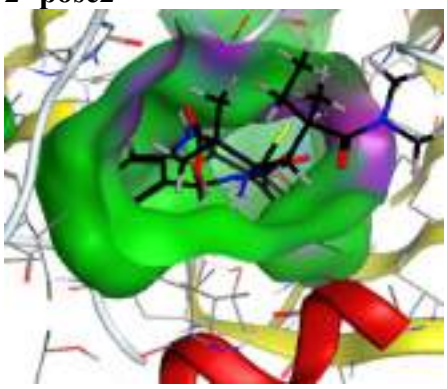
2- pose2



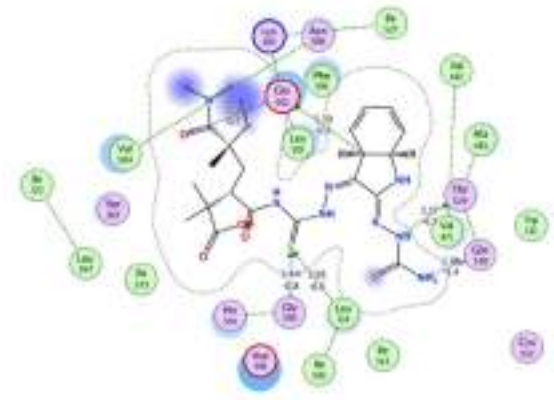
2- pose2



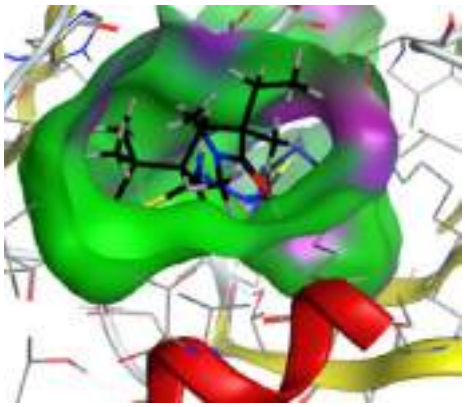
3- pose1



3- pose1



4-pose1



4-pose1

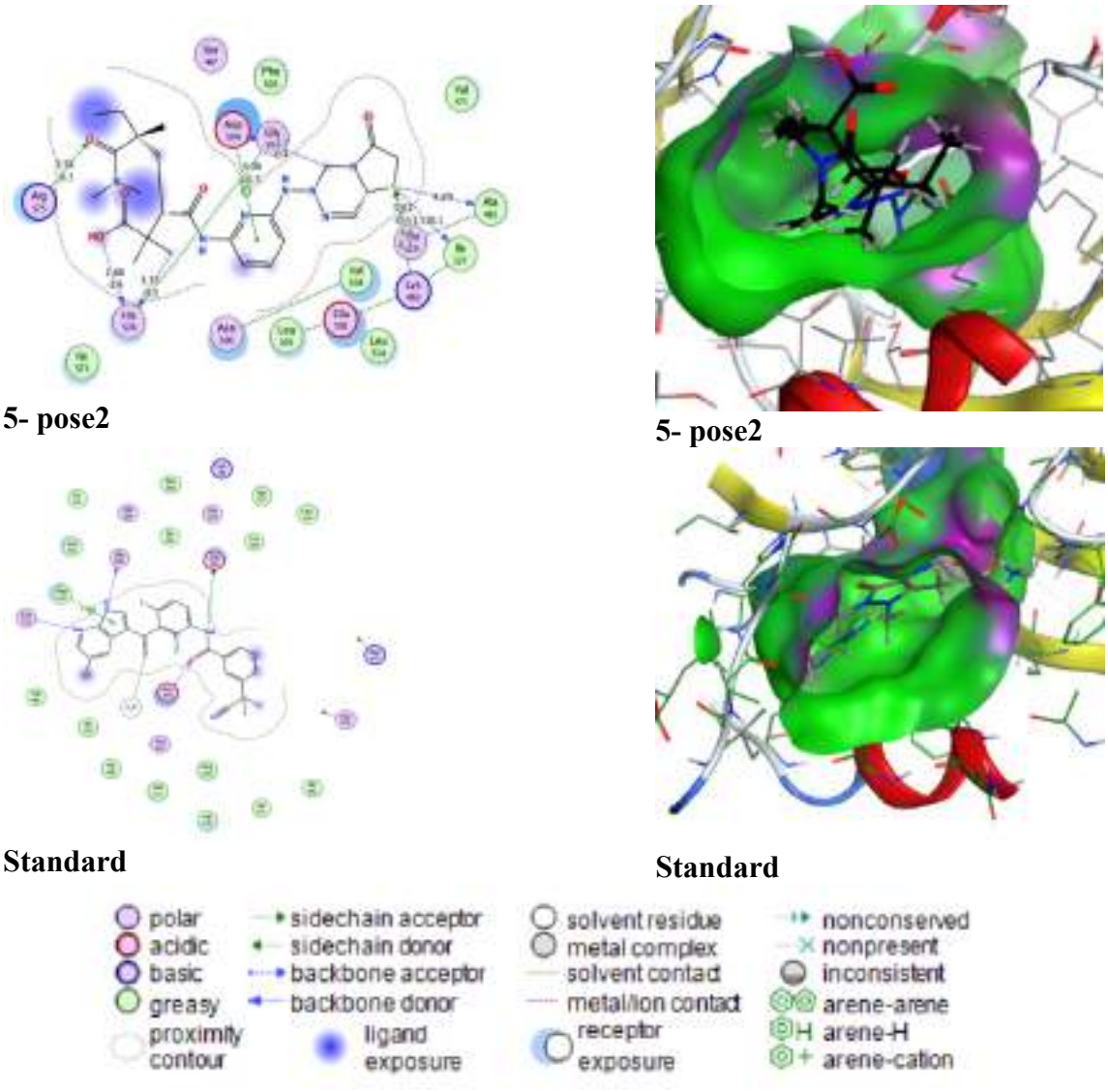


Figure (4- 324): 2D and 3D of the best pose.

4.55 Interpretation of molecular docking results

Molecular docking analysis against the 8C7Y protein revealed noticeable differences in the binding behavior, interaction stability, and energetic compatibility of the investigated compounds inside the receptor active site. In molecular docking studies, the binding affinity value represents the estimated free energy of binding between the ligand and the receptor. More negative values indicate stronger binding stability and a greater probability of forming a stable ligand–protein complex. At the same time, RMSD values are important indicators of docking reliability and pose accuracy. Generally, RMSD values lower than 2 Å indicate that the predicted ligand orientation inside the binding pocket is acceptable and structurally reliable.

Therefore, the interpretation of the present results depends mainly on the combination of binding affinity, RMSD values, and the nature of molecular interactions formed with the amino acid residues of the receptor.

The obtained docking results demonstrated that all investigated copolymers were able to fit successfully within the active pocket of the 8C7Y receptor, with binding affinity values ranging approximately from −7.7 to −9.4 kcal/mol. This range indicates that the synthesized copolymers possess favorable binding characteristics and exhibit good compatibility with the receptor cavity. However, significant variations were observed among the copolymers regarding the strength of binding and interaction patterns, suggesting that the chemical structure and functional groups of each ligand play an important role in determining docking efficiency and receptor stabilization.

Among all tested ligands, copolymer (1) exhibited the strongest binding affinity, reaching −9.42921 kcal/mol, accompanied by an RMSD value of 1.680834 Å. This result indicates that the copolyme achieved highly stable accommodation inside the active site while maintaining an acceptable geometric orientation. The high binding affinity of compound 1 may be attributed to its ability to establish multiple stabilizing interactions with important amino acid residues such as GLU 501, ASP 594, and ILE 513. The presence of both hydrogen donor and hydrogen acceptor interactions suggests that the ligand was capable of forming a strong hydrogen-bonding network within the receptor cavity. Hydrogen bonding interactions are considered among the most important contributors to ligand stabilization because they improve molecular recognition and strengthen receptor–ligand affinity. In addition, the interaction distances were within acceptable ranges, indicating favorable electronic overlap and efficient intermolecular attraction forces. Therefore, the excellent docking score observed for copolymer (1) reflects both energetic stability and proper spatial orientation inside the binding site.

The docking analysis also demonstrated that copolymer (5) displayed highly promising behavior, with a binding affinity value of −9.14807 kcal/mol and RMSD

value of 1.866477 Å. Although its binding affinity was slightly weaker than copolymer (1), it formed a larger interaction network with several receptor residues, including HIS 574, ASP 594, ALA 481, ILE 527, LYS 483, THR 529, and ARG 575. This large number of interactions indicates extensive occupation of the binding pocket and suggests that copolymer (5) has high surface complementarity with the receptor cavity. Particularly important was the interaction with HIS 574 and ASP 594, since these residues appear repeatedly among the most active ligand poses and may represent critical residues involved in receptor stabilization. Moreover, copolymer (5) exhibited both hydrogen-bond interactions and hydrophobic π-H interactions, indicating that the ligand benefits from multiple stabilization mechanisms simultaneously. Such interaction diversity usually enhances binding persistence and may improve biological activity under physiological conditions.

Copolymer (4) demonstrated intermediate docking performance with a binding affinity of −8.25522 kcal/mol and RMSD value of 1.773028 Å. Despite showing weaker binding compared with copolymers (1) and (5), the copolymer still displayed acceptable receptor affinity and structural stability. The ligand established several hydrogen-bond interactions with residues such as GLU 501, THR 529, GLN 530, LEU 514, and GLY 593. These interactions indicate that copolymer (4) possesses moderate stabilization ability within the active site. However, the lower binding affinity compared with copolymers (1) and (5) suggests that the interaction strength or electronic compatibility may not be sufficiently optimized. This may result from weaker electrostatic interactions, less favorable hydrophobic contact distribution, or partial steric mismatch inside the receptor pocket.

Copolymers (2) and (3) showed comparatively lower docking efficiencies. Copolymer (2) recorded a binding affinity of −7.86163 kcal/mol, while compound 3 showed −7.76099 kcal/mol. Although these values still indicate acceptable receptor binding, they are noticeably weaker than those obtained for copolymers (1) and (5). Interestingly, copolymer (2) exhibited the lowest RMSD value among all ligands, reaching only 1.314758 Å. This means that the predicted docking

orientation is highly geometrically reliable and stable. Nevertheless, geometric stability alone is insufficient to guarantee stronger binding affinity. The energetic contribution of the interactions remains more important than RMSD alone. Copolymers (3) formed several interactions with residues including SER 467, LYS 483, ASN 500, PHE 595, and GLY 593, but its RMSD value slightly exceeded 2 Å, suggesting relatively lower pose precision compared with the other ligands. Furthermore, some interactions appeared weaker due to larger bond distances and lower interaction energies, which may explain the reduced docking score.

Comparison with the standard copolymer revealed highly significant observations. The standard ligand exhibited a binding affinity around −8.62 kcal/mol with RMSD value of 1.924656 Å. Based on these values, copolymers (1) clearly surpassed the standard in binding strength, while copolymer (5) demonstrated very comparable and highly competitive behavior. This finding suggests that copolymers (1) and (5) may possess stronger inhibitory potential toward the 8C7Y receptor than the reference ligand itself. The superior activity of these copolymers may be related to the presence of suitable pharmacophoric groups capable of forming strong hydrogen bonds and favorable hydrophobic interactions within the active site.

Overall, the molecular docking study suggests that the investigated ligands possess promising inhibitory potential against the 8C7Y receptor, particularly copolymers (1) and (5), which demonstrated the best balance between binding affinity, RMSD stability, and interaction diversity. The results indicate that proper interaction distribution, hydrogen-bond formation, and favorable ligand orientation collectively contribute to enhanced receptor binding. Therefore, these copolymers may represent promising candidates for further biological evaluation, molecular dynamics simulation, and future drug development studies targeting the 8C7Y protein.

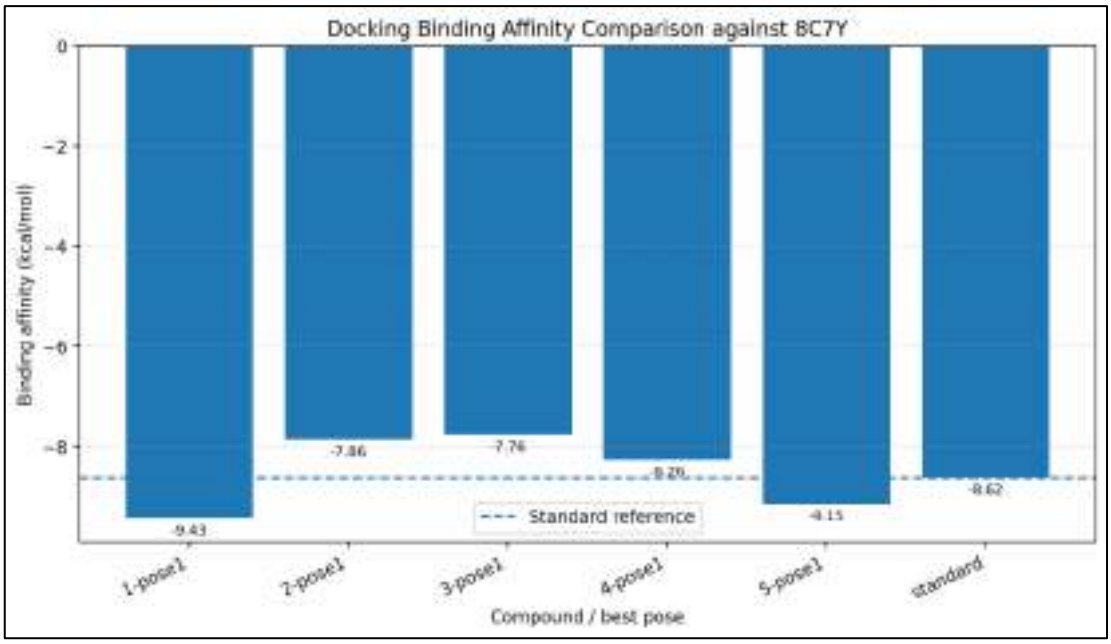


Figure (4- 325):This chart illustrates the comparative binding affinity values of all copolymers against the 8C7Y receptor. More negative values indicate stronger predicted binding strength and higher receptor affinity. The graph clearly shows the superior performance of copolymers 1 and 5 compared with the remaining ligands and the standard copolymers.

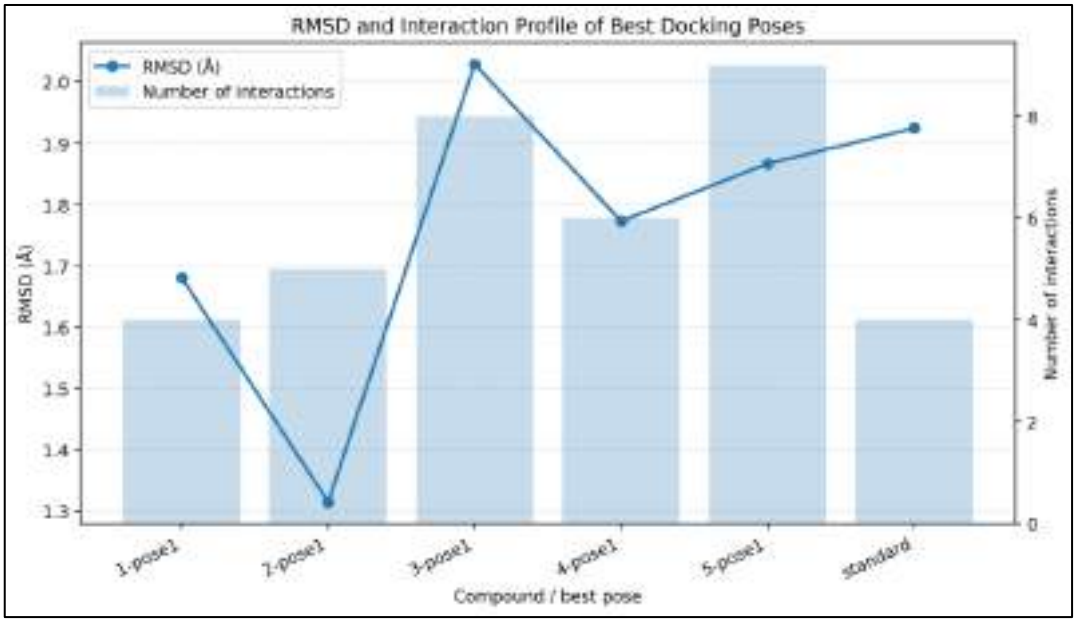


Figure (4- 326):This chart presents the relationship between RMSD values and the total number of receptor interactions for the best docking poses. Lower RMSD values indicate better structural reliability of the docking pose, while a higher number of interactions reflects stronger stabilization within the receptor cavity. Copolymer 5 exhibited the richest interaction profile, whereas copolymer 2 showed the best geometric stability.

4.56 Molecules Library Preparation

The newly copolymers **(**1, 2, 3, 4, 5**)** were synthesized and characterization to using in molecular docking process, Chemdraw Ultra 12.0 (https://chemdraw pro.software.informer.com/12.0/) software was utilized to generate the 3D structures of the copolymers **(**1, 2, 3, 4, 5**)** and followed by energy minimization. The structures were pre-optimized with semi-empirical AM1 method using Hyperchem 8.08 software. The structures were optimized using density functional theory DFT method by employing the B3LYP/6-31G basis set to obtain the most stable conformation. The convergent value of maximum force, root-mean-square (RMS) force, maximum displacement and RMS displacement are set by default and achieved "YES". All values are positive after calculating vibrational frequencies for ligands; those results indicate that the ligands are stable. The optimized structures were combined in one database on MOE software (Molecular Operating Environment (MOE), 2019) in order to study the affinity of ligands (fig.4-327). Also, figure 1 illustrates the schematic representation of the docking procedure, analysis of ligands, and reactivity.

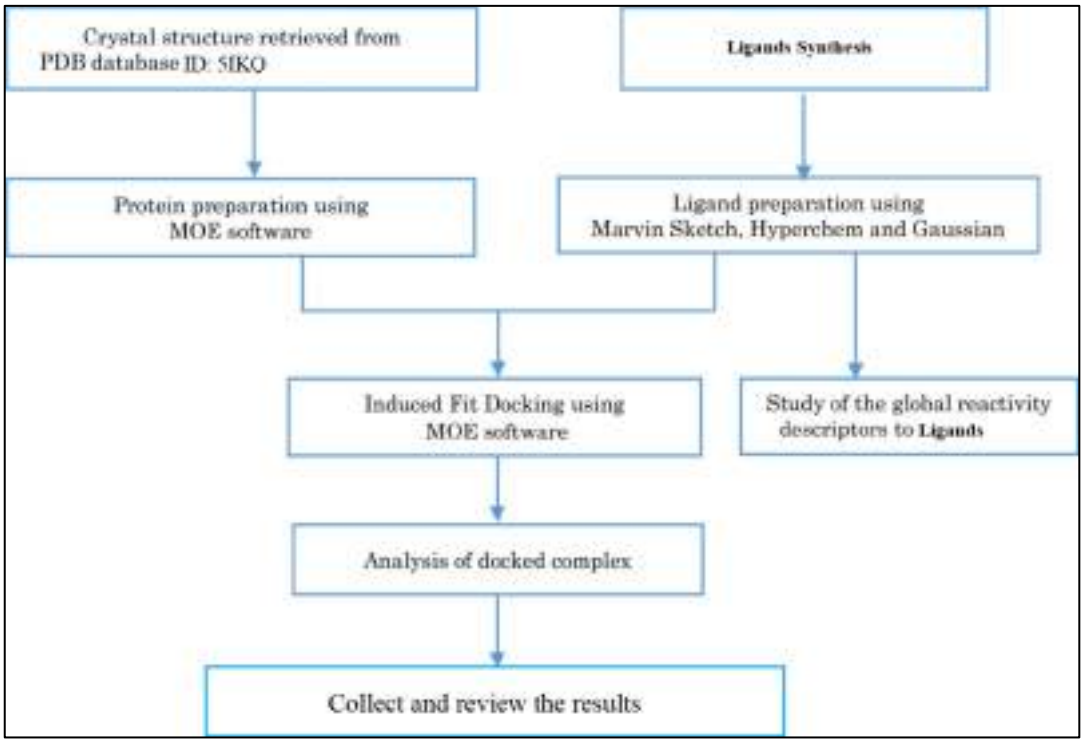


Figure (4- 327): Schematic representation of the docking procedure, analysis of ligands and reactivity.

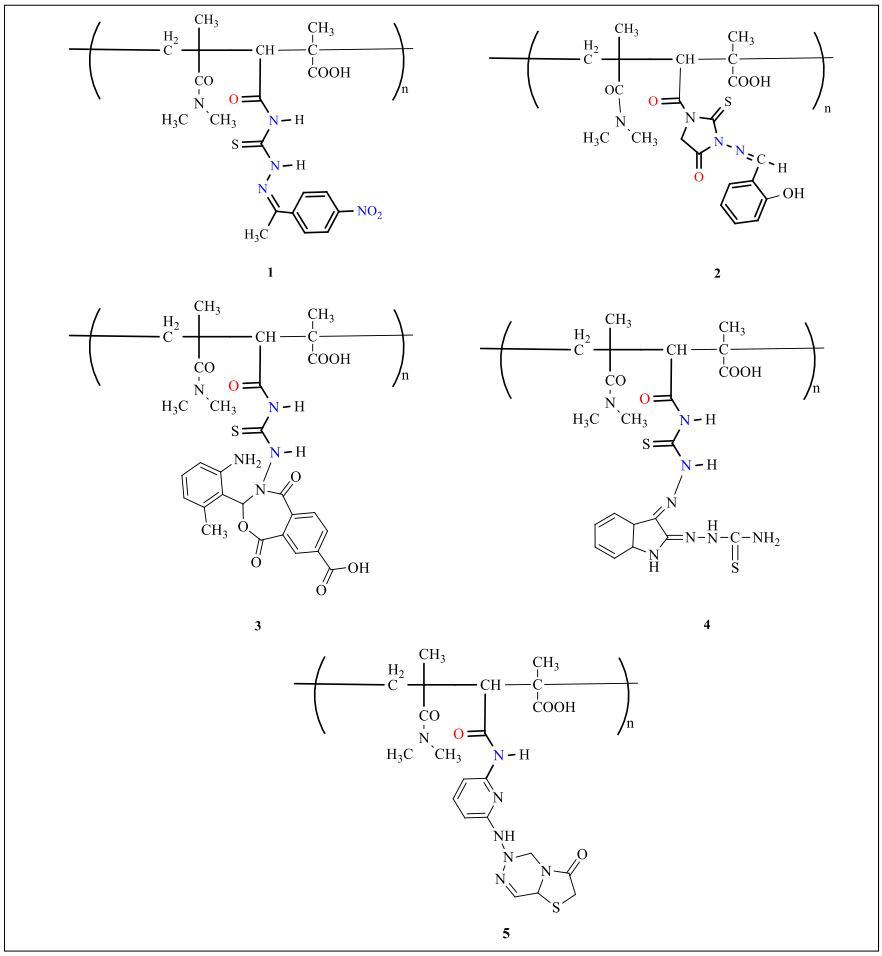


Figure (4- 328): 2D structures of selected copolymers (ligands).

4.57 Receptors preparation

The crystal structures of the proteins (5IKQ) (fig.4-329) was selected from the Protein Data Bank. Because the water molecule in the active site of the target proteins plays an important role, it was inserted in the active sites to ensure making a hydrogen bond between the ligand and the target. After that, the proteins structure was prepared by correcting the missing bonds, which were broken in X-ray diffraction, and then the hydrogen atoms were added also Importantly, PDB is a trusted source for the crystal structure of biological macromolecules worldwide.



Figure (4- 329): Crystal structures of the 5IKQ proteins.

4.58 Ligand–Protein molecular docking

All the docking and scoring calculations were performed using the molecular operation environment software (MOE) (Molecular Operating Environment (MOE), 2019). The crystal structure of the protein (5IKQ) (fig.4-330) at a resolution of 2.41 Å was obtained from the Protein Data Bank. A resolution between 1.4 and 2.5 Å is considered a good quality for docking studies. It is known that the best score of RMSD values should be less than 2 Å with an energy score less than or equal to -7 kcal/mol. These two values are often used as criteria to validate the result of the molecular docking.

4.59 Results

Molecular docking is used as a fundamental tool in the drug discovery pipeline. In the present study, MOE software was applied to perform all molecular docking calculations and predict the binding modes of the prepared copolymers (1, 2, 3, 4, 5) with the protein (5IKQ) (fig.4-331). The predicted binding affinities and features of the investigated copolymers (1, 2, 3, 4, 5) toward 5IKQ are listed in the next tables. These tables show the best binding poses of copolymers (1, 2, 3, 4, 5) against target proteins. The 2D and 3D representations of interactions of the inspected copolymers

with the key amino acid residues of the (5IKQ) proteins are illustrated in the next figures and tables. Copolymers (1, 2, 3, 4, 5) showed good binding affinity values (Table 4-12 and Table 4-13) with proteins (5IKQ). The binding and mode of interactions of the copolymers (1, 2, 3, 4, 5) with the (5IKQ) protein are shown in 2D and 3D figures. From the interactions, it has been shown that primarily there are different types of interactions (hydrogen bonding and hydrophobic interactions). Interactions were further examined for bond lengths and hydrogen bonds in the active site and were illustrated in the last figures. The results from these figures showed that copolymers (1, 2, 3, 4, 5) interact with different amino acid residues in three different interactions: H-donor, H-acceptor, and H-pi, as well as two H-acceptor and pi-H interactions with the water and different amino acids. The distance and energy binding of interaction are listed in the next tables.

Table (4- 12): The binding affinity and rmsd result of copolymers with 5IKQ

Copolymers	Mseq	Binding Affinity Kcal/mol	Rmsd (Å)	E_conf	E_place	E_score1	E_refine	E_score2
1- pose1	**1**	**-8.9212**	**2.467667**	**70.04081**	**-13.1467**	**-5.85184**	**-24.3844**	**-8.9212**
1- pose2	**1**	**-8.61888**	**1.785912**	**67.82926**	**-12.4637**	**-8.68086**	**-14.4368**	**-8.61888**
1- pose 3	**1**	**-8.22303**	**1.705931**	**102.8066**	**-11.9471**	**-5.1008**	**-8.30995**	**-8.22303**
1- pose4	**1**	**-7.90337**	**1.505062**	**87.74002**	**-18.4552**	**-6.9085**	**-7.98404**	**-7.90337**
1- pose5	**1**	**-7.65708**	**3.86451**	**39.41525**	**-14.315**	**-6.99956**	**-23.2361**	**-7.65708**
2- pose1	**2**	**-8.55305**	**1.676937**	**123.2149**	**-21.0189**	**-5.62453**	**-10.4812**	**-8.55305**
2- pose2	**2**	**-8.21299**	**1.629039**	**166.7165**	**-15.1157**	**-4.3842**	**0.169912**	**-8.21299**
2- pose3	**2**	**-8.08189**	**1.929031**	**136.1422**	**-14.8999**	**-4.22267**	**-7.59303**	**-8.08189**
2- pose4	**2**	**-8.05914**	**1.288394**	**122.1873**	**-13.8362**	**-7.3313**	**-8.34028**	**-8.05914**
2- pose5	**2**	**-7.58965**	**1.596513**	**115.5488**	**-12.7568**	**-4.68195**	**-10.0411**	**-7.58965**
3- pose1	**3**	**-9.28179**	**1.999978**	**-0.16836**	**-6.10299**	**0.557371**	**-11.8574**	**-9.28179**
3- pose2	**3**	**-8.4647**	**3.330435**	**11.20716**	**-4.26934**	**-2.75727**	**-8.86952**	**-8.4647**
3- pose3	**3**	**-8.06155**	**3.039991**	**-50.4707**	**-2.32562**	**1.431081**	**-22.7572**	**-8.06155**
3- pose4	**3**	**-7.95359**	**1.526107**	**18.82102**	**-2.65224**	**-0.70704**	**-1.17634**	**-7.95359**
3- pose5	**3**	**-7.90174**	**2.145704**	**-39.2697**	**-7.10011**	**-3.16653**	**-16.1749**	**-7.90174**
4- pose1	**4**	**-9.17947**	**1.96491**	**64.3281**	**-14.4383**	**-3.15624**	**-13.5048**	**-9.17947**
4- pose2	**4**	**-8.32525**	**1.961664**	**38.14109**	**-14.1757**	**-5.44909**	**-4.89837**	**-8.32525**
4- pose3	**4**	**-8.18621**	**1.54851**	**59.31128**	**-15.8703**	**-2.24875**	**-1.40385**	**-8.18621**
4- pose4	**4**	**-8.08169**	**3.377768**	**79.37996**	**-12.7831**	**-4.454**	**-11.8648**	**-8.08169**
4- pose5	**4**	**-8.00363**	**2.025324**	**71.31677**	**-22.1472**	**-2.87923**	**-2.41242**	**-8.00363**
5- pose1	**5**	**-9.8142**	**2.59508**	**-33.9878**	**-14.9686**	**-3.22272**	**-40.5698**	**-9.8142**
5- pose2	**5**	**-9.42482**	**1.987207**	**-3.72111**	**-13.1323**	**-5.95965**	**-24.3083**	**-9.42482**
5- pose3	**5**	**-9.2948**	**2.606561**	**-13.6099**	**-11.5126**	**-4.80875**	**-30.2435**	**-9.2948**
5- pose4	**5**	**-9.05468**	**2.305744**	**-27.0041**	**-14.1774**	**-3.23975**	**-22.4367**	**-9.05468**
5- pose5	**5**	**-9.04324**	**2.63804**	**-4.69117**	**-14.3394**	**-5.10406**	**-27.4921**	**-9.04324**
Standard	**Std**	**-7.17611**	**2.096395**	**-46.0659**	**-14.1648**	**-10.165**	**-37.0982**	**-7.17611**

Table (4- 13): Details of the best pose of protein 5IKQ

Copolymers	Binding Affinity Kcal/mol	Rmsd (Å)	Smile
1- pose1	**-8.9212**	**2.467667**	**S=C(N/N=C(/C)\c1ccc([N+](=O)[O-])cc1)NC(=O)[C@H](C(C(=O)O)(C)C)C[C@](C(=O)N(C)C)(CC)C**
1- pose2	**-8.61888**	**1.785912**	**S=C(N/N=C(/C)\c1ccc([N+](=O)[O-])cc1)NC(=O)[C@H](C(C(=O)O)(C)C)C[C@](C(=O)N(C)C)(CC)C**
1- pose 3	**-8.22303**	**1.705931**	**S=C(N/N=C(/C)\c1ccc([N+](=O)[O-])cc1)NC(=O)[C@H](C(C(=O)O)(C)C)C[C@](C(=O)N(C)C)(CC)C**
1- pose4	**-7.90337**	**1.505062**	**S=C(N/N=C(/C)\c1ccc([N+](=O)[O-])cc1)NC(=O)[C@H](C(C(=O)O)(C)C)C[C@](C(=O)N(C)C)(CC)C**
1- pose5	**-7.65708**	**3.86451**	**S=C(N/N=C(/C)\c1ccc([N+](=O)[O-])cc1)NC(=O)[C@H](C(C(=O)O)(C)C)C[C@](C(=O)N(C)C)(CC)C**
2- pose1	**-8.55305**	**1.676937**	**S=C1N(/N=C\c2c(O)cccc2)C(=O)CN1C(=O)[C@@H](C(C(=O)O)(C)C)C[C@@](C(=O)N(C)C)(CC)C**
2- pose2	**-8.21299**	**1.629039**	**S=C1N(/N=C\c2c(O)cccc2)C(=O)CN1C(=O)[C@@H](C(C(=O)O)(C)C)C[C@@](C(=O)N(C)C)(CC)C**
2- pose3	**-8.08189**	**1.929031**	**S=C1N(/N=C\c2c(O)cccc2)C(=O)CN1C(=O)[C@@H](C(C(=O)O)(C)C)C[C@@](C(=O)N(C)C)(CC)C**
2- pose4	**-8.05914**	**1.288394**	**S=C1N(/N=C\c2c(O)cccc2)C(=O)CN1C(=O)[C@@H](C(C(=O)O)(C)C)C[C@@](C(=O)N(C)C)(CC)C**
2- pose5	**-7.58965**	**1.596513**	**S=C1N(/N=C\c2c(O)cccc2)C(=O)CN1C(=O)[C@@H](C(C(=O)O)(C)C)C[C@@](C(=O)N(C)C)(CC)C**
3- pose1	**-9.28179**	**1.999978**	**S=C(NC(=O)[C@H](C(C(=O)O)(C)C)C[C@](C(=O)N(C)C)(CC)C)NN1[C@@H](c2c(N)cccc2C)OC(=O)c2c(C1=O)ccc(C(=O)O)c2**
3- pose2	**-8.4647**	**3.330435**	**S=C(NC(=O)[C@H](C(C(=O)O)(C)C)C[C@](C(=O)N(C)C)(CC)C)NN1[C@@H](c2c(N)cccc2C)OC(=O)c2c(C1=O)ccc(C(=O)O)c2**
3- pose3	**-8.06155**	**3.039991**	**S=C(NC(=O)[C@H](C(C(=O)O)(C)C)C[C@](C(=O)N(C)C)(CC)C)NN1[C@@H](c2c(N)cccc2C)OC(=O)c2c(C1=O)ccc(C(=O)O)c2**
3- pose4	**-7.95359**	**1.526107**	**S=C(NC(=O)[C@H](C(C(=O)O)(C)C)C[C@](C(=O)N(C)C)(CC)C)NN1[C@@H](c2c(N)cccc2C)OC(=O)c2c(C1=O)ccc(C(=O)O)c2**
3- pose5	**-7.90174**	**2.145704**	**S=C(NC(=O)[C@H](C(C(=O)O)(C)C)C[C@](C(=O)N(C)C)(CC)C)NN1[C@@H](c2c(N)cccc2C)OC(=O)c2c(C1=O)ccc(C(=O)O)c2**
4- pose1	**-9.17947**	**1.96491**	**S=C(N/N=C/1\C(=N/NC(=S)N)\N[C@H]2[C@@H]\1C=CC=C2)NC(=O)[C@H](C(C(=O)O)(C)C)C[C@](C(=O)N(C)C)(CC)C**
4- pose2	**-8.32525**	**1.961664**	**S=C(N/N=C/1\C(=N/NC(=S)N)\N[C@H]2[C@@H]\1C=CC=C2)NC(=O)[C@H](C(C(=O)O)(C)C)C[C@](C(=O)N(C)C)(CC)C**
4- pose3	**-8.18621**	**1.54851**	**S=C(N/N=C/1\C(=N/NC(=S)N)\N[C@H]2[C@@H]\1C=CC=C2)NC(=O)[C@H](C(C(=O)O)(C)C)C[C@](C(=O)N(C**

Copolymers	Binding Affinity Kcal/mol	Rmsd (Å)	Smile
			)C)(CC)C
4- pose4	-8.08169	3.377768	S=C(N/N=C/1\C(=N/NC(=S)N)\N[C@H]2[C@@H]\1C=CC=C2)NC(=O)[C@H](C(C(=O)O)(C)C)C[C@](C(=O)N(C)C)(CC)C
4- pose5	-8.00363	2.025324	S=C(N/N=C/1\C(=N/NC(=S)N)\N[C@H]2[C@@H]\1C=CC=C2)NC(=O)[C@H](C(C(=O)O)(C)C)C[C@](C(=O)N(C)C)(CC)C
5- pose1	-9.8142	2.59508	O=C(Nc1nc(NN2N=C[C@H]3SCC(=O)N3C2)ccc1)[C@H](C(C(=O)O)(C)C)C[C@](C(=O)N(C)C)(CC)C
5- pose2	-9.42482	1.987207	O=C(Nc1nc(NN2N=C[C@H]3SCC(=O)N3C2)ccc1)[C@H](C(C(=O)O)(C)C)C[C@](C(=O)N(C)C)(CC)C
5- pose3	-9.2948	2.606561	O=C(Nc1nc(NN2N=C[C@H]3SCC(=O)N3C2)ccc1)[C@H](C(C(=O)O)(C)C)C[C@](C(=O)N(C)C)(CC)C
5- pose4	-9.05468	2.305744	O=C(Nc1nc(NN2N=C[C@H]3SCC(=O)N3C2)ccc1)[C@H](C(C(=O)O)(C)C)C[C@](C(=O)N(C)C)(CC)C
5- pose5	-9.04324	2.63804	O=C(Nc1nc(NN2N=C[C@H]3SCC(=O)N3C2)ccc1)[C@H](C(C(=O)O)(C)C)C[C@](C(=O)N(C)C)(CC)C
Standard	-7.17611	2.096395	Clc1c(Nc2c(C(=O)[O-])cccc2)c(Cl)ccc1C

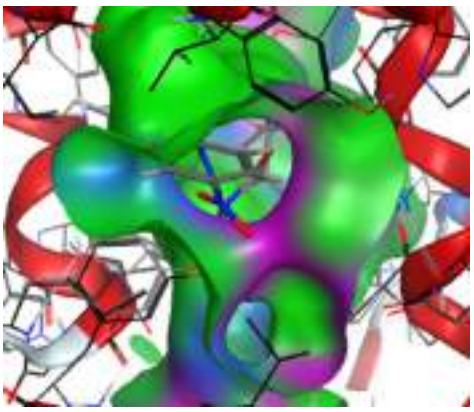
Table (4- 14): Name of copolymers and smiles

Copolymers	Binding Affinity Kcal/mol	Rmsd (Å)	Atom of compound	Atom of Receptor	Involved receptor residues	Type of interaction bond	Distance (Å)	E (kcal/mol)
1- pose2	-8.61888	1.785912	S 12	CA	SER 354 (B)	H-acceptor	3.53	-0.7
			S 12	CA	SER 354 (B)	H-acceptor	3.53	-0.7
			O 31	OG	SER 531 (B)	H-acceptor	2.25	16.7
			O 31	OG	SER 531 (B)	H-acceptor	2.56	-0.3
			6-ring	CG1	VAL 117 (B)	pi-H	3.31	-0.3
2- pose1	-8.55305	1.676937	O 3	CA	ALA 528 (B)	H-acceptor	3.06	-0.7
			O 3	CA	ALA 528 (B)	H-acceptor	3.06	-0.6
			O 8	CZ	PHE 382 (B)	H-acceptor	2.91	19.2
			S 9	CA	VAL 350 (B)	H-acceptor	3.35	-1
			S 9	CA	VAL 350 (B)	H-acceptor	3.35	-1
			6-ring	CA	SER 531 (B)	pi-H	3.82	-0.6
			6-ring	CA	SER 531 (B)	pi-H	3.82	-0.5
3- pose1	-9.28179	1.999978	S 3	CG	ARG 121 (B)	H-acceptor	3.42	-0.7
			S 3	CG	ARG 121 (B)	H-acceptor	3.48	-0.7
			S 3	CB	ALA 528 (B)	H-acceptor	3.66	-0.6
			O 6	NH2	ARG 121 (B)	H-acceptor	2.43	4.7
			O 6	NH2	ARG 121 (B)	H-acceptor	2.81	-2.5
			6-ring	CA	VAL 524 (B)	pi-H	4.35	-0.3
			6-ring	CA	VAL 524 (B)	pi-H	4.35	-0.4
4- pose1	-9.17947	1.96491	C 17	OH	TYR 356 (B)	H-donor	3.28	-0.3
			S 3	CA	ALA 528 (B)	H-acceptor	4.36	-0.4
			S 3	OG	SER 531 (B)	H-acceptor	2.85	-0.3
			S 3	CA	ALA 528 (B)	H-acceptor	4.36	-0.4
			S 3	OG	SER 531 (B)	H-acceptor	2.91	-0.8
			N 31	OH	TYR 386 (B)	H-acceptor	2.67	-0.2
			N 31	OH	TYR 386 (B)	H-acceptor	2.83	-1.8
			S 35	CG	MET 523 (B)	H-acceptor	3.68	-0.4

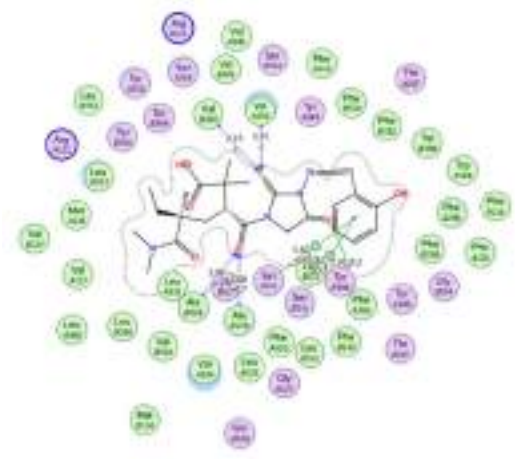
Copolymers	Binding Affinity Kcal/mol	Rmsd (Å)	Atom of compound	Atom of Receptor	Involved receptor residues	Type of interaction bond	Distance (Å)	E (kcal/mol)
			S 35	**CA**	**GLY 527 (B)**	**H-acceptor**	**4.28**	**-0.4**
			S 35	**CG**	**MET 523 (B)**	**H-acceptor**	**3.77**	**-0.3**
			S 35	**CA**	**GLY 527 (B)**	**H-acceptor**	**4.28**	**-0.5**
5- pose2	**-9.42482**	**1.987207**	**O 4**	**OG**	**SER 531 (B)**	**H-acceptor**	**3.02**	**-0.8**
			O 38	**OH**	**TYR 386 (B)**	**H-acceptor**	**3.12**	**-0.5**
			O 38	**OH**	**TYR 386 (B)**	**H-acceptor**	**3.05**	**-0.8**
			C 10	**6-ring**	**TYR 386 (B)**	**H-pi**	**4.75**	**-0.4**
			C 10	**6-ring**	**TYR 386 (B)**	**H-pi**	**4.7**	**-0.3**
			6-ring	**CD1**	**LEU 532 (B)**	**pi-H**	**3.81**	**-0.5**
			6-ring	**CD1**	**LEU 532 (B)**	**pi-H**	**3.73**	**-0.3**
Standard	**-7.17611**	**2.096395**	**O 1**	**OH**	**TYR 386**	**(B) H-acceptor**	**2.83**	**-1.4**
			O 1	**OH**	**TYR 386**	**(B) H-acceptor**	**2.83**	**-1.8**
			6-ring	**CA**	**GLY 527**	**(B) pi-H**	**4.31**	**-0.5**
			6-ring	**CG1**	**VAL 524**	**(B) pi-H**	**4.61**	**-0.2**
			6-ring	**CA**	**GLY 527**	**(B) pi-H**	**4.31**	**-0.3**



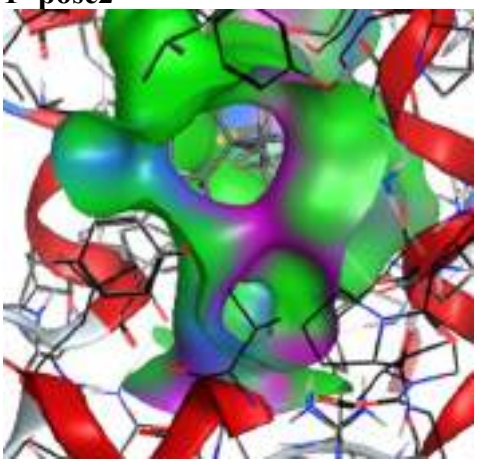
1- pose2



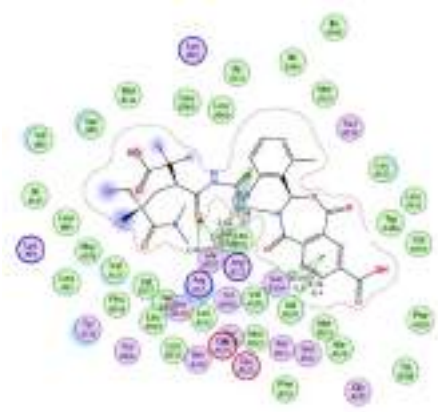
1- pose2



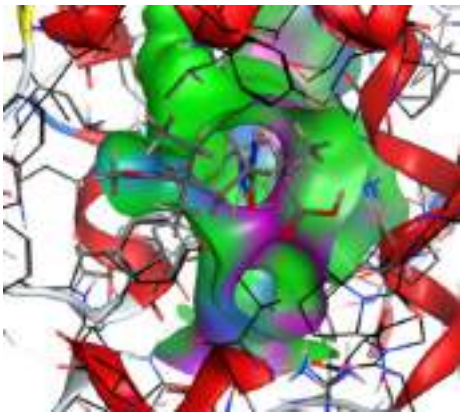
2- pose1



2- pose1



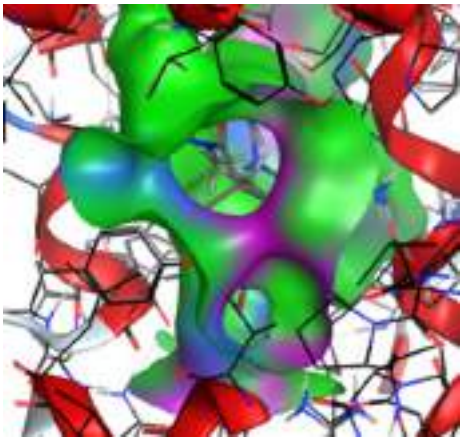
3- pose1



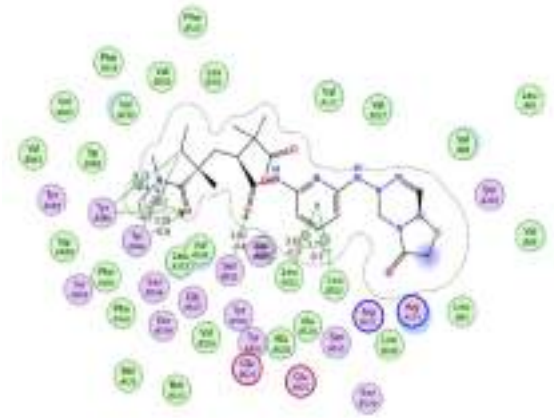
3- pose1



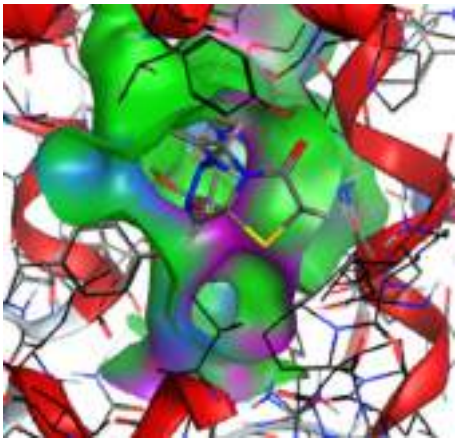
4-pose1



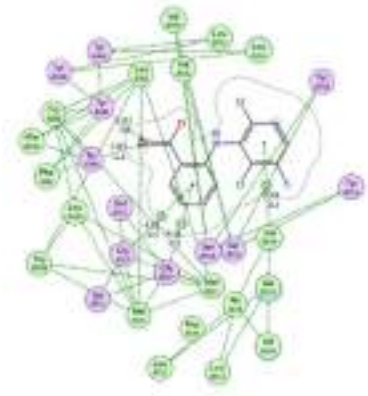
4-pose1



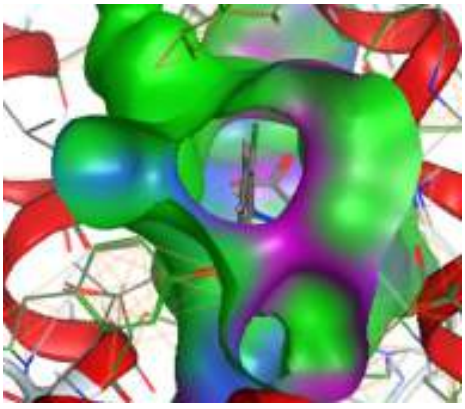
5- pose2



5- pose2



Standard



Standard



Figure (4- 330): 2D and 3D of the best pose.

4.60 Interpretation of molecular docking results

The molecular docking investigation against the 5IKQ protein demonstrated that all synthesized compounds were successfully accommodated within the receptor binding cavity, indicating favorable geometric and electronic compatibility with the active site. The obtained binding affinity values ranged approximately between −8.5 and −9.4 kcal/mol for the best poses, while the standard copolymer exhibited a weaker binding affinity of only −7.17611 kcal/mol. This difference clearly indicates that the investigated copolymers possess stronger predicted inhibitory potential toward the 5IKQ receptor compared with the reference ligand. In molecular docking studies, more negative binding affinity values indicate stronger receptor–ligand stabilization and lower binding free energy, which usually reflects greater complex stability and potentially enhanced biological activity.

At the same time, RMSD values for the best docking poses remained within acceptable limits, mostly around or below 2 Å. Such values indicate that the docking orientations are geometrically reliable and structurally stable inside the receptor cavity. Therefore, the combination of strong binding affinity and acceptable RMSD values suggests that the investigated copolymers are capable of forming energetically favorable and structurally stable complexes with the 5IKQ protein.

A deeper analysis of the docking data reveals that copolymer 5-pose2 exhibited the strongest binding affinity among all tested copolymers, reaching −9.42482 kcal/mol with an RMSD value of 1.987207 Å. This result is particularly important because it indicates that copolymer (5) possesses exceptional receptor-binding capability and favorable spatial accommodation within the active pocket. The interaction profile demonstrated that this ligand formed several stabilizing contacts

with critical amino acid residues including SER 531, TYR 386, and LEU 532. The ligand also exhibited both hydrogen-bonding interactions and π-H hydrophobic interactions. The simultaneous presence of polar and hydrophobic interactions significantly enhances receptor stabilization because hydrogen bonds contribute to directional specificity while hydrophobic interactions improve pocket occupation and reduce ligand mobility inside the cavity. In particular, repeated interactions with TYR 386 suggest that this residue may play a crucial role in stabilizing active ligands within the 5IKQ binding site.

Interestingly, copolymer 3-pose1 also demonstrated highly promising docking behavior, with a binding affinity value of −9.28179 kcal/mol and RMSD value very close to the ideal threshold at 1.999978 Å. Although its RMSD was slightly higher than some other ligands, the copolymer formed multiple interactions with ARG 121, ALA 528, and VAL 524. The interaction with ARG 121 appears especially important because arginine residues are highly polar and frequently contribute strong electrostatic stabilization through hydrogen-bonding interactions. Furthermore, the ligand established π-H interactions with VAL 524, suggesting additional hydrophobic stabilization within the receptor cavity. The overall interaction network indicates that copolymer (3) achieved efficient occupation of the active site and strong energetic stabilization, explaining its highly favorable docking score.

Copolymer (4)-pose1 also exhibited excellent docking performance with a binding affinity of −9.17947 kcal/mol and RMSD value of 1.96491 Å. One of the most remarkable features of this ligand is the extensive interaction network formed inside the receptor cavity. The ligand interacted with several residues including TYR 356, SER 531, TYR 386, MET 523, GLY 527, and ALA 528. The large number of interactions suggests high surface complementarity between the ligand and receptor pocket. Moreover, the ligand formed both donor and acceptor hydrogen bonds, which significantly improve binding stability and receptor recognition. The repeated interaction with TYR 386 observed in both copolymers (4) and (5) further supports the importance of this residue as a key stabilizing residue within the active site.

Although copolymers (1)-pose2 and 2-pose1 displayed slightly weaker binding affinities compared with copolymers (3), (4), and (5), their docking results still indicate favorable receptor binding. copolymer (1)-pose2 achieved a binding affinity of −8.61888 kcal/mol with RMSD value of 1.785912 Å. The ligand formed multiple hydrogen-bond interactions mainly with SER 354 and SER 531 in addition to a π-H interaction with VAL 117. These interactions contributed to reasonable stabilization within the active site. However, the smaller interaction network compared with compounds 4 and 5 may explain the slightly reduced binding affinity.

Similarly, copolymer (2)-pose1 exhibited a binding affinity of −8.55305 kcal/mol and RMSD value of 1.676937 Å, which represents one of the lowest RMSD values among the investigated ligands. This suggests very reliable geometric orientation inside the binding pocket. The ligand established interactions with ALA 528, PHE 382, VAL 350, and SER 531, including hydrogen bonds and π-H interactions. Despite its good geometric stability, the overall interaction strength appears weaker than the stronger-performing copolymers, which explains its comparatively lower binding affinity.

Comparison with the standard copolymer provides highly important evidence regarding the effectiveness of the synthesized ligands. The standard copolymer exhibited weaker binding affinity and fewer stabilizing interactions compared with nearly all tested copolymers. This indicates that the synthesized molecules possess improved receptor compatibility and stronger interaction capability with the 5IKQ active site. Particularly, copolymers (3), (4), and (5) significantly outperformed the standard ligand, suggesting that their structural features may provide enhanced inhibitory potential against the target protein.

From a mechanistic perspective, the superior docking behavior observed for copolymers (3), (4), and (5) may be attributed to several factors simultaneously. First, the presence of heteroatoms such as oxygen, sulfur, and nitrogen allows efficient hydrogen-bond formation with polar amino acid residues inside the receptor cavity. Second, aromatic rings contribute to hydrophobic and π-H interactions that

stabilize ligand orientation within the hydrophobic regions of the active pocket. Third, the molecular size and flexibility of these copolymers appear suitable for efficient cavity occupation without causing severe steric hindrance. These combined factors likely contribute to the observed enhancement in binding affinity and receptor stabilization.

Overall, the molecular docking study strongly suggests that copolymers (3), (4), and (5) represent the most promising candidates against the 5IKQ receptor, with copolymer (5) demonstrating the strongest overall binding affinity. The obtained results indicate that these copolymers possess excellent receptor compatibility, favorable interaction patterns, and stable docking conformations. Therefore, these ligands may be considered suitable candidates for further biological evaluation, molecular dynamics simulation studies, and future drug development investigations targeting the 5IKQ protein.

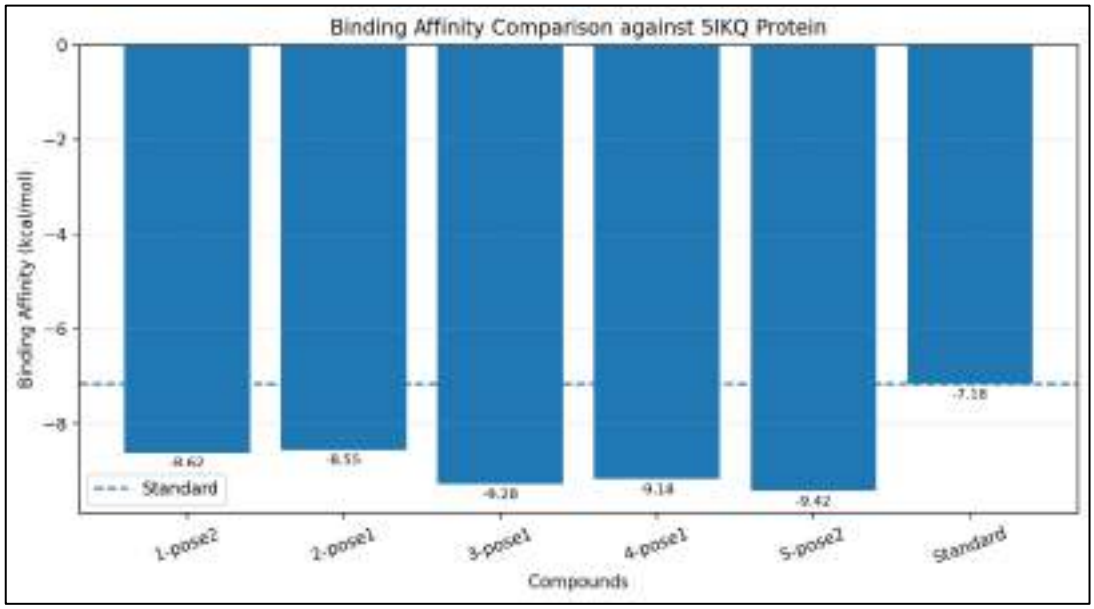


Figure (4- 331):The figure illustrates the comparative binding affinity values of the investigated copolymers against the 5IKQ receptor. More negative values indicate stronger predicted receptor binding and better complex stability. The graph clearly demonstrates the superior docking performance of compounds 3, 4, and especially copolymer 5 compared with the standard ligand.

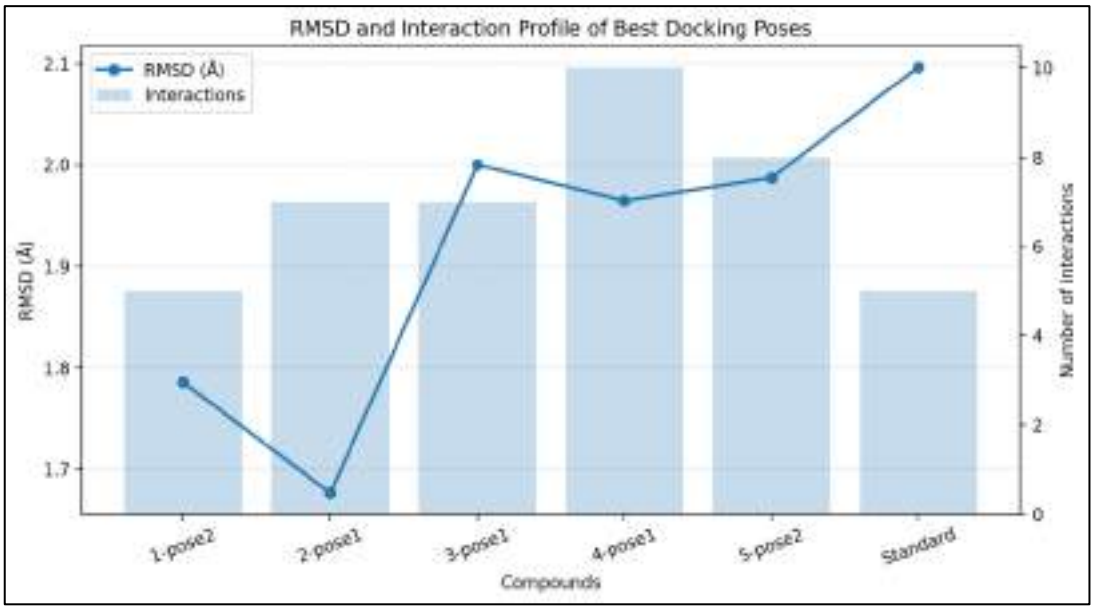


Figure (4- 332):The figure presents the relationship between RMSD values and the total number of receptor interactions for the best docking poses. Lower RMSD values indicate better docking reliability, while higher interaction counts reflect stronger receptor stabilization. Copolymers 4 exhibited the largest interaction network, whereas copolymers 3 and 5 combined strong binding affinity with highly favorable interaction profiles.

4.61 Biological activity:

4.61.1 Cytotoxic potential of copolymer (1) on colon Cell Line(HCT-116)

Copolymer(1) exhibits cytotoxic activity on colon cancer cell line. At 400 µg/mL, the viability of HCT-116 cells reached to (46.479±0.508%) compared to HdFn cells (85.048±0.143%), indicating a cytotoxic pressure. This observation is supported by its IC_{50} values (164.3 µg/mL in cancer cells *vs* 309.4 µg/mL in Hdfn cells) (fig.4-333), suggesting moderate selectivity but weak potency. Structurally, copolymer(1) contains a Schiff base (C=N) and a thiocarbonyl group (C=S), both of which can participate in nucleophilic and electrophilic interactions. However, the absence of extended π-conjugation limits electron delocalization, resulting in reduced stabilization of reactive intermediates and weaker interaction with intracellular targets such as proteins or nucleic acids. Consequently, copolymer(1) may induce mild metabolic disruption without triggering significant apoptotic signaling or oxidative stress pathways (155).

Table (4- 15): Cytotoxic potentials of copolymer(1) on colon cancer cell line vs normal cell line after 24 hrs.; 37 Cº

Conc. (µg/mL)	Cell viability (%) o copolymer(1)		
	HdFn	HTC-116	P - value
	Mean±SD	Mean±SD	
400	85.048±0.143	46.479±0.508	0.001
200	91.662±0.835	60.327±0.624	0.001
100	96.193±0.371	77.964±0.306	0.001
50	98.050±0.375	87.965±0.596	0.001
25	98.779±0.739	93.960±0.388	0.05

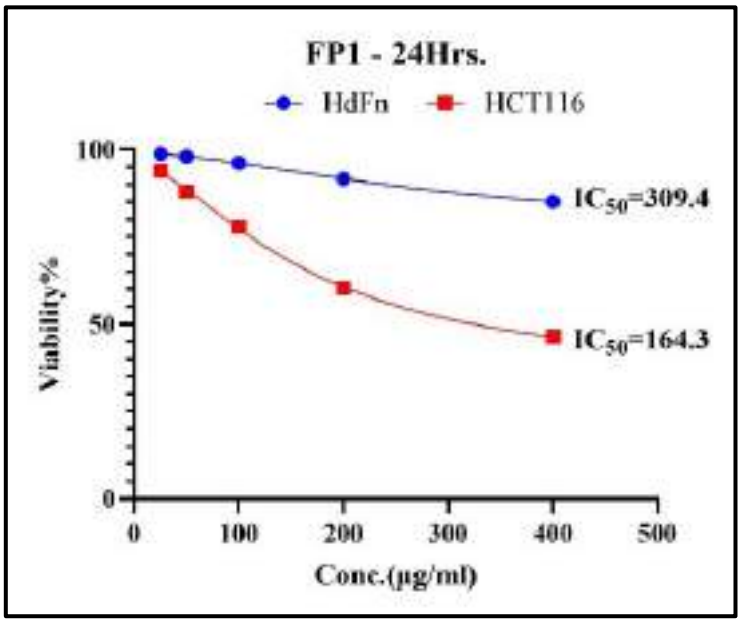


Figure (4- 333): Cytotoxic potentials o copolymer(1) on colon cancer cell line vs normal cell line after 24 hrs.; 37 Cº

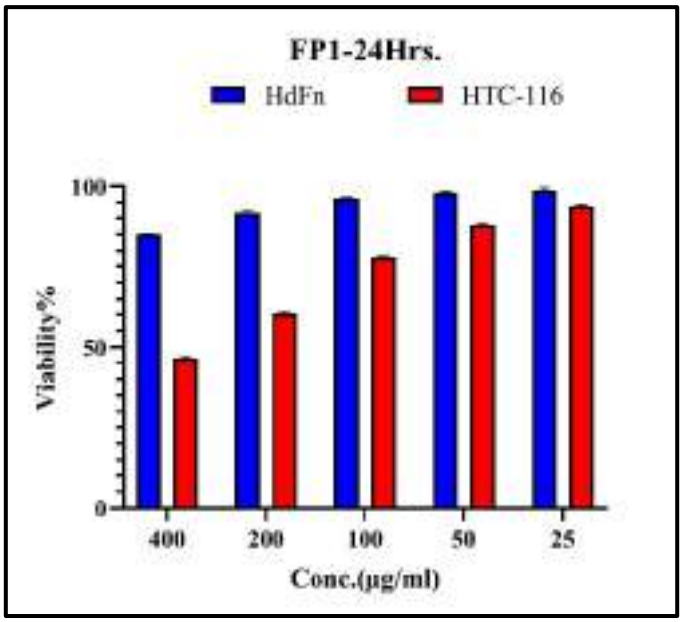


Figure (4- 334): Cytotoxic potentials of copolymer(1) on colon cancer cell line vs normal cell line after 24 hrs.; 37 C°

At 48 hours of exposure, the cytotoxic profile transitions from initial molecular interaction to a phase dominated by intracellular accumulation and sustained functional disruption. The numerical data clearly indicate that all compounds exhibit enhanced cytotoxic effects over time; however, the magnitude of this enhancement varies significantly depending on their structural characteristics. This suggests that time itself is not the primary determinant of cytotoxicity, but rather acts as an amplifying factor for the intrinsic physicochemical properties of each compound, particularly those governing cellular uptake, intracellular retention, and target interaction.

Copolymer(1) also continues to exhibited a cytotoxic activity, although a measurable improvement is observed compared to the 24-hour time point. At 400 µg/ml, the viability of HCT-116 cells decreases to 42. 058±0.894%, while HdFn cells remain relatively unaffected at cell viability of 82. 367±0.694%. copolymer(1) exhibited the most cytotoxic potential of IC_{50} (147.1 µg/ml) in cancer cells compared to 282.8 µg/ml in normal cells; (Table 4-16) and (fig.4-335). This reduction reflects a time-dependent increase in cytotoxicity; however, the overall effect remains limited. Structurally, copolymer(1) lacks sufficient conjugation and electron delocalization, which restricts its ability to stabilize within the intracellular

environment. As a result, the compound is capable of inducing mild cellular stress but fails to sustain prolonged biochemical disruption or trigger significant apoptotic signaling. Consequently, the observed cytotoxic effect progresses gradually but does not reach a level indicative of substantial cellular collapse.

Table (4- 16): Cytotoxic potentials of copolymer(1) on colon cancer cell line vs normal cell line after 48 hrs.; 37 Cº

Conc. (µg/ml)	Cell viability (%) of copolymer(1)		
	HdFn	HTC-116	P - value
	Mean±SD	Mean±SD	
400	82.367±0.694	42.058±0.894	0.001
200	89.388±0.404	54.971±0.995	0.001
100	95.054±0.599	74.068±0.509	0.001
50	97.238±0.815	85.008±0.533	0.001
25	98.690±0.273	91.911±0.611	0.05

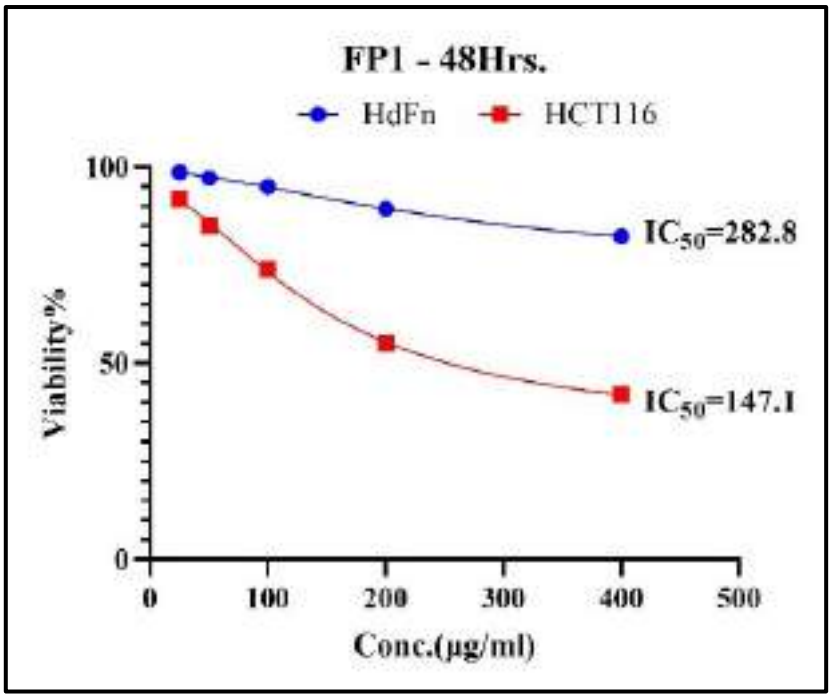


Figure (4- 335): Cytotoxic potentials of copolymer(1) on colon cancer cell line vs normal cell line after 48 hrs.; 37 Cº

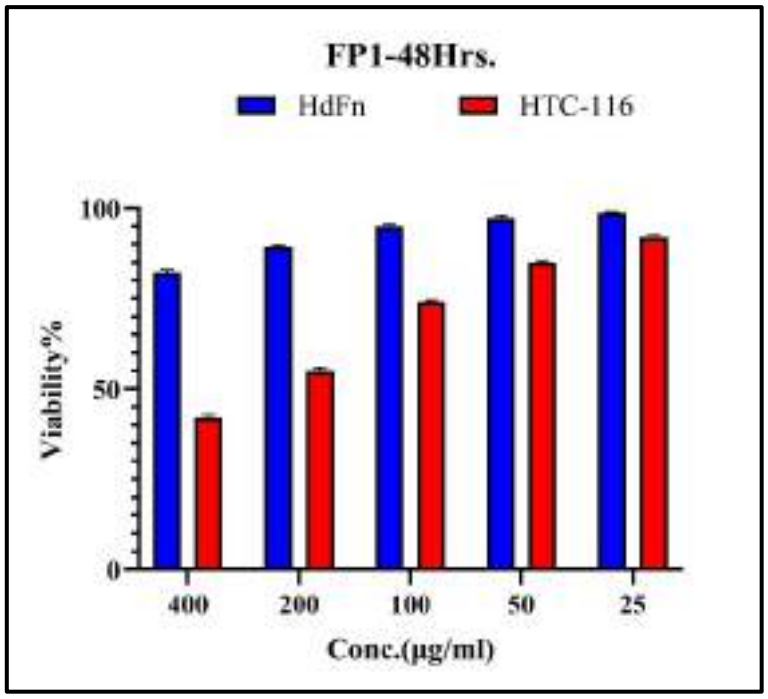


Figure (4- 336): Cytotoxic potentials of copolymer(1) on colon cancer cell line vs normal cell line after 48 hrs.; 37 C°

All compounds at 72 hours exhibited more toxicity against colon cancer cell line.The cytotoxic response reaches its maximum expression, representing the stage at which cellular adaptive mechanisms are no longer sufficient to counteract sustained biochemical stress. At this point, the observed effects reflect cumulative intracellular damage rather than transient interactions. The numerical data clearly indicate that prolonged exposure does not alter the relative ranking of the compounds but instead amplifies their intrinsic activity, confirming that cytotoxicity is fundamentally governed by structural properties rather than exposure time alone.

Copolymer(1), although showing continued improvement over time and at concentration of 400 µg/ml, the viability of HCT-116 cells decreases to 38.251±0.641 %, compared to 79.476±0.836% in HdFn cells, indicating a modest but consistent time-dependent increase in cytotoxicity. The IC_{50} values further decrease to 126.0 µg/mL in cancer cells and 217.0 µg/mL in normal cells line (Table.4-17) and (fig.4-337). Despite this improvement, the overall effect remains limited. This can be attributed to the relatively simple molecular architecture of copolymer(1) , which lacks sufficient conjugation and electron delocalization. As a

result, the copolymer is unable to stabilize within the intracellular environment or sustain multi-site interactions. Consequently, copolymer(1) induces gradual metabolic stress without triggering extensive mitochondrial dysfunction or irreversible cellular damage.

Table (4- 17): Cytotoxic potentials of copolymer(1) on colon cancer cell line vs normal cell line after 72 hrs.; 37 C°

Conc. (µg/mL)	Cell viability (%) of copolymer(1)		
	HdFn	HTC-116	P – value
	Mean±SD	Mean±SD	
400	79.476±0.836	38.251±0.641	0.001
200	85.847±0.701	48.191±0.744	0.001
100	92.254±0.644	69.079±0.679	0.001
50	94.782±0.782	81.600±0.376	0.001
25	96.488±0.146	88.156±0.715	0.01

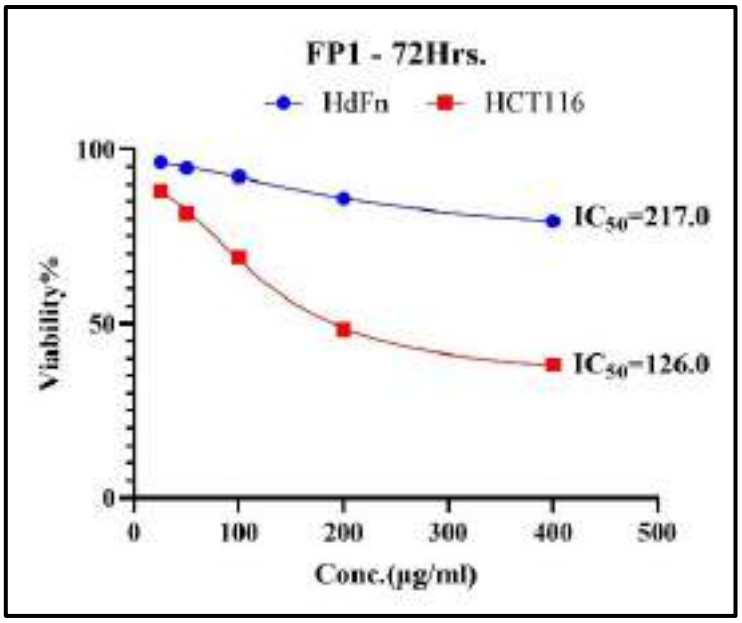


Figure (4- 337): Cytotoxic potentials of copolymer(1) on colon cancer cell line vs normal cell line after 72 hrs.; 37 C°

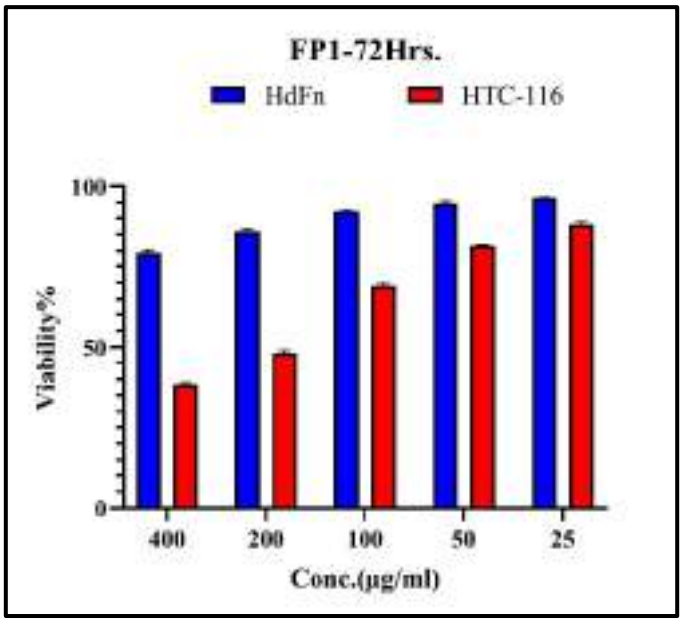


Figure (4- 338): Cytotoxic potentials of copolymer(1) on colon cancer cell line vs normal cell line after 72 hrs.; 37 C°

4.61.2 Antioxidant Activity of copolymer(1) Extract via DPPH Assay.

For copolymer(1), possessed the ability to scavenge DPPH radical at the four concentrations tested (0.0625, 0.125, 0.250 and 0.500 mg/ml). The concentrations 0.250 and 0.500 mg/ml of copolymer(1) shared an approximated radical scavenging activity (43.866±0.012 and 52.286±0.205 %, respectively), but other concentrations (0.125 and 0.0620 mg/ml) less potency than higher concentrations (35.114±0.891 and 28.420±0.649%, respectively). (fig.4-339) (Table4-18) while Vit-C showed variation between scavenging activity.

Table (4- 18): DPPH radical scavenging activity of copolymer(1) and Vit-C.

Samples	DPPH radical scavenging activity Conc. (Mean ± SD)%			
	0.500	0.250	0.125	0.0625
Vitamin-C	75.995±0.185	63.644±0.135	55.221±0.152	39.111±0.027
copolymer(1)	52.286±0.205	43.866±0.012	35.114±0.891	28.420±0.649
P value	0.001	0.01	0.01	0.05

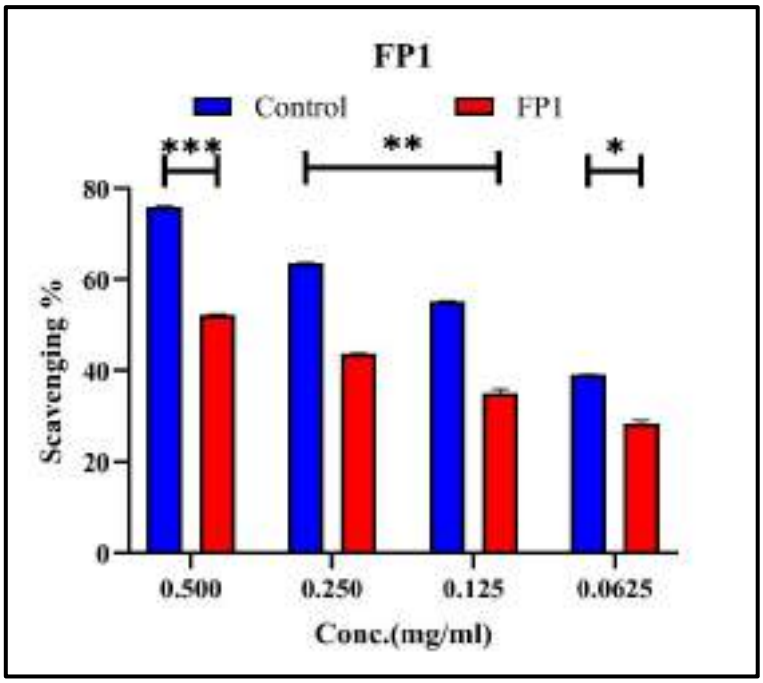


Figure (4- 339): DPPH radical scavenging activity of copolymer(1) and vitamin C

4.61.3 Cytotoxic potential of copolymer (2) on colon Cell Line(HCT-116)

Copolymer(2) demonstrated a slight enhancement in cytotoxic activity. At 400 µg/mL, HCT-116 viability decreases to 43.255±0.608%, while HdFn cells remain largely unaffected 84.212±0.707%. copolymer(2) exhibited the most cytotoxic potential withen IC_{50} values (145.6 µg/mL in cancer cells and 311.2 µg/mL in Hdfn cells) as shown in (Table 4-19) and (fig.4-340) confirm a modest improvement in potency. This increase can be attributed to the incorporation of a heterocyclic nitrogen-containing moiety, which enhances the molecule's ability to form hydrogen bonds and electrostatic interactions with intracellular biomolecules. However, the increased polarity associated with this structural feature may reduce passive diffusion across lipid membranes, thereby limiting intracellular accumulation. As a result, although copolymer(2) shows improved target interaction, its overall cytotoxic effect remains constrained by suboptimal cellular uptake(156).

Table (4- 19): Cytotoxic potentials of copolymer(2) on colon cancer cell line vs normal cell line after 24 hrs.; 37 Cº

Conc. (µg/mL)	Cell viability (%) of copolymer(2)		
	HdFn	HTC-116	P – value
	Mean±SD	Mean±SD	
400	84.212±0.707	43.255±0.608	0.001
200	90.820±0.186	56.502±0.762	0.001
100	95.720±0.439	74.252±0.726	0.001
50	97.238±0.265	87.047±0.767	0.001
25	98.498±0.163	91.761±0.545	0.01

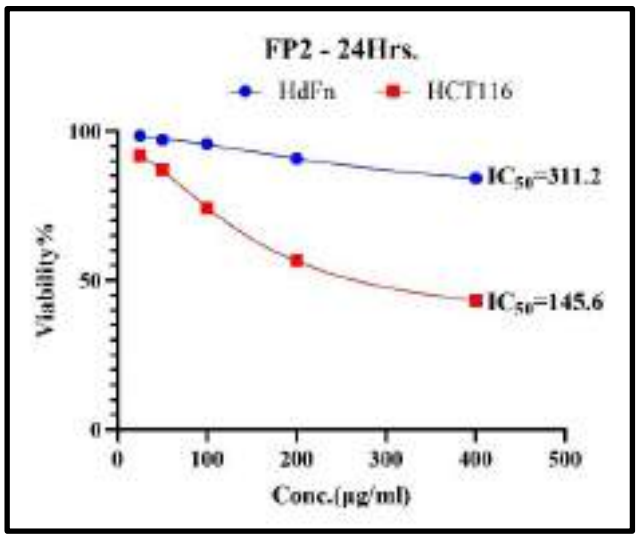


Figure (4- 340): Cytotoxic potentials of copolymer(2) on colon cancer cell line vs normal cell line after 24 hrs.; 37 Cº

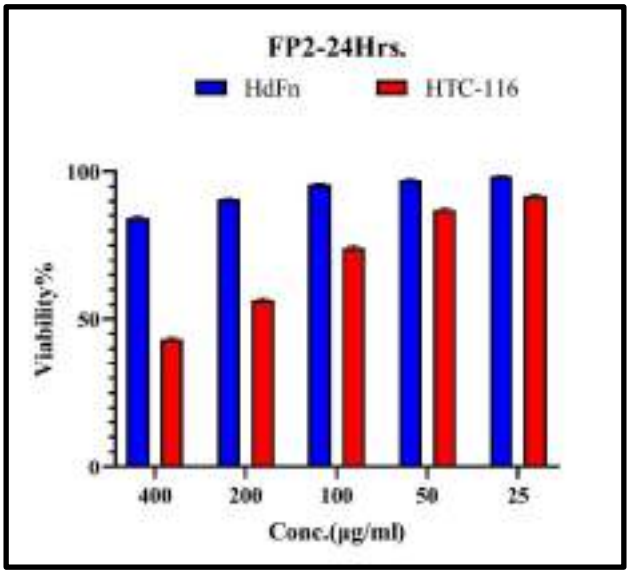


Figure (4- 341): Cytotoxic potentials of copolymer(2) on colon cancer cell line vs normal cell line after 24 hrs.; 37 Cº

Copolymer(2) demonstrated a more pronounced improvement compared to copolymer(1). At 400 µg/ml, HCT-116 cell viability decreases to 39.381±0.675%, while HdFn cells viability remain 82.301±0.665%, indicating stronger cytotoxic pressure with preserved selectivity. The IC_{50} value also become more effective at 126.1 µg/ml in cancer cells *vs*. 223.3 µg/ml in Hdfn normal cells line (Table 4-20) and (fig.4-342). This enhancement can be attributed to the presence of a heterocyclic nitrogen-containing moiety, which increases the compound's ability to engage in hydrogen bonding and electrostatic interactions with intracellular biomolecules. However, despite improved interaction potential, the absence of extended conjugation limits the compound's capacity for sustained intracellular activity. Therefore, while copolymer(2) exhibits greater efficacy than copolymer(1), its cytotoxic effect remains moderate and does not reach the level observed in more structurally optimized compounds.

Table (4- 20): Cytotoxic potentials of copolymer(2) on colon cancer cell line vs normal cell line after 48 hrs.; 37 C°

Conc. (µg/ml)	Cell viability (%) of copolymer(2)		
	HdFn	HTC-116	P – value
	Mean±SD	Mean±SD	
400	82.301±0.665	39.381±0.675	0.001
200	88.036±0.562	49.851±0.668	0.001
100	92.916±0.518	69.749±0.816	0.001
50	96.791±0.210	81.677±0.615	0.01
25	98.043±0.453	89.914±0.608	0.5

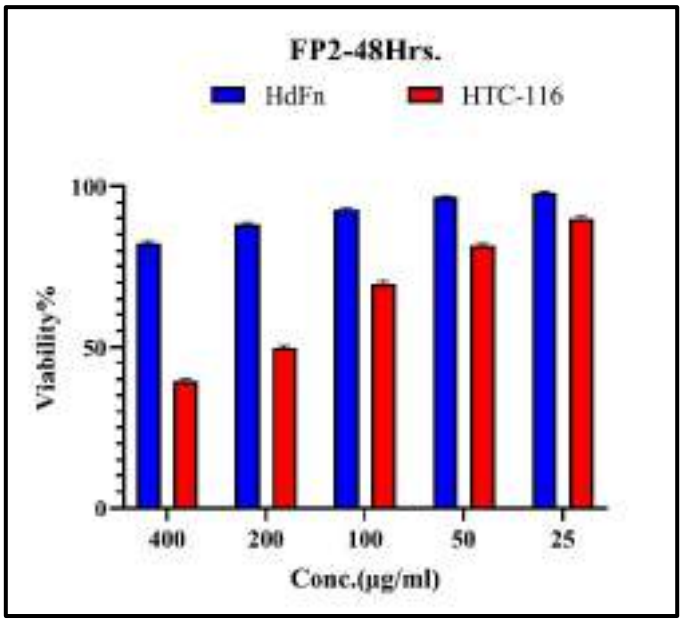


Figure (4- 342): Cytotoxic potentials of copolymer(2) on colon cancer cell line vs normal cell line after 48 hrs.; 37 C°

The cytotoxicity copolymer(2) increased by time and concentrations increased indicating a concentration and time dependent toxicity and demonstrated a more pronounced cytotoxic effect compared to copolymer(1). At 400 µg/ml, HCT-116 cell viability decreases to 33.878±0.704%, while HdFn cells remain at 78.927±0.501%, indicating stronger cytotoxic pressure withen an IC_{50} value of 108.3 µg/ml in cancer cells compared to 185.6 µg/ml in normal cells (Table 4-21) and (fig.4-343). This improvement is associated with the presence of a heterocyclic ring, which enhances the compound's ability to interact with intracellular biomolecules through hydrogen bonding and electrostatic interactions. However, the absence of extended conjugation and limited heteroatom density restrict the copolymer's capacity to maintain sustained intracellular disruption. Therefore, although copolymer(2) exhibits enhanced activity, its effect remains moderate and does not reach deeper levels of cellular impairment.

Table (4- 21): Cytotoxic potentials of o copolymer(2) on colon cancer cell line vs normal cell line after 72 hrs.; 37 Cº

Conc. (µg/mL)	Cell viability (%) of copolymer(2(		
	HdFn	HTC-116	P - value
	Mean±SD	Mean±SD	
400	78.927±0.501	33.878±0.704	0.001
200	84.299±0.593	44.529±0.533	0.001
100	90.581±0.061	61.042±0.746	0.001
50	93.791±0.303	78.279±0.317	0.001
25	96.049±0.645	85.808±0.751	0.001

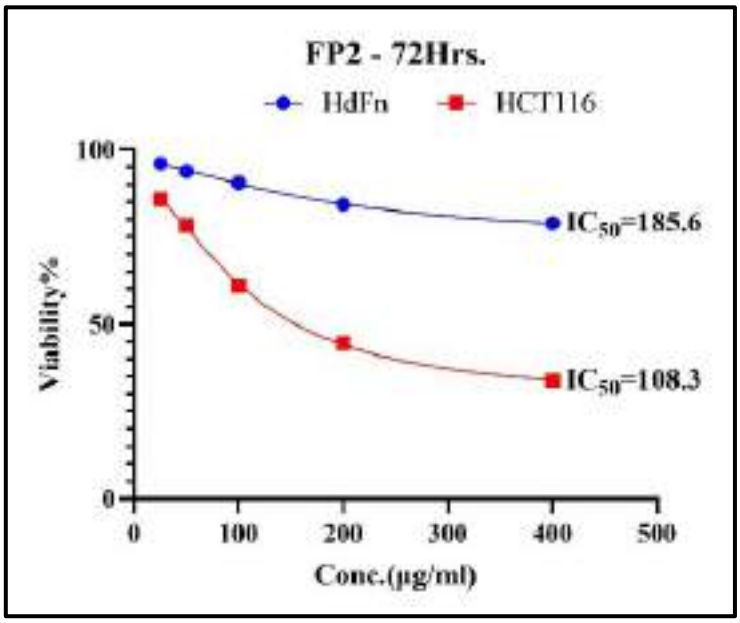


Figure (4- 343): Cytotoxic potentials of copolymer(2) on colon cancer cell line vs normal cell line after 72 hrs.; 37 Cº

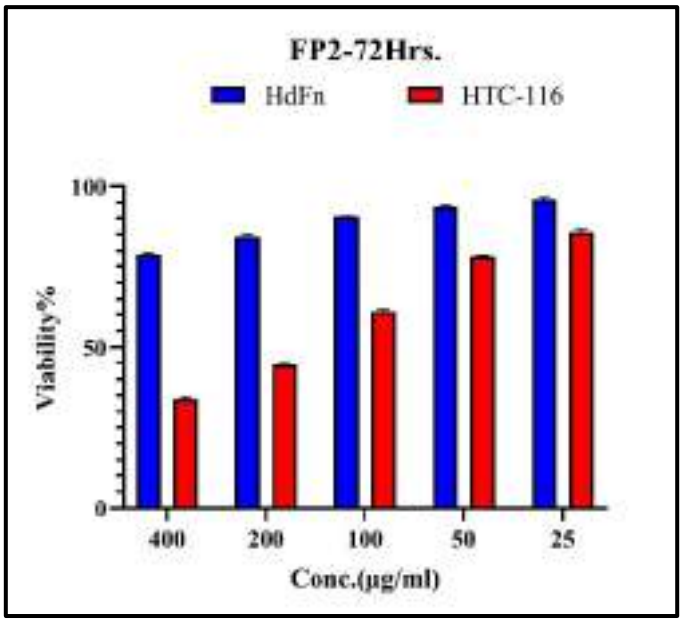


Figure (4- 344): Cytotoxic potentials of o copolymer(2) n colon cancer cell line vs normal cell line after 72 hrs.; 37 C°

4.61.4 Antioxidant Activity of copolymer(2) Extract via DPPH Assay

Copolymer(2), also exhibited a scavenging activity and these activity increased as concentration increased reached to 48.506±0.086 and 56.928±0.071% for 0.250 and 0.500 mg/ml respectively. Other concentrations 0.0620 and 0.125 mg/ml showed also scavenging activity but less than higher concentrations (30.915±0.681and 39.266±0.934%), (fig.4-345) and (Table 4-22) however Vit-c possessed the highest scavenging activity at 0.500 mg/ml reached to 75.995±0.185 % .

Table (4- 22): DPPH radical scavenging activity of copolymer(2) and Vit-C.

Samples	DPPH radical scavenging activity Conc. (Mean ± SD)%			
	0.500	0.250	0.125	0.0625
Vitamin-C	75.995±0.185	63.644±0.135	55.221±0.152	39.111±0.027
copolymer(2)	56.928±0.071	48.506±0.086	39.266±0.934	30.915±0.681
P value	0.001	0.01	0.01	0.5

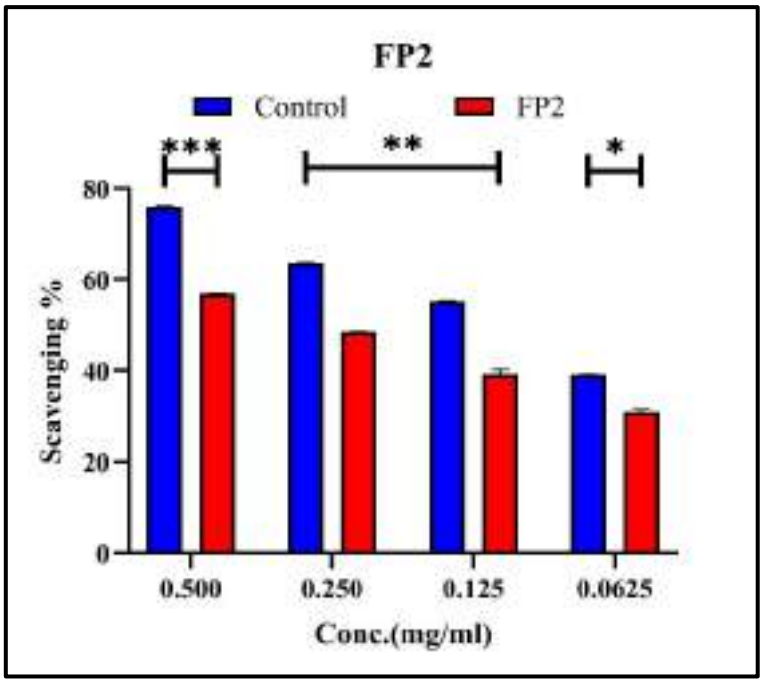


Figure (4- 345): DPPH radical scavenging activity of copolymer(2) and vitamin-C

4.61.5Cytotoxic potential of copolymer (3) on colon Cell Line (HCT-116).

Copolymer(3) exhibited a more pronounced cytotoxic effect, with HCT-116 cell viability decreasing from (89.550±0.306%) at 25 µg/ml to (39.978±0.660%) at 400 µg/ml, while HdFn cells maintain higher viability 82.742±0.650% at 400 µg/ml. The IC_{50} value further decreases to 122.3 µg/mL in cancer cells, indicating enhanced potency and selectivity, (Table 4-23) and (fig.4-346). This improvement is likely associated with increased π-conjugation and the presence of extended aromatic systems, which facilitate electron delocalization. Such structural features enhance molecular stability and enable stronger non-covalent interactions, including π–π stacking with nucleic acids and hydrophobic interactions with membrane components. Additionally, increased lipophilicity may promote improved membrane permeability, leading to higher intracellular concentrations and more effective disruption of cellular processes, particularly mitochondrial function and ATP production(157).

Table (4- 23): Cytotoxic potentials of copolymer(3) on colon cancer cell line vs normal cell line after 24 hrs.; 37 Cº

Conc. (µg/mL)	Cell viability (%) of copolymer(3)		
	HdFn	HTC-116	P – value
	Mean±SD	Mean±SD	
400	82.742±0.650	39.978±0.660	0.001
200	89.069±0.549	50.981±0.580	0.001
100	94.215±0.386	68.998±0.353	0.001
50	96.475±0.221	84.745±0.513	0.001
25	97.880±0.665	89.550±0.306	0.01

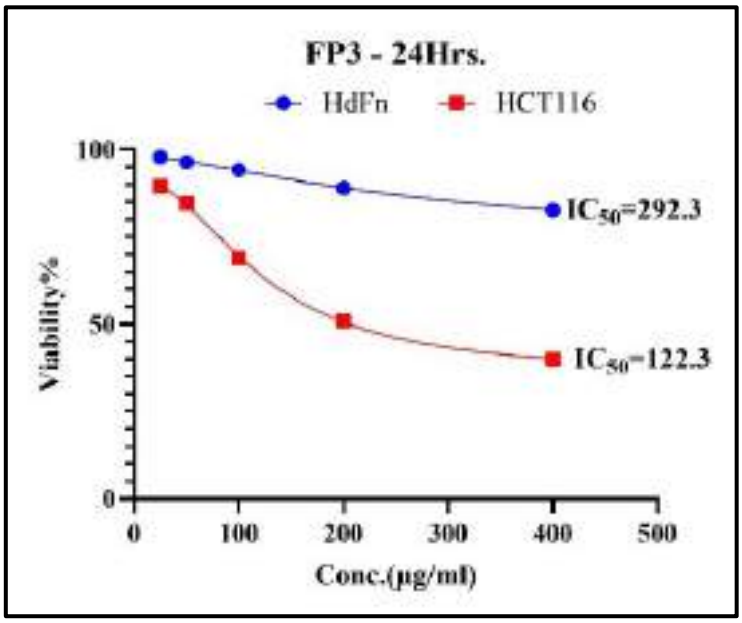


Figure (4- 346): Cytotoxic potentials of copolymer(3) on colon cancer cell line vs normal cell line after 24 hrs.; 37 Cº

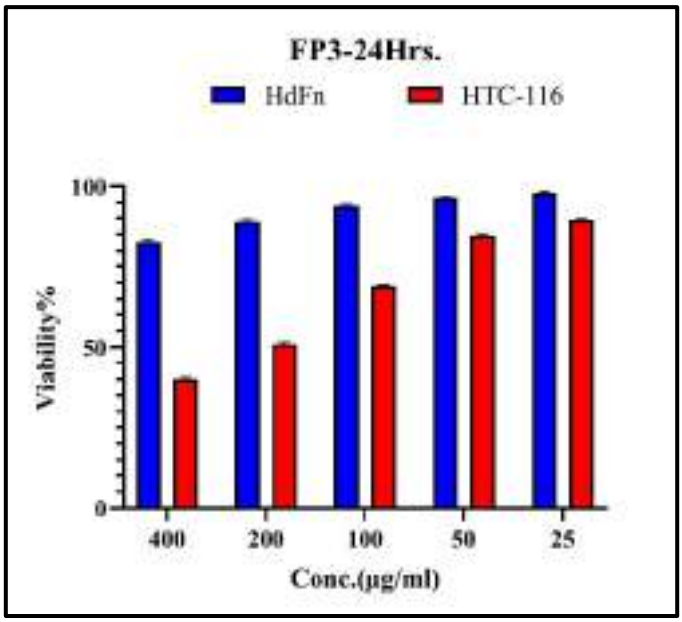


Figure (4- 347): Cytotoxic potentials of copolymer(3) on colon cancer cell line vs normal cell line after 24 hrs.; 37 C°

Copolymer(3) exhibits a more dominant cytotoxic profile at 48 hours. At 25 to 400 µg/ml, the viability of HCT-116 cells decreases further from 87.013±0.696% to 0.432%, while HdFn cells viable cell ranged from 97.835±0.172% to 77.056±0.577% respectively for same concentrations tested, indicating enhanced selectivity and potency. The IC_{50} value decreases markedly to 108.3 µg/ml in cancer cells compared to 199.4 µg/ml in Hdfn normal cells, (Table 4-24) and (fig.4-348). This substantial reduction suggests t copolymer(3) hat is capable of deeper intracellular engagement. The presence of an extended aromatic system and increased π-conjugation enhances electron delocalization, allowing the molecule to stabilize within the cellular environment and interact more effectively with intracellular targets such as DNA and mitochondrial proteins. As a result, copolymer(3) is able not only to initiate cellular stress but also to sustain it over time, leading to a more pronounced reduction in metabolic activity.

Table (4- 24): Cytotoxic potentials of copolymer(3) on colon cancer cell line vs normal cell line after 48 hrs.; 37 Cº

Conc. (µg/ml)	Cell viability (%) of copolymer(3)		
	HdFn	HTC-116	P – value
	Mean±SD	Mean±SD	
400	80.096±0.373	37.346±0.432	0.001
200	85.606±0.037	45.959±0.645	0.001
100	91.670±0.596	64.049±0.737	0.001
50	95.221±0.196	79.752±0.506	0.001
25	97.835±0.172	87.013±0.624	0.01

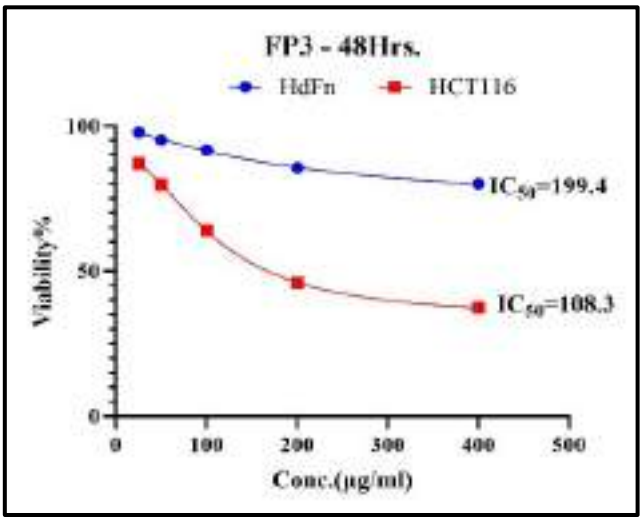


Figure (4- 348): Cytotoxic potentials of copolymer(3) on colon cancer cell line vs normal cell line after 48 hrs.; 37 Cº

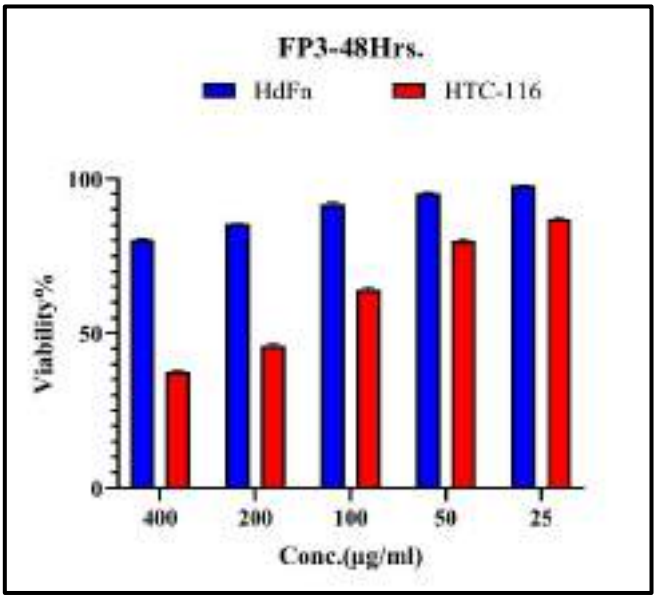


Figure (4- 349): Cytotoxic potentials of copolymer(3) on colon cancer cell line vs normal cell line after 48 hrs.; 37 Cº

Copolymer(3) exhibits a strong and consistent cytotoxic profile at 72 hours. At concentration of 400 µg/ml, the viability of HCT-116 cells reached to 32.348±0.588%, while HdFn cells maintain a viability of 74.878±0.720%, indicating improved potency and selectivity. The inhibitory concentration $_{50}$ value decreases significantly to 85.07 µg/ml in cancer cells compared to 167.9 µg/ml in normal cells, (Table 4-25) and (fig.4-350).

Table (4- 25): Cytotoxic potentials of copolymer(3) on colon cancer cell line vs normal cell line after 72 hrs.; 37 C°

Conc. (µg/mL)	Cell viability (%) of copolymer(3)		
	HdFn	HTC-116	P – value
	Mean±SD	Mean±SD	
400	74.878±0.720	32.348±0.588	0.001
200	79.811±0.622	40.616±0.800	0.001
100	87.028±0.527	55.377±0.371	0.001
50	90.510±0.423	67.929±0.497	0.001
25	94.969±0.312	79.980±0.895	0.01

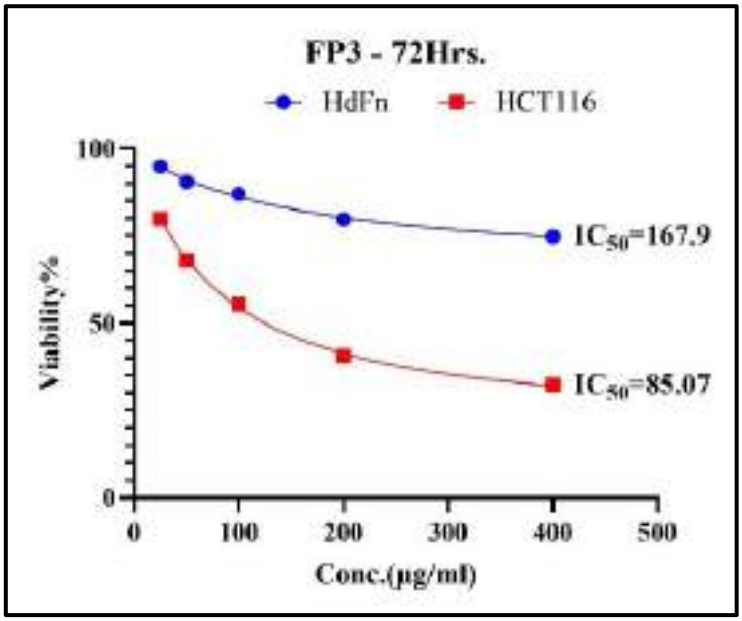


Figure (4- 350): Cytotoxic potentials of copolymer(3) on colon cancer cell line vs normal cell line after 72 hrs.; 37 C°

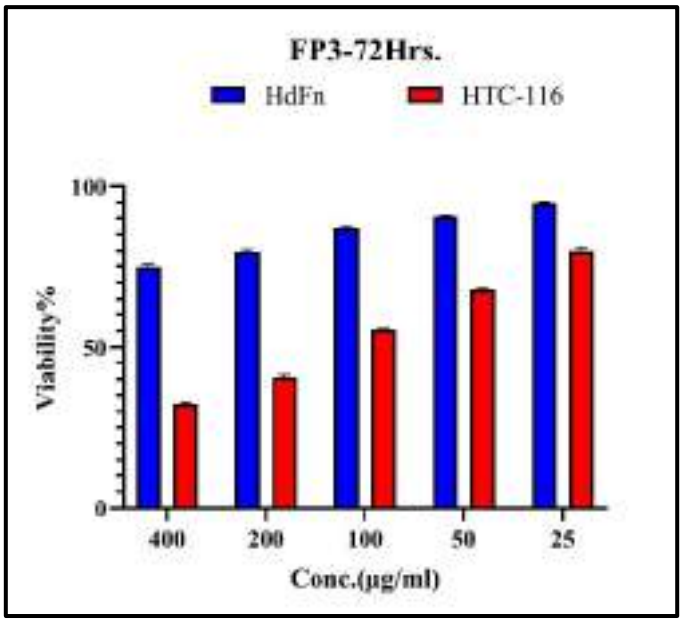


Figure (4- 351): Cytotoxic potentials of copolymer(3) on colon cancer cell line vs normal cell line after 72 hrs.; 37 C°

This marked reduction suggests that copolymer(3) is capable of inducing sustained intracellular disruption. The presence of an extended aromatic system and increased π-conjugation enhances electron delocalization, allowing the molecule to stabilize within the cellular environment and interact with critical intracellular targets, including mitochondrial proteins and nucleic acids. As a result, copolymer(3) not only initiates cellular stress but maintains it, leading to persistent metabolic dysfunction and a significant decrease in viability.

4.61.6 Antioxidant Activity of copolymer(3) Extract via DPPH Assay

Results of copolymer(3) in (Table 4-26) and (fig.4-352) revealed that higher scavenging activity compared to previous compounds at all concentrations tested 0.0620, 0.125, 0.250 and 0.500 mg/ml to be 35.628±0.804, 45.936±0.966, 55.741±0.873 and 64.318±0.213 % respectively while for Vit-C was 39.111±0.027, 55.221±0.152, 63.644±0.135 and 75.995±0.185% for 0.0620, 0.125, 0.250 and 0.500 mg/ml.

Table (4- 26): DPPH radical scavenging activity of copolymer(3) and Vit-C.

Samples	DPPH radical scavenging activity Conc. (Mean ± SD)%			
	0.500	0.250	0.125	0.0625
Vitamin-C	75.995±0.185	63.644±0.135	55.221±0.152	39.111±0.027

copolymer(3)	64.318±0.213	55.741±0.873	45.936±0.966	35.628±0.804
P value	0.01	0.5	0.5	0.5

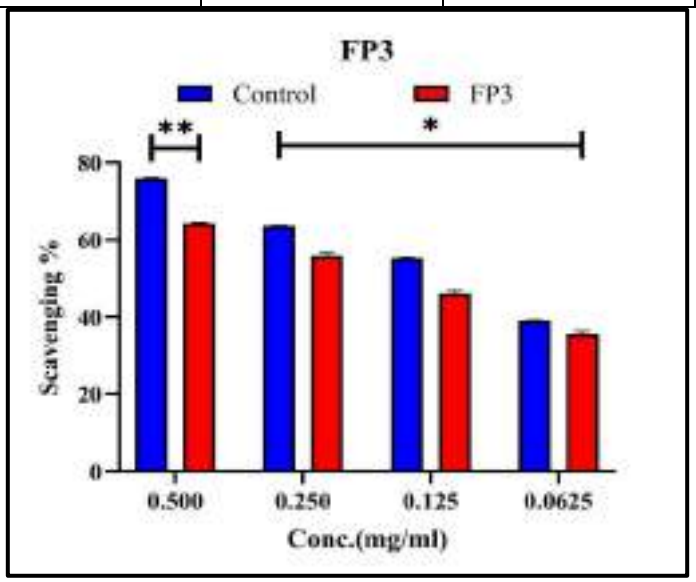


Figure (4- 352): DPPH radical scavenging activity of copolymer(3) and vitamin-C

4.61.7 Cytotoxic potential of copolymer (4) on colon Cell Line (HCT-116).

Copolymer(4) exhibits the highest cytotoxic activity among all tested compounds. At 400 µg/mL, HCT-116 cell viability decreases to 34.488±0.683%, while HdFn cells remain at 78.868±0.394%, demonstrating both high potency and selectivity. The lowest IC_{50} value further confirms its superior activity as shown in, (Table 4-27) and (fig.4-353). This enhanced effect can be attributed to its structurally complex architecture, characterized by multiple heterocyclic rings and a high density of heteroatoms, including nitrogen and sulfur. These features provide multiple potential binding sites, allowing simultaneous interaction with diverse intracellular targets.

Table (4- 27): Cytotoxic potentials of copolymer(4) on colon cancer cell line vs normal cell line after 24 hrs.; 37 C°

Conc. (µg/mL)	Cell viability (%) of copolymer(4)		
	HdFn	HTC-116	P – value
	Mean±SD	Mean±SD	
400	78.868±0.394	34.488±0.683	0.001
200	84.990±0.576	45.179±0.379	0.001
100	89.676±0.620	59.771±0.589	0.001
50	95.071±0.858	77.793±0.589	0.001
25	97.974±0.649	84.589±0.421	0.01

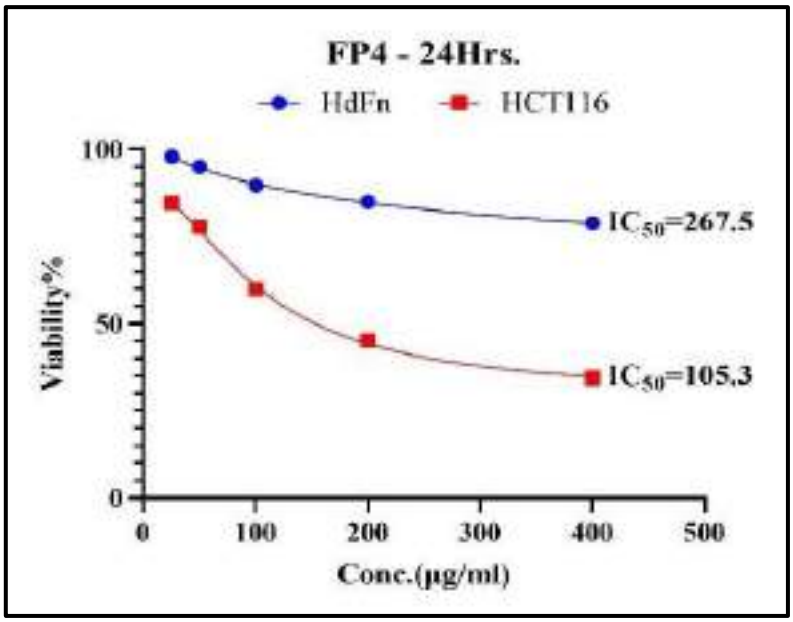


Figure (4- 353): Cytotoxic potentials of copolymer(4) on colon cancer cell line vs normal cell line after 24 hrs.; 37 Cº

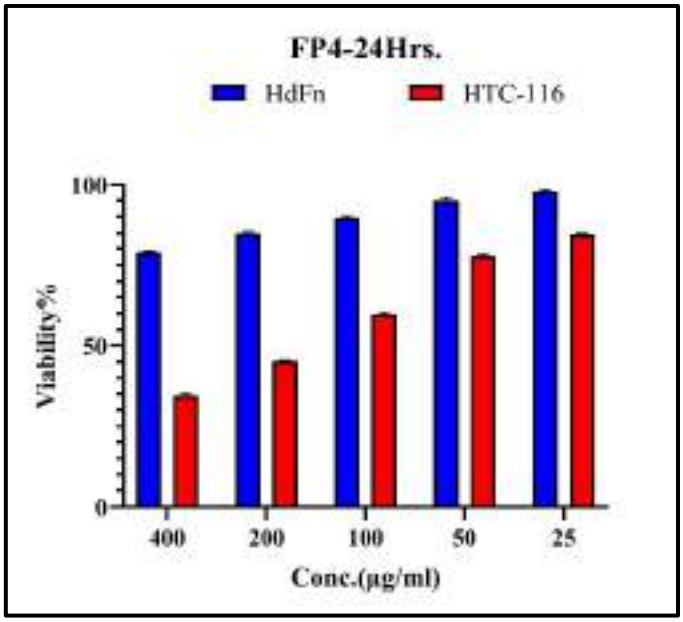


Figure (4- 354): Cytotoxic potentials of copolymer(4) on colon cancer cell line vs normal cell line after 24 hrs.; 37 Cº

Copolymer(4) remains the most potent compound, and its dominance becomes more pronounced at 48 hours of exposure. At 400 µg/ml, the viability of HCT-116 cells decreases markedly to 30.400±0.696%, while HdFn cells retain a higher viability of 70.005±0.753%, representing the largest selectivity margin among all tested copolymers. This superior activity is further confirmed by the IC_{50} values,

which reached to 38.16 µg/ml in cancer cells in comparison to 77.67 µg/mL in normal cells, indicating both high potency and maintained selectivity (Table 4-28) and (fig.4-355).

Table (4- 28): Cytotoxic potentials of copolymer(4) on colon cancer cell line vs normal cell line after 48 hrs.; 37 Cº

Conc. (µg/ml)	Cell viability (%) of copolymer(4)		
	HdFn	HTC-116	P - value
	Mean±SD	Mean±SD	
400	70.005±0.753	30.400±0.696	0.001
200	77.673±0.506	38.168±0.189	0.001
100	86.378±0.572	53.280±0.581	0.001
50	92.204±0.519	72.676±0.766	0.01
25	96.160±0.481	81.323±0.882	**

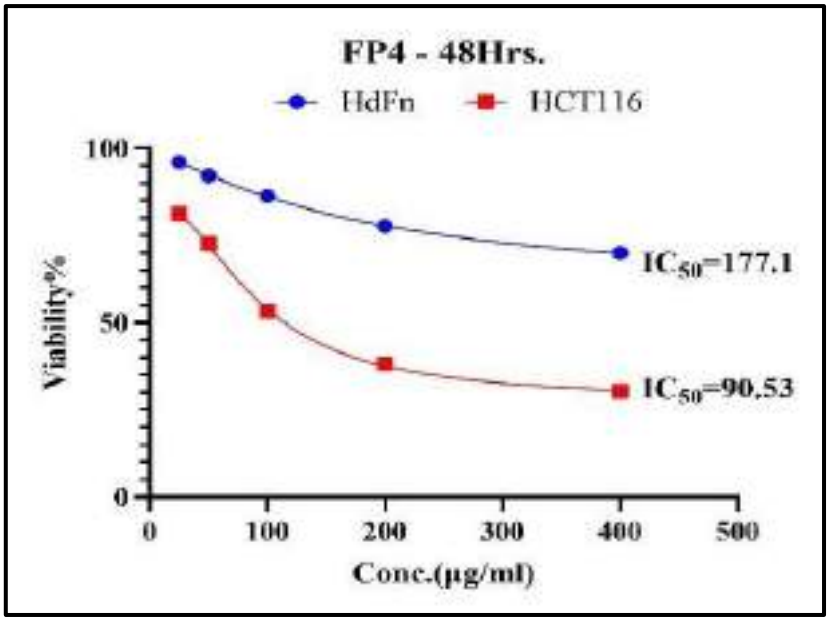


Figure (4- 355): Cytotoxic potentials of copolymer(4) on colon cancer cell line vs normal cell line after 48 hrs.; 37 Cº

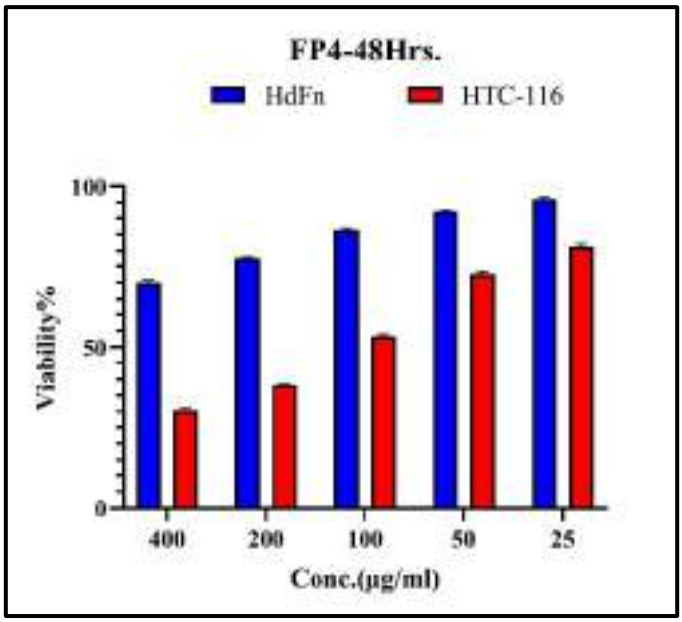


Figure (4- 356): Cytotoxic potentials of copolymer(4) on colon cancer cell line vs normal cell line after 48 hrs.; 37 C°

This substantial reduction in viability suggests that copolymer(4) has transitioned from surface-level interaction to deep intracellular activity. The enhanced cytotoxic effect can be attributed to its structurally complex architecture, characterized by multiple heterocyclic rings enriched with nitrogen and sulfur atoms. These heteroatoms introduce several potential binding and reactive sites, enabling the compound to engage in diverse molecular interactions within the cellular environment.

Copolymer(4) remains the most potent compound, and its superiority becomes absolute at 72 hours. At 400 µg/ml, the viability of HCT-116 cells decreases dramatically to 20.923±0.512%, representing the lowest value among all tested compounds, while HdFn cells retain 61.297±0.334% viability. The IC_{50} values further confirm this dominance, reaching 50.62 µg/ml in cancer cells compared to 124.0 µg/ml in normal cells. This sharp decline in viability indicates that copolymer(4) has progressed beyond metabolic disruption toward irreversible cellular damage, (Table 4-29) and (fig.4-357).

Table (4- 29): Cytotoxic potentials of copolymer(4) on colon cancer cell line vs normal cell line after 72 hrs.; 37 Cº

Conc. (µg/mL)	Cell viability (%) of copolymer(4)		
	HdFn	HTC-116	P - value
	Mean±SD	Mean±SD	
400	61.297±0.334	20.923±0.512	0.001
200	68.840±0.725	29.281±0.577	0.001
100	78.064±0.768	38.293±0.562	0.001
50	87.297±0.586	53.299±0.873	0.001
25	91.747±0.381	66.065±0.509	0.001

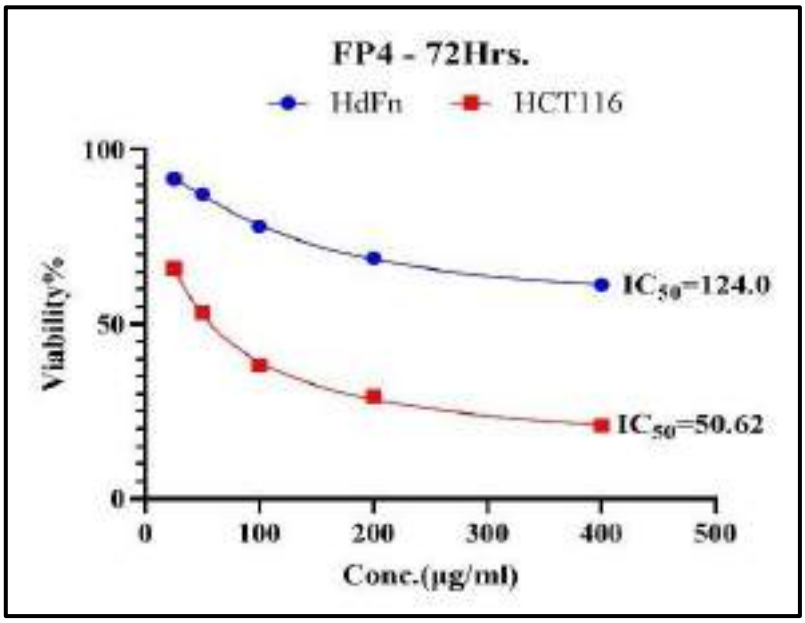


Figure (4- 357): Cytotoxic potentials of copolymer(4) on colon cancer cell line vs normal cell line after 72 hrs.; 37 Cº

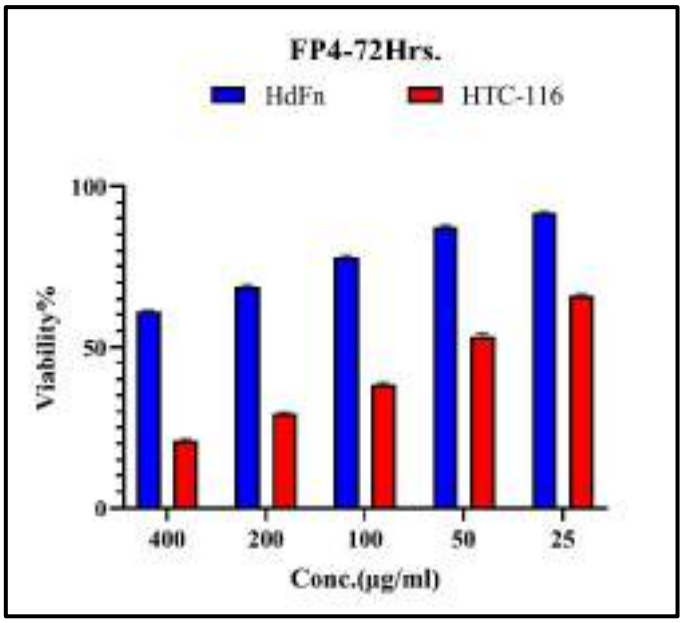


Figure (4- 358): Cytotoxic potentials of copolymer(4) on colon cancer cell line vs normal cell line after 72 hrs.; 37 C°

The exceptional activity of copolymer(4) can be attributed to its highly integrated and reactive molecular structure, characterized by multiple heterocyclic rings and a high density of nitrogen and sulfur atoms. These features provide multiple reactive and binding sites, enabling the compound to interact simultaneously with various intracellular targets. As a result, copolymer(4) does not operate through a single mechanism but induces multi-pathway disruption, including mitochondrial dysfunction, redox imbalance, and interference with essential metabolic processes.

4.61.8 Antioxidant Activity of Extract copolymer(4) via DPPH Assay.

Copolymer(4) which possessed the highest potency to DPPH scavenging activity in all tested concentrations 0.0620, 0.125, 0.250 and 0.500 mg/ml reached to 38.451±0.731, 49.866±0.842, 60.742±0.956 and 69.615±0.184% respectively, (Table 4-30) and (fig.4-359). Also, Vit-C showed variation between scavenging activity between concentration tested.

Table (4- 30): DPPH radical scavenging activity of copolymer(4) and Vit-C.

Samples	DPPH radical scavenging activity Conc. (Mean ± SD)%			
	0.500	0.250	0.125	0.0625
Vitamin-C	75.995±0.185	63.644±0.135	55.221±0.152	39.111±0.027
copolymer(4)	69.615±0.184	60.742±0.956	49.866±0.842	38.451±0.731
P value	0.5	0.5	0.5	NS

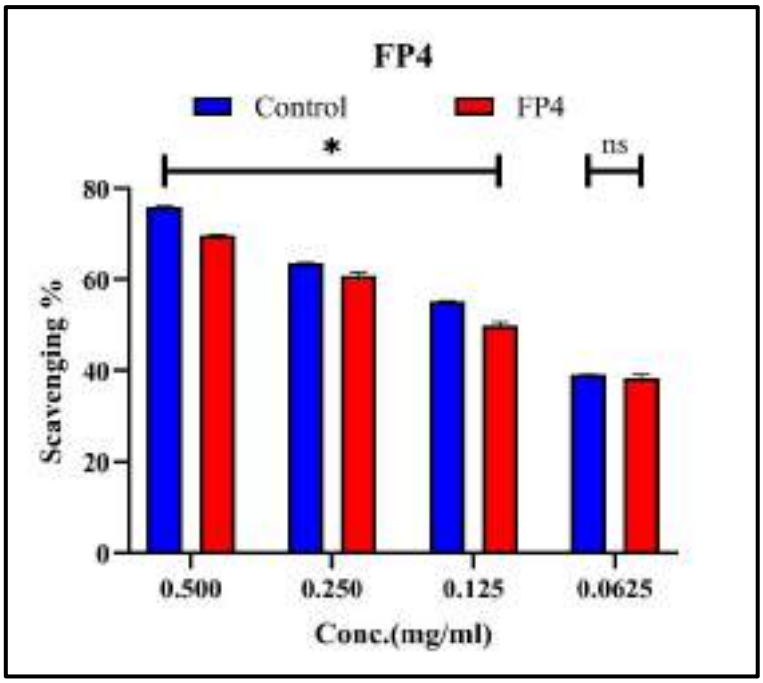


Figure (4- 359): DPPH radical scavenging activity of copolymer(4) and vitamin-C

4.61.9 Cytotoxic potential of copolymer (5) on colon Cell Line (HCT-116).

Copolymer(5) demonstrates further enhancement in cytotoxic activity. For colon cancer cell, the viability decreased from 87.040±± 0.706% to 36.981±0.592%, for 25 to 400 µg/ml, respectively, while HdFn cells showed a cell viability of 80.189±0.515%, indicating a substantial and selective cytotoxic effect. The IC_{50} values support this observation (112.4 µg/ml), reflecting improved potency compared to earlier compounds. Structurally, copolymer(5) appears to achieve a more optimal balance between polarity and lipophilicity through the presence of aromatic systems, heteroatoms (N and S), and flexible linkages such as ether groups. This balance likely facilitates both efficient membrane permeability and stable intracellular interactions. Rather than inducing rapid, non-specific damage, copolymer(5) may exert its effects through sustained interaction with key cellular

targets, potentially affecting enzymatic activity or mitochondrial integrity over time, (Table 4-31) and (fig 4-360).

Table (4- 31): Cytotoxic potentials of copolymer(5) on colon cancer cell line vs normal cell line after 24 hrs.; 37 Cº

Conc. (µg/mL)	Cell viability (%)copolymer(5)		
	HdFn	HTC-116	P – value
	Mean±SD	Mean±SD	
400	80.189±0.515	36.981±0.592	0.001
200	86.864±0.671	48.203±0.764	0.001
100	92.141±0.545	63.525±0.650	0.001
50	96.141±0.545	80.718±0.267	0.001
25	98.414±0.221	87.040±0.706	0.01

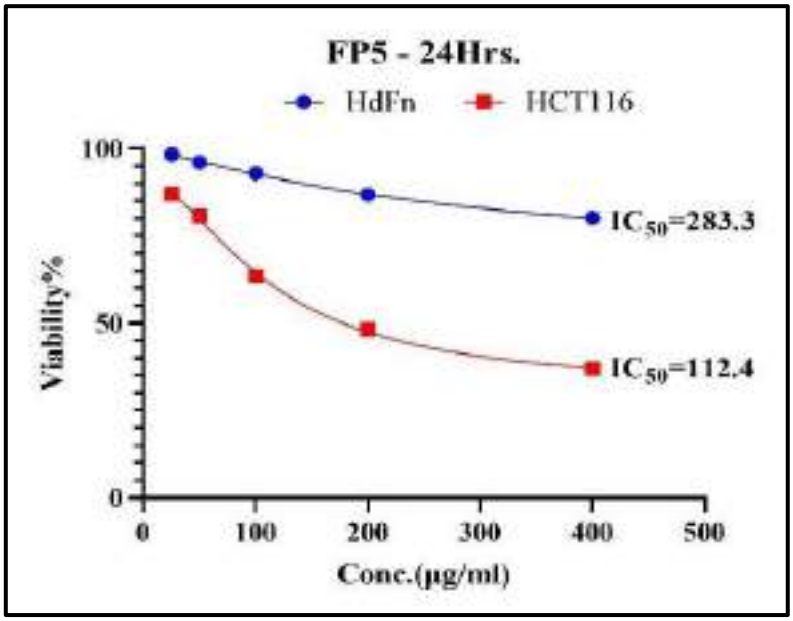


Figure (4- 360): Cytotoxic potentials of copolymer(5) on colon cancer cell line vs normal cell line after 24 hrs.; 37 Cº

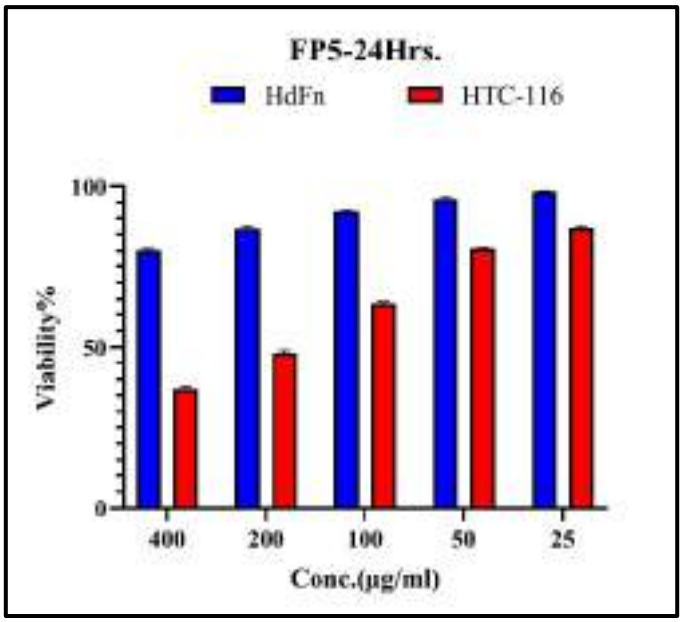


Figure (4- 361): Cytotoxic potentials of copolymer(5) on colon cancer cell line vs normal cell line after 24 hrs.; 37 Cº

Copolymer(5) continues to demonstrate strong and consistent cytotoxic activity, reinforcing its classification as a highly effective compound. Cell viability decreased as concentrations increased. At 400 µg/ml, the viability of HCT-116 cells decreases to 34.176±0.690%, while HdFn cells remain at 77.956±0.577%, indicating a significant cytotoxic effect with maintained selectivity. The IC_{50} values further confirm its potency, reaching 98.46 µg/ml in cancer cells compared to 183.7 µg/mL in Hdfn normal cells, (Table 4-32) and (fig.4-362).

Table (4- 32): Cytotoxic potentials of copolymer(5) on colon cancer cell line vs normal cell line after 48 hrs.; 37 Cº

Conc. (µg/ml)	Cell viability (%) of copolymer(5)		
	HdFn	HTC-116	P - value
	Mean±SD	Mean±SD	
400	77.956±0.577	34.176±0.690	0.001
200	83.380±0.456	42.357±0.422	0.001
100	89.313±0.562	58.485±0.578	0.001
50	93.850±0.238	76.280±0.537	0.001
25	97.539±0.017	83.873±0.696	0.001

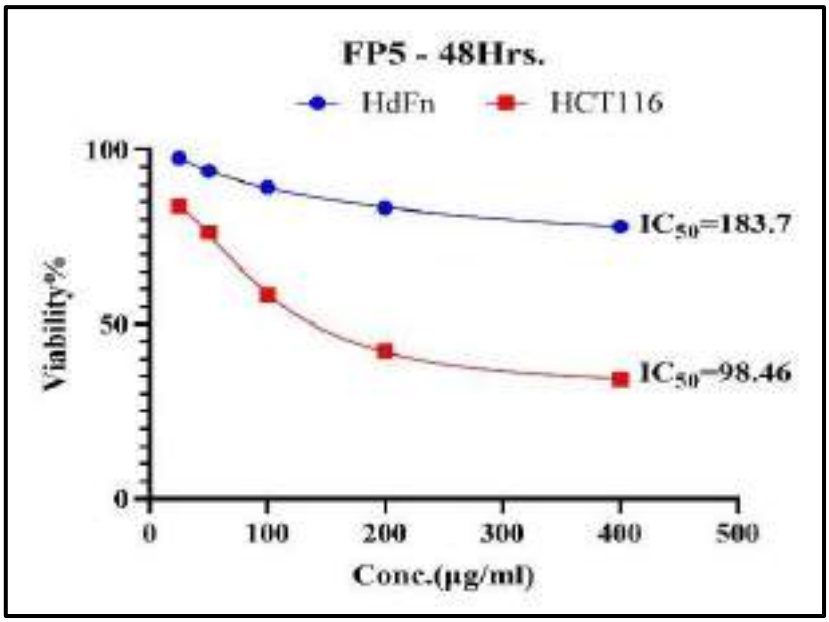


Figure (4- 362): Cytotoxic potentials of copolymer(5) on colon cancer cell line vs normal cell line after 48 hrs.; 37 Cº

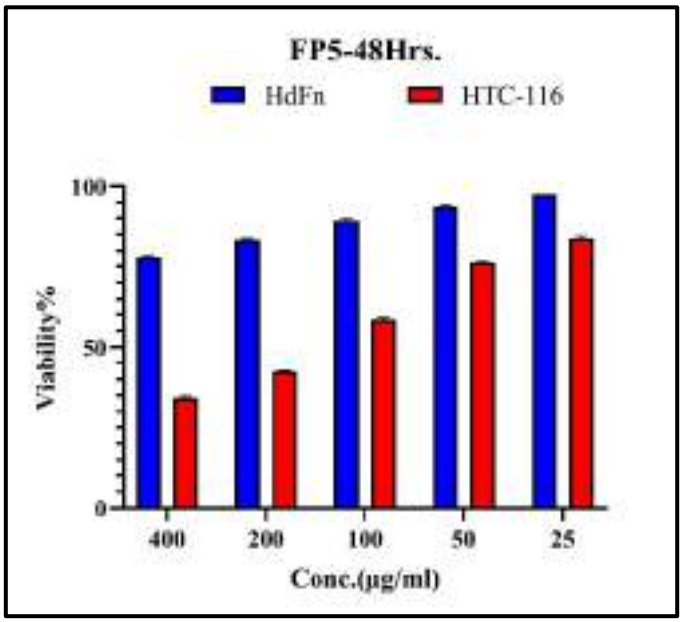


Figure (4- 363): Cytotoxic potentials of copolymer(5) on colon cancer cell line vs normal cell line after 48 hrs.; 37 Cº

This marked reduction indicates a substantial enhancement in activity over time. The superior performance of copolymer(5) can be attributed to its balanced structural architecture, which combines aromatic systems, heteroatoms, and flexible linkages. This structural balance facilitates both efficient membrane permeability and stable intracellular interactions. Consequently, copolymer(5) is able to accumulate within the cell and exert sustained biochemical disruption, rather than

transient effects, resulting in progressively increased cytotoxicity.

Copolymer(5) demonstrates a highly potent cytotoxic profile, approaching that of the most active compound. At tested concentration of 400 µg/ml, the HCT-116 cell viability decreases to 28.311±0.350%, while HdFn cells remain at 71.174±0.464%, indicating a substantial reduction in viability with preserved selectivity and the IC_{50} values further confirm this effect, reaching 36.51 µg/ml in cancer cells compared to 77.87 µg/ml in normal cells. This enhanced activity is attributed to the balanced structural composition of copolymer(5), which integrates aromatic systems, flexible linkages, and polar functional groups. This structural balance facilitates efficient membrane permeability and stable intracellular retention. Consequently, copolymer(5) is capable of sustained interaction with cellular targets, leading to cumulative intracellular damage and progressive loss of metabolic activity over time, (Table 4-33) and (fig.4-364).

Table (4- 33): Cytotoxic potentials of copolymer(5) on colon cancer cell line vs normal cell line after 72 hrs.; 37 C°

Conc. (µg/mL)	Cell viability (%) of copolymer(5)		
	HdFn	HTC-116	P - value
	Mean±SD	Mean±SD	
400	71.174±0.464	28.311±0.350	0.001
200	77.877±0.385	36.513±0.510	0.001
100	82.229±0.422	46.806±0.573	0.001
50	89.816±0.726	61.198±0.665	0.001
25	94.479±0.286	71.923±0.812	0.001

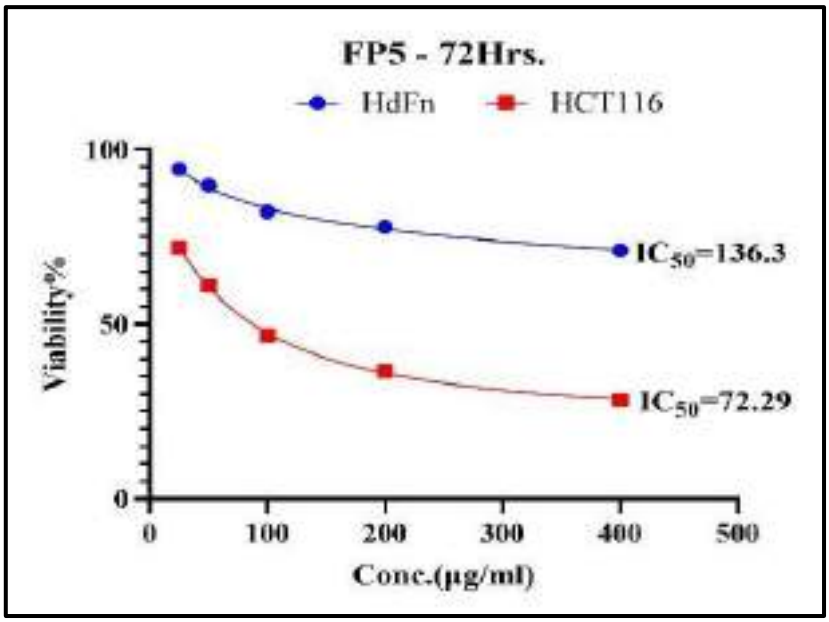


Figure (4- 364): Cytotoxic potentials of copolymer(5) on colon cancer cell line vs normal cell line after 72 hrs.; 37 C°

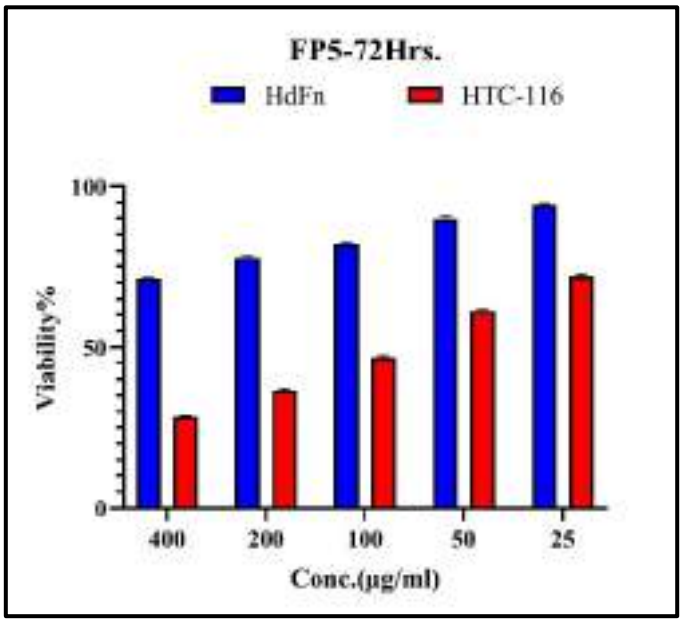


Figure (4- 365): Cytotoxic potentials of copolymer(5) on colon cancer cell line vs normal cell line after 72 hrs.; 37 C°

The chemical structures of copolymer (1) to copolymer(5) are important factors in their anticancer effects on colon cancer cell lines. Overall, these compounds include key elements like thiosemicarbazone or thioamide structures, heterocycles that include nitrogen, aromatic systems, and amide/carboxyl functional groups. These structural changes are commonly linked to induction of apoptosis, cell-cycle arrest, oxidative stress, metal chelation, and intracellular target inhibition in cancer

cells.(158, 159). In the case of copolymer(1), there is a thiosemicarbazone-like unit that is bound to an aromatic system. The significance of this kind of scaffold is that thiosemicarbazones are known to form complexes with metal ions in particular with iron and iron is vital to the growth and proliferation of colorectal cancer cells. Recent research has indicated iron chelation as a good idea in colorectal cancer as it may inhibit proliferation, disrupt the redox equilibrium, and trigger stress pathways in cancer cells. (159). Thus, the primary mechanisms by which copolymer(1) decreases the viability of colon cancer cells include metal chelation, oxidative stress and apoptosis and may have additional effects on intracellular enzymes.(158, 159).

In the case of copolymer(2), the structure seems to be composed of a pyridine-type heterocycle and a thiohydantoin-like ring. Thiohydantoin systems are frequently cited as target-directed anticancer scaffolds, as they can effectively interact with intracellular proteins and enzymes, while cancer cell-cycle arrest and apoptosis are associated with thiohydantoin-related compounds(156, 160). According to this, copolymer(2) can be a primarily intracellular enzyme inhibitor, leading to growth arrest and apoptosis of colon cancer cells.(156, 161).

Copolymer(3) appears to have a system of aromatic imide-like structures resembling phthalimide or naphthalimide, along with a thiosemicarbazone-like component. This is significant as the naphthalimide-based compounds are well-known in anticancer research as DNA-binding molecules. Recent reviews clarify that such compounds may intercalate into DNA, alter DNA topology, disrupt topoisomerases, and, subsequently, arrest the cell cycle, cause DNA damage, and trigger apoptosis.(157, 162). According to this, copolymer(3) is most likely to be the most likely to work via DNA-related mechanisms of copolymer(1)-copolymer(5).(157)

The copolymer(4) structure is highly nitrogen-rich and appears to contain a heterocyclic system with tetrazole and sulfur-based groups. The pharmacological properties of tetrazoles are beneficial, as they enhance cellular target binding, stability, and interactions. According to recent research, tetrazole-derived

compounds are promising anticancer scaffolds, and some of them may induce apoptosis and cell-cycle arrest by binding intracellular targets. Therefore, copolymer(4) have a multi-target anticancer compound that could suppress colon cancer cell growth by inhibiting key intracellular proteins and promoting apoptosis(163, 164).

In the case of copolymer(5), a heterocyclic moiety of the structure is conjugated with aromatic rings and polar groups like amide and carboxyl groups. This makes the molecule more balanced in terms of its chemical character, as it is both hydrophobic and aromatic, as well as polar at its binding sites. This kind of balance is commonly significant to cellular uptake and intracellular binding. According to this design, copolymer(5) can exert an antiproliferative effect on colon cancer cells by interacting with intracellular targets, thereby inhibiting cell cycle progression and inducing apoptosis. Overall, such fused heterocyclic aromatic systems are frequently associated with inhibition of pathways involved in tumor-cell survival and proliferation.(165, 166). Comparing the five compounds, we can indicate that copolymer(1) will be more likely to work with the help of iron chelation and oxidative stress, copolymer(2) with enzyme inhibition and cell-cycle arrest, copolymer(3) with DNA-related targeting and apoptosis, copolymer(4) with multi-target intracellular activity and its effects on apoptosis, and copolymer(5) with a more general antiproliferative intracellular action (In general, the most likely biological results in colon cancer cell lines would be decreased cell viability, proliferation suppression, apoptosis, and disruption of the cell-cycle progression.(155, 159).

4.61.10 Antioxidant Activity of copolymer(5)and copolymer(6) Extract via DPPH Assay.

Copolymer(5) showed a variation in scavenging activity ranging from 66.840±0.026 to 36.904±0.685% for 0.500 to 0.0625 mg/ml respectively and copolymer(6) agreed with results of copolymer(5), in which the scavenging activity ranged from 59.441±0.138 to 32.486±0.744% for 0.500 to 0.0625 mg/ml

respectively, (Table 4-34) and (fig.4-366) Also, Vit-C exhibited higher scavenging activity between concentration tested.

Table (4- 34): DPPH radical scavenging activity of copolymer(5) and copolymer(6), Vit-C.

Samples	DPPH radical scavenging activity Conc. (Mean ± SD)%			
	0.500	0.250	0.125	0.0625
Vitamin-C	75.995±0.185	63.644±0.135	55.221±0.152	39.111±0.027
copolymer(5)	66.840±0.026	58.086±0.117	47.552±0.914	36.904±0.685
P value	0.5	0.5	0.5	0.5
copolymer(6)	59.441±0.138	50.863±0.921	41.905±0.857	32.486±0.744
P value	0.01	0.5	0.5	0.5

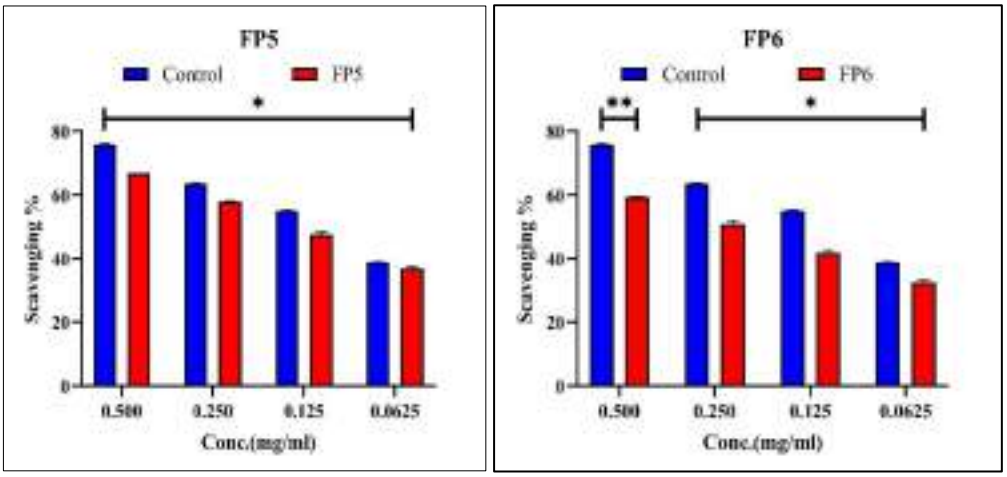


Figure (4- 366): DPPH radical scavenging activity of copolymer(5) and copolymer(6) with vitamin-C

4.61.11 Cytotoxic against of copolymer(6) on skin cancer Cell Lines(A431) in comparison with normal cell line (Hdfn).

Copolymer(6) has cytotoxic effects against skin cancer cell line especially at 400 µg/mL, the cancer cell viability was up to (37.768±0.545%) compared to (84.958.260±0.387 %) for 25 µg/mL, indicating a cytotoxic potentials. This can be confirmed by its IC50 values (131.7 µg /ml in cancer cells vs 213.6 µg/mL in Hdfn cells) (fig.4-367), indicating moderate selectivity with low potency and also normal cell viability reduced from (97.250±0.552 % to 78.260±0.921%) for 25 to 400 µg /ml repectively (Table 4-35) ,(fig.4-368).

Table (4- 35): Cytotoxic potentials of copolymer(6) on skin cancer cell line vs normal cell line after 24 hrs.; 37 C°.

Conc. (µg/mL)	Cell viability (%) of copolymer(6)		
	HdFn	A431	P -value
	Mean±SD	Mean±SD	
400	78.260±0.921	37.768±0.545	0.001
200	84.504±0.502	49.963±0.564	0.001
100	90.089±0.736	64.681±0.503	0.001
50	94.921±0.633	78.650±0.749	0.001
25	97.250±0.552	84.958±0.387	0.01

Where 0.5, 0.01, 0.001: Significant differences (P ≤ 0.05) between means.

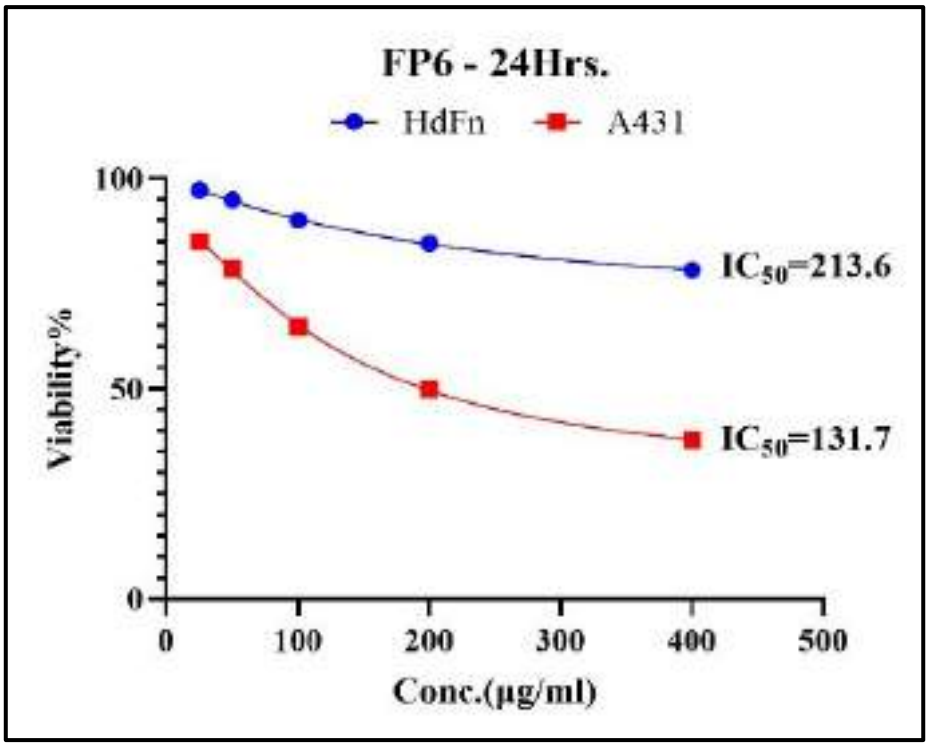


Figure (4- 367): Cytotoxic potentials of copolymer(6) on skin cancer cell line vs normal cell line after 24 hrs.; 37 C

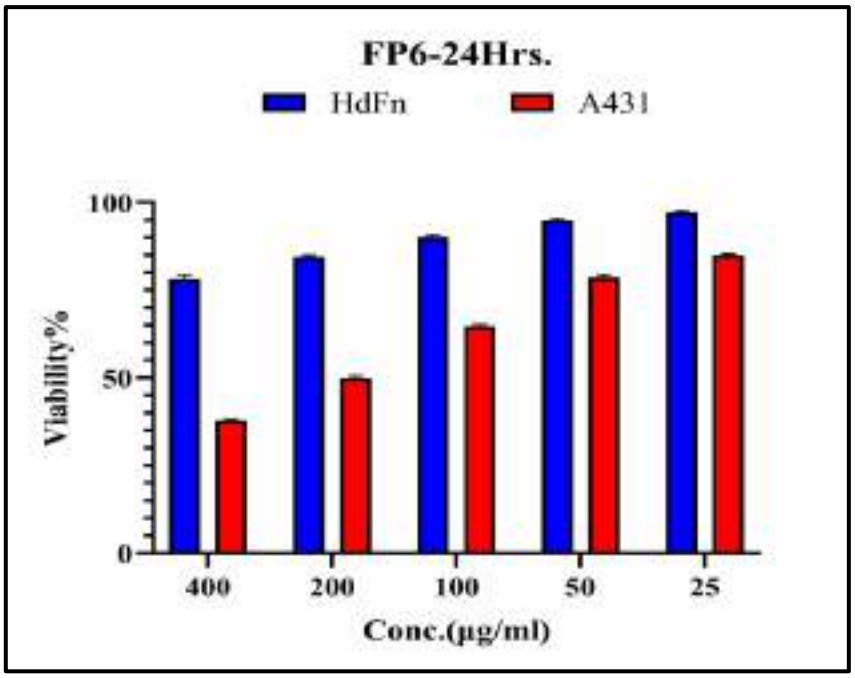


Figure (4- 368): Cytotoxic potentials of copolymer(6) on skin cancer cell line vs normal cell line after 24 hrs.; 37 C.

Copolymer(6) has a cytotoxic profile. The viability of the A431 cells at 25 to 400 µg/ml further reduces from 80.379±0.206% to 34.041±0.756% and HdFn cells also reduced to 76.187±0.285% in the same concentrations tested, The IC_{50} of the copolymer(6) is found to be significantly lower in cancer cells, at 115.4 µg/ml, and in normal cells of Hdfn, 199.3 µg /ml (fig.4-369).

Table (4- 36): Cytotoxic potentials of copolymer(6) on skin cancer cell line vs normal cell line after 48 hrs.; 37 C°.

Conc. (µg/mL)	Cell viability (%) of copolymer(6)(		
	HdFn	A431	P -value
	Mean±SD	Mean±SD	
400	76.187±0.285	34.041±0.756	0.001
200	81.835±0.925	43.225±0.903	0.001
100	88.039±0.706	60.040±0.454	0.001
50	91.983±0.406	74.012±0.499	0.001
25	95.008±0.448	80.379±0.206	0.001

Where 0.5, 0.01, 0.001: Significant differences (P ≤ 0.05) between means.

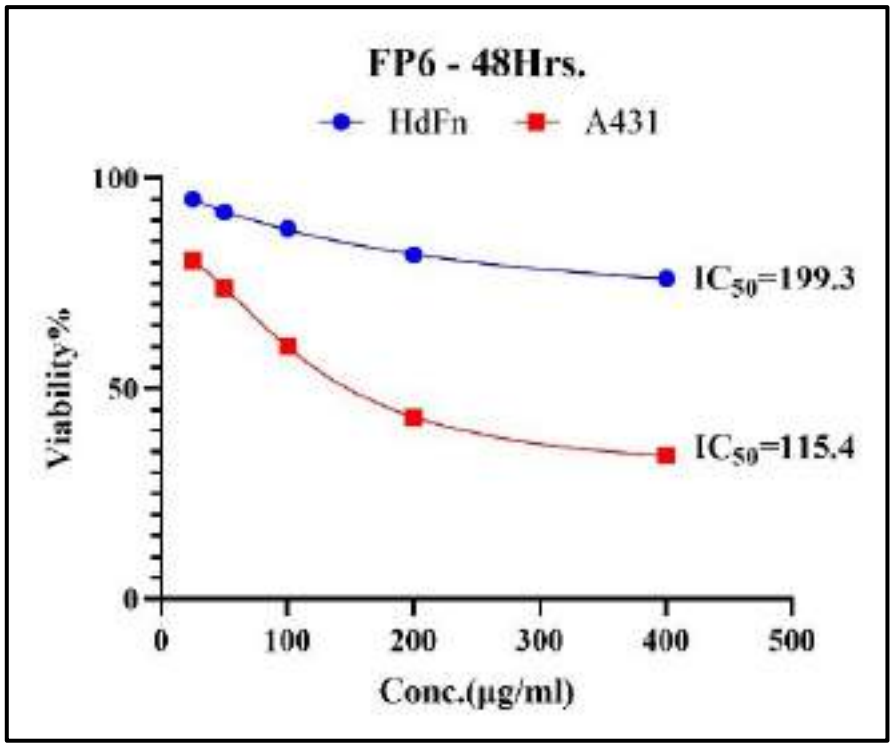


Figure (4- 369): Cytotoxic potentials of copolymer(6) on skin cancer cell line vs normal cell line after 48 hrs.; 37 C°

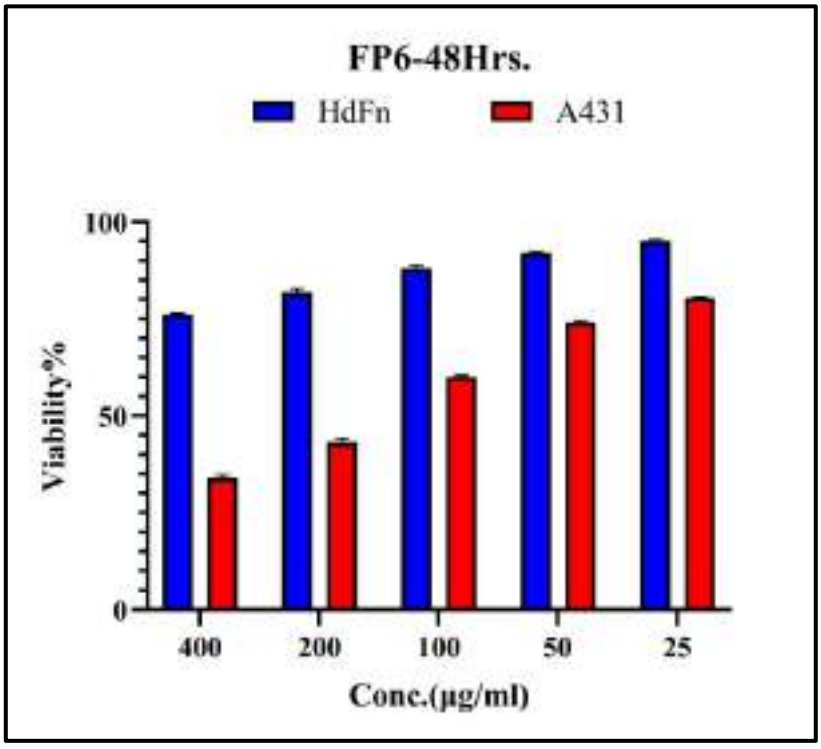


Figure (4- 370): Cytotoxic potentials of copolymer(6) on skin cancer cell line vs normal cell line after 48 hrs.; 37 C°.

Though with a constant improvement with time and a concentration of 400 µg/ml of copolymer(6), the cell viability drops to 29.023±0.707% compared to 71.996±0.595% in HdFn cells at same concentration. The IC_{50} also reduce to 98.67 µg/ml in skin cancer cell and 167.7 µg/ml in normal cells line (fig.4-371).

Table (4- 37): Cytotoxic potentials of copolymer(6) on skin cancer cell line vs normal cell line after 72 hrs.; 37 C°.

Conc. (µg/mL)	Cell viability (%) of copolymer(6)(		P -value
	HdFn	A431	
	Mean±SD	Mean±SD	
400	71.996±0.595	29.023±0.707	0.001
200	78.478±0.153	35.681±0.569	0.001
100	82.947±0.665	51.015±0.724	0.001
50	89.981±0.404	64.177±0.166	0.001
25	93.014±0.656	72.657±0.536	0.001

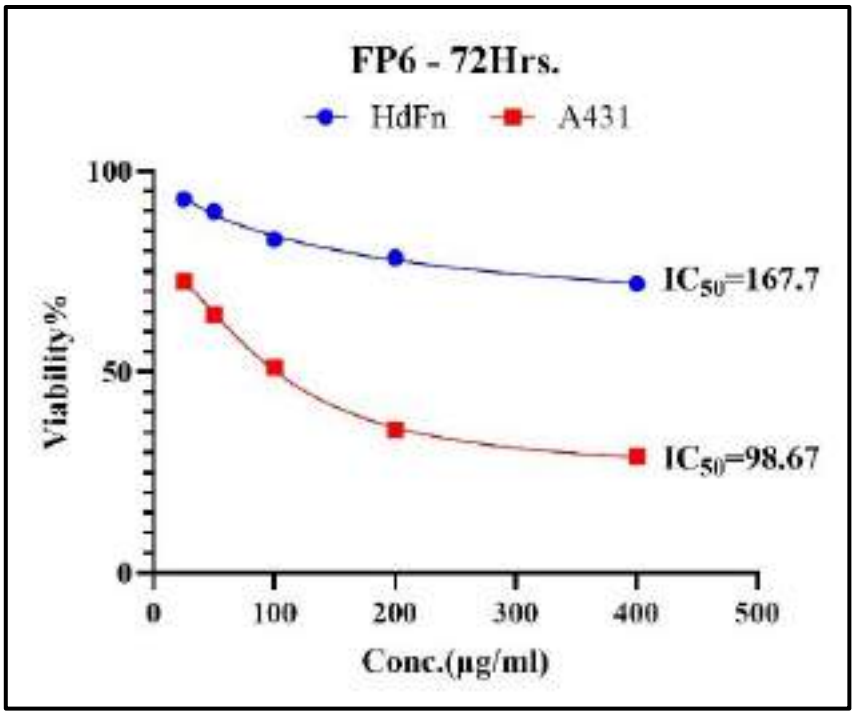


Figure (4- 371): Cytotoxic potentials of copolymer(6) on skin cancer cell line vs normal cell line after 72 hrs.; 37 C°.

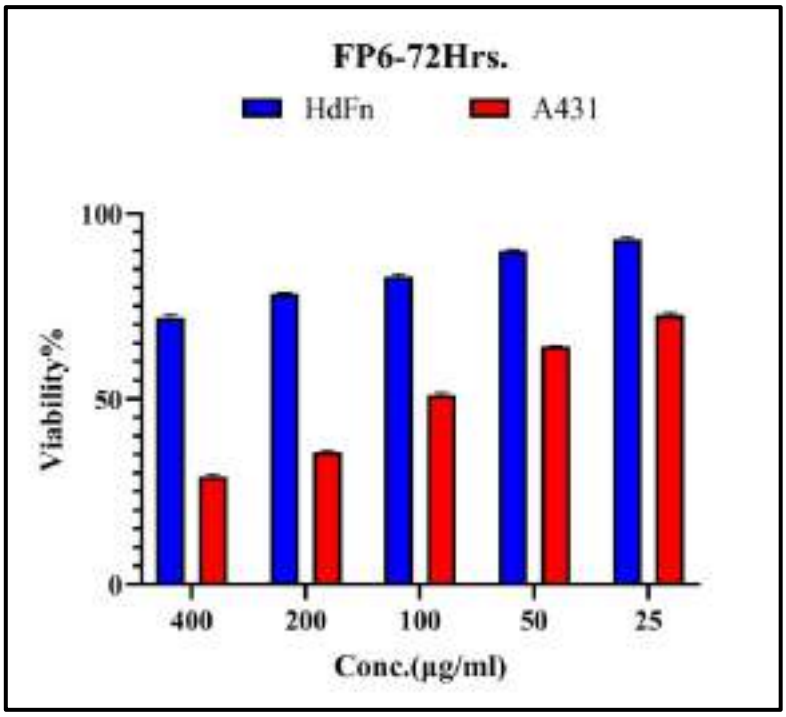


Figure (4- 372): Cytotoxic potentials of copolymer(6) on skin cancer cell line vs normal cell line after 72 hrs.; 37 C°.

4.61.12 Cytotoxic against of copolymer(7) on skin cancer Cell Lines(A431) in comparison with normal cell line (Hdfn).

Copolymer(7) showed also showed a cytotoxic effects with a cell viability of (91.554±0.674 to 45.736±0.531%) for 25 to 400 µg /ml respectively with slight cytotoxic activity. At 400 µg/mL, Hdfn cell viability decreases to 85.150±0.475%, with the IC_{50} values of (186.4 µg/mL in cancer cells and 274.3 µg/mL) in Hdfn cells as depicted in (fig.4-373), (Table 4-38) which indicated a cytotoxic capacity.

Table (4- 38): Cytotoxic potentials of copolymer(7) compound on skin cancer cell line vs normal cell line after 24 hrs.; 37 C°

Conc. (µg/mL)	Cell viability (%) of copolymer(7)		
	HdFn	A431	P -value
	Mean±SD	Mean±SD	
400	85.150±0.475	45.736±0.531	0.001
200	91.156±0.156	60.968±0.701	0.001
100	95.892±0.519	79.892±0.727	0.001
50	98.129±0.166	85.653±0.573	0.01
25	99.112±0.186	91.554±0.674	0.5

Where 0.5, 0.01, 0.001: Significant differences (P ≤ 0.05) between means.

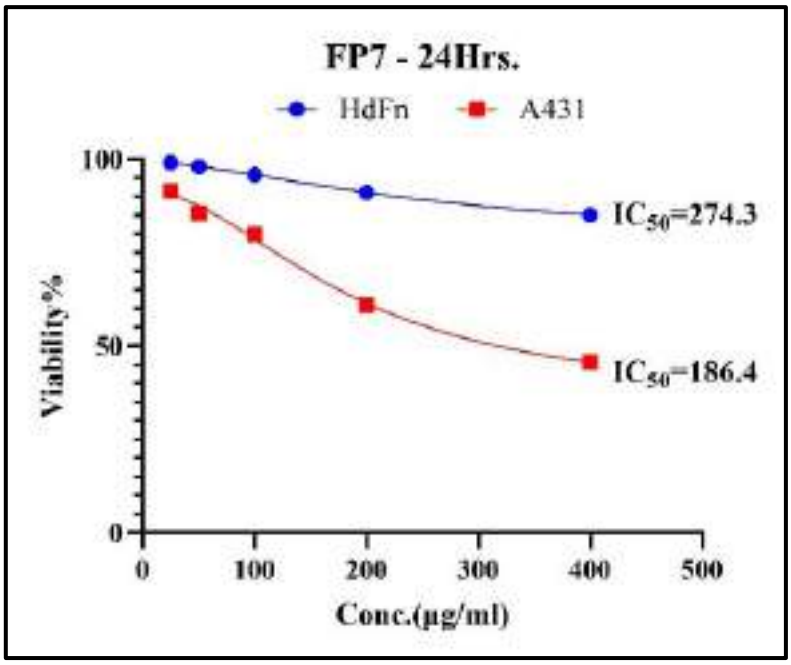


Figure (4- 373): Cytotoxic potentials of copolymer(7) on skin cancer cell line vs normal cell line after 24 hrs.; 37 C°

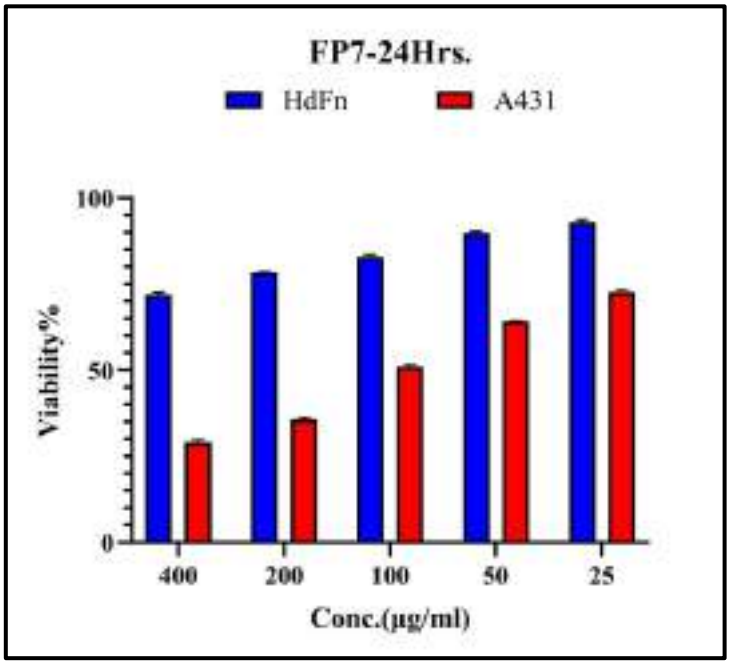


Figure (4- 374): Cytotoxic potentials of copolymer(7) on skin cancer cell line vs normal cell line after 24 hrs.; 37 C°

Copolymer(7) its dominance increases with increasing exposure time of 48 hours. The viability of A431 cells is reduced significantly to 42.993±0.641% at 400 µg/ml with HdFn cells maintaining a high viability of 81.886±0.415%, the highest selectivity margin of all the compounds tested. The high potency and selectivity of

this superior activity is further proven by the IC $_{50}$ value that was 157.0 µg/ml in cancer cells compared to 251.8 µg/mL in normal cells, indicating a high potency and selectivity (fig.4-375).

Table (4- 39): Cytotoxic potentials of copolymer(7) on skin cancer cell line vs normal cell line after 48 hrs.; 37 C°.

Conc. (µg/mL)	Cell viability (%) of copolymer(7)		
	HdFn	A431	P -value
	Mean±SD	Mean±SD	
400	81.886±0.415	42.993±0.641	0.001
200	88.288±0.356	55.159±0.266	0.001
100	93.856±0.292	74.649±0.492	0.001
50	96.980±0.584	81.713±0.705	0.01
25	98.488±0.240	87.659±0.601	0.01

Where 0.5, 0.01, 0.001: Significant differences (P ≤ 0.05) between means.

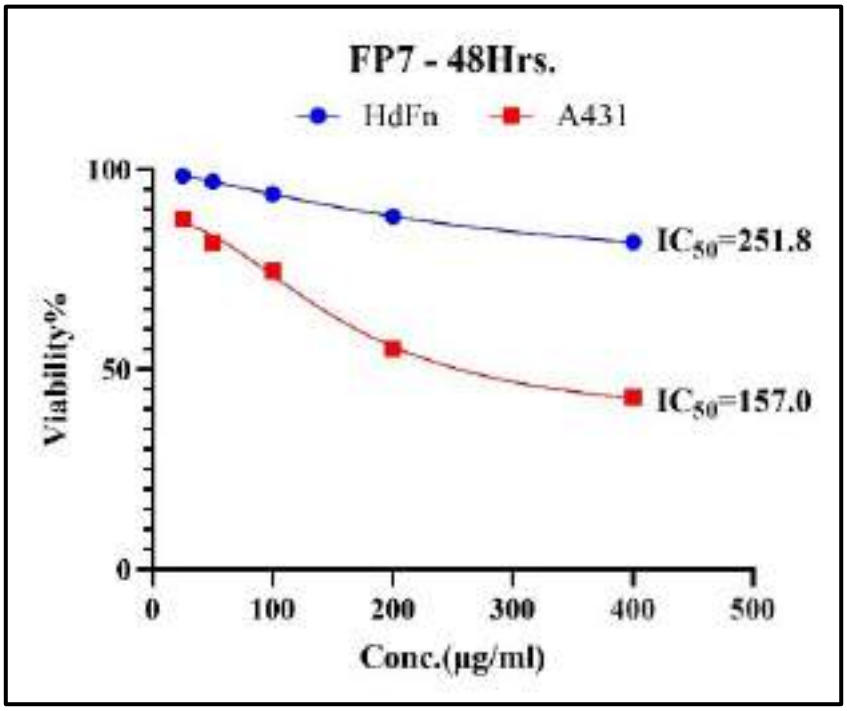


Figure (4- 375): Cytotoxic potentials of copolymer(7) on skin cancer cell line vs normal cell line after 48 hrs.; 37 C°.

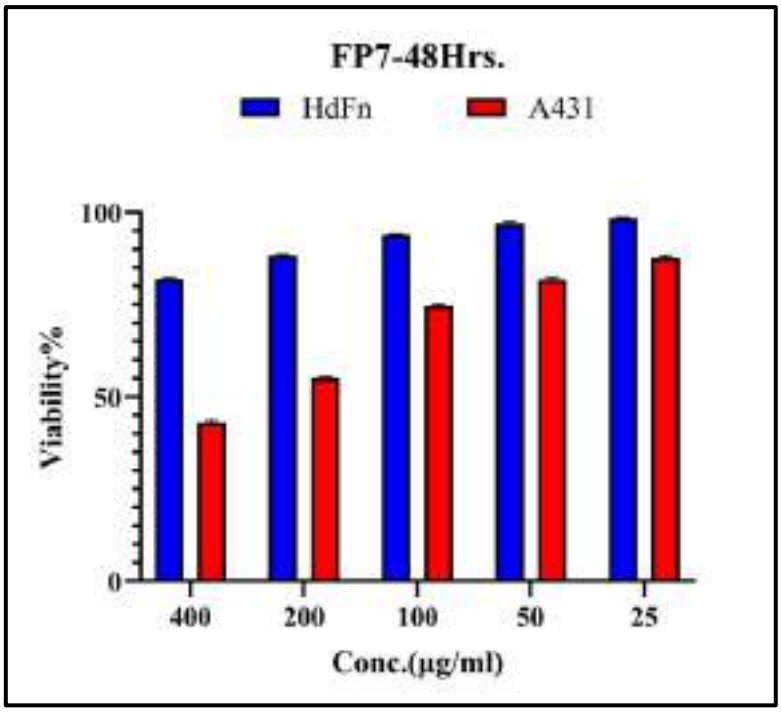


Figure (4- 376): Cytotoxic potentials of copolymer(7) on skin cancer cell line vs normal cell line after 48 hrs.; 37 C°.

Time and concentrations of copolymer(7) were found to enhance the cytotoxicity, which showed a concentration and time-dependent toxicity and exhibited a stronger cytotoxic effect after 72 hours. At 400 µg/ ml, the viability of A431 cells was reduced to 39.721±0.693% whereas HdFn cells remain unaffected and viability reached to 79.501±0.397% which implies that cytotoxic pressure is stronger in cancer cells with an IC_{50} of 136.3 µg/ ml compared to IC_{50} of 216.7 µg/ ml that get from the effect copolymer(7) on normal cell line (fig.4-377).

Table (4- 40): Cytotoxic potentials of copolymer(7) on skin cancer cell line vs normal cell line after 72 hrs.; 37 C°.

Conc. (µg/mL)	Cell viability (%) of copolymer(7)		
	HdFn	A431	P -value
	Mean±SD	Mean±SD	
400	79.501±0.397	39.721±0.693	0.001
200	85.737±0.682	49.309±0.336	0.001
100	91.684±0.408	70.092±0.398	0.001
50	95.383±0.589	78.765±0.767	0.001
25	97.180±0.161	85.304±0.859	0.01

Where 0.5, 0.01, 0.001: Significant differences (P ≤ 0.05) between means.

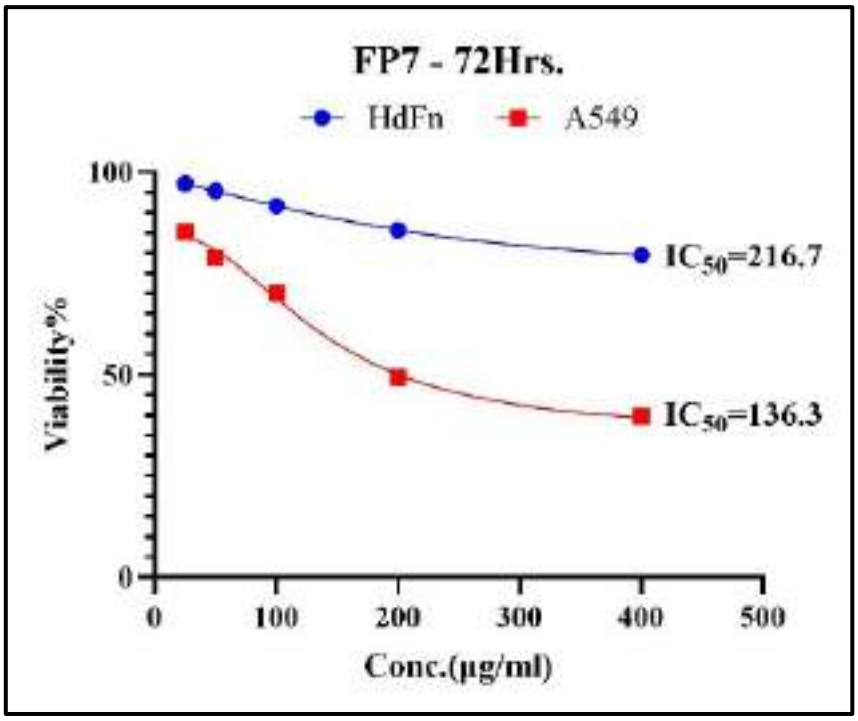


Figure (4- 377): Cytotoxic potentials of copolymer(7) on skin cancer cell line vs normal cell line after 72 hrs.; 37 C°

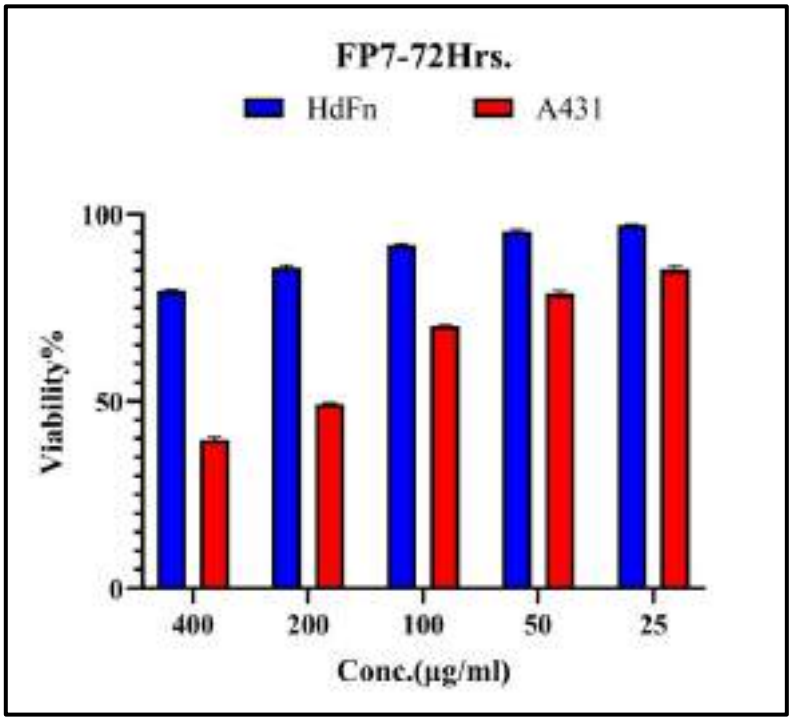


Figure (4- 378): Cytotoxic potentials of copolymer(7) on skin cancer cell line vs normal cell line after 72 hrs.; 37 C°.

4.61.13 Antioxidant Activity of copolymer(7)and copolymer(8) Extract via DPPH Assay.

(fig.4-379) and (Table 4-41) explained that copolymer(7) and copolymer(8) exhibited a less potency in scavenging DPPH in comparison to other compounds to reach (47.018±0.176 and 25.784±0.672%; 49.735±0.047 and 27.096±0.716 %) for 0.500 to 0.0625 mg/ml of respectively comparison to high Vit-C potency in all concentrations tested.

Table (4- 41): DPPH radical scavenging activity of copolymer(7) and copolymer(8), Vit-C.

Samples	DPPH radical scavenging activity Conc. (Mean ± SD)%			
	0.500	0.250	0.125	0.0625
Vitamin-C	75.995±0.185	63.644±0.135	55.221±0.152	39.111±0.027
copolymer(7)	47.018±0.176	39.106±0.095	31.269±0.927	25.784±0.672
P value	0.001	0.01	0.01	0.01
copolymer(8)	49.735±0.047	41.515±0.884	33.875±0.765	27.096±0.716
P value	0.001	0.01	0.01	0.01

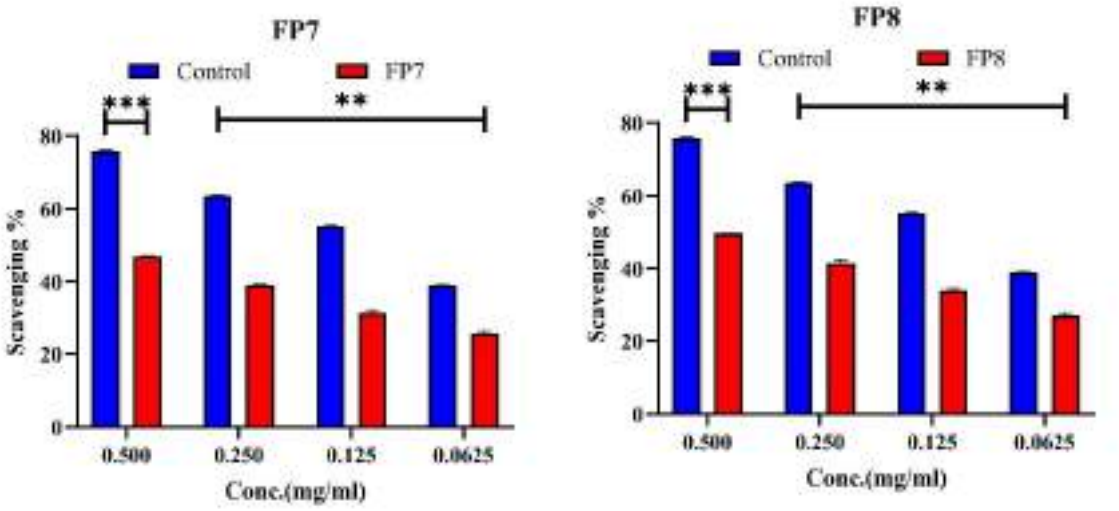


Figure (4- 379): DPPH radical scavenging activity of copolymer(7) and copolymer(8) with vitamin-C.

4.61.14 Cytotoxic against of copolymer(8) on skin cancer Cell Lines(A431) in comparison with normal cell line (Hdfn).

Copolymer(8) exhibited a cytotoxic effect, with A431 cell viability decreasing from (89.235±0.0.596%) at 25 µg/ml to (42.755±0.744%) at 400 µg/ml , while HdFn cells maintain higher viability 83.416±0.343% at 400 µg/ml. The IC $_{50}$ value also drops to 171.8 µg/mL in cancer cells, showing an increase in potency and selectivity

vs. IC $_{50}$ of 240.1 µg/mL on normal cell line (fig.4-380), (Table 4-42).

Table (4- 42): Cytotoxic potentials of copolymer(8) on skin cancer cell line vs normal cell line after 24 hrs.; 37 C°.

Conc. (µg/mL)	Cell viability (%) of copolymer(8)		
	HdFn	A431	P -value
	Mean±SD	Mean±SD	
400	83.416±0.343	42.755±0.744	0.001
200	89.385±0.329	57.030±0.784	0.001
100	94.488±0.238	75.152±0.507	0.001
50	97.217±0.514	83.819±0.995	0.01
25	98.235±0.606	89.235±0.596	0.5

Where0.5, 0.01, 0.001: Significant differences (P ≤ 0.05) between means.

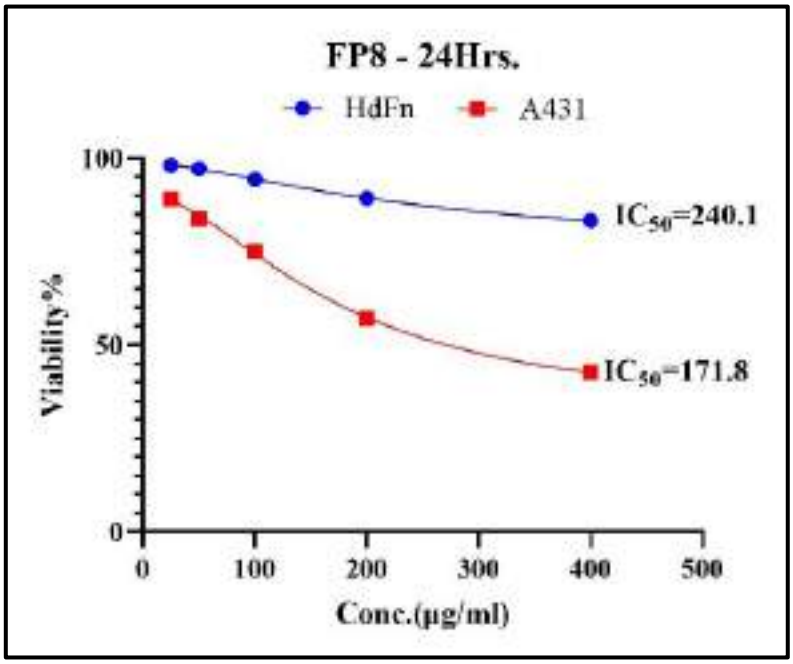


Figure (4- 380): Cytotoxic potentials of copolymer(8) on skin cancer cell line vs normal cell line after 24 hrs.; 37 C°

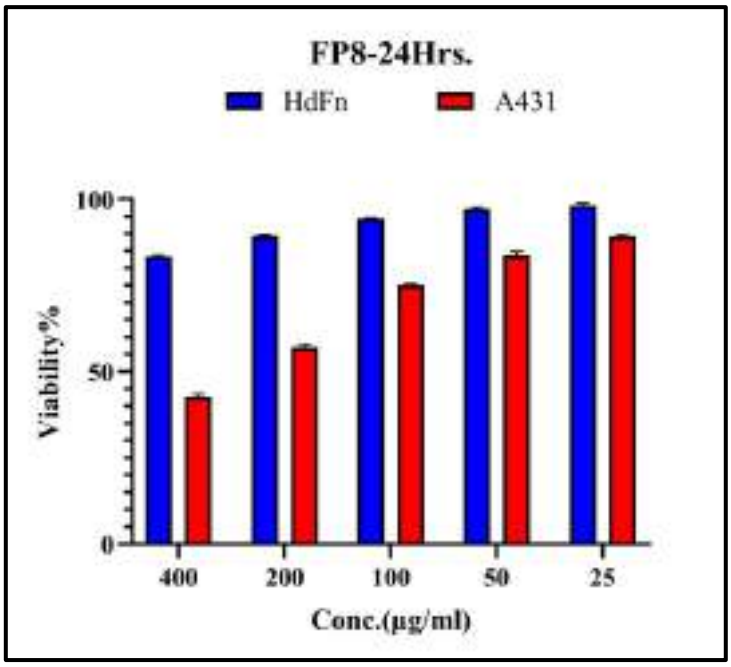


Figure (4- 381): Cytotoxic potentials of copolymer(8) on skin cancer cell line vs normal cell line after 24 hrs.; 37 C°

Copolymer(8) exhibits high and sustained cytotoxic effect, which supports the fact that the compound is a highly effective towards cancer cell. The cell viability of the A431 cells at 400 µg/ml is reduced to 39.857±0.406% but HdFn cells stand at 79.253±0.303% which shows a significant cytotoxic effect but with selectivity. IC_{50} values also affirm its potency, 145.8 µg/ml in skin cancer cells, and 222.0 µg/ml in Hdfn normal cells (fig.4-382).

Table (4- 43): Cytotoxic potentials of copolymer(8) on skin cancer cell line vs normal cell line after 48 hrs.; 37 C°.

Conc. (µg/mL)	Cell viability (%) of copolymer(8)		
	HdFn	A431	P -value
	Mean±SD	Mean±SD	
400	79.253±0.303	39.857±0.406	0.001
200	85.430±0.162	51.693±0.306	0.001
100	92.141±0.893	69.185±0.510	0.001
50	95.113±0.531	79.732±0.767	0.001
25	97.806±0.270	85.055±0.370	0.01

Where0.5, 0.01, 0.001: Significant differences (P ≤ 0.05) between means.

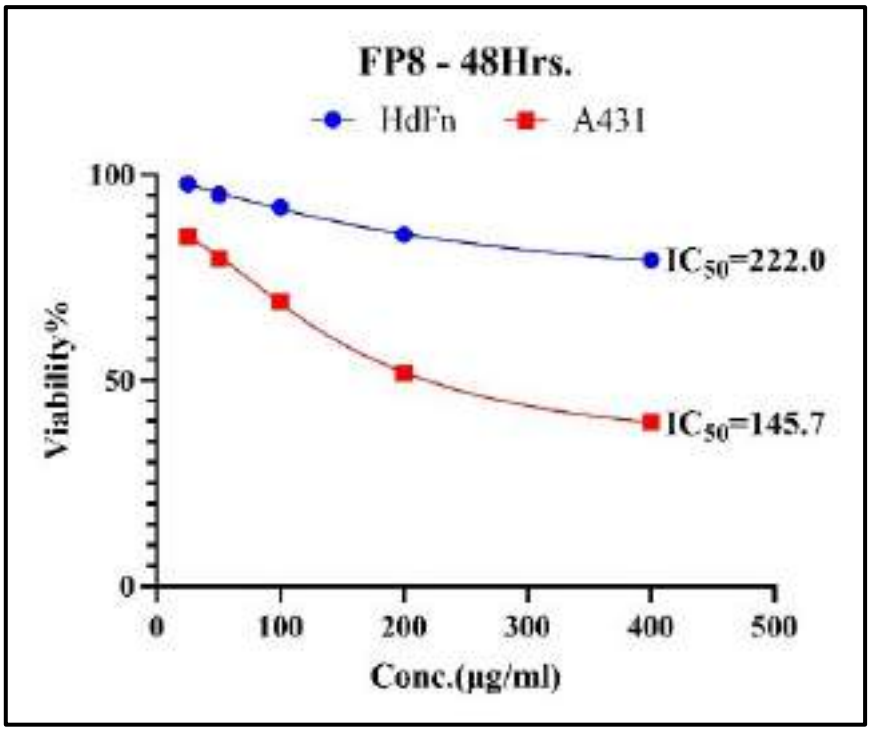


Figure (4- 382): Cytotoxic potentials of copolymer(8) on skin cancer cell line vs normal cell line after 48 hrs.; 37 C°.

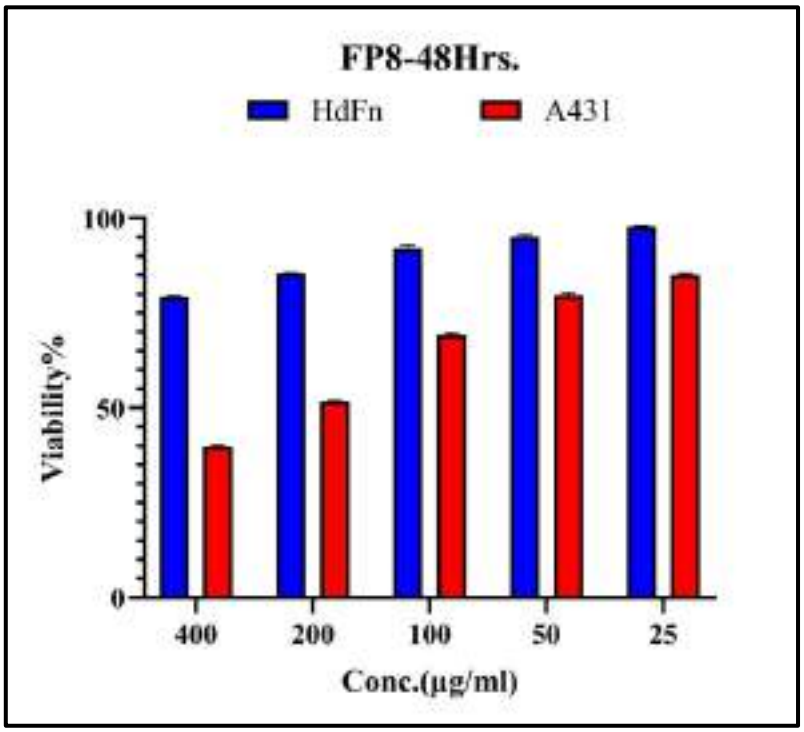


Figure (4- 383): Cytotoxic potentials of copolymer(8) on skin cancer cell line vs normal cell line after 48 hrs.; 37 C° .

At 72 hours copolymer(8) possessed the ability to reduced cancer cell viability to (37.062±0.228% starting from viability of 82.268±0.653%) for 400 to 25 µg/ml

with IC_{50} of 127.1 µg/ml. While an IC_{50} value of 196.9 µg/ml obtained after treated normal cell line with FP8 at concentrations from 25 to 400 µg/ml as shown in (Table 4-44) and (fig.4-384)

Table (4- 44): Cytotoxic potentials of copolymer(8) on skin cancer cell line vs normal cell line after 72 hrs.; 37 C°.

Conc. (µg/mL)	Cell viability (%) of copolymer(8)		
	HdFn	A431	P -value
	Mean±SD	Mean±SD	
400	77.360±0.682	37.062±0.228	0.001
200	83.879±0.707	46.366±0.750	0.001
100	89.652±0.570	63.964±0.793	0.001
50	94.838±0.122	73.310±0.875	0.001
25	96.635±0.403	82.268±0.653	0.01

Where0.5, 0.01, 0.001: Significant differences (P ≤ 0.05) between means.

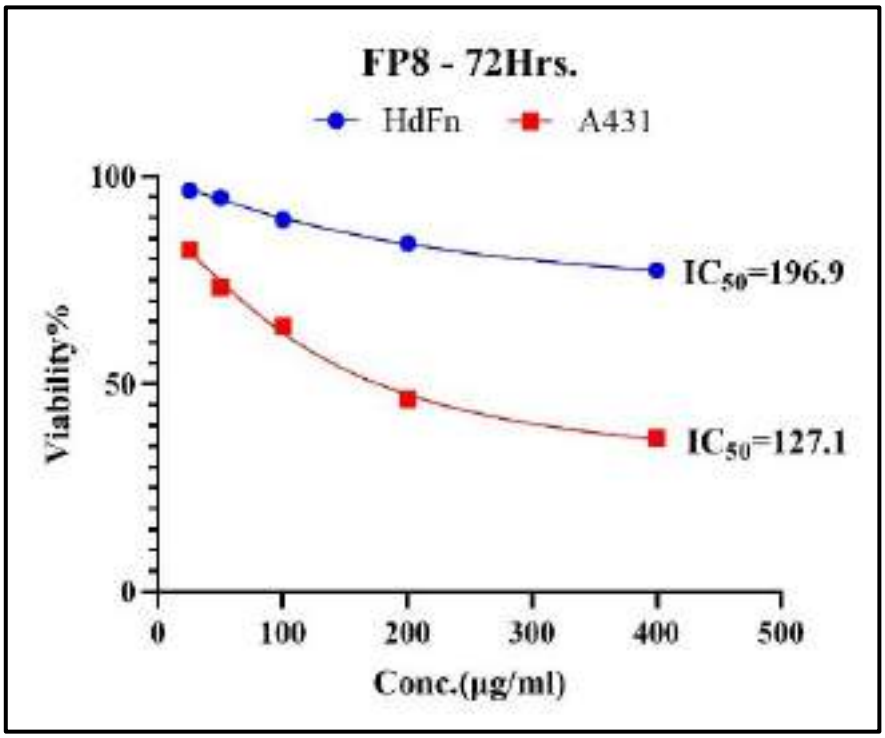


Figure (4- 384): Cytotoxic potentials of copolymer(8) on skin cancer cell line vs normal cell line after 72 hrs.; 37 C°.

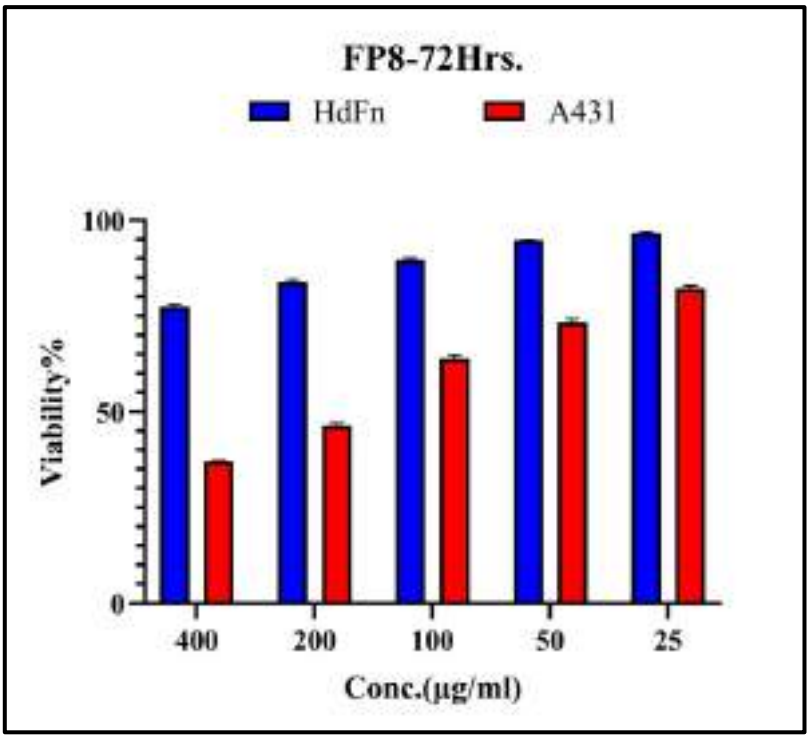


Figure (4- 385): Cytotoxic potentials of copolymer(8) on skin cancer cell line vs normal cell line after 72 hrs.; 37 C°.

4.61.15Cytotoxic against of copolymer(9) on skin cancer Cell Lines(A431) in comparison with normal cell line (Hdfn).

Copolymer(9) exhibited cytotoxic potential with IC_{50} value of 127.3 µg/ml *vs*. 205.8 µg/ml on normal cell line and cell viability decreased from (82.698±0.844 % to 35.126±0.875%) and from (96.783±0.663 to 76.011±0.348%) for cancer and normal cell from 25 to 400 µg/ml respectively. (Table 4-45)

Table (4- 45): Cytotoxic potentials of copolymer(9) on skin cancer cell line vs normal cell line after 24 hrs.; 37 C°.

Conc. (µg/mL)	Cell viability (%) of copolymer(9)		
	HdFn	A431	P -value
	Mean±SD	Mean±SD	
400	76.011±0.348	35.126±0.875	0.001
200	82.520±0.342	46.841±0.609	0.001
100	88.750±0.805	62.173±0.896	0.001
50	93.825±0.967	76.166±0.783	0.001
25	96.783±0.663	82.698±0.844	0.01

Where 0.5, 0.01, 0.001: Significant differences ($P \leq 0.05$) between means.

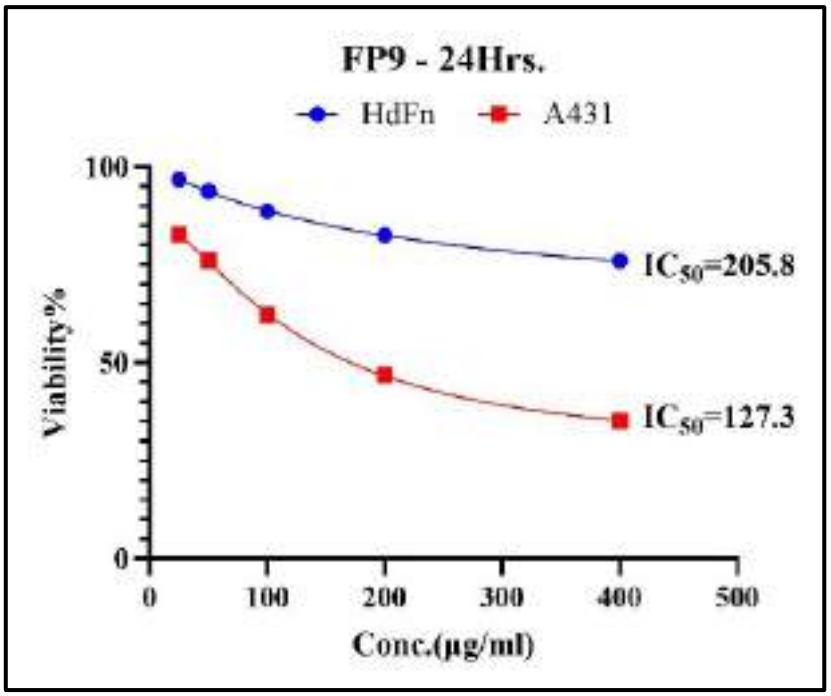


Figure (4- 386): Cytotoxic potentials of copolymer(9) on skin cancer cell line vs normal cell line after 24 hrs.; 37 C°

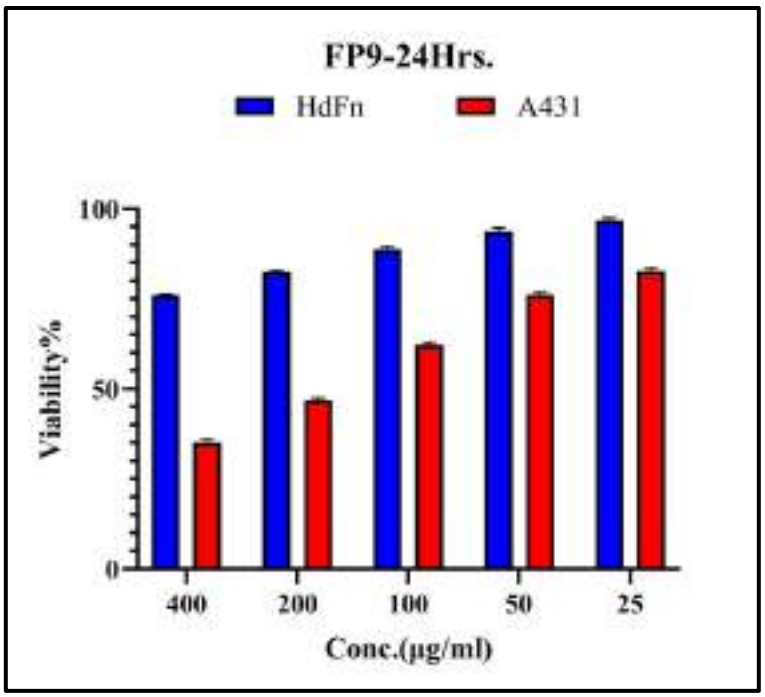


Figure (4- 387): Cytotoxic potentials of copolymer(9) on skin cancer cell line vs normal cell line after 24 hrs.; 37 C°

(Table 4-46) explained a cytotoxic potential of copolymer(9) on skin cancer cell line with reduction in cell viability at concentration dependent manner as shown that the cancer cell viability reach to (29.944±0.305% and 78.845±0.404%) for 400

to 25 µg/ml respectively with an IC_{50} value of 103.6 µg/ml in comparison to IC_{50} of 189.3 µg/ml from the effect of copolymer(9) normal cell with cell viability ranged from (93.925±0.595% to 72.854±0.595%) for 25 to 400 µg/ml.(fig.4-388).

Table (4- 46): Cytotoxic potentials of copolymer(9) on skin cancer cell line vs normal cell line after 48 hrs.; 37 C°

Conc. (µg/mL)	Cell viability (%) of copolymer(9)		
	HdFn	A431	P -value
	Mean±SD	Mean±SD	
400	72.854±0.595	29.944±0.305	0.001
200	78.914±0.613	37.563±0.910	0.001
100	85.150±0.504	55.248±0.544	0.001
50	90.249±0.637	72.104±0.705	0.001
25	93.925±0.595	78.845±0.404	0.001

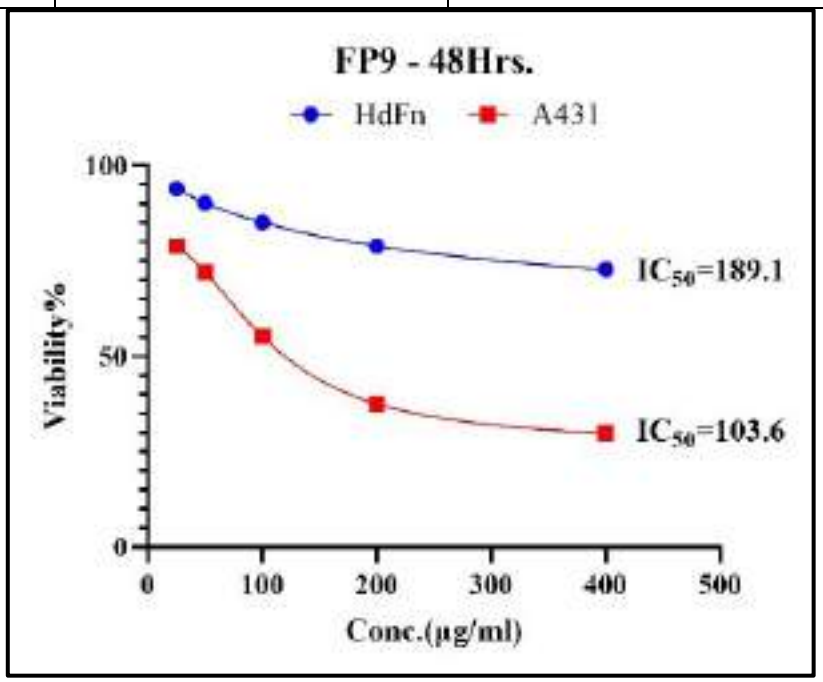


Figure (4- 388): Cytotoxic potentials of copolymer(9) on skin cancer cell line vs normal cell line after 48 hrs.; 37 C°

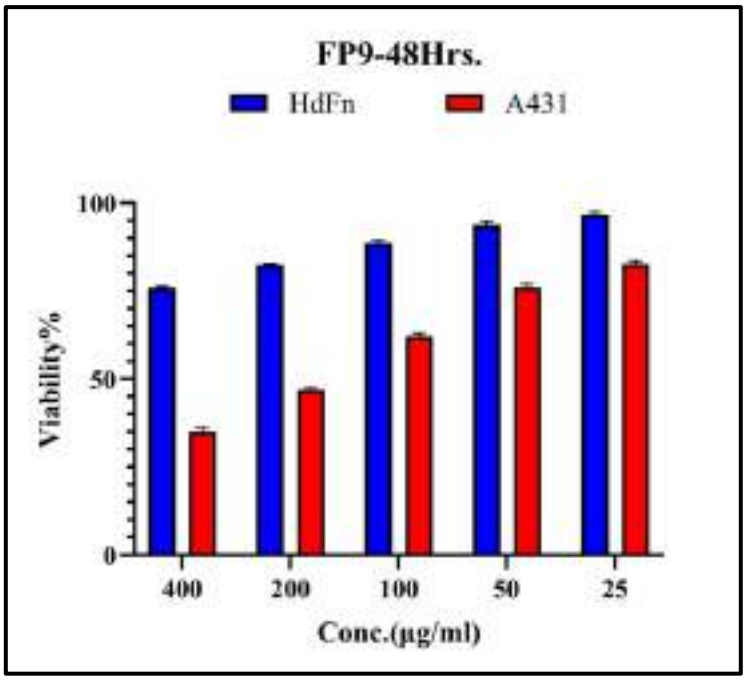


Figure (4- 389): Cytotoxic potentials of copolymer(9) on skin cancer cell line vs normal cell line after 48 hrs.; 37 C°

Copolymer(9) exhibits also revealed cytotoxic profile, close to that of the most active compound. The A431 cell viability reduces to 24.946±0.578% at the tested concentration of 400 µg/ml where's HdFn cells was 67.755±0.763% at same concentration and the IC_{50} values further support this effect showing 87.02 µg/ml in cancer cells and 150.4 µg/ml on normal cell (Table 4-47), (fig.4-390).

Table (4- 47): Cytotoxic potentials of copolymer(9) on skin cancer cell line vs normal cell line after 72 hrs.; 37 C°.

Conc. (µg/mL)	Cell viability (%) of copolymer(9)		
	HdFn	A431	P -value
	Mean±SD	Mean±SD	
400	67.755±0.763	24.946±0.578	0.001
200	74.723±0.501	31.125±0.872	0.001
100	79.945±0.551	42.017±0.341	0.001
50	87.714±0.557	56.864±0.659	0.001
25	90.488±0.266	64.156±0.648	0.001

Where 0.5, 0.01, 0.001: Significant differences ($P \leq 0.05$) between means.

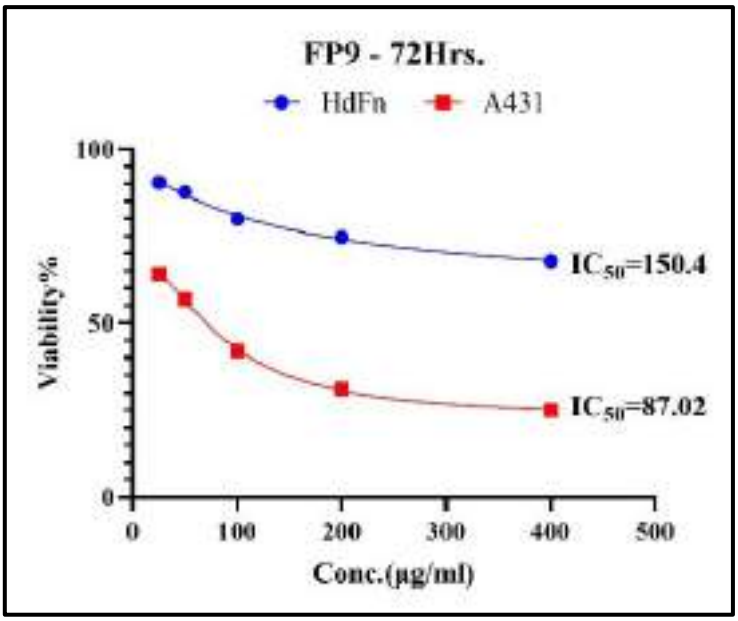


Figure (4- 390): Cytotoxic potentials of copolymer(9) on skin cancer cell line vs normal cell line after 72 hrs.; 37 C°.

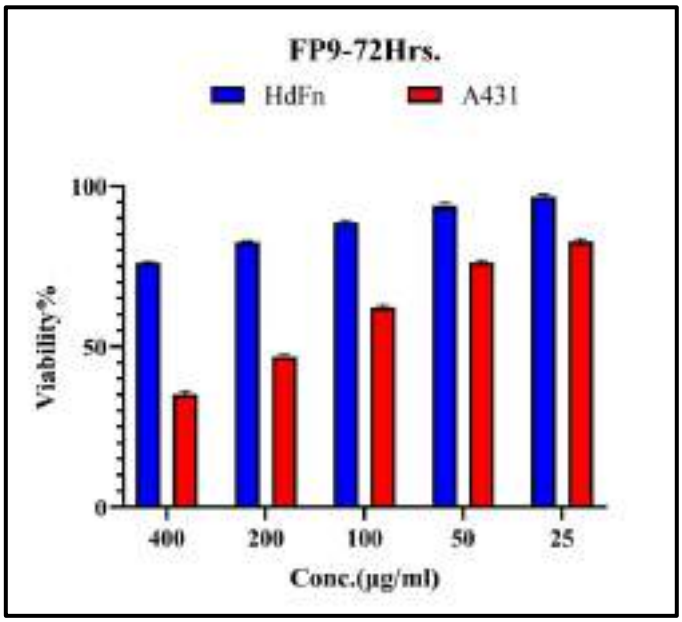


Figure (4- 391): Cytotoxic potentials of copolymer(9) on skin cancer cell line vs normal cell line after 72 hrs.; 37 C°

4.61.16 Antioxidant Activity of copolymer(9) Extract via DPPH Assay.

As results indicated in (fig.4-392) and (Table 4-48), copolymer(9) possessed a high potency to scavenge free radical (DPPH) for all tested concentrations 0.0625, 0.125, 0.250 and 0.500 mg/ml to reach 33.957±0.692, 43.781±0.788, 53.201±0.034 and 61.806±0.985% respectively and Vit-C also possessed highly DPPH scavenging activity.

Table (4- 48): DPPH radical scavenging activity of copolymer(9) and Vit-C.

Samples	DPPH radical scavenging activity Conc. (Mean ± SD)%			
	0.500	0.250	0.125	0.0625
Vitamin-C	75.995±0.185	63.644±0.135	55.221±0.152	39.111±0.027
copolymer(9)	61.806±0.985	53.201±0.034	43.781±0.788	33.957±0.692
P value	0.01	0.5	0.5	0.5

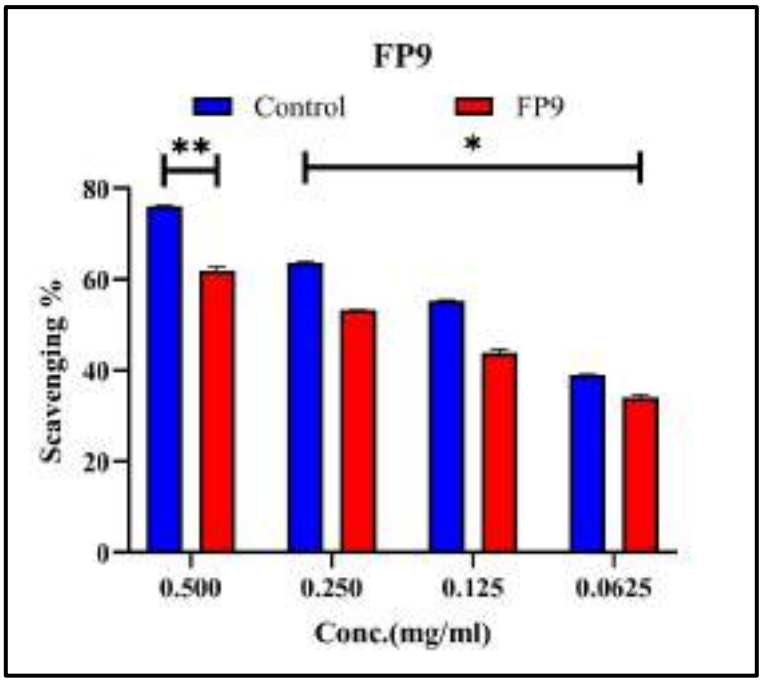


Figure (4- 392): DPPH radical scavenging activity of copolymer(9) and vitamin -C

4-62-17:-Cytotoxic against of copolymer(10) on skin cancer Cell Lines(A431) in comparison with normal cell line (Hdfn).

(Table 4-49) represented a decrease in cell viability of A431 cancer cell from (86.613±0.520% to 40.005± 0.427%) after treated cancer cell with copolymer(10) for 25 to 400 µg/ml respectively and exhibited the most potent cytotoxic activity with an IC_{50} value of 149.6 µg/ml. However an IC_{50} of 228.8 µg/ml obtained from the effect of copolymer(10) on normal cell with reduction in cell viability to 81.058±0.672% at 400 µg/ml

Table (4- 49): Cytotoxic potentials of copolymer(10) on skin cancer cell line vs normal cell line after 24 hrs.; 37 C°.

Conc. (µg/mL)	Cell viability (%) of copolymer(10)		
	HdFn	A431	P -value
	Mean±SD	Mean±SD	
400	81.058±0.672	40.005±0.427	0.001
200	87.045±0.641	53.147±0.503	0.001
100	92.527±0.532	69.347±0.460	0.001
50	96.199±0.160	81.715±0.534	0.01
25	97.975±0.413	86.613±0.520	0.01

Where 0.5, 0.01, 0.001: Significant differences (P ≤ 0.05) between means.

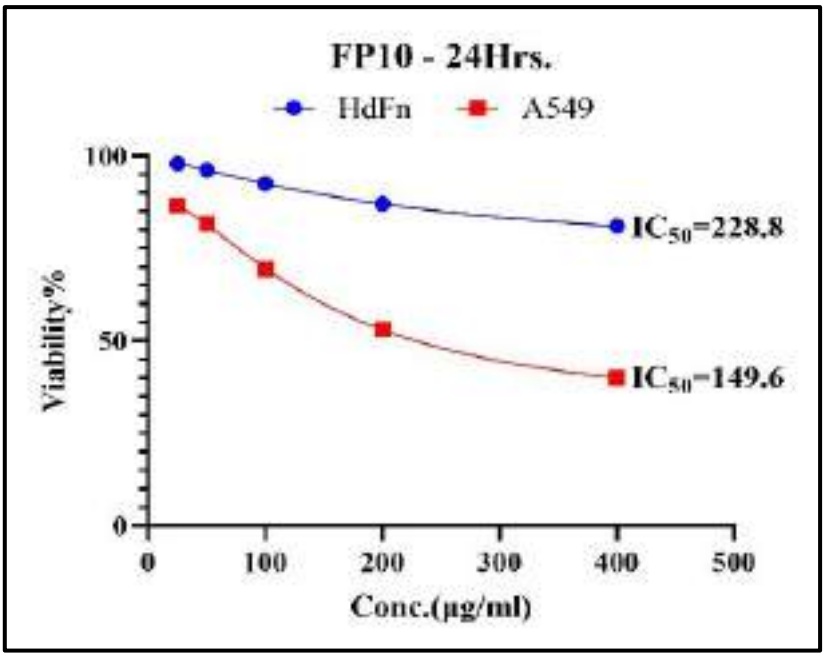


Figure (4- 393): Cytotoxic potentials of copolymer(10) on skin cancer cell line vs normal cell line after 24 hrs.; 37 C°.

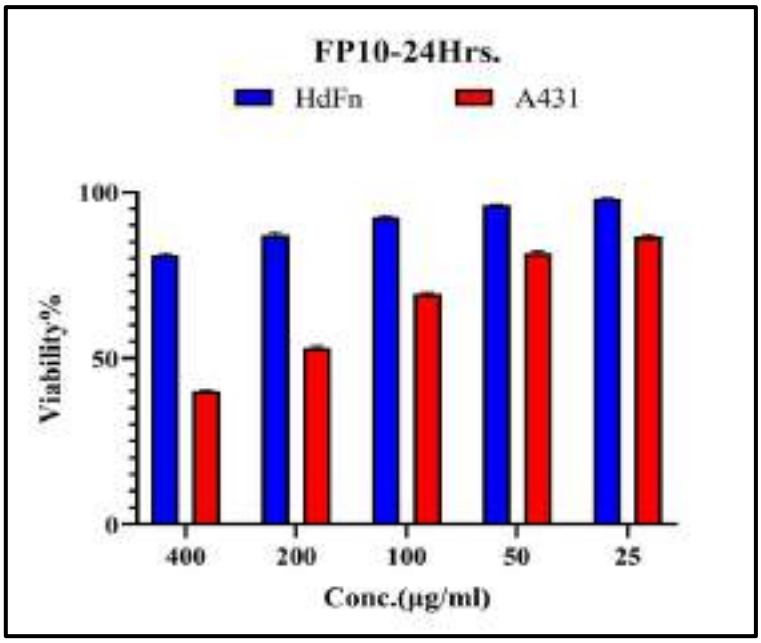


Figure (4- 394): Cytotoxic potentials of copolymer(10) on skin cancer cell line vs normal cell line after 24 hrs.; 37 C°.

(Fig.4-395) revealed that copolymer(10) possessed cytotoxic effect against skin cancer cell with reduction in cell viability at concentration dependant manner in which cell viability reduced from (83.0.82±0.494% at 25 µg/ml *vs.* cell viability of 37.398 ±0.383% for 400µg/ml with IC_{50} value of 126.5 µg/ml. copolymer(10) exhibited the most cytotoxic potent with IC_{50} of 215.7 µg/ml and reduction in cell viability to 77.097±0.680% at concentration 400 µg/ml of on normal cell line (Table 4-50)

Table (4- 50): Cytotoxic potentials of copolymer(10) on skin cancer cell line vs normal cell line after 48 hrs.; 37 C°.

Conc. (µg/mL)	Cell viability (%) of copolymer(10)		
	HdFn	A431	P -value
	Mean±SD	Mean±SD	
400	77.097±0.680	37.398±0.383	0.001
200	83.708±0.309	47.393±0.346	0.001
100	90.697±0.393	64.183±0.473	0.001
50	94.138±0.490	75.194±0.184	0.001
25	96.709±0.582	83.082±0.494	0.01

Where 0.5, 0.01, 0.001: Significant differences (P ≤ 0.05) between means.

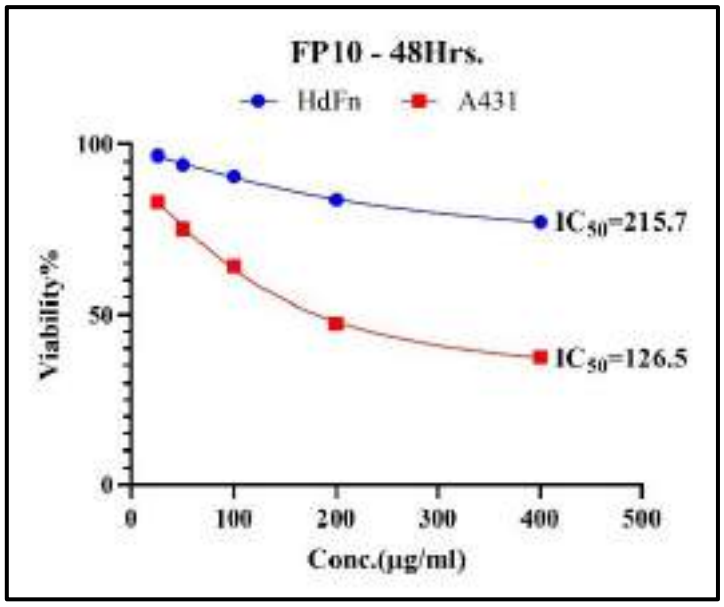


Figure (4- 395): Cytotoxic potentials of copolymer(10) on skin cancer cell line vs normal cell line after 48 hrs.; 37 C°.

After 48 h of treatment the cytotoxic activity of all copolymers was increased in comparison with the 24 h period of exposure. The viability of A431 cells decreased gradually with the increase of compound concentration, while HdFn cells had relatively higher viability. copolymer(9) again showed the highest cytotoxic effect, with a viability of A431 cells of 29.944±0.305% at 400 µg/mL, and the lowest IC50 of the compounds tested. copolymer(6) and copolymer(10) were also potent cytotoxic agents, whereas copolymer(7) displayed a relatively lower reduction in A431 viability but showed better normal-cell viability. These results suggest that the cytotoxic effect of the compounds on A431 cells was increased with the prolonged exposure. An IC_{50} value of 110.7 µg/ml was obtained after treated cancer cell with copolymer(10) and cell viability reduced from (77.793±0.662% to 31.988±0.414%) for 25 to 400 µg/ml respectively, however IC_{50} of 187.9 µg/ml and decreasing in Hdfn cell viability from (95.120±0.787 to 73.954±0.579%) after treated normal cell with copolymer(10) for 25 to 400 µg/ml respectively (Table 4-51), (fig.4-396)

Table (4- 51): Cytotoxic potentials of copolymer(10) on skin cancer cell line vs normal cell line after 72 hrs.; 37 C°

Conc. (µg/mL)	Cell viability (%) of copolymer(10)		
	HdFn	A431	P -value
	Mean±SD	Mean±SD	
400	73.954±0.579	31.988±0.414	0.001
200	81.531±0.180	40.896±0.938	0.001
100	87.184±0.508	56.758±0.449	0.001
50	94.244±0.476	69.215±0.610	0.001
25	95.120±0.787	77.793±0.662	0.001

Where 0.5, 0.01, 0.001: Significant differences (P ≤ 0.05) between means.

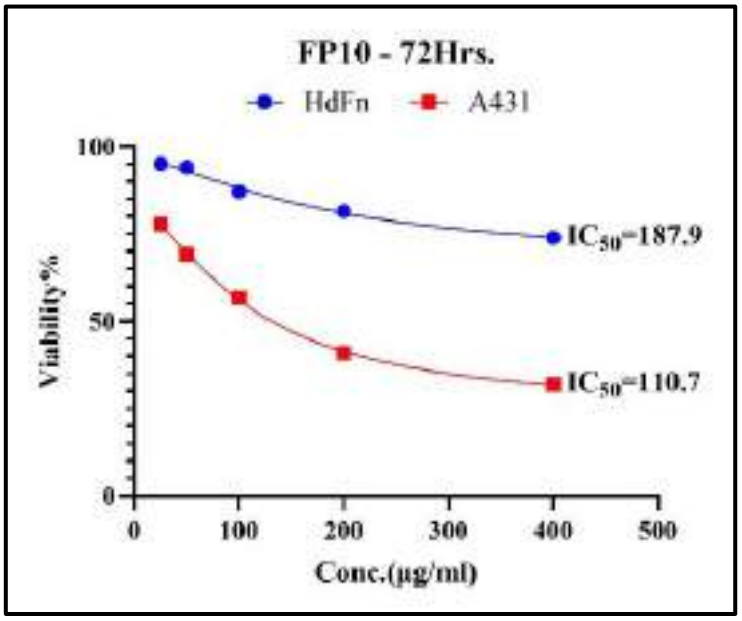


Figure (4- 396): Cytotoxic potentials of copolymer(10) on skin cancer cell line vs normal cell line after 72 hrs.; 37 C°.

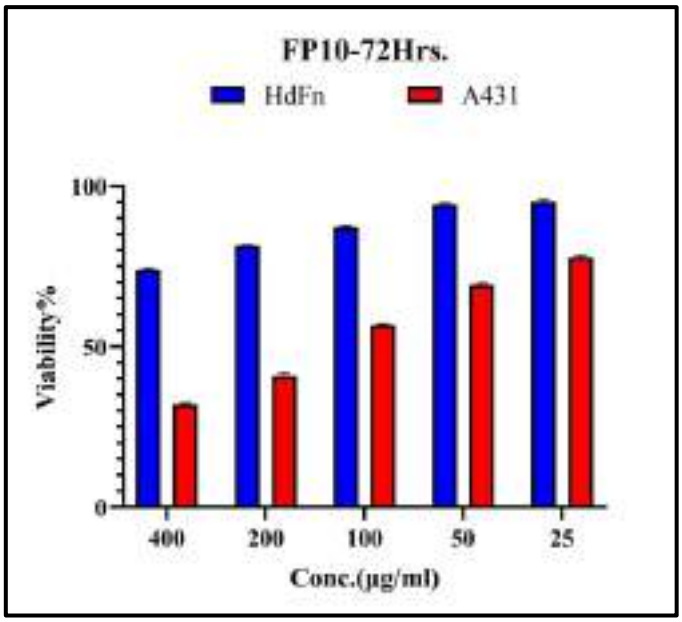


Figure (4- 397): Cytotoxic potentials of copolymer(10) on skin cancer cell line vs normal cell line after 72 hrs.; 37 C°

All the tested copolymers demonstrated the highest cytotoxic activity against A431 skin cancer cells after 72 hours of exposure. The most prominent reduction of cell viability was observed at 400 µg/mL and it appears that the reduction was dependent on concentration and time. copolymer(9) was the most active compound with the viability of A431 of 24.946±0.578% and the lowest IC50 value of 87.02 µg/mL. copolymer(6) and copolymer(10) also showed significant cytotoxic effects and were followed by copolymer(8) and copolymer(7). The viability of HdFn normal cells was also decreased, but remained higher than that of A431 cells, confirming that the compounds were more cytotoxic to cancer cells than normal cells.

Possible anticancer efficacy of compounds copolymer(6)- copolymer(10) towards skin cancer cell lines can be attributed to the chemical groups that have been found in the structures. A variety of bioactive motifs can be found in these compounds: thiosemicarbazone-like motifs, thiohydantoin/thioxo rings, aromatic imide-like motifs, fused nitrogen-rich heterocycles, carbonyl groups, and sulfur-based groups. Scaffolds of this type have been shown to kill cancer cells by generating reactive oxygen species, inducing mitochondrial dysfunction and apoptosis, arresting the cell cycle, chelating metals, and inhibiting intracellular enzymes such as ribonucleotide reductase and topoisomerase II.(157, 167, 168).

Thus, the predicted biological impact of copolymer(6)- copolymer(10) might be structure-dependent and could vary based on the active groups in each copolymer.

In the case of copolymer(6), the presence of a thiosemicarbazone-type moiety along with the presence of a nitro-substituted aromatic ring indicates the possibility of multi-target anticancer action. Thiosemicarbazone analogs have been reported to cause oxidative stress, disrupt mitochondrial function, block ribonucleotide reductase and topoisomerase II, and affect cell-cycle activity(167). Also, thiosemicarbazone metal complexes can disrupt mitochondrial energy metabolism and induce ROS production, which subsequently triggers mitochondria-mediated apoptosis(157). According to this, copolymer(6) might prevent the growth of skin cancer cells primarily by mediating mitochondrial stress via ROS, inducing apoptosis, and potentially inhibiting cellular enzymes. copolymer(7) contains a thiohydantoin/thioxo-imidazolidinone-type ring, an azomethine bond, and a phenolic aromatic ring. This structural arrangement suggests that copolymer(7) is likely to exert its activity by binding intracellular targets rather than inducing severe oxidative stress. Thiohydantoin analogs have demonstrated cytotoxic effects against cancer cell lines, with activity highly dependent on substituents on the thiohydantoin backbone(169) .Therefore, copolymer(7) may inhibit the growth of skin cancer cells by interacting with intracellular proteins or enzymes involved in cell growth, thereby disrupting the cell cycle and inducing apoptosis.

Copolymer(8) possesses an extensive aromatic imide-like skeleton, a thioamide or thiourea group, and an amino-substituted aromatic ring. Aromatic imide systems, particularly 1, 8-naphthalimide-type compounds, have been extensively investigated as anticancer scaffolds due to their capacity to interact with DNA, inhibit DNA topoisomerase II, and induce DNA damage and apoptosis (157, 170). Consequently, intracellular macromolecular targeting, particularly through DNA-based mechanisms, is likely the principal mode of action for copolymer(8). The most probable mechanism involves DNA interaction, topoisomerase inhibition, and cell-cycle arrest. a copolymer(9) features a fused nitrogen-heterocyclic system with

several sulfur- and nitrogen-donor groups, which facilitate metal interactions and intracellular binding. Thiosemicarbazone compounds have been reported to affect cancer cells by disrupting metal homeostasis, increasing reactive oxygen species (ROS) generation, impairing mitochondrial function, and inducing apoptosis (157, 168). Therefore, copolymer(9) may exert anticancer effects against skin cancer through enzyme inhibition, metal chelation, mitochondrial dysfunction, and ROS-induced apoptosis. a copolymer(10) contains a nitrogen-based fused heterocycle, a pyridine-like ring, and carbonyl groups. These structural features indicate that copolymer(10) is likely a target-directed compound rather than a simple membrane-damaging agent. Nitrogen-rich heterocyclic systems are frequently utilized in anticancer drug design due to their ability to bind enzyme pockets and modulate signaling pathways involved in cell proliferation and survival (171). Accordingly, copolymer(10) may suppress the growth of skin cancer cells by binding to intracellular targets, inhibiting cell cycle progression, and inducing apoptosis. apoptosis.

In general, copolymer(6)-copolymer(10) meOverall, the mechanisms of action for copolymer(6) –copolymer(10) are closely linked to their chemical structures. copolymer(6) primarily acts through ROS formation, mitochondrial stress, and apoptosis(157, 167). copolymer(7) is likely to function via enzyme inhibition and cell-cycle disturbance (170). copolymer(8) is most likely to affect DNA-related pathways due to its aromatic imide-like scaffold (157, 170) .C opolymer(9) may exert effects via metal chelation, mitochondrial dysfunction induction, and mediation of ROS-induced apoptosis(157, 168). copolymer(10) may inhibit cancer cell growth through heterocycle-mediated intracellular nitrogen binding(171). However, these proposed mechanisms require experimental validation by measuring IC50, apoptosis, ROS, cell-cycle progression, mitochondrial membrane potential, topoisomerase inhibition, and DNA damage markers.

4.61.17Antioxidant Activity of copolymer(10)and Extract via DPPH Assay.

Finally, copolymer(10) matches with copolymer(9) by possessing higher potency to scavenging activity against DPPH radicals and also at all concentrations 0.0625, 0.125, 0.250 and 0.500 mg/ml to reach 29.637±0.703, 37.748±0.812, 46.214±0.963 and 54.604±0.994% respectively, (fig.4-398), (Table 4-52) and also Vit-c showed highest DPPH scavenging activity.

Table (4- 52): DPPH radical scavenging activity of copolymer(10) and Vit-C.

Samples	DPPH radical scavenging activity Conc. (Mean ± SD)%			
	0.500	0.250	0.125	0.0625
Vitamin-C	75.995±0.185	63.644±0.135	55.221±0.152	39.111±0.027
copolymer(10)	54.604±0.994	46.214±0.963	37.748±0.812	29.637±0.703
P value	0.01	0.5	0.5	0.5

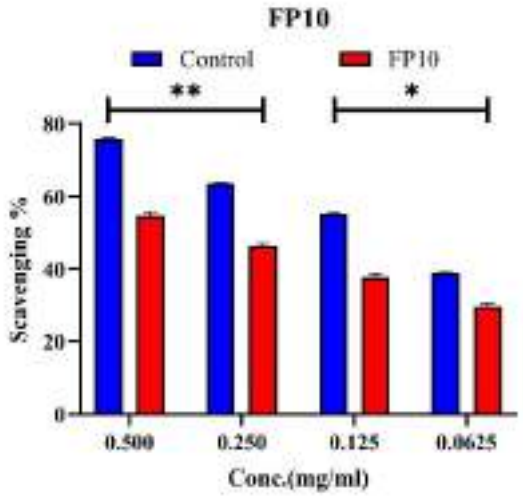


Figure (4- 398): DPPH radical scavenging activity of copolymer(10) with vitamin -C

Vitamin-C (positive control) that showed highest DPPH scavenging activity in same concentrations tested used in previous compounds and the activity of scavenging reached to 75.995±0.185, 63.644±0.135, 55.221±0.152 and 39.111±0.027% for 0.500, 0.250, 0.125, and 0.0625mg/ml (Table 4-53).

Table (4- 53): DPPH radical scavenging activity of vitamin-C.

Samples	DPPH radical scavenging activity Conc. (Mean ± SD)%			
	0.500	0.250	0.125	0.0625
Vitamin-C	75.995±0.185	63.644±0.135	55.221±0.152	39.111±0.027

The antioxidant properties of the synthesized compounds copolymer(1)–copolymer(10) are primarily attributed to their capacity to neutralize free radicals through hydrogen atom donation, electron transfer, and stabilization of the resulting radical intermediates. In the DPPH assay, radical quenching may proceed via hydrogen atom transfer (HAT), single-electron transfer (SET), proton-coupled electron transfer, or sequential proton loss electron transfer, contingent upon the molecular structure and reaction conditions. (172-174).

The antioxidant activity of copolymer(1) could be due to the presence of reactive functional groups like azomethine and sulfur containing groups. These groups can be involved in electron transfer reactions and might be responsible for direct electron donation to free radicals. The antioxidant activity of copolymer(1) is probably restricted due to lack of extension of π-electrons. Following the donation of an electron or hydrogen atom, the antioxidant molecule radical intermediate must be stabilized to prevent continuing oxidative propagation. Without general resonance delocalisation, the radical form is less stable, and the ability to act as a scavenger is limited. Thus, the antioxidant activity of copolymer(1) could be mostly attributed to direct electron donation, and its general antioxidant activity is hampered by the fact that it has a less-stabilized radical and a shorter conjugated system. This interpretation is in accordance with general structure–activity relationship of Schiff base-type antioxidants, in which presence of electron-donating substituents and conjugation have a significant effect on DPPH radical scavenging activity.(174).

The presence of the heteroatomic nitrogen components could impart better antioxidant activity to copolymer(2). Electron density can be increased in the molecule and electron transfer to free radicals can be allowed by nitrogen atoms. Also, heteroatoms can stabilize the radical intermediate by resonance and induction. However, the presence of azomethine type functionality can also play a role in radical scavenging because Schiff base structures have been known to participate in HAT and SET pathways with DPPH radicals(174). However, the antioxidant activity of copolymer(2) is dependent on the way in which these active centres are

incorporated into the conjugated system. With incomplete connection to a delocalized electronic framework, the stabilization of the radical is not complete. Therefore, copolymer(2) should exhibit antioxidant properties primarily through heteroatom-assisted electron transfer, but with moderately high stabilization potential as compared to the more highly conjugated compounds.

Copolymer(3) may have greater antioxidant capacities due to a more desirable aromatic or conjugated system. Extended π-conjugation is one of most crucial structural factors that influence the radical scavenging activity as it permits the unpaired electron, which is created following the electron donation, to be spread over a larger molecular framework. This delocalization lowers the reactivity of the anti-oxidant derived radically and raises the stability of the molecule following a free radical neutralisation. It is likely, therefore, that copolymer(3) would have an antioxidant effect due to a combined mechanism of action of transfer of electrons and resonance stabilization. It is also possible that aromatic rings can help by offering an electron rich environment for the quenching of radicals. The mechanism suggested for the compound copolymer(3) is also supported by the findings that the conjugation, ring structure and electron-donating groups play a crucial role in the antioxidant activity of Schiff base and related heterocyclic compounds(173, 174).

Structurally, copolymer(4) may be considered a good compound to possess anti-oxidant activity as it is likely to contain a number of antioxidant supporting properties in one molecule such as conjugated systems, heterocyclic rings and electron-rich heteroatoms, which include nitrogen and sulfur. All of these features can work together to improve the radical scavenging by several routes. The nitrogen atoms can play a role in facilitating the transfer of electrons, groups containing sulphur can be involved in redox related interactions, and the heterocyclic or aromatic system can contribute to the resonance delocalisation of the radical intermediate. The antioxidant activity of such a structure can thus be attributed to the delicate balance between electron donation and radical stabilization. Sulfur and nitrogen containing heterocyclic compounds such as thiosemicarbazone and

thiohydantoin derivatives are reported to have antioxidant properties owing to the ability of their N/S donor systems to donate electron and stabilize radicals(158, 175, 176). Hence, it is likely that copolymer(4) has the most efficient structure for antioxidant activity in this series.

The antioxidant activity of copolymer(5) can be justified by the balanced molecular architecture that combines aromaticity, heteroatoms and functional groups capable of interacting with free radicals. A molecule with balanced polarity, electronic flexibility and conjugation can interact effectively with DPPH radicals and still have the ability to stabilize the radical form after donation. Aromatic systems can offer resonance stabilization and nitrogen and sulfur atoms can increase electron density and facilitate redox interaction. Thus, copolymer(5) is expected to act via a mixed mechanism involving electron transfer, possible hydrogen donation and stabilization of the radical derived from the antioxidant. The high mechanistic potential of copolymer(5) indicates that the structure of this compound provides accessible radical-scavenging centers and sufficient electronic delocalization, both of which are important for antioxidant efficiency .(172, 174)

Copolymer(6) could have antioxidant effects by sulfur and nitrogen functional groups, especially if copolymer(6) has a structure similar to thiosemicarbazone. Thiosemicarbazones contain centers such as C=N, C=S, NH, N, S which can interact with free radicals, making them unique to participate in redox reactions. These groups can help to transfer electrons, donate hydrogen and stabilize the radical intermediate (158, 175). Nevertheless, the antioxidant activity of copolymer(6) may depend on availability of these active sites as well as level of conjugation within the molecule. In cases where steric hindrance prevents proper exposure of N/S donor centres and/or the conjugated system is not extended enough, the radical-scavenging effect can stay moderate. Thus, the antioxidant activity of copolymer(6) could be of a mechanistic nature, but the efficacy of it is dependent on the presence of its redox active centers.

The structure of copolymer(7) may have lower efficiency for donating hydrogen/electrons, which may explain its lower antioxidant behavior. The antioxidant activity of a molecule with a heterocyclic ring is dependent on the presence of electron-rich centers, which are also accessible, and the ability to stabilize the radical form after an electron has been donated to it. For copolymer(7) with thiohydantoin or thioxo-imidazolidinone-type ring, the antioxidant activity might be highly sensitive to the kind and position of the substituents at the ring. The electron availability and the strength of the neutralization of the radicals can be lowered by electron withdrawing substituents, lack of conjugation or steric restriction on the active sites. The antioxidant activity of thiohydantoin derivatives has been a subject of previous studies with significant variations in activity depending on substituent effects and electronic arrangement (176, 177). Therefore, copolymer(7) could have a more unfavourable electronic structure for DPPH radical scavenging.

The possible presence of aromatic or imide-like structural features may also be responsible for the limited antioxidant properties of copolymer(8). Aromaticity can help stabilize radicals, but typically the more strongly the aromatic system is able to stabilize a radical, the more functional groups it needs to have that are able to donate an electron or a hydrogen. An electron withdrawing imide or carbonyl may decrease the electron density in the molecule and lessen the ability to donate electrons to DPPH radicals. Furthermore, a rigid aromatic structure can provide stability to the parent molecule, but may not necessarily offer available radical-scavenging sites. Therefore, the structural stability of copolymer(8) can be expected, but the ability of the antioxidant centres to donate hydrogen is limited, and there is a reduced availability of electrons, or the antioxidant centres are not accessible. It is not surprising that aromaticity is not sufficient to ensure high DPPH scavenging activity, as mentioned by.

The nitrogen and sulfur-rich heterocyclic structure of copolymer(9) could be responsible for its significant antioxidant activity. These structures can offer multiple

centers that can act as electron donors and act as radical scavengers. The atoms of nitrogen and sulfur can provide electron transfer, and the heterocyclic system can provide resonance stabilization of the radical intermediate. Sulfur-containing compounds can also have an antioxidant effect by redox modulation and by neutralizing free radicals. So likely copolymer(9) will operate via heteroatom-assisted radical scavenging, both electron donation and radical stabilization play a role. Reports on thiosemicarbazone related and sulfur containing heterocyclic compounds also support this mechanism, as many of these compounds exhibit antioxidant activity on account of their N/S donor system and their framework of conjugation The nitrogen-containing heterocyclic and carbonyl groups cause copolymer(10) to exhibit moderate antioxidant behavior. The heterocyclic structure might offer a certain level of stabilization of free radicals, and the N atoms could participate in electron transfer and/or free radical interactions. But carbonyl groups can pull electron density out of the molecule, decreasing its capacity to give up electrons or hydrogen atoms. Thus, the antioxidant activity of copolymer(10) may be a compromise between the electron-poor carbonyl group effect and the electron-rich heterocyclic center. Structural balance of this kind can lead to measurable antioxidant capacity, but may not be enough to achieve the highest possible antioxidant activity when there is some restriction in electron donation. Therefore, copolymer(10) might act primarily through heterocycle assisted electron transfer, and the activity of copolymer(10) might be controlled by the electronic effect of carbonyl containing groups.

4.62 Antimicrobial and Antifungal Activity of Tested Copolymers.

4.62.1 Antibacterial Activity

Antimicrobial potentials of (copolymer(1)- copolymer(10) copolymers on Gram negative bacteria, Gram positive The antimicrobial potentials of synthesized polymers (1-10) were assessed through well diffusion assay on (Gram negative bacteria *E. coli* and *Pseudomonas aeruginosa* and Gram-positive bacteria *Staphylococcus aurous and enterococcus faecalis* and (*Candida albicans*) as fungi.

The results indicated that the diameter of inhibition zone varies depending on type of polymer, polymer concentrations and bacterial type as explained below.(178)

4.62.2 Effect of polymers on E. coli and P. aeruginosa:

The results explained that various inhibition zone were noticed as sown in (Table 4-54) and (fig.4-399). For (1) polymer, no inhibition zone showed on *E. coli* for both concentrations (100 and 50%), however an inhibition zone of (28 mm and 18 mm) obtained from effect of copolymer (1) on *P. aeruginosa* for both concentration respectively (100 and 50%). The results of

Copolymer (2) on *E. coli* and *P. aeruginosa* revealed that bacterial inhibition zone was (18 mm and 22mm) for concentration (100%) while at concentration of (50%) no inhibition zone noticed on both bacterial types.

Table (4- 54): Antibactrial activities of (copolymer1 and copolymer2) on both *Escherichia coli* and *Pseudomonas aeruginosa*

Microbial types	Zone of inhibition (mm)			
	copolymer(1)		copolymer(2)	
	100	50	100	50
Escherichia coli	---	---	18	---
Pseudomonas aeruginosa	28	18	22	---

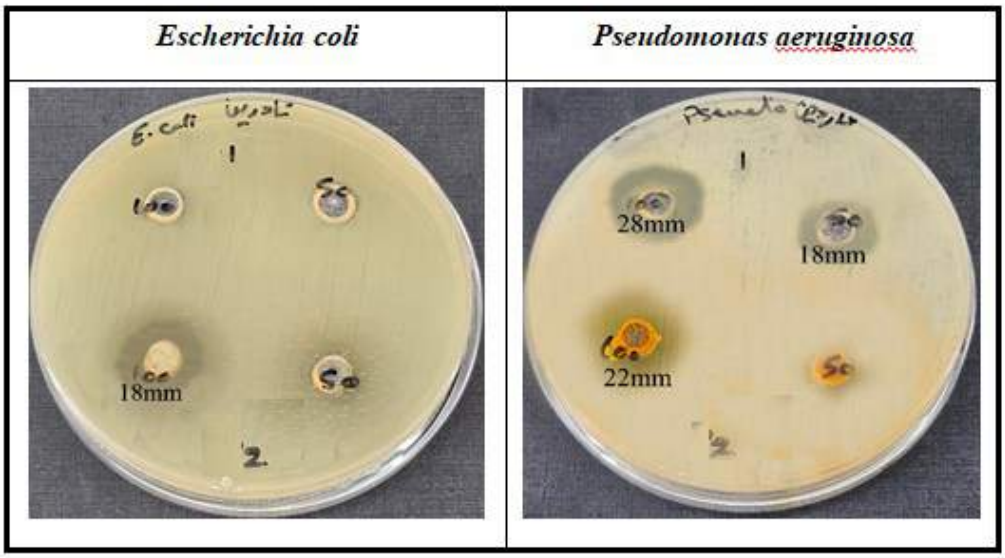


Figure (4- 399): Antibacterial activities of (copolymer(1) and copolymer(2)) on both *Escherichia coli* and *Pseudomonas aeruginosa*

The remaining polymers showed inhibition of 15mm for both copolymer(3) and copolymer(4) on *E. coli* and *P. aeruginosa* at 100% concentration. Where at 50% no inhibition zone. In compare to copolymer(4) for 100% polymers possessed the ability of inhibit bacterial growth with diameter of inhibition zone 45mm and 43mm for *E. coli* and *P. aeruginosa*, respectively where at concentration of (50%), 32mm and 28mm, respectively. As shown in (Table 4-55) ,(fig.4-400).

Table (4- 55): Antibacterial activities of (copolymer(3) and copolymer(4)) on both *Escherichia coli* and *Pseudomonas aeruginosa*

Microbial types	Zone of inhibition (mm)			
	copolymer(3)		copolymer(4)	
	100	50	100	50
Escherichia coli	**15**	**---**	**45**	**32**
Pseudomonas aeruginosa	**15**	**---**	**43**	**28**

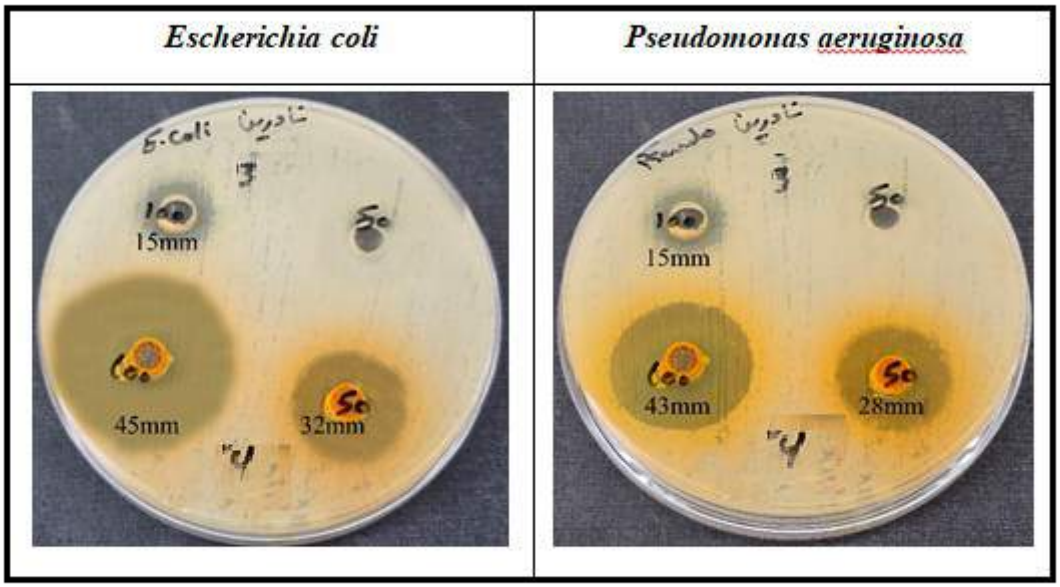


Figure (4- 400): Antibacterial activities of (copolymer(3) and copolymer(4)) on both *Escherichia coli* ad *Pseudomonas aeruginosa*

However, copolymer(5) and copolymer(6) copolymers showed inhibition of 32mm, 23mm on *E. coli* for 100% concentration respectively. In addition, for 50% of polymers tested, the formation of inhibition zone varies depending on copolymer. Also, for *P. aeruginosa* bacteria all 100% polymers possessed the ability of inhibit

bacterial growth with diameter of inhibition zone 16mm and 11mm for copolymer(3) and copolymer(4), respectively. And at concentration of (50%), only *E. coli* for copolymer(6) copolymers showed inhibition zone 19mm as shown in (Table 4-56) ,(fig.4-401).

Table (4- 56): Antibacterial activities of (copolymer(5) and copolymer(6)) on both *Escherichia coli* and *Pseudomonas aeruginosa*

Microbial types	Zone of inhibition (mm)			
	copolymer(5)		copolymer(6)	
	100	50	100	50
Escherichia coli	**32**	**22**	**28**	**19**
Pseudomonas aeruginosa	**16**	**11**	**20**	**---**

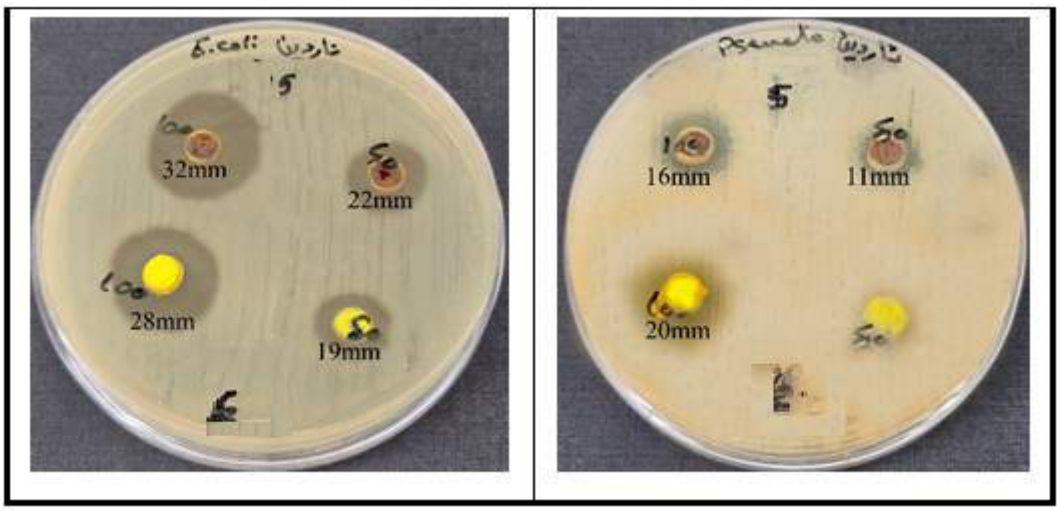


Figure (4- 401): Antibacterial activities of (copolymer(5) and copolymer(6)) on both *Escherichia coli* and *Pseudomonas aeruginosa*

The remaining copolymers showed inhibition of 20mm and 29mm on *E. coli* for 100% concentration respectively. And for 50% concentration 11mm and 13mm, respectively. In cocompare to *P. aeruginosa* only 100% concentration copolymers possessed the ability of inhibit bacterial growth with diameter of inhibition zone 19mm and 15mm, respectively) as shown in (Table 4-57) (fig.4-402).

Table (4- 57): Antibacterial activities of (copolymer(7) and copolymer(8)) on both *Escherichia coli* and *Pseudomonas aeruginosa*

Microbial types	Zone of inhibition (mm)			
	copolymer(7)		copolymer(8)	
	100	50	100	50
Escherichia coli	**20**	**11**	**29**	**13**
Pseudomonas aeruginosa	**19**	**---**	**15**	**---**

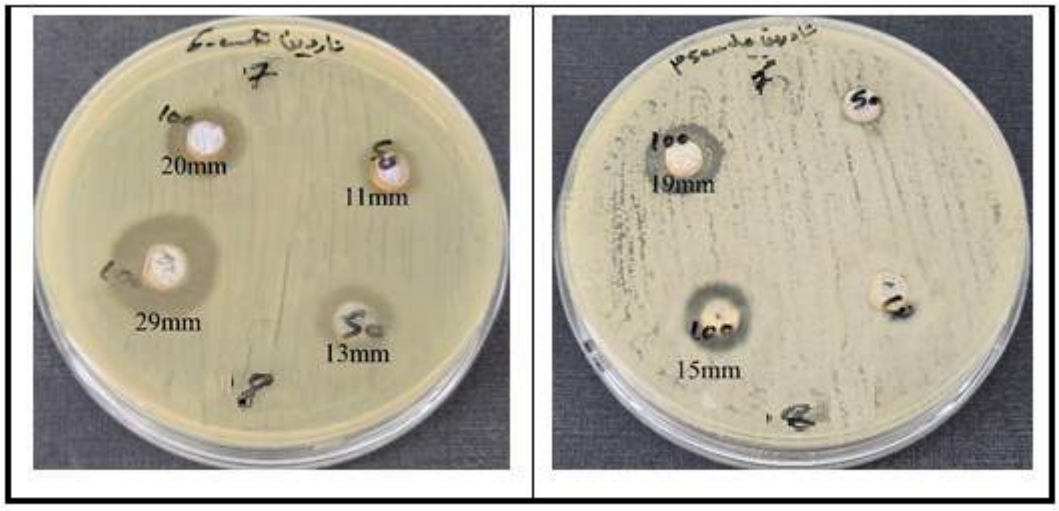


Figure (4- 402): Antibacterial activities of (copolymer(7) and copolymer(8)) on both *Escherichia coli* and *Pseudomonas aeruginosa*

The remaining copolymers showed inhibition of 45mm and 22mm on *E. coli* for 100% concentration respectively. But for 50% just copolymer(9) tested, formation inhibition zone. Also, for *P. aeruginosa* bacteria all 100% polymers possessed the ability of inhibit bacterial growth with diameter of inhibition zone 22mm and 25mm copolymer(9) and copolymer(10), respectively) but at concentration of (50%), only copolymer(10) showed inhibition zone of 11mm type as shown in (Table 4-58) (fig.4-403).

Table (4- 58): Antibacterial activities of (copolymer(9) and copolymer(10)) on both *Escherichia coli* and *Pseudomonas aeruginosa*

Microbial types	Zone of inhibition (mm)			
	copolymer(9)		copolymer(10)	
	100	50	100	50
Escherichia coli	**45**	**29**	**32**	**---**
Pseudomonas aeruginosa	**22**	**---**	**25**	**11**

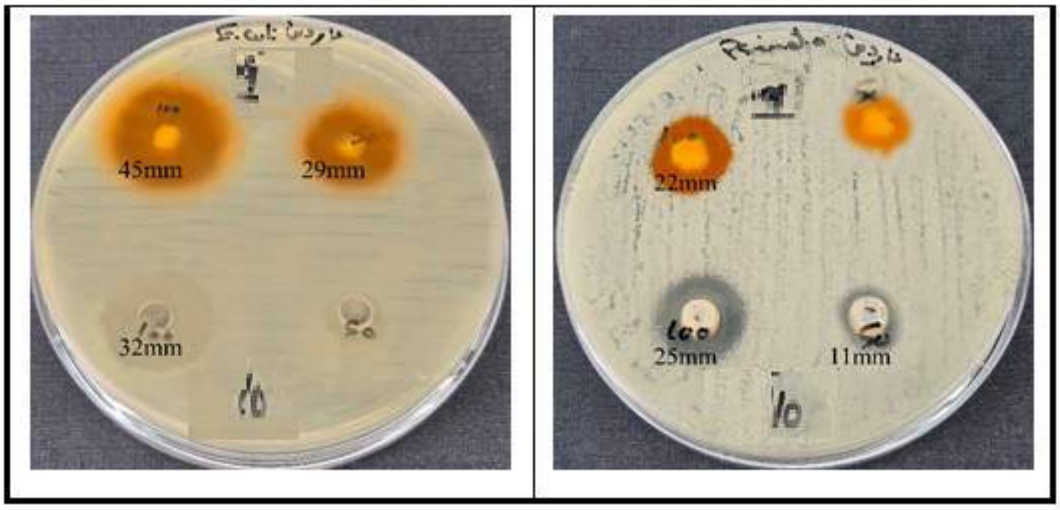


Figure (4- 403): Antibacterial activities of (copolymer(9) and copolymer(10)) on both *Escherichia coli* and *Pseudomonas aeruginosa*

For Gram positive bacteria (*Staphylococcus aureus* and *Enterococcus faecalis*) all polymers exhibited the ability to inhibit bacterial growth through varying diameters of inhibition zone.

The effects of copolymer(1), copolymer(2) on *S. aureus* at 100% concentration indicated that the zone of inhibition was 12mm and 22mm, respectively. An inhibition zone noticed at a concentration of 50% only on copolymer(2) as 11mm. Antibacterial results of copolymer(1) and copolymer(2) on *E. faecalis* also estimated and the results showed that all polymer had the ability at both concentrations to inhibit growth of bacteria with a diameter of 35mm and 27mm for copolymer(1), as well as 18mm and 12mm for copolymer(2), as shown in (Table 4-59) (fig.4-404).

Table (4- 59): Antibacterial activities of (copolymer(1) and copolymer(2)) on both *Staphylococcus aureus* and *Enterococcus faecalis*

Microbial types	Zone of inhibition (mm)			
	copolymer(1)		copolymer(2)	
	100	50	100	50
Staphylococcus aureus	12	---	22	11
Enterococcus faecalis	35	27	18	12

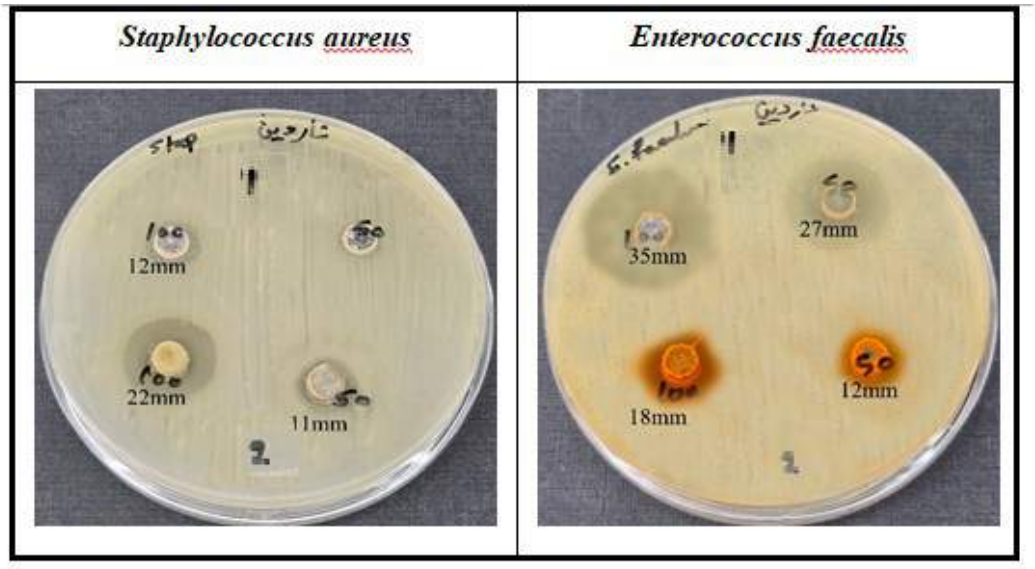


Figure (4- 404): Antibacterial activities of (copolymer(1) and copolymer(2)) on both *Staphylococcus aureus* and *Enterococcus faecalis*

The effects of copolymer(3) had no inhibition zone in both 100% and 50% in compare to copolymer(4) 29mm at 100% concentration, and 18 for 50% at on *S. aureus*. *E. faecalis* also estimated and the results showed that copolymer(3) and copolymer(4) had the ability at both concentrations to inhibit growth 38mm and 49mm, with 25mm and 31mm at 100% and 50% as shown in (Table 4-60) (fig.4-405).

Table (4- 60): Antibacterial activities of (copolymer(3) and copolymer(4)) on both *Staphylococcus aureus* and *Enterococcus faecalis*

Microbial types	Zone of inhibition (mm)			
	copolymer(3)		copolymer(4)	
	100	50	100	50
Staphylococcus aureus	---	---	29	18

Enterococcus faecalis	**38**	**25**	**49**	**31**

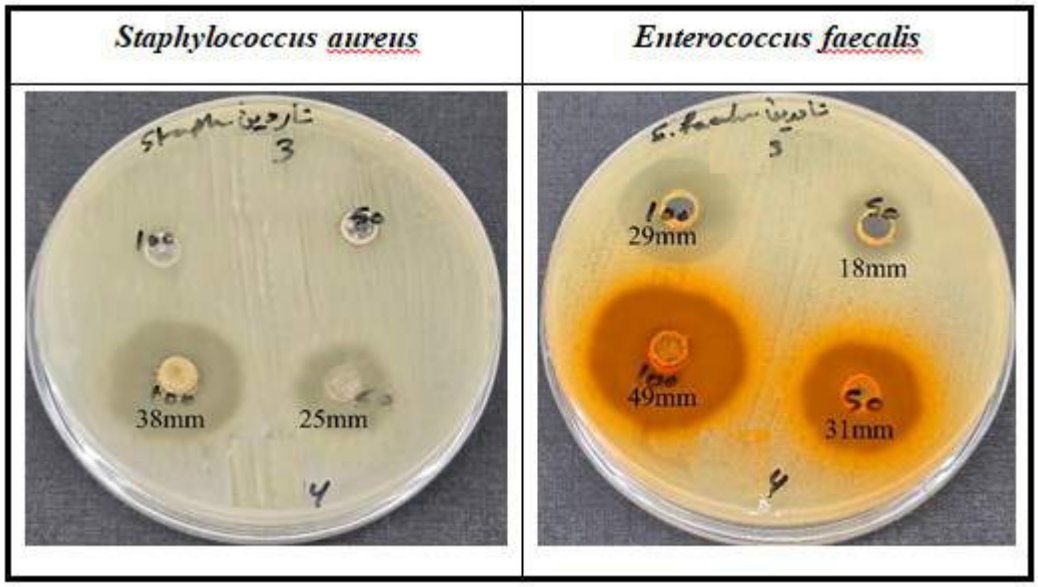


Figure (4- 405): Antibacterial activities of (copolymer(3) and copolyme4)) on both *Staphylococcus aureus* and *Enterococcus faecalis*

The effects of copolymer(5) and copolymer(6) on *S. aureus* at 100% concentration indicated that the zone of inhibition was 23mm and 32mm, respectively. Antibacterial results of copolymer(5) and copolymer(6) for *E. faecalis* also estimated and the results showed that all polymer had the ability at both concentrations to inhibit growth of bacteria with a diameter of (24mm, 15mm), (32mm, 11mm) inhibition zone at 50% as shown in (Table 4-61) (fig.4-406).

Table (4- 61): Antibacterial activities of (copolymer(5) and copolymer(6)) on both *Staphylococcus aureus* and *Enterococcus faecalis*

Microbial types	**Zone of inhibition (mm)**			
	copolymer(5)		**copolymer(6)**	
	100	**50**	**100**	**50**
Staphylococcus aureus	**23**	**16**	**32**	**26**
Enterococcus faecalis	**24**	**15**	**32**	**11**

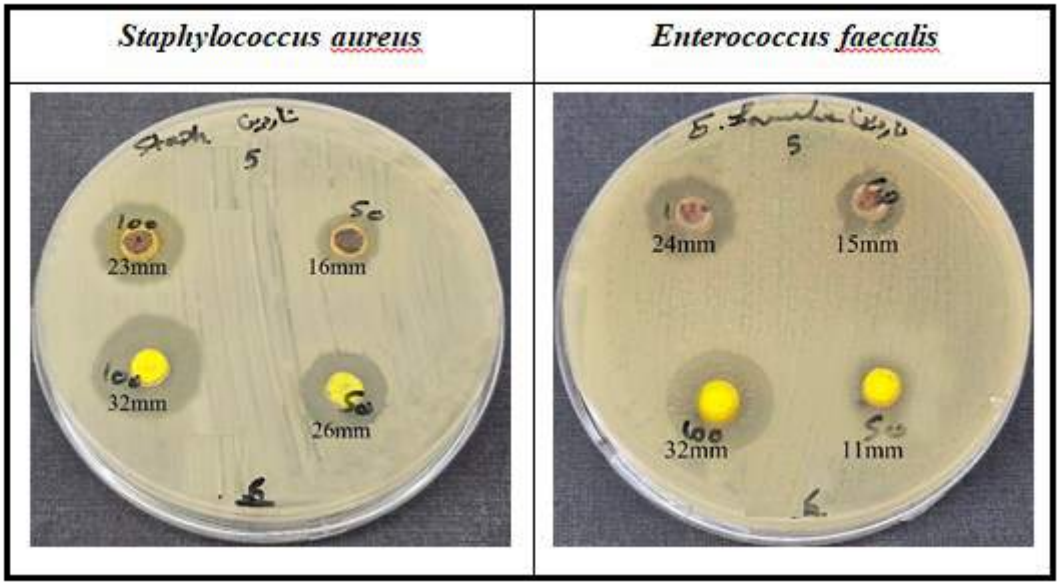


Figure (4- 406): Antibacterial activities of (copolymer(5) and copolymer(6)) on both Staphylococcus aureus and Enterococcus faecalis

The effects of copolymer(7) and copolymer(8) on *S. aureus* at 100% concentration indicated that the zone of inhibition was 15mm and 29mm. Where concentration of 50% only for copolymer(8) 11mm. *E. faecalis* also estimated and the results showed that all polymer had the ability at both concentrations to inhibit growth of bacteria with a diameter of (23mm and 13mm), (22mm), 100% and 50%, respectively as shown in (Table 4-62) (fig.4-407).

Table (4- 62): Antibacterial activities of (copolymer(7) and copolymer(7)) on both *Staphylococcus aureus* and *Enterococcus faecalis*

Microbial types	Zone of inhibition (mm)			
	copolymer(7)		copolymer(8)	
	100	50	100	50
Staphylococcus aureus	**15**	**---**	**29**	**11**
Enterococcus faecalis	**23**	**13**	**22**	**---**

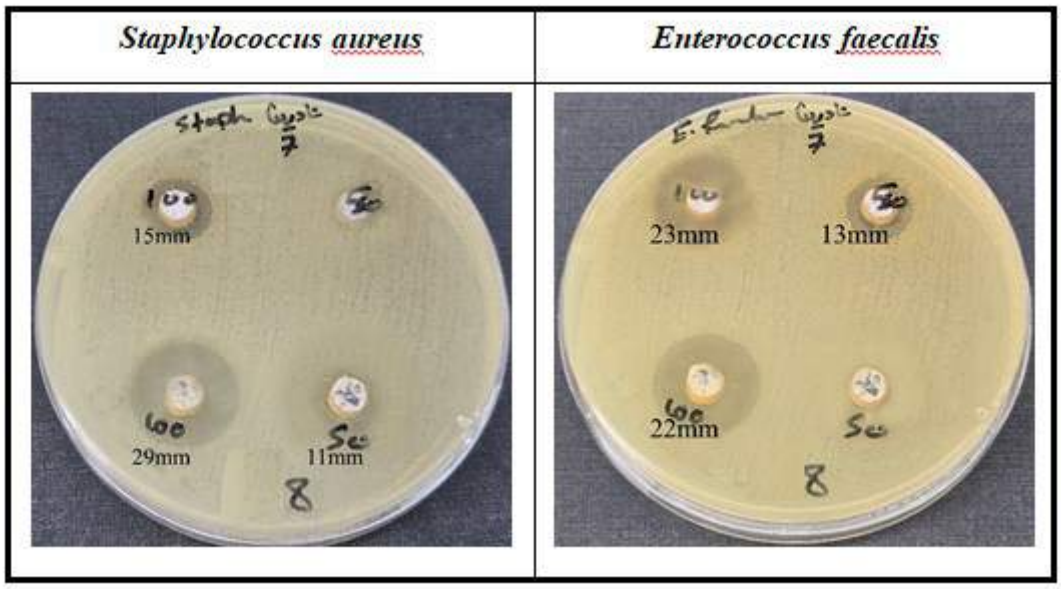


Figure (4- 407): Antibacterial activities of (copolymer(7) and copolymer(8)) on both *Staphylococcus aureus* and *Enterococcus faecalis*

The effects of copolymer(9) and copolymer(10) on *S. aureus* at 100% concentration indicated that the zone of inhibition was 32mm and 28mm, respectively. Where only copolymer(10) noticed at a concentration of 50% 11mm. Antibacterial results of (copolymer(9) and copolymer(10)) on *E. faecalis* also estimated and the results showed that both concentrations to inhibit growth of bacteria with a diameter of copolymer(9) 38mm and 21mm for 100% and 50% where copolymer(10) only at 100% concentration 22mm as shown in (Table 4-63) (fig.4-408).

Table (4- 63): Antibacterial activities of (copolymer(9) and copolymer(10)) on both *Staphylococcus aureus* and *Enterococcus faecalis*

Microbial types	Zone of inhibition (mm)			
	copolymer(9)		copolymer(10)	
	100	50	100	50
Staphylococcus aureus	32	---	28	11
Enterococcus faecalis	38	21	22	---

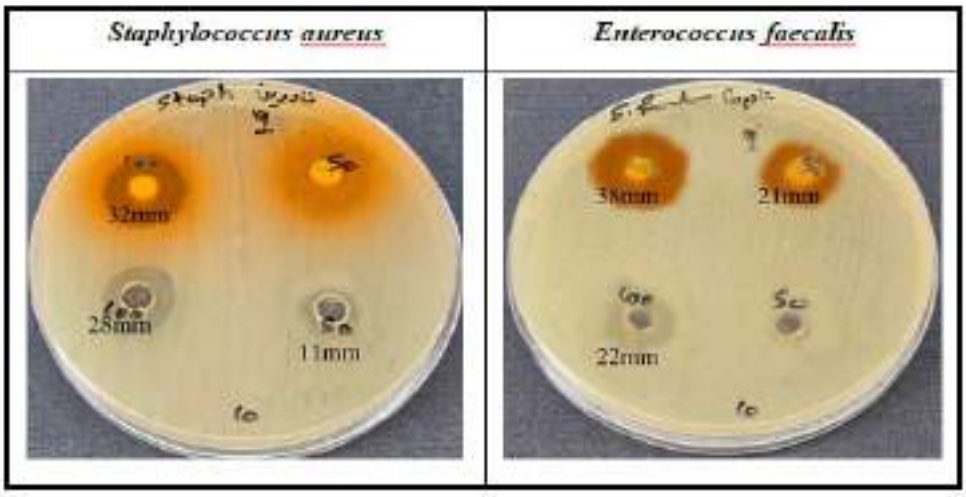


Figure (4- 408): Antibacterial activities of (copolymer(8) and copolymer(10)) on both Staphylococcus aureus and Enterococcus faecalis

4.63 Antifungal Activity

Antifungal potential also evaluated by assessing the effect of synthesized polymers on *C. albicans* and the results revealed that copolymer(1) have no inhibition growth, where copolymer(2) had 42mm and 29mm, respectively and had 32mm and 42 against *Aspergillus niger* as shown in (Table 4-64) (fig.4-409).

Table (4- 64): Antifungal activities of (copolymer(1) and copolymer(2)) on *Candida albicans* and *Aspergillus niger*

Fungal types	Zone of inhibition (mm)			
	copolymer(1)		copolymer(2)	
	100	50	100	50
Candida albicans	---	---	42	29
Aspergillus niger	-----	---	32	42

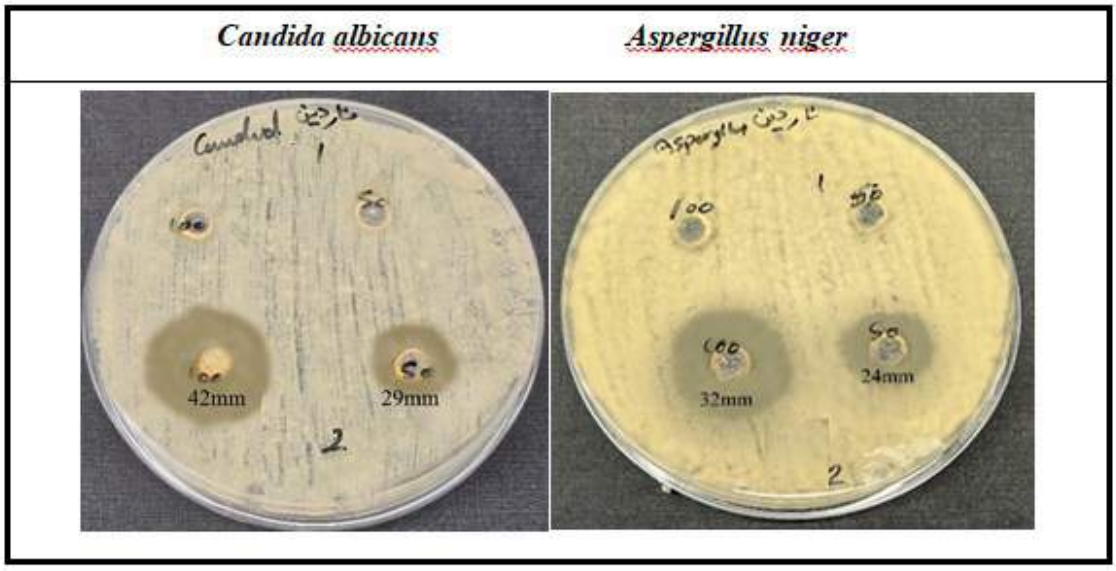


Figure (4- 409): Antifungal activities of (copolymer(1) and copolymer(2)) on *Candida albicans* and *AspergDillus niger*

Both copolymer(3) and copolymer(4) have no inhibition growth at 100% and 50% concentration and 39mm , 22mm against *Aspergillus niger*. As shown in (Table 5-65) (fig.4-410).

Table (4- 65): Antifungal activities of (copolymer(3) and copolymer(4)) on *Candida albicans* and *Aspergillus niger*

fungal types	Zone of inhibition (mm)			
	copolymer(3)		copolymer(4)	
	100	50	100	50
Candida albicans	---	---	---	---
Aspergillus niger	---	---	39	22

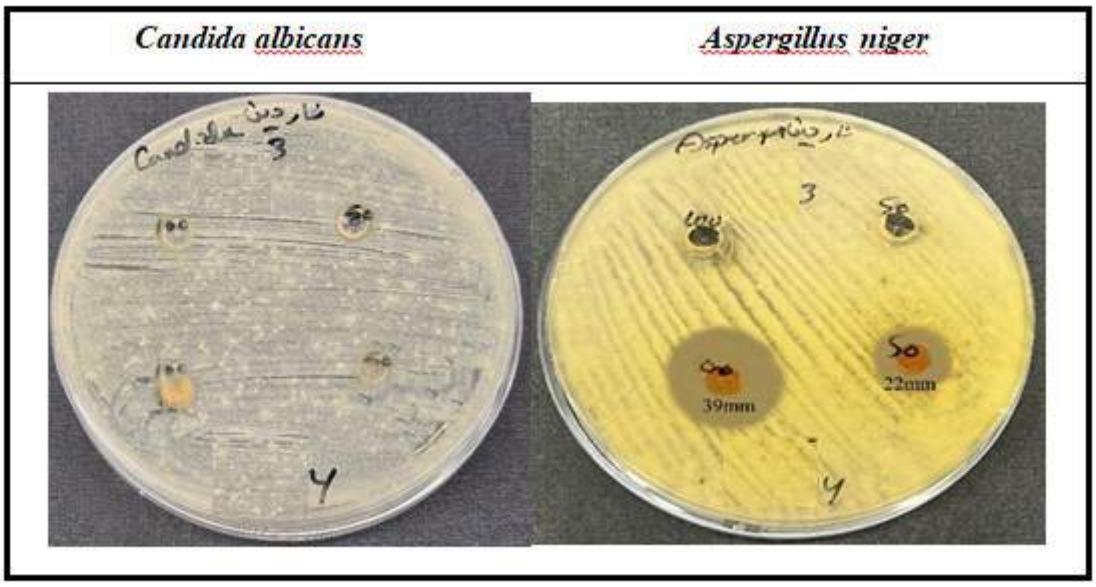


Figure (4- 410): Anti Antifungal activities of (copolymer(3) and copolymer(4)) on *Candida albicans* and *Aspergillus niger*

Copolymer(5) and copolymer(6) had possessed the most potent antifungal activity by zone of inhibition (42mm, 25mm), (33mm, 20mm) at 100% and 50%, respectively and 25mm at 100% , (28mm, 19mm) at 50% against *Aspergillus niger* as seen in (Table 4-66) (fig.4-411).

Table (4- 66): Anti Antifungal activities of (copolymer(5) and copolymer(6)) on *Candida albicans*

fungal types	Zone of inhibition (mm)			
	copolymer(5)		copolymer(6)	
	100	50	100	50
Candida albicans	**23**	**16**	**32**	**26**
Aspergillus niger	**24**	**15**	**32**	**11**

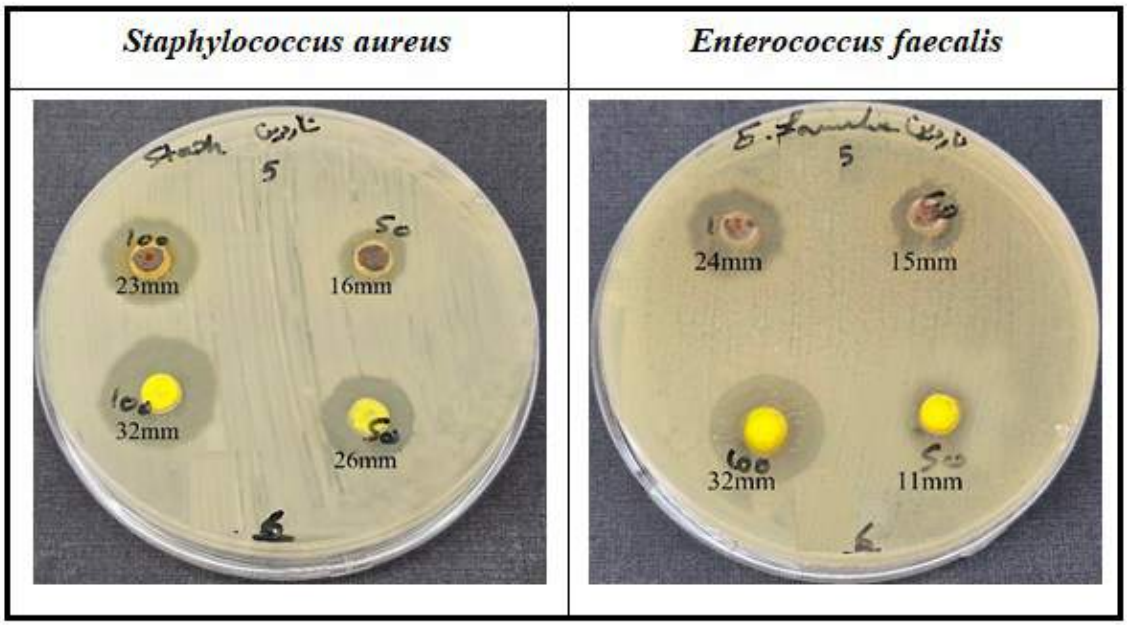


Figure (4- 411): Antibacterial activities of (copolymer(5) and copolymer(6)) on both Staphylococcus aureus and Enterococcus faecalis

Copolymer(7) and copolymer(8) at 100% concentration 12mm and 28mm where at 50% concentration only (8) 19mm against *candida albicans* and at 100% concentration 24mm and 17mm where at 50% concentration (8) 29mm and 20mm against Aspergillus niger as seen in (Table 4-67) (fig.4-412).

Table (4- 67): Anti Antifungal activities of (copolymer(7) and copolymer(8)) on *Candida albicans* and *Aspergillus niger*

fungal types	Zone of inhibition (mm)			
	copolymer(7)		copolymer(8)	
	100	50	100	50
Candida albicans	12	---	28	19
Aspergillus niger	24	17	29	20

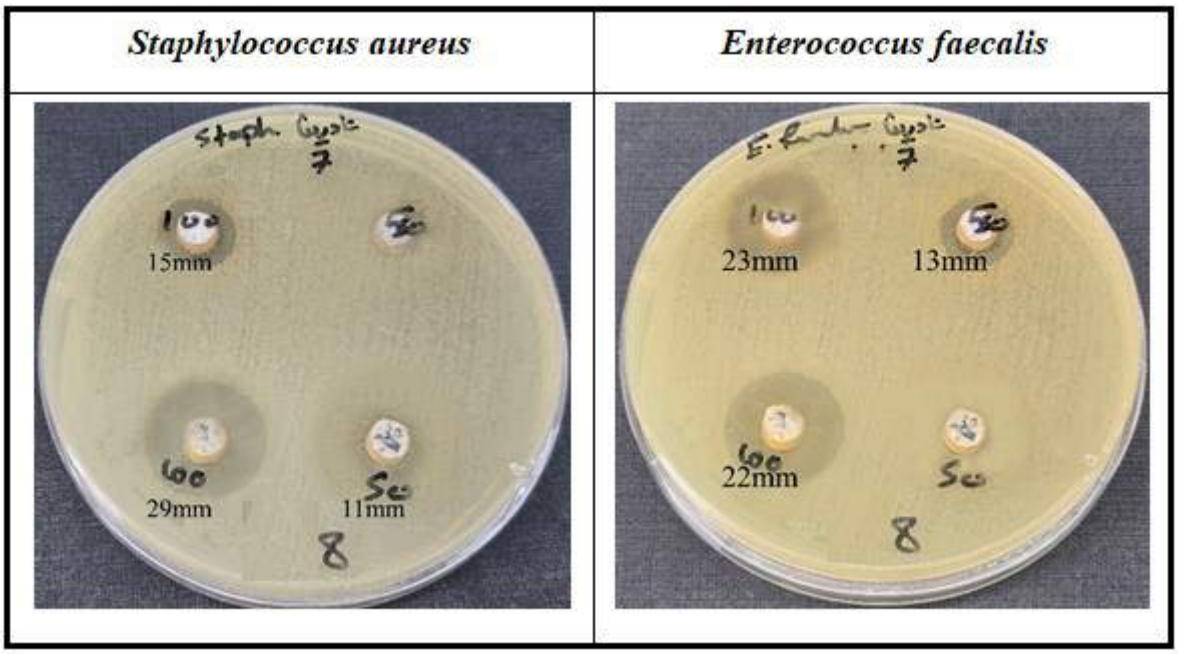


Figure (4- 412): Anti Antifungal activities of (copolymer(7) and copolymer(8)) on *Candida albicans* and *Aspergillus niger*

Where copolymer(9) and copolymer(10) showed at 100% concentration 11mm 12mm on *candida albicans* but at 100% 21mm and 50% 45mm and 29mm on *Aspergillus niger* as seen in (Table 4-68) (fig.4-413).

Table (4- 68): Anti Antifungal activities of (copolymer(9) and copolymer(10)) on *Candida albicans* and *Aspergillus niger*

fungal types	Zone of inhibition (mm)			
	copolymer(9)		copolymer(10)	
	100	50	100	50
Candida albicans	**11**	**---**	**12**	**---**
Aspergillus niger	**21**	**---**	**45**	**29**

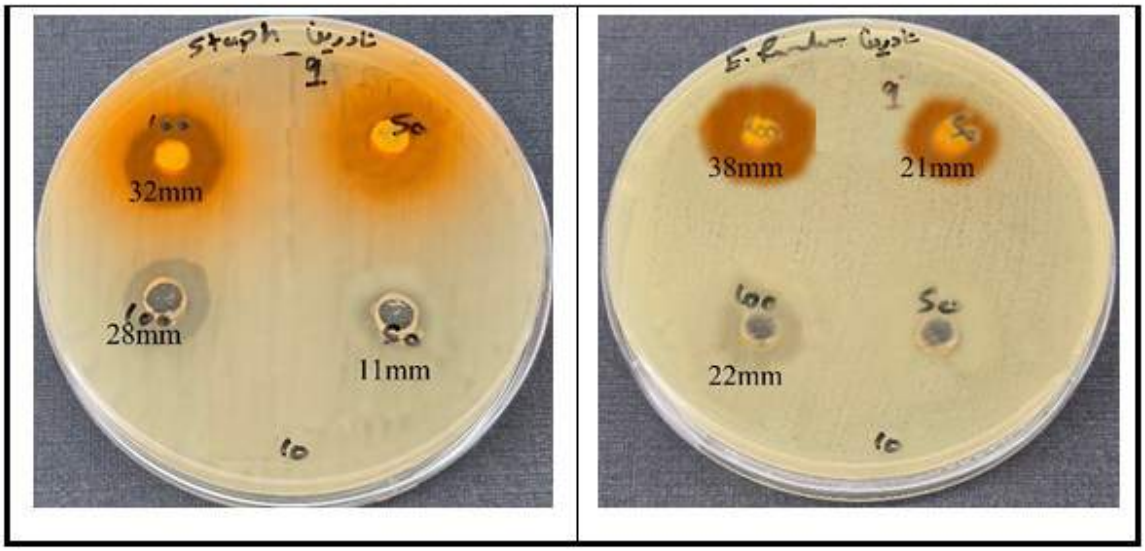


Figure (4- 413): Antifungal activities of (copolymer(9) and copolymer(10)) on *Candida albicans* and *Aspergillus niger*

The antimicrobial activity observed in the present study and the effects of the synthesized compounds do not operate through a single universal mechanism. But also, the effects are likely influenced by the chemical scaffold and the structural differences among Gram-positive bacteria, Gram-negative bacteria, and *Candida albicans*. Because of these compounds rich in sulfur- and nitrogen-containing pharmacophores, especially thiosemicarbazone-, hydrazone-, and heterocycle-based systems, antimicrobial activity is usually due to a combination of membrane disruption, enzyme inhibition, metal chelation, induction of oxidative stress, and possible binding to macromolecules, rather than to a single specific target.(164, 179, 180). The difference between Gram-positive and Gram-negative bacteria is especially important for interpreting the present results. Gram-positive bacteria have a thick peptidoglycan layer but lack an outer membrane, which also facilitates access of synthetic compounds to the cytoplasmic membrane and intracellular targets. In contrast, Gram-negative bacteria possess an outer membrane rich in lipopolysaccharide that markedly restricts compound penetration; therefore, strong activity against Escherichia coli or Pseudomonas aeruginosa usually suggests that the compound either penetrated the outer membrane efficiently, destabilized membrane integrity, or accumulated to a sufficient intracellular level to inhibit

essential targets(181, 182).

The mechanism of these chemical compounds against Candida albicans is discussed separately because fungal cells differ fundamentally from bacterial cells. Candida has a wall with beta-glucan, chitin, and mannan, while the fungal membrane depends on ergosterol. So, compounds with notable anticandidal activity are more plausibly linked to membrane stress, interference with ergosterol-associated processes, or disruption of fungal wall-associated functions rather than to the same mechanism responsible for antibacterial activity(183, 184).

Copolymer(1) seems to have a polymer-linked scaffold with carboxyl and amide groups, along with a thiosemicarbazone-like segment and an aromatic amino-substituted region. Thiosemicarbazone-based systems are often described as multitarget antimicrobial scaffolds because sulfur and nitrogen donor atoms can facilitate hydrogen bonding, metal coordination, and interactions with proteins and membrane-related targets. (185). Since copolymer(1) primarily exhibited activity against Staphylococcus aureus, Pseudomonas aeruginosa, and Enterococcus faecalis, but not against Escherichia coli or Candida albicans, its effect is probably due to interaction with bacterial surfaces and inhibition of essential bacterial enzymes rather than broad DNA-targeting mechanisms toxicity. Its effectiveness against P. aeruginosa is especially significant, as inhibiting this organism typically necessitates either penetrating the outer membrane or partially disrupting membrane integrity. (181). copolymer(2) exhibited moderate antibacterial activity but showed strong activity against Candida albicans. Since its structure appears to include a nitrogen-rich heteroaromatic system and sulfur-containing groups, its mode of action likely relies on enhanced target recognition through hydrogen bonding and heteroatom-mediated interactions.(164). The activity against Candida suggests that copolymer(2) primarily acts by disrupting fungal membranes, leading to ergosterol disruption or wall stress, rather than directly damaging DNA. If DNA were the main target, we would expect broader, less selective inhibition across various systems in organisms. (184)

Copolymer(3) shows a narrower spectrum and appears more structurally bulky and conjugated than copolymer(1) and copolymer(2).It has had a partial intracellular effect, possibly targeting bacterial enzymes or other macromolecular structures, but it has limited penetration and a narrow biological range. (179) . Copolymer(4) emerged as the strongest antibacterial compound, showing powerful activity against both Gram-positive and Gram-negative bacteria, including Pseudomonas aeruginosa. It remained inactive against Candida albicans. The compound's abundance of nitrogen-containing heterocycles and sulfur groups likely enhances its effectiveness by facilitating penetration into bacterial cells and inhibiting essential bacterial enzymes. Thiosemicarbazone-related and heteroatom-rich scaffolds are often studied for their ability to interfere with microbial metal balance, redox processes, and enzyme functions. (185). The absence of antifungal activity suggests that its effect is not merely nonspecific membrane dissolution but rather a more specific action against bacteria. copolymer(5) demonstrated a notably robust biological profile, successfully inhibiting both bacteria and Candida albicans. The structure appears to combine aromatic segments, an ether-type linkage, and heterocyclic or amide-containing moieties, suggesting a balanced polarity-lipophilicity relationship. Therefore, the most plausible mechanism for copolymer(5) is a primary membrane-oriented effect on both bacterial and fungal envelopes, followed by secondary intracellular consequences such as enzyme dysfunction induced by membrane stress (184).

Copolymer(6) appears to induce effects that may include membrane destabilization, oxidative stress, and disruption of conserved metabolic enzymes. Additionally, it involves carbonyl-containing polymer-linked groups. These actions are commonly reported to operate through multiple pathways, such as membrane perturbation, enzyme inhibition, metal chelation, oxidative stress induction, and potential interference with intracellular macromolecules. (185). Additionally, the nitro group might induce intracellular redox stress after uptake. copolymer(6) shows activity against Gram-positive and Gram-negative bacteria and Candida albicans,

acting through a combined mechanism involving membrane interaction followed by inhibition of intracellular targets. Therefore, copolymer(6) strong performance supports previous research that highlights thiosemicarbazones as promising broad-spectrum antimicrobial scaffolds. (186)

Copolymer(7) demonstrated weaker antimicrobial activity compared to copolymer(5) and copolymer(6), with its effectiveness diminishing at lower concentrations. Structurally, copolymer(7) contains a thiohydantoin, an azomethine linkage, and a phenolic aromatic ring. Unlike copolymer(6), it lacks a nitro group and appears less electronically activated, which may explain its reduced potency. The likely mechanism involves inhibiting intracellular microbial enzymes following limited uptake, rather than causing severe membrane disruption. This aligns with previous studies indicating that while thiohydantoin derivatives can exhibit antimicrobial activity, their effectiveness largely depends on their substitution patterns and physicochemical properties. (161).

Copolymer(8) features an aromatic system, a thioamide group, and an amino-substituted aromatic ring. These aromatic imide structures are often linked to intracellular target binding. In this study, copolymer(8) exhibited moderate activity against several organisms but was less effective against Pseudomonas aeruginosa, suggesting that although the compound likely targets intracellular components, its bulky structure may hinder penetration through the outer membrane of resistant Gram-negative bacteria. Consequently, copolymer(8) likely interacts primarily with intracellular targets, such as essential enzymes or other macromolecular systems, with membrane interactions playing a minor role. This aligns with previous research on naphthylamide-type compounds, which have demonstrated antibacterial effects targeting intracellular components such as DNA gyrase. (174).

Copolymer(9) is a potent antibacterial compound, but it shows weak activity against Candida albicans. Its structure includes a nitrogen-containing heterocycle, multiple thioamide-like groups, and several nitrogen-donor sites. This type of strong intracellular bacterial target binding is the primary mechanism. Sulfur- and nitrogen-

rich compounds are often linked to inhibiting bacterial enzymes and disrupting metal-dependent cellular pathways because copolymer(9) was very effective against bacteria but only weakly active against Candida, it suggests a generalized membrane disruption.(186)

Copolymer(10) contains a nitrogen-rich fused heterocycle, a pyridine-like ring, and carbonyl groups. This composition suggests that copolymer(10) is more likely a target-directed antimicrobial compound rather than a direct membrane-lytic agent. Its greater activity against bacteria than against Candida albicans suggests it may preferentially interact with bacterial intracellular enzymes or proteins involved in metabolic processes. The decrease in activity at lower concentrations also implies that copolymer(10) requires sufficient intracellular accumulation or high target occupancy to effectively inhibit microbial growth. Therefore, copolymer(10) most likely acts by binding to intracellular bacterial targets rather than causing strong membrane damage, which aligns with (174) (187).

Chapter Five
Conclusions and Recommendations and Future Work

5. Conclusions and Recommendations and Future Work

5.1 Conclusions

The Following Conclusions Can Be Drawn from This Current Thesis:

1. Many biologically active heterocyclic compounds have been obtained based on this reagent. This suggests that thiosemicarbazides can be particularly useful in the synthesis of functionalized heterocyclic compounds used in the design of novel highly effective pharmaceuticals with a broad spectrum. Series of synthesized heterocyclic compounds were synthetized such as ureidoacetamide, thiosemicarbazone, 5-Styryli-2-amino-1, 3, 4-thiadiazole, Tetrazole derivatives. thiazolidin-4-one, 1, 3-oxazepine-4, 7-dione, imide, 2, 3-dihydroquinosulin-4-one, acetamideand, 2- iminothiazolidine – 4- one and Mannich compound derivatives with good yields.
2. The cycloaddition reaction between cyclic anhydrides and imine derivatives containing strong electron with drawing group, such as bromo in ***p***- position to imine group never take place, the reason may be attributed to decrease the characteristic of π- bond in (C=N) group due to the further conjugation with nitro group and decreasing the electronic density of benzene ring in case of chlorine atom which leads to increase strength of the conjugation.
3. tetrazole derivatives were prepared from the reaction of Schiff bases derivatives that obtained from terphthaldehyde and Isatin with of sodium azide.
4. 2- iminothiazolidine – 4- one was prepared from the reaction of thiourea with of mono chloroacetic acid
5. Mannich compound derivatives were prepared from the reaction of formalin with 1, 4-phenylenediamine and Triethylenetetramine compounds.
6. New copolymers (methyl acrylic acid- Itaconic anhydride) and (N, N-dimethyl acrylamide-Citraconic anhydride) were prepared by radical photopolymerization of vinyl monomers (methyl acrylic acid, Itaconicanhydride, N, N-dimethylacrylamide and Citraconic anhydride) using

1-hydroxy cyclohexyl phenol ketone as the initiator

7. The new synthesized compounds have been immobilized through amidic bonds, through the opening of the anhydride cycle of the (methyl acrylic acid-Itaconic anhydride) and (N, N-dimethyl acrylamide-Citraconic anhydride) copolymers.
8. The physical properties, including melting points and molecular weights, were systematically cataloged, providing valuable data for future research and applications.
9. In this study a series of new heterocyclic compounds and copolymers were synthesized. The presence of functional groups was identified with the help of elemental and spectral analysis (FTIR, ^{1}HNMR and ^{13}CNMR) and Elemental Analysis (CHNS).
10. In this work, we have seen that there are many aspects of a copolymer material that may have a more or less significant role in the thermal stability and fire behavior of a polymeric material. However, it is clear that the two properties are somewhat correlated. Highly ordered structures in the copolymer structure of a material often leads to a high thermal stability and a high fire performance. Moreover, a high degree of aromaticity may cause and enhancement in the fire and thermal properties of a material. In terms of structural properties, it was observed that highly aromatic, heterocyclic copolymers with high inter-chain interactions have highly desirable thermal and fire performances.
11. Exothermic peak of copolymers appeared in the DSC measurement is due to the chain polymerization of the vinyl group and the ring-opening.
12. Molecular docking is a key tool in structural molecular biology and computer-assisted drug design. The goal of ligand-protein docking is to predict the predominant binding mode(s) of a ligand with a protein of known three-dimensional structure. Successful docking methods search high-dimensional spaces effectively and use a scoring function that correctly ranks candidate

dockings. Docking can be used to perform virtual screening on large libraries of compounds, rank the results, and propose structural hypotheses of how the ligands inhibit the target, which is invaluable in lead optimization. The setting up of the input structures for the docking is just as important as the docking itself. The thesis discusses the background and theory of molecular docking software, and covers the usage of some of the most-cited docking software.

13. The antimicrobial activity of the modified copolymers was tested against four bacterial and three fungi strains Staphylococcus aureus, Escherichia coli, pseudomonas aeroginosa, Klebsiella, Aspergillus Niger, Aspergillus Flavus and Fusarium oxysporium, respectively. It was found that the diameter of inhibition zone varied according to the type of active group in the copolymers and also the examined microorganism. In general, the copolymers were further modified and showed antimicrobial activity against the tested microorganisms. However, the compound of the modified copolymers was found to be the most effective on bacteria and fungi species.
14. The copolymers were prepared was evaluated for their cytotoxicity activity against the cancer cell lines used were the colon cancer cell line caco2 and skin cancer cell line revealed increased inhibition compare to the normal cell line. This interpretation is supported by the consistent decrease in IC_{50} values from 24 to 72 hours across all copolymers.
15. Finally, it is anticipated that the prepared antimicrobial copolymers would be of great help in the field of biomedical applications and biological water treatment should advance our understanding of derivatives' biological activities investigate these compounds' prospective applications as antibiotics and identify the structure-activity correlations associated with such applications.

5.2 Recommendations and future work

Some test results have been encouraging and further testing should be undertaken to confirm the ability of the synthesized copolymer to efficiently improve the medical application

1. The relatively new study of homopolymer self-assembly in solution means that ample opportunity exists to investigate new systems. By adapting many of the organic reactions known to occur in phenol, polymers containing functional groups not previously attainable by free radical polymerization can be synthesized.
2. Treatment of the synthesized bis-1, 3- oxazepine derivatives with various primary amines or hydrazines to obtain new bis-1, 3-diazepine derivatives.
3. Synthesis of a new series of Schiff bases containing 1, 2, 4- triazole-3-thiole derivatives from the reaction with other different aldehydes and ketones.
4. apply this route to synthesize different heterocyclic compounds on large scale and evaluation their biological activity against different kind of cancer cells, bacteria or fungus.
5. Pharmaceutical study of the synthesized copolymers in vivo.
6. Study of using of the synthesized heterocyclic compounds as accelerators in vulcanization of rubber.
7. Synthesis of a series of new copolymers for synthesized compounds with different transition metal ions and evaluate their biological activities.

References

References

1. Sikkema DJ. Rigid-chain polymers: Aromatic polyamides, heterocyclic rigid rod polymers, and polyesters. Advanced Industrial and Engineering Polymer Research. 2022;5(2):80-9.
2. Liu Y, Lam JW, Tang BZ. Conjugated polymers developed from alkynes. National Science Review. 2015;2(4):493-509.
3. Schmitt D, Abdel-Hafez SM, Tummeley M, Schunemann V, Schneider M, Presser V, et al. Surface-initiated living anionic polymerization of functional methacrylates from the surface of organic particles. Macromolecules·101-7086:(17)56;2023 .
4. Han T, Xie J, Chen F, Sze PW, Su X, Wang D, et al. Synthesis of hybridized nontraditional intrinsic luminescent polymers with ring-openable fused heterocycles by facile multicomponent polymerizations. Macromolecules. 2023;56(24):1.27-0016
5. Allen NS. Historical Perspectives and Reflections on the Degradation and Stabilization of Polymer Materials. Journal of Vinyl and Additive Technology. 2026.
6. Singh D, Dilip Saoji S. Nanoarchitectonics in Macromolecular Science: Integrating Molecular Dynamics with Smart Materials. Journal of Macromolecular Science, Part B. 2025;64(12):1611-20.
7. Aldemir A, Şeker SB. Optimization of the Solution Components Using in the Wet Wipes by the Response Surface Methodology for Reduce the Harmful Effects on the Environment. Asia-Pacific Journal of Chemical Engineering. 2025;20(5):e70060.
8. Solmaz A, İlter Z, Kaya İ. Synthesis, characterization, thermal and kinetic properties of chalcone methacrylamide polymers containing halogen group in side chain. Polymer Bulletin. 2022;79(7):5041-61.
9. von Vacano B, Mangold H, Vandermeulen GW, Battagliarin G, Hofmann M, Bean J, et al. Sustainable design of structural and functional polymers for a circular economy. Angewandte Chemie International Edition. 2023;62(1:(2e202210823.
10. Smokal V, Andriy K, Kutsevol N, Studzinsky S, Panova A. Synthesis and characterization of new quinoline containing poly (methacrylate) s with azomethine fragment. Molecular Crystals and Liquid Crystals. 2026;770(4):601-10.
11. Misin V ,Zezin A, Klimov D, Sybachin A, Yaroslavov A. Biocidal polymer formulations and coatings. Polymer Science, Series B. 2021;63(5):459-69.
12. Sonawane D, Pokharkar V. A Comparative Study of Binding Interactions of Natural Flavonoids and Conventional Drug Donepezil for Multiple Alzheimer's Disease Targets Using In silico Approach. Letters in Drug Design & Discovery. 2023;20(12):1947-58.
13. Sheir SK, Elmongy EI, Mohamad AH, Osman GY, Bendary SE, Ahmed AA, et al. Molluscicidal and Larvicidal Potency of N-Heterocylic Analogs against Biomophalaria alexandrina Snails and Schistosoma mansoni Larval Stages. Pharmaceutics. 2023;15(4):1200.
14. Singh P, Rawat S, Agrahari AK, Singh M, Chugh S, Gurcha S, et al. Nsc19723, a thiacetazone-like benzaldehyde thiosemicarbazone improves the efficacy of tb drugs in vitro and in vivo. Microbiology spectrum. 2022;10(6):e02592-22.
15. Alsafy SM, Alrazzak NA. Synthesis, characterization, and biological activity study of new heterocyclic compounds. Engineering Proceedings. 2024;59·178:(1)
16. Tang L-n, Liu G-y, Li J-h, Chen M. Palladium-catalyzed diversified synthesis of monofluorinated alkenes from allylic gem-difluorides through Pd–OH intermediate. Organic Letters. 2023;25(50):9064-9.
17. Wieczorkiewicz PA, Krygowski TM, Szatylowicz H. Substituent effects and electron delocalization in five-membered N-heterocycles. Physical Chemistry Chemical Physics. 2024;26(28):19398-410.
18. Hazra G, Masarwa A. Synthesis and Functionalization of Thiophosphonium Salts: A Divergent Approach to Access Thioether, Thioester, and Dithioester Derivatives. Organic Letters. 2023;25(34):6396.
19. Abdullah Al Awadh A. Biomedical applications of selective metal complexes of indole, benzimidazole, benzothiazole and benzoxazole: A review (From 2015 to 2022 .(Saudi Pharmaceutical Journal. 2023;31(9):1-17.

References

20. Pandey SK, Patidar L. PHARMACODYNAMIC EVALUATION OF POLYHERBS AND ITS FORMULATION FOR ANTI-TUSSIVE ACTIVITY USING CITRIC ACID INDUCED IN GUINEA PIG. Genetics and Molecular Research. 2026.
21. Alburyhi MM, Hamidaddin MA, Noman MA, Saif A, Yahya T, Al-Ghorafi MA-h. Rivaroxaban-Excipient Compatibility Studies for Advanced Drug Delivery Systems Development. European Journal of Pharmaceutical and Medical Research. 2024;11(9):370-404.
22. Hu Y, Zhang S, Xu K ,Zhuang X, Tang Y, Gong H, et al. Nano-Metal-Organic Frameworks and Nano-Covalent-Organic Frameworks: Controllable Synthesis and Applications. Chemistry–An Asian Journal. 2025;20(1):e202400896.
23. Fishman JA, editor Pneumocystis jiroveci. Seminars in respiratory and critical care medicine; 2020: Thieme Medical Publishers.
24. Awulachew MT. Acta Scientific Pharmaceutical Sciences (ISSN: 2581-5423) Volume 6 Issue 8 August 2022. Acta Scientific Pharmaceutical Sciences (ISSN: 2581-5423). 2022;6(8.(
25. Basu S, Rana S, Saha P, Ghosh P, Mukhopadhyay C. FeCl3-Catalyzed Synthesis of 6-Thioxo-hexahydroindeno [1', 2': 4, 5] imidazo [1, 5-a] pyridin-12 (6H)-ones via an Interesting [1, 2] Oxygen Shift Pathway. The Journal of Organic Chemistry. 2022;87(15):9755-63.
26. Aktekin MB, Oksuz Z, Turkmenoglu B, Istifli ES, Kuzucu M, Algul O. Synthesis and evaluation of di-heterocyclic benzazole compounds as potential antibacterial and anti-biofilm agents against Staphylococcus aureus. Chemical Biology & Drug Design. 2024;10:(2)4e14601.
27. AL-ATI GAM. Chimie Organique Hétérocyclique. 2024.
28. Mohammed LA, Farhan MA, Dadoosh SA, Alheety MA, Majeed AH, Mahmood AS, et al. A review on benzimidazole heterocyclic compounds: Synthesis and their medicinal activity applications. SynOpen. 2023;7(04):652-73.
29. McGinley J, Harmon O'Driscoll J, Healy MG, Ryan PC, Mellander PE, Morrison L, et al. An assessment of potential pesticide transmission, considering the combined impact of soil texture and pesticide properties: A meta-analysis .Soil use and Management. 2022;38(2):1162-71.
30 . Popa M, Sunel V, Stoican AD, Popa AA, Uglea CV. Poly (maleic anhydride–alt–vinyl acetate) Conjugates with Alkylating Agents: II. Organotropic Effects and Antitumoral Activity. Materiale plastice. 2008;45.274:(3)
31. Yilmaz E. Compatibilization of polyvinyl chloride-polymethyl methacrylate polymer blends with maleic anhydride-styrene-methyl methacrylate terpolymer. Journal of Applied Polymer Science. 2022;139(10):51745.
32. Fouassier J, Rabek J, Polaczek J ,Jakubiak J. Lasers in Polymer Science and Technology: Applications: Volume IV. Przemysl Chemiczny. 2023;102(3.(
.33 Smit M. Polymer-coated magnetic nanoparticles and polymer nanoparticles for the treatment of Mycobacterium tuberculosis (Mtb): Stellenbosch: Stellenbosch University; 2022.
34. Ntrivala MA, Pitsavas AC, Lazaridou K, Baziakou Z, Karavasili D, Papadimitriou M, et al. Polycaprolactone (PCL): the biodegradable polyester shaping the future of materials–a review on synthesis, properties, biodegradation, applications and future perspectives. European Polymer Journal. 2025;234:114033.
35. Tunc T, Karakus G, Sumer Z. Investigation of Cytotoxic and Antimicrobial Effects of Polyanhydride-Based Poly [(maleic anhydride)-co-(vinyl Acetate)] Conjugates Combined with Methotrexate and Gemcitabine in Breast Cancer Treatment. ACS omega. 2025;10(12):12152-62.
36. Salah ARM. Heterocyclic compounds in modern drug design: synthetic strategies and biological targets. Shorouk Academy–Department of Engineering. 2025.15-1:
37. Charushin VN, Verbitskiy EV, Chupakhin ON, Vorobyeva DV, Gribanov PS, Osipov SN, et al. The chemistry of heterocycles in the 21st century. Russian Chemical Reviews. 2024;93(7.(
38. Handschuh M. Bericht über die Verleihung des Wilhelm-Ostwald-Nachwuchs-preises 2021. Mitteilungen der Wilhelm-Ostwald-Gesellschaft eV. 2022;27(1):44.
39. Wohlgemuth R. Selective Biocatalytic Michael Addition Reactions. ChemSusChem. 2026;19(11):e202502620.

References

40. Perrin CL, Agranat I, Bagno A, Braslavsky SE, Fernandes PA ,Gal J-F, et al. Glossary of terms used in physical organic chemistry (IUPAC Recommendations 2021). Pure and Applied Chemistry. 2022;94(4):353-534.
41. Hoque M, Emon K, Malo P, Hossain M, Tannu S, Roshed M. Comprehensive guide to vitamin and mineral sources with their requirements. Indiana Journal of Agriculture and Life Sciences. 2023;3(6):23-31.
42. Aribo EO. Comparative anxiolytic, motor coordination and antioxidant effects of vitamin C and rutin on Cadmium-induced neurotoxicity in Swiss white mice. World Journal of Biology Pharmacy and Health Sciences. 2025.
43 . Dhayalan V, Kumar MP, Annie AS, Sunagatullina AS, Malakhov V, Hoffmann-Roder A, et al. Preparation and Reactivity of Organometallic Reagents Leading to Functionalized N-Heteroaromatics. Chemical Reviews. 2026;126(4):2582-652.
44. Verma C. Handbook of heterocyclic corrosion inhibitors: principles and applications: CRC Press; 2023.
45. Zhao P, Wang L, Guo X, Chen J, Liu Y, Wang L, et al. Visible light-driven α-diazoketones as denitrogenated synthons: synthesis of fluorinated N-heterocycles via multicomponent cyclization reactions. Organic Letters. 2023;25(18):3314-8.
46. Jurczyk J, Woo J, Kim SF, Dherange BD, Sarpong R, Levin MD. Single-atom logic for heterocycle editing. Nature Synthesis. 2022.64-352:(5)1;
47. Abu-Hashem AA, Abdelgawad AA, Hussein HA, Gouda MA. Synthetic and reactions routes to tetrahydrothieno [3, 2-b] quinoline derivatives (Part IV). Mini-Reviews in Organic Chemistry. 2022;19(1):74-91.
48. Morales G, Bunin BA. Combinatorial Chemistry, Part B: Elsevier; 2004.
49. Donnelly K, Baumann M. Flow synthesis of oxadiazoles coupled with sequential in-line extraction and chromatography. Beilstein Journal of Organic Chemistry. 2022;18(1):232-9.
50. Barekatain M, Johansson LC, Lam JH, Chang H, Sadybekov AV, Han GW, et al. Structural insights into the high basal activity and inverse agonism of the orphan receptor GPR6 implicated in Parkinson's disease. Science signaling. 2024;17(865):eado8741.
51. Salah ARM. Heterocyclic Compounds: Synthesis, Reactivity Models, and Applications in Drug Design. 2025.
52. Chen L-J, Ying R-N, Wang X-Q, Xie D-T, Dong J, Lin H-Y, et al. Discovery of Triketone–Indazolones as Novel 4-Hydroxyphenylpyruvate Dioxygenase Inhibiting-Based Herbicides. Journal of Agricultural and Food Chemistry. 2025;73(2):1112-21.
53. Adachi K, Ohyama K, Shimura Y, Tanaka Y, Shimizu M, Saito Y, et al. Virtual hepatic and plasma exposures of voriconazole administered to cytochrome P450 2C19 poor metabolizers predicted by simplified and full pharmacokinetic modeling systems: possible causal factor for hepatic disorders seen in a Japanese database. Biological and Pharmaceutical Bulletin. 2025;48(8):1271-6.
54. Wang Z, Debuigne A. Radical polymerization of methylene heterocyclic compounds :functional polymer synthesis and applications. Polymer Reviews. 2023;63(4):805-51.
55. Hifumi R, Tomita I. Low dielectric, good adhesive, and flame-retardant aromatic poly (ether) s with phosphine sulfide groups. Macromolecules. 2024;57(18):8763-71.
56. Saleh MY, Abdelzaher MA, Ali AH, Owaid KA. Synthesis and Characterization of some new Heterocyclic Polymer Compounds from Benzo [1, 2-d: 4, 5-d] bis (thiazole)-2, 6-diamine and [6, 6'-Bibenzo [d] thiazole]-2, 2'-diamine. Rafidain Journal of Science. 2023.69-57:(4)32;
57. Mosquera S, Ginésy M, Bocos-Asenjo IT, Amin H, Diez-Hermano S, Diez JJ, et al. Spray-induced gene silencing to control plant pathogenic fungi: A step-by-step guide. Journal of Integrative Plant Biology. 2025;67(3):801-25.
58. Mitchell S ,Martín AJ, Guillén-Gosálbez G, Pérez-Ramírez J. The future of chemical sciences is sustainable. Angewandte Chemie International Edition. 2024;63(26):e202318676.
59. Felippe IS, Babbage TL, Shaheen R, Bassetto M, Fan J-L, Pauza A, et al. Vitamin B6 (Pyridoxal 5' Phosphate) antagonises carotid body P2X3 receptors in hypertension. Cardiovascular research. 2026;122(2):285-96.

References

60. Janietz S, Brening T, Schiestel T, Götz T. Block copoly (phenylquinoxaline) s as potential ionomers for proton exchange membranes .Polymer. 2023;271:125794.
61. Alsolami ES, Alorfi HS, Alamry KA, Hussein MA. One-pot multicomponent polymerization towards heterocyclic polymers: a mini review. RSC advances. 2024;14(3):1757-81.
62. Patel A, Shah D, Patel N, Patel K, Soni N, Nagai A, et al. Quinoxaline as ubiquitous structural fragment: An update on the recent development of its green synthetic approaches. Current Organic Chemistry. 2021;25(24):3004-16.
63. Younas M, Pervaiz B, Riaz B. Lexical Meanings and Mistranslation: an Analysis of English Translation of Munshi Premchand's Short Stories. Global Language Review. 2022;7(1):209-16.
64. Hergenrother PM, Connell JW, Labadie JW, Hedrick JL. Poly (arylene ether) s containing heterocyclic units. High Performance Polymers: Springer; 2005. p.110-67 .
65. Hedrick JL. Poly (aryl ether oxadiazoles). Polymer bulletin. 1991;25(5):543-50.
66. Ahmed HS, Mohammed MMK, Khorsheed NH, Esmail EM. Review on Systematic Mapping study for synthesis of polymers containing 1, 3, 4 Thiadiazole. Al-Kitab Journal for Pure Sciences. 2025;9(01):14-33.
67. Armo R, Malviya RK. Recent Advances in Quinoxaline and Benzoxazole-Based Heterocycles for Anti-Inflammatory Drug Development. International Journal of Medical and Pharmaceutical Sciences. 2026;2(03):179-85.
68. El Alami A, El Maraghi A, Sdassi H. Review of synthesis process of benzoxazole and benzothiazole derivatives. Synthetic Communications. 2024;54(10):769-801.
69. Gerasimova TP, Zagidullin AA, Nikolaeva AN, Fayzullin RR, Saitova AM, Miluykov VA, et al. Structural flexibility of favipiravir and its structural analogues in solutions: experimental and computational insight. Organic & Biomolecular Chemistry. 2024;22(18):3668-83.
70. Han Y-T, Zhang Y, Zhong D-L, Yao K-X, Wang J-J, Yan J. CO2 adsorption and separation from flue gas using a halogenated covalent triazine-based framework. Journal of Environmental Chemical Engineering. 2026:121605.
71. Chanu LV, Singh OM. Recent progress in the synthesis of azoles and related five-membered ring heterocycles using silica-supported heterogeneous catalysts. Journal of Heterocyclic Chemistry. 2021;58(12):2207-25.
72. Thakur S, Kumar D, Jaiswal S, Goel KK, Rawat P, Srivastava V, et al. Medicinal chemistry-based perspectives on thiophene and its derivatives: exploring structural insights to discover plausible druggable leads. RSC Medicinal Chemistry. 2025;16(2):481-510.
73. Neha K, Ali F, Haider K, Khasimbi S, Wakode S. Synthetic approaches for oxazole derivatives: A review. Synthetic Communications. 2021;51(23):3501-19.
74. Bariki R, Joseph RG, El-Kadri OM, Al-Sayah MH. The development of Metal-Free porous organic polymers for sustainable carbon dioxide photoreduction. Nanomaterials. 2024;14(17):1432.
75. An B, Liu J, Fan Y, Nie W, Yang C, Yao H, et al. Novel third-generation pyrimidines-based EGFR tyrosine kinase inhibitors targeting EGFR T790M mutation in advanced non-small cell lung cancer. Bioorganic Chemistry. 2022;122:105743.
76. El-mrabet A, Haoudi A, Kandri-Rodi Y, Mazzah A. An overview of quinolones as potential drugs: synthesis, reactivity and biological activities. Organics. 2025;6(2):16.
77. Yamamoto T, Murakami R, Suginome M. Single-handed helical poly (quinoxaline-2, 3-diyl) s bearing achiral 4-aminopyrid-3-yl pendants as highly enantioselective, reusable chiral nucleophilic organocatalysts in the steglich reaction. Journal of the American Chemical Society. 2017;139(7):2557-60.
78. Salunke AK, Ghosh A, Banerjee S. Synthesis and characterization of novel poly (arylene ether) s based on 9, 10-bis-(4-fluoro-3-trifluoromethylphenyl) anthracene and 2, 7-bis-(4-fluoro-3-trifluoromethylphenyl) fluorene. Journal of applied polymer science. 2007;106(1):664-72.
79. Qiao Y, Liu C, Jia H, Zhang Y, Zhao W, Li Y, et al. Phthalocyanine-terminated poly (aryl ether) sizing: an efficient strategy in interfacial interactions optimization of CF/PPESK composites with excellent thermal-resistant. Composites Part A: Applied Science and Manufacturing. 2024;179:108057.

80. Martins P, Jesus J, Santos S, Raposo LR, Roma-Rodrigues C, Baptista PV, et al. Heterocyclic anticancer compounds: recent advances and the paradigm shift towards the use of nanomedicine's tool box. Molecules. 2015;20(9):16852-91.
81. Mondal J, Sivaramakrishna A. Functionalized triazines and tetrazines: Synthesis and applications. Topics in Current Chemistry. 2022;380(5):34.
82. Sumdani MG, Islam MR, Yahaya ANA, Safie SI. Recent advancements in synthesis, properties, and applications of conductive polymers for electrochemical energy storage devices: A review. Polymer Engineering & Science. 2022;62(2):269-303.
83. Cao Z, Aharonian F, An Q, Axikegu, Bai Y, Bao Y, et al. The first LHAASO catalog of gamma-ray sources. The Astrophysical Journal Supplement Series. 2024;271(1):25.
84. Mohd Iskak NA, Chee CF, Muhamad Sarih N ,Muhd Julkapli N. Polycarbonate synthesis via ring-opening polymerization: catalysts, mechanisms, and sustainable strategies. New Journal of Chemistry. 2026;50(20):8526-49.
85. Sun L, Wang X, Fleurat-Lessard P, Gros CP, Bolze F, Xu H. Synthesis, photophysical properties and two-photon absorption of benzothiazole/benzoxazole π-expanded carbazole dyes. Dyes and Pigments. 2022;204:110447.
86. West SM, Tran DK, Guo J, Chen SE, Ginger DS, Jenekhe SA. Phenazine-substituted poly (benzimidazobenzophenanthrolinedione): electronic structure, thin film morphology, electron transport, and mechanical properties of an n-type semiconducting ladder polymer. Macromolecules. 2023;56(5):2081-91.
87. So Y-HZ, J. M.; Murlick, C.; Ellaboudy, A. Synthesis and Photophysical Properties of Some Benzoxazole and Benzothiazole Compounds. Macromolecules (misspelled as "Mncromolecules" in the query). 1996;29(8):2783–95.
88. Han T, Deng H, Qiu Z, Zhao Z, Zhang H, Zou H, et al. Facile multicomponent polymerizations toward unconventional luminescent polymers with readily openable small heterocycles. Journal of the American Chemical Society. 2018;140(16):5588-98.
89. Chernyshov VV, Popadyuk II, Yarovaya OI, Salakhutdinov NF. Nitrogen-containing heterocyclic compounds obtained from monoterpenes or their derivatives: Synthesis and properties. Topics in Current Chemistry. 2022;380(5):42.
90. Higashihara T, Wu H-C, Mizobe T, Lu C, Ueda M, Chen W-C. Synthesis of thiophene-based π-conjugated polymers containing oxadiazole or thiadiazole moieties and their application to organic photovoltaics. Macromolecules. 2012;45(22):9046-55.
91. Abdelwahab H, AM Al-Zahrani F, Ali AA, Mahmoud A, Lin L. New thiadiazol azo disperse dyes derivatives and their application as a colored material for silk screen-printing ink for printing on polyester fabric. Pigment & Resin Technology. 2024;53(3):294-304.
92. Monclús L, Arp H, Groh K, Faltynkova A, Løseth M, Muncke J, et al. Mapping the chemical complexity of plastics. Nature. 2025;643(8071):349-55.
93. Atta S, Fawzy N, Ahmed F, Abdel-Rahman A. Synthesis of triazolyl-oxadiazolyl-thiazolyl-and thiadiazolylbenzofuran of potential biological activity. Phosphorus, Sulfur, and Silicon and the Related Elements. 2002;177(4):863-75.
94. Arash Tabei RE, Arash Mahboubi. Synthesis of new 2-(5-(5-nitrofuran-2-yl)-1,3,4-thiadiazol-2-ylimino)thiazolidin-4-one derivatives as anti-MRSA and anti-H. pylori agents. 2022;16.
95. Istanbullu H, Bayraktar G, Saylam M. Fused pyridine derivatives: synthesis and biological activities. Exploring Chemistry with Pyridine Derivatives. 2022:125-60.
96. Crispim CV, de Lima MF, Abubakar A, da Silva RR, da Silva TH, Silva DG. Miniaturized Reaction Platforms in Drug Discovery: from Synthesis to Direct-to-Biology Screening. Journal of the Brazilian Chemical Society. 2026;37(spe2):e-20260097.
97. Breugst M, Reißig HU. Die Huisgen-Reaktion: Meilensteine der 1, 3-dipolaren Cycloaddition. Angewandte Chemie. 2020;132(30):12389-404.
98. Graschtat V, Proz I, Lehmann M, Detert H. 1, 2, 4-Tris (5-aryl-1, 3, 4-oxadiazolyl)-benzenes: novel λ-shaped fluorescent liquid crystals. Journal of Materials Chemistry C. 2025;13(31):15941-7.

99. Springer-S Rahmani AM. Synthesis and characterization of novel poly(arylene ether)s containing 1,3,4-oxadiazole and triazole units through click chemistry. 2015;23:1018–25.
100. Zifeng Xu YJ, Peiyang Dong ,Guochen Ji ,Siyuan Chen, Junping Zheng. High-performance, thermally stable and recyclable triboelectric nanogenerators benefit from triple-functional silyl ether networks interspersed with engineered MXene. 2026;150.
101. Ramle AQ, Tiekink ER. Advances in the Synthesis and Reactivity of Selenadiazoles. Asian Journal of Organic Chemistry. 2025;14(9):e00577.
102. Jyoti K, Singh[1] SB. played by nanoimmunoadjuvants. Multifunctional Nanocarriers. 2022:347.
103. Baier D, Krüger A, Wagner T, Tiemann M, Weinberger C. Gas Sensing with Nanoporous In2O3 under Cyclic Optical Activation: Machine Learning-Aided Classification of H2 and H2O. Chemosensors. 2024;12(9):178.
104. Overberger C, Moore J. Ladder polymers. Fortschritte der Hochpolymeren-Forschung: Springer; 2006. p. 113-50.
105. Fujimoto K, Tang Z, Shinoda W, Okazaki S. All-atom molecular dynamics study of impact fracture of glassy polymers. I: Molecular mechanism of brittleness of PMMA and ductility of PC. Polymer. 2019;178:121570.
106. Shang J, Song P, Li G, Sun Q, Li Y, Wei Z. Crystallization and melting behavior of poly (ether ketone ketone)(PEKK) copolymers synthesized by facile one-step method. Journal of Thermal Analysis and Calorimetry. 2023;148(21):11727-41.
107. Tashiro K. Phase Transition Behavior of Polymer Crystals. Structural Science of Crystalline Polymers: Basic Concepts and Practices: Springer; 2022. p. 769-812.
108. Kobzar Y, Fatyeyeva K, Chappey C, Désilles N, Marais S. Polyoxadiazoles as proton exchange membranes for fuel cell application. Reviews in Chemical Engineering. 2022;38(7):799-820.
109. Sahoo PR, Saxena A, Kumar S. Oxadiazole in material and medicinal chemistry: CRC Press; 2024.
110. Wan Z, Liu H, Zheng Y, Ma Y, Liu K, Zhou X, et al. A review of acoustic devices based on suspended 2D materials and their composites. Advanced Functional Materials. 2024;34(3):2303519.
111. Hayek A, Alsamah A, Shalabi YA, Saleem Q, Ben Sultan MM, Alhajry RH. Molecular design of poly (imide–oxadiazole) membranes for high-pressure mixed-gas separation. Macromolecules. 2022;55(9):3747-61.
112. Selvi S, Kannan A, Jayaraj JM, Selvi T, Karthikeyan M, Prahalathan C, et al. Synthesis and biological evaluation of 3-hydroxypyrazoles as aquaporin 9 inhibitors. Journal of Heterocyclic Chemistry. 2024;61(4):669-79.
113. Saeed RS, Ghali TS, Alwitry ZA, Tomma JH, Al-rawi MS. Blending a New Polymers Containing Oxadiazole Ring with PVA: Synthesis, Thermal Analysis and Biological Activity .Iraqi Journal of Science. 2025:5284-96.
114. Poonam, Bhasin G, Srivastava R, Singh R. Oxadiazoles: moiety to synthesis and utilize. Journal of the Iranian Chemical Society. 2022;19(3):665-77.
115. Ankushrao SS, Ghanwat AA, Patil YS, Kadam VN. Synthesis ,characterization and properties of processable polyazomethines for high temperature applications. Journal of Advanced Scientific Research. 2021;12(03 Suppl 2):306-14.
116. Halder S, Chakraborty C. Porous covalent polymer framework-based molecular platform for polychromatic Vis-to-NIR electrochromic smart window to modulate solar irradiation. Solar Energy Materials and Solar Cells. 2024;270:112800.
117. AlMaadeed MAA, Ponnamma D, El-Samak AA. Polymers to improve the world and lifestyle: physical, mechanical, and chemical needs. Polymer science and innovative applications: Elsevier; 2020. p. 1-19.
118. Lee S, Jeong R, Seo M, Lee H-S. Double-activated nucleophilic aromatic substitution polymerization by bis-ortho-trifluoromethyl groups to soluble para-poly) biphenylene oxide). Polymer. 2020;188:122124.
119. Cappitti A, Vespignani L, Giomi D. Nucleophilic aromatic substitutions on 4, 5-dicyanopyridazine: application of bis-nucleophiles. Tetrahedron. 2026:135221.

120. Pinson J, Jean-Michel S. Electrochemical Induction of SRN1 Nucleophilic Substitution. Electroorganic Synthesis: Routledge; 2023. p. 29-44.
121. Pistritto VA, Schutzbach-Horton ME, Nicewicz DA. Nucleophilic aromatic substitution of unactivated fluoroarenes enabled by organic photoredox catalysis ·Journal of the American Chemical Society. 2020;142(40):17187.
122. Lister TM, Roberts GW, Hossack EJ, Zhao F, Burke AJ, Johannissen LO, et al. Engineered enzymes for enantioselective nucleophilic aromatic substitutions. Nature. 2025;639(8054):375-81.
123. Hu Y, Wei Z, Frey A, Kubis C, Ren CY, Spannenberg A, et al. Catalytic, Kinetic, and Mechanistic Insights into the Fixation of CO2 with Epoxides Catalyzed by Phenol-Functionalized Phosphonium Salts. ChemSusChem. 2021;14(1):363-72.
124. Medjidov A, Ismayilova S, Ganzayeva G, Agaeva S, Qasimova S. Properties of polymers based on aromatic diamines. Azerbaijan Chemical Journal. 2022(3):21-44.
125. Shim E, Kammeraad JA, Xu Z, Tewari A, Cernak T, Zimmerman PM. Predicting reaction conditions from limited data through active transfer learning. Chemical science. 2022;13(22):6655-68.
126. Vindizheva A, Kharaeva Z, Khashirova S, Danilova-Volkovskaya GM. Use of Polyester-Etherketone and Composites Based on it in Medical Practice. Key Engineering Materials. 2021;899-709: .14
127. Borlinghaus N, Ansari TN, von Garrel LH, Ogulu D, Handa S, Wittmann V, et al. Nucleophilic aromatic substitution reactions under aqueous, mild conditions using polymeric additive HPMC. Green Chemistry. 2021;23(11):3955-62.
128. Mayhugh AL. Room temperature methods of direct arylation for conjugated polymer and small molecule synthesis: University of Washington; 2022.
129. El Ain MA, Puiatti M, Budén ME. Construction of 3, 3'-Bicarbazoles and Indolocarbazoles by Using Visible Light. European Journal of Organic Chemistry. 2022;2022(36):e202200642.
130. Shaposhnikova V, Salazkin S. Synthesis and properties of poly (arylene ether ketones). Russian Chemical Bulletin. 2014;63(10):2213-23.
131. Zhang C, You J-A, Sun Y, Li S, Zhang S. Stepwise UV crosslinking in solvent: A novel method to enhance the solvent resistance of poly (aryl ether ketone) membranes. Journal of Membrane Science. 2023;688:122096.
132. V. Carlier BJ, J. Devaux, R. Legras, P. T. McGrail. "Nucleophilic cleavage of activated aryl ethers by a fluoride anion". Polymer. 1993;34(1):167–70.
133. Luleburgaz S, Tunca U, Durmaz H. Poly (silyl ether) s (silyl ether copolymers) via hydrosilylation of carbonyl compounds. Polymer Chemistry. 2023;14(25):2949-57.
134. Li J, Zhang S, Liu X. Synthesis of phenolphthalein/bisphenol A-based poly (arylene ether nitrile) copolymers: Preparation and properties of films. Journal of Applied Polymer Science. 2023;140(5):e53407.
135. Pu M, Fang C, Zhou X, Wang D, Lin Y, Lei W, et al. Recent advances in environment-friendly polyurethanes from polyols recovered from the recycling and renewable resources: a review. Polymers. 2024;16(13):1889.
136. Biswas T, Mittal RK, Sharma V, Kanupriya, Mishra I. Nitrogen-fused heterocycles: empowering anticancer drug discovery. Medicinal Chemistry. 2024;20(4):369-84.
137. Sahu N. Aromaticity-Guided Synthesis and Reactivity of Heterocyclic Compounds: Structural Insights and Applications. International Journal. 2025;11(2.(
138. Balaban ATO, D. C.; Katritzky, A. R. Aromaticity as a cornerstone of heterocyclic chemistry. Chemical Reviews 2004;104(5):2777-812.
139. A. F. Pozharskii ATS, A. R. Katritzky. Heterocycles in Life and Society: An Introduction to Heterocyclic Chemistry, Biochemistry and Applications. John Wiley & Sons·2011 .
140. Nistanaki SK, Nelson HM. Dewar heterocycles as versatile monomers for ring-opening metathesis polymerization. ACS macro letters. 2020;9(5):731.
141. Pozharskii AFS, A. T.; Katritzky, A. R. Heterocycles in life and society 2011.
142. Paggi JM ,Pandit A, Dror RO. The art and science of molecular docking. Annual review of biochemistry. 2024;93(1):389-410.

143. Muhammed MT, Aki-Yalcin E. Molecular docking: principles, advances, and its applications in drug discovery. Letters in Drug Design & Discovery. 2024;21(3):480-95.
144. De Blasio C. Thermogravimetric analysis (TGA). Fundamentals of biofuels engineering and technology: Springer; 2019. p. 91-102.
145. Saadatkhah N, Carillo Garcia A, Ackermann S, Leclerc P, Latifi M, Samih S, et al. Experimental methods in chemical engineering: Thermogravimetric analysis—TGA. The Canadian Journal of Chemical Engineering. 2020;98(1):34-43.
146. Bashirgonbadi A, Ureel Y, Delva L, Fiorio R, Van Geem KM, Ragaert K. Accurate determination of polyethylene (PE) and polypropylene (PP) content in polyolefin blends using machine learning-assisted differential scanning calorimetry (DSC) analysis. Polymer Testing. 2024;131:108353.
147. Khalef L, Lydia R, Filicia K, Moussa B. Cell viability and cytotoxicity assays: Biochemical elements and cellular compartments. Cell biochemistry and function. 2024;42(3):e4007.
148. Ghasemi M, Liang S, Luu QM, Kempson I. The MTT assay: a method for error minimization and interpretation in measuring cytotoxicity and estimating cell viability. Cell viability assays: Methods and protocols: Springer; 2023. p. 15-33.
149. Gulcin İ, Alwasel SH. DPPH radical scavenging assay. Processes. 2023;11(8):2248.
150. The CMS statistical analysis and combination tool: COMBINE. Computing and Software for Big Science. 2024;8(1):19.
151. Silverstein RM, Webster, F.X and Kiemle, D.J Spectrometric Identification of Organic Compounds. John Wiley & Sons. 2005.
152. Pretsch E, Buhlmann, P., Baderscher, M. . Structure Determination of Organic Compounds: Tables of Spectral Data. 2009.
153. Pavia LD, Lampman, L.G., Kris, S.G., Vyvyan, R.J. . Introduction to Spectroscopy. Brooks/Cole, Cengage Learning. 2009.
154. Vuković J, Steinmeier, D., Lechner, M. D., Jovanović, S. and Božić, B. , . Thermal Degradation of Aliphatic Hyperbranched Polyesters and their Derivatives. Polymer Degradation and Stability, . 2006;91:1903-8.
155. Garbuz O, Ivanov, V., & Petrov, A. . Thiosemicarbazone-based compounds as promising anticancer agents: Structure–activity relationship and molecular mechanisms. Bioorganic Chemistry. 2025;150.
156. Aishwarya R, Kumar, S., & Patel, D. . Thiohydantoin derivatives as potential anticancer agents: Mechanisms of action and therapeutic perspectives. European Journal of Medicinal Chemistry, 265, 115987. 20.256;25
157. Zhang Y, Li, X., & Chen, H. . DNA-intercalating agents in cancer therapy: Focus on naphthalimide derivatives. Pharmacological Research. 2024;198.
158. Garbuz O, and colleagues. Thiosemicarbazone-based compounds: cancer cell cytotoxicity and structure-dependent mechanisms. International Journal of Molecular Sciences, 26 [Full bibliographic details should be checked according to the final database record]. 2025.
159. Vidanapathirana AK, Silva, R., & Perera, M. . Iron chelation therapy in colorectal cancer: Mechanisms and therapeutic implications. Frontiers in Oncology. 2025;15.
160. Khodair AI ea. New bis-hydantoin/thiohydantoin derivatives: antibacterial activity and computational insights. Journal of Molecular Structure https://doiorg/101016/jmolstruc2024139015. 2024.
161. Khodair AI, Abdelrahman, M. H., & Hassan, H. M. . Design, synthesis and biological evaluation of novel thiohydantoin derivatives as anticancer agents. Bioorganic & Medicinal Chemistry Letters. 22024;98.
162. Magri A, Esposito, F., & Novellino, E. . Naphthalimide derivatives as DNA-targeting anticancer agents: Mechanisms and therapeutic applications. Cancer Letters. 2025;610.
163. Olejarz W, Kubiak-Tomaszewska, G., & Chrzanowska, A. Advances in tetrazole derivatives as potential anticancer agents. International Journal of Molecular Sciences. 2025;26(3):1456.
164. Maji S, Das, P., & Roy, K. . Tetrazole-based heterocycles as emerging anticancer scaffolds: A comprehensive review. Medicinal Research Reviews 2025;45(2):789–825.

References

165. Hatti KS, Sahu, N., & Verma, R. . Heterocyclic compounds in cancer therapy: Recent advances in design and biological activity. Journal of Molecular Structure. 2024;1302.
166. Sahu N, Verma, R., & Singh, P. . Recent progress in heterocyclic compounds for cancer therapy: Molecular targets and mechanisms. Current Pharmaceutical Design. 2024;30(12):1567–83.
167. Feizpour S ea. Design and biological evaluation of novel water-soluble thiosemicarbazone derivatives as anticancer agents. Scientific Reports·2025 . .
168. Veg E ea. Some biological applications and mechanistic insights of thiosemicarbazones and their metal complexes. 2025.
169. El-Deen IM ea. In vitro cytotoxicity screening of some 3-substituted-4-oxo-2-thiohydantoin derivatives against cancer cell lines. 2024.
170. Lee CC ea. Novel 1,8-naphthalimide derivatives inhibit growth and induce apoptosis in cancer cells. 2024.
171. Gallego-Yerga L ea. Novel tetrazole derivatives targeting tubulin with antimitotic effects against cancer cells. 2023.
172. Platzer M, Kiese, S., Herfellner, T., Schweiggert-Weisz, U., Miesbauer, O., and Eisner, P. . Common trends and differences in antioxidant activity analysis of phenolic substances using single electron transfer based assays. Molecules, 26(5), 1244 https//:doiorg/103390/molecules26051244. 2021.
173. Yamauchi M, and colleagues. DPPH measurements and structure–activity relationship studies on the antioxidant capacity of phenols. Antioxidants, 13(3), 309 https://doiorg/103390/antiox13030309. 2024.
174. Rana MS, Rayhan, N. M. A., Emon, M. S. H., Islam, M. T., Rathry, K., Hasan, M. M., Mansur, M. I., Srijon, B. C., Islam, M. S., Ray, A., Rakib, M. A., Islam, A., Kudrat-E-Zahan, M., Hossen, M. F., and Asraf, M. A. . Antioxidant activity of Schiff base ligands using the DPPH scavenging assay: an updated review. RSC Advances, 14, 33094–33123 https://doiorg/101039/D4RA04375H. 2024.
175. El-Sayed DS, Hassan, S. S., and colleagues. Structural and topological analysis of thiosemicarbazone-based metal complexes: computational and experimental study of bacterial biofilm inhibition and antioxidant activity. BMC Chemistry, 19, 24 https://doiorg/101186/s13065-024-01338-5. 2025.
176. Bukhari A, Nadeem, H., and colleagues. . Synthesis and evaluation of novel thiohydantoin derivatives for antidiabetic activity using in silico, in vitro and in vivo methods. Scientific Reports https://doiorg/101038/s41598-025-08731-7. 2025.
177. Seliem IA, and colleagues. . DMF-DMA catalyzed synthesis, molecular docking, in-vitro antioxidant activity and antitumor evaluation of thiohydantoin derivatives. Journal of Molecular Structure https://doiorg/101016/jmolstruc2024139015. 2024.
178. Hlila MB, Majouli, K., Jannet, H. B., Aouni, M., Mastouri, M., and Selmi, B. . Antimicrobial activity of Tunisian Euphorbia paralias L. Asian Pacific Journal of Tropical Biomedicine. 2017;7(7):629-32.
179. L P. Updated Information on Antimicrobial Activity of Hydrazide-Hydrazones. International Journal of Molecular Sciences. 2021;22(18):10367.
180. Czylkowska A ea. Thiosemicarbazone-Based Compounds: A Promising Scaffold for Antimicrobial Drug Discovery. Molecules. 2024;30(1):129.
181. Manrique PD ea. Predicting permeation of compounds across the outer membrane of Gram-negative bacteria using molecular descriptors. Communications Chemistry. 2024;103(7.(
182. Saxena D ea. Tackling the outer membrane: facilitating compound entry into Gram-negative bacteria. Nature Reviews Bioengineering. 2023:318-34.
183. Lu X ea. Next-generation antifungal drugs: mechanisms, efficacy, and resistance. Drug Resistance Updates. 2025.
184. Li Y ea. New antifungal strategies and drug development against fungal infections. Frontiers in Cellular and Infection Microbiology. . 2025.
185. Czylkowska A ea. Thiosemicarbazone-Based Compounds :A Promising Scaffold for Antimicrobial Drug Discovery. Molecules. 2024.

References

186. Czylkowska A ea. Thiosemicarbazone-Based Compounds: A Promising Scaffold for Antimicrobial Drug Discovery. . Molecules. 2024;30(1):129.
187. Butler MS ea. A Review of Antibacterial Candidates with New Modes of Action. 2024.

الخلاصة:

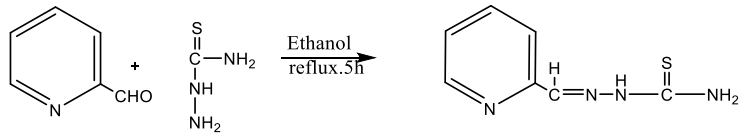
تمتلك جميع الكائنات الحية القدرة على الدفاع عن نفسها ضد مسببات الأمراض الخارجية وإصلاح تلف الأنسجة الناتج عن العدوى. وقد أدى اكتشاف الاستجابة الالتهابية إلى فوائد كبيرة في علاج الأمراض الالتهابية المرتبطة بعمليات فسيولوجية ومرضية متنوعة. لا تزال فسيولوجيا المرض غير مفهومة تمامًا، إلا أن الالتهاب معروف بأنه استجابة تكيفية تُحفزها محفزات ضارة. في المقام الأول، يُقيّم المحفز الالتهابي الحاد من خلال العدوى أو إصابات الأنسجة، مما يؤدي إلى توزيع مكونات الدم (البلازما وكريات الدم البيضاء) عبر المنطقة المصابة أو المتضررة. بالإضافة إلى ذلك، قد يؤدي هذا الحدث الموضعي إلى التهاب مزمن وأمراض المناعة الذاتية في حالات أخرى، والتي تنشأ عن خلل في وظيفة الأنسجة نتيجة لاختلال التوازن الداخلي لآلية بيولوجية واحدة أو أكثر.

تُبرز فائدة مركبات الثيوسيميكاربازيد في التخليق العضوي أهميتها في تخليق العديد من المركبات الحلقية غير المتجانسة. ويُعد تفاعلها مع الأنظمة التي تحتوي على مجموعات C=O وC=N إحدى طرق تحضير المركبات النشطة بيولوجيًا، مثل البيرازول، والثيازول، والتريازول، والثياديازول، والأوكساديازول، والتريازين، والثياديازين. وينعكس تكوين روابط C–N وC=N، بدلًا من تكوين رابطة N–N، في استخدامها الواسع النطاق لتحضير هذه المركبات الحلقية غير المتجانسة بنسب إنتاج ممتازة.

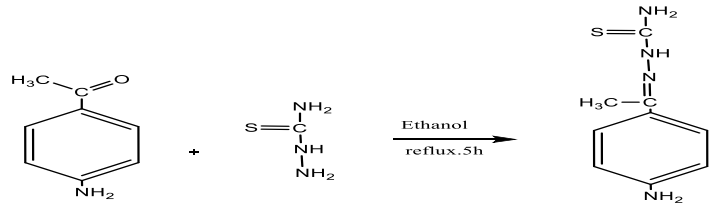
حظيت فئات جديدة من البوليمرات المشتركة، المشتقة من بوليمرات مشتركة تحتوي على مركبات حلقية غير متجانسة خماسية وسداسية الحلقات، باهتمام كبير نظرًا لتطبيقاتها المتنوعة، لا سيما في مجال العلاج الكيميائي، ومضادات الميكروبات، ومبيدات الفطريات، وذلك فيما يتعلق بتثبيت بعض المركبات النشطة بيولوجيًا على البوليمرات المشتركة (حمض ميثيل أكريليك - أنهيدريد إيتاكونيك) و(N،Nثنائي ميثيل أكريلاميد - أنهيدريد سيتراكونيك) عبر روابط كيميائية. وقد سمحت لنا الفعالية العالية لحلقة الأنهيدريد في البوليمر بالحصول على مترافقة يتم فيها تثبيت المركبات النشطة بيولوجيًا لبعض المركبات الحلقية غير المتجانسة على الدعامة البوليمرية عبر روابط أميدية. تم تحديد البنية الكيميائية للمركبات والبوليمرات المشتركة المصنعة باستخدام تقنيات طيفية مثل [FTIR، وHNMR1، وCNMR13، والتحليل العنصري .](CHNS)كما تم تحديد بعض الخصائص الفيزيائية للمركبات المصنعة، مثل نقاط الانصهار والألوان.

يتضمن هذا العمل اثني عشر جزءًا مختلفًا كما هو موضح أدناه:

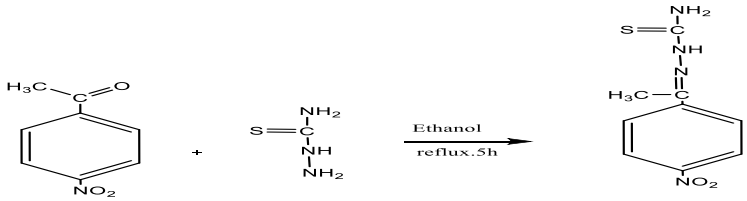
1. الجزء الأول: تناول هذا الجزء تخليق قواعد شيف جديدة للحصول على المركبات الوسيطة من ثيوسيميكاربازون (1-11) عن طريق تفاعل ثيوسيميكاربازيد مع العديد من الكيتونات والألدهيدات العطرية كما هو موضح في المخطط (1).


Ethanol
reflux.5h

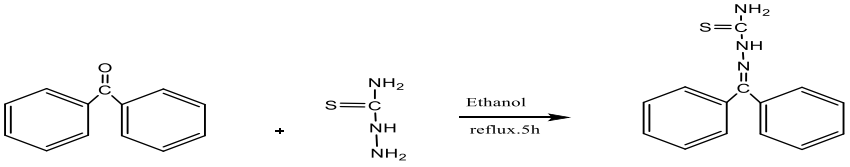
(1)


Ethanol
reflux.5h

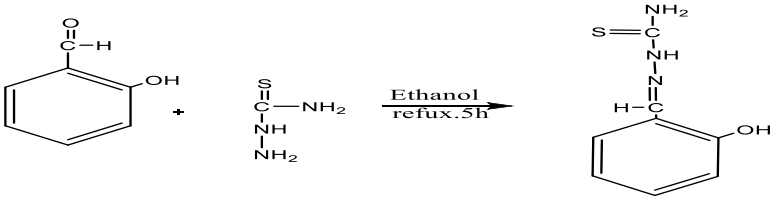
(2)


Ethanol
reflux.5h

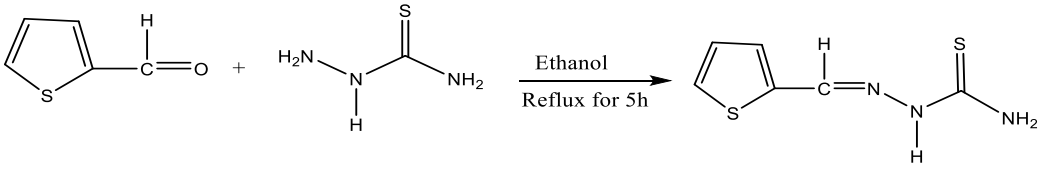
(3)


Ethanol
reflux.5h

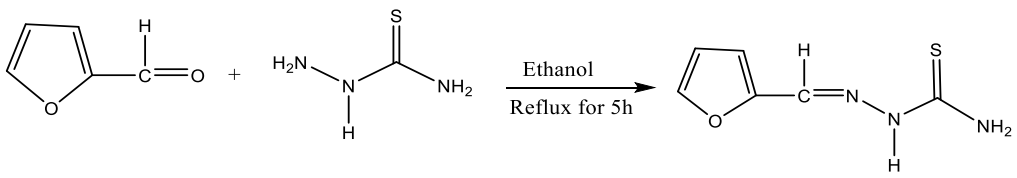
(4)


Ethanol
reflux.5h

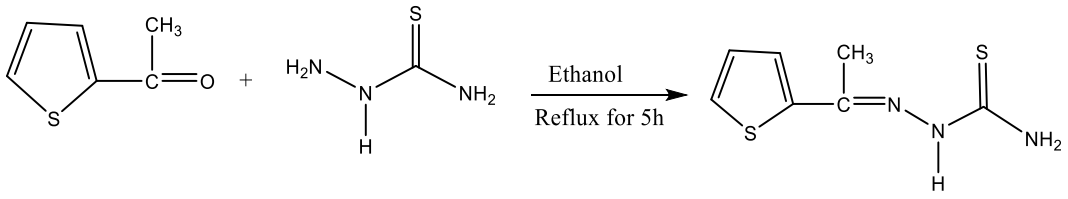
(5)


Ethanol
Reflux for 5h

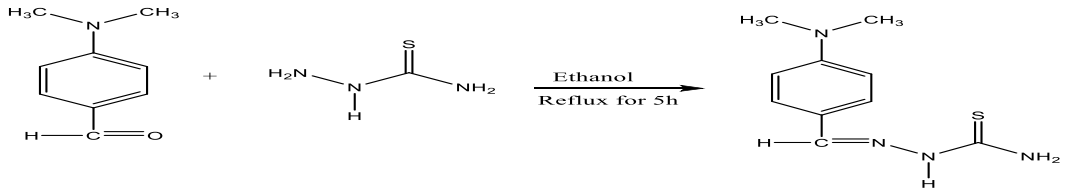
(6)


Ethanol
Reflux for 5h

(7)

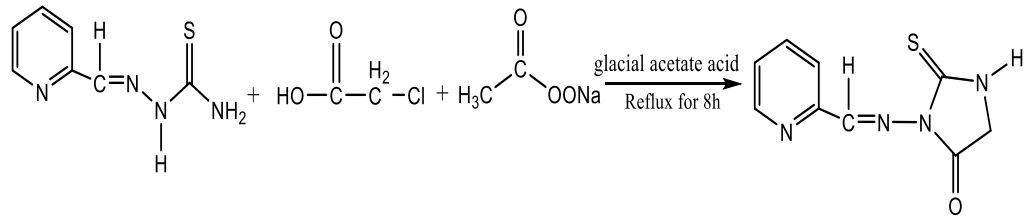


(8)

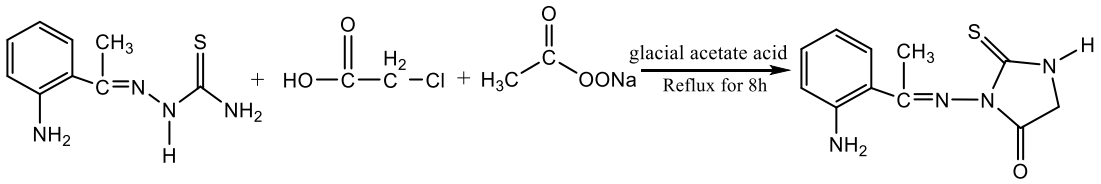


(9)

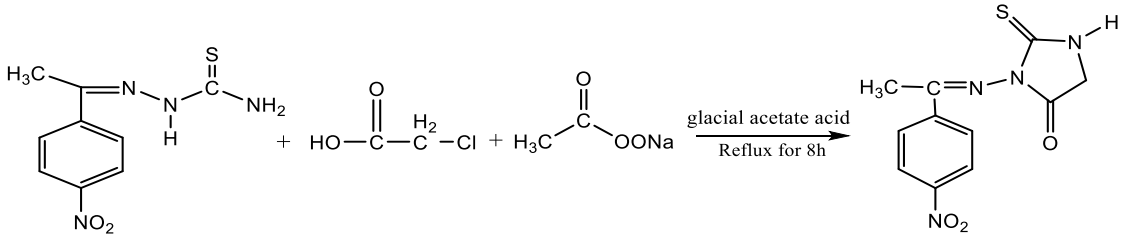
2. الجزء الثاني: بمعالجة المركبات (1، 2، 3، 4، 6، 7، 8، 9) بحمض الكلورواسيتيك وأسيتات الصوديوم اللامائية، تم تخليق سلسلة من مركبات 2-(4-بديل-بنزيليدين هيدرازونو)-1،3-ثيازوليدين-4-ون (12-21) كما هو موضح في المخطط (2).



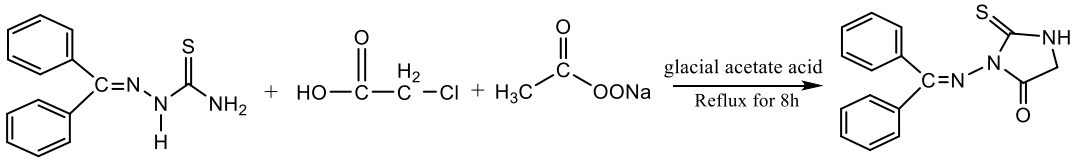
(1)



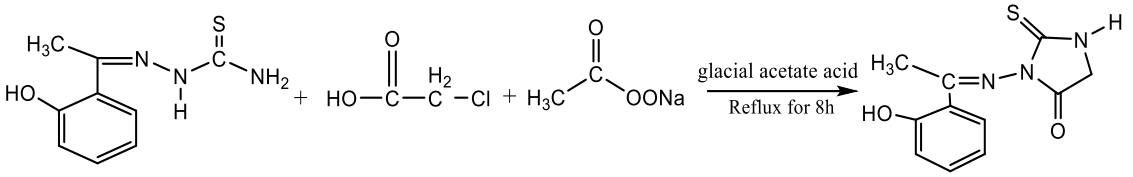
(2)



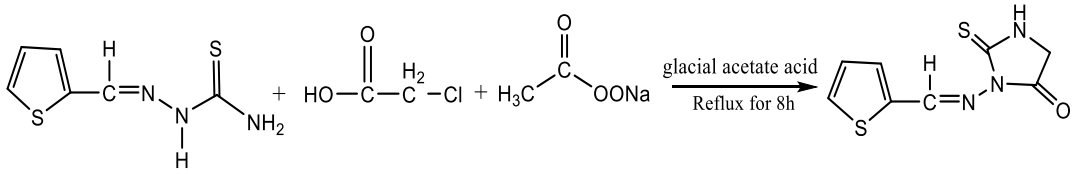
(3)



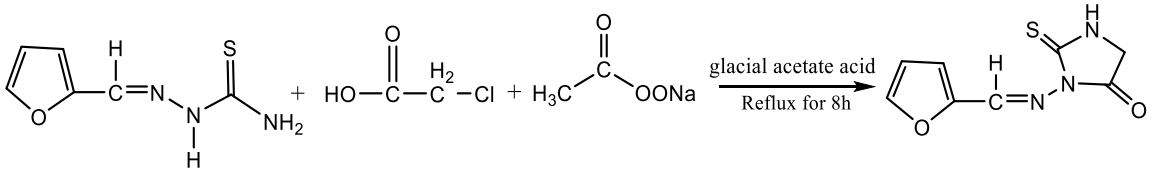
(4)



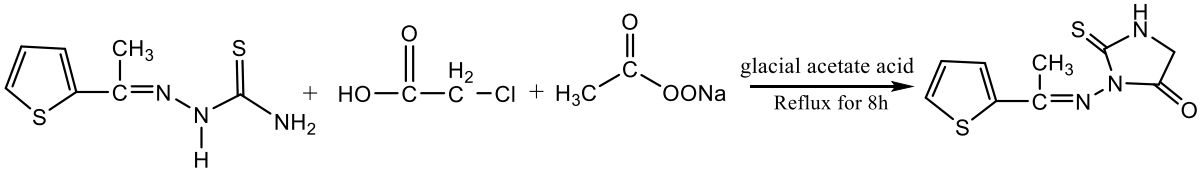
(5)



(6)

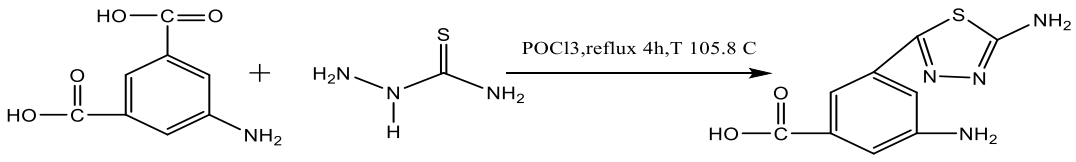


(7)

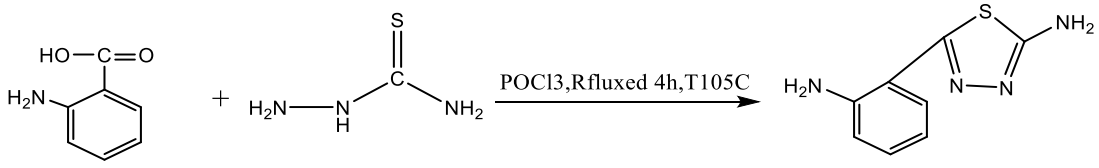


(8)

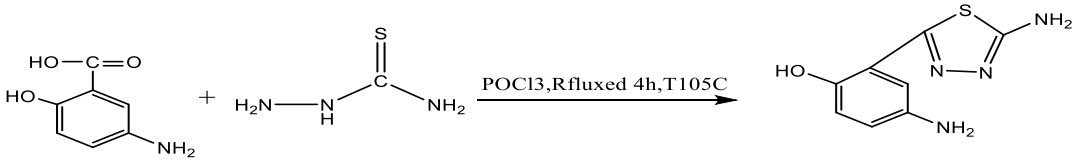
3. الجزء الثالث: تم تحضير مركبات 5-ستيريل-2-أمينو-4،3،1-ثياديازول (22-24) من تفاعل حمض 5-أمينو فثاليك، وحمض أنثرانيليك، وحمض 5-أمينو-2-هيدروكسي بنزويك مع ثيوسيميكاربازيد بوجود POCl3 كما هو موضح في المخطط (3).



(1)

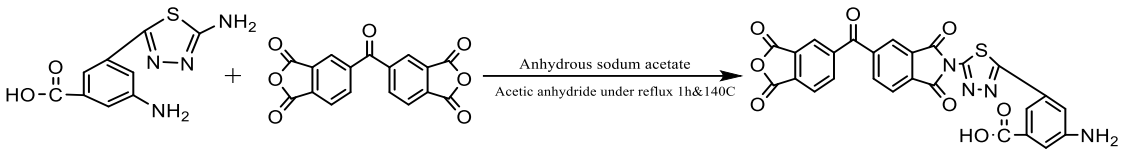


(2)

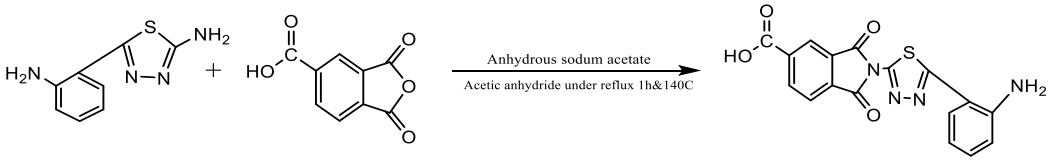


(3)

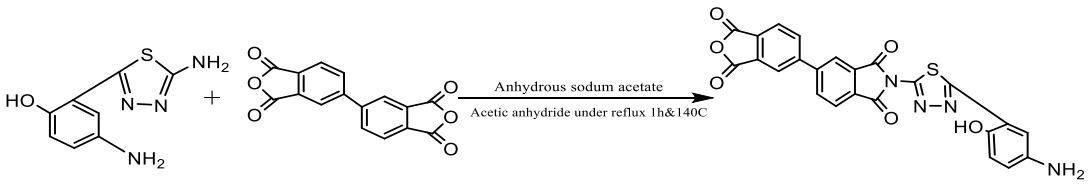
4. الجزء الرابع: تم تحضير مركبات الإيميد (22-24) من تفاعل مركبات 5-ستيريل-2-أمينو-4،3،1-ثياديازول (25-27) مع أنهيدريد حمض 3،3'،4،4'-بنزوفين رباعي الكربوكسيليك، وأنهيدريد تريميليتيك، وأنهيدريد حمض 4،4،3،3'-ثنائي فينيل رباعي الكربوكسيليك في محاليل بنسبة 3:2 من حمض الخليك والبيريدين كما هو موضح في المخطط (4).



(1)

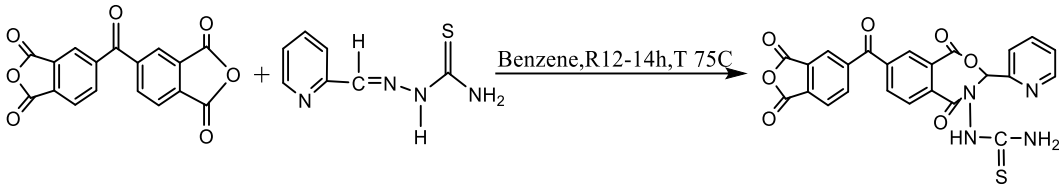


(2)

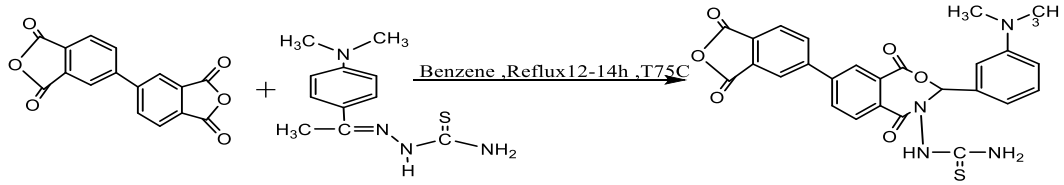


(3)

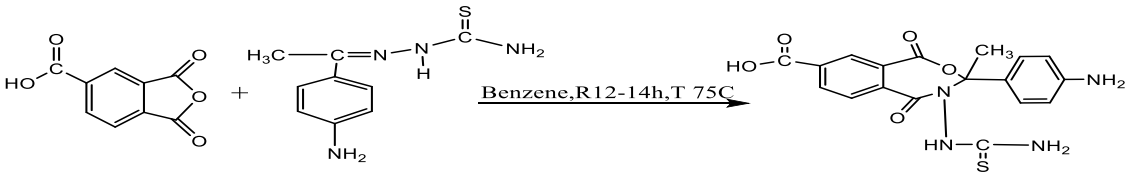
5. الجزء الخامس: تم تحقيق خطوة التدوير عن طريق معالجة مركبات ثيوسيمكاربازون (1،2،11) باستخدام أنهيدريد تريميليتيك وأنهيدريد حمض بنزوفين رباعي الكربوكسيليك 3،4،4'،3' للحصول على مركبات مشتقة من 1،3-أوكسازيبين-4،7-ديون (28-30) كما هو موضح في المخطط (5).



(1)



(2)



(3)

٦. الجزء السادس: تفاعل مركب ٢-أمينو ١،٣،٤-ثياديازول-٥-ثيول مع كلوريد الكلوروأسيتيل لإنتاج المركب (٣١)، ثم عولج باليوريا للحصول على المركب (٣٢) كما هو موضح في المخطط (٦).

٧. الجزء السابع: تم تصنيع مشتقات ٢،٣-ثنائي هيدروكينوسولين-٤-ون (٣٣-٣٥) من تفاعل مشتقات قواعد شيف (٨، ٩، ١٠) مع حمض الأنثرانيليك كما هو موضح في المخطط (٧).

٨. الجزء الثامن: تم تصنيع مشتقات التترازول (٣٨-٣٩) من تفاعل أزيد الصوديوم مع مشتقات قواعد شيف الناتجة عن تفاعل تيرفثالدهيد وإيزاتين مع ثيوسيميكاربازيد (٣٦-٣٧) كما هو موضح في المخطط (٨).

٩. الجزء التاسع: تم تحضير ٢-إيمينوثيازوليدين-٤-ون (٤٠). تم تصنيع المركبات من تفاعل الثيوريا مع حمض أحادي كلورو الأسيتيك كما هو موضح في المخطط (9).

10. الجزء العاشر: تم تصنيع مشتقات مركبات مانش (41-44) من تفاعل المركب (40) مع 1،4-فينيلين ديامين، و3،4'-ثنائي أمينو ثنائي فينيل إيثر، وثلاثي إيثيلين رباعي الأمين، و2،6-ثنائي أمينو بيريدين في وجود الفورمالين كما هو موضح في المخطط (10).

11. الجزء الحادي عشر: تم إجراء البلمرة الضوئية الجذرية لمونومرات الفينيل (حمض ميثيل أكريليك، وأنهيدريد إيتاكونيك، وN،N ثنائي ميثيل أكريلاميد، وأنهيدريد سيتراكونيك) باستخدام 1-هيدروكسي سيكلوهكسيل فينول كيتون كمحفز، مما أدى إلى إنتاج بوليمرات مشتركة (حمض ميثيل أكريليك - أنهيدريد إيتاكونيك) و(N،N ثنائي ميثيل أكريلاميد - أنهيدريد سيتراكونيك). بلمرة البوليمرات المشتركة كما هو موضح في المخطط (11)

12. الجزء الثاني عشر: تم تصنيع بوليمرات مشتركة تحتوي على مركبات حلقية غير متجانسة خماسية وسداسية الحلقات، وذلك لتثبيت بعض المركبات النشطة بيولوجيًا عبر روابط كيميائية على البوليمرات المشتركة (حمض ميثيل أكريليك - أنهيدريد إيتاكونيك) (1-44) و(N،N ثنائي ميثيل أكريلاميد - أنهيدريد سيتراكونيك) (45-64)، كما هو موضح في المخطط (12).

أظهر التحليل الحراري الوزن (TGA) أن البوليمرات المشتركة التي تحتوي على مجموعة فينيل كبديل في حلقة البيريدين والمركبات الحلقية غير المتجانسة تتمتع بأعلى استقرار حراري. ويبدو أن استخدام بديل أكبر حجمًا في الموضع 4 من حلقة البيريدين في مونومرات ثنائي الأمين يُحسّن من ذوبانية واستقرار البوليمرات المشتركة الناتجة.

دُرست درجة حرارة التحول الزجاجي للبوليمرات المشتركة باستخدام المسعر التفاضلي الماسح (.(DSC وظهرت قمة طاردة للحرارة للبوليمرات المتفرعة في قياس .DSCوازدادت درجة حرارة التحول الزجاجي للبوليمرات المشتركة مع الوزن الجزيئي، وكان هذا التغير متوافقًا مع الحسابات النظرية.

تم حساب الالتحام الجزيئي لعشرة بوليمرات اصطناعية. يُسهّل الالتحام الجزيئي تحليل التفاعلات بين مركبين، مما يُتيح تكوين مُركّب مستقر يُمكن استخدامه في تجارب مُختلفة. يُمكن استخدام نتائج دراسة الالتحام لتحديد

طاقة المُركّبات وقوتها واستقرارها. يُمكن أن يكون الليجاند المُستخدم أي جزيء صغير؛ وقد يكون البروتين المُستهدف بروتينًا أو كربوهيدرات أو حمضًا نوويًا. يُمكن تخزين البيانات المُجمّعة من دراسات الالتحام كبيانات أولية في قواعد البيانات لاستخدامها في تجارب واستخدامات مُستقبلة.

الالتحام الجزيئي هو أسلوب حسابي يُستخدم للتنبؤ بارتباط الجزيئات، التي تُسمى الليجاندات، ببروتينات المُستقبلات المُناسبة. وهو أداة تُستخدم لأغراض حسابية مُتعددة، بما في ذلك اكتشاف الأدوية. وقد أصبح أداة أساسية في تطوير الأدوية. تُستخدم هذه الطريقة لدراسة تفاعلات ارتباط الليجاند بالمستقبل باستخدام مقاييس مثل درجات الالتحام، ودرجات g، وطاقات الارتباط الحرة، وما إلى ذلك. تسمح هذه الطريقة للباحثين بدراسة الجزيئات الصغيرة والتأكد من أنها يمكن أن تعطي نتائج مفيدة قبل استخدامها في التجارب المعملية الرطبة.

تم اختبار النشاط المضاد للميكروبات للبوليمر المشترك المُعدَّل ضد مجموعة متنوعة من الكائنات الدقيقة, شملت الكائنات الحية الدقيقة موجبة الغرام (المكورات العنقودية الذهبية) وسالبة الغرام ، والإشريكية القولونية، والزائفة الزنجارية، والكلبسيلة الرئوية) ونوعان من الفطريات، والفطريات مثل (الكانديدا البيضاء, والرشاشية السوداء) . وبشكل عام، أظهرت البوليمرات المشتركة نشاطًا جيدًا مضادًا للميكروبات ضد الكائنات الدقيقة المذكورة سابقًا. يهدف هذا البحث إلى تقييم النشاط البيولوجي لبعض البوليمرات المشتركة المُصنَّعة حديثًا والتي تحتوي على مركبات حلقية غير متجانسة، وتطوير مرشحات دوائية جديدة لعلاج السرطان ضد خطوط الخلايا السرطانية، وخطوط الخلايا السرطانية التي تتضمن مجموعات دوائية مختلفة كجزيئات هجينة تمتلك خصائص مضادة للأكسدة ومضادة للميكروبات.

يُفترض أن يُسهم تصنيع بعض البوليمرات المشتركة في تعزيز فهمنا للأنشطة البيولوجية للمشتقات، ودراسة تطبيقات هذه المركبات المحتملة كمضادات حيوية، وتحديد علاقات التركيب بالنشاط المرتبطة بهذه التطبيقات. لذا، نصف هنا عملية تصنيع وتحديد ودراسة الأنشطة البيولوجية لتطوير علاجات جديدة لهذا الدواء.

تم تقييم عشرة من البوليمرات المشتركة الجديدة المصنعة من حيث نشاطها السام للخلايا ضد خطوط الخلايا السرطانية المستخدمة، وهي خط خلايا سرطان القولون ((Caco2وخط خلايا سرطان الجلد، حيث أظهرت زيادة في التثبيط مقارنةً بخط الخلايا الطبيعية. يدعم هذا التفسير الانخفاض المستمر في قيم IC_{50} من 24 إلى 72 ساعة لجميع المركبات، بالإضافة إلى استمرار الفرق بين خط خلايا سرطان القولون (HCT-116)وخط الخلايا الطبيعية (.(HdFn)

جمهورية العراق
وزارة التعليم العالي والبحث العلمي
جامعة القادسية
كلية العلوم
قسم الكيمياء

تخليق وتشخيص بوليمرات حلقية غير متجانسة جديدة ودراسة النشاط البيولوجي المحتمل

رسالة مقدمة الى

مجلس كلية العلوم/جامعة القادسية

وهي جزء من متطلبات نيل درجة الدكتوراه في علوم الكيمياء

من قبل الطالبة

نضال حسون ثامر

ماجستير علوم كيمياء/ جامعة القادسية (2021-2022)

بأشراف

أ.د. محمد علي مطر

1448هجري **2026 ميلادي**